Indexes Eng

ENGINEERING-TRANSPORTATION
LIBRARY

THE UNIVERSITY
OF MICHIGAN
MAR 10 1966
ENGINEERING
LIBRARY

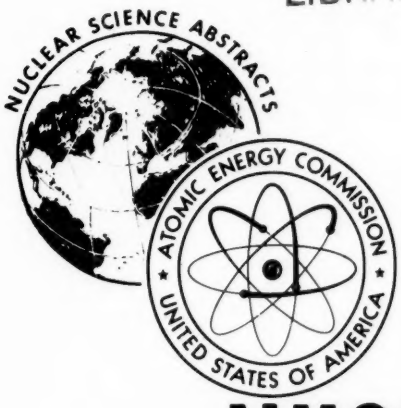


# NUCLEAR SCIENCE ABSTRACTS

Volume 20 Number 2

Abstracts 1581–3648

January 31, 1966

UNITED STATES ATOMIC ENERGY COMMISSION
Division of Technical Information

DEPOSITED BY THE
UNITED STATES OF AMERICA

# USAEC DEPOSITORY LIBRARIES

**Collections of USAEC reports are maintained in the libraries of the organizations listed below for reference use by the general public. Facilities for making photocopies are available. The USAEC also makes available through these libraries atomic energy reports of countries other than the U. S. that are abstracted in *Nuclear Science Abstracts*.**

**ALABAMA**
Auburn, Auburn University
**ARIZONA**
Tucson, University of Arizona
**ARKANSAS**
Fayetteville, University of Arkansas
**CALIFORNIA**
Berkeley, University of California
Davis, University of California
Los Angeles, University of California
San Diego, Public Library
Stanford, Stanford University
**COLORADO**
Boulder, University of Colorado
Denver, Public Library
**CONNECTICUT**
New Haven, Yale University
**DELAWARE**
Newark, University of Delaware
**DISTRICT OF COLUMBIA**
Washington, Library of Congress
**FLORIDA**
Coral Gables, University of Miami
Gainesville, University of Florida
Tallahassee, The Florida State University
**GEORGIA**
Atlanta, Georgia Institute of Technology
**HAWAII**
Honolulu, University of Hawaii
**ILLINOIS**
Chicago, John Crerar Library
Chicago, University of Chicago
Evanston, Northwestern University
Urbana, University of Illinois
**INDIANA**
Bloomington, Indiana University
Lafayette, Purdue University
**IOWA**
Ames, Iowa State University
**KANSAS**
Manhattan, Kansas State University
**KENTUCKY**
Lexington, University of Kentucky
Louisville, University of Louisville
**LOUISIANA**
Baton Rouge, Louisiana State University
New Orleans, Tulane University
**MARYLAND**
Baltimore, Johns Hopkins University
College Park, University of Maryland
**MASSACHUSETTS**
Cambridge, Harvard University
Cambridge, Massachusetts Institute of Technology
**MICHIGAN**
Ann Arbor, University of Michigan
Detroit, Public Library
East Lansing, Michigan State University
**MINNESOTA**
Minneapolis, University of Minnesota
**MISSISSIPPI**
State College, Mississippi State University
**MISSOURI**
Kansas City, Linda Hall Library
Rolla, University of Missouri School of Mines and Metallurgy
St. Louis, Washington University
**MONTANA**
Bozeman, Montana State College
**NEVADA**
Las Vegas, Nevada Southern University
Reno, University of Nevada
**NEW JERSEY**
Princeton, Princeton University
Teaneck, Fairleigh Dickinson University
**NEW MEXICO**
Albuquerque, University of New Mexico
**NEW YORK**
Albany, The University of the State of New York
Buffalo, State University of New York at Buffalo
Ithaca, Cornell University
New York, Atomic Industrial Forum, Inc.
New York, Columbia University
New York, New York University
Rochester, University of Rochester
Schenectady, Union College
Syracuse, Syracuse University
Troy, Rensselaer Polytechnic Institute
**NORTH CAROLINA**
Charlotte, Public Library of Charlotte and Mecklenburg County
Durham, Duke University
Raleigh, North Carolina State College
**NORTH DAKOTA**
Grand Forks, University of North Dakota
**OHIO**
Cincinnati, University of Cincinnati
Cleveland, Public Library
**OHIO (CONT.)**
Columbus, Ohio State University
Toledo, University of Toledo
Youngstown, Youngstown University
**OKLAHOMA**
Norman, University of Oklahoma
Stillwater, Oklahoma State University
**OREGON**
Corvallis, Oregon State University
Portland, Reed College
**PENNSYLVANIA**
Philadelphia, University of Pennsylvania
Pittsburgh, Carnegie Library
University Park, Pennsylvania State University
**PUERTO RICO**
Rio Piedras, University of Puerto Rico
**RHODE ISLAND**
Providence, Brown University
**SOUTH CAROLINA**
Columbia, University of South Carolina
**TENNESSEE**
Knoxville, University of Tennessee
Memphis, Public Library
Nashville, Joint University Libraries
Oak Ridge, Oak Ridge Associated Universities
**TEXAS**
Austin, University of Texas
College Station, Texas A & M University
Dallas, Southern Methodist University
Houston, Rice University
Lubbock, Texas Technological College
San Antonio, Public Library
**UTAH**
Salt Lake City, University of Utah
**VIRGINIA**
Blacksburg, Virginia Polytechnic Institute
Charlottesville, University of Virginia
Norfolk, Old Dominion College
**WASHINGTON**
Pullman, Washington State University
Seattle, University of Washington
**WEST VIRGINIA**
Morgantown, West Virginia University
**WISCONSIN**
Madison, University of Wisconsin
Milwaukee, Public Library
**WYOMING**
Laramie, University of Wyoming

DEPOSITED BY THE
UNITED STATES OF AMERICA

Volume 20, Number 2, January 31, 1966

# NUCLEAR SCIENCE ABSTRACTS

*A semimonthly publication of the USAEC Division of Technical Information, Edward J. Brunenkant, Director.*
*Published by the USAEC Division of Technical Information Extension, Robert L. Shannon, Extension Manager.*

*Nuclear Science Abstracts* covers the international literature on nuclear science and technology and provides the only comprehensive abstracting and indexing of this body of information. Published twice each month since 1947, *NSA* covers technical reports of the U. S. Atomic Energy Commission and its contractors, technical reports of U. S. Government agencies and other governments, universities, industrial and research organizations, as well as patents, books, and journal literature on a world-wide basis. Nearly 350,000 abstracts have appeared in *NSA* through Volume 19. The subject matter covered in *NSA* is described in issue Number 1 and in TID-4552, *Subject Scope of Nuclear Science Abstracts*, available free from the U. S. Atomic Energy Commission, Division of Technical Information Extension, P. O. Box 62, Oak Ridge, Tennessee 37830.

Abstracts are arranged according to a number of subject categories and subcategories. Definitions of categories appear in issues Number 1 and 13. If the language of the original item is not English, the language will be indicated. Translations are not abstracted where an abstract of the original item has appeared in *NSA*.

## INDEXES TO NSA

Corporate author, personal author, subject, and report number indexes appear in each issue and are cumulated quarterly, semiannually, and annually. Multi-volume cumulations have been issued as indicated on the following page. Report number indexes for all volumes (1–18) were issued at the end of Vol. 18. At the end of Vol. 19, the indexes for Vols. 1–15 were reissued to include additional public availability information. This cumulation will be a permanent shelf item and will not be reissued. Report number indexes for Vol. 19 are included as a cumulation beginning with Vol. 16.

## AVAILABILITY OF PUBLICATIONS ABSTRACTED

The public availability of all U. S. Atomic Energy Commission reports is indicated in the report number indexes. The availability of other reports, when known, is also indicated. The availability of some unnumbered reports is given in the abstract.

Dissertations abstracted in *Dissertation Abstracts* and included in *NSA* are available from University Microfilms, Inc., 315 N. First Street, Ann Arbor, Michigan 48103.

Most of the published literature abstracted in *NSA* is on deposit at the Library, Oak Ridge Associated Universities, Oak Ridge, Tennessee, (a USAEC depository library) and is available through interlibrary loan. When requesting papers from this source, it is important that *NSA* volume and abstract number be cited.

# HOW TO OBTAIN NUCLEAR SCIENCE ABSTRACTS

*NSA* is available on an exchange basis to universities, research institutions, industrial firms, and publishers of scientific information. Inquiries should be directed to the U. S. Atomic Energy Commission, Division of Technical Information Extension, P. O. Box 62, Oak Ridge, Tennessee 37830.

Government agencies may obtain *NSA* free of charge.

*NSA* is available to the general public on a subscription basis from the Superintendent of Documents, U. S. Government Printing Office, Washington, D. C. 20402, as follows:

For the 24 regular issues, $30.00 domestic, $37.00 foreign. A single issue costs $1.75, plus 25 per cent for foreign mailing. Domestic rates apply to the United States, Canada, Mexico, and Central and South American countries except Argentina, Brazil, British and French Guiana, Surinam, and British Honduras. Foreign rates apply to the countries excepted above and to all other countries throughout the world.

For the quarterly, semiannual, and annual indexes, $22.00 domestic, $25.00 foreign.

Multivolume subject and author indexes are available as follows:

Vols. 1–4 (1948–1950) Johnson Reprint Corporation, 111 Fifth Avenue, New York, N. Y. 10003, $30.00.

Vols. 5–10 (1951–1956) Superintendent of Documents, U. S. Government Printing Office, Washington, D. C. 20402, $5.25.

Vols. 11–15, Subjects, Superintendent of Documents, U. S. Government Printing Office, Washington, D. C. 20402, $19.00.

Vols. 11–15, Personal Authors, Superintendent of Documents, U. S. Government Printing Office, Washington, D. C. 20402, $14.25.

Vols. 11–15, Corporate Authors, Superintendent of Documents, U. S. Government Printing Office, Washington, D. C. 20402, $2.50.

Cumulative Report Number Index, Vols. 1–15, Revised, is available from the Superintendent of Documents, U. S. Government Printing Office, Washington, D. C. 20402, $4.00.

Cumulative Report Number Index, Vols. 16–19, is available from the Superintendent of Documents, U. S. Government Printing Office, Washington, D. C. 20402, $2.50.

Annual Indexes are available separately from the U. S. Government Printing Office as follows:

Vol. 16, Subject and Authors, $9.75.
Vol. 17, Subject and Authors, $12.25.
Vol. 18, Subject and Authors, $12.50.
Vol. 19, Subject and Authors, $12.50.

# ACKNOWLEDGMENTS

Agreements between the United States Atomic Energy Commission and the following organizations with regard to providing continuing services and specific literature coverage for *Nuclear Science Abstracts* are gratefully acknowledged:

American Institute of Physics; Atomic Energy of Canada Limited; Atomic Energy Research Establishment, United Kingdom; European Atomic Energy Community (EURATOM); Gmelin Institute; International Atomic Energy Agency; Japan Atomic Energy Bureau—Japan Atomic Energy Research Institute; Netherlands Patent Office; Reactor Centrum Nederland.

# TABLE OF CONTENTS

Volume 20, Number 2, January 31, 1966


| Category | Page |
|---|---|
| BIOLOGY AND MEDICINE | 211 |
| General | 211 |
| Ecology | 212 |
| Metabolism, Tissue Distribution, and Toxicology | 212 |
| Radiation Effects on Biochemicals | 214 |
| Radiation Effects on Tissues | 214 |
| Radiation Effects Therapy and Countermeasures | 227 |
| Radiation Hazards and Protection | 228 |
| Radiotherapy and Radiodiagnosis | 228 |
| CHEMISTRY | 233 |
| General | 233 |
| Analytical Procedures | 233 |
| Inorganic and Physical Chemistry | 241 |
| Organic Chemistry | 251 |
| Radiation Chemistry | 252 |
| Radiochemistry | 258 |
| Separation Processes and Procedures | 260 |
| ENGINEERING | 264 |
| General | 264 |
| Applications of Nuclear Explosions | 264 |
| Facilities and Equipment | 265 |
| Heat Transfer and Fluid Flow | 266 |
| Materials Testing | 268 |
| Protective Structures | 269 |
| Space Propulsion | 270 |
| GEOLOGY, METEOROLOGY, AND MINERALOGY | 271 |
| General | 271 |
| Meteorology | 271 |
| Natural Radioactivity and Fallout | 271 |
| Techniques and Equipment | 273 |
| Thorium and Uranium Minerals | 273 |
| HEALTH AND SAFETY | 275 |
| INSTRUMENTATION | 279 |
| General | 279 |
| Radiation Detection | 281 |
| Radiation Effects | 288 |
| ISOTOPE TECHNOLOGY | 289 |
| General | 289 |
| Industrial Applications | 289 |
| Power Application | 290 |
| Separation and Production | 290 |
| MATHEMATICS AND COMPUTERS | 291 |
| METALS, CERAMICS, AND OTHER MATERIALS | 292 |
| General | 292 |
| Corrosion | 294 |
| Fabrication | 297 |
| Properties and Structure | 299 |
| Radiation Effects | 311 |
| PHYSICS | 324 |
| General | 324 |
| Accelerators | 325 |
| Astrophysics and Cosmology | 328 |
| Atomic Physics | 332 |
| Cosmic Radiation | 339 |
| Direct Energy Conversion | 341 |
| Elementary Particles and Radiations | 343 |
| Field Theory, Scattering Theory, and Symmetries | 351 |
| Fluid Physics and Thermodynamics | 357 |
| Geophysics | 360 |
| Gravitation, Quantum Mechanics, and Relativity Theory | 362 |
| Low Temperature Physics | 365 |
| Neutron Physics | 370 |
| Nuclear Properties and Reactions | 375 |
| Plasma Physics and Thermonuclear Processes | 391 |
| Shielding | 401 |
| Solid State Physics | 404 |
| REACTOR TECHNOLOGY | 410 |
| General | 410 |
| Auxiliaries and Components | 411 |
| Criticality Studies | 413 |
| Design and Feasibility | 418 |
| Fuels | 418 |
| Power and Power-Breeder Reactors | 420 |
| Process Heat Reactors | 425 |
| Production Reactors | 425 |
| Propulsion and Space | 425 |
| Research and Test Reactors | 427 |
| WASTE DISPOSAL AND PROCESSING | 430 |
| GENERAL AND MISCELLANEOUS | 431 |
| CORPORATE AUTHOR INDEX | INDEX-1 |
| PERSONAL AUTHOR INDEX | INDEX-11 |
| SUBJECT INDEX | INDEX-57 |
| REPORT NUMBER INDEX | INDEX-134 |

# STAFF OF NUCLEAR SCIENCE ABSTRACTS


**MANAGING EDITOR**

John W. Norris

**ASSISTANT MANAGING EDITOR**

Donald D. Davis

**ASSOCIATE EDITORS**

Lawrence T. Whitehead
David E. Bost
Robert C. Kelly
Lee M. Thompson

**SUBJECT INDEX EDITOR**

Everett J. Hoffman

**EVALUATORS**

William D. Matheny
John H. Mitchell
Mary H. Newman

**ABSTRACTORS**

F. S. Armstrong (AECL)
Jane G. Buchanan
D. Lamar Cason
Helen G. Donald
James R. Dulaney
Wells L. Green
Mary Catherine Grissom
Fernando J. Hamilton
Phyllis C. Hansen
Thomas F. Heagerty
Carolyn D. Houston
Rose V. Jermain
Betty L. McDowell
Jean F. Peckham
Mona H. Raridon
Julia Redford
Lila B. Smith
Charles E. Stuber
Martha J. Thomas
Anne G. Ward
David C. West
Milton O. Whitson

**SUBJECT HEADING SPECIALIST**

Robert E. Upchurch

**CORPORATE AUTHOR SPECIALIST**

Clara L. Fox

**DESCRIPTIVE CATALOGING SPECIALIST**

J. Paul Meredith

**SCHEDULING AND PUBLISHING COORDINATOR**

Brainard L. Patton


Communication concerning the editorial policy and content of *NSA* should be addressed to the Managing Editor, *Nuclear Science Abstracts*, AEC Division of Technical Information Extension, P. O. Box 62, Oak Ridge, Tennessee 37830.

---


*Use of funds for printing this publication approved by the Director of the Bureau of the Budget, May 20, 1963*

Volume 20, Number 2 January 31, 1966

# NUCLEAR SCIENCE ABSTRACTS

## BIOLOGY AND MEDICINE

### General

*Refer also to abstracts 1790, 1791, and 2520.*

**1581** (BNWL-SA-341) AGE RELATED CHANGES IN HEMATOLOGICAL AND SERUM BIOCHEMICAL PARAMETERS IN MINIATURE SWINE. McClellan, R. O.; Vogt, Glenda S.; Ragan, H. A. (Battelle-Northwest, Richland, Wash. Pacific Northwest Lab.). Sept. 30, 1965. Contracts AT(45-1)-1350; AT(45-1)-1830. 14p. (CONF-650718-1). Dep. mn; CFSTI $1.00 cy, $0.50 mn.

From Symposium on Swine in Biomedical Research, Richland, Wash.

Twenty-one hematological and serum biochemical parameters were measured at 6 weeks (weaning), 3 months, 6 months, 9 months, and 12 months of age, and thereafter at 6 month intervals in miniature swine maintained as control animals in a long-term radiotoxicity study. The oldest animals under observation are now 6 years of age. Age-related changes are reported that were observed in most of the parameters investigated. (auth)

**1582** (NYO-2038-2) PRODUCTION AND STUDY OF ASPOROGENIC MUTANTS. A STUDY OF THE FINE STRUCTURE, BIOCHEMISTRY AND CONTROL OF BACTERIAL SPOROGENESIS. Annual Report, January 1, 1965–December 31, 1965. Lundgren, Donald G. (Syracuse Univ., N. Y. Dept. of Bacteriology and Botany). Contract AT(30-1)-2038. 56p. Dep. mn; CFSTI $3.00 cy, $0.50 mn.

Results are summarized from a series of studies on the cytology, control mechanisms, biochemical differentiation, physiology, and genetics of sporulation of Bacillus cereus and Bacillus subtilis. Electron microscopic studies were made of fine structure and membrane disruption during sporulation. (C.H.)

**1583** ISOTOPIC EFFECT OF TRITIUM IN THE FORM OF TRITIATED THYMIDINE ON THE ACTIVITY OF ATP: PURIFIED THYMIDINE-5'-PHOSPHOTRANSFERASE. Baugnet-Mahieu, L.; Goutier, R.; Semal, M. (Centre d'Etude de l'Energie Nucleaire, Mol, Belg.). Arch. Intern. Physiol. Biochim., 73: 556-7(June 1965). (In French).

It was previously shown that in the presence of an extract of liver regenerating in vitro, thymidine-6-$^{3}H$ is phosphorylated to a lesser degree than thymidine-2-$^{14}C$. For a $^{3}H/^{14}C$ ratio equal to unity in the incubated thymidines, the $^{3}H/^{14}C$ ratio in the mono-, di-, and triphosphate esters that were formed varied from 0.6 to 0.8. This phenomenon was analyzed with the aid of preparations of thymidine kinase purified from the liver undergoing regeneration. The formation of $^{3}H$-thymidine monophosphate (TMP) was slower than that of TMP-$^{14}C$. The amount of this reduction was inversely proportional to the concentration in enzyme protein. The tests conducted with hepatic extracts and with purified enzyme preparations excluded the possibility of enzyme inhibition by the products of the radiolysis of $^{3}H$-thymidine, as well as that of a loss of tritium in the course of incubation. Since thymine is an important point of attachment of thymidine in the active center of the enzyme, it is considered possible that the presence of tritium on the thymidine actually slows the formation of the enzyme-substrate complex. (BBB)

**1584** THE FINE STRUCTURE OF MICROCOCCUS RADIODURANS. Thornley, Margaret J.; Horne, R. W.; Glauert, Audrey M. (Strangeways Research Lab., Cambridge, Eng.). Arch. Microbiol., 51: 267-89(1965).

A study of the fine structure of Micrococcus radiodurans was undertaken to find out whether there are any unusual features that might be correlated with the extremely high radioresistance. Preliminary observations showed that the nuclear and cytoplasmic structure is normal, but that the cell surface has a multilayered structure that differs from that of any bacteria hitherto described. The fine structure was studied by electron microscopy of intact and disrupted cells using thin sectioning and negative staining techniques. The cell wall consisted of four distinct layers, each having a characteristic fine structure, one of which was tentatively identified as that responsible for maintaining the rigidity of the cells. Striations with a periodicity of 175 to 200 Å are visible in thin sections of this layer, and a pseudo-hexagonal array of dark holes is seen in surface view of negatively-stained fragments. It is concluded that this layer is the main structural element of the cell wall of M. radiodurans. The other three layers of the surface were not clearly located in thin sections. (TCO)

**1585** ISOTOPE FLOWS AND FLUX RATIOS IN BIOLOGICAL MEMBRANES. Kedem, Ora (Massachusetts General Hospital, Boston); Essig, Alvin. J. Gen. Physiol., 48: 1047-70(July 1965).

The theory of isotope flow was investigated by analysis of fluxes of isotopic species applied to opposite surfaces of a membrane. A simple and general flux ratio equation was derived that may permit evaluation of membrane permeability, even without knowledge of forces, or of the nature of active transport processes. Application of the equation may permit evaluation of the contributions of the various processes to the transport of the examined species. The formulation was applied to consideration of energetics of active transport. Results showed that net flux may be determined from measurement of two isotope fluxes, both in the absence and presence of isotope interaction. Existence of heterogeneous parallel pathways modifies predictably both the observed flux ratio and the apparent exchange resistance. Only in the absence of leak are the observed parameters equal to those in an active pathway. With increasing leak, deviations become quite appreciable; large flux ratios indicate insignificant leak. Evaluation of the contribution of metabolism to transport processes is dependent on the experimental setting. The maximum electrochemical potential difference produced

by active transport is related to the magnitude leak. The flux ratio of a short-circuited membrane is influenced by both leak and isotope interaction. (TCO)

**1586** A NEW CO-PRECIPITATION METHOD FOR THE ACTIVATION ANALYSIS SIMULTANEOUS DETERMINATION OF MANGANESE, COPPER AND ZINC IN BLOOD SERUM. Campero, A. (Atomic Energy Commission of Mexico, Mexico City. General Atomic Div., General Dynamics Corp., San Diego, Calif.); Lukens, H. R. Jr. Trans. Amer. Nucl. Soc., 8: 330(Nov. 1965).

**1587** CORRELATIONS BETWEEN TESTS OF AGING IN HIROSHIMA SUBJECTS—AN ATTEMPT TO DEFINE PHYSIOLOGIC AGE. Hollingsworth, J. W.; Hashizume, A.; Jablon, Seymour (Atomic Bomb Casualty Commission, Hiroshima-Nagasaki). Yale J. Biol. Med., 38: 11-26(Aug. 1965). (TID-22234).

Nine physiologic functions that change with age were measured in 437 subjects during their regular visits to the Atomic Bomb Casualty Commission Clinic in Hiroshima, Japan. This pilot study was undertaken to determine the feasibility of collecting such data in a population sample, and to provide data for statistical formulation of a combined physiologic age score. The study demonstrated that adequate sample data could be obtained, and that statistical treatment could construct a physiologic age for individual subjects. However, the tests were of limited value below age 40, and the validation of the concept of physiologic age requires eventual correlation with mortality. Since the ABCC program includes a highly accurate mortality survey, it is hoped that data on physiologic aging can be collected and eventually related to mortality. (auth)

## Ecology

*Refer also to abstracts 2079–2081.*

**1588** (BNL-917) ECOLOGICAL EFFECTS OF NUCLEAR WAR. Woodwell, G. M. (ed.) (Brookhaven National Lab., Upton, N. Y.). Aug. 1965. Contract AT(30-2)-Gen-16. 76p. (CONF-630805-1). Dep. mn; CFSTI $3.00 cy, $0.75 mn.

From 13th Meeting of the American Inst. of Biological Sciences, Amherst, Mass.

Separate abstracts were prepared on five papers presented at this symposium. (C.H.)

*For abstracts of individual papers see: 1589 and 2078–2081.*

**1589** (BNL-917, pp 61-8) BIOLOGICAL INTERACTIONS ASSOCIATED WITH SPRUCE BUDWORM INFESTATIONS. Macdonald, D. R. (Forest Entomology and Pathology Lab., Fredericton (New Brunswick)).

Both the spruce budworm and DDT are very severe stresses to the plant and animal communities of the boreal forest. It is interesting to note, however, that in both cases when the stress is removed there is a very rapid trend toward recovery. In fact, the spruce-fir community maintains its own built-in mechanism for repair in the form of an abundant supply of advanced tree reproduction which largely escapes destruction and forms the new forest. It is actually a self-perpetuating system, alternating between mature and immature stages, and has been called both a catastrophic climax and a dynamic climax. Even when wildfire disrupts the system, succession is only temporarily delayed unless the site is burned repeatedly and the humus layer destroyed. (auth)

**1590** (RM-3902-TAB) NOTES ON THE ESTIMATION OF FIRE DAMAGE TO NON-URBAN AREAS FROM NUCLEAR ATTACK. Doner, J. E. (RAND Corp., Santa Monica, Calif.). Oct. 1965. Contract AT(04-3)-414. 16p. Dep. mn; CFSTI $1.00 cy, $0.50 mn.

Early attempts to estimate the non-urban fire damage that would result from a widespread nuclear attack on the United States have, of necessity, depended heavily on the experience and judgment of fire suppression personnel. An elementary model was previously developed, but lack of knowledge about the very complex burning process of a forest fire and the tremendous number of inputs required for a nationwide study limit its accuracy and utility. Some possible approaches toward improving the model are suggested. (auth)

**1591** SYSTEMATIC RELATIONSHIPS BETWEEN CARBON AND OXYGEN ISOTOPES IN CARBONATES DEPOSITED BY MODERN CORALS AND ALGAE. Keith, M. L.; Weber, J. N. (Pennsylvania State Univ., University Park). Science, 150: 498-501(Oct. 22, 1965).

Analyses of organic carbonates from Jamaican coral reefs showed a positive correlation between the $^{18}O$:$^{16}O$ ratio and the $^{13}C$:$^{12}C$ ratio in some taxonomic groups of corals and algae, but essentially no correlation (nearly constant $^{18}O$) in one suborder of reef-building corals. The strontium and magnesium contents apparently were controlled mainly by skeletal mineralogy and showed no correlation with carbon or oxygen isotopic composition. The observed positive correlations between $^{13}C$ and $^{18}O$ content may be due to calcification processes utilizing carbon-oxygen compounds from two isotopically different sources or utilizing selected portions of a wide spectrum of carbon-oxygen compounds in which there is a positive correlation between $^{13}C$:$^{12}C$ and $^{18}O$:$^{16}O$ ratios. Coral and algal carbonates from Jamaican waters, with an annual temperature range of only about 4°C, exhibited a total $\delta^{13}C$ range of more than 13 per mil and a $\delta^{18}O$ range of more than 4 per mil. The wide isotopic variability resulting from vital effects of calcifying organisms must be taken into account in applying isotopic analysis to the study of sedimentary carbonate rocks, which may include reef-derived carbonates. (auth)

## Metabolism, Tissue Distribution, and Toxicology

*Refer also to abstract 1695.*

**1592** (BNL-7903) AN ESTIMATE OF THE SIZE OF THE RIBOSOMAL SITE FOR MESSENGER RNA BINDING. Takanami, M.; Zubay, G. (Brookhaven National Lab., Upton, N. Y.). [1964]. Contract AT(30-2)-Gen-16. 18p. Dep. mn; CFSTI $1.00 cy, $0.50 mn.

The properties of the binding site for messenger RNA in Escherichia coli ribosomes and their subunits were studied using a solution of ribosomes, $^{14}C$-polyribouridylic acid (poly U), and a small volume of a solution containing ribonuclease. The solution was incubated, chilled, and fractionated on a Sephadex C-100 column. Elution patterns of the mixture, the effects of increasing RNAase concentration, the results of sedimentation studies, and chromatographic patterns after cellulose-column elution were used to estimate the size of the ribosomal site for messenger RNA binding. (C.H.)

**1593** (COO-1170-4) CRITICALLY CONTROLLED INHALATION STUDY OF PATHOGENESIS OF NEODYMIUM OXIDE IN MICE AND GUINEA PIGS. Davison, Fred C.; Ramsey, Frank K. (Iowa State Univ. of Science and Tech., Ames. Inst. for Atomic Research; Iowa State Univ. of Science and Tech., Ames. Coll. of Veterinary Medicine). June 1965. Contract AT(11-1)-1170. 77p. Dep. mn; CFSTI $3.00 cy, $0.75 mn.

The effects of an aerosol of stable neodymium oxide ($Nd_2O_3$) of a known particle size range and concentration on the lungs, other major organs, blood, and body weight of mice and guinea pigs, when administered over various periods of time up to 120 days, were evaluated. An inhalation system was constructed, and the aerosol produced was characterized concerning its particle size and concentration. The final experimental design was the outgrowth of a pilot intratracheal injection experiment conducted on guinea pigs and rats. Mice and guinea pigs exposed to concentrations of approximately 30 mg $Nd_2O_3$/meter$^3$ of air, in which

about 60% of the mass was composed of particles less than 1 $\mu$ in diam, showed a gradual increase of neodymium in the lung as exposure time increased. This material was contained in macrophages in the alveoli and in the alveolar septa and was transported to the tracheobronchial lymph nodes. There were no granulomatous or other dramatic inflammatory reactions to the foreign material during the period of this experiment, and the other body organs which were evaluated histopathologically remained relatively normal. Changes in hematologic parameters were not remarkable. (auth)

**1594** (LA-DC-6507) SYNCHRONIZED MAMMALIAN CELLS. II. AN EXPERIMENTAL TEST OF A MODEL FOR SYNCHRONY DECAY. Anderson, E. C.; Petersen, D. F. (Los Alamos Scientific Lab., Univ. of California, N. Mex.). [1964]. Contract W-7405-eng-36. 7p. Dep. mn; CFSTI $1.00 cy, $0.50 mn.

A theoretical model is described which can be used to make quantitative predictions for the decay of synchrony in cell cultures on the basis of the assumption that decay is due to a random variability in generation times. A method of obtaining data of sufficient precision to permit accurate analysis of growth rate patterns is described. This was applied in a test of the model and the comparison of the single and double block methods for the induction of synchrony. Chinese hamster ovary cells were grown in tissue culture, synchronized by the thymidine block method, and total cell concentrations were measured at hourly intervals by electronic particle counting. A comparison was made of experimental data and theoretical decay predicted by the model. (C.H.)

**1595** TUMOUR UPTAKE AND DISTRIBUTION OF NIOBIUM ISOTOPES IN RATS. Matthews, C. M. E.; Gartside, J. M. (Hammersmith Hospital, London). Brit. J. Cancer, 19: 551-9(Sept. 1965).

The distribution of carrier free niobium isotopes $^{90}$Nb and $^{95}$Nb, in rats and uptake in two different transplanted rat sarcomas is described. Factors affecting this distribution, including binding to plasma proteins, are discussed. The investigation was complicated by the fact that niobium isotopes readily form colloidal solutions. (auth)

**1596** BODY CONTENT OF $^{232}$Th DAUGHTERS AFTER THOROTRAST INJECTION. Hursh, John B. (Univ. of Rochester, N. Y.). Brit. J. Radiol., 38: 776-84(Oct. 1965).

Whole-body $\gamma$ counting procedure was used to study the fate, up to four years' post-injection, of $^{232}$Th daughters in four volunteer subjects who received intravenous injections of 24 ml Thorotrast. Thoron expired in the breath was measured in two subjects yielding 9 per cent of thoron formed. A decreasing rate of excretion of the radium daughters was inferred for the time interval of the study. Calculations are made to show that at least 16 per cent of the thoron formed moves out from its site of origin and that the lung dose from expired thoron, depending on time after injection, and on $^{228}$Ra build up may vary from 15 to 45 rems per year. (auth)

**1597** ELECTRON MICROSCOPIC AUTORADIOGRAPHY OF THE INCORPORATION OF TRITIATED LEUCINE BY THE HYPOPHYSIS OF THE DRAKE IN ORGANOTYPIC CULTURE. Tixier-Vidal, Andree; Fiske, Susan; Picart, Renee; Haguenau, Francoise (College de France, Paris). Compt. Rend., 261: 1133-6(July 1965). (In French).

The incorporation of tritiated leucine was studied by electron microscopy at the level of hypophysic explants of the drake in organotypic culture. The explants are constituted almost exclusively by prolactin cells. The steps of the progression of the newly synthesized proteins are described and some particular characteristics are announced; simultaneous labeling of the nucleus and of the ergastoplasm and low proportion of labeled granulations after 2 hrs of contact. (tr-auth)

**1598** IN VIVO DISTRIBUTION OF RADIOACTIVE CHROMIC PHOSPHATE: INFLUENCE OF THE PARTICLE SIZE AND ROUTE OF INJECTION. Anghileri, L. J. (Comision Nacional de Energia Atomica, Buenos Aires). Int. J. Appl. Radiat. Isotop., 16: 623-30(Nov. 1965).

The in vivo distribution of colloidal chromic radiophosphate having different particle sizes was studied following intravenous, intramuscular, and intracavitary injection into mice. True colloidal solutions were obtained by the probable formation of a chromium–gelatin complex, and colloids with this characteristic, have a different behavior to those prepared by a simple colloidal adsorption of the particles on the gelatin. The smaller the particle size the higher the amount deposited in the liver and the amount eliminated through the bile. The same relationship to particle size was observed in bone uptake. The colloid was deposited mainly in bone marrow and retained there with the consequent risk of irradiation damage. Considerable activity was observed in leukocytes due to phagocytosis of particles. It was assumed that their death and disintegration causes a slow increase in the liver uptake. The small-particle type gave a high specific activity in the liver, gonads, and bone. With the larger particles the highest specific activity was in the bones and decreased considerably in the liver. (auth)

**1599** $^{133}$Xe PARTITION COEFFICIENTS. Gillespie, F. C. (Western Regional Hospital Board, Glasgow). Phys. Med. Biol., 10: 561-2(1965).

A method for measuring the relative concentrations of $^{133}$Xe in equal volumes of air and blood under equilibrium conditions was recently published (Isbister, W. H., et al., Phys. Med. Biol., 10: 243 (1965)). Errors found in data given using this method are reported. (P.C.H.)

**1600** EXAMINATIONS OF RADIOIODINE UPTAKE OF HUMAN FETUSES. Held, F.; Schwartz, K.-D.; Kuehne, D.; Potschwadek, B. (Univ., Rostock). Radiobiol. Radiotherap., 6: 615-18(1965). (In German).

Thirteen women, in whom an interruption of pregnancy was performed from medical indication, received $^{131}$I before this. The activity in fetus and placenta was measured. (tr-auth)

**1601** THE INFLUENCE OF PHYSIOLOGICAL INOCULUM AGE ON THE GROWTH OF A MICROBE CULTURE IN $H_2O$ AND 50 PER CENT $D_2O$. Mucka, V.; Einhorn, F.; Cabicar, J. (Fakultaet fuer Technische- und Kern-Physik, Prague). Z. Naturforsch., 20b: 610(June 1965). (In German).

The effects of $D_2O$ on the growth of the yeast Saccharomyces cerevisiae at different physiological inoculum ages was followed. The results showed that the total growth in a medium with natural $D_2O$ is a function of the inoculum age up to about 40 hr, whereas the total growth in 50% $D_2O$ is almost constant and independent of the inoculum age. It was also established that the total growth in 50% $D_2O$ lies about halfway between the minimum and maximum total growth in natural $D_2O$ concentrations. (J.S.R.)

**1602** ALPHA-ACTIVE FALLOUT PARTICLES; PHYSICAL CHARACTERISTICS RELATED TO PULMONARY EXPOSURE [Thesis]. Schiager, Keith Jerome. Ann Arbor, Mich., Univ. of Michigan, 1964. 132p.

Samples of atmospheric dust were obtained from several sources and represented air volumes ranging from thousands to millions of cubic meters. These samples were collected during the two and one-half year period following the Russian series of atmospheric weapons tests in September 1961. The density and size-distribution characteristics of atmospheric dust particles were measured for several samples. Radioactivity distributions were determined for samples collected in systems that separated the particles into various size ranges. From these measurements, the size range for fallout particles was found to be approximately one to four microns in diameter. The alpha-active elements in fallout were determined by chemical separation and alpha-energy spectroscopy. Plutonium was found to be the only alpha-active element of biological importance. Traces of uranium were detected in some samples, but the activity was less than one per cent of that of plutonium. The solubility of plutonium was found to be very slight—only nine per cent dissolved in 300 days under conditions approximating the

lung environment. Thus, removal of fallout plutonium from the lungs by physical dissolution is expected to be negligible. The concentration of plutonium in the air was determined for all of the samples used in this investigation. An average of $2 \times 10^{-3}$ picocuries per cubic meter of air was observed. Based on the measured aerosol characteristics, the average quantity of plutonium retained in the lungs of exposed individuals is estimated to be approximately two to six picocuries. (A.G.W.)

**1603** LIQUID SCINTILLATION DETERMINATION OF $^{45}Ca$ AND $^{89}Sr$ IN CHLAMYDOMONAS REINHARDTI DANGEARD AND PROTOSIPHON BOTRYOIDES KLEBS [Thesis]. Yarbrough, James David. University, Ala., Univ. of Alabama, 1964. 60p.

Chlamydomonas reinhardti Dangeard was effectively introduced into a liquid scintillation solution by utilizing an ethyl alcohol dehydration series for extraction of water and pigments, and counted in a single channel Tri-Carb liquid scintillator system. Counting of a graded series of algal cell concentrations in scintillation suspensions, revealed little internal quenching by algal concentrations of 0 – 63 mg/ml, with observable quenching at 75.6 mg/ml. Equal amounts of pre-frozen and live Chlamydomonas cells treated with calcium-45 for periods of 5, 15, 30 min, and 12 hr were introduced into the scintillation system following alcohol dehydration. The pre-frozen algal cells took up 30-44 per cent of the Ca-45 provided. The rapid uptake of Ca-45 by dead algal cells is indicative of an ion-exchange phenomenon. The live algal cells absorbed and held at least 70% of the Ca-45 available, with the exception of the 12 hr treatment sample. This increase in absorption by live over dead algal cells is considered to be the result of cellular metabolic activities. Studies of calcium and strontium absorption by Chlamydomonas reinhardti and Protosiphon botryoides Klebs involved growth of these algae in a basal nutrient medium with total Ca-Sr ratios of 0.5 : 0.5, 0.1 : 0.9 and 0.01 : 0.99 and containing Ca-45 and Sr-89. Periodic sampling and counting with a liquid scintillation system revealed discrimination for calcium by both algal species, particularly in the 0.5 : 0.5 Ca/Sr culture medium. The ratio of Ca/Sr in the algal cells to the ratio of Ca/Sr in the original medium was as high as 2.19 for Chlamydomonas and 3.32 for Protosiphon. Discrimination for Ca increased in Protosiphon as the culture developed beyond the logarithmic phase of growth. (Dissertation Abstr.)

## Radiation Effects on Biochemicals

**1604** (TID–22291) CHEMICAL EFFECTS OF IONIZING RADIATIONS ON THE INDIVIDUAL AMINO ACIDS WITHIN INTACT AND PURE PROTEIN MOLECULES. Progress Report. Friedberg, Felix (Howard Univ., Washington, D. C. Dept. of Biochemistry). Oct. 15, 1965. Contract AT(30-1)-2735. 9p. Dep. mn; CFSTI $1.00 cy, $0.50 mn.

Results are reported from studies that show definite indications for structural unfolding of the ribonuclease molecule upon gamma irradiation in the solid state (increase in viscosity and increase in negative optical rotation) concommitant with the loss in enzymatic activity. Disulfide interchange does not occur to any appreciable extent. The data establish that the number average molecular weight of the enzyme is not changed by the irradiation. (auth)

**1605** LONG-LIVED RADIATION-INDUCED ELECTRON SPIN RESONANCES IN AN AQUEOUS BIOLOGICAL SYSTEM. Swartz, Harold M.; Molenda, Robert P.; Lofberg, Robert T. (Walter Reed Army Medical Center, Washington, D. C.). Biochem. Biophys. Res. Comm., 21: 61-5(Oct. 8, 1965).

The existence of radioinduced long-lived unpaired electron species in a biological system of normal human blood is reported. It is suggested that these resonances may represent significant energy available to cause damage well after the radiation period has ended. The site of the resonances appears to be in the blood cells, inasmuch as the plasma fraction showed no ESR signals even after very high radiation doses. (P.C.H.)

## Radiation Effects on Tissues

*Refer also to abstract 2080.*

**1606** (AD–623079) URETHAN-INDUCED LUNG TUMORS IN MICE: X-RADIATION DOSE DEPENDENT INHIBITION. Foley, W. A.; Cole, L. J. (Naval Radiological Defense Lab., San Francisco, Calif.). Sept. 22, 1965. 11p. (USNRDL–TR–911). CFSTI $1.00 cy, $0.50 mn.

Adult male $LAF_1$ mice received single whole-body x ray exposures of 100, 300, 500, or 700 rads, followed one day later by single injection of urethan (1 mg/g). The mice were sacrificed 25 weeks later, and the lungs examined grossly and microscopically for tumors. All of the mice in group receiving 100 rad plus urethan exhibited lung tumors (alveologenic carcinomas), with a mean of 3.1 tumors per mouse. This lung tumor incidence was identical with that occurring in the mice which received urethan only. However, a definite reduction in lung tumor incidence and number of tumors per mouse was observed at the 500 rad dose (66% incidence and 1.8 tumors per mouse, respectively) and at 700 rad (59% incidence and 1.3 tumors per mouse). Thus, the x radiation suppression of urethan-induced lung tumors in mice is dose-dependent in the range of 500 rad to 900 rad. The data suggest that this tumor suppression is correlated with a direct radiation inhibition of alveolar cell proliferation. (auth)

**1607** (AED-C–04-18) RADIATION EFFECTS ON LIVING TISSUES AND ORGANISMS. Series C: Bibliographies. Stahlhofen, W. (comp.) (Max-Planck-Institut fuer Biophysik, Frankfurt am Main (West Germany)). Apr. 1965. 248p. Dep. mn.

A list is presented of 820 references to recent publications on radiation effects on living tissues and organisms. Author, corporate source, and subject indexes are included. (C.H.)

**1608** (AED-C–04-19) RADIATION EFFECTS ON LIVING TISSUES AND ORGANISMS. Series C: Bibliographies. Stahlhofen, W. (comp.) (Max-Planck-Institut fuer Biophysik, Frankfurt am Main (West Germany)). Apr. 1965. 314p. Dep. mn.

One-thousand three hundred and ninety-seven references are presented to recent literature (1961 to 1965) on radiation effects on living tissues and organisms. Author, report number, and subject indexes are included. (C.H.)

**1609** (BNL–9477) RESPONSE OF THE SKIN OF SWINE TO INCREASING EXPOSURES OF 250 KVP X-RAY. Archambeau, J. O.; Fairchild, R. G.; Commerford, S. L. (Brookhaven National Lab., Upton, N. Y.). [1965]. Contract AT(30-2)-Gen-16. 58p. (CONF-650718–2). Dep. mn; CFSTI $3.00 cy, $0.75 mn.

From Symposium on Swine in Biomedical Research, Richland, Wash.

The gross and histological features of the skin of swine resemble those of the human being sufficiently to warrant its use as an in vivo system for the evaluation and comparison of the effects of different ionizing radiations and the extrapolation of these results to humans. As the initial part of studies designed to compare the effects of x rays and neutrons, detailed gross and cytological effects were determined as a function of time following increasing doses of 250 kvp x ray to 10 cm in diameter fields on the shoulder and lower back of 60- to 100-lb immature swine. The effects produced following single exposures over a range from 1760 to 2800 R were evaluated on the basis of the number of moist reactions produced, that healed or failed to heal. Erythema and epilation time-dose changes were determined but not evaluated. The moist reaction begins about the 18th to 21st day and is maximally developed at about 28 days following irradiation. Healing, if it occurs, is complete or at a maximum between 35 and 49 days. The highest exposure at which a moist reaction did not occur was 2700 R. However, complete ulceration also was seen occasionally following exposures as low as 1900 R; thus there was an overlap of 800 roentgens where healing or

ulceration may occur. The exposure at which 50% of the irradiated fields were healed at the end of the observation period of 49 days was estimated to be 2350 R. These results furnish a standard with which the effectiveness of other radiations is being compared. (auth)

**1610** (BNL–9611) THE RADIOSENSITIVITY OF MARCHANTIA THALLI AS RELATED TO NUCLEAR AND INTERPHASE CHROMOSOME VOLUMES. Miller, Morton W.; Sparrow, Arnold H. (Brookhaven National Lab., Upton, N. Y.). [1965]. Contract AT(30-2)-Gen-16. 6p. (CONF-650814–3). Dep. mn; CFSTI $1.00 cy, $0.50 mn.

From Symposium on Mutational Process, Prague.

Studies on the comparative radiosensitivities of plants have shown that the size of the nucleus and/or the chromosomes is an important factor in determining tolerance. Results are reported from an attempt to determine the radiosensitivity of cells within multicellular structures, the gemmae and thalli of Marchantia polymorpha L., a thalloid liverwort. The gemmae are asexual reproductive propagules produced by the haploid thallus within a gemmae cup. The bryophytic capacity for cellular totipotency is well known and the gemmae and thalli Marchantia have this capacity for proliferation; it appears that if an intact cell has not lost its reproductive integrity it will produce a vegetative outgrowth in the absence of other inhibitory factors. The nuclear volume of apical cells ($98.9 \pm 4.9\mu^3$) of Marchantia gemmae was much larger than the nuclear volume of other vegetative cells capable of producing a vegetative outgrowth ($54.7 \pm 3.3\mu^3$). The lethal x radiation exposures for the apical and non-apical vegetative cells of the gemmae were approximately 29 kR and 55 kR respectively. The energy absorbed by the gemminiferous apical and non-apical vegetative cells at the 100% lethal exposure is $18.3 \pm 0.9 \times 10^6$ ev and $19.2 \pm 1.6 \times 10^6$ ev per chromosome, respectively. Thus actual tolerance is not different. These amounts of energy are approximately 4.7 times greater than the reported average amount of energy absorbed per chromosome for growing herbaceous angiosperms at the 100% lethal exposure. The nuclear volumes for apical and non-apical vegetative cells of Marchantia thalli are approximately 129 $\mu^3$ and 12 $\mu^3$, respectively. Apical and non-apical proliferation in thalli are eliminated by exposures of 10 kR and 55 kR, respectively. The energy absorbed at the 100% lethal exposure by the most resistant cells of the thallus was $4.0 \times 10^6$ ev per chromosome, which is insignificantly different from the amount of energy absorbed by herbaceous angiosperms irradiated at the 100% lethal exposure. (auth)

**1611** (COO–1119-4) X-IRRADIATION OF THE DEVELOPING AVIAN EMBRYO AS A FACTOR OF AGING. Period Covered: September 20, 1964–September 10, 1965. Muller, Harry D. (Colorado State Univ., Fort Collins). Sept. 24, 1965. Contract AT(11-1)-1119. 36p. Dep. mn; CFSTI $2.00 cy, $0.50 mn.

Data are reported on the body weight, reproductive capacity, blood pressure, heart rate, and mortality parameters of chickens exposed to x radiation during embryonic development, evaluated at 42 mo. of age. Body weight evaluations demonstrated that the control animals and the survivors of low doses of irradiation demonstrate heavier body weights than the survivors of $LD_{50}$ or greater doses of irradiation. Age at time of administration of the treatment appears to have less influence than the total dose administered. Sex apparently has no observable influence on these responses other than those normally found in the mature body weights of the domestic fowl. Reproductive capacity evaluations demonstrated that irradiation survivor females continue to demonstrate impaired ovulation rate. However, the ability of the male survivors to fertilize both irradiation survivor and control females is not measurably impaired. Matings between control individuals and survivor individuals, as well as matings between survivor individuals, have demonstrated that these individuals are capable of competing on a percentage basis with unexposed individuals in the production of viable progeny. Blood pressure evaluations demonstrated that the survivors of the higher doses of irradiation demonstrate lowered diastolic and systolic pressures when compared to the control individuals. Physiological impairment at a period of 36 months after exposure still demonstrates statistically significant deviation from control values. Heart rate measurements showed few significant differences between irradiation survivors or between irradiation survivors and unirradiated controls. Where these significant deviations were observed the heart rate of control individuals decreased to a point significantly less than that of several survivor groups. This was the first observation of this nature and will be carefully scrutinized for its behavior in the next test period. Mortality rates have yet to reach a sufficient level for accurate statistical probit analysis of effects of embryonic irradiation on life span. Only a few of the survivor groups have cumulative mortality rates which exceed the mortality rates of the control groups. It is possible that the prenatal irradiation treatments acted as a selective process, eliminating those which would have died during their juvenile life. Categorical breakdown of mortality causes still does not supply sufficient information to project the effects of embryonic irradiation upon the reproductive, somatic, or the interaction of the effects upon these two systems. (auth)

**1612** (EUR–2505.e) THE FEASIBILITY OF A NEW PROCEDURE FOR BIOLOGICAL DOSIMETRY. Whitfield, J. F.; Kellerer, S.; Brohee, H.; Youdale, T. (European Atomic Energy Community, Ispra (Italy). Joint Nuclear Research Center). 1965. 34p. Dep. mn.

The proportion of rat, as well as human, lymphocytes with structureless (or pycnotic) nuclei can serve as a sensitive indicator of absorbed radiation dose (following an acute exposure) provided that the irradiated cells are removed from the blood and maintained in a glucose-phosphate medium. The dosimeter is particularly sensitive to doses between 0 and 100 R. Above 100 R, the slope of the linear dose-effect curve tends to decrease and the dosimeter becomes less sensitive. (auth)

**1613** (HW-SA–3537) FAST NEUTRON EFFECTS ON PRODUCTIVITY OF YOUNG AND OLD FLOUR BEETLES, TRIBOLIUM CASTANEUM HERBST AND ALTERATIONS DUE TO TEMPERATURE AND SEX-EXPOSED. Erdman, Howard E. (General Electric Co., Richland, Wash. Hanford Atomic Products Operation). Oct. 6, 1964. Contract AT(45-1)-1350. 16p. Dep. mn; CFSTI $1.00 cy, $0.50 mn.

Virgin day-old and three-week old flour beetles, Tribolium castaneum, strain Brazil CI, were given approximately 830 and 970 rads, respectively, of fast neutrons of average energy 4.6 Mev. Ten replicates of the mating combinations control, male-exposed, female-exposed, and both-exposed were cultured at 25°C, 29°C and 32°C in 65 to 70% relative humidity. Productivity, measured as adult progeny per reproducing female per day, was scored for 14 days. Decreases in temperature progressively delayed reproductive onset. Additional delay in reproductive onset occurred when young female beetles were irradiated, indicating a greater radiation sensitivity at this stage of oogonial maturation. Thereafter, no other indication of a differential radiosensitivity of germ cells was noted. Productivity of young beetles plateaued during the second week; that of old beetles after the first day. Male- and female-exposed productivities were not significantly different within a temperature but were less than control and greater than both-exposed. Neutron irradiation effects appeared additive in that both-exposed mating combinations had the expected number of progeny compared to those in which one sex only was exposed. (auth)

**1614** (NASA-SP–71, pp 97-103) EFFECT OF HIGH-ENERGY PROTONS AND ALPHA PARTICLES ON SMALL MAMMALS. Sondhaus, Charles A. (Lawrence Radiation Lab., Univ. of California, Berkeley).

The dose distribution produced in a mammal by exposure to high-energy protons is probably the most important parameter governing the type and degree of injury. For solar proton fluxes, average linear energy transfer (LET) is elevated significantly only at the ends of particle tracks, so that the high-LET component of a primary-plus-secondary proton dose remains small even with isotropic exposure of

tissue volumes approaching the dimensions of the human body. A review of experiments on small mammals (mouse, rat) is presented. The results indicate a value of relative effectiveness about 0.7 to 0.8 times that of 250-kv x radiation for 50% mortality at 30 days, for protons at several energies above 50 Mev. In the small mammal, both the build-up of secondary particle dose and the gross nonuniformity of total dose distribution are minimal in this energy range, whether the exposure is monodirectional or isotropic. At energies below 50 Mev, the contribution of Bragg peak dose increases since the dimensions of the animal exceed the particle range. Dose distribution in the tissue is thus non-uniform, and the apparent effectiveness of exposure dose increases. Since experiments show a significant alpha-particle component in solar cosmic radiation, the effects of high-energy (910-Mev) alpha-particle irradiation of the mouse were investigated. A value of 720 rads for the $LD_{50}$ (30) dose has been found, which is identical to the value found for dose and effectiveness of high-energy protons. This result is to be expected on the basis of dose uniformity and LET similarity between these radiations. The relative effectiveness of high-energy proton and alpha radiation for acute mortality in the mouse is actually variable with time as well as dose, and depends on the time after irradiation at which mortality is evaluated. The effectiveness of both protons and alpha particles versus x rays increases at shorter times post-irradiation, exceeding unity at 6 days. This effect, due presumably to temporal differences in the predominant injury modes constituting the acute radiation syndrome in these mammals, is discussed. The influence of dose rate is also considered. (auth)

**1615** (NASA-SP-71, pp 105-14) BIOLOGICAL EFFECTS OF HEAVY IONS. Todd, Paul (California Univ., Berkeley. Donner Lab.).

The outstanding biological damage that results from heavy-ion irradiation is attributed to the lethal effects on large numbers of cells by a single particle with high probability. Relative cell losses in a homogeneous biological system exposed to the primary cosmic radiation are expected to be about 1:1:0.7 for heavy, medium, and light nuclei, respectively, assuming that a heavy nucleus inactivates each cell it traverses. (auth)

**1616** (NASA-SP-71, pp 219-23) FRACTIONAL CELL LETHALITY APPROACH TO SPACE RADIATION HAZARDS. Curtis, S. B.; Dye, D. L.; Sheldon, W. R. (Boeing Co., Seattle, Wash.).

A method of radiation hazard evaluation has been introduced in which the fractional number of cells of an organ killed or inactivated is calculated. This Fractional Cell Lethality or FCL depends only on the particle energy spectrum and the probability of cell inactivation. Recent data on inactivation cross sections of human kidney cells were used to calculate the contribution of protons, alpha particles, and M-group particles to the FCL of the kidney. The results indicate that the proton and alpha particle contributions would have been the same order of magnitude for the 12 November 1960 giant flare and that their relative contribution does not vary much with shielding thickness. For a seated astronaut, the FCL values are on the order of 5 percent under reasonable shielding at points 4 and 6 cm inside the body at the waist. When data on inactivation cross sections become available on more critical organs, containing cells not replaced by the body, this approach may yield a realistic evaluation of the hazard from high LET radiation on extended space missions. (auth)

**1617** (NP-15149) A QUANTITATIVE EVALUATION OF CELL SURVIVAL AS A FUNCTION OF RADIATION DOSE. Final Report. Colombo, G.; Levis, A. G.; Marin, G. (Padua Univ. (Italy). Istituto di Zoologia e Anatomia Comparata). [1962]. IAEA Contract No. 36. 74p. Dep. mn.

Results are reported from a series of studies on the effects of x radiation on multiplication of guinea pig kidney cells in tissue culture. The effects of doses ranging from 150 to 900R on growth rate, cell morphology, and survival were studied under various environmental conditions. Results indicated that radiation caused a general depression of mitotic activity and temporarily blocks cells entering mitosis; the radiosensitivity of cells was changed only by extreme changes in environmental conditions; the presence of giant cells appeared to be a morphological expression of lethal damage carried by the clones; and specific genetic loci appear to control radiosensitivity. A comparison was made of the effects of nitrogen mustard and x radiation on growth and morphology of cells in tissue culture. Results indicate that x radiation and nitrogen mustard do not act on a common target in causing reproductive death of cells. A nitrogen mustard-resistant strain of cells was developed and chromosome studies and studies of colony formation after x irradiation indicated no cross-resistance to x radiation in the cells. A list is included of 17 publications that report results of the studies. (44 references.) (C.H.)

**1618** (NYO-3319-6) RADIATION SENSITIZATION OF BACTERIA BY p-HYDROXYMERCURIBENZOATE. Bruce, A. K. (State Univ. of New York, Buffalo. Dept. of Biology). [1965]. Contract AT(30-1)-3319. 19p. (CONF-650715-1). Dep. mn; CFSTI $1.00 cy, $0.50 mn.

From Panel on Coordination of Research in Radiation Sensitization of Microorganisms in Food Preservation, Vienna.

The importance of sulfhydryl compounds in influencing the radiation response of bacteria has been demonstrated in several studies. Agents which selectively bind –SH groups such as N-ethylmaleimide (NEM), phenylmercuriacetate (PMA), and p-hydroxymercuribenzoate (HMB), and the less specific iodoacetate (IAA) have all been shown to sensitize bacteria to x radiation. Extracts of the highly radioresistant bacterium Micrococcus radiodurans have shown the ability to protect Escherichia coli B/r in a manner similar to 2-mercaptoethylamine (MEA), further implicating the role of chemical protection in the cell. Studies involving the quantitative measurement of the sensitizing agent HMB in the cell have shown that the radioresistant M. radiodurans binds far more HMB than does Sarcina lutea or E. coli B/r and that the amount bound is in the same order as their radioresistance. This suggests that the radiosensitivity of cells is related to radical trapping mechanisms present in the cell. Results are reported from studies on the binding characteristics of HMB in cells and the quantitative measurement of binding to several species of bacteria selected to cover a wide range of radiosensitivity. These included Micrococcus radiodurans, Escherichia coli, Proteus mirabilis, Paracolobactrum intermedia, Bacillus mycoides, Sarcina lutea, and Micrococcus albus. The kinetics of the binding of HMB and the development of radiosensitivity was compatible with sulfhydryl interaction. The amount of HMB bound was directly related to the radiosensitivity of seven bacterial species studied. (C.H.)

**1619** (TID-22293) STUDIES OF CHEMICAL PROTECTION AGAINST RADIATION INDUCED CHROMOSOME ABERRATIONS. Final Report, September 1, 1961–August 31, 1965. Mittler, Sidney (Northern Illinois Univ., DeKalb. Dept. of Biological Sciences). Contract AT (11-1)-1081. 41p. Dep. mn; CFSTI $2.00 cy, $0.50 mn.

Results are reported from a study on the mechanism of the radiation induced genetic changes. The protective effects of sulfhydryl compounds used to protect mammals, AET (aminoethylisothiourium dihydrobromide), MEA (mercaptoethylamine), and glutathione on radiation induced genetic damage of Drosophila testis were investigated. Protection was not given to spermatozoa, spermatids, spermatocytes and spermatogonia. The responses measured were production of recessive sex linked lethals, translocations, deletions, loss of X and Y chromosomes, and dominant lethals as measured by the failure of fertilized eggs to develop. MEA did increase the recessive lethals in the 3 to 6 day brood. Pre-treatment with glutathione increased the incidence of XO males in 6 to 9 day brood and post-treatment in 0 to 3 day brood. MEA and glutathione increased the percentage of eggs that failed to develop in dominant lethals tests. Preliminary tests with pre-treatment with AET on radiation induced crossing-over in the

male indicated that there was no protection but an enhancement of this radiation effect. (auth)

**1620** (UCRL–16154) RESULTS OF COMPUTATIONS OF DEPTH DOSE IN TISSUE IRRADIATED BY PROTONS. Steward, Palmer G. (Lawrence Radiation Lab., Univ. of California, Berkeley). May 25, 1965. Contract W-7405-eng-48. 117p. Dep. mn; CFSTI $4.00 cy, $0.75 mn.

A computer code was developed for the depth-dose relation due to primary protons and to cascade, evaporation, and hydrogen-proton collision (recoil) secondary protons in spheres of tissue. Recoil protons are assumed to be emitted in the forward direction, as also, on the basis of Metropolis' calculations, are cascade protons. Evaporation protons are assumed to deposit their dose locally. The results show that the depth-dose pattern varies widely with proton energy and sphere size. For certain intermediate proton energies, the primary protons cause a peak dose rate at a predictable depth in the sphere. The secondary proton dose rate increases with increasing incident-proton energy, sphere size, and depth. At the center of a sphere of 2.5-cm radius, 730-Mev protons cause a secondary proton dose which is 14% of the total dose, 35% for a 10-cm radius, and 48% for a 25-cm radius. (auth)

**1621** (UCRL–16387) STUDIES OF VICIA FABA ROOT MERISTEMS IRRADIATED WITH A $\pi^-$ BEAM. Richman, Stephen P.; Richman, Chaim; Raju, Mudundi R.; Schwartz, Bernard (Lawrence Radiation Lab., Univ. of California, Berkeley). Sept. 3, 1965. Contract W-7405-eng-48. 18p. (CONF-650924–5). Dep. mn; CFSTI $1.00 cy, $0.50 mn.

From Workshop Conference on Space Radiation Biology, Berkeley, Calif.

The biological effects of $\pi^-$ mesons, produced by the 184-in. cyclotron 90-Mev beam, were studied in Vicia faba root meristem cells. The roots were exposed in the plateau region and in the peak region of the $\pi^-$-meson Bragg curve. It is pointed out that the Bragg curve for these particles is not the usual Bragg curve obtained for a beam of $\alpha$ particles or protons. Two ionization chambers, one used as a monitor and the second as a detector, were used in determining the curve. The irradiation technique is described. Data are reported on the percentage of total anaphases that were abnormal at intervals after the end of 20-hr irradiation, the percentage of cells containing micronuclei at similar intervals, and the growth rate after irradiation measured as a fraction of the control rate. (C.H.)

**1622** (WT–820) GENETIC EFFECTS OF FAST NEUTRONS FROM NUCLEAR DETONATIONS. Projects 23.4–23.14 and 23.16 [of] OPERATION UPSHOT-KNOTHOLE. Plough, H. H.; Sheppard, C. W. (eds.) (Division of Biology and Medicine (AEC), Washington, D. C.). Jan. 1954. 58p. Dep. mn; CFSTI $3.00 cy, $0.75 mn.

A series of genetic test objects were exposed to fast neutron irradiation at Upshot-Knothole. Plant materials used included spores of several fungi, Tradescantia pollen, and seeds of Datura and of corn. Drosophila flies, Mormoniella wasps, and several mouse strains constituted the animal specimens used. The data indicate that the relative biological effectiveness (RBE) for genetic effects from detonation neutrons compared with x or $\gamma$ irradiation is high, observed values ranging from about 2 to 15 or more. The RBE for chromosome breakage from detonation neutrons is not significantly higher than that from cyclotron neutrons; this conclusion is subject to some uncertainties in dose determination. It is indicated that the RBE for the production of simple mutations by fast neutrons compared with x rays tends to be low. The values are higher for gross chromasome aberrations. The genetic tests are of some value as biological dosimeters supplementary to physical dosimetry. The studies clearly indicate that for equal doses neutrons represent a greater potential genetic hazard than other forms of radiation from nuclear detonations. (auth)

**1623** ELECTRON SPIN RESONANCE MEASUREMENTS ON IRRADIATED BACTERIOPHAGES AND THEIR NUCLEIC ACIDS. Mueller, A. Angew. Chem. Intern. Ed. Engl., 3: 241-2(Mar. 1964).

Radicals were produced in dry bacteriophages and nucleic acid prepared therefrom, by irradiation with x rays (50 kR/min) or $\gamma$ rays ($^{60}$Co, 10 krep/min) and examined qualitatively and quantitatively by means of their ESR absorption spectra. The results were compared with measurements on phage proteins and nucleic acid components (nucleotides, nucleosides, free bases). In whole phages of strains T1 and T2, radicals which show different ESR-spectral types were produced in high yield (G = 2 to 10) by irradiation. Radicals were formed in comparable yield from T2 phage nucleic acids and gave ESR spectra which corresponded to those observed in whole phages. The radical concentration in irradiated phage nucleic acid increased with dose according to an exponential function up to a saturation value between $10^{18}$ and $10^{19}$ radicals/g (63% of the saturation concentration is reached after doses of 0.4 to 1.4 mR). The radicals of the T2 protein were equal in concentration and spectral frequency to those of other sulfur-free proteins. Radical yield in d-2-Deoxyribose was G = 4. The radicals produced in the nucleosides did not show a spectrum typical of D-2-Deoxyribose, but spectra which are similar to those of the free bases. While the radical yield of irradiated nucleotides corresponded to that from nucleic acids (G = 2 to 15), the radical yield in the case of irradiated nucleosides was less (G = 0.4 to 1.0) and still smaller in the case of the pure nucleic acid bases (G = 0.1 to 1.0). The radical yield increased particularly strongly on passing from thymine via thymidine to thymidine-5-monophosphate. Directly after irradiation the spectrum of the phosphate, like that of thymine, had a large number of lines, but later changed into a quartet, which appeared very like that of stored nucleic acid. The radical concentrations in the bases, nucleosides, and nucleotides showed a similar dependence on the radiation dose as those in the nucleic acid and all the other substances investigated. It is probable that the primary radiation damage occurs at the thymine unit of the nucleic acid. (BBB)

**1624** RELATION OF THE REPAIR OF DAMAGE INDUCED BY A MONOFUNCTIONAL ALKYLATING AGENT TO THE REPAIR OF DAMAGE INDUCED BY ULTRAVIOLET LIGHT IN BACILLUS SUBTILIS. Searashi, T.; Strauss, B. (Univ. of Chicago). Biochem. Biophys. Res. Commun., 20: 680-7(Sept. 22, 1965).

The monofunctional alkylating agent, methyl methanesulfonate (MMS) inactivates transforming DNA by a chain of processes which culminate in the insertion of single strand breaks into DNA and MMS-induced damage can be repaired. Recently it was found that a mutant of B. subtilis sensitive to ultraviolet radiation (UV) was not sensitive to MMS. A simple way of accounting for this lack of MMS sensitivity in the uvr$^-$ (UV-sensitive) strain was to suppose that repair of biological damage, including UV damage, occurred by a sequence of reactions and that a block in one of the earlier reactions did not inactivate the later steps. Repair of MMS damage might require only these later steps. The properties of a newly isolated MMS-sensitive mutant which confirm some of the predictions of this hypothesis are reported. (C.H.)

**1625** INVESTIGATIONS INTO THE EFFECTS OF ULTRAVIOLET LIGHT ON THE RATE OF DEOXYRIBONUCLEIC ACID SYNTHESIS IN MAMMALIAN CELLS. Cleaver, J. E. (Cambridge Univ., Eng.). Biochim. Biophys. Acta, 108: 42-52(Sept. 6, 1965).

Ultraviolet light at 2537 Å was found to inhibit the rate of synthesis of DNA in L-strain cells according to a biphasic dose response curve. The major cause of the inhibition in the rate of DNA synthesis, as measured by $^3$H thymidine incorporation, is the effect of ultraviolet light on the final step in DNA snythesis, the assembly of the nucleotide triphosphates into DNA. During the first 4 hr following exposure ultraviolet light inhibits the rate of entry of cells into the S phase, the rate of passage through the S phase (i.e., the rate of DNA synthesis), and the rate of entry into mitosis. These ultraviolet-induced inhibitions appear to be due to separate causes and are not causes or

consequences of one another. The rate of DNA synthesis after irradiation with 240 erg/mm$^2$ of ultraviolet light falls to a minimum after 2 hr and then begins to recover. The cells irradiated with this dose eventually recover completely. After irradiation with 960 erg/mm$^2$ the rate of DNA synthesis falls to a very low level after 3 hr and no recovery is detected. (auth)

**1626** EFFECT OF RADIATION ON NUCLEAR PHOSPHORYLATION IN HUMAN MALIGNANT TUMOURS. Fahmy, A. R.; Williams, W. Jones (South Wales Radiotherapy Centre Velindre Hospital, Cardiff. Welsh National School of Medicine, Cardiff). Brit. J. Cancer, 19: 501-4 (Sept. 1965).

Nuclear phosphorylation was studied in 14 human malignant tumors. The rate of phosphorylation was inhibited by small doses of x radiation, 25 rads caused 50 per cent inhibition in all the tumors studied. The relation between dose and percentage inhibition is linear. The rate of phosphorylation did not show any appreciable difference in the tumors studied and was not related to the site of origin, histological type, grade of malignancy, or mitotic activity. (auth)

**1627** CHANGES IN THE HIGHER NERVOUS ACTIVITY OF DOGS AFTER EXPOSURE TO IONIZING RADIATION AT DIFFERENT PERIODS OF ANTENATAL DEVELOPMENT. Piontkovskii, I. A.; Airapetyants, M. G. Bull. Exp. Biol. Med. (USSR) (Engl. Transl.), 58: 1292-5(Nov. 1964).

Translated from Byul. Eksp. Biol. Med., 58: 29-33 (Nov. 1964).

Dogs were exposed to x radiation in utero as a single dose of 200 R delivered on the 13th, 20th, 45th, and 55th days of development. The conditioned reflex activity was investigated in the dogs at the age of 1 to 2 yr using the classical method of salivary reflexes conditioned to food. The most marked disturbances of the reflex-forming function of the cerebral cortex and of processes of internal inhibition were observed in dogs irradiated on the 13th day of embryogenesis. The conditioned reflexes to both sound and light were formed with great difficulty, stable differentiation was not found, conditioned-reflex activity was chaotic in character, and omission of reflexes, refusal to eat in the experimental room, and balancing and paradoxical phases were frequently observed. Irradiation on the 20th day of embryogenesis caused difficulty during the formation of the conditioned reflex to light, indicating disturbance of the functions of the optic analyzer. Irradiation on the 20th and 45th days, and to a lesser extent on the 55th day of embryogenesis caused a marked increase in de-inhibition that was mainly observed at the beginning of the stimulus. The results of tests of prolongation of differentiation indicate weakness of the process of internal inhibition in the irradiated animals. Irradiation on the 55th day had little effect on the food conditioned reflexes. (C.H.)

**1628** DESTRUCTION OF THE OTOLITH APPARATUS BY IONIZING RADIATION. FIXATION OF APPLICATORS TO THE VESTIBULE. Arlashchenko, N. I.; Grigor'ev, Yu. G.; Malinin, A. B. Bull. Exp. Biol. Med. (USSR) (Engl. Transl.), 58: 1379-81(Nov. 1964).

Translated from Byul. Eksp. Biol. Med., 58: 122-4 (Nov. 1964).

The physiology of the sensory structure of the sacs of the vestibule and of the ampullae of the semicircular canals of the membranous labyrinth and the function of the utricle as an argon of equilibrium was studied in rabbits. The close anatomical association between the semicircular canals and the divisions of the vestibule constitutes an almost insuperable obstacle to a separate study of the sensory structures of the non-auditory portion of the labyrinth. An attempt was made to damage the function of the otoliths alone by means of soft $\beta$ applicators using $^{147}$Pm. The 0.22 kev energy of the $\beta$ particles is about 1/250 of the initial amount at a distance of 250 $\mu$ from the surface of the source, a distance equal to the width of the sensitive layer of the macula. When the radioapplicator was fixed in the immediate neighborhood of the sensitive maculae utriculi it caused their damage or destruction while the ampullary apparatus remained completely functional. (C.H.)

**1629** THE EFFECT OF THE COMBINED ACTION OF RADIOACTIVE $^{131}$I AND NOISE ON CARDIAC ACTIVITY. Mukhamedov, T. (Inst. of Regional Experimental Medicine, Tashkent). Byull. Eksp. Biol. Med., 59: 43-6(Feb. 1965). (In Russian).

A study was made of the effect on cardiac activity of $^{131}$I, noise, and the combined action of these two factors in male dogs weighing 10 to 15 kg. Prolonged administration of $^{131}$I in a dose of 4 to 5 $\mu$curies/k caused a change in the EKG waves and intervals (deceleration of cardiac contractions, increase in the PQ and QT intervals and in the P wave, shifting of the ST intervals to below the isoelectric line), especially distinct in functional loading. Noise (100 to 105 db) caused moderate EKG changes (deceleration of cardiac contractions, reduction of the PQ and QT intervals and also of the P wave). The combined action of these factors produced the same changes as with $^{131}$I alone (deceleration of cardiac contraction, an increase in the PQ and QT intervals, reduction of the P wave, an increase of the R wave, shifting of the ST to below the isoelectric line, appearance of a biphasic negative T wave). However, these changes set in earlier and were more pronounced under the combined action. (ATD)

**1630** CONCERNING THE DISTURBANCE OF THYMIDINE AND DESOXYURIDINE METABOLISM IN IRRADIATED RATS. Mazurik, V. K. Byull. Eksp. Biol. Med., 59: 59-61(Feb. 1965). (In Russian).

A study was made of the 24-hour thymidine and desoxyuridine urinary excretion in intact irradiated rats. In normal conditions rats proved to excrete less thymidine than desoxyuridine. There is a considerable rise in thymidine excretion and a less considerable one of desoxyuridine. Thymidine and deoxyuridine concentrations become approximately equal. On the one hand a rise in thymidine and desoxyuridine excretion is explained by increased disintegration of the cellular elements and by intensified DNA catabolism in the rapidly regenerating tissues, and on the other hand, by a relative insufficiency of the phosphorolysis systems. (ATD)

**1631** IMMUNOLOGICAL REACTIVITY IN MONKEYS AFTER RECOVERY FROM ACUTE RADIATION SICKNESS. Dzhikidze, E. K.; Pekerman, S. M. (Inst. of Experimental Pathology and Therapy, Academy of Medical Sciences, USSR). Byull. Eksp. Biol. Med., 59: 73-7(Apr. 1965). (In Russian).

The natural mechanisms of immunity, particularly antibody formation, were studied in 77 monkeys 2 months to 5 years after recovery from irradiation with doses ranging from 150 to 700 R, from the RUM-3 and a telegamma cobalt apparatus. Antibody formation was impaired in proportion to the dose of radiation, as reflected in varying degrees of retardation or even complete inhibition of the immunological response. The humoral indices of natural immunity were not significantly affected, but the mechanisms of nonspecific cellular immunity were somewhat depressed in a number of animals during the first 10 to 12 months after irradiation. However, the extent of injury was not directly related to the dose. Phagocytosis returned to the original level 1 to 3 years later. Apparently clinical recovery was not necessarily accompanied by restoration of normal immunological reactivity. The mechanisms responsible for antibody formation were not repaired until 1 to 2 years after exposure to doses of 550 to 700 R. Normalization of immunobiological reactivity undoubtedly reflects the processes of restoration of all the physiological functions injured by radiation. (ATD)

**1632** EFFECT OF TRANSPLANTATION OF HOMOLOGOUS HEMATOPOIETIC CELLS ON ANTIBODY SYNTHESIS IN IRRADIATED ANIMALS. Shevelev, A. S. (Smolensk Medical Inst., USSR). Byull. Eksp. Biol. Med., 59: 77-80(Apr. 1965). (In Russian).

Injection of homologous bone-marrow and spleen cells into stock-bred mice x irradiated with doses that killed 9

to 60% of the animals within 30 days inhibited antibody formation much more than it did in the irradiated control mice immunized with bacterial (typhoid or dysentery) or nonbacterial (sheep erythrocytes) antigens. The effect was nonspecific and it persisted in some cases for several months. This lack of reactivity may have been the result of an immunological reaction between the transplanted hematopoietic cells of the donor and the immunologically competent cells of the host weakened by irradiation. Since these experiments involved injecting the recipients with a mixture of cells from several donors, a question arose as to the role of the transplant-to-transplant reaction in inhibiting reactivity. Rats irradiated with sublethal doses were intravenously injected with spleen cells from irradiated rats. The result was a distinct depression of antibody formation after injection of typhoid bacteria following transplantation only if the spleen cells came from a single donor. However, this did not happen when the spleen cells were a mixture of cells obtained from 5 donors. Therefore, the transplant-to-transplant reaction, at least for the primary immunological response, is not responsible for the absence of nonspecific immunological reactivity and actually prevents it from developing. (ATD)

**1633** QUANTITATIVE ANALYSIS OF DNA IN THE CELLS OF THE CORNEAL EPITHELIUM IN RATS IRRADIATED WITH X-RAYS. Veselkina, M. N. (Inst. of Cytology, Leningrad). Byull. Eksp. Biol. Med., 59: 96-9 (May 1965). (In Russian).

In a period of 24 to 120 hours after the irradiation of rats with x rays in a dose of 700 R there is a marked nuclear polymorphism. In the corneal epithelium there appear cells with satellite nuclei and a larger number of binuclear cells. The results of investigations carried out by means of cytospectrophotometry showed that after irradiation the number of polyploid nuclei containing DNA in quantities of 5 to 8 respectively grows to 30% whereas normally it is only 10%. The satellite nuclei contain an insignificant amount of DNA, which points to their formation from chromosome fragments during atypical karyokinesis. The amount of DNA in the nuclei of binuclear cells varies extensively; the minimum quantity being 1n + 1n, the maximum we have noted being 3n + 5n. (ATD)

**1634** THE INCLUSION OF $^{3}$H-THYMIDINE IN THE CELLS OF THE STRATIFIED FLAT EPITHELIUM IN RATS FOLLOWING X-RAY IRRADIATION. Zhorno, L. Ya. (Inst. of Cytology, Leningrad). Byull. Eksp. Biol. Med., 59: 99-103(May 1965). (In Russian).

In the epithelium of the tongue in albino rats, mitoses disappear after x irradiation and the percentage of cells synthesizing DNA markedly declines. In 96 hours, the number of labeled nuclei sharply increases as compared to the control ones. Consequently, irradiation interferes with the transition of the cells from the $G_1$ period to the S period and the $G_2$ period. With the advent of a compensatory process, all periods of the mitotic cycle apparently become shorter. (ATD)

**1635** THE EFFECT OF X-RAYS ON THE REGENERATIVE CAPACITY OF THE IRRADIATED NERVUS PERONEUS COMMUNIS. Evsyukov, V. I. (Central Roentgeno-Radiological Inst., Leningrad). Byull. Eksp. Biol. Med., 59: 106-9(Feb. 1965). (In Russian).

In irradiation of the extremity in a dose of 3,000 R there occurs a prolonged and considerable, statistically authentic, depression of the nerve capacity to regeneration. Thus, the capacity to repair the radiation injury is not a peculiar feature of the nerve. Irradiation (3,000 R) of the spinal cord in the area innervating the posterior extremities does not inhibit the regeneration of the nonirradiated sectioned nervus peroneus communis. Thus, the fibers of the irradiated nerve cells do not lose the capacity to regeneration. These observations lead to a supposition that inhibition of the nerve regeneration observed after its direct irradiation is chiefly caused by the injury of the connective tissue and of the syncitium of Schwann, not of the processes or axons. (ATD)

**1636** THE EFFECT OF DAMAGE ON CELL CONDUCTIVITY IN ELECTRONIC CELL SIZE DISTRIBUTION. Vittorio, P. V. (Dept. of National Defence, Ottawa). Can. J. Physiol. Pharm., 43: 1027-9(Nov. 1965).

The possible effects of cell membrane injury on cell conductivity, and therefore on the results of Coulter counter electronic cell size distribution studies, were investigated. Suspensions of normal, x irradiated, and mechanically injured rat thymus lymphocytes were incubated with $^{51}$Cr and the effects of injury on $^{51}$Cr uptake were determined for various time intervals up to 4 hr. Erythrosin B staining was also used to demonstrate the damage to the cells. Cell size distribution results obtained with the Coulter electronic counter showed no change for the same time period. (C.H.)

**1637** SOME EFFECTS OF HIGH LEVELS OF GAMMA IRRADIATION ON THE LIPIDS OF WHEAT. Tipples, K. H. (Grain Research Lab., Winnipeg, Manitoba, Can.); Norris, F. W. Cereal Chem., 42: 437-51(Sept. 1965).

Two wheat varieties were irradiated: one a hard red spring Canadian Manitoba wheat, moisture content 13.6% and protein content 13.6%; and the other an English soft white winter wheat, variety Minister, moisture content 13.5% and protein content 9.2%. Samples sealed in polythene were irradiated with a $^{60}$Co source at levels of $10^5$, $10^6$, and $10^7$ rad. The lowest level of $10^5$ rad is ~two to five times the level used for disinfestation purposes. Irradiation produced small changes in the lipid fractions of irradiated wheat. Linoleic and linolenic acids decreased slightly, but only significantly so, at the very highest dose. Unesterified acids appeared were more susceptible to radiation damage than esterified acids. Carotenoids and the antioxidant tocopherols decreased with increasing irradiation. Nevertheless, on storage of the milled wheat, linoleic and linolenic acids were autoxidized more slowly in the irradiated samples than in the control. Lipids of irradiated wheat had a higher peroxide value than those of unirradiated wheat. On storage of the flour, lipids of unirradiated wheat showed a gradual increase in peroxide value, whereas lipids of irradiated wheat did not show the same extent of increase. Silicic acid fractionation of flour lipids indicated that irradiation caused a decrease in triglyceride, galactolipid, and phospholipid, and an increase in free sterol, monoglyceride, and diglyceride. The most striking difference between lipids extracted from unirradiated and heavily irradiated wheat was the increase in the amount of free sterol. Manitoba wheat extracted with $CCl_4$ and Minister wheat extracted with chloroform-methanol, showed this increase: from 3.6 to 7.8% for Manitoba, and from 3.8 to 6.2% for Minister. As the amount of sterol ester extracted did not change, the increase in free sterol probably did not occur as a result of sterol ester splitting. Rather, free sterol presumably occurred partly in a bound form, so that not all of it was extracted by normal solvent extraction. The irradiation could have severed or weakened the linkage by which sterol was bound, thus making the sterol more completely available for solvent extraction. The observed changes in lipid on irradiation were probably linked with the formation of unacceptable odors and flavors in the wheats. (BBB)

**1638** THE EFFECT OF TEMPERATURE AND OXYGEN ON THE FREQUENCY OF CHROMOSOME ABERRATIONS IN IRRADIATED TOMATO SEEDS. Kulik, M. I. (Inst. of Cytology and Genetics, Academy of Sciences, SSSR). Dokl. Akad. Nauk SSSR, 162: 928-31(June 1, 1965). (In Russian).

A study was made of the influence of thermal and atmospheric factors during storage of irradiated seeds on the frequency of chromosome aberrations in tomatoes. Batches of tomato seeds were kept at a high temperature, others were kept in pure oxygen, and still others were subjected to gamma rays in doses of 5000, 10,000, 15,000, and 20,000 R and irradiated with fast neutrons in doses of 500, 1000, and 1500 rad. The irradiated seeds were divided into three groups: those stored in air at room temperature throughout the experiment, those stored in pure oxygen at room temperature for 20 days, and those stored in air at 45°C

for 30 days. Microscopic study of rootlets of the sprouted seeds was made to determine the number of chromosome injuries. When gamma irradiation of seeds was combined with their subsequent storage at 45°C, no cumulative effects were observed. The same was true for gamma-irradiated seeds stored in pure oxygen for 20 days. Similarly, the frequency of chromosome aberrations as a result of the combined effect of neutron irradiation and storage of seeds at high temperature or in oxygen did not equal the sum of effects caused by these factors individually. This investigation clearly shows the difference between the interaction of various factors: gamma radiation and storage at 45°C caused 59% aberrant mitoses, while the same amount of gamma radiation with storage in pure oxygen caused 71.2% aberrant mutations. Experimental results confirm the hypothesis that primary radiation products can be stored in seeds for a long time; thus, they can interact with chemical products accumulating during storage. The possibility of modifying induced mutations, for the purpose of selection, by means of the combined influence of different mutagenic factors is suggested. (A.T.D.)

**1639** THE EFFECTS OF X-IRRADIATION ON THE DNA OF ESCHERICHIA COLI. AN AUTORADIOGRAPHIC STUDY. **Shaffer, C. R.; McGrath, R. A. (Oak Ridge National Lab., Tenn.). Exp. Cell Res., 39: 604-6(Sept. 1965). (ORNL-P-649).**

Cells of a radiation resistant strain (B/r) and a radiation sensitive strain ($B_{s-1}$) of Escherichia coli were labeled with $^3H$ thymidine. Quantitative autoradiography was used to compare the distribution of radioactivity among unirradiated and x irradiated cells. During a 50 min incubation all irradiated cells, including survivors in the resistant strain, lost labeled material. The radiation sensitive cells lose much more label than the resistant ones. (auth)

**1640** THE THERMOSENSITIZING EFFECT OF IRRADIATION WITH ULTRAVIOLET LIGHT AND X-RAYS ON CELLS OF OPHIOSTOMA AND RHODOTORULA. Fries, N. (Univ. of Uppsala). Exp. Cell Res., 39: 693-7(Sept. 1965).

Increased sensitivity to a high incubation temperature can be induced in various types of cells by treating them with a short heat shock. Such a thermosensitization can also be effectuated by irradiation with ultraviolet light and x rays. This effect is described for two microorganisms, a plus strain of the heterothallic ascomycete Ophiostoma multiannulatum, which grows in liquid medium with budding cells like a yeast, whereas on an agar surface it forms densely branched mycelia, and Rhodotorula glutinis, a red yeast isolated from slime flux of birch, which forms a suspension of free cells when grown in a liquid medium, and dense, red colonies on agar plates. (C.H.)

**1641** MICROSCOPIC AND SUBMICROSCOPIC CHANGES IN THE ADRENALS IN RADIATION SICKNESS CAUSED BY RADIOACTIVE STRONTIUM. **Khomutovskii, O. A. (Bogomoletz Inst. of Physiology, Kiev). Fiziol. Zh., Akad. Nauk Ukr. RSR, 11: 514-15(July-Aug. 1965). (In Russian).**

The microscopic and submicroscopic structures of the adrenals in radiation sickness caused by a single and repeated intraperitoneal administration of chloride salts of $^{89}Sr$ and $^{90}Sr$ in quantities of 0.3 microcuries/g were studied in 150 albino rats and 25 guinea pigs. The results of the investigation show that on the first or second day of radiation sickness adrenal activity is enhanced, the number of lipoid inclusions increases in the cortical layer cells, and the RNA and RNP contents decrease. In the medullar layer, degranulation of chromaffinic cells develops. After two or three days there is, as a result of developing degenerative processes, a progressive fall in the functional activity of the cells of the cortex and medullar substance of the adrenals; the number of lipoid inclusions decreases in the cortical cells, and that of incretor granules in chromaffinic cells of the medullar substance. Chronic irradiation hindered normalization of regeneration processes, as a result of which the architectonics of the gland was disturbed. Cells with altered submicroscopic structure appeared in the cortical and medullar substance, polymorphism of mitochondria developed, RNP grains became larger, denser, and, sometimes agglutinated; the quantity of first ergastoplasmatic membranes decreased; and nuclei contained the coarsely dispersed phase of chromatin. The intensity of the morphological changes during the first period of radiation sickness and the degree of disturbance of the regeneration processes at remote periods depended directly on the quantity of absorbed energy in the adrenals during the first period of radiation sickness and on the chronic radiation dose. (ATD)

**1642** GENETIC EFFECTS OF X RAYS ON QUANTITATIVE CHARACTERS IN A HETEROGENEOUS POPULATION OF DROSOPHILA MELANOGASTER. **Tobari, Izuo; Nei, Masatoshi (National Inst. of Radiological Sciences, Chiba, Japan). Genetics, 52: 1007-15(Nov. 1965).**

An outbred population of Drosophila melanogaster was exposed to 1,000 R of x rays. The numbers of abdominal and sternopleural bristles were studied after three generations of random mating. The mean values of the two characters showed no appreciable change due to radiation. In view of the practical equality of positive and negative mutation rates in these characters, this result suggests that the frequencies of positive and negative alleles in the outbred population are nearly equal, on the average. The phenotypic variance was increased in both abdominal and sternopleural bristles. Partitioning of the phenotypic variance has shown that this increase is mainly due to the increase in genetic variance. The increase in genetic variance in sternopleural bristles was also detected by the parent-offspring covariance, which was larger in the irradiated than in the control population. The amount of variance increase per roentgen has suggested that the increase of genetic variance in the irradiated population is caused mainly by mutations at fixed or nearly fixed loci rather than at loci with intermediate gene frequencies. (auth)

**1643** GENETIC SEGREGATION IN THE UNISEXUAL WASP DEVORGILLA. **Speicher, B. R.; Speicher, Kathryn G.; Roberts, Franklin L. (Oak Ridge National Lab., Tenn. Univ. of Maine, Orono). Genetics, 52: 1035-41(Nov. 1965). (ORNL-P-1330).**

The ichneumonid wasp Devorgilla reproduces by female parthenogenesis. Egg diploidy is retained by an abortive first maturation, where the separating anaphase dyads return to a common second metaphase. One polar nucleus is then eliminated, so that two chromatids of each original tetrad are retained in the egg and two are discarded. The segregation of x-ray-induced recessive lethals was studied by counting the inviable eggs from heterozygous females. One lethal behaved as a point mutation and produced 12.77% homozygous recessive (lethal) eggs. Homozygous normal females also appeared in an approximately equal proportion. The frequency of homozygosis of each gene, being less than 16.67%, indicates that the centromeres involved separate reductionally at the first meiotic division and equationally at the second. The amount of detectable crossing over between the locus and the centromere is 25.53%. The actual map distance should be between 25.5 and a calculated 48.5 units. A second lethal mutation produced 35.77% inviable eggs and only 2.78% homozygous normal females. The disparity between these two classes, and the high total inviability, suggest the presence of a chromosome aberration. (auth)

**1644** GENETIC EFFECTS FROM SIMULTANEOUS IRRADIATION OF IMMATURE AND MATURE DROSOPHILA VIRILIS MALES. **Clayton, Frances E. (Univ. of Arkansas, Fayetteville). Genetics, 52: 1081-92(Nov. 1965).**

Male Drosophila 2½ to 5 hours and six days old were x rayed simultaneously with 500, 1000, 1500, and 2000 R. Progeny from two successive 24-hour mating periods were checked for dominant lethals and translocations. The susceptibility of sperm bundles and motile spermatozoa was similar at all dosage levels as determined by dominant lethals and translocations from period 1. From period 2,

dominant lethal and translocation rates increased following irradiation of immature males but decreased when mature males were treated; this occurred at all levels of radiation with the exception of the 500 R test, in which translocation rates for the two days were similar. (auth)

**1645** COMPARATIVE RESISTANCE OF ENTEROVIRUSES AND B. COLI IN WATER DISINFECTION WITH γ-RADIATION. Ryabchenko, V. A.; Lovtsevich, E. L. (Pamfilov Inst. of Collective Economy, Moscow; Inst. of Polymyelitis and Virus Encephalitis, Moscow). Gig. Sanit., No. 8, 26-9(Aug. 1965). (In Russian).

Experimental findings obtained prove that in water E. coli is less resistant to the action of γ rays than enteroviruses (ECHO-7 and poliomyelitis viruses). Consequently E. coli cannot be a reliable index of water decontamination efficiency by means of γ rays in respect to enteroviruses. In order to decontaminate the water from enteroviruses it is necessary to increase the radiation dose approximately 2 to 3 times as compared to that necessary for the decontamination of water containing E. coli. (ATD)

**1646** CONTRIBUTIONS TO THE STUDY OF IMMEDIATE AND EARLY X-RAY REACTIONS WITH REGARD TO CHEMOPROTECTION. X. THE EFFECT OF PYRIDOXINE-DEFICIENCY IN MICE ON THEIR RADIOSENSITIVITY. Veninga, T. S. (State Univ., Groningen, Netherlands); Morse, H. Int. J. Radiat. Biol., 9: 399-408(1965).

Feeding a pyridoxine-deficient diet to mice led to an increase of radiosensitivity. However, animals surviving whole-body x irradiation for 10 to 13 days showed increased radioresistance. Daily injections with the pyridoxine antagonist desoxypyridoxine gave rise to uniformly enhanced radiosensitivity. The rise in sensitivity is suggested to be partly due to depletion of biogenous amines. The increase in resistance to irradiation of surviving animals cannot be explained. (auth)

**1647** ON THE ROLE OF THE SYSTEMS ORTHOPHENOLS–ORTHOQUINONES IN THE INITIAL RADIATION-INDUCED PROCESSES IN AN ORGANISM. Kuzin, A. M.; Plyshevskaya, E. G.; Kopylov, V. A.; Ivanitzkaya, E. A.; Lebedeva, N. E.; Kolomiitseva, I. K.; Tokarskaya, V. I.; Mel'nikova, S. K. (Inst. of Biological Physics, Moscow). Izv. Akad. Nauk SSSR, Ser. Biol., No. 4, 507-20(July-Aug. 1965). (In Russian).

Under the action of γ irradiation on tyrosine–tyrosinase system an enzymic process of tyrosine conversion into orthoquinones is activated as a result of a radiochemical reaction. The orthoquinones are actively absorbed by native cellular nuclei and combine with DNA. The effect of orthoquinones on living tissues imitates some processes, being caused by direct irradiation. The data obtained illustrate the change of cellular nuclei fluorescence in the presence of acridine-orange, both under the action of irradiation and of orthoquinones (tyrosine oxidation products) on cellular nuclei. The same phenomenon was observed under the influence of quinones extracted from γ-irradiated plant and animal tissues. By a series of experiments an increase of orthophenols was demonstrated in irradiated plant tissues. The action of the above substances on the plant seeds caused not only the suppression of DNA synthesis but changed also the A/T ratio in DNA of plants. The effect was analogous to that of previously described γ irradiation. The injection of purified orthoquinones extracted from irradiated plant tissues into young mice caused weight drop, growth delay, and sharp decrease of leukocyte content in peripheric blood, that is, it imitated the direct action of ionizing radiation. On the basis of the experiments and the data previously communicated, an hypothesis on the initial radiation-enzymic formation of active quinones in the irradiated tissue is presented. Fast sorption of the quinones by cellular nuclei leads to the delay and disturbance of DNA synthesis, delayed to cell division, leukopenia, growth delay, and to formation of chromosomal aberrations. (ATD)

**1648** THE INFLUENCE OF IONIZING IRRADIATION ON THE GROWTH AND METABOLISM OF NUCLEIC ACIDS IN PLANTS. Korableva, N. P.; Metlizkii, L. V. (Bach Inst. of Biochemistry, Moscow). Izv. Akad. Nauk SSSR, Ser. Biol., No. 4, 521-32(July-Aug. 1965). (In Russian).

The data given show that the degree of growth process inhibition and character of disturbances arising in the course of nucleic acids metabolism under the influence of ionizing irradiation may differ in dependence on peculiarities of metabolism characteristic of one or other plant species. The tendency of ionizing irradiation to affect morphogenetic processes in plant tissues is related to their physiological and functional state. Beside the suppression of growth intensity, degeneration of meristem tissue is to be considered as one of typical manifestations of the action of ionizing radiation. The higher radiosensitivity of meristem (growth points of bulbs and tubers) in comparison with functionally formed tissues (reserve parenchyma) is related to a large extent to the easier affection of energetic and nucleic metabolism. It is quite evident that the foundations of the action of ionizing irradiation and its practical use cannot be successfully elaborated without the consideration of specificity of reaction of different species and organs of plants to the irradiation. (ATD)

**1649** THE EFFECT OF SPACE FLIGHT FACTORS UPON EVONYMYS EUROPAEA L. SEEDS. Nuzhdin, N. I.; Dosortseva, R. L.; Pastushenko-Strelets, N. A.; Samokhvalova, N. S. (Inst. of Genetics, Moscow). Izv. Akad. Nauk SSSR, Ser. Biol., No. 4, 576-80(July-Aug. 1965). (In Russian).

Air dry seeds of E. europaea L. preliminary irradiated with $^{60}$Co gamma-rays in a dose of 10 kR and unirradiated ones were on board the spacecraft Vostok-5 during its space flight. The same seeds left in Moscow and taken on board a plane to the cosmodrome served as the control. The frequency of cells with chromosome aberrations was studied in root tips grown from both experimental and control seeds. As a result of the experiments conducted it was found that in the experimental series of unirradiated seeds the frequency of cells with abnormal mitoses differed statistically from both controls. In the series with gamma-irradiation of seeds prior to the space flight differences were statistically significant only between the experiment and the control left in Moscow. Preliminary gamma-irradiation of seeds and the subsequent action of space flight factors cause an additive effect upon the occurrence of cells with abnormal mitoses. (ATD)

**1650** ROLE OF SUPERINFECTING PHAGE IN LYSIS INHIBITION WITH PHAGE T4 IN ESCHERICHIA COLI. Rutberg, Blanka; Rutberg, Lars (Karolinska Institutet, Stockholm). J. Bacteriol., 90: 891-4(Oct. 1965).

The ability of bacteriophage T4 to induce lysis inhibition upon superinfection was investigated after various treatments of the phage, including γ- and ultraviolet-induced inactivation. This ability was found not to be a property of the external protein part of the phage, nor was it dependent on the functional and possibly structural integrity of the phage genetic material. (auth)

**1651** EFFECT OF PARTICLE AGGREGATION ON THE SURVIVAL OF IRRADIATED VACCINIA VIRUS. Galasso, G. J.; Sharp, D. G. (Univ. of North Carolina, Chapel Hill). J. Bacteriol., 90: 1138-42(Oct. 1965).

The survival curve (plaque titer versus time) of vaccinia virus irradiated with ultraviolet light was found to be strongly dependent, in both shape and general slope, on the degree of aggregation among the virus particles. When special care was taken to produce completely dispersed virus, a straight steep line resulted. Some severely aggregated preparations produced a straight line also, but of much less slope. Thus, the straight line, often taken as evidence of complete dispersion, is not a reliable measure for vaccinia virus. None of the experimental curves resembled the classical multihit curve predicted by the Poisson function for the behavior of uniformly aggregated virus. The aggregation was observed, by electron microscopy, to be nonuniform, and of such a distribution that the survival curves can be qualitatively accounted for in terms of multiplicity reactivation of irradiated virus within cells that receive groups of two or more particles. The greatly in-

creased survival value of aggregates of virus, which indicates multiplicity reactivation, is worthy of note. (auth)

**1652** EFFECTS OF EXTERNAL IRRADIATION OF THE HEART ON CARDIAC OUTPUT, VENOUS PRESSURE AND ARTERIAL PRESSURE. Bishop, V. S. (Texas A and M Univ., College Station); Stone, H. L.; Yates, Jerrell; Simek, J.; Davis, J. A. J. Nucl. Med., 6: 645-50(Sept. 1965).

The resting cardiac output venous pressures and arterial pressure changes following exposure of the right chest wall to 20,000 R $^{60}$Co $\gamma$ radiation were evaluated in dogs. Results indicated that doses of ionizing radiation in the therapeutic range may produce damage to the myocardium. The effect is probably an indirect effect resulting from increased permeability and fragility of the capillaries. The injury to the myocardium resulting from therapeutic doses may not be detected under normal resting conditions. The latent period, or time from exposure to microscopic changes in the cardiac muscle, is sensitive to small changes in dose. (auth)

**1653** GLUCOSE CONTROL OF AN X-RADIATION INDUCED DIFFERENCE IN $CO_2$ PRODUCTION BY YEAST CELLS. Spoerl, Edward; Doyle, R. J. (Army Medical Research Lab., Fort Knox, Ky.). Life Sci., 4: 1843-8 (Oct. 1965).

Data are reported showing that glucose supplementation in the starvation suspension will prevent development of the difference in capacity to produce $CO_2$ previously found in x-irradiated and unirradiated yeast cultures. (TCO)

**1654** INVESTIGATIONS ON REVERSIONS TO METHIONINE INDEPENDENCE INDUCED BY MUTAGENS IN SCHIZOSACCHAROMYCES POMBE. Loprieno, Nicola; Clarke, Colin H. (Univ., Pisa. Medical Research Council Mutagenesis Research Unit, Edinburgh). Mutat. Res., 2: 312-19(Aug. 1965).

The mutagenic effect of UV light, nitrous acid, N-nitroso-N-methylurethane and N-nitroso-N-methyl-N′-nitroguanidine on the met$_4^-$, D19, h$^-$ strain of Schizosaccharomyces pombe was studied by analyzing reversion to methionine independence. A genetic analysis of the induced and spontaneous revertants gave indications of mutagen specificity among the mutagens studied; most of the induced reversions were due to suppressor mutations. Data on the different response to di-epoxybutane of the met$_4^-$, D19 site in cells of opposite mating types (h$^-$ and h$^+$) are also presented. (auth)

**1655** MUTANTS INDUCED BY IONIZING RADIATIONS AND ETHYLENEIMINE IN WINTER WHEAT. Khvostova, V. V.; Mozhaeva, V. S.; Aigaes, N. S.; Valeva, S. A. (Inst. of Biophysics, Academy of Science, Moscow). Mutat. Res., 2: 339-44(Aug. 1965).

The mutagenic effects of $\gamma$ rays, 1 to 2 Mev fast neutrons, and ethyleneimine are compared in treatments of seeds of winter wheat variety Triticum agropyron hybrid-186 (2n = 42). Ethyleneimine in a concentration of 0.01%, was found to be the most efficient mutagen: 50.8% of the $M_2$ progenies segregated for mutants. After treatment with 740 rad of fast neutrons 36.5% of the progenies contained mutants, and 10 kR $\gamma$ rays gave 6.2% progenies with mutants. Different spectra of mutants were obtained after treatment with neutrons, $\gamma$ rays, and ethyleneimine. Neutrons produced a narrow spectrum: of 207 mutants, 80% were erectoids, squareheads and speltoids and only 20% were other mutant types. From 81 mutants isolated after $\gamma$ ray treatment, 33% belonged to the class of other types. In the ethyleneimine series 100 mutants were found. Of these, 34% belonged to the class of other types. In the ethyleneimine series 100 mutants were found. Of these, 34% belonged to the above-mentioned three types of mutant affecting the spike, whereas 66% consisted of various other mutant forms. Thus ethyleneimine, besides being the most efficient mutagen, also produced the broadest mutant spectrum. With the mutagens used, mutants with valuable agronomical properties, such as resistance to lodging, resistance to fungal diseases, and high productivity were produced. (auth)

**1656** MUTATIONS INDUCED BY ETHYL METHANESULFONATE IN MAIZE. Amano, E.; Smith, H. H. (Brookhaven National Lab., Upton, N. Y.). Mutat. Res., 2: 344-51(Aug. 1965). (BNL-8824).

Single-locus mutations were induced frequently and almost exclusively by treating seeds or young seedlings of I Sh Wx stocks of Zea mays with aqueous solutions of ethyl methanesulfonate, while x irradiation of pollen produced a high proportion of multiple-locus mutations. (auth)

**1657** THE MUTAGENIC EFFECT OF TRITIATED URIDINE IN DROSOPHILA SPERMATOCYTES. Olivieri, G.; Olivieri, A. (State Univ., Leiden. Inst. of Radiopathology and Radiation Protection, Leiden). Mutat. Res., 2: 381-4(Aug. 1965).

The mutagenic effects of B particles from incorporated $^3$H-thymidine or $^3$H-uridine in Drosophila spermatocytes were studied. Since actinomycin D inhibits the incorporation of uridine, but not that of thymidine, a comparison of the mutagenic effectiveness of the two tritiated nucleosides was made with and without actinomycin D co-treatment. $^3$H-uridine was found to be a more effective mutagenic agent than $^3$H-thymidine, in spite of the effect that the specific activity of the thymidine was greater than that of the uridine. Actinomycin D strongly inhibited the labeling of the cytoplasm. Autoradiographic studies showed that $^3$H-uridine was incorporated both in the nucleus and in the nucleolus. (C.H.)

**1658** PLAQUE-FORMATION BY NON-IMMUNE AND X-IRRADIATED LYMPHOID CELLS ON MONOLAYERS OF MOUSE EMBRYO CELLS. Moeller, Goeran; Moeller, Erna (Karolinska Institutet Medical School, Stockholm). Nature, 208: 260-3(Oct. 16, 1965).

A plaque technique was used to evaluate the effect of normal and x irradiated lymphoid cells aggregated to monolayers of embryonic target cells in tissue cultures. The appearance of plaques in the monolayer culture at the site of lymphoid cell introduction was used as the criteria of aggregation of non-immune lymphoid cells on embryonic target cells. In cases where no plaques developed the monolayer cells were intact and surrounded by dense aggregates of lymphoid cells. The addition of allogenic or semi-isologous $F_1$ hybrid spleen or lymph node cells on to monolayers of parental embryo cells in several different strain combinations led to the appearance of plaques, while isogenic lymphoid cells had no detectable effect. Non-immune parental lymph node or spleen cells were found to be fully competent to induce the appearance of plaques in the majority of cases studied. X irradiation did not appear to inhibit the ability of hybrid lymph cells to cause plaques on parental embryo cells or to affect the plaque-forming efficiency of allogenic and parental lymphoid cells. The results indicate that a non-immunological recognition process is initiated by the close contact between antigenically and structurally incompatible lymphoid cells and target neoplastic and embryonic cells that results in damage or death of the target cells. (C.H.)

**1659** PHOTOREACTIVATION OF TOBACCO MOSAIC VIRUS RIBONUCLEIC ACID FOLLOWING NEAR ULTRAVIOLET IRRADIATION. Merriam, Virginia; Gordon, Milton P. (Univ. of Washington, Seattle). Proc. Nat. Acad. Sci., 54: 1261-8(Oct. 1965).

Tobacco mosaic virus (TMV) RNA inactivated by irradiation at wavelengths in the region of 300 m$\mu$ exhibits an increased photoreactivable sector with respect to that observed following 253.7 m$\mu$ irradiation. The amount of the photoreactivable lesion similar to that formed by 253.7 m$\mu$ irradiation is increased by the near UV irradiation, and the formation of a new type of repairable lesion is inferred from the dark-holding effect and the variation in apparent infectivity on assay plants grown under high- and low-intensity illumination. (auth)

**1660** EFFECT OF ALLOGENEIC BONE MARROW ON LETHALLY IRRADIATED THYMECTOMIZED MICE. Simmons, Richard L.; Wolf, Sheldon M.; Chandler, James G.; Nastuk, William L. (Columbia Univ., New York). Proc. Soc. Exp. Biol. Med., 120: 81-4(Oct. 1965).

Thymectomized and sham-thymectomized mice were lethally x irradiated and given syngeneic and allogeneic bone marrow. Whereas the irradiated syngeneic chimeras failed to reject allogeneic skin grafts in the absence of the thymus, a secondary graft-versus-host disease developed with equal rapidity in both thymectomized and sham-thymectomized allogeneic chimeras. The possibility that bone marrow precursors of lymphoid tissue differentiate via different routes in irradiated syngeneic and allogeneic chimeras is suggested. (auth)

**1661** EFFECT OF X-RAYS ON HEMOLYSIN PLAQUE FORMING CELLS. Uyeki, Edwin M. (Battelle-Northwest, Richland, Wash.). Proc. Soc. Exp. Biol. Med., 120: 115-17(Oct. 1965). (BNWL-SA-133).

All measured parameters of the primary antibody response of C57L × A/He mice injected with sheep red cells were uniformly depressed by 500 R of x ray. With adequate x ray doses, the production of anti-body forming cells was radiosensitive, irrespective of the several time intervals employed between x ray and antigenic stimulation. At lower x ray doses the numbers of hemolysin plaque forming cells are clearly influenced by this time interval. A bi-phasic response to x rays in the production of antibody forming cells was demonstrated, i.e., a relatively insensitive period in between two sensitive periods. (auth)

**1662** INTERACTIVE EFFECTS OF X-IRRADIATION AND BARBITURATES. Nair, V.; Finer, S.; Shah, D. (Chicago Medical School). Proc. Soc. Exp. Biol. Med., 120: 246-52(Oct. 1965).

The effects of varying doses of cephalic x irradiation on barbiturate hypnosis were examined in rats. An enhancement of hypnosis was found in the irradiated animals, the effect depending on the dose of radiation and the time post-irradiation. At relatively higher doses (5,000 and 10,000 R), the duration of thiopental hypnosis was significantly prolonged. Similarly, in the 10,000 R irradiated rats, the time of onset of hypnosis for the slow acting barbital was considerably shortened. Using pentobarbital, it was possible to demonstrate the enhancement effect, both with respect to onset and duration of hypnosis. It was also shown that even at the high doses of radiation employed, head x irradiation produced no inhibition of the phenobarbital induction of microsomal enzyme activity as evidenced by the pharmacological effects. (auth)

**1663** THE RADIOBIOLOGY OF YEAST. James, A. P.; Werner, M. M. (Atomic Energy of Canada Ltd., Chalk River, Ont.). Radiat. Bot., 5: 359-82(Nov. 1965).

Data are summarized from a number of studies on the effects of radiation on yeast and diverse factors that modify these effects. Topics discussed include the initial effects of radiation on cell division, lethal effects, mutations, mitotic recombination, heterallelic recombination, modifying factors, and extrachromosomal factors. (197 references). (C.H.)

**1664** COMPARATIVE SENSITIVITY TO GAMMA RADIATION OF YEAST MITOSIS AND MEIOSIS. Miller, J. J.; Kingsley, V. V.; Ramirez, C. (McMaster Univ., Hamilton, Ont.). Radiat. Bot., 5: 383-90(Nov. 1965).

Following exposure to $^{60}$Co gamma radiation at dosages from 2000 to 50,000 rad, cells of Saccharomyces cerevisiae were placed in media favorable to either growth or sporulation. Ability to grow was less sensitive to radiation than ability to sporulate. The inactivation curve for multiplication by budding was sigmoidal, but inactivation of the sporulation mechanism was exponential. The radiation-sensitive phase of sporulation was the reductional nuclear division that precedes spore wall formation. The average number of spores per ascus was not altered by irradiation. (auth)

**1665** RECURRENT IRRADIATION FOR OAT BREEDING. Khadr, F. H.; Frey, K. J. (Cotton Inst., Alexandria, Egypt). Radiat. Bot., 5: 391-402(Nov. 1965).

A second cycle of thermal neutron irradiation for expanding the genetic variability for 3 polygenic attributes, relative to the pedigreed procedure and relative to the first cycle of irradiation, was evaluated in 4 oat populations: irradiated Clintland; irradiated Beedee; the hybrid of Clintland × Beedee; and the irradiated hybrid. The 5 lines with the highest 100 seed weight from each population were re-irradiated and also pedigreed. The sampling procedure involved populations; parents within populations; families within parents; and lines within families. Lines derived from populations by these 2 methods and lines from the original populations were grown in a replicated experiment, and were measured for 100-seed weight, heading date, and plant height. The progress from selecting the parent strains for 100-seed weight was as great as or greater than that predicted in both the irradiation-derived and the hybrid-derived material. For both the selected (seed weight) and unselected (plant height and heading date) attributes, the new populations developed via recurrent irradiation showed expanded variability over either the original or the pedigreed populations. However, the second irradiation treatment did not generate as much variability as the first. There were no significant shifts in the population means as a result of the re-irradiation treatment. For all attributes, the variances, generated from treating hybrid-derived materials with either one or two doses of irradiation, were somewhat smaller than the sum of hybridization- and irradiation-derived variances which had been estimated independently. The degree of conformity between the actual and predicted variance was attribute-oriented. (auth)

**1666** ELECTRON MICROSCOPIC STUDY ON THE DEVELOPMENT OF NORMAL AND X-RAY IRRADIATED CELLS OF WHEAT EMBRYOS. Von Wangenheim, K. H. (Kernforschungsanlage, Juelich, Ger.). Radiat. Bot., 5: 403-16(Nov. 1965). (In German).

The normal development of mesophyll cells of germinating wheat embryos was investigated and compared with the development of embryos which had been irradiated with high x ray doses (200 to 800 kR). Air dry irradiated seeds were capable of germination and developed into small plantlets of up to 19 mm in length. Nuclei in various mitotic stages were rarely found in the embryonic tissues. Their existence can be explained by the occurrence of prophasic nuclei which were found occasionally in the resting embryos. Lipoid droplets were distinguishable from spheromsomes and from round or elliptic and strongly osmiophilic bodies. During germination the resorption of reserve materials (lipoid bodies and round or elliptic bodies) proceeds normally in the irradiated tissues. No obvious alteration has been found during the development of the endoplasmatic reticulum, the central vacuole and the chloroplasts. After the irradiation of pregerminated seeds a significant decrease in diameter of mitochondria has been determined and an increase in fixation instability seems to occur. The embryos, which had been irradiated in the dry state, do not reveal such conspicuous disturbances comparable to those found in zoological objects after x irradiation, despite the high x ray doses. The cells developed normally and the speed of this development is approximately the same as that of the cells of the controls. Between 12 and 21 days after soaking the irradiated seeds on moist filter paper, the plantlets die even under sterile conditions. (auth)

**1667** RBE OF 14 Mev NEUTRONS IN DRY BARLEY SEEDS. Harle, J. R. (Atomic Energy of Canada Ltd., Chalk River, Ont.). Radiat. Bot., 5: 417-22(Nov. 1965).

To determine the RBE of fast neutrons under controllable experimental conditions, dry barley seeds containing 1% moisture were exposed in vacuo to 14 Mev neutrons or to $^{60}$Co gamma rays. After irradiation, the seeds were soaked in water in the presence or absence of oxygen. Reduction in early growth of the seedlings was used as a measure of radiation damage. Post-irradiation treatment with oxygen did not alter the effects of neutron radiation, but increased the effects of gamma radiation by a factor of 9.3. The RBE of fast neutrons was found to be 29 in the absence of oxygen and 3 with post-irradiation oxygen treatment. (auth)

**1668** COMPARISON OF REPRODUCTIVE INTEGRITY IN THE STAMEN HAIR AND ROOT MERISTEM OF TRADESCANTIA PALUDOSA FOLLOWING ACUTE GAMMA IRRADIATION. Alvarez, M. R.; Sparrow, A. H. (Brook-

haven National Lab., Upton, N. Y.). Radiat. Bot., 5: 423-30(Nov. 1965). (BNL—9283).

The inactivation of the essentially single-cell system of the Tradescantia stamen hair was compared with the changes reflected in the cell population of the aerial root meristem following acute exposure to gamma radiation. Floral buds of Tradescantia paludosa (clone B2-2) having immature stamen hairs were irradiated with exposures ranging from 35 to 150 R. Flowers scored 10 to 16 days post irradiation showed a decrease in the number of normal hairs per filament which was proportional to the exposure. Since loss of the reproductive integrity of the terminal cell results in a stunted hair, the dose-response obtained was considered to represent single-cell survival. Active aerial roots of the same species were also irradiated at exposures ranging from 50 to 400 R. The number of cells comprising the meristem at 4 days post irradiation was determined for each exposure. Cell counts showed a decrease in the cell population of the meristem proportional to the exposure. The survival curves obtained for the essentially single-cell stamen hair system and for the cells comprising the root meristem did not differ significantly in either intercept or slope. Since the interphase chromosome volumes of the terminal stamen hair cells and the cells of the root meristem were not significantly different, it was concluded that no radioresistance was conferred to the cells of the root meristem by virtue of their close contact with each other and possible intercellular connections within the tissue. (auth)

**1669** RADIOSENSITIVITY OF RICE SEED IN RELATION TO WATER CONTENT AND FREE RADICALS. Myttenaere, C.; Bourdeau, Ph.; Helcke, G.; Masset, M. (Euratom, Joint Research Centre, Ispra, Italy). Radiat. Bot., 5: 443-51(Nov. 1965).

Dormant seeds of 5 varieties of lowland rice, Oryza sativa L. were equilibrated at water content varying from 6.4 to 27.6% and x irradiated (210 kv) at exposure doses up to 50 kR. Germination was little affected by irradiation up to the 50 kR dose. Effects on survival, height growth, and seed production of the plants indicated that radiosensitivity was minimal at intermediate water content, (14 to 16.6% for the whole seed or 10 to 13% for the embryo) and increased rapidly above and below this range. ESR measurements gave a good correlation between the concentration of slow-decaying free radicals and radiation damage in dry-to-moderately moist seeds but not in the upper part of the moisture range. Significant differences in radiosensitivity were detected among varieties. (auth)

**1670** THE EFFECT OF A SINGLE RADIATION EXPOSURE ON THE BLOODPICTURE OF GUINEA-PIGS IN DEPENDENCE ON DOSE AND TIME. Horst-Meyer, H. zur; Petroff, Ch. (Univ., Berlin). Radiobiol. Radiotherap., 6: 499-504(1965). (In German).

Examination of guinea pigs following whole-body x irradiation under the conditions of deep therapy with 50 doses showed a decrease in the absolute number of granulocytes with the minimum on the 10th day. With the lymphocytes after a not significant decrease on the first day an absolute lymphocytosis occurs up to the 100th day of the experiment. With an exposure of 100 R and 200 R the cellular depression of granulocytes was more intense than of lymphocytes which already increase again from the fifth day after 100 R. The results point to the reparation of damage in lymphocytes beginning sooner than in granulocytes. (tr-auth)

**1671** THE REACTION ON IONIZING RADIATION IN THE SYSTEM OF ADENOHYPOPHYSIS—THYROID GLAND —GONADS. Kascenko, L. A. Radiobiol. Radiotherap., 6: 517-21(1965). (In German).

The morphological and functional changes occurring in the endocrine glands under the effect of radiation are characterized by some stereotyped phenomena. In the early stages of radiation injury in the endocrine glands those mechanisms are altered which assure the hormonal distribution. They are affected before the mechanisms of synthesis. In the early stages of radiation reaction in the radiation injured glands an increased contact of products of the cellular secretion is to be found. In the gonads the decrease or complete loss of sensitivity of the irradiated glands to the specific hormonal stimulators was found. This peculiarity of radiation injury obviously is of universal character. Both effects the blockage of the hormonal distribution and loss of sensibility to hormonal stimuli, are a disturbance of the hormonal relations between the glands in the irradiated organism and lead to disintegration of the endocrine system. (tr-auth)

**1672** EXAMINATIONS OF THE BLOOD-PICTURE AFTER INTRACAVITARY ADMINISTRATION OF $^{198}$Au. Horst-Meyer, H. zur; Ziemack, H. (Univ., Berlin). Radiobiol. Radiotherap., 6: 595-9(1965). (In German).

Under the intracavitary administration of $^{198}$Au a granulocytopenia and lymphopenia occur in the human being at the end of the first week. The decrease of the cell count in the peripheral blood must not be considered as a radiation injury of the hematopoietic tissues but a consequence of a change in distribution. After a stimulus (abscess), as well as after the administration of prednisone, the cell count in the peripheral blood will be promptly normalized. (tr-auth)

**1673** THE MOLECULAR WEIGHT OF FACTOR XII (HAGEMAN FACTOR) ESTIMATED WITH IONIZING RADIATION. Haanen, C.; Morselt, G.; Schoenmakers, J.; Maters, M.; Braams, R. (Univ. of Nijmegen, Netherlands. Univ. of Utrecht). Scand. J. Haematol., 2: 248-52(1965).

The sensitivity of a dry enzyme to inactivation by ionizing radiation has been found to be approximately proportional to the molecular weight of the enzyme molecule, thus the study of the radiation sensitivity of dried enzymes or other functional proteins can lead to an approximate estimate of the molecular weight of the protein under investigation. The method was applied to obtain information concerning the molecular weight of Factor XII (Hageman factor), a factor present in mammalian plasma, which initiates the clotting process when blood or plasma comes into contact with glass. Samples of bovine Factor XII preparations were pipetted onto glass coverslips, dried in vacuum, and exposed in vacuum to a beam of fast protons (1.8 Mev) from a Van de Graaff accelerator. Crude bovine Factor XII and highly purified bovine Factor XII were prepared and Factor XII-activity was tested in a standardized system. From a comparison of the radiation sensitivity of Factor XII with those of three different enzymes, the molecular weight of Factor XII was estimated at approximately 80,000. (C.H.)

**1674** EFFECT OF GAMMA RADIATION ON DIETARY AND HORMONAL INDUCTION OF ENZYMES IN RAT LIVER. Pitot, Henry C. (Univ. of Wisconsin, Madison); Peraino, Carl; Lamar, Carlos Jr.; Lesher, Sam. Science, 150: 901-3(Nov. 12, 1965).

The dietary induction of serine dehydrase, produced by the oral intubation of hydrolyzed casein to protein-depleted rats, is markedly inhibited by doses of $\gamma$ radiation of 400 R or higher provided the irradiation is given within an hour after the initial dose of casein. If the irradiation is delayed until 7 hours after the initial dose of casein, induction is not inhibited. In contrast, the cortisone induction of tyrosine $\alpha$-ketoglutarate transaminase is not inhibited by doses of $\gamma$ radiation up to 3200 R; in some instances hormonal induction of this enzyme appears to be enhanced by irradiation. (auth)

**1675** EFFECT OF WHOLE-BODY AND PARTIAL-BODY X-IRRADIATION ON THE EXTRACTABLE CELLULAR COMPONENTS OF THE LUNG WITH SPECIAL CONSIDERATION TO THE ALVEOLAR MACROPHAGE [Thesis]. Moyer, Robert Findley. Los Angeles, Univ. of California, 1965. 116p.

A series of experiments involving the extraction of cells from the lungs of rabbits and rats was conducted to establish the radioresponsiveness of the cellular components within the alveoli. With the exception of a small preliminary study, all irradiation was conducted using the brems-

strahlung produced by a 6-Mev linear electron accelerator (17.8 mm Cu HVL). The $LD_{50,30}$ for totally irradiated Sprague-Dawley rats under the exposure conditions used was approximately 900 rads. Rats were exposed to (a) whole-body doses of 500, 750 and 1000 rads and (b) a partial-body dose of 1000 rads to either the cranial and abdominal regions combined or to the thoracic region alone. Thoracic irradiation and whole-body irradiation at the three dose levels all reduced macrophage numbers to approximately 50% of control values during the second week after irradiation. More extensive studies with rats exposed to 1000 rads showed a three phase reaction to alveolar macrophages, (a) elevation during the first post-irradiation week, (b) reduction from the second to fifth week and (c) recovery after five weeks. Alveolar macrophage size was elevated throughout the 37-day period of observation and reached maximal values near the end of the second week. The frequency of binuclear macrophages increased abruptly during the second week after irradiation. Lung weight increased approximately 20% in irradiated rats during the third week and remained elevated at the end of the 37-day period of observation. The number of polymorphonuclear leucocytes extracted from the lung increased to approximately ten times control levels during the second and third weeks after 1000 rads of whole-body irradiation and subsequently decreased in an exponential manner. Small aphagocytic mononuclear cells were found in lung washes from all control animals. Large concentrations of these cells were correlated with the presence of small clear spots on the lung surface. This cell type was markedly reduced during the first two weeks after whole-body irradiation, and the extent of this reduction was proportional to the fraction of the body irradiated. (Dissertation Abstr.)

**1676** THE EFFECTS OF TOTAL-BODY IRRADIATION WITH X-RAYS AND SUPPLEMENTARY INJECTIONS OF LIVER HOMOGENATE UPON THE SURVIVAL PERIOD IN INBRED LINES OF THE SYRIAN HAMSTER, MESOCRICETUS AURATUS (WATERHOUSE) [Thesis]. Skavaril, Russell Vincent. Columbus, Ohio, Ohio State Univ., 1964. 69p.

Three inbred lines of the Syrian hamster, Mesocricetus auratus (Waterhouse), were developed to study the relationship of genotype, sex, and x-ray dose to the length of survival in a 30-day observation period following a single, whole-body exposure to x rays. All experimental animals were 40 to 50 days old, and the range of x-ray dose employed was 450 to 975 roentgens. Single or double substitution of the mutant gene e or $c^d$ for its corresponding wild-type allele was found to increase the resistance of the hamster to x rays. The e substitutions were found to be considerably more resistant than either the wild-type line or the $c^d$ substitutions. Significant differences were observed between the responses of the two sexes in certain genotypes, i.e., E/E +/+, E/e +/+, and E/E $c^d/c^d$. The wild-type male hamster was found to be slightly more resistant than the wild-type female, but the more resistant sex did not remain constant as gene substitutions were made at the the e or $c^d$ locus. There were no differences in lengths of survival periods within or between lines when a dose of 450 roentgens was given. Significant differences between lines were observed at doses greater than 450 roentgens. A single injection of isologous whole-liver homogenate prepared in buffered saline and given with irradiation was found to increase the length of survival period. Such an increase was not observed when the supplementary injection was buffered saline. The exact nature of the effect, which was found to be attributable to the liver in the homogenate, was dependent upon sex, genotype, and x-ray dose. However, the effect of an increased survival period was found to be independent of whether the supplementary injection of isologous whole liver homogenate was given before or after x rays. (A.G.W.)

**1677** GENETIC EFFECTS OF IRRADIATION ON PREWEANING AND POSTWEANING GAINS OF PIGS [Thesis]. Park, Young Il. Ames, Iowa, Iowa State Univ. of Science and Tech., 1964. 85p.

The genetic influence of irradiation of sire and maternal grandsire on preweaning and postweaning gains of pigs was investigated. The data came from 9,348 pigs of the Duroc and Hampshire breeds raised from the spring of 1960 through the spring of 1963. About half of the sires and maternal grandsires used were exposed to 300 R of x rays directed locally to their testes in a single dose at a rate of 100 R per minute, five or more months before they were used for breeding. The other boars were used as controls. This produced four treatment combinations from a two-by-two factorial arrangement of sire treatment and maternal grandsire treatment. A statistical method of analyzing an $R \times 2^2$ table was derived and utilized. The estimates of the main effect (control minus irradiated) of sire treatment, that of maternal grandsire treatment and the interaction between sire treatment and maternal grandsire treatment, are tabulated. The effects of sire treatment and maternal grandsire treatment varied considerably from block to block, except probably for the effect of maternal grandsire treatment on preweaning gain. The phenotypic variances and the heritabilities are estimated within breed-year-season-parity group. Most of the increased phenotypic variances of offspring by irradiated sires appeared not to be additively genetic. The larger litters at weaning tended to have smaller gains and the regressions of the gains on litter size were larger in offspring by irradiated sires than in those by control sires. The results suggest that the offspring by irradiated sires have a reduced buffering capacity or are more susceptible to differences in environments than the offspring by control sires. (Dissertation Abstr.)

**1678** AN INVESTIGATION INTO THE BASIS OF VARIATION OF PURINE ANALOGUE RESISTANCE IN AN ESTABLISHED MURINE CELL LINE [Thesis]. Morrow, Kenneth John Jr. Seattle, Univ. of Washington, 1964. 137p.

Resistance to analogs of hypoxanthine and guanine was studied in an established line of murine origin. Two discrete levels of resistance were studied. Cells resistant to an intermediate concentration occur with a frequency of about $10^{-3}$, and cells resistant to a high level of the analog occur with a frequency of $10^{-5}$. Variants are not induced by the selecting agent but are rather pre-existing in the population. No phenotypic lag was detected. The mutation rate from sensitive to intermediate was $10^{-4}$ and from sensitive or intermediate to resistant was $10^{-6}$. Mutagenesis studies with uv and x rays, with and without a lag period before addition of the selecting agent, were negative. Reversion experiments in the reverse direction, with a lag, gave an increase over control values in preliminary experiments. The biochemical basis of resistance was found to reside in the loss of the enzyme inosinic acid pyrophosphorylase. Chromosomal analysis and physical measurements of the DNA failed to disclose any detectable difference between sensitive and resistant cell lines. A model is proposed to account for the results, which suggests the existence of two separate loci, or a single complex locus, in either case present in a diploid condition. Intermediate mutants are believed to be due to an alteration that partially destroys enzyme activity. The resistant mutants are believed to be due to a separate alteration in another locus, or region of the same locus, which abolishes enzyme activity when present in double dose and decreases it so as to yield an intermediate clone when present in a single dose. The resistants produce revertants with a low frequency due to a back mutation in one of the alleles; these revertants are intermediate in their resistance and give off sensitive and resistant cells at the same rate, possibly as the result of a recombinational event. (A.G.W.)

**1679** THE RESISTANCE OF CLOSTRIDIUM PERFRINGENS TYPE A SPORES TO GAMMA RADIATION [Thesis]. Midura, Thaddeus Francis. Ann Arbor, Mich., Univ. of Michigan, 1964. 157p.

The resistance of Clostridium perfringens spores to ionizing radiation was investigated. A classic strain and an atypical, heat resistant strain were selected as representative of Cl. perfringens Type A. Spores were produced in Ellner's medium and in a trypticase soy broth medium. The

number of viable spores was determined by dilution counts using tryptone-yeast extract agar medium and the Prickett tube technique. Approximately $1 \times 10^6$ spores per ml suspended in M/15 phosphate buffer were irradiated with gamma rays from cobalt-60. The procedure was repeated using spores of the atypical Type A strain in cooked meat broth, and spores of the classic strain in M/15 phosphate buffer. The radiation resistance of the spores was determined by the enumeration of the survivors. Under the conditions of the experiments, the survivor curves show that the logarithm of the per cent survivors was exponential with increasing gamma radiation doses up to approximately one megarad. The D values for spores of the atypical strain suspended in M/15 phosphate buffer and in cooked meat broth were 0.23 and 0.30 megarads respectively. For spores of the classic strain, a D value of 0.25 megarads was obtained. Spores of the classic and atypical strains of Cl. perfringens are characterized by differing heat resistance, yet all the strains tested demonstrated similar radiation resistance. The spores of Cl. perfringens were more resistant to the effects of ionizing radiation when suspended in cooked meat broth than when suspended in M/15 phosphate buffer. (Dissertation Abstr.)

**1680** THE NATURE OF RECOGNITION OF ANTIGENIC DETERMINANTS [Thesis]. DiLeone, Gilbert Robert. Kingston, R. I., Univ. of Rhode Island, 1964. 98p.

Two approaches were used to test the hypothesis that the carrier of antigenic determinants functions at the level of cellular recognition by examination of the primary and secondary immune responses to protein and azoprotein antigens. The serologically unrelated protein antigens used in the first approach were human gamma globulin (HGG) and bovine serum albumin (BSA). Using these proteins as carriers three azoproteins were prepared: BSA-azo-p-arsanilic acid (BSA-PAA), BSA-azo-p-aminobenzoyl-L-glutamic acid (BSA-PABLG) and HGG-azo-p-arsanilic acid (HGG-PAA). These antigens, in various combinations and sequences, were given as primary and secondary intravenous injections to a number of groups of New Zealand white rabbits. The results indicated that the carrier protein determines the time of peak titer of the secondary response to homologous azolinked haptens. Moreover, attachment of haptens to proteins does not significantly change the responses to the protein carrier. The second approach to the problem was to study the effect of irradiation on the primary and secondary antibody responses to native serologically related protein antigens, human gamma globulin (HGG) and bovine gamma globulin (BGG). All rabbits received a primary injection of BGG. Some of these rabbits were given whole body x irradiation one day later. Twenty-four hours after irradiation a second injection of either BGG or HGG was given to individual irradiated or normal unirradiated rabbits. Some of another group of BGG sensitized rabbits were given whole body irradiation 29 days after primary injection and all were given a secondary injection of either BGG or HGG on day 30. Rabbits of a separate control group were irradiated 24 hours prior to injection of either BGG or HGG. The results indicated that a secondary type response to cross-reacting determinants does not occur after secondary injection of heterologous HGG. A better secondary response to cross-reacting sites occurred after two injections of BGG. Whole-body irradiation inhibited the immune response to determinants entering the animal for the first time, regardless of the fact that the antibody forming system may have been previously sensitized to part of the antigen molecule. (Dissertation Abst.)

**1681** INVISIBLE RADIATIONS. Godward, M. B. E. (Queen Mary Coll., London). pp 551-66 of Physiology and Biochemistry of Algae. New York, Academic Press, 1962.

The actions of uv, x, $\gamma$ rays, fast electrons, protons, $\alpha$ particles, and neutrons on algae are reviewed. The effect of 1-Mev electrons on various species of algae are also presented. The observed effects of 1,000,000-rad doses of 1-Mev $\beta$ rays upon cultures of Chlorella pyrenoidosa subsequently kept in continuous light began with a fall in the viable cell count, which continued to decrease more slowly for 18 days after irradiation, and then increased again. A second dose of the same magnitude produced similar effects. The recovered cells were somewhat larger than normal, but their growth rate was equal to that of the control culture. In comparable tests at 10,000 rad, no difference was observed between the effects of x rays and high-energy $\beta$ rays. (TCO)

**1682** RADIATION INDUCED INACTIVATION OF RIBONUCLEASE. Thomson, D. H.; Stratton, K. 4p. (CONF-650560-6). Gmelin, AED-CONF-65-157-11.

From 13th Annual Meeting of the Radiation Research Society, Philadelphia.

Results are reported from a study of the effects of $^{60}Co$ $\gamma$ radiation on bovine pancreatic ribonuclease at various temperatures. The samples were prepared by freeze drying aliquots of solution in pyrex tubes and the irradiations were carried out in a cooling medium. The enzyme activity showed an exponential dose relationship and from these plots $D_{37}$ doses were obtained. Data are presented on the $D_{37}$ doses obtained at various temperatures from 77°K up to 366°K for samples irradiated in the presence and absence of air. Increased sensitivity in the presence of oxygen was observed down to liquid $N_2$ temperatures where the oxygen effect disappears. (C.H.)

**1683** EFFECT OF INHALING 95% OXYGEN AND 5% CARBON DIOXIDE ON THE RADIOCURABILITY OF MURINE TUMORS. Inch, W. R.; McCredie, J. A.; Kruuv, J. (Ontario Cancer Treatment and Research Foundation, London; Univ. of Western Ontario, London). 19p. (CONF-650560-1). Gmelin, AED-CONF-65-157-8.

From 13th Annual Meeting of the Radiation Research Society, Philadelphia.

Inhalation of 5% carbon dioxide and 95% oxygen at atmospheric pressure, increased blood flow and radiocurability of the poorly vascularized C3H isoimplant tumors in mice compared with breathing 100% oxygen. The rate of cure of the C3HBA isotransplant, which has a better blood supply, was increased compared with air but not with pure oxygen. (auth)

**1684** RADIATION EFFECTS ON THE FREE RADICAL PROPERTIES OF MELANIN. Stratton, K.; Pathak, M. 5p. (CONF-650560-5). Gmelin, AED-CONF-65-157-14.

From 13th Annual Meeting of the Radiation Research Society, Philadelphia.

The protective function of melanin against actinic damage in human skin was investigated. Samples of human hair and skin and of guinea pig hair were exposed to ultraviolet or $\gamma$ radiation at room temperature and 77°K and the electron spin resonance spectra determined. All the pigmented preparations gave ESR signals both at room temperature and at 77°K without irradiation. Bleaching of black hair with hydrogen peroxide reduced the melanin signal to approximately the size of that obtained from blond hair. Ultraviolet radiation did not produce any ESR signals at room temperature, with life times greater than a few minutes, in any of these materials. Measurements of the relative radical yields as a function of ultraviolet dose showed that the radical yield in white skin is almost 50% higher than in heavily pigmented skin. Gamma radiation produced free radicals in skin irradiated at low temperatures, in hair samples, in melanin granules, and in melanosomes. The hair spectrum at room temperature was a fairly characteristic protein spectrum with a strong cystine radical component. The spectrum of irradiated skin changed with increasing dose in a consistant manner. It was concluded that the photoprotective effect of melanin in pigmented skin may be related to the reduced total radical yield of such skin. (C.H.)

**1685** CYCLIC FLUCTUATIONS IN THE RADIOSENSITIVITY OF MICE AFTER EXPOSURE TO SUBLETHAL WHOLE BODY IRRADIATION. Kallman, Robert F.; Silini, Giovanni (Stanford Univ., Palo Alto, Calif.). 11p. (CONF-650560-2). Gmelin, AED-CONF-65-157-12.

From 13th Annual Meeting of the Radiation Research Society, Philadelphia.

The kinetics of the recuperation of mice from sublethal whole-body x irradiation was studied. In a series of exper-

iments designed to define the shape of the recuperation curve, particularly during the first 12 to 18 hours after conditioning irradiation, experiments were done which permitted the calculation of per cent residual injury at closely spaced times during this interval. These experiments were of the kind generally known as split-dose or two-fraction experiments: a conditioning dose $D_c$ was given to a large lot of mice at time zero, and a graded series of second doses was given at several evenly spaced post-conditioning times. The 30 day mortalities of equal sized groups thus irradiated were subjected to appropriate statistical calculations, and from these data calculations were made of per cent residual injury. Three different conditioning doses were tested, namely 150, 300, and 450 R, and all experiments were done with C57BL mature male mice. It was found that in each case the recuperation curve, i.e., the curve of per cent residual injury, showed characteristic fluctuations, with a minimum in the curve (a period of marked second-dose refractoriness) falling at 4 to 9 hours and a maximum at 8 to 10 hours. The times at which these minima and maxima occurred were apparently independent of the size of the conditioning dose. Additional data points were usually obtained in the experiments of this series at later times, usually at 6 or 12 hour intervals to a latest time of 48 hours. The data were suggestive of the continuation of the initial fluctuations as a cyclic phenomenon in the period between approximately 12 and 48 hours. (auth)

**1686** LONG-TERM ANGIOGRAPHIC AND CLINICAL EVALUATION AFTER IRRADIATION OF ONE KIDNEY IN DOGS. Ranniger, Klaus (Univ. of Chicago). 6p. (CONF-650560-4). Gmelin, AED-CONF-65-157-9.

From 13th Annual Meeting of the Radiation Research Society, Philadelphia.

Radiation nephritis did not occur in all dogs which received more than 2500 rads x radiation and were followed for at least two and one-half years. Radiation nephritis was not seen in four animals which received 1000 or 2000 rads to one kidney and which were followed for at least two and one-half years. Selective renal arteriography showed abnormal findings at least two months prior to the onset of other clinical signs of nephritis. Arteriography was a reliable indicator of yearly radiation nephritis in all cases. Bio-assay tests for the presence of pressure substances in the renal venous blood were negative in two dogs with hypertension. Histological studies bear out the arteriographic findings in respect to larger vessels. (auth)

## Radiation Effects Therapy and Countermeasures

**1687** EFFECTS OF 1-β-D-ARABINOFURANOSYLCYTOSINE HYDROCHLORIDE ON REGENERATING BONE MARROW. Papac, R. J.; Calabresi, P.; Hollingsworth, J. W.; Welch, A. D. (Yale Univ., New Haven). Cancer Res., 25: 1459-62(Oct. 1965).

1-β-D-Arabinofuranosylcytosine (ara-$C^3$ or cytosine arabinoside), a pyrimidine nucleoside analog, is capable of inhibiting marrow regeneration in lethally x irradiated mice in which marrow recolonization by donor marrow cells from normal mice occurs. When administered on the 4th day after irradiation and marrow injection, the drug induces significant marrow suppression. Depending upon the relative amounts of the compounds and the intervals of time between their administration, reversal of the effect of cytosine arabinoside on the bone marrow can be accomplished by deoxycytidine. When the metabolic block induced by cytosine arabinoside is circumvented by deoxycytidine, with release of the biosynthesis of DNA, the administration of certain cytotoxic agents yields enhanced suppression of the regenerating bone marrow of mice. (auth)

**1688** THE ACTION OF PROTECTIVE AGENTS FOLLOWING IRRADIATION WITH SUBLETHAL DOSES. Yarmonenko, S. P.; Konopolyannikov, A. G.; Suvorov, N. N.; Fedoseev, V. M. Dokl. Akad. Nauk, SSSR, 162: 205-7(May 1, 1965). (In Russian).

Results are reported from experiments that seem to refute the view that radioprotective agents have little or no value when low doses of radiation are used if one accepts as a criterion of protection the agents' effect on loss of bone-marrow cells rather than on deaths of experimental animals. Their experiments involved 1900 white rats exposed to whole-body x irradiation with 270, 400, and 700 R. The animals were injected intraperitoneally with the radioprotective agents s, β-aminoethylisothiuronium dihydrobromide and 5-methoxytryptamine hydrochloride 10 to 15 minutes before irradiation. At the time of maximum aplasia of bone marrow (3 days after irradiation), the protected animals, regardless of the irradiation dose used, had 2½ to 3 million more cells (10 to 12% of the total cell population) than did the control. Thus, the value of the factor of decrease in dose as a criterion of the protective agent's effectiveness remains constant, regardless of the dose. The data also confirm the view that the value of chemical protection lies in decreasing the dose and thus preserving a mass of hemopoietic cells that serve as a source of subsequent regeneration. This was also shown by experiments in which the radioprotective agents were highly effective in cases of repeated irradiation with sublethal doses. (ATD)

**1689** RESTRICTION OF OBSTETRIC RADIOLOGY. Vickers, Anthony A. (Worchester Royal Infirmary, Eng.). Lancet, 1: 1318-22(June 19, 1965).

Hazards to the fetus and maternal gonads (primarily leukemia and genetic damage, respectively) as a result of diagnostic radiologic examination of obstetric patients are considered and means to lessen them are proposed. For various studies of the incidence of leukemia in relation to previous exposure to x rays, the results are inclusive. Genetic damage, though more remote in time, is a much more insidious and potentially grave risk to the population as a whole. The effect of the Medical Research Council (MRC) and Adrian Committee reports, over the seven-yr period 1956-62, was studied from the records of the 1757 patients referred for radiological investigations of pregnancy from hospital maternity units. The number of x-ray examinations decreased until clinic attendances rose sufficiently to increase the x-ray figures again. The proportion of x-rayed patients fell distinctly initially after the MRC report (1956), but rose slightly after the Adrian Committee's report (1960). Improvements in the methods used are enumerated. It is concluded that the radiologist should not try to find answers that the obstetrician can find out without irradiation. (TCO)

**1690** REDUCTION OF SENSITIVITY TO $^{60}$Co GAMMA RAYS IN PHASEOLUS MUNGO L. THROUGH PRE- OR POST-IRRADIATION HEAT TREATMENT OF THE SEED. Santos, Ibarra S. Sci. Rev., 5: 25-31(Apr. 1964).

Seeds of an isogenic line of mungo (Phaseolus mungo L.), containing 8% moisture and with 100% viability were treated by irradiation alone, heat treatment followed by irradiation, and irradiation followed by heat treatment. The seeds were exposed to a $^{60}$Co source for 25 hr and at three different distances at which they received 60, 100, and 160 kr, respectively. Heat treatment consisted of exposure to a temperature of 80°C for 7½ hr. The results showed that with heat treatment, especially post-irradiation, a much higher dose of gamma rays can be applied to seeds. The significance of this finding in the mungo radiation breeding program is discussed. (P.C.H.)

**1691** REMOVAL OF RADIOISOTOPES FROM MAN. Spencer, Herta; Rosoff, Betty (Veterans Administration, Hines, Ill.). Trans. Amer. Nucl. Soc., 8: 333(Nov. 1965).

**1692** STUDIES ON THE CHLOROPHYLL CHELATE COMPOUNDS AS CHEMICAL PROTECTORS AGAINST RADIATION INJURY. Kasugai, Noboru (Nanpo and Co., Ltd., Tokyo). Yakugaku Zasshi, 84: 1152-7(Dec. 1964). (In Japanese).

A large number of chelated complexes of chlorophyll

with metal ions and biologically important acids and bases were prepared and tested for toxicity and radioprotective activity in CF1 mice. Among the complexes tested were the sodium or potassium salts of Mg, Co, Mn, V, Ag, Zn, and Au chlorophyllin coordinated with methionine, adenine, folic acid, or ammine ion. The complexes were prepared with phytochlorin derived from chlorophyll. Prior to studies to examine them as chemical protectors against radiation injury, animal experiments of the chlorophyll metal chelate compounds showed very low toxicity. The protective effect of the compounds against radiation injury was determined by comparative study on survival between treated and untreated mice following lethal whole-body $^{60}Co$ $\gamma$ irradiation. Survival rate of the treated groups were found to be superior to the untreated groups, and the hexacoordinated chlorophyllin metal (Co, Mg, Mn, and V) chelate compounds were found to be most effective. The compounds were most effective when given before irradiation but were still slightly active when injected postirradiation. Thus, one of the most protective compounds (Na chlorophyll-Co chelate) gave a 30-day survival rate of 70% in mice exposed to 720 R doses of $\gamma$ rays when injected 5 min before irradiation, compared with 15% 30-day survivors when injected 5 min after irradiation. Of the control mice, 100% mortality was reached by the 20th postirradiation day. (BBB)

**1693** INFLUENCE OF CERTAIN CHEMICALS ON THE SENSITIVITY OF RAT EMBRYOS TO X-IRRADIATION [Thesis]. Loawhakasetr, Pathom. Corvallis, Oreg., Oregon State Univ., 1965. 113p.

The effect of 2-aminoethyl-2-thiopseudourea·Br·HBr (AET), 2-mercaptoethylamine·HCl (MEA) and trisodium calcium chelate of diethylenetriaminepentaacetic acid ($CaNa_3$DTPA) on the radiosensitivity of rat fetus was investigated. A total of 1256 fetuses were critically examined. Exposure of rats to 200 R whole-body x-irradiation at 9.5 days of gestation resulted in a high incidence of uterine resorption (50%) and eye defects in fetuses (90%) when examined at 19th day of gestation, and only about 27% of the fetuses survived to term. When AET (50 mg per rat) or MEA (25 mg per rat) was given to rats through I.P. injection before x irradiation, the incidence of uterine resorption and fetal abnormalities was significantly reduced. Irradiated pregnant rats receiving AET or MEA prior to irradiation were able to give birth to young of normal litter size and birth weight. These offspring, though some still carried eye defects, survived beyond puberty and showed apparent normal growth and reproduction. Greater protection to fetuses against x irradiation was obtained when AET and MEA were given simultaneously to pregnant rats shortly before irradiation than when either of the two chemicals was administered separately. The study also revealed that the chelating agent $CaNa_3$DTPA had a detrimental effect on fetal development. It induced uterine resorption and eye defects in fetuses when administered to rats at 9.5 days of gestation. At a low dose level (62.5 mg per rat) it protected the fetus slightly against the irradiation effect. A synergistic action in damaging of the rat fetuses was observed when large doses of $CaNa_3$DTPA were administered to pregnant rats prior to 200 R whole-body x irradiation. (Dissertation Abstr.)

## Radiation Hazards and Protection

**See also HEALTH AND SAFETY**

**1694** SOME BIOLOGICAL ASPECTS OF THE USE OF SPHEROIDIZED FUEL IN SPACE NUCLEAR POWER SYSTEMS. Langham, Wright H. (Los Alamos Scientific Lab., N. Mex.). Trans. Amer. Nucl. Soc., 8: 331-2(Nov. 1965).

**1695** ACCUMULATION OF RADIOACTIVE FISSION PRODUCTS IN HAIR. Strain, William H. (Univ. of Rochester, N. Y.); Danahy, Daniel T.; O'Reilly, Richard J.; Thomas, Martin R.; Wilson, Robert M.; Pories, Walter J. Trans. Amer. Nucl. Soc., 8: 332-3(Nov. 1965).

## Radiotherapy and Radiodiagnosis

**1696** (CONF-641126-1) UN NUEVO COLOIDE MARCADO CON $^{99m}$Tc. INFORME NO. 152. (Preparation of a $^{99m}$Tc Labelled Colloid. Note No. 152). Garzon, O. L.; Palcos, M. C.; Radicella, R. (Comision Nacional de Energia Atomica, Buenos Aires (Argentina)). 1965. 7p. Dep. mn.

From 1st Symposium on Nuclear Medicine, Mendoza, Argentina.

The preparation of $^{99m}$Tc labelled colloidal antimony sulphide is described. The 0.1 hydrochloric acid solution containing $^{99m}$Tc is added to an equal volume of $H_2S$ free, PVP stabilized, preformed antimony sulphide colloidal solution. After neutralization, the colloid is sterilized by heating at 120°C for 30 minutes. The colloidal particles retain more than 98% of the $^{99m}$Tc. Clear liver scannings are obtained by intravenous administration of the labelled colloid. (auth)

**1697** THE MEASUREMENT OF PATIENT DOSE. Ardran, G. M.; Crooks, H. E. (Oxford Univ.). Brit. J. Radiol., 38: 766-70(Oct. 1965).

The performances of two commercially available integrating exposure meters (the Diamentor and the Philips Diagnostic Monitor) were compared under practical conditions in diagnostic radiology. The advantages and disadvantages of measuring exposure in R × cm$^2$ or mW-sec are discussed together with the difficulties of converting their readings into the energy absorbed by the patient in g-rads. The conclusion is drawn that both types of instrument have considerable value in estimating patient exposure or dose but require calibration and a knowledge of the circumstances under which they are used before their potential accuracy can be utilized. (auth)

**1698** IMAGE CONTRAST AND RADIATION PROTECTION: A FIGURE OF MERIT. PART I. NARROW BEAMS. Spiegler, G.; Keane, B. E. (Royal Sussex County Hospital, Brighton, Eng.). Brit. J. Radiol., 38: 771-5(Oct. 1965).

Factors that may affect the radiation dose received by the patient during diagnostic radiography are reviewed. These include the x-ray tube, filtration, cones and grids, kilovoltage, filters, beam cross section, body thickness, and depth. Alterations in these factors may increase protection but also affect image quality. The beneficial and adverse effects of hardening the beam, a change of filtration, and a change of tube tension are considered. (C.H.)

**1699** EXIT DOSES FOR LUNG FIELDS MEASURED BY LITHIUM FLUORIDE THERMOLUMINESCENCE. Svarcer, Vesna; Fowler, J. F.; Deeley, T. J. (Hammersmith Hospital, London). Brit. J. Radiol., 38: 785-90 (Oct. 1965).

Lithium fluoride thermoluminescence dosimetry powder has been used in gelatine capsules of 10 mm length and 4 mm diameter to measure the exit doses in patients having treatment to the thorax by means of 8 MV x rays. It was found that exit doses for fields passing through the lungs were up to 60 per cent higher than the doses calculated on the assumption of homogeneous unit density tissue; the dose received at the tumor would thus be increased by about half this value. Such increases can be satisfactorily explained because the beam has passed through lung tissue containing air instead of unit density tissue. Where growth of fluid or fibrosis was present in the lung, the excess dose was less marked, and the exit dose became nearer to that expected for unit density tissue. In most cases it was possible to explain the observed exit doses, but the magnitude of the variation could not have been assessed from radiographs and clinical examination. It is therefore not possible to apply general correction factors, without exit dose measurement (or quantitative tomography) on each patient. Lithium fluoride powder makes it possible to make a large number of measurements on patients during routine treatment. Such measurements may prove useful for more precise estimates of the dose given in radiotherapeutic procedures, especially where results of lung treatments are being analyzed with respect to dose. (auth)

**1700** BONE MARROW TRANSPLANTATION IN ACUTE LEUKEMIA. Thomas, E. D.; Epstein, R. B. (Univ. of Washington, Seattle). Cancer Res., 25: 1521-4(Oct. 1965).

Studies of whole-body irradiation and marrow transplantation as related to the treatment of acute leukemia in man and mice are reviewed. A discussion is given of current problems of procurement and preservation of marrow, of difficulties in securing allogenic marrow grafts, and of the potential application of cross-circulation to problems in acute leukemia. (auth)

**1701** ADOPTIVE IMMUNOTHERAPY OF ACUTE LEUKEMIA: EXPERIMENTAL AND CLINICAL RESULTS. Mathe, G.; Amiel, J. L.; Schwarzenberg, L.; Cattan, A.; Schneider, M. (Hopital Paul-Brousse, Villejuif, France. Institut Gustave Roussy, Villejuif, France). Cancer Res., 25: 1525-31(Oct. 1965).

The theoretical principle of treatment of acute leukemia by adoptive immunotherapy is to permit allogenic, immunologically competent cells to act against the host's leukemic cells and the basic leukemogenic factors present in the host. Such an effect may be obtained by a graft of allogenic hematopoietic cells following total-body x irradiation. If the patient is able to survive the secondary syndrome that is induced by the homograft, an eradication of the leukemia may well be obtained. It has been demonstrated that this mode of therapy is effective in the treatment of spontaneous, transplanted, and viral leukemias in mice. Clinical trials of adoptive immunotherapy of acute leukemia in man are described. The results show that it is possible to obtain a sustained graft of hematopoietic cells and that such a graft has a distinct value as an antileukemic agent. (auth)

**1702** REPORT ON THE SYMPTOMATOLOGY OF RADIATION-CAUSED GROWTH DISTURBANCES TO THE VERTEBRAL COLUMN. Kolar, J.; Stasek, Vl.; Palecek, L.; Lokajicek, M. (Charles Univ., Prague). Fortschr. Geb. Roentgenstr. Nuklearmed., 103: 319-26(1965). (In German).

The radiological changes in the vertebral column due to irradiation during childhood are described on the basis of observations on twenty-eight patients. These included abnormal bone structure, changes in the direction of growth and in the shape of the vertebral bodies, consisting of irregular surfaces, short processes etc.; wedge vertebrae; scoliosis, and neoplasms. The sequence and dynamics of these changes in relation to the dose of radiation, its frequency, and the age of the child are discussed. The development of a scoliosis depends not only directly on the changes in the spine, but also on disturbed growth in the pelvis. (tr-auth)

**1703** ON THE X-RAY DIAGNOSIS RADIATION BURDENS TO YOUTHS AND ADULTS. Pape, R. (Roentgeninstitut des Wilhelminenspitals, Vienna); Zakovsky, J. Fortschr. Geb. Roentgenstr. Nuklearmed., 103: 326-43 (1965). (In German).

The determination of incident and gonad doses occurring on 2000 hospital patients and 1000 out-patients during diagnostic radiography was established, and the results were compared with the examinations on 30,000 young persons of the age 14 to 18 years and 1.4 million persons insured with two health insurance companies. In the abdominal investigations, which involve a higher radiation burden, juveniles participate only with 6 pc, adults however with 45 to 77 pc of the cases sent for an x ray examination. The significant reduction of dose by using 6 mm Al for screening is discussed at 90 to 100 kv with less than 1 mA. The importance of the distance of the primary beam edge from the gonads is emphasized. The calculated gonad dose agrees very well with measurements on 982 patients in routine examinations. With the examinations extremities, head, and chest the gonads are usually exposed to much less than $^1/_{1000}$th of the incident dose, with male patients to approximately 0.2 to 0.3 mR per one chest radiograph and screening, with women to about 1 mR. With investigations on the upper abdomen the gonads are on an average exposed to 3 to 30 mR. With investigations on the lower abdomen shielding of the male gonads against direct radiation is nearly always possible. On men the gonad dose is then of the order of 20 to 100 mR, on women about ten times as much. On children and adolescents the values are smaller. The doses established for the blood-forming organs are too small to cause damage. For Austria (for 1963) an annual gonad dose per person of 8 mR to 40 mR was worked out depending on the screening technique and tube filtration used. (tr-auth)

**1704** PATIENT DOSIMETRY IN X-RAY DIAGNOSIS. INCIDENT RADIATION ENERGY, SKIN SURFACE DOSE, AND INTEGRAL DOSE. Schinz, H. R.; Wideroee, R. Fortschr. Geb. Roentgenstr. Nuklearmed., 103: 344-8 (1965). (In German).

The significance and purpose of x-ray diagnostic dosimetry, the determination of the skin-area dose and of the integral dose and the ionization-area value, or incident area-dose are discussed. If the quality of the radiation is known, the latter measuring value can serve to work out the incident radiation energy and the integral dose. Comparative large scale investigations are unfortunately often undertaken without due reference to the qualities of radiation used. For the sake of conceptional clarity it would be of an advantage to make use of the value area-skin dose, which in the diagnostic range is numerically equal to the value $R \cdot cm^2$ used up to now. Using the ancillary concepts of effective length, the integral dose may readily be worked out from the skin-area dose. (tr-auth)

**1705** AN ECONOMIC METHOD OF OBTAINING PHOTOSCAN. Sharma, S. M.; Ramanathan, P. (Atomic Energy Establishment, Trombay, India; Tata Memorial Hospital, Bombay). Int. J. Appl. Radiat. Isotop., 16: 668 (Nov. 1965).

Photoscanning technique gives a better contrast and resolution than conventional dot scanners. Experiments were undertaken to develop a cheaper film for photoscans. Hard extra white glossy printing papers gave the best results. The ideal speed and light source iris setting (f) were found to be 24 cm/min and 4, respectively. (F.J.H.)

**1706** CHRONIC SYNOVIAL EFFUSIONS TREATED WITH INTRA-ARTICULAR RADIOACTIVE GOLD. Makin, Myer; Robin, Gordon C. (Hadassah Hospital, Jerusalem). J. Am. Med. Assoc., 188: 725-8(May 24, 1964).

Technique, dosage, complications, and clinical results are described in the use of colloidal $^{198}Au$ in benign joint disease, mainly osteoarthritis. The successful use of $^{198}Au$ in the treatment of malignant peritoneal and pleural effusions prompted its trial in cases of persistent synovial effusion in which orthodox methods had failed. This trial was carried out on 25 joints in 22 patients with persistent effusions. Of the 23 knee joints injected, 20 were given a dose of 10 mC and three, 5 mC. The dose was estimated empirically on the assumption that the area of the synovium in the average adult knee joint is 200 $cm^2$. The estimated mean therapeutic dose given to the synovial surface was 5000 R. Although this was based on a presumed surface area which could not be accurately measured, an attempt was made to deliver a dose of 2000 to 7000 R to the irradiated surface. The objective was to reduce synovial hyperemia and to produce mild subsynovial fibrosis. In the two ankle joints injected, a dose of 3 mC was used. Within a week of $^{198}Au$ injection there was usually a marked increase in the amount of fluid in the joint. This reactive effusion did not require reaspiration and disappeared within a few weeks. There were no delayed complications as a result of treatment. Follow-up examinations made at frequent intervals following injection, extending to six years, showed a gradual resorption of the fluid during the month following injection. In one patient, who had received only 5 mC, there was an initial good response but five months after injection, effusion recurred and remained despite a second injection of 10 mC of $^{198}Au$. In the other two patients who received only 5 mC, relief of effusion took place but the improvement was much less marked than after the full dose of 10 mC. Thus, it was possible to reduce the overproduction of synovial fluid by $\beta$-ray surface irradiation of the synovium.

This gave a high dose of radiation on the synovial surface alone, without the high skin dosage and tissue penetration that would be necessary with an external radiation source. A colloidal suspension of $^{198}Au$, as was used, after a short time, settles on the surface as a thin film and emits $\beta$ and $\gamma$ radiation. The $\gamma$ emission, having a high penetration, almost completely escapes from the body and has little irradiating effect. The $\beta$ rays are largely absorbed within a tissue thickness of 1 to 2 mm. Most of their radiation effect therefore is directed against the synovial lining of the joint and the $\beta$ rays have very little effect on the extrasynovial tissues. The danger of radiation sequelae restricted this treatment to patients over 40 years of age. Because of the poor penetration of the $\beta$ emission, it is probable that only the synovium and the superficial layers of the joint cartilage were irradiated and the adjacent bone and soft tissue did not receive any significant radiation. It is concluded that $^{198}Au$ is a useful therapeutic agent in the treatment of persistent synovial effusion where orthodox methods have consistently failed. (BBB)

**1707** PROTON RADIOBIOLOGY. Debois, Jean M. J. Belge Radiol., 48: 351-70(1965). (In French).

The study of the radiobiology of protons was accelerated by the prospect of space navigation. The peculiarities of a proton beam absorption show certain advantages as compared with the, until now clinically applied, radiations but, on the other hand, they give rise to new problems of application. Most of the clinical applications have been made in the field of neuroradiology, namely radiological hypophysectomy and localized stereotactic destruction of cerebral tissue. A review is presented of the different radiobiological studies with discussion of their particular aspects. The study of the R.B.E. is still too fragmentary to allow definitive conclusions. Theoretically, the proton beam seems already to deserve its place in radiotherapy but great technical and financial difficulties are the major obstacle to a more widespread application. (52 references.) (tr-auth)

**1708** RADIOTHERAPY OF PITUITARY TUMOURS. Bradley, J. M. (Peter MacCallum Clinic, Melbourne). J. Coll. Radiol. Austral., 9: 36-43(Feb. 1965).

A series of 30 cases of pituitary tumors, treated by x ray therapy, is reviewed and the results of other methods of radiation treatment are discussed. Failure to control the tumors of this series appears, in the majority of cases, to be due to underdosage. It is considered that doses of 4,000 to 5,000 rads of fractionated megavoltage radiation, administered in four weeks, are required to control a sufficiently high proportion of these tumors and that this dosage range is not likely to produce much morbidity. While the risk of radiation carcinogenesis appears to be low, hypopituitarism as a delayed effect may be a more frequent complication than has been realized in the past. (auth)

**1709** THE USE OF POSITRON EMITTER IN THE DETERMINATION OF CORONARY BLOOD FLOW IN MAN. Cohen, Alberto; Zaleski, Edward J.; Luebs, Eide-Dittmar; Bing, Richard J. (Wayne State Univ., Detroit). J. Nucl. Med., 6: 651-66(Sept. 1965).

The concepts underlying a coincidence counting method for the measurement of coronary blood flow using $^{84}Rb$, a positron emitter, is described. Coronary blood flow is calculated by the logarithmic extrapolation of the myocardial clearance values of $^{84}Rb$ to zero time. At this time, the myocardial extraction ratio is unity. The accuracy of the method has been established in experiments on the isolated dog heart. All calculations are objectively performed by a digital computer. The resting coronary blood flows in individuals above and below the age of 40 and in males and females were not statistically different. In addition, there were no significant differences in the resting coronary blood flows in patients with and without coronary artery disease. The observation that sublingual administration of nitroglycerin increases the coronary blood flow in individuals without coronary artery disease while failing to increase it in patients with coronary artery disease has been used as a diagnostic test in the recognition of coronary artery disease. (auth)

**1710** AN ORGANIC PLASTIC, LOCALIZING WHOLE-BODY COUNTER. Andrews, Howard L. (Puerto Rico Nuclear Center, Mayaguez); Peterson, Dorothy C.; Murphy, Raymond E.; Myers, E. June. J. Nucl. Med., 6: 667-78 (Sept. 1965).

The energy resolution of organic plastic scintillators is quite adequate for the assay of most of the radioactive nuclides commonly used in clinical and experimental medicine. No difficulty was encountered in a period of over two years in maintaining the detecting efficiency of an 18 detector system employing 72 photomultiplier tubes. The ability of a multidetector system to localize depends primarily upon the calibration procedures and only secondarily on the detector response. Multicompartment measurements proved feasible in simple configurations and can be extended to organs and more complex nuclide distributions. (auth)

**1711** CEREBRAL BLOOD FLOW MONITORING BY EXTERNAL DETECTION OF INHALED RADIOACTIVE XENON. Johnson, Albert E.; Gollan, Frank (Veterans Administration Hospital, Coral Gables, Fla. Univ. of Miami, Coral Gables, Fla.). J. Nucl. Med., 6: 679-86 (Sept. 1965).

The accuracy of the $^{133}Xe$ disappearance rate from tissue as a measurement of blood flow was ascertained by comparing the results with electromagnetically monitored flow in the isolated perfused head of a dog. The measurement of cerebral blood flow in man by external monitoring of inhaled $^{133}Xe$ agrees with results in the literature using other inert gases and methods of administration and counting. Good correlation also exists between the carbon dioxide effect on cerebral blood flow and the disappearance rate of inhaled radioactive xenon from the cerebral cortex. Serial studies in the same subject may be of great value in recording changes in blood flow as a result of cerebrovascular disease, an experimental procedure, or a drug. Since this method can be readily repeated without trauma or hazard, it may lend itself for widespread clinical investigations. (auth)

**1712** THE DEMONSTRATION OF EXTRACRANIAL NEOPLASMS WITH $^{99m}Tc$ PERTECHNETATE. Bolliger, Theodore T.; Witcofski, Richard L.; Whitley, Joseph E.; Maynard, C. Douglas (Bowman Gray School of Medicine, Winston-Salem, N. C.). J. Nucl. Med., 6: 687-9(Sept. 1965).

Extracranial neoplasms have been visualized by scintiscanning as a result of their selective localization of $^{99m}Tc$ pertechnetate. The initial experience in 11 known neoplasms is presented. Compared with reported results with $^{197}Hg$ chlormerodrin, $^{99m}Tc$ pertechnetate had the advantages of immediate and rapid scanning; it has the limitation of activity in normal blood pools, as well as in certain abdominal organs. (auth)

**1713** CONCERNING RADIATION-INDUCED BRAIN NECROSIS (CLINICAL OBSERVATION). Kirsanova, G. I.; Doschenko, N. M. Med. Radiol., 10: No. 7, 72-5(July 1965). (In Russian).

Damage to the brain was observed at doses of 5000 to 10,000 R. The clinical picture of the brain damage is described in a 22 year old carpenter who was given a x-ray dose of about 1500 R to the head in the treatment of microspore infection. First his hair fell out, and a slow-healing sore formed in the parietal region. No hair growth on the head was noted over a period of 2½ years. The blood picture was normal. A year and 5 months after irradiation the patient noticed an uncontrolled twitching of the right foot which was followed by epileptic paroxysms of increasing severity over a period of weeks. A total of 2 years and 2 months later attacks of Jackson's epilepsy continued to plague the patient. Microscopic examination of a biopsy sample of the skin from the parietal region of the head showed atrophy of the malpighian layer with necrotic foci and neutrophilic infiltrates. Hair bulbs and sweat glands were absent. The bioelectrical activity of the muscles had

been altered. The patient was operated on 2 years and 6 months later, since the clinical data indicated the development of a glioma. Under microscopic observation the brain tissue appeared edematous with extensive necrotic foci. No cancerous growth was noted. The clinical picture is characteristic of radiation damage to the brain without the usual symptoms of radiation sickness. (TTT)

**1714** DEVELOPMENT AND DOSIMETRY OF AN EPITHERMAL NEUTRON BEAM FOR POSSIBLE USE IN NEUTRON CAPTURE THERAPY. I. EPITHERMAL NEUTRON BEAM DEVELOPMENT. Fairchild, R. G. (Brookhaven National Lab., Upton, N. Y.). Phys. Med. Biol., 10: 491-504 (1965). (BNL-8260).

The possibility exists of destroying neoplastic cells in vivo by introducing a suitable neutron-capturing isotope such as $^{10}B$ and subsequently irradiating the area with a beam of thermal neutrons (energy < 0.5 ev). An advantage can be gained by using epithermal neutrons (energy 10 kev to 0.5 ev), since they provide deeper penetration in tissue than do thermal neutrons. The Brookhaven Medical Research Reactor was used to obtain an epithermal neutron beam giving a thermal neutron flux density of $1.42 \times 10^{10}$ n/cm$^2$-sec at 3 cm depth in tissue; the beam used gave the highest number of epithermal neutrons per unit of contaminating radiations. (auth)

**1715** RADIOISOTOPE SCANNING DISPLAY. Perry, B. John; Pullan, B. Phys. Med. Biol., 10: 562-4(1965).

The importance of an apparent change in uptake over a given area of a scan and a knowledge of the clinically normal pattern of uptake is discussed. A display system that involves tape recording the scan with subsequent fast playback is presently being developed. (P.C.H.)

**1716** THE PATHOGENESIS OF LATE CONSEQUENCES OF RADIATION THERAPY. Aleksandrov, S. N. Radiobiol. Radiotherap., 6: 511-15(1965). (In German).

The pathogenesis of late consequences of x radiation action is based on the total permanent disturbances in organisms occurring as a consequence of direct irradiation. These may include the loss of a part or all elements of some kinds of cells which cannot be replaced, nonhereditary disturbances in the irradiated cells that remain permanent, and hereditary changes in somatic cells. As the biological system represents a unit, these primary changes become the cause of the development of secondary disturbances not directly connected with irradiation. An essential part of these disturbances in mammals is of compensatory character and causes a state of permanent compensated tension characterizing organisms which survives acute or chronic radiation sickness. All these primary and secondary disturbances determine changes in the reactivity of the organism, and lead to decreased protective adaptability of the irradiated biological objects which is expressed in an increased sensibility to different injuring effects and intercurrent diseases. This increases the extent of secondary disturbances in the irradiated organism and causes late changes of reactivity and a decrease of adaptability. The biological chain reaction, beginning with the permanent primary disturbances, leads to a premature depletion of adaptive potencies of the organism, i.e., to a shortening of life of the irradiated biological objects which represents an integral result of late radiation pathology. (tr-auth)

**1717** GENERATION AND PREVENTION OF SEVERE RADIATION LESIONS. Koerbler, J.; Frank, P. Radiobiol. Radiotherap., 6: 527-35(1965). (In German).

During the last few years the authors were consulted in many cases of injuries caused by the therapeutic use of x rays. This is considered as a proof that even with modern equipment severe injuries can occur. Some important facts must be remembered to avoid these accidents. The therapist should be content in many cases with a pallative effect and in some he must be aware that no therepeutic effect at all is obtainable. Every effort to enforce the favorable result leads to complications. The treatment of benign lesions by x rays should in every case be refused; the results being always poor or even problematic and the hazards great. An entrance field too small for a relatively large dose is another source of danger. The concentration of a big part of radiant energy on a narrow spot must result in damage. In postoperative treatment by x-rays it should be emphasized that surgical intervention diminishes the resistance of tissues against irradiation. It is of greatest importance to point out the fact that the general condition of the patient is largely responsible for his reaction to the assault of radiant energy. In a state of malnutrition the organism is less resistant and more inclined to injury by radiation. This is of paramount importance now when irradiation therapy is used more and more in the underdeveloped nations when the population is in a permanent state of deficient nutrition. (tr-auth)

**1718** THE CONCENTRATED SERIAL IRRADIATION METHOD FOR TREATING CARCINOMA OF THE SKIN. Dimitrov, M.; Pentschev, P. (Geschwulstforschungsinstitut, Sofia). Radiobiol. Radiotherap., 6: 563-8(1965). (In German).

The late results are reported for the use of the concentrated serial x irradiation method in 622 patients with 728 tumors of the skin. The method aims at obtaining the carcinogenic effect with higher tumor dose, but decrease of damages to the tissue by means of a rhythmically performed irradiation. In patients in stages I and II, primary recovery was obtained in 97.3% and a definite recovery was achieved in 99.8%, radiation injuries occurred in 1.6%. Patients tolerated the treatment very well. Radiation response is lower than in conventional fractionated irradiation and cosmetic effects were very good. (tr-auth)

**1719** ABOUT LATE CHANGES OF THE SKIN AFTER IRRADIATION OF HAEMANGIOMAS. Muenchow, H.; Dressler, S. (Radiologischen Klinik der Medizinischen Akademie, Dresden). Radiobiol. Radiotherap., 6: 575-83 (1965). (In German).

Data are reported on 279 infantile hemangiomas of the skin which were treated 10 to 13 years ago with radium irradiations according to Chaoul. The relations between late changes of the skin, the kind of treatment, the doses administered, and the extent of the primary findings are discussed. The time of beginning the treatment as well as the duration of regression are discussed. The authors give their opinion on spontaneous regression on the base of some observations. Only a small percentage of hemangiomas proved to be extended so that the risk of an increased radiation exposure must be taken. The majority of hemangiomas do not exceed 3 cm diameter. It is recommended to observe the proportionality of growth by measuring the size of neighboring regions of the body and to start therapy not before the beginning of a disproportional increase in size considering the tendency to spontaneous regression. The necessity to protect the irradiated regions of the skin against secondary stimuli of thermic, chemical, and mechanical kind is emphasized. (tr-auth)

**1720** ABOUT PROTRACTED X-IRRADIATIONS IN BRONCHIAL CARCINOMA. Pape, R. (Roentgeninstitut des Wilhelminenspitales, Vienna). Radiobiol. Radiotherap., 6: 585-90(1965). (In German).

Only a small number of patients with bronchial carcinoma may be x irradiated in such a way that an effective influence is possible. There remained only 65 cases out of 314 in which the success of a lowest tumor dose of 3000 R over a period of some months could be followed and checked. Not only the dose height but also the method of radiation application seem to be important in these cases. A radiation treatment will be recommended which is protracted over many months, the single irradiations not being given daily but about 3 to 4 times a week with pauses between the series not being longer than one month. Total surface doses of more than 30,000 R could be obtained with stationary fields without radiation fibroses appearing. These principles of treatment might eventually be used in megavolt and cobalt irradiation. (tr-auth)

**1721** THE DEPENDENCE OF BUILD-UP RATIO ON THE FIELD SIZE AND THE SOURCE-SURFACE DISTANCE.

Ashton, Thomas; Zamecnik, Jiri (General Infirmary, Leeds, Eng.). Radiology, 85: 956-8(Nov. 1965).

The buildup ratio for several field sizes was measured for radiation from a cobalt-60 teletherapy unit and for x rays from a 4-Mev linear accelerator. The results disclose that for constant field size on the surface, the buildup ratio increases rapidly at first and then more slowly, becoming almost constant at a distance of 300 cm from the source, in contrast to constant diaphragm conditions when the buildup ratio decreases at the larger distances. (auth)

**1722** A DEVICE TO FACILITATE THREADING OF $^{60}$Co BEADS. Legal, J.; Campbell, E. M. (Manitoba Cancer Treatment and Research Foundation, Winnipeg, Can.). Radiology, 85: 959-61(Nov. 1965).

A device is described which permits threading of cobalt-60 beads into a chain. The procedure is almost entirely mechanical and, in comparison to manual threading, results in manifold reduction in radiation exposure to the technician. (auth)

**1723** $^{60}$Co ROTATIONAL THERAPY CALCULATOR. Scott, Walter P. Radiology, 85: 965-7(Nov. 1965).

A design for a cobalt-60 rotational therapy calculator is presented. This may be used either independently or in combination with other calculators. Although it is designed primarily for telecobalt-60 rotational therapy, it may just as well be employed for fixed fields with the ratio scale representing percentage depth dose, wedge factor, et al. The mechanics of proceeding from given tumor/air ratio and roentgen air dose to roentgen tumor dose, required time, speed of rotation, and conversion to rads are outlined. (auth)

**1724** THE RELATIVE TOXICITY OF ANGIOGRAPHIC CONTRAST MEDIA. Foster, J. H.; Killen, D. A.; Sessions, R. T.; Rhea, G. W.; Winfrey III, E. W.; Collins, H. A. (Vanderbilt Univ., Nashville). Vascular Diseases, 1: 8-20 (Jan. 1964).

Toxicity of the following contrast agents was studied in dogs: Angio-Conray, sodium iodide, Hypaque, Urokon, Miokon, Neo-Iopax, Diodrast, Thorotrast ($ThO_2$), and Ditriokon. The results of a 5-sec injection of 15 ml of the various contrast media into the aorta at the renal level in 125 dogs are listed. The contrast media tested represent a cross-section of the media which have been used clinically in the past or are presently being utilized. Every animal receiving Urokon was permanently paraplegic, as were most of the animals in the Neo-Iopax group. The spinal cord injury in the paraplegic animals was found on histologic study to be massive destruction of the gray matter. A high incidence of paresis was encountered in the Miokon and Diodrast groups. Only an occasional instance of paresis was found in the Hypaque and Ditriokon groups and these animals ususally recovered completely. With Thorotrast and Angio-Conray there were no instances of paresis or paraplegia; thus with these two media there was no evidence of neurologic injury. Renal injury was also assessed. Renal tubular necrosis was encountered in all of the Urokon-treated animals and in 2 of 14 Ditriokon animals. When varied doses (2 to 30 ml) of Urokon, Hypaque, and Thorotrast were injected into a pair of lumbar arteries, as little as 2.0 ml of Urokon produced paraplegia, whereas as much as 30 ml of Hypaque or Thorotrast failed to produce paraplegia in a single instance. Chemical and physical properties of a number of contrast media are listed. The abdominal aortic injection test and the intravenous injection test both indicated that Angio-Conray is the least toxic concentrated organic iodide medium available, but repeat injection studies and selective renal artery injection studies indicated that Angio-Conray is nephrotoxic. Angiographic contrast media are neurotoxic and nephrotoxic. In sufficient concentrations they will cause injury to any organ system in the body. These facts must be kept in mind by anyone doing contrast angiography. The search for a safer and more satisfactory medium must continue. (BBB)

**1725** THE GENERAL REACTION AND RADIATION INJURIES IN RADIOTHERAPY OF PATIENTS WITH CARCINOMA OF THE CERVIX UTERI. Strashinin, A. S. (Central Research Roentgeno-Radiological Inst., Ministry of Public Health, USSR). Vop. Onkol., 11: No. 9, 3-7 (1965). (In Russian).

Data are presented concerning the general reaction and local radiation injuries observed in the course of radiotherapy of 306 patients with carcinoma of the cervix uteri. The general reaction was observed in 23% of patients, leucopenia in 52.6%, dermal radiation injuries in 50%, and local intestinal and bladder injuries in 4% of cases. Different changes of the gastrointestinal tract were revealed in 35 out of 47 patients subjected to x-ray exploration five and more years after radiotherapy. Dystonia and dyskinesia were the most frequently observed changes of different parts of the small and large intestine. It is concluded that all the patients are liable to dispensary control after radiotherapy for cervix uteri cancer. This control is desirable not only in connection with a necessity to follow up the results of radiotherapy but also for investigation and treatment of the gastrointestinal tract disorders. (ATD)

# CHEMISTRY

## General

*Refer also to abstracts 1976 and 2520.*

**1726** (EUR–2508.e) BIBLIOGRAPHY CONCERNING TRANSPLUTONIUM ELEMENTS. Demine, O. (European Atomic Energy Community). Sept. 1965. 254p. Dep. mn.

References (1171) on transplutonium elements, isotopes, and compounds are given to U. S. and foreign journals, books, and reports published from 1945 to May 1965. References are given for properties, purification, preparation, separation and recovery, natural occurrence, production, and uses. Separate author, subject, and corporate author indexes are included. (P.C.H.

**1727** (NASA-SP–5032) HANDLING HAZARDOUS MATERIALS. Cloyd, D. R. (Williams (Clyde) and Co., Columbus, Ohio); Murphy, W. J. (Temple Univ., Philadelphia, Pa. Research Inst.). Sept. 1965. 95p. GPO $0.45.

Data are presented on some highly reactive materials that have been studied in the search for fuels and oxidizers for space work, including liquid hydrogen, pentaborane, fluorine, chlorine trifluoride, ozone, nitrogen tetroxide, and hydrazine and its derivatives. Both the hazards that have restricted the use of these materials and the procedures by which they have been handled and stored safely are described. References are given to work done by NASA and other investigators. (C.H.)

## Analytical Procedures

### See also Separation Processes and Procedures

*Refer also to abstracts 1586, 2055, 2056, 2099, 2367, and 2444.*

**1728** (AD–618552) THE ENRICHMENT AND DETERMINATION OF TRITIUM IN WATER [Thesis]. Burns, Ralph William Jr. (Ohio State Univ., Columbus). 1965. 85p. CFSTI $3.00 cy, $0.75 mn.

Various methods that have been used for the enrichment of tritium are reviewed and developments in liquid scintillation spectrometry are presented. In addition, other methods that are used for the determination of tritium are reviewed and compared with liquid scintillation spectrometry. In an attempt to find a more sensitive and a more convenient method for the determination of tritium in large volumes of water, the preferential adsorption of tritiated water by various materials was investigated. (auth)

**1729** (AD–619244) DETERMINATION OF ZIRCONIUM IN ZIRCONIUM METAL AND ZIRCONIUM POWDER. Test Report. Norwitz, George (Frankford Arsenal, Philadelphia, Pa.). July 1965. 17p. CFSTI $1.00 cy, $0.50 mn.

An accurate method is proposed for the determination of zirconium in zirconium metal and zirconium powder. The sample is dissolved in a mixture of hydrofluoric, nitric, perchloric, and sulfuric acids, the solution is evaporated to dryness, salts are dissolved in dilute hydrochloric acid, mandelic acid is added, the solution is heated at 80°C for 40 minutes, zirconium mandelate is filtered off, the residual zirconium in the filtrate is recovered by heating at 80°C overnight, and the combined precipitates are ignited over a blast burner to zirconium dioxide. An investigation was made of the factors involved in the dissolution of the sample, precipitation with mandelic acid, ignition of the precipitate, and size of the sample. The effect of hafnium and possible interferences was considered. (auth)

**1730** (BNL–9601) THE $^{99m}$Tc GENERATOR. Richards, P. (Brookhaven National Lab., Upton, N. Y.). Oct. 14, 1965. Contract AT(30-2)-Gen-16. 29p. Dep. mn; CFSTI $2.00 cy, $0.50 mn.

A combination of useful nuclear properties of 6-hour $^{99m}$Tc of interest in nuclear medicine led to the development of a simple, rugged, and compact generator which makes the short-lived isotope available for use at locations far removed from sources of production. Parent $^{99}$Mo is produced as a separated carrier-free fission product or by neutron bombardment of molybdenum. Each method has advantages and disadvantages. The separated fission product, because it yields higher product concentrations, is the most widely used material in the nuclide generator. The daughter $^{99m}$Tc is milked by elution with physiological saline solution. The process separates $^{99m}$Tc from the parent $^{99}$Mo in a form requiring little further processing for clinical use. The $^{99}$Mo remaining in the generator continues to decay forming fresh $^{99m}$Tc of which the activity reaches a maximum every 23 hours, permitting several milkings per day. (auth)

**1731** (BNL–9614) REFINEMENT IN METHODS OF NEUTRON ACTIVATION ANALYSIS OF ANCIENT GLASS OBJECTS THROUGH THE USE OF LITHIUM DRIFTED GERMANIUM DIODE COUNTERS. Sayre, Edward V. (Brookhaven National Lab., Upton, N. Y.). [1965]. Contract AT(30-2)-Gen-16. 28p. (CONF-650640-2). Dep. mn; CFSTI $2.00 cy, $0.50 mn.

From 7th International Glass Congress, Brussels.

With new lithium drifted germanium diode solid state detectors, which record photopeaks with nearly ten times the resolution of large crystal scintillation detectors, it was possible to determine nondestructively the concentrations of some rare earth oxides in ancient glasses. Of these the concentration of europium oxide, although below spectrographically detectable limits, showed a pronounced and significant reverse correlation with the concentrations of magnesium and potassium oxides. It has been suggested that the alkali used in the preparation of ancient glasses which are characterized by low concentrations of magnesium or potassium oxides might have been natron, the naturally deposited sodium carbonate from the lakes of the Wadi Natroun in Egypt. If natron contained a sufficiently high concentration of europium oxide its use in these glasses would be indicated. However specimens of both ancient and modern natron were found not to contain the relatively high europium concentrations which characterize the low magnesium and potassium ancient glasses. (P.C.H.)

**1732** (CEA-R–2850) TRAITEMENT PAR ORDINATEUR DES SPECTRES $\gamma$. APPLICATION AU DOSAGE DE MELANGES DE RADIOELEMENTS NATURELS OU ARTIFICIELS. (Computer Processing of $\gamma$ Spectra. Application to the Determination of Mixed Natural or Artificial Radioelements). Coulomb, Rene; Goldsztein, Marcel; Schiltz, Jean-Claude (Commissariat a l'Energie Atomique, Fontenay-aux-Roses (France). Centre d'Etudes Nucleaires). Aug. 1965. 66p. Dep. mn.

A program, written in Fortran II for IBM 7094 II, permitting resolution by means of least squares of a mixture of natural or artificial radioelements, is described. The spectra are processed in measurement groups, making up a homogeneous study, which comprise standards and samples. This highly versatile program may either ensure the processing of a great number of daily analyses, or be used pending development of radiochemical methods. The numerical or graphical controls, error computations, and the printing of results in clear and legible form were multiplied. In spite of this, the calculation times are exceedingly short. Several independent studies which include about sixty spectra may be processed in less than five minutes. (auth)

**1733** (DP–979) PROCESS SCALE SEPARATION OF HYDROGEN ISOTOPES BY GAS CHROMATOGRAPHY.

West, David L. (Du Pont de Nemours (E. I,) and Co., Aiken, S. C. Savannah River Lab.). Oct. 1965. Contract AT(07-2)-1. 24p. Dep. mn; CFSTI $1.00 cy, $0.50 mn.

The technical feasibility of a gas chromatographic process for separating hydrogen isotopes was demonstrated. In this process, batches of hydrogen isotopes are swept by helium through ferric-oxide-treated alumina at 77°K. The six molecular species of hydrogen which are resolved by the alumina are stripped from the helium by refrigerated charcoal, and the helium is recirculated. Capacities in the range of hundreds of liters (at STP) per day are feasible. (auth)

**1734** (EG-Report-36) ON LINE GAS ANALYSIS. Hignett, K. C. (United Kingdom Atomic Energy Authority, Risley (England). Engineering Group). May 1965. 47p. Dep.; BIS $2.40; HMSO 12s. 6d.

The method of Continuous Gas Analysis as applied to chemical processing and nuclear reactor systems is reported. The case for the on line method is discussed and is followed by considerations of various principles on which selection of the adequate system may be based. Some sampling techniques and their associated problems are examined. Finally the operating principles and performance of the more common analysis systems are explained. (auth)

**1735** (EUR-2408.e) IDENTIFICATION CHART FOR GAMMA EMITTING RADIONUCLIDES FORMED BY (n,γ) REACTIONS. Girardi, F.; Guzzi, G.; Pauly, J. (European Atomic Energy Community, Ispra (Italy). Joint Nuclear Research Center). 1965. 14p. Dep. mn.

A chart for the identification of unknown gamma emitting radionuclides was prepared. It gives the energy and the intensity of the main gamma peaks of those radioisotopes formed by (n,γ) reaction which are of interest in activation analysis. The nuclides considered were represented in the order of half-life and in the alphabetic order of elements. The energy scale was chosen in such a way as to show the superimposition of gamma rays of slightly different energy in the same way as it appears on the oscilloscope of the multichannel analyzers. An effort was made to reduce the size of the chart to make it easy to handle and to read. (auth)

**1736** (GA-3491) APPLICATIONS OF NEUTRON-ACTIVATION ANALYSIS IN SCIENTIFIC CRIME DETECTION. Quarterly Report for the Period Ending July 31, 1962. Guinn, V. P. (General Atomic, San Diego, Calif. John Jay Hopkins Lab. for Pure and Applied Science). Sept. 18, 1962. Contract AT(04-3)-167. 36p. Dep. mn; CFSTI $2.00 cy, $0.50 mn.

The use of neutron activation for analysis of gunpowder residue on hands is reported. Also initial results on the examination of commercial-plastic samples, and soils, greases, and inks are discussed. (P.C.H.)

**1737** (GA-3664) APPLICATIONS OF NEUTRON-ACTIVATION ANALYSIS IN SCIENTIFIC CRIME DETECTION. Quarterly Report for the Period Ending October 31, 1962. Buchanan, J. D.; Ruch, R. R. (General Atomic, San Diego, Calif. John Jay Hopkins Lab. for Pure and Applied Science). Nov. 15, 1962. Contract AT(04-3)-167. 27p. Dep. mn; CFSTI $2.00 cy, $0.50 mn.

The use of activation analysis in crime detection for the determination of elements in gunpowder residues on hands, commercial plastics, greases, automobile-tire rubber, fingernails, and determination of arsenic in hair in suspected arsenic poisoning is discussed. (P.C.H.)

**1738** (GA-4041) APPLICATIONS OF NEUTRON-ACTIVATION ANALYSIS IN SCIENTIFIC CRIME DETECTION. Quarterly Report for the Period Ending January 31, 1963. Guinn, V. P.; Ruch, R. R.; Bellanca, Sandra C. (General Atomic, San Diego, Calif. John Jay Hopkins Lab. for Pure and Applied Science). Feb. 28, 1963. Contract AT(04-3)-167. 19p. Dep. mn; CFSTI $1.00 cy, $0.50 mn.

The use of activation analysis for the identification of gunshot residues and the characterization and identification of materials that are introduced as evidence in criminal cases. Special attention was given to the characterization of various materials of forensic interest (greases, soils, paints, glass, wood, paper) relative to the attention devoted to the gunshot residue problem. In addition, law-enforcement problems of interest to the Food and Drug Administration (Hg in wheat, Br in foods) were also investigated. (P.C.H.)

**1739** (GA-4297) APPLICATIONS OF NEUTRON-ACTIVATION ANALYSIS IN SCIENTIFIC CRIME DETECTION. Quarterly Report for the Period Ending April 30, 1963. Guinn, V. P.; Madigan, Sandra C.; Ruch, R. R. (General Atomic, San Diego, Calif. John Jay Hopkins Lab. for Pure and Applied Science). May 31, 1963. Contract AT(04-3)-167. 22p. Dep. mn; CFSTI $1.00 cy, $0.50 mn.

The use of activation analysis in criminalistics and law enforcement included studies of gunpowder residues, sediment pollution of rivers, oil pollution of harbors, soils, drugs, tobacco, hair, and mercury contamination in wheat. (P.C.H.)

**1740** (GA-4576) APPLICATIONS OF NEUTRON-ACTIVATION ANALYSIS IN SCIENTIFIC CRIME DETECTION. Quarterly Report for the Period Ending July 31, 1963. Ruch, R. R.; Madigan, Sandra B.; Guinn, V. P. (General Atomic, San Diego, Calif. John Jay Hopkins Lab. for Pure and Applied Science). Aug. 30, 1963. Contract AT(04-3)-167. 24p. Dep. mn; CFSTI $1.00 cy, $0.50 mn.

The use of activation analysis for gunpowder residue analysis, paint analysis, milo grain samples, oils, drugs, and hair in crime detection is reported. (P.C.H.)

**1741** (IA-1031) SOLVENT EXTRACTION. Marcus, Y. (Israel Atomic Energy Commission, Yavne. Soreq Nuclear Research Center). June 1965. 13p. Dep. mn.

Development in solvent extraction, which includes the adoption of the extraction chromatography technique, the extraction of complex anions by ion-pair formation, and the use of new systems (e.g. liquid metals, molten salts, two non-aqueous solvents), is discussed. (P.C.H.)

**1742** (INR-636/XIII/J) USUWANIE IZOTOPOW PROMIENIOTWORCZYCH Z ROZTWOROW WODNYCH PRZY UZYCIU ZELU KRZEMOWEGO. (Removal of Radioisotopes from the Water Solutions by the Use of Silica Gel). Horski, Jozef (Institute of Nuclear Research, Warsaw (Poland)). May 1965. 83p. Dep.

Studies were made on the use of silica gel for the removal of radioisotopes from aqueous solutions. The following radioisotopes separately or all together in mixture were used: $^{90}Sr$, $^{95}Zr$, $^{106}Ru$, $^{137}Cs$, $^{144}Ce$. In some experiments $^{131}I$ in the presence of stabile isotopes was also used. In some cases nonisotopic electrolytes or capillary active agents were added. HCl, $CO_2$, $H_3PO_4$, $Na_2HPO_4$, or $FeCl_3$ were used for precipitation of the silica gel. Three ways for decontamination were proved: the removal of radioisotopes in static or dynamic condition with use of the silica gel previously precipitated and dried, and the third one the precipitation of the silica gel in the decontaminated solutions. (auth)

**1743** (JUL-216-RW) PHYSIKALISCH-CHEMISCHE ANALYSENMETHODEN ZUR UNTERSUCHUNG VON REAKTORMATERIALIEN UND KERNBRENNSTOFFEN. (Physico-Chemical Analysis Methods for Study of Reactor Materials and Nuclear Fuels). Nickel, H. (Kernforschungsanlage, Juelich (West Germany). Institut fuer Reaktorwerkstoffe). Jan. 1965. 142p. Dep. mn.

Several methods were tested with respect to their applicability to the studies of solids used in reactor technology. Results showed that activation analysis is at least equal to other commonly used methods. The hot extraction of oxygen in vacuum gave satisfactory results. The physical-chemical processes in boron and iron containing graphite electrodes in arc excitation and their influence on the spectrochemical results were determined in the study of the quantative analysis. The x-ray-diffraction method was found to be well suited to the quantitative analysis of U–Th mixed oxides. 211 references are cited. (P.C.H.)

**1744** (NAS-NS-3030(Rev.)) RADIOCHEMISTRY OF SELENIUM. Molinski, V. J.; Leddicotte, G. W. (Union Carbide Corp., Tuxedo, N. Y. Mining and Metals Div.). Nov. 1965. Contract W-7405-eng-26. 55p. Dep. mn; CFSTI $1.00 cy, $0.50 mn.

Nuclear Science Series of National Academy of Sciences–National Research Council, Washington, D. C. Committee on Nuclear Science.

A review is presented on nuclear and chemical properties of Se, methods of sample dissolution and of separation reactions, descriptions of counting techniques, and radiochemical separation procedures for Se. 81 references are cited. (P.C.H.)

**1745** (RT/CHI(65)-25) MESSA A PUNTO DI UN METODO DI ANALISI DEI POLIFENILI PER GAS-CROMATOGRAFIA SU COLONNE A CLORURO DI LITIO E APPLICAZIONE NEL CONTROLLO DELLA PREPARAZIONE DI ISOMERI PURI DEI QUATERFENILI. (Method of Gas-Chromatographic Analysis of Polyphenyls in Lithium Chloride Columns and its Application to the Control and Preparation of Pure Quaterphenyl Isomers). Bordonali, C.; Patimo, C. (Comitato Nazionale per l'Energia Nucleare, Rome (Italy)). June 1965. 23p. Dep. mn.

A method of gas-chromatographic analysis on lithium chloride columns is described, together with its application on the purity control of the quaterphenyl isomers. The method used to prepare the pure isomers of the quaterphenyls was also then examined. (auth)

**1746** (TID-22199) A STUDY OF SENSITIVITY OF INCREMENTAL DERIVATIVE POLAROGRAPHY. Final Report. (Adelphi Univ., Garden City, N. Y.). June 1965. Contract AT(30-1)-2923. 11p. Dep. mn; CFSTI $1.00 cy, $0.50 mn.

Studies were made on sensitivity improvement in the incremental derivative polarograph, a method for charging current compensation, and a criterion for resolution in the case of mutually overlapping polarographic waves. (P.C.H.)

**1747** (UCRL-11616(Rev.)) THE EXTRACTION OF $HClO_4$ BY TRILAURYL AMINE. I. AROMATIC DILUENTS. Bucher, J. J.; Diamond, R. M. (Lawrence Radiation Lab., Univ. of California, Berkeley). Sept. 1964. Contract W-7405-eng-48. 32p. Dep. mn; CFSTI $2.00 cy, $0.50 mn.

The role the organic diluent plays in the extraction of $HClO_4$ and $HReO_4$ into dilute solutions of trilauryl amine (TLA) was studied, and the nature of the extracted complexes determined. With the exception of tetrachloroethylene, the diluents used (benzene, mesitylene, sym-triethylbenzene, chlorobenzene, anisole, o-dichlorobenzene, nitrobenzene) were aromatic. Their dielectric constants covered a range from 2.3 to 35. It was found that the extraction can be correlated roughly with dielectric constant, but is also dependent upon the basic properties of the diluent. Inference is made that these solvents interact with the hydrogen of the ammonium cation by means of their $\pi$-electron system and also through specifically basic groups when present in the molecule. With nitrobenzene as the solvent, the predominant species in the organic phase was dissociated $TLAH^+$ and $ClO_4^-$ ions; with chlorobenzene, anisole and o-dichlorobenzene, it was a simple ion pair of $TLAH^+ClO_4^-$; and for the remaining low-dielectric solvents, electrostatic polymers were found in the relatively concentrated solutions (up to 0.1 M $TLA \cdot HClO_4$), and ion pairs only in very dilute concentrations. (auth)

**1748** (UJV-1369/65) OBNARUZHENIE POVREZHDENIYA URANOVYKH TEPLOVYDELYAYUSHCHIKH ELEMENTOV PRI NEAKTIVNYKH ISPYTANIYAKH V POTOKE $CO_2$. (Discovery of Damage in Uranium Fuel Elements in Nonactive Test in $CO_2$). Zaiits, V.; Vlchek, I.; Gudechek, M. (Ustav Jaderneho Vyzkumu, Ceskoslovenska Akademie Ved, Rez). [1965]. 20p. Dep. mn.

During the testing of fuel elements in a nonradioactive closed loop under nominal service conditions of pressure, temperature, flow rate, humidity, etc., the U contained in the element may become oxidized, entering the gas circuit in the form of U oxide aerosols. In order to find the damaged elements rapidly, a radiometric method was developed for detecting U-containing aerosols by passing the $CO_2$ stream through cellulose filters and analyzing the filter residue. A flow rate of 1 $cm^3$/sec per $cm^2$ of the filter was found to yield the best results. A scintillation detector with a photomultiplier was used for the radiometric determination of the deposit. The sensitivity of the method allowed a concentration of 2.77 mg/$m^3$ to be detected and concentrations of 27.7 mg/$m^3$ to be measured. The method is considered a reliable tool for recognizing the beginning of the deterioration of fuel elements subjected to loop testing. Further experiments are needed to adapt the method for the study of the kinetics of the deterioration reaction. (TTT)

**1749** (USNRDL-TR-912) A COMPENDIUM OF RADIOCHEMICAL PROCEDURES FOR THE DETERMINATION OF SELECTED FISSION PRODUCTS IN SEA WATER. Lai, M. G.; Goya, H. A. (Naval Radiological Defense Lab., San Francisco, Calif.). Aug. 19, 1965. Contract AT(49-5)-2084. 39p. Dep. mn; CFSTI $2.00 cy, $0.50 mn.

Procedures are described for analyzing seawater samples for the following fission-product nuclides: $^{137}Cs$, $^{89}Sr$, $^{90}Sr$, $^{91}Y$, $^{141}Ce$, $^{144}Ce$, $^{140}Ba$, $^{95}Zr$, $^{103}Ru$, $^{106}Ru$, $^{99}Mo$, and $^{131}I$. All procedures employ either solvent extraction, precipitation, or ion exchange chromatography to separate the fission products from seawater. (auth)

**1750** (UCRL-Trans-1245(L)) THE SEPARATION OF CATIONS ON A PAPER-CHROMATOGRAPHIC BASIS. Blasius, E.; Gottling, W. Translated for Univ. of California Lawrence Radiation Lab., Livermore, from Z. Anal. Chem., 162: 42319(1958). 18p. Dep. mn; JCL $1.60 fs, $0.80 mf.

A method is described for the separation of groups of elements by paper chromatography. This includes the Cr, Al, Zn, alkaline earth, and alkali metal groups. The group precipitations were found to be satisfactory, since the substances are present in sufficiently large quantities. The methods of detecting the pots on the paper are more sensitive than the methods normally used in microanalysis. Results for each group are briefly summarized. (P.C.H.)

**1751** GAS CHROMATOGRAPHIC DETERMINATION OF PERMANENT GASES IN HELIUM AT REDUCED SAMPLE PRESSURES. Attrill, J. E.; Boyd, C. M.; Meyer, A. S. Jr. (Oak Ridge National Lab., Tenn.). Anal. Chem., 37: 1543-6(Nov. 1965). (ORNL-P-1036).

Commercially available components were used to adapt a process chromatograph for the injection of samples taken at the pressure of the sample source. The sample loop on the linear sampling valve was connected to a vacuum system through a three-way solenoid valve, which, when actuated, connected the evacuated loop to the sample source. The actuation and return of the sampling valve was delayed to permit the loop to fill to source pressure and to prevent the injection of carrier gas back into the sample source. Sample consumption was reduced and analytical data recorded in terms of partial pressures of components within the system sampled. Percentage concentrations of $H_2$, $O_2$, $N_2$, $CH_4$, CO, and $CO_2$ were determined in helium at 100 mm of Hg. (auth)

**1752** DETERMINATION OF $^{155}Eu$ IN FISSION PRODUCTS USING REDUCTION BY LITHIUM AMALGAM. Bubernak, Joseph; Lew, Marion S.; Matlack, George M. (Los Alamos Scientific Lab., N. Mex.). Anal. Chem., 37: 1574-6(Nov. 1965). (LA-DC-6508).

The method and factors involved in the separation of europium from other fission products using the electrolytic cells are described. The procedure for separation of Eu from solution by extraction using a lithium amalgam is given. Eu was stripped from the mercury phase using 1M nitric acid and carried through the final steps. The precipitate was filtered, dried by vacuum desiccation, and weighed to determine the chemical yield. Mounted on an aluminum plate the gamma activity of $^{155}Eu$ was counted

with the counter threshold set for a minimum energy cut-off of about 30 kev. Interfering ions, effects of electrolysis time, stability of lithium amalgam, optimum amalgam quantity and extraction time, reproducibility of analysis, and decontamination from other fission products are discussed. (F.J.H.)

**1753** DETERMINATION OF MAGNESIUM IN URANIUM BY ATOMIC ABSORPTION SPECTROMETRY. Humphrey, J. Richard (Atomics International, Canoga Park, Calif.). Anal. Chem., 37: 1604-5(Nov. 1965).

Atomic absorption spectrophotometry was used to determine magnesium in uranium. The uranium sample was dissolved in hydrochloric acid and the solution was divided into three or more aliquots to which were added different quantities of a magnesium standard solution. Atomic absorption measurements were made at 285 mμ using an atomic absorption spectrophotometer equipped with a magnesium hollow cathode lamp. The effects of varying the acid and uranium concentrations were investigated. The effects of some impurities commonly found in uranium were also studied. The results are stated in terms of the ratio of the absorbance in the presence of the impurities to that in their absence. (F.J.H.)

**1754** RADIOCHEMICAL DETERMINATION OF $^{90}Sr$ IN WATER USING ION EXCHANGE. Talvitie, N. A.; Demint, Robert J. (Department of Health, Education, and Welfare, Salt Lake City). Anal. Chem., 37: 1605-7(Nov. 1965).

$^{90}Sr$ was determined in water by preferential adsorption on cationic resin from an EDTA medium followed by selective elution of ingrown $^{90}Y$ with ammonium 2-methyllactate. The column was eluted with hard water. (The hardness was added as calcium ions having maximal carrying capacity for $^{90}Sr$ at concentrations of 100 mg per liter.) The recovery of $^{90}Sr$ from water, with no corrections other than for reagent blank and for ingrowth and decay of $^{90}Y$, was 98% with a relative standard deviation of 2%. (F.J.H.)

**1755** DETERMINATION OF MERCURY IN WHEAT AND TOBACCO LEAF BY NEUTRON ACTIVATION ANALYSIS USING $^{197}Hg$ AND A SIMPLE EXCHANGE SEPARATION. Kim, Chong K.; Silverman, Joseph (Univ. of Maryland, College Park). Anal. Chem., 37: 1616-17(Nov. 1965).

A mercury exchange method was developed and applied to the separation of mercury from irradiated samples of wheat and tobacco. The method is highly selective so that further purification is not required. The results obtained from neutron activation analysis of tobacco and wheat for mercury are given. The mercury recovery was incomplete when an open vessel was employed, but recovery was consistently about 90% when the acid digestion was carried out in a reflux system. $^{197}Hg$ was chosen for counting because of the large cross section (3000 b) for its production and its convenient half life. (F.J.H.)

**1756** ON THE ELECTROPHORESIS OF $^{227}Ac$. Aitzetmueller, K.; Buchtela, K.; Grass, F. (Oesterreichische Hochschule, Vienna). Atomkernenergie, 8: 269-72(July-Aug. 1965). (In German).

The electrophoretic behavior in α-hydroxyisobutyric acid of actinium 227 and its decay products was investigated using cellogel-strips. The sequence of mobilities was Fr + Tl > Ra > Ac > Pb > Bi > Th in the direction to the cathode, and Po to the anode. It is demonstrated that commercially available Ac-227 contained approximately 15% radium D (lead 210). (auth)

**1757** THE EVAPORATOR COLLECTOR, A SIMPLE APPARATUS FOR CONTINUOUS SAMPLING WITH SIMULTANEOUS CONCENTRATION OF THE SAMPLE. Aurand, K.; Behrens, H. (Institut fuer Wasser-, Boden- und Lufthygienne, Berlin). Atomkernenergie, 8: 304-6(July-Aug. 1965). (In German).

A description is given of a simple apparatus for continuous sampling of tap water with simultaneous automatic evaporation. That apparatus is concentrating several hundred liters of water in a flask. The concentrated sample in the flask can be forwarded by mail in a special box for investigation. That process allows to detect directly radionuclides in concentrations of about 0.1 pCi/l according the radionuclide and partly lower concentrations by direct γ-spectroscopy of the concentrated sample. (auth)

**1758** MEASUREMENT OF SOFT β-RADIATION IN BIOLOGICAL MATERIAL WITH THE AID OF LIQUID SCINTILLATORS. III. DETERMINATION OF $^{35}S$ AFTER DISSOLVING THE SAMPLE IN NITRIC ACID. Horesovsky, O.; Franc, Z. (Research Inst. for Pharmacy and Biochemistry, Prague). Collect. Czech. Chem. Commun., 30: 3218-19(Sept. 1965).

A method is described for the determination of sulfur-35 in biological materials. The method consists of partial degradation of the sample by $HNO_3$ and $H_2O_2$ from which a white evaporation residue is obtained. The whole operation is carried out in glass measuring vessels so that all manipulations are excluded which lead to losses. Another advantage consists in the possibility of processing colored and otherwise difficultly soluble samples, such as feces, bones, skin, spleen, and blood. (P.C.H.)

**1759** DETERMINATION OF $^{233}Pa$ IN THE AIR. Bulanova, I. D.; Vorobiev, A. M. Gig. Sanit., No. 7, 71-2(July 1965). (In Russian).

An analytical method was developed to separate $^{233}Pa$ from $^{233}U$, thorium, and fission products such as $^{137}Cs$, $^{90}Sr$, $^{144}Ce$, $^{106}Ru$, and $^{95}Zr-^{95}Nb$. The method depends on the extraction of $^{233}Pa$ by methylisobutylketone (MIBK) from 5 to 10N HCl. Complexing of $^{233}Pa$ by adding fluoride prevents the extraction of $^{233}Pa$ by MIBK. At least 10 $m^3$ of air are drawn through a membrane filter which is then ignited in a porcelain crucible in a muffle furnace at 500 to 600°C for one hour. The residue is taken up in a few ml of 8N HCl + 0.5N HF, and is extracted with MIBK. The organic layer is discarded. Then 2 ml of MIBK and 150 mg of solid $AlCl_3 \cdot 6H_2O$ are added to the aqueous layer. The excess aluminum breaks the $^{233}Pa$ fluoride complex, and the $^{233}Pa$ extracts into the MIBK. The aqueous layer is discarded. The organic layer is washed with 2 to 8N HCl, and the $^{233}Pa$ is backextracted with 8N HCl + 0.5N HF. Two cycles are required to purify the $^{233}Pa$. The $^{233}Pa$ yield is 92 to 94%. The $^{233}Pa$ is counted on an end window counter with a window thickness of 1 to 2 $mg/cm^2$. The absolute activity is determined by comparison with a $^{147}Pm$ standard, or by calculation. (TTT)

**1760** ELECTROMETRIC STUDY ON THE QUANTITATIVE PRECIPITATION OF SAMARIUM(III) AS NORMAL TELLURITE. Prasad, Sarju; Pathak, Keshawa Chandra (Banaras Hindu Univ., Varanasi). Indian J. Chem., 3: 341-2(Aug. 1965).

A conductometric titration method for the microdetermination of samarium(III) as normal tellurite is described. A solution of samarium(III) nitrate is titrated against standard sodium tellurite solution maintaining an overall concentration of 40% ethanol (by volume) in the reaction mixture. By this procedure samarium(III) can be estimated within 1–2% of error. The effect of varying ethanol concentration on the reaction was investigated and the breaks recorded in the titration curves show the formation of a normal samarium tellurite corresponding to the samarium: tellurium molar ratio of 2:3. (auth)

**1761** EXTRACTION OF THORIUM, PROTACTINIUM, URANIUM, RUTHENIUM, AND ZIRCONIUM BY LONG CHAIN AMINES. Venkateswarlu, K. S.; Subramanyan, V.; Dhaneswar, M. R.; Shanker, R.; Lal, Manohar; Shankar, J. (Atomic Energy Establishment, Trombay, India). Indian J. Chem., 3: 448-51(Oct. 1965).

Extraction studies of thorium, protactinium, uranium, ruthenium, and zirconium with long chain amines (Primine JMT, Amberlite LA-2 and triisooctylamine) were carried out from sulfuric acid solutions. The nature of the extracted species was inferred from the results. In uranium and ruthenium extractions, mixtures of Amberlite LA-2 and triisooctylamine give higher distribution ratios as compared to the individual reagents. (auth)

**1762** ION EXCHANGE BEHAVIOUR OF URANIUM(VI) IN AQUEOUS SODIUM TRIPHOSPHATE AND ITS SEPARATION FROM RARE EARTHS. Apte, B. G.; Subbaraman, P. R.; Gupta, J. (National Chemical Lab., Poona, India). Indian J. Chem., 3: 454-7(Oct. 1965).

Complex formation of uranyl ion with sodium triphosphate was investigated using ion exchange equilibration methods and applied successfully to the elution-separation of uranium-rare earth mixtures. Clear-cut separations were obtained both on cation and anion exchangers; but the anion exchange method was faster and more flexible being applicable equally to uranium as well as rare earth concentrates. The conditional formation constants of both uranyl and rare earth triphosphate complexes rose with pH as expected but the former were more stable than their rare earth counterparts. The predominant uranyl complex species in a solution of pH 3-4 appeared to be $UO_2HP_3O_{10}^{2-}$ but the sodium salt separating out at this pH had the composition $Na_3UO_2P_3O_{10} \cdot 6H_2O$. (auth)

**1763** LOW-TEMPERATURE ADSORPTION AND GAMMA SCINTILLATION SPECTROMETRY FOR MEASURING $^{41}Ar$. Bevis, H. A.; Dunavant, B. G. (Univ. of Florida, Gainesville). Int. J. Appl. Radiat. Isotop., 16: 527-35(Sept. 1965).

A technique for measuring $^{41}Ar$ by low-temperature adsorption on charcoal and $\gamma$-scintillation spectrometry was developed. Following the design and fabrication of an adsorber cartridge, several parameters that affect collection efficiency were investigated, including the type of charcoal, particle size, sampling rate, and charcoal regeneration. The parameters were optimized to form the proposed technique which, after calibration, was field tested at the University of Florida reactor facility. The sampling device functioned well and the radiological analysis of the sample was made without difficulty. The sensitivity of the system is estimated to be about $10^{-9}$ $\mu$C of $^{41}Ar/cm^3$ of air, with an accuracy of ±15%. (auth)

**1764** PURITIES OF SOME COMMERCIALLY AVAILABLE $^{14}C$-LABELED HYDROCARBONS BY GAS-LIQUID RADIOCHROMATOGRAPHY. Muhs, M. A.; Bastin, E. L.; Gordon, B. E. (Shell Development Co., Emeryville, Calif.). Int. J. Appl. Radiat. Isotop., 16: 537-44(Sept. 1965).

Gas-liquid radiochromatography (GLRC) was used to measure the chemical and radiochemical purity of a number of commercially available $^{14}C$-labeled hydrocarbons. All of the compounds tested had satisfactory chemical purity (>99%) but poor radiochemical purities (0 to 50%). All of the hydrocarbons found to be radiochemically impure were successfully purified by preparative scale gas chromatography using GLRC as the test method. The study suggested that impurities in labeled compounds arose from two sources: in the synthesis step, which results in traces of impurities of comparable volatility as the parent compound but of higher specific activity, and during storage (self radiolysis) which results in high boiling contaminants (polymers) of specific activity comparable to the parent compound. Results indicated that analyses for these impurities should involve GLRC to determine volatile radioactive impurities, and a total activity balance between the injected and the eluted material to determine nonvolatile radioactive impurities. (auth)

**1765** AN AUTOMATED SYSTEM FOR RAPID AND PRECISE FAST NEUTRON ACTIVATION ANALYSIS. Vogt, J. R.; Ehmann, W. D.; McEllistrem, M. T. (Univ. of Kentucky, Lexington). Int. J. Appl. Radiat. Isotop., 16: 573-80(Oct. 1965).

An automated fast neutron activation analysis system is described, which permits the rapid and nondestructive analysis of large numbers of samples with accuracy and precision. A 250-kv Cockcroft–Walton-type accelerator is used to provide a fast neutron flux of $4.5 \times 10^9$ n $cm^{-2}$ $sec^{-1}$ using the $T(d,n)^4He$ reaction. An automated irradiation control system was developed to control the irradiation and counting processes. The system includes a solenoid-operated beam-stop for turning the neutron beam on and off, and two solenoid-operated spinner assemblies for rotating the sample container in the neutron beam and in front of the scintillation detectors. As many as 60 oxygen analyses or 10 silicon analyses per hr were run using this system. Problems associated with sample preparation, irradiation, data accumulation, and data reduction are discussed and the application of the system to the determination of silicon is described. (auth)

**1766** SIMULTANEOUS ASSAY OF $^{90}Sr$ AND $^{90}Y$ BY LIQUID SCINTILLATION SPECTROMETRY. Uyesugi, G. S.; Greenberg, A. E. (California State Dept. of Public Health, Berkeley). Int. J. Appl. Radiat. Isotop., 16: 581-7 (Oct. 1965).

A liquid scintillation technique is described whereby $^{90}Sr$ can be assayed with high efficiency in the presence of $^{90}Y$. This permits the estimation of $^{90}Sr$ by direct counting and eliminates the need to allow ingrowth of $^{90}Y$, chemical separation of the yttrium daughter, and calculation of $^{90}Sr$ from the $^{90}Y$ counts. (auth)

**1767** A RAPID METHOD FOR DISSOLVING TISSUE FOR LIQUID SCINTILLATION COUNTING. Petroff, C. P.; Patt, H. H.; Nair, P. P. (Sinai Hospital of Baltimore, Inc.; Johns Hopkins Univ., Baltimore). Int. J. Appl. Radiat. Isotop., 16: 599-601(Oct. 1965).

An efficient technique is described for the rapid dissolution of tissues for liquid scintillation counting incorporating the advantages of previously published studies to obtain high counting efficiencies without phase separation. A 2N solution of methanolic KOH was employed as the solubilizing agent, and ethylene glycol monobutyl ether was used to bring about complete miscibility of the tissue digest with the toluene scintillator solution. (auth)

**1768** PRECISION METHOD FOR THE ROUTINE MEASUREMENT OF $^{14}C$ AND $^3H$ IN PROPORTIONAL COUNTERS. Jordan, P.; Lykourezos, A. P. (Eidgenoessische Technische Hochschule, Zurich). Int. J. Appl. Radiat. Isotop., 16: 631-44(Nov. 1965). (In German).

The factors that determine the precision and accuracy of the proportional counter measurements of $^3H$ and $^{14}C$ were examined in detail. A method is described, which permits the maintenance of the standard error at the 0.1% level and detects immediately any abnormal source of error. (auth)

**1769** DETERMINATION OF CHLORINE AND SODIUM IN SELENIUM BY NON-DESTRUCTIVE NEUTRON ACTIVATION ANALYSIS. Gobrecht, H. (Technische Univ., Berlin); Bock-Werthmann, W.; Tausend, A.; Braetter, P.; Willers, G. Int. J. Appl. Radiat. Isotop., 16: 655-9(Nov. 1965).

A nondestructive determination of Cl and Na traces in selenium by means of $\gamma$-scintillation spectrometry is described. The influence of these elements on the semiconductor properties of selenium is mentioned. The nuclear data of the matrix is discussed. The best activation and measurement conditions for the BER (Berlin Reactor), which allowed the determination of 0.01 ppM Na and 10 ppM Cl, are indicated. It was necessary to apply a method of spectrum subtraction to the determination of low Cl concentrations. (auth)

**1770** SORPTION OF RADIOACTIVE SUBSTANCE IN A CHROMATOGRAPHIC COLUMN. Nakhutin, I. E.; Ochkin, D. V. Inzh.-Fiz. Zh., 9: 112-16(July 1965). (In Russian).

An analytical expression was derived for a stationary distribution of the concentration of a radioactive substance in a gas along the chromatographic column. The linear isotherm was assumed. Transport of the material in the gas to the surface of sorbent grains and the diffusion inside grains were taken into account. If the rate of diffusion in grain is low, adsorption will occur only in the surface layer. In this case effective capacity of the sorbent is decreased. The temperature relation was also considered. (auth)

**1771** DETECTION OF PHOSPHOLIPIDS ON PAPER CHROMATOGRAMS BY NEUTRON ACTIVATION. Johnson, Peter; Weber, Evelyn J.; Carter, H. E.; Krober, M. S.

(Univ. of Illinois, Urbana). J. Lipid Res., 6: 425-7 (July 1965).

Improved techniques are described for detection of phospholipids on paper chromatograms by neutron activation (with the formation of $^{32}P$ compounds). It was found that irradiation of phospholipids on paper chromatograms for a short time at low neutron flux can produce sufficient radioactivity for the detection of even small quantities of these lipids, and the paper retains its strength. Irradiation is carried out after development of the chromatograms to eliminate problems arising from radioinduced degradation of the lipids. Radioactivity from impurities even with low neutron flux is relatively high in the case of both Whatman and Schleicher and Schull filter papers, but it was found that treatment of the paper with formaldehyde followed by overnight washing with water effectively removes impurities which would otherwise be activated during neutron irradiation. In the method described, samples of crude corn phosphatides (10–50 μg) were applied in aqueous pyridine as a series of 1.25-in. wide streaks across a large sheet of HCHO-treated chromatography paper which was then developed 18–24 hr in redistilled n-butanol-acetic acid-water (4 : 1 : 5). The paper was dried, cut into 1⅝-in. wide strips, and placed in cylindrical Plexiglas vials which were then irradiated in the Triga Mark II Reactor for 7 hr at 250 kw with a thermal neutron flux of $2 \times 10^{12}$ neutrons/sec cm$^2$. Irradiated samples were allowed to decay for at least 48 hr before scanning for $^{32}P$ on a linear-response autoscanner. Autoradiography was also carried out. Background from the paper was at a low enough level to allow very small amounts of phospholipids to be detected ($10^{-4}$ μg P). Peaks from chromatographed samples could be measured weeks after irradiation, as shown by the separation of phytoglycolipid and phosphatidyl inositol from a mixture of corn phosphatides. (BBB)

**1772** CHROMOTROPE 2B AS A CHROMOGENIC AGENT FOR THE PHOTOMETRIC DETERMINATION OF THE RARE EARTHS. Dey, Arun K.; Sangal, Satendra P.; Sinha, Surendra N.; Munshi, Kailash N. (Univ. of Allahabad, India). Microchem. J., 9: 282-7(Sept. 1965).

Chromotrope 2B (CTB) was found to form colored chelates with rare earths and was used as a chromogenic reagent for their photometric determination. It was found that the reagent is very sensitive towards the rare earths. The effect of temperature, rate of color formation, and color stability are discussed. (F.J.H.)

**1773** FLUOROMETRIC DETERMINATION OF SCANDIUM AND GALLIUM WITH DERIVATIVES OF SALICYLALDEHYDE. Holzbecher, Zavis (Inst. of Chemical Technology, Prague). Microchem. J., 9: 288-300(Sept. 1965).

Derivatives of salicylaldehyde and resorcylaldehyde form fluorescing metal complexes that can be extracted from solutions saturated with sodium perchlorate with isoamyl alcohol. The intensity of the blue fluorescence depends on the acidity of the solutions. This fact was used for a selective and sensitive fluorimetric determination of Sc and Ga by means of acetylhydrazone of salicylaldehyde or formylhydrazone of resorcylaldehyde, respectively. The determination limits were 0.07 μg Ga or 0.05 μg Sc in 1 ml of amyl alcoholic extract. The determination of microgram amounts of these elements was not disturbed by Li, Na, $Tl^{1+}$, Ag, Pb, Hg, Be, Ca, Sr, Ba, Mg, Cd, La, $Ce^{3+}$, $Cr^{3+}$, Mn, and small amounts of Co, Ni, In, or As. The serious interference of $Cu^{2+}$ and $Fe^{3+}$ could be avoided by masking these elements with thiosulfate. Scandium or gallium, respectively, in the presence of Al, Y, or Zn, respectively, can be determined indirectly by measuring the fluorescence intensity of the mixture at different pH values and solving simultaneous equations. To determine Ga and Sc or Al, in a mixture the fact that the fluorescence of the Sc or Al complex is quenched by NaF much more than the fluorescence of the Ga complex can be used. The composition of the Sc complex of acetylhydrazone of salicylaldehyde was studied by a fluorometric method. (auth)

**1774** SOME INVESTIGATIONS ON DETERMINATION OF ISOTOPIC COMPOSITION OF NATURAL BORON ISOTOPES. Riedel, Jozef Tadeusz (Inst. for Nuclear Research, Polish Academy of Sciences, Warsaw). Przegl. Elektron., 6: 385-91(Aug. 1965). (In Polish).

The basic principles of mass spectrometry, as applied to a system for measuring the relative isotopic abundances of natural isotopes, are discussed. A technique for measuring the isotopic abundances of boron is described, which has an attainable accuracy of 0.02%. The effects of memory of the apparatus, corrections arising from the time for carrying out an analysis, and the sensitivity to sample cleanliness and sample handling (i.e., distillation of liquid $BF_3$) are also discussed. (TTT)

**1775** THORIUM, PROTACTINIUM, AND URANIUM EXTRACTION BY MEANS OF NEOCUPFERRON. Lapitskii, A. V.; Rudenko, N. P.; Saed, Abdel Gavad. Radiokhimiya, 7: 139-42(1965). (In Russian).

The extraction of U(VI), Pa, and Th from hydrochloric acid solutions using neocupferron in chloroform and of thorium with solutions of neocupferron in hexanol was investigated. On the basis of the results obtained, an hypothesis on the possibility of the extraction separation of Th, Pa, and U using neocupferron discussed. (tr-auth)

**1776** BEHAVIOR OF THORIUM, PROTACTINIUM, AND URANIUM DURING EXTRACTION BY MEANS OF BENZOHYDROXAMIC ACID AND N-BENZOYLPHENYLHYDROXYLAMINE. Rudenko, N. P.; Saed, Abdel Gavad; Lapitskii, A. V. Radiokhimiya, 7: 142-5(1965). (In Russian).

It was established that U and Pa as well as Th are extracted with benzohydroxamic acid in the pH interval from 3 to 5. From this it follows that with these reagents it is possible to achieve separations of U, Th, and Pa. The composition of the complexes Pa–benzohydroxamic acid and U–benzohydroxamic acid corresponds to the ratio 1 : 1. N–benzoylphenylhydroxylamine forms with $^{223}Pa$ a stable complex in concentrated solutions of HCl. Complexes with Pa can be re-extracted with 0.5M HF. U in acid medium does not form complexes with N–benzoylphenylhydroxylamine. Th also does not form similar compounds. The possibility of the separation of Pa from Th using benzoylphenylhydroxylamine is discussed. (tr-auth)

**1777** EFFECTS OF KETONES ON POLONIUM BEHAVIOR IN HYDROCHLORIC SOLUTIONS. Starik, I. E.; Ampelogova, N. I.; Kuznetsov, B. S. Radiokhimiya, 7: 199-203(1965). (In Russian).

The behavior of polonium in 0.001 to 1M HCl solutions in the presence of acetone was investigated using electromigration, electrodialysis, dialysis, and sorption on ion exchange resins and by means of electrochemical separation on copper. It was found that the presence of acetone in the hydrochloric solution displaces the equilibrium between the different Po compounds to the side of the formation of negatively charged chlorocomplexes. It was discovered that the separation of Po on copper from 0.1 to 0.001M HCl solutions with complex formation depends on the concentration of the acetone in the solution with the minimum separation occurring in the range of 10 to 30% acetone by volume. (tr-auth)

**1778** DETERMINATION OF $^{7}Be$ IN SAMPLES OF ATMOSPHERIC AEROSOLS AND ATMOSPHERIC PRECIPITATION IN THE PRESENCE OF FISSION FRAGMENTS. Gedeonov, L. I.; Rys'ev, O. A.; Susorova, N. A. Radiokhimiya, 7: 254-5(1965). (In Russian).

A method for the radiochemical separation of $^{7}Be$ in which the $^{7}Be$ is separated as the hydroxide in the presence of Trilon B, is described. The Trilon B acts as a masking complex-forming agent. In addition to $^{7}Be$, $^{89}Sr$, and $^{90}Sr$ can be separated from the same sample of rain water. The analytical procedure used producing the hydroxide and the oxide is described. The γ spectrum of BeO shows that the half life of the separated emitter (54 days) and the γ energy corresponded to those of $^{7}Be$. The method can be applied to atmospheric aerosols without any modifications. (tr-auth)

**1779** COMPLEX EMANATION-THERMAL METHOD. Zaborenko, K. B.; Melikhov, L. L.; Portyanoi, V. A. Radiokhimiya, 7: 319-24(1965). (In Russian).

An installation for the complex emanation-thermal analysis, permitting continuous recording on an electron potentiometer during heating under controlled conditions of emanation, shrinkage, and weight and also permitting a differential thermal analysis of the compound, was constructed. Since all the measurements are carried out under ideal analytical conditions, the complex analysis gives the most complete information on processes occurring during heating of solid substances and their mixtures. Work on the installation during three summers showed its good characteristics and the advantages of the use of the emanation-thermal method for the solution of problems of theoretical and applied chemistry. (tr-auth)

**1780** PREPARATION OF SPECIMENS AND CORRECTIONS FOR SELF-ABSORPTION DURING MEASUREMENT OF THE ACTIVITY OF SOFT BETA EMITTERS. Levin, V. I.; Brezhneva, N. E.; Ratnikova, M. G. Radiokhimiya, 7: 346-50(1965). (In Russian).

The simple linear function $K = 1 + \beta\underline{x}$ can be used for the determination of the self-absorption correction for soft $\beta$ emitters in samples. The $\beta$ coefficient is near in size to the mass absorption coefficient $\mu$, determined by the formula $e^{-\mu\underline{x}}$. At $\mu\underline{x} \leq 1$ and $\mu\underline{x} \geq 1$ the linear formula for the self-absorption correction approaches the formula based on the exponential absorption law. (tr-auth)

**1781** DISPERSION METHOD FOR RELATIVE MEASUREMENTS OF RADIOACTIVITY. Luk'yanov, V. B.; Korobkov, V. I. Radiokhimiya, 7: 350-5(1965). (In Russian).

By using dispersion analysis it was established that in measurement of the comparative and absolute radioactivities of samples prepared on filter paper, irregularities of the distribution of the activity of the sample appeared along the surface. The contribution of different origins of dispersion was evaluated in the total error of the test. The efficiency of the utilization of the dispersion method of analysis for evaluation of the precision of radiometric determination is shown. The introduction of dispersion analysis in applied radiochemical laboratories makes it possible to develop standard schemes of design for different radiometric methods. (tr-auth)

**1782** EXTRACTION OF URANIUM(VI) FROM CARBONATE SOLUTIONS BY QUATERNARY PHOSPHONIUM AND ARSONIUM BASES. Laskorin, B. N.; Filippov, E. A.; Goncharenko, G. I.; Skvortsov, N. V.; Skorovarov, D. I. Radiokhimiya, 7: 356-7(1965). (In Russian).

Phosphonium $[R_4P] + Cl^-$ and arsonium salts $[R_4As] + Cl^-$ were tested to determine the effects of the concentration of carbonate ions and nature of the diluent on the extraction of uranium (VI). The organic phase consisted of a 0.1M solution of the quarternary base in chloroform or butyl ethyl ketone containing 7 vol % n-octanol. Aqueous solutions 0.008M of uranium containing 0.1M ammonium bicarbonate and 0.1-1.0M sodium carbonate were employed. The extraction was carried out by vigorously shaking the combined aqueous and organic phases. It was found that the arsonium and phosphonium compounds have practically the same extractive properties, but the addition of 8-hydroxyquinoline caused the distribution ratio to be much higher in the case of the arsonium compounds. It was concluded that the extraction of uranium (VI) from carbonate media by the phosphonium and arsonium compounds is rather ineffective owing to a decrease in the distribution coefficient caused by an appreciable solubility of the complex in the aqueous phase; however, the addition of 8-hydroxyquinoline raised the distribution ratio because of the formation of the complex $[UO_2(C_9H_6ON)_3]^-$, which has no affinity for water. (OTS)

**1783** BEHAVIOUR OF THORIUM NITRATE SOLUTIONS IN AMBERLITE $^{120}$Ir. Grade, Maria Regina Sales (Comissao de Estudos de Energia Nuclear, Lisbon). Rev. Port. Quim. (Lisbon), 6: 123-4(1964). (In Portuguese).

The behavior of thorium nitrate solutions with Th present in small dilutions in amberlite IR-120 ion exchange resins was investigated. The effect of iron on the capacity of the resin for the Th and for its elution from the resin was determined. The conditions for the elution of Th and Fe were determined. The results showed that in both the fixation of Th and its elution 4 M $HNO_3$ was the most suitable reagent. (J.S.R.)

**1784** APPLICATION OF ACTIVATION ANALYSIS TO THE DETERMINATION OF SOME IMPURITIES IN NUCLEAR-GRADE URANIUM. Kosta, L.; Cook, G. B. (International Atomic Energy Agency, Neideroesterreich, Austria). Talanta, 12: 977-87(Nov. 1965).

Activation analysis was applied to the determination of nine trace elements in some uranium compounds including three samples of nuclear pure uranium oxides. The method of analysis was based on the preseparation of uranium by ion exchange, using three different systems according to the impurities involved. The elements considered were: thorium, lanthanum, chromium, copper, cobalt, manganese, sodium, tungsten, and molybdenum. No chemical yield corrections were necessary because the method provided quantitative recoveries. Technique and results are discussed and it is shown that reagent blanks do not represent a serious problem. The impurities studied can be determined in relatively small sample aliquots with a precision ($2\sigma$) of ±20% in concentration ranges down to a few ppB. (auth)

**1785** SOME RECENT DEVELOPMENTS IN RADIOACTIVATION ANALYSIS. A REVIEW OF IMPROVEMENTS IN THE ANALYTICAL TECHNIQUE. Girardi, Francesco (Euratom Joint Nuclear Research Centre, Italy). Talanta, 12: 1017-41(Nov. 1965).

Different techniques of activation analysis are considered and recent basic or technical improvements are reviewed. Developments in related fields such as radiochemistry of $\gamma$ spectrometry are reported only when especially referring to activation analysis. (188 references). (auth)

**1786** DETERMINATION OF TRACE AMOUNTS OF CADMIUM AND SILVER BY SUBSTOICHIOMETRIC RADIOISOTOPIC DILUTION ANALYSIS. Landgrebe, A. R.; McClendon, L. T. (National Bureau of Standards, Washington, D. C.) Trans. Amer. Nucl. Soc., 8: 315-16(Nov. 1965).

**1787** AN IMPROVED MODEL FOR THE LEAST-SQUARES ANALYSIS OF GAMMA-RAY SPECTRA IN ACTIVATION ANALYSIS. McGuire, S. W.; Hartley, H. O.; Wainerdi, Richard E. (A and M College of Texas, College Station). Trans. Amer. Nucl. Soc., 8: 325(Nov. 1965).

**1788** RECOMMENDED DELAY IN COUNTING AFTER NEUTRON ACTIVATION. Pollack, Louis R. (San Francisco Naval Shipyard). Trans. Amer. Nucl. Soc., 8: 325-6(Nov. 1965).

**1789** NEUTRON ACTIVATION ANALYSIS OF HALOGENS IN THE ATMOSPHERE. Winchester, John W. (Massachusetts Inst. of Tech., Cambridge). Trans. Amer. Nucl. Soc., 8: 326-7(Nov. 1965).

**1790** THE DETERMINATION OF IODINATED COMPOUNDS BY NEUTRON ACTIVATION OF $^{129}$I-DESCRIPTION OF THE TECHNIQUE. Ouellette, Robert P.; Balcius, Joseph F.; Brownell, Gordon L. (Massachusetts General Hospital, Boston). Trans. Amer. Nucl. Soc., 8: 330-1(Nov. 1965).

**1791** THE DETERMINATION OF VANADIUM IN BLOOD BY NEUTRON ACTIVATION ANALYSIS WITH PREIRRADIATION SEPARATION. Lukens, H. R.; Heydorn, K.; Choy, T. (General Atomic Div., General Dynamics Corp., San Diego, Calif.). Trans. Amer. Nucl. Soc., 8: 331(Nov. 1965).

**1792** NUMERICAL METHODS FOR SOLUTION OF COMPLEX GAMMA SPECTRA. Schunicht, Bernard F. (General Electric Co., Schenectady, N. Y.). Trans. Amer. Nucl. Soc., 8: 339-40(Nov. 1965).

**1793** ON SEVERAL VERSIONS OF DEVICES FOR SPECTRAL-ISOTOPIC DETERMINATION OF GASES IN METALS. Sakorina, N. A.; Laseeva, G. S.; Petrov, A. A.; Skvortzova, G. V.; Favorskaya, M. P. Vestn. Leningr. Univ., No. 10, Ser. Fiz. Khim., No. 1, 152(1965). (In Russian).

Several methods were developed and tested for the spectral-isotopic determination of gases in metals by means of the optical quantum generator, h-f generator, or the discharge tube with a hollow cathode. (auth)

**1794** DETERMINATION OF URANIUM IN ORES. Mukashev, F. A.; Syromyatnikov, N. G. (Satpaev Inst. of Geology, Academy of Sciences, Kazakh SSR). Zavodsk. Lab., 31: 806(1965). (In Russian).

For determining >0.002% U in ore, uranium was reduced with a few granules of zinc in 4 N HCl. Colorimetric analyses with arsenazo III were carried out on parallel samples, in one of which uranium was reduced, and in the other it was not reduced. The presence of >5 mg Fe and >250 μg Ti interfered with the reduction of uranium. The following procedure is recommended. A sample of 0.1 to 0.5 g is boiled with a mixture of HCl and $H_2O_2$, and evaporated to dryness. The residue is treated with 4N HCl, which is made up to a volume of 100 ml. Two aliquots containing 10 to 15 μg of uranium are placed in 25 ml calibrated vessels. About 1 mg of ascorbic acid is added to one of the aliquots to reduce iron (with slight heating), and 1 ml of saturated oxalic acid is added to complex zirconium. Then 1 ml of a 0.05% solution of arsenazo III is added, and the solution brought up to volume with 4N HCl. A total of 23 ml of 4N HCl, 1 ml of saturated oxalic acid, and six granules of zinc metal are added to the other aliquot. After reducing for an hour the solution is filtered, and 1 ml of 0.05% solution of arsenazo III is added. The difference in optical densities of the two solutions is a measure of the uranium (IV). The results are reproducible to ±10% as compared to the radiochemical method. (TTT)

**1795** POLAROGRAPHIC DETERMINATION OF EUROPIUM AND YTTERBIUM IN THE PRESENCE OF POTASSIUM CHLORIDE. Il'kova, S. B.; Gubel'bank, S. M. Zavodsk. Lab., 31: 806-7(1965). (In Russian).

The contents of Eu and Yb were determined polarographically in 30% KCl. The half-wave potentials were found to be −0.55 v for Eu, and −1.35 v for Yb with respect to a mercury anode. The height of the wave was proportional to the concentration of Eu or Yb in the rare earth concentrate. A change in pH from 3 to 5.5 did not change the height of the wave for europium. At lower pH the diffusion current increased, possibly, because of hydrogen discharge. At a pH of >5.5 the rare earths precipitated. The pH stability limits were 4.5 to 5.5 for Yb. Other rare earths with the exception of cerium (>40%) had no substantial effect on the half-wave potential or the magnitude of the diffusion current of Eu and Yb. The relative error was 5 to 7% for Eu, and 7 to 10% for Yb. The minimum concentration of Eu and Yb to be determined was 0.01 to 0.03 mg/ml. (TTT)

**1796** EXTRACTION OF RARE EARTH AMYGDALATE SALTS BY BUTANOL. Tishchenko, M. A.; Lauer, R. S.; Poluektov, N. S. (Inst. of General and Inorganic Chemistry, Odessa). Zh. Neorgan. Khim., 10: 1925-8(Aug. 1965). (In Russian).

It was established that amygdalates of the cerium elements are extracted with butanol from aqueous solutions at pH 3.5 to 6. The distribution coefficients of Nd amygdalate was investigated in dependence on the concentration of the amygdalic acid. By means of the method of isomolar series, it was found that in the extraction of compounds with one atom of Nd, 4 molecules of amygdalic acid were necessary. This gives a basis to conclude that with the extracted compounds $NdM_3 \cdot MH$, where MH is amygdalic acid, appears. (tr-auth)

**1797** FALLING STREAM STANDARD SAMPLING SYSTEM (Engineering Materials). (Mallinckrodt Chemical Works, St. Louis, Mo.). (CAPE-1261).

25 drawings.

The system is used to sample U concentrate for payment purposes that cannot be obtained satisfactorily by auger. The advantages are its compactness, observation windows, variability of flow rates, and tightness thus limiting air influx and dust leaks. The system consists of a roller conveyor, weigh-in scale, and drum elevator which lifts the drum to an upper conveyor on which it rolls into a dumping station. Here the lid is removed, a large dumping cone is clamped on, and the drum and cone are inverted and lowered into place. The concentrate enters the upper surge hopper where it is stirred to avoid bridging. The output is fed through a rotary valve to a vibratory feeder which empties into the first-stage cutter box. Here a Geary-Jennings sampler directs a portion of the flow down to a second vibratory feeder supplying the second-stage cutter box. Rejected materials fall into a lower surge hopper. In the second-stage cutter box another Geary-Jennings sampler cuts the stream and its output goes down a chute into the sample collection drum. All reject materials drop into the lower surge hopper from which empty drums are filled. The drums are located on a drum packer from which an output conveyor leads across a weigh-out scale. A secondary sample splitter is used to evaluate the system. (For details, see TID-4100). (P.C.H.)

**1798** LAMINAR FLOW OXYGEN-ACETYLENE BURNER (Engineering Materials). (Lawrence Radiation Lab., Univ. of California, Livermore). (CAPE-1271).

12 drawings.

The burner is used to introduce atoms into an optical beam path from a hollow cathode lamp. Radiation absorption from the lamp is measured spectrophotometrically. The characteristics provided by the burner for atomic absorption spectrophotometry are: aspiration of the sample through a proven, commercial atomizer; efficient premixing of the atomized cloud of sample and combustibles; burning of the sample in a high-temperature flame under fuel rich conditions which assures even refractory elements appearing as atoms in the optical beam path; and a flame port which conforms to the beam path in shape to maximize absorption. The possibility of flashback is minimized by use of a nozzle design permitting low hydrostatic internal pressures and a water-cooled flame port which prevents overheating. In the event of a flashback, a blow-out port is included. The rugged construction of the equipment will withstand the explosion shockwave. (For details, see TID-4100). (P.C.H.)

**1799** SODIUM SAMPLER (Engineering Materials). (Oak Ridge National Lab., Tenn.). (CAPE-1268).

13 drawings.

The vacuum distillation, analytical sampler is used for the determination of oxygen in sodium and NaK. Alkali metal is transferred, under pressure, to the sampler where a fixed volume of the metal is retained in a hemispherical cup, and the metal is distilled from the oxide. After the sampler has cooled, the oxide residue is dissolved and the amount of oxide oxide in the metal is determined. The apparatus, which is constructed of stainless steel, consists of two main sections: a sampler cup insert and a distillation chamber held together with clamps. The insert heater is a 500 v heating element wound around a suitable base. Thermocouples used to measure the temperature of the sampler cup are inserted through the base. A cooled sight glass of fused quartz 9⅝ in. long, .906 in. OD, and .787 in. ID is provided. (For details, see TID-4100) (P.C.H.)

**1800** PROCESS FOR THE DISPERSION OF UNIFORM DROPLETS OF A LIQUID IN A SECOND LIQUID. Hure, Geoffroy Graham Jacques; Saint-James, Rose (to Commissariat a l'Energie Atomique). Canadian Patent 712,562. June 29, 1965. Priority date May 9, 1962, France.

The process is characterized by the formation of homogeneous droplets of controlled diameter dispersed in another liquid. The diameter depends on the flow rate through the injector opening and on the vibration frequency impressed on liquid A which is to be dispersed in liquid B. Such control is useful in solvent extraction columns where

the diameter of the droplets may be optimized for maximum extraction efficiency. (F.S.A.)

**1801** METHOD OF ANALYZING WATER SAMPLES FOR DEUTERIUM CONTENT. Arnett, Edward M. U. S. Patent 3,208,826. Sept. 28, 1965. Filed Feb. 23, 1961.

A gas chromatographic method is described for analyzing aqueous samples containing mixed light and heavy water for deuterium content. The sample is passed through a tube containing $CaH_2$ to generate $H_2$ and HD directly related in deuterium content to that of the original water sample. Measured portions of the gases produced are trapped in a gas sampler associated with the gas chromatographic device. The mixed gases are released into a stream of carrier gas of $H_2$ to pass through a column packed with a surface active material to separate extraneous gases from the $H_2$–HD sample. The deuterium content of the sample is determined by measuring its thermal conductivity relative to the carrier gas. (B.L.M.)

## Inorganic and Physical Chemistry

**1802** (AD-618038) ON THE ANISOTROPY OF EXCHANGE IN YTTERBIUM IRON GARNET. Levy, Peter M. (Pennsylvania Univ., Philadelphia). July 1965. Contract Nonr55136. 10p. (TR-24). CFSTI $1.00 cy, $0.50 mn.

Exchange splittings of the lowest 2F5/2 and 2F7/2 doublets of Yb(3+) in YbIG were evaluated in terms of exchange potential parameters given previously. A good four parameter fit of the experimental exchange splittings was obtained by adopting essentially zero values for the rare earth-iron exchange interactions that take place through the nearest neighbor oxygen ions. The chief result was that the rare earth-iron exchange interaction takes place primarily through the next-nearest neighbor oxygens (2.43A); the nearest neighbor oxygens (2.37A) are comparatively inert. (auth)

**1803** (AD-619266) RADIATIVE PROPERTIES OF GASES. VOLUME I. GENERAL DISCUSSIONS. Miller, R. V.; Golden, S. A. (Rocketdyne, Canoga Park, Calif.). Aug. 12, 1965. Contract Nonr462300. 218p. CFSTI $6.00 cy, $1.25 mn.

Theoretical studies of the basic radiative properties of high temperature gases are described. The primary emphasis was devoted to methods of calculating spectral absorption coefficients of electronic transitions in diatomic molecules. The smeared line model was used to calculate absorption coefficients in fifty such transitions. Ancillary work included studies of methods of calculating numerical potential functions of the Rydberg-Klein-Rees type, solutions to the Schroedinger equation with such potential functions, and computational procedures for evaluating Franck-Condon and r-centroid factors. (auth)

**1804** (AWRE-O-68/65) URANIUM CORROSION STUDIES. PART 2. THE RATE OF REACTION OF POLISHED URANIUM AND WATER VAPOUR AT VARIOUS TEMPERATURES. Grimes, J. H.; Morris, J. R. (Atomic Weapons Research Establishment, Aldermaston (England)). Sept. 1965. 22p. Dep.; BIS $0.65; HMSO 3s. 3d.

The rate of reaction of uranium and water vapor was determined at temperatures in the range 30 to 80°C. An activation energy of 9 kcal/g mole was derived. Comparisons are made between the rate of corrosion of uranium found by the measurement of oxide film growth and that found by other methods. (auth)

**1805** (AWRE-O-69/65) THE SORPTION OF METHANOL BY CORRODED URANIUM. Perry, G. S. (Atomic Weapons Research Establishment, Aldermaston (England)). Oct. 1965. 18p. Dep.; BIS $0.60; HMSO 3s.

The sorption of methanol by partly oxidized uranium which has not seen a temperature >75°C was investigated. The isotherms approached type II and showed considerable irreversibilities, and the chemisorbed methanol was removed only by heating at 300°C in vacuo. There was also some evidence for the chemisorption of a permanent gas, probably hydrogen, which was displaced by the sorbed methanol. Because of complications caused by chemisorbed methanol, it was not possible to assess the extent of the porosity of the corroded uranium. (auth)

**1806** (BM-RI-6697) HEAT OF FORMATION OF NEODYMIUM TRICHLORIDE. Stuve, J. M. (Bureau of Mines, Reno, Nev. Reno Metallurgy Research Center). Mar. 1965. 4p. Bureau of Mines Free.

Heat of solution measurements of high-purity neodymium metal and neodymium trichloride ($NdCl_3$) in 4.360 molal hydrochloric acid (HCl) were used to determine the standard heat of formation ($\Delta H_f^0$) of $NdCl_3$. From solution data obtained, the heat of formation of $NdCl_3$ (c) was computed as −248,970 ±260 cal/mole at 298.15°K. (auth)

**1807** (CEA-R-2827) ANISOTROPIE DU TENSEUR DE DEPLACEMENT CHIMIQUE DES FLUORS DANS $UF_6$ [theses]. (Anisotropy of the Fluorine Chemical Shift Tensor in $UF_6$ [thesis]). Rigny, Paul (Commissariat a l'Energie Atomique, Saclay (France). Centre d'Etude Nucleaires). 1965. 30p. Dep. mn.

Submitted to Univ., Paris.

An $^{19}F$ magnetic resonance study of polycrystalline $UF_6$ is presented. The low temperature complex line can be analyzed as the superposition of two distinct lines, which is attributed to a distortion of the $UF_6$ octahedron in the solid. The shape of the two components is studied. Their width is much larger than the theoretical dipolar width, and must be explained by large anisotropies of the fluorine chemical shift tensors. The resulting shape functions of the powder spectra are determined. The values of the parameters of the chemical shift tensors yield estimates of the characters of the U–F bonds, and this gives some information on the ground state electronic wave function of the $UF_6$ molecule in the solid. (auth)

**1808** (COO-958-5) CORRELATED EPR-OPTICAL SPECTRA OF POTASSIUM IN ETHYLAMINE–AMMONIA MIXTURES. Dalton, L. R.; Rynbrandt, J. D.; Hansen, E. M.; Dye, J. L. (Michigan State Univ., East Lansing. Dept. of Chemistry). [1965]. Contract AT(11-1)-958. 69p. (CONF-650401-16). Dep. mn; CFSTI $3.00 cy, $0.75 mn.

From American Chemical Society, Detroit.

Extensive electron paramagnetic resonance (EPR) studies of potassium in ethylamine–ammonia mixtures were made over a temperature range of −180° to +100°C and at varying ammonia concentrations up to 68 mole percent. Hyperfine splittings, g values, linewidths, and spin concentrations were measured. Optical spectra were measured from −65° to +35°C for a number of the solutions. Correlation of optical and EPR results rules out the assignment of the visible absorption to the monomeric species responsible for hyperfine splitting. The unusual temperature dependence of the EPR spectra cannot be explained in the light of current models, nor can the ammonia dependence be quantitatively interpreted. A model involving equilibrium between atoms and monomers quantitatively describes the temperature dependence. To explain the dependence upon ammonia concentration, it is necessary to consider two monomeric species, one fully solvated by ethylamine and the other involving replacement of ethylamine by one molecule of ammonia. Above about eight mole percent ammonia, computer analysis of the EPR spectra showed the building-in of an extra absorption consisting of a single broad line. The intensity of this absorption relative to the four-line pattern continued to increase until the lines merged at about 25 mole percent ammonia. Under varying conditions, the optical spectra showed the three peaks characteristic of metal–amine solutions. Relative intensities were very sensitive to temperature and ammonia concentration. At low ammonia concentrations, only the visible absorption was obtained while the intermediate and infrared absorptions occurred at higher concentrations. The latter two peaks were favored by high temperature, while the visible ab-

sorption was more pronounced at lower temperatures. These spectra are discussed in the light of current models for metal–amine solutions. (auth)

**1809** (COO–1149-30) HEAT CAPACITY AND THERMODYNAMIC PROPERTIES OF ZIRCONIUM TETRAFLUORIDE FROM 5 TO 307 deg K. Westrum, Edgar F. Jr. (Michigan Univ., Ann Arbor. Dept. of Chemistry). Nov. 1964. Contract AT(11-1)-1149. 12p. Dep. mn; CFSTI $1.00 cy, $0.50 mn.

The heat capacity of $ZrF_4$ was determined from 5 to 307°K by adiabatic calorimetry. No thermal anomaly was detected and a normal sigmoid curve represents the data. The heat capacity ($C_p$), entropy ($S^0$), enthalpy function $[(H^0 - H_5^0)/T]$, and free energy function $[-(F^0 - H_5^0)/T]$ are, respectively, 24.79, 25.00, 14.03, and 10.97 cal/(gfm °K) at 298.15°K. (auth)

**1810** (EUR–2458.f) ETUDES THERMODYNAMIQUES PAR SPECTROMETRIE DE MASSE. ETUDE THERMODYNAMIQUE DU SYSTEME URANIUM–OXYGENE PAR SPECTROMETRIE DE MASSE. LA CHALEUR DE SUBLIMATION DE L'URANIUM. (Thermodynamic Studies by Mass Spectrometry. Thermodynamic Study of the Uranium–Oxygen System by Mass Spectrometry. The Heat of Sublimation of Uranium). Pattoret, A.; Smoes, S.; Drowart, J. (Brussels Univ. (Belgium). Faculte des Sciences). Aug. 1965. Contract 003-63-3 DIRB. 60p. Dep. mn.

Uranium vapor pressures and partial pressures of uranium and UO and $UO_2$ molecules in the system U(1) + $UO_2$(s) were measured by mass spectrometry. The heat of sublimation calculated from the uranium pressures is $\Delta H_{5,s}^0(U) = 125.5 \pm 2.5$ kcal/atmg. The consistency of this value with the thermodynamic data for the evaporation of uranium oxides and carbides was critically examined and found to be satisfactory. (auth)

**1811** (EUR–2486.e) THERMAL AND MECHANICAL STUDIES OF SOLID-SOLID CONTACTS. Mustacchi, C.; Giuliani, S. (European Atomic Energy Community, Ispra (Italy). Joint Nuclear Research Center). 1965. 52p. Dep. mn.

Bearing curves of solids with several surface finishes were studied. Experimental and theoretical analyses were made of the thermal situation of a solid-solid contact with particular emphasis on the fuel-pellet-clad interaction in a nuclear reactor fuel element. (auth)

**1812** (EUR–2495.e) WATER SOLUBILITY IN MOLTEN ALKALI NITRATES. Bertozzi, G. (European Atomic Energy Community, Ispra (Italy). Joint Nuclear Research Center). 1965. 12p. (CONF-650502–9). Dep. mn.

From Electrochemical Society, San Francisco.

Water vapor solubility in pure lithium nitrate and in lithium-sodium and lithium-potassium nitrate mixtures, at water vapor pressures up to 30 torr, in the temperature range 230 to 280°C is reported. The dissolution process is reversible, i.e. no hydrolysis reactions occur. The ion-dipole interaction energy is taken into account, and it is shown to be the most relevant parameter in determining the dissolution process. Thermodynamic quantities for the solution equilibrium are given. (auth)

**1813** (EUR–2515.e) SOME EXPERIMENTAL DATA ON THE INTERACTION OF KRYPTON WITH URANIUM OXIDE SURFACES. Gautsch, O.; Mustacchi, C.; Wahl, H. (European Atomic Energy Community, Ispra (Italy). Joint Nuclear Research Center). Sept. 1965. 34p. Dep. mn.

Polycrystalline $UO_2$ surfaces were bombarded with Kr ions of a few Kev energies to obtain secondary electron yields, sputtering ratios, and saturation values. Ion gettering of Kr by $UO_2$ was also investigated. (auth)

**1814** (NAA-SR-6333) PRESSURE DROP FOR FLOWING VAPORS CONDENSING IN A STRAIGHT HORIZONTAL TUBE. Baroczy, C. J.; Sanders, V. D. (Atomics International, Canoga Park, Calif.). June 1, 1961. Contract AT(11-1)-Gen-8. 44p. Dep. mn; CFSTI $1.00 cy, $0.50 mn.

A method for calculating condensing static pressure drop of a saturated vapor flowing in a straight round tube on which there is a prescribed heat flux is described. The method postulates that this system is equivalent to a quasi-static, two-phase, two component fluid flow system in which no condensation takes place. The effect of condensation is accounted for by a variable liquid to vapor flow weight ratio which is a function of the condensation rate. The method utilizes an improved Lockhart-Martinelli type of two-phase, two component pressure drop correlation that was devised especially for it, and is proposed for general use. The pressure drop is obtained by a point-by-point calculation and numerical integration over the range of condensation. The results of the method were compared with measured pressure drops for condensing steam and the agreement was favorable. Some numerical examples are given. (auth)

**1815** (NRL–6241) HIGH-TEMPERATURE PROPERTIES OF SODIUM. Stone, J. P.; Ewing, C. T.; Spann, J. R.; Steinkuller, E. W.; Williams, D. D.; Miller, R. R. (Naval Research Lab., Washington, D. C.). Dec. 24, 1964. Contract NASA C-76320. 64p. CFSTI $3.00 cy, $0.75 mn.

An experimental program is in progress to measure various thermophysical properties of sodium, potassium, and cesium. A final reporting of the experimental results for sodium (saturation and superheat properties of the vapor, density, and specific heat of the liquid) is presented together with a thermodynamic treatment of the data. Two equations of state are advanced, one virial and one quasi-chemical, and additional saturation and superheat properties of the vapor are derived from these equations. Either of two paths can be used to compute thermodynamic properties, the monomeric gas path or the liquid path, but results obtained by the former procedure are believed to be more accurate. Enthalpy, entropy, specific volume, specific heat, and compositional information (weight fraction of dimer, weight fraction of tetramer, and average molecular weight) are tabulated for some 700 selected vapor states in the temperature range from 1625 to 2575°F and in the pressure range from 0.2 to 25 atm. (auth)

**1816** (ORNL-TM–1258) CHLORIDE VOLATILITY EXPERIMENTAL STUDIES: THE REACTION OF $U_3O_8$ WITH CARBON TETRACHLORIDE AND MIXTURES OF CARBON TETRACHLORIDE AND CHLORINE. Gens, T. A. (Oak Ridge National Lab., Tenn.). Aug. 26, 1965. Contract W-7405-eng-26. 20p. Dep. mn; CFSTI $1.00 cy, $0.50 mn.

In a proposed process for recovering uranium as volatile chlorides ($UCl_5$ and $UCl_6$) by chlorinating spent uranium oxide fuel elements, one of the problems relates to minimizing the production of nonvolatile chlorides ($UCl_4$ and $UO_2Cl_2$). In 1-hr experiments in which coarse $U_3O_8$ powder (surface area, 0.38 $m^2/g$) was treated with 85% Ar–15% $CCl_4$ vapor, the amount of $UCl_4$ found in the nonvolatile chloride products, consisting of $UO_2Cl_2$ and $UCl_4$, decreased from 57 mole % to 30 mole % as the temperature was increased from 400°C to 550°C. The mole percentage of $UCl_4$ was about half as large when finely divided $U_3O_8$ (surface area, 0.55 $m^2/g$) was used. The three conclusions are: When chlorine was substituted for argon, no $UCl_4$ was found at 400 to 550°C; therefore, the uranium oxide was more rapidly converted to volatile chlorides. Most of the $U_3O_8$ is first converted rapidly to $UO_2Cl_2$, and the $UO_2Cl_2$ is then chlorinated to produce $UCl_6$ and $UCl_5$ (when chlorine is not added to $CCl_4$, $UCl_4$ is also found). It was not possible to determine whether the primary chlorination reaction or the decomposition of higher uranium chlorides was the major source of $UCl_4$. (auth)

**1817** (TID–22323) THE SCATTERING OF LIGHT BY ANISOTROPIC DISCS WITH THEIR PRINCIPAL POLARIZABILITY DIRECTION AT AN ANGLE TO THE RADIUS. ONR Technical Report No. 76. Stein, Richard S.; Clough, Stuart B. (Massachusetts Univ., Amherst. Polymer Research Inst.). June 30, 1965. Contracts AT(30-1)-3003-3; Nonr 3357(01). 52p. Dep. mn; CFSTI $3.00 cy, $0.50 mn.

Equations are presented for the scattering of light by

two-dimensional polymer spherulites in which the optic axes of the uniaxial crystals are oriented at an arbitrary angle $\beta$ to the radii. For the case where the axes lie in the plane of the disc, the scattering patterns are identical to those calculated for $\beta = 0$, except that they are rotated through the azimuthal angle by the amount $\beta$. Of special interest is the case where the crystals rotate helicoidally about the radii (banded spherulites). The equations predict scattering maxima whose position is related to the period of rotation and the angle $\beta$. (auth)

**1818** (UCRL-11976) SPECTROSCOPIC INVESTIGATION OF HIGH TEMPERATURE SPECIES ISOLATED IN INERT GAS MATRICES [Thesis]. Brabson, G. D. (Lawrence Radiation Lab., Univ. of California, Berkeley). Aug. 1965. Contract W-7405-eng-48. 131p. Dep. mn; CFSTI $4.00 cy, $1.00 mn.

The matrix isolation technique was applied to three systems, and the isolated species were studied by visible-ultraviolet and infrared spectroscopy. The 3 systems included Hg, and $S_2$ in Ne, Ar, Kr, Xe, and $N_2$, and graphite vapor in Ar, Kr, and $N_2$. Mercury spectra were found to be shifted to shorter wavelength by 940, 1270, 775, 10 and 845 $cm^{-1}$, respectively. Fluorescent experiments on $S_2$ showed that vibrational motion is rapidly quenched by the matrix; the strongest bands belong to the (O,v'') progression. The spectrum of $C_3$ was observed, but spectra attributable to $C_2$ were not found in the region from 2000 to 12,000 Å. (P.C.H.)

**1819** (UCRL-14287) LATTICE MODELS FOR COOPERATIVE PHENOMENA. I. SURVEY AND COMPARISON OF APPROXIMATE METHODS. Brush, Stephen G. (Lawrence Radiation Lab., Univ. of California, Livermore); Kikuchi, R. (Hughes Research Labs., Malibu, Calif.). Sept. 1, 1965. Contract W-7405-eng-48. 47p. Dep. mn; CFSTI $2.00 cy, $0.50 mn.

Methods for estimating the thermodynamic properties of physico-chemical systems undergoing cooperative phase transitions are discussed. The Lenz-Ising model can be used to represent mixtures, magnets, and gas-liquid systems; in each case, it is assumed that atoms are arranged in a lattice structure, each lattice site being characterized by a two-valued parameter which may represent the type of atom, spin up or down, or atom or hole. The history of the Lenz-Ising model is reviewed, from its original formulation by Wilhelm Lenz in 1920 up to the present time. The following approximate methods are described: quasi-chemical; cluster variation; eigenvalue variation; and periodic boundary conditions. Thermodynamic properties of the simple cubic lattice, predicted by these approximations, were computed and compared with exact values obtained by series expansions and Padé approximant extrapolations. It was concluded that while none of these approximate methods gives accurate results in the neighborhood of the transition temperature or critical point, it is possible to obtain fairly good values of thermodynamic properties at sufficiently high or low temperatures by using the quasi-chemical or cluster-variation methods. Approximately 100 references are cited. (P.C.H.)

**1820** (AEC-tr-6619) THERMAL DECOMPOSITION OF URANYL NITRATE. Lebeau, Paul. Translated from Compt. Rend., 154: 1612-14(1912). 5p. Dep. mn; JCL $1.10 fs, $0.80 mf.

The thermal decomposition of uranyl nitrate begins at a temperature close to 100 °C. It gives rise first to nitric acid and uranic hydrate. After reaching the melting point of the salt, partial dehydration of the mass, with formation of anhydrous nitrate whose destruction is superimposed on that of the hydrated salt, takes place. This explains the formation of the mixture of uranic anhydride and its hydrate which is obtained in the decomposition of the molten salt. (P.C.H.)

**1821** (AEC-tr-6620) DEHYDRATION AND DECOMPOSITION OF THE HYDRATES OF URANYL NITRATE. FORMATION OF A MONOHYDRATE. de Forcrand, M. Translated from Compt. Rend., 156: 1044-8(1913). 6p. Dep. mn; JCL $1.10 fs, $0.80 mf.

Studies were made on the dehydration of the ordinary hexahydrate of uranyl nitrate in the cold in a $H_2SO_4$ bell jar, at atmospheric pressure and in vacuo. Dehydration of the dihydrate by heat was also studied. The results showed that to obtain an anhydrous product containing only traces of uranic acid, it would be necessary not to go above 125–130°C, and to work with $CO_2$ charged with nitric vapors. However, at this temperature it is necessary to prolong the experiment to more than 60 hr. (P.C.H.)

**1822** (ANL-Trans-233) BEHAVIOR OF ZIRCONIUM DICHLORIDE IN MOLTEN MIXTURES OF ALKALI AND ALKALI EARTH METALS. Sheiko, I. N.; Barchuk, V. T. Translated by Elmar K. Wilip (Argonne National Lab., Ill.), from Ukr. Khim. Zh., 30: 577-81(1964). 8p. Dep. mn; CFSTI $1.00 cy, $0.50 mn; JCL $1.10 fs, $0.80 mf.

The behavior of $ZrCl_2$ was studied in the following molten systems: $KCl-LiCl$, $KCl-NaCl$, $NaCl-CaCl_2$, $KCl-MgCl_2$, $NaCl-MgCl_2$, $NaCl-BaCl_2$, $NaCl-AlCl_3$, and $KCl-NaCl-ZrCl_4$. It was found that $ZrCl_2$ does not suffer changes in the melts up to 400°C. Temperature increase above 400°C leads to a noticeable disproportionation and to an increase of the metal content in the melt. The disproportionation process depends on the nature of the melt and on the temperature and duration of the experiment. It was found that $ZrCl_2$ is practically insoluble in all investigated melts and is present in an equilibrium with the metal on particles produced by the disproportionation of $ZrCl_2$. The amount of $ZrCl_2$ in the melt depends essentially on the temperature and on the stability of the suspension of metallic Zr. (auth)

**1823** INFRARED RADIATION OF SOLIDS REFRACTORY MATERIALS. Grenis, Albert F.; Levitt, Albert P. (Army Materials Research Agency, Watertown, Mass.). Amer. Ceram. Soc. Bull., 44: 901-6(Nov. 1965).

Apparatus and techniques were developed for determining the infrared radiation characteristics of solids, including flame-sprayed ceramic coatings, at elevated temperatures. The normal spectral emittance, integrated normal total emittance, and infrared radiation intensity curves of selected solids for different surface conditions were determined at a temperature of 1300°K in the wavelength region extending from 1.0 to 10.0 $\mu$. Infrared radiation properties for the flame-sprayed ceramic coatings, aluminum oxide, chromic oxide, and zirconium oxide, and for solid boron nitride are discussed. It was found that flame-sprayed chromic oxide most closely simulated a blackbody in the wavelength region studied. (auth)

**1824** THERMAL CONDUCTIVITY OF HELIUM AT TEMPERATURES 0 TO 1000 deg C AND PRESSURES 1 TO 200 ATM. Vargaftik, N. B.; Zimina, N. H. At. Energ. (USSR), 19: 300-3(Sept. 1965). (In Russian).

Experiments were carried out on He thermal conductivity at temperatures from 0 to 1000°C and pressures from 110 to 760 mm Hg. These and other published data, for pressures up to 200 atm, are analyzed and compared with calculations using the Enskog formula for the thermal conductivity of a compressed gas, for various temperatures and pressures. Variations of the temperature discontinuity as a function of the reciprocal pressure and the correction for the temperature discontinuity are derived and examined. (M.J.T.)

**1825** SOME HEATS OF SOLUTION IN LIGHT AND HEAVY WATER. Davies, D. H.; Benson, G. C. (National Research Council of Canada, Ottawa). Can. J. Chem., 43: 3100-3(Nov. 1965). (NRC-8613).

The heats of solution of sodium chloride, sodium fluoride, sodium methanesulfonate, sodium benzenesulfonate, and sodium p-toluenesulfonate were determined at several concentrations in light and heavy water at 25°C. The heat of solution is considerably higher in heavy water for all of these except sodium fluoride which is the same in each. (F.S.A.)

**1826** RELATIVE ISOTOPIC DISPLACEMENTS IN THE SPECTRUM OF NEODYMIUM. SPECIFIC MASS

EFFECT. Gerstenkorn, Simon; Helbert, Jean-Marie; Chabbal, Robert (C.N.R.S., Bellevue, France. Commissariat a l'Energie Atomique). Compt. Rend., 261: 1232-5(Aug. 2, 1965). (In French).

The isotopic displacement between the isotopes 142, 144, 146, 148, and 150 of neodymium was measured using a Fabry-Perot photoelectric spectrometer. Measurements with a precision of the order of a per cent were obtained by the use of isotopes enriched to more than 93% and because of a new method for the calibration of spectra. Six lines were studied and an important variation of the relative isotropic displacement was established. In the case where this variation is caused by a specific effect, it is shown that this effect for one of the transitions studied is equal to at least 10 times the Bohr effect (10 mk). (tr-auth)

**1827** NATURE OF THE IRREVERSIBLE POLYMORPHIC TRANSFORMATIONS OF RARE EARTH OXIDES. Boganov, A. G.; Rudenko, V. S. (Inst. of Silicate Chemistry, Academy of Sciences, USSR). Dokl. Akad. Nauk SSSR, 161: 590-3(Mar. 21, 1965). (In Russian).

To determine the existence of high-temperature polymorphic transformations in the oxides of Pr, Nd, Sm, Gd, Tb, and Dy, x-ray diffraction studies were carried out with a special vacuum x-ray camera at 2200 to 2300°C. In addition, the weight loss in the region of the transition point was measured, the influence of the gas medium (oxidizing, reducing, vacuum) and its pressure on the transition temperature was studied, and chemical analyses for "excess" oxygen (above the sesquioxide ratio 2 : 3) were performed iodometrically. The temperature of the C → A transition for $Pr_2O_3$ varied between 700 and 1350°C as a function of the medium and in such a way that the structural change for compositions of this oxide, which are close to the sesquioxide value, was directly related not only to the thermodynamic conditions, but to the change in the composition of the compound; in this sense, the C → A transformation in $Pr_2O_3$ could not be considered a true polymorphic transformation. In $Nd_2O_3$, $Sm_2O_3$, and $Gd_2O_3$, the transformations from C to A and B forms were related to their partial reduction to a composition with an oxygen content lower than the sesquioxide value. The distinctly reversible nature of the transformations in $Tb_2O_3$ and $Dy_2O_3$ and their irreversible character in $Pr_2O_3$, $Nd_2O_3$, $Sm_2O_3$, and $Gd_2O_3$ are thought to have the same fundamental cause associated with slight changes in composition occurring in rare earth oxides in the transition range during heating. (CFSTI)

**1828** ISOTOPIC EXCHANGE OF HYDROGEN ATOMS IN CYCLOPENTADIENYL RINGS OF COBALTICINIUM COMPOUNDS. Kursanov, D. N.; Setkina, V. N.; Baranetskaia, N. K.; Dvoriantseva, G. G.; Materikova, R. B. Dokl. Akad. Nauk SSSR, 161: 847-50(Apr. 1, 1965). (In Russian).

The kinetics of the hydrogen exchange of $Co(C_5H_5)_2OH$ in deuteromethanol (27.1 at. %) in the presence of MeONa was studied. The reaction was carried out at 50°C in a current of dry nitrogen and stopped at various times by pouring off the reaction mixture and acidifying with hydrochloric acid. The exchange rate constant was $6.0 \times 10^5$ to $6.9 \times 10^5$ $sec^{-1}$. With a reaction time increasing from 62 to 360 min, the amount of hydrogen that exchanged increased from 22.5 to 58.2%. When the reaction mixture was boiled for 13 hr, the exchange was 80 to 90% of the equilibrium value. Infrared spectrum adsorption lines were measured for the frequency range 400 to 4000 $cm^{-1}$ and are tabulated for 2000 to 3200 $cm^{-1}$. Nuclear magnetic resonance spectrum measurements were made of the cobalticinium chloride in saturated $D_2O$ solutions with dioxane as the internal standard. (TTT)

**1829** MASS SPECTRA OF WATER IONIZED IN A STRONG ELECTRICAL FIELD. Gol'denfel'd, I. V.; Nazarenko, V. A.; Pokrovskii, V. A. (Inst. of Physical Chemistry, Academy of Sciences, Ukrainian SSR). Dokl. Akad. Nauk SSSR, 161: 861-3(Apr. 1, 1965). (In Russian).

Ionization of water by tungsten, molybdenum, platinum, and gold point discharges and also by a nichrome wire discharger at a potential gradient of the order of $10^7$ to $10^8$ volts per centimeter was studied. In the case of the tungsten point discharger the mass spectra had strong lines corresponding to ions of 19, 37, 55, and 73 mass equivalent that were assigned to $(H_2O)_nH^+$ ions (where n is 1, 2, 3, and 4). The very weak mass spectral lines corresponding to 17 and 18 mass equivalents were assigned to $OH^+$ and $H_2O^+$ ions. The occurrence of lines corresponding to very small mass numbers was attributed to the products of decomposition of water aggregates according to formula $(H_2O)_nH^+ \rightarrow (H_2O)_mH^+ + (H_2O)_{n-m}$. These line assignments were confirmed in a separate study on ionization of $D_2O$. In order to examine the possibility of isotopic analysis, mixtures of light and heavy waters with known contents of deuterium were ionized and mass spectra were taken. Distribution of line intensities was determined from the formula $I_l = [C_k^l/(1 + \Delta)^k]\Delta^l$, where $\Delta$ is the atomic ratio of deuterium to hydrogen in the water blend, and l is the number of deuterium atoms. The number of lines as well as line intensity ratios calculated from this formula agreed with the mass spectra taken for a 1 : 1 mixture of $H_2O$ and $D_2O$. Formation of "metastable" ions (according to the first formula above) was reflected in the appearance of j(k − j + 2) lines instead of one line corresponding to pure $H_2O$. Distribution of intensities of these lines was determined from the formula $I_{li} = [C_k^l/(1 + \Delta)^k]\Delta^l(C_k^{l-i}C_l^i/C_{kj})$, where j is the sum of hydrogen and deuterium atoms in a "metastable" ion, i is the number of deuterium atoms in a "metastable" ion, l and k are as above and correspond to the starting "metastable" ion. Similar results were obtained with the molybdenum point discharger and the nichrome wire discharger. In the case of a rare metal point discharger (Pt,Au) the mass spectra showed an intensive $H_3O^+$ line, and the $H_2O^+$ to $H_3O^+$ ion ratio depended on the potential gradient. (CFSTI)

**1830** THE REPLACEMENT OF A HALOGEN BY A PROTON IN HALOGENOFERROCENES. Nesmeyanov, A. N.; Kursanov, D. N.; Nefedova, M. N.; Setkina, V. N.; Perevalova, E. G. (Inst. of Elementoorganic Synthesis, Academy of Sciences, USSR). Dokl. Akad. Nauk SSSR, 161: 1349-51(Apr. 21, 1965). (In Russian).

In studying the isotopic exchange of hydrogen in acid media an unexpected reaction of iodoferrocene with the acid was detected. In treating solutions of iodoferrocene in organic solvents (benzene, methylene chloride) with deuterotrifluoroacetic acid (95 at. % deuterium) there was a rapid formation of the ferricine cation and a complex compound of iodoferrocene with iodine. The ferricine cation after reduction by sodium sulfite yielded ferrocene containing 9.5 at. % deuterium, which corresponded exactly to the replacement of the iodine atom by deuterium. In the case of bromo- and chloroferrocene the substitution of deuterium for the halogen also was observed but to a lesser extent than with iodoferrocene. (CFSTI)

**1831** THE REDUCTION OF TUNGSTEN OXIDES BY HYDROGEN. Parsons, D. S. (Sylvania Electric Products Inc., Towanda, Pa.). Electrochem. Technol., 3: 280-3 (Sept.-Oct. 1965).

The kinetics of reduction of tungstic oxides by hydrogen was studied. In a static bed above 898°K (625°C), the rate was limited by the diffusion of water vapor out of the bed. A theoretical diffusion equation and an empirical reduction equation were developed and compared. These describe the reduction in terms of time, diffusion-path length, oxide bulk density, and absolute temperature. Another empirical equation based on this one was developed to describe the metal-powder particle size as measured by a sub-sieve sizer, in terms of the reduction time, temperature, bed depth, and $WO_3$ particle size. (auth)

**1832** CALCINATION AND SINTERING STUDY OF CERIA. Subba Rao, V. V. (National Chemical Lab., Poona). Indian J. Chem., 3: 343-5(Aug. 1965).

The thermal decomposition behavior of cerous carbonate and hydrated ceria was studied in the temperature range 30−1200° by measuring the surface areas and densities of the decomposition products. The mass loss at each stage was also determined and correlated. Cerous carbonate shows only one maximum at 340° in the plots of surface

area against temperature of calcination. Hydrated ceria shows no maximum; on the other hand the area decreases rapidly from 300° onward. The absence of a maximum could be due to the fact that no new phase structure is formed on heating ceria gel but only water of hydration is lost. These results were compared with those obtained with cerous oxalate. (auth)

**1833** LABELLING OF GLYCINE BY DIRECT EXCHANGE WITH HEAVY WATER. Paul, S. D.; Ramamurthy, J.; Chawla, A. S. (Atomic Energy Establishment Trombay, Bombay). Indian J. Chem., 3: 369(Aug. 1965).

The preparation of glycine $d_2$, $d_3$, and $d_5$ is described involving labeling of glycine by direct exchange with heavy water alone or in the presence of platinum black, as the catalyst. In the case of glycine $d_5$ the extent of deuteration obtained in single equilibration is 70%. (auth)

**1834** THE CRYSTAL STRUCTURE OF RARE EARTH AND YTTRIUM OXYBROMIDES. Mayer, I.; Zolotov, S.; Kassierer, F. (Hebrew Univ., Jerusalem). Inorg. Chem., 4: 1637-9(Nov. 1965).

Rare earth and yttrium oxybromides were prepared and their crystal structure studied. These compounds crystallize in the PbFCl-type tetragonal structure, with space group $D_{4h}^7P4/nmm$, and 2 molecules in the unit cell. Lattice constants and atomic parameters were calculated. Metal–bromide and bromide–bromide distances are discussed. (auth)

**1835** COLLOIDAL PROPERTIES OF PLUTONIUM IN DILUTE AQUEOUS SOLUTION. Lindenbaum, A.; Westfall, W. (Argonne National Lab., Ill.). Int. J. Appl. Radiat. Isotop., 16: 545-53(Sept. 1965).

The colloidal properties of Pu(IV) in solutions suitable for injection were investigated as a function of pH, time after pH adjustment, and relative concentrations of Pu and complexing citrate ions. Polymerization was increased with increasing pH and depressed by a large molar excess of citrate. The rate of depolymerization was directly proportional to citrate concentration, time and acidity. Differences in the rates of polymerization and depolymerization are demonstrated. The polydisperse nature of Pu(IV) colloids is shown by kinetic dialysis studies, which demonstrate a mixture of diffusible species. Apparent discrepancies between values for the fraction of diffusible Pu obtained by ultrafiltration and by dialysis are related to reversible polymerization. Techniques are described for the preparation of Pucitrate solutions of minimal colloidality and for rapid estimation of colloidal formation by the ultrafiltration procedure. The relation between the colloidal properties of Pu and its distribution in animal tissues is discussed. (auth)

**1836** USE OF $^{14}C$ TO MEASURE CARBON DIOXIDE REMOVAL IN A SYNTHETIC AMMONIA PLANT. Fries, B. A.; Hull, D. E.; Dupzyk, R. J.; Lamoree, D. J. (California Research Corp., Richmond). Int. J. Appl. Radiat. Isotop., 16: 561-4(Oct. 1965).

Use of the total-sample method was extended to measurement of the leakage of carbon dioxide through an oil-filled knockout trap in a large synthetic ammonia plant. Approximately 1 mC of $^{14}CO_2$ was injected into the plant, and gas samples were withdrawn from points ahead of and beyond the trap. The $^{14}CO_2$ was recovered from the samples and counted in a liquid scintillation counter. The high sensitivity of the method was illustrated by the detection of approximately 1 $\mu$C of $^{14}C$ in a gas stream flowing at over $6 \times 10^6$ standard $ft^3$/hr. The trap is shown to be 99.9% efficient in $CO_2$ removal. (auth)

**1837** WETTING OF METALLIC CARBIDES BY LIQUID COPPER, NICKEL, COBALT AND IRON. Ramqvist, Lars (Stora Kopparbergs Berlags AB, Soederfors Bruk, Sweden). Int. J. Powder Met., 1: No. 4, 2-21(Apr. 1965).

The wetting properties of the metallic carbides of groups IV, V, and VI, of mixed carbides, and of nonstoichiometric carbides by liquid Co, Cu, Fe, and Ni were investigated. Measurements showed that a correlation exists between the wetting angle and the heat of formation of the carbides; the wetting decreases with the greater stability of the carbides. (auth)

**1838** THE ISOTOPIC EXCHANGE OF CYCLOHEXANE WITH DEUTERIUM OVER EVAPORATED FILMS OF GERMANIUM AND SILICON. Gudkov, B. S.; Balandin, A. A.; Savin, E. P. (Zelinskii Inst. of Organic Chemistry, Academy of Sciences, USSR). Izv. Akad. Nauk SSSR, Ser. Khim., No. 6, 1120-1(1965). (In Russian).

Deuterium exchange between $C_6H_{12}$ and $D_2$ was carried out with a mole ratio of ~1 : 60 at a pressure of 23 mm Hg std on an evaporated film of Ge or Si of 7 mg. A control experiment showed no exchange in the absence of Si or Ge. The mass-spectrometric results showed that Si is a better catalyst for deuterium exchange than Ge. After two hr exchange at 175°C the content of $C_6H_{11}D_1$ was 2.87% for Ge and 0.97% for Si as a catalyst. The content of $C_6H_{10}D_2$ was 1.43% for Ge and 0.37% for the Si catalyst. The contents of $C_6H_9D_3$, $C_6H_8D_4$, $C_6H_7D_5$, $C_6H_6D_6$ and $C_6H_5D_7$ were 0.71, 0.40, 0.17, 0.09, and 0.03%, respectively, for Ge as a catalyst. The values were a factor of 3 to 4 lower for Si as a catalyst. (TTT)

**1839** THERMAL EXPANSION OF THREE GROUP IVA CARBIDES TO 2700 deg C. Richardson, James H. (Aerospace Corp., El Segundo, Calif.). J. Amer. Ceram. Soc., 48: 497-9(Oct. 21, 1965).

X-ray thermal expansion measurements on arc-cast carbides of titanium, zirconium, and hafnium are reported. The coefficients of thermal expansion for these materials from room temperature to 2700°C are $9.5 \pm 0.3 \times 10^{-6}$/°C, $7.6 \pm 0.2 \times 10^{-6}$/°C, and $7.3 \pm 0.2 \times 10^{-6}$/°C, respectively. (auth)

**1840** CZOCHRALSKI GROWTH OF RARE-EARTH MOLYBDATES OF TYPE $M_2(MoO_4)_3$. Kestigian, M. (Sperry Rand Research Center, Sudbury, Mass.). J. Amer. Ceram. Soc., 48: 544-5(Oct. 21, 1965).

Large, optical-quality single crystals of rare earth molybdates [$M_2(MoO_4)_3$] were prepared by the Czochralski technique. Appropriate quantities of the respective oxides were intimately mixed and calcined in oxygen at 1000°C in platinum vessels for 16 hr. The calcined material was melted and the temperature of the melt adjusted so that nucleation occurred when a small-diameter precious-metal rod was dipped into the melt. Rotation rates of 35 to 150 rpm were used during the seed withdrawal step. Large, optical quality single crystals of gadolinium molybdate $Gd_2(MoO_4)_3$, europium molybdate $Eu_2(MoO_4)_3$, and several mixed rare earth molybdates such as $[(GdEu)_2(MoO_4)_3]$ and $[(EuTh)_2(MoO_4)_3]$ were grown. Preliminary x-ray diffraction studies indicated temperature-sensitive structure changes in these compounds. (F.J.H.)

**1841** ISOTOPE EFFECT ON THE PARAMAGNETIC RESONANCE OF TRIPLET EXCITONS. Buckman, Trent D.; Griffith, O. Hayes; McConnell, Harden M. (Stauffer Lab. of Physical Chemistry, Stanford, Calif.). J. Chem. Phys., 43: 2907-8(Oct. 15, 1965).

The rate of triplet-exciton jumping in ionic molecular crystals was previously deduced under the assumption that nuclear hyperfine interactions make a substantial or dominant contribution to the observed exciton-resonance linewidths. The magnetic resonance of excitons in (morpholinium)$^+$ (perdeutero TCNQ)$^-$ and in $(\phi_3AsCH_3)^+$ (perdeutero TCNQ)$_2^-$ were observed and do, in fact, support the above assumption. The triplet exciton and impurity linewidths in the morpholinium salt are shown as the applied field is rotated in the (001) plane. It is noted that there is a marked similarity between the exciton linewidth anisotropy and the free-radical linewidth anisotropy in this plane. This suggests that the free-radical impurity is TCNQ$^-$, that this radical has an orientation similar to that of the (TCNQ)$_2^-$ pairs on which the triplet excitons move, and that the exciton linewidth anisotropy does indeed arise from nuclear hyperfine interactions, as mentioned previously. (J.F.P.)

**1842** STEPWISE EXCITATION OF FLUORESCENCE OF $CaWO_4$ ACTIVATED WITH $Er^{3+}$. Bakumenko, V. L.;

Vlasov, A. N.; Kovarskaya, E. S.; Kozina, G. S.; Favorin, V. N. JETP Lett. (USSR) (Engl. Transl.), 2: 16-18(July 1, 1965).

Stepwise excitation of fluorescence of $Er^{3+}$ was observed in single-crystal $CaWO_4:Er^{3+}$. The exciting monochromatic beams were aimed at the crystals opposite to each other through smaller faces. The radiation from the first passed through a filter absorbing the exciting light and was then registered with a FEU-27 photomultiplier. The stepwise excitation of fluorescence at wavelengths near 543 nm was observed when the wavelength of one of the exciting beams was approximately 1.5 $\mu$ and corresponded to the region of infrared absorption of $Er^{3+}$ in the $^4I_{15/2} \rightarrow {}^4I_{13/2}$ transition, while the wavelength of the second exciting beam corresponded to the 710–850 region. No fluorescence was excited by any of the beams separately, and the effect was observed only when the sample was simultaneously excited by both beams. The transition scheme responsible for the effect is shown. The dependence of the fluorescence intensity on the excitation wavelengths is also shown. The conversion coefficient was also estimated taking the infrared exciting beam as the signal and the red one as the pump. (J.F.P.)

**1843** ON THE EFFECT OF $H_2^+$ EXCITATION ON THE CROSS SECTION FOR THE ION-MOLECULAR REACTION $H_2^+ + H_2 \rightarrow H_3^+ + H$. Tunitskii, N. N.; Spezhakova, G. E. (Karpov Inst. of Physics and Chemistry, Academy of Sciences, USSR). Kinetika i Kataliz, 6: 563(May-June 1965). (In Russian).

It is known that $H_2^+$ ions formed by electron bombardment can undergo oscillatory excitation. If the $H_2^+$ ion is in the ground state, the probability ratio, $\beta$, of the reverse and direct reactions of the intermediate complex can be expressed by the phase volumes of the reacting systems $\Delta G$: $\beta = (\alpha_1 M_2/\alpha_2 m_1)^{0.5}(G_1/\Delta G_2)$. For the reaction $H_2^+ + H_2 \rightarrow H_3^+ + H$, the value of $\beta$ lies between 0.3 and 0.6. From the formula $W = [1/(1+\beta)]$, the probability W of the breakdown of $H_4^+$ into $H_3^+ + H$ is equal to about 0.6 to 0.8. Thus, if the molecular ion $H_2^+$ undergoes oscillatory excitation, the probability of the complex breaking down into $H_3^+ + H$ decreases, and there is a distinct probability of the reverse reaction to form the initial products. It also follows that the true cross section for the formation of $H_3^+$ should decrease with increasing energy of the ionizing electrons from 40% to about 20%. (TTT)

**1844** THE EFFECT OF COMPLEX FORMATION ON REACTIONS BETWEEN POSITRONIUM AND INORGANIC IONS. Goldanskii, V. I.; Firsov, V. G.; Shantarovich, V. P. (Inst. of Chemical Physics, Academy of Sciences, USSR; Inst. of Theoretical and Experimental Physics, Academy of Sciences, USSR). Kinetika i Kataliz, 6: 564-5 (May-June 1965). (In Russian).

The rate constants $k_p$ and $k_H$ for chemical reactions of the positronium and of the H atom were compared. In a $Fe(ClO_4)_2$ solution the values of $k_H$ and $k_p$ are $6.7 \times 10^6$ and $2 \times 10^9$ $mol^{-1}$ $sec^{-1}$, respectively. The ratio of $k_p$ to $k_H$ is $3 \times 10^3$. Similiarly in a $Fe_2(SO_4)_3$ solution the value of $k_H$ is $4.8$ to $9 \times 10^6$ $mol^{-1}$ $sec^{-1}$ and the value of $k_p$ is $1.2 \times 10^{10}$ $mol^{-1}$ $sec^{-1}$. In this case the ratio of $k_p$ to $k_H$ is 1.4 to $2.5 \times 10^3$. In the presence of a $[Fe(CN)_6]^{3-}$ solution the value of $k_H$ is $3.9 \times 10^4$ l $mol^{-1}$ $sec^{-1}$ with $k_p/k_H = 3.1 \times 10^5$. Apparently the $Fe^{2+}$ ion forms a hydride-like compound (positronide). (TTT)

**1845** NORMAL COORDINATE ANALYSIS OF $XeF_4$ IN THE UREY-BRADLEY FIELD. Yeranos, Walter A. (Northern Illinois Univ., De Kalb). Mol. Phys., 9: 449-54(1965).

Using published infrared and Raman data, the normal coordinates, the Urey-Bradley force constants, and the contribution of these force constants to the different normal modes of $XeF_4$ were determined. The analysis was carried out using a Fortran II program written specifically for the IBM 1620 computer, and within the formalism of Wilson's G–F matrix method. Furthermore, using a recently reported semi-empirical M.O. scheme for $XeF_4$, the vibronic interactions responsible for the symmetry forbidden $2a_{2u} \rightarrow 3e_u$ electronic transition at 44.15 kK are discussed qualitatively. (auth)

**1846** INVESTIGATION OF THE SOLUBILITY OF CERTAIN ACTINIUM COMPOUNDS. I. DETERMINATION OF THE SOLUBILITY OF ACTINIUM OXALATE. Ziv, D. M.; Shestakova, I. A. Radiokhimiya, 7: 166-75 (1965). (In Russian).

The solubility of actinium oxalate in water and in 0.01N $HNO_3$ was determined. The solubility of $Ac_2(C_2O_4)_3$ in water was 2.15 mg/l. The activity product of $Ac_2(C_2O_4)_3$ was calculated as $2.0 \times 10^{-26}$. The solubility product of $Ac_2(C_2O_4)_3$ in $HNO_3$ was calculated from its solubility in water as $4.1 \times 10^{-26}$. It was shown that in the presence of excess ions of the same type in solution the solubility significantly increases; the experimentally determined value for the solubility of $Ac_2(C_2O_4)_3$ was 12.4 mg/l and the theoretically calculated solubility was 0.06 mg/l. (tr-auth)

**1847** INVESTIGATION OF THE SOLUBILITY OF CERTAIN ACTINIUM COMPOUNDS. II. DETERMINATION OF THE SOLUBILITY AND EVALUATION OF THE RELATIVE BASICITY OF ACTINIUM HYDROXIDE. Ziv, D. M.; Shestakova, I. A. Radiokhimiya, 7: 175-87(1965). (In Russian).

$Ac(OH)_3$ was obtained by the method of inverse precipitation. The solubility of $Ac(OH)_3$ in water and in electrolyte–$NH_4NO_3$ was determined and the activity product of $Ac(OH)_3$ was calculated as $2.1 \pm 0.8 \times 10^{-19}$. The aging of $Ac(HO)_3$, purified of its decay products, in 0.001 N $NH_4NO_3$ was completed almost completely within a week. As a result of the aging the activity product of $Ac(OH)_3$ was reduced. The activity product of the aged hydroxide is $1.3 \pm 0.15 \times 10^{-21}$. A rapid and fairly significant decrease of the pH in the system $Ac(OH)_3$–$NH_4NO_3$–$H_2O$ can show a radiolytic effect caused by the $\alpha$ radiation of the decay products of Ac. The pH for the precipitation of $Ac(OH)_3$ from nitric acid solutions with Ac concentration of $1.21 \times 10^{-2}$ M was calculated as 8.61 on the basis of solubility data obtained by ultramicro methods. $Ac(OH)_3$ displayed a much stronger basicity than lanthanum hydroxide. (tr-auth)

**1848** ON THE PENTAVALENT NEPTUNIUM COMPLEXING ABILITY. Chudinov, E. G.; Shvetsov, I. K. Radiokhimiya, 7: 188-91(1965). (In Russian).

On the basis of the instability constant of complex compounds of pentavalent neptunium with the instability constants of compounds formed with different metals with ligands, it was found that the complexing ability of pentavalent neptunium is close to that of the divalent transition elements Zn, Mn, and Cd. (tr-auth)

**1849** THE STATE OF Pu(IV) AT pH = 1.0 TO 12.0 AND PLUTONIUM CONCENTRATION $2 \times 10^{-5}$M. Grebenshchikova, V. I.; Davydov, Yu. P. Radiokhimiya, 7: 191-5 (1965). (In Russian).

By comparison of results on the adsorption and desorption of Pu(IV) with silica gel using ultrafiltration and centrifugal methods it was found that at concentrations of $2 \times 10^{-5}$M tetravalent Pu exists in solution up to pH = 1.4 in the ionic form, but beginning with pH = 1.4 to 12.0 it exists in the colloidal state with distinct degrees of dispersion of the colloidal particles. Overcharging of the colloidal particles of Pu(IV) was observed at pH = 8.0 to 8.5. (tr-auth)

**1850** ON THE SYNTHESIS OF SOME POLONIUM $\alpha$-NAPHTHYL DERIVATIVES. Nefedov, V. D.; Toropova, M. A.; Zhuravlev, V. E.; Levchenko, A. V. Radiokhimiya, 7: 203-7(1965). (In Russian).

By the use of classical methods of synthesis and the Grignard reagent the following $\alpha$-naphthyl derivatives of Po were prepared and identified by paper chromatography: $Po(\alpha\text{-}Cl_{10}H_7)_2$, $Po(\alpha\text{-}C_{10}H_7)_2Cl_2$, $Po(\alpha\text{-}C_{10}H_7)_2Br_2$, $Po(\alpha\text{-}C_{10}H_7)_2I_2$, $Po(\alpha\text{-}C_{10}H_7)_2F_2$, $Po(\alpha\text{-}C_{10}H_7)_3Cl$, $Po(\alpha\text{-}C_{10}H_7)_3Br$, $Po(\alpha\text{-}C_{10}H_7)_3I$, $Po(\alpha\text{-}C_{10}H_7)_3Cl \cdot HgCl_2$. (tr-auth)

**1851** KINETICS OF $UO_2$ AND Fe(III) REACTIONS IN PERCHLORIC ACIDS. Kanevskii, E. A.; Filippov, A. P. Radiokhimiya, 7: 207-14(1965). (In Russian).

A method for the determination of the order of reaction for the dissolution of solids with respect to one of the solution components is proposed. For all such heterogeneous

processes a method for the determination of the velocity constant of parallel reactions was developed. It was established that the interaction of $UO_2$ and the ions $Fe^{3+}$, $FeOH^{2+}$, $Fe(OH)_2^+$, and $Fe(OH)_4^{+}$ in perchloric acid solutions is a first order reaction with respect to Fe(III). The formation of U(VI) is connected to the rapid disproportionation reaction of U(V). The velocity constants of the parallel reactions (III, 1) – (III, 4) have the following values: $K_1 \cong K_4 \cong 1$, $K_2 \cong 10$, and $K_3 \cong 10{,}000$. Therefore the hydrolyzing ions $Fe(OH)^{2+}$, $Fe_2(OH)_2^{4+}$, and particularly $Fe(OH)_2^+$, are characterized to a great extent by large oxidizing activities in the given heterogeneous processes in comparison with the $Fe^{3+}$ ions. (tr-auth)

**1852** PHYSICO-CHEMICAL STUDIES OF SOME RADIUM COMPOUNDS. I. IONIC REFRACTION OF RADIUM. Vdovenko, V. M.; Dubasov, Yu. V. Radiokhimiya, 7: 214-20(1965). (In Russian).

The indexes of refraction and the density of aqueous solutions of radium bromide and chloride were measured. The molar refraction of the compound was calculated with an infinitely large light wave as equal to 29.8 ± 0.6 and 23.5 ± 1.2 $cm^3$, respectively. From the data on the refraction of $RaBr_2$ and $RaCl_2$ the ion refraction of radium was calculated equal to 5.9 ± 0.8 $cm^3$. From the results it was found that the comparatively small increase of the ionic refraction of radium with respect to barium can be explained by the small screening charge of the radium nucleus by the $4f^{14}$ electrons. (tr-auth)

**1853** INVESTIGATION OF Ru(IV) SOLUTIONS IN PERCHLORIC AND SULFURIC ACIDS. Vdovenko, V. M.; Lazarev, L. N.; Khvorostin, Ya. S. Radiokhimiya, 7: 232-40(1965). (In Russian).

Conditions for the preparation of solutions of the monomer form of Ru(IV) in perchloric acid by reduction of $RuO_4$ solutions with hydrogen peroxide were found. It was established that the monomer ions of Ru(IV) exist in the solution in the form of doubly charged cations, probably $RuO^{2+}$. The existence in the sulfuric acid solution of polymer compounds with an oxidation degree for ruthenium of 3.5 was found. The complex formation of $RuO^{2+}$ with $HSO_4^-$ ions was investigated by the cation exchange method. It was found that in the concentration interval of $8.8 \times 10^{-3}$ to 1.0M for $HSO_4^-$ ions the complex $RuOSO_4$ was formed. The equilibrium constant for the reaction of the formation of this complex was $K_1 = 12.5 \pm 1.2$ at $\mu = 2.0$ and $K_1 = 6.6 \pm 1$ at $\mu = 4.0$. (tr-auth)

**1854** CERTAIN POLONIUM π-ANISYL DERIVATIVES. Nefedov, V. C.; Zhuravlev, V. E.; Toropova, M. A.; Gracheva, L. N.; Levchenko, A. V. Radiokhimiya, 7: 245-6 (1965). (In Russian).

By use of the Grignard reaction the following π-anisyl derivatives of polonium were prepared and identified (by paper chromatography) for the first time; $Po(\pi\text{-}CH_3\text{-}O\text{-}C_6H_4)_2$, $Po(\pi\text{-}CH_3\text{-}O\text{-}C_6H_4)_2Cl_2$, $Po(\pi\text{-}CH_3\text{-}O\text{-}C_6H_4)_2F_2$, $Po(\pi\text{-}CH_3\text{-}O\text{-}C_6H_4)_3Cl$, $Po(\pi\text{-}CH_3\text{-}O\text{-}C_6H_4)_3Br$ and $Po(\pi\text{-}CH_3\text{-}O\text{-}C_6H_4)_3I$. (tr-auth)

**1855** ON COMPLEXING OF ACTINIDE ELEMENTS. Geletseanu, I.; Lapitskii, A. V. Radiokhimiya, 7: 280-3 (1965). (In Russian).

On the basis of theoretical representations on energy bonds obtainable with 7s, 6d, and 5f electrons and of the theory of ligand fields on materials with a large number of experimental models, obtained from literature data, the stability of the complex compounds of the actinide elements was compared. Factors affecting the stability of the complex compounds formed of actinide elements with different ligands were considered. (tr-auth)

**1856** ON LANTHANUM CITRATE COMPLEXES OF 1:1 COMPOSITION. Ivanchenko, A. F.; Kirin, I. S.; Makashev, Yu. A. Radiokhimiya, 7: 283-8(1965). (In Russian).

A complex of lanthanum citric acid was separated in the solid form. The pH-metric investigations and measurements of electrical conductivity by the method of isomolar series of aqueous systems containing $La^{3+}$ and the groups $Cit^{3-}$, $HCit^{2-}$, and $H_2Cit^-$ are reported. The maximum and minimum points of some parameters of the systems with the ratios Cit/La of 1:1 forming in solution the complexes $LaH[Cit]^+$ and $[LaCit]^0$ were determined. The solubility of freshly precipitated lanthanum complexes in water was determined at the temperature of 25.0 ± 0.0°C and was found to equal $2.6 \pm 0.2 \times 10^{-3}$M. The composition of the compounds separated in the solid state was determined. The chemical formula of the complex in the precipitate is $[LaCit(H_2O)] \cdot 2H_2O$. (tr-auth)

**1857** PARTIAL THERMODYNAMIC EQUILIBRIUM IN NONEQUILIBRIUM SYSTEMS. I. REACTION OF PLUTONIUM WITH HYDROGEN PEROXIDE IN PRESENCE OF OTHER ALLOYS. Nikol'skii, B. P.; Posvol'skii, M. V.; Krylov, L. I. Radiokhimiya, 7: 298-305(1965). (In Russian).

The reaction of plutonium with $H_2O_2$ under conditions of complex compatibility leads to the establishment of thermodynamic equilibrium between valent and electron forms of Pu, the activity of which is assigned to similar solutions with the ratio of the kinetic factors of the oxidation and reduction reactions of $H_2O_2$. The ratio of the valent form at equal weight depends on the nature of the addend and also on the total concentration of Pu in the solution. With increases of total concentration of Pu in the solution the percentage of the "oxidized" form decreases. In buffered solutions of malonic and maleic acid the equilibrium is displaced to the side of the formation of the oxidized form, in solutions of complexes it is displaced to the side of the reduced form. This is connected to the comparative stability of the complexes formed by the different valent forms of Pu with the peroxide groups and with the different organic ligands. (tr-auth)

**1858** ENTROPY CHARACTERISTICS OF THE SMALLEST AND LARGEST HYDRATIONS OF RARE EARTH AND ACTINIDE IONS. Krestov, G. A. Radiokhimiya, 7: 305-10(1965). (In Russian).

The entropy characteristics of the smallest and largest hydrations of monoatomic ions of the rare earth and actinide elements were determined. The singularities of the changes of the entropy of water in the range of the smallest and largest hydrations and their dependence on the basic characteristic of the ions (charge and radius) are indicated and the interconnection of these quantities with the coordination numbers is shown. (tr-auth)

**1859** THERMAL CAPACITY OF SOME FRANCIUM AND ASTATINE CRYSTALLINE COMPOUNDS AT 0 TO 300 deg K. Krestov, G. A.; Lapin, V. A. Radiokhimiya, 7: 311-15(1965). (In Russian).

On the basis of the determination of the thermal capacity and entropy of crystalline halides of the alkali metals, by application of the frequency of corresponding gaseous molecules, thermal capacity and entropy were calculated for the solid halides of francium and for the astatides of the alkali metals in the temperature interval from 0 to 300°K. The regularities and fluctuations of these magnitudes are shown. (tr-auth)

**1860** APPLICATION OF A COMPLEX EMANATION-THERMAL METHOD FOR STUDYING THE KCl–$CaCl_2$ CONSTITUTION DIAGRAM. Zaborenko, K. B.; Polyakov, V. P.; Shoroshev, Yu. G. Radiokhimiya, 7: 324-9(1965). (In Russian).

The effectiveness of the complex emanation-thermal method for the investigation of the phase transformations in salt systems was investigated. It has numerous advantages with respect to other methods of physical-chemical analysis both in methodic relations and in completeness of the information received. The complex character of the process of fusion is shown for $CaCl_2$. (tr-auth)

**1861** APPLICATION OF COMPLEX EMANATION-THERMAL METHOD IN STUDIES OF THE CaO–$Fe_2O_3$ CONSTITUTION DIAGRAM. Zaborenko, K. B.; Polyakov, V. P.; Shoroshev, Yu. G. Radiokhimiya, 7: 329-35(1965). (In Russian).

The possibilities for use of the emanation-thermal method during investigation of the phase transformation in oxide systems are shown for studies of the phase diagram of $CaO-Fe_2O_3$. The temperature for the formation of polycalcium ferrite was determined to be 1130°C. The temperature of the other phase transformations obtained from the emanation curves agreed with the literature data. The complex emanation-thermal method has all of the advantages of dynamic methods (in comparison with quenching methods) and can be used successfully during the study of phase diagrams of oxide systems. (tr-auth)

**1862** PRODUCTION AND PREPARATION OF POLYMETHYLMETHACRYLATE KRYPTONATES. Trofimova, A. M.; Pankov, A. M.; Kovarskii, A. P. Radiokhimiya, 7: 359-61(1965). (In Russian).

A simple method for the preparation of kryptonates on a base of solid organic materials was suggested. A polymethylmethacrylate kryptonate was prepared that had a very high stability with respect to the kryptonates prepared using other organic materials. (tr-auth)

**1863** ADVANCED HIGH TEMPERATURE THERMAL ANALYSIS APPARATUS EMPLOYING DERIVATIVE AND DIFFERENTIAL TECHNIQUES. Rupert, George N. (Los Alamos Scientific Lab., N. Mex.). Rev. Sci. Instrum., 36: 1629-36(Nov. 1965). (LA-DC-7022).

The techniques of thermal analysis, derivative thermal analysis, differential thermal analysis, and thermal derivative thermal analysis (temperature vs derivative-of-temperature curves), are combined in this apparatus. High sensitivity is available for detecting small heat effects (less than 0.2 cal/sec) produced by rapid phase transitions in cooling or heating samples, and accurately determining their temperatures. Light from the incandescent samples is sensed by photoconductive diodes. Thermocouples with suitable amplifiers may be used for lower temperature studies. The diode currents after processing are displayed on a dual-trace storage oscilloscope. The temperatures of the samples, which are heated indirectly by induced radio frequency currents, are measured using a calibrated beam splitter and optical pyrometer. A description of a light source used to demonstrate the various displays by simulating thermal arrests in the cooling or heating curve of an incandescent sample is included. Illustrations are given for typical thermal analysis displays in the Nb-C, Ti-C, and V-C systems. (auth)

**1864** MELTING POINTS OF CURIUM AND AMERICIUM TRIFLUORIDES. Burnett, J. L. (Oak Ridge National Lab., Tenn.). Trans. Amer. Soc., 8: 335(Nov. 1965).

**1865** DIFFUSION COEFFICIENT OF WATER IN WATER AND IN SOME ALKALINE EARTH CHLORIDE SOLUTIONS AT 25 deg C. Jones, J. R.; Rowlands, D. L. G.; Monk, C. G. (Univ. Coll. of Wales, Aberystwyth). Trans. Faraday Soc., 61: 1384-8(July 1965).

A continually sampled capillary tube method was used to obtain the self-diffusion coefficient of water in water and in 0.25, 0.5, and 1.0M alkaline earth chloride solutions (Mg, Ca, Sr, and Ba chlorides) by using trace amounts of tritium. The trends with salt concentrations were examined by reference to viscosities, ion hydration, and ion sizes. The values of diffusion constant (D) of Sr in 0.25, 0.5, and 1M $SrCl_2$ solution were 2.121, 2.033, and 1.77 ($\times 10^{-5}$), respectively. The average result for the diffusion coefficient in water ($D(H_2O)$) was $2.22 \times 10^{-5}$ cm $sec^{-1}$. This is 1.5% lower than previously obtained, viz, $2.25 \times 10^{-5} \pm 1\%$, using both deuterium and tritium as tracers in a sheared boundary apparatus. To see how far the diffusion coefficients in the salt solutions are related to the viscosities of the solutions, values of $D(H_2O)/\eta$ were calculated where $\eta$ is the viscosity relative to that of water. The resulting calculations are all lower than the D(expt.) values. For all the solutions reported, D(expt.) decreases almost linearly with increasing salt concentrations. This feature may be expressed by: $D(soln) = D(H_2O)(1 - hM)$, where h is a parameter and M is salt molarity. Except for two solutions (0.52M LiBr, difference = 5.5%; 40.5M NaCl, difference = 4%), an average agreement of about ±1% between D(expt.) and D(calc.) was obtained by using this equation, on choosing a suitable value of h. If the hydration effect is the important one, i.e., $hM = f$ (f = fraction of water attached to the ions), the h values should be related to the average hydration numbers of the ions. Alternatively, if ion size is the important factor, i.e., $ax = hM$, the h values should be related to the sizes of the hydrated ions. (BBB)

**1866** FORMAL KINETICS OF SOME COMPETITIVE BIMOLECULAR REACTIONS AND CALCULATION OF KINETIC ISOTOPE EFFECT IN THE DISTRIBUTION OF ISOTOPIC MOLECULES. Skorobogatov, G. A. Vestn. Leningr. Univ., No. 10, Ser. Fiz. Khim., No. 1, 128-41 (1965). (In Russian).

The system of the reactions of $A \rightarrow B + (D)$, $A + B \rightarrow C + (E)$, $A + C \rightarrow F + (G)$, $A \rightarrow H$ is considered for the case, when B and C components are mixtures of any number of similar compounds, e. g. isotopic molecules. It is shown that the corresponding formal-kinetic problem is described by the system of differential equations always reduced to the integral and not expressed in elemental functions. In the less common case of the system of the reactions of $A + B \rightarrow C + (E)$, $A + C \rightarrow F + (G)$ the formal-kinetic problem is reduced as before to the integral not expressed in elemental functions, but for calculating the final distribution (i.e. under infinite time) of all the components it is enough to solve the algebraic equation with one unknown. The results obtained can be applied for calculating the kinetic isotope effect in the distribution of isotopic molecules. (auth)

**1867** ON THE ABSORPTION OF THE BLUE SOLUTIONS OF EUROPIUM AND BERYLLIUM IN LIQUID AMMONIA. Ostertag, Werner; Ruedorff, Walter; Suhr, Harald (Universitaet, Tuebingen, Ger.). Z. Naturforsch., 20b: 599-601(June 1965). (In German).

The absorption spectra of blue europium and beryllium solutions were measured. The results were used to establish whether the nature of these blue metal solutions is the same as that of the blue alkali ammonia solutions. It was determined that Eu is present in solution as the $Eu^{2+}$ ion. (J.S.R.)

**1868** PHYSICO-CHEMICAL PROPERTIES OF CRYSTAL HYDRATES OF TERBIUM SUBGROUP RARE EARTH SULFATES. Zaitseva, L. L.; Ilyashenko, V. S.; Konarev, M. I.; Konovalov, L. N.; Lipis, L. V.; Chebotarev, N. T. Zh. Neorgan. Khim., 10: 1761-70(Aug. 1965). (In Russian).

The octohydrate sulfates of Eu, Gd, and Tb were investigated in the temperature interval from 20 to 1200°C using thermographic, thermogravimetric, and x-ray methods of analysis. On the basis of thermogram and x-ray diagram analyses it was established that the dehydration process of the octohydrates, accompanied by variations of the crystal structure, proceeds in two steps. The first stage of the process is connected with the formation of crystal hydrides containing two molecules of water and the second stage is connected with the formation of a completely dehydrated salt. The lattice parameters of the octohydrates were calculated and the results showed an isostructure between the salts. It was established that the dehydrate has a cubic structure with the lattice constant $a = 6.36 \pm 0.02$ Å. The crystal structure of the dehydrated sulfates of Eu, Gd, and Tb were determined. It was established that the dehydrated salts have a cubic lattice the constants of which decrease with increasing atomic number of the rare earths. (P.C.H.)

**1869** WATER SOLUBILITY OF COMPLEX COMPOUNDS OF LANTHANUM, CERIUM, PRASEODYMIUM, NEODYMIUM, AND SAMARIUM ACETATES WITH THIOUREA. Frontasev, V. P.; Sakharova, Yu. G.; Sakharova, N. N. (Saratov State Univ., USSR). Zh. Neorgan. Khim., 10: 1816-21(Aug. 1965). (In Russian).

Complex acetate compounds of La, Ce, Pr, Nd, and Sm with thiourea have good water solubility, which increases with increasing temperature. The essential difference in the solubility of the compounds studied was established at

20, 30, and 40°C. The existence of complex compounds in saturated aqueous solutions, with the exception of Sm compounds, was limited by the temperature interval. Their decomposition was observed with separation from the solution of simple acetates of the corresponding rare earths. A new complex compound of Sm acetate with thiourea with the composition $Sm(C_2H_3O_2)_3 \cdot CS(NH_2)_2 \cdot 0.5H_2O$ was synthesized. (tr-auth)

**1870** REACTIONS OF YTTRIUM GROUP RARE EARTH CHLORIDES WITH SODIUM FLUOSILICON. Chalova, E. P.; Bleshinskii, S. V. (Inst. of Inorganic and Physical Chemistry, Academy of Sciences, USSR). Zh. Neorgan. Khim., 10: 1853-6(Aug. 1965). (In Russian).

The reactions of chlorides of the yttrium rare earth elements with sodium fluosilicate were investigated in aqueous solutions at 25 ± 0.1°C. The composition of the precipitate was determined. It was established that the rare earth elements are completely precipitated by molar additions of $Na_2SiF_6$ to the chloride with formation of the fluoride. The fluoride is formed in all cases, and does not depend on the quantity of $Na_2SiF_6$ introduced. The sodium fluosilicate can be used for the selective precipitation of the rare earth elements as fluorides at pH 2 to 2.5. (tr-auth)

**1871** THE $UO_2$–$PbO_2$ SYSTEM. Kirkinskii, V. A.; Makarov, E. S. Zh. Neorgan. Khim., 10: 1872-6(Aug. 1965). (In Russian).

The interaction and phase equilibrium in the $UO_2-PbO_2$ system was studied by x-ray and microscopic analysis methods. The interaction of the components begins after not very long prolonged annealing at 150 to 200°C, i.e., at temperatures considerably lower than in the $UO_2-PbO_2$ system. The activation energy necessary for the oxidation-reduction reaction is considerably lower than the activation energy for reactions leading to the regulation of U and lead and the formation of lead uranate, which begins even at 400°C. At temperatures from 200 to 250°C oxidation-reduction reactions proceed between the original components with the formation of $UO_{2+x}$ (where x varies from 0.1 to 0.4) and $Pb_2O_3$ or $Pb_2O_4$ with different ratios. At 300°C the original uranium oxide is oxidized to $U_3O_8$ and $PbO_2$ is reduced to $Pb_3O_4$. The interaction of the components at 400 and 500°C leads to the formation of the compound $PbUO_{4-x}$ of cubic syngony, if in the original mixture $UO_2$ is in excess and $PbUO_4$ of rhombic syngony with excess $PbO_2$. No solid solutions between $UO_2$ and $PbO_2$ were detected. (P.C.H.)

**1872** THE $YCl_3$–NaCl–KCl SYSTEM. Korshunov, B. G.; Drobot, D. V.; Shevtsova, Z. N. (Moscow Inst. of Fine Chemical Tech.). Zh. Neorgan. Khim., 10: 1901-5 (Aug. 1965). (In Russian).

Interactions of the components in the $YCl_3-NaCl-KCl$ system was investigated by thermal analysis during their crystallization from melts. The fusibility diagram of the system was constructed, the transformation below the surface of the liquidus was noticed, and the boundary range of the crystallization phase was determined. The formation of γ phases on the basis of 3 components was noted in the system. The composition of the γ phase corresponded to $KNa_3Y_2Cl_{10}$ and congruent melting was found at 545°C. An hypothesis was made on the formation of similar compounds in the system $RCl_3-NaCl-KCl$ for rare earth elements with an ionic radius smaller than that of yttrium. (tr-auth)

**1873** SOLUBILITY OF YTTRIUM AND ERBIUM PHOSPHATES. Vagina, N. S. Zh. Neorgan. Khim., 10: 1938-9(Aug. 1965). (In Russian).

The interaction of yttrium and erbium salts with potassium phosphate was investigated. It was established that in the pH interval from 4.4 to 4.6 the ratio of Y and Er to $PO_4^{3-}$ is 1:1. The solubility of the simple Y and Er phosphates in water and salt solutions and sulfuric acid was determined at different concentrations at 25 ± 0.1°C. (tr-auth)

**1874** A STUDY OF BONDING IN IRON COMPOUNDS USING THE MOESSBAUER EFFECT [Thesis]. Erickson, Nils Eric. Seattle, Univ. of Washington, 1964. 213p.

A series of studies was designed to investigate the relationship between certain features of Mössbauer spectra and the bonding characteristics of iron in various types of compounds. The Mössbauer spectra of a number of low-spin ferrous and ferric mixed cyanide-di-imine complexes were studied in which it was found that the chemical isomeric (CI) shift is an approximate additive property of the numbers and types of ligands bonded to the iron. This observation indicates that it is possible to study the relative effects of various groups on Mössbauer CI shifts by looking at appropriately substituted compounds even though it is not possible to prepare the fully substituted species. Thus, by investigating $[Fe(CN)_5NO]^{-2}$ and $[Fe(CN)_5CO]^{-3}$, an ordering of the most common strong-field ligands was made in terms of their ability to produce negative CI shift values. This ordering is $NO^+ > CO > CH_3NC > CN^- \gg$ bipy > phen, which is the same ranking these ligands have in the spectrochemical series. The CI shift data are interpreted in terms of increasing 3d electron delocalization as the dominant factor in producing negative shifts. This interpretation is borne out by the observation that the field gradient in the ferric cyanide-di-imine complexes decreases as the CI shift becomes more negative. In high-spin compounds it was found that there was no longer a correlation between CI shift and spectrochemical series ranking of ligands, but there was a correlation with the nephelauxetic series ranking of ligands. This is also taken as evidence that 3d electron delocalization is the major factor in determining CI shifts. It was found that when one plots the difference in CI shifts between similar ferrous-ferric compounds versus the average shift of the pair, the resulting curve is linear and is valid for both high- and low-spin compounds. The difference in shift decreases as the average shift becomes more negative. It was also found that there is a linear relationship between the average CI shift of the ferrous-ferric cyanide-di-imine complexes and the redox potentials of these pairs. A Mössbauer study of the compound $Na_2Fe(CO)_4$ containing iron with a formal oxidation state of minus two is reported. This substance produces one of the largest negative shifts known. Also reported are Mössbauer studies of cis-trans isomerism in iron compounds where the isomerism arises from the relative positions of two groups around a single metal atom. It is found that in contrast to binuclear species, there is a significant difference in CI shifts and quadrupole splitting between the two isomers. (Dissertation Abstr.)

**1875** A LIGHT-SCATTERING STUDY OF THE NATURE OF NIOBIUM(V) IN AQUEOUS SOLUTION [Thesis]. Conrad, Raymond Walter. Auburn, Ala., Auburn Univ., 1964. 102p.

The size of the species obtained by dissolving hydrated niobium pentoxide in an aqueous solution of oxalic acid was determined from turbidity measurements using the Debye theory of light scattering. The species was shown to be mononuclear when fresh moist hydrated niobium pentoxide is used to prepare the solutions. The use of dried hydrated niobium pentoxide yielded a species in solution with a higher degree of aggregation. Differential refractive index measurements showed the mononuclear species to have a 3:1 oxalate:niobium mole ratio. An investigation of the nature of the alkali metal niobate species in strongly basic solution was performed, using the multi-component theory of light scattering. This theory was applied to the results of turbidity and depolarization measurements on solutions of the niobate, and the species in solution was shown to be ca hexameric with an unsymmetrical structure. (Dissertation Abstr.)

**1876** ROTATIONAL SPECTROSCOPY OF THE ALKALI FLUORIDES [Thesis]. Veazey, Sidney Edwin. Durham, N. C., Duke Univ., 1965. 90p.

Rotational transitions of the alkali metal fluorides CsF, $Rb^{87}F$, $Rb^{85}F$, KF, NaF, and $Li^7F$ were experimentally measured in the millimeter and submillimeter wave regions where no previous measurements existed.

The work was accomplished with a high-temperature molecular-beam microwave spectrometer previously utilized for study of the alkali bromides, iodides, and chlorides. A more reliable oven was constructed and used to vaporize the alkali fluorides at temperatures up to 1100°C. Measurements on rotational transitions as high as $J = 27 \rightarrow 28$ and in the first three vibrational states gave $Y_{01}$, $Y_{11}$, and $Y_{12}$ more accurately for the most part than previous measurements, and gave $Y_{02}$ and $Y_{21}$ for the first time. From these, the first four coefficients in Dunham's potential expansion, mass ratios of isotopes, $Y_{10}$ and $Y_{20}$, moments of inertia, and internuclear distances were derived. (Dissertation Abstr.)

**1877** THE FAR INFRARED SPECTRUM OF $D_2O$ [Thesis]. Slone, Hasel James Jr. Columbus, Ohio, Ohio State Univ., 1964. 112p.

The far infrared spectrograph at the Ohio State University was used to obtain the spectrum of $D_2O$ in the spectral region from 7 $cm^{-1}$ to 115 $cm^{-1}$. The experimental positions and relative intensities of the pure rotation absorption spectrum were obtained. Absorption maxima were located with an accuracy of about 0.05 $cm^{-1}$. Lines 0.3 $cm^{-1}$ apart were partially resolved throughout the spectrum. An analysis of the spectrum provided ground state rotational constants and ground centrifugal distortional constants. The method of determining the distortional constants is described. Some problems in the optical design of the multiple traversal absorption cell used are discussed. (Dissertation Abstr.)

**1878** FACTORS INFLUENCING PERMEABILITY AND DIFFUSION OF RADON IN SYNTHETIC SANDSTONES [Thesis]. Evans, Hilton B. Salt Lake City, Univ. of Utah, 1959. 104p.

Artificial sandstone cores were constructed in which the porosity, cement content, and grain size were controlled. Except for the two ends, the cores were sealed in lucite. The relation between the permeability $\kappa$ (millidarcys) and the fractional porosity $\Phi$ of artificial cores, in which only the porosity varied, was found to be of the form $\kappa = \alpha e^{\beta\Phi}$ (where $\alpha$ and $\beta$ are factors dependent on the grain size and cement content). The relation between the permeability $\kappa$ (millidarcys) and the mean grain size g (cm) of cores in which only the grain size varied was found to be of the form $\kappa = \gamma g^{\sigma}$ (where $\sigma$ and $\gamma$ are factors dependent on the porosity and cement content). A diffusion system, consisting of two ionization chambers connected by a section of tygon tubing containing an artificial core, was developed to measure the apparent diffusion coefficient of radon in an argon-saturated core. Empirical methods were developed to correct the observed diffusion coefficients for the effect of the length of the tubing connecting the two chambers and for the effect of nonequilibrium between radon and the decay products in the chambers. The apparent diffusion coefficients of cores, in which the porosity and grain size were constant, were found to increase with decreasing cement content. For cores in which only the porosity varied, the apparent diffusion coefficients increased with increasing porosity. No clear relationship could be established between the apparent diffusion coefficient and the mean grain size of cores in which only the grain size varied although the general trend indicated that the apparent diffusion coefficient increased with increasing grain size. (Dissertation Abstr.)

**1879** CESIUM SORPTION BY HYDROBIOTITE [Thesis]. Fruh, Erwin Gustav. Madison, Wis., Univ. of Wisconsin, 1965. 301p.

Sorption of cesium by mixed layer silicate clays was investigated in laboratory batch tests. The presence of other solutes in the completely mixed cesium-clay suspension decreased or inhibited cesium sorption. A model was developed to relate the effect of the various experimental conditions on the sorption of the cesium by the clays. The experimental results show the possible significance of the behavior-chemistry and transport of various trace-pollutants by suspended particulates in the aquatic environment. (A.G.W.)

**1880** THE THERMODYNAMICS OF THE RHENIUM–OXYGEN AND MOLYBDENUM–OXYGEN SYSTEMS AND THE DEFECT STRUCTURE OF ALPHA TANTALUM PENTOXIDE [Thesis]. Foster, James Sheridan. Columbus, Ohio, Ohio State Univ., 1964. 148p.

The standard free energy of formation of $ReO_2$ was determined with solid-electrolyte, galvanic cells having $Zr_{0.85}Ca_{0.15}O_{1.85}$ electrolytes. Reference electrodes of $Ni-NiO$ and $Cu-Cu_2O$ were used. The following equation was derived for temperatures from 950° to 1100°K: $\Delta F^{0}_{ReO_2} = -102750 + 40.67T$ (±300) cal/mole. Attempts were made to determine the melting point of $ReO_3$ at temperatures up to 600°C, and no evidence of melting was observed. However, evidence of decomposition to $ReO_2$ and gaseous $Re_2O_7$ was found. Standard free energy equations for the rhenium oxides, $ReO_2$, $ReO_3$, and $Re_2O_7$, were derived from this investigation from data in the literature, and from some estimated values of heat capacities. A phase diagram for the rhenium–oxygen system was proposed. The range of stability of $MoO_2$ was established by measuring the standard free energy of formation of $Mo_4O_{11}$ with solid-electrolyte, galvanic cells having either $Ni-NiO$ or $Fe-Fe_xO$ as the reference electrode. The equation derived for $\Delta F^{0}_{Mo_4O_{11}}$ for temperatures from 920° to 1090°K was $\Delta F^{0}_{Mo_4O_{11}} = -679500 + 223.3T$ (±1250), cal/mole. A peritectic reaction involving the decomposition of $Mo_4O_{11}$ to $MoO_2$ and liquid $MoO_3$ at 825°C was observed. Standard free energy versus temperature and phase diagrams based on this investigation and data in the literature were derived. The defect structure of alpha tantalum pentoxide was studied at temperatures from 1404° to 1499°C in atmospheres with oxygen partial pressures ranging from one to $10^{-9}$ atmospheres by measuring the resistance of a polycrystalline specimen. Complex behavior was observed involving maxima in the resistance at intermediate oxygen pressures. For pressures below the maxima the data were rationalized on the basis of an anion deficient structure containing doubly ionized oxygen vacancies. At high pressures, an anion-excess structure with doubly ionized oxygen interstitials present was indicated, although the data did not fit the model very well. An explanation of the behavior at high oxygen pressures involving interaction of the oxygen interstitials and splitting of their acceptor levels was proposed. A heat of formation of oxygen vacancies equal to 200,000 cal/mole was calculated along with a value of 99,000 cal/mole for the heat of formation of oxygen interstitials. (Dissertation Abstr.)

**1881** STUDIES IN FLUORINE CHEMISTRY: I. SOME FLUORINE CONTAINING COMPOUNDS OF XENON. II. THE ROLE OF WATER IN THE SYNTHESIS OF TRIFLUOROACETYL HYPOFLUORITE [Thesis]. Gard, Gary Lee. Seattle, Univ. of Washington, 1964. 84p.

Xenon difluoride was shown to react with water giving xenon, oxygen, and hydrogen fluoride. In the presence of potassium iodide, iodine is liberated. With sulfur trioxide only fluorination occurs liberating free xenon. Xenon hexafluoride reacts with water to give xenic acid, with hydrogen chloride to give chlorine, and with perfluorocyclopentene to give perfluorocyclopentane. It also reacts with antimony pentafluoride to give solid adducts ($XeF_6 \cdot SbF_5$, $XeF_6 \cdot 2SbF_5$, and $2XeF_6 \cdot SbF_5$). These adducts were characterized by their physical properties and powder spectra. Proof for these adducts was obtained both by analysis and synthesis. In a study of the role of water vapor in allowing trifluoroacetyl hypofluorite to be formed by the reaction of fluorine with trifluoroacetic acid vapor, it was found that the yield of the hypofluorite was negligible when water was absent and that increasing the amount of water vapor up to a certain limit caused an increase in the yield of the hypofluorite. Above this limit, additional water appeared to have no influence on the yield. It appears likely that the role of water in the reaction is to form a reactive intermediate by reaction with fluorine or trifluoroacetic acid. Attempts to prepare a "solid hypofluorite" with antimony pentafluoride were unsuccessful, but a convenient preparation of $SF_5OF$ and $SF_5OOSF_5$ was developed. Peroxydisulfuryl difluoride was found to act as a fluorinating

agent and possibly as an oxygenating-fluorinating reagent. (Dissertation Abstr.)

**1882** THERMODYNAMIC PROPERTIES OF MOLYBDENUM(III) CHLORIDE IN MOLTEN ALKALI METAL CHLORIDES. Selis, Sidney M. (General Motors Corp., Warren, Mich.). 16p. (CONF-650502-8). Gmelin, AED-CONF-65-169-11.

From Electrochemical Society, San Francisco.

Using emf methods, partial thermodynamic values in molten LiCl–KCl were precisely determined from 460 to 540°C in the Mo concentration range of 0.01 to 1 mole per liter. At 460°C the free energy of formation of the molybdenum(III) chloride in a decimolar solution was $-67{,}000 \pm 100$ calories per mole, and the corresponding entropy change was $-23 \pm 1$ calories per degree per mole. Extrapolated to 450°C, the potential of Mo/Mo(III) (1 molar in LiCl–KCl) vs Pt/Pt(II) (1 molar) was $-0.603 \pm 0.002$ v. There was a strong solvent cation effect due to coulombic, steric, and other contributions, and the excess free energy of $MoCl_3$ in KCl was much more negative than in LiCl–KCl. (auth)

**1883** CESIUM PRODUCTION. Blue, Robert D.; Moolenaar, Robert J. (to Dow Chemical Co.). U. S. Patent 3,201,229. Aug. 17, 1965. Filed Dec. 20, 1961.

A method for the production of Cs from a cesium halide consists of heating a bath of the cesium halide and an alkali metal halide in a closed container to a temperature at which the bath is molten and maintaining the bath at a temperature below the boiling point of Cs while the bath is electrolyzed to produce the alkali metal and gaseous halogen. The halogen is removed from contact with the bath as it is formed. The direct current source is disconnected and the container is evacuated. The metal–salt bath is heated to a temperature above the boiling point of Cs to simultaneously reduce and distill the Cs. (B.L.M.)

**1884** PRODUCTION OF HEAVY WATER. Guernsey, Edwin Owens (to Socony Mobil Oil Co., Inc.). U. S. Patent 3,206,365. Sept. 14, 1965. Filed Feb. 8, 1963.

A dual-temperature steam-hydrogen catalytic exchange process is described for making heavy water in which a continuously recirculating supply of hydrogen is made to transfer a portion of its deuterium content to steam in a low temperature zone and then to replenish its deuterium content by transfer from fresh steam in a high temperature zone. The exchange in both the low and high temperature zones is carried out in the presence of fissionable material suitably mixed with the catalyst. (auth)

**1885** PROCESS OF PREPARATION OF URANIUM COMPOUNDS FROM URANIUM–MOLYBDENUM ALLOYS. Bourgeois, Michel; Faugeras, Pierre (to Commissariat a l'Energie Atomique). U. S. Patent 3,208,815. Sept. 28, 1965. Priority date Aug. 3, 1960, France.

A process for the preparation of substantially Mo-free $UO_2F_2$, $UF_4$, and uranium oxides from U–Mo alloys consists of initiating a reaction between the alloy and a gaseous mixture composed of HF and an oxygen-containing gas at a temperature of between 100 and 200°C. The reaction eliminates Mo as a volatile oxyhalide and leaves a nonvolatile residue containing the uranium compound. The reaction is continued until substantially all the Mo has been eliminated. (B.L.M.)

## Organic Chemistry

*Refer also to abstract 1817.*

**1886** (CONF-641123-1) CHROMATOGRAFO PREPARATIVO DE FASE MOVIL GASEOSA. Informe No. 140. (Preparative Chromatograph of Moving-Gas Phases. Report No. 140). Bonard, Rustam T.; Videla, Gerardo J. (Comision Nacional de Energia Atomica, Buenos Aires (Argentina)). 1965. 14p. Dep. mn.

From 11th Argentina Chemical Conference, Bahia Blanca, Argentina.

The basic characteristics of a gas chromatograph design for the preparation of substances to be used in organic synthesis, especially of compounds labelled with radioisotopes, in the production of carriers of a suitable purity of infrared and mass spectrometry, and in gaseous chromatography were described. In the construction, the derivative problems of preparative chromatography were taken into consideration with emphasis on the fast injection and vaporization of large quantities of the sample and the recovery of the fractions separated. This apparatus is simple in construction and operation and resolves economically problems of preparative gaseous chromatography with an efficiency comparable to more elaborate commercial instruments. (tr-auth)

**1887** (NP–15523) TRITIACION DE FURFURAL. INFORME NO. 153. (Tritiation of Furfural. Report No. 153). Rodriguez Pasques, Rafael H. (Comision Nacional de Energia Atomica, Buenos Aires (Argentina)). 1965. 10p. Dep. mn.

Tritiated furfural was prepared by irradiating arabinose with recoil tritons indirectly produced in a nuclear reactor. Furfural was subsequently derived from the tritiated arabinose by chemical reaction. The method is comparatively simple. The specific activity obtained was 56 microcuries per gram of furfural. (auth)

**1888** HYDROGEN ISOTOPE EFFECTS IN AROMATIC SUBSTITUTION REACTIONS. Zollinger, H. (Swiss Federal Inst. of Tech., Zurich). Advan. Phys. Org. Chem., 2: 163-200(1964).

Applications of kinetic isotope effects in the study of mechanisms of aromatic substitution reactions are reviewed. The study of hydrogen isotope effects was divided into three stages: measurement of an isotope rate ratio ($k_H/k_D$, $k_H/k_T$, $k_D/k_T$, or $k_X/k_Y$ for groups other than hydrogen); elucidation of the parameters that influence the magnitude of the measured isotope effect (solvent, temperature, catalysts, etc.) and investigation of other kinetic characteristics of the reaction (acid or base catalysis, etc.); and interpretation of all results in terms of a detailed mechanism, separation of the measured isotope effect into primary and secondary effects, and interpretation of the causes for small isotope effects. Electrophilic aromatic substitution was considered in orientation studies. The reaction forms of reagents (pre-equilibria) and the mechanism of the substitution proper, i.e., the order of sequence in time of the additive combination of the electrophilic reagent and the release of the proton (or other group to be substituted) were studied. The mechanism of nucleophilic aromatic substitution was also considered along with homolytic aromatic substitution. That the mechanism of the homolytic substitution of aromatic compounds is not clear was demonstrated by two examples. The magnitude of hydrogen isotope effects led to conclusions concerning the bonding of hydrogen in the proton transfer transition state. (170 references) (BBB)

**1889** A RADIOTRACER STUDY OF PRODUCT CONTAMINATION BY CATALYTIC NICKEL. Braier, H. A.; Mott, W. E.; Schmid, B. K. (Gulf Research and Development Co., Pittsburgh). Int. J. Appl. Radiat. Isotop., 16: 611-12(Oct. 1965).

In hydrogenation experiments using a nickel-containing catalyst, samples were analyzed for nickel content by a direct radiotracer method. $^{63}Ni$ was added to the catalyst to a specific activity of 3.26 mC/g nickel. Samples were analyzed for total nickel by x-ray spectroscopy. The traces of nickel were separated from the bulk of the material, deposited on filter paper, and counted with a windowless counter. As little as $2 \times 10^{-5}$ $\mu$C of $^{63}Ni$ could be detected in 1 g of product with a standard deviation of about 20%. Data indicated that while traces of catalytic nickel entered the product during all stages of the hydrogenation experiment, the quantity was very small compared with the total nickel in the product. (M.C.G.)

**1890** PREPARATION OF $^{131}I$-LABELLED INSULIN AND ISOLATION BY GEL FILTRATION. Abdel-Wahab,

M. F. (Middle Eastern Regional Radioisotope Centre for Arab Countries, Cairo); El-Kinawi, S. A. Int. J. Appl. Radiat. Isotop., 16: 668-70(Nov. 1965).

A method for labeling beef or pork insulin with $^{131}I$ is described. The method is based on the reaction of insulin with nascent $^{131}I$ followed by a separation of the radioactive insulin using an extraction column. For confirmation of the purity of the labeled insulin an antigen-antibody reaction was used. (F.J.H.)

**1891** DEUTERIUM ISOTOPE EFFECTS IN THE DECOMPOSITIONS OF ACETYL PEROXIDE AND TWO t-BUTYL PERESTERS. Koenig, T. W.; Brewer, W. D. (Univ. of Oregon, Eugene). Tetrahedron Letters, No. 32, 2773-8(Aug. 1965).

The rates of decomposition of acetyl peroxide(I) t-butyl phenylperacetate(III) and t-butyl $\alpha$-phenylperpropionate(V) and their corresponding deuterated analogs (II, IV, VI, ($\alpha$-D) and VII ($\beta$-$D_3$)) were determined. The rates of decomposition of the acetyl peroxides were measured through the disappearance of the infrared carbonyl absorption in isooctane with and without added styrene. There was an easily discernible decrease in the rate of disappearance of II and III with deuterium substitution at the $\alpha$-position. The values of $k_H/k_D$ per deuterium atom were 1.17 and 1.14 for II and III, respectively. These values agreed with those observed for $\beta$-scission of the cumyloxy radical. There was also a small rate reduction for III on substitution of deuterium at the $\beta$ position. This value was much smaller than that observed in most solvolytic reactions. Induced decomposition by abstraction of the $\alpha$ hydrogen or deuterium may contribute to the observed $\alpha$-isotope effects for II and III. Styrene, an effective inhibitor for induced decompositions, was present in 0.5M concentration in these kinetic runs. A reduction in the rate constants for the decompositions of II and III was observed with the addition of styrene. The rate of disappearance of acetyl peroxide was reduced by the presence of styrene and the rates observed by the galvinoxyl method were still smaller, probably indicating that some induced decomposition occurred, which may be first order and thus not impart any curvature to the rate plots. There was no indication of any significant change in the observed rates of decomposition of acetyl peroxide with deuterium substitution; thus there was little or no methyl radical character in the rate-determining transition state for its decomposition. (BBB)

**1892** CATALYTIC REACTIONS OF ALIPHATIC ALCOHOLS OVER THORIUM OXIDE [Thesis]. Legg, John Wallis. Gainesville, Fla., Univ. of Florida, 1964. 72p.

Six thorium oxide catalysts were prepared by the precipitation of thorium hydroxide from thorium nitrate solution with ammonia. The hydroxide was dried, pelleted and heated under vacuum at 600° for four to twenty-nine hours. The surface area of each of the catalysts was measured. The products of the reactions of ethanol, 1-propanol, 2-propanol, 1-butanol, and 2-butanol over thoria were separated and identified. Each of the alcohols dehydrated to produce water and the appropriate olefin; 2-butanol produced 1-butene but no 2-butene. 2-Propanol and 2-butanol lost hydrogen to produce acetone and methyl ethyl ketone, respectively. 1-Propanol and 1-butanol both reacted to lose carbon monoxide and hydrogen; in the process 3-pentanol was formed from 1-propanol and 4-heptanone from 1-butanol. The tendency to dehydrate was found to be 2-propanol > 2-butanol ≥ ethanol ≫ 1-propanol > 1-butanol. An increase in catalyst surface area caused a considerable but nonlinear increase in the dehydration of ethanol, 2-propanol, and 2-butanol, but little increase in the dehydration of 1-propanol and 1-butanol. These results led to a proposal, similar to that of Schwab's, that dehydration occurs by the concerted elimination of water in pores. The alcohol molecule is proposed to attach to the pore walls in such a way as to make favorable formation of the olefin. The mechanism permits the explanation of four peculiarities of thoria as a dehydration catalyst: (a) the non-formation of ethers, (b) the preferential formation of 1-olefins from secondary 2-alcohols, (c) the production of methyl vinyl carbinol from, 2, 3-butanediol and (d) the greater dehydration reactivities of alcohols of smaller size. (Dissertation Abstr.)

# Radiation Chemistry

**See *also* BIOLOGY AND MEDICINE — Radiation Effects on Biochemicals Radiation Effects on Tissues**

*Refer also to abstracts 2164, 2433, and 3065.*

**1893** (AD-618228) LOW TEMPERATURE POLYMERIZATION STUDIES. Progress Report No. 6, April 1–June 30, 1965. Mortion, Maurice (Akron Univ., Ohio. Inst. of Rubber Research). July 15, 1965. Contract AF04(611)-9694. 65p. CFSTI $3.00 cy, $0.75 mn.

Results are reported for studies on the polymerization or attempted polymerization of the following monomers by gamma radiation (7.6 × 100,000 Rads per hour) at reduced temperatures: fluoral, acrylonitrile, vinyl fluoride, vinylidene fluoride, trifluoroethylene, tetracyanoethylene, perfluorobutene-2, hexafluoropropylene, vinyl triethoxysilane, para-nitrostyrene, and benzaldehyde. (TAB)

**1894** (AD-623095) THE RADIATION-INDUCED DECOMPOSITION OF MILLIMOLAR CONCENTRATIONS OF HYDROGEN PEROXIDE IN AERATED "PURE WATER". Balkwell, W. R.; Oldham, S. B. (Naval Radiological Defense Lab., San Francisco, Calif.). Aug. 19, 1965. 19p. (USNRDL-TR-903). CFSTI $1.00 cy, $0.50 mn.

The decomposition of hydrogen peroxide in aerated "pure water" was studied as a function of dose and initial hydrogen peroxide concentration, $(H_2O_2)_0$, in the 1 to 100 millimolar concentration region. Irradiations were performed with a 2000-curie $^{60}Co$ source at a dose rate of 12.8 kilorads per minute. The decomposition of hydrogen peroxide was found to follow first-order kinetics with respect to peroxide in the 1 to 100 millimolar concentration range. The specific peroxide decomposition rate constant, $K_1$, was observed to decrease with an increase in initial peroxide concentration. The decomposition yield of hydrogen peroxide, $G\text{-}(H_2O_2)$, at a given dose was found to increase significantly with increasing initial peroxide concentration and to be proportional to the square root of the initial peroxide concentration up to about 40 millimolar peroxide. The peroxide decomposition yield for a given initial peroxide concentration was observed to decrease continually during irradiation. The rate of decrease was found to be greater for higher initial concentrations of peroxide. (auth)

**1895** (AERE-R-4988) THE RADIOLYTIC REACTION BETWEEN GRAPHITE AND CARBON DIOXIDE. PART VI. GAS FLOW EXPERIMENTS IN DIDO. THE EFFECT OF ADDED OXYGEN. Dominey, D. A.; Morley, H.; Waite, R. J. (Atomic Energy Research Establishment, Harwell (England)). Aug. 1965. 16p. Dep.; BIS $0.60; HMSO 3s. 0d.

The addition of small amounts of oxygen to carbon dioxide accelerates the radiolytic oxidation of graphite. The effect is not directly proportional to oxygen concentration and it is probable that energy is transferred from $CO_2$ to $O_2$ in the gas phase and that graphite is oxidized by the resulting active species. The inhibiting action of $CH_4/CO/CO_2$ mixtures is destroyed by the addition of oxygen, not by destruction of the methane itself but by removal of the protective layer formed on the graphite by decomposition of methane. (auth)

**1896** (IS-T-23) RECOIL CHEMISTRY OF $^{11}C$ IN LIQUID HYDROCARBONS [Thesis]. Clark, Donald Eldon (Ames Lab., Iowa State Univ. of Science and Tech.). July 1965. Contract W-7405-eng-52. 97p. Dep. mn; CFSTI $3.00 cy, $0.75 mn.

Submitted to Iowa State Univ. of Science and Tech., Ames.

The chemical behavior of recoil carbon-11 atoms in

various $C_5-C_7$ hydrocarbons was investigated. The recoil atoms were produced by the $^{12}C(\gamma,n)^{11}C$ reaction with the bremsstrahlung beam of an electron synchrotron. Standard gas chromatographic methods coupled with scintillation flow counting techniques were used for radioassay of the labeled products. This study was principally concerned with the product yields of ethane, ethylene, and acetylene from the different target compounds, although methane yields were also determined in all cases. The initial phase of the investigation established the effects of iodine as a radical scavenger and radiation dose on the product yields. Iodine affected the yields of all of the volatile products except for acetylene. Radiation dose had the effect of changing the yields; the changes appeared to be primarily due to radiolytically produced hydrogen which was able to reduce some of the labeled species. When irradiation times of about five minutes or less were used, the results were approximately the same as would have been obtained for the idealized "zero dose" case. The two-carbon product yields, as well as the $(C_2H_6 + C_2H_4)/C_2$ ratios, were shown to be dependent upon the structure of the target molecules. These results are discussed in terms of the decomposition modes available to the assumed activated complexes resulting from insertion-type reactions of three primary species $^{11}C$, $^{11}CH$, and $^{11}CH_2$. Mixtures of benzene and methylcyclopentane were irradiated and the yields of volatile products were determined. Within experimental error, the yields were shown to be strictly dependent upon the molar concentrations of the two components. This was interpreted as being an indication that the reaction cross sections for equivalent labeled species with the two different molecules have similar energy dependences. This study appears to confirm that three neutral species, $^{11}C$, $^{11}CH$ and $^{11}CH_2$, are responsible for the products formed in these systems. The reactions by which the products are formed seem to proceed via mechanisms involving the insertion of these three recoil fragments into C–H and C=C bonds of the parent compounds. (auth)

**1897** (NASA-TN-D-3032) EXPERIMENTAL STUDY OF TRANSIENT EFFECTS IN DIELECTRIC MATERIALS CAUSED BY ELECTRON IRRADIATION. Storti, George M.; Phillips, Donald H.; Frank, Clifford S. (National Aeronautics and Space Administration, Langley Station, Va. Langley Research Center). Oct. 1965. 58p. CFSTI $3.00 cy, $0.75 mn.

Voltage pulses in capacitors and insulated wires during low-energy electron irradiation were studied. Various dielectric materials (polyethylene terephthalate, polytetrafluoroethylene, polystyrene, ceramics, polypyromellitimide, regenerated cellulose, polyvinyl alcohol, a copolymer of polyvinyl chloride and polyvinylidene chloride, mica paper, and silicone-impregnated mica paper) were tested over a range of incident electron kinetic energies, temperatures, and dose rates. Some dielectrics were found to have relatively few voltage pulses occurring as a result of irradiation, whereas others pulsed rapidly and with large amplitudes. The number of pulses was found to vary with the incident electron kinetic energy. Because of the thinness of most of the samples tested, the greatest number of pulses was obtained at the lower energies (30 to 100 kev), and, in all cases, the number of pulses decreased markedly as the electron energy was increased. Temperature also had an important effect on the number of pulses. Irradiation at low temperatures resulted in a greater number of pulses. Dose-rate effects on the number of pulses were significant except at the lowest temperatures at which the tests were conducted. Some of the results are compared with results obtained from previously published work on the x-ray-induced conductivity in dielectric materials. A degree of qualitative correlation was found with this prior work; i.e., those materials found to possess long postirradiation current decay constants in the x-ray work tended to be more susceptible to electron-induced transients. (auth)

**1898** (RRL-2310-164) QUARTERLY REPORT [ON RADIATION RESEARCH], JULY 1, 1965–SEPTEMBER 30, 1965. Fundamental Research No. 6041. (Radiation Research Labs., Mellon Inst., Pittsburgh, Pa.). Oct. 8, 1965. Contract AT(30-1)-2310. 10p. Dep. mn; CFSTI $1.00 cy, $0.50 mn.

Abstracts are presented of reports on the ESR spectrum of $FO_2$ radical formed in electron irradiation of $CF_2$ in presence of $O_2$, ESR studies of radioinduced radicals, and kinetics of reaction of radicals with HI. The radiolysis of liquid $CH_4$ and the effects of propene and $C_2D_4$ on the product yields were studied. Hydrogen yields in irradiated liquid Ar–$C_2H_4$ and $C_2H_4$ at −161°C are reported. Work on the direct photolysis of ethylene gas is described. Results of runs on the flash photolysis of $C_2H_6$ in the far uv are given. The mercury ($^1P_1$) photosensitized decomposition of methylcyclopropane and recombination coefficients for the ions produced in irradiated alkanes and alkenes are reported briefly. During the pulse radiolysis of solutions of $HClO_4$–$Fe(ClO_4)_3$, a transient absorption which formed at 345 mμ with a half life of 45 μsec was determined to be due to reaction of $Fe^{3+}$ ion and OH radical. (D.L.C.)

**1899** (BNL-tr-23) RADIOCHEMICAL PROCESSES TAKING PLACE DURING RADIOLYSIS OF CARBON TETRAFLUORIDES. Khramchenkov, V. A. Translated by Stephen Amoretty (Brookhaven National Lab., Upton, N. Y.). 10p. Dep. mn; CFSTI $1.00 cy, $0.50 mn; JCL $1.10 fs, $0.80 mf.

The feasibility of molecular fluorine separation by radiolysis of carbon tetrafluorides is reported. It was experimentally proven that, when chemically similar compounds (perfluorodienes) are subjected to radiolysis, the radiochemical breakdown processes in the hard phase, in contrast with the processes that occur in the liquid phase, predominate over the processes of polymerization of molecules. The composition of the gaseous products of radiolysis of perfluorodienes is due to the process of dissociation of the carbon tetrafluoride radical breakdown. Due to the absence of $CF_4$ in the gaseous products of radiolysis of perfluoridienes, it is assumed that the excitation energy, which produces the C–F bond when the heavy carbon tetrafluoride radical interacts with fluorine atom, is localized in the carbon tetrafluoride chain. (auth)

**1900** SCINTILLATION DECAY IN CALCIUM TUNGSTATE. Sayer, M.; Hardy, W. R. (Queen's Univ., Kingston, Ont.). Can. J. Phys., 43: 1925-33(Nov. 1965).

Measurements of the luminescence decay time were made for a number of single crystals of calcium tungstate for excitation by cathode rays, α and γ radiation. The value of the decay time was found to depend both on the crystal used and on the nature of the excitation. For γ-ray excitation, the decay time was in the range 6.1 to 6.8 μ sec. The values obtained for cathode-ray excitation were, in general, 20-30% higher for all crystals, while for α excitation, several crystals showed no change in decay time, while others showed a decay time 20% faster. Measurements of the temperature dependence of the decay time and thermoluminescence experiments indicate that these differences in behavior can be attributed to differences in the density of energy traps and nonradiative centers in the crystal and to a rise in temperature in the excited channel. (auth)

**1901** RADIOLYSIS OF ACETONE IN THE LIQUID PHASE. QUANTITATIVE STUDY. Kucera, J. (Inst. of Nuclear Research, Czechoslovak Academy of Sciences, Rez). Collect. Czech. Chem. Commun., 30: 3080-6(Sept. 1965).

Radiation yields of acetonylacetone, acetic acid, acetates, acetylacetone, isopropanol, pinacol, formaldehyde, acetaldehyde, 2,3-butanediol, diacetonealcohol, 2-methyl-2,4-pentanediol, and diacetyl were determined in liquid acetone irradiated with γ-$^{60}$Co-radiation. From analysis of the relative amounts of products and examination of the possible reactions it is shown that, in addition to the generally accepted radiolysis reactions of acetone, it is necessary to postulate the reaction $CH_3COCH_3^* \rightarrow CH_4 + CH_2 = CO$, giving rise to part of the methane formed, as well as other, at

present unknown reactions, which either give rise to hydrogen atoms or scavenge acetonyl radicals. (auth)

**1902** FORMATION OF ORDERED POLYVINYLIDENE CHLORIDE BY RADIATION POLYMERIZATION FROM THE GAS PHASE ONTO AN ORDERED POLYMER FILM. Vlasov, A. V.; Tokareva, L. G.; Tsvankin, D. Ya.; Tsetlin, B. L.; Shablygin, M. V. (Inst. of Organoelemental Compounds, Academy of Sciences, USSR; All-Union Scientific Research Inst. of Synthetic Fibers, USSR). Dokl. Akad. Nauk SSSR, 161: 857-60(Apr. 1, 1965). (In Russian).

Readily crystallizable vinylidene chloride was polymerized from the gas phase on a stretched film of high density polyethylene under x irradiation. The study was made to examine the possibility of producing highly ordered layers of polyvinylidene. Condensation of vinylidene was prevented by selecting appropriate reaction conditions. Radiation intensity was 6 rads per sec. The film temperature under irradiation was 60°C and the partial pressure of vinylidene monomer was 500 mm Hg. The rate of polymerization was 5%/hr based on the weight of the starting monomer charge. The radiation polymerization efficiency was 1500 molecules per 100 ev. The infrared absorption spectra indicated that polyvinylidene coating deposited on a stretched polyethylene film is highly ordered and crystalline. Polyvinylidene deposited on a relaxed polyethylene support was disordered. This behavior was also confirmed by the results of x-ray diffraction studies. The polymerization of vinylidene chloride was initiated on a polyethylene radical produced by absorption of a hydrogen atom from a macromolecule of the polymer base. It was concluded that spatial orientation and crystallinity induced by the polymer base is different from that exhibited by ordinary stereospecific polymers. (CFSTI)

**1903** RADIATION POLYMERIZATION OF HEXAMETHYLCYCLOTRISILOXANE IN THE SOLID PHASE. Trofimova, G. M.; Barkalov, I. M.; Kuz'mina, S. S.; Yenikolopyan, N. S.; Gol'danskii, V. I. (Inst. of Chemical Physics, Academy of Sciences, USSR). Dokl. Akad. Nauk SSSR, 161: 882-5(Apr. 1, 1965). (In Russian).

Kinetics of hexamethylcyclotrisiloxane(I) polymerization in the solid phase and under X-ray irradiation was studied in detail. Thermographic analysis of the reacting system indicated a phase change around −10°C. From −196 to −10°C the initial rate of polymerization was independent of temperature and the size of the monomer crystals. The activation energy was equal to zero for coarse crystals and 3.9 kcal/mol for fine crystals. From 0°C to the boiling point, the initial rate of polymerization was dependent on temperature and monomer crystallinity and size. The activation energy of the polymerization reaction was equal to 8.5 kcal/mol. In both temperature ranges the rate of polymerization was proportional to the radiation intensity. (CFSTI)

**1904** CALORIMETRIC ANALYSIS OF THE KINETICS OF RADIATION POLYMERIZATION. Barkalov, I. M.; Gol'danskii, V. I.; Rapoport, V. B. (Inst. of Chemical Physics, Academy of Sciences, USSR). Dokl. Akad. Nauk SSSR, 161: 1368-70(Apr. 21, 1965). (In Russian).

A special heat-conducting calorimeter was built according to the principle of Calvier's microcalorimeter for making measurements directly in a radiation field. Two identical vessels of pure copper with the test sample and a calibrating device are surrounded by casings, which are identical in their thermophysical properties and through which flows practically all the heat given off in the sample and calibrating device. The thermal flows, which pass between these casings, create between their inner and outer surfaces temperature drops, which are controlled by a battery of thermocouples connected differentially to a galvanometer. The measuring vessels with their casings are placed in a massive copper block that provides an even temperature field around the batteries of thermocouples. The block is placed in a thermostatic copper casing in which the liquid of the thermostat circulates. Between the thermostatic casing and the block are 4 copper screens, each 0.2 mm thick. The radiation of the operating vessel of the calorimeter can be conducted both from the end of the calorimeter through a channel and also radially through the walls of the thermostatic chamber. A calorimeter of this design was used in work on the following three problems: investigation of the kinetics of radiation polymerization of polyesteracrylates; measurement of the heats of fusion and phase transitions in certain monomers; and investigation of the kinetics of solid phase polymerization directly during radiation. (CFSTI)

**1905** THE USE OF ORGANOMETALLIC COMPOUNDS IN PLASTIC SCINTILLATORS FOR THE DETECTION AND RESOLUTION OF GAMMA RAYS. Dannin, J.; Sandler, S. R.; Baum, B. (Borden Chemical Co., Philadelphia). Int. J. Appl. Radiat. Isotop., 16: 589-97(Oct. 1965).

Tin-loaded plastic and lead-loaded liquid and plastic scintillators were evaluated for γ-photopeak resolution. Polyvinyltoluene scintillators containing physically incorporated triphenyl-4-ethylphenyltin and copolymerized p-triphenyltinstyrene showed well-resolved photoelectric peaks towards $^{137}Cs$ and $^{203}Hg$ γ rays. Photoelectric peaks were absent in the spectra of liquid and plastic scintillators containing triphenyl-2,4-dimethylphenyllead. Quenching studies indicated that the scintillation efficiency is approximately independent of whether the organometallic was incorporated by physical means or by copolymerization and is dependent on the type of flour. Efficiency was also improved through the use of naphthalene as a secondary solvent. (auth)

**1906** IONIC PROCESSES IN γ-IRRADIATED ORGANIC SOLIDS: RECOMBINATION LUMINESCENCE. Skelly, David W.; Hamill, William H. (Univ. of Notre Dame, Ind.). J. Chem. Phys., 43: 3497-3506(Nov. 15, 1965).

Several aromatic hydrocarbons, ketones, and amines phosphoresced when their γ-irradiated dilute solutions in 3-methyl pentane were exposed to near-infrared light at 77°K or were warmed slightly. Triphenylamine (TPA) was examined in some detail. Optical absorption spectroscopy provides evidence for color centers tentatively identified as $TPA^+$, $TPA^-$, as well as solvent-trapped electrons ($e^-$). Formation of $TPA^+$ was attributed to transfer of the electron vacancy in the molecular matrix. Infrared bleaching of ($e^-$) and $TPA^-$-induced phosphorescence of TPA with corresponding decrease of $TPA^+$. Addition of organic halide ($e^-$ trap) decreased $TPA^-$ and ($e^-$), and ethanol (hole trap) decreased $TPA^+$; both decreased phosphorescence which was attributed to ion recombination. (auth)

**1907** ABSTRACTION OF HYDROGEN ATOMS BY ENERGETIC RECOIL TRITIUM ATOMS: CORRELATION WITH C-H BOND-DISSOCIATION ENERGIES IN HYDROCARBONS. Root, J. W.; Breckenridge, W.; Rowland, F. S. (Univ. of Kansas, Lawrence; Univ. of California, Irvine). J. Chem. Phys., 43: 3694-3704(Nov. 15, 1965).

The yields of HT from hot abstraction reactions by energetic tritium atoms reacting with various substances RH were measured in a large excess of $C_2D_4$. The energetic tritium atom fluxes are reasonably similar in such systems and permit comparison of absolute HT yields from different R−H bond types. A more accurate comparison is possible when the HT yields are normalized to the yields of either the hot abstraction or substitution reactions with $C_2D_4$. The hot HT yields so measured from hydrocarbons show an excellent correlation with the bond-dissociation energies of the C−H bonds involved, with higher yields from weaker bonds. The abstraction of H from $CD_3CH_2CD_3$ was favored by approximately 1.4, per bond, over H from $CH_3CD_2CH_3$. No significant differences were observed in the $DT/C_2D_3T$ ratios from reaction with $C_2D_4$ in the various mixtures with different substances. A preference of 1.27 ± 0.02 was observed for the abstraction of H from $C_2H_4$ vs D from $C_2D_4$. No isotopic molecule difference was observed between the energetic addition reaction of tritium atoms to the olefinic position in $C_2H_4$ vs $C_2D_4$. (auth)

**1908** COLOR CENTERS IN SODIUM FLUORIDE. Amenu-Kpodo, Kwasi; Neubert, Theodore J. (Illinois

Inst. of Tech., Chicago). J. Phys. Chem. Solids, 26: 1615-19(1965). (COO-1044-11).

A survey was made of color centers produced in NaF crystals by x-irradiation. Measured at 80°K, the F-band occurred at 333 mμ (3.72 ev) and the M-band at 498 mμ (2.49 ev). At room temperature the comparative wavelengths are 341 and 505 mμ, respectively. The $R_1$- and $R_2$-bands and the K-band occur at 395 (3.14), 435 (2.85), and 282 mμ (4.40 ev), respectively, measured at 80°K. Four V-type bands were observed at liquid $N_2$ temperature at 288 (4.31), 267 (4.64), 249 (4.98) and 233 mμ (5.32 ev). These disappeared on warming to room temperature. Study of growth kinetics at four temperatures indicated that x-irradiation at $CO_2$ temperatures is an efficient means of production of high concentrations of F-centers with only minor formation of M-centers. At room temperature and 100°C, x-irradiation produced M-centers at concentrations proportional to the square of the F-center concentration. (auth)

**1909** RADIATION CROSSLINKING OF NYLON 66 AND POLY(VINYL ALCOHOL). Bernstein, Bruce S.; Odian, George; Orban, Gyula; Tirelli, Sebastian (Radiation Applications, Inc., Long Island City, N. Y.). J. Polymer Sci. Pt. A, 3: 3405-12(Oct. 1965).

Low-dose $^{60}Co$ irradiation of nylon 66 and poly(vinyl alcohol) in the presence of methanol–water–allyl methacrylate (AMA) mixtures caused cross-linking of the polymers. In both cases, cross-linking was facilitated by the presence of the polyfunctional monomer and did not occur in its absence. Nylon gel fractions of 40% were obtained after a dose of 3 Mrad; poly(vinyl alcohol) gel fractions of over 75% were obtained after 5 Mrad. With both polymers, the gel fraction was dependent on the radiation dose, AMA level, and water level during radiation. (auth)

**1910** DIVINYL COPOLYMERIZATION INITIATED BY HIGH INTENSITY, LOW ENERGY ELECTRONS. Burlant, W.; Hinsch, J. (Ford Motor Co., Dearborn, Mich.). J. Polymer Sci. Pt. A, 3: 3587-97(Oct. 1965).

Solutions of unsaturated esters in styrene were copolymerized by 0.04 Mev electrons at dose rates of 0.44 to 85.8 Mrad/min. Disappearance of each monomer and gel fractions was measured as a function of dose rate. Rates noted under these conditions of high linear energy transfer exhibited linear dependence on intensity, followed by a region independent of intensity. The data suggested that polymerization occurs in discrete volume elements, and that chain growth is initiated by hot radicals. For 65% ester solutions, the polymerization rate of the bulk sample, $d\alpha_t/dt$, is given by $d\alpha_t/dt = \{(k_p^{*2}/k_t)[M_2^0]\}V$, where $k_p^*$ is an activated propagation rate constant tenfold greater than that for more conventional polymerizations, $k_t$ is the termination rate constant, $[M_2^0]$ is the starting ester concentration, and V, proportional to the radiation intensity, is the volume fraction of the sample occupied by the reacting elements. The volume of the element in which polymerization is occurring, estimated from experimental data and using reasonable values for the life of a growing radical, is $3 \times 10^9$ $A^3$, a value consistent with what is known of electron impact processes in liquids. (auth)

**1911** HIGH ENERGY ELECTRON IRRADIATION OF TRIHYDROPERFLUOROALKYL ACRYLATE MONOMERS: STATISTICAL EVALUATION OF FACTOR INTERDEPENDENCY. Degering, Ed. F.; Caldarella, Gerald J.; Haines, George H. J. Polymer Sci. Pt. A, 3: 3635-42 (Oct. 1965).

A 2,2,2,2-factorial design was used for the radioinduced polymerization of 1,1,3-trihydroperfluoropropyl and 1,1,7-trihydroperfluoroheptyl acrylates with a 2-Mev electron accelerator in order to more critically determine the effect of variables. From the data obtained, it is concluded that: degassing, flame-out, and time-lapse are significant, dependent main effects for both monomers, and atmosphere is a significant, dependent main effect for the heptyl ester. The atmosphere and flame-out, degassing and time-lapse, and flame-out and time-lapse interactions were independently significant for the propyl ester, whereas for the heptyl ester the atmosphere and flame-out were independently significant, but degassing and flame-out, degassing and time-lapse, and flame-out and time-lapse were dependently significant. The degassing, flame-out, and time-lapse interaction was independently significant for the heptyl ester. It was concluded that experimental variables may be significantly interdependent. (auth)

**1912** GAMMA-RAY INITIATED POLYMERIZATION OF N-VINYLSUCCINIMIDE IN THE LIQUID PHASE. Hardy, Gyula; Varga, Jozsef; Nagy, Gabor; Helcz, Attila. Magy. Kem. Folyoirat, 71: 313-15(July 1965). (In Hungarian).

Kinetics of the gamma radioinduced liquid-phase polymerization of N-vinylsuccinimide were characterized by a high rate of the chain transfer reaction to the molecules of the monomer, and by a great value of the ratio $k_p/k_z^{\frac{1}{2}}$. The latter fact may be explained by the small value of $k_z$ caused by steric hindrance by the bulky polar substituent of the vinyl group, or by a gel-effect existing from the beginning of the polymerization process. (auth)

**1913** RADIATION-INDUCED LIQUID- AND SOLID-PHASE POLYMERIZATION OF ACETYLENE. Tabata, Y.; Saito, B.; Shibano, H.; Sobue, H.; Oshima, K. (Tokyo Univ.). Makromol. Chem., 76: 89-98(1964).

The polymerization was investigated in the liquid phase at −78°C and in the solid phase at −196°C as affected by $^{60}Co$ γ radiation at dose rates of $3 \times 10^4$ to $10^5$ R/hr. The effects of diphenylpicrylhydrazyl (DPPH) and benzoquinone on the polymerization were examined, and the ir spectra of the polymer was measured. No induction period was observed in both liquid and solid state polymerizations, the initial rate of polymerization was proportional to the dose rate in the region studied. This suggests that the mechanism of the polymerization in the liquid phase at −78°C is an ionic one. The effects of DPPH and benzoquinone on the polymerization indicate that the radical scavengers do not inhibit the polymerization, and also suggest that the polymerization proceeds by an ionic mechanism in the liquid state. The results also indicated that dimethylformamide appreciably retards the polymerization and methylene chloride considerably accelerates the polymerization. These facts suggest that the polymerization of acetylene in the liquid phase proceeds by a cationic mechanism. The polymer obtained in the liquid state polymerization was a relatively bulky powder, and the polymer obtained by the solid state polymerization was a rigid material (deep brown). Other properties of the polymers obtained are discussed. (TCO)

**1914** GAMMA-RAY INDUCED POLYMERIZATION OF FORMALDEHYDE. Yamaoka, Hitoshi; Hayashi, Koichiro; Okamura, Seizo (Faculty of Engineering, Kyoto Univ.). Makromol. Chem., 76: 196-209(1964).

In the $^{60}Co$ γ-ray induced polymerization of formaldehyde, the effects of solvent, and the copolymerization with vinyl monomers were studied. The rate of polymerization in methylene chloride and toluene increased markedly with increasing monomer concentration and was found to be proportional to second order of the monomer concentration except for the initial range. In diethyl ether solution the rate of polymerization was proportional to first order of monomer concentration except when the concentration was very low. The rate of polymerization was found to be proportional to first order with respect to dose rate in these solutions as well as in bulk. Intrinsic viscosity values, molecular weights, and thermal stability of polymers prepared in diethyl ether were higher than those prepared in the other solutions and in bulk. Copolymerizations with vinyl monomers were also carried out. The ease of copolymerization in bulk and in methylene chloride solution was found in the following order; isobutene > styrene ≫ methyl methacrylate (MMA) = acrylonitrile (AN). The results of copolymerization of formaldehyde with α-methylstyrene showed that the rate of copolymerization decreased markedly with the increase of α-methylstyrene in the monomer mixture. Also in ethyl ether, with MMA the

polymer composition did not show a considerable difference between a copolymer and formaldehyde homopolymer even at 50:50 monomer ratio. Similar results were obtained in copolymerization with AN. The results indicate that the radioinduced polymerization of formaldehyde proceeds predominantly by an ionic mechanism in solution, and copolymerization in methylene chloride and in toluene by cationic, and in diethyl ether, by an anionic mechanism. (TCO)

**1915** RADIATION-INDUCED COPOLYMERIZATION OF TETRAFLUOROETHYLENE WITH ISOBUTENE AT LOW TEMPERATURE. Tabata, Yoneho; Ishigure, Kenkichi; Oshima, Keichi (Tokyo Univ.). Makromol. Chem., 85: 91-101(1965).

Studies showed that tetrafluoroethylene copolymerizes with isobutene and that a crystalline, alternating copolymer can be obtained over a wide range of the monomer composition in the copolymerization. The copolymerizations were carried out by $^{60}Co$ $\gamma$ irradiation at −45 and −78°C. The monomer reactivity ratios, $r_1(C_4H_8)$ and $r_2(C_2F_4)$, were determined from an elementary analysis of the copolymers to be 0.2 and 0 at −45°C, respectively; while the reactivity ratios at −78°C could not be determined exactly, but were roughly estimated to be $r_1(C_4H_8) \cong r_2(C_2F_4) \cong 0$. The alternating tendency of this copolymer may be due to the opposite polarities of the monomers, that is, the electron-withdrawing property of the fluorine atoms of tetrafluoroethylene and the electron-donating property of methyl groups of isobutene. It is suggested on the basis of the monomer composition dependence of the copolymerization rate that the termination reaction takes place mainly via a degradative chain transfer of the growing radical to isobutene at a high isobutene concentration in the monomer mixture. (BBB)

**1916** ELECTRON SPIN RESONANCE OF IRRADIATED METHACRYLIC ACID. Sakai, Yoshiro; Bamford, C. H. (Government Industrial Research Inst., Nagoya, Japan). Nagoya Kogyo Gijutsu Shikensho Hokoku, 13: 444-7(Dec. 1964). (In Japanese).

Electron spin resonance absorption was studied with methacrylic acid irradiated by uv light in the solid state at temperatures ranging from +10 to −40°C. The radical concentrations became maximum at −5°C. At −5°C there may be a transition in the crystal, enhancing the mobility of the molecule and radical formation at this temperature. Irradiation at temperatures above −5°C yielded radicals that gave the characteristic methacrylate spectrum, consisting of nine lines (a quintet with a weaker quartet) having an equal spacing of 11.6 G. Below this temperature each of the four weak lines were split into two with the formation of a 13-line spectrum. When the irradiation time was constant, the splitting became more noticeable as the temperature of irradiation was lowered to about −30°C. The results are interpreted in terms of the conformation. The nonequivalence of the two methylene hydrogen atom was assumed, and by the calculation using Symons's relation, it was found that the whole methylene group rotated about the C−C bond by 5° from the symmetrical conformation, but there was no distortion of the $H^{(1)}$ C $H^{(2)}$ angle. In the symmetrical conformation the angles ($\theta_1$, $\theta_2$) between the methylene H atoms both equal 60°, whereas in the new conformation, $\theta_1 = 55°$ and $\theta_2 = 65°$. (BBB)

**1917** RATE CONSTANT FOR THE REACTION OF $O^-$ WITH OXYGEN. Adams, G. E.; Boag, J. W.; Michael, B. D. (Mount Vernon Hospital, Northwood, Eng.). Nature, 205: 898-9(Feb. 27, 1965).

The rate constant for the reaction $O^- + O_2 \rightarrow O_3^-$ was measured by irradiating a solution of aerated 0.1N KOH with a short pulse of fast electrons and observing directly the growth of the transient species $O_3^-$ which has an absorption maximum at 4300 Å. The electron pulse had a duration of only 0.2 μsec and delivered a dose of about 1 krad to the solution. To increase the $O^-$ concentration the solution was saturated with nitrous oxide, which reacts with the electrons to give $O^-$. To reduce the speed of the reaction of $O^-$ with oxygen, the solution was saturated with air instead of pure oxygen. Growth curves for the species $O_3^-$, obtained by means of a monochromator, photomultiplier, and oscillograph set to record at 4300 Å, indicated the duration of the electron pulse by the initial negative peak due to Cherenkov emission. These curves give a linear first-order plot, and the mean slope is $0.76 \times 10^6$ $sec^{-1}$. Since the oxygen concentration was 250 μM the second-order rate constant, k, was $2.6 \times 10^9$ $M^{-1}$. It was not possible to determine a complete absorption spectrum for $O^-$ itself, but there was some evidence that it absorbs at wavelength near 2600 Å. The decay with time is shown for the absorption at 2600 ± 100 Å when an initially deaerated solution of 0.1N KOH containing about 8 mM nitrous oxide is irradiated by a single 2-μsec pulse. (TCO)

**1918** INVESTIGATIONS OF THE INFLUENCE OF RADIOACTIVE RAYS ON PHARMACEUTICALS. Buechi, J.; Iconomou, N. (Pharmazeutisches Inst., Zurich). Pharm. Acta Helv., 40: 257-74(1965). (In German).

The significance of radioactivity and radioisotopes in pharmacy is discussed. Basic definitions and radiation units are defined. A review of the literature on the influence of radiation on chemical materials, pharmaceuticals, and pharmaceutical preparations was made. The behavior of solvents was considered, with particular emphasis on the behavior of water. Radiation-chemistry reactions of organic materials were examined. The radiosterilization of pharmaceuticals is discussed; a table of radiation resistance of various microorganisms is given. (BBB)

**1919** VARIATION OF THE RELATIVE CONCENTRATIONS OF $\alpha$ AND F CENTERS IN KBr IRRADIATED AT 5°K. Ritz, V. H.; Kabler, M. N. (Naval Research Lab., Washington, D. C.). Phys. Lett., 19: 259-60(Nov. 1, 1965).

An explanation is given for a large and unanticipated variation with dose of the ratio of $\alpha$-center concentration to F-center concentration (designated $\alpha/F$) in normally pure KBr at 5°K. This variation is shown where $\alpha/F$ is plotted as a function of average F-center concentration for four different radiation qualities: unfiltered x rays from a Be window, W-target tube operating at a constant voltage of either 7 or 15 kev, and 0.60 or 1.90 Mev electrons from a Van de Graaff accelerator. The results shown are discussed. It is concluded that $\alpha/F$ is essentially independent of radiation quality, even though the $\alpha$- and F-center growth rates each depend on quality. Also the form of $\dot{F}_t$ which the present model requires is consistent with the viewpoint that the majority of $\alpha$ centers, in particular those created directly at the rate $\dot{\alpha}_0$, are poor electron traps and thus participate little in the electron transfer process. (J.F.P.)

**1920** EFFECT OF SOLVENT ON SPECTRA PRODUCED BY PULSE RADIOLYSIS OF SOLUTIONS OF ORGANIC ELECTRON SCAVENGERS. Keene, J. P. (Christie Hospital and Holt Radium Inst., Manchester, Eng.); Kemp, T. J.; Salmon, G. A. Proc. Roy. Soc. (London), Ser. A, 287: 494-509(Sept. 28, 1965).

Pulse radiolysis of some organic electron scavengers in solvents covering a range of polarity indicates the type of product found spectroscopically to be a function of the polarity and the reactivity of the solvent. In solvents of low polarity, large yields of the triplet state of the solute are produced except in cases where the excited solute can abstract a hydrogen atom from the solvent. In solvents of intermediate polarity (tetrahydrofuran and triethylamine), much lower yields of triplet states are formed, and increased yields of anions and neutral radicals are obtained. However, anion yields are still much less than those recorded for glassy solutions at 77°K. Naphthalene is unable to reduce $G(\phi_2COH)$ when solutions of benzophenone in either an ether or an aliphatic amine are pulsed, and it was concluded that for these solvents triplet benzophenone is not a major precursor of $\phi_2COH$, although it plays a significant role in cyclohexane. Aqueous solutions of molecules known to have highly characteristic triplet-triplet

absorption spectra give very low or undetectable yields of triplet states. The yield of the naphthalene-hydrogen atom adduct increases through the series; benzene, cyclohexane, tetrahydrofuran, diethyl ether, triethylamine, methanol, water, i.e., it follows the yield of separated ion pairs. Evidence as to the nature of the precursors of this species and those of the triplet states of the solutes is presented. (auth)

**1921** REACTIONS OF TRITIUM RECOIL ATOMS AND $^{14}C$ WITH HETEROCYCLIC AMINES. Avdonina, E. N.; Baranovskii, I. B.; Wung, Hao-ming; Nesmeyanov, An. N. Radiokhimiya, 7: 220-7(1965). (In Russian).

The products of the reaction of tritium recoil atoms and $^{14}C$ with pyridine and picoline were investigated in various phase states in the presence of receptor radicals and in the composition of complex compounds. It was established that the radiation stability and radiochemical yields of the series of products are increased with increase of the possibility of energy dispersion in the system. In the presence of nickel compounds the introduction of tritium into the organic molecule increases because of the abrupt intensification of the isotope exchange with HT under exposure conditions. (tr-auth)

**1922** FORMATION OF POLYMERS LABELED WITH $^{14}C$ DURING ETHYLENE-AMMONIA IRRADIATED IN NUCLEAR REACTOR. Dzantiev, B. G.; Shevchenko, A. P. Radiokhimiya, 7: 368-70(1965). (In Russian).

It was found that small additions (2 to 5%) of ethylene and ammonia lead to an abrupt increase of the fraction of recoil $^{14}C$ held in the form labeled polymers. In the achievement of maximum labeling the yield depended very little on the composition of the ethylene–ammonia system. The yield of the $^{14}C$-labeled polymers at the maximum had a linear dependence on the thermal neutron flux. (tr-auth)

**1923** EFFECTS OF REACTOR RADIATION ON THE THERMOPHYSICAL PROPERTIES OF MONOISOPROPYLDIPHENYL. Rasskazov, D. S.; Babikov, Yu. M.; Belinskaya, N. T.; Lyapunov, O. I. (Moscow Inst. of Power Engineering). Teploenergetika, No. 8, 83-4(Aug. 1965). (In Russian).

The irradiation of MIPD in a circulating loop of an organic reactor resulted in the formation of polymer at a temperature of 200 to 250°C. The weight content of the polymer had an effect on the viscosity and density of the organic moderator and coolant. The viscosity is given by the relation, $\eta_r/\eta_{calc.} = (1 + 0.035\ p)$, where $\eta_r$ is the viscosity of the irradiated MIPD and $\eta_{calc.}$ is the viscosity of pure MIPD in nsec/m$^2$, and can be calculated at temperatures of 50 to 370°C from the relation: $\eta_{calc.} = 65.6/(t + 60)^{2.13}$. The percent of polymer after irradiation is given by p. Similarly the density of the irradiated MIPD is given by the equation: $d_r = d_{calc.} + 1.5\ p$. Here $d_r$ is the density of the irradiated MIPD, and $d_{calc.}$ is the density of pure MIPD calculated as follows: $d_{calc.} = 984 - 0.473 + -0.811 \times 10^{-3}\ t^2$. These empirical relations hold at polymer values of p = 0 to 30%. (TTT).

**1924** CHARGED-PARTICLE SLOWING-DOWN SPECTRA FOR FAST-NEUTRON IRRADIATION OF WATER. Faw, R. E.; Miller, L. F. (Kansas State Univ., Manhattan). Trans. Amer. Nucl. Soc., 8: 316-17(Nov. 1965).

**1925** RADIATION-INDUCED POLYMERIZATION OF STYRENE AT LOW TEMPERATURES. Phalangas, C. J.; Srinivasan, S.; Silverman, Joseph (Univ. of Maryland, College Park). Trans. Amer. Nucl. Soc., 8: 320(Nov. 1965).

**1926** THE EFFECT OF PRESSURE ON SOLID-STATE POLYMERIZATION OF TRIOXANE. Ballantine, D. S. (Brookhaven National Lab., Upton, N. Y.). Trans. Amer. Nucl. Soc., 8: 320-1(Nov. 1965).

**1927** INTERPRETATION OF RADIOLYSIS OF TERPHENYLS—APPARENT KINETICS AND FAST-NEUTRON EFFECT. Mason, Edward A.; Timmins, Tom H. (Massachusetts Inst. of Tech., Cambridge). Trans. Amer. Nucl. Soc., 8: 420-1(Nov. 1965).

**1928** TEMPERATURE, DOSE-RATE AND TRACK-DENSITY EFFECTS IN THE RADIOLYSIS OF ORTHO- AND META-TERPHENYL. Boyd, A. W.; Connor, H. W. J. (Atomic Energy of Canada Ltd., Ontario). Trans. Amer. Nucl. Soc., 8: 421-2(Nov. 1965).

**1929** 160,000-CURIE $^{60}Co$ FACILITY. Harvey, H. W.; Hoh, J. C.; Podolski, W. F.; Youngquist, C. H. (Argonne National Lab., Ill.). Trans. Amer. Nucl. Soc., 8: 629-30(Nov. 1965).

**1930** INVESTIGATIONS OF POLYMERIZATION RADIATION. [PART] V. Ivanov, V. S.; Bezhan, I. P.; Levando, L. K. Vestn. Leningr. Univ., No. 10, Ser. Fiz. Khim., No. 1, 157-9(1965). (In Russian).

As a result of $^{60}Co$ $\gamma$ rays on p-phenylenedi-N-maleimide and 4,4′-diphenylenedi-N-maleimide at 240–260°C in the solid state, thermostable insoluble cross-linked polymers were formed. (auth)

**1931** ENERGY TRANSFER IN THE $\gamma$-RADIOLYSIS OF THE BENZENE–BENZOPHENONE–ISOPROPANOL SYSTEM. Schulte-Frohlinde, D.; von Sonntag, C.; Lang, G. (Kernforschungszentrum, Karlsruhe, Ger.). Z. Physik. Chem. (Frankfurt), 45: 257-68(June 1965). (In German).

The G values of hydrogen, methene, acetaldehyde, and acetone in the $\gamma$ radiolysis of isopropanol–benzene mixtures were determined with and without the addition of 1% benzophenone and 1% p-hydroxybenzophenone. From the results it was concluded that a part of the acetone formed comes from a reaction of the electron-excited benzophenone. The electron excitation energy produced the benzene excited by the radiation effects. (tr-auth)

**1932** INFLUENCE OF THERMAL NEUTRON REACTOR RADIATION ON THE POTENTIAL OF OXIMER-CURY ELECTRODE. Gromova, A. I.; Morozova, I. K.; Gerasimov, V. V. Zashita Metal., 1: 452(July-Aug. 1965). (In Russian).

Two mercury oxide electrodes were connected by a glass tube 4.5 m long filled with a 0.1N NaOH solution. The lower electrode was placed in a mixed neutron and gamma field in the center of the active reactor zone, and the upper electrode was placed 1 m away in the same gamma field with the neutron flux reduced by a factor of $>10^3$. After an hour at full power at a neutron flux of $10^{12}$ neutrons cm$^{-2}$ sec$^{-1}$, the difference in the potentials of the upper and lower electrodes was 5 to 10 mv, and did not vary for the next 4 hr of reactor operation. Another control experiment showed that the gamma radiation had no effect in causing the difference in potential between the two electrodes. It was concluded that reactor radiation has only a small effect on the potential of a mercury oxide electrode, and that this comparison electrode can be placed in the active zone of a reactor in case of necessity. It should be noted that a gas bubble was noted in the joint of the connecting tube as a result of radiolytic effects on the solution. (TTT)

**1933** ENERGY DEPOSITION BY FISSION FRAGMENTS: OPTICAL EXCITATION OF NITROGEN [Thesis]. Sears, John Thomas. Princeton, N. J., Princeton Univ., 1965. 89p.

Measurements of nitrogen luminescence excited by fission fragments and by alpha rays were used to study competitive emission and quenching processes in the gas. The results indicate a cross section for electronic quenching of $C^3\Pi_u$ molecules by ground state molecules that is 0.04 that of the thermal kinetic cross section for collision. The $C^3\Pi_u$ molecules probably follow a nonradiative collision route to the $B^3\Pi_g$ state. At pressures >15 mm Hg, Stern-Volmer kinetics are obeyed while at lower pressures, anomalous results are attributed to a cascade from a higher excited state, viz., $E^3\Sigma_g^+ \rightarrow C^3\Pi_u$. A novel kinetic analysis was developed that gives the power law dependency of energy loss by fission fragments in a gas from the pressure at which maximum luminosity is observed. For nitrogen, the relationship $E = E_0(1-f)^{1.70\pm0.07}$ is valid for $0.4\ E_0 < E < E_0$. E is the kinetic energy of a fission fragment of original energy $E_0$ that has traveled a fraction, f, of its total range. Experiments with fission fragments and alpha rays indicate

that, if compared at the same velocity, near the beginning of their ranges, both particles exhibit the same efficiency for excitation of the second positive system ($C^3\Pi_u \rightarrow B^3\Pi_g$). This result lends support to an earlier finding that the lower overall ionization efficiency of fission fragments relative to that of alpha rays is due to the onset of Rutherford collisions at the end of the fission fragment track. (Dissertation Abstr.)

**1934** HOT ATOM CHEMISTRY OF SURFACES; NATURE OF THE CHEMICAL REACTIVITY OF ISOMERIC RADIOBROMINE ATOMS [Thesis]. Kazanjian, Armen Roupen. Los Angeles, Univ. of California, 1965. 119p.

When an alkyl halide is irradiated with neutrons, the subsequent gamma emission from the halogen nucleus endows the halogen atom with sufficient recoil energy to break its chemical bond and eventually form new bonds with fragments produced by collisions. The fraction of hot (energetic) atoms that finally result in organic compounds is called the organic retention. In an investigation of the effects on retention of caging (the physical containment of a chemical species by the surrounding solvent molecules), a variable cage was produced by adsorbing varying numbers of molecular layers of n-propyl bromide on inert substrates such as Molecular Sieve or porous Vycor. The $(n,\gamma)$ reaction was then carried out by neutron irradiation. Subsequent separation and counting of the organic and inorganic phases yielded the retention as a function of the number of adsorbed layers. The results showed that caging is effective within a few molecular layers. An explanation is proposed for the fact that the $(n,\gamma)$ and isomeric transition processes in bromine have identical results even though the isomeric transition (unlike the $(n,\gamma)$ reaction) produces bromine atoms with high positive charge (up to +13) and supposedly very little recoil energy. The two nuclear processes were distinguished experimentally by using a gas ($CF_3Br$) whose ionization potential was larger than that of the Br atom. This preserved a positive charge on the Br atoms and made ion-molecule reactions possible. Since the fractions of positive ions were different in the two processes, the retentions were different: 5–9 percent for the $(n,\gamma)$ reaction and 20–22 percent for the isomeric transition. Unsuccessful attempts were made to reduce the retention in the isomeric transition by adding substances with low ionization potentials to neutralize the $Br^{+1}$ ions. (A.G.W.)

**1935** ELECTRON SPIN RESONANCE OF SEVERAL MOLECULES IN THE SOLID STATE [Thesis]. Griffith, O. Hayes. Pasadena, Calif., California Inst. of Tech., 1965. 224p.

Single crystals of ester-urea, ketone-urea, and ether-urea inclusion compounds were x irradiated and investigated by electron spin resonance. Eleven inclusion compounds formed between urea and the straight-chain alkyl esters yielded radicals of the type $RCH_2\dot{C}HCOOR'$. The $\alpha$ and $\beta$ proton coupling constants of two radicals were studied over the temperature range 352 to 7°K. The splittings caused by the alcohol (R') protons were resolved in many cases. Information regarding the structure of the inclusion compounds was obtained. The long-lived radical $RCH_2\dot{C}HCOR'$ was detected in all six ketone-urea crystals. The spin density in the 2p orbital adjacent to the carbonyl group is 0.81 ± .04. The ether radicals were of the type $R\dot{C}HOR'$ and the spin density on the carbon atom is approximately 0.70 ± .08. The ketone radical and ether radical spin distributions obtained from the $\pi$-electron theory are in qualitative agreement with the experimental spin distributions. In addition, single crystals of fumaric acid-urea were X-irradiated and studied by electron spin resonance. The dominant radical ($HO_2CCH_2\dot{C}HCO_2H$) in this case is formed by addition of a hydrogen atom. The fumaric acid-urea crystal is not a hexagonal inclusion compound. The major orientations of the radical were determined with respect to the external crystal morphology. Electron spin resonance studies of the triplet state of pyrene and triplet exciton states in ion radical salts are also briefly reported. (Dissertation Abstr.)

**1936** THE DECOMPOSITION OF WATER VAPOR INDUCED BY ALPHA RADIATION [Thesis]. Ambrosiani, Vincent F. Syracuse, N. Y., Syracuse Univ., 1964. 98p.

The alpha-radiation-induced decomposition of water vapor at 120°C was studied using the ion yield method. Experiments were performed at 50, 100 and 200 mm Hg using alpha particles from radium bromide at two intensities. The ion yield decreased slightly from 0.9 to 0.75 as the pressure increased from 50 to 200 mm Hg. The decrease was interpreted as a typical Lindemann deactivation process involving the excited water molecule. The ion yield increased with dose rate, rising from 0.9 to 1.5 at 50 mm Hg as the dose rate increased from $7.2 \times 10^{12}$ to $12.5 \times 10^{12}$ ev/sec. The effect was somewhat less at higher pressures. The dose rate effect involves ion molecule reactions that lead to hydrated protons. These are unreactive in the gas phase and diffuse to the wall where they are neutralized and H atoms are liberated. High dose rates increase the probability that OH will react in the gas before reaching the wall and thus will tend to produce higher yields. At higher pressures most OH radicals react in the gas phase and increasing the dose rate produces a smaller effect on the yield. The major steps in the mechanism are given. Contradictory ion yield data in the literature are brought into qualitative agreement by considering vessel surface-to-volume effects. The ion yield is unaffected by increases in the field strength up to $X/P \sim 4$. At this point, the curve starts to rise with a constant slope. The shape of the curve is independent of pressure and dose rate. The overall results and mechanism for water vapor radiolysis parallel those obtained for ammonia. (A.G.W.)

# Radiochemistry

## See also Separation Processes and Procedures

*Refer also to abstract 2142.*

**1937** (BNL–9281) GAMMA RADIATION SOURCE AND IRRADIATOR DESIGN. Oltmann, A.; Kuhl, O. A. (Brookhaven National Lab., Upton, N. Y.). June 1965. Contract AT-30-2-GEN-16. 31p. (CONF-651110–3). Dep. mn; CFSTI $2.00 cy, $0.50 mn.

From American Society of Mechanical Engineers, Annual Winter Meeting, Chicago.

BNL has designed and assisted in the design, fabrication, and installation of a number of gamma facilities now in use and currently being built. The design of the BNL standard source is described from its inception to the latest version. The design, fabrication, and operation of a variety of irradiation facilities now in use for research purposes are discussed in some detail. The design of semi-production type, for commercial applications, is also discussed. (M.O.W.)

**1938** (EUR–2452.e) SELF-RADIOLYSIS AND METHODS FOR STORAGE OF TRITIATED ORGANIC COMPOUNDS. Ciranni, G.; Guarino, A.; Pizzella, R.; Possagno, E.; Rabe, B.; Rabe, G. (Rome Univ. (Italy). Istituto di Chimica Farmaceutica). 1965. 74p. Dep. mn.

Tritium-labeled cyclohexane, 2.952 mC/mg, and n-propanol, 2.272 mC/mg, were prepared and stored for a period of 90 and 120 days. Storing conditions were as follows: with air; in vacuum; in solution of benzene, and adsorbed on: cellulose; 1:2-benzanthracene; active charcoal; silica gel, and ferric oxides. The autoradiolysis of cyclohexane in vacuum gave $G_{(H_2)} = 4.3$. Only small amounts of cyclohexene and cyclohexane-dimers resulted, but high yield of polymers with more than 12 C-atoms as well as some isomerization products and lower hydrocarbons were produced. In the HT-formation isotope effects were evident. From n-propanol ($G_{(H_2)}$ in vacuo = 3.0), aldehydes, isopropanol, and allyl alcohol but no glycols or polymers were formed. High specific activity methyl butyrate-2,3-$^3$H and methyl stearate-9,10-$^3$H were stored for approximately three months. Rather high G-values were found for the parent acids and for the destroyed ester molecules. Phenyl alanine-$^3$H was stored un-

der vacuum, in air, and adsorbed on cellulose powder, on $Fe_2O_3$-$Fe_3O_4$, diphenylbenzene, and acid alumina. The best storing conditions proved to be storage in the solid state, under vacuum. Clathrates containing high specific activity methyl stearate-9,10-$^3$H were stored for approximately 70 days. The following host molecules were employed: desoxycholic acid, cycloveratryl, tri-o-thymotide and β-cyclodextrin. The gaseous self-radiolysis products decrease significantly up to ~ 90% (HT from choleic clathrate). (P.C.H.)

**1939** (EUR-2476.i) MARCATURA DI PROTEINE PER VIA ELETTROCHIMICA. (Electrochemical Labelling of Proteins). Rosa, U.; Donato, L.; Ambrosino, C.; Pennisi, F.; Massaglia, A.; Scassellati, G. (Societa Ricerche Impianti Nucleari, Sluggia (Italy). Centro Ricerche Nucleari). 1965. 50p. Dep. mn.

An electrolytic labeling method was used for $^{125}$I or $^{131}$I labeled human serum albumin and insulin for use in studies on protein metabolism. Data are given on the apparatus used and the techniques employed for the preparation and control of the end product. The effects of iodination on the protein molecule were studied on the basis of the physicochemical (e.g. electrophoretic mobility) and, in particular, biological properties (the catabolic rate in normal subjects in the case of serum albumin and convulsive and hypoglycemic activity in that of insulin). A preliminary study was undertaken to determine the chemical effects as a function of the degree of iodination. The —SH groups in albumin and S—S groups in insulin were titrated amperometrically. The distribution of the iodine in the residual tyrosine was studied by means of enzymatic hydrolysis of the protein and chromatographic analysis of MIT and DIT in the hydrolysate. The first results obtained from the project are described and discussed. (tr-auth)

**1940** (RFP-638) AQUEOUS RADIOACTIVE WASTE TREATMENT PLANT AT ROCKY FLATS. Ryan, E. S.; Vance, J. N.; Maas, M. E. (Rocky Flats Div., Dow Chemical Co., Golden, Colo.). Oct. 25, 1965. Contract AT(29-1)-1106. 19p. (SM-71-43; CONF-651202-4). Dep. mn; CFSTI $1.00 cy, $0.50 mn.

From Symposium on Practices in the Treatment of Low and Intermediate Level Radioactive Waste, Vienna.

The operation of an aqueous radioactive waste treatment plant at Rocky Flats is described, including details of construction, flow charts, operating data, and problems encountered. Plans for additional processing of the effluent are also discussed. (auth)

**1941** PREPARATION OF RADIUM STANDARD SOLUTIONS. Yura, Osamu; Kimura, Miwako. Denki Shikensho Iho, 29: 259-63(Mar. 1965). (In Japanese).

Three kinds of radium chloride solution, 20.2, 2.02, and 0.202 μg-Ra per gram, each contained in flame-sealed 5 ml glass ampoules, were prepared to supply standards for radon testing. The original radium chloride sample was carefully calibrated, in comparison with the radium primary standard precisely certified at Union Minière du Haut Katanga, Belgium, in terms of mg-Ra unit using an ionization chamber, and was dissolved in barium aqueous solutions. An NBS radium standard sample assured no discrepancy between the two laboratories within the accuracy of the calibration. (auth)

**1942** $^{60}$Co (3000 C) STANDARD γ-RAY IRRADIATION FACILITIES AND MEASUREMENTS OF DOSE RATES DISTRIBUTIONS. Moriuchi, Yasuyuki; Takebe, Masahiro.. Denki Shikensho Iho, 29: 315-23(Apr. 1965). (In Japanese).

Necessary conditions for the establishment of exposure standards whose intensities are higher than $10^3$ R/hr are described. A γ-ray irradiator of $^{60}$Co (about 3 kC) which has been set up at the Tanashi Branch of Electrotechnical Laboratory is described together with its irradiation room, and its attached equipments. The results of measurements of leakage or scattered γ-ray dose rates distributions inside or outside of this room are also described. The γ-ray source which is set in the lead vessel 1.5 m above the floor level can be issued horizontally through the shutter hole. If the horizontal γ-ray beam flux of about 0.03 steradian collimated by the shutter hole is used, the so-called inverse square law is established within ±0.3% of relative accuracy in the distance of about 1 to 7 m from the source. Under these conditions, the standard γ-ray field of any intensity from about 400 R/min to 0.8 R/min is easily available. (auth)

**1943** COMPUTER PROGRAMS FOR PAIRED AND TRIAD RADIOIODINE LABEL TECHNIQUES IN RADIOIMMUNOCHEMISTRY. Pressman, D.; Pressman, R. (Roswell Park Memorial Inst., Buffalo). Int. J. Appl. Radiat. Isotop., 16: 617-22(Nov. 1965).

Paired and triad label techniques using $^{131}$I and $^{125}$I as a pair or $^{131}$I, $^{125}$I, and $^{130}$I as a triad are of considerable importance in immunochemical and protein structure studies. They provide a means for direct measurement of antibody and control proteins picked up in vivo in the case of tissue-localizing antibodies. They also provide a means of studying the chemical composition of protein molecules. Computer programs, written in FORTRAN II language, analyze counting measurements on tissues, which have taken up proteins labeled with a pair or triad of radioisotopes. The programs are also applicable to measurements on products obtained by various procedures carried out on a mixture of proteins so labeled. The method of analysis is discussed and the mathematical relationships programmed are presented. (auth)

**1944** PRELIMINARY STUDIES ON NEUTRON ACTIVATION OF TETRAETHYL GERMANIUM. Nowak, M. (Inst. of Nuclear Research, Warsaw). Int. J. Appl. Radiat. Isotop., 16: 649-53(Nov. 1965).

Tetraethylgermane was activated in the thermal column of the nuclear reactor EWA. The compounds of radioactive germanium and arsenic formed were separated by extraction with aqueous solution of inactive tracers or by high-tension paper electrophoresis. The possibility of obtaining germano-organic compounds labeled with $^{75}$Ge and $^{77}$Ge free of radioactive arsenic compounds was confirmed experimentally. (auth)

**1945** THE SEPTUM CAP TECHNIQUE AND ITS MANY-SIDED APPLICATIONS. Luhleich, H. (Gesellschaft fuer Kernenergieverwertung in Schiffbau und Schiffahrt mbH, Geesthacht-Teseperhude, Ger.). Kerntechnik, 7: 326-9(July 1965). (In German).

For investigations under exclusion of air, a suitable experimental technique, the septum cap technique, is described. A great deal of radiochemical work under such conditions can be done with the help of this technique. Septum caps, hypodermic needles and hypodermic syringes are the most important resources. For the rest all apparatus commonly used for chemical and physicochemical investigations can be adapted to the septum cap technique by insignificant changes. The single operations can be done easily and safely. (auth)

**1946** BEHAVIOR OF POLONIUM IN KETONES AND MIXED AQUEOUS-ACETONE SOLUTIONS. Starik, I. E.; Kuznetsov, B. S.; Ampelogova, N. I. Radiokhimiya, 7: 196-9(1965). (In Russian).

It was established that during the dissolution of polonium chlorides in anhydrous ketones (acetone, methylethyl ketone, and methylisobutylketone) ionized compounds are formed in which the polonium enters into the structure of complex anions. In mixed aqueous-acetone solutions, polonium is present in a pseudocolloidal form. (tr-auth)

**1947** EVALUATION OF CROSS SECTIONS FOR NUCLEAR REACTIONS $^{45}$Sc(n,α)$^{42}$K, $^{42}$Ca(n,p)$^{42}$K, AND $^{43}$Ca(n,p)$^{43}$K. PRODUCTION OF CARRIER-FREE $^{42}$K AND $^{43}$K. Kurchatova, L. N.; Levin, V. I. Radiokhimiya, 7: 336-41(1965). (In Russian).

The effective cross section for the reaction $^{45}$Sc(n,α)$^{42}$K was evaluated. For neutrons with energy distributions close to the fission spectra the effective cross section was 0.1 to 0.3 mb. The effective cross sections of the reactions $^{42}$Ca(n,p,)$^{42}$K and $^{43}$Ca(n,p)$^{43}$K were determined to be 3.2 ± 0.02 and 2.3 ± 0.1 mb, respectively. A method for the sepa-

ration of the radioactive $^{42}K$ and $^{43}K$ from neutron-irradiated calcium oxide was developed, which is based on the separation of calcium by means of the quenching of the calcium oxide and precipitation of calcium in the form of carbonate with subsequent anion exchange purification of $^{42}K$ and $^{43}K$. For increased yield and radioisotopic purity of the carrier-free $^{42}K$ in target quantities, calcium oxide enriched in the $^{42}Ca$ isotope was used. During use of such targets, $^{42}K$ was obtained with admixtures of $^{43}K \leq 1$ to 2% $^{24}Na \leq 0.5\%$ and long lived radioisotopes $\leq 0.1\%$. (tr-auth)

**1948** PRODUCTION OF $^{205}At$ AND $^{203}At$ DURING BOMBARDMENT OF BISMUTH BY 400-Mev PROTONS. Mal'tseva, N. S.; Mekhedov, V. N. Radiokhimiya, 7: 341-5(1965). (In Russian).

A method for the chemical separation of At from Bi samples irradiated with high-energy particles was developed. With this method it is possible to measure the $\alpha$ spectra and to identify the light isotopes with half lives >7 min. The results of measurements of the yields of medium and heavy At isotopes obtained using a semiconductor $\alpha$ spectrometer agreed with earlier determinations. The comparative probability for the formation of light isotopes of At from Bi with 400-Mev protons was only $\frac{1}{3}$ the yield of heavy isotopes and the nuclei indicated are produced perhaps by secondary reactions. The $\alpha$-active isotopes of At with half lives of more than 10 days and less than 10 years are not formed at high energies and almost all do not exist in nature. (tr-auth)

**1949** THE ASTATINE ISOTOPES PRODUCED IN $^{3}He$ BOMBARDMENT OF BISMUTH. Lee, Ikchoon. Ta Han Hua Hsueh Hui-Chih, 7: 159-64(June 1963). (In Korean).

Samples of Bi targets (3 to 4 mg/cm$^2$ thick) prepared by evaporating Bi from a W boat in a high vacuum on 60-$\mu$ thick Al disks were bombarded in the external beam of $^{3}He$ of a cyclotron with a maximum energy of 30 Mev and a beam current of 1.5 $\mu$amp for 20-min periods. Then the target was dissolved in a few drops of concentrated $HNO_3$ and diluted in 8N HCl. Carrier-free At isotopes were extracted by means of diisopropyl ether and analyzed by an $\alpha$-ionization chamber and a 100-channel pulse height analyzer. The main product, $^{209}At$, was formed by the ($^{3}He$,3n) reaction. $^{211}At$, $^{210}At$, $^{208}At$, and $^{207}At$ were also identified. A semiquantitative calculation of the relative yield of each isotope was made. (OID)

**1950** NITRATION AND SUCCINOYLATION OF TRITIUM-LABELED TOLUENE. Eastham, J. F.; Bloomer, J. L.; Hudson, F. M. (Univ. of Tennessee, Knoxville). Tetrahedron, 18: 653-6(1962).

In the nitration of toluene, it has been established that tritium and hydrogen are substituted at the same rate and that therefore loss of hydrogen in this substitution reaction requires less activation energy than does formation of some prior transition state, presumably one in which the aromatic ring has become positively charged due to attack by nitronium ion. The nature of secondary hydrogen isotope effects and the existence of such effects in the nitration of toluene are considered. New experimental data presented for the mononitration of $\alpha$-, m- and p-tritiated toluene samples reveal no secondary isotope effects. It is suggested that the remarkable freedom of this aromatic nitration from hydrogen isotope effects (primary or secondary) constitutes evidence that in the transition state for the reaction, the aromatic ring has accepted very little charge from the nitronium ion. In another electrophilic substitution, p-succinoylation of toluene-p-t, the result that the succinoylation product retains most of the tritium of the starting material is rationalized. It is possible to explain retention of tritium on the ring (even from the para position) in p-succinoylation of toluene with two assumptions: the tritium and hydrogen on all positions of toluene are continuously maintained in equilibrium by exchange with the carboxyl group (or its $AlCl_3$ complex) of the product; and tritium or hydrogen on the ring positions of the product does not exchange. The consequence of these assumptions is that tritium removed into the carboxyl group of product is rapidly reintroduced onto the ring of unreacted toluene, thereby giving little net loss of activity. (BBB)

# Separation Processes and Procedures

**See *also* Analytical Procedures**
**ISOTOPE TECHNOLOGY — Separation and Production**

*Refer also to abstracts 3320 and 3447.*

**1951** (AECL–2279) ABSTRACTS OF CANADIAN PATENTS ON THE PRODUCTION OF HEAVY WATER. Armstrong, F. S. (Atomic Energy of Canada Ltd., Chalk River (Ontario)). July 1965. 33p. Dep.; AECL $1.00.

Abstracts of 43 patents are included for the period from 1937 to mid-1965. The abstracts are divided into three groups according to the nature of the process involved: distillation processes; isotopic exchange processes; and water electrolysis processes. Separate inventor and assignee indexes are included. (P.C.H.)

**1952** (ANL–6859) ENGINEERING DEVELOPMENT OF FLUID-BED FLUORIDE VOLATILITY PROCESSES. PART 4. FLUIDIZED-PACKED BEDS: STUDIES OF HEAT TRANSFER, SOLIDS-GAS MIXING, AND ELUTRIATION. Gabor, John D.; Mecham, William J. (Argonne National Lab., Ill.). Mar. 1965. Contract W-31-109-eng-38. 127p. Dep. mn; CFSTI $4.00 cy, $1.00 mn.

Various properties of fluidized-packed beds were studied from a basic point of view: bed expansion and pressure drop, solids mixing, gas mixing, effective bed thermal conductivity, heat-transfer coefficients at the column wall and fixed packing surface, and elutriation. Data and theoretical discussions of mechanisms are presented. In addition, the empirical and theoretical results are applied to process design and, where possible, compared with pilot-plant data. (P.C.H.)

**1953** (IS-T–34) PREDICTION OF THE APPROACH TO STEADY-STATE OF A MIXER-SETTLER EXTRACTOR [Thesis]. Halligan, James Edmund (Ames Lab., Iowa State Univ. of Science and Tech.). July 1965. Contract W-7405-eng-82. 66p. Dep. mn; CFSTI $3.00 cy, $0.75 mn.

Four mathematical models were proposed, based on assumed flow characteristics in the settling chambers, to predict the nitric acid concentration in the various streams in a mixer-settler extractor as a function of time for the system nitric acid-water-tributyl phosphate in Varsol. These models were programmed on an IBM-7074 computer using DIAN, a system for programming a digital computer in terms of analog components. The model that assumed perfect mixing and 100% stage efficiency in the mixing chambers, homogeneity of the aqueous phase in the settling chamber, and plug flow of the organic phase in the settling chamber was found to predict the nitric acid concentrations most accurately. This model was called the Hybrid Model because it was obtained by combining the best features of two of the other models. All four of the assumed models predicted the actual results more closely as the number of stages in the cascade increased. In the absence of other information, the Hybrid model is recommended for prediction of results for tube-type mixer-settler extractors for systems in which the properties of the phases are similar to that of water and a 50% tributyl phosphate-50% Varsol mixture. (auth)

**1954** (KY–287) ON THE ELECTROLYTIC GENERATION OF FLUORINE FROM URANIUM HEXAFLUORIDE. Rossmassler, W. R.; Harris, R. L.; Mayo, T. J. (Paducah Gaseous Diffusion Plant, Ky.). May 1, 1959. Contract

W-7405-eng-26. 49p. Dep. mn; CFSTI $2.00 cy, $0.50 mn.

Several possible methods for recovering the fluoride value from gaseous diffusion plant waste $UF_6$ are discussed. Recovery as elemental fluorine, while the most difficult method, offers the greatest opportunities for recovering the maximum value. Studies searching for a fused salt melt containing $UF_6$ and suitable for electrolysis are described. The systems studied included the alkali metal fluorides in various combinations with $UF_4$, $UF_5$, and $UF_6$. The requirements for a suitable electrolyte are defined, but no material meeting all the requirements was found. Consequently, fluorine production was not achieved. (auth)

**1955** (NP-15403) EUROCHEMIC SAMPLING SYSTEM. Clement, J. M.; Shank, E. M. (European Company for the Chemical Processing of Irradiated Fuels, Mol (Belgium)). Feb. 1965. 106p. (ETR-169). Dep. mn; CFSTI $4.00 cy, $0.75 mn.

The Eurochemic main process sampling system is a combination of principles based on experience from the French C.E.A., the U.S.A.E.C., and Eurochemic. The system contains means for recirculating radioactive process solutions through a sampling bottle (re-circulation loop), for handling and viewing the sampling operation (sampling blister), and for transporting the sample to the analytical laboratory (transport facility). Each of the above systems is described in detail, including implantation. The sampling requirements for Eurochemic are summarized along with a review of the design evolution. The finalized re-circulation loop is compared with the Thorex sampler and with the pre-project design. It is felt that the final system represents a reasonable combination of experience and opinions. The sampling systems used for the Intermediate Waste Storage Unit, the final Plutonium facility, and the Inactive Make-up units are not described. These systems do, however, incorporate many of the principles of the main process samplers. (auth)

**1956** (ORNL-1696) DEVELOPMENT OF THE EXCER PROCESS. [PART] I. Higgins, I. R.; Roberts, J. T. (Oak Ridge National Lab., Tenn.). Apr. 13, 1956. Contract W-7405-eng-26. 55p. Dep. mn; CFSTI $3.00 cy, $0.50 mn.

The Excer process is an aqueous process for converting uranyl nitrate solution to solid $UF_4$. The uranyl nitrate solution is fed to a cation-exchange resin column where the uranium is sorbed. The nitrate passes through and appears in the effluent as nitric acid. The uranium is eluted with excess 6.4 M hydrofluoric acid, as $UO_2F_2$ and is then reduced to $UF_4.3/4H_2O$ slurry in an electrolytic cell. The wet product cake is centrifuged and finally dried to anhydrous $UF_4$ at about 400°C. The centrifuge supernatant is concentrated by evaporation and recycled through the electrolytic cell. In laboratory tests, gross beta decontamination factors were 6-33, and corrosion products were removed by factors as high as 2600. The current efficiency in the electrolytic cell was approximately 90% for reductions as high as 99%. The equipment must be almost wholly plastic or plastic-lined because of the corrosive action of hydrofluoric acid. Utilization of HF in the process is essentially stoichiometric. A cost estimate indicated that uranium could be converted from uranyl nitrate solution to anhydrous $UF_4$ for about 25¢ per pound. A suggested modification of the process, in which an improved cell design is used and HF concentration equipment is eliminated, should reduce the cost to 20¢ per pound. (auth)

**1957** (CEA-tr-X-616) SEPARATION DU THORIUM D'AVEC LES TERRES RARES PAR L'EMPLOI DE RESINES ECHANGEUSES ANIONIQUES. (Separation of Thorium from Rare Earths by Use of Anion Exchange Resins). Yagi, I. Translated into French from Kogyo Kagaku Zasshi, 63: 788-93(1960). 28p. Dep. mn; JCL $2.60 fs, $1.04 mf.

The behavior of macroquantities of thorium and of traces of rare earths (Ce, La, $^{144}Ce-^{144}Pr$, $^{152-154}Eu$, $^{90}Y$, $^{147}Nd-^{147}Pm$) in a nitric acid solution was studied on a strongly basic anion exchange resin (Amberlite IRA-410). The possibility of separating Th from the rare earth traces was examined. The results have shown that the following conditions are necessary for such a separation. Nitric acid must be used for the regeneration of the resin. The concentration of the nitric acid in the standard solution ought to be 6 N and the concentration of the Th to be separated should be 0.001 to approximately 0.01 M. The elution solution should be 6 N nitric acid followed by water. These conditions make it possible to increase the decontamination coefficient of Th in the presence of $^{144}Ce-^{144}Pr$ to a value of 35. The separation of Th from the other elements is much lower. These results have established the conditions essential for the industrial production of high purity compounds of Th. (tr-auth)

**1958** PRECONCENTRATION OF TRACE ELEMENTS BY PRECIPITATION ION EXCHANGE USING ORGANIC-HYDROCHLORIC ACID SYSTEMS. Ruch, R. R.; Tera, Fouad; Morrison, G. H. (Cornell Univ., Ithaca, N. Y.). Anal. Chem., 37: 1565-8(Nov. 1965).

The approach to preconcentration of trace elements by precipitation ion exchange was extended and improved by the use of organic-HCl eluent systems. The matrix and traces are first sorbed on a cation exchange column; the matrix is then precipitated by the organic-HCl eluent, followed by nonselective elution of the traces. The separation is based on the insolubility of the matrix and the low selectivity of the traces in 70% p-dioxane-30% concentrated hydrochloric acid by volume. As many as 40 trace elements may be preconcentrated in greater than 90% yields, matrix-free or with only small amounts of matrix from the following matrices: Li, Na, K, Rb, Mg, Ca, Sr, Ba, Sc, Y, and La. Using 81% dioxane-10% ethanol-9% concentrated HCl (by volume) as eluent, matrices such as Ni, Cr, Mn, Pb, and Al demonstrated sufficient insolubility and delayed column breakthrough, as well as favorable trace recovery, to be of value in preconcentration. (auth)

**1959** ANION EXCHANGE STUDIES OF THORIUM, RARE EARTHS, AND SCANDIUM IN AMMONIUM THIOCYANATE-ORGANIC SOLVENT-WATER MIXTURES. Pietrzyk, Donald J.; Kiser, Donald L. (Univ. of Iowa, Iowa City). Anal. Chem., 37: 1578-80(Nov. 1965).

Thorium, rare earths, and scandium anion exchange in $NH_4SCN$-organic solvent-water mixture was studied. The distribution coefficients of the metal ions on Dowex 1X8 in various concentrations of acetone and 0.1M $NH_4SCN$, ethanol and 0.1M $NH_4SCN$, and $NH_4SCN$ and 70% ethanol are given along with values for water-$NH_4SCN$-methanol (ethanol or acetone) systems. Data on separation of metal ions on the Dowex 1X8 columns are given. (F.J.H.)

**1960** DECONTAMINATION OF SODIUM FROM PRODUCTS OF REACTIONS WITH WATER IN THE CIRCULATION LOOP. Subbotin, V. I.; Kirillov, P. L.; Kozlov, F. A.; Ivanovskii, N. N.; Makarov, V. M. At. Energ. (USSR), 19: 298-300(Sept. 1965). (In Russian).

Experiments were carried out on the removal of NaH, created in the reaction $Na + \frac{1}{2} H_2 \rightarrow NaH$, and on the removal of NaH and $Na_2O$, from the reaction $4Na + H_2O \rightarrow Na_2O + 2NaH$, from sodium coolant by means of filtration through a cold trap. Results of measurements of the removal temperatures are given for typical examples. (M.J.T.)

**1961** CONTRIBUTIONS TO THE ELECTROPHORESIS OF RADIOACTIVE RARE EARTHS. Buchtela, K.; Aitzetmueller, K.; Grass, F. (Oesterreichische Hochschule, Vienna). Atomkernenergie, 8: 264-8(July-Aug. 1965). (In German).

The electrophoretic separation of mixtures of radioactive rare earths was investigated using foils of acetyl cellulose. The separated activities were identified by their half lives and by $\gamma$ spectrometry. Electrophoresis in $\alpha$-hydroxyisobutyric acid is compared with ion exchange chromatography. A straight line is obtained if one draws the peak positions of ion exchange elution in logarithmic scale versus normalized electrophoresis positions in a linear scale. Predictions are

given for the electrophoretic behavior of trivalent actinides. The predicted position for Am was verified by experiment. (auth)

**1962** PURIFICATION OF URANIUM FROM FISSION PRODUCTS BY MEANS OF FRACTIONAL PRECIPITATION OF $UO_2$ BY REDUCTION OF $UO_2Cl_2$ FROM ALKALI CHLORIDE MELT. Avogadro, A.; DePlano, A.; Krawczynski, S.; Loo, P. Van Atomkernenergie, 8: 301-3(July-Aug. 1965). (In German).

On dissolving irradiated $UO_2$ by means of chlorination in an alkali-chloride melt and reducing it with $H_2$ to $UO_2$, the alkalines, as Cs, as well as the alkaline earths, as Ba, and the rare earths, as La, remain in the bath. Ce and Zr-Nb precipitate with the uranium. If the precipitation of $UO_2$ is, however, done in a fractional way, a logarithmic distribution of the two last-mentioned elements between the salt bath and the precipitated $UO_2$ is observed, which allows a separation of these two elements from the bulk of uranium. With an artificial mixture of all elements with fission yields greater than 1%, the decontamination factors for a simulated burn-up of 3%, obtained by precipitation of 5% $UO_2$, have been for Zr-Nb: DF = 1000; for Ce: DF = 7. The elements Te, Mo and Ru could be separated by means of volatilization of the chlorine compounds. (auth)

**1963** INVESTIGATION OF ADSORPTION OF TECHNETIUM FROM AQUEOUS SOLUTIONS ONTO RUSSIAN-MADE ANION EXCHANGE RESIN. Ryabchikov, D. I.; Pozdnyakov, A. A. (Inst. of Geochemistry and Analytic Chemistry, Academy of Sciences, USSR). Dokl. Akad. Nauk SSSR, 161: 896-8(Apr. 1, 1965). (In Russian).

Technetium separation from various waste aqueous solutions in the nuclear energy industry was studied. Adsorptive properties of some anion exchange resins were examined. Separation coefficients for technetium isotopes in acid solution were determined. Concentrations of technetium isotopes were measured by monitoring $\gamma$ and $\beta$ radiation. Isotopic equilibration was achieved after 50 to 60 min contact between the solution and the anion exchange resin. One anion exchange resin extracted technetium from weakly acidic, neutral, and basic concentrated solutions of $NaNO_3$, from solutions of HCl of any concentration, and also from 6 to 7M of $H_2SO_4$ and from 3 to 4M $HNO_3$. Because of small adsorption of technetium from perchlorate solutions, these solutions could be used for desorbing technetium from the anion exchange resin. All technetium can be desorbed from a resin to a 1.5 to 2M aqueous solution of $HClO_4$. Adsorption of technetium on strongly basic anion exchange resins was reversible. High sorptivity of $TcO_4^-$ ions was due to small hydration of these ions. (CFSTI)

**1964** URANIUM ORE REFINING PLANT. Sumitani, Shozo; Muramatsu, Takio (Ebara Mfg. Co., Ltd., Japan). FAPIG (Tokyo), No. 36, 33-7(Apr. 1965). (In Japanese).

A uranium ore refining plant is described. The refining of uranium ore usually includes two steps. The preliminary step is mineral-acid digestion (followed by ion exchange or solvent extraction) or carbonate-infusion (followed by alkali precipitation). In the final step $UF_4$ is produced by the dry or wet method and reduced with Mg or Ca. Mineral-acid digestion method tends to introduce impurities. The Furukawa-Denko refining plant employs the infusion method with bicarbonate or oxalate and $UF_4$ is produced by cycling the fluoride double salt. The process for the bicarbonate infusion method is $UO_3 + 2NaHCO_3 \rightarrow Na_2UO_2(CO_3)_2 + NaOH$, $Na_2UO_2(CO_3)_2 + (RR'NH_2)_2CO_3 \rightarrow (RR'NH_2)_2UO_2(CO_3)_2 + Na_2CO_3$, and $(RR'NH_2)UO_2(CO_3)_2 + Na_2CO_3 \rightarrow Na_2UO_2(CO_3)_2 + (RR'NH_2)_2CO_3$. The Excer method uses the sulfuric acid infusion. Nitric acid infusion is also carried out. The final refining step includes a conversion process, $UO_2CO_3 + 2HCl \rightarrow UO_2Cl_2 + CO_2 + H_2O$, a fluorination process, $UO_2Cl_2 + HCOOH + 5NH_4F + 2SO_2 \rightarrow UF_4 \cdot NH_4F + 2NH_4Cl + 2NH_4HSO_3 + CO_2$, and a thermal decomposition process, $UF_4 \cdot NH_4F \rightarrow UF_4 + NH_4F$. The Excer process uses electrolytic reduction. (NSA of Japan)

**1965** SEPARATION OF MOLYBDENUM FROM RHENIUM BY THE EXTRACTION OF Mo(VI) FROM Re(IV) WITH AMYL ACETATE. Yatirajam, V.; Prosad, R. (Kurukshetra Univ., India). Indian J. Chem., 3: 345-7 (Aug. 1965).

A procedure for the complete and rapid separation of molybdenum(VI) from rhenium(VII) is described. Mo(VI) and Re(VII) are first reduced in hydrochloric acid solution by hydrazine dihydrochloride to Mo(V) and Re(IV) respectively. Mo(V) is then selectively oxidized back to Mo(VI) by bromine, leaving Re(IV) unaffected. Mo(VI) is extracted from the solution with amyl acetate. (auth)

**1966** STUDY ON REMOVAL OF IODINE FROM ATMOSPHERE BY SPRAY. I. REMOVAL OF IODINE BY SPRAY UNDER ATMOSPHERIC PRESSURE. Maekawa, Tatsuo; Nishizawa, Yukinori; Shibayama, Tetsuo; Kawaguchi, Osamu (Mitsubishi Atomic Power Industries, Inc., Japan). Nippon Genshiryoku Gakkaishi., 7: 563-9(1965). (In Japanese).

The removal of elementary iodine from the atmosphere by spray was studied using a steel drum fitted with an iodine generating system, a spray nozzle, an electric heater, and a gas-phase sampling system. The experiments were carried out over a temperature range of 25 to 80°C under atmospheric pressure, and the removal rate of iodine was estimated by gas chromatography. The results are expressed by the equation, $-dC/dt = (k_p + \alpha F)C$, where C is concentration of iodine in air, t is spraying time, $k_p$ is plateout rate constant, F is spray rate, and $\alpha$ is washout rate constant. The plateout rate constant increased with increasing temperature, but the washout rate constant was independent of temperature. (auth)

**1967** EFFECTS OF SALTING-OUT AGENTS ON THE URANIUM AND PLUTONIUM ACTIVITY COEFFICIENTS IN NITRIC ACID SOLUTIONS. Shuvalov, O. N. Radiokhimiya, 7: 265-70(1965). (In Russian).

The effects of $Al(NO_3)_3$, $Mg(NO_3)_2$, and $NH_4NO_3$ on the activity coefficients of $U^{6+}$, $Pu^{6+}$, and $Pu^{4+}$ in solutions of uranium and nitric acid were determined. The Kharned coefficients were determined for $U^{6+}$ and $Pu^{6+}$. It is shown that the activity coefficients of $Pu^{4+}$ and the extraction constants of $HNO_3$ in the presence of salting-out agents lie on a smooth curve. (tr-auth)

**1968** RADIOCOLLOIDS IN SORPTION SYSTEMS. II. ISOTHERM OF COLLECTIVE SORPTION IN A SYSTEM WITH ALTERNATING SORBENT MASS. Egorov, Yu. V.; Nikolaev, V. M. Radiokhimiya, 7: 273-80(1965). (In Russian).

From the independent sorptive behavior of each type of particle in microcomponent radiocolloids for systems with variable mass of the sorbent, the isotherm of the collective sorption ("gross isotherm") of such radiocolloids was investigated. The physical significance of the parameters of the isotherms investigated, revealed in its asymptotic alternates (sufficently small and sufficently large mass of the sorbent) was explained. It was established that in the general outlines the isotherm obtained coincides with the hyperbolic isotherm with the polyempirical parameters, proposed and confirmed by earlier authors. The method for the graphic and analytical analysis of such isotherms for multicomponent radiocolloids is shown. The two-type variants (the different sorbing types of particles belonging to one isotope and the cases where one type of particle is not sorptive) are shown in detail. (tr-auth)

**1969** EFFECTS OF THE GAS MACROCOMPONENT ON THE DISTRIBUTION OF $^{85}Kr$ AND $^{133}Xe$ BETWEEN GASEOUS PHASE AND SOLID CARBON SORBENT. Trofimov, A. M.; Pankov, A. M. Radiokhimiya, 7: 293-8 (1965). (In Russian).

The temperature dependence of the absorption coefficients of $^{85}Kr$ and $^{133}Xe$ on different activated carbons from air, He, Ar, and $CO_2$ was investigated. The temperature limits, in which the linear rule of the distribution on gas microcomponents operates, were established. For example, with absorption on activated carbon from carbon dioxide this rule operated at temperatures above 263°K, but from Ar and air it was valid above 230°K. The heats of absorption of microquantities of Kr and Xe on different activated carbons from He, Ar, air, and $CO_2$ were calculated. The

absorption isobars of gas macrocomponents, He, Ar, air, and $CO_2$, on the activated carbon were determined. (tr-auth)

**1970** FLUORINATION OF $UO_2$–$PuO_2$ FISSION-PRODUCT OXIDE PELLETS IN A FLUIDIZED-BED REACTOR. Anastasia, L. J. (Argonne National Lab., Ill.); Alfredson, P. G.; Steindler, M. J. Trans. Amer. Nucl. Soc., 8: 357-8(Nov. 1965).

**1971** FLUID-BED FLUORIDE VOLATILITY PROCESSING OF IRRADIATED FUELS IN A HOT CELLS. Chilenskas, A. A.; Turner, K. S.; Holmes, J. T.; Kincinas, J.; Potts, G. (Argonne National Lab., Ill.). Trans. Amer. Nucl. Soc., 8: 615(Nov. 1965).

**1972** PROCESS AND APPARATUS FOR DECONTAMINATION OF MILK PRODUCTS BY ELECTRODIALYSIS. (to Ionics, Inc.). British Patent 1,005,125. Sept. 22, 1965. Priority date June 8, 1962, United States.

An electrodialysis cell for removing radioactive ionized contaminants from milk has electrodes situated at each end and has repeating units each having three adjacent compartments. The center compartment is bounded on both sides by ion-exchange membranes of the same selectivity, and the adjacent compartments are defined on their outer sides by an ion-exchange membrane of the opposite selectivity. The contaminated milk is passed through the center compartment, and electrolyte solutions containing nonradioactive ions for reconstituting the mineral content of the milk are passed through the outer compartments. A direct current passed transversely through the compartments and membranes causes electrical migration of ions so that the milk withdrawn contains fewer radioactive ions than initially present and has substantially the mineral concentration of normal milk. (A.G.W.)

**1973** PURIFICATION OF URANIUM YELLOWCAKE. (to Rio Algom Mines Ltd.). British Patent 1,006,007. Sept. 29, 1965. Priority date Oct. 18, 1961, Canada.

A process for removing impurities in uranium yellow cake containing predominant amounts of ammonium diuranate consists of the following steps: treating the yellow cake with an aqueous solution of a carbonic acid salt to form a soluble uranium carbonate complex, separating the insoluble impurities, acidifying the uranium carbonate complex solution to a pH of up to 5.2 to precipitate a diuranate and release carbon dioxide, separating the supernatant liquor, redissolving the precipitate by acidifying to a pH of approximately 3.0, and treating the resultant solution with a precipitating agent to recover a substantially pure diuranate. Carbonates and bicarbonates of potassium, sodium, or ammonium are suitable for the carbonic acid solution, and quantities sufficient to dissolve >90% of the U must be used. (A.G.W.)

**1974** THIOCYANATE EXTRACTION OF BERYLLIUM. Biermann, Wendell Joseph (to Beryloy Ltd.). British Patent 1,006,900. Oct. 6, 1965. Filed June 25, 1962.

In a process for extraction of Be from a Be-containing aqueous solution, thiocyanate ion is added to the solution and the pH is set at 2 to 3 by addition of $H_2SO_4$. Beryllium is then selectively extracted by suitable organic solvents, particularly those having ketone or hydroxy groups on chains containing 6 to 8 carbons. A dilute ammonia solution is used for removing the Be from the organic solvent in the form of a beryllium hydroxide precipitate in the water phase. Substantially full recovery of the reagents and solvents used is possible. (A.G.W.)

**1975** REMOVAL OF RADIOACTIVE STRONTIUM AND CESIUM FROM MILK. Migicovsky, Bert B. (to Canadian Patents and Development Ltd.). U. S. Patent 3,207,607. Sept. 21, 1965. Priority date Aug. 19, 1959, Canada.

In a process for removing radioactive Sr and Cs from milk, the milk is treated with an ion exchange resin substantially saturated with Ca, K, and Na ions in the proportions in which the ions are present in milk to cause the radioactive elements to be absorbed by the resin. The milk may be either agitated with the resin or passed through a column containing the resin. (B.L.M.)

# ENGINEERING

## General

**1976** (VDDIT–94) PREVENTIVE MAINTENANCE IN CHEMICAL AND MINING INDUSTRIES. A Literature Search. Holm, Hans I.; Lind, Jan-Erik (Aktiebolaget Atomenergi, Stockholm (Sweden)). Sept. 1965. 10p. Dep. mn.

Forty-four references on proper preventive maintenance programs in chemical and mining industries are given to journals published from July 1963 to June 1965. (P.C.H.)

**1977** A NONDESTRUCTIVE ELECTRICAL METHOD OF STUDYING THE DENSITY DISTRIBUTION OF A RANDOMLY PACKED BED. Zablocki, H. S.; Rudo, F. S.; Cutler, J. A.; Coler, M. A. (Markite Corp., New York). Trans. Amer. Nucl. Soc., 8: 582(Nov. 1965).

**1978** VIBRATION OF FUEL ASSEMBLIES IN PARALLEL FLOW. Pavlica, R. T.; Marshall, R. C. (Combustion Engineering, Inc., Windsor, Conn.). Trans. Amer. Nucl. Soc., 8: 599-600(Nov. 1965).

## Applications of Nuclear Explosions

**1979** (AD–614814) MICROMETEOROLOGICAL PHENOMENA OF UNDERWATER NUCLEAR EXPLOSIONS. Young, George A. (Naval Ordnance Lab., White Oak, Md.). Jan. 14, 1965. 37p. (NOLTR–64-187). CFSTI $2.00 cy, $0.50 mn.

The above-surface phenomena of Test Baker in Operation Crossroads (1964) are described in detail with emphasis on the primary base surge. Some recent theoretical results concerning the surge structure and behavior are summarized. The base surge from the Teapot ESS Underground Test is briefly described and compared with the Baker surge. (auth)

**1980** (AD–614990) SIMULATION OF AIR-BLAST-INDUCED GROUND MOTION, PHASE I. Period Covered: December 1963–August 1964. D'Arcy, Gerald P.; Auld, Harry E.; Leigh, Gerald G. (Air Force Weapons Lab., Kirtland AFB, N. Mex.). Apr. 1965. 81p. (WL-TR–65-11). CFSTI $3.00 cy, $0.75 mn.

An analytical and experimental program was performed to determine the most promising techniques for simulating the air-blast-induced ground motions from a large-yield nuclear weapon. Two techniques were then selected for further development. One of the selected techniques employs a detonable gas mixture and the other a primacord matrix to generate a traveling shock wave which loads the ground. The nuclear air-blast overpressure environment is described and the simulation produced by either scheme is compared with this environment. The primacord technique was then selected because it was found to be the most practical and economical. Sufficient data are presented to enable the design of simulation experiments which use either technique. (auth)

**1981** (PNE–605F) STRONG-MOTION SEISMIC MEASUREMENTS. Project DUGOUT. Lowrie, L. M.; Mickey, W. V. (Coast and Geodetic Survey, Rockville, Md. Washington Science Center). May 1965. Contract AT(29-2)-746. 43p. Dep. mn; CFSTI $2.00 cy, $0.50 mn.

The 100-ton DUGOUT row charge cratering experiment was monitored with strong-motion seismographs at distances from 146 meters to 1.58 kilometers. Measurements of transitory earth particle displacements and accelerations were made along two recording station lines, one perpendicular to the row, the other in line with the row. The primary purpose of the program was to determine whether there was any azimuthal variation in the propagation of seismic energy dependent upon the configuration of the charge. Maximum earth particle motions indicated symmetrical seismic wave propagation beyond 250 meters. Fourier spectrograms from recordings obtained at 600 meters showed more high frequency content in line with the charge, but at 1.5 kilometers spectrograms were remarkably similar in the two recording station directions. For stations on the two recording lines at a distance of 1.5 kilometers particle motion diagrams showed some similar waveforms and no obvious dissimilarities which could be correlated with the charge configuration. First motion travel times, indicating a velocity of 2.2 km/sec, were in contrast with laboratory determinations which suggested compressional wave velocities between 3.5 km/sec and 4.5 km/sec for the basaltic material of Buckboard Mesa. This is attributed to vesicularity and other inhomogeneities in the basalt. The conversion of total available source energy to seismic energy was estimated at about 0.3 percent. (auth)

**1982** (PNE–807F) WEATHER AND RADIOLOGICAL SURVEILLANCE. Project HANDCAR. Final Report. (Weather Bureau, Las Vegas, Nev. Public Health Service, Las Vegas, Nev. Reynolds Electrical and Engineering Co., Inc., Mercury, Nev.). Nov. 12, 1965. 53p. Dep. mn; CFSTI $3.00 cy, $0.50 mn.

Project Handcar, a contained 10-kt nuclear explosion in dolomite, was detonated at a depth of 402 m on Nov. 5, 1964. Results are presented of weather and surface radiation protection and of off-site and on-site surveillance. No radiation exposure resulted. (D.L.C.)

**1983** (PNE–2000) ISTHMIAN CANAL STUDIES, 1964. ANNEX III. APPENDIX 1. NUCLEAR EXCAVATION PLAN. Graves, Ernest Jr.; Holmes, Robert S. (Army Engineering Nuclear Cratering Group, Livermore, Calif.); Nordyke, Milo D.; Cauthen, Lewis J. Jr.; Williamson, Marvin M. (Lawrence Radiation Lab., Univ. of California, Livermore). Sept. 1964. Contract W-7405-eng-48. 67p. Dep. mn; CFSTI $1.00 cy, $0.75 mn.

A plan for using nuclear explosions to dig the channel for an Isthmian sea-level canal is described for two alternative routes: Sasardi-Morti (Route 17) and Atrato-Truando (Route 25). This plan begins with the concept of nuclear excavation and the design of the nuclear explosions. The hazardous effects of the explosions and their control are discussed. The nuclear operations required to carry out the excavation detonations are described, and the cost is estimated. The development program required before the excavation can be undertaken is summarized. (D.L.C.)

**1984** (PNE–2001) ISTHMIAN CANAL STUDIES, 1964. ANNEX III. APPENDIX 1. INCLOSURE A. EXCAVATION WITH NUCLEAR EXPLOSIONS. (Army Engineering Nuclear Cratering Group, Livermore, Calif.). Sept. 1964. Contract W-7405-eng-48. 119p. Dep. mn; CFSTI $1.25 cy, $0.75 mn.

The design of the nuclear explosions required to excavate the channel for the Isthmian sea-level canal is described for two alternative routes: Sasardi-Morti (Route 17) and Atrato-Truando (Route 25). The size and number of the nuclear devices, the dimensions and engineering properties of the craters, detonation programs, and emplacement drilling are considered in detail. It is concluded that Route 17 would require 294 devices with a total yield of 166.4 Mt in 14 separate detonations, while Route 25 would use 262 devices with a total yield of 270.9 Mt in 21 separate detonations. (D.L.C.)

**1985** (PNE–2003) ISTHMIAN CANAL STUDIES, 1964. ANNEX III. APPENDIX 1. INCLOSURE C. SAFETY EVALUATION FOR AIR BLAST, GROUND SHOCK, THROW-

OUT, AND DUST. Cauthen, Lewis J. Jr.; Korver, John A.; Nordyke, Milo D.; Preston, Roger G. (Lawrence Radiation Lab., Univ. of California, Livermore); Reed, Jack W.; Vortman, Luke J. (Sandia Corp., Albuquerque, N. Mex.). Sept. 1964. Contract W-7405-eng-48. 34p. Dep. mn; CFSTI $1.00 cy, $0.50 mn.

The nature of each of the hazards is outlined. Close-in and intermediate- and long-range air blast are considered. Comparisons are made of predicted air blast and ground shock levels with damage criteria. Throwout and dust from cratering explosions are analyzed. (D.L.C.)

**1986** (PNE–2004) ISTHMIAN CANAL STUDIES, 1964. ANNEX III. APPENDIX 1. INCLOSURE D. NUCLEAR OPERATIONS. (Nevada Operations Office (AEC), Las Vegas). Sept. 1964. Contract W-7405-eng-48. 55p. Dep. mn; CFSTI $1.00 cy, $0.50 mn.

The nuclear operations program is made up of the activities required to emplace and fire the nuclear explosives, conduct the safety programs, and provide operational direction and management. The elements of the nuclear operations program include project management, operations coordination and area control, explosives security, nuclear explosives operations, meteorology, radiological safety and terrestrial bioenvironmental program, marine bioenvironmental program, air blast prediction, and seismic effects. Each of the elements is described, and cost estimates are given. (D.L.C.)

**1987** (UCRL–13189) WEAPONS EFFECTS DISPLAY SYSTEM STUDY. Final Report. Henderson, R. L.; Campbell, J. C.; Gaydos, H. F.; Kester, S. G. (System Development Corp., Santa Monica, Calif.). Sept. 7, 1965. Contract W-7405-eng-48. 50p. Dep. mn; CFSTI $2.00 cy, $0.50 mn.

For Univ. of California Lawrence Radiation Lab., Livermore.

The general characteristics of a Weapons Effects Display System whose purpose is to provide a simple, direct means of solving specific weapons effects problems and a means whereby important functional relations could be presented and related to the physical world in a meaningful manner are reported. Basically the system consists of an operator control console for inserting and controlling problem data, an analog computer to perform the necessary calculations, and a display unit to present the problem solution. The two aspects of the problem, the human factors problem and the problem of physically generating the displays, are treated separately. (P.C.H.)

## Facilities and Equipment

*Refer also to abstracts 1799, 1953, 2352, and 3522.*

**1988** (NAA-SR–11198) DEVELOPMENT OF THE THERMOELECTROMAGNETIC PUMP FOR THE 3-kwe MERCURY RANKINE SYSTEM. Hanlin, H. H. (Atomics International, Canoga Park, Calif.). Sept. 1, 1965. Contract AT(11-1)-Gen-8. 69p. Dep. mn; CFSTI $3.00 cy, $0.75 mn.

A thermoelectromagnetic pump is developed to circulate the heat-transfer fluid in a Rankine-cycle space power system. This device combines a d-c conduction pump and thermoelectric generator into a single, all-metallic unit. The thermoelectric elements, chromel and constantan, extract heat from the fluid being pumped, convert a portion of it directly into electricity to supply the conduction pump, and reject the waste heat to the secondary working fluid, mercury, as it enters the boiler. This pump type offers several advantages: it has no moving parts; and complete sealing of the liquid metals for highest reliability and complete utilization of rejected heat for highest system efficiency is possible. The design performance objective of 1 psi, 12 gpm NaK-78 at 1200°F is achieved, and an endurance run to 6000 hours is demonstrated. The complete development program, sign method and equations, laboratory procedures, and important test results are described. (auth)

**1989** (NYO–841-2) SUMMARY REPORT ON PERFORMANCE OF AIR CLEANING SYSTEM FOR U. S. BUREAU OF MINES BOMAEC-30 INCINERATOR. Dennis, Richard; Silverman, Leslie (Harvard School of Public Health, Boston, Mass.). Dec. 1964. Contract AT(30-1)-841. 156p. Dep. mn; CFSTI $5.00 cy, $1.00 mn.

Evaluation of combustion and gas cleaning equipment tests are presented for studies on the BOMAEC-30 institutional type incinerator developed for low level, radioactive waste disposal. The BOMAEC-30 unit consists of a cylindrical, stainless steel-lined, chamber with all combustion air admitted tangentially above the waste charge. Results of several tests with sawdust and office wastes indicated that: only dry (<10% moisture) materials could be burned completely without auxiliary gas firing; the design burning rate objective of 30 lbs. per hour could not be attained in most tests; and the operating methods were not amenable to a safe, rapid means of waste incineration. A water spray cooling tower and glass fabric filtration system did not furnish adequate gas cleaning. (P.C.H.)

**1990** (TID–3545(Rev.1)) HOT LABORATORIES. An Annotated Bibliography. Bost, William E. (comp.) (Division of Technical Information Extension (AEC), Oak Ridge, Tenn.). Nov. 1965. 194p. Dep. mn; CFSTI $5.00 cy, $1.00 mn.

References (1286) on design, equipment, and operation of laboratories for work with radioactive materials are given to U. S. and foreign journals, reports, books, and patents published from 1947 through 1964. Separate availability, author, and report number indexes are included. (P.C.H.)

**1991** 150 kOe LIQUID NITROGEN COOLED PULSED FLUX-CONCENTRATOR MAGNET. Brechna, H.; Hill, D. A.; Bailey, B. M. (Massachusetts Inst. of Tech., Cambridge). Rev. Sci. Instrum., 36: 1529-35(Nov. 1965). (MIT–2098-154).

A 150 kOe flux-concentrator magnet is described, having a 90 $cm^3$ conical bore 7 cm long and of 10.4 cm maximum diameter. The field is held at peak value ±10% for 30 to 50 msec per pulse. The flux concentrator is energized by a transformer-rectifier set delivering 600 V at 3800 A for the duration of the pulse; it is cooled by a closed loop of circulating subcooled liquid nitrogen, which in turn is cooled external to the magnet by liquid nitrogen boiling at atmospheric pressure. (auth)

**1992** CLEANING BLOCKED COOLANT PASSAGES IN WATER-COOLED MAGNETS. Markley, F.; Malm, J.; Chernick, C.; Hughes, J. (Argonne National Lab., Ill.). Rev. Sci. Instrum., 36: 1670-1(Nov. 1965).

The blocked coolant passage is drained, dried by flushing with nitrogen gas, cleaned of grease using acetone, equipped with Teflon gaskets in place of the normally used rubber gaskets, evacuated, and exposed to fluorine gas at pressures up to 700 mm Hg. The fluorine reacts with the blocking substances, and unblocks the passage. The passage is exposed to fluorine for about 30 min during this cleaning. (T.F.H.)

**1993** REMOTELY OPERABLE FUEL-ROD PROFILOMETER. Duncan, R. N.; Barden, J. L.; Atkinson, J. S. (General Electric Co., San Jose, Calif.). Trans. Amer. Nucl. Soc., 8: 584(Nov. 1965).

**1994** THE THORIUM–URANIUM RECYCLE FACILITY. Irvine, A. R.; Lotts, A. L.; Olsen, A. R. (Oak Ridge National Lab., Tenn.). Trans. Amer. Nucl. Soc., 8: 614 (Nov. 1965).

**1995** CONTAMINATED FILTER REMOVAL EQUIPMENT. Hahs, C. A. (Oak Ridge National Lab., Tenn.). Trans. Amer. Nucl. Soc., 8: 619-20(Nov. 1965).

**1996** CENTRAL LABORATORY FOR HOT CHEMISTRY AT KFA-JUELICH. Davis, J. M. (Kernforschungsanlage, Juelich, Ger.); Javary, B.; Schloesser, L.; Tarbe de St. Hardouin, A. Trans. Amer. Nucl. Soc., 8: 621 (Nov. 1965).

**1997** HOT LABORATORY OF JAPAN ATOMIC ENERGY RESEARCH INSTITUTE. Murakami, M.; Yso, Y.; Sasaki, Y.; Kayashi, K.; Matsumoto, T.; Sakakura, A.; Tomimura, K. (Japan Atomic Energy Research Inst., Tokyo). Trans. Amer. Nucl. Soc., 8: 621-2(Nov. 1965).

**1998** THE BABCOCK AND WILCOX HOT-CELL FACILITY. Womack, Robert E. (Babcock and Wilcox Co., Lynchburg, Va.). Trans. Amer. Nucl. Soc., 8: 622-3 (Nov. 1965).

**1999** NEW FONTENAY-AUX-ROSES ALPHA-BETA-GAMMA RADIOMETALLURGY LABORATORY—DESIGN AND CONSTRUCTION. Valentin, A.; Portal, A. (Centre d'Etudes Nucleaires de Saclay, Gif-sur-Yvette, France). Trans. Amer. Nucl. Soc., 8: 623(Nov. 1965).

**2000** EVOLUTION OF THE HIGH-LEVEL CAVES AT THE SAVANNAH RIVER LABORATORY. Coogler, A. L.; Deily, G. J.; Hale, R. J. (E. I. duPont de Nemours and Co., Aiken, S. C.). Trans. Amer. Nucl. Soc., 8: 623-4 (Nov. 1965).

**2001** ALPHA-GAMMA FACILITY FOR FUEL STUDIES. Banslaben, A. J.; Chow, J. G. Y. (Brookhaven National Lab., Upton, N. Y.). Trans. Amer. Nucl. Soc., 8: 625(Nov. 1965).

**2002** AUTOMATIC TILTING DEVICE FOR RADIOACTIVE ARTICLES. Escavis, Armand; Gerard, Victor; Mas, Roland (to Commissariat a l'Energie Atomique). British Patent 1,004,499. Sept. 15, 1965. Priority date Aug. 22, 1963, France.

An automatic remotely controlled pivoting device is designed to transfer a fuel element or any radioactive article from a vertical position into a horizontal position. A runway overhung on a pivot shaft is adapted to receive and bear the radioactive article. A counterweight applies torque to the actuating shaft to return the runway to the vertical position, and a damping system retards the runway near the ends of its pivoting movement. Locking pawls lock the runway in its two end positions. (A.G.W.)

**2003** IMPROVEMENTS IN REMOTE CONTROL AND AUTOMATION DEVICES FOR PLANT IN RADIOACTIVE SURROUNDINGS. Boulenger, Bernard; Fuzellier, Jean; Pratviel, Pierre; Couture, Jacques; Faugeras, Pierre (to Commissariat a l'Energie Atomique). British Patent 1,004,867. Sept. 15, 1965. Priority date Oct. 6, 1960, France.

In a system for remotely controlling the movement of members in a radioactive environment, a transmitter located outside the radioactive environment for transmitting binary control data and consisting of a pulse generator for producing a train of pulses preceded by a reference pulse is connected by a single-line circuit to receivers connected to different members to be controlled. Each receiver includes a decoding circuit, a control circuit, a comparison circuit, and a recording circuit. (A.G.W.)

**2004** DEVICE FOR THE TRANSMISSION OF MOVEMENTS AND APPLICATION OF SAID DEVICE TO REMOTE-HANDLING APPLIANCES. Fortin, Antoine; Fortin, Marcel; Vertut, Jeau (to Commissariat a l'Energie Atomique). British Patent 1,006,272. Sept. 29, 1965. Priority date Apr. 25, 1962, France.

A device is patented for coupling a shaft mounted in one of two components relatively movable about an axis to another shaft mounted in the other component so that rotation of one shaft is transmitted to the other and the coupling device does not obstruct the relative movement of the components. The shafts carry pinions meshing with an intermediate toothed wheel or with members of an intermediate toothed wheel assembly, and the toothed wheel or one member of the assembly is rotatable about the axis about which the components are movable. The relative movement may be an angular movement about an axis perpendicular to the axes of the shafts or a rotation about an axis parallel to the axes of the shafts. A remote-handling appliance embodying the device is described. (A.G.W.)

**2005** DEVICE FOR THE LEAK-TIGHT TRANSMISSION OF MOVEMENT THROUGH A WALL. Archer, Jacques; Boiron, Pierre (to Groupement Atomique Alsacienne Atlantique). British Patent 1,006,414. Sept. 29, 1965. Priority date Nov. 13, 1962, France.

In a device for transmission of movement through a wall, the driving shaft and the driven shaft rotate about the same axis and are coupled at a point located off-center with respect to the axis in such a manner as to transmit a torque from one to the other while ensuring perfect leak-tightness between the two shafts by means of a deformable cylindrical membrane. The arrangement is such that the membrane is free from any twisting efforts about its axis and is subjected only to minimum mechanical bending stress. (A.G.W.)

**2006** A SYSTEM FOR MECHANICALLY MOUNTING A RADIOACTIVE SAMPLE. Ferrier, Charles; Lefebvre, Gilbert (to Commissariat a l'Energie Atomique). British Patent 1,006,484. Oct. 6, 1965. Priority date Apr. 11, 1963, France.

A system is patented for mounting a radioactive sample in a cavity in a ballasting block so that a surface is exposed for polishing. The sample is provided with a cylindrical sheath of coating material and held in the cavity by means of a flexible plastic cup. The cup has a longitudinal slot that can be closed up to hold the sample by the action of a screw carried by the block. Apparatus for supporting and transporting the block and for positioning the sample by remote control from outside a radioactive cell are included. (A.G.W.)

## Heat Transfer and Fluid Flow

**See *also* PHYSICS — Fluid Physics and Thermodynamics**

*Refer also to abstracts 3323, 3459, 3461, 3515, and 3516.*

**2007** (AD-618026) COMBINED CONVECTION AND RADIATION IN RADIOISOTOPE THRUSTORS [Thesis]. Dibiase, James A. (Air Force Inst. of Tech., Wright-Patterson AFB, Ohio. School of Engineering). June 1965. 149p. (GSP-65A/ME/65-1). CFSTI $4.00 cy, $1.00 mn.

Heat transfer by the combined effects of convection and radiation was investigated for radioisotope propulsion systems. Fully developed laminar flow was considered, with the transverse temperature profiles assumed to be the fully developed profiles for the local conditions. The governing equations were derived for non-insulated and insulated systems and the equations were solved numerically on an IBM-7094 computer. The assumptions used in the theoretical analysis were tested experimentally for the insulated case by simulating the radioisotope with a resistance heater and using hydrogen as a propellant. The theoretical and experimental data are compared for the range of flow rates tested. (auth)

**2008** (AD-622825) INVESTIGATION OF LIQUID METAL BOILING HEAT TRANSFER. Progress Report, May–August 1965. Balzhiser, Richard E.; Caswell, Bruce F.; Padilla, Andrew Jr.; Barry, Robert E.; Gahman, Robert L.; Merte, Herman Jr. (Michigan Univ., Ann Arbor. Liquid Metals Lab.). Aug. 1965. Contract AF 33(657)-11548. 45p. CFSTI $2.00 cy, $0.50 mn.

Critical heat flux determinations were made with rubidium. The burnout results along with other liquid metal burnout data are correlated with a dimensionless relation. A film boiler was operated and yielded data over pressure range of 2 – 19mm mercury. The data obtained fall slightly above the predictions of Berenson for potassium film boiling at a pressure of a 0.1 atm. Data obtained for which the surface temperature exceeded the saturation temperature by greater than 700°F yielded reasonable consistent results when the flux was calculated by two independent procedures. At lower values of the surface temperature, unusual behavior was encountered which is probably related to transi-

tional effects which began to occur on the wall of the vessel near the boiling plate. For values of $T_{surf} - T_{sat}$ from 700 – 900°F and over the pressure range of 2 – 19mm of mercury, the heat fluxes obtained ranged from 4,000 to 8,000 Btu/(hr)(ft$^2$). A forced circulation apparatus was operated to yield condensing coefficients for sodium over a temperature range of 1240 to 1525°F and a range of heat fluxes from 215,000 to 583,000 Btu/(hr)(ft$^2$). The condensing coefficient was observed to be essentially constant over these ranges at a value of 10,800 ± 3,300 Btu/(hr)(ft$^2$)(°F). (P.C.H.)

**2009** (EUR-2490.e) FORCED CONVECTION BURNOUT AND HYDRODYNAMIC INSTABILITY EXPERIMENTS FOR WATER AT HIGH PRESSURE. PART I. PRESENTATION OF DATA FOR ROUND TUBES WITH UNIFORM AND NON-UNIFORM POWER DISTRIBUTION. Biancone, F.; Campanile, A.; Galimi, G.; Goffi, M. (FIAT, Turin (Italy). Sezione Energia Nucleare). Aug. 1965. Contract 008-61-12 PNII. 104p. Dep. mn.

Forced convection burnout studies were made on water at high pressure. Burnout and hydrodynamic instability data are presented for a first series of experiments performed on round tubes over a wide range of conditions. The effect of non-uniform power distribution along the heater on burnout power as well as on the location of the point at which burnout inception occurs, was investigated. A description of the experimental facility and test sections employed is also included. (P.C.H.)

**2010** (IPV-19) BERAKNING AV TRYCKFALL I ROR OCH BRANSLEELEMENT AV LEDRORSTYP. (Calculation of Pressure Drop in Ducts and Fuel Elements With Shroud). Lange, H.; Steinman, O. (Aktiebolaget Atomenergi, Stockholm (Sweden)). May 10, 1960. 35p. Dep. mn.

Calculations using the IPV-3 and IPV-5 were completed with consideration of subcooled boiling. The corresponding pressure drop terms were introduced with one proportionality constant, whose size was determined experimentally. The constant was not general or characteristic depending principally on the increase in subcooled boiling not taken into consideration. Methods were not previously available for pressure drop measurements from fuel elements with a too-large hydraulic diameter. Equations were derived for computer calculation. Results are given for the calculation of fuel elements for the R3/Adam and for a 100 Mv(e) tube reactor. (tr-auth)

**2011** (LA-DC-7189) MOVING PICTURE COMPUTER OUTPUT. Welch, J. Eddie (Los Alamos Scientific Lab., Univ. of California, N. Mex.). [1965]. Contract W-7405-eng-36. 27p. (CONF-651022-1). Dep. mn; CFSTI $2.00 cy, $0.50 mn.

From Users of Automatic Information Display Equipment, Annual Meeting, New York.

A description is given of the way in which results from fluid dynamics calculations can be displayed using the S-C 4020 Microfilm Recorder. Included are figures showing plots of pressure contours, velocity vectors, stream function contours, streak lines, and fluid configuration. Special emphasis is given to the production of moving pictures from 4020 plots. Selected frames were chosen from several cinema sequences illustrating calculations of the flow of water from a broken dam, the passage of a blast wave through a bomb shelter tunnel, the flow of water around an obstacle in a channel, the meteor with a missile surface, and the flow of water from a sluice gate. (auth)

**2012** (NYO-3304-6) INVESTIGATION OF BOILING FLOW REGIMES AND CRITICAL HEAT FLUX. Report No. 602. Bergles, A. E.; Goldberg, P.; Clawson, L. G.; Roos, J.; Bourne, J. G. (Dynatech Corp., Cambridge, Mass.). Oct. 15, 1965. Contract AT(30-1)-3304. 38p. Dep. mn; CFSTI $2.00 cy, $0.50 mn.

Results for the first series of flow regime tests involving the core electrical probe are discussed in detail. In addition to the normal dependence on mass velocity and quality, the flow regime boundaries are significantly affected by inlet temperature, length, and pressure. The flow patterns were not altered by minor changes in probe instrumentation or variations in water purity. Critical heat flux data are presented and compared with several correlations which have been proposed for bulk boiling of water at high pressure. Test-section oscillations were observed under certain conditions; however, this instability does not appear to have significantly affected flow conditions in the test section. A simplified analytical model is presented which appears to explain the experimental trends as well as indicate the current magnitude of the unstable oscillation frequency. (auth)

**2013** (ORNL-P-1661) EXPERIENCES AND DEVELOPMENTS IN INSTRUMENTATION FOR LIQUID METAL EXPERIMENTS. Metz, H. J.; Yarosh, M. M. (Oak Ridge National Lab., Tenn.). [1965]. Contract W-7405-eng-26. 42p. (CONF-650946-2). Dep. mn; CFSTI $2.00 cy, $0.50 mn.

From 4th High Temperature Liquid-Metal Heat Transfer Technology Conference, Argonne, Ill.

A large potassium system and its attendant instrumentation, which was built at ORNL, is described in some detail. A discussion of operating experience with some of the instrumentation is followed by more detailed information on the instruments themselves. (M.O.W.)

**2014** (ORNL-P-1678) AN ACOUSTIC INSTRUMENT FOR MEASURING SUBCOOLING IN BOILING SYSTEMS. Kartluke, H.; Wichner, R. P.; Hoffman, H. W. (Oak Ridge National Lab., Tenn.). [nd]. Contract W-7405-eng-26. 8p. (CONF-650946-3). Dep. mn; CFSTI $1.00 cy, $0.50 mn.

From 4th High Temperature Liquid-Metal Heat Transfer Technology Conference, Argonne, Ill.

An acoustic instrument capable of indicating the degree of undersaturation in a known fluid at unknown temperature and pressure conditions is described. This incipient-boiling detector (developed by Aeroprojects Incorporated) has been tested with water and shown to be effective as a means for monitoring the flow in pressurized water reactors where boiling is undesirable and dangerous. The current study is directed to evaluating this device for possible similar application in liquid-metal cooled fast reactors. Preliminary tests in liquid potassium are discussed. The results were inconclusive; further experiments with a higher power oscillator are planned. (auth)

**2015** (ORNL-P-1681) PRESSURE DROP WITH FORCED-CONVECTION BOILING OF POTASSIUM. Wichner, R. P.; Hoffman, H. W. (Oak Ridge National Lab., Tenn.). [1965]. Contract W-7405-eng-26. 14p. (CONF-650946-4). Dep. mn; CFSTI $1.00 cy, $0.50 mn.

From 4th High Temperature Liquid-Metal Heat Transfer Technology Conference, Argonne, Ill.

Results are given for the pressure drop with boiling potassium in forced-convection flow through a vertical, circular tube. The data, which comprise a single series of measurements (Series D), were obtained in a 6-ft long × 0.270-in.-ID tube having pressure taps at 1-ft spacings over the final 4 ft of the channel. The pressure-measurement system and its deficiencies are discussed; the primary difficulty appears to be "aging" of the diaphragms in the pressure transmitters over long exposure times at high temperatures. The pressure distribution along the boiler was estimated using both homogeneous and Lockhart-Martinelli descriptions of the flow; the calculated exit pressures compared favorably with the measured values. (auth)

**2016** (SC-DC-65-1765) HEAT TRANSFER AND TEMPERATURE DISTRIBUTION IN FINNED RADIATORS. Technical Report ME-15. Wildin, Maurice W. (New Mexico Univ., Albuquerque. Bureau of Engineering Research). Aug. 1965. Contract AT(29-1)-789. 74p. Dep. mn; CFSTI $3.00 cy, $0.75 mn.

For Sandia Corp., Albuquerque, N. Mex.

Some fundamental concepts and material properties used in radiant heat transfer are defined, relations between material properties are discussed, and methods of rigorously

formulating a couple of fairly broad classes of problems are presented. Simplifications in formulation which result from various assumptions are also discussed. As an example of the value and limitations of analyzing limiting cases, the problem of radiant heat transfer between infinite parallel flat plates which are neither purely specular nor purely diffuse reflectors was solved. An approximate method was used which assumes that the directional distribution of energy reflected from an element of a plate can be described by combining a diffuse field and a specularly reflected beam. The numerical results showed that the spectral net heat flux is quite insensitive to the relative amounts of diffusely and specularly reflected energy. (P.C.H.)

**2017** (TID-22312) THE EFFECT OF SURFACE CONDITIONS ON POOL BOILING HEAT TRANSFER OF SODIUM. Progress Report, March–October 1965. Shai, Isaac (Massachusetts Inst. of Tech., Cambridge. Dept. of Mechanical Engineering). Oct. 5, 1965. Contract AT (20-1)-3357. 6p. Dep. mn; CFSTI $1.00 cy, $0.50 mn.

Various tests were performed in investigating the surface effects on pool boiling heat transfer of sodium. Due to unstable boiling at high temperatures and the inability to clean the boiler after each test, proper results could not be attained. A new design for the boiler is given and some results are reported. (M.O.W.)

**2018** (TRG-Report-920) A FEASIBILITY STUDY ON THE USE OF POWDERS AS HEAT TRANSFER MEDIA IN IRRADIATION CAPSULES. Evans, J. L. (International Research and Development Co. Ltd., Newcastle-upon-Tyne). Aug. 1963. Contract CON/R/160559/D/EM2. 20p. Dep.; BIS $0.50; HMSO 2s. 6d.

Because of the experimental difficulties associated with the use of sodium above its boiling point, ceramic powders have been suggested as heat transfer media in irradiation capsules. The desirable properties of such powders are high thermal conductivity, compatibility with the materials of the capsule, and sufficient flexibility to allow unimpeded distortion of the irradiation specimen. The factors affecting these properties are discussed and a high degree of flexibility has been found to be incompatible with a high conductivity. The use of powders for high heat rating applications is therefore not feasible. Experiments to determine the physical properties of powders for low heat rating applications are suggested. (auth)

**2019** SOME FEATURES OF BIPHENYL THERMAL TURBINES AND THEIR MAXIMUM POWER. Danilin, V. S.; Zakharov, I. I.; Loginov, A. A.; Chernyaev, V. A. At. Energ. (USSR), 19: 257-61(Sept. 1965). (In Russian).

The most important properties of biphenyl turbines are examined for atomic heat and electric power plants of up to 50 Mw. It is shown that the limiting factor with regard to the maximum power of these turbines is not the strength, but the degree to which the flow section can be expanded. The fundamental gas-dynamic properties of biphenyl are also briefly discussed. A method is proposed for estimating the maximum power of a central-heating turbine using biphenyl at various rotor speeds. The results show that a biphenyl turbine for a nuclear central-heating plant with a power of 20–50 Mw should have a low rotor speed and be of the double-flow type in a single housing. (M.J.T.)

**2020** FLOW OF SLURRY THROUGH A PIPE. I. ENTRANCE REGION OF LAMINAR FLOW. Michiyoshi, Itaru (Kyoto Univ.); Mizuno, Kenichi; Hoshiai, Yoichi. Nippon Genshiryoku Gakkaishi., 7: 554-62(1965). (In Japanese).

Analyses were made of the flow of slurry in a circular pipe. A theoretical analysis of the laminar flow of Bingham plastic fluid in the entrance region of a circular pipe, by the variational method, is described. Ascertaining the theoretical results by experiments performed with an alumina (about 2 $\mu$ diameter)–water slurry, it was concluded that the length of the entrance region is shorter with Bingham plastic fluid than with Newtonian fluid. It was also found that the correction factor, representing the effect of pressure drop in the entrance region on the pressure difference between the inlet and a given point downstream of the entrance region, is smaller than in the case of Newtonian fluid. These results were correlated with the specific radius of plug of the Bingham fluid flow. (auth)

**2021** A VISUAL AND FRICTIONAL PRESSURE-DROP STUDY OF NATURAL-CIRCULATION SINGLE-COMPONENT TWO-PHASE FLOW AT LOW PRESSURES. Huang, M. N.; El-Wakil, M. M. (Univ. of Wisconsin, Madison). Trans. Amer. Nucl. Soc., 8: 595-6(Nov. 1965).

**2022** LOCAL FILM COEFFICIENTS OF TURBULENCE PROMOTED ML-1-TYPE FUEL ELEMENTS. Kattchee, N.; Soulis, R. (William M. Brobeck and Associates, Berkeley, Calif.). Trans. Amer. Nucl. Soc., 8: 600-1(Nov. 1965).

**2023** THE CRITICAL HEAT FLUX FOR BOILING LIQUID METAL SYSTEMS. Caswell, B. F.; Balzhiser, R. E. (Univ. of Michigan, Ann Arbor). New York, American Inst. of Chemical Engineers, 1965, Preprint No. 22, 13p., $0.50. (CONF-650812-13). ORINS.

From ASME-AIChE Heat Transfer Conference and Exhibit, Los Angeles.

Burnout heat flux was studied in pool-boiling and forced-circulation systems encompassing both metallic and nonmetallic fluids. Noyes previously suggested modifications to the Zuber equation, which permitted correlation of burnout data for fluids covering a large range of Prandtl number. Attempts to improve this correlation by dimensional analysis produced two expressions, one of which incorporates a Prandtl number term to bring metallic and nonmetallic data together and a second that correlates all liquid metal burnout data. These correlations were further tested with additional data for water, sodium, and rubidium. The experimental data and proposed correlations are discussed. (M.C.G.)

**2024** A DEVICE FOR THE SEPARATION OF STEAM FROM A LIQUID. (to Licentia Patent-Verwaltungs-G.m.b.H.). British Patent 1,006,571. Oct. 6, 1965. Priority date June 22, 1961, Germany.

A device for the separation of a steam-liquid mixture consists of a cylindrical casing into which the mixture is introduced at the top in a tangential direction. The casing has a central steam discharge opening at the top and liquid discharge openings in the lower half of the cylindrical wall of the casing. The bottom of the casing is either closed by a plate or is provided with a streamlined core of diameter smaller than that of the casing. Various devices are included for deflection of the water discharged from the openings. (A.G.W.)

## Materials Testing

*Refer also to abstracts 2240 and 2272.*

**2025** (BNWL-SA-349) RECENT APPLICATIONS OF EDDY CURRENT TESTING AT BATTELLE-NORTHWEST. Brown, R. L. Jr.; Spanner, J. C. (Battelle-Northwest, Richland, Wash. Pacific Northwest Lab.). Oct. 5, 1965. Contract AT(45-1)-1830. 32p. (CONF-651031-1). Dep. mn; CFSTI $2.00 cy, $0.50 mn.

From American Society of Metals Meeting, Detroit.

A brief discussion of the basic principles of eddy current testing serves as an introduction to functional descriptions of a number of tests which have been developed as part of a continuing program in nondestructive testing R&D at Battelle-Northwest. Specific applications have been selected to illustrate the versatility of electro-magnetic methods as applied to a wide variety of testing and measurement problems. A newly developed technique which received considerable national publicity due to a substantial improvement in signal interpretation capability is described. An ultra-stable eddy current test, developed to satisfy the continuing need for increased sensitivity which results from improved materials fabrication processes, is also described. Applications, which are discussed, include the testing of

some 150,000 feet of installed steam generator tubing, the testing of small diameter Inconel tubing, and an eddy current motion analyzing system which was developed to perform vibration measurements in a nuclear reactor. (auth)

**2026** (UCRL–13188) SCATTERED LIGHT IN PHOTOTHERMO-ELASTICITY. Brown, G. W.; Kerper, P. (California Univ., Berkeley. Inst. of Engineering Research). Aug. 1965. Contract W-7405-eng-48. 19p. (MD–65-5). Dep. mn; CFSTI $1.00 cy, $0.50 mn.

A photoelastic technique is developed for determining stress distributions in mockups of engineering components under various thermal environments. The technique consists in shining light through the mockup, then analyzing the polarization of the scattered light. The intensity of the scattered light is increased by means of photomultiplier recording methods. (T.F.H.)

**2027** SENSITIVITY OF THE SCINTILLATION METHOD IN GAMMA-RAY DEFECTOSCOPY. Arkhangel'skii, A. A.; Volkovyskii, P. Yu. At. Energ. (USSR), 19: 308-9(Sept. 1965). (In Russian).

The dependence of the dimension of the minimum detectable defect, $\Delta x_{min}$, on the thickness of the machine part and on the integral gamma flux incident on the machine part is studied, assuming that measurement sensitivity is determined by statistical error — i.e., by fluctuations in the number of gamma quanta — and not by instrument error. A formula is derived for the variation of the sensitivity with the incident integral flux and the machine-part thickness. Results of calculations are compared with those of previous experiments, for the variation of sensitivity with the square root of the inverse source activity and the variation of $\Delta x_{min}$ with machine-part thickness, for a $^{60}Co$ source. (M.J.T.)

**2028** EXAMINATION OF HEAVY STEEL CASTINGS WITH THE BETATRON. Bates, W. (F. H. Lloyd and Co. Ltd., Wednesbury, Eng.). Brit. J. Non-Destruct. Testing, 7: 55-73(Sept. 1965).

Experience showed that the betatron provides not only faster inspection due to much shorter exposure times, but achieves a higher standard of flaw discrimination than the previously used isotope techniques. Inspection time was limited by handling the castings rather than exposure time. The low scatter properties of the betatron enables a more quantitative assessment of the defect size. (W.L.G.)

**2029** DIFFRACTION EFFECTS IN GAMMA RADIOGRAPHY. Halmshaw, R. (Ministry of Defence, Fort Halstead, Eng.). Brit. J. Non-Destruct. Testing, 7: 63-5(Sept. 1965).

A cast austenitic stainless steel tube was radiographed by placing an $^{192}Ir$ source on the inside center-line of the tube with film wrapped around the outside. The resultant radiographs showed a large number of randomly oriented dark streaks up to 2 in. long and with several starlike intersections of three streaks. These streaks did not occur when other types of gamma sources were used nor with the $^{192}Ir$ source placed outside the tube. It is concluded that the stars are the result of a diffraction effect. (W.L.G.)

**2030** NONDESTRUCTIVE ANALYSES OF IRRADIATED MIT REACTOR FUEL ELEMENTS BY GAMMA-RAY SPECTROSCOPY. Sovka, J. A.; Rasmussen, N. C. (Massachusetts Inst. of Tech., Cambridge). Trans. Amer. Nucl. Soc., 8: 383-4(Nov. 1965).

**2031** A HIGH-TEMPERATURE TENSILE TESTING MACHINE FOR IRRADIATED STRUCTURAL MATERIALS. Teats, R.; Watts, E. C. (Battelle-Northwest, Richland, Wash.). Trans. Amer. Nucl. Soc., 8: 617(Nov. 1965).

**2032** REMOTELY OPERATED TEST EQUIPMENT FOR MATERIALS TESTING IN COMBINED CRYOGENIC AND NUCLEAR RADIATION ENVIRONMENT. Weleff, W.; McQueen, H. S. (Aerojet-General Nucleonics, San Ramon, Calif.). Trans. Amer. Nucl. Soc., 8: 617-18(Nov. 1965).

**2033** DEVELOPMENT OF PHOTOGRAMMETRIC TECHNIQUES FOR MEASURING SURFACE CONTOURS OF SMALL SAMPLES. Solomon, Y. (Westinghouse Electric Corp., Pittsburgh); Bohn, S. W.; Dimond, W. J. Trans. Amer. Nucl. Soc., 8: 618(Nov. 1965).

**2034** IMPROVEMENTS RELATING TO RADIOGRAPHIC EXAMINATION. Swanson, Kenneth MacGregor (to United Kingdom Atomic Energy Authority). British Patent 1,004,262. Sept. 15, 1965. Filed July 4, 1961.

In a radiographic method for producing an image of a body by means of penetrating radiation, a shield having at least one collimating tube extending through it is interposed between the body and a radiation-sensitive surface. A compound pivotal motion causing the tube to scan the body is imparted to the shield by a motor. The shield is spherical and pivots about its center; the collimating tube passes through the center. (A.G.W.)

## Protective Structures

*Refer also to abstract 2084.*

**2035** (AD–615017) NON-LINEAR RESPONSE OF REINFORCED CONCRETE SPHERICAL DOMES TO AIR BLAST LOADING. Mayor, Richard P.; Hansen, Robert J. (Massachusetts Inst. of Tech., Cambridge. Dept. of Civil Engineering). Nov. 1963. Contract DA49 146XZ129. 173p. (R63-53; DASA–1442). CFSTI $5.00 cy, $1.00 mn.

A method was developed to predict the response of a concrete dome to an air blast load. The problem is physically non-linear because of the stress-strain laws considered for steel and concrete and also geometrically non-linear because finite displacements are taken into account. The stress-strain relations, and the equations of motion were derived directly in finite difference form for computer use by postulating a lumped mass model to simulate shell behavior. A simplified representation in terms of the model of the behavior of reinforced concrete is also presented. A predictor-corrector method was used to integrate the equations and attention is given to computer efficiency and storage limitations. Finally, some results for the axis-symmetric case are compared to other studies that have been made. (auth)

**2036** (AD–618030) ENVIRONMENTAL EFFECTS ON SPACE STRUCTURES. Report No. 6-74-64-17. Keeney, R. L. (Lockheed Missiles and Space Co., Sunnyvale, Calif.). Apr. 1964. 76p. CFSTI $3.00 cy, $0.75 mn.

Current estimates of the nature and magnitude of environmental effects caused by space vacuum, radiation, and meteoric particles on spacecraft structures are presented. Methods to counteract the deleterious effects of the space environment on spacecraft structures and their contents are discussed and preferable ones recommended. (TAB)

**2037** (DP–968) LEAK TESTING OF THE HWCTR CONTAINMENT BUILDING. Kale, S. H.; Gorrell, T. C.; Kiger, E. O.; Arnett, L. M. (Du Pont de Nemours (E. I.) and Co., Aiken, S. C. Savannah River Lab.). Oct. 1965. Contract AT(07-2)-1. 40p. Dep. mn; CFSTI $2.00 cy, $0.50 mn.

Special techniques were developed to measure the total leak rate from the containment building and to determine the location of small leaks. The containment structure was a composite steel and prestressed reinforced concrete building. The series of tests conducted showed that the leak tightness of the building initially decreased with time. The periodic tests that are described permitted leaks to be found and repaired, so that the leakage was maintained at an acceptably low value. (auth)

**2038** THE ATTENUATION OF IN-AND-DOWN SCATTERED RADIATION. Batter, John F. (Conesco, Springfield, Va.). Trans. Amer. Nucl. Soc., 8: 652-3(Nov. 1965).

**2039** ROOF STRUCTURE FOR RADIATION SHELTER. Hayes, Edward J. (to Kelsey-Hayes Co.). U. S. Patent 3,206,896. Sept. 21, 1965. Filed Mar. 21, 1962.

A prefabricated roof structure for fallout shelters in private homes is described. The roof is composed of a number of longitudinally extending panels, each having a number of substantially V-shaped longitudinally extending channels transversely spaced from each other and interconnected by means of a flat connecting web portions. Each panel is supported at opposite ends by the shelter walls. A number of T-shaped supporting bars are disposed between and supported upon the side walls, and each bar is located so that its upright portion is placed in longitudinally supporting relationship within the channels on the panels for additional support of the panels. The T-shaped bars and the V-shaped channels have substantially the same depth and define a generally smooth surface contiguous with an upper surface of the walls. A number of interconnected wall members are connected to the walls of the shelter and extend upwardly beyond the panels to define an enclosure for holding a radiation absorbing material, such as sand or gravel. (B.L.M.)

**2040** RADIATION SHELTER. Hayes, Edward J.; Rumbles, William E. (to Kelsey-Hayes Co.). U. S. Patent 3,208,410. Sept. 28, 1965. Filed Sept. 22, 1961.

A prefabricated radiation shelter adapted for individual home installation is described. The shelter is easily assembled; protects the occupants from falling debris and damage from physical impact of at least a limited degree; and uses sand, gravel, water, or some other inexpensive readily available material as the radiation absorbing or insulating material. The shelter design uses standard panels and wall sections so that shelters of varying size and shape may be constructed from the same basic components. (B.L.M.)

# Space Propulsion

**See also ISOTOPE TECHNOLOGY — Power Application**
**REACTOR TECHNOLOGY — Propulsion and Space**

*Refer also to abstracts 2007 and 2668.*

**2041** COLD-PLASMA INDUCTION MOTORS FOR PROPULSION OF SPACECRAFT. Nihoul, Jacques C. J. (Cambridge Univ., Eng.). Rev. Universelle Mines, 20: 135-40(May 1964). (In French).

The discussion of the different plasma propulsion units shows the advantages of the induction system and the prospects of a cold-plasma propeller. The theory of a simple apparatus functioning on this principle is established. The conditions of isothermal flow and the operational precautions permitting a satisfactory yield with a cold-plasma are examined. An example for the application for such a propulsion unit is given and the system proposed is evaluated practically. (tr-auth)

**2042** PLASMA GENERATOR. Patrick, Richard M. (to Avco Corp.). U. S. Patent 3,209,189. Sept. 28, 1965. Filed Mar. 29, 1961.

A plasma generator is made up of a gas acceleration space closed at one end and divergent at the opposite end, an inner electrode intermediate between the ends of the space, and an outer electrode located within the space and encircling the inner electrode. The gas acceleration space has a substantially minimum transverse distance at the electrodes. Means are provided for establishing a direct current discharge across the electrodes and for establishing a magnetic field within the space substantially parallel to the defining walls of the space to prevent connection of the electrodes by the magnetic lines of force. Gas is introduced into the space near its closed end. (B.L.M.)

# GEOLOGY, METEOROLOGY, AND MINERALOGY

## General

**2043** GEOLOGICAL SURVEY RESEARCH, 1965. CHAPTER C. Geological Survey Professional Paper 525-C. Washington, D. C., U. S. Government Printing Office, 1965. 224p. $2.00.

Forty-four papers are presented on structural geology, mineralogy and petrology, geophysics, geochemistry, geochronology, paleontology and stratigraphy, glacial and pleistocene geology, geomorphology, economic geology, marine geology, data analysis, analytical methods, quality of water, limnology and surface water, ground water, relation between ground water and surface water, and hydrologic instrumentation. A separate abstract was prepared for one paper. (F.J.H.)

*For an abstract of the individual paper see: 2057.*

## Meteorology

**See also Site Survey and Selection**

*Refer also to abstract 1979.*

**2044** (NDRE-51) PARTICULATE NUCLEAR BOMB DEBRIS AS A METEOROLOGICAL TRACER. Storeboe, P. B. (Forsvarets Forskninginstitutt, Kjeller (Norway)). Mar. 1965. 92p. (CONF-747-6). Dep. mn.

From 4th Symposium on Radioactivity in Scandinavia Risoe, Denmark, Oct. 1964.

The suitability of particulate nuclear bomb debris as tracer material in meteorological research was investigated. Particle size is a very important parameter, and much emphasis was laid on an attempt to assess the size through inference from direct and indirect observations, as well as through computations. Even for air bursts, a significant part of the debris may be in the micron range at the moment of cloud stabilization. Sources of systematic and unsystematic errors during sampling are discussed. It is pointed out how representativity and reasonable sampling procedures vary with the problem under study, and a number of pure debris effects are indicated. Potentialities and limitations of particulate nuclear bomb debris as meteorological tracer material are then discussed in connection with a critical survey over applications made in the past. It is especially difficult to carry through long-time studies by help of the debris. (auth)

**2045** (UCRL-13162) CRYOGENIC AIR SAMPLER FOR HIGH ALTITUDE APPLICATION. Final Technical Report. (National Engineering Science Co., Pasadena, Calif.). June 17, 1965. Contract W-7405-eng-48. 132p. Dep. mn; CFSTI $4.00 cy, $1.00 mn.

For Lawrence Radiation Lab., Univ. of California, Livermore.

A description is given of the design of a high altitude cryogenic air sampler, designated Cryoprobe II. By cryogenic pumping methods the Cryoprobe II is to collect a 5 to 25 gram atmospheric sample in the altitude regime from 85 to 137 kilometers. In a preceding program, basic theory investigations established the feasibility of using a surface cooled to near absolute zero for condensing atmospheric samples when passing through the sampling regime at supersonic velocity. The design of the Cryoprobe II payload was thoroughly analyzed with respect to impact loads, heat transfer, stress analysis, electrical requirements, system stability, and buoyancy. All design requirements were fulfilled. Fabrication drawings and specifications have been prepared. Outstanding design questions are discussed and a manufacturing plan and current cost estimate for building and testing the first two samples are presented. (auth)

## Natural Radioactivity and Fallout

**See also HEALTH AND SAFETY**

*Refer also to abstracts 1602, 2520, and 3095.*

**2046** (BIO/04/64) DATA ON ENVIRONMENTAL RADIOACTIVITY COLLECTED IN ITALY, JULY-DECEMBER 1963. (Comitato Nazionale per l'Energia Nucleare, Rome (Italy)). Apr. 1964. 204p. Dep. mn.

Data are presented on the gross $\beta$ radioactivity due to fallout fission products in samples of air, rain water, and surface waters; the content of $^{90}Sr$, $^{89}Sr$, and $^{137}Cs$ in samples of milk and other foods collected at 16 sites located throughout Italy from July through Dec. 1963. (C.H.)

**2047** (EUR-2509.e) ENVIRONMENTAL RADIOACTIVITY, ISPRA 1964. de Bortoli, M.; Gaglione, P.; Malvicini, A.; Van Der Stricht, E. (European Atomic Energy Community, Ispra (Italy). Joint Nuclear Research Center). 1965. 66p. Dep. mn.

Results are summarized from measurements of environmental radioactivity performed during 1964 at 7 sites in Italy. Data are given on the concentrations of strontium-90, cesium-137, and other radionuclides in fallout, air, soil, waters, herbage, animal bones, and foods. (auth)

**2048** (USNRDL-TR-888) GAMMA-EMISSION DATA FOR THE CALCULATION OF EXPOSURE RATES FROM NUCLEAR DEBRIS. VOLUME II. INDUCED ACTIVITIES. Crocker, G. R.; Wong, D. T. (Naval Radiological Defense Lab., San Francisco, Calif.). Aug. 13, 1965. Contract AT(49-7)-1963. 80p. Dep. mn; CFSTI $3.00 cy, $0.75 mn.

Photon energies and photon abundances have been compiled and summarized for some induced activities that may result from nuclear events. The data are presented in tabular form, including photon energies and abundances for the gamma rays, x rays, and beta particles emitted per disintegration. A list of multipliers is also presented for converting activities of the radionuclides to infinite-plane exposure rates. (auth)

**2049** SOME MEASUREMENTS ON HOT PARTICLES DURING 1962 and 1963. Halter, J.; Huber, O.; Gasser, M. (Univ., Freiburg, Switzerland). Atomkernenergie, 8: 295-300(July-Aug. 1965). (In German).

In 1962 and 1963 air of the lower stratosphere and the upper troposphere has been examined for the presence of hot particles. These were most numerous in the summer of 1962. In some of the strongest hot particles a quantitative determination of the $^{95}Zr$-$^{95}Nb$ and $^{141}Ce$ and $^{144}Ce$ activity was possible. The decay curve of the $^{95}Zr$-$^{95}Nb$ photopeak allows the determination of the approximate date of origin of the hot particles. Other gamma emitting fission products have not been found in the hot particles; upper limits of their activity are given. (auth)

**2050** INITIAL ANALYSIS OF THE FISSION PRODUCTS OVER BERLIN FROM THE RED CHINESE ATOMIC BOMB TEST OF OCTOBER 16, 1964. Fett, Walter (Freie Univ., Berlin). Berlin Wetterk., 20: 1-11(Mar. 4, 1965). (In German).

The fission product activity in the troposphere above Berlin was measured by a probe. It amounted to 60 $\mu$R/hr, an increase of ~ one third over the cosmic irradiation present in the area. Close to one half of the additional radioactivity was concentrated within a layer ~1 km in thickness. It was located at an altitude corresponding to a pressure of ~300 mbar. The concentration of the activity could be estimated only approximately as ranging between 0.5 and $1 \times 10^5$ pC/m$^3$. In addition, it was estimated that an air column 1 km$^2$ in size contained ~$10^2$ C of fission products. The concentration of fission products in rainfall on 23 October 1964 was increased more than tenfold over

the value indicated by the long-term trend. More than 1.5 months passed before it returned to the lower value. It required 7 days for the fission product cloud to encircle ¾ of the earth's surface as compared to the 9 days required for fission product clouds to reach the area from Soviet tests conducted 25° closer to Berlin. The presence of fresh fission products in the air dose to the earth's surface was delayed by 4 days from the time they appeared in rainfall. The peak activity was noted during the October-November period, and amounted to ~0.9 pC/m$^3$. The effective age of the 24-hr samples measured was 300 days, while the ratio of activity between the upper and lower boundaries of the troposphere above Berlin was ~0.5 × 10$^5$: 1. (BBB)

**2051** LEAD ISOTOPE RATIOS FROM THE COBALT-NORANDA AREA CANADA. Kanasewich, E. R. (Univ. of Alberta, Edmonton); Farquhar, R. M. Can. J. Earth Sci., 2: 361-84(Aug. 1965).

Lead isotope ratios indicated that very old galenas in Archean volcanics and sediments in the vicinity of Timmins, Ontario; Noranda and Val d'Or, Quebec, had additions of younger lead of the type found near Cobalt, Ontario. The mixture of leads of two distinct ages produced isotopic ratios that are linearly related. The greatest degree of mixing occurred in areas such as Kirkland Lake, which are close to the boundary between Archean rocks and the Bruce-Cobalt Series. Most of the lead appeared to be derived from a subsialic source region. From the relationship of the anomalous lead line and the single-stage growth curve commonly accepted for ordinary leads it was found that lead sulfide mineralization occurred 3,250 ± 150 million yr ago in Archean rocks of Ontario and Quebec. The leads associated with mines along the northeastern edge of the Cobalt basin were separated from their uranium and thorium source region 2,300 ± 150 million yr ago. Leads from Chibougamau, Quebec, appeared to be related in age to the Cobalt leads. Fifty lead isotope ratios illustrated the claim that single-stage lead models must not be applied indiscriminately to isolated analyses of galena. It also produced evidence for the existence of crustal rocks in North America prior to 3,200 million yr ago. (auth)

**2052** GEOCHEMICAL ASPECTS OF THE Th/U RATIO INVESTIGATION IN ROCKS. Kovalev, V. A. (Lab. of Geochemical Problems, Minsk). Geokhimiya, No. 9, 1171-3(Sept. 1965). (In Russian).

The Th/U ratio can be used to estimate the intensity of weathering processes. U is more mobile than Th. Black schists and phosphorites show a low Th/U ratio (less than two). Littoral sands and alluvial deposits show a high Th/U ratio (greater than 7). Most clay deposits show an intermediate Th/U ratio of 2 to 7. Leaching experiments with 3% HCl on a 0.01 mm fraction of mineral showed that only 40% of the Th could be leached out, while 70% of the U was removed from the mineral. The Th accumulated in the heavier, accessory minerals, and was not leached out readily. (TTT)

**2053** THE PROBLEM OF HOT PARTICLES IN THE ATMOSPHERIC AIR (A SURVEY). Bykhovskii, A. V.; Malakhov, S. G. Gig. Sanit., No. 7, 87-97(July 1965). (In Russian).

A systematic study of global fallout during the nuclear testing period of 1957 to 1958 showed that the activity in the hot particle varied from 10$^{-8}$ to 10$^{-13}$ C. The number of particles with an activity of 10$^{-8}$ C was only a few percent of the number of particles with an activity of 10$^{-13}$ C. The particle size was estimated at 10 to 20 $\mu$ as the upper limit from Stokes law, and at 0.5 $\mu$ as the lower limit from the activity content of the particle. By autoradiography and microscopic observation the particle size was found to vary from 1 to 20 $\mu$ with an increase in radioactivity of the particle with increasing particle size. The following activities were detected in the hot particles by gamma spectrometry: $^{141}$Ce, $^{144}$Ce, $^{95}$Zr + $^{95}$Nb, $^{103}$Ru, $^{131}$I, $^{143}$Pr, $^{147}$Nd, $^{140}$Ba, and $^{140}$La. In addition, $^{237}$U, $^{239}$Np, $^{132}$Te, $^{99}$Mo, $^{89}$Sr, and $^{90}$Sr were also detected. The possible carcinogenic effect of the radioactive particles in human lungs is discussed. It is noted that a hot particle with an activity of 7 × 10$^{-10}$ C will give a dose of 3500 to 4500 rads to the surrounding tissue over a distance of 50 $\mu$ from the particle. This dose exceeds the minimum carcinogenic dose observed in animal experiments. It is noted that a particle with an activity of 1 × 10$^{-12}$ C will cause the death of about 1000 cells, but there is no evidence that the organism undergoes any significant damage as a result. (TTT)

**2054** REPORT ON RADIOACTIVE FALLOUT: PROGNOSIS ON THE CONTAMINATION OF FOODSTUFFS AND EXTERNAL RADIATION IN SCANDINAVIA IN 1962-1963. Medd. Sundhedsstyr., No. 114, 853-6(Mar. 23, 1962). (In Danish).

A report is given of a conference of scientists from 5 Nordic countries held in January 1962 to discuss radioactive fallout in Scandinavia resulting from the 1961 Soviet nuclear weapons tests at Novaja. The hazards of heavy local radioactive fallout and means of preventing contamination were emphasized, and a prediction made for the year 1962-1963. The total yield of the nuclear blast was estimated at 120 Mt, about 25 Mt of which was fissionable material. To establish a basis for estimating fallout, comparison was made between the 1961 test and those of 1958, the ratio being 2 to 1. Strontium-90 fallout was estimated at about 10 mC/km$^2$ in areas with 70 cm/yr precipitation. The estimated specific activity in precipitation in 1962 was about 15 pC/l of $^{90}$Sr and 25 pC/l of $^{137}$Cs over the whole Scandinavian region. Included in this estimate is fallout from earlier explosions, about 1 to 2 mC/km$^2$ of $^{90}$Sr and 2 to 3 mC/km$^2$ of $^{137}$Cs. Levels of $^{137}$Cs and $^{90}$Sr in the biosphere for 1962 are compared. The level of $^{90}$Sr in food was estimated to be about twice as great in 1962 as in the preceding year. Bone and bone marrow doses were tabulated and estimated to be equal. External effects in 1962-3 would consist mainly of $^{95}$Zr/$^{95}$Nb doses acting in the spring of 1962. The external contribution to the 30-yr gonadal dose would come from $^{137}$Cs. In addition, an internal dose of 100 pC/gK of $^{137}$Cs or 4 mrem in 2 yr is predicted, and five times as great a dose in infants. Carbon-14 doses cannot be estimated exactly, but would probably be twice that from the previous weapons tests. Doses to newly formed bone tissue would be about 0.05 rem, and 0.02 rem to surrounding tissue, or about 10% of the dose from background radiation in 1962-3. The 30-yr gonadal dose for the period beginning Jan. 1, 1962, would be about 0.05 rem or 1 to 2% of background radiation during the past 30 yr. These averages were considered 50% accurate. Exceptions would be a few areas where precipitation is greater or diet unusual. Extensive tabulated data are given showing the estimated doses for Denmark, Finland, Norway, Sweden, Iceland, and Scandinavia in general. (BBB)

**2055** NONDESTRUCTIVE ACTIVATION ANALYSIS OF COBALT IN IRON METEORITES. Rancitelli, L.; Fisher, D. E. (Cornell Univ., Ithaca, N. Y.). Trans. Amer. Nucl. Soc., 8: 328-9(Nov. 1965).

**2056** THE NEUTRON ACTIVATION-ANALYSIS DETERMINATION OF RARE-EARTH ELEMENTS IN SILICATE ORES. Lukens, H. R. Jr.; Graber, F. (General Atomic Div., General Dynamics Corp., San Diego, Calif.). Trans. Amer. Nucl. Soc., 8: 329(Nov. 1965).

**2057** FRACTIONATION OF URANIUM ISOTOPES AND DAUGHTER PRODUCTS IN URANIUM-BEARING SANDSTONE, GAS HILLS, WYOMING. Rosholt, John N. Jr.; Ferreira, Carlos P. pp C58-61 of Geological Survey Research, 1965. Chapter C. Geological Survey Professional Paper 525-C. Washington, D. C., U. S. Government Printing Office, 1965.

At a sandstone-type uranium deposit in the Wentz mine in Natrona County, Wyo., isotopic ratios of $^{234}$U/$^{238}$U for 14 samples taken at, or just above, the present level of standing water showed that the deposit had a relatively consistent $^{234}$U deficiency ranging from 7 to 29%. $^{230}$Th/$^{234}$U and $^{231}$Pa/$^{235}$U ratios indicated that the time interval since uranium emplacement near the level of standing water is about 80,000 yr and that the time interval gen-

erally is greater with increasing distance above the water. The source uranium also appeared to be deficient in $^{234}U$, and the deficiency was maintained in ore by relatively continuous preferential leaching of this isotope. (auth)

## Techniques and Equipment

*Refer also to abstract 1981.*

**2058** (NVO–98-10) HAWAIIAN RUN-UP PROGRAM. Preliminary Program Plan, Progress Report. Tucker, Charles T.; Wilson, George (National Marine Consultants, Anaheim, Calif.). Oct. 15, 1965. Contract AT(26-1)-98. 62p. Dep. mn; CFSTI $3.00 cy, $0.75 mn.

The Hawaiian Run-Up Program consists of the long-term emplacement of two Type I and ten Type III systems in the Hawaii area. Two modified Type I systems will be installed in deep water about 30 miles off the Southwest (Kona) Coast of Hawaii, and ten Type III systems will be emplaced along the coast of the island. The collection and analysis of various wave data are the program objectives. Included are discussions on the design and buildup of equipment, installation of equipment Type I and III, operation, data processing, and refit program. (M.O.W.)

**2059** (NVO–98-11) ABSOLUTE PRESSURE SENSORS. Interim Progress Report. Folwell, Philip A. (National Marine Consultants, Anaheim, Calif.). Oct. 1965. Contract AT(26-1)-98. 37p. Dep. mn; CFSTI $2.00 cy, $0.50 mn.

The method selected for monitoring and recording waves at deep water sites has necessitated the use of a buoy mounted pressure sensor at a depth of 600 to 1000 feet. The testing and calibration work to demonstrate the suitability of the transducer for the application, and to determine its characteristics so that accurate analyses of operational data can be made, are described. The design of the transducers is included. An investigation was performed to analyze possible hydrodynamic influences on the pressure measurement. The results are presented. (M.O.W.)

**2060** STUDIES ON SANDY SURFCOASTS WITH $^{46}Sc$. Petersen, M. (Ministerium fuer Ernaehrung, Landwirtschaft und Forsten, Kiel). Atomkernenergie, 8: 285-94 (July-Aug. 1965).

Methods of investigation using radioactive tracers are qualified for direct measurements at the bottom of waters and give information on the kinetic of erosions and the transport of sand. A description of the nuclides and the tracer amounts used is given. If the use of a boat for the measurements is not possible in the surf special measuring techniques are necessary. A new radioactive method by marking the grains of sand was developed. In three coastal areas 100 kg of sand marked with $^{46}Sc$ (2 to 3 C) were put into the surf by helicopters and the diffusion was observed. For measurements from the helicopter a special immersion probe supplied with a radiation detector was constructed. At the same time the luminoform method was proved. From results of 1268 radiation measurements and 336 analyzed sand samples a description of the diffusion of marked sand is given for areas of the same radiation intensity. (auth)

**2061** A NEW TECHNIQUE USING RADIOACTIVE TRACERS FOR STUDIES IN PHYSICAL OCEANOGRAPHY. Srivastava, P. S. (Naval Headquarters, New Delhi). Indian J. Pure Appl. Phys., 1: 263-5(July 1963).

Methods employing $^{60}Co$ are described for measuring the oscillation of the air-water interface, movement of water, and eddy diffusion, and also for determining the pattern and extent of eddy diffusion in the ocean. (BBB)

**2062** SYNTHESIS OF TRIMETHYLBENZENES FOR MEASURING NATURAL RADIOCARBON BY MEANS OF SCINTILLATION METHOD. Butomo, S. V.; Reikhsfel'd, V. O.; Makovetskii, K. L. Radiokhimiya, 7: 364-6(1965). (In Russian).

A method for the synthesis of mesitylene and pseudocumene for radiocarbon dating by the scheme $C \rightarrow CaC_2 \rightarrow Mg_2C_3 \rightarrow H_3C - C \equiv C_6H_3(CH_3)_3$ with a total carbon yield of 50% was developed. It was found that isomers with trimethylbenzene have high scintillation efficiencies and do not yield n-xylene. The good scintillation efficiency of trimethylbenzene and the possibility of producing it from natural materials makes it possible to propose mesitylene and pseudocumene as a carrier of the $^{14}C$ activity during measurement of the half life of radiocarbon. (tr-auth)

**2063** THE RESULTS OF EXPERIMENTAL APPLICATION OF X-RAY-RADIOMETRIC WELL-LOGGING IN THE CENTRAL KAZAKHSTAN. Meier, V. A.; Nakhabtzev, V. S. Vestn. Leningr. Univ., No. 12, Ser. Geol. Geogr., No. 2, 65-73(1965). (In Russian).

A new method for studying elementary composition of ores in bore-holes by the characteristic x-ray emission, called radiometric well-logging, was tested. To reduce the disturbing influence of changes of material composition and density of medium on quantitative determinations the background of scattered radiation was used as internal standard. It was found that some heavy elements in multi-component ores can be determined by the new method. The accuracy of radiometric well-logging is believed to be not less than that of ordinary chemical analysis of ores by their cores. (auth)

## Thorium and Uranium Minerals

**2064** ON TWO GENETIC TYPES OF POST-MAGMATIC THORIUM-RARE EARTH DEPOSITS. Nevskii, V. A.; Kozlova, P. S. At. Energ. (USSR), 19: 277-81 (Sept. 1965). (In Russian).

Two genetic types of postmagnetic thorium-rare earth deposits are described. One of them is associated with surface ore-bearing beds, the other, with deep beds. In deposits of the first type, a close spatial connection is discovered with the matrix magmatic rocks formed at an insignificant depth from the surface. These deposits are characterized by a complex polycomponent and polymineral composition and an insignificant vertical range of mineralization. The deposits of the second type do not have the spatial connection with magmatic rocks formed at a significant depth from the surface at sufficient distance from the ore-bearing bed. The mineral composition of the ores of the deposits is comparitively simple. The vertical range of mineralization constitutes many hundreds of meters for containing the type of mineralization at the depth. (tr-auth)

**2065** RARE EARTH AND THORIUM CONTENT IN SOILS OF TOMSK REGION. Pashneva, G. E.; Slavnina, T. P.; Serebrennikov, V. V. (Tomsk State Univ., USSR). Izv. Sibirsk. Otd. Akad. Nauk SSSR, No. 4, Ser. Biol.-Med. Nauk, No. 1, 48-52(1965). (In Russian).

The concentration of rare earth elements, Y, and Th in leached black earth podzolic, turf podzolic, light gray wood, dark gray wood, meta, and river alluvial soils of the tomsk region was determined. The concentration of Th and rare earth elements in the soils depends on the quantity of humus and increases with the increase of the concentration of humus in the soil. The distribution of Th in these soils depends on the development of turf and podzolic processes. The concentration of Th increases in the upper humus-accumulation horizon because of biogenesis and in the alluvial horizon because of the erosion of its eluvial horizon where the concentration of Th is lower than in the $A_1$, $B_1$, and $B_2$ horizons. The per cent relation of rare earth elements shows that in the soils studied the rare earth elements of a cerium group predominate, with the exception of turf podzolic and light ray wood soil which have a comparatively high concentration of Er. (tr-auth)

**2066** RADIOACTIVE EQUILIBRIUM IN THE NINGYOTOGE URANIUM ORES, ESPECIALLY BETWEEN IONIUM AND URANIUM. Murano, Tohru (Atomic Fuel Corp., Tokyo). Mineral. J. (Tokyo), 4: 12-29(Feb. 1963).

The radioactive equilibrium states in the uranium ores of the Ningyotoge mine were investigated in relation to their $^{230}Th$ content and to their microscopic features. Among the U daughter products, $^{230}Th$ and $^{234}U$ affect the equilibrium states over a long time, because they have long half lives and are situated in the upper positions of the uranium decay series. Uranium deposits in the Ningyotoge mine are formed in Neocene Tertiary lucustrine sediments, chiefly conglomerate and shale, lying horizontally on a granite base. In the unoxidized zone, uranium occurs principally as ningyoite, accompanied by pyrite and carbonaceous matter. Uraninite is also found in very small quantities, and in the oxidized zone the main uranium mineral is autunite. An analytical method for $^{230}Th/U$ was examined and applied to the ores. The method does not require determination of the chemical yield in the separation of thorium and offers a simple means for obtaining the absolute value of $^{230}Th/U$. To investigate the different states in phases of a specimen, variation of $^{230}Th/^{234}Th$ ratio under chemical leaching was followed. Autoradiography and radioactivity measurements were also made. It was suggested that the states of radioactive equilibrium in the Ningyotoge ores are a result of the differentiation of thorium from uranium. This may occur by oxidation and chemical leaching and by crystallization of uranium minerals. The radionuclides in a radiocolloid formed $^{230}Th$ and its daughter products. (BBB)

# HEALTH AND SAFETY

*See also* **BIOLOGY AND MEDICINE — Radiation Hazards and Protection**
**GEOLOGY, METEOROLOGY, AND MINERALOGY — Natural Radioactivity and Fallout**

*Refer also to abstracts 1588, 1590, 1689, 1727, 1966, 1985, 2038, 2171, 2289, 2341, 2520, 2655, 2657, 2995, 3243, 3244, 3272, 3275, 3276, 3379, and 3575.*

**2067** (AD–614824) BULGUR WAFER AND ADJUNCTS FOR FALLOUT SHELTER RATIONS. Annual Report, July 1963–June 1964. Shepherd, Allan D.; Beavers, Darrell V.; Ferrel, Robert E.; Horvat, Robert J.; Ng, Hawkins (Agricultural Research Service, Albany, Calif. Western Regional Research Lab.). Jan. 1965. Contract OCD-OS62-54. 52p. CFSTI $3.00 cy, $0.50 mn.

Long-term (five-year) studies of the storage life of bulgur wafers and adjuncts (food to serve with the wafers to vary fallout shelter menus) are in progress. Taste panel results after 16 months of storage indicate that the shelf-life of bulgur wafers may be increased by nitrogen-gas packing and by use of malt sirup rather than corn sirup in the formulation. Chemical-physical analyses are being made on duplicate samples of wafers in a search for a test that correlates with organoleptic evaluation. Trends are not yet well enough developed to permit meaningful correlation. Identity of components of the vapors from rancidifying bulgur and from a model compound, methyl linoleate (linoleic acid comprises more than half of the fatty acids in wheat), is being sought by means of a new technique which combines gas-liquid chromatography and rapid-scan mass spectrometry. Wheat products prepared by hot-air puff-drying and by gun puffing were evaluated as wafer ingredients potentially cheaper than regular puffed bulgur. Material obtained by hot-air puff-drying shows some promise as a suitable alternate wheat ingredient for wafers. Several new adjuncts are proposed, including a pectin jelly prepared with cold water to replace the originally developed jellies requiring hot water for preparation. (auth)

**2068** (AD–614895) THE CHINESE NUCLEAR EXPLOSION, N-NATION NUCLEAR DEVELOPMENT AND CIVIL DEFENSE. Zilbert, E. R. (RAND Corp., Santa Monica, Calif.). Apr. 1965. 26p. (P–3074(RAND)). CFSTI $2.00 cy, $0.50 mn.

The October 1964 explosion of an atomic device by China is reviewed, with thought as to possible similar activities by other countries such as India and Brazil. The United States Government is taken to task for having implemented no fallout shelter program. (TAB)

**2069** (AD–615003) SHELTER OCCUPANCY STUDIES AT THE UNIVERSITY OF GEORGIA. Appendices. (Georgia Univ., Athens). Dec. 31, 1964. Contract OCD-PS64-77. 149p. CFSTI $4.00 cy, $1.00 mn.

From 8-21 February, 1964, a 13-day simulated fallout shelter occupancy test was conducted by the University of Georgia Psychological Laboratories. This test was the fifth in a series of such studies. Its primary purpose was the evaluation of shelter survival without a trained shelter manager. Other purposes included relative food preference tests, commode chemical tests, and cognitive vigilance tests. Thirty shelterees, 15 males, 15 females, aged 7-70, participated. Stress conditions included restricted food and water rations, minimal living space (8 $ft^2$/person), a chemical commode, reduced ventilation, and sleeping accommodations of corrugated fiberboard placed over a concrete floor. The shelter manager was appointed, although he received no prior training in management methods or familiarization with shelter material. A Shelter Manager Handbook, with additional instructional material, was stocked with the OCD shelter supplies. The handbook provided information on use of stocked items, as well as a suggested daily activity and training program. (TAB)

**2070** (AD–615004) SHELTER OCCUPANCY STUDIES AT THE UNIVERSITY OF GEORGIA. Final Report. Hammes, John A. (Georgia Univ., Athens). Dec. 31, 1964. Contract OCD-PS64-77. 123p. CFSTI $4.00 cy, $1.00 mn.

From 1962-1964 the University of Georgia conducted six simulated community fallout shelter occupancy tests for the Office of Civil Defense. Investigated variables included organizational and environmental factors. Men, women, and children, aged 3-70 years, participated. Recent test results and overall implications for the National Shelter Program are reported. (auth)

**2071** (AD–615005) SHELTER OCCUPANCY STUDIES AT THE UNIVERSITY OF GEORGIA. Final Summary Report. Hammes, John A. (Georgia Univ., Athens). Dec. 31, 1964. Contract OCD-PS64-77. 20p. CFSTI $1.00 cy, $0.50 mn.

Results of occupancy tests on simulated community fallout shelters are discussed. Information is included on personnel management, leadership, sanitary engineering, sleep, temperature, food, water, physical fitness, ventilation, personality, and environmental and physiological stress. (TAB)

**2072** (AD–618006) FEASIBILITY STUDY OF A FILTRATION UNIT FOR THE REMOVAL BY THE INDIVIDUAL OF CBR AGENTS FROM WATER. Rogers, Morris R.; Kaplan, Arthur M. (Quartermaster Research and Engineering Command, Natick, Mass.). June 1961. 38p. (CP–19). CFSTI $3.60 cy, $0.50 mn.

The feasibility of developing a small filtration unit for an individual to remove CBR agents from his water supply was studied. A literature search indicated that laboratory and engineering studies have established the principles by which all three agents can be effectively removed from contaminated water. These methods include chlorination, sedimentation, coagulation, demineralization, and filtration. A simple filtration unit capable of removing or reducing the CBR agents in water to a safe level is considered feasible and could be used by the individual under emergency conditions to treat water supplies. (auth)

**2073** (AD–618101) ATMOSPHERIC DIFFUSION STUDIES AT THE NARF SITE. Period Covered: October 1, 1963–September 30, 1964. Bradbury, H. G. (General Dynamics/Fort Worth, Tex.). June 1965. Contract AF29(601)-6213. 113p. (FZK–206; WL-TR–64-156). CFSTI $4.00 cy, $0.75 mn.

Four atmospheric diffusion experiments were conducted in the Nuclear Aerospace Research Facility area at General Dynamics/Fort Worth in order to study the dispersal and dilution factors of the atmosphere as they pertain to the release of airborne radioactivity in the NARF area. Fluorescent dye was released to the atmosphere from a point near the Reactor Operations Building and sampled downwind to measure depletion factors under varying meteorological conditions. The tests were performed with air temperature gradients ranging from slightly unstable to mildly stable (inversion) situations. The sampling data obtained were applied in the evaluation of the parameters associated with the statistical diffusion equation. Although the four tests were too few in number to provide substantial statistical data, the results show that under the poorest diffusion conditions experienced, the effluent depletion factors ranged from approximately 0.0001 to 0.000001 between 88 and 704 m from the release point. These factors are considerably less than those actually being applied under nuclear safety considerations within the NARF reactor operations area. (auth)

**2074** (AHSB(RP)M–40) COMPUTED DEPOSITION RATES PER UNIT RELEASE RATE OF WINDBORNE MATERIAL. Bryant, Pamela M. (Authority Health and Safety Branch, United Kingdom Atomic Energy Authority, Harwell (England)). Sept. 1965. 34p. Dep.

Methods for calculation of dry deposition rates, washout by rain, and combined (wet and dry) deposition rates, all with respect to unit rate of release to atmosphere are described. Computed values of these deposition rates corresponding to several alternative values of deposition velocity and of the washout coefficient over a range of stack heights and distances, are given in tabular form for use as ready-reckoners. A computer program, given in the appendix, includes calculation of derived working limits for continuous release rates of $^{90}Sr$ and $^{137}Cs$ to atmosphere in a milk producing area in Great Britain and these values are included. (auth)

**2075** (AHSB(S)R-92) REVIEW OF U.K.A.E.A. CRITICALITY DETECTION AND ALARM SYSTEMS 1963/64. PART I. PROVISION AND DESIGN PRINCIPLES. Aspinall, K. J.; Daniels, J. T. (Authority Health and Safety Branch, United Kingdom Atomic Energy Authority, London (England)). 1965. 51p. Dep.; BIS $1.60; HMSO 8s.

Results are presented of a review of the criticality detection and alarm arrangements adopted at the different Establishments of the UKAEA and a distillation of the principles which should underlie the future provision and design of criticality detection and alarm systems. The discussions are confined to gamma detection which is used throughout the UKAEA. The basic tenets are: (a) The object is not the more rudimentary one of detecting any abnormal radiation, it is one of balancing the hazards from abnormal radiation against the hazards and costs associated with the instant evacuation of working plant. Therefore the alarm is not to be operated unless the radiation is of such a nature as could emanate from accidental criticality, but when the radiation is of such nature then the alarm must be triggered reliably and quickly. (b) Where an alarm system is provided it should be designed to be operated by the minimum foreseeable initial excursion regardless of whether or not the circumstances may be that such an initial excursion of itself could result in unacceptable doses to men. Arguments, resting largely on analyses of data from past incidents as reported by Stratton, are deployed to derive those detailed technical criteria needed by designers of detection and alarm systems, and to quantify them where appropriate. Recommendations are made for a detection threshold for general use, a detection threshold for special use in areas of high ambient gamma background, dose/fission ratios, and system response time. Reliabilities of detection systems and of alarm noise generation, transmission, and propagation are discussed. Lastly, evacuation principles and facilities are discussed and recommendations made concerning evacuation area boundaries and methods. (auth)

**2076** (ANL–7068) LABORATORY INVESTIGATIONS IN SUPPORT OF FLUID-BED FLUORIDE VOLATILITY PROCESSES. PART VIII. ANALYSIS OF AN ACCIDENTAL MULTIGRAM RELEASE OF PLUTONIUM HEXAFLUORIDE IN A GLOVEBOX. Trevorrow, L. E.; Kessie, R. W.; Steindler, M. J. (Argonne National Lab., Ill.). July 1965. Contract W-31-109-eng-38. 20p. Dep. mn; CFSTI $1.00 cy, $0.50 mn.

A 5.7-g sample of plutonium hexafluoride was accidentally released to the interior of a glovebox. An analysis of the penetration of plutonium through the filter system of the glovebox was carried out. Data obtained from an air-sampling instrument located in the effluent air stream of the filter system indicated that 2.4 μg of plutonium were released to the atmosphere during this incident. Air and surface concentrations of plutonium at sampling points beyond the exhaust stack were below the limits of detection. The performance of the high-efficiency filters of the glovebox ventilation system was generally within the range predicted from small-scale experiments that had been carried out before the incident to simulate the type of accidental release that occurred. Detailed analysis of the distribution of plutonium following the release indicated possible design improvements that could be made in the once-through air ventilation system in use. (auth)

**2077** (AWRE-O–41/65) THE SODIUM FLAME PHOTOMETER TEST FOR HIGH EFFICIENCY FILTERS. Dyment, J.; Thomason, I. D. (Atomic Weapons Research Establishment, Aldermaston (England)). May 1965. 44p. Dep.; BIS $1.40; HMSO 7s.

The sodium flame test was originally devised at CDEE, Porton, for testing respirator filters and later extended to large air filters. The use of flame photometry as a filter test is reviewed briefly in relation to the requirements of a test for high efficiency ventilation filters. The basis of the method and experimental examination of the principal features of the CDEE design are described. Detailed attention is given to the operating characteristics of the detector unit, the size distribution of the test cloud, and comparison of the method with the British methylene blue and American DOP test methods. An estimate of the capital and installation costs for one of these rigs is given; it is concluded that the method is satisfactory for testing filters for radioactive installations, and has certain advantages over the other methods considered. (auth)

**2078** (BNL–917, pp 1-10) PHYSICAL DAMAGE FROM NUCLEAR EXPLOSIONS. Miller, Carl F. (Stanford Research Inst., Menlo Park, Calif.).

The hazards of nuclear explosions for man are described in terms of areas around the blast designated as damaged, radep, and free. The general effects of initial ionizing radiation, thermal radiation, blast and shock, and residual ionizing radiation or fallout are summarized with respect to the hazards that would result in case of nuclear war, and specific criteria are given for the definition of such areas. The 3-psi overpressure contour or the distance within which there is thermal ignition in houses, whichever gives the larger area, is used to define the damaged area; the outer perimeter of the radep area is defined by the 100 R infinity exposure dose contour. The areas so defined are illustrated for a 5-MT-yield surface detonation. Calculations for the radep and free areas resulting from a 20,000-MT hypothetical attack on North America are summarized. Some of the available data on the radiological properties of fallout, such as its gamma decay rate, rate of nuclide dissolution, and rate of contamination of foliage, are presented and discussed. (auth)

**2079** (BNL–917, pp 11-19) EFFECTS OF FIRE ON MAJOR ECOSYSTEMS. Broido, A. (Forest Service, Berkeley, Calif. Pacific Southwest Forest and Range Experiment Station).

In heavily built-up urban areas, mass fires are to be expected if nuclear attack should occur. In wildlands, thermal radiation from nuclear detonation can ignite exposed kindling fuels over large regions. Whether such ignitions spread and merge to form a catastrophic fire depends on the same factors that influence the spread of any wildland fire. Should a mass fire occur, its gross characteristics during the period of active burning are expected to differ considerably from those of large-scale peacetime fires. However, the greatly shortened burning time of the mass fire compared to a conventional large fire pertains to the over-all burning period. The conventional fire covers piecemeal an area in which, for the mass fire, the burning periods everywhere coincide. The duration of either fire at any given point should be much the same. Hence, the ecological consequences of the fires that may occur after a nuclear catastrophe are not expected to differ seriously from the consequences of holocausts of the past. Although large fires have been with us since prehistoric times, interpretations of their effects on major ecosystems are still quite controversial – whether one considers the effect on plant succession, on animal life, on plant diseases and pests, on the chemical composition of the soil, or on such physical factors as temperature and humidity. (auth)

**2080** (BNL–917, pp 20-38) EFFECTS OF IONIZING RADIATION ON ECOLOGICAL SYSTEMS. Woodwell, G. M.; Sparrow, A. H. (Brookhaven National Lab., Upton, N. Y.).

The potential effects of fallout radiation on the natural ecological systems forming the homeostatic matrix within which civilization exists are defined broadly. Ecosystems have three basic patterns: geographic pattern, such as deserts, grasslands, forests, and tundras; temporal patterns which are successions; and patterns of internal structure and function. The latter can be defined in many ways, but the distribution and flow of energy among the various populations is used in this discussion. Three sources of information are available for analysis of the potential effects of fallout radiation on these patterns: data from experimentally irradiated ecosystems, data from radiobiological studies of many organisms, and data from other parallel catastrophes in which ionizing radiation was not a factor. Emphasis is placed on the first two sources. Experimentally irradiated ecosystems contributing data to this analysis include those around the Lockheed reactor in northern Georgia and recent experiments in an oak-pine forest and in fields at Brookhaven National Laboratory. Radiobiological data of particular use are the correlations recently developed at Brookhaven between the radiosensitivity of plants and chromosome volume. These analyses show patterns of radiosensitivity among the plant populations of natural ecosystems; communities of herbaceous annuals, for instance, would probably withstand fallout radiation exposures up to 4000R with minor effects, while most coniferous forests would be devastated by 2000R or less. Field experiments with small, open, irradiated ecosystems have shown no clear tendency for devastating population explosions of insets after radiation damage, but experience is limited. Changes in herbivorous insect populations have followed, in general, the abundance of food. Three categories of radiation effects on ecosystems were established for predicting potential fallout effects: minor effects involving temporary inhibition of growth or reduction of reproductive capacity in plants, intermediate effects involving the initiation of new plant successions, and severe effects involving the potential alteration of the capacity of the site to support life. This latter range of effects might occur after erosion or loss of essential nutrients. Prediction of severe effects is subject to large uncertainties introduced by ecological factors in addition to irradiation. (auth)

**2081** (BNL-917, pp 39-60) IONIZING RADIATION AND HOMEOSTASIS OF ECOSYSTEMS. Platt, Robert B. (Emory Univ., Atlanta, Ga.).

Radiation effects and subsequent recovery in ecosystems near the air-shielded Lockheed nuclear reactor constitute the closest approximation of short-term radiation effects without heat and blast on vegetation. The two periods of high-level irradiation, 14 months apart, closely resembled fallout exposures, both in intensity and in duration. The course of recovery apparently has been well established in the five years since the first exposure and the four years since the second. Thus, it has been possible to establish ecological effects on vegetation for doses up to 300,000 rads, plotted against developmental stages from abandoned agricultural fields to climax forests. Since the pine-dominated stage is highly sensitive to radiation, the hardwood stage intermediately sensitive, and the herbaceous stage among the least sensitive, results from these three developmental stages have wide applicability to similar areas throughout the world. In the event of a 20,000-MT attack on the United States with 100% fission, it has been estimated that 2 to 5% of the country would receive 15,000R or more within 2 weeks, and 10% would receive 5000 to 10,000R. The remaining 85 to 88% would receive <5000R, the greatest percentage on the order of 1000 to 2000R. In view of these data, a broad generalization may be made for radiation effects from a nuclear war on this country's vegetation. From 5 to 20% of the forest ecosystems may have the tree overstory seriously damaged or killed. Another 20% may be visibly affected, but without the loss of the overstory; recovery for this percentage would be relatively fast. The damage may not be fully evident for several months to a year. If fire occurred, the damage would be increased. For the rest of the country (grasslands, deserts, and tundra), temporary changes may occur in the species composition in 2 to 10% of the area, the remainder being relatively little affected. Therefore, direct radiation effects from nuclear war on vegetation are not likely to seriously limit man's reconstruction of his renewable resources. Other ecological effects may be far more limiting, such as radioactive contamination or effects on animals and food resources. (auth)

**2082** (CEA-Bib.-59) QUELQUES ASPECTS DE RADIOHYDROLOGIE. Etude Bibliographique. (Some Aspects of Radiohydrology. Literature Survey). Bittel, Robert (Commissariat a l'Energie Atomique, Saclay (France). Centre d'Etudes Nucleaires). Sept. 1965. 46p. Dep. mn.

Various aspects of hydrological problems arising from the presence of radioisotopes in rivers between the point of disposal and the places at which the water is used by man are reviewed. 151 references are cited. (P.C.H.)

**2083** (CEX-65.4) BIOLOGICAL TOLERANCE TO AIR BLAST AND RELATED BIOMEDICAL CRITERIA. White, Clayton S.; Bowen, I. Gerald; Richmond, Donald R. (Lovelace Foundation for Medical Education and Research, Albuquerque, N. Mex.). Apr. 1965. Contract AT(29-1)-1242. 253p. Dep. mn; CFSTI $2.75 cy, $1.25 mn.

Experience with animals exposed in a variety of above and below ground structures during full-scale field operations at the Nevada Test Site in 1953, 1955, and 1957 is reviewed. The data were assembled and summarized to illustrate the nature of the blast-induced problems of significance in open and closed protective shelters. Potential hazards were related to the following: various patterns of variation in environmental pressure; translational events associated with transient, high-velocity winds, ground shock, and gravity involving the impact of energized inanimate objects on the one hand and the consequences of whole-body displacement on the other; non-line-of-site thermal phenomena including hot objects and rapidly moving hot, dust-laden air and debris; and dust, in the respirable size range, sufficiently high in concentration even in closed shelters as to warrant design measures to minimize or eliminate the occurrence of small particulates whether arising from wall spalling or otherwise. Tentative biological criteria, conceived to help assess human hazards from blast-related phenomena, were presented. Relevant data from the literature and research in environmental medicine were set forth to aid the reader in appreciating how the criteria were formulated, what information was extrapolated from animal data, and wherein best estimates were employed. Various concepts were noted to emphasize areas in which more thinking and research must continue if more refined, complete, and adequate criteria are to be forthcoming for assessing man's response to blast-induced variation in his immediate environment. (117 references) (auth)

**2084** (EURAEC-374(Vol.2)) DESIGN AND ECONOMIC STUDY OF SPENT FUEL SHIPPING. (Stanray Corp., Chicago, Ill.). May 1, 1962. Contract AT(11-1)-963. 196p. Dep. mn; CFSTI $5.00 cy, $1.00 mn.

Work Performed under United States-Euratom Joint Research and Development Program.

Information is included on: fuel reprocessing; cask design for shipping; regulations for the safe transport of radioactive materials; transportation in the U. S.; and economic and legal aspects of shipping and receiving spent fuels for reprocessing. (P.C.H.)

**2085** (SC-R-65-991) SAFETY AS A DESIGN FEATURE IN SYSTEMS. Swain, A. D. (Sandia Corp., Albuquerque, N. Mex.). Sept. 1965. Contract AT(29-1)-789. 14p. (CONF-650915-2). Dep. mn; CFSTI $1.00 cy, $0.50 mn.

From Systems Engineering Conference, Chicago.

Designing safety features into systems is a more effective way to reduce accidents than campaigning to make people more careful. Hazards can be drastically and permanently reduced through design action in modifying the hazardous situation, whereas reduction through modifying people is limited and requires continuing reinforcement. Moreover, reinforcement gets exceedingly more

difficult to achieve because of the human tendency to "tune out" stimuli a person comes to consider as noise. Safety in systems is a design problem, one to be resolved by objective engineering techniques. (auth)

**2086** (BNL-tr-42) GLOBAL FALLOUT OF NUCLEAR EXPLOSION PRODUCTS. Lavrenchik, V. N. Translated by Stephen Amoretty (Brookhaven National Lab., Upton, N. Y.), from Chapter 3 of Global'noye Vypadeniye Produktov Yadernykh Vzrynov, Atomizdat, Moscow, 1965. 44p. Dep. mn; CFSTI $2.00 cy, $0.50 mn; JCL $4.60 fs, $1.52 mf.

A review is presented on sample collection and determination of activity of fallout on the earth, in atmosphere, and in the stratosphere. Special attention is given to the determination of $^{14}C$ and tritium. Approximately 100 references are cited. (P.C.H.)

**2087** MEASUREMENT OF THE BACKGROUND EXTERNAL RADIATION EXPOSURE OF THE URBAN POPULATION IN THE USSR. Bochvar, I. A.; Keirim-Markus, I. B.; Moiseev, A. A.; Prosina, T. I.; Yabubik, V. V. At. Energ. (USSR), 19: 311-12(Sept. 1965). (In Russian).

Preliminary results are presented of the measurement of the background external exposure of small groups of people from 26 cities in the USSR. The studies were started in the second half of 1963. Individual dosimeters of the infrared spectroscopic type using thermoluminescent aluminophosphate glass were employed, allowing gamma doses from 0.02 to $2 \times 10^6$ rads to be measured. Ten people from each city wore the dosimeters continually for 167 to 325 days. The drop in instrument readings during the time of exposure was measured for control dosimeters. A table of results and error limits is given. Analysis of the data showed that the exposure levels depend largely on the type of rocks and soils in the cities; attempts to observe a correlation between exposure dose and latitude or height above sea level were unsuccessful. (M.J.T.)

**2088** LEGAL QUESTIONS ON THE COMMERCIAL ENTRY OF THE SAVANNAH INTO GERMAN WATERS. Karr, H.; Loosch, R. (Bundesministerium fuer Wissenschaftliche Forschung, Bad Godesberg, Ger.). Atomwirtschaft, 10: 533-5(Oct. 1965). (In German).

The commercial entry of the nuclear ship Savannah operated by a private shipping line raises various legal questions which did not arise as long as the ship was operated directly by the American government. Since on the first commercial voyage German ports were approached, new reactor operation agreements were granted. Especially a new solution for the insurance was necessary. The further development of the legal ground for the commercial operation of nuclear vessels is of special interest to the German Republic because of the proposed operation of the German nuclear ship Otto Hahn. (tr-auth)

**2089** DESIGN AND CONSTRUCTION OF ALPHA EMITTER LABORATORY. Abe, Shiro (National Inst. Radiol. Sci., Chiba, Japan). Genshiryoku Kogyo, 11: 59-63(Jan. 1964). (In Japanese).

An $\alpha$-emitter inhalation laboratory (a ferroconcrete, two-story building of total floor-space 484.4 $m^2$) was constructed to make studies on alpha inhalation injuries and their mechanism. The characteristics of $\alpha$ emitters are described. The laboratory design is discussed. Rooms in the laboratory are separated from one another to reduce contamination. Handling of high-level $\alpha$ emitters is concentrated in the middle of the laboratory. The laboratory is divided into three radiation control areas, according to the $\alpha$ activity. Personnel working in the high-level area wear protective clothing. In the intermediate-level area, $\alpha$ emitters are handled in glove boxes. Fire fighting facilities and equipment, ventilation system, radiation monitors, etc., are described. (NSA of Japan)

**2090** RADON CONCENTRATION IN DIFFERENT ENVIRONMENTS AND THE FACTORS INFLUENCING IT. Hague, A. K. M. M. (Borough Polytechnic, London); Collinson, A. J. L.; Brooke, C. O. S. Blyth. Phys. Med. Biol., 10: 505-14(1965).

Using a scintillation counter technique, a systematic study of radon concentration was made in various environments and conditions viz., normal living accommodation with adequate and inadequate ventilation, completely sealed offices and laboratories, industrial premises, air-conditioned offices and premises of dealers and users of luminescent powders. Radon concentration indoors was found to depend upon several factors, including the nature of building materials, ventilation conditions, temperature, and weather conditions. (auth)

**2091** DOSE MODELS FOR EVALUATING THE RADIATION HAZARD FROM REACTOR DEBRIS. Ellett, W. H. (Naval Radiological Defense Lab., San Francisco); Berger, M. J.; Hogan, O. L. Trans. Amer. Nucl. Soc., 8: 568 (Nov. 1965).

**2092** GAMMA RADIATION CHARACTERISTICS—ANGULAR DISTRIBUTION OVER A DESERT-TERRAIN FALLOUT FIELD. Frank, A. L. (Naval Research Lab., Washington, D. C.). Trans. Amer. Nucl. Soc., 8: 657 (Nov. 1965).

**2093** SAFETY FIRST IN THE QUEST FOR ECONOMIC NUCLEAR POWER. Horan, John R. (Atomic Energy Commission, Idaho Operations Office, Idaho Falls). Trans. Pacific Coast Oto-Ophthalmol. Soc., 45: 11-24(1964).

Safety features in the development of nuclear reactors for power generation are discussed, especially with respect to the program of the AEC's National Reactor Testing Station (NRTS) in Idaho. It is concerned with building, testing, operating, and evaluating various types of nuclear reactors and allied plants for various uses, including not only electric power production, but also the propulsion of vessels and and vehicles. The accomplishments of the NRTS in the field of reactor development and safety are enumerated. Some public health safety features offered by nuclear power generators not offered by conventional power plants are mentioned. (BBB)

**2094** SOCIAL IMPLICATIONS OF THE PEACEFUL USES OF NUCLEAR ENERGY. Klineberg, Otto (ed.). Technology and Society Series. Liege, United Nations Educational, Scientific and Cultural Organization, 1964. 169p.

The social, moral, and cultural problems involved in the peaceful utilization of atomic energy are discussed. The views of eight authors on various aspects of the problems are presented. (C.H.)

**2095** NUCLEAR MATERIALS MANAGEMENT AND ITS RELATIONSHIP TO NUCLEAR SAFETY AND CRITICALITY CONTROL. Tingey, F. H. (Phillips Petroleum Co., Idaho Falls, Idaho). Vienna, International Atomic Energy Agency, 1965, Preprint No. SM-67/22, 7p. (CONF-650803-46). ORINS.

From IAEA Symposium on Nuclear Materials Management, Vienna.

The preclusion of those conditions which would result in an inadvertent collection of fissionable material in quantity, geometry and environment to produce a neutron chain reaction is of fundamental importance to all those actively engaged in the nuclear industry. Basically the responsibility for preventing inadvertent criticality in any area of plant operation lies with line supervision. In devising preventative measures at least three different types of problems need be considered. These are: (a) The scientific or technical problems connected with evaluating the hazard presented by a proposed quality of fissile material in a given geometry and environment. (b) The engineering problems presented by the restrictions dictated from the scientific or technical considerations. (c) The purely administrative problems presented in implementing the restrictions and requirements imposed from the technical and engineering considerations. (auth)

# INSTRUMENTATION

## General

*Refer also to abstracts 2520, 2531, and 3473.*

**2096** (AD-617928) ANTENNA INSIDE A MAGNETO-PLASMA-FILLED PARALLEL-PLATE WAVEGUIDE. Rao, B. Rama (Cruft Lab., Harvard Univ., Cambridge, Mass.). Mar. 15, 1965. Contract AF19(628)-2406. 23p. (AFCRL-65-401). CFSTI $1.00 cy, $0.50 mn.

An antenna inside a magnetoplasma-filled parallel-plate waveguide is considered. Its behavior at the Pythagoras (upper hybrid resonance) frequency and the plasma resonance frequency was studied. The effect of the magnetoplasma medium on the feed-point singularity of the antenna current was also investigated. (auth)

**2097** (AD-618396) PROPAGATION CONSTANT ALONG A CYLINDRICAL ANTENNA IMMERSED IN A WARM PLASMA. PARTS I AND II. Seshadri, S. R.; Galejs, J. (Sylvania Electronic Systems, Waltham, Mass. Applied Research Lab.). Apr. 1965. Contract AF19(628)-2410. 35p. (SR-6; AFCRL-65-371). CFSTI $2.00 cy, $0.50 mn.

I. A lossless plasma is considered. The propagation constant is shown to be close to that of the plasma mode in an unbounded plasma in the frequency range for which the electromagnetic (EM) and the plasma (P) space waves are excited, that is for frequencies above the plasma frequency. This applies to antennas without or with an insulating sheath. II. An insulated antenna in a lossy plasma is considered. A guided wave with a propagation constant close to that of the electromagnetic mode in an unbounded plasma is now possible in addition to the guided plasma wave, that is the only one which satisfies the radiation condition for a lossless plasma. It is, therefore, appropriate to include in the approximation for the current distribution along the antenna parts which have propagation constants of the order of magnitude of P and EM waves. (auth)

**2098** (AD-618398) WAVEGUIDE ADMITTANCE FOR RADIATION INTO PLASMA LAYERS—THEORY AND EXPERIMENT. Galejs, Janis; Mentzoni, Michael H. (Sylvania Electronic Systems, Waltham, Mass. Applied Research Lab.). Apr. 1965. Contract AF19(628)-2410. 26p. (SR-8; RR-451; AFCRL-65-373). CFSTI $2.00 cy, $0.50 mn.

Measured admittance of an X-band waveguide radiating into dielectric and plasma layers was compared with variationally computed admittance figures. The waveguide admittance measurements for polystyrene sheets of varying thicknesses compared closely with calculations. The admittance measurements for plasma layers were made during the diffusion controlled afterglow of a pulsed discharge contained in a bell-shaped vessel. The plasma density was measured over approximately 70 percent of the thickness of the plasma layers and was found to be nearly constant in this range which excluded regions near the boundary. Numerical solutions of the equations for ambipolar diffusion during the afterflow in a rectangular geometry showed that the lateral plasma density variations are negligible in the vicinity of the waveguide. The measured admittance and plasma density data are shown to agree with calculations made for homogeneous plasma layers, if a correction is made for elevated ion temperatures for times of approximately 10 to 22 microsec. following the discharge. Several computational models consider plasma stratifications near the boundary of the plasma layer but they do not improve the agreement between measurement and calculations. (TAB)

**2099** (AECL-2291) A HIGH SENSITIVITY HEAVY WATER LEAK DETECTOR. Bayly, J. G. (Atomic Energy of Canada Ltd., Chalk River (Ontario)). Oct. 1965. 47p. Dep.; AECL $1.50.

A process instrument for measuring changes in the D/H ratio of water has now passed from the experimental to the prototype stage. The infrared transmissions in a sample and in a reference stream are compared at two wavelengths to give an analysis which is insensitive to contaminants commonly found in water yet responds to 0.5 ppm $D_2O$ near the natural abundance (150 ppm), and can have a range to at least 5000 ppm. At least thirty water streams can be analysed per hour, and maintenance problems are expected to be negligible. (auth)

**2100** (IS-1193) ELECTRONICS IN MASS SPECTROMETRY. Flesch, Gerald D.; Svec, Harry J. (Ames Lab., Iowa State Univ. of Science and Tech.). June 1965. Contract W-7405-eng-82. 81p. Dep. mn; CFSTI $3.00 cy, $0.75 mn.

A review of the fundamental behaviors of the electronic circuits involved in magnetic mass spectrometers is given in non-technical language. Emission regulated current supplies and ion current amplifiers are considered. Both vacuum tube and transistor circuits are discussed. The subject is presented in such a way that one should be able to find somewhere in the compiled circuits, an example of most of the circuits usually found in commercial and home built instruments. (auth)

**2101** (JINR-P-2319) UCHET IMPUL'SNOSTI V RABOTE PROMEZHUTOCHNOI PAMYATI. (Account of the Pulsed Mode in Intermediate Memories). Zabiyakin, G. I.; Shetet, T.; Shibaev, V. D. (Joint Inst. for Nuclear Research, Dubna (USSR). Lab. of Neutron Physics). 1965. 10p. Dep. mn.

The data on the calculation of the intermediate memory are generalized. Using the intermediate memory model the dependencies are obtained of the losses of the intermediate memory applied as a derandomizer in the pulsed regime by varying the number of storage elements, the average random rate of the pulse arrival, the time interval during which the pulses arrive and the rewriting rate. The plotted curves allow to calculate the characteristics of the intermediate memory used as a derandomizer in the pulsed regime. (auth)

**2102** (JUL-273-PP) CROWBAR- UND POWER-CROWBAR-SCHALTUNGEN UND IHRE BERECHNUNG. (Crowbar and Power Crowbar Circuits and Their Calculation). Belitz, H.-J.; Kugler, E. (Kernforschungsanlage, Juelich (West Germany). Institut fuer Plasmaphysik). June 1965. 46p. Dep. mn.

The crowbar is a switching element that makes it possible to so control an ignited condenser discharge by external switches that high current pulses of selected form and length can be obtained. The two crowbar circuits considered transform the initial state of the discharge which is characterized by a fast current rise to another dynamic state that corresponds to a slow decrease of the current. The voltages and currents in the individual branches of an oscillatory circuit with crowbar were calculated and a FORTRAN program for the numerical calculations was given. (tr-auth)

**2103** (LA-DC-7055) ANALYTICAL MODEL FOR STUDY OF THERMOCOUPLE ERROR ATTRIBUTED TO ELECTRICAL CONDUCTION IN INSULATION. Tallman, C. R. (Los Alamos Scientific Lab., Univ. of California, N. Mex.). [1965]. Contract W-7405-eng-36. 31p. (CONF-651002-7). Dep. mn; CFSTI $2.00 cy, $0.50 mn.

From Instrument Society of America, 20th Annual Conference, Los Angeles.

The most satisfactory thermocouple used to date is a refractory-metal sheathed, BeO-insulated thermocouple using thermo-elements of W/W-26 Re. An analytical model is presented for the study of errors observed in thermocouples of the above materials of $\frac{1}{8}$ inch OD or less, which can be attributed to the progressive failure of the insulator with increasing temperature. (M.O.W.)

**2104** (MATT-362) A FERROMAGNETIC RESONANCE MAGNETOMETER. Ernst, W. P.; Skislak, A. H. (Princeton Univ., N. J. Plasma Physics Lab.). Sept. 1965. Contract AT(30-1)-1238. 14p. (CONF-650512-12). Dep. mn; CFSTI $1.00 cy, $0.50 mn.

From Symposium on Engineering Problems of Controlled Thermonuclear Research, Livermore, Calif.

A ferromagnetic magnetometer system is described that is capable of measuring transient magnetic field values with the accuracy of 1 part in $10^4$. The use of stoichiometric yttrium iron garnet material enables one to perform point field measurements where large gradients are present. (M.O.W.)

**2105** (UCRL-16357(Rev.)) TECHNIQUES OF MAGNETIC-FIELD MEASUREMENT. Watson, Peter G.; DiGregorio, Ronald F. (Lawrence Radiation Lab., Univ. of California, Berkeley). Aug. 31, 1965. Contract W-7405-eng-48. 20p. (CONF-650922-18). Dep. mn; CFSTI $1.00 cy, $0.50 mn.

From 1st International Symposium on Magnet Technology, Stanford, Calif.

A survey of magnetic measurement techniques is presented. Emphasis is placed on the inherent advantages and limitations of each method, on improvements, and on the degree of accuracy attainable. Magnetic measuring systems are considered. Factors such as positioning equipment, data recording and processing, and overall cost of measurement are discussed in terms of two systems—the "search-coil Zip-Track" system and the "Rapid Mapper." (auth)

**2106** (UJV-1346/65) ELEKTRONICKE PRISTROJE PRO MIKROVLNNY SPEKTROMETR. (Electronic Devices for Microwave Spectrometers). Blaho, Dusan (Ustav Jaderneho Vyzkumu, Ceskoslovenska Akademie Ved, Rez). 1965. 15p. Dep. mn.

An electronic apparatus developed at the Institute for Nuclear Research for microwave spectrometry has the following features: the low-frequency selective amplifier for the basic frequency in the range of 30 to 265 cycles per sec., has a latitude of less than 6.5% for a fall off of ±3dB, a maximum input sensitivity of $2 \times 10^{-8}$ volts and a maximum voltage gain of $10^7$, the synchronous detector for frequencies of 30 and 230 cycles has a maximum input amplitude of 0.5 volt with a maximum output voltage of 1.5; for a load resistance greater than 10 megohms, the time constant of the integrating circuit has a range of 0.5 to 6 seconds, the low frequency oscillator operates at 30 or 230 cycles, and it has a stabilized power supply for the klystron and for the modulator, which can apply saw-tooth, sinusoidal, or square-wave voltages to the reflector of the klystron. (TTT)

**2107** NUCLEAR INSTRUMENTATION—A GENERAL SURVEY. Euro Nucl., 2: 481-5(Oct. 1965).

Developments in the field of nuclear instrumentation are reviewed. Reactor power instrumentation and control, instrumentation for gas analysis and for flux measurement, health physics instrumentation, instruments using radioisotopes, detectors, low-level electronics, modular electronics, and automation are discussed. (M.C.G.)

**2108** TERA-OHMMETER WITH A RADIOACTIVE GENERATOR CURRENT. Loog, P. K.; Pikver, R. I.; Rezben, V. A.; Saks, O. V. Izmeritel. Tekh., No. 6, 28-31 (June 1965). (In Russian).

The voltage drop over a high-ohm resistance is determined in measuring currents on the order of $10^{-16}$ amps. High-ohm standard resistances are not stable for long periods of time, and have other disadvantages. Hence, a current generator was developed creating voltage drop $U_x$ over a resistance $R_x$. The voltage drop $U_x$ depends linearly on the magnitude of the resistance $R_x$. The voltage drop $U_x$ is measured by an electron voltmeter. An ionization chamber containing a radioactive source serves as the current generator which is calibrated by charging a standard condenser C with a current I to a voltage $U_0$ over a time $t: I = U_0C/t$. The $^{90}Sr-^{90}Y$ source with an activity of 0.5 mC gives a maximum current of $10^{-10}$ amps which can be attenuated by a factor of 10, 100, or 1000 by metal filters. A temperature change of 10°C or a pressure change of 4000 n/m$^2$ gives a 3 to 4% current change. These errors can be eliminated by calibrating the current just before use. With this device resistances from $10^9$ to $10^{13}$ ohms can be measured with an error of <1%. Standard condensers are used in the place of standard resistors. (TTT)

**2109** USE OF NUCLEAR MAGNETIC DOUBLE RESONANCE IN THE ANALYSIS OF HIGH-RESOLUTION NMR SPECTRA. Lippmaa, E. (Inst. of Cybernetics, Academy of Sciences, Estonian SSR). Izv. Akad. Nauk Est. SSR, Ser. Fiz. Mat. Tekh. Nauk, 14: No. 1, 125-8 (1965). (In Russian).

A universal proton-proton nuclear double resonance spectrometer must allow all possible techniques (field sweep, frequency sweep, INDOR) to be used with a broad (60 db) range of perturbing and measuring field strengths, to be spin-stabilized and as free from noise and spurious signals as possible. The amplitudes of the perturbing field $H_2$ and measuring field $H_1$ must be independent of their frequencies—a near impossibility with modulation methods. In some experiments $H_2$ must be available for further pulse or frequency modulation. For these reasons a 40 Mc spectrometer, stabilized by spin generator and using frequency synthesis to obtain $H_1$ and $H_2$ has been built. Until now the apparatus has been used for tickling and spin decoupling experiments with good results. The drift is about 0.1 cps/min, resolution $1.2 \times 10^{-8}$. (auth)

**2110** FOCUSSING OF ELECTRON BEAM FROM BIASED ELECTRON GUN. A STUDY WITH OXIDE-CORED CATHODE AS WELL AS TUNGSTEN HAIR-PIN FILAMENT. Kamigaito, Osami (Nagoya Univ., Japan). Jap. J. Appl. Phys., 4: 604-10(Aug. 1965).

Various characteristics of electron beams (diameter, total current, brightness, etc.) from electron guns such as used in electron microscopes and other equipments were studied systematically. General results are described which are independent of detailed gun design. It was found that the image of the cathode tip is formed on a plane at a certain bias voltage. At this bias voltage, the brightness measured on the plane is maximum, which agrees with theory. It was made clear that the decrease of brightness from the maximum is mainly due to the finite size of apertures used for the measurement. Near the cut-off voltage, space charge limitation also makes the brightness lower. These results contradict the conclusions of Haine & Einstein. The nature of the so-called hollow beam was studied. This is due to electrons from the sides of the cathode. Thus it does not appear for oxide-cored cathodes. (auth)

**2111** THE TELECOMMUNICATION EQUIPMENT OF THE NUCLEAR RESEARCH ESTABLISHMENT AT JUELICH (GERMANY) AS AN EXAMPLE OF ADAPTING TELECOMMUNICATION MEANS TO SPECIAL OPERATIONAL CONDITIONS. Rittinghaus, K. F.; Wiedemann, K. NTZ-Nachr. Z., 16: 256-63(May 1963). (In German).

The telecommunication equipment of the nuclear research establishment at Jülich (Germany) was planned on the basis of the expected operational requirements with particular consideration of the safety requirements. The equipment includes telecommunication devices mainly employed for safety purposes, and contains as a main section the safety center. It also includes conventional telecommunication equipment which is provided for the general operation of the research establishment. After two years of construction, the equipment was put into operation during 1962 to 1963. A report is given of a number of special requirements and their technical solutions which have resulted from the purpose and the size of the nuclear research establishment. (auth)

**2112** SMALL NMR PROBE FOR USE IN INHOMOGENEOUS FIELDS. Breuer, H. (Univ. of Saskatchewan, Saskatoon). Rev. Sci. Instrum., 36: 1666-7(Nov. 1965).

A magnetic field probe having a diameter of 1 cm, whose operation is based on NMR signals in $MnSO_4$, is designed for field measurements in the vacuum chamber of a double-

focusing 180° magnet. Means used for rendering the field homogeneous in the region of the probe are described. (T.F.H.)

**2113** ABSOLUTE-VELOCITY MOESSBAUER SPECTROMETER. Spijkerman, J. J.; Ruegg, F. C. (National Bureau of Standards, Washington, D. C.). Trans. Amer. Nucl. Soc., 8: 344(Nov. 1965).

**2114** EVALUATION OF THERMOCOUPLES FOR USE TO 2600 deg C IN MIXED-OXIDE FUEL. Novak, P. E.; Asamoto, R. R. (General Electric Co., San Jose, Calif.). Trans. Amer. Nucl. Soc., 8: 388-9(Nov. 1965).

**2115** A ($^{90}$Sr + $^{90}$Y)/URANIUM RADIATION GAUGE FOR HYDROCARBON DENSITY MEASUREMENTS. Meno, F.; Mott, W. E. (Gulf Research and Development Co., Pittsburgh). Trans. Amer. Nucl. Soc., 8: 581-2(Nov. 1965).

**2116** THE REMOTE DETERMINATION OF GAS PRESSURE AND VOLUME FOR ENCAPSULATED FUEL ELEMENTS. Mahagin, D. E.; Feldman, M. J. (Argonne National Lab., Idaho Falls, Idaho). Trans. Amer. Nucl. Soc., 8: 616-17(Nov. 1965).

**2117** REMOTE UNDERWATER DEVICES FOR THE EVALUATION AND REDUCTION OF IRRADIATED YANKEE FUEL ASSEMBLIES. Kitzes, S.; Miner, D.; Santavy, J. A. (Westinghouse Electric Corp., Pittsburgh). Trans. Amer. Nucl. Soc., 8: 618-19(Nov. 1965).

**2118** FAST ELECTRONICS IN NUCLEAR PHYSICS. Orman, P. R. (Atomic Energy Research Establishment, Harwell, Eng.). pp 415-52 of Nuclear Structure and Electromagnetic Interactions. New York, Plenum Press, 1965.

Various characteristics of components and circuits for fast electronic systems are described. The choice of components; amplification, pulse height analysis and scaling; and fast timing circuits are discussed. (L.B.S.)

**2119** EIGHTH NATIONAL POWER INSTRUMENTATION SYMPOSIUM. Proceedings, New York, May 12–14, 1965. Pittsburgh, Instrument Society of America, 1965. (CONF-650536).

Thirteen papers are included; separate abstracts have been prepared for three. Papers not abstracted consider boiling system dynamics, power system automation and control, power plant instrumentation development, and computer applications in power systems. (L.B.S.)

*For abstracts of individual papers see: 3532–3534.*

**2120** IMPROVEMENTS IN AND RELATING TO SYSTEMS FOR MEASURING THE PERMEABILITY OF POROUS BARRIERS. Pozwolski, Alexandre Edgar (to Commissariat a l'Energie Atomique). British Patent 1,004,206. Sept. 15, 1965. Priority date Aug. 31, 1962, France.

A system is patented for measuring the permeability of a porous barrier relative to that of a standard barrier. Two equal-volume chambers are connected by a differential pressure gage, and each chamber communicates with a gas reservoir through a porous barrier, one of which is the barrier of unknown permeability while the other is a standard barrier of known permeability. The permeability to be measured is deduced from the pressure gage reading and the known permeability of the standard barrier. (A.G.W.)

## Radiation Detection

*Refer also to abstracts 1792, 1905, 2075, 2195, 2432, 2860, 3019, and 3362.*

**2121** (AD–614832) DEVELOPMENT OF RADIAC SET AN/TDQ-2 FOR DETECTION OF PULSED X-RADIATION FROM HIGH POWERED ELECTRONIC EQUIPMENT. Final Report. McCall, Richard C.; Jasins, Alfred C. (Controls for Radiation, Inc., Cambridge, Mass.). Mar. 30, 1965. Contract AF30(602)-2791. 60p. (RADC-TDR–64-259). CFSTI $3.00 cy, $0.75 mn.

A remote area monitor was developed for the purpose of detecting and measuring steady or pulsed x radiation emission from high powered electronic equipment associated with radar installations. The system consists of six detectors connected to a central console by 250 ft cables. Each detector consists of a two foot square plastic scintillator coupled to a plastic light pipe which converges to a single photomultiplier, an internal calibration source and an amplifier. R-F shielding is also provided. The central console utilizes six interchangeable modules with five decade logarithmic scales to indicate the radiation dose-rate from 1 mR/hour to 100 R/hour. A push button switch is incorporated for each channel to check the calibration of the detector. In addition, an alarm system in the console provides both visual and audible signals when any one detector exceeds a pre-set radiation level. A fail-safe circuit was designed which indicates failure of detector operation by means of a bright light mounted on each module. The entire system was designed to operate on its own emergency power supply during power failure of up to 50 hours. (auth)

**2122** (AD–622626) LOW DOSE MEASUREMENTS WITH MODIFIED SILVER–PHOSPHATE GLASS DOSIMETER READER. Menkes, C. K. (Naval Radiological Defense Lab., San Francisco, Calif.). Aug. 30, 1965. 39p. (USNRDL-TR–889). CFSTI $2.00 cy, $0.50 mn.

Greater precision in measuring gamma-ray doses below 1.0 R with silver-activated phosphate glass is achieved by modification of the Toshiba FGD-3B Fluoro Glass Dosimeter Reader. Twenty-five milliroentgen (25 mR) was read on 6mm × 6mm × 3.3mm glass square dosimeters with an accuracy of about 5%, suggesting that results of this precision should be obtainable with more sensitive glass dosimeters down to 10 mR or less. Fluorimetric emission spectra and measurements made after replacement of the red filter by a yellow filter in the Toshiba reader indicate that the predose of Toshiba silver phosphate glass has a relatively significant fluorescence in the region of the irradiation-induced fluorescence. (auth)

**2123** (ANL–7085) A NEUTRON MONITOR FOR SIMULTANEOUS MEASUREMENT OF FLUENCE AND DOSE EQUIVALENT. Dvorak, Robert F.; Dyer, Norman C. (Argonne National Lab., Ill.). Aug. 1965. Contract W-31-109-eng-38. 12p. Dep. mn; CFSTI $1.00 cy, $0.50 mn.

A neutron detector which has application as both an area monitoring instrument and a criticality dosimeter is under development. The detector simultaneously measures both dose equivalent and fluence from an exposure to fast neutrons. The moderator consists of a 12-in.-diameter, aluminum-encased paraffin sphere. The neutron sensors are nine thermal activation foils located within the moderator. The neutron fluence is determined by activation of six foils symmetrically located one inch below the surface of the moderator. For this foil array, the summed activity is nondirectional and proportional to the fluence within 10 percent over the investigated energy range from 20 kev to 2.3 Mev. The neutron dose equivalent is determined from activation of three symmetrically interlocked foils at the center of the moderator, and the summed activity is proportional to the dose equivalent within 75 percent over the same energy range. A response correction technique is described which, for monoenergetic neutrons, brings the dose equivalent to within about 10 percent. The average sensitivity of the monitor over the stated energy range, using indium foils, is 76 cpm per mrem/hr and 25 cpm per n/cm$^2$-sec at the end of one half-life exposure at uniform radiation level. (auth)

**2124** (BNL–9590) MEGACHANNEL ANALYZERS. Soucek, B.; Spinrad, R. J. (Brookhaven National Lab., Upton, N. Y.). [1965]. Contract AT-30-2-GEN-16. 14p. (CONF-651001–5). Dep. mn; CFSTI $1.00 cy, $0.50 mn.

From IEEE Nuclear Science Symposium, San Francisco.

The need for multiparameter multi-channel analyzers

which span a range of millions of channels is easily demonstrated. To meet this need three basically different techniques were developed: event recording, multi-window preselection, and associative-memory analysis. Criteria for choosing between the various systems or combinations of them are reviewed. Within each analyzer class, design features which have proved effective in hardware and software implementations are presented. Two new systems, presently operational at our laboratory, are described. The first, a computer time-shared, magnetic tape, three-dimensional event recorder, has additional facilities for accumulating analysis and display of any three single dimensional spectra. Display selection parameters and window boundaries are all inserted by direct light pen manipulation on the data field. A second megachannel analyzer system, which uses computer programmed associative-memory techniques offers the user a more effective utilization of core memory than was attainable in the past. Finally, certain features such as speed, event entry, and memory utilization are reviewed in the context of the various systems. (auth)

**2125** (CEA-R-2816) UN OBTURATEUR MECANIQUE POUR SPECTROGRAPHE DONT LE TEMPS D'EXPOSITION VARIE DE 1,5 MICROSECONDE A 3 MILLISECONDES. (Mechanical Time Shutter for Spectrograph With Exposure Times from 1.5 mu s to 3 ms). Becker, Lothar; Drawin, Hans-Werner (Commissariat a l'Energie Atomique, Fontenay-aux-Roses (France). Centre d'Etudes Nucleaires). June 1965. 22p. (EUR-2440.f). Dep. mn.

A mechanical time-shutter for exposure times from 1.5 μsec to 3 msec is described. The apparatus is designed for spectrographic observations of pulsed electrical discharges that show rapidly varying spectral emissivities. For the mechanical part of the shutter, a specially formed fast rotating disk having a slit is used. Triggering of the discharge is achieved by the rotating disk, in connection with photocells. Both the instant at which the exposure shall begin and the duration of exposure, can be selected on a special electronic control device. All functions, namely rotation of the disk, ignition of the discharge, exposure, and switch-off of the disk are controlled electronically. The principle and the main electronic control parts of this instrument are described. (auth)

**2126** (CONF-650657-1) PRECISION X-RAY SPECTROSCOPY. Bearden, J. A. (Johns Hopkins Univ., Baltimore, Md.). [1965]. Contract AT(30-1)-2185. 14p. Dep. mn; CFSTI $1.00 cy, $0.50 mn.

From International Conference on Physics of X-Ray Spectra, Ithaca, N. Y.

The high resolving power of the double crystal spectrometer is discussed in terms of the geometry of its crystals. The precision required in the alignment and crystal tilt angles in order to achieve an instrumental precision greater than one part per million in x-ray wavelengths is discussed. The correct form of the expression for correcting these values for finite vertical divergence is pointed out. An optical-level procedure for adjusting and aligning a double-crystal spectrometer and a simple method of grinding crystals parallel to a desired plane for testing and use are described. (M.O.W.)

**2127** (ISS-64/15) CRITERI PER LA SCELTA DELLE CONDIZIONI DI LAVORO MIGLIORI NELLE MISURE DI PREPARATI RADIOATTIVI (RASSEGNA). (Criteria for the Choice of the Best Working Conditions in the Measurements of Radioactive Sources (A Review)). Corti, F. (Istituto Superiore di Sanita, Rome (Italy). Laboratori di Fisica). May 6, 1964. 158p. Dep. mn.

Problems of statistical character appearing in radioactivity measurements are considered. The different methods used in performing these measurements are compared graphically. A method was studied to fix the factor of merit for every counter, on the basis of which the best possible conditions for measurements are determined. A general criterion was deduced to choose the most convenient counter among the different ones available for these measurements. (auth)

**2128** (JINR-E-2324) IONIZATION MEASUREMENT IN A STREAMER CHAMBER. Asatiani, T. L.; Gazaryan, K. A.; Zhmyrov, V. N.; Matevosyan, E. M.; Nazaryan, A. A.; Sharkhatunyan, R. O. (Joint Inst. for Nuclear Research, Dubna (USSR). Lab. of Nuclear Problems). 1965. 34p. Dep. mn.

The problems of ionization measurement in a streamer chamber filled with neon are investigated. The ionizing power of protons coming at 90° to the electric field with energies of 660, 106, 57, 47, and 33 Mev was measured with three time values of streamer track formation. The track brightness is shown to serve as a good parameter for measuring ionization in the streamer chamber. The track brightness versus ionization of protons coming at 55 – 67° to the electric field was measured at 660, 106, and 57 Mev. Ionization in the streamer chamber filled with helium was preliminary measured. (auth)

**2129** (JINR-P-2312) SIMMETRICHNAYA SISTEMA PROVOLOCHNYKH ELEKTRODOV IZOTROPNOI ISKROVOI KAMERY. (A Symmetric System of Wire Electrodes for an Isotropic Spark Chamber). Matyushin, A. T.; Matyushin, V. T. (Joint Inst. for Nuclear Research, Dubna (USSR). Lab. of High Energy). 1965. 12p. Dep. mn.

Possibilities of optimization in the construction of an isotropic spark chamber are considered. It is shown that the chamber with a symmetric system of wire electrodes has some advantages over an "open" system and provides great accuracy in determining the track coordinates, in particular "z-projection." (auth)

**2130** (JINR-P-2340) POLUAVTOMATICHESKII PRIBOR DLY A PROSMOTRA I IZMERENIY A SNIMKOV S ISKROVYKH KAMER. (Semi-Automatic Device for Scanning and Measuring Spark Chamber Photographs). Legar, F.; Maly, M.; Shon, O. (Joint Inst. for Nuclear Research, Dubna (USSR). Lab. of High Energy; Joint Inst. for Nuclear Research, Dubna (USSR). Lab. of Nuclear Problems). 1965. 28p. Dep. mn.

A semi-automatic device for scanning and measuring the spark chamber photographs was developed and constructed. The device has the following technical characteristics: it is meant for measuring the angles of track deflection on the photographs taken with standard 35-mm motion picture cameras, the magnification on the screen is tenfold, the device is provided with a black screen which allows to work by daylight, the film is automatically driven, the device has two regimes for driving the film: frame by frame and continuous, forward and backward, and the device records automatically the angular coordinates on the paper tape. (auth)

**2131** (JINR-P-2344) SMESHCHENIE RAZRYADOV ISKROVOI KAMERY V MAGNITNOM POLE. (Displacement of Spark Chamber Discharges in a Magnetic Field). Korenchenko, S. M.; Morozov, A. G.; Nekrasov, K. G. (Joint Inst. for Nuclear Research, Dubna (USSR). Lab. of Nuclear Problems). 1965. 12p. Dep. mn.

The discharges of the spark chamber placed in a magnetic field are displaced with respect to the ionizing particle track if they are affected by the clearing electric field which is normal to the magnetic field. Using the experimental data of this work obtained with a spark chamber filled with neon and the data of others the dependence of the magnitude of the discharge displacement on the applied fields, on the pulse delay in the chamber supply and on the gas parameters was derived. For noble gases, neon, helium, and their mixtures, good agreement is obtained between the theoretical estimate for the discharge displacement and the experimental data. (auth)

**2132** (JINR-P-2368) PROVOLOCHNAYA ISKROVAYA KAMERA S VNESHNIMI AKUSTICHESKIMI DATCHIKAMI. (Wire Spark Chamber With External Acoustic Transducers). Ambro, P.; Karzhavin, Yu. A.; Matyushin, V. G.; Matyushin, A. T.; Shoshev, P. (Joint Inst. for Nuclear Research, Dubna (USSR). Lab. of High Energy). 1965. 7p. Dep. mn.

A wire filmless chamber is described in which the Cartesian coordinates of the spark are recorded with

external acoustic transducers. Such a chamber allows to record simultaneously several sparks arising in the discharge gap. (auth)

**2133** (NASA-SP-71, pp 245-50) AN APPLICATION OF THE GENERALIZED CONCEPT OF DOSIMETRY TO SPACE RADIATIONS. Wright, H. A.; Hurst, G. S.; Wagner, E. B. (Oak Ridge National Lab., Tenn.). (ORNL-P-706).

The application of the generalized concept of dosimetry to the dosimetry of high-energy protons is illustrated. Calculations are made of the distribution of energy losses in an array of silicon detectors exposed to an isotropic flux of monoenergetic protons. The array consists of a main crystal of dimensions $1 \times 1 \times 1$ cm bounded on each of its six faces by a crystal of dimensions $0.1 \times 1 \times 1$ cm. A computer code is used to plot the distribution of energy losses for several selected energies up to 400 Mev. An energy loss operator is defined that transforms an energy loss distribution function into a dose function. This operator can be used to calculate the rem dose accurately at selected energies, and within a given tolerance at intermediate energies. An electronic circuit is described that selects energy-loss signals from the detector and routes them to the appropriate section of a data processor, thus permitting the calculation of the dose received from radiation by high-energy protons of arbitrary energy spectrum. (auth)

**2134** (TID-22335) A FEASIBILITY STUDY OF A HIGH SENSITIVITY FAST NEUTRON DOSIMETER. Summary Report. Swartz, J. M.; Chase, B. H.; Thurston, M. O. (Continental Electronics Corp., Columbus, Ohio). Dec. 31, 1963. Contract AT(11-1)-1226. 54p. Dep. mn; CFSTI $2.00 cy, $0.50 mn.

The development of a fast neutron dosimeter based on the radioinduced degradation of the excess electron and excess hole lifetimes is described. The dosimeter is envisioned for use as a personnel radiation monitor. (T.F.H.)

**2135** GAMMA AND NEUTRON DOSIMETRY USING COLORED POLYVINYL ALCOHOL FILMS IN NUCLEAR REACTORS. Lavrentovich, Ya. I.; Levon, A. I.; Mel'nikova, G. N.; Kabakchi, A. M. At. Energ. (USSR), 19: 273-6 (Sept. 1965). (In Russian).

It is shown that radiation discoloration of a polyvinyl alcohol film containing methylene blue can be used for the dosimetry of gamma and neutron radiation in nuclear reactors. The degree of discoloration is a linear function of dose in the range of $10^4$ to $10^6$ rad and is practically independent of changes in linear energy transfer, dose intensity, and temperature within wide limits. Films containing boric acid besides the dye allow thermal neutron fluxes in the range of $10^{12}$ to $10^{14}$ n/cm$^2$ to be detected. The measurement error in all cases does not exceed ±10%. (tr-auth)

**2136** THE EFFICIENCY OF $^3$H/Zr SOURCES IN NONDISPERSIVE X-RAY SPECTROMETRIC ANALYSIS. Betin, Yu. P.; Bursukova, M. I.; Verkhovskii, B. I.; Shelkov, L. S. At. Energ. (USSR), 19: 297-8(Sept. 1965). (In Russian).

The relative efficiency of a zirconium-tritium source for the excitation of x-ray emission in elements was studied. The arrangement of the source, probe, and proportional counter is described. The variation of emitted x-ray intensity with energy is presented for the excitation of K radiation in elements with Z from 16 to 30 and of L radiation in elements with Z from 48 to 73. (M.J.T.)

**2137** ON THE IMPAIRMENT OF IONIZATION CHAMBER HOMOGENEITY BY CONDUCTING COVERING. Bregadze, Yu. I. At. Energ. (USSR), 19: 309-11(Sept. 1965). (In Russian).

The decrease of energy deposited in the gas volume of a homogeneous ionization chamber, caused by a conducting covering, is estimated as a function of the fast-neutron energy, the gas volume, and the thickness of the covering. Calculations are carried out for a flat ionization chamber of hydrogenous material, filled with a wall-equivalent gas, in a flux of fast neutrons incident perpendicular to the wall. Results are presented of the variation of the ratio of energy deposited in the chamber volume with conducting covering to energy deposited in the volume of a strictly homogeneous chamber with the distance between the chamber walls. (M.J.T.)

**2138** SEMICONDUCTOR PARTICLE DETECTORS. Varga, Dezsoe. At. Kozlemen., 7: 155-75(June 1965). (In Hungarian).

Recent increase in the use of semiconductor particle detectors is due to the newly developed simplified fabrication processes, greater variety in the parameters of the commercially available types and the large reduction in their price. It is possible to prepare reliably operating, thick sensitive layers, extending the use of semiconductor detectors into the field of $\beta$ and $\gamma$ spectrometry, in addition to the spectrometry of heavy particles. The action of the detectors is based on the interaction of the high-energy charged particles with the electrons of the solid. As a result of the collisions, the electrons of the semiconductor are lifted from the valency or deeper-lying zones to the conductance zone. This results in the creation of electron-hole pairs, originally located at various levels, but collected within $10^{-12}$ sec at both sides of the forbidden zone. The energy liberated during this process creates additional pairs. In the case of Si, an energy of $\epsilon_0 = 3.6$ ev is needed for creating a pair. It can be experimentally demonstrated that the number N of carrier couples generated in a crystal is directly proportional with the energy E of the particle, $N = E/\epsilon_0$. The electrons and holes recombine ultimately in the semiconductor. For good detection, the recombination losses must be minimized. Requirements concerning homogeneous crystal detectors, such as halides, diamond, CdS, Si, diffuse p-n detectors, surface barrier detector and Li-ion compensation detectors are reviewed and the limits of energy resolution under various conditions are given. (30 references). (TTT)

**2139** A LOW-LEVEL DEVICE FOR THE MEASUREMENT OF HIGH ENERGY $\beta$-RADIOACTIVE GASES. Fleck, C. M.; Weiss, H. (Oesterreichische Hochschule, Vienna). Atomkernenergie, 8: 249-53(July-Aug. 1965). (In German).

Coincidence-anticoincidence equipment is described for the measurement of $\beta$-radioactive gases or aerosols with energies in the range of 0.2 to 10 Mev. The gases and aerosols are measured as they flow through the apparatus. Therefore the equipment is especially suitable for continuous monitoring of air and may be used in connection with a promptly acting alarm device. A shield of 200 g/cm$^2$ iron increases the sensitivity so that natural radioactive gases of air can be measured. As an example the detection limits are given for $^{41}$Ar and $^{16}$N, which are produced during reactor operation. A method of discriminating between these two nuclides is described. (auth)

**2140** THE OPERATION OF HALOGEN-FILLED G-M COUNTERS UP TO HIGH GAMMA DOSE RATES. Weiss, H. (Oesterreichische Hochschule, Vienna). Atomkernenergie, 8: 255-60(July-Aug. 1965). (In German).

G-M counters could be suitable detectors for radiation monitors if they would not saturate and give smaller pulses with increasing dose rate. For the commercially available counters, Philips type 18529, 18509 and 18550 which are halogen filled, the pulse rate and pulse height were measured being a function of gamma ($^{60}$Co) dose rate up to values of $1.4 \times 10^4$ R/hr – in some cases up to $8 \times 10^4$ R/hr. The influence of shunt capacitance (capacitance of counter socket) is described. Next to the pulse counting technique, measuring the integrated current of G-M counters is a simple method for monitoring radiation. Though, depending on the various types of counters the current – dose rate characteristic is showing a remarkable maximum before saturation occurs. This results in a small usable operation range. range. After investigation of this phenomenon a simple circuit is described which prevents the occurence of the maximum and thus gives a quasi – logarithmic characteristic close to the saturation value. With this curcuit an operation range for the 18529 type counter up to 5000 R/hr was possible. Diagrams are given for determining the influence on the current characteristics of various counter voltages and series resistances. (auth)

**2141** AUTOMATION IN RADIATION MEASUREMENT TECHNIQUES. Bosch, J. (Frieseke and Hoepfner GmbH, Erlangen, Ger.). Atomwirtschaft, 10: 515-20(Oct. 1965). (In German).

The present state of the technology makes possible an extensive automation in the range of radiation measurements. There are available numerous electronic and mechanical units such as automatic samplers, units for logical linkages, counting or computing devices, multichannel pulse-height analyzers, data distribution, and mechanical and electrical calculators. An automatic feedback of the measurement results to the experiment is being carried out in nuclear physical measurements in high-energy physics. (tr-auth)

**2142** ANALYSIS AND DATA PROCESSING OF MULTIPARAMETRIC MEASUREMENT VALUES. Linz, H. (Frieseke and Hoepfner GmbH, Erlangen, Ger.). Atomwirtschaft, 10: 525-8(Oct. 1965). (In German).

Multidimensional pulse-height analyzers that were used for a long time in nuclear physical experiments were recently introduced into the area of nuclear chemistry. In radioisotopic mixtures with several photolines individual radioisotopes could not be identified with certainty. In addition to the coincidence spectrometry, multidimensional analyzers can be used advantageously for the recording of decay curves of very short-lived radioisotopes. (tr-auth)

**2143** MODERN DETECTORS IN RADIATION PROTECTION. Kiefer, H.; Maushart, R. (Kernforschungszentrum, Karlsruhe, Ger.). Atomwirtschaft, 10: 529-33 (Oct. 1965). (In German).

Geiger counters and film packets do not always completely satisfy the present requirements of personnel dosimetry. An effective radiation protection is possible with numerous special measurement devices with special detectors. The basic considerations that lead to the development and introduction of modern detectors were explained using 3 examples. The large-surface proportional counter, glass dosimeters, and semiconductor detectors are considered. (tr-auth)

**2144** FUNCTIONAL PERFORMANCE OF A GEIGER-MUELLER COUNTER. Grillet, Leon (Faculte des Sciences, Rennes, France). Bull. Soc. Sci. Bretagne, 37: 56(1962). (In French).

Normally, operation which corresponds to the threshold voltage is characterized by a slight slope in the counting level. Usually adjustment of the applied voltage upward brings about oscillating function. When a counter of the type L.C.T. 3 G 12 is used, this type of operation is seen near 248 v. The rapid oscillations extend over an amplitude of several volts, and then finally terminate in a counting state. Function is irreversible. When the voltage is reduced, the same phenomenon of oscillatory function is not observed with a very wide amplitude at the lower voltage. However, this phenomenon is reproducible when the initial procedures are used. If a variable condenser of several hundred picofarads is connected across the terminals of the tube, the frequency is decreased or increased by the value of the capacitance. This facilitates observation of the form of the oscillations. They appear to be relaxation oscillations. These observations have been confirmed by oscillograms. (BBB)

**2145** SPURIOUS SCATTERING IN NUCLEAR EMULSIONS. Sood, P. M.; Chohan, V. S.; Datta, Bhagwat (Panjab Univ., Chandigarh, India). Indian J. Pure Appl. Phys., 3: 291-5(Aug. 1965).

The role of non-planarity in causing spurious scattering in nuclear emulsions was investigated by studying the dislocations in pellicles of a stack in regions exactly one above the other along the XY and XZ planes. Studies in different depth regions of three pellicle emulsions showed that spurious scattering is maximum near the air surface and minimum in the middle, while its magnitude at the glass surface does not show a fixed trend. The dislocations responsible for spurious scattering do not always obey a normal distribution. (auth)

**2146** ON THE RELATIVE TIME DISTRIBUTION OF PULSES IN THE $4\pi\ \beta-\gamma$ COINCIDENCE TECHNIQUE. Williams, A.; Campion, P. J. (National Physical Lab., Teddington, Middx., Eng.). Int. J. Appl. Radiat. Isotop., 16: 555-60(Sept. 1965).

A time-to-pulse-height converter is used to show that the relative time distribution of pulses in a $4\pi\ \beta-\gamma$ coincidence system using a gas counter for the $4\pi\ \beta$ detector is asymmetrical. The same technique can be used to set the relative delay between channels with some considerable precision. (auth)

**2147** THE METHOD OF SMALL SOLID ANGLE FOR MEASURING $\alpha$-PARTICLE FLUX AND DETERMINING THE RELATIVE STOPPING POWER OF MICA AND CERTAIN GASES. Shchebolev, V. T. Izmeritel. Tekhn., No. 5, 52-5(May 1965). (In Russian).

A circular $^{233}U$ source was mounted on an external stand at a distance h from the end window of a proportional alpha counter. The geometry of the arrangement was determined by the diameter of the end-window opening $2R_1$, by the diameter of the alpha source $2R_2$ and by the distance h. Because of the finite thickness t of the end-window diaphragm, it was necessary to calculate an effective source radius $R_2 = R_2 + \Delta R_2(h)$. The relative stopping power of the mica window was found to be 1.45 mg/cm$^2$, which agree well with a theoretical value of 1.44 calculated for 5-Mev alpha particles ($E_\alpha$ of $^{233}U$ equals 4.82 Mev). By determining the count rate as a function of gas pressure at various distances of h, the relative molecular stopping power was found to be 0.184 for helium, 0.942 for argon, 0.915 for methane, and 1.51 for carbon dioxide. The values were 0.223 for 99% He + 1% Ar, 0.235 for 98% He + 2% Ar, 0.278 for 95% He + 5% Ar, 0.250 for 97% He + 3% Ar, and 0.350 for 90% He + 10% Ar. The reflection of alpha particles from the source backing can be neglected on counting at a small solid angle of $\sim 10^{-5}$. (TTT)

**2148** ON THE OPTIMUM MEASURING CONDITION OF GAMMA AND BETA SPECTROMETERS. Schult, O. W. B. (Technische Hochschule, Munich). Kerntechnik, 7: 309-15(July 1965). (In German).

The ratio between the peak counting-rate and the square root of the background, obtained from the measurement with an existing gamma or beta spectrometer, can be considered as a measure for the observability of a weak line. This quantity is calculated. It depends on the size of the source and (in case of the beta spectrometer) also on the slit in front of the detector. From the analysis of the dependence of the ratio defined above, and the resolution, on the geometry, certain limits can be put on the dimensions of the source and the slit. Within these limits, there are optimum experimental conditions. The best channel setting is explained if a scintillation counter is used as detector. Two graphs show how the total measuring time has to be split into the interval for the peak measurement and the time for the determination of the background when the statistical error should be a minimum, and a curve which allows for a very simple calculation of the error. (auth)

**2149** A SIMPLE OSCILLOGRAPHIC GAMMA SPECTROMETER WITH, AS DESIRED, LINEAR OR PARABOLIC ENERGY SCALE. Grueter, H. (Universitaet, Muenster, Ger.). Kerntechnik, 7: 316-19(July 1965). (In German).

Oscillographic pulse-height analyzers using the grey wedge method permit quite easily an almost complete analysis of all detector pulses. In the measuring arrangement a simple unit consisting of pulse stretcher and vertical-voltage generator in connection with a cathode-ray oscillograph integrates a commercial scintillation counting device to a gamma spectrometer. Caused by the exponential form of the vertical beam deflection the level of photographic pulse registration follows the curve of oscillation frequency in the spectrum. For photographic registration on extremely hard industrial film (Gevaert O 81) turned out best. The set is mainly used for the mea-

surement of artificial radioactivity caused by fission products. (auth)

**2150** A FAST METHOD IN GAMMA SPECTROMETRY. Rinn, F. H. (Siemens and Halske AG, Karlsruhe, Ger.). Kerntechnik, 7: 320-1(July 1965). (In German).

The method of single-channel spectrometry for registration of gamma spectra is exact but time-consuming; multichannel spectrometry, on the contrary, is exact and fast but complicated. Finally the oscillographic spectroscopy with subsequent photographic registration is exact, the apparatus required is limited, the method is faster than the one-channel method, but nevertheless not fast enough. A remarkable time-saver without increase of expenditure turns out to be the combination of the oscillographic method and the single-channel method using a pulse-height analyzer with adjustable measuring range. The productivity of this method is shown. (auth)

**2151** A METHOD TO COMPENSATE THE NATURAL AIR-RADIOACTIVITY BY MEANS OF BETA-ALPHA-PSEUDOCOINCIDENCES. Gebauer, H. (Frieseke and Hoepfner GmbH, Erlangen, Ger.). Kerntechnik, 7: 322-5(July 1965). (In German).

A description is given of an apparatus which makes the compensation of the natural air-radioactivity possible by means of $\beta$-$\alpha$-pseudocoincidences. A flat methane-flow counter is used as detector. To give a practical example the control of the $^{239}$Pu activity concentration in a hot laboratory is discussed. (auth)

**2152** RADON MEASUREMENTS BY SCINTILLATION METHODS. Toth, Arpad (Sanitary Service, Pecs, Hungary). Magy. Fiz. Folyoirat, 13: 129-55(1965). (In Hungarian).

Scintillation methods were found very useful for determining $^{222}$Rn, $^{220}$Rn, and $^{219}$Rn for purposes of radiation protection, raw material prospecting, geophysical and physicochemical studies, etc. The measurements are usually carried out at a very low level of activity. These $\alpha$ counters present the advantage of being inexpensive, unaffected by humidity, cosmic and $\gamma$ radiation; they do not require a special filling gas and possess a resolution better than 1 msec. The ZnS scintillating layer may be easily replaced. A novel counting system based on ZnS(Ag) scintillator was developed; it operated reliably for periods of 8 hours per day without changing the background as a result of electric noise. Under conveniently reached conditions, activities as low as 0.2 pC of $^{222}$Rn could be determined within 2 hours with an accuracy of ± 20%. The constructional details given illustrate that the needed components, such as multipliers, pulse recorders, integral discriminating circuits, etc., may be procured easily, without any major changes in the electronics. (TTT)

**2153** DIGITAL COMPUTERS IN NUCLEAR RADIATION COUNTING. Nucleus (Chicago), No. 19, 1-11(Mar. 1965).

Problems solvable by the digital computer in the field of radioisotope technology are discussed. Although these problems are commonly resolved by graphic approximation methods or simplified manual procedures, the digital computer offers a more sophisticated method which permits a more adequate data interpretation. A number of common problems are considered. These include the counting rate and statistics, background subtraction, decay corrections, various derived parameters, the flow of isotopes through various sytems, and dual labeling. The method of computer programing is also described. (J.F.P.)

**2154** CHARGE-SENSITIVE TRANSISTOR PREAMPLIFIER FOR USE WITH SEMICONDUCTOR NUCLEAR RADIATION DETECTORS. Karwowski, M.; Wlodarski, W.; Pawlowski, Z. Nukleonika, 10: 189-93(1965). (In Polish).

The performance characteristics and stability of the preamplifier are described in detail for a 6-transistor preamplifier utilizing OC-170 transistors. The limiting gain is $8 \times 10^{-4}$ V/1000 ion pairs for a signal from a zero-capacity source, and this gain is held to within 3% of the limiting value for 0-400 pF of source capacitance. The linearity is 1% from 0–3v output, and the gain variation is less than 2% for a supply voltage change of 30%. Temperature characteristics curves are presented. A $^{210}$Po alpha pulse-height spectrum is shown for the preamplifier connected to the output of a 20 mm$^2$ surface-barrier diode and to the input of a ZPT-0173 amplifier feeding a type AA-102 pulse height analyzer. A half-width of about 1% is obtained with this arrangement for the 5.298 Mev alpha line. (TTT)

**2155** SEMICONDUCTOR NUCLEAR RADIATION DETECTORS AND THEIR APPLICATIONS. Chwaszczewska, Janina; Dakowski, Miroslaw; Przyborski, Wincenty; Sowinski, Mieczyslaw. Przeglad Elektron., 6: 174-9 (Apr. 1965). (In Polish).

The advantages of semiconductor radiation detectors are briefly discussed, and the state of the art of semiconductor-detector design and fabrication in Poland is outlined. Surface-barrier detectors have been constructed with gold layers of 40-100 micrograms/cm$^2$ thickness, with areas of 4 mm$^2$ to 2 cm$^2$ for single detectors and up to 14 cm$^2$ for a mosaic of detectors, and with a resolution of 16 Kev for 8.776 Mev alphas (using a single 12mm$^2$ detector). Sensitive layers of 400-500 microns have been achieved. Also, dE/dx type detectors have been built with thicknesses of 25 to 70 microns. Surface barrier diodes with guard rings have made depths of 1.2 to 1.5 mm. The guard ring reduces the leakage current on the sensitive inner gold conductor and thereby allows the use of higher voltages across the sensitive layer. For thicknesses above 1 mm, lithium drifted germanium detectors have been constructed. Thicknesses of 3 mm have been obtained. The demands placed on the electronic circuitry required to obtain high resolution information from the millivolt-level signals produced by these semiconductor type devices are discussed. (TTT)

**2156** THE DOSIMETRY OF HIGH ENERGY ELECTRONS. Seidel, W.; Wulff, W. Radiobiol. Radiotherap., 6: 619-24(1965). (In German).

Several photographic methods were compared for depth dose plots of high energy electrons. It was found that with lower expense photographic equidensitometry of isodose determination is equivalent to the conventional procedures in flat and oblique arrangement of the film. As an example, abrupt dose gradients on interfaces are represented. (tr-auth)

**2157** THE DOSIMETRY OF CONVENTIONAL AND HIGH ENERGY RADIATION WITH SCINTILLATION DOSIMETER. Hegewald, H. (Humboldt-Univ., Berlin). Radiobiol. Radiotherap., 6: 625-30(1965). (In German).

The use of scintillation detectors as x radiation dosimeters has the advantage that very small measuring volumes may be used and an energy independent measurement may be obtained over a relatively wide energy range. The radiation effect on the photomultiplier, Cherenkov radiation, and luminescence, cause perturbations which may cause measuring errors. A series of measuring methods was developed which eliminate wholly or partly the perturbing influences. The methods described in the literature are summarized and their advantages and disadvantages are discussed. The direct modulation of the scintillation light by means of the electro-optical rotation of the oscillation plane of linearly polarized light by excited Piezo-crystals is proposed. (tr-auth)

**2158** PREPARATION AND CHARACTERISTICS OF THE IFA EN$_2$ NUCLEAR EMULSION. Apostol, A.; Nicolae, Marieta; Pop, Rodica. Rev. Roumaine Phys., 10: 169-78 (1965). (In French).

A method for the preparation and the characteristics of an emulsion sensitive to the ionization minimum were presented. The emulsion is designed for use in nuclear physics and in $\beta$ and $\beta + \gamma$ autoradiography. After a critical discussion of the factors determining the polydispersion of the

microcrystals of the emulsion and the homogeneity of the grain sensitivity, the preparation method is described. The precipitation method in acid milieu by ammonium silver nitrate using diluted solutions of the reagents was employed. After some hours of chemical aging the chemical is sensitized with gold. The sensitivity to $\alpha$ particles, the sensitivity to the ionization minimum, clouding, reproducibility, and the conservation delay of the sensitivity were determined for a large number of the emulsions. The results for the characteristics of this emulsion showed that it is well suited for use in nuclear physics and in autoradiography. (tr-auth)

**2159** MASS SPECTROMETER SOURCE LOADING LOCK AND ISOLATION VALVE. Munro, R.; Ridley, R. G. (Atomic Weapons Research Establishment, Berks, Eng.). Rev. Sci. Instrum., 36: 1538-9(Nov. 1965).

An all-metal sliding bar vacuum lock is described employing a new type of vacuum seal involving the deflection of the wall of the lock housing. A pressure of $2 \times 10^{-7}$ Torr can be maintained in the main source region of a mass spectrometer during the introduction of solid samples into the source. An isolation valve utilizing a similar principle is also described. (auth)

**2160** APPLICATION OF PILE-UP DISTORTION CALCULATIONS. Soucek, Branko (Brookhaven National Lab., Upton, N. Y.). Rev. Sci. Instrum., 36: 1582-7(Nov. 1965). (BNL-9015).

Factors studied include: relative distortion of the distribution peak (peak position, as well as peak count); distortion of the distribution shape; influence of the detector output waveform on spectral distortion; influence of radiation source intensity (pulse rate) on spectral distortion; influence of detector resolution (dimensions and type of detector) and amplifier resolution (noise, drift); discontinuities in spectra produced by pile-up, etc. Quantitative curves are given. Results are obtained on the basis of theories of pile-up effect. The domain of validity of results is shown, as well as a comparison between different approaches (analytical and numerical) for calculation of spectral distortions due to pile-up effect. (auth)

**2161** EFFECT OF SOLLER SLITS ON X-RAY INTENSITY IN A MODERN DIFFRACTOMETER. Stoecker, W. C.; Starbuck, J. W. (Mallinckrodt Chemical Works, St. Charles, Mo.). Rev. Sci. Instrum., 36: 1593-8(Nov. 1965).

The properties of Soller slits in a modern diffractometer are discussed in relation to the effect they have on the x-ray intensity distribution within the plane that contains the line focus and diffractometer axis. On the basis of an idealized Soller slit collimator, equations are derived for computing relative x-ray intensity in terms of the distance from the edge of the specimen. An independent mathematical derivation substantiates these equations and also shows the effect of varying the number of slits while keeping other properties of the collimator unchanged. When the equations are used to calculate the over-all intensity profiles of two diffractometers at the specimen position, the results are found to be in reasonable agreement with photographically determined profiles. Similar equations are used to explain the effect of the receiving Soller slits on the diffracted rays. (auth)

**2162** COMPACT VERSATILE X-RAY COLLIMATOR WITH ADJUSTABLE PINHOLES. Love, Warner E.; Hendrickson, Wayne A.; Herriott, Jon R.; Lattman, Eaton E.; McCorkle, G. Lewis (Johns Hopkins Univ., Baltimore). Rev. Sci. Instrum., 36: 1655-6(Nov. 1965).

The x-ray collimator described has rectangular apertures, which are defined by the flat heads of four screws, aligned in opposing pairs with axes perpendicular to the beam. The first pair of screws defines a sheet-type beam, and the second pair (perpendicular to the first pair) transmits the rectangular beam. The screws are set in tapped holes, so that the beam cross section may be varied continuously. The collimator described consists of three graduated apertures of the type described. (T.F.H.)

**2163** ARGON GAS SCINTILLATION DETECTOR. Cojocaru, V.; Ivanceanu, I.; Marinescu, L.; Mihai, I.; Petrascu, M. (Inst. of Atomic Physics, Bucharest). Studii Cercetar. Fiz., 16: 917-21(1964). (In Rumanian).

A scintillation counter using technical Ar was developed for studying fission fragments. The 4.5-cm diameter and 9.5-cm high chamber could be observed through a 5-mm thick optical glass disc; the system also included a photomultiplier with a high load resistance at the anode. A layer of Po deposited on a Ag support served as the $\alpha$ radiation source. Before filling the chamber with gas, it was evacuated to a pressure of $10^{-2}$ mm of Hg, then filled in open circuit at a rate of 0.5 cm/sec. The gas used for filling consisted of Ar in amounts ranging from 80 to 99.7%; $N_2$ from 0.24 to 20% and 0.05% each of $O_2$ and ($CO_2$ + CO). A systematic study of the correlation between pressure and resolution revealed that the optimum resolution is reached at a pressure of about 500 mm of Hg; at that pressure, the mixture of Ar + 10% $N_2$ yielded the best results: in that case a potential of about 2 v was obtained at the exit of the photomultiplier at an amplitude resolution of about 30%. This was verified separately by means of an NaI crystal and a 1 mC $^{137}Cs$ source. Use of the instrument is quite simple; no outgassing or gas stream purification were found to be necessary. (TTT)

**2164** ABSOLUTE EFFICIENCIES AND RADIATION DAMAGE IN POLYCRYSTALLINE PHOSPHORS IRRADIATED WITH HIGH-ENERGY ELECTRONS. Belcher, Ralph L.; Silverman, Joseph (Univ. of Maryland, College Park). Trans. Amer. Nucl. Soc., 8: 322(Nov. 1965).

**2165** MEASUREMENT OF MEGARAD DOSES OF $^{60}Co$ GAMMA RAYS WITH UVT LUCITE. Muller, A. C.; Rizzo, F. X. (Brookhaven National Lab., Upton, N. Y.). Trans. Amer. Nucl. Soc., 8: 323(Nov. 1965).

**2166** THE APPLICATION OF LITHIUM-DRIFTED GERMANIUM DETECTORS TO NEUTRON ACTIVATION ANALYSIS—STUDIES IN GEOCHEMISTRY AND OF 15th CENTURY PRINTING. Schroeder, Gerald L.; Kraner, Hobart W.; Evans, Robley D. (Massachusetts Inst. of Tech., Cambridge). Trans. Amer. Nucl. Soc., 8: 327(Nov. 1965).

**2167** PULSE-SHAPE DISCRIMINATION TECHNIQUE FOR A DUAL-CRYSTAL COMPTON REDUCTION DETECTOR. Lam, Carroll F. (Air Force Hospital, Wright Patterson AFB, Ohio); Wainerdi, Richard E. Trans. Amer. Nucl. Soc., 8: 340(Nov. 1965).

**2168** SIGNIFICANCE OF THE EXPONENTIAL FUNCTION IN QUENCHING CORRECTION IN LIQUID-SCINTILLATION COUNTING AND ITS APPLICATION TO CHANNELS-RATIO METHOD. Peng, C. T. (Univ.of California, San Francisco). Trans. Amer. Nucl. Soc., 8: 340-1(Nov. 1965).

**2169** GEOMETRICAL EFFECTS ON EFFICIENCIES OF WELL-TYPE GAMMA-RAY SCINTILLATION DETECTORS. Snyder, B. J. (Westinghouse Astronuclear Lab., Pittsburgh). Trans. Amer. Nucl. Soc., 8: 341-2(Nov. 1965).

**2170** ABSOLUTE COUNTING WITH WELL-TYPE SCINTILLATION DETECTORS. Wagner, Paul R.; Pollack, Louis R. (San Francisco Bay Naval Shipyard). Trans. Amer. Nucl. Soc., 8: 342-3(Nov. 1965).

**2171** DIRECT-FIELD GAMMA SPECTROMETRY FOR RAPID QUANTITATIVE ASSESSMENT OF ENVIRONMENTAL CONTAMINATION. Lowder, W. M.; Condon, W. J. (U. S. Atomic Energy Commission, New York). Trans. Amer. Nucl. Soc., 8: 343(Nov. 1965).

**2172** GAMMA SCANNING WITH ANTICOINCIDENCE SPECTROMETERS. Holm, Dale M.; Sanders, W. Mort (Los Alamos Scientific Lab., N. Mex.). Trans. Amer. Nucl. Soc., 8: 343-4(Nov. 1965).

**2173** ALPHA PARTICLE ENERGIZED NEUTRON-FLUX MONITOR. Kinzer, Jackson (Atomics International, Canoga Park, Calif.). Trans. Amer. Nucl. Soc., 8: 579(Nov. 1965).

**2174** EXPERIMENTAL EVALUATION OF SELF-POWERED NEUTRON-FLUX MONITORS FOR PWR IN-CORE USE. Worsham, H. J. Jr.; Ball, R. M. (Babcock and Wilcox Co., Lynchburg, Va.). Trans. Amer. Nucl. Soc., 8: 579-80(Nov. 1965).

**2175** INVESTIGATION OF THERMOLUMINESCENT DOSIMETRY FOR MEASURING GAMMA HEATING IN A CRITICAL ASSEMBLY. Stanford, G. S.; Johnson, T. W. (Argonne National Lab., Ill.). Trans. Amer. Nucl. Soc., 8: 587-8(Nov. 1965).

**2176** ON THE PROPAGATION OF DISCHARGES IN SELF-EXTINGUISHING COUNTERS. IV. Franke, H. G.; Huster, E.; Krafft, O. (Univ., Muenster, Ger.). Z. Physik, 188: 274-81(1965). (In German).

Measurements with a Geiger counter with inserted grid between wire and cathode solved the problem whether the discharge process is built up by the photoeffect in the gas or at the cathode of the counter. For negative voltages $U_g$ of the grid (cathode grounded) only the volume inside of the grid is sensitive to discharges. It was found, that within the limits of error, the threshold did not depend on the masking degree of the cathode. From this it follows that mainly the photoeffect in the gas contributes to the discharge process. But the distributions of time of the discharge spread along the wire at $U_g < 0$, $U_g > 0$ and in a counter with a massive cathode has shown that also the photoeffect at the cathode contributes to the discharge process. (auth)

**2177** RECENT ADVANCES IN NUCLEAR RADIATION DETECTORS. Ferguson, A. T. G. (Atomic Energy Research Establishment, Harwell, Eng.). pp 375-414 of Nuclear Structure and Electromagnetic Interactions. New York, Plenum Press, 1965.

Recent developments in gaseous ionization chambers, scintillation counters, and solid state devices relevant to low-energy nuclear physics are outlined. Applications of semiconductor counters to charged particle, gamma-ray, and neutron spectroscopy are discussed. (L.B.S.)

**2178** THE RESPONSE OF LITHIUM FLUORIDE TO REACTOR NEUTRONS. Simpson, R. E. (Walter Reed Army Medical Center, Washington, D. C.). 42p. (CONF-650637-4). Gmelin, AED-CONF-65-151-2.

From International Conference on Luminescent Dosimetry, Palo Alto, Calif.

Results from a study of the glow curves of TLD-100 (7.5% $^6$Li) and TLD-700 (0.09% $^6$Li) under gamma exposure are characteristically similar. However, under reactor exposures in a field of known thermal neutron and gamma fluxes, indicate significant difference in the 220°C and 275°C glow peaks for approximately the same integrated area under the curves. It is postulated that these differences are primarily due to the specific ionization of ejected electrons from gamma versus that resulting from the $^6$Li(n,$\alpha$)$^3$H reaction of the thermal neutrons. In the first instance, ionization is the result of energetic electrons whereas in the latter case, ionization is dominated by a 4.8 Mev $\alpha$ and $^3$H reaction products. In essence the phosphor becomes a "source" as a function of the thermal neutron flux. The glow curve characteristics have been significantly demonstrated by shielding the phosphors against thermals using $^6$Li and cadmium covers. By this technique a true gamma dose is obtained producing the characteristic gamma glow curve both for the TLD-100 and TLD-700. The average response of the TLD-700 LiF has been determined to be 0.7 rad per $10^{10}$ nvt thermal neutrons while the response of the normal phosphor is greater than 200 rad per $10^{10}$ nvt. Having determined the responses of these materials to thermal neutrons and considering the relative independence to gamma energy permits the use of the TLD-700 phosphor for determining gamma dose within a reactor environment. The TLD-100 material may be used as an auxiliary thermal neutron plus gamma detector where such data are desired. (auth)

**2179** SYSTEM DESIGN IN LOW BACKGROUND INTERNAL GAS SAMPLE COUNTING OF $^{14}$C AND TRITIUM. Sharp, Rodman A.; Ellis, John G. (Beckman Instruments, Inc., La Jolla, Calif.). 14p. (CONF-650652-8). Gmelin, AED-CONF-65-158-11.

From International $^{14}$C and $^3$H Dating Conference, Pullman, Wash.

Good results in low background internal gas sample counting of carbon-14 and tritium depend on careful optimization of an integrated system including design of detector, cosmic ray guard counter, shielding, and electronics and choice of counting gas. Recent advances leading to a simplified and economical high-performance internal gas sample counting system are described. The relative merits of internal gas sample counting and liquid scintillation counting for low level carbon-14 and tritium measurements are compared. (auth)

**2180** IMPROVEMENTS IN INSTRUMENTS FOR COUNTING OR ANALYSING BETA RAYS. (to Hoshasen Igaku Sogo Kenkyusho). British Patent 1,005,582. Sept. 22, 1965. Priority date Mar. 6, 1961, Japan.

A low-background $\beta$-ray scintillation spectrometer utilizes an organic phosphor in which a recess is formed. The inside surface of the recess is coated with an electroconductive material and acts as the cathode of a G-M counter. Beta particles enter the phosphor through the G-M counter, trigger both counters, and give coincidence output signals. By use of appropriate circuitry the coincidence output can be used to measure the energy distribution of $\beta$-rays emitted from a sample or it can be used to count $\beta$-rays in a given energy range. (A.G.W.)

**2181** RADIATION DOSIMETER. Yokoto, Ryosuke; Nakajima, Saburo (to Tokyo Shibaura Electric Co. Ltd.). British Patent 1,005,948. Sept. 29, 1965. Filed Aug. 27, 1963.

A method of measuring the radiation dose to which a radiation-sensitive phosphate glass block had been exposed consists of irradiating the central portions of the block with a parallel beam of ultraviolet radiation and measuring the fluorescent radiation emitted at right angles to the direction of the incident ultraviolet radiation. Means are provided for reducing contamination of the surfaces of the block and for irradiating the block without irradiating its holder. (A.G.W.)

**2182** IMPROVEMENTS RELATING TO SOLID STATE RADIATION DETECTORS. Rouse, Robert Lindsay (to Associated Electrical Industries Ltd.). British Patent 1,006,233. Sept. 29, 1965. Filed May 8, 1962.

A method of manufacturing p-i-n junction semiconductor radiation detectors includes the steps of treating a semiconductor alloy of Si and Ge (at least 10% Ge) by a lithium ion drift process at a high temperature to form a p-n junction, applying a reverse electrical bias to the junction at a lower temperature to increase the thickness of the depletion zone and form a p-i-n junction, and connecting electrical leads to the device for connection to external circuitry. Appropriate circuitry may include a biasing source connected to apply a reverse bias to the p-i-n detector and a pulse height analyzer for measuring the output. The device may be cooled below ambient temperature. (A.G.W.)

**2183** IMPROVEMENTS IN AND RELATING TO ELECTROMETER SYSTEMS. Ganouna-Cohen, Gilbert (to Commissariat a l'Energie Atomique). British Patent 1,006,475. Oct. 6, 1965. Priority date Aug. 8, 1962, France.

An electrometer system for measuring small electrical charges liberated in an ionization chamber includes a fixed electrode coupled to the ionization chamber collector electrode and a movable electrode coupled to one of the poles of a source of electrical potential. The outer casing of the ionization chamber is coupled to the other pole of the source. A screen or flap moves to vary the masking of an element sensitive to radiation emitted by a radiation

source in response to movement of the movable electrode. When the sensitive element detects a predetermined relative movement of the electrode, an arrangement of relays and switches decreases the potential difference between the fixed and movable electrodes. (A.G.W.)

## Radiation Effects

*Refer also to abstract 2433.*

**2184** (AD-614618) EXPLORATORY DEVELOPMENT OF THE Q-FACTOR TECHNIQUE. Quarterly Progress Letter No. 4 for Period Ending March 31, 1965. Report No. 2899. Frank, Max (Bendix Corp., Southfield, Mich. Research Labs. Div.). Apr. 10, 1965. Contract AF29(601)-6316. 63p. CFSTI $3.00 cy, $0.75 mn.

Mean composite radiation damage constants, including the percent relative dispersion, are reported as a function of emitter current density for 22 different n-p-n silicon transistor types irradiated in a neutron environment of 7 × 10 to the 13th power n/cm$^2$, E > 0.1 Mev. A technique is described for the resolution of reciprocal gain into damage effect components in the base and space charge regions. The technique yields different damage constants for each region and results in a more accurate description of the radiation effects. Results are given for the application of this method to the 2N1613 transistor. A discussion is included of the determination of transistor physical parameters required for prediction of radiation damage, using the Boothroyd-Trofimenkoff model with data derived for the 2N1613 transistor. Results are shown from an isochronal annealing experiment performed on two pairs of 2N1613 transistors, one pair previously irradiated in neutrons and the other in a Cobalt-60 environment, each pair consisting of an actively and a passively irradiated unit. (auth)

**2185** (AD-618194) EXPLORATORY DEVELOPMENT OF THE Q-FACTOR TECHNIQUE. Quarterly Progress Letter No. 5 for Period Ending June 30, 1965. Report No. 3034. Frank, Max (Bendix Corp., Southfield, Mich. Research Labs. Div.). July 13, 1965. Contract AF29(601)-6316. 18p. CFSTI $1.00 cy, $0.50 mn.

Data for predicting transistor gain degradation in a neutron radiation environment were obtained from experimental studies of the variation of the radiation damage constant K as a function of temperature and current during both measurement and irradiation. Relatively small spreads in the values of K were obtained when the individual base transit times were measured and the radiation exposures were precisely determined. Radiation damage effect data from 20 different n-p-n silicon transistor types were obtained and normalized to the same minority carrier concentration in the base region, using the transit time and the V sub BE-I sub C characteristics of the specific transistors. The resulting relative dispersions of the damage constant for minority carrier densities of 10 to the 15th power/cc and 10 to the 16th power/cc were typically 15 to 20 percent. These dispersions indicate that electrical measurements of transistor physical parameters can provide reasonably accurate predictions of the gain degradation for a wide variety of transistors without additional radiation testing of specific transistor types. (auth)

**2186** (ECOM-2415) PULSED NUCLEAR RADIATION INDUCED TRANSIENTS IN ELECTRICAL CABLES (DRF NO. 1). Schlosser, William; Newberg, Joseph; Key, Joseph A. (Army Electronics Labs., Fort Monmouth, N. J.). July 1964. 36p. CFSTI $2.00 cy, $0.50 mn.

The pulse nuclear radiation induced transients in the individual conductors of RG-62A/U and RG-59B/U coaxial cables and a multiconductor ribbon cable due to exposure to the DRF-Mark F TRIGA reactor were studied as a function of applied voltage and repetitive exposure. The cable response consists of three current constituents: a replacement current, a conduction current, and a charging current. The predominance of the replacement component over the conduction component of the observed current after repetitive exposure was noted. The charging current is attributed to the introduction of charges in an initial exposure and to the redistribution of charges in an exposure accompanying an applied voltage change. The magnitudes of the induced currents were considerably lower than those observed for these cables at SPRF. An r-f signal transmitted through an RG-62A/U cable was attenuated by an amount that was also considerably lower than the attenuation observed at SPRF. (auth)

**2187** (ECOM-2545) PULSED NUCLEAR RADIATION EFFECTS ON RESISTORS AND CABLES, SPRF IV. Lascaro, Charles P.; Schlosser, William; Newberg, Joseph (Army Electronics Labs., Fort Monmouth, N. J.). Dec. 1964. 35p. CFSTI $2.00 cy, $0.50 mn.

Various cable and resistor types and an operating micromodule multi-virbrator circuit were exposed to a pulsed nuclear radiation environment (SPRF) and their transient response measured during the pulse. The initial RG-59 B/U cable response was determined to be voltage dependent and averaged 0.15 μa per volt superimposed on a zero voltage "replacement" current of −15 μa. A miniature low noise cable, with conductive interfaces, gave the lowest and most stable response of all cables tested. The attenuation of three different types of r-f cables was measured and the signal in JT-205 with foamed polyethylene was attenuated approximately 20%. The US-DEV −15 cable with perforated tape teflon averaged 0.3% and for RG-8 A/U, a solid polyethylene dielectric, attenuation averaged 0.5%. Carbon composition, deposited carbon film, nichrome film, tin oxide, wirewound, cermet, and gas-filled "Minuteman" resistors of various wattages were tested in an unpotted, conformally coated, and potted condition. All low value resistors tested (less than 1500 ohms) maintained tolerance levels even in unpotted conditions. For the unpotted higher-value resistors (10 K ohm) the shunting effect of the ionized air may cause a resistance change of the order of 2% which can be reduced to 1% by conformal coating. The 100 K ohm "Minuteman" gas-filled resistor showed an effective decrease of 7% during exposure. A free running multivibrator in a microcircuit modular configuration underwent both transient and permanent damage. (auth)

**2188** CARRIER REMOVAL IN SILICON AS THE CAUSE OF RADIATION-INDUCED FLUCTUATIONS IN THE BASE RESISTANCE AND EMITTER EFFICIENCY OF SILICON TRANSISTORS. Andrews, P. A.; Mayburg, S. (Controls for Radiation, Inc., Cambridge, Mass.). Proc. IEEE (Inst. Elec. Electron. Eng.), 53: 1653-4(Oct. 1965).

Variations in the resistivity of thin slices of silicon were investigated both before and after irradiation by using a four-point probe of 0.010-inch spacing. A p-type slice of silicon 0.015 inches in thickness was probed, with the results showing nonuniformity in resistivity. Then, the sample was irradiated by a flux of $10^{17}$ per cm$^2$ of 1.4-Mev electrons in such a way that one half of the sample was exposed and the other half was shielded with enough aluminum to stop the electrons. Bremsstrahlung was produced when the electrons were stopped so that the unirradiated part of the slice received part of the high-energy gamma rays. Some damage was produced in this portion of the silicon, since there was an increase in resistivity there. The resistivity increase in the irradiated region was found to be nonuniform. The reasons for these resistivity fluctuations are discussed. The effects of carrier removal are considered. (J.F.P.)

**2189** RELATIONSHIP OF WAVELENGTH OF TRANSFER SYSTEM TO QUENCHING OF RADIOISOTOPES IN DYES. Jaffee, Max; Ford, Leonard A. (Food and Drug Administration, Washington, D. C.). Trans. Amer. Nucl. Soc., 8: 318-19(Nov. 1965).

**2190** PULSED NUCLEAR IRRADIATION EFFECTS ON ELECTRONIC PARTS. Hendershott, D. (General Electric Co., Philadelphia). Trans. Amer. Nucl. Soc., 8: 371-2(Nov. 1965).

**2191** CRYOGENIC IRRADIATION OF RESISTANCE TEMPERATURE TRANSDUCERS FOR NERVA. Greenhow, W. A.; Schenz, R. F.; Gilchrist, Ed (Aerojet-General Nucleonics, San Ramon, Calif.). Trans. Amer. Nucl. Soc., 8: 372-3(Nov. 1965).

# ISOTOPE TECHNOLOGY

## General

*Refer also to abstracts 1786 and 2520.*

**2192** (BLG-68-11) CONDITIONS DE TRAVAIL ET DE SECURITE DANS LES LABORATOIRES DU DEPARTEMENT DES RADIOISOTOPES A MOL. (Working Conditions and Safety in Laboratories of the Department of Radioisotopes at Mol). Constant, R.; Mekers, J. (Centre d'Etude de l'Energie Nucleaire, Brussels (Belgium)). Mar. 1965. 17p. Dep. mn.

The new installations for the production and distribution of radioisotopes at Mol are described. (tr-auth)

**2193** A MULTIPURPOSE $^{60}$Co GAMMA IRRADIATION FACILITY. Linden, D. B.; Teas, H. J. (Puerto Rico Nuclear Center, Mayaguez). Int. J. Appl. Radiat. Isotop., 16: 661-5(Nov. 1965).

A multipurpose $^{60}$Co $\gamma$-irradiation facility was developed for use in biological, chemical, and solid-state physics research. The facility uses water as a shield so that direct visual observations of the source and mechanisms involved in irradiation procedures can be made. The source can be arranged in several geometries providing a dose-rate range of 3500 to 1,500,000 R/hr and providing a field up to 18 in. in dia. Temperature control as well as control of the gaseous environment of the sample during irradiation is possible with different sample holders. Materials that were irradiated include: seeds, bacterial cultures, small animals, maize tassels, bananas, chick embryos, insects, organic crystals, chemical solutions, and vegetative cuttings of plants. (auth)

**2194** BULK-GRAIN-IRRADIATOR DESIGN. Reiback, Earl; Morton, Maxwell R. (Vitro Lab., West Orange, N. J.). Trans. Amer. Nucl. Soc., 8: 323-4(Nov. 1965).

**2195** CALORIMETRIC CALIBRATIONS OF HIGH-SPECIFIC-ACTIVITY GAMMA SOURCES. Rothbart, Michael A.; Galanter, Leonard; Rizzo, Francis X.; Muller, Albert C. (Brookhaven National Lab., Upton, N. Y.). Trans. Amer. Nucl. Soc., 8: 580-1(Nov. 1965).

## Industrial Applications

**2196** (AD-614910) COMPILATION OF A BIBLIOGRAPHY ON THE WHOLESOMENESS OF IRRADIATED FOODS. Reber, Elwood F.; Raheja, Krishan; Davis, Dorothy (Massachusetts Univ., Amherst. Dept. of Food and Nutrition). 1964. Contract DA49 193MD2571. 25p. CFSTI $1.00 cy, $0.50 mn.

Approximately 200 references are given to journals and reports published from 1955 through 1964. The references are arranged according to subject. (P.C.H.)

**2197** POSSIBILITY OF USING RADIATIONS IN THE PRESERVATION OF WINE. Paunovic, R. (Faculty of Agronomy, Belgrade). Ann. Technol. Agr., 12: 143-53 (1963). (In French).

Experimental data pertinent to the use of ionizing radiation to pasteurize wine are reviewed. During the preservation of wines irradiated with doses below the lethal dose, the number of yeast cells is reduced to a certain level. According to the radiation dose and the conditions of preservation, yeast growth can be reinstituted. Lethal doses for wine yeasts vary between 1 and 1.2 Mrad. For spores, lethal doses are even greater than for vegetative forms. The possibility of reducing lethal doses by combining the radiation treatment with low or high temperatures is considered. In addition, ionizing radiations alter some essential components of wine such as an increase in the aldehyde content, a reduction of the quantity of sulfur dioxide, and marked changes in anthocyanins, flavones, cinnamic acids, and tannins. Gaseous products are formed ($H_2$, CO, and $CH_4$) as well as many identified or unidentified volatile or nonvolatile compounds. It is likely that $H_2$ affects the variation of rH in irradiated wines to a great extent. Irradiation alters the organoleptic properties of wine; the lowest doses can improve them, while lethal doses often have the opposite effect. Before this process can be used, more experiments are needed, especially from the point of view of an increase of yeast sensitivity to radiation, improvement in irradiation technology, as well as in research on the innocuousness of irradiated wines. (TCO)

**2198** ECONOMIC EFFICIENCY OF NUCLEAR RADIATION IN PRODUCTION AND PROCESSING OF AGRICULTURAL PRODUCTS. Prokof'ev, N. S. At. Energ. (USSR), 19: 282-6(Sept. 1965). (In Russian).

A graph-analysis method of determining the economic efficiency of gamma isotope devices intended for use in the production and processing of agricultural products is described. The efficiency and expediency of the use of ionizing radiation in agriculture is shown for concrete examples, and recommendations are given for the optimal parameters of the devices for production goals. (tr-auth)

**2199** SAFETY OF IRRADIATED FOODSTUFFS. Food Cosmetics Toxicol., 2: 71-2(Apr. 1964).

The importance of toxicologic studies of food preserved by ionizing radiation is emphasized, and recent reports of feeding experiments with irradiated food are assessed. In one recent study, canned chicken stew, $\gamma$ irradiated with doses of 2.79 and 5.58 Mrad and cabbage subjected to 0.279 and 0.558 Mrad were fed to weanling rats and their second and third generations for periods up to 2 yr. When activities of several enzymes were assayed as indices of toxicity changes in duodenal enzymatic activity of young rats were elicited by foodstuffs exposed to the highest dosage of irradiation. Thus elevated levels of esterase and peptidase were associated with depressed levels of alkaline phosphatase and monoamine oxidase. Young males proved more resistant than females to these changes. In another chronic toxicity study, three successive generations of rats, raised for periods up to 2 yr on diets containing peaches irradiated with 0, 2.79 or 5.58 Mrad and supplemented with a mixture of vitamins, were entirely normal. In the case of irradiated beef, a decreased content of methionine was reported. Irradiated beef caused a hemorrhagic diathesis (tendency to spontaneous hemorrhage), possibly due to deficiency of methionine. Thus, although added methionine appeared to be effective in preventing the occurrence of hemorrhages in the adult and weanling groups, excessive dietary methionine elicited reductions in the growth of rats fed irradiated beef. No such effects were observed in the groups fed nonirradiated beef. Methionine is capable of restoring pyrothrombin rates of animals in the irradiated-beef group to normal in a linear dose-response relation. The higher incidence of hemorrhagic diathesis in animals receiving irradiated beef emphasizes the need to undertake toxicological investigations on each foodstuff subjected to irradiation before assurances of the safety of the foodstuff can be given. (BBB)

**2200** A SIMPLE RADIOISOTOPE VISCOMETER. Auslaender, J. S.; Fuia, H. N. (Polytechnical Inst., Bucharest). Int. J. Appl. Radiat. Isotop., 16: 667-8(Nov. 1965).

A radioisotope device used for measuring the viscosity of liquids is described, which uses the rate of fall of a ball containing $^{60}$Co. Measurements were made on silicon oil using an 8 mm dia steel ball containing 0.68 mC $^{60}$Co, a sample container of 10 cm effective length, a G-M counter and a scaler. The accuracy obtained from a single run with six to nine estimates of the velocity was 1 to 2%, while the average of the four runs gave an accuracy of 0.7%. The velocity measured in a glass vessel was 0.1186 ± 0.0005

cm/sec. Only one detector is used in the method described. (F.J.H.)

**2201** RADIOTRACER STUDIES OF INDUSTRIAL PROCESSES AND WASTE DISCHARGES. Erwall, L. G.; Ljunggren, K.; Mattsson, H. (Isotope Tech. Lab., Sweden). Trans. Amer. Nucl. Soc., 8: 314(Nov. 1965).

**2202** $^{82}$Br TAGGED BROMOBENZENE AS AN INDUSTRIAL TRACER. Braier, H. A.; Mott, W. E. (Gulf Research and Development Co., Pittsburgh). Trans. Amer. Nucl. Soc., 8: 314-15(Nov. 1965).

**2203** THE PRESERVATION OF IRRADIATED MEAT. Moll, A. Voeding, 24: 802-3(Dec. 15, 1963). (In Dutch).

Samples of beef, pork, veal, lamb, and two types of poultry were irradiated and preserved for 1, 4, 9, or 16 months. One portion of each type was cooked before irradiation; it was then preserved at 22°C; the others were irradiated raw and maintained at 22°C or 5°C. The samples were then tested for flavor by a panel. After a period of 6 months, cooked fat meats had a bad taste, whether the sample was preserved at 22°C or at −3°C. For raw-irradiated meat preserved at 22°C, the flavor deteriorated so rapidly that after 9 months it was completely inedible; this was particularly the case with beef. The raw meat which was irradiated was much less preservable and much less flavorful than the previously cooked sample; this was particularly true for samples preserved over longer periods of time. Deterioration of appearance was also marked for uncooked samples. (BBB)

# Power Application

## *See also* ENGINEERING — Space Propulsion

*Refer also to abstract 3548.*

**2204** (GA-6695) SNAP-15A-RADIOISOTOPE THERMOELECTRIC GENERATOR. Campana, R. J. (General Atomic, San Diego, Calif. John Jay Hopkins Lab. for Pure and Applied Science). Oct. 1, 1965. Contract AT(04-3)-167. 19p. (CONF-651001-4). Dep. mn; CFSTI $1.00 cy, $0.50 mn.

From IEEE Nuclear Science Symposium, San Francisco.

The design and development of the SNAP-15A thermoelectric generator are described. The performance of the 15A is compared with semiconductor and metal thermocouples. Test results to date, a safety and hazards evaluation, and a description of uses and applications are included. (M.O.W.)

**2205** (MND-3169-52) SNAP-19 SUPPORT STRUCTURE DESIGN DEVELOPMENT AND QUALIFICATION TESTS. Britton, W. R. (Martin Co., Baltimore, Md. Nuclear Div.). Jan. 1965. Contract AT(30-1)-3169. 62p. Dep. mn; CFSTI $3.00 cy, $0.75 mn.

The development tests conducted on the SNAP 19 Support Structure Assembly are described. Included are descriptions of test procedures, test results, and comparison with the dynamic analysis. Tests were performed on two full-scale support structures with dummy generators simulating the weight and centers of gravity of operational thermoelectric generators. (auth)

**2206** $^{147}$Pm BETAVOLTAIC ELECTRICAL POWER SOURCES. Sundermann, D. N.; (Battelle Memorial Inst., Columbus, Ohio). Trans. Amer. Nucl. Soc., 8: 318(Nov. 1965).

**2207** AERO HEATING RESULTS FROM THE RFD-2 FLIGHT TEST. Clark, A. J. Jr. (Sandia Corp., Albuquerque, N. Mex.). Trans. Amer. Nucl. Soc., 8: 545(Nov. 1965).

# Separation and Production

## *See also* CHEMISTRY — Separation Processes and Procedures

*Refer also to abstract 3542.*

**2208** (NP-15575) CATALOGUE OF RADIOISOTOPES, RADIOACTIVE PREPARATIONS, SPECIAL PURPOSE SOURCES, SERVICE IRRADIATIONS [AND] SPECIAL SERVICES. Overseas Edition, March, 1965. (Australian Atomic Energy Commission, Coogee). 114p. Dep. mn; Australian AEC Free.

Descriptions are given of radioisotopes that are presently being produced by the Australian Atomic Energy Commission in its high flux reactor HIFAR. Information is included on: $^{60}$Co; medical preparations; radiography sources; specifications and prices of unprocessed and processed radioisotopes; ordering procedure for radioisotopes; packaging and transport of radioisotopes; and neutron and gamma irradiation service. (P.C.H.)

**2209** (SGAE-PH-26/1965) A NUMERICAL METHOD FOR THE CALCULATION OF IMAGE ABERRATIONS OF INHOMOGENEOUS MAGNETIC SECTOR FIELDS BETWEEN CONICAL POLE FACES. Ruedenauer, F.; Viehboeck, F. P. (Vienna Univ. (Austria). Institut fuer Physikalische Chemie; Oesterreichische Studiengesellschaft fuer Atomenergie G.m.b.H., Seibersdorf. Physik-Institut). [1965]. 24p. Dep. mn.

Owing to their increased dispersion, mass separators with inhomogeneous magnetic sector fields may be useful for production of highly enriched isotopes. As suggested by Boerboom, Tasman et al., the required inhomogeneity may be acquired by conically shaped pole faces. A numerical method is described which allows a three-dimensional ray-tracing through inhomogeneous magnetic sector fields. For several cases (among them the case of stigmatic focussing of the second order) the curve of direction focussing as well as the image shape along this curve are calculated. (auth)

**2210** A PROPOSED PROCESS FOR PRODUCING LARGE QUANTITIES OF $^{237}$Np AND $^{238}$Pu IN COMMERCIAL POWER REACTORS. Ranshoff, J. A. (Neutron Products Inc., Washington, D. C.); DeFelice, Joseph A. Trans. Amer. Nucl. Soc., 8: 334(Nov. 1965).

**2211** SEPARATION OF CURIE QUANTITIES OF $^{90}$Y FROM $^{90}$Sr BY AN ELUTION PROCESS. Orr, P. B. (Oak Ridge National Lab., Tenn.). Trans. Amer. Nucl. Soc., 8: 334-5(Nov. 1965).

**2212** CYCLOTRON ISOTOPE PRODUCTION AND OTHER SERVICE IRRADIATIONS. Beaver, J. E.; Holley, W. L. (Oak Ridge National Lab., Tenn.). Trans. Amer. Nucl. Soc., 8: 335-6(Nov. 1965).

# MATHEMATICS AND COMPUTERS

*Refer also to abstract 1620.*

**2213** (BNL-9609) THE ROLE OF COMPUTERS IN PROCESSING SCANNING DATA. Robertson, James S. (Brookhaven National Lab., Upton, N. Y.). [nd]. Contract AT(30-2)-Gen-16. 6p. (CONF-650544-2). Dep. mn; CFSTI $1.00 cy, $0.50 mn.

From Symposium on Fundamental Problems in Scanning, Chicago.

The basic operational processes of computers are discussed. (T.F.H.)

**2214** (KAPL-M-6483) CURFIT. CURVE FITTING PROGRAM. Warrington, James A. (Knolls Atomic Power Lab., Schenectady, N. Y.). July 15, 1965. Contract W-31-109-eng-52. 35p. Dep. mn; CFSTI $2.00 cy, $0.50 mn.

CURFIT is a package program, which contains a variety of functions that can be fit to a given set of data points. There are at present five fits available: polynomial; exponential; cosine; series of cubics; and Fourier series. This collection is sufficient for most everyday applications. Input preparation is easy, owing to use of a comma loader. The program is written in FORTRAN-IV and is currently running on the Philco 2000-212. (auth)

**2215** NUCLEAR POWER APPLICATIONS AND HILBERT-SCHMIDT APPLICATIONS IN THE BANACH SPACES. Saphar, Pierre; Julia, Gaston. Compt. Rend., 261: 867-70(July 1965). (In French).

Ruston and Grothendieck have shown that the classical theory of Fredholm for integral equations can be developed in a natural manner to the level of Banach spaces in the framework of nuclear applications or trace applications. Smithies has also constructed a generalized Fredholm theory for the Hilbert-Schmidt applications of a Hilbert space within itself. In the present study an attempt is made to carry these applications further. (tr-auth)

**2216** BRANCHING RULES AND CLEBSCH-GORDAN SERIES OF SEMI-SIMPLE LIE ALGEBRAS. Straumann, N. (CERN, Geneva). Helv. Phys. Acta, 38: 481-98(Aug. 1965).

Explicit formulas (branching rules) are derived for the decomposition of an irreducible representation of a semi-simple Lie algebra L relative to semi-simple subalgebras L′. These formulas are valid for a large class of subalgebras L′. As a special case, an explicit formula for the Clebsch-Gordan series of semi-simple Lie algebras is obtained. (auth)

**2217** PREDICTION ANALYSIS OF THE EXPONENTIAL FUNCTION. Wolberg, J. R. (Israel Inst. of Tech., Haifa). Trans. Amer. Nucl. Soc., 8: 587(Nov. 1965).

**2218** DATA PROCESSING. Kane, J. V. (Bell Telephone Labs., Murray Hill, N. J.). pp 453-510 of Nuclear Structure and Electromagnetic Interactions. New York, Plenum Press, 1965.

Lectures are presented on data processing in the form of six references; viz., a stored, program computer as a multiparameter radiation analyzer; a two-dimensional pulse height analyzer; interface for an SDS 910 general purpose computer; a nuclear radiation recorder analyzer; the design of experiments using compiler language computer programs; and data simulation with an on-line computer as a diagnostic and analytical tool. (L.B.S.)

# METALS, CERAMICS, AND OTHER MATERIALS

## General

*Refer also to abstracts 3320, 3452, 3497, 3555, 3556, and 3647.*

**2219** (AMRA-CR-64-05/4) RESEARCH INVESTIGATION OF PHASE-REINFORCED HIGH TEMPERATURE ALLOYS PRODUCED DIRECTLY FROM THE MELT. Final Report. Lemkey, F. D.; Bayles, B. J.; Salkind, M. J. (United Aircraft Corp., East Hartford, Conn. Research Labs.). July 31, 1965. Contract DA-19-020-AMC-00434(X). 94p. (UACRL-D910261-4). CFSTI $3.00 cy, $0.50 mn.

An investigation was performed to produce high-temperature, high-strength, whisker-reinforced alloys directly from the melt. The technique of unidirectional solidification was applied to the $Ni_3B$–Ni, Ni–NiBe, Ti–TiB, and Ta–$Ta_2C$ eutectic systems. Composites were produced of aligned Ni lamellae in a $N_3B$ matrix, NiBe lamellae in a N solid solution matrix, and aligned $Ta_2C$ whiskers (29% by volume) in a Ta matrix. An attempt to produce a composite of TiB whiskers in Ti by unidirectionally solidifying the Ti–B eutectic led to the discovery that this system is an anomalous eutectic. The TiB was found to grow in a random manner. Tensile tests showed that whisker reinforcement was successfully achieved in the Ta–$Ta_2C$ system. Room temperature fracture strengths in excess of 150,000 psi were measured on Ta–$Ta_2C$ eutectic specimens in the direction of the aligned $Ta_2C$ phase. The experimentally determined ultimate strength was predicted by the rule of mixtures modified for discontinuous fibers. The fracture mechanism was found to be cleavage of $Ta_2C$ whiskers followed by plastic flow of the matrix. Preliminary elevated temperature tests indicate a rapid decrease in fracture strength with increasing temperature. It was concluded from the decreasing number of fractured carbide whiskers with increasing temperature and from the absence of whisker pullout that the whisker aspect ratio and the shear strength of the matrix are the limiting factors for effective load transfer. (auth)

**2220** (ANL–7059) PREPARATION OF METALS BY MAGNESIUM–ZINC REDUCTION. PART III. REDUCTION OF PLUTONIUM DIOXIDE. Knighton, J. B.; Steunenberg, R. K. (Argonne National Lab., Ill.). June 1965. Contract W-31-109-eng-38. 12p. Dep. mn; CFSTI $1.00 cy, $0.50 mn.

Plutonium metal was prepared on a laboratory scale by the direct reduction of plutonium dioxide with liquid magnesium–zinc alloy in the presence of fluxes composed of alkali and alkaline earth halides. The reduction rate of plutonium dioxide, unlike those of uranium and thorium oxides, was relatively independent of the flux composition. The most satisfactory reductions at 800°C were obtained with a magnesium concentration of about 10 wt % in the liquid-metal phase. A 30-gram ingot of metallic plutonium was produced by vacuum distillation of magnesium and zinc from the liquid-metal product solutions. The use of plutonium dioxide instead of fluorides as the starting material has the advantage of a greatly decreased neutron-emission hazard resulting from ($\alpha$,n) reactions. Plutonium losses arising from incomplete reduction in this process were less than 1%. (auth)

**2221** (ANL–7082, pp 62-73) NUCLEAR SAFETY. (Argonne National Lab., Ill.).

Development of a hodoscope for monitoring fuel during meltdown experiments is reported. Research on effects of a standard approximation in calculation of fuel-temperature distributions is also reported along with fuel pin thermal-stress calculations. Operation of TREAT is summarized, and development of the large TREAT loop is discussed. Information is included on reactions of stainless steel-clad and Zircaloy-2-clad fuels with steam. (J.R.D.)

**2222** (EURAEC–1390) PREPARATION OF ZIRCONIUM ALLOYS AND U–Mo ALLOYS. Special Report No. 18. Sari, C. (Centre d'Etude de l'Energie Nucleaire, Mol (Belgium); Societe Belge pour l'Industrie Nucleaire, Brussels). [1960]. Contract 27-60-7 RDB. 66p. (EUR–2349; BN–6408-2). Dep. mn; CFSTI $3.00 cy, $0.75 mn.

Work Performed under United States–Euratom Joint Research and Development Program.

Powders of zirconium, Zircaloy-2, zirconium–10 to 15% niobium, and uranium–10 to 12% molybdenum were produced either by the hydride route or by a direct comminution of selected turnings. For the reduction of the hydride, a fluidized bed process was developed. The results of a study on the hydriding kinetics of some zirconium and uranium alloys are also given. (auth)

**2223** (GEMP–51A) HIGH-TEMPERATURE MATERIALS PROGRAM. Progress Report No. 51, Part A. (General Electric Co., Cincinnati, Ohio. Nuclear Materials and Propulsion Operation). Sept. 30, 1965. Contract AT (40-1)-2847. 59p. Dep. mn; CFSTI $3.00 cy, $0.75 mn.

Laboratory testing of Fe–Cr–Al–Y-fueled specimens exceeded 9500 hours at 950°C, and 7000 hours at 1100°C in air with virtually no U (<0.02%) detected on the cladding surface. Analysis of the fueled 2541-clad Fe–$UO_2$ specimen from in-pile test LTFC-1, which operated for 1007 hours at 1100°C, revealed no structural damage from irradiation. The diametric growth ranged from 0.2 to 0.7%. Weight gain data for a series of Fe–Cr–Al–Y alloys were obtained at 900 and 1100°C in static air for 9000 hrs. The lowest oxidation rates are shown by 2541 alloys containing 0.3 to 0.5% Y. Creep-rupture tests of arc-cast W at 2000 and 2200°C (62 and 67% of the absolute melting temperature, respectively) indicate a transition in the creep mechanism within this temperature range. Specimens annealed at 2400°C and tested at 2000°C are more creep resistant and have a greater rupture life than specimens annealed at 2000°C and tested at 2000°C. The reverse is shown for specimens tested at 2200°C. Multi-temperature creep tests of arc-cast W at constant stress (load) yield an apparent activation energy for creep of 160 kcal/mole. This is in reasonably good agreement with the quoted value of 140 kcal/mole for self-diffusion. Creep-rupture tests of W–25Re–30Mo (at. %) were performed at 1600 and 2200°C. The results indicate a possible material structural change at 2200°C and 0.352 kg/mm$^2$ (low stress). This was not indicated for the other test conditions. Along with the familiar Andrade and parabolic creep equations, two additional equation forms were found to yield excellent results in first-stage creep evaluations. Special least-squares computer programs were written to enable all the equation constants to be calculated. Refinements in the radial heat flow technique, which has been used in the past for measuring the thermal conductivity of ceramic materials, have recently allowed measurements to be made for high conductivity materials. Data for Mo were obtained from 900 to 2000°C and are in excellent agreement with previously published data for Mo. This apparatus also proved useful in measuring the electrical resistivity of refractory metals from room temperature to 2300°C. The thermoelectric properties of Cr–20 Os and Mo–10Ru–10 Os were measured as a function of temperature; Cr–20 Os was found to be a good negative thermoelement material. The resistivity of BeO was shown to be much higher than that of $ThO_2$; its activation energy, however, is less than that of $ThO_2$, suggesting that impurities control its resistivity. Studies of the effect of Re content of less than 25% in the W–Re–Mo system showed that the alloys containing 10 and 12.5% Re could not be processed using the techniques established for W–25Re–30Mo or the alloys containing 19, 21, 23, or 27% Re with 30Mo content. Other alloys containing varying amounts of Re with Mo contents of 10 and 20% were par-

tially processed. Mo–W–Re alloys with high Mo contents were prepared and hot-rolled into sheet. Alloys containing 20, 25, and 30% Re were readily processed, but difficulty was encountered with alloys containing 5, 10, or 15% Re and 15 or 30% W. Room-temperature bend tests were conducted on hot-rolled sheet (20 to 30% Re) that was heated for 10 hours at 2000°C in $H_2$ before bending. These alloys showed a high degree of ductility. Sheet and tubing were also made from W–3Re and W–5Re alloys. Welds on sheet stock made from these binary systems were strong and non-porous. Additions of 1, 2, or 5% Re to Mo reduced voids and porosities in the welds. Special purification techniques to remove $O_2$, $N_2$, and C impurities in unalloyed and alloyed Mo result in an increase in ductility and an improvement in weldability. (W.L.G.)

**2224** (GEMP–52A) HIGH-TEMPERATURE MATERIALS PROGRAM PROGRESS REPORT NO. 52, PART A. (General Electric Co., Cincinnati, Ohio. Nuclear Materials and Propulsion Operation). Oct. 20, 1965. Contract AT(40-1)-2847. 51p. Dep. mn; CFSTI $3.00 cy, $0.50 mn.

Separate abstracts were prepared for the 7 sections of the report. (W.L.G.)

*For abstracts of individual sections see: 2257, 2320–2322, and 2422–2424.*

**2225** (IS-T-40) THE PREPARATION OF VANADIUM METAL BY THE ALUMINUM REDUCTION OF VANADIUM PENTOXIDE [Thesis]. Krupp, William Edward (Ames Lab., Iowa State Univ. of Science and Tech.). Feb. 1965. Contract W-7405-eng-82. 65p. Dep. mn; CFSTI $3.00 cy, $0.75 mn.

A process is described for preparing high purity vanadium metal in kilogram quantities. Vanadium pentoxide is bomb-reduced with aluminum metal in the presence of iodine, which acts as a thermal booster. The resulting vanadium–aluminum alloy is consolidated by arc casting and purified by electron beam melting. Vanadium metal containing a level of impurities equivalent to that obtained by the crystal-bar iodide process was consistently produced in yields of 80%. Use of this metal to replace the crystal-bar refining step resulted in a considerable cost reduction. (auth)

**2226** (RT/CHI(65)–30) PREPARATION OF URANIUM DIOXIDE AND CARBIDE PARTICLES BY SOL-GEL METHODS. Cogliati, G.; Lanz, R.; Mezi, E. (Comitato Nazionale per l'Energia Nucleare, Rome (Italy)). Sept. 1965. 9p. Dep. mn.

A process for the preparation of spherical uranium carbide or oxide particles was developed. This process consists of the following phases: preparation of a colloidal uranium (IV) solution; dispersion of the colloidal solution in an organic solvent immiscible in water and gelation of the particles by extraction of nitric acid; and drying and thermal treatment of the gel particles. (auth)

**2227** MEASUREMENT OF THE MICROSCOPIC DISTRIBUTION OF OXYGEN AND CARBON IN METALS BY $^3$He ACTIVATION. Holm, Dale M. (Los Alamos Scientific Lab., N. Mex.). Trans. Amer. Nucl. Soc., 8: 327-8(Nov. 1965).

**2228** HIGH-TEMPERATURE COMPATIBILITY TESTING OF MOLTEN PLUTONIUM FUEL-CONTAINER SYSTEMS. Andelin, R. L. (Los Alamos Scientific Lab., N. Mex.). Trans. Amer. Nucl. Soc., 8: 346-7(Nov. 1965).

**2229** COMPATIBILITY OF COMMERCIAL CLADDING ALLOYS WITH IMPROVED METALLIC FAST REACTOR FUELS. Walter, C. M.; Lahti, J. A.; Kelman, L. R. (Argonne National Lab., Ill.). Trans. Amer. Nucl. Soc., 8: 348-9(Nov. 1965).

**2230** THORIUM–URANIUM–PLUTONIUM ALLOYS AS POTENTIAL FAST POWER BREEDER FUELS. Blumenthal, B. (Argonne National Lab., Ill.). Trans. Amer. Nucl. Soc., 8: 349-50(Nov. 1965).

**2231** FUEL-ELEMENT PERFORMANCE IN PRESSURIZED WATER REACTORS. Allio, R. J. (Westinghouse Electric Co., Pittsburgh). Trans. Amer. Nucl. Soc., 8: 359(Nov. 1965).

**2232** RECENT DATA ON THE PERFORMANCE OF DEFECTED LOW-DENSITY POWDER $UO_2$ FUELS IN REACTOR SERVICE. Arlt, W. H.; Duncan, R. N.; Pashos, T. J.; Mathay, P. W. (General Electric Co., San Jose, Calif.). Trans. Amer. Nucl. Soc., 8: 365(Nov. 1965).

**2233** HIGH-TEMPERATURE STUDIES OF URANIA IN A THERMAL GRADIENT. Fryxell, R. E.; Aitken, E. A. (General Electric Co., Cincinnati). Trans. Amer. Nucl. Soc., 8: 381-2(Nov. 1965).

**2234** EFFECTIVE AXIAL AND RADIAL THERMAL EXPANSION OF $UO_2$ WITH A RADIAL THERMAL GRADIENT. Asamoto, R. R.; Perry, K. J.; Zebroski, E. L. (General Electric Co., San Jose, Calif.). Trans. Amer. Nucl. Soc., 8: 383(Nov. 1965).

**2235** MATHEMATICAL MODEL FOR PREDICTING COATED-PARTICLE BEHAVIOR. Prados, J. W.; Scott, J. L. (Oak Ridge National Lab., Tenn.). Trans. Amer. Nucl. Soc., 8: 387-8(Nov. 1965).

**2236** COMPATIBILITY OF REFRACTORY METALS WITH BOILING ALKALI METALS. DeVan, J. H.; DiStefano, J. R.; Jansen, D. H. (Oak Ridge National Lab., Tenn.). Trans. Amer. Nucl. Soc., 8: 390-1(Nov. 1965).

**2237** DETERMINATION OF THE SOLUBILITY OF SEVERAL TRANSITION METALS IN MOLTEN POTASSIUM. Ginell, W. S.; Teitel, R. J. (Douglas Aircraft Co., Inc., Santa Monica, Calif.). Trans. Amer. Nucl. Soc., 8: 393-4 (Nov. 1965).

**2238** COMPATIBILITY OF SOME REFRACTORY ALLOYS IN FLOWING NONISOTHERMAL LITHIUM. DeVan, J. H.; Sessions, C. E. (Oak Ridge National Lab., Tenn.). Trans. Amer. Nucl. Soc., 8: 394-5(Nov. 1965).

**2239** CARBON AND NITROGEN TRANSFER IN A TYPE-316 STAINLESS-STEEL Cb–1% Zr, LIQUID-POTASSIUM SYSTEM. Goldmann, K.; Hyman, N.; Kostman, S.; McKee, J. (United Nuclear Corp., White Plains, N. Y.). Trans. Amer. Nucl. Soc., 8: 396(Nov. 1965).

**2240** SCREENING TESTS OF TURBINE NOZZLE AND BLADE MATERIALS. Cunningham, C. W.; DeVan, J. H.; Fuller, L. E.; Jansen, D. H.; MacPherson, R. E. (Oak Ridge National Lab., Tenn.). Trans. Amer. Nucl. Soc., 8: 401(Nov. 1965).

**2241** TANTALUM BASE ALLOYS FOR ALKALI METAL CONTAINMENT. Ammon, R. L.; Buckman, R. W. Jr.; Begley, T. (Westinghouse Astronuclear Lab., Pittsburgh). Trans. Amer. Nucl. Soc., 8: 401-2(Nov. 1965).

**2242** MATERIALS DEVELOPMENT FOR SLIDING-CONTACT APPLICATIONS IN 1000 deg F POTASSIUM SPACE POWER SYSTEMS. Allen, C. M. (Battelle Memorial Inst., Columbus, Ohio); Basham, S. J.; Morris, John L. Trans. Amer. Nucl. Soc., 8: 403(Nov. 1965).

**2243** ON CAVITATION DAMAGE IN LIQUID-METAL PUMPS. Thiruvengadam, A.; Preiser, H. S. (Hydronautics, Inc., Laurel, Md.). Trans. Amer. Nucl. Soc., 8: 405(Nov. 1965).

**2244** THE EFFECT OF CARBON-CONTAMINATED SODIUM ON AUSTENITIC STAINLESS STEEL. Hetzler, F. J.; Lauritzen, T. A. (General Electric Co., San Jose, Calif.). Trans. Amer. Nucl. Soc., 8: 413(Nov. 1965).

**2245** DESIGN EVALUATION OF A FUSED-SALT MOLTEN-METAL EXTRACTOR. Felt, R. E.; Burkhart, L. E. (Iowa State Univ., Ames, Iowa). Trans. Amer. Nucl. Soc., 8: 593-4(Nov. 1965).

**2246** INERT-ATMOSPHERE ENCLOSURE FOR ENVIRONMENTAL TESTING. Ludlow, J. O.; Coleman, L. F.; Malecha, R. F.; Schraidt, J. H.; Slawecki, M. A. (Argonne National Lab., Ill.). Trans. Amer. Nucl. Soc., 8: 627-8(Nov. 1965).

**2247** OPERATING EXPERIENCE WITH THE KAPL-RADIOACTIVE MATERIALS LABORATORY METALLOGRAPHY FACILITY. Wemple, B. D.; Jackson III, D. C.; LaRocque, D. D. (General Electric Co., Schenectady, N. Y.). Trans. Amer. Nucl. Soc., 8: 628-9(Nov. 1965)

**2248** WATERPROOF NUCLEAR RADIATION SCREENING SUBSTANCE. Baumgartner, Kurt; Strahle, Erwin. British Patent 1,004,248. Sept. 15, 1965. Priority date Mar. 13, 1962, Germany.

A bitumen-bound asphalt composition in the form of blocks or sheets can be used for screening against $\alpha$, $\beta$, and $\gamma$ radiation and neutrons. The composition includes up to 98% of at least one heavy-atom substance such as barium sulfate, lead oxide, thorium oxide, or bismuth oxide. The composition is made by dispersing the heavy-atom substance in melted, solvent-liquefied, or emulsified bitumen. It can be used for floor, ceiling, or wall coverings, to form containers for radioactive wastes, or to solidify radioactive wastes by binding with the solid substance. (A.G.W.)

**2249** IMPROVEMENTS RELATING TO THE MANUFACTURE OF GRAPHITE. Jenkins, Mansell John (to United Kingdom Atomic Energy Authority). British Patent 1,004,904. Sept. 15, 1965. Filed July 9, 1962.

A method for preparing coke particles for the production of an isotropic form of polycrystalline graphite is patented. A mass of a solid cokable substance is heated under an inert atmosphere maintained at a sufficiently high pressure to preserve the solid phase of the mass and to control the rate of liberation of the volatile products. The residual mass is comminuted to yield roughly spherical or equiaxial particles. The particles may be further shaped by abrasion following a calcination step. (A.G.W.)

**2250** IMPROVEMENTS IN OR RELATING TO REFRACTORY URANIUM COMPOUNDS. Accary, Andre; Dubuisson, Jacques; Rousset, Pierre (to Commissariat a l'Energie Atomique). British Patent 1,005,393. Sept. 22, 1965. Priority date Dec. 31, 1960, France.

In a process for preparation of powders of refractory uranium compounds, a metal-ceramic composition is formed by sintering the uranium compound and uranium metal together. The composition is then treated with an agent that causes disintegration of the composition and separation of the desired compound in powder form. The disintegrating agent may be hydrogen in the case of uranium carbide, hydrochloric acid in the case of uranium nitride, and either hydrogen or hydrochloric acid in the case of uranium silicide. Preferably the composition is subjected to a grain-refining heat treatment prior to disintegration. (A.G.W.)

**2251** PLASMA-JET-GUN. Kugler, Tibor; Vesely, Vladimir. U. S. Patent 3,206,587. Sept. 14, 1965. Filed Feb. 13, 1963.

A plasma–jet–gun is provided for depositing coatings from high-melting materials. The gun includes a housing having a channel for stabilizing the trunk of an electric arc and passageway means for introducing plasma generating gas into the channel. An interior metallic electrode faces the inner end of the channel, and an exterior electrode is adjacent to the outer end of the channel for establishing the electric arc in the channel. The electrodes are mounted for rotation about an axis parallel to the axis of the channel, and drive means is provided for rotating the electrodes. A cooling liquid is circulated through passageway means for cooling the housing and the electrodes. (B.L.M.)

**2252** METHOD OF DISSOLVING CERAMICS CONTAINING BERYLLIA. Vondra, Benedict L. Jr. (to Nuclear Materials and Equipment Corp.). U. S. Patent 3,208,816. Sept. 28, 1965. Filed Dec. 8, 1961.

A method of dissolving a chemically highly stable ceramic comprised of BeO and at least one of the class consisting of $UO_2$, $ZrO_2$, $Al_2O_3$, $ZrB_2$, and $TiB_2$ consists of reducing the ceramic to at least 100 mesh, producing an aqueous slurry of the powder, adding the equivalent of about .01 mole of Hg to the slurry, preheating the slurry to 60°C, and adding a concentrated acid to dissolve the slurry. The acid may be HF, HCl, $HNO_3$, $H_2SO_4$ or mixtures of any of these. Alternatively, silver may be added to catalyze the dissolution rather than Hg. (B.L.M.)

## Corrosion

*Refer also to abstracts 1748, 1804, and 1805.*

**2253** (AECL–2297) NUCLEATION AND GROWTH OF HYDRIDES IN ZIRCONIUM ALLOYS. Roy, C. (Atomic Energy of Canada Ltd., Chalk River (Ontario). Chalk River Nuclear Labs.). Sept. 1965. 28p. Dep.; AECL $1.00.

Studies of the $H_2$(T) distribution in Zr alloys were undertaken by autoradiography. The heating of Zr alloy specimens (which had been hydrided, annealed above the $H_2$ dissolution temperature, and quenched) at temperatures as low as 80°C promoted $H_2$ segregation at grain-boundaries (in Zr and Zircaloy-2) and phase boundaries (in Zr–2.5 wt% Nb). This effect was most obvious in small grained material. In large grained Zr oriented hydrides also developed within the grains, apparently along the slip planes. Thus metallographic mounting techniques should not be used in studying quenched specimens without careful consideration. About 4000 ppm $O_2$ in solid solution in Zircaloy-2 (annealed in the $\alpha + \beta$ region) gives rise to a higher $H_2$ concentration in the $O_2$ stabilized $\alpha$ grains than in the transformed $\beta$ grains, when hydriding was carried out at a lower temperature (650°C). Plastic deformation may enhance hydride nucleation by increasing the dislocation density. This effect was suggested by observations of slight $H_2$ concentration in cold-worked, as opposed to recrystallized, regions in Zr; hydride precipitation along slip bands in strained and annealed Zr specimens; and along slip planes in thermally cycled Zr and Zircaloy-2. (auth)

**2254** (BM–RI–6680) STRESS CORROSION CRACKING OF VANADIUM, MOLYBDENUM, AND A TITANIUM–VANADIUM ALLOY. Carter, J. P.; Kenahan, C. B.; Schlain, David (Bureau of Mines, College Park, Md. College Park Metallurgy Research Center). Mar. 1965. 18p. Bureau of Mines Free.

Vanadium, molybdenum, and a titanium–10% vanadium alloy were evaluated for their susceptibility to stress corrosion cracking in a number of corrodents. Tests were conducted utilizing conventional U-bend techniques with subsequent evaluation in a pneumatic constant-load apparatus. Vanadium and molybdenum were generally resistant to stress corrosion cracking in the media studied. U-bend specimens of vanadium showed evidence of stress corrosion cracking in 6 N hydrochloric and 18 N sulfuric acids; however, tensile stress specimens exposed to these solutions did not exhibit stress cracking. Similar results were obtained when U-bend specimens of molybdenum were immersed in 10% formic acid. Titanium–10% vanadium alloy was susceptible to stress corrosion cracking in 2.85 N hydrochloric acid solution. Heat treating the alloy greatly reduced its corrosion rate and its susceptibility to stress corrosion cracking in this medium. (auth)

**2255** (EURAEC–1323) FURTHER DEVELOPMENT OF THE ZIRCONIUM ALLOY $ZrNb_3Sn_1$ FOR USE AS CLADDING MATERIAL IN WATER-COOLED NUCLEAR REACTORS. Quarterly Report No. 5, October 1–December 31, 1964. Ruckdeschel, W. (Metallgesellschaft A. G., Frankfurt am Main (West Germany)). Mar. 24, 1965. Contract 019-63-11 TEED. 20p. (EUR–2305). Dep. mn; CFSTI $1.00 cy, $0.50 mn.

Work Performed Under United States–Euratom Joint Research and Development Program.

The comparative corrosion tests on ten Zr–3Nb–1Sn alloys with Fe, Cr, V, and Sb additions in steam at 400 and 450°C were concluded. Short-time tensile tests were performed on corroded samples at room temperature. In addition, the $H_2$ pick-up was determined by analysis. The

2000 hour corrosion test produced high weight increases and $H_2$ contents. Simultaneously, both the tensile strength and the elongation decreased substantially in all the alloys. At both corrosion temperatures, reduction of the Sn content improved the corrosion behavior but decreased the strength. The ternary alloys containing Sb, Fe, and Cr showed the lowest $H_2$ pick-up at both temperatures. (auth)

**2256** (EURAEC–1449) QUARTERLY REPORT NO. 3, APRIL–JUNE 1965. (Compagnie des Ateliers et Forges de la Loire, Paris (France). Department des Recherches). Contract 033-64-9 TEE F (RD). 29p. (EUR–2383). Dep. mn; CFSTI $2.00 cy, $0.50 mn.

Work Performed under United States–Euratom Joint Research and Development Program.

The effects of test temperature on the mechanical properties of four austenitic and four austeno-ferritic stainless steels were measured. Two silicon austeno-ferritic steels, Uranus 50 Si and Uranus ST Si, exhibited superior yield strengths and breaking stresses without a decrease in elongation. Austenitic steels, Uranus SD and ICN 164 BC, cracked under stress in a boiling 42% $MgCl_2$ solution. Uranus S austenitic and Uranus ST, Uranus ST Si, and Uranus 50 austeno-ferritic stainless steel remained uncracked after 1000 hours. All austenitic stainless steels cracked under stress in a chlorinated solution at 150°C with an initial pH of 8. The austeno-ferritic steels remained uncracked after 1000 hrs in chlorinated solutions at 150°C with an initial pH of 8 and 9. (W.L.G.)

**2257** (GEMP–52A, pp 47-52) PHYSICO-CHEMICAL STUDIES OF CLAD $UO_2$ IN POTENTIAL MELTDOWN ENVIRONMENTS. (General Electric Co., Cincinnati, Ohio. Nuclear Materials and Propulsion Operation).

Testing of 0.38-mm-thick Zircaloy-4 sheet specimens in steam with the specimen heated at approximately 0.3°C per second shows the specimen breaks at about 1300°C because of embrittlement and subsequent mechanical failure. Oxidation consumed about 0.13 mm of the metal from each side. Isothermal corrosion of Zircaloy-4 in steam plus air atmosphere shows an accelerated corrosion rate when the air is introduced into the steam. Zircaloy-4 in contact with $UO_2$ at 1900°C shows substantial reaction after 5 minutes at temperature. (auth)

**2258** (MSAR–65-149) EFFECT OF HIGH TEMPERATURE SODIUM ON AUSTENITIC AND FERRITIC STEELS. Quarterly Progress Report, July–September 1965. (MSA Research Corp., Callery, Pa.). Oct. 22, 1965. Contract AT(11-1)-765. 29p. Dep. mn; CFSTI $2.00 cy, $0.50 mn.

Slight changes in mechanical properties were noted for type 316 stainless steel specimens exposed for 4000 hrs and tested in 1200°F He. An increase in rupture life and a corresponding decrease in ductility was observed for type 316 stainless steel exposed for 4000 hrs to 1200°F high-carbon Na and tested in 1200°F He. Specimens exposed for 4000 hrs to 1200°F high-oxygen Na exhibited a slight decrease in rupture life. Tests on $2\frac{1}{4}$ Cr–1 Mo steel specimens exposed for 4000 hrs to 1100°F He indicate a reduction in the creep-rupture life due to thermal aging. (W.L.G.)

**2259** (SC-DC–65-1789) DENDRITIC EROSION IN DIELECTRICS. Work, Richard N. (Sandia Corp., Albuquerque, N. Mex.). Oct. 1965. Contract AT(29-1)-789. 8p. (CONF-651028–1). Dep. mn; CFSTI $1.00 cy, $0.50 mn.

From Conference on Electrical Insulation, Buck Hill Falls, Pa.

A possible mechanism for dendritic erosion in dielectrics is considered, and its relation to the characteristics of growth is discussed qualitatively. The model described draws heavily from the theory of breakdown in gases, and uses the many points of similarity between the growth of discharges in solids and in gases. (P.C.H.)

**2260** (SC-DR–65-519) ION PLATED COATINGS FOR THE CORROSION PROTECTION OF URANIUM. Bland, R. D.; McDonald, J. E.; Mattox, D. M. (Sandia Corp.; Albuquerque, N. Mex.). Oct. 1965. Contract AT(29-1)-789. 26p. Dep. mn; CFSTI $2.00 cy, $0.50 mn.

The feasibility of using the ion plating process to coat depleted uranium with a protective coating of aluminum was demonstrated. It is found that coatings of less than $5 \times 10^{-4}$ inches in thickness provide good corrosion protection for the uranium when exposed to a condensing water vapor atmosphere at 95°C for up to 96 hours. Comparison is made between various techniques of surface preparation and various deposition parameters. Vacuum evaporated coatings are found to be totally inadequate for corrosion protection. Some suggestions for future investigations are presented. (auth)

**2261** (UCRI–326) PRINCIPLES GOVERNING THE BEHAVIOR OF SOLID MATERIALS IN SEVERE HIGH TEMPERATURE ENVIRONMENTS. Quarterly Progress Report, July 1–September 30, 1965. Walsh, Patrick N. (Union Carbide Research Inst., Tarrytown, N. Y.). Sept. 30, 1965. Contract DA-01-021-AMC-11926(Z). 64p.

The reaction of $O_2$ with W was studied in the induction-heated stagnation-flow reactor at $O_2$ pressures between 2 and 12 torr. At each pressure, the reaction rate increases with temperature with an apparent activation energy near 22 kcal below 2900°K; about 2900–3000°K a maximum in reaction rate is observed, and above 3000°K the rate decreases with further temperature increase. The data agree exactly with previous measurements elsewhere and agree reasonably well with extrapolations of the kinetic model deduced from previous mass-spectrometric studies in this laboratory. The effect of $H_2$ on the oxidation of W by $H_2O$ was investigated in the same apparatus over a wide range of $H_2/H_2O$ ratios. The presence of $H_2$ decreases the reaction rate, but has little effect on the activation energy. The oxidation of pyrolytic, ZTA, and ZTE graphites was investigated in the arc-image stagnation-flow reactor. For all three the reaction rate increases with temperature at the lowest temperatures, maximizes between 1850 and 2100°K depending on the graphite, then decreases with further temperature increase; around 2600-2700°K, the rate again begins to increase with temperature for pyrolytic and ZTE graphite. The vaporization rates of the three graphites were measured under conditions simulating the oxidation studies; the vaporization rates are in good agreement with those calculated from tabulated C vapor pressures. The reactivity of Ta in flowing HF was high and independent of temperature above 2000°K; it is apparently diffusion-limited. TiC, ZrC, HfC, NbC, and TaC, on the other hand, were quite resistant to corrosion by HF at 2500°K but showed strong temperature dependences of reactivity. Oxygen and hydrogen atoms were the principal products observed at high temperatures in a mass-spectrometric study of the $H_2O$–W reaction. At equal incident oxygen-mass flux rates, the rates of production of O atoms from the reactions of $O_2$ and $H_2O$ were identical from 1870 to 2640°K; the rates of production of $WO_2$ were also identical at high temperatures, but at 1634°K $O_2$ was five times as effective in producing $WO_2$; $O_2$ produced $WO_3$ more efficiently than did $H_2O$ over the whole temperature range investigated. A W nozzle insert fitted with three probe-type thermocouples was successfully test-fired at the Army Missile Command. Temperature measurements were uncertain because one of the thermocouples lost contact with the insert. An unsymmetrical erosion was obtained because the injector plate holes became partially plugged during the firing. TaC cylinders, up to 1.2" diameter, were isostatically pressed to about 65% of theoretical density. Heating in $H_2$ for two hours at 2300°C raised the density to 73–75% of theoretical and effectively removed the Co sintering aid. Over 95% of the pores of such a skeleton were then infiltrated at 1425°C with Ag–10 wt % Cu alloy. OFHC Cu infiltrated other TaC samples much more reproducibly than did other forms of Cu. Incompletely infiltrated skeletons could be further loaded by a second heating with OFHC Cu; reheating also appeared to improve the homogeneity of the composites. A Cu–2 wt % Be alloy infiltrated TaC very erratically, possibly because of its relatively high impurity content. Hot-

pressed TaC and NbC bars with densities near 90% of theoretical were nearly 100% filled by Ag–10 wt % Cu alloy; this alloy was generally superior to Cu as an infiltrant. (auth)

**2262** (WCAP-2056(Pt.6)) HIGH TEMPERATURE SUPERCRITICAL PRESSURE WATER LOOP—CORROSION TESTS. (Westinghouse Electric Corp., Pittsburgh, Pa. Atomic Power Div.). Aug. 1965. Contract AT(30-1)-2948. 157p. Dep. mn; CFSTI $5.00 cy, $1.00 mn.

The description and results of two extended corrosion out-of-pile loop tests in a supercritical pressure and temperature, oxygenated water environment, using Westinghouse 16-20 stainless alloy thin cladding under high heat flux are given. In one of the tests, chlorides were added to the water. Corrosion data from these tests on 16 Cr-20 Ni stainless alloy with heat fluxes of ~300,000 Btu/hr ft$^2$, resulting in a cladding temperature up to 1200°F (at clean metal), indicate that corrosion is a problem in supercritical fluid containing some (2 to 10 ppM) oxygen. (auth)

**2263** THE EFFECT OF YTTRIUM ON THE HIGH TEMPERATURE OXIDATION RESISTANCE OF SOME Fe-Cr BASE ALLOYS IN CARBON DIOXIDE. Francis, J. M.; Whitlow, W. H. (Central Electricity Generating Board, Berkeley, Eng.). Corrosion Sci., 5: 701-10(Oct. 1965).

The effect of a 1% Y alloying addition on the oxidation resistance of Fe–25% Cr and Fe–25% Cr–5% Al alloys was examined in $CO_2$ at 1000°C. Thermogravimetric measurements were made over the exposure range 0–100 h, together with a structural evaluation of the oxide films formed. Internal oxidation of both alloys takes place under these conditions, and the presence of small amounts of the resultant $Y_2O_3$ phase in the metal/oxide interface can contribute to the improved adhesion of the surface oxide. This was shown to be essentially independent of either cation or anion transport in the protective oxide layer. The appearance of an internal oxide precipitate is coincident with the depletion of the second phase ($YFe_3$) particles that are dispersed in the grain boundaries throughout the matrix alloy. The only general conclusions that can be drawn from the weight gain/time data for the alloys are that the improvement in the initial oxidation resistance attained by the addition of Y to the Fe–25% Cr alloy is similar to that of a 5% Al addition, and that addition of Y to the Fe–Cr–Al alloy causes no improvement in the isothermal oxidation behavior but does improve the compactness and adhesion of the oxide scale. (auth)

**2264** MATERIAL RESISTANCE TO MERCURY CORROSION. Nejedlik, J. F.; Vargo, E. J. (Thompson Ramo Wooldridge Inc., Cleveland). Electrochem. Technol., 3: 250-8(Sept.-Oct. 1965).

Material resistance to mercury corrosion was determined in glass reflux type capsules at 900°F. The materials studied included unalloyed metals and iron, nickel, and cobalt alloys. The resistance defined as weight loss per unit area of pure metals to mercury attack showed a periodic variation with atomic number, and the resistance was clearly correlated with the periodic variation of solute solubility in liquid metal. Several major effects of alloying on the corrosion rate of iron, cobalt, and nickel alloys were noted. Base metals possessing good corrosion resistance suffered a decrease in resistance with increasing alloying element content. Conversely, an improvement results from the addition of alloying elements for those base metals possessing poor resistance. Nickel additions were generally detrimental. Chromium additions up to 14% by weight in BCC alloys were generally not deleterious. (auth)

**2265** CORROSION OF STEELS AND TANTALUM BY MOLTEN CADMIUM-MAGNESIUM-ZINC SYSTEMS. Kyle, Martin L.; Nelson, Paul A.; Burris, Leslie Jr. (Argonne National Lab., Ill.). Electrochem. Technol., 3: 258-62 (Sept.-Oct. 1965).

Corrosion of 1020 carbon steel, types 405, and 304 stainless steel, and tantalum by the cadmium-magnesium-zinc ternary system was investigated at temperatures of 500, 750, and 850°C. Carbon steel (1020) and type 405 stainless steel exhibited excellent corrosion resistance to cadmium-magnesium alloys at temperatures up to 750°C. Corrosion rates of these materials increased with increasing concentrations of zinc in the ternary alloy. Type 304 stainless steel was severely corroded due to nickel leaching by the solvents. Except at high zinc concentrations (>95 wt%), tantalum exhibited good corrosion resistance at temperatures up to 850°C. The effect of stress on the corrosion behavior was not investigated experimentally, but other evidence including practical experience indicated that this was not a significant factor for the conditions of this investigation. (auth)

**2266** CORROSION OF REFRACTORY METALS BY ZINC–MAGNESIUM–URANIUM AND HALIDE SALT SYSTEMS. Nelson, P. A.; Kyle, M. L.; Bennett, G. A.; Burris, L. Jr. (Argonne National Lab., Ill.). Electrochem. Technol., 3: 263-9(Sept.-Oct. 1965).

Corrosion tests at temperatures up to 1000°C were conducted to determine the resistance of tantalum, molybdenum, tungsten, and some alloys of these metals to zinc and zinc-rich solutions containing magnesium and uranium, both in the absence and presence of molten chloride salts. Tungsten, while showing the best corrosion resistance, was subject to slight intergranular attack at 1000°C. The alloy Mo-30% W was deemed to be useful for certain applications although the alloy suffered molybdenum leaching at 800°C. Tantalum and molybdenum were severely attacked and Ta-10% W failed by stress-induced liquid metal embrittlement. (auth)

**2267** THE EFFECT OF OXYGEN ON THE PRECIPITATION OF HYDROGEN FROM ZIRCONIUM. Hardie, D. (Univ. of Newcastle-upon-Tyne, Eng.). J. Nucl. Mater., 17: 88-90(Aug.-Sept. 1965).

The effect of oxygen on the uptake and terminal solubility of hydrogen by zirconium was studied. A sample of zirconium containing 185 ppm hydrogen was oxidized for 72 hr at 800°C. It was then cut into three pieces, which were heated for 30 min at 540, 640, and 825°C, respectively and then air-cooled. They were then heated for 30 min at 300°C and furnace-cooled to allow slow precipitation of hydride. All three specimens were polished and etched in a 50% mixture of nitric and acetic acid to which several drops of hydrofluoric acid were added in order to reveal the hydride distribution. The structures were essentially the same except that they were spread over a greater distance in the specimen that was heat-treated at 825°C. The essential characteristics were a dark oxide layer, a brittle layer with a high oxygen concentration and no visible hydride precipitate, another layer with some oxygen and some hydrogen content, and the inner core of coarse intergranular hydride. (F.J.H.)

**2268** THE RELATIVE AGGRESSIVENESS OF Li, Na, K, Rb AND Cs BOILING AND CONDENSING IN Nb–1Zr CAPSULES. Romano, A. J.; Fleitman, A. H.; Klamut, C. J. (Brookhaven National Lab., Upton, N. Y.). Trans. Amer. Nucl. Soc., 8: 391(Nov. 1965).

**2269** CORROSION STUDIES OF TUNGSTEN, MOLYBDENUM AND RHENIUM IN LITHIUM. De Mastry, John A. (Battelle Memorial Inst., Columbus, Ohio). Trans. Amer. Nucl. Soc., 8: 391-2(Nov. 1965).

**2270** ALKALI-METAL CORROSION STUDIES ON MATERIALS FOR ADVANCED SPACE POWER SYSTEMS. Harrison, Robert W. (General Electric Co., Cincinnati). Trans. Amer. Nucl. Soc., 8: 392-3(Nov. 1965).

**2271** ALKALI METAL. REFRACTORY ALLOY COMPONENT AND COMPATIBILITY EVALUATION TESTS. Hoffman, E. E.; Holowach, J. (General Electric Co., Cincinnati). Trans. Amer. Nucl. Soc., 8: 396-8(Nov. 1965).

**2272** DESIGN AND OPERATION OF AN ALKALI METAL. REFRACTORY ALLOY CORROSION TEST FACILITY. Holowach, J.; Hoffman, E. E. (General Electric Co., Cincinnati). Trans. Amer. Nucl. Soc., 8: 398-400(Nov. 1965).

**2273** CORROSION STUDIES IN THE NaK 78 TYPE-316 STAINLESS-STEEL Cb 1 percent Zr-ALLOY SYSTEM. Lloyd, D. B.; Taboada, A. (Oak Ridge National Lab., Tenn.). Trans. Amer. Nucl. Soc., 8: 406(Nov. 1965).

**2274** PARTIALLY SELECTIVE CORROSION OF TYPE-316 STAINLESS STEEL IN HIGH-TEMPERATURE SODIUM. Brush, E. G. (General Electric Co., Pleasanton, Calif.). Trans. Amer. Nucl. Soc., 8: 412-13(Nov. 1965).

**2275** STATIC AND DYNAMIC CORROSION BY TIN, BISMUTH AND BISMUTH–SODIUM ALLOY UP TO 1000 deg C. Shimotake, H.; Hesson, J. C. (Argonne National Lab., Ill.). Trans. Amer. Nucl. Soc., 8: 413-15(Nov. 1965).

**2276** A ZIRCONIUM ALLOY. (to Siemens-Schuckertwerke Aktiengesellschaft). British Patent 1,004,205. Sept. 15, 1965. Priority date Sept. 29, 1962, Germany.

A Zr alloy having good corrosion resistance in steam at 400–500°C contains 0.005–1% Y and at least 0.05% of one or more of the elements Nb, Sn, Cu, Fe, Cr, Ni, Mo, W, V, Ta, and Pd, each up to 5%, the balance being Zr. The alloy is suitable for use as a fuel can or structural material in a nuclear reactor. (A.G.W.)

**2277** IMPROVEMENTS IN BERYLLIUM–MAGNESIUM ALLOYS. Caillat, Roger; Darras, Raymond; Leclercq, Daniel; Salesse, Marc; Vachet, Pierre (to Commissariat a l'Energie Atomique). British Patent 1,004,547. Sept. 15, 1965. Priority date Mar. 14, 1963, France.

A Be alloy containing 0.1–0.5% by weight of Mg has high oxidation resistance in either dry or moist pressurized $CO_2$ gas at 650–750°C. In addition, a low neutron-capture cross section and good resistance to deformation make the alloy particularly suitable for use in nuclear reactors cooled by $CO_2$ gas. (A.G.W.)

## Fabrication

*Refer also to abstracts 2350, 2354, 3509, and 3510.*

**2278** (BMI–1746) HOT ISOSTATIC COMPACTION OF GRAPHITE. Carmichael, Donald C.; Ownby, P. Darrell; Hodge, Edwin S. (Battelle Memorial Inst., Columbus, Ohio). Oct. 5, 1965. Contract W-7405-eng-92. 37p. Dep. mn; CFSTI $1.00 cy, $0.50 mn.

The effects of temperature, pressure, and graphite starting material on the density, isotropy, and strength of dense graphite material prepared by hot isostatic compaction of graphite powders were examined. Process equipment was developed to permit operation at temperatures up to 2700°C under a 1600-atom isostatic pressure of inert gas. The isotropy of graphite compacts was determined by neutron diffraction. Relatively isotropic, high-purity graphites were produced having modest isotropic tensile strength and extremely high density (up to 2.24 g per $cm^3$, or 99% of theoretical). (auth)

**2279** (CEA-R-2828) ETUDE DE L'OXYDATION DES POUDRES D'URANIUM A BASSE TEMPERATURE ET SON APPLICATION AU FRITTAGE DE POUDRES D'URANIUM OXYDE [These]. (Study of the Low Temperature Oxidation of Uranium Powders and Its Application to the Sintering of Uranium Oxide Powders [Thesis]). Conte-Albert, Madeleine (Commissariat a l'Energie Atomique, Saclay (France). Centre d'Etudes Nucleaires). 1965. 87p. Dep. mn.

Submitted to Paris Univ. (France).

The uranium oxygen reaction was studied with a view to obtaining U–$UO_2$ samples containing about 20% by weight of $UO_2$ starting from spherical grain uranium powder ($36\ \mu < \phi < 50\ \mu$). The techniques used were micrography, thermogravimetry, sintering under pressure, and radiocrystallography. At 170°C in air or argon + oxygen mixtures, the uranium oxide formed was always $UO_2$ and was uniformly distributed around the initial uranium spheres. These mixed powders can easily be sintered under pressure in the $\gamma$-phase. The density of the samples obtained was 85 to 90% of the theoretical density. The influence of $UO_2$ on the properties of uranium was found by the use of dilatometry and thermal cycling in the $\alpha$ phase. The temperatures at which the phase changes $\alpha \rightleftharpoons \beta$ and $\beta \rightleftharpoons \gamma$ occurred were lowered, the remanent expansion was decreased. High density samples resisted thermal cycling; the characteristic defects of uranium, high distortion and wrinkled surface, almost disappeared. Heat treatments in a secondary vacuum at 1050°C caused crystallization of $UO_2$ in a geometrical form and the appearance of a phase of the fcc crystalline type having the composition $U_WC_XO_YN_Z$. This phase caused a new decrease in the $\alpha \rightleftharpoons \beta$, $\beta \rightleftharpoons \gamma$ transformation temperatures for the uranium. After ten dilatometric cycles the remanent expansion of the sample was about 0.5%. The resistance to thermal cycling of a low density sample that was heat-treated was similar to that of a high density sample that had not undergone a heat treatment. (auth)

**2280** (DP–989) URANIUM DIOXIDE FUEL TUBES FOR IRRADIATION IN THE VBWR. Ferrara, Anthony S. (Du Pont de Nemours (E. I.) and Co., Aiken, S. C. Savannah River Lab.). Oct. 1965. Contract AT(07-2)-1. 25p. Dep. mn; CFSTI $1.00 cy, $0.50 mn.

Experimental fuel tubes containing crushed arc-fused uranium dioxide were fabricated for irradiation testing in the Vallecitos Boiling Water Reactor (VBWR). Two of the four tubes delivered were compacted by vibration alone and two were compacted by vibration plus swaging; bulk $UO_2$ densities were 84 and 92% of the theoretical value, respectively. The elements were approximately three feet long, 2.06 inches in outside diameter, and 0.3 inch in wall thickness including 0.030-inch-thick cladding of low-nickel Zircaloy-2. (auth)

**2281** (EURAEC–1408) ELECTRO SLAG WELDING OF REACTOR STEELS. Final Report No. 1. (Schweisstechnische Lehr- und Versuchsanstalt, Duisburg (West Germany)). Feb. 25, 1965. Contract 046-61-3 RDA. 104p. (EUR–2367). Dep. mn; CFSTI $4.00 cy, $0.75 mn.

Work Performed under United States–Euratom Joint Research and Development Program.

A summary of the development of techniques and welding alloys for the electro-slag welding of thick sections of Mn, Cr–Mo, Mn–Mo–Ni–V and ASTM 302B steels for use in reactors is presented. (W.L.G.)

**2282** (HW-SA–3755) THE REMOTE REFABRICATION OF REACTOR FUELS. Shuck, A. B.; Lotts, A. L.; Drumheller, K. (General Electric Co., Richland, Wash. Hanford Atomic Products Operation). [Aug. 27, 1964]. Contract AT(45-1)-1350. 140p. Dep. mn; CFSTI $4.00 cy, $1.00 cy.

The purposes, problems, and principles of remote fabrication of reactor fuels are outlined, along with remote fabrication and remote inspection, rejuvenation, and repair of PRTR fuels at Hanford. The processing and fabrication of intermediate radiation level Th–$^{233}$U fuel is also described, along with processing and refabrication of EBR-II fuel. Plans for the fabrication of target elements for the High Flux Isotope Reactor are discussed. (P.C.H.)

**2283** (KAPL–3110) ELECTRON-BEAM TUBE-TO-TUBESHEET WELDING. Murphy, H. J. (Knolls Atomic Power Lab., Schenectady, N. Y.). Aug. 9, 1965. Contract W-31-109-eng-52. 33p. Dep. mn; CFSTI $2.00 cy, $0.50 mn.

Electron-beam welding was investigated for application to the welding of Ni–Cr–Fe Alloy 600 tube-to-tubesheet joints. Equipment of both the low- and high-voltage type was considered. Metallographic and ultrasonic evaluations were performed. The results showed that Alloy 600 tubes can be electron-beam-welded to a weld-metal composition tubesheet without the formation of tube or tubesheet fissures, but the joining of Alloy 600 tubes to an Alloy 600 tubesheet may produce intergranular fissuring of the tubesheet. This effect is particularly pronounced in ghost-grained Alloy 600. Porosity, although inherent in partial-penetration electron-beam welds, was considered innocuous since any porosity >12 mils in diameter can be located by ultrasonic inspection to ensure a minimum leak path. Ul-

trasonic inspection can be performed to measure the depth of joint fusion within ~12 mils as well as to locate porosity >12 mils in effective diameter. The limiting problem in the application of electron-beam welding to tubesheet joints is one of weld nugget-joint alignment. (auth)

**2284** (NP-15093) FABRICATION AND PROPERTIES OF TUNGSTEN SINGLE CRYSTALS. PART I. GROWTH OF SINGLE CRYSTAL TUNGSTEN TO BE USED FOR ROLLING INTO SINGLE CRYSTAL SHEET. Edwards, G. W. (Linde Div., Union Carbide Corp., Indianapolis, Ind.). PART II. ROLLED SINGLE CRYSTAL TUNGSTEN SHEET. Raymond, L. (Aeronutronic Div., Philco Corp., Newport Beach, Calif.). Final Report, March 1, 1964-February 26, 1965. May 14, 1965. 70p.

A method for deforming single crystals of tungsten such that monocrystallinity is maintained throughout the deformation process was developed. Items of hardware that retain their single crystal character can be fabricated. An item of hardware, which is also a single crystal, is desirable in certain applications for two reasons. The recrystallization phenomenon with its associated brittleness is absent. Thus, the single crystal will remain ductile even if heated to the melting point. Because of the single crystallinity of material, it can be welded by a state-of-the-art technique and maintain its single crystallinity even in the weld bead. Thus, recrystallization and brittleness associated with weldments are also avoided. The method for cold deformation of tungsten single crystals requires extreme care in its present state of development. The starting single crystal boules from which billets are fabricated must be of high purity and of low dislocation concentration and lineage. In order to maintain monocrystallinity, single or duplex slip must be employed. Therefore, careful orientation of the starting billet is necessary in order that the desired slip system alone be active. For deformation by rolling, the billet orientations (110)[001] or (100)[011] are necessary to encourage duplex slip. Other orientations allow multiple slip and do not yield single crystals. Furthermore, deformation of less than 10% per pass is necessary. If deformations of more than 10% are produced, multiple slip will occur even on properly oriented billets. Periodically, the surface of the billet must be chemically polished so that multiple slip caused by friction between the billet surface and the rolls is removed. If this surface is not removed, then subsequent recovery heat treatment will cause recrystallization of this highly strained area. (W.L.G.)

**2285** DISSOLUTION AND PRECIPITATION OF URANIUM CARBIDES. Giraud-Heraud, Francois (Laboratoires de la Societe Industrielle de Combustible Nucleaire, Veurey, France). Compt. Rend., 261: 1308-11 (Aug. 2, 1965). (In French).

The carbides formed during the casting of U and its alloys are redissolved by heating to high temperature. After a rapid cooling from the liquid state or from L + UC region, they reappear in the form of dendrites or of fine precipitants oriented with respect to the solid solution. (tr-auth)

**2286** CAPILLARY PHENOMENA IN THE DENSIFICATION PROCESS DURING SINTERING IN THE PRESENCE OF THE LIQUID PHASE. Naidich, Yu. V.; Lavrinenko, I. A.; Eremenko, V. N. (Inst. of Materials Problems, Academy of Science, Ukrainian SSR). Int. J. Powder Met., 1: 41-8(Apr. 1965).

The effects of wetting and capillary phenomena on the kinetics of sintering in the presence of a liquid phase are discussed from a fundamental as well as from a practical point of view. Examples are given for the E–Cu and W–Ag systems. Equations were developed that correlate the forces between the particles with the angle of contact between the solid and the liquid components. An optimum amount of the liquid phase was determined for maximum shrinkage of the composite material during sintering. (auth)

**2287** THE EFFECT OF PARTICLE SIZE ON SINTERING KINETICS IN ALUMINA POWDER. Kothari, N. C. (Univ. of Queensland, Brisbane). J. Nucl. Mater., 17: 43-53(Aug.-Sept. 1965).

Sintering studies on $\alpha$-alumina powder were conducted to determine the influence of particle size (0.08 to 0.1, 0.2 to 0.3, and 0.8 to 1.0 $\mu$m) and sintering atmosphere on the rate of sintering in the temperature range from 200 to 1600°C. The shrinkage initiation temperature did not depend on the particle size of the powder and sintering atmosphere. It was found that the apparent diffusion coefficient increases with decreases in particle size. The results obtained indicated that bulk diffusion is the principal mechanism of material transport. The temperature dependence of the rate of sintering was characterized by an activation energy of 133 ± 5 kcal/mole. (auth)

**2288** THE SYNTHESIS OF SPHERICAL NUCLEAR FUELS IN A 4000 deg KELVIN PLASMA. Gibson, James O. (Vitro Lab., West Orange, N. J.). Trans. Amer. Nucl. Soc., 8: 352(Nov. 1965).

**2289** NONREMOTE FABRICATION OF $^{233}U$ FUEL ELEMENTS. Hins, A. G.; Wynveen, R. A.; Pilarski, E. M. (Argonne National Lab., Ill.). Trans. Amer. Nucl. Soc., 8: 352-4(Nov. 1965).

**2290** ZERO-POWER REACTOR-III FUEL FABRICATION. Collett, J. G.; Benson, E. M.; Gerrish, R. W. Jr.; Bruggeman, L. D. (Nuclear Materials and Equipment Corp., Apollo, Pa.). Trans. Amer. Nucl. Soc., 8: 354-5 (Nov. 1965).

**2291** DEVELOPMENT OF $ThO_2$-PELLET FABRICATION. Forscher, F.; Vondra, B. L.; Beltram, C. (Nuclear Materials and Equipment Corp., Apollo, Pa.). Trans. Amer. Nucl. Soc., 8: 355-6(Nov. 1965).

**2292** PREPARATION OF CERAMIC-REFRACTORY METAL SEALS FOR SPACE POWER SYSTEMS. Griesenauer, Neal M.; De Mastry, John A. (Battelle Memorial Inst., Columbus, Ohio). Trans. Amer. Nucl. Soc., 8: 356-7(Nov. 1965).

**2293** BERYLLIUM RADIATOR FABRICATION. Turner, Gary F. (Lockheed Missiles and Space Co., Sunnyvale, Calif.). Trans. Amer. Nucl. Soc., 8: 407-8 (Nov. 1965).

**2294** BRAZED GRAPHITE-METAL COMPOSITES FOR SPACE RADIATORS. DelGrosso, Anthony (Douglas Aircraft Co., Inc., Santa Monica, Calif.). Trans. Amer. Nucl. Soc., 8: 408-9(Nov. 1965).

**2295** A MODEL FOR PREDICTING THE EFFECT OF LOOP GEOMETRY ON THE CORROSION RATE OF MATERIALS IN SODIUM. Mottley, J. D. (Westinghouse Electric Co., Pittsburgh). Trans. Amer. Nucl. Soc., 8: 410-11 (Nov. 1965).

**2296** OBSERVATIONS CONCERNING LOCALIZED CORROSION IN PUMPED SODIUM SYSTEMS. Comprelli, R. A.; Hetzler, F. J.; Young, R. S. (General Electric Co., San Jose, Calif.). Trans. Amer. Nucl. Soc., 8: 411-12 (Nov. 1965).

**2297** STARTUP EXPERIENCE WITH THE EBR-II FUEL CYCLE FACILITY. III. FUEL FABRICATION. Feldman, M. J.; Bacca, J. P.; Eschen, V. G.; Mahagin, D. E. (Argonne National Lab., Idaho Falls, Idaho). Trans. Amer. Nucl. Soc., 8: 613-14(Nov. 1965).

**2298** LIVERMORE SLUG FABRICATION FACILITY. Hubbell, W. H.; Coops, M. S. (Univ. of California, Livermore). Trans. Amer. Nucl. Soc., 8: 626(Nov. 1965).

**2299** MODIFICATION OF THE KAPL REMOTE ANNEALING FACILITY. Altamari, L. A. (General Electric Co., Schenectady, N. Y.). Trans. Amer. Nucl. Soc., 8: 626-7(Nov. 1965).

**2300** IMPROVEMENTS IN OR RELATING TO NIOBIUM-COATED URANIUM CARBIDE ARTICLES. Theison, Roger (to European Atomic Energy Community). British Patent 1,005,102. Sept. 22, 1965. Priority date Jan. 24, 1962, Germany.

In a method of coating a uranium carbide article with Nb, the article is subjected to a fine-cleaning step by ion discharge within an evacuated enclosure and then to a Nb-deposition step by electron bombardment with molten Nb metal within the same enclosure. The article may also be coated with an intermediate binding substance such as copper within the enclosure between the above two steps. Apparatus for carrying out the method is described. The Nb-coated article may be sealed into a sintered Al casing to form a reactor fuel element. (A.G.W.)

**2301** RADIATION SHIELDING MATERIAL. Taylor, Roderick; Vassiliou, Basil Emmanuel (to Nuclear Power Plant Co. Ltd. and A.E.I.-John Thompson Nuclear Energy Co. Ltd.). British Patent 1,005,196. Sept. 22, 1965. Filed July 27, 1962.

A process is described for the fabrication of a nuclear radiation shielding material composed of 15 to 85 wt % of a substantially ferrous material chosen from one or more of the following materials, cast iron, steel, iron and alloys of iron with small proportions of Ni, Cr, Si, or Mn and 15 to 85 wt % of carbon. The carbon may be coke, anthracite, carbon black, graphite, petroleum coke, tar, pitch, or SiC. The particle size of the ferrous material is in the range of 20μ to ¼ in., and the grain size of the carbon is in the range of 30 mesh to 20μ. The materials are mixed; the temperature of the mix is raised to 120 to 250°C; the bonding agent is added while mixing is continued; the mixture is formed into blocks of the desired shape by mechanical means; and the blocks are cooled prior to firing in a furnace in a reducing atmosphere at a temperature of 900 to 1500°C. (B.L.M.)

**2302** IMPROVEMENTS IN OR RELATING TO THE MANUFACTURE OF SHAPED BODIES FROM PARTICULATE MATERIAL. (to Armour Research Foundation of Illinois Inst. of Tech.). British Patent 1,005,871. Sept. 29, 1965. Priority date Sept. 23, 1960, United States.

A method of manufacturing solid shaped bodies from particulate material is particularly applicable to manufacture of carbon or graphite bodies. The particulate material is blended with a binder consisting of at least 50% by weight of prepolymerized furfuryl alcohol and from 0 to 50% by weight of pitch, and heat and pressure are applied to the mixture to form the desired shape. The binder is then graphitized and the body is hardened by baking. Thermatomic carbon may be included in the composition to increase the green density and promote higher shrinkage during graphitizing. (A.G.W.)

**2303** A METHOD OF FABRICATION OF FINNED TUBES AND APPARATUS THEREFOR. Portal, Pierre; Trieule, Andre (to Commissariat a l'Energie Atomique). British Patent 1,006,644. Oct. 6, 1965. Priority date May 13, 1963, France.

A method and apparatus are patented for the fabrication of tubes having a smooth internal surface and an external surface provided with fins inclined to the axis of the tube. A tubular workpiece is placed in a die made up of a series of grooved elements each corresponding to an angular sector of the fins required in the finished piece. An expander head is passed through the workpiece so as to force a predetermined thickness of material into the grooves of the die. At the same time the pressure of air enclosed between the fins and the die is limited. (A.G.W.)

**2304** APPARATUS FOR TREATING THE INTERIOR OF A TUBULAR ELEMENT. Thome, Paul; Foulquier, Henri; Malmaison, Rueil; Frehling, Jean (to Commissariat a l'Energie Atomique). U. S. Patent 3,207,408. Sept. 21, 1965. Filed Apr. 5, 1962.

An apparatus is provided for treating the interior of a tubular element, particularly for coupling a second tubular element to the interior of the first element by welding. The apparatus includes a composite elongated body that is introducible within the tubular element and a tool mounted on the end part of the member within the body. Means are provided for remote control and radial displacement of the tool and for turning the assembly formed by at least the internal element of the assembly and the tool about the axis of the tubular element. The body includes a number of concentric members including the internal member carrying the tool and an external tubular member angularly displaceable about the axis. The apparatus is particularly useful for effecting a fluid-tight coupling between pipe elements by internal welding when the ends of the pipes being coupled are inaccessible from the outside. (B.L.M.)

**2305** HIGH-TEMPERATURE NUCLEAR FUEL STRUCTURES AND THEIR PRODUCTION. Benesovsky, Friedrich; Rudy, Erwin (to United Kingdom Atomic Energy Authority). U. S. Patent 3,207,697. Sept. 21, 1965. Filed Mar. 14, 1962.

A high temperature material suitable for use as a reactor fuel is characterized by its high stability and resistance to reduction in a C rich environment and consists essentially of a monocarbide of at least one nuclear fuel metal carbide, (UC) a metal carbide, and carbon. The carbide of the nuclear fuel metal and the metal carbide are present in proportions such that the nuclear fuel metal carbide content of the pseudo binary mixed crystals is 0.5–30 mol %. The metal carbide is selected from the group consisting of ZrC, NbC, and mixtures of the two. The material may also contain from 0.5 to 2 mol % ThC. At least a portion of the C present is in the form of an outer coating overlaying the mixed crystals of the remaining constitutents. (B.L.M.)

**2306** RADIATION SHIELDING COMPOSITION COMPRISING CARBON AND LEAD DISPERSED IN CEMENT. Hall, William C. (to Chemtree Corp.). U. S. Patent 3,207,705. Sept. 21, 1965. Filed Apr. 19, 1962.

A material having good radiation shielding properties consists of from 25–50% comminuted carbon by gross volume, from 25–50% comminuted lead by gross volume, and cement to form a solid structure. The carbon and lead is dispersed evenly throughout the cement, and the material has a density of 1.6 g/cm$^3$, substantially lower than ordinary concrete. (B.L.M.)

## Properties and Structure

*Refer also to abstracts 1822, 2890, and 3493.*

**2307** (AD-613023) REFRACTORY METALS—AN ASSESSMENT. Burte, Harris M.; Cooper, Thomas D.; Elbaum, Jerome K. (Air Force Materials Lab., Wright-Patterson AFB, Ohio). Jan. 1965. 44p. (AFML-TR-64-334). CFSTI $2.00 cy, $0.50 mn.

The refractory metals (Nb, Mo, Ta, and W) and their alloys offer attractive potential as metallic materials for high temperature applications. Their general characteristics (e.g., high melting point, ductile-brittle transition, oxidation characteristics) are discussed in relation to a critical assessment of the feasibility of their use in current and future aerospace applications. Coatings for oxidation protection, fabrication, and joining, are shown to be areas of technology limiting the use of these materials, and therefore requiring further efforts. In spite of the current limitations, the high temperature capability is being utilized and for some future applications, improvements in strength, ductility, and coating characteristics are expected to increase reliability and capability. (auth)

**2308** (AD-614637) INVESTIGATION OF THE FORMABILITY CHARACTERISTICS OF THE POLYPHASE TITANIUM ALLOY Ti-6Al-6V-2Sn-4Zr. Ayvazian, Arthur M.; Colton, Robert M. (Army Materials Research Agency, Watertown Arsenal, Mass.). Mar. 1965. 21p. (AMRA-TR-65-05). CFSTI $1.00 cy, $0.50 mn.

Studies were conducted on a 1000-pound ingot of titanium alloy Ti-6Al-6V-2Sn-4Zr, in order to determine the metal working characteristics. Five actual titanium components were formed from this material by extrusion and press forming. The results indicated that the ease of formability compared favorably with that of the commercial alloy Ti-6Al-6V-2Sn. The mechanical properties of test specimens taken from parts formed from both alloys disclosed that for the alloy Ti-6Al-6V-2Sn-4Zr the tensile strength was substantially higher and ductility and toughness were lower at the same yield strengths. (auth)

**2309** (AD-615024) THE EFFECT OF DEFORMATION AND HEAT TREATMENT ON THE MECHANICAL PROPERTIES OF THE Ti-6Al-6V-2Sn-4Zr-1Fe-1Cu ALLOY. Smoot, Perry R. (Army Materials Research Agency, Watertown, Mass.). Mar. 1965. 20p. (AMRA-TR-65-04). CFSTI $1.00 cy, $0.50 mn.

The effects of deformation and heat treatment variables on the mechanical properties of a promising experimental alloy, Ti-6Al-6V-2Sn-4Zr-1Fe-1Cu, was determined utilizing material from a commercially procured ingot. Forging, solution, and aging temperatures and aging times were varied and the resultant notched and unnotched tensile and impact properties were obtained to establish the highest yield strength obtainable in combination with adequate ductility, as defined by Specification MIL-T-46038. This optimum combination of properties was obtained at a yield strength level of 200 ksi, with an elongation of 9 percent, a reduction of area of 26 percent, and Charpy V-notch impact energy of 6 foot-pounds at −40°F. (auth)

**2310** (AD-618681) EFFECTS OF ALLOYING UPON CERTAIN PROPERTIES OF 55.1 NITINOL. Goldstein, D. M.; Buehler, W. J.; Wiley, R. C. (Naval Ordnance Lab., White Oak, Md.). May 28, 1965. 42p. (NOLTR-64-235). CFSTI $2.00 cy, $0.50 mn.

Ternary alloys of the intermetallic compound TiNi were hot hardness tested. Although hardness can be increased by such alloying, neither the base material nor the alloys offer promise for long time service use above 800°F. Silicon, aluminum, iron, and cobalt were effective room temperature hardeners. A unique interfacial compatibility between TiNi and tungsten bulk metal was discovered. It is believed that this will enable introduction of a new metal-metal composite system of fibrous tungsten in a Nitinol matrix. A rod of such material is shown to be capable of room temperature swaging, suggesting improved methods of working highly refractory metals. Silver-free TiNi brazing alloys for joining tungsten metals are a natural result of such compatibility. (auth)

**2311** (AD-618925) THE USE OF STRAIN SOFTENING TO IMPROVE THE PROPERTIES OF REFRACTORY METALS. Final Report. Ripling, E. J.; Zager, S. (Materials Research Lab., Inc., Richton Park, Ill.). Mar. 1965. Contract NOw64-0247c. 46p. CFSTI $2.00 cy, $0.50 mn.

The strain softening characteristics of a cold rolled mild steel, the cobalt base alloy V-36 and a number of refractory alloys were investigated. It was found that softening by flexing was able to significantly improve the notch bend ductility and smooth tensile ductility of the steel. The ductility of the cobalt base alloy, on the other hand, was not significantly altered by flexing. Although the smooth bend properties of molybdenum and tungsten were not altered beyond the as-received scatter range, flexing produced a significant improvement in the notch bend ductility especially of the 0.5 Ti-Mo alloy. Test results on cold rolled molybdenum sheet also indicated that a stronger product with improved formability could be obtained by substituting cold rolling plus flexing for the present process of warm rolling plus stress relieving. (auth)

**2312** (AD-619197) EVALUATION OF CERIUM OXIDE AS A LASER HOST: GROWTH AND EVALUATION OF $CeO_2$ AND $ThO_2$. Quarterly Report No. 3. Linares, Robert C. (Perkin-Elmer Corp., Norwalk, Conn.). 1965. Contract Nonr466000. 5p. CFSTI $1.00 cy, $0.50 mn.

Investigation of the properties and crystal growth of $ThO_2$ was begun. Work was also continued on attempts to grow large crystals of $CeO_2$ by slow cooling of the flux and by the gradient technique. (auth)

**2313** (AD-619208) RECRYSTALLIZATION VARIABLES OF FLAT ROLLED MOLYBDENUM–COBALT ALLOYS. Schnitzel, R. H.; Taebel, W. A.; Lambert, V. E. (Westinghouse Electric Corp., Bloomfield, N. J.). 1951. Contract NOrd10276. 23p. (NAVORD-3073). CFSTI $1.00 cy, $0.50 mn.

The relation between microstructure and mechanical properties, and the recrystallization variables, temperature, amount of deformation, impurity content, and type of molybdenum powder, were studied for rolled Mo–Co alloys. Temperature and time at temperature were found to be the most important variables. The ½ hour recrystallization temperature, as determined metallographically for Mo-0.15 Co alloy worked 50% was 950°C. The alloy was completely recrystallized at 1100°C. The anneal that gave the most desirable combination of tensile strength and ductility was ½ hour at 1000°C followed by a slow furnace cool. The alloy was 10 to 30% recrystallized by this anneal. Increasing the cobalt content from .01 to .15 percent did not appear to alter the recrystallization range of temperature. (auth)

**2314** (ARL-65-140) SOME STUDIES ON MONOCLINIC ZIRCONIUM DIOXIDE FROM ROOM TEMPERATURE TO 1095 deg C. Lang, S. M.; Franklin, E. W.; Tylutki, N. J. (Owens-Illinois Technical Center, Toledo, Ohio). Apr. 30, 1965. Contract AF33(615)-1258. 29p.

Strain and/or annealing relaxation phenomena were expected to occur in the [111] and [11$\bar{1}$] planes of monoclinic zirconia ($ZrO_2$) in the temperature range up to 1095°C; these could not be detected. However, ambiguities were noted in the [211], [21$\bar{1}$], and [10$\bar{2}$] planes within that temperature range for samples not heat-treated at or above the monoclinic-tetragonal transformation; the [211] anomaly is at least an order of magnitude more pronounced than the others. A number of low angle diffraction maxima for monoclinic $ZrO_2$ were resolved, using both normal film and diffractometer techniques. The detectability of from 0.1 to 0.3 wt.% of zircon ($ZrSiO_4$) in so-called pure zirconia samples indicates that a revision of the $ZrO_2$-$SiO_2$ equilibrium diagram would be appropriate. For monoclinic system lattice constants calculations, an algebraically exact solution method was developed that computes the constants for all possible sets of four indexed reflection maxima. Sample temperature measurement in the high-temperature x-ray diffractometer apparatus was the poorest of the experimental parameters; however, the precision of temperature control and the speed of response of the control system were exceptionally good. (P.C.H.)

**2315** (CONF-650632-3) THE LATERAL STRAIN BEHAVIOR OF GRAPHITE—AN ANISOTROPIC MATERIAL. Digesu, F. J.; Pears, C. D. (Southern Research Inst., Birmingham, Ala.). [1963]. Contract AT(40-1)-2694. 33p. Dep. mn; CFSTI $2.00 cy, $0.50 mn.

From 7th Biennial Conference on Carbon, Cleveland.

Seven elastic constants describe the strain behavior of an anisotropic material such as graphite. These constants define three different ratios of lateral to axial strain (Poisson's ratios), two elastic moduli, and two shear moduli. The elastic relationships permit the calculation of two of the constants from the experimental measurement of the other five. The five constants to be measured require careful selection since only one is completely independent. A discussion of the relationships between the constants plus models for a molded and an extruded graphite are presented. Experimental data for CFZ and ATJ graphite to 5500°F are presented and the experimental values of Poisson's ratio, elastic moduli, and shear moduli are compared to the values calculated from the theoretical relationships. Also, experimental measurements of the tri-directional strains in the plastic range are analyzed. (auth)

**2316** (COO-1198-220) SEMICONDUCTIVITY IN GLASS SYSTEMS $V_2O_3$–$P_2O_5$ AND $V_2O_5$–$P_2O_5$. Roeder, P. J.; Friedberg, A. L. (Illinois Univ., Urbana. Materials Research Lab.). [1963]. Contract AT(11-1)-1198. 21p. Dep. mn; CFSTI $1.00 cy, $0.50 mn.

Glass in the form of small bars was cast from melts in the systems $V_2O_3$–$P_2O_5$ and $V_2O_5$–$P_2O_5$. The glass bars, opaque and of a dark color, represented compositions in the range of 60 to 90 mole % vanadia ($V_2O_3$ or $V_2O_5$). Glasses containing more than 90 mole % vanadia were not successfully fabricated since devitrification and associated rupturing of the small glass bars occurred on cooling these high vanadia melts. For glasses in both systems, the electrical resistivity for glasses extended from $10^5$ to $10^6$ ohm-cm at 25°C to $10^1$ to $10^2$ ohm-cm at

the annealing temperatures of the glasses (200–240°C). Resistivity decreased with increase in vanadia content. Comparing the two systems, resistivity of the $V_2O_3$ glasses was significantly lower for high vanadia content, but the $V_2O_5$ glasses exhibited lower resistivity for low vanadia content. Comparison of a-c and d-c measurements confirmed that conduction was electronic. Resistivity values showed no dependence on oxygen partial pressures present during measurement. (auth)

**2317** (EURAEC–1380) DIFFUSION OF RARE GASES IN SOLIDS. Quarterly Report No. 14, January–March 1965. (Hahn-Meitner-Institut fuer Kernforschung, Berlin (West Germany)). Apr. 1965. Contract 028-64-1 TEE (RD). 21p. (EUR–2343). Dep. mn; CFSTI $1.00 cy, $0.50 mn.

Work Performed Under United States–Euratom Joint Research and Development Program.

Postactivation tests on UC single crystals show that their behavior is marked by an activity burst followed by only slight release; on commencement of heating or at higher temperatures, increasing release results mainly due to sample evaporation. Generally speaking, the same pattern was found for the diffusion of Ar-39 in single crystals of KCl and KBr, i.e., under 470°C at higher activation energy is observed. The following value was found for the high-temperature diffusion range: $D = 9 \times 10^{-4} \exp(-8600/RT)$ for 470–600°C. The diffusion of T in AgLi was markedly inhibited below 350–375°C, as with the K-halides. This trend was confirmed both in isothermal tests and in experiments with continuously rising temperature. A detailed account is given of the analysis of tests involving the measurement of the gas release rate, together with a description of an apparatus for separating carrier-free Ar, Kr and Xe. (auth)

**2318** (GA–5918(Pt.1)) ADVANCED, GRAPHITE-MATRIX, DISPERSION-TYPE FUEL SYSTEMS AND RESEARCH ON GRAPHITE. Quarterly Progress Report for the Period Ending November 14, 1964. Bokros, J. C.; Goeddel, W. V.; Koyama, K.; Lonsdale, H. K.; Price, R. J.; White, J. L.; Zumwalt, L. R. (General Atomic, San Diego, Calif. John Jay Hopkins Lab. for Pure and Applied Science). Dec. 1, 1964. Contract AT(04-3)-167. 59p. Dep. mn; CFSTI $3.00 cy, $0.75 mn.

Examination of pyrolytic-carbon coating deposited from 1900 to 2400°C showed that both isotropic and granular deposits were produced, depending on the methane concentration. Mechanical properties of pyrolytic carbons deposited under various conditions were found to be structure-sensitive. Laminar deposits were found to have the highest strength, and isotropic coatings accommodated the largest elastic strains before fracture. Granular deposits were shown to be inferior in strength to either of the other types and also underwent less elastic strain to fracture than isotropic deposits. Measurement of the mechanical properties of annealed laminar structures, which were deposited at 1400°C under various conditions, showed that laminar deposits anneal quite differently. Low-density, laminar structures were the least annealable, and high-density, laminar structures were the most annealable. In general, the largest changes in properties occurred in structures in which the largest changes in crystallite size and layer spacing occurred. The mode of fracture of pyrolytic carbons deposited under various conditions was also found to be structure-sensitive. Laminar structures fractured perpendicular to the layer planes in the as-deposited condition, and parallel in the annealed condition, while granular structures exhibited interlaminar fractures in individual grains. Thermal conductivity values for various pyrolytic-carbon structures were obtained by thermal diffusivity measurements. The results showed a correlation between thermal conductivity and preferred orientation (e.g., the most highly oriented structures (laminar) had the lowest conductivity). Tracer-level diffusion studies conducted on various pyrolytic-carbon structures using $^{228}Th$ as the diffusive species indicate that the diffusion coefficient is strongly dependent on the structure. Experimental work to determine concentration profiles and diffusion coefficients of metallic fission products in pyrolytic carbon is described. A method for measuring the degree of graphitization taking place in carbonaceous materials during heat treatment and in graphitic materials during irradiation is described. The method measures manometrically the kinetics of oxidation by a hot dichromate solution. The phenomenon of enhanced plasticity in hot-working graphite bodies containing solid ZrC particles appears to be restricted to bodies with low pitch contents; bodies prepared with a 20 wt % pitch matrix show no significant change in hot-working rate, and the properties are not adversely affected, as are those for bodies prepared with 10 wt % pitch matrix. Significant improvements in the properties of hot-worked graphite bodies were obtained by hot-working the carbide-containing bodies under temperatures at which the carbide is liquid. During hot-working, the excess liquid is squeezed from the body, leaving a highly densified matrix with a fine dispersion of carbide particles. Bodies prepared with MoC or ZrC show compressive strengths greater than 20,000 and 9,000 psi in the strong and weak directions, respectively. (W.L.G.)

**2319** (GE-TM–65-6-13) THERMODYNAMIC BEHAVIOR OF HYPOSTOICHIOMETRIC $UO_2$. Aitken, E. A.; Brassfield, H. C.; Fryxell, R. E. (General Electric Co., Cincinnati, Ohio. Nuclear Materials and Propulsion Operation). [1964]. Contract AT(40-1)-2847. 30p. (CONF-650704–34; SM–66-83). Dep. mn; CFSTI $2.00 cy, $0.50 mn.

From IAEA Symposium on Thermodynamics, Vienna.

The ability of the $UO_2$-type structure to accommodate excess oxygen is well-known. Recent evidence has indicated that this structure is stable also in the hypostoichiometric state at high temperatures and low oxygen partial pressures, but its manifestation occurs as a uranium metal precipitate in the oxide after cooling from high temperatures. Further evidence is presented of its existence at high temperatures, and the variation in thermodynamic properties across its homogeneity range is described. Hypostoichiometric $UO_2$ evaporates congruently in a convenient experimental region. For example, during free vaporization in slowly flowing hydrogen (–40°C dew point) at 2400°C the composition evaporates congruently at an O/U of 1.88. If the temperature is decreased or the moisture content increased the congruent O/U ratio increases. The water content of the hydrogen must be at least one percent to maintain uranium dioxide at the stoichiometric value at 2400°C. When $UO_2$ pellets are sealed in Ta cans and heated above 1700°C, the O/U ratio of the pellet changes and reaches an equilibrium value which is governed by the oxygen activity of the atmosphere surrounding the can. $UO_2$ does not react with tantalum but because of the high solubility of oxygen in tantalum, the latter functions as a membrane. Congruent evaporation experiments and use of tantalum containers as membranes provide an experimental means for determining the relationship of the oxygen activity in $UO_2$ as a function of stoichiometry. The partial molar free energy of oxygen, $\bar{G}_{O_2}$, derived from these measurements increases almost linearly on the oxygen deficient side with increasing oxygen to uranium ratio. Near the stoichiometric composition $\bar{G}_{O_2}$ rises steeply. Using these results, together with estimated $\bar{G}_{O_2}$ values on the oxygen excess side obtained from the literature, it is shown that the data at a given temperature are consistent with a statistical model. The model assumes that the stoichiometry is achieved by allowing oxygen ions to be distributed in lattice or interstitial positions. The Frenkel energy for oxygen is 60 kcal/g atom which agrees favorably with previous estimates from oxygen self-diffusion data. The relationship between $\bar{G}_{O_2}$ and the partial pressure of the gaseous oxides, UO and $UO_2$, is discussed and some general comments are made about extending this experimental method to other compounds. (auth)

**2320** (GEMP–52A, pp 23–5) EVALUATIONS OF THE PLASTIC FATIGUE PROPERTIES OF HEAT RESISTANT ALLOYS. (General Electric Co., Cincinnati, Ohio. Nuclear Materials and Propulsion Operation).

Eight low-cycle fatigue specimens of type 304 stainless

steel were tested at 800°C for two separate strain ranges. All specimens were subjected to fully reversed cyclic straining. A list of 14 recently published papers and reports related to the project is included. (W.L.G.)

**2321** (GEMP-52A, pp 43-5) FISSION PRODUCT TRANSPORT PROCESSES IN REFRACTORY-METAL FUEL SYSTEMS. (General Electric Co., Cincinnati, Ohio. Nuclear Materials and Propulsion Operation).

Studies of Kr transport in Ta at elevated temperatures are described. Optimum discharge conditions for simultaneously loading and diffusing measurable levels of $^{85}Kr$ into large-grained tantalum at 1730°C were established. Submicron sectioning work was continued on the W–Mo–Re alloys. (auth)

**2322** (GEMP-52A, pp 53-4) PHYSICO-CHEMICAL STUDIES OF Fe-Cr-Al-CLAD FUEL SYSTEMS. (General Electric Co., Cincinnati, Ohio. Nuclear Materials and Propulsion Operation).

Nine Fe–Cr–Al cladding alloys containing 5 to 25 wt % Cr and 4 to 10 wt % Al were prepared for use in phase studies with U. Fe–15Cr–4 Al-clad capsules with U cores were prepared and are under test at temperatures in the range 600° to 1200°C. (auth)

**2323** (GEMP-314) ON THE MECHANISM OF THE RHENIUM-ALLOYING-EFFECT IN GROUP VI-A METALS. Wukusick, C. S. (General Electric Co., Cincinnati, Ohio. Nuclear Materials and Propulsion Operation). Nov. 20, 1964. Contract AT(40-1)-2847. 19p. Dep. mn; CFSTI $1.00 cy, $0.50 mn.

The mechanism by which Re improves the ductility of Group VI-A metals, Cr, Mo, and W was investigated. Spinodal decomposition is postulated to be the mechanism. The essential feature of the mechanism is the removal of interstitial impurities from solution in the matrix by formation of clusters in a more or less oriented array. Dislocation mobility is improved by the removal of interstitial impurities. Data favorable to the postulation include the solubility–temperature relations, elastic constants of the base metals, crystal structure of the solutes, hardness data, and shape and distribution of equilibrium precipitates in Cr–Ru alloys. (P.C.H.)

**2324** (HW-SA-3765) STRUCTURE OF DEFORMED INTERNALLY OXIDIZED ALLOYS. Brimhall, J. L.; Huggins, R. A. (Stanford Univ., Calif. Dept. of Materials Science). [Nov. 4, 1964]. Contract AT(45-1)-1350. 30p. Dep. mn; CFSTI $2.00 cy, $0.50 mn.

For General Electric Co., Richland, Wash. Hanford Atomic Products Operation.

The structure of deformed internally oxidized alloys of silver containing magnesium and copper containing aluminum were studied by thin film transmission electron microscopy. With low to moderate amounts of strain, the deformation structure in the dispersion-hardened alloys was found to consist of a high density of dislocations arranged in a random distribution or in a very fine, but poorly defined, cell structure, depending on the fineness of the dispersion and amount of deformation. In contrast, both pure copper and silver show relatively large, distinct cell structures. The particular structures in the alloys are believed to result from particles acting as both dislocation sources and deflectors. The lack of a pronounced deformation texture and regions of severe local plastic curvature after heavy deformation can also be traced to the formation of dislocations on many slip systems and a lack of local concentrations of dislocations of predominantly one sign. (auth)

**2325** (HW-SA-3767) INFLUENCE OF A FINELY DISPERSED SECOND PHASE ON RECRYSTALLIZATION. Brimhall, J. L.; Klein, M. J.; Huggins, R. A. (Stanford Univ., Calif. Dept. of Materials Science). [Nov. 5, 1964]. Contract AT(45-1)-1350. 36p. Dep. mn; CFSTI $2.00 cy, $0.50 mn.

For General Electric Co., Richland, Wash. Hanford Atomic Products Operation.

The annealing behavior of internally oxidized alloys of silver containing magnesium and copper containing aluminum was studied by transmission electron microscopy. In agreement with observations on pure materials, annealing of the dispersion-hardened alloys involves the formation of subgrains from the cell structure and the subsequent growth of the subgrains into the matrix. The kinetics of both subgrain formation and growth are extremely slow in the dispersion-containing alloys, compared to pure silver and copper. This retardation could be attributed to the nature of the deformed structure, which does not contain regions of severe plastic curvature. As a result, the formation of mobile interfaces by misorientation accumulation is difficult. Particle interaction with dislocation motion during subgrain formation and direct particle interaction with the migrating subgrain boundaries during growth are discussed. (auth)

**2326** (IFA-FR-39) L'ETUDE DES DIAGRAMMES LIQUIDS ET DES PROPRIETEES THERMODINAMIQUES DES SYSTHEMES $SiO_2-ThO_2$ ET $SiO_2-ThO_2-UO_2$. (Study of Liquidus Diagrams and Thermodynamic Properties of $SiO_2-ThO_2$ and $SiO_2-ThO_2-UO_2$ Systems). Lungu, S. (Institutul de Fizica Atomica, Academis R. P. R., Bucharest (Romania)). 1965. 10p. Dep. mn.

Equilibrium diagrams are presented corresponding to liquidus curves for the systems $SiO_2-ThO_2$ and $SiO_2-ThO_2-UO_2$ in hydrogen atmosphere. The investigations evidenced a non-miscibility range in the binary systems and a zone of non-miscibility in the ternary system which connect the non-miscibility ranges of the binary systems for $SiO_2-ThO_2$ and $SiO_2-UO_2$. The study of the free energy curve in $SiO_2-ThO_2$ system relatively to pure liquidus phases gives the maximum value of ~1 kcal/mol for the internal energy and the anomalies characteristic to silicates for the great concentrations of $SiO_2$. (auth)

**2327** (IKF-12) DIE OPTISCHEN EIGENSCHAFTEN VON $TiO_2$ ALS REFLEKTOR FUER PLASTISCHE SZINTILLATOREN. (The Optical Properties of $TiO_2$ as a Reflector for Plastic Scintillators). Mayer, R.; Wensel, A. (Institut fuer Kernphysik, Universitaet Frankfurt (West Germany)). July 1965. 12p. Dep. mn.

The optical properties of $TiO_2$ (NE 560) as a reflector for plastic scintillators were studied. The reflector was applied to the plane face of a hemisphere made of lucite which has approximately the same index of refraction as plastic scintillator. The total diffuse reflecting power is 0.876. This value was determined by comparison to a MgO standard. The angular dependence of the reflecting power indicates that $TiO_2$ behaves as an ideal diffuse reflector only for angles from normal up to 60°. The contribution of regular reflection to total reflection as a function of the angle of incidence was determined using an approximative integration method. Reflection coefficients for regular reflection were calculated using Fresnel's formulas. (auth)

**2328** (INR-625/XIV/R) VZAIMNAYA DIFFUZIYA URANA I NIKELYA. (Interdiffusion in the Nickel–Uranium System). Matyya, G.; Gabrytski, S. (Institute of Nuclear Research, Warsaw (Poland)). 1965. 28p. Dep.

Interdiffusion in the N–U system was investigated over the temperature range 550–720°C. The values of the activation energies for the diffusion zone and for intermetallic phases $UNi_5$ and $U_6Ni$ were determined. The results show that there must be some solubility range within the $U_6Ni$ phase. (auth)

**2329** (IS-T-35) STUDIES OF THE MAGNETORESISTANCE OF THALLIUM [Thesis]. Milliken, John Crosby (Ames Lab., Iowa State Univ. of Science and Tech.). May 1965. Contract W-7405-eng-82. 74p. Dep. mn; CFSTI $3.00 cy, $0.75 mn.

The transverse magnetoresistance of thallium at 4.2 and 1°K was measured as a function of field direction and magnitude for magnetic fields up to 54 kO. The occurrence and direction of open orbits on the Fermi surface were analyzed to clarify the structure of c-axis posts and to study magnetic breakdown of the energy gap between

the third and fourth Brillouin zones. The results indicated the diameter of the posts to be less than 0.091 $A^{0-1}$. Complete magnetic breakdown was not achieved at fields of 54 kO. For orientations where magnetic breakdown occurred, the breakdown fields decreased with an increase in the electron mean free path. (auth)

**2330** (KAPL–3091) PRIMARY AND SECONDARY RECRYSTALLIZATION OF ALPHA ZIRCALOY-4. Washburn, D. F. (Knolls Atomic Power Lab., Schenectady, N. Y.). Oct. 1964. Contract W-31-109-eng-52. 39p. Dep. mn; CFSTI $2.00 cy, $0.50 mn.

An investigation was undertaken to determine the primary and secondary recrystallization kinetics of cold-worked Zircaloy-4. Reactor-grade Zircaloy-4 in the form of hot-rolled plates, 0.790 and 0.150 in. thick, were cold-rolled 10, 20, 40, and 60 or 68%. Samples of the cold-rolled material were subsequently annealed in a helium atmosphere at temperatures ranging from 500 to 800°C (932 to 1472°F). Various annealing times, up to a maximum of 10,000 min (167 hr), were used. Recovery and recrystallization were followed by determining the hardness changes of the isothermally annealed samples of both the thin and thick plates. The results showed that the rates of recrystallization in both the thin and thick plates were essentially the same. Recovery had a strong effect on x-ray line-broadening, but did not cause much change in hardness. Recrystallization, after all amounts of cold work, occurred in two hours of less at 700°C, but was very sluggish at lower temperatures. Increasing the amount of cold work caused an increase in the rate of recrystallization and a decrease in the temperature at which a significant decrease in hardness occurred in a reasonable length of time. With 10% cold work, recrystallization occurred by the growth of existing grains rather than by the nucleation and growth of new grains. The activation energy for recrystallization decreased from about 105 kcal/mole for 20% cold work to about 80 kcal/mole for 40 to 60% cold work. Metallographic examination showed that the amount of cold work had pronounced effects on the secondary recrystallization process. (P.C.H.)

**2331** (KAPL–3103) PRIMARY AND SECONDARY RECRYSTALLIZATION OF BETA-QUENCHED ZIRCALOY-4. Washburn, D. F. (Knolls Atomic Power Lab., Schenectady, N. Y.). Nov. 1964. Contract W-31-109-eng-52. 26p. Dep. mn; CFSTI $2.00 cy, $0.50 mn.

An investigation of primary and secondary recrystallization was undertaken on beta-quenched Zircaloy-4 with various degrees of cold-work. Hot-rolled, reactor-grade plate, 0.150 in. thick, was water-quenched after being heat-treated at 1060°C (1940°F) for one hour. The beta-quenched plate was subsequently cold-rolled 10, 20, or 40%. Small samples were heat-treated in a helium atmosphere at temperatures in the range of 500 to 800°C (932 to 1472°F). Recrystallization was followed by hardness measurements, x-ray line-broadening, and metallographic examination. The occurrence of secondary recrystallization was determined by metallographic examination. In addition to the cold-worked material, the as-quenched Zircaloy-4 was also examined by similar methods to determine the changes brought about by the approach to equilibrium of the beta-quenched material in the absence of cold-work. An extremely large variation in x-ray intensity of the $(10\bar{1}5)$ peak was observed in the beta-quenched material. At annealing temperatures in the range of 500 to about 600°C, an increase in hardness was observed after short annealing times. After 10% cold-work, it appeared that alpha grains formed by the growth of transformed beta (alpha prime) platelets. In the case of larger amounts of cold work, i.e., 20 and 40%, new alpha grains formed by nucleation and growth of new grains rather than by the migration of existing alpha boundaries. The formation of abnormally large grains by secondary recrystallization was not observed in the 10% cold-worked material, although normal grain growth occurred at the higher annealing temperatures. In the as-quenched and 40% cold-worked materials, abnormal grain growth or secondary recrystallization occurred and led to the presence both of very large and comparatively fine grains. (P.C.H.)

**2332** (LA–3307) COMPATIBILITY OF REFRACTORY METALS WITH SOLID SOLUTION (UC)(ZrC) AT ELEVATED TEMPERATURES. Davidson, K. V.; Riley, R. E.; Taub, J. M. (Los Alamos Scientific Lab., Univ. of California, N. Mex.). Feb. 1965. Contract W-7405-eng-36. 17p. Dep. mn; CFSTI $1.00 cy, $0.50 mn.

The results of time-temperature thermal treatments designed to investigate the compatibility of refractory metals such as tungsten, molybdenum, and niobium in the presence of solid solution (UC)(ZrC) are reported. Also given are details of the techniques used to fabricate specimens. (auth)

**2333** (NASA-CR-54457) GENERATION OF LONG TIME CREEP DATA OF REFRACTORY ALLOYS AT ELEVATED TEMPERATURES. Quarterly Report No. 8, March 26–June 26, 1965. Sawyer, J. C.; Steigerwald, E. A. (TRW Equipment Labs., Thompson Ramo Wooldridge Inc., Cleveland, Ohio). July 7, 1965. Contract NAS 3-2545. 56p.

Creep data obtained under ultrahigh vacuum conditions are presented for molybdenum-base alloys TZC and TZM, niobium alloy Cb132M, and arc-melted tungsten, arc-melted tungsten–25% rhenium, and Sylvania A. The results indicate that in the 1800 to 2200°F temperature range the TZC alloy possesses the greatest degree of creep resistance. (auth)

**2334** (NP–15530) PROPIEDADES DE UNA ALEACION DE COBRE DE ALTA RESISTENCIA AL ABLANDAMIENTO Y ALTA CONDUCTIVIDAD. Informe No. 146. (Properties of Copper Alloys of High Resistance and High Conductivity. Note No. 146). Obrutsky, D.; Sarrate, M.; Wortman, O. (Comision Nacional de Energia Atomica, Buenos Aires (Argentina)). 1965. 14p. Dep. mn.

The precipitation in Cu–Zr alloys with various concentrations of Zr was studied using hardness tests, conductivity, thermal electromotive force, dilatometry, x rays, and cutting. The tests verified that additions of 0.08% Zr increase significantly the recrystallization temperature. The maximum increase of hardness was observed for aging for 5 minutes at 500°C. Apparently only one mechanism is responsible for the aging. The precipitated samples have a characteristic Widmanstatten structure. The mechanical properties are dependent on the orientation and this dependency is larger when the concentration of Zr is largest. The activation energy for the precipitation was 23,000 cal/mole. The mechanical properties are comparable and the conductivity is superior to alloys of Cu–Cr. (J.S.R.)

**2335** (NYO–2394-9) LINEAR DISLOCATION ARRAYS IN HETEROGENEOUS MATERIALS. Technical Report No. 9. Chou, Y. T. (Brown Univ., Providence, R. I. Div. of Engineering). Oct. 1964. Contract AT(30-1)-2394. 18p. Dep. mn; CFSTI $1.00 cy, $0.50 mn.

A simple class of dislocation pile-ups in materials composed of soft and hard phases was examined. The analysis is based on the assumption that an array of discrete dislocations may be replaced by a continuous distribution of elementary dislocations. Two special cases considered are: a pile-up of screw dislocations in the soft matrix against a welded boundary; and a pile-up of edge dislocations against a slipping boundary, i.e., a boundary which can transmit normal but not shear stresses. It is shown that, in a heterogeneous material, the length of the piled-up array depends linearly on the number of dislocations in the pile-up, as is the case in a homogeneous material. The number of dislocations in a given array, however, is generally less in the heterogeneous than in the pure matrix material. The results indicate that the two-phase material would work harden more than the pure matrix, provided the mean free path is not small. (auth)

**2336** (ORNL–P–1634) COMPARATIVE CREEP-RUPTURE PROPERTIES OF D-43 AND B-66 ALLOYS.

Stephenson, R. L. (Oak Ridge National Lab., Tenn.). [1964]. Contract W-7405-eng-26. 23p. (CONF-651025-2). Dep. mn; CFSTI $1.00 cy, $0.50 mn.

From Symposium on Physical Metallurgy of Refractory Metals, French Lick, Ind.

Creep-rapture properties of D-43 (Nb-10% W-1% Zr-0.1% C) and B-66 (Nb-5% V-5% Mo-1% Zr) were determined to 1000 hr so that a valid comparison of their suitability for high-temperature structural applications could be made. The results showed that D-43 alloy was characterized by a stable microstructure at temperatures up to 1204°C. In contrast, B-66 alloy was characterized by rapid diffusion-controlled processes (rapid grain-boundary motion and low recrystallization temperature) and as a result exhibits inferior long-time high-temperature creep properties. (P.C.H.)

**2337** (ORNL-P-1677) EQUILIBRIUM SOLID SOLUTIONS OF NITROGEN IN Cb-1 percent Zr BETWEEN 1200-1800 deg C. Inouye, H. (Oak Ridge National Lab., Tenn.). [1965]. Contract W-7405-eng-26. 19p. (CONF-651025-1). Dep. mn; CFSTI $1.00 cy, $0.50 mn.

From Symposium on Physical Metallurgy of Refractory Metals, French Lick, Ind.

An ultrahigh vacuum technique capable of measuring sorption rates as low as $4 \times 10^{-3}$ ppm N/hr and pressures of $10^{-10}$ torr of nitrogen was used to measure the thermodynamic properties of solutions of nitrogen in Nb-1% Zr between 1200-1800°C. In the composition range 31-278 ppm N, the solutions obeyed Sievert's law. An anomalous solution behavior that was dependent on the $X_N$, the amount of nitrogen in solution, occurred between 1200-1400°C and was attributed to an oxygen-nitrogen interaction. The partial molar free energy expression for the dissolution of nitrogen in the normal solutions was $\Delta\overline{F}^0 = -51{,}500 + 20.74T$. (auth)

**2338** (ORNL-P-1735) MAGNETIC STRUCTURE PROPERTIES OF Tb-Sc ALLOYS. Child, H. R.; Koehler, W. C. (Oak Ridge National Lab., Tenn.). Oct. 1965. Contract W-7405-eng-26. 12p. (CONF-651106-2). Dep. mn; CFSTI $1.00 cy, $0.50 mn.

From Conference on Magnetism and Magnetic Materials, San Francisco.

The results of a neutron diffraction study of the magnetic structure properties of the Tb-Sc alloy system are reported. Five binary alloys with Tb content from 90 to 25 atomic percent were examined by powder techniques from 300°K down to liquid helium temperatures to determine the magnetic ordering temperatures and the magnetic structures. The dilution by Sc causes the spiral magnetic phase of Tb to remain stable over a temperature interval larger than in the pure metal. However, the Néel points of the Tb-Sc alloys fall well below those found for Tb-Y and the initial turn angles are smaller in this system. $T_N$ falls more rapidly for Tb-Sc alloys than for Tb-Y alloys as a function of the effective spin variable $x = c(g-1)^2J(J+1)$, where c is the atomic percent of Tb, and reaches 0°K at x about 2.5. The 25% Tb alloy shows no visible magnetic order down to 1.3°K in contrast to the Tb-Y system where magnetic order was observed with as little as 5 at.% Tb. The universal curve of $T_N$ vs. x previously found for rare earth alloys is not obeyed in the Tb-Sc system. (auth)

**2339** (ORNL-P-1753) DEFORMATION, CREEP, AND FRACTURE IN ALPHA-ZIRCONIUM ALLOYS. Picklesimer, M. L. (Oak Ridge National Lab., Tenn.). [1965]. Contract W-7405-eng-26. 59p. (CONF-651017-2). Dep. mn; CFSTI $3.00 cy, $0.75 mn.

From Electrochemical Society Meeting, Buffalo.

The anisotropy of mechanical properties observed in $\alpha$-zirconium alloys can be related to the preferred orientation of the material. The influence of preferred orientation on anisotropy of yield strengths, plastic flow, creep, fracture, their strain rate and temperature sensitivities, and the stability of such textures to further deformation are discussed in terms of the deformation systems observed in single crystals. It was concluded that other deformation systems are forced to operate because of the restraint of neighboring grains in polycrystalline materials. 59 references are cited. (auth)

**2340** (ORNL-TM-1131) EVALUATION OF NIOBIUM-VANADIUM ALLOYS FOR APPLICATION IN HIGH-TEMPERATURE REACTOR SYSTEMS. Roche, T. K. (comp.) (Oak Ridge National Lab., Tenn.). Oct. 1965. Contract W-7405-eng-26. 34p. Dep. mn; CFSTI $2.00 cy, $0.50 mn.

Alloys in the Nb-V system were evaluated for potential use in high-temperature reactor systems capable of long-time operation. These alloys were attractive because of their good tensile properties as reported by other investigators. Properties of immediate interest that were examined included fabricability, corrosion behavior in Li, strength, weldability, aging response, and stability in high vacuums. The greatest emphasis was placed on alloys with about 40% V and small additions of Ti and Zr. This concentration of V has been shown to be near optimum for good tensile properties. A complete evaluation of the alloys was not carried out because several drawbacks were uncovered early in the program. For example, difficulty was experienced in fabricating seamless tubing of the alloy Nb-39% V-1% Ti, and this same alloy was subject to metal losses by evaporation at elevated temperatures in high vacuums. The most disappointing result was the lack of creep strength at elevated temperatures. This report presents the results obtained to justify the conclusion that other Nb alloys presently available would be more satisfactory for this application. (auth)

**2341** (SC-DC-65-1637) AN EXPERIMENTAL INVESTIGATION OF THE BEHAVIOR OF BERYLLIUM METAL IN SIMULATED LAUNCH PAD ABORT ENVIRONMENTS. Final Report. Blumenthal, J. L.; Santy, M. J. (TRW Systems, Redondo Beach, Calif.). July 30, 1965. Contract AT(29-1)-789. 213p. Dep. mn; CFSTI $6.00 cy, $1.25 mn.

For Sandia Corp., Albuquerque, N. Mex.

Comprehensive laboratory investigation of the chemical behavior of beryllium metal in a wide range of simulated launch abort environments was completed. A two phase laboratory program was conducted. The first phase of the program aimed at determining, as a function of temperature and pressure, with each of the major combustion gas species, the rate at which bulk beryllium metal was converted into combustion products (oxides, nitrides, etc.) and whether or not the reaction products formed were in a particle size range which could become airborne. The kinetics of the reactions of beryllium with the combustion gases oxygen, nitrogen, air, nitric oxide, carbon monoxide, carbon dioxide, hydrogen, and water vapor were investigated in the temperature range from 800 to 1500°C and over the pressure range from 0.1 mm Hg to atmospheric pressure. The second phase of the laboratory program involved semi-quantitative observations of the behavior of beryllium in selected flame environments which were fully determined thermochemically. It was found that the degree of interaction between the flame environment and the beryllium components and the amount of airborne contamination which is released will increase rapidly with increasing beryllium metal temperature, concentration in the flame environment of water vapor and/or oxygen, and the total pressure of the environment. Other results are discussed extensively. (P.C.H.)

**2342** (SC-DR-58-61) THE MECHANICAL PROPERTIES OF WROUGHT DEPLETED URANIUM AND OF WELDS JOINING THIS MATERIAL. Nelson, V. G. (Sandia Corp., Albuquerque, N. Mex.). Mar. 1961. Contract AT(29-1)-789. 30p. Dep. mn; CFSTI $2.00 cy, $0.50 mn.

A test program was conducted to establish design allowables for tensile properties in wrought depleted uranium and in welds joining this material. Typical values of Charpy impact were determined for the uranium and the butt welds. Free bend bars were cut across the weld joints and tested to study the behavior of welds in bending and to determine the modulus of rupture in bending. Typical values for longitudinal and transverse shear in fillet welds were determined. Data are tabulated. (P.C.H.)

**2343** (SC-TM-65-242) THERMAL PROPERTIES OF SELECTED METALS AT AMBIENT TEMPERATURE. Pousma, J. G. (Sandia Corp., Albuquerque, N. Mex.). May 1965. Contract AT(29-1)-789. 3p. Dep. mn; CFSTI $1.00 cy, $0.50 mn.

A table of thermal and mechanical properties of some familiar metals was generated to serve as a design help where thermal characteristics of the material are important. (auth)

**2344** (TRG-Report-1072) A COMPARISON OF PROCEDURES FOR DISSOLVING IGNITED PLUTONIUM OXIDES FOR ANALYSIS. Black, R. M.; Drummond, J. L. (Reactor Group, United Kingdom Atomic Energy Authority, Risley (England)). July 20, 1965. 9p. Dep.; BIS $0.40; HMSO 2s.

A comparison of all available methods for dissolving ignited plutonium dioxide, on an analytical scale, showed that the rate of solution in a hydrobromic/0.15M hydrofluoric acid mixture was about six times as fast as in nitric/hydrofluoric acid. An improved apparatus made from a transparent inert plastic (FEP) was used for refluxing mixed oxides with nitric/hydrofluoric acid. Plutonium oxide previously sintered at 1600°C in air was most rapidly attacked by fusion with sodium bisulfate under reflux at 800°C. (auth)

**2345** (UCRL-11030) RESISTANCE MEASUREMENTS AT HIGH PRESSURES. Jura, George (Lawrence Radiation Lab., Univ. of California, Berkeley). Nov. 8, 1963. Contract W-7405-eng-48. 23p. Dep. mn; CFSTI $1.00 cy, $0.50 mn.

The accuracy of resistance determinations on semiconductors as a function of pressure is reviewed and discussed. Uses of resistance measurements are also considered. A technique is described that might permit a precision approaching that at atmospheric pressure. (P.C.H.)

**2346** (UCRL-11471) SUPERCONDUCTIVITY OF THE CUBIC MODIFICATION OF MoC. Toth, Louis E.; Rudy, Erwin; Johnston, Jean; Parker, Earl R. (Lawrence Radiation Lab., Univ. of California, Berkeley). June 1964. Contract W-7405-eng-48. 17p. Dep. mn; CFSTI $1.00 cy, $0.50 mn.

The superconducting transition temperatures of the metallic carbides and nitrides with the NaCl structure were interpreted on the basis of the tight-binding model of Bilz (Z. Phys. 153: 338(1958)). It was found that total valence electron concentrations from 9 to 10 are required for high critical temperatures in these compounds. The cubic modification (NaCl) of molybdenum carbide was found to be superconducting at 13.0°K in agreement with the Bilz band model. (auth)

**2347** (UCRL-12146) THE CRYSTAL STRUCTURE OF TETRAMETHYL AMMONIUM HEXAHYDROHEXABORATE. Schaeffer, Riley; Johnson, Quintin; Smith, Gordon S. (Lawrence Radiation Lab., Univ. of California, Livermore). Oct. 19, 1965. Contract W-7405-eng-48. 7p. Dep. mn; CFSTI $1.00 cy, $0.50 mn.

A complete x-ray structure analysis of tetramethyl ammonium hexahydrohexaborate was made. Crystals grown from water solution were examined by precision and Weissenberg methods. The structure was solved by noticing that the antifluorite structure can accommodate the octahedral $B_6H_6^{2+}$ ion at the origin and the tetrahedral (disregarding hydrogen) $N(CH_3)_4^+$ ion at $\pm 1/4$, $1/4$, $1/4$. Preliminary structure factor calculations verified this model. Data are tabulated. (P.C.H.)

**2348** (UCRL-16051) GRAIN BOUNDARY ENERGY [Thesis]. Kennedy, Kurt D. (Lawrence Radiation Lab., Univ. of California, Berkeley). Aug. 1965. Contract W-7405-eng-48. 39p. Dep. mn; CFSTI $2.00 cy, $0.50 mn.

The interfacial energy of [001] tilt boundaries in pure copper and copper +0.02% silver were determined by measuring the dihedral angles formed by chemical grooving in molten salt. Boundary energies were determined for three boundary orientations and nine temperatures between 200 and 1000°C. The temperature coefficient of boundary energy was similar to the temperature coefficient of the shear modulus. The boundary energy of copper at 300°C was reduced 30% by the addition of 0.02% silver but was unaffected at 1000°C. The reduction of grain boundary energy of the copper doped with silver was ascribed to silver atoms occupying sites at the boundary. The presence of silver atoms at boundary sites relieved some of the elastic strain energy of the boundary. Thermodynamic and lattice parameter data predicted segregation of silver to copper grain boundaries to approximately the same extent as indicated by reduction of grain boundary energy. (auth)

**2349** (UCRL-16320) TWO ASPECTS OF ALLOY THERMOCHEMISTRY: A. VARIATION OF PROPERTIES WITH COMPOSITION IN ORDERED PHASES. B. SOLUTE INTERACTIONS IN DILUTE LIQUID ALLOYS [Thesis]. Orr, Raymond Leonard (Lawrence Radiation Lab., Univ. of California, Berkeley). Sept. 17, 1965. Contract W-7405-eng-48. 98p. Dep. mn; CFSTI $3.00 cy, $0.75 mn.

A. A method is presented for calculating the compositional variation of the configurational thermodynamic properties of ordered intermetallic phases which exist over a range of composition by means of the substitutional defect mechanism. The treatment, which is an extension of the one of Wagner and Schottky, is applied to the simple quasi-chemical model analogous to that employed in the Bragg and Williams treatment of the variation of degree of order with temperature. The configurational thermodynamic properties are expressed as functions of the deviation from ideal stoichiometry and a composition dependent parameter which represents the atomic distribution. By minimizing the Gibbs energy with respect to the distribution parameter, an expression is obtained relating the equilibrium distribution with composition for given degrees of order at the stoichiometric composition. Solutions of this expression then permit the configurational properties to be evaluated as functions of composition for specified degrees of order at ideal stoichiometry. The method of treatment is derived in detail for phases having the CsCl-type superlattice structure, and the results of corresponding treatments for AuCu-type and $AuCu_3$-type superlattice phases are also given. Existing entropy of formation data for the AgMg, AuCd, and AuCu ordered phases are compared with values predicted by the treatments. Good correlations are obtained, leading to reasonable interpretations of the actual values in terms of the configurational and thermal contributions to the total entropies of formation. It is proposed that the methods developed could provide the basis for more elaborate or extensive treatments, either which incorporate other defect mechanisms or which employ higher-order approximations of the quasi-chemical model. B. Calorimetric measurements are reported for the heats of solution of gold and indium in a number of liquid tin-rich alloys at a temperature of 705°K. From the data, the partial molar enthalpies of gold are determined as a function of dilute solute concentrations in the binary Au–Sn system and in the ternary systems, Ag–Au–Sn, Au–Ni–Sn, and Au–In–Sn. Partial molar enthalpies of indium are determined for dilute solute concentrations in the In–Sn, Ag–In–Sn, and Au–In–Sn systems. The data are expressed in terms of the interaction parameter concept introduced by Wagner and more recently extended by Lupis and Elliott. Values are obtained for the gold-gold, silver-gold, nickel-gold, gold-indium, and silver-indium enthalpy interaction parameters in liquid tin. Values of enthalpy interaction parameters are also evaluated from existing data for the temperature variation of the Gibbs energy interaction parameter in four liquid ternary alloy systems. The results are interpreted in terms of solute atom distributions through comparisons with values of the enthalpy interaction parameters predicted by the random solution and Henry's law models for the dilute solution. (auth)

**2350** (USBM-RC-1205) QUARTERLY METALLURGICAL PROGRESS REPORT NUMBER 28, AUGUST 1–SEP-

TEMBER 30, 1965. (Bureau of Mines, Albany, Oreg. Albany Metallurgy Research Center). Contract AT(11-1)-599. 19p. Dep. mn; CFSTI $2.00 cy, $0.50 mn.

Five articles are included; separate abstracts were prepared for 4. The remaining article contains brief information on thorium alloy systems. (P.C.H.)

*For abstracts of individual papers see: 2351–2354.*

**2351** (USBM-RC-1205, pp 3-7) HIGH MELTING POINT CARBIDES (HfC). Beall, R. A.; Kato, H. (Bureau of Mines, Albany, Oreg. Albany Metallurgy Research Center).

Various compositions of C–Ta–Hf were prepared, and five TaC–C and TaHfC–C castings were evaluated for quality. Mechanical properties were determined and evaluated for 15 HfC–C castings at elevated temperatures. Data on tensile properties are tabulated. (P.C.H.)

**2352** (USBM-RC-1205, pp 9-10) COLD-MOLD INDUCTION MELTING. Beall, R. A.; Clites, P. G. (Bureau of Mines, Albany, Oreg. Albany Metallurgy Research Center).

Progress in the development of a furnace for induction melting reactive metals in a water-cooled copper crucible is reported. Melting tests with titanium revealed a surprisingly deep molten pool, which resulted in considerable improvement in the appearance of the ingot sidewalls. (P.C.H.)

**2353** (USBM-RC-1205, pp 11-14) INVESTIGATION OF THE SYSTEM UC–UN–UO. Kelly, Hal J.; Henry, Jack L.; Paulson, Danton L.; Blickensderfer, Robert (Bureau of Mines, Albany, Oreg. Albany Metallurgy Research Center).

Phase studies were made on the pseudoternary system UC–UN–UO near the solid solution region at 1,700°C to establish phase boundaries and the extent of the solid solution range. Results are discussed. (P.C.H.)

**2354** (USBM-RC-1205, pp 15-19) W–Re–Mo ALLOY DEVELOPMENT. Kato, H. (Bureau of Mines, Albany, Oreg. Albany Metallurgy Research Center).

Tungsten and Mo powders were sieved to remove +325 mesh particles, blending tests were made, and the first trial sleeves were pressed and sintered. Steps were taken to recover W-25 Re scrap. Several blending tests were also made on W–Re–Mo mixtures of adjusted composition. Results showed that the alloy composition after blending and sintering was higher in Re and lower in Mo than the target composition supposedly blended. Engineering properties of W–Re sheet bar extrusions are undergoing evaluation. (P.C.H.)

**2355** (WAPD-T-1757(Rev.)) HYDRIDE HABIT IN ZIRCONIUM AND IN UNSTRESSED AND STRESSED ZIRCALOY-4. Babyak, W. J. (Bettis Atomic Power Lab., West Mifflin, Pa.). Aug. 1965. Contract AT(11-1)-Gen-14. 39p. Dep. mn; CFSTI $2.00 cy, $0.50 mn.

The habit planes for hydride precipitation in large grains of alpha zirconium and Zircaloy-4 were determined in specimens containing 161 and 136 ppm hydrogen, respectively. In zirconium, the hydride platelets precipitated on various pyramidal planes inclined to the basal plane at angles ranging from 10 to 50 and 75 and 90°C. Hydrides were most frequent at inclinations of about 20 and 90°C. In Zircaloy-4, the hydride habit was significantly different than that in zirconium. Hydride platelets were inclined to the basal plane at angles ranging from 5 to 25°C with the predominant inclination equal to 12°; no platelets were found near the prism plane position. In both zirconium and Zircaloy-4, hydrides were principally, but not exclusively, parallel to $\{10\bar{1}1\}$ type planes. When the Zircaloy-4 grains were subjected to tension stresses of 12,100 and 19,400 psi during hydride precipitation, the hydride habit was essentially unchanged except that precipitation favored those habit planes which were more nearly perpendicular to the stress direction. The stress-orientation effect increased with the magnitude of the stress. (auth)

**2356** (AERE-Trans-1030) THE VALUE OF THE SELF-DIFFUSION PARAMETERS OF ZIRCONIUM. Federov, G. B. Translated by J. J. Cornish (U.K.A.E.A. Atomic Energy Research Establishment, Harwell, Eng.), from Met. i Metalloved. Chistykh Metallov, Sb. Nauchn. Rabot, No. 4, 34-40(1963). 8p. Dep., BIS $0.30; HMSO 1s. 9d.

Calculated values for the self-diffusion of zirconium and its alloys are reviewed and evaluated. It is assumed that the difference in the self-diffusion parameters is determined to a considerable extent by different degrees of stabilization of the initial zirconium. (P.C.H.)

**2357** (AERE-Trans-1032) STUDY OF DIFFUSION OF CARBON AND MOLYBDENUM IN CHROMIUM. Gruzin, P. L.; Zemskii, S. V.; Rodina, I. B. Translated by J. J. Cornish (U.K.A.E.A. Atomic Energy Research Establishment, Harwell, Berks, Eng.), from Met. Metalloved. Chistykh Metallov, Sb. Nauch. Rabot, No. 4, 243-50(1963). 9p. Dep.; BIS $0.30; HMSO 1s. 9d.

The coefficients of diffusion of carbon in chromium as a function of temperature were determined. It was established that the level of the diffusion mobility of carbon in chromium is much lower than in iron, which corresponds to processes of carbon precipitation from the solid solution of these metals. The temperature dependence of the coefficients of diffusion of molybdenum was determined for chromium and nickel. These results are required for an examination of the processes which take place during the work of protective coatings. (auth)

**2358** (AERE-Trans-1034) BEHAVIOUR OF KRYPTON AND XENON IN URANIUM METAL. RELEASE OF KRYPTON AND XENON FROM METALLIC URANIUM. Nagasaki, Ryukichi; Kawasaki, Satoru. Translated by S. G. Brickley (U.K.A.E.A. Atomic Energy Research Establishment, Harwell, Eng.), from Nippon Genshiryoku Gakkaishi, 6: 646-55(1964). 20p. Dep., BIS $0.80; HMSO 4s.

The diffusion coefficients of Kr and Xe in irradiated U are considered using the experimental results obtained and the diffusion equations, and the factors influencing the coefficients are discussed. When the sample was heated under inert gas atmosphere, the apparent diffusion coefficient increased. For highly irradiated samples, the diffusion coefficient was smaller than in less highly irradiated samples. When the sample was heated in an inert gas atmosphere, the release of gases was suddenly increased at the transformation temperature of the samples, and the gas release was also increased by thermal cycling. It is very probable that the gas bubbles migrate as a result of the surface diffusion of the matrix atoms. (P.C.H.)

**2359** (NASA-TT-F-338) PHYSICAL METALLURGY OF TITANIUM. Kornilov, I. I. (ed.). Translation of Metalloved. Titana, Akad. Nauk SSSR, Gos. Kom. Sov. Min. SSSR Chern. Tsvetin. Met., Inst. Met., Tr. Pyatogo Soveshch., Moscow, 1963(1964). 356p. CFSTI $7.00 cy, $1.75 mn.

Forty-six articles on metal chemistry of titanium, interaction of titanium with gases and the corrosion properties of alloys, and mechanical and technological properties of titanium alloys are included. (P.C.H.)

**2360** (ORNL-tr-814) THE INFLUENCE OF TRAPS ON DIFFUSION (RARE GAS DIFFUSION IN SOLIDS). Gaus, H. (Hahn-Meitner-Institut fuer Kernforschung, Berlin (West Germany)). Translated for Oak Ridge National Lab., Tenn., from Preprint. 25p. Dep. mn; JCL $2.60 fs, $0.95 mf.

It is generally assumed that the diffusion of gas in solids is modified by traps, which capture the gas atoms for a time and re-emit them. In this case, an analytical calculation was performed for a small diffusion depth (arbitrary body form). Simple approximation formulas, valid for different time intervals, were obtained for the resulting gas release. With these formulas, values of certain parameter combinations may be obtained directly from the experimental curves. In the atomic picture, the meaning of the absorption-emission probability is then discussed on

the basis of the theory of Eyring, Zener, and others. A simple expression was obtained especially for the quotient of absorption emission probability. In connection with the mentioned release formulas, this expression may explain the two-fold activation enthalpy found recently by others. (auth)

**2361** (WAPD-Trans-21) INVESTIGATIONS ON THE $UO_2$–$ThO_2$–$ZrO_2$ SYSTEM. Brisi, Cesare. Translated for Bettis Atomic Power Lab., West Mifflin, Pa., from Atti Accad. Sci. Torino: Pt. I. Classe Sci. Fis., Mat. Nat., 94: 67-76(1959/1960). 12p. Dep. mn; JCL $1.60 fs, $0.80 mf.

The solids obtainable by heating mixtures of $UO_2$, $ZrO_2$, and $ThO_2$ at 1400°C in a current of hydrogen were examined. Under these conditions in the area leanest in zirconium dioxide, a cubic phase whose maximum $ZrO_2$ content gradually decreases from 17 to little more than 1 mole % as the thorium dioxide present increases is formed. The zirconium dioxide can, in turn, dissolve about 8 mole % of uranium dioxide. The solubility limits found on preparations heated to 1000°C practically coincide with those found on solids obtained at higher temperature. (auth)

**2362** MEASUREMENT OF THE FORMATION ENERGY OF THE ELECTRON-HOLE PAIR IN n-TYPE SILICON. Kantola, Martti; Sutela, Vaeinoe; Rantala, Veikko (Univ. of Turku). Ann. Acad. Sci. Fenn., Ser. A VI, 175: 1-6(1965).

The formation energy of the electron-hole pair in n-type silicon was measured, using a Si-Au surface-barrier detector and the 5.147-Mev alpha peak of $^{239}Pu$. The results yield a formation energy of 3.22 ± 0.16 ev, which gives evidence that the value 3.5 ev from the theory of Schockley is too large. (L.B.S.)

**2363** CHANGE OF BERYLLIUM PROPERTIES AFTER AGEING TREATMENT. Azhazha, V. M.; D'yakov, I. G.; Papirov, I. I.; Tikhinskii, G. F. At. Energ. (USSR), 19: 269-72(Sept. 1965). (In Russian).

The change of residual resistance and mechanical properties of metal-ceramic beryllium as a result of its aging at various temperatures was studied. It is shown that the trends of the dependences of the residual resistance and the plastic characteristics of beryllium on time and temperature of aging are similar in their general features. By means of heat treatment of hot-pressed beryllium in the optimum regime, as in the aging of other sorts of beryllium, a significant increase of its plastic properties can be achieved. (tr-auth)

**2364** DIFFUSION OF THE FISSION PRODUCT $^{147}Pm$ IN ALUMINIUM OXIDE. Bobleter, O.; Fiedler, W.; Grass, F. (Oesterreichische Hochschule, Vienna). Atomkernenergie, 8: 261-3(July-Aug. 1965). (In German).

The diffusion of $^{147}Pm$ through sintered alumina was investigated by the method of beta-absorption in the temperature range of 1350 to 1540°C. From the diffusion coefficients of various temperatures follows the equation: $D = 1.18 \times 10^8 \cdot \exp(157{,}000/RT)\ cm^2 sec^{-1}$. As a proof to these results the decrease of the residual activity on the sample was calculated and examined by means of the abrasive method. (auth)

**2365** PROTON MAGNETIC RESONANCE STUDIES ON HYDROGEN DIFFUSION IN THE NIOBIUM–HYDROGEN SYSTEM. COMMENTS ON STRUCTURE OF β-NIOBIUM HYDRIDE. Stalinski, B.; Zogal, O. J. (Inst. of Structural Research, Polish Academy of Sciences, Wroclaw). Bull. Acad. Pol. Sci., Ser. Sci. Chim., 13: 397-402(1965).

The results of an investigation on self-diffusion of hydrogen atoms in the system Nb–H are given, and the structure of the β-phase is disucssed. A comparison of theoretical and experimental second moments was used for determining the hydrogen atom positions in the rigid lattice of the hydride. The results indicated that diffusion occurs via the vacancy mechanism. (P.C.H.)

**2366** THE BINARY SYSTEM URANIUM–URANIUM MONOCARBIDE. Guinet, Philippe; Vaugoyeau, Henri; Blum, Pierre L. (Centre d'Etudes Nucleaires, Grenoble, France). Compt. Rend., 261: 1312-14(Aug. 2, 1965). (In French).

The liquidus of the uranium–uranium monocarbide system was determined by the saturation method, and the solidus by putting the liquid and the solid in equilibrium. The eutectic temperature was determined by differential thermal analysis. The diagram is of the simple type with the eutectic shifted to the uranium side. A substoichiometric monocarbide exists where the minimum concentration of carbon is 4.36% and the temperature is 2150°C. (tr-auth)

**2367** THE PARTITIONING OF OXYGEN BETWEEN ZIRCONIUM AND LIQUID POTASSIUM. Litman, A. P. (Oak Ridge National Lab., Tenn.); Prados, J. W. Electrochem. Technol., 3: 228-33(Sept.-Oct. 1965). (ORNL-P-984).

The distribution of oxygen between zirconium and liquid potassium was studied at 815°C. The rate of oxygen uptake by zirconium samples exposed to a dilute solution of oxygen in liquid potassium was correlated with a diffusion model for oxygen movement through the solid. Mass transfer calculations based on literature values for the diffusion coefficient of oxygen in zirconium are in reasonable agreement with experimental rates of oxygen uptake. The distribution ratio for oxygen between zirconium and potassium is sufficiently reproducible at 815°C to afford a useful analytical procedure for the determination of oxygen in potassium. This procedure, termed the gettering-vacuum fusion technique, gave complete recovery of oxygen from doped potassium samples at oxygen levels of less than one hundred to several thousand parts per million. Recoveries were not influenced by the prior thermal history of the alkali metal. (auth)

**2368** DIFFUSIVITY OF URANIUM IN VARIOUS LIQUID METAL SOLUTIONS. Hesson, J. C.; Hootman, H. E.; Burris, L. Jr. (Argonne National Lab., Ill.). Electrochem. Technol., 3: 240-4(Sept.-Oct. 1965).

The diffusivities of uranium in liquid cadmium, zinc, bismuth, and aluminum were measured as a function of temperature by the capillary-bath technique. The diffusivities of uranium in units of $10^{-5}$ $cm^2/sec$ in these solvent metals over the indicated temperature ranges were as follows: cadmium, 1.3 to 2.3 (450 to 650°C); bismuth, 2.3 to 5.1 (490 to 725°C); zinc, 1.3 to 2.8 (600 to 800°C); and aluminum, 0.5 to 4.5 (700 to 850°C). The diffusivities of uranium in these solvents were somewhat less than those predicted by the Einstein–Stokes equation. (auth)

**2369** ON CERTAIN MAGNETIC PROPERTIES OF Ni–Eu ALLOYS. Chechernikov, V. I.; Speranskii, N. M.; Terekhova, V. F.; Rozhkova, R. S. (Moscow State Univ.). Fiz. Metal. Metalloved., 20: 157-9(July 1965). (In Russian).

Ni–Eu alloys containing 0.77, 2.0, 3.26, 3.6, and 6.38 at. % Eu were prepared in an arc furnace under a helium atmosphere. The alloys were homogenized at 1100°C for 100 hr. Microstructural analyses showed that the alloys contained two phases. The amount of the second phase increased with increasing content of europium. The second phase was apparently a eutectic of Ni (α) + $Ni_{17}Eu_2$. The lattice constants of the $Ni_{17}Eu_2$ compound were found to be a = 8.36 and c = 8.09 Å with c/a = 0.968. The alloy hardness increased with increasing europium content. The alloy with 6.38 at. % Eu had a hardness of 271 $kg/cm^2$, which exceeded the hardness of pure nickel (70 $kg/cm^2$) by almost a factor of four. The magnetic susceptibility χ of the Ni–Eu alloys was determined from 300 to 1000°C in a vacuum of $10^{-3}$ to $10^{-4}$ mm Hg std. A plot of $1/\chi$ as a function of temperature gave a straight line. The results showed that the Ni–Eu alloys followed the Curie–Weiss law in the following form: $\chi = \chi_k + [c/(T - \theta)]$. Here $\chi_k$ is the susceptibility that does not depend on temperature. The value of $\chi_k$ is greater for the alloy than it is for nickel. The value of $\theta$ remained constant from 3 to 6.38 at. % Eu. (TTT)

**2370** THE THERMAL CONDUCTIVITY OF SODIUM IN THE TEMPERATURE RANGE 90–850 deg C. Evange-

listi, Roberto; Isacchini, Franco (Centro Studi Nucleari della Casaccia, Rome). Int. J. Heat Mass Transfer, 8: 1303-17(Oct. 1965).

An experiment that was carried out to determine the effect of temperature on thermal conductivity of sodium, in the temperature range from 90 to 850°C is described. The experimental method is based on a mathematical model. The apparatus and the test procedure are described, with reference to the major features of the measurement device. The experimental results were compared with previously published data. (auth)

**2371** HIGH-TEMPERATURE PLASTIC DEFORMATION OF POLYCRYSTALLINE BERYLLIUM OXIDE. Barmore, Willis L.; Vandervoort, Richard R. (Univ. of California, Livermore). J. Amer. Ceram. Soc., 48: 499-505(Oct. 21, 1965).

High-density specimens were plastically deformed under four-point transverse bending. Tests were conducted in vacuum in the region 1400 to 1700°C under stresses of 1000 to 4500 psi. The activation energy for creep was 99.0 kcal/mole. Creep rate was directly proportional to the applied stress and inversely proportional to the square of the grain diameter. The deformation behavior is ascribed to a Nabarro-Herring type mechanism. Results showed that creep was the same in tension and compression. (auth)

**2372** STRENGTH OF GRAPHITE TUBE SPECIMENS UNDER COMBINED STRESSES. Ely, Richard E. (United States Army Missile Command, Redstone Arsenal, Ala.). J. Amer. Ceram. Soc., 48: 505-8(Oct. 21, 1965).

Tubular specimens of two rocket nozzle-grade graphites were tested under ten biaxial stress states at room temperature. The static biaxial load was applied by internal fluid pressure and axial loads. Fracture strengths were compared with the maximum normal stress, the maximum strain energy, and the Stassi-D'Alia theories. Correlations between the results and the theories usually were not of a general nature. (auth)

**2373** GRAIN GROWTH IN POROUS COMPACTS. Kingery, W. D.; Francois, B. (Center for Nuclear Studies, Grenoble, France). J. Amer. Ceram. Soc., 48: 546-7(Oct. 21, 1965).

Examination of micrographs of pore compacts of $UO_2$ and $Al_2O_3$ during normal grain growth made it clear that the pores remain on grain boundaries, and more commonly at grain interactions. This indicated that pores must migrate along with the boundaries in normal grain growth. Pore migration can be accomplished by evaporation-condensation, surface diffusion, or volume diffusion as a result of a difference in curvature of the pore faces when a moving boundary is asymmetrically located on a pore. There is an essential difference, however, between pores located on grain boundaries (the ones that change in size) and a second phase, in that the grain boundaries between pores act as effective vacancy sinks separating and thus blocking pore-pore vacancy transfer. (F.J.H.)

**2374** RECOVERY OF YIELD STRESS IN Pu-1 wt percent Ga. Pavlick, J. E. (Dow Chemical Co., Golden, Colo.). J. Nucl. Mater., 17: 1-4(Aug.-Sept. 1965).

The recovery of yield stress in a Pu–1 wt% Ga alloy was studied at room temperature after recovery anneals between 120 and 240°C for specimens, which were strained 4.8% in tension. The amount of recovery followed a logarithmic function of annealing time for each annealing temperature. The activation energy for the recovery process between 160 and 240°C was found to be approximately 20 kcal/mole. (auth)

**2375** ISOCHRONAL RECOVERY OF WORK HARDENING IN ALUMINIUM–ALUMINA ALLOYS. Nobili, D. (C.C.R., Euratom, Ispra, Italy); De Maria, R. J. Nucl. Mater., 17: 5-19(Aug.-Sept. 1965).

The isochronal recovery of work hardening in Al–$Al_2O_3$ SAP-type alloys was studied by combining several techniques, mainly electrical resistivity and metallographic observations. The effects of the oxide content on the amount of defects produced by cold work and on the way they anneal out were observed. The influence of impurities was also considered. It was noticed that work hardening gave rise to a high lattice strain increasing with oxide content and also dependent on particle spacing. Annealing took place in stages. The last corresponded to recrystallization and was preceded by a recovery process giving rise to polygonization and growth of the grains. This was characterized by the presence of substages: three peaks were observed in less pure alloys and a single peak, centered at ≈200°C, in the samples prepared from pure aluminum. This substage seemed to be connected with annealing of vacancies. For a given degree of work hardening, recrystallization took place at temperatures rapidly rising with the oxide content. Probably this behavior resulted from competition between recovery and recrystallization increasing with the dispersed phase. (auth)

**2376** THE MECHANISM OF STRAIN-AGEING IN COMMERCIALLY PURE NIOBIUM. Szkopiak, Z. C.; Miodownik, A. P. (Battersea Coll. of Technology, London). J. Nucl. Mater., 17: 20-9(Aug.-Sept. 1965).

The strain-aging process in commercially pure niobium was studied using both yield-point return and internal friction measurements. After a 6% pre-strain specimens were aged at temperatures ranging from 100 to 165°C for periods of up to 160 hr. The yield-point return results showed that the strain-aging process obeys a $t^{\frac{1}{3}}$ law up to about 65% completion of the aging process. The activation energy was found to be 25800 ± 1000 cal/mol, which is in good agreement with the reported activation energy for the diffusion of oxygen in niobium (26600 cal/mol). The internal friction results offered complementary information to the yield point return measurements, and showed that while oxygen diffuses to dislocations during the early stages of strain-aging, it subsequently returns into solid solution after more extensive aging. The most likely explanation of this effect is that oxygen atoms are replaced at the dislocations by carbon atoms. An attempt was made to calculate the dislocation density and dislocation atmosphere density for the fully strain-aged condition at 155°C. (auth)

**2377** SURFACE STRUCTURE IN BETA-QUENCHED URANIUM. Drobnjak, DJ. (Inst. of Nuclear Sciences Boris Kidrich, Belgrade). J. Nucl. Mater., 17: 37-42 (Aug.-Sept. 1965).

Metallographic observations were made on $\beta$-quenched uranium specimens. The results showed that the structure that frequently appeared on the surface differs considerably from that in bulk material. The $\alpha$ grains forming the surface structure appeared in three essentially different forms: fine martensitic platelets, coarse martensitic plates, and fine equiaxed grains. The former $\beta$ grain boundaries were clearly distinguishable. In most of the former $\beta$ grains fine platelets were the only transformation products, while in the rest of them coarse plates co-existed either with fine platelets or equiaxed grains. A mechanism to account for the appearance of the surface structure is discussed. (auth)

**2378** THE TENSILE PROPERTIES OF PLUTONIUM-GALLIUM ALLOYS IN THE TEMPERATURE RANGE 20–100°C. Miller, D. C.; White, J. S. (Atomic Weapons Establishment, Aldermaston, Eng.). J. Nucl. Mater., 17: 54-9(Aug.-Sept. 1965).

The room-temperature compositional dependence of UTS, flow stress, elongation, reduction in area, density, and hardness was determined for plutonium-gallium alloys having compositions lying within the range of 0 to 5.6 at. % Ga. The tensile properties were also measured at 60 and 100°C for $\delta$-stabilized alloys having compositions in the range from 1.1 to 5.6 at. % Ga. These data together with those previously determined for plutonium–aluminum and plutonium–cerium alloys enabled some deductions to be made regarding the solution hardening of $\delta$-stabilized plutonium. (auth)

**2379** MIXED OXIDE SYSTEMS OF LANTHANIDE AND ACTINIDE ELEMENTS. III. X-RAY STUDY IN THE SYSTEM NEPTUNIUM OXIDE-EUROPIUM OXIDE. Haug, H.; Weigel, F.; Oertel, W. (Univ., Munich; Univ. of Cali-

fornia, Berkeley). J. Nucl. Mater., 17: 73-8(Aug.-Sept. 1965). (In French).

The lattice parameters of mixed oxides containing known proportions of neptunium oxide and europium oxide were determined by x-ray diffraction to a high precision. In the neptunium oxide–europium oxide system two phases, A and B, appeared in the range from 0 to 45 mol % $EuO_{1.5}$. Phase A, which had the cubic fluorite structure with $\alpha_0$ = 5.432 Å, was $NpO_2$. Phase B was mixed oxide, also possessing the fluorite structure; its parameter decreased by about 0.005 Å in the range from 0 to 45 mol % $EuO_{1.5}$. The homogeneity range of phase B was 45 to 50 mol % $Eu_2O_3$ and broadened out somewhat with rising temperature. Above 50 mol % $EuO_{1.5}$, the fluorite phase gradually changed, via a badly distorted intermediate range, to C-type $Eu_2O_3$. From comparative consideration of the $(Eu_{0.5}M_{0.5})O_2$ phases, with M = Th, Pa, U, Np, or Pu, conclusions were drawn concerning the valence of the actinide ions in the lattice. Neptunium appeared to exhibit valence 5. (auth)

**2380** RECOVERY AND STRAIN-HARDENING OF ALPHA PHASE PLUTONIUM. Pavlick, J. E.; Hanson, I. G. (Dow Chemical Co., Golden, Colo.). J. Nucl. Mater., 17: 91-4(Aug.-Sept. 1965).

A study was undertaken to determine if recovery of the yield stress of alpha–plutonium occurred after small deformations and to determine the strain-hardening exponent of alpha–plutonium. The strain hardening of alpha–plutonium was determined by measuring the increase in plastic strain with increasing load. Recovery anneals were performed on specimens deformed either 3 or 5% in compression for various times at 109°C. The strain-hardening exponent of alpha–plutonium is 0.07. The alpha–plutonium showed recovery characteristics at 109°C. Strain-hardening characteristics were observed up to at least 5% plastic deformation. (F.J.H.)

**2381** THE MECHANICAL PROPERTIES OF NUCLEAR CERMETS. Cope, Lawrence H. (United Kingdom Atomic Energy Authority, Risley, Eng.). Metallurgia, 72: 165-77(Oct. 1965).

Low- and medium-volume nuclear cermets, possessing a continuous metallic matrix, and having no real bond with the ceramic phase, are shown to resemble the matrix metal in their manner of plastic deformation, and to resemble voided metal in their tensile stress properties. Their macroscopic ultimate tensile stress is proportional to the minimum matrix load-bearing section. The achievable strength of a well-consolidated cermet can be calculated from the minimum matrix cross-sectional area presented at an equatorial section through a plane of spheres, equivalent in volume to that of the ceramic investment, packed in a simple cubic lattice. The concept of a "minimum matrix interstitial volume" is introduced, which appears to account quantitatively for the observed decrease in cermet tensile elongation values to fracture as the ceramic volume is increased. Cermet elastic constants, and the reduction of area in the fracture zone, appear to be influenced by the comparative incompressibility of the ceramic phase particles. It is postulated that the measured mechanical properties of nuclear cermets provided a reliable indication of the metallurgical quality and of the potential integrity under irradiation. (auth)

**2382** DEVELOPMENT OF ZIRCONIUM DIOXIDE BASE REFRACTORY MATERIALS. Gel'man, V. A. Ogneupory, No. 6, 39-42(1965). (In Russian).

The composition of an electrofused zirconium alumina refractory material, possessing high stability to the fusion of refractory aluminum silicate glass at 1750°C, was worked out. With the purpose of testing this refractory material industrial glass furnaces designed for cooking glass at temperatures higher than 1750°C and industrial technology for its manufacture were developed. (tr-auth)

**2383** METALLIC HEAT CONDUCTIVITY BELOW 1 deg K. Lindenfeld, P.; Lynton, E. A.; Soulen, R. (Rutgers Univ., New Brunswick, N. J.). Phys. Lett., 19: 265(Nov. 1, 1965).

The thermal conductivity of a moderately pure copper specimen and of a dilute indium–tin alloy was measured down to 0.45°K. No departures from the expected variation with temperature were found within the accuracy of (±1%) of the experiment. In the temperature range below 1.5°K, the curves of K/T against T for all specimens are straight horizontal lines, indicating an electronic conductivity limited entirely by elastic scattering. The curve for In–Sn shows a slight upward trend above 1.5°K corresponding to the expected lattice conductivity. In no case was there any evidence for an anomalous deviation greater than one per cent. (J.F.P.)

**2384** X-RAY PHASE ANALYSIS OF BINARY OXIDES IN THE $UO_2$–$MoO_2$–$MoO_3$ SYSTEM. Kovba, L. M.; Trunov, V. K. Radiokhimiya, 7: 316-19(1965). (In Russian).

The system $UO_2$–$MoO_2$–$MoO_3$ was investigated by x-ray phase analysis. The formation of the binary oxides $UMo_2O_8$, $UMo_7O_{22}$, and $UMo_{11}O_{35}$ was established. The lattice parameters of the binary oxides obtained were determined and it is shown that they have the same sub-cell. (tr-auth)

**2385** NEW COMPOUNDS OF THE $MgCu_2$ TYPE IN ALLOYS OF RARE-EARTH METALS WITH Fe, Co, AND Ni. Kripyakevich, P. I.; Teslyuk, M. Yu.; Frankevich, D. P. (Moscow State Univ.). Soviet Phys.-Cryst. (Engl. Transl.), 10: 344-5(Nov.-Dec. 1965).

Translated from Kristallografiya, 10: 422-3(May-June 1965).

$TbFe_2$, $LuFe_2$, $YbCo_2$, $LuCo_2$, $TmNi_2$, and $LuNi_2$ alloys were prepared in an arc furnace with a cooled copper base from rare-earth metals and Fe, Co, and Ni. X-ray structural examination of nonheat-treated samples showed a cubic face-centered structure. The lattice spacings are tabulated, which were determined from x-ray diffraction photographs with asymmetrical packing. The conclusion that the compounds have the $MgCu_2$-type structure was confirmed by a comparison of the x-ray line intensities for the $LuFe_2$ alloy with those calculated for $MgCu_2$. (L.B.S.)

**2386** IMPROVED METALLIC FAST POWER BREEDER FUELS. Kelman, L. R.; Savage, H.; Walter, C. M.; Blumenthal, B.; Dunworth, R. J.; Rhude, H. V. (Argonne National Lab., Ill.). Trans. Amer. Nucl. Soc., 8: 347-8(Nov. 1965).

**2387** THERMAL CONDUCTIVITY OF GRAPHITE. Carter, Robert L. (Univ. of Missouri, Columbia). Trans. Amer. Nucl. Soc., 8: 368-9(Nov. 1965).

**2388** LOW-TEMPERATURE DUCTILITY AND STRENGTH OF VAPOR-DEPOSITED TUNGSTEN. Schaffhauser, A. C. (Oak Ridge National Lab., Tenn.). Trans. Amer. Nucl. Soc., 8: 369-70(Nov. 1965).

**2389** FISSION-PRODUCT BEHAVIOR IN FUEL-ELEMENT CLADDING MATERIALS. Morrison, D. L.; Howes, J. E. Jr.; Sunderman, D. N.; Gilchrist, Ed (Battelle Memorial Inst., Columbus, Ohio). Trans. Amer. Nucl. Soc., 8: 373-4(Nov. 1965).

**2390** DETERMINATION OF THE MELTING POINT OF $UO_{2+x}$. Latta, R. E.; Fryxell, R. E. (General Electric Co., Cincinnati). Trans. Amer. Nucl. Soc., 8: 375 (Nov. 1965).

**2391** THE MELTING POINT OF PLUTONIA–URANIA MIXED-OXIDE FUELS. Lyon, W. L.; Baily, W. E. (General Electric Co., San Jose, Calif.). Trans. Amer. Nucl. Soc., 8: 376(Nov. 1965).

**2392** NEW EVIDENCE TO DELINEATE THE $UO_2$ MOLTEN BOUNDARY. Lyons, M. F.; Weidenbaum, B.; Hausner, H.; Pashos, T. J. (General Electric Co., Pleasanton, Calif.). Trans. Amer. Nucl. Soc., 8: 376-8(Nov. 1965).

**2393** A DEVICE FOR OUTPILE THERMAL SIMULATION OF REACTOR-FUEL MICROSTRUCTURES. Kerr,

J. M.; Harbinson, E. N.; Johnson, C. R. (Babcock and Wilcox Co., Lynchburg, Va.). Trans. Amer. Nucl. Soc., 8: 386-7(Nov. 1965).

**2394** HIGH-TEMPERATURE CREEP OF TANTALUM. Green, W. V. (Los Alamos Scientific Lab., N. Mex.). Trans. Met. Soc. AIME, 233: 1818-25(Oct. 1965). (LA-DC-7099).

Creep of tantalum was measured at temperatures from 0.6 to 0.89 of the absolute melting temperature. The creep curves included first, second, and third stages. Steady-state creep rate depended on the fourth power of stress. The activation energy for creep throughout this temperature range was approximately 114 kcal per mole, measured by the ΔT technique. Subgrain formation occurred as a result of creep strain, and pile-up dislocation arrays were observed in etch-pit patterns. (auth)

**2395** THE EFFECT OF HEAT TREATMENT ON THE MICROSTRUCTURE AND SUPERCONDUCTING PROPERTIES OF A 45 percent Nb (Cb)-55 percent Zr ALLOY. Shukovsky, H. B. (Massachusetts Inst. of Tech., Cambridge); Ralls, K. M.; Rose, R. M. Trans. Met. Soc. AIME, 233: 1825-32(Oct. 1964).

Studies of the phase structure, critical current density, and resistive critical magnetic field of a 45% Nb–55% Zr superconducting alloy after final-size heat treatments are reported. A combination of optical metallography, x-ray diffraction, and electrical-resistivity measurements were used to determine the phase structure. Superconductivity measurements, made with heat-treated wires, were correlated with microstructure. Although no quantitative relationship between microstructure and critical current density was found, it is shown that the critical current density is highest when the microstructure is finely divided by fibering, coring, precipitation, or fine-scale phase dispersions. The resistive critical field was very sensitive to the compositions of the phases present. Since the alloy investigated was near the maximum resistive critical field for the Nb–Zr system, any phase decomposition resulted in lower $H_r$. Elimination of the effects of cold work lowered $H_r$ also. A possible interpretation of the latter in terms of internal surface superconductivity is suggested. (auth)

**2396** EFFECTS OF GRAIN SIZE ON TENSILE AND CREEP PROPERTIES OF ARC-MELTED AND ELECTRON-BEAM-MELTED TUNGSTEN AT 2250 deg TO 4140 deg F. Klopp, William D.; Witzke, Walter R.; Raffo, Peter L. (Lewis Research Center, Cleveland). Trans. Met. Soc. AIME, 233: 1860-6(Oct. 1965).

The tensile and creep properties of arc-melted and electron-beam-melted tungsten over the temperature range from 2250 to 4140°F were studied. The tensile and creep strengths varied with grain size with the finer-grained materials the stronger. The activation energy for transient creep at 2250 to 3500°F was 95,000 cal per (g) (mole), while that for steady creep at 3300 to 4000°F was 141,000 cal per (g) (mole). At 2875 to 3300°F the apparent activation energy for steady creep decreased with decreasing temperature. It is suggested that cross slip is rate controlling during transient creep, while dislocation climb is rate controlling during steady creep above 3300°F. (auth)

**2397** THERMAL DIFFUSION OF DISSOLVED HYDROGEN ISOTOPES IN IRON AND NICKEL. Gonzalez, O. D.; Oriani, R. A. (U. S. Steel Corp., Monroeville, Pa.). Trans. Met. Soc. AIME, 233: 1878-86(Oct. 1965).

A thermo-osmosis technique was used to measure the heat of transport, Q*, of hydrogen and of deuterium dissolved in α-iron and in nickel, and of hydrogen in $\gamma$-$Fe_{0.6}Ni_{0.4}$ in the temperature range from 400 to 600°C. For all these systems, Q* was negative and had a large temperature coefficient; an isotope effect could be established for the solutes only in nickel. The magnitude of Q* was considerably larger than the activation energy, E, for migration in the case of these isotopes in α-iron, so that all variants of the Wirtz model must be rejected. The phenomenological definition of Q* was developed to show that Q* is related to the mechanisms by which the activation energy is dissipated back into the lattice, and that Q*/E is a function of the ratios of the mean free paths of electrons and of phonons to the distance of jump of the diffusing atom. A correlation is shown to exist between the sign of Q* in thermal diffusion and that of the effective charge in electromigration, and may be understood as due to the large ratio of the mean free path of electrons to that of phonons. (auth)

**2398** DETERMINATION OF DIFFUSIVITY OF CARBON IN TANTALUM AND COLUMBIUM CARBIDES BY LAYER-GROWTH MEASUREMENTS. Resnick, R.; Steinitz, R.; Seigle, L. (General Telephone and Electronic Labs., Inc., Bayside, N. Y.). Trans. Met. Soc. AIME, 233: 1915-18(Oct. 1965).

The rates of growth of the carbide phases MC and $M_2C$ in the Ta–C and Nb–C systems were measured at various temperatures and the results used to estimate the rate of carbon diffusion in the intermetallic phases. Sheets of high-purity tantalum (50 ppM Nb, <25 ppM Ti, 10 ppM Fe, 5 ppM Cr, <50 ppM Mo, W, and all other metals, 15 to 75 ppM $O_2$, 10 to 30 ppM $N_2$, and 10 to 30 ppM C) were heated to temperatures between 1800 and 2700°C in a carbon resistor furnace under an atmosphere of argon plus methane to maintain an excess of carbon at the sample surface. The thicknesses of the carbide layers were measured with a filar micrometer and plotted logarithmically as a function of time. The equations used to calculate the layer thicknesses are given. The activation energy for diffusion in NbC was close to that obtained for TaC. Values of the diffusivity of carbon in $Nb_2C$, calculated from layer-growth data, decreased with increasing temperature. According to the previously published phase diagrams, $\Delta C_2$ for this phase increases by a factor of 20 between 1900 and 2300°C. The increase in $\Delta C_2$ should be accompanied by a proportionate increase in $k_2$, but this was evidenced in the measured layer-growth data, thus indicating a possible error in the location of the phase boundaries. (F.J.H.)

**2399** MODIFICATION OF MAGNESIUM ALLOYS WITH ZIRCONIUM AND LANTHANUM. Lashko, N. F.; Morozova, G. I.; Tikhova, N. M. Tsvetn. Metal., No. 9, 79-82(Sept. 1965). (In Russian).

The fine-grained structure of magnesium alloys containing Zr was not due to the separation of α-Zr via a peritectic reaction, but was probably due to the formation of a refractory zirconium compound, or an intermetallic compound. In the Mg–Zn–Zr–lanthanide system, intermetallic compounds Zn(Zr, lanthanide) were formed lattice parameters varying from 3.336 to 3.76 Å. Thus, the Zn(Zr,La) phase with a CsCl type of structure had a lattice parameter of 3.45 Å. A Mg alloy containing 2.6% Nd had a relatively large grain size compared to the same alloy containing an additional 0.5% Zr. The growth in grain size of many Mg alloys was limited by a high eutectic temperature and by a low solubility of alloying element. Thus, Zn and Al with low eutectic temperatures of 341 and 436°C, respectively, and with high solubilities of 3.3 and 11.5 at. % in Mg alloys formed Mg alloys with a large grain size. Nd and Ce with eutectic temperatures of 552 and 590°C, respectively, and with low solubilities of 0.4 to 0.6 and 0.13 to 0.3 at. %, respectively, in Mg alloys gave fine-grained structures in Mg alloys. The phases $Mg_{12}Ce$ and $Mg_{12}Nd$ with a $Mg_{12}Th$ type of structure were formed in these systems. (TTT)

**2400** TERNARY URANIUM(V) OXIDES. Kemmler, Sibylle (Universitaet, Tuebingen, Ger.). Z. Naturforsch., 20b: 599(June 1965). (In German).

The crystal structure and densities of the ternary uranium(V) oxides $MnU_2O_6$, $CoU_2O_6$, and $NiU_2O_6$ are reported. The black $MnU_2O_6$ has a cubic fluoride structure and is isomorphic with the other two oxides. The dark brown $CoU_2O_6$ crystallizes in hexagonal form. The reddish brown $NiU_2O_6$ is isomorphic with $CoU_2O_6$ with which it forms mixed crystals. (J.S.R.)

**2401** THE SIGNIFICANCE OF RECENT DEVELOPMENTS IN FRACTURE MECHANICS IN GREAT BRITAIN

IN RELATION TO THE SAFETY OF REACTOR PRESSURE VESSELS. Irvine, W. H. (United Kingdom Atomic Energy Authority, Risley, Eng.). pp 429-37 of Flow and Fracture of Metals and Alloys in Nuclear Environments. ASTM Special Technical Publication No. 380. Philadelphia, American Society for Testing and Materials, 1965.

Theoretical and experimental evidence suggested that fast fracture in plated structures is controlled by structural behavior and material properties. Recent work involving tests to failure on 5-ft dia, 14-ft long, cylindrical steel pressure vessels containing 6 to 24-in. long slits, confirmed that for constant-load conditions (such as those existing in a pneumatic test) crack arrest does not occur; while under conditions nearer to the constant-strain case (such as those in a hydraulic test), the extent of crack propagation was controlled by fracture toughness and total energy available. In addition, the work indicated that a correlation of the form $f_s^2 l^2$ = function of $(\phi, f_y, f_u)$ exists between the critical parameters, crack length l, gross stress $f_s$, Charpy energy absorption $\phi$, yield stress $f_y$, and ultimate tensile stress $f_u$. When considered in conjunction with the relationship between the main parameters and plastic zone size, this correlation suggested that, in addition, the critical condition was affected by the path along which instability was approached; for instance, by increase in crack size, increase in stress, or change in material properties. Since energy availability controls fracture appearance through plastic zone size, strain rate, and crack speed, cleavage and shear fracture may exist side by side at the same temperature, and it was suggested that the interpretation of service and test failures of steel structures should be based on an analysis of factors such as load history, stress level, flaw size, and Charpy value, rather than on a fracture appearance temperature approach. The safety implications of these effects in relation to proof testing, annealing out of radiation damage and material monitoring are discussed. (auth)

**2402** THE IMPORTANT MATERIALS PARAMETERS AFFECTING THE PERFORMANCE OF NUCLEAR REACTOR PRESSURE VESSELS. Wylie, R. D. (Southwest Research Inst., San Antonio, Tex.). pp 438-50 of Flow and Fracture of Metals and Alloys in Nuclear Environments. ASTM Special Technical Publication No. 380. Philadelphia, American Society for Testing and Materials, 1965.

The two failure mechanisms of most concern in nuclear reactor pressure vessels are brittle fracture and low-cycle fatigue. Steel selection and fabrication history determine the properties of the vessel prior to service. The ability to detect defects incident to vessel fabrication is an important factor in fracture consideration. Suggestions are made relative to an engineered selection of nondestructive-test requirements dependent on stress level. (auth)

**2403** THE EQUILIBRIUM PHASE DIAGRAMS FOR THE TANTALUM–TANTALUM BROMIDE AND TANTALUM–TANTALUM IODIDE SYSTEMS [Thesis]. Boatman, James Claude. Ames, Iowa, Iowa State Univ. of Science and Tech., 1964. 95p.

The tantalum-tantalum bromide and the partial tantalum-tantalum iodide equilibrium phase diagrams were obtained using differential thermal analysis, x-ray powder diffraction, solubility experiments, and equilibrium experiments. Four phases other than $TaBr_5$ were found in the tantalum-tantalum bromide system, i.e., $TaBr_4$, $TaBr_{2.83}$, $TaBr_{2.5}$, and $Ta_6Br_{14}$. The phases that were found other than $TaI_5$ in the tantalum-tantalum iodide system were $TaI_4$ and $Ta_6I_{14}$. (TCO)

**2404** REACTIONS OF URANIUM CARBIDE IN A FUSED KCl–LiCl/ZINC SYSTEM [Thesis]. Robinson, William Courtney Jr. Ames, Iowa, Iowa State Univ. of Science and Tech., 1964. 132p.

The reaction of uranium monocarbide with liquid zinc was investigated in the temperature range of 540-800°C. At temperatures below 725°C the uranium monocarbide reacts with the liquid zinc to form a uranium-zinc compound and an oxygen enriched uranium monocarbide phase. There is no reaction at 800°C. This indicates that the standard free energy of formation of uranium monocarbide is equal to the free energy of $UZn_{8.5}$ at about 725°C. No other uranium carbide phase was ever observed as a reaction product. The reactions of uranium monocarbide in a $LiCl-KCl-ZnCl_2$/zinc system were investigated in the temperature range 580-802°C. The salt phase was analyzed for uranium and zinc and the mole fraction ratio $K_N = N_{UCl_3}/(N_{ZnCl_2})^3$ was calculated. The $K_N$ proved to be a function of the moles $ZnCl_2$/moles UC charged with the uranium remaining in the zinc phase present as an oxygen enriched uranium monocarbide at values of $K_N$ greater than 20 and as $UO_2$ at values of $K_N$ less than 15. All of the uranium in the uranium monocarbide charged was never oxidized into the salt even when $K_N$'s as low as 0.21 were obtained. These results indicate that the uranium monocarbide lattice is being stabilized by oxygen. An EMF cell of the type $U/LiCl-KCl-UCl_3/UO_xC_{1-x}$, C was utilized to investigate the increase in chemical potential of uranium in the uranium oxycarbide phase as a function of oxygen composition from 0.35 to 0.82 mole fraction UO and temperature from 460 to 760°C. Extrapolation of the data obtained to zero oxygen concentration was found to yield the free energy of formation of UC as a function of temperature. The equation obtained was $\Delta F^0_{UC} = -16{,}915 - 1.90T$. (Dissertation Abstr.)

**2405** CONDUCTION CHARACTERISTICS OF TANTALUM OXIDE FILMS [Thesis]. Feisel, Lyle Dean. Ames, Iowa, Iowa State Univ. of Science and Tech., 1964. 74p.

Observations are reported on the electric conduction characteristics of a $Ta_2O_5$ film as the insulating material in a metal-insulator sandwich. A model of a metal-insulator interface is formulated. The phenomenon of negative resistance and the use of a metal-insulator-metal sandwich as a cold cathode emitter are treated. (TCO)

**2406** GRAIN REFINED BERYLLIUM. (to Stauffer Chemical Co.). British Patent 1,005,436. Sept. 22, 1965. Priority date Sept. 29, 1960, United States.

Beryllium containing 0.01–0.3% by weight of boron uniformly incorporated in it is fine-grained, fabricable, and weldable. The two materials are mixed in a finely divided state, melted under vacuum, and allowed to solidify. Finely divided Al may also be added to the mixture to combine with any oxygen present as an impurity. (A.G.W.)

**2407** NIOBIUM ALLOYS. Begley, Richard T.; Buckman, Raymond W. Jr.; Ammon, Robert L. (to Westinghouse Electric Corp.). U. S. Patent 3,206,305. Sept. 14, 1965. Filed Feb. 25, 1963.

Niobium base alloys characterized by high strength at elevated temperatures and good hot and cold working properties consist of 20 to 40 wt % Ta, 2 to 20 wt % V, up to about 5 equivalent % by weight of one of the two, Hf or Zr, and the balance Nb. The equivalent % of Hf or Zr is determined by the equation: Zr % + ½ Hf % = equivalent %. (B.L.M.)

# Radiation Effects

## See *also* CHEMISTRY — Radiation Chemistry

*Refer also to abstracts 2030, 2036, 3309, and 3496.*

**2408** (AD-614899) IRRADIATION EFFECTS ON REACTOR STRUCTURAL MATERIALS. Period Covered: November 1, 1964–January 31, 1965. Steele, L. E.; Hawthorne, J. R.; Serpan, C. Z. Jr.; Klier, E. P.; Watson, H. E. (Naval Research Lab., Washington, D. C.). Feb. 15, 1965. Contract AF49(5)-2110. 25p. (NRL-MR-1593). CFSTI $1.00 cy, $0.50 mn.

Results are reported for: simultaneous irradiation of five heavy section plates of A302-B steel; comparative irradiation of Charpy-V specimens of weld heat affected zone and base plate of A212-B and A302-B steel, and progress in the continuing study of the effects of nuclear environment upon properties of reactor steels including irradiation of capsules in the Heavy Water Components Test Reactor, re-

moval of the grid plate of the Organic Moderated Reactor Experiment, and disassembly and examination of surveillance capsules from the Big Rock Point Reactor. (auth)

**2409** (AD–617319) IRRADIATION EFFECTS ON REACTOR STRUCTURAL MATERIALS, 1 FEBRUARY–30 APRIL 1965. Quarterly Progress Report. Steele, L. E.; Hawthorne, J. R.; Watson, H. E. (Naval Research Lab., Washington, D. C.). May 15, 1965. Contract AT49(5)-2110. 32p. (NRL-Memo–1611). CFSTI $2.00 cy, $0.50 mn.

Information is reported on: irradiation embrittlement of several heats of ASTM Type A302-B steel at 550 F; notch ductility and tensile properties of an Fe-Cr-Al-Y alloy before and after irradiation; simultaneous irradiation of Charpy-V and drop weight specimens of A212-B, A302-B, and A350-LF1 (Modified) steels; effect of stress during irradiation on the notch ductility of A350-LF1 (Modified) steel; and a remotely operated milling machine for hot cell operations. (auth)

**2410** (AD–617918) TABLES OF CAPACITOR DISCHARGE IN TRANSIENT GAMMA RADIATION ENVIRONMENTS. Landis, DeWitt (Lockheed Missiles and Space Co., Sunnyvale, Calif.). Mar. 1, 1965. 185p. CFSTI $5.00 cy, $1.25 mn.

Data on the response of various types of capacitors to various transient gamma radiation environments are tabulated. The tables were generated on the Burroughs B5500 digital computer at Stanford University. The capacitor parameters represent only the average response of many similar capacitors to many different radiation environments. Unit-to-unit and manufacturer-to-manufacturer variations in the capacitors make it impossible to predict the effects of radiation exactly, so the tables should be considered as giving only a typical response of the particular capacitor to the given radiation environment. Assuming, however, that the capacitor parameters used are exact, then it is believed that the numbers given in the tables, with a few exceptions, are accurate to three significant figures. Additional tables are given on the voltage left across a capacitor at various times after t = O for a fixed resistance shorted across the capacitor at time t = O. (TAB)

**2411** (AD–618078) SEMICONDUCTOR DESIGN EFFECTS ON RADIATION RESISTANCE. Quarterly Report No. 1, December 15, 1964–March 15, 1965. Belardi, Richard J.; Honnold, Vincent R. (Hughes Aircraft Co., Newport Beach, Calif. Research, Development and Engineering Dept.). Contract DA28 043AMC00418E. 53p. CFSTI $3.00 cy, $0.75 mn.

All the standard 2N708 transistors and all of the special transistors, except the PNP, were fabricated. These special devices, incorporating a total of fourteen surface variations, were organized under the following general categories: surface damage, epitaxial layers, thermal oxide layers, pyrolytic oxide layers, and surface potential changes. The test circuit used with the Hughes Linac for measuring the radiation response was designed to limit to a minimum the interference from electromagnetic noise and the circuit time constant and still provide sufficient signal strength. Irradiation data were obtained on a total of six surface variations with the experimental error (as indicated by root-mean square deviations) less than 3%. Although specific conclusions concerning the numerous surface variations cannot be made until all the special devices have been irradiated and the data statistically analyzed, initial data tends to indicate that surfaces which are more satisfactory from a device manufacturing veiwpoint are also more satisfactory from a transient radiation environment. (auth)

**2412** (AD–618079) STUDY FOR GENERALIZED MODEL FOR SEMICONDUCTOR RADIATION RESPONSE PREDICTION. Quarterly Progress Report No. 1, December 15, 1964–March 15, 1965. Raymond, James P.; Chang, William W. (Northrop Corp., Van Nuys, Calif.). June 1965. Contract DA28 043AMC00423E. 146p. (NVR–3840; ECOM–00423-1). CFSTI $5.00 cy, $1.00 mn.

The lumped-model technique was applied to the characterization of the radioinduced transient response observed in diodes and transistors. A significant result of the diode analysis was the comparison of the lumped-model response to the solution of the differential equations in describing the diode photocurrent. Application of the lumped-model analysis to the ionizing radiation effects in a grown junction transistor was also straightforward and encouraging. A general expression for the common-emitter transient response was developed in terms of the transistor and common-emitter circuit parameters. This expression allows the calculation of the total transient collector photocurrent as a function of the source resistance, and the quiescent operating current. The experiments necessary to determine the diode and transistor lumped-model parameters were defined. These experiments were completed with the grown-junction transistors specimens, completing the information required for numerical prediction of the transistor response. (auth)

**2413** (AD–618688) LABORATORY EXPERIMENTAL ANALYSIS OF GAMMA RADIATION EFFECTS ON SILICON ALLOY JUNCTION SEMICONDUCTOR DIODES. Frank, Burton V. (Picatinny Arsenal, Dover, N. J. Nuclear Engineering Directorate). May 1965. 148p. (TM–1633; SMUPA-TK–935). CFSTI $4.00 cy, $1.00 mn.

The behavior of silicon diodes of the alloy-junction type was examined, during gamma irradiation, in terms of basic diode theory, and radiation induced effects in bulk semiconductor materials. Some twenty-seven IN483B Diodes were exposed to a constant gamma dose rate of 1,000,000 Roentgens per hour from a 9,110 Curie cobalt-60 source under constant geometry test conditions. Measurements were made at various gamma dose levels ranging up to $1.67 \times 10^8$ Roentgens, corresponding to an irradiation exposure time of 167 hours. As was expected, the change in the reverse diode characteristics was significant, whereas there was negligible change observed in the forward diode characteristics. Correlation between the semiquantitative predictions from diode theory and actual experimental data indicate that the transient effects of gamma radiation on silicon diodes are relatively predictable. The procedure developed for predicting the ionization current is summarized. Diode post-irradiation recovery measurements, under reverse bias conditions, showed that the diode is directly affected by the exposed gamma dose. (auth)

**2414** (AECL–2272) THE EFFECT OF NEUTRON IRRADIATION AND HYDROGEN CONCENTRATION ON TENSILE PROPERTIES OF THE CANDU COOLANT TUBE SPACER ALLOY. Ells, C. E.; Sawatzky, A. (Atomic Energy of Canada Ltd., Chalk River (Ontario)). June 1965. 28p. Dep.; AECL $1.00.

The effect of neutron irradiation on tensile properties of the Zr–2.5 wt % Nb–0.5 wt % Cu alloy was evaluated for neutron fluxes up to $3 \times 10^{20}$ n/cm$^2$ (E > 1.0 Mev). Specimen temperature during irradiation was normally 300°C. The material was studied in a heat treated condition, quenched from ≈40°C below the $\beta$-transus and aged 6 hrs at 535°C. Hydrogen concentrations up to 250 ppm were used in some tests. The dose dependence of hardening followed the saturation equation proposed by Makin and Minter, $\Delta\sigma = A[1 - \exp(-B\phi)]^{\frac{1}{4}}$, with a saturation increment of 27,000 psi in the 0.2% yield stress above the unirradiated value of ≈75,000 psi at 300°C. Irradiation up to the maximum studied had little effect on reduction in area, although the uniform elongation was decreased. Increasing the hydrogen concentration had very little effect on the tensile properties in the unirradiated condition, but tended to lower the reduction in area of specimens irradiated to ≈$10^{20}$ n/cm$^2$. (auth)

**2415** (AECL–2276) HIGHLY RATED HOLLOW $UO_2$ PELLETS IRRADIATED IN COLLAPSIBLE SHEATHING—DIMENSIONAL STABILITY, METALLOGRAPHY AND AUTORADIOGRAPHY. Bain, A. S. (Atomic Energy of Canada Ltd., Chalk River (Ontario)). July 1965. 45p. Dep.; AECL $1.50.

Hollow $UO_2$ pellets were sheathed in collapsible Zircaloy-2, then irradiated at power ratings which produced central temperatures estimated to range from 2400 to over 2800°C (melting point of $UO_2$). The axial voids were either 4 or 0.5% of the volume of the fuel. A 4 vol % void significantly reduced the diametral expansion of the sheath, but if melting of the $UO_2$ occurred, appreciable ovality was measured. With 0.5 vol % voids the diametral expansions were similar to those obtained from solid pellet fuel with the same central temperatures. Two elements failed during the first loading. One failure was attributed to sheath corrosion brought on by the high surface heat fluxes, combined with coolant flow disruption due to sheath ovality, and lack of a fairing section directly upstream. The other failure occurred where a small section of sheathing collapsed into a gap formed when the outward movement of $UO_2$ fragments was not even. Examination of fractured and polished cross sections defined a limit of melting of the $UO_2$ at reactor shutdown; from the data a value of $\Lambda$ (500, 2800°C) of 71.5 W/cm was calculated. Autoradiography of some polished cross sections showed an active ring outside the area that was considered molten at reactor shutdown. Taking this as the limit of melting at maximum power output a value of $\Lambda$ (500, 2800°C) of 69.5 W/cm was calculated. An average of these yielded a value of $\Lambda$ (500, 2800°C) = 70.5 ± W/cm. (auth)

**2416** (AECL–2289) MELTING OF $UO_2$ DURING IRRADIATIONS OF SHORT DURATION. Bain, A. S.; Aragones, M.; Guerrero, H. (Atomic Energy of Canada Ltd., Chalk River (Ontario)). Aug. 1965. 22p. Dep.; AECL $1.00.

Six elements were irradiated for ten minutes in the Hydraulic Rabbit of NRX. The power ratings were sufficient to cause central melting of the $UO_2$ fuel. Four of the elements contained 1 volume percent tungsten spheres in the $UO_2$. When the $UO_2$ melted, the tungsten spheres sank and settled at the demarcation between the melted and non-melted fuel. From these results it was concluded that in $UO_2$ irradiated at constant power for ten minutes the limit of melting is the boundary between the central zone and the dense band of $UO_2$, as observed most easily on fractured cross-sections. (auth)

**2417** (BNWL–112) HIGH-TEMPERATURE GRAPHITE IRRADIATIONS: 800 TO 1200 deg C. Interim Report No. 1. Helm, J. W. (Battelle-Northwest, Richland, Wash. Pacific Northwest Lab.). Sept. 1965. Contract AT(45-1)-1830. 79p. Dep. mn; CFSTI $3.00 cy, $0.75 mn.

A temperature-monitored irradiation test was conducted in the K7 position of the Engineering Test Reactor (ETR) to determine the behavior of several types of graphite at temperatures from 800 to 1200°C and neutron exposures up to $4.5 \times 10^{21}$ nvt, E > 0.18 Mev. Mean sample temperatures agreed within ±100°C from one reactor cycle to the next. The graphites irradiated were: conventional-coke graphites, CSF and TSGBF; needle-coke graphites, KC, EGCR, and TSX; and raw-coke graphites, 63-16, 63-17, and 63-38. The physical distortion of the graphites tested showed a dependence on the temperature of irradiation, although this varied considerably for the various graphites. All the transverse samples of the conventional and needle-coke graphites contracted except one TSGBF sample, which expanded 3.3%. The samples irradiated at 1200°C generally contracted more than those at 800°C. The samples of the raw-coke graphites contracted much less than those of the other graphites and in some cases expanded slightly in both the transverse and parallel orientations. The raw-coke graphites, which all had nearly the same initial CTE and were very isotropic, showed differences in irradiation behavior, indicating the less-graphitic phase has an effect on the radiation-induced physical distortion. (P.C.H.)

**2418** (CEA-R–2801) CONSIDERATIONS GENERALES SUR LES IRRADIATIONS D'ECHANTILLONS DANS LES REACTEURS. (General Views About Sample Irradiations in Reactors). Seguin, Maurice (Commissariat a l'Energie Atomique, Grenoble (France). Centre d'Etudes Nucleaires). July 1965. 38p. Dep. mn.

Irradiation of fissile or non-fissile materials, carried out under circumstances becoming more and more severe in reactors of increasing flux is resulting in an evolution of irradiation rigs. A survey of problems arising from irradiating under various circumstances leads to the conclusion that it is possible to devise one capsule type suitable to every particular case, and for a wide temperature range. Consequently, once the various irradiation parameters are known, a general method of calculation can be followed so as to determine the various sizes of the parts of the capsule. These calculations might sometimes be corrected through benefits gained from previous irradiations. (auth)

**2419** (DP–973) DEPLETION OF DEIONIZER RESIN IN AN SRP REACTOR SYSTEM. Baumann, Elizabeth W. (Du Pont de Nemours (E. I.) and Co., Aiken, S. C. Savannah River Lab.). Aug. 1965. Contract AT(07-2)-1. 14p. Dep. mn; CFSTI $1.00 cy, $0.50 mn.

An axial core section was removed from a depleted deionizer from an SRP reactor system, and the ion exchange resins were examined for absorbed ions, retained solids, and residual and regenerable exchange capacity. Total depletion of the initial capacity of the cation exchange resin was 60% and that of the anion exchange resin was 90%. Destruction of exchange sites by radiation and absorption of resin degradation products accounted for 30% of the depletion of each resin. (auth)

**2420** (DPST–65–83–8) USAEC–AECL COOPERATIVE PROGRAM. Monthly Progress Report, August 1965. Hilborn, H. S. (comp.) (Du Pont de Nemours (E. I.) and Co., Aiken, S. C. Savannah River Lab.). Sept. 30, 1965. Contract AT(07-2)-1. 7p. Dep. mn; CFSTI $1.00 cy, $0.50 mn.

Cracks that occurred in Zircaloy-2 tubing while in a reactor are produced by bending the adjacent area of the tube after removal from the reactor were examined with an electron microscope. Preliminary results indicate that the irradiated Zr matrix exhibits low macroscopic ductility because no strain hardening occurs. Plastic strain is initiated in one area and continues there until fracture. (W.L.G.)

**2421** (EXP-NRX–22902) RE-IRRADIATION OF A HIGH BURN-UP $UO_2$–ZIRCALOY FUEL ELEMENT AT AN INCREASED HEAT RATING. MacDonald, R. D. (Atomic Energy of Canada Ltd., Chalk River (Ontario)). July 1965. 31p. (AECL–2277). Dep.; AECL $1.00.

Element LT, having achieved a burnup of approximately 8500 Mwd/U at an average $\int \lambda d\theta = 29$ W/cm during the X-2-t test, was re-irradiated for an additional reactor cycle at a 50% greater heat rating ($\int \lambda d\theta$ about 45 W/cm). During this final cycle, the element diameter increased 0.4% over its previous value. Enough residual ductility remained in the sheath of LT at its operating temperature to allow this additional strain to be accommodated without a cladding failure. The extent of discernible grain growth probably increased slightly after the final cycle, but measurement errors made the conclusion uncertain. Almost no additional grain growth took place in the $UO_2$ near the center of the pellets. The fission xenon release, 21% of that formed, was similar to the amount that would have been expected had the element been punctured at the conclusion of the X-2-t test. (auth)

**2422** (GEMP–52A, pp 11-21) EFFECT OF RADIATION ON REFRACTORY METALS AND ALLOYS. (General Electric Co., Cincinnati, Ohio. Nuclear Materials and Propulsion Operation).

Creep-rupture tests of W–25Re sheet material at 850°C showed that the rupture lives of irradiated specimens ($2 \times 10^{19}$ nvt, $E_n \geq 1$ Mev) were greater than those of control specimens by a factor of approximately 20. The Grant–Monkman equation relating rupture time and minimum creep rate was shown to be applicable to the W–25Re data in the 800 to 900°C temperature range. The control and the irradiated data gave a reasonable fit to the equation even though there were differences in the strengths of the various materials. Hot-hardness measure-

ments of W single crystals irradiated to three fast neutron dosage levels showed that a significant change in the nature of the irradiation-induced defects and in their influence on the hardness properties occur in the dosage region of approximately $2.4 \times 10^{19}$ to $7.3 \times 10^{19}$ nvt. Room-temperature hardness values following elevated temperature anneals of W single crystals irradiated to a fast neutron dose of approximately $7.3 \times 10^{19}$ nvt increased about 23% over the values observed in the as-irradiated specimens after annealing at temperatures up to 500°C. Tensile tests of polycrystalline W specimens irradiated at reactor ambient temperatures to a fast neutron dose of approximately $1.1 \times 10^{20}$ nvt showed that the brittle-to-ductile transition temperature is increased by about 300°C with a ductile fracture occurring at about 500°C in the irradiated specimens. (W.L.G.)

**2423** (GEMP-52A, pp 27-35) EFFECT OF RADIATION ON HEAT RESISTANT METALS AND ALLOYS. (General Electric Co., Cincinnati, Ohio. Nuclear Materials and Propulsion Operation).

Irradiation of Hastelloy N specimens at 650°C for one-half of an ETR cycle plus the remainder at reactor ambient temperatures appears to further reduce the rupture life of the specimens when compared to those which were irradiated for a full ETR cycle at reactor ambient temperatures. Annealing Hastelloy N control and irradiated specimens at 870°C for 4 hours tends to improve the ductility but not the rupture life of specimens when tested at 650°C. This heat treatment, however, did increase the time of the control specimen and decreased the time to rupture of the irradiated specimen when tested at 815°C. (auth)

**2424** (GEMP-52A, pp 37-42) RADIATION EFFECTS IN BeO. (General Electric Co., Cincinnati, Ohio. Nuclear Materials and Propulsion Operation).

Measurements to determine the soaking times required in density determinations of BeO indicated that 4 hrs soaking following vacuum impregnation was adequate for bulk density measurements with diethylphthalate and that 100 hrs soaking was required for apparent density measurements with toluene. Postirradiation expansion, porosity, and strength measurements on several new BeO compositions irradiated at 100°C showed some differences from previously tested materials; however, there was no improvement in the dosage at which microcracking occurred. The new compositions included NGK-grade BeO with 2 wt % Be metal, UOX with 1 and 2% Be metal, and Thermalox 995A, a relatively new nuclear grade of BeO from Brush Beryllium Co. (auth)

**2425** (IDO-14665) MEASUREMENT OF HEAT GENERATION RATE OF HIGHLY RADIOACTIVE CALCINED ALUMINA. Rhodes, D. W.; Jacobson, M. E. (Phillips Petroleum Co., Idaho Fall, Idaho. Atomic Energy Div.). Oct. 1965. Contract AT(10-1)-205. 17p. Dep. mn; CFSTI $1.00 cy, $0.50 mn.

The calorimetric measurement of the heat generation rate of highly radioactive (~20 curies per pound) calcine produced by the fluidized bed calcination of aluminum nitrate-nitric acid wastes in the Waste Calcining Facility at the Idaho Chemical Processing Plant is described. The results agreed closely with values calculated by using the concentration, decay patterns, and decay energies of the radioisotopes in the waste. (auth)

**2426** (LA-3387) RADIATION DAMAGE TO ALKALI HALIDES AND OTHER SIMPLE IONIC CRYSTALS. Pretzel, Frank E. (Los Alamos Scientific Lab., Univ. of California, N. Mex.). July 1965. Contract W-7405-eng-36. 23p. Dep. mn; CFSTI $1.00 cy, $0.50 mn.

Ionizing radiation produced interstitial-vacancy pairs in ionic halide crystals by a more efficient mechanism than the knock-on process. Observations obtained by x-ray diffraction and optical absorption studies are explained in terms of the probable mechanism of radiation damage. Comparisons were made with radiation damage in LiH and other ionic crystals. (auth)

**2427** (NASA-SP-55) SYMPOSIUM ON THERMAL RADIATION OF SOLIDS HELD AT SAN FRANCISCO, CALIFORNIA, MARCH 4-6, 1964. Katzoff, S. (ed.) (National Aeronautics and Space Administration, Washington, D. C.). 1965. 630p. (ML-TDR-64-159; CONF-532). CFSTI $3.75 cy, $2.75 mn.

Fifty-five articles are included; one was abstracted separately in NSA. One article was previously abstracted in NSA as 18: 26097. The remaining 53 articles include information on: fundamentals of radiation studies on solids; surface effects; measurement techniques; space environmental effects; and applications. Separate author and subject indexes are included. (P.C.H.)

*For an abstract of the individual paper see: 2428.*

**2428** (NASA-SP-55, pp 365-79) NUCLEAR ENVIRONMENTAL EFFECTS ON SPACECRAFT THERMAL CONTROL COATINGS. Breuch, R. A.; Pollard, H. E. (Lockheed Missiles and Space Co., Palo Alto, Calif.).

A total of 250 different standard, developmental, and research thermal-control coatings were irradiated in vacuum with a nominal integrated dose of $10^{10}$ ergs/g(C) gamma and $10^{14}$ fast neutrons/cm$^2$. A preliminary summary of the effects of nuclear radiation on the optical properties of some selected coating materials is presented. The materials include inorganic (silicate bonded) systems, plasma-sprayed ceramic coatings, chemically polished metals, acrylic- and epoxy-base coatings, silicone dispersion systems (air-cured), and adhesive-applied silicone films. Optical properties before and after irradiation are given. Also presented are plots of total hemispherical emittance measured during irradiation. Effects of accelerated simultaneous nuclear and ultraviolet irradiation on solar-reflector coatings and the effects of sample temperature during irradiation are included. (auth)

**2429** (ORNL-3837) IRRADIATION BEHAVIOR OF HIGH BURNUP $ThO_2$-4.45 percent $UO_2$ FUEL RODS. Rabin, S. A.; Ullmann, J. W.; Long, E. L. Jr.; Osborne, M. F.; Goldman, A. E. (Oak Ridge National Lab., Tenn.). Oct. 1965. Contract W-7405-eng-26. 66p. Dep. mn; CFSTI $3.00 cy, $0.75 mn.

Fuels $UO_2$ and $ThO_2$-$UO_2$ pellet specimens were irradiated in the Materials Testing Reactor (MTR), Engineering Test Reactor (ETR), and the Chalk River Reactor (NRX) to burnups at least as high as 96,000 Mwd/MT(U + Th). At the time of inception, there was no intent to evaluate the performance of the fuel per se. However, in view of the interest in thorium-bearing fuels at ORNL and in high burnup fuels in general, it was decided to examine in detail several of the irradiated $ThO_2$-$UO_2$ fuel rods and glean as much information as possible about their behavior. Three such rods were examined. The significant features of these irradiations are that, although the cladding temperatures were low, the fuel operated at heat ratings equivalent to those in power reactors today and the burnups range from 37,000 to 96,000 Mwd/MT(U + Th). The fabrication of these specimens is described and pertinent preirradiation data are presented. The in-reactor operating conditions and behavior are given, and the results of postirradiation examination are described and interpreted. (auth)

**2430** (ORNL-P-1713) IRRADIATION EFFECTS IN STAINLESS STEELS AT HIGH TEMPERATURES. Martin, W. R.; Weir, J. R. Jr. (Oak Ridge National Lab., Tenn.). [1965]. Contract W-7405-eng-26. 15p. (CONF-650620-2). Dep. mn; CFSTI $1.00 cy, $0.50 mn.

From Sodium Components Development Program Information Meeting, Chicago.

The effects of irradiation on the elevated-temperature mechanical properties of structural materials is described using type 304 stainless steel as an example. The general result is that the grain boundary fracture process, but not the deformation process, is affected. All data suggest the primary cause to be helium generated from $(n,\alpha)$ reactions. Several metallurgical techniques for improving the ductilities of irradiated alloys are suggested, and experimental data are given for type 304 stainless steel for which the degree of improvement is demonstrated. (auth)

**2431** (ORNL-TM-1255) AN IRRADIATION EXPERIMENT TO STUDY THE COMPATIBILITY OF BeO WITH GRAPHITE AT 1500 deg C. PART I. PREIRRADIATION DESCRIPTION AND INITIAL OPERATION. Brandon, C. A. (Oak Ridge National Lab., Tenn.). Nov. 1965. Contract W-7405-eng-26. 67p. Dep. mn; CFSTI $3.00 cy, $0.75 mn.

An irradiation experiment to determine the inpile compatibility of beryllia with graphite at 1500°C is being conducted in the F-1 core position of the ORR. The irradiation which began on March 14, 1965, is scheduled to be completed in approximately nine months after a fast neutron (E > .18 Mev) dose of ~$2 \times 10^{21}$ nvt. The experimental facility and the irradiation capsule design and assembly are described. The detailed results of preirradiation spectrographic, gravimetric, photographic and dimensional analyses are tabulated. The proposed postirradiation examination procedure is outlined. The initial operation, through May 13, 1965, has been at the design conditions. (auth)

**2432** (REIC-Memo-26) RADIATION EFFECTS ON GLASS: AN ANNOTATED BIBLIOGRAPHY. Gilmour, B. A.; Heenan, W. F. (Radiation Effects Information Center, Battelle Memorial Inst., Columbus, Ohio). Sept. 15, 1965. Contract AF33(615)-1124. 31p. Dep. mn; CFSTI $2.00 cy, $0.50 mn.

Approximately 150 abstracts are presented on radiation effects on glass, glass devices, and glass dosimeters. The abstracts include those processed by the Radiation Effects Information Center since 1958. They are arranged alphabetically by author. (D.L.C.)

**2433** (REIC-Memo-27) COMPILATION OF NUCLEAR, PULSED, AND SPACE RADIATION EFFECTS PROJECTS. (Radiation Effects Information Center, Battelle Memorial Inst., Columbus, Ohio). Oct. 15, 1965. Contracts AF33(615)-1124; W-7405-eng-92. 102p. Dep. mn; CFSTI $4.00 cy, $0.75 mn.

A list is presented of the contracts and their objectives and scope. The list is arranged under the following categories: general, electronics and electrical systems, nuclear weapons effects, propulsion systems, polymers, organic and inorganic materials, ceramic materials, metals, experimental methods, and miscellaneous. Two indexes (agency and contract number) are included. (D.L.C.)

**2434** (TID-22342) SOLID STATE INVESTIGATIONS UTILIZING ELECTRON-BOMBARDMENT PHENOMENA. Annual Progress Report, 1965. Pomerantz, Martin A. (Bartol Research Foundation, Swarthmore, Pa.). Oct. 29, 1965. Contract AT(30-1)-2730. 77p. Dep. mn; CFSTI $3.00 cy, $0.75 mn.

Measurements are reported of the effects of alpha-particle irradiation on the electric conductivity of diamond; the effects of electron irradiation on the electric conductivity of diamond, RbBr, and NaBr; electron-beam-induced desorption of Th atoms from W and Re surfaces; electron diffraction by Al and W surfaces; and gas adsorption onto W surfaces. (T.F.H.)

**2435** (WAPD-T-1720) FATIGUE AND BURST TESTS ON IRRADIATED IN-PILE STAINLESS STEEL PRESSURE TUBES. Waldman, L. A.; Doumas, M. (Bettis Atomic Power Lab., Pittsburgh, Pa.). Sept. 1964. Contract AT-11-1-GEN-14. 44p. Dep. mn; CFSTI $2.00 cy, $0.50 mn.

A study was initiated to evaluate the loss of ductility of irradiated in-pile stainless steel pressure tubes by relatively quick and simple methods in an effort to extend their operating lifetime limit. The tests associated with this study used representative conditions of pressure cycling and geometry to determine the bursting pressure and fatigue life of both unirradiated control specimens and sections of an irradiated in-pile tube. Results showed that irradiation increases the tensile strength and the low-cycle fatigue life of these stainless steel tubes subjected to pressure cycling. Using these results, an extension in the lifetime limit of operating in-pile pressure tubes was established as part of a continuing test program. (auth)

**2436** (WERL-8844-4) PART I. VARIATIONS IN THE EMBRITTLEMENT OF IRRADIATED PRESSURE VESSEL STEELS. Wessel, E. T.; Eichelberger, T. W. (Westinghouse Research Labs., Pittsburgh, Pa.). Jan. 15, 1965. Contract AT-11-1-GEN-14. 41p. Dep. mn; CFSTI $2.00 cy, $0.50 mn.

The basic aspects of the deformation and fracture characteristics of several heats of ASTM A302B steel were investigated in terms of the Petch parameters. Both irradiation sensitive and insensitive were represented in the data that were analyzed. In the irradiated condition, the friction stress, $\sigma_i$, increased with increased neutron exposure for all heats. The sensitive heats exhibited a much greater increase in $\sigma_i$ than did the insensitive heats. The grain boundary resistance, $k_y$, decreased with increased exposure, particularly at the higher exposure levels (>$10^{18}$ nvt). The relative change in $\sigma_i$ and/or $k_y$ is the predominate factor controlling sensitivity to irradiation damage. It appears that the differences in $\sigma_i$ and $k_y$ and the corresponding bulk differences in irradiation sensitivity may be attributed to gross differences in microstructure. (auth)

**2437** (WERL-8844-6) VARIATION IN SENSITIVITY TO IRRADIATION DAMAGE—PRESSURE VESSEL STEELS. PART III. Wessel, E. T.; Eichelberger, T. W.; Armstrong, R. W. (Westinghouse Research Labs., Pittsburgh, Pa.). Jan. 15, 1965. Contract AT-11-1-GEN-14. 234p. Dep. mn; CFSTI $6.00 cy, $1.25 mn.

Work was conducted to determine the reasons for the differences in the amount of damage, denoted by the increase in transition temperature, resulting from neutron irradiation in various heats of A302B steel. The basic and theoretical factors determining the transition temperature were studied using a Cottrell-Petch type of analysis. The effects of chemistry, heat treatment, microstructure, prestraining, thermal aging, and strain aging were studied. Based on favorable Petch parameters, the quenched and tempered structures were superior to those obtained by slower cooling methods from the austenitizing temperatures. (auth)

**2438** THE EFFECT OF ELECTRON IRRADIATION ON THE MECHANICAL PROPERTIES OF STEEL SUBJECTED TO A THERMAL MECHANICAL TREATMENT. Bystrov, L. N.; Ivanov, L. I.; Bannykh, O. A. (Baikov Inst. of Metallurgy, USSR). Fiz. Metal. Metalloved., 19: 791-2 (May 1965). (In Russian).

A chromium–manganese steel containing 0.4% C, 6% Mn, and 1% Cr was heated to 1050°C, cooled to 550°C, hot rolled at 550°C to a reduction of 80%, and quenched in water. After this treatment the steel had an austenitic-martensitic structure. Its hardness was 49.5 HRC units. The hardness was 43 HRC units after quenching from 1050°C. Thin plane samples 2 mm thick were irradiated with 5-Mev electrons at doses of 6 to $8 \times 10^{14}$ electrons/cm$^2$, and were subjected to rupture tests 24 hours after irradiation. The electron irradiation led to a decrease in plasticity with $\theta$ = 140.8 kg/mm$^2$ for the unirradiated samples and $\theta$ = 138 kg/mm$^2$ for the irradiated samples. The yield point $\theta_{0.2}$ was 80.7 kg/mm$^2$ for the controls as compared with 69.3 kg/mm$^2$ for the irradiated samples. The relative elongation at rupture was 3.5% for the controls as compared to 4.3% for the irradiated samples. These anomalous results can be explained if it is assumed that the steel is in a metastable state after the thermal mechanical treatment. Irradiation promoted the transition from a metastable state to an equilibrium state. Irradiation had the effect of a low-temperature anneal in this case. (TTT)

**2439** X-RAY AND GAMMA CONDUCTIVITY OF GaSe SINGLE CRYSTALS. Guseinova, E. S.; Mekhtiev, R. F. Izv. Akad. Nauk Azerbaidzh. SSR, Ser. Fiz.-Tekhn. Mat. Nauk, No. 1, 63-5(1965). (In Russian).

Results are reported of an investigation of the increased conductivity induced by x rays and gamma rays in low-

resistivity (100–200 ohm-cm) and high-resistivity ($10^4$ ohm-cm) p-GaSe single crystals. All measurements were made at room temperature. The x rays were produced by a standard URS-70 apparatus with iron tube, and the gamma rays were from a $^{60}Co$ source. For both types of radiation the increase in conductivity was 8 to 10 times for high-resistivity samples and several multiples of 10% for low-resistivity samples. The results also show that the effect of visible light is not additive with the effects of the x rays or gamma rays. The reason for this is the presence of two different relaxation mechanisms for the x ray or gamma ray conductivity, each responding differently to visible light. The results are compared with other data and some of the differences are explained. (ATD)

**2440** EFFECTS OF FAST NEUTRON IRRADIATION ON SILICON ELECTRIC PROPERTIES DURING p-n TRANSITIONS IN FUSED DIODES PREPARED WITH SILICON BASE. Zaidman, S. A.; Sevryukova, L. M. (Kuznetsov Inst. of Physics and Tech., Academy of Sciences, Siberian SSR). Izv. Vyssh. Ucheb. Zavendenii, Fiz., No. 4, 96-9 (1965). (In Russian).

Si doped with P with a resistivity of 5 to 7 ohm cm was exposed to irradiation with fast neutrons for a period of 150 hr (integrated flux of $15.2 \times 10^{10}$ n/cm$^2$) resulted in an increase in the density of dislocations from $8 \times 10^4$ per cm$^2$ to $8.39 \times 10^6$ per cm$^2$. All measurements were performed directly on the crystals, from which p-n junctions were then fabricated by alloying Si with Al. Since fabrication of p-n junctions requires heating to 670°C, the effect of heating on annealing of radiation defects was also investigated. Although the lifetime of minority carriers $\tau$ increased by about 10 $\mu$sec after annealing, the density of dislocations remained approximately the same. The increase in $\tau$ was attributed to annealing of vacancies and interstitials. Of all the defects produced by fast neutron bombardment of Si, the dislocations exerted the strongest effect on $\tau$. During the alloying of Al with Si, the point defects in Si are annealed, although the generation of additional dislocations results in a decrease of $\tau$. A decrease of $\tau$ in the diode can also be associated with the increase in the donor concentration from the side of the ohmic contact, which is made of gold and an antimony alloy. The irradiation of silicon with fast neutrons and the reduction of the restoration time of reverse resistance result in an increased reverse current in the p-n junction. (ATD)

**2441** A PRELIMINARY INVESTIGATION OF HELIUM GAS PRECIPITATION IN IRRADIATED COPPER–BORON ALLOYS. Russell, B.; Hastings, I. J. (Univ. of Queensland, Brisbane). J. Nucl. Mater., 17: 30-6(Aug.-Sept. 1965).

Changes that occurred in the lattice parameter of a neutron-irradiated copper–boron alloy during the early stages of annealing were measured. After irradiation at 100°C, the lattice parameter was larger than that of the unirradiated alloy. During annealing, the lattice parameter decreased until it became smaller than that of the unirradiated alloy, and then increased. After complete annealing, the lattice parameter was equal to that of the original untreated alloy. Initially the helium atoms, which were formed by an $(n,\alpha)$ reaction from $^{10}B$, occupied interstitial positions. During annealing, each helium atom captured two vacancies and entered substitutional solution, before migrating to form gas bubbles. This process caused the lattice to contract. As bubbles formed, helium left the solution and the concentration of helium-vacancy complexes was reduced. There was a corresponding expansion of the lattice parameter. The activation energy for the first stage was 0.76 ± 0.1 ev. The activation energy for the second stage was 0.96 ± 0.1 ev, which is possibly the energy required to move a helium atom-vacancy complex through the lattice. (auth)

**2442** THE OXIDATION OF IRRADIATED BERYLLIUM IN CARBON DIOXIDE. Bennett, M. J.; Crick, N. W.; Blythe, P. C.; Antill, J. E. (Atomic Energy Research Establishment, Harwell, Eng.). J. Nucl. Mater., 17: 60-72 (Aug.-Sept. 1965).

The effect of prior irradiation on the oxidation of beryllium in carbon dioxide between 600 and 1000°C was investigated using beryllium irradiated to $1.2 \times 10^{20}$ and $2.8 \times 10^{21}$ n/cm$^2$ (>1 Mev), respectively. The radiation effects were entirely associated with the swelling caused by the helium produced by nuclear transmutation. No significant effect was obtained when the swelling was less than 5% but there was an appreciable increase in the magnitude of oxidation coinciding with maximum (~30%) swelling. This increase in oxidation was accompanied by the development of an intergranular void network in the metal due to the swelling and could be explained solely by the increased area available for reaction. With further oxidation the voids became blocked with oxide and the available area decreased. The development of the void network with increasing swelling was demonstrated by the oxidation experiments and by open pore-volume measurements on samples swollen to varying extents in vacuo. (auth)

**2443** THERMAL RESISTANCE DUE TO MICROCRACKING IN NEUTRON-IRRADIATED BERYLLIUM OXIDE. Dullow, R. J.; McDonald, D. L.; Pryor, A. W. (Australian Atomic Energy Commission Research Establishment, Lucas Heights, New South Wales). J. Nucl. Mater., 17: 83-5(Aug.-Sept. 1965).

A series of thermal conductivity measurements demonstrated both the magnitude of the effect of microcracking on the thermal conductivity of BeO, and the annealing of this thermal resistance at high temperatures. The thermal conductivity measurements were made at 78°K. Results obtained on four samples for which x ray examination had demonstrated the onset of microcracking following neutron irradiation are given. The annealing behavior of the microcracks was studied by observing the decrease in thermal resistance at 78°K after successive 1-hr anneals at intervals up to 1200°C. A 1-hr anneal at 1200°C was sufficient to remove all trace of the thermal resistance increase due to microcracking. It was concluded that microcracking will have serious effects on the thermal conductivity of BeO undergoing neutron irradiation. (F.J.H.)

**2444** MEASUREMENT OF THE HELIUM CONTENT IN NEUTRON-IRRADIATED COPPER–BORON ALLOYS. Russell, B.; Heffernan, B. J. (Univ. of Queensland, Brisbane). J. Nucl. Mater., 17: 86-7(Aug.-Sept. 1965).

The reaction by which helium is formed from $^{10}B$ during slow neutron irradiation is $^{10}B + h + 2e \rightarrow {}^4He + {}^7Li$. One mole of $^7Li$ is formed for each mole of He and the lithium is almost completely stable after formation in the reactor. An atomic absorption technique was developed for measuring the concentration of $^7Li$ in copper/lithium-bearing liquid solutions to an accuracy of at least 1 ppm. From this value the amount of helium could be calculated. (F.J.H.)

**2445** X-RAY LINE BROADENING IN NEUTRON IRRADIATED MAGNESIUM OXIDE. Walker, D. G.; Hickman, B. S. (Australian Atomic Energy Commission, Lucas Heights, Sydney). Phil. Mag. (8), 12: 445-51(Sept. 1965).

X-ray diffraction line broadening in magnesium oxide after neutron irradiation at 75 to 100°C was investigated. Only slight broadening occurred for a neutron dose of $4.2 \times 10^{19}$ nvt (> 1 Mev), whereas appreciable broadening was present for specimens irradiated to $2.1 \times 10^{20}$ nvt and $4.5 \times 10^{20}$ nvt. At $2.1 \times 10^{20}$ nvt all the observed broadening could be attributed to strain but a particle size contribution was present at $4.5 \times 10^{20}$ nvt. The results are interpreted in terms of the formation of interstitial dislocation loops at doses above $10^{20}$ nvt. At $2 \times 10^{20}$ nvt, the measured line breadths are in close agreement with those calculated using data from density measurements. With doses above $4 \times 10^{20}$ nvt, interaction between dislocation loops leads to the formation of a structure similar to that of a cold-worked metal. (auth)

**2446** YOUNG'S MODULUS OF PYROLYTIC CARBON IN RELATION TO PREFERRED ORIENTATION. Price,

R. J. (General Atomic Div., General Dynamics Corp., San Diego, Calif.) Phil. Mag. (8), 12: 561-71(Sept. 1965). (GA-6053).

Expressions are derived which express Young's modulus of an anisotropic aggregate of hexagonal crystallites in terms of the single-crystal elastic constants and functions of the preferred orientation, assuming either a constant tensile strain or a constant tensile stress throughout the aggregate. Measurements of Young's modulus and preferred orientation on a number of pyrolytic carbons with different anisotropies show that the "constant stress" model represents a good approximation of the behavior of these materials. Young's modulus of polycrystalline nuclear graphite, whose dislocations have been pinned by a low-temperature neutron irradiation, agrees with the same model. (auth)

**2447** THE NUCLEATION OF RADIATION DAMAGE IN GRAPHITE. Reynolds, W. N.; Thrower, P. A. (A.E.R.E., Harwell, Berks, Eng.) Phil. Mag. (8), 12: 573-93(Sept. 1965) (AERE-R-4862).

A quantitative survey was carried out of the sizes and densities of the defects found by transmission electron microscopy of irradiated graphite crystals. Three regimes are considered, viz. isothermal irradiations between 150° and 1200°C, seeding irradiations in which the crystals were given a short preirradiation at a lower temperature before the isothermal irradiation, and the behavior during thermal annealing. In each regime a comparison was made with the corresponding macroscopic property changes observed on polycrystalline material. This behaves like crystals with added traps about 0.37 ev in depth, causing heterogeneous nucleation of interstitial clusters, at a density of about one per crystallite plane. The vacant lattice sites have an energy of 5.5 ± 1 ev, only about half that predicted by recent theoretical calculations. Interstitial loops migrate by a conservative climb process with an activation energy of 2.6 ev, which is reduced to 1.8 ev in the presence of continued irradiation. The difference is attributed to the thermal activation energy of formation of jogs on the loops. At higher temperatures, vacancy-controlled annihilation is associated with an activation energy of 5.4 ev which refers to interplanar vacancy motion. The behavior of some macroscopic property changes on irradiation and annealing implies the presence of a saturating population of submicroscopic defects which are susceptible to radiation annealing. The chief limitation to the model at present is the comparative ignorance of the properties of vacancies and their interactions with interstitials. (auth)

**2448** HIGH-POWER OPERATION OF $PuO_2$–$UO_2$ FAST REACTOR FUEL. Knight, Ford; Rabin, S. A.; O'Neill, G. L.; Baily, W. E. (General Electric Co., San Jose, Calif.). Trans. Amer. Nucl. Soc., 8: 345(Nov. 1965).

**2449** IRRADIATION OF $UO_2$–$PuO_2$ HIGH-POWER-DENSITY FUEL ELEMENTS IN PRTR. Freshley, M. D.; Panisko, F. E.; Skavdahl, R. E. (Battelle-Northwest, Richland, Washington). Trans. Amer. Nucl. Soc., 8: 365-6(Nov. 1965).

**2450** FISSION-PRODUCT AND HEAVY-ELEMENT DISTRIBUTIONS IN HIGH-PERFORMANCE $UO_2$ FUEL RODS. Davies, J. H.; Boyle, R. F.; Hanus, J. F. (General Electric Co., Pleasanton, Calif.). Trans. Amer. Nucl. Soc., 8: 378-9(Nov. 1965).

**2451** OBSERVATIONS ON MICROSTRUCTURAL CHANGES WITH BURNUP IN MIXED-OXIDE FUELS. Baily, W. E.; Craig, C. N.; Wolff, U. E. (General Electric Co., San Jose, Calif.). Trans. Amer. Nucl. Soc., 8: 379-80(Nov. 1965).

**2452** AN IN-PILE STUDY OF THE THERMAL CONDUCTIVITY AND ELECTRICAL PROPERTIES OF $UO_2$ AND $UO_{2-x}$. MacEwan, J. R. (Atomic Energy of Canada Ltd., Ontario); Harvey, A.; Notley, M. J. F.; Maki, H. Trans. Amer. Nucl. Soc., 8: 380(Nov. 1965).

**2453** RELATIVE IN-PILE THERMAL CONDUCTIVITY OF STOICHIOMETRIC AND HYPOSTOICHIOMETRIC MIXED OXIDES OF PLUTONIA AND URANIA. Baily, W.E.; Craig, C. N. (General Electric Co., San Jose, Calif.). Trans. Amer. Nucl. Soc., 8: 381(Nov. 1965).

**2454** BURNUP ANALYSIS OF LUMPY FUEL. Robkin, M. A. (General Electric Co., Pleasanton, Calif.). Trans. Amer. Nucl. Soc., 8: 385(Nov. 1965).

**2455** CONSIDERATIONS ON THE ANNEALING OF IRRADIATED PRESSURE-VESSEL STEEL. Seman, D. J.; Pasierb, E. J. (Bettis Atomic Power Lab., Pittsburgh). Trans. Amer. Nucl. Soc., 8: 416-17(Nov. 1965).

**2456** THE EFFECT OF THERMAL-NEUTRON IRRADIATION AT A FIXED FAST-NEUTRON DOSE ON THE CREEP-RUPTURE PROPERTIES OF HIGH-TEMPERATURE ALLOYS. Moteff, J.; Lovell, A. J.; Kingsbury, F. D. (General Electric Co., Cincinnati). Trans. Amer. Nucl. Soc., 8: 417(Nov. 1965).

**2457** THE EFFECT OF NEUTRON IRRADIATION ON THE HARDNESS PROPERTIES OF THE Bcc METALS, TUNGSTEN AND MOLYBDENUM. Moteff, J.; Kamphouse, J. L.; Smith, J. P. (General Electric Co., Cincinnati). Trans. Amer. Nucl. Soc., 8: 417-18(Nov. 1965).

**2458** RADIATION DAMAGE IN INCOLOY-800. Busboom, H. J.; Comprelli, F. A.; Spalaris, C. N. (General Electric Co., San Jose, Calif.). Trans. Amer. Nucl. Soc., 8: 418(Nov. 1965).

**2459** RADIATION EFFECTS ON MATERIALS AT LIQUID-HYDROGEN TEMPERATURE. Weleff, W.; Dixon, C. E.; Funk, C. W. (Aerojet-General Nucleonics, San Ramon, Calif.). Trans. Amer. Nucl. Soc., 8: 419-20(Nov. 1965).

**2460** EXPERIMENTAL RESULTS ON THE EFFECTS OF HIGH-RADIATION FIELDS ON THE ELECTRICAL CONDUCTIVITY OF METAL OXIDES. Bregar, John F.; Davis, Monte V.; Anderson, William E. (Univ. of Arizona, Tucson). Trans. Amer. Nucl. Soc., 8: 422-3(Nov. 1965).

**2461** IRRADIATION OF IMPACTED $UO_2$–$PuO_2$. Bailey, W. J. (Battelle-Northwest, Richland, Wash.). Trans. Amer. Nucl. Soc., 8: 424(Nov. 1965).

**2462** THE FISSION-PRODUCT GAS PRESSURES IN $UO_2$ FUEL ELEMENTS DURING IRRADIATION. Notley, M. J. F.; DesHaies, R.; MacEwan, J. R. (Atomic Energy of Canada Ltd., Ontario). Trans. Amer. Nucl. Soc., 8: 424-5(Nov. 1965).

**2463** HIGHLY RATED HOLLOW $UO_2$ PELLETS IRRADIATED IN COLLAPSIBLE SHEATHING. Bain, A. S. (Atomic Energy of Canada Ltd., Ontario). Trans. Amer. Nucl. Soc., 8: 425-6(Nov. 1965).

**2464** IRRADIATION EVALUATION OF FUEL ELEMENTS FOR THE PBRE AND AVR REACTORS. Scott, J. L.; Morgan, J. G.; DeCarlo, V. A. (Oak Ridge National Lab., Tenn.). Trans. Amer. Nucl. Soc., 8: 426-7(Nov. 1965).

**2465** CONTROLLED IRRADIATION TESTING OF URANIUM-ALUMINUM FUELS FOR THE ADVANCED TEST REACTOR. Walker, V. A.; Gibson, G. W. (Phillips Petroleum Co., Idaho Falls, Idaho). Trans. Amer. Nucl. Soc., 8: 427(Nov. 1965).

**2466** IRRADIATION BEHAVIOR OF ZIRCONIUM-URANIUM ALLOY FUEL TUBES. Angerman, C. L.; Caskey, G. R. Jr. (E. I. duPont de Nemours, Aiken, S. C.). Trans. Amer. Nucl. Soc., 8: 427-8(Nov. 1965).

**2467** INTERNAL CONVERSION. BeO-BASE FUEL ELEMENT. Bohlander, K. M.; Turner, P. P. (General Electric Co., Cincinnati). Trans. Amer. Nucl. Soc., 8: 428-9(Nov. 1965).

**2468** THE BEHAVIOR OF WATER VAPOR IN $UO_2$ DURING IRRADIATION. Kubit, C. J.; McClintock, D. R.; Ferrari, H. M. (Westinghouse Electric Co., Pittsburgh). Trans. Amer. Nucl. Soc., 8: 429-30(Nov. 1965).

**2469** RESPONSE OF LOW-BURNUP-IRRADIATED MIXED-OXIDE ($PuO_2$–$UO_2$) FUEL TO TRANSIENT OVERPOWER. Hanson, J. E. (General Electric Co., San Jose, Calif.). Trans. Amer. Nucl. Soc., 8: 560-1(Nov. 1965).

**2470** FLOW AND FRACTURE OF METALS AND ALLOYS IN NUCLEAR ENVIRONMENTS. ASTM Special Technical Publication No. 380. A Symposium presented at the Sixty-Seventh Annual Meeting American Society for Testing and Materials, Chicago, Illinois, June 21-26, 1964. Philadelphia, American Society for Testing and Materials, 1965. $24.00. 471p. (CONF-512).

Proceedings of the Symposium on Flow and Fracture of Metals and Alloys in Nuclear Environments are presented. Separate abstracts were prepared for 11 of the 28 papers. The remaining 17 papers were previously abstracted in NSA and appeared as abstracts 18: 24191, 27955, 30229, 32222, 32226, 34218, 39813, and 40003 and 19: 2859, 4715, 7972, 7996, 9429, 9731, 23119, 23157, and 30820. (M.C.G.)

*For abstracts of individual papers see: 2401, 2402, and 2471–2479.*

**2471** MECHANISMS OF RADIATION-INDUCED MECHANICAL PROPERTY CHANGES. Barnes, R. S. (Atomic Energy Research Establishment, Harwell, Eng.). pp 40-68 of Flow and Fracture of Metals and Alloys in Nuclear Environments. ASTM Special Technical Publication No. 380. Philadelphia, American Society for Testing and Materials, 1965.

At temperatures of interest for reactor materials some point defects cluster together with their own kind, and if large enough, their geometry and the type of point defect involved can be determined in the electron microscope. Depending upon their structure and the temperature, these clusters can move through the solid under the influence of externally applied elastic stresses, or internal stresses. The interaction of dislocation lines with point defect clusters dominates the radio-induced mechanical property changes. The hardening, which irradiation induces, is dependent on the nature, size, number, and distribution of these clusters, which frequently depend on impurities and the temperature. However, above a certain temperature the clusters either become too large to be effective, or they disappear. The mechanical properties can be modified if irradiation introduces impurities by nuclear transmutation. In practically all but some of the most pure materials, transmutations occur, and if the transmutation has a high probability and the product is noxious, the effects can be important. Because of their low solubility, and because they are normally gaseous at the temperatures of concern, the inert gas elements, which are frequent transmutation products, can have marked effects on the mechanical properties. These elements cluster together and form gas bubbles, which at suitable temperatures migrate bodily through the solid, colliding, and coalescing with others to form larger bubbles, and collecting on dislocation lines, precipitates, and boundaries within the solid. The bubbles impede the motion of dislocations through the solid and harden it, the effects depending mainly on the size and distribution of the bubbles and the number of gas atoms produced. However, the bubbles on the grain boundaries enlarge under tensile stress and can weaken the solid and reduce its ductility. (auth)

**2472** IRRADIATION HARDENING AND EMBRITTLEMENT IN BODY-CENTERED CUBIC TRANSITION METALS. Wronski, A. S. (European Research Associates, Brussels); Sargent, G. A.; Johnson, A. A. pp 69-85 of Flow and Fracture of Metals and Alloys in Nuclear Environments. ASTM Special Technical Publication No. 380. Philadelphia, American Society for Testing and Materials, 1965.

The hardening and embrittlement of body-centered-cubic transition metals by neutron irradiation near room temperature is discussed. Results on the dependence of irradiation hardening in molybdenum on neutron dose and strain rate are reviewed. A critical assessment was made both of the results to be found in the literature and of these results, and it was concluded that the underlying mechanisms of irradiation hardening are still obscure. Evidence presently available suggests, however, that for doses up to about $10^{18}$ nvt (<1 Mev) these effects are due principally to the pinning of dislocations by point defects, while at higher doses the interaction of moving dislocations with defect clusters and dislocation loops also becomes important. Recent work carried out on yielding and flow in several unirradiated body-centered-cubic transition metals, especially niobium, is reviewed. (auth)

**2473** COMPUTER STUDIES OF NEUTRON IRRADIATION AND ANNEALING IN FINITE BCC IRON SPECIMENS. Beeler, J. R. Jr. (General Electric Co., Cincinnati). pp 86-104 of Flow and Fracture of Metals and Alloys in Nuclear Environments. ASTM Special Technical Publication No. 380. Philadelphia, American Society for Testing and Materials, 1965.

The primary damage state in neutron-irradiated $\alpha$–iron was computed as a function of specimen size and neutron energy. A Monte Carlo technique was used to compute the concentration and energy spectrum of primary knock-on atoms (PKA) produced by neutrons. In a second set of calculations, the number of displaced atoms produced by a PKA was computed as a function of its energy. These calculations consisted of simulating the entire elastic collision cascade of an energetic atom in the exact crystal structure of $\alpha$–iron. In addition to providing the displacement function for a PKA as a function of energy, they also gave an atomic level description of the defect distribution in a collision cascade (displacement spike). By combining the results of these two sets of computations it was possible to describe the damage state in an iron specimen as a function of its size and of neutron energy. The results strongly suggested that the damage state produced in small specimens is essentially different from that produced in large specimens, as are their annealing characteristics. The conditions of tension test specimen size and shape, which insure that annealing kinetics data obtained from irradiated wires are applicable to these specimens, were determined. Calculations on the mechanisms for damage saturation, on annealing behavior, and on saturation and embrittlement in pressure shells as a function of depth, are also described. (auth)

**2474** EFFECTS OF IRRADIATION IN IRON AND STEELS. Harries, D. R.; Eyre, B. L. (Atomic Energy Research Establishment, Harwell, Eng.). pp 105-19 of Flow and Fracture of Metals and Alloys in Nuclear Environments. ASTM Special Technical Publication No. 380. Philadelphia, American Society for Testing and Materials, 1965.

The effects of irradiation under a variety of neutron flux and temperature conditions on the transition temperature of a low-carbon, low-alloy steel containing 0.0036 wt % boron were investigated. This steel exhibited greater embrittlement than nominally boron-free steels irradiated under similar conditions; the differences in behavior were analyzed in terms of the additional displaced atoms and cluster of defects, respectively, produced in the iron lattice by the energetic products of the $^{10}B(n,\alpha)^{7}Li$ reaction in the boron steel. Tension specimens prepared from three mild steels were tested at room temperature after irradiation to approximately the same neutron dose at accurately controlled temperatures in the range from 100 to 350°C; the reactor was operated at three power levels, giving relative neutron dose rates of 1 : 4 : 100. The increases in yield stresses were functions of the irradiation temperature and the type of steel but, in agreement with preliminary results reported previously, were not dependent on the neutron dose rate. The absence of a neutron dose rate effect suggested that the nucleation of the damage in steels is not diffusion controlled, and it is probable that the radiation hardening does not depend on the number of displaced atoms but on the number of defect clusters formed in the displacement spikes. It was suggested that the dependency of the radiation hardening on the type of steel is associated with differences in the active nitrogen content. The effects of irradiation, $2.0 \times 10^{20}$ n/cm$^2$ (fission) at 60°C, followed by annealing at temperatures up to 500°C on the damage in pure iron were

studied using thin-film electron microscope and microhardness techniques. The damage observed in the as-irradiated condition was considered to be interstitial point defect clusters. The clusters disappeared and the radioinduced increase in microhardness recovered over a relatively narrow annealing temperature range suggesting that interstitials and vacancies are annealing simultaneously by a process of mutual annihilation. (auth)

**2475** RECOVERY OF DEFECTS IN NEUTRON-IRRADIATED TUNGSTEN. Moteff, J.; Smith, J. P. (General Electric Co., Cincinnati). pp 171-87 of Flow and Fracture of Metals and Alloys in Nuclear Environments. ASTM Special Technical Publication No. 380. Philadelphia, American Society for Testing and Materials, 1965.

Isochronal resistivity recovery spectra of irradiated tungsten indicated three resolved peaks at 16, 22, and 31% of the absolute melting temperature of this material. Isochronal annealing of the tungsten hardness increment indicated that irradiation affects the athermal component of the hardness, observed at temperatures above 0.15 $T_m$, and not the strong temperature-dependent component, which becomes prominent below this temperature. In addition, the hardness recovery occurred at 0.35 $T_m$; the 0.16, 0.22, and 0.31 $T_m$ peaks were absent. The recovery stages of resistivity at 0.31 $T_m$ and of the hardness at 0.35 $T_m$ in body-centered-cubic metals corresponded to the recovery stage observed for both types of properties in most irradiated face-centered-cubic metals, which occurred at approximately 0.50 $T_m$. (auth)

**2476** THE NATURE AND ANNEALING BEHAVIOR OF IRRADIATION DAMAGE IN MOLYBDENUM. Eyre, B. L.; Roberts, A. C. (Atomic Energy Research Establishment, Harwell, Eng.). pp 188-201 of Flow and Fracture of Metals and Alloys in Nuclear Environments. ASTM Special Technical Publication No. 380. Philadelphia, American Society for Testing and Materials, 1965.

Structural defects were observed using transmission electron microscope techniques in molybdenum after neutron or fission-fragment irradiation at about 60°C. There was no detectable change in the observable damage on annealing for 1 hr at temperatures up to 600°C, but at 650°C the defects increased in size and became resolvable as dislocation loops. These loops originated from interstitial atoms and the loop size increased with annealing in the range from 650 to 950°C. After annealing at 1200°C a well-developed dislocation network was observed and only a few loops remained. No correlation between recovery of microhardness and the observable damage was apparent. Possible reasons are given for the absence of aggregates of vacant lattice sites. (auth)

**2477** THE EFFECT OF IRRADIATION TEMPERATURE ON THE POST-IRRADIATION STRESS-STRAIN BEHAVIOR OF STAINLESS STEEL. Martin, W. R.; Weir, J. R. (Oak Ridge National Lab., Tenn.). pp 251-68 of Flow and Fracture of Metals and Alloys in Nuclear Environments. ASTM Special Technical Publication No. 380. Philadelphia, American Society for Testing and Materials, 1965. (ORNL-TM-906).

The results of an investigation on the influence of irradiation temperatures from 150 to 750°C, and post-irradiation test temperatures of 25 to 850°C on the mechanical properties of AISI Type 304 and 347 stainless steels tested at various strain rates are described. The irradiations were conducted in an Oak Ridge Research Reactor core position. Subsize tension specimens were irradiated to $7 \times 10^{20}$ nvt (fast) and $9 \times 10^{20}$ nvt (thermal). The yield stress was not affected by irradiation at any test temperature above 600°C. At lower irradiation and testing temperatures the yield and ultimate engineering tensile stresses were strongly dependent on irradiation temperature. The true tensile and fracture stresses at test temperatures below 600°C were unaffected regardless of the irradiation temperature; they were slightly reduced at test temperatures above 600°C in the high strain-rate tests. Increases in yield strength due to irradiation were associated with decreases in the uniform elongation, but not fracture strain for test temperatures below 600°C. At higher testing temperatures radiation effects on the ductility parameters were strongly strain-rate sensitive. The ductility parameters decreased markedly with decreasing strain-rate and increasing deformation temperature. At this neutron exposure the influence of irradiation at deformation temperatures less than 600°C was reflected only in the stress-strain relation and not in the fracture stress or strain. However, the radiation effect for deformation at 600°C and above concerned the fracture process and not the deformation relationship. The effect on the fracture process appeared to be a result of changes in the grain boundary fracture behavior. (auth)

**2478** GAS FORMATION AND COMPRESSION FRACTURES IN IRRADIATED BERYLLIUM. Beeston, J. M. (Phillips Petroleum Co., Idaho Falls, Idaho). pp 395-417 of Flow and Fracture of Metals and Alloys in Nuclear Environments. ASTM Special Technical Publication No. 380. Philadelphia, American Society for Testing and Materials, 1965.

The displacement and gaseous atom production rate was calculated for fast neutrons and for the primary nuclear reactions $^9Be(n,2n)2^4He$ and $^9Be(n,\alpha)^6He$ for beryllium in a lattice piece in the Materials Testing Reactor (MTR). The results of compression tests on samples cut from lattice piece LB-15 are given. Electron microscope fractographs are presented, which show gas bubble growth only at the higher exposures. X-ray-diffraction patterns indicated no change in hexagonal line patterns and lattice parameter changes of less than 0.2% for the higher exposures, $1.45 \times 10^{22}$ n/cm$^2$. The bowing of the MTR lattice pieces was analyzed in terms of the presence of the gaseous atoms, and the fracture of MTR lattice pieces and compression samples was examined in relation to fracture criteria. The strain corresponded to a growth of about 0.2% per $1 \times 10^{22}$ nvt > 1 Mev. (auth)

**2479** THE USE OF MATERIALS PROPERTIES BY THE REACTOR VESSEL DESIGNER. Langer, B. F. (Bettis Atomic Power Lab., Westinghouse Electric Corp., Pittsburgh). pp 418-28 of Flow and Fracture of Metals and Alloys in Nuclear Environments. ASTM Special Technical Publication No. 380. Philadelphia, American Society for Testing and Materials, 1965.

The information that the pressure vessel designer must obtain from the materials engineer in order to provide protection against crack growth and brittle fracture is discussed. The most meaningful fatigue tests in the low-cycle range were found to be those in which strain, rather than stress, is the controlled parameter. The correlation between fatigue properties, strength properties, and ductility is considered because the principal effects of neutron bombardment are to increase the strength and lower the ductility. Irradiation also raises the transition temperature, meaning that the reactor vessel designer must consider the possibility of brittle fracture occurring late in life. (auth)

**2480** RADIATION DAMAGE IN SEMICONDUCTORS. 7th International Conference on the Physics of Semiconductors, Paris-Royaumont, 1964. 3. Paris, Dunod, 1965. 426p. (CONF-679).

Papers presented at the 7th International Conference on the Physics of Semiconductors on radiation damage in semiconductors are given. Separate abstracts were prepared for 38 of the 47 papers. Three papers were previously abstracted for NSA and appeared as 19: 2665, 26877, and 26880. (M.C.G.)

*For abstracts of individual papers see: 2481—2518.*

**2481** RADIATION DAMAGE IN SEMICONDUCTORS. Fan, H. Y. (Purdue Univ., Lafayette, Ind.). pp 1-8 of Radiation Damage in Semiconductors. Paris, Dunod, 1965.

The present understanding of radiation damage in germanium and silicon is reviewed to illustrate problems in the study of radiation effects on semiconductors. The

nature of defects and production of primary defects are discussed. (M.C.G.)

**2482** LOW TEMPERATURE IRRADIATION OF SEMICONDUCTORS AND IONIZATION EFFECTS. MacKay, J. W.; Klontz, E. E. (Purdue Univ., Lafayette, Ind.). pp 11-25 of Radiation Damage in Semiconductors. Paris, Dunod, 1965.

The roles of temperature and charge state in governing the stability of close-pair defects in irradiated semiconductors and the effects of these factors on the production of stable defects are discussed. The stability of close-pair defects in Ge, InSb, and Si was studied at low temperatures and the ionization effects determined. It is shown how a model of close-pairs may be applied to describe some of the features of the behavior of semiconductors at higher temperatures. (M.C.G.)

**2483** APPLICATION OF HOT CARRIER TECHNIQUES TO THE STUDY OF RADIATION DAMAGE IN GERMANIUM. Callcott, T. A.; Mackay, J. W. (Purdue Univ., Lafayette, Ind.). pp 27-33 of Radiation Damage in Semiconductors. Paris, Dunod, 1965.

Hot carrier techniques were used to measure the electric resistivity and Hall coefficient of Sn-doped germanium samples with exhaustion range carrier concentrations as small as $10^{14}$ $cm^{-3}$. Short pulsed fields of 10 to 20 volts/cm ionized electrons frozen out on the chemical donor states without appreciably raising the lattice temperature and without affecting electrons in lower lying states. Conductivity versus electric field curves are shown. Carrier removal rates were obtained and annealing effects studied in pure n-type germanium bombarded by 1-Mev electrons at 4.2°K. In addition, evidence was obtained strongly supporting the supposition that the major defect introduced by energetic electron irradiation at 4.2°K is a double acceptor. (M.C.G.)

**2484** METASTABLE DEFECT ANNEALING IN GERMANIUM. Rzewuski, H. (Inst. of Nuclear Research, Warsaw). pp 35-40 of Radiation Damage in Semiconductors. Paris, Dunod, 1965.

Annealing kinetics of metastable defects in germanium did not confirm the MacKay and Klontz model of point defects, in which a metastable defect consists of a close vacancy-interstitial pair with the annealing threshold at a temperature ≈65°K. Germanium samples were bombarded with 1-Mev electrons. Approximate values for short time constants for recombination processes of metastable defects induced by the irradiation are ~100 μsec. (M.C.G.)

**2485** ELECTRON IRRADIATION OF p-TYPE Ge AT 0°C. Klontz, E. E.; MacKay, J. W.; Flanagan, T. M. [Purdue Univ., Lafayette, Ind.]. pp 41-46 of Radiation Damage in Semiconductors. Paris, Dunod, 1965.

The behavior of radioinduced defects in p-type germanium having an initial Fermi level in the vicinity of 0.2 ev was studied. During irradiation the conductivity and hole concentration increased with increasing defect concentrations. The rate of increase of carrier concentration was not large, but the total number of holes was initially small, so that the sensitivity was high and a factor of two increase in conductivity was not unusual. That the annealing observed was not a simple recombination of vacancies and interstitials was evident when experiments were carried out on samples of intermediate purity. At liquid nitrogen temperature the net effect of the irradiation-produced centers was to contribute a small number of holes to the valence band while annealing removed several times this number. It was concluded that the annealing observed is due to a rearrangement of the defects accompanied by shifting of their associated electronic energy states. (M.C.G.)

**2486** STRUCTURAL PROPERTIES OF DEFECTS IN SEMICONDUCTORS. Vook, F. L. (Sandia Lab., Albuquerque, N. Mex.). pp 51-66 of Radiation Damage in Semiconductors. Paris, Dunod, 1965.

Results of measurements of length change, x-ray lattice parameters, small angle x-ray scattering, electron microscopy, and thermal conductivity as they help to determine the structural properties of radioinduced defects in semiconductors are reviewed. Length change and x-ray measurements were found to be useful to distinguish between isolated point defects, clusters of point defects, and spike regions. Electron microscopic observations proved to be useful in exploring the detailed structural nature of disordered regions in germanium. Thermal conductivity provided a sensitive method for studying the stability and structural nature of defects in Ge, Si, GaAs, and InSb. (M.C.G.)

**2487** EFFECTS OF FAST NEUTRONS ON THE THERMAL CONDUCTIVITY OF SILICON BETWEEN 80 AND 300°K AND RECOVERY THROUGH ANNEALING. Albany, H. J.; Vandevyver, M. (Centre d'Etudes Nucleaires de Saclay, Gif-sur-Yvette, France). pp 67-72 of Radiation Damage in Semiconductors. Paris, Dunod, 1965. (In French).

The thermal conductivity $\kappa$ of a silicon single crystal irradiated at 70°C with an integrated flux of $1.2 \times 10^{18}$ fast neutrons $cm^{-2}$ and its evolution after annealings were analyzed on the basis of the Callaway model. The large $\kappa$ decrease after neutron bombardment was found to be associated with an increase of both $\tau^{-1} = A\omega^4$ and $\tau^{-1} = c/L$ phonon scatterings; the important decrease of the parameter L in comparison with the geometrical sizes of the single crystal was connected with the formation of defect clusters giving rise to a wavelength independent scattering. The evaluation of the cluster number compared to primary atom number is discussed. Recovery evolution with isochronal annealings up to 400°C is considered in reference with the L and A parameter variations with the annealing temperatures. (auth)

**2488** EFFECT OF FAST NEUTRON IRRADIATION ON THERMAL CONDUCTIVITY OF TERNARY ARSENIDES. Leroux-Hugon, P.; Weill, G. (C.N.R.X., Bellevue, France). pp 73-7 of Radiation Damage in Semiconductors. Paris, Dunod, 1965. (In French).

The influence of irradiation by fast neutrons on thermal conductivity was investigated on the ternary semiconducting compounds $CdSnAs_2$ and $ZnSnAs_2$. The results were interpreted in terms of two types of defects: point defects and clusters. Irradiation of both ordered and disordered forms of $ZnSnAs_2$ allow the influence of the degree of order on the sensitivity of the material to neutrons to be studied. Annealing experiments showed recovery that may be accounted for in the case of $CdSnAs_2$, by a second order mechanism with an activation energy of about 0.65 ev. (auth)

**2489** EFFECTS OF PROTON IRRADIATION ON SILICON. Authier, A.; Montenay-Garestier, M. T. (Faculte des Sciences, Paris). pp 79-86 of Radiation Damage in Semiconductors. Paris, Dunod, 1965. (In French).

Silicon samples irradiated with 0.7-Mev protons from a Van de Graaff generator were studied using x-ray topographical techniques. Fringes were observed in the image of the irradiated region. These fringes appeared when the irradiation was carried out within a narrow range of temperatures. Their number depended on the dose, eventual annealing, and the nature of the reflecting plane used. (auth)

**2490** A REVIEW OF EPR STUDIES IN IRRADIATED SILICON. Watkins, G. D. (General Electric Research Lab., Schenectady, N. Y.). pp 97-113 of Radiation Damage in Semiconductors. Paris, Dunod, 1965.

It was found that radiation damage in silicon is in general a very complex process. A variety of defect structures were produced, even with 1.5-Mev electron irradiation. Many different important defect structures were apparently formed depending on chemical purity (both electrically active and inactive impurities), Fermi level, temperature of irradiation, kind of irradiation, etc. There was a relative simplicity, however, for irradiation at ≲20°K, although

impurities still played a dominant role. This was true even for a 4°K irradiation, and this was interpreted as indicating possible long range motion of the interstitial silicon atoms at this temperature. The early annealing stages (60 through 180°K) after such a low temperature irradiation can then be identified with the onset of vacancy migration and its simple trapping by other defects. However, for irradiations above ~60°K, both vacancies and interstitials may be mobile during the irradiation and the process and resultant defect structures can be correspondingly more complex. (M.C.G.)

**2491** THE INTERACTION OF RADIATION DEFECTS WITH IMPURITIES AND OTHER DEFECTS IN SEMICONDUCTORS. Vavilov, V. S. (Lebedev Inst. of Physics, Moscow). pp 115-29 of Radiation Damage in Semiconductors. Paris, Dunod, 1965.

Photoconductivity measurements were made of silicon grown under special conditions and containing oxygen in concentrations not exceeding $10^{14}$ $cm^{-3}$ irradiated with fast electrons. The concentration of chemical impurities having deep levels was not detectable by electrical methods. After irradiation there was an absence of spectral steps corresponding to the A or E centers and to the residual impurities. The structureless photoconductivity region, mainly situated near the fundamental band edge and having a "tail" to approximately 4 $\mu$ was considered to be due to point defect pairs separated by different distances. Radioinduced defects in lithium-doped silicon were also studied. The nature of radioinduced defects in very pure germanium single crystals and in germanium doped by gold was determined. (M.C.G.)

**2492** ELECTRON SPIN RESONANCE CENTER IN ZnSe AFTER ELECTRON BOMBARDMENT AT LOW TEMPERATURE. Locker, D. R.; Kulp, B. A. (Aerospace Research Labs., Wright-Patterson AFB, Ohio). pp 131-4 of Radiation Damage in Semiconductors. Paris, Dunod, 1965.

A microwave cavity was constructed in order to study electron spin resonance centers in ZnSe following low-temperature electron bombardment. It was found on some samples that bombarding electrons with energies less than 240 kev do not produce spin centers. When higher electron energies were used a spin resonance was observed after bombardment that was proportional to the total number of electrons hitting the sample. Electron spin resonance spectra were also observed for selenium-coated ZnSe samples after low-temperature electron-induced diffusion. (M.C.G.)

**2493** THE CORRELATION OF E.S.R. CENTRES AND OPTICAL ABSORPTION BANDS IN ELECTRON-IRRADIATED DIAMOND. Duncan, I. (The Univ., Reading, Eng.). pp 135-42 of Radiation Damage in Semiconductors. Paris, Dunod, 1965.

The optical absorption spectra of a type IIa diamond before and after 1.0-Mev electron irradiation are shown. Possible correlations between the strength of the radioinduced G band in the spectra and the strengths of the various features in the ESR spectrum were investigated. A linear relation was observed between centers giving rise to the G band and those giving rise to one of four systems in the ESR spectra. (M.C.G.)

**2494** ARSENIC IMPURITY DEFECT INTERACTIONS IN $\gamma$-IRRADIATED GERMANIUM. Curtis, O. L. Jr.; Crawford, J. H. Jr. (Oak Ridge National Lab., Tenn.). pp 143-9 of Radiation Damage in Semiconductors. Paris, Dunod, 1965.

Observations were made on germanium irradiated with $^{60}Co$ gamma radiation at 0°C. Lifetimes were obtained from the transient decay of photoconductivity in bulk specimens following injection by pulses of light. Arsenic-doped Ge exhibited an important annealing stage at room temperature. About two-thirds of the radioinduced damage annealed at room temperature. Lifetime vs reciprocal temperature curves were obtained for a number of As-doped samples. They indicated minority carrier trapping. The thermal break-up of the trapping centers was also studied. (M.C.G.)

**2495** OPTICAL TRANSITIONS OF ELECTRONS IN FAST NEUTRON IRRADIATED ANTIMONY-DOPED GERMANIUM. Ligenza, S. (Inst. of Nuclear Research, Swierk, Poland). pp 151-3 of Radiation Damage in Semiconductors. Paris, Dunod, 1965.

Optical methods were used for studying the positions of defect energy levels in n-type germanium irradiated with fast neutrons. Irradiation of the antimony-doped n-type germanium single crystals was carried out at 100°C and photoconductivity measurements were made. Data are presented in graphs and can be explained by a set of local defects energy levels. (M.C.G.)

**2496** FORMATION OF DEFECTS AT LOW TEMPERATURE IN Si IRRADIATED BY $^{60}Co$ $\gamma$ RAYS. Flores, J. Merlo; Messier, J. (Centre d'Etudes Nucleaires Saclay, France). pp 155-60 of Radiation Damage in Semiconductors. Paris, Dunod, 1965. (In French).

Studies were made by Hall effect and resistivity measurements on high resistivity n-type silicon of the formation conditions at low temperature of a level at 160 Mev in the conduction band. The temperature dependence of the introduction rate for this level as well as its formation velocity at low temperature did not identify it with the association vacancy-oxygen observed by electron resonance. On high resitivity p-type silicon the anneal at 175°K of a defect formed by bombardment at 77°K was observed. This defect seemed closely related to the one responsible for the level placed at 270 Mev in the valence band. (auth)

**2497** RADIATION DAMAGE IN SEMICONDUCTING III-V COMPOUNDS. Eisen, F. H. (North American Aviation Science Center, Canoga Park, Calif.). pp 163-71 of Radiation Damage in Semiconductors. Paris, Dunod, 1965.

Semiconductor radiation damage studies undertaken in the III–IV compounds are reviewed. Low values of threshold displacement energies were observed. Post-irradiation recovery seemed to be due to the annihilation of primary defects and not to be influenced by the impurities in the samples. The effects of the charge states of the defects on their rates of annihilation were determined. Data are presented for InSb, GaAs, InP, InAs, Ge, and Si. (M.C.G.)

**2498** FLUORESCENCE STUDIES ON II-VI COMPOUND SEMICONDUCTORS. Kulp, B. A. (Aerospace Research Labs., Wright-Patterson Air Force Base, Ohio). pp 173-7 of Radiation Damage in Semiconductors. Paris, Dunod, 1965.

Fluorescence studies of radioinduced defects in CdS and ZnSe semiconductors are reviewed. (M.C.G.)

**2499** SOME ELECTRICAL TRANSPORT STUDIES ON n-TYPE II-VI SEMICONDUCTORS. Woodbury, H. H.; Aven, M. (General Electric Research Lab., Schenectady, N. Y.). pp 179-85 of Radiation Damage in Semiconductors. Paris, Dunod, 1965.

The effects of electron irradiation and thermal treatments on the electrical transport properties of CdTe, CdS, and ZnSe n-type semiconductors were studied with special emphasis on the double acceptor defect. A tentative model is proposed for the double acceptor center, which was found to be the dominant defect produced in n-type CdS, ZnSe, and CdTe. (M.C.G.)

**2500** NEUTRON AND GAMMA IRRADIATIONS OF INDIUM ANTIMONIDE AT 78 deg K. ANNEALING OF DEFECTS. Verdone, M.; Georgopoulos, C.; Dautreppe, D. pp 205-12 of Radiation Damage in Semiconductors. Paris, Dunod, 1965. (In French).

The irradiation at 78°K of n-type indium antimonide, $n_0 = 7.10^{13}$ $cm^{-3}$, showed up an important effect due to the radiation. This is confirmed by $\gamma$ irradiation using $^{60}Co$. For both these irradiations, isochronous annealing indicated the existence of 5 recovery stages. Isothermal annealing the different stages gave kinetics of first order for the first two. The activation energies of three of these stages are: $E_2 = 0.62$, $E_3 = 0.73$, and $E_4 = 0.79$ ev. The variation of the carrier concentration as a function of the temperature after each annealing stage, enables 5 defect

levels, introduced by irradiation and localized in the forbidden band to be defined. These levels are situated at 0.01 and 0.03 ev below the conduction band, and at 0.034, 0.060, and 0.080 ev above the valence band, respectively. A temperature-dependent defect model is proposed, which accounts for the experimental results. (auth)

**2501** STUDIES OF RADIATION DEFECTS IN GaAs BASED ON PROTON- AND ELECTRON-BOMBARDMENT INDUCED LIGHT EMISSION. Loferski, J. J.; Wu, Ming Hsien (Brown Univ., Providence). pp 213-17 of Radiation Damage in Semiconductors. Paris, Dunod, 1965.

Defects induced in GaAs by electron and proton bombardment were studied by examination of the spectral composition and intensity of the luminescence from the irradiated crystals. It was concluded that the threshold for introduction of radiation defects in GaAs lies between 275 and 288 kev. The spectrum associated with proton-bombardment-induced defects differed markedly from that associated with electron-bombardment defects. (M.C.G.)

**2502** THE EFFECT OF NEUTRON IRRADIATION ON THE ELECTRICAL PROPERTIES OF $Mg_2Ge_{0.8}Si_{0.2}$. Barnes, C. E.; Kikuchi, C.; Mason, D. R. (Univ. of Michigan, Ann Arbor). pp 219-23 of Radiation Damage in Semiconductors. Paris, Dunod, 1965.

Single crystals of $Mg_2Ge_{0.8}Si_{0.2}$ were irradiated with a neutron flux of $4 \times 10^{12}$ n/sec cm$^2$ and the effects of radiation of the electric conductivity and Hall effect were determined. The Hall constant decreased both with increasing temperature and increasing amounts of irradiation. The electric conductivity increased with increasing irradiation. Results indicated that the donor centers induced by irradiation have rather deep-lying levels. It was suggested that the increase in mobility with irradiation may be due to a decreasing effective mass, possibly caused by the creation of internal stresses during irradiation. (M.C.G.)

**2503** THE EFFECT OF FAST NEUTRON BOMBARDMENT ON THE ELECTRICAL PROPERTIES OF p- AND n-TYPE SILICON CARBIDE. Nagels, P.; Denayer, M. (S.C.K.-C.E.N., Mol, Belg.). pp 225-33 of Radiation Damage in Semiconductors. Paris, Dunod, 1965.

Studies were made of the influence of the defects introduced during fast neutron irradiation on the electronic behavior of SiC and to establish the reasons for the deterioration of SiC semiconductor devices. Data indicated that n-type SiC remained n-type under irradiation but that p-type changed to n-type. It was therefore concluded that the predominant defect produced by neutron bombardment is an effective donor state. A tentative model of the defect energy states produced by bombardment was deduced. (M.C.G.)

**2504** RADIATION DAMAGE PRODUCED BY FAST ELECTRONS IN SILICON CARBIDE. Mitchell, F. W. J.; Moore, M. J. (Univ. of Reading, Eng.). pp 235-44 of Radiation Damage in Semiconductors. Paris, Dunod, 1965.

Changes in the semiconducting properties of SiC as a function of fast electron irradiation were studied using 2-Mev electrons at 2 $\mu$a/cm$^2$. The carrier concentration was found to decrease with electron irradiation in both n-type and p-type specimens. It was concluded that both donor and acceptor levels are produced in the band gap when atoms are displaced by fast electron irradiation. The net effect of the two types of state depended on the position of the Fermi level. (M.C.G.)

**2505** EFFECTS OF NEUTRON AND PROTON BOMBARDMENTS ON THE EXCITON SPECTRUM OF $Cu_2O$. Nikitine, S.; Grosmann, M.; Schwab, C.; Deiss, J. L.; Soxhlet, P.; Song, K. S. (Univ., Strasbourg). pp 245-52 of Radiation Damage in Semiconductors. Paris, Dunod, 1965. (In French).

The perturbation of the exciton spectrum of $Cu_2O$ by neutron and proton irradiation, in comparison with the Stark effect for the exciton and the substitution of silver atoms for those of copper, was studied. It is shown that the deformation potential resulting from large defects created in the $Cu_2O$ lattice by the energetic particles is the cause of the effects observed, and in particular of the appearance of fine exciton structure. The results of calculations for a model in which the dislocation loop is considered as the large defect involved are presented. (auth)

**2506** DEFECT MOBILITY AND ANNEALING IN IRRADIATED GERMANIUM AND SILICON. Hasiguti, R. R.; Ishino, S. (Tokyo Univ.). pp 259-73 of Radiation Damage in Semiconductors. Paris, Dunod, 1965.

Diagrams of annealing stages for defects in irradiated germanium and silicon are shown. Five main annealing stages in irradiated n-type germanium and two to four main stages in irradiated p-type germanium were observed in the range from 4 to 550°K. Some defects in silicon were identified and the annealing behavior of these defects clarified. The experimentally estimated migration energies of a vacancy and an interstitial were very different in germanium and silicon. (M.C.G.)

**2507** DRIFT MOBILITY OF RADIATION-INDUCED DEFECTS IN SILICON. Davoust-Saltiel, E.; Baruch, P. (Ecole Normale Superieure, Paris). pp 275-80 of Radiation Damage in Semiconductors. Paris, Dunod, 1965.

Measurements were made of the drift mobility of radiation defects in silicon at 0 to 120°C. After irradiation a large decrease in electron concentration was found at 78°K. However, a large part of this decrease was reversible. Three different annealing steps were identified: near room temperature, near 110°C, and near 200°C. Each step was sensitive to the electric field. (M.C.G.)

**2508** RADIATION-ENHANCED DIFFUSION IN SILICON. Pfister, J. C. (Ecole Normale Superieure, Paris). pp 281-5 of Radiation Damage in Semiconductors. Paris, Dunod, 1965.

Studies were made of the enhancement of diffusion produced by the controlled creation of point defects in silicon by irradiation with protons or electrons. The samples were heated during irradiation to 600 to 1200°C so that diffusion could take place. The lifetime of proton-induced defects was near 100 sec at 850 to 900°C and the diffusion length depended on the crystalline perfection of the sample. Electron-bombardment studies showed enhanced diffusion at 900 to 1000°C. Values of 4 to 5 $\mu$ were obtained for defect diffusion length. It was concluded that vacancies are created by irradiation and that these enhance impurity diffusion. (M.C.G.)

**2509** RIPENING OF DEFECTS, INDUCED BY FAST NEUTRONS IN GERMANIUM, IN THE COURSE OF LOW-TEMPERATURE ANNEALING. Konopleva, R. F.; Novikov, S. R.; Rubinova, E. E.; Ryvkin, S. M. (Ioffe Physico-Technical Inst., Leningrad). pp 287-94 of Radiation Damage in Semiconductors. Paris, Dunod, 1965.

Specimens of n-type and p-type germanium were irradiated in a reactor at liquid nitrogen temperature with various doses of fast neutrons (up to $5 \times 10^{15}$ n/cm$^2$). The radiation effects on the properties of the samples were determined and then the specimens were annealed at different temperatures ranging from 100 to 600°K. Four clearly pronounced annealing stages were observed. Irradiation resulted in a compensation of both n- and p-material, which indicated a simultaneous introduction of donor and acceptor centers. However, the maximum degree of compensation was not achieved immediately on irradiation but following an additional warming at temperatures above 77°K. A number of energy levels appeared in the forbidden band of germanium at the first stage of annealing. The activation energies for the ripening of defects and annealing of donors are 0.17 and 0.55 ev, respectively. The extreme position of the Fermi level in specimens irradiated at low temperature lay close to the center of the forbidden band. (M.C.G.)

**2510** GAMMA IRRADIATION OF LITHIUM DRIFTED p-i-n JUNCTIONS IN SILICON. Ammerlaan, C. A. J. (Univ. of Amsterdam). pp 295-302 of Radiation Damage in Semiconductors. Paris, Dunod, 1965.

The effects of gamma radiation on silicon were studied using lithium-drifted p-i-n junctions. Irradiations were performed at room temperature for a 100-hr period. Measurements were made of the capacity of the junction versus the applied reverse bias. The time dependence of the ion density in a reverse biased junction at room temperature after irradiation is shown. When no reverse bias was applied to the junction, some increase of the junction capacity, instead of anneal, was observed. (M.C.G.)

**2511** FIELD AND CHARGE DEPENDENCE OF RADIATION DAMAGE IN SILICON. Fang, P. H. (Goddard Space Flight Center, Greenbelt, Md.). pp 303-6 of Radiation Damage in Semiconductors. Paris, Dunod, 1965.

The photovoltaic short circuit current of a Si cell with shallow p-n junction subjected to electron radiation was measured as a function of photon energy before and after irradiation. The silicon spatial radiation damage function was calculated. (M.C.G.)

**2512** STUDY OF RECOMBINATION PROCESSES OF ELECTRON-HOLE PAIRS IN GERMANIUM IRRADIATED BY $^{60}$Co $\gamma$ RAYS BY MEANS OF THE PHOTOVOLTAIC EFFECT IN p-n JUNCTIONS. van Dong, Nguyen; Zahedi-Moghadam, A. (Centre d'Etudes Nucleaires de Saclay, Gif-sur-Yvette, France). pp 307-12 of Radiation Damage in Semiconductors. Paris, Dunod, 1965. (In French).

Using the photovoltaic effect in p-n junctions, the recombination mechanism of electron-hole pairs during irradiation as influenced by the structural defects introduced in n- and p-type germanium by $^{60}$Co $\gamma$ rays was followed. At 310°K, the level of the recombination centers was located 0.26-ev below the conduction band and the capture cross sections for holes and electrons were respectively: $\sigma_p = 4 \times 10^{-15}$ cm$^2$ and $\sigma_n = 3 \times 10^{-15}$ cm$^2$. The value for $\sigma_n$ was probably underestimated, because the number of defects introduced in p-type samples seemed smaller than in n-type. These results seemed to indicate that interstitials are responsible for the recombination. At 80°K in n-type samples, a shallow level located 0.05 ev below the conduction band, with a capture cross section for holes $\sigma_p \geq 2 \times 10^{-14}$ cm$^2$, was found. It was concluded that in this case carrier recombination is due to close vacancy-interstitial pairs. In p-type samples at low temperature, the lifetime was practically not influenced by irradiation. This was attributed to a spontaneous annealing of vacancy-interstitial pairs due to purely electrical interactions. (auth)

**2513** THRESHOLDS AND CROSS SECTIONS. Mitchell, E. W. J. (Univ. of Reading, Berkshire, Eng.). pp 367-74 of Radiation Damage in Semiconductors. Paris, Dunod, 1965.

The values of displacement energy found for semiconductors range from about 5 to 100 ev. Problems associated with determining displacement energies are discussed. The importance of the energy variation of damage rates is considered. It was concluded that the energy dependence of the threshold curve is important not only to separate collision from ionization effects, but also to obtain unequivocal conclusions about the interpretation of anisotropies of the electron threshold energies. (M.C.G.)

**2514** EFFECTS OF ELECTRON IRRADIATION ON THE MOBILITY OF ELECTRONS IN GALLIUM ARSENIDE. Grimshaw, J. A. (Univ. of Reading, Berkshire, Eng.). pp 377-84 of Radiation Damage in Semiconductors. Paris, Dunod, 1965.

Changes in electron mobility in irradiated gallium arsenide were studied and interpreted in terms of the ionized scattering theory. Hall effect and electric conductivity measurements were made both before electron irradiation and as a function of dose and incident energy at 80°K, and as a function of temperature between 80 and 290°K. Mobility changes appeared independent of the kinetic energy of displaced atoms up to 1.0-Mev beam energy. The reduction in mobility induced by bombardment at 80°K was greater than would be caused by increased scattering due to the introduction of one singly charged acceptor as each carrier is removed from the conduction band. (M.C.G.)

**2515** MEASUREMENT OF ANISOTROPY OF DISPLACEMENT ENERGY IN SILICON. George, G. G.; Gunnersen, E. M. (Atomic Weapons Research Establishment, Aldermaston, Berks., Eng.). pp 385-92 of Radiation Damage in Semiconductors. Paris, Dunod, 1965.

Room-temperature irradiations at doses of $8.7 \times 10^{12}$ electrons/cm$^2$ were used to study the anisotropy of displacement energy in silicon. It was established that at energies in the region of 500 kev, the change in carrier concentration is approximately a linear function of dose. It was concluded that close above the threshold, the (111) displacements are easier than (110), which in turn are easier than (100), and that this anisotropy does not disappear until above 1200 kev. (M.C.G.)

**2516** THE NATURE AND YIELD OF PHOTON AND NEUTRON INDUCED DEFECTS IN SEMICONDUCTORS. Cleland, J. W.; Bass, R. F.; Crawford, J. H. Jr. (Oak Ridge National Lab., Tenn.). pp 401-6 of Radiation Damage in Semiconductors. Paris, Dunod, 1965.

An extensive series of determinations of the rates of introduction of lattice defects in a variety of semiconductors by irradiation from changes in electrical properties is described. The effects of gamma radiation and thermal neutrons on Ge, GaAs, and Si are reported in tables. (M.C.G.)

**2517** STUDIES OF HIGH-ENERGY ELECTRON (10-60 Mev) AND PROTON (20-130 Mev) RADIATION DAMAGE IN SILICON AND GERMANIUM. Corelli, J. C.; Cheng, L. J.; Taylor, C. A.; Merrill, O. H. (Rensselaer Polytechnic Inst., Troy, N. Y.). pp 407-16 of Radiation Damage in Semiconductors. Paris, Dunod, 1965.

The characteristics and properties of defects induced in silicon and germanium by electrons at 10 to 60 Mev and protons at 20 to 130 Mev are described. (M.C.G.)

**2518** CARRIER LIFETIME STUDIES IN HIGH-ENERGY ELECTRON-IRRADIATED SILICON. van Lint, V. A. J.; Harrity, J. W. (General Atomic Div., General Dynamics Corp., San Diego, Calif.). pp 417-23 of Radiation Damage in Semiconductors. Paris, Dunod, 1965.

Irradiation of silicon by high-energy electrons (~30 Mev), which produce on the average a small number of (~4.3) of total displacements per primary recoil event, was studied. The measurements were performed over a large range of excess-carrier concentrations to verify the consistency of the Shockley-Read theory with the recombination process and, hence, to determine both the low-injection and high-injection lifetime parameters. (M.C.G.)

# PHYSICS

## General

**2519** (AD-615152) SOLID STATE RESEARCH USING HIGH MAGNETIC FIELDS. Final Report, July 1-October 31, 1964. Lax, Benjamin; Bitter, Francis (National Magnet Lab., Massachusetts Inst. of Tech., Cambridge). Feb. 15, 1965. Contract AF19(604)-7344. 46p. (AFOSR-65-0733). CFSTI $2.00 cy, $0.50 mn.

Research on solid state, low temperature, and plasma physics is described. Within these areas such phenomena as super-conductivity, magneto-optical effects, cyclotron and magnetic resonance, and transport effects in metals, semimetals, and semiconductors were investigated. (TAB)

**2520** (IA-920) RESEARCH LABORATORIES SEMI-ANNUAL REPORT FOR THE PERIOD JULY-DECEMBER 1963. (Israel Atomic Energy Commission, Yavne. Soreq Research Establishment). 196p. Dep. mn.

Progress and trends in the research program are reported, and operational services are described. Information is included on operation of the IRR-1 Reactor and isotope production. Research progress is reported on elementary particle theory, reactor physics, nuclear physics, solid state physics, inorganic chemistry, radiation chemistry, nuclear chemistry, analytical chemistry, and applications technology. Biological and medical research are summarized. Results of research on nuclear hazards are presented along with research progress on nuclear and mechanical instrumentation. A bibliography of reports and papers associated with the project is included. (JRD)

**2521** (LNF-65/28) ACTIVITY AT THE NATIONAL LABORATORIES OF FRASCATI, JULY 1, 1964-JUNE 30, 1965. Report No. 15. (Laboratori Nazionali di Frascati, Comitato Nazionale per l'Energia Nucleare (Italy)). Aug. 1965. 32p. Dep. mn.

Research carried out by the following groups during June-July 1964 is presented; high-energy nuclear physics, Adone project, LEALE, machine, cryogenic, magnetic measurements, electronics, technological, health physics, and computing. (M.O.W.)

**2522** (ORNL-P-1516) SOME PROBLEMS IN THE DESIGN OF AN 8TH ORDER POWER OPTIMIZED COIL. Luton, J. N. Jr. (Oak Ridge National Lab., Tenn. [1965]. Contract W-7405-eng-26. 11p. (CONF-650512-14). Dep. mn; CFSTI $1.00 cy, $0.50 mn.

From Symposium on Engineering Problems of Controlled Thermonuclear Research, Livermore, Calif.

A review of the problems encountered in the design of magnet coils to produce a given field with a minimum of power is presented. Previous work has shown that the current density distribution which produces the maximum field strength for a given power is under the restriction that the coil be of a certain order. Using this concept, work aimed at producing a field of about 60 kG, homogeneous over a 12" sphere, with a solenoid which consumes 7 Mw is presented. (M.O.W.)

**2523** (SC-RR-65-449) MATHEMATICAL MODELS OF MAGNETIC FLUX COMPRESSION. Freeman, John R.; Lane, Frank O.; Byatt, William J. (Sandia Corp., Albuquerque, N. Mex.). Oct. 1965. Contract AT(29-1)-789. 33p. Dep. mn; CFSTI $2.00 cy, $0.50 mn.

One- and two-dimensional models of magnetic flux compression devices are derived. Analytical solutions for the magnetic field as a function of time are obtained under the assumption of an infinitely conducting liner system, while field solutions for the case of a finite, temperature dependent liner conductivity are obtained numerically. Data are presented showing the relation between the initial conditions of the device and $B_{max}$, the maximum field obtained. For the case of infinite conductivity, this relationship can be expressed as; $B_{max}/B_0 = 1 + KE_0/ME_0 \simeq KE_0/ME_0$, where $B_0$ is the initial magnetic field, $KE_0$ is the initial kinetic energy, and $ME_0$ is the initial magnetic energy in the system. This expression is valid for both the one- and two-dimensional models. Results for $B_{max}/B_0$ are shown graphically for the case of a finite, temperature dependent conductivity. Data relating to the turnaround radius, or minimum liner separation, are also presented. Assuming infinite conductivity in the one-dimensional model, this relationship is

$$\frac{l_T}{l_0} = \frac{1}{1 + \dfrac{KE_0}{ME_0}} \simeq \frac{ME_0}{KE_0}$$

where $l_0$ is the initial liner separation and $l_T$ is the minimum liner separation. For the two-dimensional model this expression becomes

$$\frac{r_T}{r_0} = \frac{1}{1 + \dfrac{KE_0}{ME_0}} \simeq \frac{ME_0}{KE_0}$$

where $r_0$ is the initial liner radius and $r_T$ is the turnaround radius. Turnaround radius data are shown graphically for the case of a finite, temperature dependent conductivity. (auth)

**2524** (NP-tr-1292(Draft)) DISCUSSION OF THE REPORT ON THE ACTIVITIES OF THE DEPARTMENT OF GENERAL AND APPLIED PHYSICS FOR THE YEAR 1963/64, PRESENTED BY ACADEMICIAN-SECRETARY L. A. ARTSIMOVICH. Translated for Culham Lab., Abingdon, Eng., from Vestn. Akad. Nauk SSSR, No. 2, 15-50(1965). 57p. (CTO/201(Draft)). Dep. mn; CFSTI $3.00 cy, $0.50 mn; JCL $5.60 fs, $1.91 mf.

**2525** HIGH-FREQUENCY INDUCTION CURRENTS AND THEIR USES AT VERY HIGH TEMPERATURES. Reboux, J. Ingrs. Techniciens, No. 177, 115-25(1964). (In French).

The results that have been obtained in the laboratory or industrially in metallurgy, chemistry, and physics of very high temperatures are summarized. The various developments that can be predicted from the present data are indicated. (J.S.R.)

**2526** MATERIALY IV VSESOYUZNOGO SOVESHCHANIYA PO SEGNETOELEKTRICHESTVA (ROSTOV-NA-DONU, 12-18 SENTYABRYA, 1964 g.). (Report, 4th All-Union Conference on Ferroelectricity, Rostov-on-the-Don, USSR, Sept. 12-18, 1964). Izv. Akad. Nauk SSSR, Ser. Fiz., 29: 874-1052(June 1965). (CONF-640917).

Forty-six papers are presented on ferroelectricity, which include the following: theoretical studies on relaxation kinetics; phase transitions; dipole structure; ferroelectric and magnetically ordered ferroelectric states; and experimental investigations of various ferroelectric and antiferroelectric materials on phase transitions; x-ray diffraction studies; crystal structure; magnetic resonance; spectroscopy; dielectric properties; Barkhausen effect; polarization, domain structure; optical properties; electro-optical effect; electro-caloric effect; thermal conductivity; ultrasound absorption; physical properties near Curie point; electron paramagnetic resonance spectra; mechanism of relaxation polarization; effect of doping on electric properties; structure and properties of ferroelectric-ferromagnetic solid solutions; magnetic properties, and thermal expansion. (L.B.S.)

**2527** ON SPONTANEOUS PARTICLE RADIATION IN RESONATOR WITH SEVERAL COUPLED MODES. Agabekyan, A. S.; Grasyuk, A. Z.; Oraevskii, A. N. (Lebedev Inst. of Physics, Moscow). Izv. Vyssh. Ucheb. Zavedenii, Radiofiz., 8: 631-3(1965). (In Russian).

The effects of coupling between the various modes of oscillation of a resonator on the spontaneous radiation of excited particles in the resonator are studied. The probability

of spontaneous transition of a particle in unit time from a state corresponding to the higher of two noncrossing discontinuous bands with known average energies to some state of the lower band is investigated. For the two limiting cases of the line width much less and much greater than the resonator transmission band, coupling between the modes is found to decrease the probability of spontaneous radiation. (M.J.T.)

**2528** PROPOSAL FOR A SOURCE OF COMPLETELY POLARIZED DEUTERONS. Von Ehrenstein, D. (Argonne National Lab., Ill.); Hess, D. C.; Clausnitzer, G. Phys. Letters, 19: 114-16(Oct. 1, 1965).

A previously proposed method for obtaining polarized deuterium ions is described. It is proposed to use two 6-pole magnets, each followed by an adiabatic-passage region in the use of the atomic-beam magnetic-resonance apparatus. A selection of theoretically possible transitions is given, and the design of the apparatus is shown. The possible modes of operation are discussed. One of the most crucial points of the proposal is whether beam intensity is lost in the second 6-pole magnet. But the selection of atoms with acceptable velocity, which has already taken place in the first 6-pole magnet, is responsible for the largest intensity loss. After this has happened most of the particles can be transmitted through the second 6-pole magnet. (J.F.P.)

**2529** SOME EFFECTS IN THE ELECTROMAGNETIC INTERACTIONS OF PARTICLES WITH COLLIDING CLUSTERS. Derbenev, Ya. S. (Inst. of Nuclear Physics, Academy of Sciences, Siberian SSR). Yadern. Fiz., 2: 119-23(July 1965). (In Russian).

One-dimensional betatron oscillations of a particle interacting with a cluster are investigated, using the first approximation of the averaging method. It is shown that the interaction leads to a large number of stable equilibrium orbits. The main characteristics of motion in the stability region of these orbits are discussed. (auth)

**2530** APPLICATIONS OF NONLINEAR PARTIAL DIFERENTIAL EQUATIONS IN MATHEMATICAL PHYSICS. PROCEEDINGS OF A SYMPOSIUM IN APPLIED MATHEMATICS OF THE AMERICAN MATHEMATICAL SOCIETY, HELD IN NEW YORK CITY, APRIL 20–23, 1964. Finn, R. (ed.). Proceedings of Symposia in Applied Mathematics. Volume XVII. Providence, American Mathematical Society, 1965. 239p. (CONF-640402).

General nonlinear theory, finite elasticity of compressible fluids, the magnetohydrodynamics of viscous fluids, general relativity, and quantum field theory are discussed. Seventeen papers are included. (J.F.P.)

## Accelerators

*Refer also to abstracts 3258–3264, and 3371.*

**2531** (AD–618304) RADIATION FACILITY SUPPORT AND SOLID-STATE STUDIES. Final Report. Wall, James A.; Glassbrenner, Charles J.; Mayburg, Sumner; Fritts, Martin (Controls for Radiation, Inc., Cambridge, Mass.). June 16, 1965. Contract AF19(628)-4036. 76p. (AFCRL–65-375). CFSTI $3.00 cy, $0.75 mn.

AFCRL linear accelerator acceptance tests are described. A health physics manual was prepared and other safety procedures established for safe operation of the linac facility. Instruments for measuring linac beam current were developed when necessary. A special ozone detector was developed for rapid measurement of the high levels of ozone developed near the linac. A low temperature thermal conductivity apparatus was designed and assembly has been essentially completed. It was designed so that thermal conductivity can be measured on samples that have been bombarded at low temperatures. Determination of the concentration of oxygen in silicon to levels as low as 10 to the 13th power atoms/cm$^3$ by means of photonuclear activation analysis is discussed. Initial tests of the technique were performed. The optimum operating electron energy of the AFCRL linac for photoactivation of oxygen is computed to be 19.4 Mev. (auth)

**2532** (BNL–9505) THE BROOKHAVEN RADIO-FREQUENCY BEAM SEPARATOR. Hahn, H.; Halama, H. J.; Foelsche, H. W. J. (Brookhaven National Lab., Upton, N. Y.). [1965]. Contract AT(30-2)-Gen-16. 12p. (CONF-650923–8). Dep. mn; CFSTI $1.00 cy, $0.50 mn.

From 5th International Conference on High Energy Accelerators, Frascati, Italy.

A Panofsky type radiofrequency beam separator with two deflectors and central beam stopper is being constructed in the Accelerator Department at Brookhaven. The separator will work in beam No. 4 to the 80-inch bubble chamber. The operating frequency is about 2856 Mc and the distance between deflectors 40 m, leading to operating momenta with two-contaminant rejection for $K^{\pm}$ at 12.8, 9.05, 7.39 Bev/c and for $\bar{p}$ at 18.1 Bev/c. High-purity beams are possible only if the deflections of the unwanted particles cancel exactly. The ensuing stringent conditions of phase stability are discussed and a solution by means of a phase servo system is indicated. The deflectors are 3-m-long iris-loaded waveguides operating in a backward wave hybrid mode, with a phase velocity equal to the particle velocity. The deflectors are powered from RCA 8568 klystrons. The associated 65-Mw modulators are built with hydrogen thyratrons KU 274. The klystron is driven by pulsed 6442 triode amplifiers. The common phase-stable r-f source consists of a phase locked cw klystron (726C) followed by a twt amplifier (RCA 4054V1). The performance of the completed microwave system is tested and found entirely satisfactory for this application. (auth)

**2533** (BNL–9536) CURRENT MAGNET DESIGN PRACTICE IN THE U. S. A. Grisoli, J. J. (Brookhaven National Lab., Upton, N. Y.); Brechna, H. (Stanford Linear Accelerator Center, Stanford Univ., Calif.); Hernandez, H. P.; Kilpatrick, R. A.; Lou, K. H. (Lawrence Radiation Lab., Univ. of California, Berkeley); Krizek, R. (Argonne National Lab., Ill.). Sept. 1965. Contract AT-30-2-GEN-16. 31p. (CONF-650922-17). Dep. mn; CFSTI $2.00 cy, $0.50 mn.

From 1st International Symposium on Magnet Technology, Stanford, Calif.

Magnets in use at ANL, LRL, SLAC, and BNL are described. Types of cores, core construction and coil design are reviewed with the intention of giving a broad picture of the current magnet design practices in the U.S.A. Many aspects are common to all the laboratories and will not necessarily be repeated. (auth)

**2534** (BNL–9587) EVALUATION OF PHASE-SPACE DENSITY MEASUREMENT TECHNIQUES. van Steenbergen, A. (Brookhaven National Lab., Upton, N. Y.). Sept. 1, 1965. Contract AT(30-2)-Gen-16. 22p. (CONF-650923–14). Dep. mn; CFSTI $1.00 cy, $0.50 mn.

From 5th International Conference on High Energy Accelerators, Frascati, Italy.

For a particle beam propagating along the z-axis and assuming a simple distribution in the $z,p_z$ projection of the six-dimensional phase-space volume in $(x,y,z,p_x,p_y,p_z)$, the total beam can be represented by, $N_{tot} = \iiiint \rho(x,x',y,y')\,dxdx'dydy'$ and the integrated partial density function is given by $D(x,x') = \iint \rho(x,x',y,y')\,dydy'$. Consequently, $N_{tot} = \iint D(x,x')\,dxdx'$. The following beam phase-space distribution measurement methods are considered, the two pairs of crossed slits method, the two slit method, and the crossed slits plus photographic film method. (M.O.W.)

**2535** (CERN–65-31) A MISSING BUNCH PHASE-LOCK SYSTEM FOR PROTON STORAGE RINGS. Schnell, W. (European Organization for Nuclear Research, Geneva (Switzerland)). Sept. 2, 1965. 13p. Dep. mn.

A system is described that is capable of distinguishing particles inside and outside the regions of stable oscillation in proton storage rings. The purpose of the system is to maintain phase-lock beam control, independently of the particle density in the surrounding stack. The operation of the system is discussed in the case of the Intersecting Storage Rings to be added to the CERN proton synchrotron. (T.F.H.)

**2536** (JINR-P-2341) O VOZMOZHNOSTI STABILIZATSII INTENSIVNOSTI SINKHROTSIKLOTRONA. (On a Possibility of Stabilization of the Synchrocyclotron Intensity). Danilov, V. I.; Enchevich, I. B.; Marchenko, B. N.; Polferov, E. A.; Safonov, A. N.; Shestov, A. V. (Joint Inst. for Nuclear Research, Dubna (USSR). Lab. of Nuclear Problems). 1965. 9p. Dep. mn.

A possible method is suggested to stabilize the synchrocyclotron intensity. It is based on the introduction of the negative feedback between the beam current transducer and one of the parameters by means of which it is possible to vary the intensity. As such a parameter, the voltage applied to the focusing electrodes was chosen. (auth)

**2537** (LA-DC-7268) DESIGN OF A SOURCE OF NEGATIVE POLARIZED HYDROGEN IONS USING CHARGE EXCHANGE IN CESIUM AND ARGON. McKibben, J. L. (Los Alamos Scientific Lab., Univ. of California, N. Mex.). [1965]. Contract W-7405-eng-36. 5p. (CONF-650928-8). Dep. mn; CFSTI $1.00 cy, $0.50 mn.

From International Conference on Polarization Phenomena of Nucleons, Karlsruhe, Ger.

The use of the metastable state in hydrogen as a means of producing a beam of polarized ions is briefly discussed. Based on the concept of charge exchange in argon and cesium, an apparatus was designed which will produce a relatively large intensity of polarized negative hydrogen ions. A discussion on the operation of the equipment is presented. (M.O.W.)

**2538** (LA-DC-7281) HIGH ENERGY PROTON LINEAR ACCELERATORS. Nagle, Darragh E. (Los Alamos Scientific Lab., Univ. of California, N. Mex.). [1965]. Contract W-7405-eng-36. 34p. (CONF-650923-20). Dep. mn; CFSTI $2.00 cy, $0.50 mn.

From 5th International Conference on High Energy Accelerators, Frascati, Italy.

Recent advances in proton linac design are reported. A survey is given of the parameters of some current designs, then some specific problems of waveguide linacs are considered, namely the theory of waveguide tanks, the choice of modes for the tank, the influence of unwanted modes, the optimal design of the accelerating cavities, methods of fabrication, sources of r-f power, and tests with electron beams. Finally some remarks are made about the particle motion and the effects of errors, and the possibilities for proton linacs above 1-Bev. (M.O.W.)

**2539** (SLAC-47) PROPERTIES OF SYMMETRIC QUADRUPOLE MAGNET TRIPLETS. Brown, K. L.; Hindmarsh, A. C. (Stanford Linear Accelerator Center, Stanford Univ., Calif.). Aug. 1965. Contract AT(04-3)-400. 49p. Dep. mn; CFSTI $2.00 cy, $0.50 mn.

A symmetric quadrupole magnet triplet, consisting of two identical quadrupoles aligned with a quadrupole of the opposite polarity midway between them, is capable of focusing a beam in both the horizontal and vertical planes simultaneously. Results of an investigation are given for symmetric triplets of configurations most frequently used, namely, those in which the middle magnet is either twice the length of the other two or of the same length. Properties are given for point-to-point focus and the parallel-to-point focus configurations. In the first case, a beam emerging from a point object is focused to a point image in the horizontal and vertical planes simultaneously. In the second case, an entering parallel beam is focused to a point image in both planes simultaneously. The tabulations are normalized for applicability to systems of any aperture or magnet length. (M.O.W.)

**2540** (UCRL-16223) THE DESIGN OF EXPERIMENTAL FACILITIES AT THE PROPOSED 200-Gev ACCELERATOR. Keefe, Denis (Lawrence Radiation Lab., Univ. of California, Berkeley). Aug. 25, 1965. Contract W-7405-eng-48. 24p. (CONF-650923-15). Dep. mn; CFSTI $1.00 cy, $0.50 mn.

From 5th International Conference on High Energy Accelerators, Frascati, Italy.

The experimental uses of the proposed 200-Bev accelerator are discussed in connection with the design of experimental facilities for the accelerator. (M.O.W.)

**2541** (UCRL-16228) THE IMPROVED BEVATRON AND ITS PERFORMANCE AT HIGH INTENSITY. Chupp, W. W.; Elioff, T.; Wenzel, W. A. (Lawrence Radiation Lab., Univ. of California, Berkeley). Aug. 26, 1965. Contract W-7405-eng-48. 21p. (CONF-650923-13). Dep. mn; CFSTI $1.00 cy, $0.50 mn.

From 5th International Conference on High Energy Accelerators, Frascati, Italy.

As a result of the recent major improvement program, the Bevatron was substantially improved in performance and experimental capability. The successful operation of the new injection system and the addition of considerable shielding permit continuous high intensity operation. Performance characteristics, particularly with respect to the operational techniques used for simultaneous experiments, are described. The properties of the new external proton beam, now required for a majority of the experiments, and the plans for further beam extensions and development of additional experimental areas are discussed. (auth)

**2542** (UCRL-16236) 200 Bev ACCELERATOR HANDLING SYSTEMS IN REGIONS OF HIGH RESIDUAL RADIOACTIVITY. Salsig, William W. (Lawrence Radiation Lab., Univ. of California, Berkeley). Sept. 1965. Contract W-7405-eng-48. 13p. (CONF-650923-10). Dep. mn; CFSTI $1.00 cy, $0.50 mn.

From 5th International Conference on High Energy Accelerators, Frascati, Italy.

Analyses are given of the performance and feasibility of shielded manipulator vehicles for use in handling and maintenance of components of high-energy accelerators. The shielded vehicles studied permit semi-remote handling and direct (through arm holes) handling. (T.F.H.)

**2543** (UCRL-16238) DESIGN STUDY FOR A 200 Gev ACCELERATOR FACILITY. Smith, Lloyd (Lawrence Radiation Lab., Univ. of California, Berkeley). Sept. 1965. Contract W-7405-eng-48. 13p. (CONF-650923-23). Dep. mn; CFSTI $1.00 cy, $0.50 mn.

From 5th International Conference on High Energy Accelerators, Frascati, Italy.

A design study for a proposed 200-Bev proton synchrotron is presented. Brief descriptions of the main ring magnets, accelerator system, injection system, and costs and schedules are included. (M.O.W.)

**2544** (UCRL-16309) DESIGN PROBLEMS ASSOCIATED WITH HIGH-CURRENT-DENSITY WATER-COOLED SEPTUM MAGNETS. Green, Michael A. (Lawrence Radiation Lab., Univ. of California, Berkeley). Aug. 1965. Contract W-7405-eng-48. 16p. (CONF-650922-4). Dep. mn; CFSTI $1.00 cy, $0.50 mn.

From the 1st International Symposium on Magnet Technology, Stanford, Calif.

The problems studied for high-current-density (above 5 ka/cm$^2$) water-cooled magnets include heat transfer, current optimization in rectangular conductors, basic concepts of achievement of high current densities, burnout, pumping and handling of coolant, coolant cavitation, and erosion, corrosion, and electrolysis. (T.F.H.)

**2545** (UCRL-16386) COST ESTIMATING MAGNET SYSTEMS WITH THE AID OF A COMPUTER. Hernandez, H. P.; Schwarz, R. W.; Yourd, R. B. (Lawrence Radiation Lab., Univ. of California, Berkeley). Sept. 3, 1965. Contract W-7405-eng-48. 19p. (CONF-650922-19). Dep. mn; CFSTI $1.00 cy, $0.50 mn.

From 1st International Symposium on Magnet Technology, Stanford, Calif.

The COMA Fortran Program briefly outlined can be used to compute twelve basic magnet geometries, including quadruple, box, "C," and "H" types. For the 6-meter spherical-bubble-chamber magnet of conventional iron-copper arrangement, the COMA Program was used, with the subroutine EFFIC added. Magnetic fields up to 70 kG were studied, and optimum coil dimensions and core thicknesses found. At 50 kG the capital plus operational cost for an operating time of 20,000 hours was 32-million dollars. For the 8-Bev Injector Synchrotron Gradient Magnet System, the MAGHYP Program aided in parameter selection and cost estimate. Cost optimization showed that the parameter

selections can be made more accurately than future market conditions can be predicted. (auth)

**2546** (UCRL-16389) MAGNET DESIGN APPLICATIONS OF THE MAGNETOSTATIC COMPUTER PROGRAM CALLED SIBYL. Dorst, Joseph H. (Lawrence Radiation Lab., Univ. of California, Berkeley). Sept. 7, 1965. Contract W-7405-eng-48. 13p. (CONF-650922-16). Dep. mn; CFSTI $1.00 cy, $0.50 mn.

From 1st International Symposium on Magnet Technology, Stanford, Calif.

The computer program SIBYL was used extensively in the design studies of magnets for a 200-Bev synchrotron at the Lawrence Radiation Laboratory, Berkeley. The code was written for static evaluation of two-dimensional magnets including the effects of finite non-uniform permeability of the iron. The general operation of the code and some of the special features are described. The code is especially useful for studying small differences between similar magnets. Applications include evaluation of the effects of iron saturation as a function of current, shaping of the pole base of AGS-type gradient magnets, shaping of magnet poles for good medium-field profiles, and partial evaluation of quadrupole magnets. The validity or accuracy of the computed results is discussed. The comparisons of calculated and measured fields of the CERN Proton Synchrotron Magnet indicate the attainable quality of computed results. At 14.4 kG, within the limits of the vacuum chamber, the gradient computed by SIBYL was within 1% of the measured gradient. (auth)

**2547** (UR-875-98) MUON AND ANTIPROTON TRAP AT SLAC. Greene, D.; Lobkowicz, F.; Tinlot, J. (Rochester Univ., N. Y. Dept. of Physics and Astronomy). Sept. 28, 1965. Contract AT(30-1)-875. 20p. (CONF-650923-19). Dep. mn; CFSTI $1.00 cy, $0.50 mn.

From 5th International Conference on High Energy Accelerators, Frascati, Italy.

It is proposed to construct a strong focussing ring of quadrupole and bending magnets in order to trap muons and antiprotons in the momentum range of 5 to 10 Bev/c. The interaction of the trapped particles can be studied directly in a 16 m long magnetfree section of the trap. The advantages of the scheme are good energy resoltuion of the trapped beam, high interaction rates with thin targets due to multiple traversals, high beam purity and large dutycycle. Parameters of the cell structure and straight sections are presented. The injection system into the ring and the targeting of the high intensity Stanford linear accelerator electron beam are discussed. (auth)

**2548** DUTY CYCLE IMPROVEMENT OF PARTICLE BEAMS AT A 680 Mev JINR SYNCHROCYCLOTRON. Danilov, V. I.; Enchevich, I. B.; Zamolodchikov, B. I.; Polferov, E. A.; Rozanov, E. I.; Smirnov, V. I.; Testov, V. G. At. Energ. (USSR), 19: 289-92(Sept. 1965). (In Russian).

A method for increasing the beam pulse length, tested on the JINR synchrocyclotron, is described. An expression for the duration of the interaction of the proton beam with the target in a continuous spectrum of amplitudes of radial oscillations is given. From this expression it can be seen that the pulse duration can be increased by increasing the interval of amplitudes of the radial oscillations and decreasing the velocity of radial movement of the beam. The use of two magnet coils for stretching the beam is described. The variation of the frequency of the accelerating voltage and the current in the stretching coils with time, the shape of the beam pulses, and the dependence of the intensity of the extended beam on the current in the coils are presented. (M.J.T.)

**2549** MICROTRON—AN EFFECTIVE ACCELERATOR. Sochor, Vaclav. Cesk. Cas. Fys., 15: 422-37(1965). (In Czech).

A survey is given of papers dealing with the problems of the microtron, i.e., a high-frequency circular accelerator of electrons. Its principle and problems not yet solved are discussed, along with new designs that have been proposed for increasing the effectiveness of the accelerator. A comparison is made with other types of accelerators; its advantages and disadvantages and the possibilities for its use are pointed out. A table of some of the microtrons in operation and their parameters is included. (auth)

**2550** CHERENKOV RADIATION OF CHARGED PARTICLES IN CIRCULAR WAVEGUIDE WITH GYROTROPIC FERRITE FILLING. Gazazyan, E. D.; Mergelyan, O. S. (Central Physico-Technical Lab., Academy of Sciences, Arm. SSR). Izv. Vyssh. Ucheb. Zavedenii, Radiofiz., 8: 629-31(1965). (In Russian).

The Cherenkov effect in a circular waveguide, filling with a medium with magnetic permeability tensor possessing magnetic gyrotropy, is studied. The medium can represent a ferrite placed in a constant magnetic field. The energy losses of the particles of the medium by radiation are calculated, and the spectrum of the emitted waves is investigated for the field of a point charge moving in a gyrotropic ferrite and a charged particle moving along the axis of a circular waveguide of fixed radius. (M.J.T.)

**2551** DEVELOPMENT OF SERVO-MANIPULATORS FOR HIGH-ENERGY ACCELERATOR REQUIREMENTS. Flatau, Carl R. (Brookhaven National Lab., Upton, N. Y.). Trans. Amer. Nucl. Soc., 8: 616(Nov. 1965).

**2552** SKYSHINE CONSIDERATION FOR ACCELERATOR SHIELDING DESIGN. Distenfeld, Carl; Colvett, Robert (Brookhaven National Lab., Upton, N. Y.). Trans. Amer. Nucl. Soc., 8: 638-9(Nov. 1965).

**2553** STRAY NEUTRON SPECTRA AT LARGE PULSED-PARTICLE ACCELERATOR SITES. O'Brien, K.; Sanna, R.; Alberg, M.; McLaughlin, J. (Atomic Energy Commission, New York). Trans. Amer. Nucl. Soc., 8: 639(Nov. 1965).

**2554** SHIELDING ATTENUATION OF NEUTRONS FROM 80-Mev ALPHA-PARTICLE BOMBARDMENT OF ELEMENTAL TANTALUM. Wadman, William W. (Univ. of California, Livermore). Trans. Amer. Nucl. Soc., 8: 640(Nov. 1965).

**2555** SEMI-EMPIRICAL SHIELDING METHOD FOR HIGH-ENERGY ELECTRON ACCELERATORS. De Staebler, H. (Stanford Linear Accelerator Center, Calif.). Trans. Amer. Nucl. Soc., 8: 640-1(Nov. 1965).

**2556** SHIELDING PROBLEMS AT THE NRL LINAC FACILITY. Murray, K.; Zimmer, G. W. (Naval Research Lab., Washington, D. C.). Trans. Amer. Nucl. Soc., 8: 641(Nov. 1965).

**2557** SHIELDING OF BREMSSTRAHLUNG FROM AN ELECTRON ACCELERATOR TARGET. Barrett, Mathew J. (Nuclear Utility Services, Washington, D. C.). Trans. Amer. Nucl. Soc., 8: 642(Nov. 1965).

**2558** RADIATION SHIELDING CONSIDERATIONS FOR TANDEM ACCELERATORS. Burrill, E. Alfred (High Voltage Engineering, Burlington, Mass.). Trans. Amer. Nucl. Soc., 8: 642-3(Nov. 1965).

**2559** SHIELDING CONSIDERATIONS FOR THE PROPOSED LOS ALAMOS MESON PHYSICS FACILITY. Cochran, D. R. F.; Israel, H. I. (Los Alamos Scientific Lab., N. Mex.). Trans. Amer. Nucl. Soc., 8: 643(Nov. 1965).

**2560** STRONG CURRENT HIGH ENERGY PARTICLE ACCELERATORS—"MESON FACTORIES." Dzhelepov, V. P.; Dmitirievskii, V. P.; Zamolodchikov, B. I.; Kol'ga, V. V. Usp. Fiz. Nauk, 85: 651-78(Apr. 1965). (In Russian).

High-energy particle accelerators in which the particles are accelerated to approximately 1 Bev and which produce sufficiently large current, up to 1 ma (meson factories) are discussed. Such accelerators are capable of producing nucleon, meson ($\pi$), and meson ($\mu$) currents which are hundreds and thousands of times larger than existing equipment can supply. The prospects afforded by such accelerators, the physical principles of accelerating particles in relativistic cyclotrons, stability theory, linear resonance effects, phase motion, nonlinear resonance effects, methods of beam extraction, modeling of relativistic

cyclotrons, and presently designed high-current accelerators in the USA and in the USSR are discussed. The question of radiation shielding and the production of particle beams with such accelerators, as well as the use of a linear proton accelerator as a high-current source, are also discussed. (ATD)

**2561** ON THE ACCELERATION OF PARTICLES WITH VARIABLES CHARGES IN AN ELECTROSTATIC FIELD. Vyalov, G. N.; Fiks, M. M. (Inst. of Theoretical and Experimental Physics, Moscow). Yadern. Fiz., 2: 112-16(July 1965). (In Russian).

The acceleration of particles with variable change in an electrostatic field is considered. The intensity of an ion beam which can be reached in the considered type of accelerator is discussed. It is shown that in principle high intensity ion beams of all elements can be obtained with the limiting energy $W_k \approx 0.125\ A_0 Z_0^5$ Mev. (auth)

# Astrophysics and Cosmology

*Refer also to abstract 2855.*

**2562** (AD-614715) THEORETICAL INVESTIGATIONS OF THE EXPANSION OF H(II) REGIONS. Final Report, October 1, 1963–December 31, 1964. Vandervoort, Peter O. (Chicago Univ., Ill.). Apr. 12, 1965. 9p. CFSTI $1.00 cy, $0.50 mn.

The essential phenomenon is the ionization of hydrogen in the interstellar gas by the radiation emitted in the Lyman continuum by a newly formed star of early spectral type. As the gas is ionized it is heated as well. The volume of ionized gas (the H II region) tends to expand, generating a compression wave moving out through the surrounding neutral interstellar gas (the H I region). The general objective of research in this area has been the construction of theoretical models of the manner in which the gas becomes ionized in an H II region and of the gas-dynamical response of both the neutral gas and the ionized gas to the ionization and heating of the gas. (TAB)

**2563** CATALOGUE OF STRENGTHS AND POLARITIES OF MAGNETIC FIELDS OF SUNSPOTS FOR THE PERIOD OF THE INTERNATIONAL GEOPHYSICAL YEAR (1 JULY 1957–31 DECEMBER 1958). Stepanov, V. E.; Shaposhnikova, E. F.; Petrova, N. N. Ann. Int. Geophys. Yr., 23: 1-266(1962).

Data are presented in the form of 533 daily maps containing some mean values of the field strengths measured at six observatories during the IGY. Tables are also presented of the total number of days with magnetic observations of sunspots for each observatory; of data about the instrument, polarizing optics, methods of observations and measurements used; and of the mean magnetic field strengths measured at different observatories. The system of the catalog is discussed. (L.B.S.)

**2564** THE TEMPERATURE STRUCTURE OF EARLY-TYPE MODEL STELLAR ATMOSPHERES. II. A GRID OF STELLAR MODELS. Strom, S. E.; Avrett, E. H. (Harvard Univ., Cambridge, Mass.). Astrophys. J., 12: 1-97(Aug. 1965).

The essential numerical data are presented for a grid of accurate non-gray stellar models, covering the range $10000°K < T_{eff} < 20000°K$ and log g = 3 and 4. Details of the calculational procedures used in computing this grid are discussed. Included as sources of continuous opacity are H, $H^-$, $H_2^+$, He I, He II, electron, and Rayleigh scattering. In all cases, constancy of the flux and flux derivative is preserved to better than 0.2 per cent. Some of the models overlap, and are in good agreement, with those recently published by Mihalas. (auth)

**2565** THE SYNTHESIS AND DESTRUCTION OF ELEMENTS IN PECULIAR STARS OF TYPES A AND B. Fowler, William A. (California Inst. of Tech., Pasadena); Burbidge, E. Margaret; Burbidge, G. R.; Hoyle, Fred. Astrophys. J., 142: 423-50(Aug. 15, 1965).

A discussion is given of the properties of the peculiar A and B stars and especially their anomalous abundances and positions in the H-R diagram. It is known that the compositions can only be explained if it is supposed that the high abundances of heavy elements, particularly in the rare-earth region, and the abundances in the vicinity of the iron peak were produced in a region in which a process of rapid neutron addition has occurred; it is shown here that the conditions are suitable for this when the star has reached a degenerated core configuration, the key reaction being $^{13}C(\alpha,n)$. This implies that either the peculiar A and B stars are at an advanced phase of evolution, i.e., they have passed through a giant phase and have returned to the vicinity of the unevolved main sequence, or else that such a process has gone on in a close binary companion and mass was transferred to the surface of the peculiar star. This latter possibility is open to observational test since, if this were true, all stars of this type should have close evolved companions. In addition to an r-process of this type, it is also shown that to produce the underabundance of the light elements, especially helium, and also to obtain the high $^3He : {}^4He$ ratio seen in 3 Centauri A a vast amount of surface spallation followed by shallow mixing must have occurred. The stars have therefore had a very complicated evolutionary history, with surface spallation and then interior nucleosynthesis followed by rapid mixing. It appears that the properties of degenerate cores and the possibility of rapid heating and energy generation and release at this phase are of the utmost importance in explaining these stars. The theory described here for explaining the observed phenomena cannot be explored in more detail until evolutionary tracks for stars in this mass range have been developed in detail. On the observational side some discussion is given of stars that may be at different parts of the evolutionary track that these stars are traversing. One conclusion derived from considerations of neutron capture processes merits special notice. It is believed that the excess phosphorus concentration found in $\kappa$ Cnc and 3 Cen, for example, is produced in a Si-P-S cycle, and an excess concentration of $^{30}Si$ in such stars is predicted. (auth)

**2566** STUDIES IN STELLAR EVOLUTION. II. LITHIUM DEPLETION DURING THE PRE-MAIN-SEQUENCE CONTRACTION. Bodenheimer, Peter (Univ. of California, Berkeley). Astrophys. J., 142: 451-61(Aug. 15, 1965).

Pre-main-sequence theoretical evolutionary tracks were calculated for configurations of six different masses between 0.5 and 1.2 $M_\odot$ in order to determine the extent to which lithium is destroyed in the convective envelopes as a function of mass. The evolutionary sequences are started with an initial amount of lithium based on observed abundances. At each time step in the calculation, reaction rates are calculated in detail, and the resulting chemical compositions are homogenized over the convective envelope. The evolutionary tracks are carried over to the main sequence in order to provide a basis for comparison with recent observations of lithium abundances in main-sequence stars in the Hyades cluster and in the solar neighborhod. The theoretical depletion as a function of position on the main sequence agrees well with the general trend of the observations, for calculations based both on the solar mass-luminosity relation and on the mass-luminosity relation that was observed for the Hyades. (auth)

**2567** STRUCTURE AND EVOLUTION OF MEDIUM-MASS STARS. IV. THE EARLY EVOLUTION OF A STAR OF 2 SOLAR MASSES. Auman, J. R. (Northwestern Univ., Evanston, Ill.). Astrophys. J., 142: 462-72(Aug. 15, 1965).

The evolution of a $2M_\odot$ star was studied until the star possessed a helium core containing approximately 10% of the star's mass. Radiation pressure and electron degeneracy were included in the equation of state. Both the proton-proton cycle and the carbon-nitrogen-oxygen cycle were included in the calculation of the nuclear-energy production. Improved surface boundary conditions were used. The evolutionary track of a $2M_\odot$ star is similar to that of the more massive stars. Electron degeneracy increases the pressure by 13% in the core of the most evolved model in this study. The ratio of the radiation

pressure to the total pressure becomes as high as 4% near the surface of the star. The relative amounts of time that the 2M⊙ star spends in the hydrogen-depletion, the hydrogen-exhaustion, and the helium-core phases are approximately 72 : 3 : 25. (auth)

**2568** NEUTRON-STAR ATMOSPHERES. Orszag, Steven A. (Princeton Univ., N. J.). Astrophys. J., 142: 473-8(Aug. 15, 1965).

Computations of the x-ray spectra of neutron stars are made taking into account possible absorption edges. The results indicate that the cooler models ($T_e = 5 \times 10^6$ °K) have considerably larger edges than the hotter models ($T_e = 10^7$ °K) and that the edges of magnesium, silicon, and neon probably have the greatest chance to be detected. (auth)

**2569** ON THE EXPLOSION OF A SUPERNOVA INTO THE INTERSTELLAR MAGNETIC FIELD. [PART] I. Bernstein, Ira B.; Kulsrud, Russell M. (Princeton Univ., N. J.). Astrophys. J., 142: 479-90(Aug. 15, 1965). (MATT-295)

The earlier stages of the explosion of a supernova into the interstellar magnetic field are modeled as the uniform expansion from a point of a perfectly conducting piston into an ideal magnetohydrodynamic fluid immersed in a constant magnetic field. The resulting similarity solution is determined in the limit where the magnetic pressure is much greater than the material pressure, and where the piston speed is much less than the Alfvén speed. (auth)

**2570** ON THE EXPLOSION OF A SUPERNOVA INTO THE INTERSTELLAR MAGNETIC FIELD. [PART] II. Kulsrud, Russell M. (Princeton Univ., N. J.); Bernstein, Ira B.; Kruskal, Martin; Fanucci, Jerome; Ness, Nathan. Astrophys. J., 142: 491-506(Aug. 15, 1965).

The problem of the earlier stages of the explosion of a supernova into the interstellar medium with a uniform magnetic field was discussed previously. The limit in which the magnetic field is weak is investigated. This limit corresponds to the Alfvén speed in the interstellar magnetic field being small compared to the expansion velocity of the supernova debris. The magnetohydrodynamic flow produced by the supernova is calculated to second order in the field strength. It is found that the expansion procedure breaks down near the supernova-debris interface, where a boundary region occurs in which the magnetic field is large, no matter how small its interstellar value. The physical quantities at the debris are evaluated. It is suggested that this large field may be subject to a Rayleigh-Taylor instability and burst through the supernova-debris interface, producing a filamentary structure with large magnetic fields such as is observed in the Crab nebula. Other comparisons with the Crab nebula are made. (auth)

**2571** THE PROPERTIES OF NON-STATIONARY IONIZATION FRONTS. [PART] I. Vandervoort, Peter O. (Univ. of Chicago). Astrophys. J., 142: 507-20(Aug. 15, 1965).

A simple model of an ionization front that departs slightly from a stationary structure is considered. The model corresponds to the case considered by Kahn in which recombination of ionized hydrogen and cooling by radiative processes are negligible. An ionization front will be non-stationary when the time scale for an element of the gas to cross the front is not negligible relative to the time scale for changes in the structure of the front. The case in which the variation of the structure results from the variation of the flux of ionizing radiation incident on the front is considered in detail. The equations governing the structure are solved by an iterative method, and the departure of the front from a stationary structure is found to the first order in the ratio of the two time scales. The formulation of the problem of the structure of the front in the case when the neutral gas ahead is not homogeneous is briefly discussed. Finally, it is remarked that, in general, the problem of the structure of a non-stationary front must be formulated as an initial-value problem and not simply as a boundary-value problem. (auth)

**2572** THE PROPERTIES OF NON-STATIONARY IONIZATION FRONTS. [PART] II. Vandervoort, Peter O. (Univ. of Chicago). Astrophys. J., 142: 521-30(Aug. 15, 1965).

The boundary relations at a non-stationary ionization front are derived in the approximation that the recombination of ionized hydrogen and cooling through the emission of radiation by collisionally excited ions are negligible within the front. The departures of these boundary relations from the boundary relations for a quasi-stationary front depend on certain integral quantities characterizing the variation of the structure of the front. As in the case of a quasi-stationary front the solution of boundary relations for the state of the gas emerging from a non-stationary front is real only if certain inequalities are satisfied. These inequalities imply that under certain conditions of the so-called M-type a quasi-stationary front cannot exist. Since a non-stationary front can exist under any conditions, this does not imply (as is commonly believed) that an ionization front will not propagate directly into the neutral gas when conditions are of the M-type. Some simple examples of the response of a quasi-stationary ionization front to the onset of conditions of the M-type are discussed. (auth)

**2573** THERMAL INSTABILITY. Field, George B. (Princeton Univ., N. J.). Astrophys. J., 142: 531-67 (Aug. 15, 1965).

The stability of a dilute gas in mechanical and thermal equilibrium is studied with a view to applications to non-gravitational condensation phenomena in astronomy. It is shown that, under a wide range of conditions, thermal equilibrium is unstable and can result in the formation of condensations of higher density and lower temperature than are found in the surrounding medium. The instability criterion is shown to differ considerably from certain criteria proposed previously. The modifications due to finite speed of sound, to thermal conduction, to a magnetic field, to rotation, to an external gravitational field, and to expansion of the medium are studied. Applications are made to the solar chromosphere and corona, to the interstellar medium in the galactic disk and halo, to planetary nebulae, and to intergalactic matter. It is shown that the principle of thermal instability is closely related to the formation of solar prominences, to condensations in planetary nebulae, and to condensation of galaxies from the intergalactic medium. (auth)

**2574** A STATISTICAL MODEL OF THE FORMATION OF STARS AND INTERSTELLAR CLOUDS. Field, George B.; Saslaw, William C. (Princeton Univ., N. J.). Astrophys. J., 142: 568-83(Aug. 15, 1965).

Oort's model for the formation and destruction of interstellar clouds is formulated mathematically with simplifying assumptions. An equation for the time-dependent cloud-mass spectrum is obtained and solved. It is found that the rate of star formation is proportional to the square of the gas density, in agreement with Schmidt's empirical model, and that the calculated proportionality constant agrees approximately with the observed value. The form of the cloud-mass spectrum, approximately a $m^{-\frac{3}{2}}$ law, also agrees roughly with observation. (auth)

**2575** SOLAR-FLARE FREQUENCY AND OBSERVING-TIME PATTERNS. Warwick, Constance S. (National Bureau of Standards, Boulder, Colo.). Astrophys. J., 142: 767-72(Aug. 15, 1965).

An intermittent pattern of solar-flare patrol leads to an increase in the total number of flares detected per hour of observation and also in the proportion of long-lived, large flares relative to small, brief flares. These effects are illustrated by examples drawn from the world-wide flare patrol. (auth)

**2576** THE WILSON EFFECT AND SUNSPOT STRUCTURE. Wilson, P. R. (Joint Inst. for Laboratory Astrophysics, Boulder, Colo.). Astrophys. J., 142: 773-81 (Aug. 15, 1965).

A method is described for interpreting sunspot-intensity profiles at different heliocentric angles in terms of the at-

tenuation coefficient distribution in the spot. Since the currently available data on sunspot profiles at various angles are qualitative rather than quantitative, the method cannot be applied in detail at present. However, it is hoped that the availability of such a method will encourage observers in the admittedly difficult task of obtaining such data. In order to demonstrate what may be done at present, a simplified form of the method is applied to Loughhead and Bray's photographs of a sunspot as it passed across the disk of the Sun from limb to limb. It is shown that the mean attenuation coefficient in the umbra of this spot is between 1 and 2 orders of magnitude less than in the surrounding photosphere. A difference of 1 order of magnitude is shown to be consistent with the assumption that the umbra of the spot is in radiative equilibrium. (auth)

**2577** THE LITHIUM ISOTOPE RATIO IN TWO HYADES F STARS. Merchant, A. E.; Bodenheimer, Peter; Wallerstein, George (Univ. of California, Berkeley). Astrophys. J., 142: 790-3(Aug. 15, 1965).

The lithium isotope ratio is reported for two stars in the Hyades, a cluster that contains a group of stars of presumably common origin. The proximity of the Hyades allows observations of main-sequence stars with a considerable range in color, permitting the investigation of the possible effect of the deepening of the outer convection zone with advancing spectral type. Four spectrograms were secured for each of the two stars with the 40-in. camera of the 120-in. coudé spectrograph. Most of the lines previously used plus four additional lines were employed to obtain the stellar radial velocity from each plate. The wavelengths of the lithium line on each plate and the color and logarithmic ratio of Li/Ca as compared to the sun are given. Also the value of $^6Li/(^6Li + {}^7Li) = \langle\lambda_{Li}\rangle - 6707.811)/0.158$, where $\langle\lambda_{Li}\rangle$ is the mean wavelength for each star. Theory and observations are not in complete agreement. Two explanations for this are given; both of these achieve consistency, but are based on incomplete observational and theoretical evidence. (J.F.P.)

**2578** ON THE DEVELOPMENT OF SOLAR FLARES WITHIN THE CALCIUM NETWORK. Bumba, V.; Howard, Robert (Carnegie Institution of Washington, D. C.; California Inst. of Tech., Pasadena). Astrophys. J., 142: 796-8(Aug. 15, 1965).

An examination is made of flare patrol films from July 1 to December 31, 1958. These spectroheliograms were made at intervals of one per minute on the $K_2$ line of Ca II. From this examination a relation was determined between flare development and the structure of the preexisting calcium network. It is established that the regions of calcium emission are also areas of concentration of more or less radial magnetic fields. There was complete coverage for 200 flares which were close enough to the center of the disk to establish connection with the calcium network. Photographs of the flares are shown, and their distribution and importance are given. The results indicate that on a small scale flares always originate at concentrations of flux lines, although this does not exclude the possibility that zero points in the field are somehow involved in the flare process. (J.F.P.)

**2579** RELATIVISTIC STABILITY OF A MAGNETOTURBULENT MASSIVE STAR. Pacholczyk, A. G. (Joint Inst. for Laboratory Astrophysics, Boulder, Colo.). Astrophys. J., 142: 805-6(Aug. 15, 1965).

It is pointed out that a massive object of the Hoyle and Fowler type which has developed a magnetoturbulent field through a previously proposed mechanism can achieve the hydrogen burning stage long before it reaches the relativistic-instability point. An equation is written for the stage in which the rotational energy of the star is practically converted into the energy of the magnetoturbulent field. The relativistic term in this equation leads to instability as soon as $\partial E/\partial R < 0$, that is when the radius of the star decreases below its critical value. (J.F.P.)

**2580** ON THE ELECTROMAGNETIC RADIATION WITH CONTINUOUS SPECTRA DURING SOLAR FLARES. Korchack, A. A. Geomagn. Aeronomiya, 5: 601-25(July-Aug. 1965). (In Russian).

The question of the origin of continuous solar electromagnetic radiation, that is, radiation having a continuous frequency spectrum, is analyzed with particular attention given to hard x-radiation. The question of the mechanisms of radiation as well as the origin of the entire spectrum of nonthermal electromagnetic radiation originating during flares is examined on the basis of extensive data obtained during the recent period of high solar activity. Though analysis of the available results of observations yields no final conclusion on the character of the spectrum of the electromagnetic radiation of flares, it appears unlikely that either the entire spectrum from radio waves to gamma rays could be described by a smooth curve or that it originates as a result of a single radiation mechanism. Theoretically, electrons accelerated in a flare generate three types of radiation, namely, magneto-bremsstrahlung, bremsstrahlung, and Compton. The strength of the Compton radiation in the solar atmosphere is determined solely by the energy of the electrons, while the strength of the synchrotron radiation must also depend on the magnetic field strength. The strength of the bremsstrahlung depends on the density of the medium. A comparative analysis of all three types of mechanism shows that hard x-radiation in a flare can only be of a Compton nature in the case where it occurs in the corona with a concentration $< 3 \times 10^8$ cm$^{-3}$. It is also possible that hard x-radiation in the upper chromosphere or in even denser regions of the flare occurs as the result of the bremsstrahlung of nonrelativistic and weakly relativistic electrons. If the spectrum of these electrons continues into the region of relativistic energies, then the centimeter radio bursts, which usually occur simultaneously with the x-radiation, can be attributed to the synchronous radiation of relativistic electrons. The different durations of these two bursts can possibly be attributed to different energy losses in nonrelativistic and ultrarelativistic energy regions. The continuous optical radiation in flares can be explained by the synchrotron radiation of relativistic electrons. If this is correct, then it might be expected that during this radiation the spectrum of the centimeter radio bursts must always increase with frequency, while the flux of hard x-radiation with photon energies >20 kev must exceed the values observed hitherto by several orders. However, it must be concluded that as yet no conclusive solution to the question of the nature of the continuous optical flare radiation has been obtained. (ATD)

**2581** ON THE SURFACE BOUNDARY CONDITION FOR STARS. Faulkner, J.; Griffiths, K.; Hoyle, F. (Cambridge Univ., Eng.). Monthly Notices Roy. Astron. Soc., 129: 363-93(1965).

The computation of stellar models depends in many cases in an important way on the photospheric boundary conditions and on the behavior of various physical quantities in the immediate sub-photospheric regions. This is particularly so for stars with deep outer convection zones. A method is presented for integration downwards from the photosphere through any convective zone that may exist. The method does not depend on mixing length theory, although similar results could be obtained from such a theory if the mixing length l was regarded as continuously variable with $l \simeq dh/d \ln T$. Results are presented in detail for the particular case of the sun. For other stars we have given our results in the form of functions $P_5(M, T_e, L, A, X)$, $h_5(M, T_e, L, A, X)$, where $P_5$ is the pressure and $h_5$ is the depth below the photosphere at which the temperature is $10^5$K. These quantities are given as functions of the mass M, effective temperature $T_e$, luminosity L, metal concentration A, and hydrogen concentration X. Allowance is made for the possible existence of an appreciable amount of mass in the surface layers by the inclusion of a mass variable in the integration scheme. An empirical prescription is given for determining $M_5$, the mass interior to $10^5$K, in terms of $P_5$, $h_5$, and the total mass and radius of the star. (auth)

**2582** A CORRELATION BETWEEN THE OPTICAL AND RADIO ASPECTS OF A CLASS 3 FLARE. McKenna,

Susan M. P. (Dublin Inst. for Advanced Studies). Monthly Notices Roy. Astron. Soc., 129: 437-42(1965).

It is shown that variations in the Hα intensity of a bright dot which appeared over the umbra of a sunspot during the Class 3 flare of 1960 November 10, were synchronous with variations in the level of the accompanying 20 cm radio emission. No such correlation existed between the characteristics of the radio emission and the behavior of other Hα regions within the flare although it is possible that minor contributions to the radio emission were made when certain of the Hα regions expanded over minor spots. An examination of all the available single frequency records on centimeter, decimeter, and meter wavelengths reveals that those radio bursts accompanying variations in the intensity of the Hα spot were Type IV events and the ionospheric record indicates that these changes in the visible and radioradiation were accompanied by simultaneous variations in the flare x-ray radiation. (auth)

**2583** OCCURRENCE OF SINGULARITIES IN OPEN UNIVERSES. Hawking, S. W. (Cambridge Univ., Eng.). Phys. Rev. Lett., 15: 689-90(Oct. 25, 1965).

It is shown for a class of universe models that the claim that in the absence of certain restrictions on the flow of matter or exact symmetries there will not be a physical singularity is false, using methods similar to those of Penrose for the case of a collapsing star. (L.B.S.)

**2584** VIBRATIONAL ENERGY OF NEUTRON STARS AND THE EXPONENTIAL LIGHT CURVES OF TYPE-I SUPERNOVAE. Finzi, Arrigo (Univ., Rome; Centro Nazionale di Astrofisica del Centro Nazionale di Richerche, Frascati, Italy). Phys. Rev. Letters, 15: 599-601(Oct. 11, 1965).

For type-I supernova, an alternative confirmation of the neutron-star hypothesis may be based on the possibility it seems to offer for explaining their exponential light curves. It is suggested that the energy released exponentially originates in the neutron star. There seem to be only two ways in which $4 \times 10^{49}$ erg, the estimated energy released, can be stored in a neutron star: in the form of thermal energy or in the form of vibrational energy, previously suggested. But the thermal energy is ruled out because at the corresponding temperature, thermal energy is released mainly in the form of neutrinos. It is suggested that the theoretical value $10.1 \times 10^{49}$ ergs and the value $4 \times 10^{49}$ deduced from observation could be improved by taking into account the temperature dependence of the dissipation of vibrational energy by beta reactions. The probable mechanism by which the vibrational energy is converted into visible light is described briefly. (J.F.P.)

**2585** X-RAY SPECTRA FROM SCORPIUS (SCO-XR-1) AND THE SUN OBSERVED ABOVE THE ATMOSPHERE. Chodil, G.; Jopson, R. C.; Mark, Hans; Seward, F. D.; Swift, C. D. (Univ. of California, Livermore). Phys. Rev. Letters, 15: 605-7(Oct. 11, 1965).

To obtain more precise information about the spectrum of the x-ray source in Scorpius (SCO-XR-1), a proportional counter sensitive to photons with quantum energies between 2 and 20 kev was flown on a rocket. With this detector and a special telemetry system it was possible to measure the spectrum in this energy region with high resolution. A plot is given of counts greater than 1.7 kev versus azimuth during the 250 seconds that the counter was above 104 km. The spectral distribution of the radiation from SCO-XR-1 and the sun is shown. Significant differences are observed between the two spectra. The Scorpius source has a significant flux extending as high as 20 kev. A plot is given for the measured intensity of the source as a function of energy. (J.F.P.)

**2586** HIGH ENERGY γ-RAY ASTRONOMY. Faudrowicz, Adam. Postepy Astron., 13: 3-12(Jan.-Mar. 1965). (In Polish).

Some theoretical concepts and two satellite measurements of gamma-ray intensity in space are described. The comparison of theoretical and experimental data of various authors is given. (auth)

**2587** COSMIC NEUTRINOS. Jatczak, Jerzy (Lodz Univ., Poland). Postepy Fiz., 16: 279-93(1965). (In Polish).

The production of neutrinos in stars and the release of stellar energy by neutrino radiation is discussed from the point of view of energy balance in the universe. A brief review of neutrino production in thermonuclear reactions, and a discussion of neutrino–antineutrino pair production by processes involving relatively low production cross sections indicates that for massive stars with dense cores the predominant mechanism of energy release is by neutrino radiation. The amount of stellar energy going into neutrino production is enormous in these cases, and it is probable that the density of "matter" in the universe in the state of neutrinos constitutes a large fraction of the averaged total matter density. The possibility of determining this fraction by the measurement of neutrino flux and energy spectrum is also discussed. (TTT)

**2588** ADIABATIC EXPONENT FOR IRON-HELIUM TRANSITION AND PAIR CREATION. Kaminisi, Keisuke (Kumamoto Univ., Japan). Progr. Theoret. Phys. (Kyoto), 34: 424-32(Sept. 1965).

The adiabatic exponent $\Gamma_1$ for a gaseous material being in equilibrium with those particles such as iron nucleus, $\alpha$, neutron, electron, positron, and photon is studied in some detail. The present investigation shows $\Gamma_1$ becomes smaller than $4/3$ over a rather wide range of dissociation rate of iron into helium. If only a few per mill of iron disintegrate into helium, then $\Gamma_1 < 4/3$ and the material would fall down into the state of hydrostatic instability. The result suggests that the disintegration of iron can be regarded as the most promising mechanism which causes the sudden collapse of the core of massive stars. (auth)

**2589** ON THE STRUCTURE AND ENERGETICS OF LARGE SCALE HYDROMAGNETIC DISTURBANCES IN THE SOLAR PHOTOSPHERE. Starr, Victor P.; Gilman, Peter A. (Massachusetts Inst. of Tech., Cambridge). Tellus, 17: 334-40(Aug. 1965).

It is suggested that the solar differential rotation is maintained against frictional dissipation by large scale quasi-horizontal hydromagnetic disturbances, which possess tilted structures similar to upper level troughs in the westerlies of the earth's atmosphere. On the sun, these tilts would be directed from the equator toward the east limb in each hemisphere. Horizontal Reynolds stresses in these disturbances thus convert eddy kinetic energy into kinetic energy of the zonal flow, while horizontal Maxwell stresses convert the mean zonal kinetic energy into "eddy" magnetic energy. In order for the disturbances as a whole to feed kinetic energy into the differential rotation, the horizontal eddy magnetic fields must be somewhat less than 7 gauss at the level considered. Measurements of the large scale patterns of the line of sight component of the magnetic field, made by Howard, show clearly the required tilt in the patterns toward the east limb in each hemisphere. These measurements also show that the patterns do have a very large horizontal scale, possessing a longitudinal wave number of about 6, and a latitudinal extent of about 60°. The magnitudes of these fields appear to be compatible with horizontal eddy magnetic fields less than 7 gauss. The braking action by the symmetric steady component of the horizontal Maxwell stress appears from the observations to be small compared with that due to the eddy component. (auth)

**2590** THE ORIGIN OF METEORITES. Levin, B. Yu. Usp. Fiz. Nauk, 86: 41-69(May 1965). (In Russian).

The changes that have occurred in the scientific explanations of the origin and nature of meteorites during the last decades are reported, making use of recent information on the abundance of elements and their isotopic ratios from the point of view of nuclear physics. The various hypothe-

ses advanced concerning the nature of meteorites are outlined and the experimental and cosmogonical evidence in their favor or against them are briefly discussed. The topics discussed are: meteorites and asteroids, atmospheric selection, cosmogonical considerations, some properties of meteorites, hypotheses of the "fire liquid" origin of meteorites, hypotheses of primordial nature of chondrules, hypothesis of unmolten parent bodies, and conclusions. (ATD)

## Atomic Physics

*Refer also to abstract 2434.*

**2591** (ANL-7030) OPTIMUM DESIGN OF HIGH-PRESSURE, LARGE-DIAMETER, DIRECT-NUCLEAR-PUMPED, GAS LASERS. DeShong, James A. Jr. (Argonne National Lab., Ill.). June 1965. Contract W-31-109-eng-38. 48p. Dep. mn; CFSTI $2.00 cy, $0.50 mn.

The principles of laser operation are discussed with emphasis on gas lasers. Previous work on small-diameter, direct-nuclear-pumped, gas lasers is surveyed. Techniques are developed for optimizing laser tube dimensions and gas pressure to obtain most efficient use of the nuclear fragment energy. These techniques are applied to calculate high-pressure, large-diameter, laser tubes for $^{235}U$ and for $^{10}B$ which both exhibit theoretical efficiencies two orders of magnitude larger than previous small-diameter tubes. The $^{10}B$ laser appears feasible, because electrically pumped lasers of similar dimensions and pressure have operated in the pulse mode with up to 80-W output. The $^{235}U$ laser is much larger in diameter and may require multiple-path operation. (auth)

**2592** (BNL-9556) ELECTRONIC BAND STRUCTURE AND OPTICAL PROPERTIES OF RARE-EARTH METALS. Dimmock, J. O. (Lincoln Lab., Massachusetts Inst. of Tech., Lexington); Freeman, A. J. (National Magnet Lab., Massachusetts Inst. of Tech., Cambridge); Watson, R. E. (Brookhaven National Lab., Upton, N. Y.). [1965]. Contract AT-30-2-GEN-16. 18p. (CONF-650804-10). Dep. mn; CFSTI $1.00 cy, $0.50 mn.

From 5th Rare Earth Research Conference, Ames, Iowa.

The optical properties of the heavy rare-earth metals are discussed in the light of recent non-relativistic augmented plane wave (APW) calculations of the electronic energy band structures of Gd and Tm. The calculations show that the bands near the Fermi energy are of mixed s-d character, originating from atomic 5d and 6s states, are relatively flat, and yield a high density of states. The selection rules for interband optical transitions both with and without spin-orbit coupling included are given for the symmetry points in the Brillouin zone. This results in the prediction of considerable polarization dependent structure in the optical absorption and reflectivity of rare-earth metals in the infrared and visible regions. An anomaly also should exist in the uv region due to transitions between the 4f levels and the conduction bands above the Fermi energy. In Gd this anomaly is expected to occur at about 7 ev. Since the heavy rare-earth metals all order magnetically at low temperatures, an additional anomaly may arise due to transitions between magnetically split energy bands. Estimates of the energies of these splittings are made and compared with the energies of the infrared structure observed by Schüller in Ho and by Cooper and Redington in Dy. (auth)

**2593** (EUR-2524.e) PRECISE REDETERMINATION OF THE $P_K\omega_K$ VALUE AND THE FLUORESCENCE YIELD OF Cr. Bambynek, W.; De Roost, E.; Spernol, A.; Van Der Eijk, W.; Vaninbroukx, R. (European Atomic Energy Community, Geel (Belgium). Central Nuclear Measurements Bureau). Sept. 1965. 8p. Dep. mn.

The K-shell fluorescence yield of Cr was measured to be $\omega_K = 0.277 \pm 1.5\%$ by determining the absolute KX-ray emission rates and the absolute disintegration rates of $^{54}Mn$ sources. The KX-ray emission rates were measured using a large $4\pi$ pressure proportional counter and a medium geometry solid angle arrangement. The disintegration rates were determined by means of a calibrated $\gamma$ spectrometer and the $4\pi(AX,\gamma)$ coincidence method. A detailed discussion of all corrections and errors is given. (auth)

**2594** (N64-23208) QUANTUM THEORY OF VIBRATIONAL ENERGY EXCHANGE AND THE EFFECT OF AN ATTRACTIVE POTENTIAL. Allen, R. T.; Feuer, P. (Purdue Univ., Lafayette, Ind. School of Aeronautical and Engineering Science). Mar. 1964. 34p. (A and ES-64-4).

A first order time-dependent perturbation theory is described for the calculation of transition probabilities in the interaction of an atom with an atomic oscillator. The relation of this theory to the theory of distorted waves is discussed. The method is applied to the special case of an interaction potential of the form $V(r) = Ce^{-2Ar} - Ge^{-Ar}$. It is also applied to the calculation of transition probabilities for a diatomic molecule reflected from a solid surface, taking into account the effect of an attractive potential. (auth)

**2595** (NASA-TN-D-3050) PARTIAL WAVE CALCULATION OF THE DIATOMIC MOLECULE $(HeH)^{++}$. Rabinovich, Harris (National Aeronautics and Space Administration, Greenbelt, Md. Goddard Space Flight Center). Oct. 1965. 17p. CFSTI $1.00 cy, $0.50 mn.

The solutions to the Schrödinger equation for the diatomic molecule $(HeH)^{2+}$ in the Born-Oppenheimer approximation were expanded in a series of partial waves and radial equations were derived. These radial equations were solved numerically for the first three orders of approximation and the energy eigenvalues and wavefunctions were obtained for seven different $\Sigma$ states at various values of the internuclear separation. The numerical wavefunctions were used to calculate dipole transition integrals and dipole moments. (auth)

**2596** (UCRL-16241) STUDY OF OPTICAL PUMPING TRANSIENTS IN $^{87}Rb$ AND APPLICATION TO DISORIENTATION CROSS SECTIONS [thesis]. Yellin, Joseph (Lawrence Radiation Lab., Univ. of California, Berkeley). July 9, 1965. Contract W-7405-eng-48. 170p. Dep. mn; CFSTI $5.00 cy, $1.00 mn.

The shapes of optical pumping transients in $^{87}Rb$ with and without buffer gas are shown to be expressible as a sum of two exponentials when the pumping occurs in the presence of a buffer gas, and as a single exponential when no buffer gas is present. These results are shown to agree with a phenomenological model of optical pumping for which a single relaxation time is assumed. It is shown that from a study of the transient structure of the optical pumping signal as a function of buffer-gas density, information can be obtained about the reorientation of a polarized rubidium atom as a result of buffer-gas collisions. From such a study an effective cross section, $\sigma$(eff), for disorientation of a polarized $^{87}Rb$ atom in the excited state through collisions with He, Ne, and Ar is determined. This effective cross section is related to the cross section for disorienting a polarized $^{87}Rb$ atom in the $5^2P_{\frac{1}{2}}$ state, $\sigma(\frac{1}{2},\frac{1}{2})$, and to the cross section for transfer of excitation of the $^{87}Rb$ atom from the $5^2P_{\frac{1}{2}}$ state to the $5^2P_{\frac{3}{2}}$, $\sigma(\frac{1}{2},\frac{3}{2})$, by $\sigma$(eff) = $\sigma(\frac{1}{2},\frac{1}{2}) + \sigma(\frac{1}{2},\frac{3}{2})$. Using measured values of $\sigma(\frac{1}{2},\frac{3}{2})$, values are deduced for $\sigma(\frac{1}{2},\frac{1}{2})$. The cross sections are: $\sigma(\frac{1}{2},\frac{1}{2})(Rb-He) = 1.5(0.8) \times 10^{-17}$ cm$^2$; $\sigma(\frac{1}{2},\frac{1}{2})(Rb-Ne) = 4.4(2.2) \times 10^{-17}$ cm$^2$; and $\sigma(\frac{1}{2},\frac{1}{2})(Rb-Ar) = 2.5(1.8) \times 10^{-16}$ cm$^2$. (auth)

**2597** DETERMINATION OF THE EFFECTIVE CROSS-SECTION FOR COLLISIONS OF NEUTRAL CALCIUM WITH ARGON. Letfus, V. (Astronomical Inst., Czechoslovak Academy of Sciences, Ondrejov). Bull. Astron. Inst. Czech., 16: 256-60(1965).

A new method for the determination of the effective cross section by means of collisions of atoms of two elements, using the combined absorption-and-hook method for the determination for the absolute number of f resonance lines, was described. The method was applied to Parcevskij and

Penkin determination for the resonance lines Ca 1 Λ 4227 and the effective cross section $\Sigma = 3.7 \times 10^{-17}$ cm$^2$ was determined for collisions with argon. (tr-auth)

**2598** CALCULATION OF THE COLLISION [CROSS] SECTIONS OF THE 2s → np TYPE IN THE IONS OF THE ISOELECTRONICS SERIES OF LITHIUM. Bely, Oleg; Lallemand, Andre (Observatoire de Paris, Meudon). Compt. Rend., 261: 909-12(July 1965). (In French).

The collision [cross] sections corresponding to the dipolar transitions of the 2s → np type (n = 2, 3, . . ., 7) were calculated for ions of Be(II), N(V), and Ne(VIII) by the Coulomb-Born method. The analysis of the results show that they can easily be extended to any 2s → np dipolar transition in any ion of the isoelectronic series of lithium. (tr-auth)

**2599** RADIATIVE LIFE OF THE 6 $^3P_0$ STATE OF THE ISOTOPES $^{199}$Hg AND $^{201}$Hg. Bigeon, Marie-Claude; Cojan, Jean-Louis Compt. Rend., 261, 913-18(July 1965). (In French).

Absorption measurements by mercury vapor of the forbidden ray (6 $^1S_0$–6 $^3P_0$) emitted by the isotopes $^{199}$Hg and $^{201}$Hg make it possible to measure the radiative life of the 6 $^3P_0$ state as $\tau_{199} = 1.63$ sec for $^{199}$Hg and $\tau_{201} = 2.52$ sec for $^{201}$Hg. (tr-auth)

**2600** THE ENERGY SPECTRA OF SCATTERED IONS AS INFLUENCED BY THE CRYSTAL STRUCTURE OF THE TARGET. Mashkova, E. S.; Molchanov, V. A.; Soshka, V. (Moscow State Univ.). Dokl. Akad. Nauk SSSR, 161: 813-16(Apr. 1, 1965). (In Russian).

A previously described technique (Dokl. Akad Nauk SSSR, 155, 70(1964)) was used with a somewhat improved geometry to determine the effect of the target's crystal structure on the energy spectrum of the scattered ions, irradiating a Cu target of various orientation with singly-charged, 30-kev Ar ions. The target was rotated around the ⟨110⟩ axis lying in its plane. The energy spectrum of the ions scattered from the (100) face consisted of a number of peaks corresponding to the Ar ions with and without charge. When the scattering angle was increased, the peaks were shifted toward lower energies and were sumultaneously broadened. Similar tests with Cu crystals cut at an angle of 18° with respect to the crystal face revealed that the crystal structure of the target affects markedly the scattering of the ions; for a complete understanding of these effects, calculations similar to those indicated by D. E. Harrison (AERE-R-4694(1964)) must be carried out. (TTT)

**2601** A NEW METHOD OF CALCULATING THE MAGNETIC MOMENT OF THE ELECTRON. Kushnirenko, A. N. Dopovidi Akad. Nauk Ukr. RSR, No. 7, 884-8(1965). (In Russian).

A new variation is given of the formula for the mean value of a physical magnitude for calculating the magnetic moment of the electron. (auth)

**2602** MEASUREMENT OF THE ENERGY LOSS PER ION PAIR IN VARIOUS GASES FOR NITROGEN AND OXYGEN IONS IN THE ENERGY REGION FROM 0.14 TO 0.7 Mev. Leimgruber, R.; Huber, P.; Baumgartner, E. (Univ., Basel). Helv. Phys. Acta, 38: 499-513(Aug. 1965). (In German).

The average energy loss per ion pair (W-value) of nitrogen and oxygen ions in $N_2$, Ar, and He has been measured in the energy range of 0.14 to 0.7 Mev. The W-value in this range depends upon the velocity and the mass of the incoming ions for $N_2$ and Ar. In nitrogen the W-value for nitrogen ions varies from 40.6 ev (at 608 kev) to 48.2 ev (at 141 kev) and for oxygen ions from 42.0 ev (at 535 kev) to 49.2 ev (at 148 kev). In argon the W-value for nitrogen ions varies from 26.3 ev (at 543 kev) to 29.1 ev (at 158 kev) and for oxygen ions from 27.8 ev (at 474 kev) to 3.15 ev (at 164 kev). In He the W-value was measured for both nitrogen and oxygen ions over the energy range of 0.13 to 0.36 Mev and no variation with energy was observed. (auth)

**2603** THE IONIZATION POTENTIAL OF Tm(I). Murakawa, Kiyoshi (Tokyo Univ.). J. Phys. Soc. Jap., 20: 1733(Sept. 1965).

The hyperfine structure of some strong lines of Tm I was investigated using a liquid-air cooled hollow discharge tube and a Fabry–Perot etalon. The ionization potential of Tm I was deduced from the hfs to be 6.51 ± 0.08 ev. (L.B.S.)

**2604** THE THEORY OF TRANSFORMATION MATRICES. Shelepin, L. A. (Lebedev Inst. of Physics, Moscow). Lietuvos Fiz. Rinkinys, Lietuvos TSR Mokslu Akad., Lietuvos TSR Aukstosios Mokyklos, 5: No. 1, 23-30(1965). (In Russian).

The theory of transformation matrices is considered in a form convenient for use in atomic spectroscopy. The review of the matrix properties is given, including a general discussion of symmetry properties and a connection with the theory of fractional parentage coefficients. New possibilities of the theory of transformation matrices using Regge symmetry are discussed. (auth)

**2605** TWO-ELECTRON MATRIX ELEMENTS OF SPIN-SPIN INTERACTION ENERGY OPERATOR. Rudzikas, Z. B.; Vizbaraite, Ya. I.; Jucys, A. P. (Kapsukas State Univ., Vilnius, USSR; Inst. of Physics and Mathematics, Academy of Sciences, Lithuanian SSR). Lietuvos Fiz. Rinkinys, Lietuvos TSR Mokslu Akad., Lietuvos TSR Aukstosios Mokyklos, 5: No. 1, 37-47(1965). (In Russian).

The expressions for two-electron reduced matrix elements of the spin–spin interaction energy operator are given. The coefficients of the radial integrals are expressed in terms of orbital quantum number of one of two electrons the corresponding quantum number of the other electron being fixed and equal to 0, 1, and 2. The method of using the mirror reflection symmetry for checking the corresponding formulas is described. (auth)

**2606** TWO-ELECTRON MATRIX ELEMENTS OF THE SPIN-ORBIT INTERACTION ENERGY OPERATOR. Rudzikas, Z. B.; Vizbaraite, Ya. I.; Karazija, R. I.; Jucys, A. P. (Kapsukas State Univ., Vilnius, USSR; Inst. of Physics and Mathematics, Academy of Sciences, Lithuanian SSR). Lietuvos Fiz. Rinkinys, Lietuvos TSR Mokslu Akad., Lietuvos TSR Aukstosios Mokyklos, 5: No. 1, 49-61(1965). (In Russian).

The expressions for two-electron reduced matrix elements of the spin–orbit interaction energy operator are given. The coefficients of the radial integrals are expressed in terms of orbital quantum number of one of two electrons the corresponding quantum number of the other electron being equal to 0, 1, and 2. The method of using the mirror reflection symmetry for checking the corresponding formulas is described. (auth)

**2607** THE FIELD FORM OF THE PERTURBATION THEORY FOR THE SYMMETRICAL MOLECULES. I. GENERAL CONSIDERATION. INTEGRATION OF THE FEYNMAN DIAGRAMS OVER PARTNERS OF THE IRREDUCIBLE REPRESENTATION. Bolotin, A. B. (Kapsukas State Univ., Vilnius, USSR). Lietuvos Fiz. Rinkinys, Lietuvos TSR Mokslu Akad., Lietuvos TSR Aukstosios Mokyklos, 5: No. 1, 71-83(1965). (In Russian).

The general statements of the field form of the perturbation theory in the MO LCAO approximation are developed. The case of the symmetrical molecules is considered. Molecular orbitals (MO LCAO) are constructed taking into account the system's local and total symmetry. The rules of the calculation of the Feynman diagrams and integration over partners of the irreducible representation are formulated. (auth)

**2608** THE FIELD FORM OF THE PERTURBATION THEORY FOR THE SYMMETRICAL MOLECULES. II. INTEGRATION OF THE FEYNMAN DIAGRAMS OVER ANGLES IN THE MO LKAO APPROXIMATION. Bolotin, A. B. (Kapsukas State Univ., Vilnius, USSR). Lietuvos Fiz. Rinkinys, Lietuvos TSR Mokslu Akad., Lietuvos TSR Aukstosios Mokyklos, 5: No. 1, 85-94(1965). (In Russian).

It is shown that the reduction of the multicenter integrals to one center enables separation of the angular part of the matrix elements of the electron interaction operator from the radial part. In this case, Feynman's diagrams

are written as a product of the angular and radial parts. In the angular part the graphical summation over quantum number gives Γj-coefficients. The general rules to obtain the contribution to the energy correction for the Feynman diagram are formulated. (auth)

**2609** ATOMIC WAVE FUNCTIONS, COLLISION CROSS-SECTIONS, AND TRANSITION PROBABILITIES OF Fe IONS. Krueger, T. K.; Czyzak, S. J. (Aerospace Research Labs., Wright-Patterson AFB, Ohio). Mem. Roy. Astron. Soc., 69: 145-57(1965).

Atomic wave functions of Fe ions (Fe V–Fe XVII) were calculated using the Hartree–Fock self-consistent field method with exchange. Wave functions, $\epsilon_{\alpha\alpha'}$, $\bar{r}$, $\bar{r}^2$, and $\sigma$ are tabulated. Probabilities were calculated for forbidden transitions in Fe X, XI, XIII, XIV, and XV, some of which are observed in the solar corona; the energy levels and forbidden transition probabilities for Fe XII were also estimated. Preliminary cross-section calculations, involving only p-waves, for forbidden transitions in Fe XI, XII and XIII were made and the problems involved in these calculations are discussed. For allowed transitions in Fe XV and Fe XVI probabilities were calculated and collision cross-sections for the latter ion only. The results are discussed in some detail. (auth)

**2610** PRESSURE DISSOCIATION AND MOLECULAR HYDROGEN. Vardya, M. S. (Univ. of California, Berkeley). Monthly Notices Roy. Astron. Soc., 129: 345-50 (1965).

The partition functions for molecular hydrogen, with an estimate of pressure dependence included, were calculated, using extension of Heitler-London theory to three electron system. These partition functions were used to evaluate the equilibrium constants and internal energies for $H_2$ as a function of temperature and pressure. Tables of partition functions, equilibrium constants, and internal energies were given for T = 1,000 to 15,000°K and for pressures as high as $7.7 \times 10^9$ dyne/cm$^2$. (auth)

**2611** THE MODEL POTENTIAL FOR POSITIVE IONS. Abarenkov, I. V.; Heine, V. (Cavendish Lab., Cambridge, Eng.). Phil. Mag. (8), 12: 529-37(Sept. 1965).

Some experience is reported of numerical calculations with atomic pseudopotentials in the sense of Austin et al., (1962). The pseudo-potentials and/or the pseudo-wave functions are not sufficiently smooth to give really good convergence to an expansion of the model wave function in a crystal in terms of plane waves. The pseudo-potential of an ion is therefore replaced by a simple model potential with two parameters. These are adjusted to reproduce exactly the observed spectroscopic energy levels of an electron in the field of the ion. In this way a model potential is set up to represent the ion, useful for calculations in solids and liquids. Some numerical results are given and more extensive tables are available from the authors. (auth)

**2612** GROUP THEORY OF THE KEPLER PROBLEM. Sundarshan, E. C. G.; Mukunda, N.; O'Raifeartaigh, L. (Univ. of Wisconsin, Madison. Syracuse Univ., N. Y.). Phys. Lett., 19: 322-6(Nov. 1, 1965).

The problem of the hydrogen atom is investigated further from a group theoretical point of view, both in the classical and quantum mechanical cases. First the arbitrary function and arbitrary parameter are interpreted. It is found that the interpretation of the arbitrary parameter is nontrivial and leads to an important property of the group 0(4,1). Also it is found that all the results generalize immediately to the case of the hydrogen atom in n dimensions. Finally, the positive and zero energy states, as well as the bound states, are investigated. (J.F.P.)

**2613** ON THE EXCITATION CROSS SECTION OF SPIN EXCHANGE BETWEEN $^{85}$Rb AND $^{87}$Rb. Elbel, M.; Wieder, H. (Physikalisches Institut, Marburg, Ger.). Phys. Letters, 18: 276-7(Sept. 1, 1965). (In German).

The spin exchange cross section between $^{85}$Rb and $^{87}$Rb was measured by polarization of Rb vapor of natural isotopic composition with Rb resonance light. The pole reversal of the magnetic guide field modified the transparency. This was measured and can be represented as a sum of two exponential functions with different constants. These two time constants were determined as a function of the temperature of the Rb cell. A value of $2.6 \times 10^{-14}$ cm$^2$ was found for the effective cross section. The deviation of this value from the more accurate measurement of $1.7 \pm 0.21 \times 10^{-14}$ cm$^2$ made earlier can be attributed to the measurement accuracy, incomplete solution of the equation describing the exchange, and uncertainties in the vapor pressure determination. (J.S.R.)

**2614** MEASUREMENT OF THE VELOCITY DEPENDENCE OF THE TOTAL SCATTERING CROSS SECTIONS FOR THE SCATTERING OF He, $H_2$, AND $D_2$ MOLECULAR BEAMS ON RARE GASES. Dueren, R.; Feltgen, R.; Gaide, W.; Helbing, R.; Pauly, H. (Universitaet, Bonn). Phys. Letters, 18: 282-3(Sept. 1, 1965). (In German).

Measurements were made of the velocity dependence of the total scattering cross section for the scattering of He, $H_2$, and $D_2$ beams on Ne, Ar, Kr, and Xe. The results for He scattered on Xe, Kr, Ar, and Ne are given on a double logarithmic scale. The effective cross section for the scattering of $H_2$ and $D_2$ on Kr is also given as a function of the primary beam velocity. (J.S.R.)

**2615** ON THE ANGULAR DEPENDENCE OF P (Θ) POLARIZATION OF 3.5 ± 1 ev ELECTRONS ON FREE Hg ATOMS. Deichsel, H.; Reichert, E.; Steidl, H. (Universitaet, Mainz). Phys. Letters, 18: 284(Sept. 1, 1965). (In German).

Earlier measurements were extended to electron energies of 3.5 ± 1 ev with a double scattering experiment. The modifications made in the measurement method are indicated. The results showed that for 3.5 ± 1 ev electrons P values up to 0.3 occur. Also P changes from large positive to large negative values within small scattering ranges. Theoretical values for electron energies below 100 ev are not available. (J.S.R.)

**2616** CHANNELING OF 13 kev $D^+$ IONS IN GOLD CRYSTALS. Andreen, C. J.; Hines, R. L.; Morris, W.; Weber, D. (Northwestern Univ., Evanston, Ill.). Phys. Letters, 19: 116-18(Oct. 1, 1965).

Some experimental results are reported on channeling at low energies in single crystal gold films using 13 kev $D^+$ ions, and the results are compared with the predictions of the transparency model. The films are grown by vacuum deposition onto a substrate of rocksalt. They are removed by dissolving the rocksalt in water and are then mounted on 75 mesh Cu electron microscope grids 3 mm in diameter. Typical distributions of the transmitted ion intensity in (100) and (110) planes and the energies of the transmitted ions are shown. The voltage across the analyzer plates is always set to give the maximum intensity for every combination of the polar angle between the film normal and the incident beam axis and the azimuthal angle of rotation about the film normal. The intensity in ⟨001⟩ dropped 8% in the 200 seconds needed to make the measurements. This drop in intensity with time is believed to be the combined effect of radiation damage and hydrocarbon buildup. When the azimuthal angle is set to give high index directions, the transmitted intensity drops below the detection limit of the electrometer. This means that no randomly scattered beam is found with this detector geometry. Measurements made on about 50 foils without the energy-analyzer have so far given well established channeling peaks in directions given. (J.F.P.)

**2617** ELASTIC SCATTERING OF SLOW ELECTRONS BY ATOMIC OXYGEN. Myerscough, Valerie P. (Univ. of California, Berkeley). Phys. Letters, 19: 120-1(Oct. 1, 1965).

The problem of elastic scattering of slow electrons by atomic oxygen is considered in the static central field exchange approximation which leads for the configuration $[0(^3P)k^2s]^4P$, $^2P$ to the radial equations for the continuum electron. The results for the doublet and quartet s-phase shifts $\delta^2P$, $\delta^4P$ are presented together with the scattering

lengths, and the s-wave elastic scattering cross section. Previous results are also given, and reasonable agreement with them is found. (J.F.P.)

**2618** VIBRATION AND ROTATION OF $N_2^+$ EXCITED BY 10-65-kev IONS. Sheridan, J. R. (Univ. of Alaska, College); Clark, K. C. Phys. Rev., 140: A1033-40(Nov. 15, 1965).

Cross sections for excitation of the $[B(^2\Sigma_u^+) - X(^2\Sigma_g^+)]$ first negative bands of $N_2^+$ resulting from impact of $H^+$, $D^+$, $He^+$, $Ne^+$, and $N^+$ have been measured in the energy range 10 to 65 kev, and at pressures such that radiation occurs much sooner than subsequent collisions of the excited molecule. Intensity ratios of bands in this system and rotational distributions in the 3914-Å (0,0) and 4278-Å (0,1) bands have been directly measured and compared with those obtained from electron impact. Supplementary determinations of total charge-exchange cross sections have been made. Cross sections for excitation of Balmer alpha radiation in charge-exchange collisions of $H^+$ and $D^+$ with $N_2$ have been measured in the same energy range. Little or no increase of vibration occurs in $H^+$, $D^+$, and $e^-$ impact, but a definite enhancement varying with ion velocity is produced by the heavier ions $He^+$, $Ne^+$, and $N^+$. Rotation, however, remains in a thermal distribution at room temperature. (auth)

**2619** LEVEL-CROSSING SPECTROSCOPY WITH AN ELECTRIC FIELD: STARK SHIFT OF THE $3^2P$ TERM IN LITHIUM. Budick, B.; Marcus, S.; Novick, R. (Columbia Univ., New York). Phys. Rev., 140: A1041-3(Nov. 15, 1965).

The method of level-crossing spectroscopy has been extended to a study of the Stark effect on the 3P term of lithium. Lithium atoms in a broad atomic beam are subjected to collinear electric and magnetic fields. The field values required to produce a level crossing or degeneracy are determined by observing the change in the angular distribution of the fluorescence resulting from the optical excitation of the 3P term. The magnetic field required to produce the crossing is found to shift to higher values as the electric field is applied. The shift increases as the square of the electric field and is given by $\Delta H = +0.056\,(11)E^2$, where $\Delta H$ is in gauss and E is in kilovolts per centimeter. The coefficient is in good agreement with the value 0.048 obtained from second-order perturbation theory and the Bates and Damgaard approximation. (auth)

**2620** THEORY OF RESONANCE BROADENING OF SPECTRAL LINES BY ATOM-ATOM IMPACTS. Ali, A. W.; Griem, H. R. (Univ. of Maryland, College Park). Phys. Rev., 140: A1044-9(Nov. 15, 1965).

The broadening of spectral lines due to dipole–dipole interactions with ground-state atoms of the same element is calculated with the impact and classical path approximations. Summation over all contributing intermediate states accounts for the multiplicity of the levels involved and results in a width proportional to the geometrical mean of absorption and emission oscillator strengths. Higher multipole interactions are shown to be almost always negligible, and for Lyman-$\alpha$ the iterated solution of the time-dependent Schrödinger equation describing the collisions is extended to fourth order. Estimated errors of its calculated width and of the widths of other lines are about 5% in the validity regime of the impact approximation, apart from any uncertainties in oscillator strengths and statistical weight factors. (auth)

**2621** LIFETIME OF THE $3^1P$ STATE OF HELIUM. Fowler, R. G.; Holzberlein, T. M.; Jacobson, C. H. (Univ. of Oklahoma, Norman). Phys. Rev., 140: A1050-1(Nov. 15, 1965).

The pressure dependence of the lifetime of the helium transition $3^1P-2^1S$ has been measured over a wide range of pressure, ranging from free escape to complete blockading. The values of lifetimes so obtained are in good agreement with theory. At pressures beyond 1 mm Hg, quenching is observed corresponding to a probable molecular formation. (auth)

**2622** ELECTRON SHAKE-OFF RESULTING FROM K-SHELL IONIZATION IN NEON MEASURED AS A FUNCTION OF PHOTOELECTRON VELOCITY. Carlson, Thomas A.; Krause, Manfred O. (Oak Ridge National Lab., Tenn.). Phys. Rev., 140: A1057-64(Nov. 15, 1965). (ORNL-P-1400).

The relative abundances of the differently charged ions that result from photoionization in the K shell of neon were measured with a specially designed mass spectrometer. Results were obtained as a function of the x-ray energy from 17.5 to 0.93 kev using characteristic lines from a variety of targets. The charge spectrum resulting from 1.5-kev x rays is as follows: $Ne^{1+}$ 5.7 ± 0.6%, $Ne^{2+}$ 70.2 ± 0.5%, $Ne^{3+}$ 20.8 ± 0.3%, $Ne^{4+}$ 3.0 ± 0.2%, $Ne^{5+}$ 0.28 ± 0.07%. At higher energies the spectrum, with the exception of charge 1, remains essentially the same. At lower energies, however, the relative abundances for ions of charges greater than 2 begin to drop at about 500 ev above the K edge of neon. From these data and from previous data on the extent of double electron emission in the KLL Auger process, the extent of electron shake-off arising from photoionization has been evaluated. Specifically, it was found that when the photoelectron leaves the K shell of neon with a velocity more than $1.5 \times 10^9$ cm/sec there is a 16% probability for a single electron shake-off, which agrees well with calculations based on the sudden approximation. Simplified calculations on multiple electron ejection were also shown to be in agreement with the observed abundances of the more highly charged ions. Direct collision and electron correlation are discussed as other possible sources for extra electron emission and the data are used to set upper limits to these contributions. (auth)

**2623** TOTAL IONIZATION IN NITROGEN BY HEAVY IONS OF ENERGIES 25 TO 50 kev. Boring, J. W.; Strohl, G. E.; Woods, F. R. (Univ. of Virginia, Charlottesville). Phys. Rev., 140: A1065-9(Nov. 15, 1965).

The total ionization produced by ions stopped in nitrogen gas has been measured in the energy range 25 to 50 kev. The measurements were made using an ion accelerator for producing the incident particles and a cylindrical ionization chamber with a differentially pumped open window. The following ions were studied: $H^+$, $He^+$, $C^+$, $N^+$, $O^+$, and $Ar^+$. The average energy loss per ion pair, W, ranges from 34.6 ev for 25-kev protons to 115.2 ev for 25-kev argon ions. A calculation indicates that a large part of the variation of W with initial ion energy and atomic species may be attributed to the variation of the energy ultimately going into the kinetic energy of the atoms of the gas. (auth)

**2624** INELASTIC COLLISIONS OF SLOW ATOMS. Callaway, Joseph (Univ. of California, Riverside); Bauer, Ernest. Phys. Rev., 140: A1072-84(Nov. 15, 1965).

A general approximate method for computing the cross sections for certain inelastic collision processes is developed. It is based on the possiblity of obtaining, with the use of the impact-parameter method, an exact expression for the transition amplitude in a special case. The dependence of the cross section on the parameters of coupling constant, velocity, and energy difference between states is discussed for a two-level model. Detailed calculations are made of cross section for collisions of the type $A(^2P_{\frac{1}{2}}) + B \rightleftharpoons A(^2P_{\frac{3}{2}}) + B$, where A is an excited atom of an alkali metal and B is an atom of a noble gas. An Appendix contains a review of the effective long-range interaction of atoms. (auth)

**2625** X-RAY YIELDS FROM K-SHELL IONIZATION BY $\alpha$ PARTICLES. Sharma, R. P.; Thosar, B. V.; Prasad, K. G. (Tata Inst. of Fundamental Research, Bombay). Phys. Rev., 140: A1084-7(Nov. 15, 1965).

The characteristic K x-ray yields are measured in Sn, Te, Ce, $^{144}Sm$, $^{152}Sm$, $^{154}Sm$, $^{160}Gd$, $^{186}W$, and Pb, by bombarding them with $\alpha$ particles of energy 4 and 3 Mev. No excess of x-ray yield has been observed in the atoms of deformed even–even nuclei, when the observed data were corrected for the x-ray contribution due to internal conversion by using the theoretical values of K-shell internal-conversion coefficients. The observed variation of the

number of K-shell vacancies per microcoulomb with the atomic number indicates that the E2 internal-conversion coefficients and also the probability for K-shell ionization are unaffected by nuclear deformation. (auth)

**2626** $2^{1,3}P$, $3^{1,3}P$, AND $4^{1,3}P$ STATES OF He AND THE $2^1P$ STATE OF $Li^+$. Schiff, B.; Lifson, H.; Pekeris, C. L.; Rabinowitz, P. (Weizmann Inst. of Science, Rehovoth, Israel). Phys. Rev., 140: A1104-21(Nov. 15, 1965).

A method is outlined for calculating nonrelativistic eigenvalues and wave functions for a two-electron P state of odd parity, and for evaluating the mass polarization and all of the relativistic corrections, apart from the radiative terms. Calculations have been made for the low-lying P states of He and the $2^1P$ state of $Li^+$ using up to 560 terms in the expansion of the wave function. The nonrelativistic eigenvalues converge to within an accuracy of from $10^{-4}$ $cm^{-1}$ to $10^{-2}$ $cm^{-1}$. The values of the mass polarization and of the relativistic corrections converge more rapidly than this, so that the total theoretical ionization energy is estimated to be correct to within an error of not more than $10^{-2}$ $cm^{-1}$, i.e., considerably less than the experimental error, in the case of all of the states considered. The difference between the theoretical and experimental term values is in no case greater than 0.1 $cm^{-1}$ in absolute magnitude, and is presumed to be due to the contributions from the radiative terms, which have not been included in the calculation. The term value obtained for the $2^1P$ state of $Li^+$ confirms the identification of the line at 9581.42 Å in the $Li^+$ spectrum as belonging to the $2^1S-2^1P$ transition. (auth)

**2627** OPTICAL LINEWIDTH AND LINE-SHAPE STUDIES OF ENERGY TRANSFER MECHANISMS BETWEEN RARE-EARTH IMPURITY IONS. Yen, W. M. (Stanford Univ., Calif.); Greene, R. L.; Scott, W. C.; Huber, D. L. Phys. Rev., 140: A1188-96(Nov. 15, 1965).

Optical linewidth and line-shape studies of transitions of 4f impurity ions in doubly doped systems are reported, and it is shown that interactions which involve excitation transfer between the impurity systems produce homogeneous broadening and line-shape changes in the optical transitions. In particular, the behavior of the 5985-Å line of $Pr^{3+}$ in doubly doped $LaF_3$: $Pr^{3+}$, $Nd^{3+}$ as a function of $Nd^{3+}$ concentration was studied. The 5985-Å $Pr^{3+}$ transition at 4.2°K involves two long-lived electronic states of the $Pr^{3+}$ ion; it follows that in the singly doped $LaF_3$: $Pr^{3+}$ the transition shows a Gaussian shape which is characteristic of inhomogeneous strain and imperfection broadening. As $Nd^{3+}$ is added to the system, a broader Lorentzian component begins to appear in the 5985-Å $Pr^{3+}$ transition and eventually (at $Nd^{3+}$ concentrations of ~1% or above) completely dominates the width and shape of the transition. The Lorentzian component of the transition line shape was successfully separated using a Fourier-transform technique and the width of this component was studied as a function of the $Nd^{3+}$ concentration. The width is found to increase linearly with increasing $Nd^{3+}$ concentration up to concentrations of 2%; at higher concentrations, the linewidth saturates and approaches an asymptotic value of ~2 $cm^{-1}$. This homogeneous component was construed to be evidence of a rapid short-range energy transfer mechanism between the $Pr^{3+}$ and $Nd^{3+}$ systems at the terminating $(^3H_6)_1$ level of the 5985-Å $Pr^{3+}$ transition. Various mechanisms are investigated as causes of the energy transfer process; it is concluded that the spin-exchange interaction is the most probable cause for the transfer. Results of other spectroscopic measurements on the doubly doped $LaF_3$: $Pr^{3+}$, $Nd^{3+}$ system are also presented. (auth)

**2628** SECONDARY-ELECTRON EMISSION FROM MOLYBDENUM DUE TO POSITIVE AND NEGATIVE IONS OF ATMOSPHERIC GASES. Mahadevan, P.; Magnuson, G. D.; Layton, J. K.; Carlston, C. E. (General Dynamics/Convair, San Diego, Calif.). Phys. Rev., 140: A1407-12 (Nov. 15, 1965).

Secondary-electron yields from a clean surface of Mo have been measured for $H^+$, $H_2^+$, $H_3^+$, $H^-$, $O^+$, $O_2^+$, $O^-$, $O_2^-$, $N^+$ and $N_2^+$ in the kinetic energy range 40 ev to 2 kev. These measurements have been made under ultrahigh vacuum of order $10^{-10}$ torr. The rate of variation of the electron yield $\gamma$ with kinetic energy of the incident ion decreases as the ion mass increases, consistently from $H^+$ to $O_2^+$. Evidence is presented to show that kinetic emission is much less affected by monolayer coverage of the surface than potential emission is. For clean surfaces, the negative-ion yields represent most closely the kinetic-emission characteristics of the bombarding particles. (auth)

**2629** LARGE-ANGLE COLLISIONS IN AN ALUMINUM SURFACE BOMBARDED BY 50-kev ARGON IONS. Dahl, Poul; Magyar, John (Univ. of Connecticut, Storrs). Phys. Rev., 140: A1420-8(Nov. 15, 1965).

The ejection of charged atomic particles from the surface of an Al target during irradiation by 50-kev $Ar^+$ ions was studied. At several angles to the incident beam an analysis of emitted ions was performed by electrostatic deflection to a single-particle detector. The spectra show sharp peaks superimposed on a continuum. The peaks correspond to single collisions. From accurate measurements of peak positions, the inelastic energy loss in the Ar on Al collisions is obtained by methods assuming pure single collisions. The values are about 450 ev for the Al recoil peaks at angles from 77 to 50°, and higher values (up to 600 ev) are found for more violent collisions. Variation of the angle which the surface forms to the incident beam did not influence the peak positions. This result supports the single-collision assumption. Absolute measurements of spectral intensities were also performed, and the number of target atoms per $cm^2$ that would account for the measured peak intensities was derived by applying generally accepted theoretical scattering cross sections. Typically, single-collision scattering is obtained from target atoms with density comparable to or less than the density in a {100} crystal plane. Theoretical estimates of multiple scattering are used in a discussion of the peak formation. The target was a single crystal, but the surface included an oxygen impurity, and no lattice-directional effect was observed. The continuum is interpreted; the discussion is based on the absolute intensity measurements and on the theory for penetration of heavy ions in the kev region for random distribution of target atoms. (auth)

**2630** DIRECT DETECTION OF TWO-PHOTON EMISSION FROM THE METASTABLE STATE OF SINGLY IONIZED HELIUM. Lipeles, M.; Novick, R.; Tolk, N. (Columbia Univ., New York). Phys. Rev. Lett., 15: 690-3(Oct. 25, 1965).

A description is given of an experiment designed to detect the decay in flight of a slow (12 ev) beam of metastable helium ions. The results give evidence of the direct detection by coincidence counting techniques of the two-photon decay of the metastable $2^2S_{\frac{1}{2}}$ state of singly ionized helium. (L.B.S.)

**2631** CHARGE-TRANSFER EXCITATION OF $CO^+$ COMET-TAIL BANDS BY SLOW $N_2^+$ IONS. Utterback, Nyle G. (General Motors Defense Research Labs., Santa Barbara, Calif.); Broida, H. P. Phys. Rev. Letters, 15: 608-9(Oct. 11, 1965).

Optical spectra were observed from collisions between low-velocity $N_2^+$ ions and CO molecules in a beam-type experiment under thin-target conditions. The reaction was identified as charge transfer to an excited state, $N_2^+ + CO \rightarrow N_2 + CO^+(A^2\Pi)$. Although this excitation reaction is endothermic by 1 ev, the cross section decreased less than a factor of two when the kinetic energy in the center-of-mass system was decreased from 100 to 8 ev, indicating that translational energy was efficiently converted to excitation energy. The excitation cross section was large. All light emission observed was identified as bands belonging to the $CO^+$ comet-tail system. The feasibility was shown of using optical techniques to study collision processes, at least for some species. The spectrum of light emitted in the $N_2^+$ interaction and the relative cross section for excitation are illustrated. (J.F.P.)

**2632** DISSOCIATION OF $H_2^+$ BY ELECTRON IMPACT. Dunn, Gordon H.; Zyl, Bert Van; Zare, Richard N. (Joint

Inst. for Laboratory Astrophysics, Boulder, Colo.). Phys. Rev. Letters, 15: 610-12(Oct. 11, 1965).

The absolute cross section as a function of electron energy is measured for the sum of certain $H_2^+$ processes. A schematic diagram of the experiment is shown. Ions are formed by bombardment of $H_2$ gas at about 0.4 $\mu$ by 200-ev electrons. The 10-kev ion beam is mass-analyzed and is passed through various differentially pumped chambers before entering the collision region. Here the ion beam is crossed by a variable-energy modulated electron beam. Protons resulting from the dissociation of $H_2^+$, are separated from the parent ion beam with a 45° parallel-plate electrostatic analyzer. Measured values of the cross sections are shown. These are compared with theoretical estimates. (J.F.P.)

**2633** PHOTOELECTRON SPECTROSCOPY WITH A SPHERICAL ANALYZER. THE VIBRATIONAL ENERGY LEVELS OF $H_2^+$. Frost, D. C.; McDowell, C. A.; Vroom, D. A. (Univ. of British Columbia, Vancouver). Phys. Rev. Letters, 15: 612-14(Oct. 11, 1965).

The use of a spherical energy analyzer to study the photoelectron energy distribution in an ionized gas is reported. The separations of the first five vibrational energy levels of $H_2^+(^2\Sigma_g^+)$ and the relative probabilities of ionization were measured. The photon source was a microwave discharge in helium, which emits essentially 584 Å (21.21 ev) in the energy range above the hydrogen ion potential. If $H_2^+$ can be formed in more than one vibrational state, a group of photoelectrons are expected corresponding to each. The differences between the group energies should give the vibrational level spacing, and the relative intensities will be proportional to the transition probabilities from $H_2(^1\Sigma_g^+)$ for 584 Å radiation. Restriction is made to observations on the $^2\Sigma_g^+$ ground electronic state. An analyzer was built wherein photoelectons are produced in a small volume at the center of a spherical grid system, so that initial ejection is always normal to the retarding field. This gives a greatly improved resolution. A diagram of the apparatus is shown. A photoelectric retarding curve is shown, and the threshold energies of five energy groups clearly visible also are show (J.F.P.)

**2634** CAPTURE AND LOSS OF ELECTRONS BY FAST IONS IN ATOMIC COLLISIONS. Nikolaev, V. S. Usp. Fiz. Nauk, 85: 679-720(Apr. 1965). (In Russian).

A systematization of the extensive experimental material obtained in recent years on the cross sections for the loss and capture of electrons by ions of almost all light elements, up to argon inclusive is given. New data are included on the equilibrium distribution of charges in ion beams, and a summary is presented of work on stripping and charge exchange of fast positive ions and atoms at velocities exceeding $2.19 \times 10^8$ cm/sec. The subjects covered are: main relations for the determination of the charge composition of an ion beam passing through matter, equations for the determination of the charge composition of an ion beam in condensed media, measurement of the equilibrium distribution of charges in an ion beam as the density of the medium is increased, experimental procedure, mass-spectrometric method for determining effective cross sections, determination of cross sections by the method of attenuation of an ion beam in a magnetic field, and procedure for determining the equilibrium charge composition of ion beams. Other topics are: electron loss by fast ions, effective cross sections for electron loss, average probability of electron removal, principal result of theoretical papers, comparison of experiment and theory, capture of electrons by fast ions, main results of theoretical papers, results of experimental research on the capture of one electron, comparison with theory, and average probability of electron capture. Also covered are: competition between capture and loss of electron, equilibrium distribution of charges in ion beams, main laws governing equilibrium distributions, causes of regularities observed in the equilibrium charge composition of ion beams passing through rarefied gases, interpretation of singularities in the equilibrium charge composition of ion beams in dense media, and methods of calculating the average ion charge. (ATD)

**2635** COMPUTATIONAL IMPROVEMENTS IN PHASE SHIFT CALCULATIONS OF ELASTIC ELECTRON SCATTERING. Buehring, Wolfgang (Universitaet, Heidelberg). Z. Physik, 187: 180-96(1965). (In German).

A method of calculating the scattering phase shifts from the Dirac radial equations containing a rather general potential is described. The method takes advantage of the fact that a system of linear differential equations can be solved with the help of power series. Application of the method is demonstrated for the case of low-energy scattering (uniformly distributed nuclear charge screened by the atomic electrons) and for the case of high-energy scattering (uniform or more complicated nuclear charge distribution without atomic screening). (auth)

**2636** THE RAINBOW EFFECT AND INTERFERENCE PATTERNS IN MOLECULAR COLLISIONS. Hundhausen, E.; Pauly, H. (Universitaet, Bonn). Z. Physik, 187: 305-37(1965). (In German).

Crossed beam measurements of differential elastic scattering cross sections for collisions of alkali atoms with mercury and xenon atoms as well as with different molecules are presented. Special attention is given to the rainbow effect including supernumerary rainbows and to interference effects connected with rainbow scattering. The observation of well resolved primary and supernumerary rainbows together with interference patterns make the determination of a three parameter potential model possible. Partial wave numerical calculations of differential cross sections are used to evaluate potential parameters and to discuss the limits of the semiclassical rainbow theory. Elastic scattering between reactive collision partners is also investigated and interpreted in terms of a simple optical model. (auth)

**2637** MEASUREMENT OF THE EFFECTIVE CROSS SECTION FOR THE LINE BROADENING OF HIGH-FREQUENCY TRANSITIONS IN THE $6\,^3P_2$ STATE OF MERCURY BY COLLISIONS WITH RARE GAS IONS. Tittel, Klaus (Universitaet, Tuebingen, Ger.). Z. Physik, 187: 421-32(1965). (In German).

The linewidth of high frequency transitions between Zeeman-levels of the metastable $6\,^3P_2$-state of mercury is measured as function of the pressure of various noble gases. The measurements are made for all noble gases in the pressure range from $10^{-3}$ to about $2 \cdot 10^{-2}$ torr. The cross sections for linebroadening due to atomic collisions are derived from the pressure dependence of the linewidth. These cross sections $\sigma$ were found to be $(71 \pm 10) \cdot 10^{-16}$ cm$^2$ for He, $(82 \pm 10) \cdot 10^{-16}$ cm$^2$ for Ne, $(153 \pm 12) \times 10^{-16}$ cm$^2$ for Ar, $(204 \pm 28) \cdot 10^{-16}$ cm$^2$ for Kr and $(291 \pm 41) \cdot 10^{-16}$ cm$^2$ for Xe. (auth)

**2638** EFFECTIVE CROSS SECTION FOR THE EXCITATION OF MOLECULAR VIBRATIONS BY FAST ELECTRONS. Geiger, J.; Wittmaack, K. (Technische Universitaet, Berlin). Z. Physik, 187: 433-43(1965). (In German).

The differential cross section for the excitation of infrared inactive and—in dipole approximation—infra-red active fundamental vibrations by fast electrons is calculated. The energy loss spectra of $CO_2$, $N_2O$, $C_2H_4$ are measured with 33 kev electrons in the small energy loss range up to 0.5 ev. The experimentally determined cross sections for the excitation of active fundamental molecular vibrations, which are of order $10^{-21}$ cm$^2$, agree well with values calculated from the integrated absorption intensity of the corresponding rotation-vibration bands. (auth)

**2639** IONIZATION PRODUCED IN COLLISIONS BETWEEN ALKALI METAL ATOMS AND GAS MOLECULES. Kikiani, B. I.; Ogurtsov, G. N.; Fedorenko, N. V.; Flaks, I. P. (Ioffe Inst. of Physics and Tech., Leningrad). Zh. Eksp. Teor. Fiz., 49: 379-85(Aug. 1965). (In Russian).

The total cross sections for production of free electrons $\sigma_-$, ionization cross section $\sigma_+$, and stripping cross section

$\sigma_1$ are measured for single collisions between Li, Na, K, and Cs atoms with the atoms of all the inert gases and with $H_2$ and $N_2$ molecules. In the investigated energy range (3 to 30 kev) all cross sections continuously increase with growth of velocity of the impinging particles. As a rule the $\sigma_-$, $\sigma_+$, and $\sigma_1$ cross sections for a given alkali metal atom also increase with increase of the atomic number of the target particles. This rule breaks down when the atomic numbers of the colliding particles are close to each other (e.g., Na–Ne, K–Ar, Cs–Xe) in which case the ionization cross sections are appreciably larger. The stripping cross sections for Li atoms in He, $H_2$, and $N_2$ are compared with the available experimental data and the $\sigma_-(v)$ curves with the theoretical curve deduced by Firsov. It is shown that theory yields excessive values for the cross sections $\sigma_-$ of ionization processes in which alkali metal atoms participate. Factors affecting the ratio between cross section $\sigma_+$ and $\sigma_1$ are discussed. (auth)

**2640** SCATTERING OF pμ ATOMS ON PROTONS. Dzhelepov, V. P.; Ermolov, P. F.; Filchenkov, V. V. (Joint Inst. for Nuclear Research, Dubna, USSR). Zh. Eksp. Teor. Fiz., 49: 393-405(Aug. 1965). (In Russian).

Further experimental studies are presented on pμ atom scattering on protons carried out to determine the spin state of the pμ atom prior to muon decay or muon capture by the proton. The range distributions of the pμ atoms are obtained using a diffusion chamber at various hydrogen densities and admixture concentrations (carbon, oxygen). An analysis of the distributions and the data on the pμ atom lifetimes show that they can be satisfactorily described by choosing for the effective cross section the value $\sigma_{p\mu+p} = (1.75 \pm 0.19) \cdot 10^{-9}$ cm$^2$. The best agreement is attained if it be assumed that the pμ atom is produced with an energy of several ev. An analysis of the data based on familiar theoretical expressions for the scattering cross sections in various spin states of the pμ atom leads to the following conclusions: (1) The cross section for elastic scattering of pμ atoms on protons is $(1.67 \pm 0.30) \cdot 10^{-19}$ cm$^2$ for the singlet spin state of the pμ atom (F = 0). This value is much greater than that predicted by the theory. Such intensive resonance scattering may be due to the existence of a low energy virtual level in the pμp system. (2) The most probable transition rate from the triplet state of the pμ atom to the singlet state is $\sim 10^{10}$ sec$^{-1}$ (for liquid hydrogen density) and as a result muon capture by protons in liquid as well as in gaseous hydrogen should proceed in a pμ atomic state with F = 0. Only at gas pressures of the order of an atmosphere muon depolarization prior to capture may not be complete due to inverse transitions which are possible under these conditions. (3) The rate of formation of ppμ mesic molecules in the para-state is negligibly small compared to their rate of formation in the orthostate, although it is higher by an order of magnitude than the value calculated by Cohen et al. It is also shown that transition of the muon from the proton to carbon and oxygen nuclei predominantly occurs on the higher Cμ and Oμ atomic orbits and the probability for direct transition to the 1 s level is smaller than 3%. (auth)

**2641** EXPERIMENTAL DETECTION OF THE ISOTOPIC SHIFT OF THE MOLYBDENUM $K_{\alpha 1}$ X-RAY LINE. Sumbaev, O. I.; Mezentsev, A. F. (Ioffe Inst. of Physics and Tech., Leningrad). Zh. Eksp. Teor. Fiz., 49: 459-69 (Aug. 1965). (In Russian).

By applying the method of alternatively introducing the measured sources into the field of vision of a diffraction spectrometer, which was previously employed for observing the chemical shift of the K-series x-ray lines of comparatively heavy elements, it has been possible to detect a volume isotopic shift of the $K_{\alpha 1}$ x-ray line of molybdenum isotopes. For $^{92}MoO_3 - {}^{100}MoO_3$, $^{94}MoO_3 - {}^{100}MoO_3$, and $^{92}MoO_3 - {}^{94}MoO_3$, the energy differences for the line were respectively 0.030 ± 0.005 ev, 0.027 ± 0.008ev, and 0.001 ± 0.005 ev. The relative sensitivity of the method is thus as high as 0.00003%. The results obtained are in satisfactory agreement with the theoretical predictions: $\Delta E(92 \text{ to } 100)_{exp} / \Delta E(92 \text{ to } 100)_{theor} = 1.15 \pm 0.19$. A comparison of the experimental errors with theoretical estimations of the magnitude of the effect for a number of other elements shows that the isotopic shift of the x rays may be used as a new method for investigating the properties of nuclei. Its main advantage over the optical isotopic shift is that the nuclear part of the effect can be separated more accurately due to the possibility of taking into account the mutual effect of the electron shells of the atom in a simpler and more accurate manner. (auth)

**2642** CALCULATION OF THE EFFECTIVE CROSS SECTION FOR LOSS OF K-ELECTRONS BY FAST HYDROGEN-LIKE IONS DURING ENCOUNTERS WITH HYDROGEN AND HELIUM ATOMS. Dmitriev, I. S.; Zhileikin, Ya. M.; Nikolaev, V. S. (Moscow State Univ.). Zh. Eksp. Teor. Fiz., 49: 500-14(Aug. 1965). (In Russian).

The cross sections for loss of K electrons by fast hydrogen-like ions of any element due to encounters with hydrogen of helium atoms is calculated in the nonrelativistic Born approximation. Approximate expressions for the cross sections in limiting cases are obtained which are convenient for practical application. For small charge ions the Born approximation yields cross sections which are identical with those calculated in the free collision approximation. The calculated cross sections can also be used for estimating the cross sections for electron loss from other shells. (auth)

**2643** THEORY OF s–f-EXCHANGE FOR NON-VANISHING ORBITAL MOMENTA. Vonsovskii, S. V.; Svirskii, M. S. (Inst. of Physics of Metals, Academy of Sciences, USSR; Chelyabinsk State Pedagogical Inst., USSR). Zh. Eksp. Teor. Fiz., 49: 682-90(Aug. 1965). (In Russian).

s–f-exchange interaction is considered in the case when the total momentum of the f-shell, J, is a good quantum number. The hamiltonian for s–f exchange related to changes in J is established and its effect on indirect exchange interaction and superconductivity is analyzed. The results obtained by Brout-Suhl and Mattis are critically discussed. (auth)

**2644** PROFOUND STRIPPING AND THE SCATTERING OF $Kr^+$ IONS IN SINGLE COLLISIONS WITH Ne, Ar, Kr AND Xe ATOMS. Pivovar, L. I.; Novikov, M. T.; Dolgov, A. S. (Inst. of Physics and Tech., Kiev). Zh. Eksp. Teor. Fiz., 49: 734-42(Sept. 1965). (In Russian).

The angular distributions of charges in a beam of krypton ions after single collisions with Ne, Ar, Kr, or Xe atoms are measured in the 250 to 850 kev energy range. The total differential cross sections for scattering of $Kr^+$ ions in the indicated gases are also measured. From the results obtained it can be concluded that electrons of the inner M shell of the krypton ions are considerably involved in the interaction and the dependence of the mean $Kr^+$ ion ionization energy on the nature of the target atoms can be established. It is found that in single collisions and angles $\theta \neq 0$ the mean ion charge is proportional to the ion velocity. The data obtained also permit one to determine the integral cross sections for electron loss and capture by $Kr^+$ ions. The measurements are performed for angles lying between 0 and 3°. (auth)

**2645** SATELLITES OF X RAY SPECTRA. Sachenko, V. P.; Demyokhin, V. F. (Rostov-on-Don State Univ., USSR). Zh. Eksp. Teor. Fiz., 49: 765-9(Sept. 1965). (In Russian).

A mechanism is proposed to explain the appearance of multiply ionized atoms; it is similar to autoionization of atoms in β-decay. The calculated intensities of the x-ray Kα- and some Kβ-satellites are in agreement with the experimental data. It is shown that nonradiative transitions significantly influence the relative intensity of the $KL_I$-$KL_{II\,III}$-satellites. The effect of chemical bond on the satellite intensity is considered. (auth)

**2646** DESTRUCTION OF ATOMIC PARTICLES BY AN ELECTRIC FIELD AND BY ELECTRON IMPACT. Smirnov, B. M.; Chibisov, M. I. Zh. Eksp. Teor. Fiz., 49: 841-51(Sept. 1965). (In Russian).

Decay of an atomic particle in a stationary homogeneous

electric field is considered. An asymptotically exact (in the limit of small field strengths) expression is obtained for the probability of electron detachment per unit time. The result obtained is employed for determining the binding energy of an electron in a negative helium ion on basis of the experimental dependence of the ion lifetime on the strength of the external electric field in which it decays. The electron affinity energy of a helium atom is 0.06 ± 0.005 ev. The cross section for disintegration of a negative ion by electron impact as a result of which an s-electron is liberated is calculated. It is assumed that the break up cross section is large compared with the characteristic size of the negative ion and that the impinging electron moves in a classical orbit. These assumptions are justified by the results. Two mechanisms of destruction of a negative ion are considered: squeezing out of a weakly bound electron of the negative ion by the static field of the impinging electron and its removal as a result of variation in time of the field of the incident electron. It is shown that at high collision velocities the second mechanism yields a result which corresponds to the Born approximation. The dependence of the $H^-$ disintegration cross section on the velocity of the incident electron is compared with the results of other calculations. (auth)

**2647** ATTACHMENT OF ELECTRONS TO ATOMS IN TRIPLE COLLISIONS. Chibisov, M. I. Zh. Eksp. Teor. Fiz., 49: 852-6(Sept. 1965). (In Russian).

The probabilities for attachment of electrons in triple encounters e + A + B and e + e + A are expressed in terms of the corresponding cross sections for disintegration of the atomic systems $A^-$ and $B^-$. The method employed is based on the statistical principle of detailed equilibrium. It is shown that at densities of the target gas of $10^{13}$ to $10^{15}$ $cm^{-3}$ attachment of electrons to neutral atoms in triple encounters is more probable than photoattachment. The pressure and temperature ranges in which the rate of the reaction e + e + A = $A^-$ + e is greater than that of the reaction e + A + A = $A^-$ + A in a gas in thermal equilibrium. (auth)

**2648** ELECTRON DETACHMENT IN SLOW COLLISIONS BETWEEN NEGATIVE IONS AND ATOMS. II. ACCOUNT OF THE FINITE SIZE OF THE SYSTEM. Demkov, Yu. N. (Leningrad State Univ.). Zh. Eksp. Teor. Fiz., 49: 885-94(Sept. 1965). (In Russian).

A reaction of the A + $A^-$ → A + A + e type is considered. The effective potential of system $A_2$, in the field of which a weakly bound electron moves, is represented by two short-range potential wells. It is assumed that when the nuclei approach each other the bound state of $A_2^-$ vanishes and it disintegrates. The angular and energy distributions of the emitted particles are calculated for symmetric and antisymmetric states. It is shown that account of the finite size of the system unexpectedly weakly changes the energy spectrum of the electrons. A general equation set is deduced for the motion of a particle in the field of moving short range potential wells of variable depth. (auth)

**2649** EXPERIMENTAL DETERMINATION OF ATOMIC TRANSITION PROBABILITIES USING A D.C. ARC PLASMA JET [Thesis]. Oakberg, Theodore Cameron. Cincinnati, Univ. of Cincinnati, 1964. 120p.

The use of a small d-c arc plasma jet as a source of emission spectra for atomic transition probability measurements was investigated and transition probabilities for several optical transitions in the spectrum of mercury were measured. The plasma jet used was a d-c electric arc in an atmosphere of helium with a trace of mercury vapor present. The arc was operated at atmospheric pressure with a current of 12.5 amperes. The Fowler-Milne method was used to determine the excitation temperature of the neutral mercury lines in the arc. The ionization equations and a Boltzmann distribution of excited energy states were solved using digital computer techniques, and yielded the maximum number densities of various excited states of mercury atoms as a function of concentration of mercury in the arc. A spectroscopic determination of the maximum intensity per unit volume was made for the 3650 Å spectrum line. The absolute transition probability (gA value) was determined for the 3650 Å spectrum line. The gA value of the 3650 Å spectrum line was found to be gA = 62. × $10^7$ $sec^{-1}$. Measurements of the relative transition probabilities of eight mercury lines, combined with this absolute measurement, gave absolute transition probabilities for eight spectrum lines of neutral mercury. An extensive survey of previous determinations of atomic transition probabilities for neutral mercury is included. It is believed that the uncertainty in the transition probabilities of eight spectrum lines of mercury is reduced from a factor of 5 or 10, to approximately 50 per cent. (A.G.W.)

**2650** DIATOMIC FORCES AND FORCE CONSTANTS FROM THE HELLMANN-FEYNMAN THEOREM; APPLICATION TO $H_2$ [Thesis]. Benston, Margaret Lowe. Seattle, Univ. of Washington, 1964. 132p.

When appropriate coordinates are used, the electrostatic theorem and the virial theorem are obtained as the two simplest cases of the Hellmann-Feynman theorem for intramolecular forces. For approximate electronic wave functions these two theorems may not be exact, and errors involved were investigated for $H_2$ using simple molecular orbital and valence bond approximations for the wave function. Large errors were found in the electrostatic force for all of the functions used. The virial theorem was also in error when unscaled functions were used, but, for scaled functions, it gave exactly the first derivative of the theoretical energy curve. The equations for the quadratic force constants, $k_2$, and the first anharmonic constant, $k_3$, are also discussed from the standpoint of the independent variables involved, and some new expressions are given. Calculations of these force constants were done for $H_2$. A variation-perturbation solution of the equations for $k_2$ and $k_3$ was developed following Sinanoglu's general outline. In this approach a trial wave function derivative is optimized by a variational procedure. The method was applied to $H_2$. (A.G.W.)

## Cosmic Radiation

### *See also* Elementary Particles and Radiations
### Nuclear Properties and Reactions

*Refer also to abstracts 2586 and 3239.*

**2651** (INR-608/VI/PH) O MOZLIWOSCIACH WYSTEPOWANIA W ODDZIALYWANIACH PROMIENIOWANIA KOSMICZNEGO JETOW WTORNYCH O BARDZO WYSOKIEJ WARTOSCI CZYNNIKA LORENTZA OBLICZONEGO METODA CASTAGNOLI. (A Possible Occurrence of Very High Lorentz Factor Calculated Using Castagnoli's Formula in Secondary Jets of Ultra High Energy). Czachowska, Z. (Institute of Nuclear Research, Warsaw (Poland)). Feb. 1965. 31p.

In cosmic ray jets there are secondary events with $\gamma_C'$ higher than $\gamma_C$ of primary interaction. The influence of dynamical properties in particular the masses of the colliding bodies in primary and secondary interactions on the ratio of $\gamma_C'/\gamma_C$ was analyzed. (auth)

**2652** (NASA-SP-71, pp 1-4) MAN-MADE RADIATIONS IN SPACE. von Braun, Wernher (National Aeronautics and Space Administration, Huntsville, Ala. George C. Marshall Space Flight Center).

A brief outline is given of the problems of natural and artificial radiations in space, as they affect manned space missions. (T.F.H.)

**2653** (NASA-SP-71) REVIEW OF GALACTIC AND SOLAR COSMIC RAYS. McDonald, F. B. (National Aeronautics and Space Administration, Greenbelt, Md. Goddard Space Flight Center).

The charge distributions, energy spectra, and spatial distributions of the galactic cosmic radiation are reviewed. The frequency and size distributions, charge and energy spectra, and propagation characteristics of solar cosmic radiation are also outlined. (T.F.H.)

**2654** (NASA-SP-71, pp 47-55) THE UPDATING AND DISSEMINATION OF THE KNOWLEDGE OF TRAPPED

RADIATION—MODEL ENVIRONMENTS. Vette, James I. (Aerospace Corp., El Segundo, Calif.).

A program is described whose purpose is the collection, assimilation, updating, and analysis of satellite data on trapped cosmic radiation, in order to produce a model of the trapped radiation environment. The output is in the form of tables and graphs, and the system has some predicting ability. The center that analyzes the data also disseminates the analyses. (T.F.H.)

**2655** (NASA-SP-71, pp 85-96) THE RADIOBIOLOGICAL CONSEQUENCES OF DOSE DISTRIBUTIONS PRODUCED BY SOLAR-FLARE-TYPE SPECTRA. Jones, Robert K. (Lovelace Foundation for Medical Education and Research, Albuquerque, N. Mex.); Adams, Duane E.; Russell, Irving J. (Air Force Weapons Lab., Kirtland AFB, Ohio).

It is concluded that no single one of three high-flux solar flares examined would represent a serious radiation hazard to an astronaut in a polar orbit, even if he were to experience the full flux in a Gemini vehicle shielded only by the magnetosphere. No consideration is given to synergisms between weightlessness, acceleration, vibrational, or psychological stresses. (auth)

**2656** (NASA-SP-71, pp 265-86) THE EFFECT OF CHARGED-PARTICLE ENVIRONMENTS ON MANNED MILITARY SPACE SYSTEMS. Keller, F. L.; Pruett, R. G. (Aerospace Corp., El Segundo, Calif.).

For future space missions, especially those which will be manned, the threat posed by the charged-particle environment could impose certain restrictions on either the vehicle and/or its mission. These radiation threats, which could have a marked influence on future manned space systems, are evaluated and discussed. The threat from cosmic rays is discussed. Data are presented on the nature of solar flares and their effects. The geomagnetically trapped belts, their effects on man and equipment, the importance of shielding, and an estimate of internal radiation dose to the crews behind various shielding are also studied. (T.F.H.)

**2657** (NASA-SP-71, pp 287-99) THE IONIZING RADIATIONS IN SUPERSONIC TRANSPORT FLIGHTS. Foelsche, Trutz (National Aeronautics and Space Administration, Langley Station, Va. Langley Research Center).

Commercial supersonic transport planes are envisioned to cruise at altitudes up to 23 km. The exposure to crew and passengers from galactic and solar cosmic rays at these altitudes on polar routes is estimated and compared with the maximum permissible dose rates (MPD) cited in the guidelines of the Federal Radiation Council or the International Commission for Radiation Protection. The dose equivalent in rem from galactic cosmic radiation at cruise altitudes on polar routes is estimated as $\leq$2 mrem/hr. This implies that the crew should experience $\leq$20 percent of the MPD for radiation workers (5 rem/year), at 20 hours/week flight duty or 10 hours in 23 km altitude, if evasive measures during intense and energetic solar flare events are taken. The calculated dose rate is considered as an upper limit because the fast neutron flux and the buildup factors of secondaries in the airplane are assumed conservatively high. Estimates of dose rates for the most important intense and energetic flare events (solar cosmic radiation) show that in cruise altitudes at high latitudes and in impact zones, e.g., during the February 23, 1956 event, 1 to 4 rem/hr might have been reached. If evasive measures are carried out in these cases, such as descending to 12 km, the radiation doses received by passengers from solar and galactic cosmic rays appear negligible ($\approx$10 percent of the MPD of 0.5 rem/year at 2 polar flights/month) except for the effects of certain characteristic biological effective components of galactic cosmic rays which appear only in high altitudes, i.e., heavy primaries and stars. (auth)

**2658** (NASA-SP-71, pp 527-33) AN EXAMINATION OF THE RELATIVE MERITS OF STOCHASTIC AND NONSTATISTICAL METHODS OF COMPUTING PRIMARY IONIZATION DOSES. Liley, B.; Schaedle, G. C. (North American Aviation, Inc., Downey, Calif.).

Several questions concerning computation of primary ionization doses for solar-flare-proton rigidity spectra with stochastic and nonstatistical methods are discussed. The topics considered include: geometrical representations for dose computations; the effect of spacecraft area density distribution function parameters on the degree of geometrical detail or precision which is desirable for dose computations with nonstatistical methods; convergence properties for the Monte Carlo method of dose computation as a function of rigidity and the geometry distribution parameters; the necessity of accounting for nuclear collisions when computing primary ionization doses. The effect of nuclear collisions on the convergence of the primary ionization dose; dose computational accuracy of the statistical primary ionization dose; and relative merits of nonstatistical and statistical methods of dose computation trade-offs between dose computational accuracy and cost. (T.F.H.)

**2659** TABLES OF IGY COSMIC RAY DATA. PART I. Simpson, J. A. (ed.). Ann. Int. Geophys. Yr., 26: 1-536(1963).

Tables are presented of cosmic-ray data from continuously recording monitors throughout the world during the period of July 1, 1957 to Dec. 31, 1958. (L.B.S.)

**2660** TABLES OF IGY COSMIC RAY DATA. PART II. Simpson, J. A. (ed.). Ann. Int. Geophys. Yr., 27: 537-1121(1963).

Cosmic-ray data tabulations for the period from July 1, 1957 to Dec. 31, 1958 are continued. A list of balloon, aircraft, and rocket flights is included, together with a list of investigators from whom further information may be obtained. (L.B.S.)

**2661** TABLES OF IGY COSMIC RAY DATA. PART III. Simpson, J. A. (ed.). Ann. Int. Geophys. Yr., 28: 1-677(1963).

The international program for experiments and continuous measurements of cosmic radiation, which began with the International Geophysical Year, was continued through the year 1959. Data tabulations for the IGY are presented. (L.B.S.)

**2662** COSMIC RAYS AND THEIR FORMATION OF A GALACTIC HALO. Parker, E. N. (Univ. of Chicago). Astrophys. J., 142: 584-90(Aug. 15, 1965).

It is demonstrated that a magnetic gas cloud confined by gravity has no equilibrium configuration if cosmic rays are generated within it. By application of the theorem to the galaxy, it is shown that cosmic rays lead to inflation of the galactic magnetic fields, producing a halo of cosmic rays and field around the galaxy. Present observational estimates of cosmic-ray life, magnetic-field strength, etc., indicate an outward inflation rate of the order of $10^2$ km/sec, although this number may be revised with improved observations. This cosmic-ray halo extends far out from the disk and nucleus of the galaxy, presumably limited by instabilities which eventually free the cosmic rays and fields at a great distance. The field inflation acts as a pressure regulator on the cosmic rays generated in the galactic disk and nucleus, so that the life of a cosmic-ray particle in the disk of the galaxy is determined mainly by the rate of generation of cosmic rays. Present estimates of the cosmic-ray life are based on the rather uncertain value of the density of interstellar gas. The gas is intimately associated both with the dynamics of the galactic fields and the calculated rate of cosmic-ray production. (auth)

**2663** SPACE EXPLORATIONS AND THE RADIATION BELTS. Delahaye, R. P.; Allain, Y.; Tabusse, E. (Centre d'Etude et de Recherches de Medecine Aeronautiques, Paris). Concours Med., 86: 1665-76(Mar. 14, 1964). (In French).

Data recorded during recent space flights have confirmed the existence of two radiation belts. The internal (Van Allen) belt is annular and is situated between 600 and 700 km above the earth between latitudes 40°N and 40°S. The area is habitable for man, although at the center of the belt at an altitude of 4000 km the intensity reaches 20 R/hr. A Pb

shield of 4 g/cm² can reduce this intensity appreciably. The second, external radiation belt has the shape of a torus, and extends between latitudes 50°N and 50°S, its average thickness is 10000 km and its altitude is from 15000 to 70000 km. This belt is composed of electrons with spectral energies similar to those emitted by an aurora borealis. The dose intensity is probably from 10 to 20 R/hr. For a satellite orbiting the earth at an altitude less than 400 km for several yr it has been calculated that the perigee should be greater than 250 km and its apogee should be less than 400 km. Studies from recently launched satellites indicate that the radiation dose encountered is of the order of 10 R/hr with shielding of 1 g/cm². Although enough information is available to estimate roughly the isointensity curves encountered in the radiation belts, no exact presentation of the reasoning that indicates that this radiation would be safe for human space travel has been presented precisely. (BBB)

**2664** RANGE DISTRIBUTION OF COSMIC RAY MUONS UNDERGROUND. Oda, H.; Murayama, T. (Nagoya Univ., Japan). J. Phys. Soc. Jap., 20: 1549-54(Sept. 1965).

Range distribution of high energy muons are calculated by a numerical method taking into account the fluctuation in energy loss by radiation and direct electron pair production. With the obtained distribution, the effect of the range fluctuation on the depth-intensity relation of cosmic ray muons is studied and compared with similar works. (auth)

**2665** COSMIC RAYS AND THE PHYSICS OF ELEMENTARY PARTICLES. Feinberg, E. L. Usp. Fiz. Nauk, 86: 733-46(Aug. 1965). (In Russian).

The problems of cosmic rays and of the formation of particles composing atmospheric showers are still in a hypothetical state. The generation of new particles having short lifetimes depends upon the energy and the mass of the particles. The use of accelerators made it possible to discover the existence of mesons and positrons by overcoming the threshold energies in laboratory experiments. The mass and the lifetime of the $\mu$-meson were determined, and also its instability. Mesons ($\pi$) were detected in atmospheric showers, and their bulk generation was achieved in particle interactions with energies of $10^{10}$ ev. The symmetry of elementary particles consists of combinations in which new primary particles appear. There are assumed particles with fractional charges of $+\frac{2}{3}e$, $+\frac{1}{3}e$, and $-\frac{1}{3}e$, where e is the elementary charge. However, these particles are not found in accelerator experiments. The interactions of elementary particles may be divided into three types: (1) strong or meson interactions which are characteristic of nucleons, $\pi$-mesons, hyperons, etc.; (2) electromagnetic interactions, which play an important role in the behavior of electrons, positrons, $\mu$-mesons, and photons; (3) weak interactions characteristic of neutrinos and other particles. The electromagnetic interaction of $\mu$-mesons makes it possible to check quantum electrodynamics by experiments with those particles whose magnetic moments are precisely measured. Weak interactions of the neutrino type studied with low energies of 1 Mev are characterized by conversion of two Fermi particles into two other similar particles. An interaction between a photon and electron yields a Fermi particle. If two colliding particles characterized by strong interaction have high energies, the result is the generation of many new particles as $\pi$-mesons, nucleons, etc. This is the principal peculiarity of strong interactions. In the case of electromagnetic interactions, the probability of emission of two photons due to collision of an electron with a nucleus is one-half that of emission of one photon. The emission of soft photons is called the "infrared catastrophe" because the law of probability is wrong in this case. An infrared catastrophe takes place in any case of strong interactions. The process of elastic scattering during interactions does not have simple properties even at energies of 30 Bev, and asymptotic development is not attained by energies greater than the rest energy. This indicates that another threshold exists in addition to the $Mc^2$ energy threshold. Studies of cosmic rays showed that collisions of two nucleons in which mesons ($\pi$) are created are not the source of meson emission, but meson fluxes originate in accumulations of mesonic matter surrounding the collision. Mesonic matter is generated by superhigh energies. Mesons composed of this matter have masses greater than the mass of a nucleon. (ATD)

**2666** DETECTABILITY OF LUNAR X-RAYS. Haymes, R. C.; Juday, R. D. (Rice Univ., Houston, Tex.). 15p. (CONF-650422-16). Gmelin, AED-CONF-65-118-36.

From American Geophysical Union, Program for Section of Seismology Annual Meeting, Washington, D. C.

Several theories that imply the generation of x rays by the moon were examined. The x-ray fluxes to be expected at the top of the earth's atmosphere are estimated and compared. For example, it is found that an x-ray flux is to be expected when the moon is full and Kp high, as a consequence of the configuration of the auroral electrons in space deduced from the long tail model of the magnetosphere. The x-ray photons are caused by energetic electrons in the tail that bombard the lunar surface. Alternatively, Gold has suggested that lunar x rays are produced by the bombardment by solar-wind electrons; this results in a lunar phase dependence that is different from the long tail model. The background is discussed and it is concluded that the lunar x-ray flux may be detectable. Experiments of this kind may provide useful tools for investigating the models. (auth)

## Direct Energy Conversion

**2667** (AD-614907) A CONTINUATION OF THE BASIC STUDY OF SLENDER CHANNEL ELECTROGASDYNAMICS. Final Report, February 1963-August 1964. Kahn, Bernard (Wright Aeronautical Div., Curtiss-Wright Corp., Wood-Ridge, N. J.). Jan. 1965. Contract AF33(657)-10892. 97p. (ARL-65-4). CFSTI $3.00 cy, $0.75 mn.

Power generation studies involving electrogasdynamic energy conversion are reported. A detailed experimental and analytical program was made on the phenomenon of generating electric power by causing a supply of unipolar ions to be forced to flow against an opposing induced electric field in an energy conversion channel. The analytical program includes studies on the mobility of charged aerosol particles, the performance of electrogasdynamic generators, and optical methods to determine particle size and number density in a steady flow. Experimental investigations include the measurement of mobility, the examination of the EGD interaction using colloidal ions, attempts to measure pressure drops due to friction and electrical body forces and electrical field distribution. The advantage of designing converters in which the length is considerably greater than the diameter was explored further, with the conclusion that electrical forces must act on the charged particles over a distance that remains compatible with limitations due to electrical breakdown and particle deposition. (auth)

**2668** (AD-615124) KINETIC STUDY OF ROCKET EXHAUST GASES. Final Report for Period Ending April 30, 1965. Report No. 103-12. (Malaker Labs., Inc., High Bridge, N. J.). Contract DA30 069ORD2918. 49p.

The feasibility of devices for extraction of electrical energy from rocket engine exhaust streams was investigated. An extensive literature search was conducted, a comprehensive bibliography prepared (published in PB-153 966) and an analytic study performed based on a physical model deduced from the most accurate experimental evidence available. Subsequently, a study of the subtle changes induced in the solid propellant combustion process by introduction of additives was undertaken. These additives, in general, modify the burning rates of propellant material. Various optical diagnostic techniques were employed to identify species concentration by flame zones and to obtain localized temperatures and total visible radiation values with good time resolution. (auth)

**2669** (AED-C-15-07) DIRECT CONVERSION OF NUCLEAR ENERGY INTO ELECTRIC ENERGY. Series C. Bibliographies. (Battelle Institut e.V., Frankfurt am Main (West Germany)). Mar. 1965. 80p. Dep. mn.

A bibliography, consisting of both published literature and progress reports for the period 1963–1964, is presented on the direct conversion of nuclear into electrical energy. Report number, author, and subject indexes are included. (M.O.W.)

**2670** (LA-DC-7330) THE PROSPECTS FOR NUCLEAR REACTOR-MHD COMMERCIAL POWER PRODUCTION. Booth, Lawrence A. (Los Alamos Scientific Lab., Univ. of California, N. Mex.). [1965]. Contract W-7405-eng-36. 48p. (CONF-650328-1). Dep. mn; CFSTI $2.00 cy, $0.50 mn.

From 11th Annual Gas Turbine Conference and Products Show, Zurich.

Cycle analysis and preliminary plant component designs are made for prospective nuclear reactor–MHD commercial power plants, and the problems of development of the plant components are discussed. The concept of commercial MHD power production is compared with other nuclear reactor power plants, and recommendations as to the feasibility of the MHD concept are made. The results of the study, conducted by an ad hoc committee of staff members at the Los Alamos Scientific Laboratory, indicate that nuclear reactor–MHD power production is infeasible for the foreseeable future. The development of the major components for prospective plants is too extensive with the present undefined criteria, and, more importantly, at this time the apparent failure to gain a reduction in total power costs will not allow the nuclear MHD plant to compete with more conventional nuclear powered plants. (auth)

**2671** EXPERIMENTAL STUDIES OF STRONG HALL EFFECTS AND U x B INDUCED IONIZATION. Klepeis, James; Rosa, Richard J. (Avco Corp., Everett, Mass.). AIAA (Am. Inst. Aeron. Astronaut.) J., 3: 1659-66(Sept. 1965).

Using a graphite inert gas heater, many different MHD-generator channel and electrode configurations were tested. Typical flow conditions were 100 gm/sec argon at 1 atm pressure seeded with 0.1 to 1.0 mole % cesium vapor at 1800 to 2000°K. The aim of the work was to study MHD channel and electrode performance at high values of the Hall parameter (5 to 15) and to look for the occurrence of extra-thermal ionization. Straight segmented-electrode channels did not perform well, apparently due to a nonuniformity created by extrathermal ionization over the electrode walls. A disk geometry in which the current in the U × B direction closes upon itself performed much better. Enhancement of the power output due to U × B induced ionization was observed. The results correlate well with those obtained in applied electric field experiments and with theory when energy loss due to radiation is included. However, an instability was also observed when large increases in ionization were sought. (auth)

**2672** EXPERIMENTAL INVESTIGATIONS ON THE BOUNDARY BETWEEN FLOWING PLASMA AND COOLED METAL ELECTRODES. Grycz, B. (Institut fuer Starkstromtechnik, Bechovice, Czechoslovakia). Beitr. Plasmaphysik, 5: 229-53(1965). (In German).

A plasma burner, which is briefly described, was constructed in order to investigate the behavior of flowing plasmas with respect to cooled metal electrodes. The flow behavior and the estimated plasma properties are discussed. The difference method for the measurement of the electrical conductivity of the plasma and the measured conductivity obtained are described. The results of the measurement of the contact potential between the plasma and the cooled metal are reported. Measurements of the current-voltage characteristics for the metal–plasma boundary are described. The values obtained had significant deviations, whose origins are in the oscillations of the fuel chamber regime. The results obtained are contradictory and unexplainable. (J.S.R.)

**2673** SPECTROSCOPIC MEASUREMENT OF FLAME TEMPERATURE IN MAGNETOHYDRODYNAMIC GENERATOR. Kimura, Masaomi; Yamanaka, Nobuji. Denki Shikensho Iho, 29: 313-24(Apr. 1965). (In Japanese).

Values of flame temperature in a magnetohydrodynamic generator measured with a spectroscope were compared with those measured by the modified sodium-resonance line reversal method with an interference filter. The difference between the two kinds of values is about −20°K, and is considered to have resulted from the too wide half width of the interference filter which allows some light leakage of the continuous background. The spectral distributions of the flame (propane + $O_2$) are also investigated. Because of the strong self reverse, potassium (K-lines 7665 and 7699 Å) does not seem suitable to the line reversal method when the temperature distribution in the flame is not uniform. The line reversal temperatures Na-, K-, and Cs-lines do not agree with each other though they are measured simultaneously in the same flame. The difference is supposed to be caused from the fact that each of the lines has an individual temperature corresponding to its individual pseudo-Boltzmann distribution which is not a true Maxwell-Boltzmann distribution. (auth)

**2674** OPTIMAL MAGNETOHYDRODYNAMIC GENERATOR. Pleshanov, A. S. Dokl. Akad. Nauk SSR, 162: 302-5(May 11, 1965). (In Russian).

A general solution is presented for the problem of optimization of the operating conditions of a magnetohydrodynamic generator (MHDG) in a simplified one-dimensional approximation, neglecting the induced magnetic field, viscosity, and thermal conductivity. The problem reduces to the integration of one equation with four functions, which must be determined by variational calculus. The optimization of the MHDG is based on the principle of minimum of integral rate of entropy production. The generalized function chosen for optimization is a linear combination of the final value of the entropy and the volume of the MHDG. From the point of view of the reciprocity principle, this is equivalent to minimization of the volume of the MHDG at a specified power. It is then shown that in an optimal MHDG, the conversion into electric energy is carried out uniformly over the channel, while the conversion itself occurs uniformly both in the thermal and in the mechanical forms of the energy. A relation is derived which ensures a minimum of the final value of the entropy for a known volume of the MHDG, or, in accordance with the reciprocity principle, a minimum volume of the MHDG for a known final value of the entropy. The possible concrete realization of the optimal MHDG is briefly discussed. (auth)

**2675** A CESIUM PLASMA DIODE. Pariser, Bert (Columbia Univ., New York, N. Y.). J. Eng. Educ. 54: 196-200(Jan. 1964).

A small experimental cesium plasma diode is described. Its construction and performance, and an explanation of conventional vacuum diodes are considered. A diagram of the experimental apparatus is shown. An ionization gauge RCA 1949 was modified and used as the diode. The gauge consists of two center tapped tungsten filaments, one of which was used, a grid of molybdenum, and a cylindrical molybdenum plate. After the system had been operated as a vacuum diode, the top part of the cross was opened and a cesium capsule was inserted. The system was then sealed off again, ready to be run as a cesium plasma diode. When the plasma diode was run as an active element (no external voltage from plate to filament) a volt-ampere curve was obtained. The open circuit voltage (filament-plate) was 0.2 v. The maximum output power at 1800°K was 24 μw. Experiments with this plasma diode yielded number densities of electrons from $3.87 \times 10^9/cm^3$ and the electron temperature ranged from 12,600°K to 16,300°K. (BBB)

**2676** A METHOD OF AND AN ARRANGEMENT FOR THE CONVERSION OF HEAT FROM A NUCLEAR FISSION REACTION INTO ELECTRIC ENERGY. (to Licentia Patent-Verwaltungs-G.m.b.H.). British Patent 1,006,613. Oct. 6, 1965. Priority date July 5, 1961, Germany.

In a method for direct conversion of heat from nuclear fission into electric energy, a liquid electric conductor is used as a working medium. Evaporation of part of the

working medium by heat from the fission reaction imparts to the nonevaporated part of the medium a movement through a magnetic field extending perpendicular to the direction of movement. The electromotive force produced perpendicular to the direction of movement and to the magnetic field causes a current to flow through an outer load circuit. Suitable conductors include liquid metals, electrolytes, or fused salt baths. Two proposed conversion units are analogous to a reciprocating engine and to a continuous flow machine. (A.G.W.)

**2677** IMPROVEMENTS IN MAGNETOHYDRODYNAMIC GENERATORS. Croitoru, Zicu (to Electricite de France). British Patent 1,006,799. Oct. 6, 1965. Priority date Mar. 13, 1962, France.

Electrodes for a magnetohydrodynamic generator are designed to provide increased area of contact with the plasma and increased electron injection into the plasma. The electrodes have grooved surfaces and are so mounted that the grooves have some exposed surfaces substantially transverse to the magnetic field. (A.G.W.)

# Elementary Particles and Radiations

## *See also* Field Theory, Scattering Theory, and Symmetries

*Refer also to abstracts 2560, 2665, and 2865.*

**2678** (AD–614843) APPROACH TO ELECTRON-PION SCATTERING. Doebner, H. D.; Simon, D. (Marburg Univ. (West Germany). Institut fuer Theoretische Physik). 1964. Contract AF61(052)-658. 25p. (AFOSR–65–0649).

It is shown that a usual Mandelstam representation completed with a suitable choice for pole terms and single dispersion integrals, obtained straightforwardly from unitarity using quantum electrodynamics and the resonance structure of the pion, provides a method to discuss electron-pion scattering on the same lines as strong interaction theory. The double spectral functions are constructed from a system of integral equations in a strip approximation, and corrections to the one-photon exchange amplitude are expressed by integrals over the imaginary part of the form factor in the annihilation channel. (TAB)

**2679** (AD–618664) POLARIZATION MEASUREMENTS ON THE RECOIL PROTON FROM PION (O) PHOTOPRODUCTION. Lundquist, D.; Allaby, J. V.; Ritson, D. M. (Stanford Univ., Calif. High-Energy Physics Lab.). June 1965. Contract Nonr22567. 12p. (HEPL–388). CFSTI $1.00 cy, $0.50 mn.

Polarization of the recoil proton in $\pi^0$ photoproduction off hydrogen was measured for photons in the range 500–1000 Mev, using the Stanford Mark III linear accelerator. Protons were detected at an angle b and momentum analyzed using a 90 degree magnetic spectrometer. The scattered protons were detected by two counter telescopes placed symmetrically to left and right of the carbon target and making angles ±C with respect to the direction of a proton emerging from the spectrometer. The measured asymmetry was obtained from the usual formula: e = L – R/L + R and the proton polarization P(b) was then obtained by substituting the known carbon analyzing power A(c) in the equation e(b,c) = P(b) A(c). Using parity conservation it can be shown that P(b) = –P(b). Thus the running time was equally divided between measurements with the spectrometer at +b and –b. This technique enabled residual artificial asymmetries to be removed, since these do not change sign when b becomes –b. Preliminary results are presented and compared to existing data from various laboratories. (auth)

**2680** (COO–818–58) POSITRON SPECTRUM FROM FISSION ANTINEUTRINOS ON PROTONS. [Thesis]. Nezrick, Frank A. (Case Inst. of Tech., Cleveland, Ohio). 1965. Contract AT(11-1)-818. 135p. Dep. mn; CFSTI $4.00 cy, $1.00 mn.

The $P(\bar{\nu}_e, \beta^+)n$ reaction was observed in a 3.2 liter gadolinium loaded decalin based liquid scintillator target placed between two cylindrical NaI crystals 29 cm in diameter and 7.6 cm deep. The crystals were set to see 0.511 Mev $\beta^+$ annihilation radiation. A prompt triple coincidence of all three detectors followed by the delayed capture of the neutron is the signature for the reaction. This detector was operated within a 27 ton lead shield at one of the Savannah River Reactors. The data were obtained during 2500 hours of operation at the rate of 0.20 events per hour, with a signal to background ratio of approximately 3/1. The observed signal was demonstrated to be due to reactor antineutrinos. The positron spectrum obtained and hence the $\bar{\nu}_e$ spectrum from fission is consistent with prediction except for a larger observed component above 4.0 Mev. (auth)

**2681** (IFA-CR–55) TRANSVERSE MOMENTUM DISTRIBUTION IN HIGH-ENERGY MESON PRODUCTION. Friedlaender, E. (Institutul de Fizica Atomica, Academia R. P. R., Bucharest (Romania)). July 1965. 37p. Dep. mn.

A survey of experimental data on the transverse momentum distributions of 5738 secondaries from high-energy inelastic interactions is analyzed. It is shown that the data cannot be fitted satisfactorily by the linear exponential distribution. The baryon data are well described by a Boltzmann distribution while the pion data are a superposition of two Boltzmann distributions with widely differing parameters. (auth)

**2682** (JINR-P-2320) ANALIZ REAKTSII $\pi^- + p \rightarrow \pi^- + \pi^+ + n$ I $\pi^- + p \rightarrow \pi^- + \pi^0 + p$ PRI KINETICHESKOI ENERGII $\pi^-$-MEZONOV 338 Mev. (Analysis of $\pi^- + p \rightarrow \pi^- + \pi^+ + n$ AND $\pi^- + p \rightarrow \pi + \pi^0 + p$ REACTIONS AT THE $\pi^-$ Kinetic Energy of 338 Mev). Blokhintseva, T. D.; Grebinnik, V. G.; Zhukov, V. A.; Libman, G.; Nemenov, L. L.; Selivanov, G. I.; Yuang Rung-fang (Joint Inst. for Nuclear Research, Dubna (USSR), Lab. of Nuclear Problems). 1965. 12p. Dep. mn.

The differences in the cross sections of the isobar channels for the $\pi^- + p \rightarrow \pi^-\pi^+ + n$(I) and $\pi^- + p \rightarrow \pi^-\pi^0 + p$(II) reactions are determined at the $\pi^-$ meson kinetic energy of 338 Mev. If the isobar transitions occur in $T = \frac{1}{2}$ state the total cross section for (II) within the experimental error is equal to the sum of the cross sections of the isobar channels. Under this assumption the total cross section for (I) is not described by the sum of the cross sections of the corresponding isobaric channels. The effect of $\pi\pi$ interaction manifests itself in the $\pi^+\pi^-$ effective mass spectrum but not in the $\pi^-\pi^0$ mass spectrum. The presence of the $(\frac{3}{2},\frac{3}{2})$ isobar affects the angular distributions of secondary particles from (I). (auth)

**2683** (JINR-P-2327) UPRUGOE RASSEYANIE $\pi^+$-MEZONOV NA PROTONAKH NA UGOL 180° PRI VYSOKIKH ENERGIYAKH. (Elastic $\pi^+$-p Scattering at 180° at High Energies). Vovenko, A. S.; Gus'kov, B. N.; Likhachev, M. F.; Lyubimov, A. L.; Matulenko, Yu. A.; Savin, I. A.; Stavinskii, V. S. (Joint Inst. for Nuclear Research, Dubna (USSR). Lab. of High Energy). 1965 9p. Dep. mn.

The differential elastic, $\pi^+$-p scattering cross section at a solid angle of 180° and at momenta of 4.10 and 4.85 Bev/c in the laboratory system was measured. The results were compared with those obtained previously (Phys. Lett. 17: 68 (1965)) using the same experimental method. In the calculation of the effective cross section values, corrections were made for the nuclear interaction of the primary and backscattered $\pi^+$ mesons and recoil protons in the H-containing target and the counter, the $\mu$ mesons in the beam, the decay of the scattered $\pi$ mesons, and the efficiency of the scintillation counter, the electronic system and the spark chamber used. The results indicated a narrow peak close to 180° at 4.0 Bev and a $\pi^+$-p back scattering peak at 4.85 Bev/c. The existence of a peak in the elastic $\pi^+$ back scattering in the high-energy range beyond 3 Bev is not due to resonance but is a characteristic of high-energy elastic scattering. (TTT)

**2684** (JINR-P–2374) NEKOTORYE ZAMECHANIYA O RADIATSIONNYKH RASPADAKH K-MEZONOV. (Some

Remarks on Radiative Kaon Decays). Mal'tsev, E. I.; Chuvilo, I. V. (Joint Inst. for Nuclear Research, Dubna (USSR). Lab. of High Energy). 1965. 14p. Dep. mn.

Experimental data on radiative kaon decays are treated. A model with an intermediate boson pole involving a $S^0$ meson is discussed. (auth)

**2685** (LA-DC-7250) A MEASUREMENT OF $C_{NN}$ IN NEUTRON-PROTON SCATTERING AT 23 Mev. Bendt, P. J.; Malanify, J. J.; Roberts, T. R.; Simmons, J. E. (Los Alamos Scientific Lab., Univ. of California, N. Mex.). [1964]. Contract W-7405-eng-36. 5p. (CONF-650928-10). Dep. mn; CFSTI $1.00 cy, $0.50 mn.

From International Conference on Polarization Phenomena of Nucleons, Karlsruhe.

Results of an experiment to measure the neutron-proton correlation function, $C_{NN}$, at 180° c.m. and $E_n$ = 23 Mev are described. The experiment consists in measuring differences in the intensity of scattered particles when a polarized beam of neutrons is incident on a polarized proton target. (M.O.W.)

**2686** (LNF-65/22) A POSSIBLE EXPERIMENT WITH A PROTON POLARIZED TARGET. Note No. 283. Bounin, P. (Laboratori Nazionali di Frascati, Comitato Nazionale per l'Energia Nucleare (Italy)). July 19, 1965. 28p. Dep. mn.

The principles of construction of a polarized proton target and a possible experiment in which a deviation of the Born approximation formula in elastic e-p scattering might be detected are described. A particular experiment which fits very well with the possibilities of the Frascati Laboratory and which is suggested by recently published results is proposed. (M.O.W.)

**2687** (LNF-65/25) THEORETICAL ASPECTS OF COLLIDING BEAM EXPERIMENTS. Note No. 284. Gatto, R. (Laboratori Nazionali di Frascati, Comitato Nazionale per l'Energia Nucleare (Italy)). Aug. 5, 1965. 41p. (CONF-650908-10). Dep. mn.

From International Conference on Thermionic Electrical Power Generation, London.

The theoretical aspects of colliding beam experiments are summarized. The topics discussed are; electromagnetic reactions: $e^+ + e^- \rightarrow 2\gamma$, $e^+ + e^- \rightarrow e^+ + e^-$, $e^+ + e^- \rightarrow e^+ + e^- + \gamma$, $e^+ + e^- \rightarrow \mu^+ + \mu^-$, $e^- + e^- \rightarrow e^- + e^-$, $e^- + e^- \rightarrow e^- + e^- + \gamma$, etc.; vacuum polarization effects, $e^+ - e^-$ annihilation into strong interacting particles, the one-photon channel, resonant contributions, annihilation into pions, intermediate $\rho^0$, $\omega^0$, and $\varphi^0$, two-photon channel, annihilation into fermion-pairs, weak-vector-meson production, and weak interactions. (M.O.W.)

**2688** (UCRL-14335) INELASTIC PROTON-PROTON SCATTERING AT 5.10 Bev. Parks, J. G. (Lawrence Radiation Lab., Univ. of California, Livermore). Sept. 20, 1965. Contract W-7405-eng-48. 33p. Dep. mn; CFSTI $2.00 cy, $0.50 mn.

Inelastic proton-proton collisions were examined at a bombarding energy of 5.10 Bev using nuclear emulsions. Cross sections and reaction parameters were obtained and compared with the results of experiments at other energies. The scattering data were analyzed in terms of the invariant mass and the effective target mass approach. Phase space predictions, based upon approximate solutions of the phase space integrals and a computer method for obtaining estimates of background, were employed to study the invariant mass distributions. The adequacy of the effective target mass approach was examined. (auth)

**2689** (UCRL-16140) TOTAL AND DIFFERENTIAL CROSS SECTIONS FOR THE REACTION $\pi^- p \rightarrow \eta n$. Richards, W. Bruce; Chiu, Charles B. (Lawrence Radiation Lab., Univ. of California, Berkeley). Sept. 29, 1965. Contract W-7405-eng-48. 14p. (CONF-650927-3). Dep. mn; CFSTI $1.00 cy, $0.50 mn.

From American Physical Society, Honolulu, Hawaii.

Data on $\pi^- p \rightarrow \eta n$ are recorded using a $4\pi$ steel spark chamber. The angular distributions, cross sections, and differential cross sections are measured for $\pi^-$ initial energies of 592 to 1319 Mev. (T.F.H.)

**2690** (AEC-tr-6591) DETERMINATION OF THE KINEMATICS OF THE REACTION $\pi^- + p \rightarrow \pi^- + \rho + \pi^+ + \pi^-$ Grigor'ev, V. K.; Grishin, A. P. THE STUDY OF THE $\pi^- + p \rightarrow \pi^- + \rho + \pi^0$ REACTION AT AN ENERGY OF 2.8 Bev. Grigor'ev, V. K.; Grishin, A. P.; Trostina, K. A. (Gosudarstvennyi Komitet po Ispol'zovaniyu Atomnoi Energii SSSR, Moscow. Institut Teoreticheskoi i Eksperimental'noi Fiziki). Translated from Report-224. 1964. 15p. Dep. mn; CFSTI $1.00 cy, $0.50 mn; JCL $1.60 fs, $0.80 mf.

The reaction $\pi^- + p \rightarrow \pi^- + p + \pi^0$ in a 17 liter propane-xenon bubble chamber is studied. The dominant mode of the reaction is $\rho$-meson formation. The feasibility of kinematic analysis of four-prong stars in bubble chambers without magnetic fields is shown. Errors appearing during such an analysis are studied. (auth)

**2691** THE LANDAU THEORY OF FERMI SYSTEMS. II. APPLICATIONS. Kisdi, David. At. Kozlemen., 7: 129-54(June 1965). (In Hungarian).

The phenomenological theory of Landau concerning the excited states close to the ground state of normal Fermi systems is based on the variation of the distribution function, $\delta n(k)$, which makes it possible to calculate the energy of the excited state from the energy of a quasiparticle and the interaction of two quasiparticles. The theory should be applied only to low-excitation states of normal systems. Keeping that limitation in mind, it was concluded that the Landau theory represents a simple and effective tool that may be used for analyzing a whole series of properties of Fermi systems. The specific heat of such systems at low temperatures is proportional to T, regardless of the material in question; on this basis the theory may be used for the qualitative description of the properties and for the interpretation of the physical behavior of Fermi systems. The experimentally determined physical parameters allow the identification of the interaction of quasiparticles; data derived from the specific heat, sound velocity and susceptibility may be used to calculate various collective oscillation modes. On the basis of the Schrödinger equation of Fermi systems, the energy and the interaction of the quasiparticles may be derived using the multibody method and the data obtained may be used together with the Landau theory to derive quantitative values concerning the physical parameters of the system. (TTT)

**2692** ELECTROMAGNETIC 2 $\pi$ DECAY OF $K_2^0$. Kundu, S. K. (Australian National Univ., Canberra). Australian J. Phys., 18: 395-400(Oct. 1965).

As alternatives to the observed $K_2^0 \rightarrow 2\pi$ decay the processes $K_2^0 \rightarrow 2\pi + \gamma$ and $K_2^0 \rightarrow K_1^0$ magnetic conversion are considered. It is shown that the former process is quite unlikely with the photon energy as suggested from experiment, while the second one is not so unlikely. Also suitable experiments are suggested to observe the processes considered here. (auth)

**2693** RECENT ADVANCES IN ELEMENTARY PARTICLE PHYSICS. Stafford, G. H. (Rutherford High Energy Lab., Chilton, Eng.). Brit. J. Appl. Phys., 16: 1429-33(Oct. 1965).

A brief review is given of some recent advances in elementary particle physics research. Reference is made to the way in which the relatively new 7 Bev proton synchrotron (NIMROD) at the Rutherford High Energy Laboratory in Berkshire has already begun to contribute to this international field. (auth)

**2694** ON THE RESONANCES IN Y-$\pi$ SCATTERING. Lukaszuk, L. (Inst. for Nuclear Research, Warsaw). Bull. Acad. Polon. Sci., Ser. Sci. Math. Astron. Phys., 13: 235-8(1965).

The problem of the two-channel p-wave Y-$\pi$ scattering is discussed in the Chew-Low static theory with crossed cuts and $\Sigma$-$\Lambda$ mass difference treated exactly. Two coupling constants $f^2_{\Lambda\Sigma\pi}$, $f^2_{\Sigma\Sigma\pi}$, and a cut-off K (which is taken common for $\Lambda\pi$ and $\Sigma\pi$ channels) are the parameters which are determined from the experimental data concerning Y*. (J.F.P.)

**2695** POSSIBLE INFLUENCE OF THE CHANNEL $\gamma + N \rightarrow \pi + \bar{N}$ ON THE PHOTOPRODUCTION AMPLITUDE.

Pokorski, S. (Univ. of Warsaw). Bull. Acad. Polon. Sci., Ser. Sci. Math. Astron. Phys., 13: 243-8(1965).

In the dispersion approach to the photoproduction of mesons ($\pi$) on nucleons a discussion of cuts is given. The regions of convergence of Legendre expansion is found for amplitudes in variables describing second and third channel, respectively. (J.F.P.)

**2696** LEPTON ANNIHILATION OF PROTON-ANTIPROTON PAIRS WITH ALLOWANCE FOR FORM FACTORS AND POLARIZATION CORRELATIONS. Sokolov, A. A.; Kerimov, B. K.; Sadykhov, F. S.; Yakhyaev, R. Sh. (Moscow State Univ.; Inst. of Physics, Academy of Sciences, USSR). Dokl. Akad. Nauk SSSR, 161: 1317-19(Apr. 21, 1965). (In Russian).

Recent experiments at CERN on the electromagnetic structure of the proton indicated that the upper limit of the cross section of the $\tilde{p} + p \rightarrow \mu^+ + \mu^-$ process is $\sigma \leq 10 \times 10^{-33}$ cm$^2$ while the theoretically derived value is $\sigma = 247 \times 10^{-33}$ cm$^2$. The experiments pointed to the influence of form factors in the pulse transmission process. These form factors were more closely investigated in the annihilation process $\tilde{p} + p \rightarrow \tilde{l} + l$ (where $l = e^-$ or $\mu^-$; $\tilde{l} = e^+$ or $\mu^+$), attempting to take into account also the polarization effects of the particles participating in the process. Formulas were derived for the differential cross section under consideration of these form factors and of the polarization states of all the initial and final particles in the center of inertia system. Integration of the expression yielded an equation for the total cross section of the lepton annihilation of polarized protons and polarized antiprotons. In contrast to the differential cross section, the total $\sigma$ does not contain proton–lepton polarization correlations. The expressions obtained determine the effect of form factors and of the spin states of proton, antiproton and the formed lepton and antilepton. It was found that the energy dependence of the cross section of the annihilation process is strongly affected by the form factors and by the correlation of the formed lepton–antilepton pair. Consideration of these effects leads to a reduction of the total cross section. (TTT)

**2697** PARITY CONSERVING AMPLITUDES OF HADRON DECAYS OF BARYONS IN THE $\tilde{U}(12)$ SYMMETRY SCHEME. Gedalin, E. V.; Kancheli, O. V.; Matinyan, S. G. (Inst. of Physics, Academy of Sciences, Georgian SSR). JETP Lett. (USSR) (Engl. Transl.), 2: 5-7(July 1, 1965).

Another possibility is considered for the results of the application of the $\tilde{U}(12)$ symmetry to hadron decays of hyperons: the spurion enters on an equal basis with real particles with respect to the transformation properties of $\tilde{U}(12)$ symmetry. The lowest representations of $\tilde{U}(12)$ symmetry, containing a CP even scalar, are 4212 and 5940. These are used to describe the weak spurion, H. With respect to SU(3) this spurion should be a sixth member of a vector. (J.F.P.)

**2698** VIOLATION OF CP INVARIANCE IN $K^0$-MESON DECAYS AND THE NON-INVARIANT VACUUM. Grib, A. A. (Leningrad State Univ.). JETP Lett. (USSR) (Engl. Transl.), 2: 8-10(July 1, 1965).

It is shown that CP invariance can be violated, but only in processes with mesons ($K_1^0$) and mesons ($K_2^0$). The reason for the violation is the method of construction of these mesons from the mesons ($K^0$) and ($\overline{K^0}$). In this method there is a transition to a different nonequivalent representation of the von Neumann ring creation and annihilation operators, that is, a transition to a different vacuum. The mesons ($K_1^0$) and mesons ($K_2^0$) do not have any definite CP. The appearance of a different vacuum and the definition of the mesons ($K_1^0$) and mesons ($K_2^0$) are the consequences of strong interactions between the mesons ($K^0$) and ($\overline{K^0}$). A system of mesons ($K^0$) and mesons ($\overline{K^0}$) which interact strongly with one another is assumed. (J.F.P.)

**2699** POSSIBLE CONNECTION BETWEEN $K_2^0$ DECAY AND STATISTICAL IRREVERSIBILITY. Chernavskii, D. S. (Lebedev Inst. of Physics, Moscow). JETP Lett. (USSR) (Engl. Transl.), 2: 14-16(July 1, 1965).

Another approach is given to the problem of the lack of CP invariance in the meson ($K_2^0$) decay into two mesons ($\pi$). The Fermi-Landau theory is used since statistical theory is generally applicable to a system of interacting particles with a large number of degrees of freedom. This is the system assumed in the case of meson ($K_2^0$) decays. (J.F.P.)

**2700** ELASTIC BACKWARD SCATTERING OF NEGATIVE PIONS BY NEUTRONS IN THE 1.4-4.0 Bev/c MOMENTUM INTERVAL. Alikhanov, A. I.; Bayatyan, G. L.; Brakhman, E. V.; Galaktionov, Yu. V.; Eliseev, G. P.; Ech, F. A.; Zel'dovich, O. Ya.; Landsberg, L. G.; Lyubimov, V. A.; Sidorov, I. V. JETP Lett. (USSR) (Engl. Transl.), 2: 57-9(July 15, 1965).

The elastic backward scattering reaction $\pi^- + n \rightarrow \pi^- + n$ was investigated in the 1.38 – 4.05 Bev/c momentum range. This reaction was investigated with an installation capable of registering with high efficiency inelastic events of the type $\pi^- + n \rightarrow \pi^- + n + k\pi^{\pm 0}$. A diagram is shown of this installation. The event was registered in a cylindrical spark chamber, inside of which a target ($D_2O$ or $H_2O$) was placed. The absolute cross sections obtained are listed. The angular distribution of elastic $\pi^-$n backward scattering is also shown at an average meson ($\pi$) momentum of 2.8 Bev/c. A peak is seen in the region of $\cos\theta = -1$. (J.F.P.)

**2701** A MEASUREMENT OF POLARIZATION IN NEUTRON-PROTON SCATTERING IN THE ENERGY RANGE 20-120 Mev. Langsford, A. (Atomic Energy Research Establishment, Harwell, Eng.); Bowen, P. H.; Cox, G. C.; Huxtable, G. B.; Riddle, R. A. J. Nucl. Phys., 74: 241-60(1965). (AERE-R-4973).

The values of the polarization in neutron-proton scattering were measured in eleven energy bands between 20 and 120 Mev in the angular range 20 to 160° cm, using time-of-flight techniques. The accuracy of the measurement is greatest, typically 2 to 3%, in the middle of the energy range where little other data are available. There is fairly good agreement between experiment and the YLAN4M phase-shift analysis predictions in the general angle and energy dependence of the polarization values. Attention is drawn to the fact that some discrepancies exist which exceed the combined experimental and phase-shift prediction errors. (auth)

**2702** THE POSITIVE EXCESS OF $\mu$ MESONS AT HIGH ENERGIES. Cohen, L. (Univ. of Southampton, Eng.); Fowler, G. N.; Poulopoulos, P. Nucl. Phys., 74: 619-24 (1965).

Experimental data on the positive excess of $\mu$ mesons at high energy are compared with theoretical predictions based on a Monte Carlo calculation of the parent $\pi$ meson production process supplemented by a contribution from isobars. It is found that some isobar contribution is essential to fit the experimental data. (auth)

**2703** $\tilde{U}(12)$ IRREGULAR COUPLING RELATIONS FOR STOPPED PROTON PAIR ANNIHILATION INTO MESONS. Hussain, F.; Rotelli, P. (Imperial Coll., London). Nucl. Phys., 74: 669-72(1965).

Analysis is made of the decay of stopped proton-antiproton pairs into a vector and a pseudoscalar meson according to $\tilde{U}(12)$ symmetry with arbitrary irregular (derivative) couplings. (auth)

**2704** THE SELF-CONSISTENT CALCULATION OF THE MAGNETIC MOMENTS OF THE NUCLEONS. Petras, M. (Univ. Komenskeho, Brastislava). Nucl. Phys., 74: 689-93(1965).

The isovector part of the magnetic moments of the nucleons is calculated on the basis of the self-consistency condition. The results support the idea of self-consistency in the $\pi$N system and the bound state structure of the nucleons. (auth)

**2705** THE MULTIPLE COMPTON SCATTERING OF LOW ENERGY GAMMA RADIATION. Brockwell, P. J. (Australian National Univ., Canberra). Phil. Mag. (8), 12: 515-28(Sept. 1965).

The emergent angular and spectra distributions of low

energy gamma radiation after multiple Compton scattering by a homogeneous plane slab are determined by a method which is based on the theory of Markov processes and the replacement of the set of all possible directions of motion in space by a finite set of directions corresponding to thirty points uniformly spaced on the unit sphere. (auth)

**2706** POLARIZATION IN THE ELASTIC SCATTERING AT BACKWARD ANGLES OF 30 Mev PROTONS FROM DEUTERONS. Johnston, A. R. (Queen's Univ., Belfast); Gibson, W. R.; Megaw, J. H. P. C.; Griffiths, R. J.; Eisberg, R. M. Phys. Lett., 19: 289-91(Nov. 1, 1965).

The results of measurements of the polarization in elastic scattering using a 30-Mev polarized proton beam of a linear accelerator are reported. The protons were scattered from a 0.51 mm thick deuterated polyethylene target. Elastic scattering events in the horizontal plane from deuterium were identified by detecting the recoiling deuterons using a double focusing magnetic spectrometer which easily separated them from elastically scattered protons and charged particles from nuclear reactions in the target over the deuteron recoil angular range. Two experiments were carried out with different arrangements for intensity monitoring. Very good agreement was obtained between the results of the two experiments which are listed. The maximum positive polarization found at 30 Mev is $+0.209 \pm 0.017$ at 140.5°. (J.F.P.)

**2707** LOW ENERGY BARYON–NUCLEON SCATTERING. Dosch, H. G. (Univ., Heidelberg); Mueller, V. F. Phys. Lett., 19: 320-1(Nov. 1, 1965).

An attempt is made to derive the effective range and shape dependent parameters as functions of the corresponding scattering length for the S waves ($^1S_0$ and $^3S_1$) of both $\Sigma^+p$ and $\Lambda p$ scattering. It is assumed in treating low energy baryon-baryon scattering that the mass differences between the baryons can be neglected and the partial wave amplitudes obtained from dispersion relations. In these the scattering lengths are introduced as subtraction constants and the left hand singularities generated by one-boson exchange with physical masses and $SU_3$ coupling constants. The numerical results for the effective range and for the shape dependent parameter are given. (J.F.P.)

**2708** DETERMINATION OF THE $\pi\pi$ SCATTERING PHASE SHIFTS UP TO 1.3 Gev C. M. ENERGY. Wolf, G. (Deutsches Elektronen Synchrotron, Hamburg). Phys. Lett., 19: 328-30(Nov. 1, 1965).

An attempt is made to combine all experimental data on the elastic $\pi\pi$ interaction and to analyze them in terms of the $\pi\pi$ scattering phase shifts. From the main results of the analysis, a set of phase shifts is obtained which in a consistent way fit the existing data on $\pi\pi$ scattering, the width of the meson ($\rho$) is found to be 170 Mev, and the existence of a T = 0, J = 0 $\pi\pi$ resonance is confirmed. A mass of 0.74 Bev and a full width at half maximum of 90 Mev were found for this resonance. The values of the $\pi\pi$ phase shifts from threshold to a cms energy of $\omega$ = 1.3 Bev are summarized graphically. The behavior of the phase shifts and that of the calculated $\pi\pi$ cross sections are shown. Comparisons are made between calculated and measured values. (J.F.P.)

**2709** SUM RULES FOR $\pi^0$-$\pi^0$ SCATTERING RESULTING FROM ANALYTICITY AND CROSSING SYMMETRY. Wanders, G. (Univ., Lausanne, Switzerland). Phys. Lett., 19: 331-3(Nov. 1, 1965).

Some physically meaningful properties of a relativistic scattering amplitude are derived. These properties are rigorous consequences of analyticity and crossing symmetry. The $\pi^0$-$\pi^0$ scattering amplitude is considered. (J.F.P.)

**2710** RESONANCE $Y_1^*$ FROM SELF-CONSISTENCY AND BROKEN UNITARY SYMMETRY. Swiecki, M. (Joint Inst. for Nuclear Research, Dubna). Phys. Lett., 19: 333-4(Nov. 1, 1965).

The bootstrap calculations of the mass and coupling constants (partial widths) of the $Y_1^*$ resonance (mass 1385 Mev, quantum numbers T = 1, S = −1, J = $\frac{3}{2}$, and P($Y_1^*N$) = +1) were performed. The first aim of these calculations was the exploration of the breaking of unitary symmetry with respect to masses and coupling constants of strongly interacting particles. Another aim was the comparison of the results of bootstrap calculations for the $Y_1^*$ resonance with those of Singh and Udgaonkar (Phys. Rev. 130: 1177 (1963)) performed for the $N_{33}^*$ resonance. The $Y_1^*$ resonance was explored as accurately as possible. That is the degeneration of the external masses was not assumed, and that calculations were performed by analogy with those of Singh and Udgaonkar, conserving important characteristic features of the multichannel bootstrap problem. The multichannel Balaźs approximation was used with a universal matching point for all six amplitudes. The agreement with experiment indicates that breaking of the unitary symmetry gives physical masses and almost symmetric coupling constants. It is also concluded that the broken symmetry can be obtained from dynamical considerations. (J.F.P.)

**2711** SPIN, PARITY AND ISOSPIN OF Y*(1760). Armenteros, R. (CERN, Geneva); Ferro-Luzzi, M.; Leith, D. W. G.; (and others). Phys. Lett., 19: 338-41 (Nov. 1, 1965).

Evidence for the reaction sequences $K^- + p \rightarrow Y^*(1760) \rightarrow Y^*(1520) + \pi^0$, $Y^*(1520) \rightarrow \Sigma^\pm\pi^\mp$, and $Y^*(1520) \rightarrow \Lambda\pi^+\pi^-$ is presented. From the first reaction the isospin of Y*(1760) is established to be 1. The production angular distribution of Y*(1520) in the overall center of mass is found to be most consistent with a spin-parity assignment $J^P = \frac{5}{2}^-$ for Y*(1760), while the decay distribution in the second reaction confirms this assignment. Of the 10,000 measured events in which a charged $\Sigma$ was produced, nearly 3,000 were found to fit the three-body reaction $\Sigma^\pm\pi^\mp\pi^0$. The invariant-mass distribution of $\Sigma^\pm\pi^\mp$ from the three-body reactions for all $K^-$ momenta is shown. The salient feature is the production of Y*(1520), with some evidence for Y*(1385) and Y*(1405) production. A Breit-Wigner equation was fitted to the data under the assumption that the entire cross section arises from the formation of a single resonance. The results of the experiment are interpreted and discussed. (J.F.P.)

**2712** THE REAL PART OF THE PROTON-NEUTRON SCATTERING AMPLITUDE AT 19.3 Gev/c. Bellettini, G.; Cocconi, G.; Diddens, A. N.; Lillethun, E.; Matthiae, G.; Scanlon, J. P.; Wetherell, A. M. (CERN, Geneva). Phys. Lett., 19: 341-5(Nov. 1, 1965).

Results of an experiment to measure proton-deuteron scattering for the same incident momentum and using the same apparatus as that previously used to measure proton-proton small angle elastic scattering and total cross section at 19.3 Bev/c by G. Bellettini et al. (Physics Letters 14: 164(1965)) are reported. The primary object was to obtain information about elastic proton-neutron scattering by comparing the results for the p-p and the p-d systems. The differential cross section for elastic p-d scattering was measured using thin-plate sonic spark chambers in an arrangement of magnetic spectrometers. It was not possible to distinguish between true-elastic events in which the deuteron was scattered coherently and quasi-elastic events in which the deuteron was broken up by the interaction. But inelastic events where one or more mesons ($\pi$) were produced were excluded. In extracting information about the p-n system from the measured p-p and p-d cross sections the treatment given by Harrington (Phys. Rev. 135: 183(1964)) was used. (J.F.P.)

**2713** $\pi^-$ MESON-NEUTRON ELASTIC BACKWARD SCATTERING AT 1.4–4.0 Gev/c. Alikhanov, A. I.; Bayatyan, G. L.; Brakhman, E. V.; Eliseev, G. P.; Galaktionov; Landsberg, L. G.; Lyubimov, V. A.; Sidoriv, I. V.; Yetch, F. A.; Zeldovich, O. Ya. (Inst. for Theoretical and Experimental Physics, Moscow). Phys. Lett., 19: 345-8 (Nov. 1, 1965).

The elastic backward scattering reaction $\pi^- + n \rightarrow \pi^- + n$ at 1.38 to 4.05 Bev/c was investigated. The experimental arrangement is shown. Absolute cross sections were obtained for 1700 events due to this reaction. Total uncertainty in the values of cross sections due to these corrections is 25%. The mean value of the cross section was obtained in the angular interval 160 to 180° cms. The de-

pendences of the mean values of the cross section on incident momentum are shown. The irregularity in the momentum region 2 to 3 Bev/c is possibly the effect of the resonance Δ (2360). The angular distribution of $\pi^-n$ scattering (obtained by the subtraction method and averaged in the momenta interval 2.1 to 3 Bev/c) is also shown. A peak is found in the region $-0.95 > \cos\theta^* > -1$. The small width of this peak is noted. (J.F.P.)

**2714** A NEW MEASUREMENT OF THE LIFETIME OF THE POSITIVE PION. Eckhause, M.; Harris, R. J. Jr.; Shuler, W. B.; Siegel, R. T.; Welsh, R. E. (College of William and Mary, Williamsburg, Va.). Phys. Lett., 19: 348-50(Nov. 1, 1965).

The lifetime of the positive meson ($\pi$) was measured by a digital timing technique for mesons ($\pi$) stopped in a plastic scintillation counter. This method permits improvement in precision by more than an order of magnitude over previous measurements. The counter arrangement is shown. Mesons ($\pi$) were brought to rest in a counter at the rate of 250/sec. A second scintillation counter for counting mesons ($\mu$) was optically separated from the $\pi$ counter by a thin sheet of aluminized plastic. A large fraction of mesons ($\mu$) from the mesons ($\pi$) decaying in the $\pi$ counter penetrated into the $\mu$ counter. Thus the meson ($\pi$) stop signal and the meson ($\mu$) decay signal occurred in different counters, permitting measurement of the time interval for each decay event by means of a 100 Mc digital time analyzer. About $2.5 \times 10^6$ events with time intervals between 40 and 250 nsec after the meson ($\pi$) stop signal were used in the analysis. The weighted mean of 15 runs yielded a value of $26.1 \pm 0.02$ nsec for the mean lifetime of the positive meson ($\pi$). (J.F.P.)

**2715** EVIDENCE FOR $\kappa^0(725)$ IN THE REACTION $\pi^-p \rightarrow K^0\Lambda^0\pi^0$ AT 1.5 AND 1.8 Gev/c. Kim, Y. S. (Ohio State Univ., Columbus); Burleson, G. R.; Kalmus, P. I. P.; Roberts, A.; Romanowski, T. A. Phys. Lett., 19: 350-2 (Nov. 1, 1965). (COO-1261-18).

The reaction $\pi^- + p \rightarrow K^0 + \Lambda + \pi$ in a $CH_2$ target was studied in 1.5 and 1.8 Bev/c exposures of the spark chamber-magnet system to a proton synchrotron. In this reaction evidence is found for the production of $\kappa(725)$ at both momenta. From an analysis of about 6,000 2, 3, and 4 $V^0$ pictures, 154 $K^0\Lambda^0\pi^0$ events at 1.5 Bev/c and 259 $K^0\Lambda^0\pi^0$ events at 1.9 Bev/c were identified and accepted. Of these events 75% are attributed to hydrogen and the rest to the carbon protons in the $CH_2$ target. In order to analyze the data as $K^0\Lambda^0\pi^0$ the erroneous fitting of $K^0\Sigma^0\pi^0$ as $K^0\Lambda^0\pi^0$ is assumed not to introduce artificial peaks into the $K\pi$ or $\pi\Lambda$ mass distribution. The effective mass distributions are shown for the $\pi^0\Lambda^0$ system for the beam momenta 1.5 and 1.8 Bev/c, respectively. The effective mass distributions for the $K^0\pi^0$ system are also given. Assuming the peaks are due to the production of $\kappa(725)$, the mass of this resonance is found to be 735 ± 5 Mev and its width less than 20 Mev. (J.F.P.)

**2716** EVIDENCE FOR A PION-NUCLEON INELASTIC $S_{31}$ RESONANCE. Donnachie, A. (Univ. College, London); Lea, A. T.; Lovelace, C. Phys. Letters, 19: 146-9(Oct. 1, 1965).

From phase-shift analysis and from partial-wave dispersion relations, the main content of the 800-Mev $\pi^+p$ shoulder was found to be an inelastic $S_{31}$ resonance. Such an object is required by SU(6) in the $70^-$ multiplet to which the known $D_{13}$ resonance belongs. Previous $\pi p$ phase-shifts up to 700 Mev are refined and extended to higher energies, using not only new experiments, but also greatly improved theoretical predictions based on partial wave dispersion relations. A semiphenomenological technique was previously developed, whereby the experimental phases and elasticities in a particular partial wave are simultaneously fitted by a parameterization which satisfies the dispersion relation exactly, and has the correct long-range forces. The difference from the previous work is that both rescattering and short-range forces are now included, so that all partial waves can be predicted theoretically, not only the small ones. The latest phases and elasticities are shown. (J.F.P.)

**2717** AN $\Omega^-$ PARTICLE PRODUCED BY A 6 Gev/c $K^-$ MESON IN HYDROGEN. Colley, D. C. (Univ. of Birmingham, Eng.); Dodd, W. P.; Haque, M. M. (and others). Phys. Letters, 19: 152-4(Oct. 1, 1965).

The observation of an event corresponding to the production of an $\Omega^-$ particle is reported. A 1.5 m hydrogen bubble chamber was exposed to 6 Bev/c mesons ($K^-$) from a mass separated beam. A photograph and a separate sketch of the event are shown, and an explanation is given of its interpretation. The measured and fitted values of the track parameters are given for one of nine separate measurements all of which are mutually consistent. A plot of probability of fit against $\Omega^-$ mass is also shown. It is concluded that the mass is 1666 ± 8 Mev. The $\Omega^-$ length is 7.48 cm and its proper lifetime is $1.85 \times 10^{-10}$ seconds. (J.F.P.)

**2718** POSITIVE PION PHOTOPRODUCTION WITH COHERENT BREMSSTRAHLUNG. Gorenstein, P. (Laboratori Nazionale di Frascati, Italy); Grilli, M.; Spillantini, P.; Nigro, M.; Schiavuta, E.; Soso, F.; Valente, V. Phys. Letters, 19: 157-60(Oct. 1, 1965).

Results of a measurement of the asymmetry ratio $A = (\sigma_\perp - \sigma_{||})/\sigma_\perp + \sigma_{||})$ with linearly polarized photons are reported. The quantities $\sigma_\perp(\sigma_{||})$ are defined as the differential cross section for the photoproduction of positive mesons ($\pi$) by photons with the electric vector perpendicular (parallel) to the production plane. The source of polarized photons was a coherent bremsstrahlung beam. Electrons accelerated to an energy of 1 Bev interacted with a suitably aligned single crystal diamond target and produced a bremsstrahlung beam. The intensity and polarization peaks were varied by changing the angle of the [110] crystal axis with respect to the incident electron direction. Measurements were made at five angles between 45 and 145° in the center of mass system. The experimental results after background corrections are shown. These include the mean value of the polarization obtained from a Born approximation calculation of coherent bremsstrahlung taking into account the experimental resolution. The asymmetry ratio and the angular dependence of $\sigma_\perp$ and $\sigma_{||}$ are also shown. (J.F.P.)

**2719** $\varphi$ SUPPRESSION IN $K^-p$ REACTIONS. Fried, H. M.; Taylor, J. G. (Univ. of California, Los Angeles). Phys. Rev. Lett., 15: 709-10(Oct. 25, 1965).

It is pointed out, within the context of the one-baryon-exchange model, that the ratio R of $\varphi$ to $\omega$ production in the backward direction in $K^-p$ reactions may be expected to be small as a consequence of $\varphi - \omega$ mixing. (L.B.S.)

**2720** FURTHER DISCUSSION OF PARTICLE-MIXTURE THEORIES OF $K^0 \rightarrow 2\pi$ DECAY. Kabir, P. K. (Institut de Physique Nucleaire, Lyon); Lewis, R. R. Phys. Rev. Lett., 15: 711-14(Oct. 25, 1965).

The implications of a recently reported result on the apparent CP invariance violation in $K_2^0$ decays are discussed, with particular reference to particle-mixture theories of long-lived $K^0 \rightarrow 2\pi$ decays. (L.B.S.)

**2721** BOOKSTRAP CALCULATION FOR THE MASS OF THE INTERMEDIATE VECTOR BOSON. Gotsman, E. (Israel Atomic Energy Commission, Yavneh); Horn, D. Phys. Rev. Lett., 15: 714-15(Oct. 25, 1965).

S-matrix methods are applied to interactions between leptons; in particular, the bootstrap technique is used to estimate the mass of the intermediate vector boson. The calculation is limited to the type of process, that of elastic neutrino–antineutrino scattering, for which only one helicity amplitude has to be considered. The single-channel bootstrap calculation yielded a self-consistent determination of the mass and the coupling constant of the exchanged particle, $M_W \approx 1258 M_p$ and $f^2 = 11.2$, respectively. (L.B.S.)

**2722** RENORMALIZATION OF THE STRANGENESS-CHANGING AXIAL-VECTOR COUPLING CONSTANT AND THE CABIBBO FORM OF UNIVERSALITY. Levinson, C. A. (Univ. of Pennsylvania, Philadelphia); Muzinich, I. Phys. Rev. Lett., 15: 715-18(Oct. 25, 1965).

The results and some details are given of calculations of the renormalization of the strangeness-changing axial-

vector coupling constant. Assuming the Cabibbo form of universality and taking into account the SU(3) structure of the total hadronic weak current, the reduced matrix elements of the currents related to weak-interaction experiments are determined by the Cabibbo theory. (L.B.S.)

**2723** ABSORPTION TIME OF NEGATIVE Σ HYPERONS IN LIQUID HYDROGEN. Burnstein, R. A.; Snow, G. A.; Whiteside, H. (Univ. of Maryland, College Park). Phys. Rev. Letters, 15: 639-41(Oct. 11, 1965).

A measurement of the capture time for the hyperon-proton system ($\Sigma^-$,p) is reported. It is found that $T_{expt} \sim 3 \times 10^{-12}$ sec, in agreement with the rapid-absorption-mechanism model. The data were obtained by observing the decay of $\Sigma^-$ hyperons in a hydrogen bubble chamber. The fraction of $\Sigma^-$ hyperons decaying at rest furnishes the information for obtaining the absorption time. The observed reactions are: $K^- + p \rightarrow \Sigma^- + \pi^+$ ($K^-$ at rest), $\Sigma^- \rightarrow \pi^- + n$, $n + p \rightarrow n + p$. The experiment established that the cascade time for the hyperon-proton system, ($\Sigma^-$,p), is similar to the cascade times for other lighter strongly interacting particles in hydrogen. This result strongly suggests that ($\bar{p}$,p) capture should proceed in a similar way with predominant s-wave capture. Also the technique used, with its superior velocity resolution, offers a means for testing energy-loss theory in the region from $\beta = 0.02$ to $\beta = 0.004$. The results thus far indicate that the observed number of $\Sigma^-$ decays in the region $\beta = 0.02$ to $\beta = 0.004$ is in excess of predictions. (J.F.P.)

**2724** OBSERVATION OF A PEAK IN $K^- + p \rightarrow \Lambda + \eta$ NEAR THRESHOLD. Berley, D.; Connolly, P. L.; Hart, E. L.; Rahm, D. C.; Stonehill, D. L.; Thevenet, B.; Willis, W. J.; Yamamoto, S. S. (Brookhaven National Lab., Upton, N. Y.). Phys. Rev. Lett., 15: 641-5(Oct. 11, 1965). (BNL-9481)

The results of measurements of the cross section for the reaction: $K^- + p \rightarrow \Lambda + \eta$ at a number of $K^-$ momenta near the threshold are reported. A sharp peak in the cross section is observed. The excitation functions predicted by possible singularities in the reaction matrix are compared with the data. Examples of this reaction are found among events of the types $K^- + p \rightarrow \Lambda$ + neutral missing mass, $K^- + p \rightarrow \Lambda + \pi^+ + \pi^- + \pi^0$. These events were observed in approximately 150,000 pictures taken with the hydrogen bubble chamber exposed to a separated $K^-$ beam at five mementa above the threshold for the reaction studied, which occurs at 724.5 Mev/c. The resulting cross sections are plotted as a function of the momentum of the $\eta$ in the $\Lambda\eta$ center-of-mass system. The cm system total energy is shown on a separate scale. The relation between the two scales is very nonlinear near threshold. The cross section exhibits a sharp peak just above threshold with a maximum near 1 mb, to be compared with the $J = \frac{1}{2}$ unitary limit of 3.6 mb, for a state with isospin equal to zero. The unusual aspect of the observed excitation function is the rapid decrease in the cross section. Several interpretations for this peak are considered. (J.F.P.)

**2725** THE INTERACTION OF π MESONS WITH NUCLEONS IN THE ACCELERATOR ENERGY REGION. Eskreys, A. (Inst. of Nuclear Research, Krakow). Postepy Fiz., 16: 257-78(1965). (In Polish).

The accumulation of experimental results on the interaction of mesons ($\pi$) with nucleons is reviewed for mesons ($\pi$) energies of 0 to 20 Bev. The experimental data include the total cross section as a function of meson energy and a discussion of the resonance-like structure of this cross section. An analysis of the interaction processes includes elastic scattering cross sections and angular distributions, and production of secondary particles both by direct and resonance interactions. The data are only explained by theory in a fragmentary way, with Regge poles explaining only elastic p-p scattering well, and with the one-particle exchange theory agreeing with experiment only below 2 Bev. The statistical theory appears to be most promising. Many useful models have been developed on the basis of this approach. (TTT)

**2726** RANGE OF VALIDITY OF THE ONE-BOSON-EXCHANGE MODEL. Hama, Yogiro; Hoshizaki, Norio (Kyoto Univ.). Progr. Theoret. Phys. (Kyoto), 34: 455-61 (Sept. 1965).

The validity of the one-boson-exchange model is discussed in connection with the nucleon-nucleon scattering. From a consideration of the asymptotic behavior of the phase shifts calculated with this model as the incident energy goes to infinity, it is shown that an appropriate limitation in energy must be imposed in order that the theory does not present contradiction with the Levinson theorem. A practical limit of applicability of the model is effectively established in terms of the impact parameter whose critical value is fixed to be $0.4 \sim 0.6\ \hbar/\mu_\pi c$; for those values of the impact parameter smaller than this, the theory does not work. An alternate estimate of the critical value is given in terms of the ranges of the forces due to the exchange of each boson, showing a reasonable agreement with the former value. A discussion concerning the inclusion of other bosons not yet discovered is also given. (auth)

**2727** NOTE ON RECENTLY DISCOVERED RESONANT STATES IN THE MESON FAMILY. Minami, Shigeo; Sugano, Reiji (Osaka City Univ.). Progr. Theoret. Phys. (Kyoto), 34: 501-3(Sept. 1965).

The new meson resonance states are described within the framework of the 189-dimensional representation; and the existence of the other resonant states, which have not yet been observed, is predicted. Their masses are estimated by using a well-known mass formula. In order to describe the resonant states, the 189 or 405 dimensional representation may be considered in the SU(6) scheme. The 189-dimensional representation is chosen for simplicity. (J.F.P.)

**2728** INTERPRETATION OF WILSON CHAMBER PHOTOGRAPHS BY THE REPROJECTION METHOD. A. ESTIMATION OF THE CONIC REPROJECTION. Neagu, D. V. Rev. Roumaine Phys., 10: 483-99(1965). (In Russian).

The effect of the conic reprojection of photographs on the experimental determination of the momentum of a charged particle in motion in a uniform magnetic field was studied. Using the radius of curvature of the conic projection, formulas were obtained for calculating the radius of curvature of the trajectory in space or of the radius of curvature of the orthogonal projection of the trajectory. In order that the numerical values of the parameters used in the formula be obtained as simply as possible, a very simple measurement method was developed. (tr-auth)

**2729** INTERPRETATION OF WILSON CHAMBER PHOTOGRAPHS BY THE REPROJECTION METHOD. B. ESTIMATION OF THE NON-HOMOGENEITY OF THE MAGNETIC FIELD. Neagu, D. V. Rev. Roumaine Phys., 10: 501-19(1965). (In Russian).

Effects of the nonhomogeneity of the magnetic field on experimental determination of the momentum of a charged particle, when the photographs are redone by the reprojection method, were analyzed. If the distribution of the magnetic field is known, formulas can be obtained to calculate the momentum of the particle using the radius of curvature of the conic projection of the trajectory. Organization of the measurement processes so that the numerical values used in the formulas can be obtained relatively quickly is described. The precision of the method is discussed and some of the experimental results are reported. The results reported show that the correction factors introduced are efficient in almost all situations of practical importance. (tr-auth)

**2730** A SEMI-EMPIRICAL EQUATION FOR THE EXTERNAL BREMSSTRAHLUNG YIELD FROM BETA EMITTERS. Truscello, Vincent C. (Martin Co., Baltimore); Silverman, Joseph. Trans. Amer. Nucl. Soc., 8: 321-2(Nov. 1965).

**2731** AN EXACT SOLUTION OF THE EQUATIONS OF RADIATIVE TRANSFER. Siewert, C. E. (Middle East Technical Univ., Ankara); Zweifel, P. F. Trans. Amer. Nucl. Soc., 8: 504(Nov. 1965).

**2732** RELATIONS BETWEEN ELECTROMAGNETIC AMPLITUDES ACCORDING TO THE UNITARY SYMMETRY

MODEL. Rekalo, M. P. (Inst. of Physics and Tech., Kharkov). Ukr. Fiz. Zh., 10: 813-23(Sept. 1965). (In Ukrainian).

Relations between photoproduction amplitudes of mesons on baryons are derived on the basis of unitary symmetry of strong interactions. Besides the electromagnetic interaction disturbing unitary symmetry, account is taken in the first order of the theory of perturbations of a moderately strong interaction. (auth)

**2733** ASYMPTOTIC EQUALITY OF THE CROSS SECTION OF $\pi^{\pm}$-MESON GENERATION FROM THE NEUTRINO AND ANTINEUTRINO. Nguyen-van-Hieu; Fam-K'ui-tu (Kiev State Univ.; Joint Inst. for Nuclear Research, Dubna, USSR). Ukr. Fiz. Zh., 10: 824-9(Sept. 1965). (In Ukrainian).

A relation of cross symmetry was established between the invariant amplitudes of the processes of $\pi^{\pm}$-meson production from the neutrino and antineutrino: $\nu + p \rightarrow l^- + \pi^+ + p$ and $\bar{\nu} + p \rightarrow l^+ + \pi^- + p$. Asymptotic expressions were obtained for the cross sections of these processes at high energies. Using the Fragmen-Lindelef theorem, it is possible to show that the differential cross sections of these processes are asymptotically equal. The differential relations may be integrated over some intervals, which yield integral relations that are more convenient for experimental checking. (auth)

**2734** ON THE CHERENKOV RADIATION IN ANISOTROPIC MEDIA. Lu, Chen-fa. Wu Li Hsueh Pao, 21: 1083-8(May 1965). (In Chinese).

The special features of Cherenkov radiation, including the consideration of magnetic moments of the elementary particles are treated in a conventional manner for the isoelectric medium $D_i = \epsilon_i E_i (i = x,y,z)$, $B = \mu H$, and the iso-ferromagnetic body $B_i = \mu_i H_i$, $D = \epsilon E$. By considering the magnetic moments of elementary particles as point magnetic moments, i.e., $M = m_0 \delta(x - v_0 t)$, as set of conditions which control the Cherenkov radiation may be established. In view of the possibility that the direction of M may differ from the direction of the motion of the elementary particles, two conditions must be considered: (1) M is parallel to the direction of motion and produces no complementary electric dipole, = 0; (2) the direction of the magnetic moment is perpendicular to the direction of motion, resulting in the generation of a complimentary dipole, $P = [v^0 \cdot M]/C$. Consideration of a completely isotropic medium is an oversimplification; the two wave quanta and the two polarizing directions in an anisotropic medium will be represented by one wave quantum and two linear polarizing waves possessing the same refractivity and adding up to an elliptical wave. Expressions are derived for various conditions. (TTT)

**2735** ANALYSIS OF THE REACTION $\gamma + p \rightarrow K^+ + \Sigma^0$. Tsarev, V. A. (Lebedev Inst. of Physics, Moscow). Yadern. Fiz., 2: 109-11(July 1965). (In Russian).

Previously obtained relations are used to analyze the experimental data on the reaction $\gamma + p \rightarrow K^+ + \Sigma^0$. The obtained values of the parameters $g^2_{NK\Sigma}$, $\mu_T$, $\mu_{\Sigma^0}$ are compared with results, following from unitary symmetry. (auth)

**2736** CALCULATION OF THE $\bar{\nu} + p \rightarrow n + \mu^+ + \gamma$ CROSS-SECTION. Frankfurt, L. L. (Ioffe Inst. of Physics and Tech., Leningrad). Yadern. Fiz., 2: 117-18(July 1965). (In Russian).

The possibility of detecting the process $\bar{\nu} + p \rightarrow n + \mu^+ + \gamma$ is considered. It is shown that the cross section of this process can be calculated in an approximation in which almost all of the $\bar{\nu}$ energy is transmitted to the $\mu$, $\gamma$ pair. The cross section lies just at the limit of experimental detection possibilities. (auth)

**2737** DETERMINATION OF ISOTOPICAL COMPONENTS OF THE $\gamma + N \rightarrow N + \pi$ AMPLITUDE AT THE $\gamma$-RAY THRESHOLD ENERGY. Adamovich, M. I.; Larionova, V. G.; Lebedev, A. I.; Kharlamov, S. P.; Yagudina, F. R. (Lebedev Inst. of Physics, Moscow). Yadern. Fiz., 2: 135-43(July 1965). (In Russian).

The differential cross sections of the process $\gamma + p \rightarrow n + \pi^+$ for the pion emission angles (in l. s.) 16, 24, 36, 56, 64 and 76° were measured in the photon energy region 165 to 230 Mev. The $\pi^+$-meson photoproduction amplitude in the S-state $E_{0+}(\gamma + p \rightarrow n + \pi^+)$ for the pion momentum q = 0 was obtained by extrapolating the empirical dependence of the cross section on q to the threshold. Data on the process $\gamma + n \rightarrow p + \pi^-$ were analyzed in the same way and the amplitude $E_{0+}(\gamma + n \rightarrow p + \pi^-)$ was obtained for q = 0. These amplitudes together with results concerning $E_0(\gamma + p \rightarrow p + \pi^0)$ are used to find the isoscalar $E^0_{0+}$ and isovector $E^-_{0+}$ and $E^+_{0+}$ parts of the photoproduction amplitude $E_{0+}$, which are then compared with the theoretical predictions. (auth)

**2738** PHOTONIC DECAYS OF HYPERONS AND $SU_6$-SYMMETRY. Matinyan, S. G. (Inst. of Physics, Academy of Sciences, Georgian SSR). Yadern. Fiz., 2: 151-3(July 1965). (In Russian).

The $SU_6$-symmetry is applied to obtain relations between the amplitudes of photonic weak decays of baryons. It is shown that in the limit of $SU_6$-symmetry all photonic decays of baryons belonging to the octet conserve parity. E1-transitions are also absent in all decays involving the $\Omega^-$-hyperon. Four relations are obtained between the M1-transition amplitudes for the photon decays of baryons. (auth)

**2739** PRODUCTION OF SLOW $\pi$-MESONS ON LIGHT NUCLEI AND THE $\pi$-$\pi$ INTERACTION. Veselovskii, G. S.; Grashin, A. F.; Demidov, V. S.; Kuznetsov, E. V.; Kuzhetsov, E. P.; Ponosov, A. K.; Protasov, V. P.; Sergeev, F. M.; Shalamov, Ya. Ya. (Inst. of Theoretical and Experimental Physics, Moscow). Yadern. Fiz., 2: 496-500(Sept. 1965). (In Russian).

The production of slow $\pi^{\pm}$ mesons in collisions of $\pi^-$ mesons with initial momentum 2.8 Bev/c and freon–mixture nuclei was investigated in 17- and 200-liter bubble chambers. Those events were selected in which the $\pi$ mesons were stopped in the working material of the chamber. The Q-distribution of the dipion is obtained in the region $Q \leq 100$ Mev. The distribution for the $\pi^+\pi^-$ pairs differs from that for the $\pi^+\pi^+$ and $\pi^-\pi^-$ pairs, which can be explained by assuming a strong $\pi$-$\pi$ interaction in the isospin state T = 0. (auth)

**2740** SOLUTION OF THE EQUATION FOR HIGH-ENERGY NEUTRON-DEUTERON SCATTERING. Belozerov, N. N. (Inst. of Theoretical and Experimental Physics, Moscow). Yadern. Fiz., 2: 552-61(Sept. 1965). (In Russian).

A solution of the Skornyakov–Ter-Martirosyan equation is obtained for energies much higher than the deuteron binding energy. More precisely, the corresponding equation for the partial amplitudes is solved. The Danilov method is used to exclude the s-wave ambiguity. (auth)

**2741** THE EFFECT OF SINGULARITIES OF TRIANGULAR DIAGRAMS WITH DECAY MASSES ON THE MASS SPECTRA OF THE SYSTEMS $\pi + \Delta_{1238}$, $\pi + \Sigma_{1385}$ and $\pi + \phi$. Anisovich, V. V.; Fomin, V. V. (Ioffe Inst. of Physics and Tech., Leningrad). Yadern. Fiz., 2: 562-4(Sept. 1965). (In Russian).

The influence of the triangular singularities of various graphs on the cross sections of the reactions $\pi^- + p \rightarrow \pi + \Delta_{1238}$, $K + p \rightarrow \pi + \Sigma_{1385}$ and on the mass spectrum of the $\pi + \phi$ system is investigated. These diagrams can lead to anomalies in the cross sections or mass spectra, attaining values of the order 10 to 20% of the background for $M_{\pi\Delta_{1238}} = 2.37$ Bev, $M_{\pi\Sigma_{1385}} = 2.62$ Bev, and $M_{\pi\phi} = 1.4$ Bev. (auth)

**2742** SEARCH FOR ANOMALOUS HYDROGEN. Kukavadze, G. M.; Memelova, L. Ya.; Suvorov, L. Ya. (Inst. of Theoretical and Experimental Physics, Moscow). Zh. Eksp. Teor. Fiz., 49: 389-92(Aug. 1965). (In Russian).

An attempt is made to detect with the aid of a mass spectrometer elementary particles with a mass greater than that of the proton. It is shown that in the earth's atmosphere the concentration of positive charged particles with a mass greater than that of deuterium may be smaller than $1.5 \cdot 10^{-12}$ if the concentration is defined as the rate of the

number of particles sought to the total number of particles in a given air sample. (auth)

**2743** TWO-PHOTON EMISSION IN ELECTRON COLLISIONS. Baier, V. N.; Galitskii, V. M. (Novosibirsk State Univ., USSR). Zh. Eksp. Teor. Fiz., 49: 661-71(Aug. 1965). (In Russian).

The cross section for double bremsstrahlung radiation emitted as a result of collision of two high-energy electrons, integrated over all finite states except the photon frequencies, is calculated in the center of inertia system under the assumption that one of the emitted photons is soft and the other possesses an arbitrary energy. (auth)

**2744** ON A CERTAIN POSSIBILITY OF MEASURING THE MAGNETIC MOMENT OF THE $\Sigma^+$ HYPERON. Yakovleva, I. V. Zh. Eksp. Teor. Fiz., 49: 707-10(Aug. 1965). (In Russian).

The possibility of measuring the magnetic moment of the $\Sigma^+$ hyperon on the basis of depolarization of $\Sigma^+$ hyperons from the $\pi^+ + p \rightarrow \Sigma^+ + K^+$ reaction in a photographic emulsion is discussed. A formula is obtained which describes the behavior of the polarization of $\Sigma^+$ hyperons in matter, the possible existence of an external magnetic field being taken into account. (auth)

**2745** FINAL STATE PION-NUCLEON INTERACTIONS AT 2.27 Bev [Thesis]. Hunter, Raymond Eugene. Tallahassee, Florida State Univ., 1964. 161p.

Pion–nucleon interactions were studied through negative pions bombarding protons in a liquid hydrogen bubble chamber at an incident pion momentum of 2.27 Bev/c. Only those final states involving four charged particles were analyzed. No final states involving strange particles were included. In addition to finding the known resonances, including the N* (1238), $\rho$-meson, $\omega$-meson, $\eta$-meson, f-meson, $A_1$-meson, and B-meson, evidence was found for one and possibly two previously unreported resonances involving three pions in the isotopic spin state of two or three. These resonances, denoted as the $E_1$ and $E_2$ mesons, were found at masses of 740 and 940 Mev. No statistically significant evidence was found for the reported $\sigma$-meson in any of the final states, nor was any strong evidence found for the inelastic production of the higher N* resonances. Cross sections for all resonances and final states were calculated and compared, where possible, with previously reported values near the present energy. The Peierls' mechanism for production of the N* (1512) was tested with negative results. The cascade model for decay of the higher N* resonances was tested. The results were inconclusive. (Dissertation Abstr.)

**2746** STUDY OF THE REACTION $\pi^- + p \rightarrow \pi^- + \rho^0 + p$ AT 7.0 Bev/c [Thesis]. Cason, Neal Martin. Madison, Wis., Univ. of Wisconsin, 1964. 84p.

Two hundred and thirteen events of the type $\pi^- + p \rightarrow \pi^- + \pi^- + \pi^+ + p$ occurring in a hydrogen bubble chamber at an incident beam momentum of 7.0 Bev/c were analyzed. The event separation was performed utilizing kinematic fitting and ionization criteria. The contamination of the sample due to other final states is less than 10%. The cross section for this reaction was measured to be 1.7 ± 0.2 mb. The partial cross sections for the production of resonant final states were measured with the results: $\sigma(\pi^- + p \rightarrow \pi^- + \pi^- + N^{*2+}) = 0.55 \pm 0.11$ mb; $\sigma(\pi^- + p \rightarrow \pi^- + \rho^0 + p) = 0.38 \pm 0.10$ mb; and, $\sigma(\pi^- + p \rightarrow N^{*0} + \rho^0) = 0.035 \pm 0.013$ mb. The $N^{*2+}$ isobar mass and width were found to be 1216 ± 14 Mev and 114 ± 30 Mev respectively. The $\rho^0$ parameters are $M^* = 773 \pm 12$ Mev and $\Gamma = 57^{+28}_{-18}$ Mev. $\rho^0$ production is peripheral and is dominated by the production of a final state in which the $\pi^-$ and $\rho^0$ have anomalously low relative energy. The low effective mass enhancement occurs between threshold and 1600 Mev. The effect is consistent with $\pi-\rho$ s-wave scattering in the zero-range approximation with a scattering length of 1.0 fermi. The internal angular distributions were studied as a function of $\pi-\rho$ effective mass, but no definite conclusions were made. (Dissertation Abstr.)

**2747** PHOTOPRODUCTION OF RHO MESONS [Thesis]. Franklin, Allan David. Ithaca, N. Y., Cornell Univ., 1965. 115p.

The reaction $\gamma + p \rightarrow p + \pi^+ + \pi^-$ was investigated with particular emphasis on $\rho^0$ meson photoproduction. The mass distribution of the two-pion system was measured over the range 465 to 795 Mev, and evidence on the angular distribution of $\rho^0$ photoproduction was obtained. Two of the final state particles were counted and their angles and momenta were measured by means of spark chambers located in two magnetic spectrometers. This provided just enough information to determine the kinematics assuming only three particles in the final state. In general, the particles detected were the recoil proton and one of the pions, both $p\pi^+$ and $p\pi^-$ combinations. In order to detect the $\rho^0$ near zero degrees two pions were detected. The mass of the two-pion system was determined to an accuracy of ±3%. It was concluded that $\rho^0$ photoproduction is a significant contribution to $\pi$ pair photoproduction for $\gamma$-ray energies near 1150 Mev. Pion pairs are not produced in a pure isotopic spin state but must be produced in a mixture of even and odd isotopic spin states. The $\rho^0$ photoproduction cross section, for $\gamma$ rays of 1150 Mev, peaks at a center of mass angle of about 60° and falls off both forward and backward of this angle. A comparison of this angular distribution to that predicted by the one-pion exchange model is also shown. (Dissertation Abstr.)

**2748** REGENERATION OF $K_1^0$ MESONS AND THE $K_1^0-K_2^0$ MASS DIFFERENCE [Thesis]. Christenson, James Harlowe. Princeton, N. J., Princeton Univ., 1964. 118p.

The regeneration of $K_1$ mesons in solid materials was studied, using a beam of $K_2$ mesons produced at the Brookhaven AGS. A pair of magnet-spark chamber spectrometers were employed to momentum analyze the pions from the $K_1$ decays. The transmission regeneration is found to be indeed coherent. The mass difference was measured with a regenerator consisting of two pieces of copper, separated by a gap of variable width. This method is independent of all nuclear parameters and yields a mass difference of .50 ± .10. Two independent analyses of data taken with various thicknesses of copper as regenerators yield mass differences consistent with the gap measurement. Mass differences larger than 1 are strongly rejected by our data. The forward regeneration cross sections for C, Cu, Fe, and W were measured and found to agree with optical model calculations. All data find explanation within the framework of the regeneration theory. (Dissertation Abstr.)

**2749** A STUDY OF SOME RARE DECAY MODES OF THE $K^+$ MESON [Thesis]. Cline, David Bruce. Madison, Wis., Univ. of Wisconsin, 1965. 146p.

Several rare decay modes of the $K^+$ meson were searched for in a large sample of $K^+$ decays in the LRL heavy-liquid bubble chamber filled with $C_3F_8$. The decay mode $\pi^+\pi^+\mu^-\nu_\mu$ ($K^-_{\mu_4}$) violates the $\Delta S = \Delta Q$ rule, whereas, $\pi^+\pi^-\mu^+\nu_\mu$ ($K^+_{\mu_4}$) does not. No $K^-_{\mu_4}$ events were found and one possible $K^+_{\mu_4}$ event was found. The $K^+_{\mu_4}$ interpretation of the event is estimated to be more probable than an interpretation of the event as back-ground by a factor of 10. The 90% confidence upper limits on the branching ratio for $K^-_{\mu_4}$ and $K^+_{\mu_4}$ are $2.5 \times 10^{-6}$ and $1.1 \times 10^{-5}$, respectively. Of 81 examples of the decay mode $\pi^+\pi^0\gamma$, 63 events were suitable for determination of the $\pi^+$ spectrum. A maximum likelihood fit to the spectrum was made using the most general Lorentz invariant and gauge invariant transition matrix element. The spectrum appears to be dominated by inner bremsstrahlung radiation. The branching ratio for $\pi^+\pi^0\gamma$ decay was found to be $(2.4^{+1.1}_{-0.8}) \times 10^{-4}$ per $K^+$ decay for $\pi^+$ kinetic energies between 55 and 80 Mev. The decay modes $\pi^+e^+e^-$, $\pi^+\mu^+\mu^-$, and $\pi^+\nu\bar{\nu}$ were also sought. One possible example of $\pi^+e^+e^-$ decay was found in an effective sample of $9.4 \times 10^5$ stopped $K^+$ meson decays. A background study revealed that this event could also be due to background. No candidates for the other decay modes were found. An upper limit on the ratio of the neutral leptonic current coupling constant to the charged current coupling constant is suggested. (Dissertation Abstr.)

# Field Theory, Scattering Theory, and Symmetries

**See also Elementary Particles and Radiations**

*Refer also to abstract 3435.*

**2750** (AD-618659) AN EMPIRICAL MASS FORMULA INVOLVING THE ELECTRON MASS. Frosch, Reinhart (Stanford Univ., Calif. High-Energy Physics Lab.). June 1965. Contract Nonr22567. 10p. (HEPL-382). CFSTI $1.00 cy, $0.50 mn.

A search for a rest mass quantum in the order of magnitude of a few Mev is reported. The search was stimulated by the observation that the accepted value of the electromagnetic mass splitting of the pion is very consistent with 9m (m = electron rest mass), and that the value of the proton mass is very close to an integral multiple of 9m. (TAB)

**2751** (IC/65/51) REMARK ON CROSSING SYMMETRY AND PARASTATISTICS. Barut, A. O.; Ghika, G.; Limic, N. (International Centre for Theoretical Physics, Trieste (Italy)). May 1965. 6p. Dep. mn.

It is shown that under the following two assumptions identical particles cannot obey parastatistics; (1) every physical amplitude must belong to an irreducible representation of the permutation group of identical particles, and (2) the amplitudes satisfy the crossing property. (M.O.W.)

**2752** (IC/65/77) MASS FORMULAE IN U(6) ⊠ U(6) THEORY. Delbourgo, R.; White, R. (International Centre for Theoretical Physics, Trieste (Italy)). Oct. 28, 1965. 7p. Dep. mn.

An analysis similar to that used by Okubo and Marshak was used to obtain elementary particle mass relations from U(6) ⊗ U(6) theory. (M.O.W.)

**2753** (JINR-P-2300) MEZONNYI TOK V NARUSHENNOI SIMMETRII U(12) I OPYTY NA VSTRECHNYKH PUCHKAKH. (Meson Current in Broken Symmetry U(12) and Experiments With Colliding Beams). Winternitz, P.; Makarov, A. A.; Nguyen Van Hieu; Tkachev, L. G.; Uglirzh (Joint Inst. for Nuclear Research, Dubna (USSR). Lab. of Theoretical Physics). 1965. 7p. Dep. mn.

The general structure of the matrix element of the meson current is studied in the broken $\tilde{U}(12)$ symmetry. Further this current is used to calculate the cross sections for the production of meson pairs in colliding electron-positron beams. (auth)

**2754** (JINR-P-2309) ISSLEDOVANIE INFRAKRASNYKH OSOBENNOSTEI SECHENIYA RASSEYANIYA METODOM FUNKTSIONAL'NOGO INTEGRIROVANIYA. (An Investigation of Infrared Singularities in the Cross Sections by the Functional Integration Method). Barbashov, B. M.; Volkov, M. K. (Joint Inst. for Nuclear Research, Dubna (USSR). Lab. of Theoretical Physics). 1965. 14p. Dep. mn.

Using the functional integration method the high energy scattering of scalar particles with mass m is studied. This process is treated on the basis of the model of scalar particles with the lagrangian $L = g:\psi^2(x)\,\phi(x)$ where the field $\psi(x)$ possesses a mass $\phi(x)$ and $\phi(x)$ – the zero mass. The contribution of the virtual quanta of the field $\phi(x)$ with $k^2 = 0$ leading to the infrared singularity in the elastic process amplitude is taken into account exactly. Beyond the framework of perturbation theory the compensation procedure of the infrared divergences is made by taking into account the processes involving the emission of an infinite number of real quanta of a field $\phi(x)$ with a total energy not exceeding a certain quantity $\Delta$. (auth)

**2755** (JINR-E-2329) ALGEBRA OF THE CURRENTS AND DISPERSION RELATIONS. Efremov, A. V.; Matveev, V. A.; Tavkhelidze, A. N.; Khelashvili, A. A. (Joint Inst. for Nuclear Research, Dubna (USSR). Lab. of Theoretical Physics). 1965. 6p. Dep. mn.

It is shown that the results obtained from the algebra of currents and those of the algebra of charges plus the requirement of the local commutativity are equivalent. (auth)

**2756** (JINR-P-2342) MASSOVYE FORMULY V SU(12) CONTAINS Sp(6) x SU(2)-SIMMETRII. (Mass Formula in SU(12) Contains Sp(6) x SU(2) Symmetry). Nikolov, A. V.; Todorov, I. T.; Fakirov, D. G. (Joint Inst. for Nuclear Research, Dubna (USSR). Lab. of Theoretical Physics). 1965. 18p. Dep. mn.

A study is presented of the SU(12)-symmetry in which the basic multiplets ("trions") consist of particles with half-integer spin and with integer electric and baryon charges. Mass formulas were obtained for mesons and baryons entering correspondingly into representations 143 and 364 under the assumption that the mass operator in the broken SU(12)-symmetry conserves not only spin, isotopic spin, and strangeness, but also the supercharge. In particular, for usual particles (with a hypercharge equal to zero) the well-known mass formulas obtained in the SU(6)-symmetry scheme are reproduced. (auth)

**2757** (NYO-2262-98) SURVEY AND CLASSIFICATION OF SOLUBLE FIELD THEORY MODELS. Fried, H. M. (Brown Univ., Providence, R. I. Dept. of Physics). June 1, 1965. Contract AT(30-1)-2262. 13p. (CONF-650653-6). Dep. mn; CFSTI $1.00 cy, $0.50 mn.

From American Physical Society, Summer Meeting, New York.

A survey of the known soluble and semi-soluble models of quantum field theory is presented. By field theory one here means sets of coupled Green's functions, and the measure of solubility of a theory is just the degree to which these functions can be found. (M.O.W.)

**2758** (UR-875-100) FIELD-THEORETIC MODELS OF ELEMENTARY PARTICLES. Marshak, R. E. (Rochester Univ., N. Y. Dept. of Physics and Astronomy). Oct. 11, 1965. Contract AT(30-1)-875. 43p. (CONF-650947-1). Dep. mn; CFSTI $2.00 cy, $0.50 mn.

From International Conference on Elementary Particles, Kyoto.

A survey of progress to date towards deriving a unified theory for elementary particles is presented. Only the quantum field theory approach is discussed. Future lines of investigation are suggested and some encouraging results recently obtained with the quark model are pointed out. (M.O.W.)

**2759** (UR-875-102) PRESENT STATUS OF WEAK INTERACTIONS. Marshak, R. E. (Rochester Univ., N. Y. Dept. of Physics and Astronomy). Oct. 15, 1965. Contract AT(30-1)-875. 42p. (CONF-650947-2). Dep. mn; CFSTI $2.00 cy, $0.50 mn.

From International Conference on Elementary Particles, Kyoto.

Four topics are studied: $SU_3$ group, Cabibbo angle, and algebra of currents; non-leptonic processes; C P violation; and intermediate vector boson and high energy neutrino experiments. (auth)

**2760** A SIMPLE ASYMPTOTIC FORMULA FOR CHARGE BRANCHING RATIOS IN THE STATISTICAL MODEL. Zalewski, Kacper (Inst. of Physical Chemistry, Krakow). Acta Phys. Pol., 28: 207-15(Aug. 1965).

The integral yielding charge branching ratios (according to the statistical model) is evaluated using the steepest descents method. An expansion of the exact result into inverse powers of the number of particles with non-zero isospins is thus obtained. The approximate results are compared with the exact ones for three 10-particle systems. The error when using the first approximation is about 1%. (auth)

**2761** ISOTROPIC TENSORS. Kotanski, Andrzej (Jagellonian Univ., Krakow). Acta Phys. Pol., 28: 285-90(Aug. 1965).

A theorem indicating the general form of an isotropic tensor is proved. It is a generalization of the Wigner-Eckart theorem and, on the other hand, of the reduction theorem from previous work. The present theorem is

valid for a large class of groups, in particular for the rotation, Lorentz, and $SU_n$ groups. (auth)

**2762** SOME PROPERTIES OF THE FORWARD SCATTERING AMPLITUDE AT HIGH ENERGIES. Wit, R. (Joint Inst. for Nuclear Research, Dubna, USSR). Acta Phys. Pol., 28: 415-21(Sept. 1965).

The connection between the high-energy behavior of Re T(s, 0) and Im T(s, 0) by means of Phragmén-Lindelof theorem and argument principle was considered. (auth)

**2763** ASYMPTOTIC AND THRESHOLD VALUES OF THE SCATTERING AMPLITUDES IN SOME STATIC MODELS. Wit, R. (Joint Inst. for Nuclear Research, Dubna, USSR). Acta Phys. Pol., 28: 407-14(Sept. 1965).

The asymptotic behavior of the scattering amplitudes for the neutral pseudoscalar static model and the Chew-Low theory by means of the Phragmen-Lindelof theorem was investigated. Some information about the threshold and asymptotic values of the amplitudes with the aid of the argument principle was obtained. (auth)

**2764** ON ELECTROMAGNETIC MASS FORMULAE IN THE UNITARY SYMMETRY. Pindor, M. (Univ. of Warsaw). Bull. Acad. Polon. Sci., Ser. Sci. Math. Astron. Phys., 13: 257-61(1965).

The consequences of an extra term in $P^\mu$ responsible for electromagnetic interaction are studied. Some mass formulas, exact in strong and electromagnetic interactions, are derived under the following assumptions: known supermultiplets of particles belong to definite representations of SU(3), and the operator $P^\mu$ has some specific transformation properties with respect of SU(3). (J.F.P.)

**2765** THE TECHNIQUE OF NORMAL PRODUCTS IN TERMS OF FUNCTIONAL INTEGRALS. Rzewuski, J. (Univ. of Wroclaw, Poland). Bull. Acad. Polon. Sci., Ser. Sci. Math. Astron. Phys., 13: 263-6(1965).

An attempt is made to account for normal product techniques in the functional formulation of the S-matrix theory. The technique of normal products which is used to avoid certain trivial divergences in quantum field theory is expressed in the language of functional integrals in the functional formulation of quantum field theory. (J.F.P.)

**2766** ELEMENTARY PARTICLE SYMMETRIES. Kibble, T. W. B. (Imperial Coll. of Science and Tech., London). Contemp. Phys., 6: 436-52(Aug. 1965).

The number of known elementary particles is now very large, and to reduce their diverse properties to order it is useful to look for symmetries between them. Symmetry properties of various kinds, and the conservation laws associated with them, are discussed here. After giving a brief survey of the general types of particle encountered in nature, first the symmetries related to space and time, and associated with the conservation laws of momentum, energy, angular momentum, and parity are discussed. Later the so-called internal symmetries, in which different particles are regarded as different states of a single basic entity are discussed. Theories of this type—particularly the "eightfold way"—have had considerable success in systematizing the properties of the known particles. (auth)

**2767** A PROOF OF NAKANISHI'S INEQUALITY. Boyling, J. B. (Cambridge Univ., Eng.). J. Math. Phys. (N. Y.), 6: 1469-71(Oct. 1965).

Nakanishi's conjectured inequality for the coefficients of the external masses and invariants in the Feynman denominators for scattering processes is proved by a determinantal method suggested by the analogy between Feynman diagrams and electrical networks. (auth)

**2768** MIXING OF REGGE POLES AND CUTS IN A FIELD-THEORY MODEL. Swift, Arthur R. (Cambridge Univ., Eng.). J. Math. Phys. (N. Y.), 6: 1472-81(Oct. 1965).

The Regge poles generated by ladder diagrams in a $\lambda \phi^3$ theory are mixed with the moving cuts generated by a class of nonplanar graphs containing an internal ladder. Since the contribution from the cut-generating diagram is of order $t^{-2}\ln^m t$, where t is the asymptotic variable, the $t^{-2}$ behavior of the pure ladder graphs is examined and the trajectory of the Regge pole near $l = -2$ is calculated. The Mellin transform method is used throughout. The transformed amplitude corresponding to a single cut insertion is given by a product of the form pole–cut–pole, where it is only the second Regge trajectory that mixes with the cut. The cut itself depends on the leading trajectory. This result substantiates the predictions as to form of other work based on unitarity, but differs in that the cut and pole depend on different trajectory functions. Finally, multiple insertions of the cut diagrams are shown to generate an amplitude with two moving poles on each sheet of the cut. (auth)

**2769** BRANCHING RULES FOR SIMPLE LIE GROUPS. Whippman, M. L. (Univ. of Pennsylvania, Philadelphia). J. Math. Phys. (N. Y.), 6: 1534-9(Oct. 1965).

If $\Gamma$ is an irreducible representation of a group G, and H is a subgroup of G, then $\Gamma$ furnishes a representation of H which is, in general, reducible, and the branching rules specify which irreducible representations of H occur in the decomposition of this representation. Branching rules are derived for various choices of G and H, including most possibilities that have been discussed as higher symmetry groups. (auth)

**2770** RECURSION RELATIONS FOR THE WIGNER COEFFICIENTS OF UNITARY GROUPS. Brody, T. A.; Moshinsky, M.; Renero, I. (Universidad de Mexico, Mexico City). J. Math. Phys. (N. Y.), 6: 1540-6(Oct. 1965).

The polynomials in the components of a set of n-dimensional vectors that form a basis for an irreducible representation of $SU_n$ are shown to be part of the basis of the group $U_{nr}$, in which the subgroup $U_n \times U_r$ is explicitly reduced and $r \geq n - 1$. Using this result, the concept of auxiliary Wigner coefficient is introduced, for which the problem of multiplicity does not arise and the phase convention is related to that of Gel'fand and Zetlin; recursion relations for this auxiliary coefficient are obtained in a straightforward way, and the connection between it and the ordinary Wigner coefficient is shown to be simple. The recursion relations are being programmed for an electronic computer to allow the systematic evaluation of the Wigner coefficients of $SU_3$ and $SU_4$. (auth)

**2771** ALGEBRAIC TABULATION OF THE CLEBSCH-GORDAN COEFFICIENTS FOR REDUCTION OF THE PRODUCT $(\lambda,\mu) \otimes (3,0)$ OF IRREDUCIBLE REPRESENTATIONS OF SU(3). Pandit, L. K.; Mukunda, N. (Univ. of Rochester, N. Y.). J. Math. Phys. (N.Y.), 6: 1547-57(Oct. 1965). (UR-875-73).

Tables of Clebsch–Gordan coefficients of SU(3) for the reduction of the product $(\lambda,\mu) \otimes (3,0)$ of representations of SU(3) are constructed by use of the tensor method. Derivations of some crossing and symmetry relations for the $SU_3$ Clebsch–Gordan coefficients are given, and the Clebsch–Gordan coefficients for the product $(\mu,\lambda) \otimes (0,3)$ are related to those mentioned above. The phase convention used in compiling the tables is stated and explained. (auth)

**2772** N-PARTICLE KINEMATICS AND GROUP-THEORETICAL TREATMENT OF PHASE SPACE. I. NONRELATIVISTIC. Levy-Leblond, Jean-Marc; Lurcat, Francois (Universite de Paris, Orsay, France). J. Math. Phys. (N. Y.), 6: 1564-70(Oct. 1965).

A group-theoretical study is made of the kinematics of n nonrelativistic particles. A systematic method is given to construct a new complete set of commuting observables. The method is based on the existence of a group (the "great group") which acts transitively on the phase-space manifold and preserves the phase-space volume element; the observables are then Casimir operators of the great group and of some of its subgroups, including the usual three-dimensional rotation group. Among these collective observables, in addition to the total angular momentum, the most interesting is the "togetherness operator" which describes the simultaneous localization of the n particles. This oper-

ator is a generalization to n > 2 of the square of orbital angular momentum; its use allows a generalization to n particles the familiar centrifugal barrier arguments. (auth)

**2773** THREE-PARTICLE NONRELATIVISTIC KINEMATICS AND PHASE SPACE. Levy-Leblond, Jean-Marc; Levy-Nahas, Monique (Universite de Paris, Orsay, France). J. Math. Phys. (N. Y.), 6: 1571-5(Oct. 1965).

The kinematics of a nonrelativistic three-particle system is studied with the help of the general method devised by Lévy–Leblond and Lurcat. Basis states are constructed which are eigenstates, in addition to the total momentum–energy, angular momentum, etc., of new observables; among these, the "togetherness tensor" describes the simultaneous localization of the three particles and therefore is of great physical interest. All of these observables arise as Casimir operators of a "great group" acting on the three-particle phase-space manifold in a transitive way, and of some of its subgroups. In the present case, by trying to keep all the particles on the same footing ("democracy" arguments), one is led to choose the $SU_3$ group as a particularly convenient "great group." The Dragt classification of non-relativistic three-particle states are thus recovered completely. The explicit calculation of the basis functions is done in a new way, by analytical methods, solving partial derivative equations. This enables us to establish the most general form of these basis functions. (auth)

**2774** S-MATRIX THEORY AND DOUBLE SCATTERING. Iagolnitzer, Daniel (Centre d'Etudes Nucleaires, Saclay, France; Ecole Nationale des Ponts et Chaussees, Paris). J. Math. Phys. (N. Y.), 6: 1576-83(Oct. 1965).

In the double scattering case, it is shown that the introduction of a pole in the S-matrix elements, is consistent with a description in terms of successive interactions. It is then shown that among Olive's class of possible "propagators" $c(k^2 - m^2 + ie)^{-1} - (1 - c)\cdot(k^2 - m^2 - ie)^{-1}$, only the usual value c = 1 gives a consistent result. (auth)

**2775** RACAH ALGEBRA FOR AN ARBITRARY GROUP. Derome, JeanRobert; Sharp, W. T. (Univ. of Toronto). J. Math. Phys. (N. Y.), 6: 1584-90(Oct. 1965).

The 3j- and 6j-symbols are studied for a general group without assuming that the group is ambivalent or multiplicity-free. The choice of multiplicity label r that distinguishes the equivalent irreducible representations that may arise in a Kronecker product of irreducible representations is left arbitrary and no special choices of phase are made. It is found that the 3j- and 6j-symbols obtained have essentially the same properties as the familiar 3j- and 6j-symbols for the rotation group in three dimensions. (auth)

**2776** TIME-DEPENDENT PERTURBATION THEORY. Hammer, C. L.; Weber, T. A. (Ames Lab., Ames, Iowa). J. Math. Phys. (N.Y.), 6: 1591-?(Oct. 1965). (IS-807).

A time-dependent perturbation theory which is based upon the U-matrix approach is presented using the interaction $e^{-\alpha t}(1 + e^{-\beta t})^{-1}V(x)$ with $\beta$ real, $\alpha$ complex and $\beta >$ Re $\alpha > 0$. Thus the adiabatic or time-independent approximation ($\beta \to 0$) and the sudden approximation ($\beta \to \infty$) can be obtained using just one formalism. The usual series for the U matrix is derived and shown to converge for a semi infinite range if the interaction is of the form $|t|^{-\delta}$, $\delta > 1$, for large times t. Two interesting results are: The derivation of the "golden rule" from the discrete-state time-dependent perturbation theory presented in most text books of quantum mechanics leads to erroneous physical interpretations because the energy-level shift is ignored. When considering scattering between states in the continuum, it is found that a characteristic feature of time-dependent interactions is a discrete momentum spectrum of final states which, in the relativistic case, leads to a mass spectrum. These spectra cannot be obtained using the S matrix. (auth)

**2777** RELATIVISTIC GENERALIZATION OF SU(3) SYMMETRY. BARYON CURRENT. Granovskii, Ya. I.; Pantyushin, A. A. (Inst. of Nuclear Physics, Academy of Sciences, USSR). JETP Lett. (USSR) (Engl. Transl.), 2: 28-9(July 1, 1965).

For the baryon wave function a symmetrical spinor of third rank is chosen which has 364 components. When the moderately strong interaction occurs, this supermultiplet breaks into SU(3) multiplets with definite values of spin and parity. Such a supermultiplet agrees with experimental data and justifies the choice of the baryon wave function. The magnetic moments of the baryons are calculated. It is noted that weak current can be considered in the same manner. (J.F.P.)

**2778** RELATIVISTIC OSCILLATOR MODELS OF ELEMENTARY PARTICLES. Ginzburg, V. L.; Manko, V. I. (Lebedev Physical Inst., USSR Academy of Sciences, Moscow). Nucl. Phys., 74: 577-88(1965).

Relativistically invariant sets of equations for particles described by the center-of-mass coordinates $x_i$ and three four-vectors $u_i^\alpha$ (i = 1, 2, 3, 4; $\alpha$ = 1, 2, 3) are considered. The $u_i^\alpha$ coordinates are internal variables which in this scheme obey oscillator type equations. It is shown that the solutions of the equations in the rest system form $SU_3$ group representations. In particular, equations can be obtained for which some of the solutions in the case of half-integer spins correspond to octets and decuplets with different spin values whereas in the case of an integer spin they correspond to octets and a singlet. Various problems arising in connection with the results obtained are discussed. (auth)

**2779** UNSTABLE BOSON EXCHANGE INTERACTIONS AND THE POLE APPROXIMATION FOR RESONANCE PARTICLES. Lassila, K. E. (Iowa State Univ., Ames; Univ. of Helsinki); Cumming, J.; McEwan, J. Nucl. Phys., 74: 593-600(1965).

A calculation is performed in an attempt to clarify the extent to which an unstable particle exchange interaction can be approximated by that obtained when stable particles are assumed. Scalar unstable bosons exchanged between spinless, heavy nucleons are considered for simplicity, and the contribution to the scattering amplitude by such a process is calculated. In coordinate space, a quantity which can be compared with the Yukawa potential is obtained. The Yukawa tail is reduced considerably for the exchange of a scalar particle with the mass and width of the $\rho$ meson when when the nucleon-nucleon separation is large. The results are also discussed from the point of view of the pole approximation. The effects found are sufficiently large to warrant a more thorough treatment than presently available in the literature. (auth)

**2780** THE BOUNDARIES OF THE SINGULARITY MANIFOLD ASSOCIATED WITH AN ARBITRARY FEYNMAN GRAPH. Andersson, Bo (Univ. of Lund, Sweden). Nucl. Phys., 74: 601-18(1965).

A method to characterize the boundary of the Landau surface of an arbitrary Feynman graph is presented and applied to some particular diagrams. (auth)

**2781** SHELL MODEL OF HADRONS. Malyuta, Yu. M. (Physics Inst., Academy of Sciences, Kiev). Nucl. Phys., 74: 625-8(1965).

A shell model of hadrons, based on groups SU[6(2l + 1)] and SU[3(2j + 1)], is proposed. The diagram technique is applied to the derivation of baryon mass formulas in the SU(12) symmetry model. (auth)

**2782** COULOMB REGGE POLES IN QUANTUM ELECTRODYNAMICS. Shabad, A. Ye. (Lebedev Physical Inst. of the USSR Academy of Sciences, Moscow). Nucl. Phys., 74: 629-41(1965).

Electron-electron and electron-positon scattering is considered. The assumption of the existence of simple Regge poles is introduced in agreement with the Born approximation. Three triplet scattering amplitudes connected by two particle unitarity are shown to have a common pole at j = 0, E = 0 lying at the Coulomb trajectory; the residues at the pole actually factorize. At E = 0 the residue vanishes in the amplitude for which the value of the total angular momentum j = 0 is, in general, physical since at this particular value of the energy the state j = 0 is impossible in the amplitude under consideration. (auth)

**2783** SUM RULES FOR MASSIVE VECTOR GAUGE FIELDS. Segre, Gino (CERN, Geneva). Nucl. Phys., 74: 673-6(1965).

Sum rules are derived and their relevance to elementary particle symmetry schemes is discussed, assuming the canonical commutation relations between bare and dressed massive vector gauge fields. (auth)

**2784** SOME CONSEQUENCES OF THE DE SANTIS MODEL FOR WEAK INTERACTIONS. Majumdar, Rabi (Univ. of Delhi). Nucl. Phys., 74: 683-8(1965).

Various decay modes and high energy neutrino-induced reactions are analyzed, following the isobaric spin assignments for the strongly interacting particles and leptons recently introduced by De Santis as an alternative scheme for weak interactions incorporating the usual $\Delta I = \frac{1}{2}$ rule and CP conservation. As a consequence $\Gamma(\Lambda \rightarrow n\pi) = \Gamma(\Xi^0 \rightarrow \Lambda\pi)$ is derived apart from phase-space considerations. Further, an I' spin for $\Omega^-$ consistent with the present model is assigned, and its various decay modes are obtained as a test of the model. The decay modes of intermediate vector bosons which are no longer schizons so far as I' spin is concerned are considered. In analyzing neutrino-induced reactions it is noted that the familiar results obtained by the $\Delta I = \frac{1}{2}$ rule do not follow unless the De Santis model is supplemented by rather arbitrary dynamical assumptions which, however, may be the consequences of a higher symmetry from which the present model can be derived. (auth)

**2785** IDENTITIES FROM THE LIPPMANN-SCHWINGER EQUATION AND THE EHRENFEST'S THEOREM IN SCATTERING THEORY. Saavedra, I. (Univ. Chile, Santiago). Phys. Lett., 19: 326-7(Nov. 1, 1965).

An identity which generalizes the optical theorem is derived, and it is postulated that Lippmann's result (Phys. Rev. Letters, 15: 11(1965)) is not a generalized version of the Ehrenfest's theorem since the right-hand side of the identity is not a quantum mechanical expectation value. (C.E.S.)

**2786** ON THE DIVERGENCE OF TERNARY SCATTERING OPERATOR IN TWO DIMENSIONS. Stecki, J. (Universite, Brussels). Phys. Letters, 19: 123-4(Oct. 1, 1965).

It was recently asserted that for some classes of dynamical events $[\Omega i\psi]$ is not convergent in 2 dimensions and that the next, 4-particle, operator will be found divergent in 3 dimensions as well. There is only one concrete calculation so far available in which such divergence is apparently found. But it is shown that the concrete argument is not valid and it is seen that the k-integral does converge for small k, as was previously argued. The prescription inherent in the definitions of the scattering operators such as $\psi$ is illustrated; namely, that the limit $\epsilon \rightarrow 0$ is to be taken after all other operations. It is also found by straightforward integration that $\int_0^\infty k\,dk \int_0^\pi d\phi\ (kv\cos\phi - i\epsilon)^{-n}$ is finite for all $n \geq 1$ in the limit $\epsilon \rightarrow 0$. (J.F.P.)

**2787** ON THE METHOD OF DASHEN AND GELL-MANN. Coleman, S. (CERN, Geneva). Phys. Letters, 19: 144-6(Oct. 1, 1965).

It is proven that if the hybrid collinear group does not leak, in the method of Dashen and Gell-Mann(Phys. Lett., 17: 142(1965)), it commutes with the hamiltonian. Thus the Dashen–Gell-Mann theory contains an internal contradiction. The argument is stable, in the sense that the contradiction persists if small leakage is allowed. This does not mean that the idea of a diminishing chain of symmetry groups must be sacrificed. The argument depends on the identification of the group generators with integrals of local currents; only this need be abandoned. This is a minimal retreat: none of the agreements of the theory with experiment depend on this identification, with possibly one exception. (J.F.P.)

**2788** CONFIRMATION OF AN $SU(6)_w$ SCATTERING RELATION. Olsson, Martin G. (Univ. of Wisconsin, Madison). Phys. Rev. Lett., 15: 710-11(Oct. 25, 1965).

It is shown that the isospin ratio for s-wave isobar production is accurately predicted by $SU(6)_w$, and that the ratio is not accounted for by the simplest dynamical models. (L.B.S.)

**2789** ELECTRODYNAMICS OF INTERMEDIATE BOSONS AND CP NONINVARIANCE. Wu, Tai Tsun (Harvard Univ., Cambridge, Mass.). Phys. Rev. Lett., 15: 718-20(Oct. 25, 1965).

The charged vector-meson theory of Lee and Yang is reinvestigated in light of an explanation of previous experimental results that CP invariance is violated in weak interactions, for the case $\kappa = 0$. The validity of the principle of minimal electromagnetic interaction is assumed. It is further assumed that the electromagnetic coupling constant appears in the combination $\partial_\mu$ only. The Lagrangian density is considered in the $\xi$-limiting formalism of Lee and Yang, and it is argued that $\xi$ should not be renormalized. The results are applied to the electromagnetic properties of the W meson. (L.B.S.)

**2790** SYMMETRY PROPERTY OF THE S MATRIX ON THE BASIS OF THE JOST FUNCTION METHOD. Sasakawa, Tatuya; Tsukamoto, Tatsuo (Kyoto Univ.). Progr. Theoret. Phys. (Kyoto), 34: 442-54(Sept. 1965).

Under the assumption that the spinless particle of s wave is scattered by the spinless target with an arbitrary enumerative number of discrete excited states, all symmetry relations are derived on the basis of the Jost function method for any number of open and closed channels. This method explicitly describes the symmetric structure of the S matrix from which the symmetry properties originate. As an application of the method, the threshold behavior is also discussed without employing the channel radius. (auth)

**2791** NOTE ON THE FOUR-PARTICLE SCATTERING THEORY. Takahashi, Yasutaro (Tokyo Coll. of Science); Mishima, Nobuhiko. Progr. Theoret. Phys. (Kyoto), 34: 498-9(Sept. 1965).

An equation is derived for four-body scattering amplitude formulated by a similar method used by Faddeev and an equation for composite-composite scattering reduced from the equation for the four-body scattering amplitude by making some approximations. The formalism given is easily extended to multiparticle scattering by reconstructing the systematic solution of multiparticle scattering problems solved by Weinberg. (J.F.P.)

**2792** COLLECTIVE DESCRIPTION OF A SYSTEM OF INTERACTING BOSE PARTICLES. Fukui, Yoshihiko; Sunakawa, Sigenobu (Tohoku Univ., Sendai). Progr. Theoret. Phys. (Kyoto), 34: 499-501(Sept. 1965).

In the development of a method describing the collective behavior of a system of Bose particles, the velocity operator corresponding to the exact canonical conjugate of the density operator was defined, and it was suggested without proof that the hamiltonian of a system is transformed into a certain form. A proof is given that this expression is correct for the case of Bose particles without the condition: rot $v(x)/> = 0$. In the case of Fermi particles the proof is not valid since the possibility that P vanishes is not excluded. (J.F.P.)

**2793** ON THE IRREDUCIBLE REPRESENTATIONS OF THE GROUP $C_2$. Raszillier, I. Rev. Roumaine Phys., 10: 179-86(1965). (In French).

The irreducible representations of the $C_2$ group were deduced and the possibility of calculation of the Racah tensors was indicated. (tr-auth)

**2794** THE GROUP $C_2$ AND THE SYMMETRY OF WEAK INTERACTION. Yang, Gao-zheng. Wu Li Hsueh Pao, 21: 1080-2(May 1965). (In Chinese).

D'Espagnat's method developed for $SU_3$ groups is applied to the $C_2$ group in a discussion of the weak interaction symmetry. The weak interaction Lagrangian L, [L = $(\bar{A}B)W$] which must satisfy the two non-leptonic decay selection rules $\Delta S \neq 2$ and $|\Delta I| = \frac{1}{2}$ must belong to the expression "4". In order to make sure that the electric charges corresponding to the ground level of the expression are integers, L does not vary according to the $C_2$ group expressing "4" but according to the $C_2 x U_1$ groups expression "4", where $U_1$ is a normalized unit group, the base of which depends on the number of K mesons. The number of K mesons for the expression "4" and the transpose "4*" are K = +1 and K = −1, respectively. From the properties of the $C_2$ group and the Dirac $\delta$ function with the coupling

constants, written in the order $\bar{A}\gamma B$, an expression is obtained for the weak current and the W boson interaction Lagrangian, deriving also the value for the coupling constant of the intermediate bosons. Under assumption of conservation of momentum, the $\Delta S = \Delta Q$ and $\Delta S = 0$ leptonic decays were calculated with the explicit interaction Lagrangians. (TTT)

**2795** STRUCTURE OF $Sp_4$ AND $SO_5$ MULTIPLETS. Malkin, I. A.; Mandel'tsveig, V. G. (Inst. of Theoretical and Experimental Physics, Moscow). Yadern. Fiz., 2: 154-62(July 1965). (In Russian).

Arbitrary irreducible representations of the groups $Sp_4$ and $SO_5$ are reduced with respect to their subgroups $SU_2 \otimes SU_2$, $U_1 \otimes SU_2$ and $U_1' \otimes SU_2'$ using a method suggested previously. Results of the calculations are given in diagrams. (auth)

**2796** MASS RELATIONS IN REDUCIBLE UNITARY MULTIPLETS. Menskii, M. B. (Moscow State Univ.). Yadern. Fiz., 2: 162-70(July 1965). (In Russian).

A system of mass relations is obtained for an arbitrary mixed (reducible) unitary multiplet in the first order with respect to moderately strong interactions. The system is not complete. The results can easily be generalized to any order with respect to moderately strong interactions. (auth)

**2797** SOLUTION OF THE BETHE-SALPETER EQUATION IN A CHARGED VECTOR MESON THEORY. Slavnov, A. A. (Steklov Inst. of Mathematics, Academy of Sciences, USSR). Yadern. Fiz., 2: 190-7(July 1965). (In Russian).

The Bethe-Salpeter equation is investigated for the scattering of leptons interacting by means of a charged vector meson. A new iteration method is suggested to solve the equation. The finiteness of each successive approximation and the convergence of the iteration series are proved for zero momenta of the initial particles, under the additional assumption that it is possible to rotate the contour of integration with respect to $\kappa_0$. (auth)

**2798** THE POSSIBLE NON-CONSERVATION OF CP-PARITY AND THE NATURE OF THE $\Delta T = \frac{1}{2}$ RULE. Zel'dovich, B. Ya.; Okun, L. B. (Inst. of Theoretical and Experimental Physics, Moscow). Yadern. Fiz., 2: 198-9 (July 1965). (In Russian).

The Wolfenstein representation for the lagrangian of the weak nonleptonic interaction with $\Delta Y = 1$ is formulated in terms of the model with three fundamental hadron fields. Two associated phenomena in the Wolfenstein model are discussed: the nonconservation of CP and the $\Delta T = \frac{1}{2}$ rule for the lagrangian of the nonleptonic interaction with $|\Delta Y| = 1$. The consequences for interaction amplitudes with $\Delta T = \frac{1}{2}, \frac{3}{2}$, and $\frac{5}{2}$ and the effects of the observed probability of the $K_2^0 \to 2\pi$ decay on the corrections to the CP-nonconserved amplitudes are considered. (M.J.T.)

**2799** THE SCATTERING OF ELECTRONS ON PARTICLES WITH HIGHER SPINS. Dubovik, V. M. (Lebedev Inst. of Physics, Moscow). Yadern. Fiz., 2: 487-95(Sept. 1965). (In Russian).

The general parametrization method for relativistic matrix elements is used to obtain an expression for the cross section for the scattering of relativistic electrons on particles with arbitrary integral or half-integral spins. The choice and normalization of form factors are discussed. (auth)

**2800** ON THE OSCILLATOR MODEL FOR ELEMENTARY PARTICLES. Manko, V. I. (Lebedev Inst. of Physics, Moscow). Yadern. Fiz., 2: 512-16(Sept. 1965). (In Russian).

It is shown that it is possible to interpret the symmetry properties of baryons (following from the unitary symmetry hypothesis) on the basis of a model consisting of two three-dimensional oscillators with different frequencies. The following relation between the masses is obtained in this model: $Y^* - \Sigma = \Xi^* - \Xi$. A unitary octet, singlet, and 27-plet with masses in the region 1.6 Bev are predicted. The problem of multiplet mixing is discussed. (auth)

**2801** ELECTROMAGNETIC DECAYS AND THE MASS-SPLITTING OF VECTOR MESONS IN UNITARY SYMMETRY. Tao, Wong-tyk; Nguyen Van Hieu (Joint Inst. for Nuclear Research, Dubna, USSR). Yadern. Fiz., 2: 529-32(Sept. 1965). (In Russian).

The possibility of determining the mass renormalization constant for the unitary octet vector mesons, on the basis of an investigation of the neutral vector meson decay into $\mu^+\mu^-$ and $e^+e^-$ pairs, is treated. (auth)

**2802** UNITARY AND SPIN CONTENT OF SU(6) SUPERMULTIPLETS. Pereiomov, A. M.; Popov, V. S.; Malkin, I. A. (Inst. of Theoretical and Experimental Physics, Moscow). Yadern. Fiz., 2: 533-42(Sept. 1965). (In Russian).

A method is developed, making it possible to determine the unitary multiplets with given spin contained in an SU(6) supermultiplet. A table is given for the reduction of all the SU(6) representations given by Young patterns with the total number of boxes f = 3, 6, and 9. The SU(6) supermultiplets are reduced to Wigner multiplets with fixed hypercharge and $\Lambda$-quark spin: $SU(6) \to SU(4) \otimes SU(2) \otimes U(1)$. A table for the reduction of the Kronecker product of the simplest SU(6) representations is given. (auth)

**2803** FORM FACTORS AND INTERACTION CONSTANTS FOR THE 56-PLET OF THE GROUP SL(6). Nguyen Van Hieu; Smorodinskii, J. A. (Joint Inst. for Nuclear Research, Dubna, USSR). Yadern. Fiz., 2: 543-51(Sept. 1965). (In Russian).

The structure of vector- and axial-current matrix elements between states of the 56-plet in the SL(6) symmetry group is investigated. It is shown that these matrix elements depend on six independent form factors $f_i(t)$. The matrix elements of a number of electromagnetic and weak interaction processes and also meson-baryon strong-interaction vertex functions are expressed in terms of these form factors. (auth)

**2804** A GENERAL METHOD FOR CALCULATIONS WITH PHENOMENOLOGICAL AMPLITUDES. Kolkunov, V. A. (Inst. of Theoretical and Experimental Physics, Moscow). Yadern. Fiz., 2: 565-9(Sept. 1965). (In Russian).

The calculation of total cross sections, lifetimes, and other quantities is considered for processes described phenomenologically. It is shown that in such a case any multiple integral can be reduced to a simple one, which can easily be estimated analytically. (auth)

**2805** ON REPRESENTATIONS OF THE ROTATION GROUP WITH COMPLEX SPIN. Sannikov, S. S. Yadern. Fiz., 2: 570-81(Sept. 1965). (In Russian).

Representations of the rotation group corresponding to an arbitrary real or complex spin $\lambda$ are considered. The main features of these representations are their irregularity and multivaluedness. Irreducible representations are realized in infinitely dimensional spaces with indefinite metric and weak topology. The considered representations are unitary in an indefinite metric. The representations are realized as analytic functions of a complex variable by functions on the group (the matrix element) and also as functions on a sphere. The Clebsch–Gordan coefficients for the reduction of direct products of representations are found. (auth)

**2806** ON THE BARYON CHARGE DEGENERACY IN THE QUARK MODEL WITH EVEN-CHARGE MESONS. Okun, L. B. (Inst. of Theoretical and Experimental Physics, Moscow). Yadern. Fiz., 2: 582(Sept. 1965). (In Russian).

The compound model in SU(6) symmetry in which fundamental fermions (quarks) interact via exchange of neutral scalar mesons $\phi$ is considered. It is emphasized that in this model there is a strict degeneracy between states with different values of baryon charge. This degeneracy is associated with the fact that the $\phi$-meson interaction lagrangian is invariant with respect to the charge conjugation of each of the three quarks. The diquark systems of interactions of one quark with another quark or its antiparticle are treated as examples. (M.J.T.)

**2807** ON CERTAIN MASS FORMULAS IN THE QUARK MODEL. Azimov, Ya. I.; Anisovich, V. V.; Ansel'm, A. A.; Danilov, G. S.; Dyatlov, I. T. (Ioffe Inst. of Physics and Tech., Leningrad). Yadern. Fiz., 2: 583-4(Sept. 1965). (In Russian).

Relations between masses of particles, arising in the nonrelativistic quark model, are examined and compared with mass formulas derived using SU(6) symmetry. The formula $\frac{1}{2}(\Xi - N) = 3(\eta - K)$, obtained in the framework of a simple potential model, and the Gell-Mann-Okubo formula are discussed. Relations between the electromagnetic mass differences of the pion and kaon and of the K* and $\rho$ resonances are derived in the quark model, and the value of the constant in them is examined. (M.J.T.)

**2808** THE CONVERGENCE BEHAVIOUR OF EXPANSIONS IN THE CLASSICAL COLLISION THEORY. Leibfried, G.; Plesser, Th. (Technische Hochschule, Aachen). Z. Physik, 187: 411-20(1965).

In the classical collision theory the scattering angle $\vartheta$ depends on the impact parameter b and on the kinetic energy $E_r$ of the relative motion. This angle $\vartheta$ (b, $E_r$) is expanded for two limiting cases: (1.) Expansion in powers of the potential $V(r)/E_r$ (momentum approximation). (2.) Expansion in powers of the impact parameter b (central collision approximation). The radius of convergence of the series, which depends on b and $E_r$, is given for various potentials V(r). For case 1 a b-dependent criterion is deduced for the alternating of the series. Then the error is smaller than the first neglected term. (auth)

**2809** OBSERVATIONS ON THE QUANTUM STATISTICAL RING SUM OF A SYSTEM OF PUNCTIFORM CHARGE CARRIERS. Kelbg, G. (Universitaet, Rostock, Ger.). Z. Physik. Chem. (Leipzig), 229: 167-72(1965). (In German).

The Slater sum and the quantum statistical ring sum of a system of charged particles were determined without consideration of the symmetry effect. The relation of the theory developed in a work by De Witt to the pseudopotential method was also found. (tr-auth)

**2810** ON THE PERMISSIBLE RATE OF DECREASE OF THE FORWARD SCATTERING AMPLITUDE AT HIGH ENERGIES. Wit, R. (Joint Inst. for Nuclear Research, Dubna, USSR). Zh. Eksp. Teor. Fiz., 49: 538-41(Aug. 1965). (In Russian).

The permissible rate of decrease of the forward scattering amplitude is estimated on basis of the Phragmén-Lindelöf theorem and theory of the Herglotz functions. As an example of application of the results a proof is presented of the incompatibility of the two-particle unitarity condition and analyticity in the Lie model. (auth)

**2811** THREE-PARTICLE PARTIAL AMPLITUDES AND THE UNITARITY CONDITIONS FOR COMPLEX VALUES OF THE ANGULAR MOMENTA. Azimov, Ya. I.; Anselm, A. A.; Gribov, V. N.; Danilov, G. S.; Dyatlov, I. T. (Ioffe Inst. of Physics and Tech., Leningrad). Zh. Eksp. Teor. Fiz., 49: 549-71(Aug. 1965). (In Russian).

On basis of some of the simplest Feynman diagrams the possibility is investigated of analytically continuing the partial amplitudes for transition of two particles into three to complex values of the total angular momentum j. The unitarity conditions with respect to energy of the two produced particles are set up and their properties are studied. The properties of the three-particle contribution to the unitarity condition for the scattering amplitude are discussed for complex values of j in connection with the appearance of Mandelstam branching points. (auth)

**2812** A CHARACTERISTIC OF THE GENERALIZED FREE FIELD. Vasil'ev, A. N. (Leningrad State Univ.). Zh. Eksp. Teor. Fiz., 49: 781-3(Sept. 1965). (In Russian).

A transformation of local field is considered which consists in transition from a field $\varphi(p)$ to the field $\varphi_a(p) = a(p^2)\varphi$, where $a(p^2)$ is an infinitely differentiable power growth function and $\varphi(p)$ is a field operator in the momentum representation. If a is not a polynomial, then the field $\varphi_a$ in the general case is nonlocal. However, if $\varphi(p)$ decreases at a sufficient rate for $|p^2| = |p_0^2 - \vec{p}^2| \to \infty$ (in particular as $\exp[-\mu|p^2|]$ for a certain $\mu > 0$), then the field $\varphi_a$ is local for any a and in this case the initial field $\varphi$ may only be a generalized free field. (auth)

**2813** FOCUSING SINGULARITY IN p-SPACE OF CONSTANT CURVATURE. Mir-Kasimov, R. M. (Joint Inst. of Nuclear Research, Dubna, USSR). Zh. Eksp. Teor. Fiz., 49: 905-13(Sept. 1965). (In Russian).

It is shown that the focusing singularity encountered in field theory for p-space of constant curvature can be removed if the S-matrix is set up in accordance with the group of motions of this space. (auth)

**2814** INTERACTION OF ELECTROMAGNETIC WAVES IN A PARTIALLY IONIZED GAS [Thesis]. Oakes, Melvin Ervin Louis. Tallahassee, Florida State Univ., 1964. 134p.

The effect of inelastic collisions on the theory of the interaction of electromagnetic waves in a partially ionized gas with properties approximating those of the lower ionosphere was studied. By using the Boltzmann transport equation with an appropriate inelastic term, the energy balance equation for the electrons is derived. On the assumptions that the isotropic part of the electron distribution function is Maxwellian and that the only inelastic effect of importance is rotational excitation of $N_2$, an equation describing the behavior of the electron temperature is determined. The solution of this equation is discussed. For the high-frequency case the equation admits double values for the electron temperature. There is also an instability in the electron temperature similar to that obtained by Gurevich for a strongly ionized gas in the low frequency limit. The rate of energy loss by the electrons in exciting the rotational states is found to be of the same order of magnitude as that found by ionospheric cross modulation experiments. The reflection of an electromagnetic wave from the boundary of a weakly ionized gas, through which a strong amplitude modulated electromagnetic wave is passing, is also investigated. (Dissertation Abstr.)

**2815** VARIATIONAL BOUNDS FOR MULTI-CHANNEL SCATTERING [Thesis]. Sugar, Robert Louis. Princeton, N. J., Princeton Univ., 1964. 65p.

Variational principles are presented, which give upper and lower bounds on all elements of the reactance matrix in potential scattering. The bounds on the reactance matrix lead to bounds on the elastic and inelastic cross sections. Single channel, multichannel, and multiparticle processes are considered. Examples are presented including upper and lower bounds on the s-wave phase shift for electron-hydrogen scattering. (Dissertation Abstr.)

**2816** QUANTUM MECHANICAL APPROACH TO STRONG INTERACTIONS [Thesis]. Susskind, Leonard. Ithaca, N. Y., Cornell Univ., 1965. 74p.

The bootstrap theory is examined from a quantum mechanical viewpoint. A Hilbert space is constructed in which each particle is a bound state of other particles. The mode of description of such a Hilbert space is in terms of a "pseudo basis" describing free but physical particle states. The self-consistency of such a theory is examined, and bootstrap equations are derived from the condition that the bound states of the system be exactly those states that go into the formulation of the Hilbert space. It is then shown that these equations have group theoretical solutions in which the particles obey a symmetry such as $SU_2$ or $SU_3$. (Dissertation Abstr.)

**2817** EFFECTS OF $\pi$ AND $\rho$ EXCHANGE IN THE PERIPHERAL MODEL OF ISOBAR PRODUCTION [Thesis]. Resnick, Lazer. Ithaca, N. Y., Cornell Univ., 1965. 65p.

The production of the $J = 3/2$, $T = 3/2$ isobar in proton–proton collisions from 2 to 10 Bev is examined in the framework of the peripheral model. The model in which the isobar is treated as an elementary particle of spin $3/2$ is found to give a qualitatively wrong angular distribution. The Ferrari-Selleri model for $\pi$ exchange is ex-

amined and the continuation of the $N\pi \rightarrow N\pi$ scattering amplitude off-shell is rederived. The off-shell total amplitude is found to be proportional to the off-shell Born term, and it is noted that the partial wave projection of the latter must be treated more carefully than heretofore. This model is found to give a qualitatively correct angular distribution and reasonable energy dependence for isobar production, though a phenomenological form-factor is still required to allow a fit to experiment. This form-factor is somewhat steeper than that found before but again there is no evidence of energy dependence. The contribution of $\rho$-exchange in this peripheral model is then examined. The formulation is in terms of helicity amplitudes; and off-shell helicity amplitudes for $N\rho \rightarrow N\pi$ defined, and an equation for them is derived. This is solved in approximation to give a result analogous to the case for $N\pi \rightarrow N\pi$. Using the hypothesis of a universal vector current to which the $\rho$ couples, the $\rho$-exchange contribution is calculated. It is found to be very rapidly increasing with the energy and already in disagreement with known experimental data between 2 and 10 Bev. (Dissertation Abstr.)

**2818** HIGH ENERGY BEHAVIOR OF THE SCATTERING AMPLITUDE FOR CROSSED-BOX LADDER GRAPHS IN THE BETHE-SALPETER EQUATION [Thesis]. Kubis, Joseph John. Princeton, N. J., Princeton Univ., 1964. 71p.

The Bethe-Salpeter scattering amplitude for crossed-box ladder graphs in the $\phi^3$ theory with scalar particles is asymptotic to $t^{-l}$ for high values of t, the energy variable in the crossed channel. The integral equation for the partial-wave amplitude with positive signature has a convergent Fredholm solution in the right half l-plane, Re $l > -\frac{3}{2}$, except for an essential singularity at $l = -1$. The leading term in the kernel is a pole at $l = -1$ with a non-separable residue, which leads to an infinite number of poles clustered around $l = -1$ in the dominant part of the solution. This is the "Gribov disease," caused by a non-zero spectral function $\rho(u,t)$. In the weak coupling limit the trajectory of the right-hand-most pole in the cluster is expressed in dispersion form by using two-particle unitarity. (Dissertation Abstr.)

**2819** THE VALIDITY OF THE THOMAS-FERMI MODEL OF FINITE NUCLEAR MATTER [Thesis]. Peressini, Eugene Ramon. Los Angeles, Univ. of Southern California, 1965. 142p.

The validity of the Thomas-Fermi approximation as applied to nuclear type many-body distributions is established. Some validity criteria are obtained, which specify the relationships between the distribution's Fermi energy, binding energy of the last particle, and slope of the binding potential necessary to insure that the Thomas-Fermi model gives an accurate surface order description of the system. The decisive quantity in these relations is the ratio, $k/(dV/dx)^{\frac{1}{3}}$, thus a potential that has a sharp surface region (such as the nuclear potential) appears much more gradual when viewed from momentum space. When these criteria are satisfied, the Thomas-Fermi estimate of many of the bulk properties of the distribution is quite accurate because of a systematic compensation of single particle errors. Attention is also given to the applicability of some general correction schemes previously proposed to improve the Thomas-Fermi model. The discussion is restricted by averaging over the small wave mechanical oscillations that occur in the distribution. It is shown that the Thomas-Fermi solution is exactly this average solution in the harmonic oscillator potential limit, which indicates that the Weizsäcker correction cannot be generally valid since it predicts a non-vanishing correction for this potential. A new first-order correction to the Thomas-Fermi density matrix, valid for potential wells near to the harmonic oscillator, is obtained, which is not of the Weizsäcker form and which does vanish for the harmonic oscillator well. Finally, the Thomas-Fermi model is used to describe the surface order properties of finite nuclear matter using a reasonable pseudo-potential form to describe the nucleon two-body potential. (Dissertation Abstr.)

# Fluid Physics and Thermodynamics

**See also Plasma Physics and Thermonuclear Processes**

**2820** (AD-614645) ON THE HYDROMAGNETIC STABILITY OF A LIQUID LAYER UNDER THE ACTION OF A MAGNETIC FIELD AND A GRAVITATIONAL FORCE. Urrutia, Jose Luis; Change, I-Dee (Stanford Univ., Calif. Dept. of Aeronautics and Astronautics). Feb. 1965. Contract Nonr22530. 61p. (SUDAER-218). CFSTI $3.00 cy, $0.75 mn.

An analytical study was made on the stability of an electrically conducting liquid layer subjected to a gravitational field and a magnetic field. The main purpose was to determine the effect of a magnetic field on the stability criteria of the layer. (TAB)

**2821** (AD-618296) RESEARCH ON MAGNETOGASDYNAMICS. Final Scientific Report. Pack, D. C. (Strathclyde Univ., Glasgow (Scotland). Dept. of Mathematics). Feb. 15, 1965. 7p. (AFOSR-65-1069). CFSTI $1.00 cy, $0.50 mn.

An analysis was made of the rectilinear, adiabatic but non-isentropic, unsteady flow of a perfectly conducting ideal gas moving in the presence of a transverse magnetic field. Detailed properties of certain generalized simple waves were obtained. The upstream influence effects in the flow of a perfectly conducting fluid over an insulating wall were found on the basis of linearized theory. The question of the physical realization of the solutions found by Cabannes for flow of perfectly conducting gas past a wedge in a magnetic field aligned with the stream was examined by a combination of analytical and heuristic arguments. Magnetogasdynamic deflagrations under the Chapman-Jouguet condition were studied and work was initiated on similarity solutions for cylindrical magnetogasdynamic detonations and flames. (auth)

**2822** (AWRE-O-60/65) AN INVESTIGATION OF THE PRESSURE WAVE PROPAGATED FROM THE OPEN END OF A 30 x 18 IN. SHOCK TUBE. James, D. J. (Atomic Weapons Research Establishment, Aldermaston (England)). Sept. 1965. 46p. Dep.; BIS $1.60; HMSO 8s. 0d.

Experiments carried out to measure the shock wave and its associated air flow propagated from the open end of a 30 × 18 in. shock tube are described. These measurements were taken for four different shock wave overpressure levels inside the tube ranging from 10–38 psi. From these measurements an estimate is made of the shock parameters from a 50 psi wave in the tube. (auth)

**2823** THE ENERGY POOL IN MAGNETOHYDRODYNAMICS. Sexl, Theodor (Universitaet, Vienna). Acta Phys. Austriaca, 19: 356-60(1965). (In German).

The energy balance in magnetohydrodynamics was formulated. The total energy in a stationary volume was then altered so that energy flows through the closed envelope of the random volume and magnetic energy was transformed into heat in the volume itself. (tr-auth)

**2824** AN MHD CHANNEL FLOW WITH TEMPERATURE DEPENDENT ELECTRICAL CONDUCTIVITY. Heywood, John B. (Massachusetts Inst. of Tech., Cambridge). AIAA (Am. Inst. Aeron. Astronaut.) J., 3: 1752-4(Sept. 1965).

It is demonstrated by analyzing a particularly simple model how peculiar velocity distributions can occur in magnetohydrodynamic channel flows even when the temperature distribution is approximately parabolic and the effect of the MHD terms in the energy equation is small. This is in contrast to previous work where velocity overshoots are a direct result of temperature overshoots inside the boundary layer. A channel flow is chosen as the model since at high Hartmann numbers this illustrates several features of a boundary layer in that viscous forces are only important close to the channel walls. The steady, fully

developed flow of an electrically conducting gas through a channel of rectangular cross section is considered. (J.F.P.)

**2825** PRECISION MEASUREMENTS OF THE TOWNSEND ENERGY RATIO FOR ELECTRON SWARMS IN HIGHLY UNIFORM ELECTRIC FIELDS. Crompton, R. W.; Elford, M. T.; Gascoigne, J. (Australian National Univ., Canberra). Australian J. Phys., 18: 409-36(Oct. 1965).

A detailed account is given of the solution to the problems associated with the use of the Townsend-Huxley method of measuring the ratio of drift speed to diffusion coefficient for very low energy electron swarms. The elimination of radial components of the electric field within the diffusion chamber is shown to be the major experimental problem, especially in the case of the comparatively weak electric fields which must be used for some of the measurements in the near-thermal region. The experimental techniques and procedures, which are described in some detail, enable measurements to be made in this region with an accuracy comparable to that which has been achieved at higher electron energies. (auth)

**2826** PLASMA EFFECTS, MULTIPLICATION AND SECONDARY EMISSION OF ANOMALOUS HYDROGEN GLOW DISCHARGES. Wieczorek, L. W.; Hnatzsche, E. (Physikalisch-Technisches Institut der Deutschen Akademie der Wissenschaften, Berlin). Beitr. Plasmaphysik, 5: 254-8(1965). (In German).

On the basis of statistical calculations of the anomalous cathode drop in $H_2$ for voltages between 0.2 and 10 kv, the $\Gamma$, $\Delta$, and M were obtained with the incorporation of steady state conditions. It was shown that in the distribution function the ions of both atomic and molecular ions must be considered. A new interpretation of the measurements of Heisen and Welenhofer with plausible values for $\Gamma$ and $\Delta$ is given. (J.S.R.)

**2827** THERMODYNAMIC FLUID IN THE JORDAN-THIRY THEORY. Pigeaud, Pierre; Lichnerowicz, Andre. Compt. Rend., 261: 893-6(July 1965). (In French).

The concept of dynamic fluids developed by Pham Mau Quan is integrated exactly in the framework of the pentadimensional theory, taking into consideration the introduction of two metrics in $V_5$. After a choice of energy tensor density making it possible to recover the equations of motion correctly in conform metrics of $V_4$, it is shown that this choice corresponds to a particularly simple expression of the source tensor of the $\Theta_{\alpha\beta}$. The continuity equation, which is expressed explicitly in terms of conform metrics in the quotient variety, is reduced to the relativistic equation if the electromagnetic phenomena are neglected. (tr-auth)

**2828** SPONTANEOUS RADIATION-EMISSION FLUCTUATIONS OF GAS DISCHARGES AND THEIR MEASUREMENT USING A SUITABLE RADIATION DETECTOR. Gubler, W.; Strutt, M. J. O. (Swiss Federal Inst. of Tech., Zurich). Electron Letters, 1: 152-3(Aug. 1965).

The equations describing the spontaneous fluctuations of photon radiation are given by Bose-Einstein statistics. These equations are applied to calculate the statistical fluctuations of photon radiation emitted by a nonhomogeneous plasma. By using a photodetector, the radiation fluctuations are transformed into corresponding output-current fluctuations. The detector must have special properties of sensitivity, noise, frequency response and transmission characteristics. The InSb photodetector described here has the required properties. (auth)

**2829** RELATIVISTIC VARIATIONAL PRINCIPLE FOR A CHARGED HYDROMAGNETIC COMPRESSIBLE FLUID. Sharma, S. R.; Sharma, N. K. (Univ. of Rajasthan, Jaipur, India). Indian J. Theor. Phys., 11: 39-46 (June 1963).

A relativistic energy principle for a charged, hydromagnetic, non-viscous and compressible fluid has been formulated in arbitrary coordinates. The variations of the variational parameters yield the equations of continuity, field equations and the equations of the fluid flow for the relativistic charged fluid. (auth)

**2830** RECENT STUDIES OF THE CLASSICAL ELECTRON GAS. Carley, D. D. (Univ. of Florida, Gainesville; Western Michigan Univ., Kalamazoo). J. Chem. Phys., 43: 3489-96(Nov. 15, 1965).

Radial distribution functions are computed for classical particles interacting with Coulomb, shielded Coulomb, and truncated Coulomb forces. The methods used to obtain these distribution functions include the Percus-Yevick and convolution hypernetted-chain-integral equations, the Monte Carlo method, the Debye-Hückel equation, and the perturbation methods of Lado and of Broyles and Sahlin. Comparisons between these methods indicate that for the Coulomb and the shielded Coulomb interactions the Debye-Hückel approximation is quite good for values of $\theta > 3.0$; $\theta = kTa/q^2$, where a is the ion-sphere radius. For values of $\theta < 1.0$ the error in the Debye-Hückel approximation increases rapidly with decreasing $\theta$. The Lado perturbation equation is an improvement over that of Broyles and Sahlin for small separation distances. The solutions obtained cover a range in $\theta$ from 0.4 to 20.0. (auth)

**2831** A SIMPLE DEMONSTRATION OF THE HARTMANN LAYER. Heiser, W. H. (Massachusetts Inst. of Tech., Cambridge); Shercliff, J. A. J. Fluid Mech., 22: 701-7(Aug. 1965).

The theory of the motion of a finitely conducting, viscous liquid between long, concentric, rotating cylinders under a radial magnetic field in the case of high Hartmann number is given. Because the current and vorticity contents of a Hartmann layer are related, it is easy to predict the behavior in both steady and unsteady states. Experiments with mercury which confirm the theory closely are described. (auth)

**2832** MICROCANONICAL ENSEMBLE IN QUANTUM STATISTICAL MECHANICS. Griffiths, Robert B. (Carnegie Inst. of Tech., Pittsburgh). J. Math. Phys. (N. Y.), 6: 1447-61(Oct. 1965).

The infinite-volume limit of thermodynamic functions calculated in the quantum microcanonical ensemble is shown to exist for a fairly wide class of spin systems and quantum gases. The entropy is set equal to the logarithm of the number of eigenstates in an energy interval which increases linearly with the size of the system, but is otherwise arbitrary. The limiting entropy per unit volume agrees with that calculated in the canonical formalism, and possesses certain convexity properties required for thermodynamic stability. A precise criterion, in terms of the energy spectra of large systems, is given for determining the limit of the thermodynamic entropy as the temperature approaches zero. This is not determined by the degeneracy of the ground state, contrary to the discussion of the "third law of thermodynamics" found in some textbooks. (auth)

**2833** MAGNETIC PROPERTIES OF CHARGED IDEAL QUANTUM GASES IN n DIMENSIONS. May, Robert M. (Univ. of Sydney). J. Math. Phys. (N. Y.), 6: 1462-8(Oct. 1965).

The mathematical model of an ideal gas of charged bosons or fermions in an n-dimensional space is considered, treating n as a continuous variable. The investigation shows the extent to which the magnetic behavior depends on the dimensionality of the system. In particular, the charged Bose gas in a homogeneous magnetic field does not condense unless $n > 4$, in contrast to the field-free gas which condenses for $n > 2$: however so long as $n > 2$ and $T < T_c$ this system completely expels homogeneous magnetic fields weaker than a certain critical field, $H_c$. ($T_c$ is the field free transition temperature.) This field expulsion comes explicitly from the condensed ground-state bosons for $n > 4$; but it is still present, and $H_c$ has the same form, for $4 > n > 2$ where there is no condensation. (auth)

**2834** HYDROMAGNETIC SWITCH-ON SHOCKS. Sarason, Leonard (New York Univ., New York). J. Math. Phys. (N. Y.), 6: 1508-18(Oct. 1965).

In one-dimensional hydromagnetic flow, switch-on shocks have been shown to be nonevolutionary, e.g., by Syrovatskii. Such shocks, however, may be considered as

a superposition of a switch-on shock and an Alfvén shock, and some results of such an assumption are examined. If the two shocks remain superimposed, the shock pair is, in fact, evolutionary. If the pair splits under the influence of incoming waves, a first-order nonlinear analysis indicates that highly stable situations can occur. But there is a non-uniqueness implicit in the ansätz, and the possibility that a solution always exists which is stable except between shocks cannot be excluded. (auth)

**2835** EXPERIMENT OF GASEOUS BREAKDOWN IN A LONGITUDINAL MAGNETIC FIELD. Nakamura, Sadao; Mitani, Kenji (Kyoto Univ.). J. Phys. Soc. Jap., 20: 1722 (Sept. 1965).

The formative time lag of breakdown was investigated in a low pressure neon discharge in magnetic fields of 0 to 700 gauss. The graphical relation obtained between the formative time lags and the magnetic field intensity is shown to agree fairly well with theory. (L.B.S.)

**2836** ANALOGUE COMPUTATION OF INSTABILITY GROWTH RATES IN FINITE CONDUCTIVITY MAGNETO-HYDRODYNAMICS. Kontos, J. (Nuclear Research Center Democritus, Athens). Nucl. Fusion, 5: 162-3(June 1965).

The application of analog computer methods is demonstrated for the study of magnetohydrodynamic equilibrium problems involving cylindrical coordinates and finite conductivity. It is shown by comparison with numerical results that a satisfactory estimate can be obtained for instability growth rates. (L.B.S.)

**2837** CO-OPERATIVE MODES OF MOTION IN SIMPLE LIQUIDS. Chen, S. H.; Eder, O. J.; Egelstaff, P. A.; Haywood, B. C. G.; Webb, F. J. (Atomic Energy Research Establishment, Harwell, Eng.). Phys. Lett., 19: 269-71(Nov. 1, 1965).

The differential cross section was measured for the scattering of cold neutrons by four liquids each having appreciable coherent scattering. The liquids are neon, argon, deuterium, and carbon tetrafluoride. The differential cross sections for each liquid are plotted against the neutron wavelength. For each of these liquids coherent effects are visible in the form of discrete peaks in the differential cross sections whose position and magnitude vary strongly with scattering angle. It is shown from the results that in the simplest liquids cooperative motions of the molecules are sufficient to produce coherent inelastic scattering phenomena similar to those observed in liquid metals and polycrystalline solids. (J.F.P.)

**2838** RELATIVISTIC GENERALIZATION OF PLASMA WAVES THEORY IN THE MAGNETOHYDRODYNAMIC APPROXIMATION OF TWO FLUIDS. Deutsch, R. V. Rev. Roumaine Phys., 10: 531-6(1965). (In Russian).

The base equations of two-fluid magnetohydrodynamics were formulated in a covariant form. As the basis of these equations, the problem of the propagation of weak monochromatic waves was studied. The dispersion equation obtained can be written in a form identical to that obtained in the usual two-fluid magnetohydrodynamics, but the expressions of characteristic frequency are different. There exists therefore the possibility of generalizing the results of two-fluid magnetohydrodynamics to relativistic waves. (tr-auth)

**2839** CUMULATION OF ENERGY AND ITS BOUNDARY. Zababakhin, E. I. Usp. Fiz. Nauk, 85: 721-6(Apr. 1965). (In Russian).

Several cases of unbounded cumulation are reviewed. This is defined as a process in which the energy density increases spontaneously without limit, and shows that dissipation phenomena (viscosity, thermal conductivity) do not always limit the growth of energy. On the other hand, it is shown that in those cases where stability analysis of the cumulation process can be made the growth of the cumulated energy density is always limited by instability. A hypothesis is therefore advanced that any unbounded cumulation is of necessity unstable and furthermore that the instability results not merely in a modification of the cumulation but in its complete cessation. The cumulation phenomena analyzed are the filling of bubbles in liquids, converging shock waves, and converging electromagnetic shock waves (both cylindrical and conical). The instability of cumulation is analyzed using as an example a thin cylindrical shell of an ideal liquid, moving toward the axes and rotating slowly. It is shown that in this case a small perturbation eliminates the unbounded cumulation, but the smaller the cumulation the larger the attained energy density. It is pointed out that no examples proving or disproving the advanced hypothesis have yet been found, although a connection is indicated between this hypothesis and certain studies of the possible collapse of the universe, and also the pinch effect in pulsed discharges in gases. (ATD)

**2840** ON THE THEORY OF GAS HEATING IN AXIALLY SYMMETRIC WALL-STABILIZED LUMINOUS ARCS. I. VARIOUS SOLUTION METHODS. Patt, H. J.; Schmitz, G. (Technische Hochschule, Aachen). Z. Physik, 188: 1-22(1965). (In German).

The properties and the dependence upon parameters of those quantities are investigated, which are characteristic for the gas-heating process in electric arcs with axial gas flow. Starting with the equations of the one-fluid-model of plasma physics three methods are derived, to calculate analytically or numerically the thermal and electrical entities of the inlet region of the arc. With these results expressions can be given for the thermal and electrical inlet length. Further the azimuthal component of the velocity and its inlet length are determined. (auth)

**2841** RELATIVISTIC FREE MOLECULE FLOW [Thesis]. Softley, Eric James. Providence, Brown Univ., 1964. 85p.

The effects of particles that form a very rarefied gas impacting on a typical physical surface are examined in the framework of the theory of special relativity. The integrated momentum and energy transfer to the surface are obtained, valid for all relative velocities and kinetic temperatures. A simple monatomic (point mass) gas is assumed. The Minkowskian coordinate system is introduced and the relativistic distribution function written in this coordinate system. The effects of particles striking the physical surface are obtained by integration. The integrations are discussed in both the gas system (with the observer at rest in the gas) and the body system. It was possible, in general, to integrate only in the gas system. The transformation to the body system was derived and applied to bring the results for the incident particle to a physically significant system. Two possible limits for the re-emitted particles are chosen, the specular limit and the purely diffuse limit, and the integrated momentum and energy to the body are obtained for these two cases. Discussion of the results and comparisons with non-relativistic results is made for selected cases, including the "stagnation" region, with the flow normal to the surface. When the non-dimensional velocity of the gas relative to the body, $\alpha$ (the ratio of the velocity to that of light), is close to unity it is possible to distinguish the leading terms for the momentum and energy transfer. It is shown that even though the momentum and heat transfer to a body traveling through this simple gas may become infinitely large as $\alpha$ approaches unity they do so such that when $\alpha$ is 0.9 the factors are approximately half an order of magnitude. (Dissertation Abstr.)

**2842** IONIZATION, ELECTRON ATTACHMENT, AND INELASTIC COLLISIONS IN THE MICROSCOPIC THEORY OF MOLECULAR AND IONIZED GASES [Thesis]. McCormack, Francis Joseph. Tallahassee, Florida State Univ., 1964. 170p.

The classical kinetic theory of molecular and ionized gases is extended to include ionization, electron attachment, and inelastic collisions. The scattering probabilities for ionization, attachment, and inelastic collisions are defined and evaluated. In terms of these, the collision integrals in the Boltzmann and Maxwell transport equations are determined in a form convenient for detailed calculations involving these terms. For the case of molecular gases it is shown how the inelastic scattering probabilities can conveniently be used to express the principles of de-

tailed balancing and microscopic reversibility. This scattering probability is also employed to obtain a general expression for the rate of exchange of energy between two gases colliding inelastically, which is valid for arbitrary particle masses and inelastic cross sections and collision frequencies. By expanding the scattering probabilities in the collision term in a Taylor series, an approximate form of the Boltzmann equation for slightly ionized gases in the presence of a time-dependent electric field is obtained, which takes into account electron–molecule or ion ionization, attachment, and inelastic collisions. The inelastic collision term is obtained for arbitrary collision frequency, and it is shown how this expression can be simplified under the assumption of a low inelastic collision frequency, or low molecular excitation energy of the electrons, or both. Assuming a low inelastic collision frequency it is shown how the differential equation for the isotropic part of the electron distribution can be derived without recourse to the principle of detailed balancing, the latter being strictly valid only for equilibrium conditions. By making both the above assumptions and further assuming a low inelastic energy transfer, a formal solution of this equation is effected by an iterative procedure. The solution indicates explicitly that inelastic collisions are responsible for a small correction term to the distribution function, which would be obtained if one considered only elastic collisions. Finally, it is pointed out how one can determine the effects of ionization, attachment, and inelastic collisions on the general conductivity expression for a slightly ionized gas. (Dissertation Abstr.)

**2843** STATISTICAL MECHANICS OF AN ASSEMBLY OF QUASIPARTICLES. Girardeau, M. D. (Univ. of Oregon, Eugene). Phys. Rev., 140: A1139-40(Nov. 15, 1965).

The expressions obtained by Morita and Tanaka for the exact thermodynamic functions of an assembly of quasiparticles with diagonal interactions are rederived by a much simpler method due to Bogoliubov, Zubarev, Tserkovnikov, Wentzel, and others. (auth)

**2844** RELATIVISTIC SHOCK STRUCTURE. Koch, Paul A. (Columbia Univ., New York). Phys. Rev., 140: A1161-5(Nov. 15, 1965).

The equations for a relativistic fluid with viscous and thermal dissipation are discussed and are applied to a plane shock wave in ionized hydrogen. It is shown that if the shock velocity is greater than a critical value ($v/c > \sqrt{2/3}$ at low temperatures), the shock profiles show an increase in velocity or a decrease in the heat-transfer parameter $\gamma T$ at the upstream end of the shock layer. This qualitative change from the nonrelativistic case is due to the relativistic interaction of heat transfer and momentum transfer. (auth)

**2845** CALCULATION OF THE YANG-LEE DISTRIBUTION OF ZEROS. Byckling, Eero (Inst. of Tech., Otaniemi, Finland). Phys. Rev., 140: A1165-8(Nov. 15, 1965).

The connection between the zeros of the grand partition function Z and the function $\chi = \lim V^{-1} \ln Z$ at infinite volume is discussed. Assuming a functional equation for $\chi$ given, conditions for the lines containing zeros and an expression for the density of zeros are derived. Explicit results are given in a special case with an attractive interaction potential. (auth)

**2846** A CONTINUED-FRACTION REPRESENTATION OF THE TIME-CORRELATION FUNCTIONS. Mori, Hazime (Kyoto Univ.). Progr. Theoret. Phys. (Kyoto), 34: 399-416(Sept. 1965).

A continued-fraction expansion of the Laplace transform of the time-correlation functions is obtained, which enables us to express the generalized susceptibilities and the transport coefficients in terms of the static correlation functions of a set of quantities. This expansion has a different feature from the moment and cumulant expansions, and has a convenient form to introduce the long-time approximation as well as the short-time approximation. Its application to the anomalous relaxation and transport phenomena near the second-order phase transition points is discussed. An expansion formula is also obtained for the time evolution of dynamical quantities in order to describe the various modes of motion involved according to their characteristic time constants. These two expansions are closely related to the time-correlation function formalism of irreversible processes, and allow physical intuition in calculating dissipative properties. (auth)

# Geophysics

*Refer also to abstract 1789.*

**2847** (AD-614716) METHOD OF DETERMINING ALPHA = $n(H+)/n_e$ AND THE ION TEMPERATURE FROM MEASUREMENT OF PROTON-WHISTLERS. Report No. 65-9. Shawhan, Stanley D.; Gurnett, Donald A. (State Univ. of Iowa, Iowa City). Apr. 1965. Contract Nonr150906. 30p. CFSTI $2.00 cy, $0.50 mn.

A statement is made of the theory and of the formulas used to derive the concentration of H(+) ion relative to the electron concentration and the ion temperature from the measurement of proton-whistlers. The potential results are discussed of measuring proton-whistlers from all of the Injun III VLF data based on a preliminary study of local summer day and winter night. Other measurements are suggested that can be made on VLF data to obtain the concentrations of He(+) and O(+) relative to the electron density. (TAB)

**2848** (AD-615111) SUNSPOT CYCLE AND IONOSPHERIC STORMS. Environmental Research Papers. Cormier, Raymond J.; Smallwood, K. L. (Air Force Cambridge Research Labs., L. G. Hanscom Field, Mass.). Feb. 1965. 45p. (AFCRL-65-125). CFSTI $2.00 cy, $0.50 mn.

A study was made on ionospheric storms and the F(2) region electron density and nondeviative absorption variations accompanying them. Data for a year of medium (1960) and a year of low (1963) sunspot number are analyzed. An index of ionospheric storminess, which is an indicator of the amount of expansion and contraction of the h-f useful frequency spectrum caused by ionospheric sotrms, is also discussed. The data used are the amplitude recordings, made at Concord, Mass., of several WWV frequencies originating from Beltsville, Maryland. The path length involved is 590 km. Discussion is presented on: the usefulness and ease of calculation of the storm index; the apparent solar (cos x) control of the F(2) region during a year of low sunspot number; the absorption (mostly nondeviative) accompanying ionospheric and magnetic storms; the differences in average ionospheric storm variations between two years of the sunspot cycle; and the appearance or disappearance of a pronounced f(0)F(1) cusp on the Ft. Belvoir ionosonde data which indicate whether an ionospheric storm is accompanied by enhanced or depressed F(2) region electron densities. (auth)

**2849** GEOMAGNETICALLY TRAPPED RADIATION. Baker, M. B. (Douglas Aircraft Co., Inc., Santa Monica, Calif.). AIAA (Am. Inst. Aeron. Astronaut.) J., 3: 1569-79(Sept. 1965).

A comprehensive description is given of the trapped charged-particle environment that can be used to find the radiation doses to which a space vehicle will be exposed. The trapped radiation environment is also described, including a discussion of the sources and loss mechanisms, the dynamics of the particle motions, the sources of data, compilation techniques, and graphic displays of the fluxes. The fluxes and energy spectra integrated over sample trajectories are also presented. The detonation of the Starfish device is also described. (J.F.P.)

**2850** OBSERVATIONS OF THE NIGHT AIRGLOW (1 JULY 1957–31 DECEMBER 1959). Yao, I. G. (ed.). Ann. Int. Geophys. Yr., 24: 1-322(1962).

A series of tables is presented of hourly values of the absolute zenith intensity of the airglow, arranged according to station and wavelength. Tables are also included of

upper atmosphere emissions; OH bands in the airglow together with predicted intensities; and stations participating in the IGY–IGC airglow program. A brief discussion on instruments and procedures is presented. (L.B.S.)

**2851** AURORAL SPECTROGRAPH DATA. Carrigan, Anne; Devlin, James J.; Norman, S. J.; Oliver, J. (eds.). Ann. Int. Geophys. Yr., 25: 1-374(1964).

Data tabulations from the auroral patrol spectrograph program are presented. Data from twenty-nine stations which operated as part of the IGY programs of Canada, New Zealand, the Soviet Union, the United Kingdom, and the United States are included. A brief description is given of the control spectrograph instruments, which were distributed at various sites in the northern and southern hemispheres. A large number of spectrograms were obtained, which provided an almost continuous record of the night sky activity. (L.B.S.)

**2852** AURORAL MORPHOLOGY AS SHOWN BY ALL-SKY PHOTOGRAPHS. Akasofu, S.-I.; Kimball, D. S. (Univ. of Alaska, College). Ann. Int. Geophys. Yr., 38: 1-299(1965).

Results are presented of an intensive study of auroral morphology from the IGY all-sky auroral camera (asca) records obtained at more than one hundred stations distributed over both the Arctic and Antarctic. Two-hundred selections of photographs giving evidence for the conclusions drawn are also presented along with magnetic records and synoptic sketches of particular types of auroral distribution. The results yield significant information concerning planetary development of the auroral substorms that accompany the polar magnetic storms. A working model of simultaneous auroral activity over the entire polar region is proposed; the all-sky photographs are arranged on the basis of the model. (L.B.S.)

**2853** INFLUENCE OF NEGATIVE IONS ON DIFFUSION OF CHARGED PARTICLES IN LOWER IONOSPHERE. Ginzburg, E. I. (Novosibirsk Electrotechnical Inst. of Communication, USSR). Izv. Vyssh. Ucheb. Zavedenii, Radiofiz., 8: 626-7(1965). (In Russian).

The coefficient of diffusion of charged particles (electrons and positive and negative ions) in the lower ionosphere is calculated using the macroscopic equations to describe the motion of these particles, under the assumption that the particle concentration changes little over the mean free path length and during the time of free flight. A linearized system of these equations together with the equation for an arbitrary electric field is solved by expansion of the unknown functions in a Fourier integral. It is found that, if the effect of the negative ions on the diffusion is disregarded, the coefficient of diffusion is substantially lowered. (M.J.T.)

**2854** THE RELATION OF SPREAD-F ECHOES TO MAGNETIC DISTURBANCES. Briggs, B. H. (Univ. of Adelaide). J. Atmos. Terrest. Phys., 27: 991-4(Sept. 1965).

The correlation between the occurrence of spread-F echoes at Slough and the magnetic K-index is examined for a complete solar cycle. Cross-correlograms for the two quantities show that variations of occurrence of spread-F echoes lag by 0.5–2 days on variations of the K-index. It is shown that the K-index often shows a marked 27-day recurrence tendency, but that there is no such recurrence tendency for spread-F echoes. (auth)

**2855** SOLAR-TERRESTRIAL EVENTS IN RELATION TO THE PHASE OF THE SOLAR CYCLE. Das Gupta, M. K.; Basu, D. (Univ. of Calcutta). J. Atmos. Terrest. Phys., 27: 1029-32(Sept. 1965).

Solar-terrestrial events are investigated with respect to recent data. These include sunspots, calcium plages, solar flares, meter wave radio bursts (200 Mc), short wave radio fadeout, and geomagnetic storms. Some of the interesting results of the preliminary analysis are reported. Data from each of the individual events studied were divided into several classes depending on the magnitude of the activity. The criteria for the classifications are shown, and a tabulation of the results of the analysis is given. The general characteristics of these data are described, and it is found that the occurrences of outstanding and large sunspot groups and calcium plages as well as other outstanding events avoid, for the most part, the peak phase of solar activity. It is concluded that the effect, in general, must be of solar origin rather than any modulation effect in the sun-earth space. It is suggested that the highly disturbed sun and its atmosphere prevent the formation of very large centers of activity and hence the occurrence of any outstanding event during the peak phases of the solar cycles. (J.F.P.)

**2856** EFFECT OF SPACE CHARGE CONVECTION ON THE MAGNETIC FIELD TRANSITION TOWARDS THE PLASMA REGIME. Hosokawa, Iwao (National Aerospace Lab., Mitaka, Japan). J. Phys. Soc. Jap., 20: 1736-7(Sept. 1965).

In previous investigations of the pressure balance condition of a unidirectional rarefied plasma flow and a wall of magnetic field H, it was concluded that the magnetic field, whose direction is assumed to be invariant, should continually decrease from $H_0$ (field in the vacuum side) to zero towards the plasma regime through a very thin transition layer. The existence of a small amount of charge separation in the transition layer was assumed in order to prevent a large electric polarization. The problem is examined further, and an answer is given to the question of how much an effect of the space charge convection should arise on H and $H_0$. (L.B.S.)

**2857** A NEW SPECULATION ON TERRESTRIAL HELIUM LOSS. Ferguson, E. E.; Fehsenfeld, F. C.; Schmeltekopf, A. L. (National Bureau of Standards, Boulder, Colo.). Planet. Space. Sci., 13: 925-8(Oct. 1965).

A new mechanism for the loss of terrestrial helium is proposed. The mechanism involves the reaction $He(2^3S) + O \rightarrow He + O^+ + e$. This reaction is very likely the dominant helium metastable loss process in the atmosphere. It is speculated that the excess of the reaction, 6.2 ev, may go largely to the helium atom as kinetic energy, in view of recently reported experiments on similar reactions. The production rate of $He(2^3S)$ metastables is about that of neutral helium in the earth's atmosphere, $\sim 10^6$ atoms/cm$^2$ sec so that this mechanism could lead quantitatively to a steady state terrestrial helium atmosphere. No other satisfactory mechanism for this has yet been proposed. (auth)

**2858** AMBIPOLAR DIFFUSION AND DRIFT MOTIONS IN THE F2-REGION. Gliddon, J. E. C. (Univ. of Illinois, Urbana). Planet. Space Sci., 13: 959-67(Oct. 1965).

The conditions for ambipolar diffusion in a magnetic field are discussed, and it is shown that the plasma equations of momentum-transfer yield unambiguous steady-state solutions under the conditions stated. The consistency of the solution with Maxwell's equations is discussed. It is further shown that steady-state solutions exist when an external electric field acts normally to the magnetic field lines. (auth)

**2859** CORPUSCULAR BOMBARDMENT AND $N_2^+$ RADIATION. Dalgarno, A.; Latimer, I. D.; McConkey, J. W. (Queen's Univ., Belfast). Planet. Space Sci., 13: 1008-9(Oct. 1965).

A review is given of more precise measurements of cross sections for electron reactions with atmospheric nitrogen in atmospheric electron absorption. Included in the results shown are cross section ratios for the production of an ion pair to the cross section for the production of a 3914 Å photon for electron impact energies up to 300 ev. The ratio is nearly constant and is given a value of 17. Also some quantitative information about typical auroras is given. (J.F.P.)

**2860** THORON ($^{220}$Rn) MEASUREMENTS IN THE ATMOSPHERE AND THEIR APPLICATION IN METEOROLOGY. Israeel, Gerhard W. (Technische Hochschule, Aachen). Tellus, 17: 383-8(Aug. 1965).

With new equipment which allows the continuous recording of the atmospheric thoron content down to $0.5 \times 10^{-14}$

C/1, the thoron content of the atmosphere, at different levels was measured. The measurements were carried out from June until September 1964. The results show a close relation between the thoron content and the meteorological variables. The thoron concentration and its decrease with height shows a remarkable diurnal variation with a maximum at noon and a minimum during the night. The thoron at this station in influenced by wind direction. Rain diminished the thoron content by 50%; the recovery time to reach the initial concentration is about 10 hours. It could be shown that the turbulent diffusion coefficient K increases linearly between 1 m and 4 m. A mean value of $K = 330 \pm 30$ cm$^2$/s at 1 m level was found. (auth)

**2861** PRINCIPAL HYPOTHESES CONCERNING THE ORIGIN OF THE EARTH'S RADIATION BELTS. Skuridin, G. A.; Pletnev, V. D. Usp. Fiz. Nauk, 85: 605-50(Apr. 1965). (In Russian).

Pointing out the failure of earlier attempts to interpret the available experimental material on the basis of a single hypothesis, numerous theoretical and experimental aspects of the origin of radiation belts are reviewed. It is shown that the problem of investigating the earth's radiation belt is in its present stage a problem of studying the capture and motion of protons and electrons in the earth's magnetosphere. Of particular importance is the study of the interaction between the interplanetary plasma (solar wind) and the earth's magnetic field, since it may explain the various physical phenomena (magnetic storms, auroras, currents in the outer atmosphere of the earth, etc.) which occur in the earth's immediate vicinity. The history of investigations of the various cosmic ray particle fluxes outside the earth's atmosphere, and especially the development of the concept that the earth's magnetic field can serve as a trap for charged particles, is traced in a brief review of the work by Stoermer, Schmidt, Alfven, and others. The various theories advanced for the kinematics and dynamics of the earth's radiation belts immediately after their discovery and following the acquisition of data with rockets and space probes is then discussed. The main emphasis is on the analysis of the dynamic and kinematic properties from the point of view of conservation of adiabatic invariants of the motion of the charged particles in the magnetic field, which is equivalent to a consideration of the equilibrium state of the radiation belts in an unperturbed magnetic field. The various methods of obtaining the distribution of the particles is described, as a function of the energy and of the spatial coordinates, from the laws of motion of the charged particles in the geomagnetic field as determined by means of the theory of adiabatic invariants. Some experimental data obtained by investigation of the radiation belts are discussed. These include the geometrical structure of the radiation belts in the stationary state, the proton component, the electron component, and data on the various dynamic formations occurring in the belts. Various hypotheses concerning the origin of the earth's radiation belts are discussed, including the neutron albedo hypothesis and various hypotheses based on the effective interaction of a plasma with the magnetic field. (ATD)

**2862** ADVANCES IN SPACE RESEARCH. Proceedings of the First Inter-American Symposium on Space Research, Buenos Aires, November 1960. New York, Pergamon Press, 1964. 445p. (CONF-601101).

A general review is given of the basic principles of research with sounding rockets. Papers are presented on aerodynamics including base flow, theory and equipment used in research, solid propellant rockets, research on solid propellants and certain structural aspects, and also scientific research of the upper atmosphere, considering the use of balloons as another relatively low cost tool in this type of investigation. Space communications, meteorological satellites, and the SNAP-3 system were also discussed. (J.F.P.)

**2863** SPACE PHYSICS WITH ARTIFICIAL SATELLITES. Al'pert, Ya. L.; Gurevich, A. V.; Pitaevskii, L. P. New York, Consultants Bureau, 1965. 248p. $25.00.

Authorized Translation from the Russian by N. H. Nickle.

The phenomena related to the movement of a satellite through a highly rarefied plasma is investigated and generalized. A systematic kinetic approach is used. The case of a body with velocity greater than the thermal motion of neutral particles and ions and with dimension larger than the Debye radius, and the case of a body with dimension comparable to or smaller than the Debye radius and velocity comparable to that of the particles are considered. The results of calculations of the disturbances in the concentration of neutron particles, ions, and electrons, and the consequent disturbances of the electric and magnetic fields in the satellites vicinity are considered. An investigation is made of the scattering of radiowaves in the satellite's wake, calculations are made of the disturbances of the plasma in the vicinity of a body at rest, and the question of the influence of an alternating electric field on the plasma is treated. (J.F.P.)

## Gravitation, Quantum Mechanics, and Relativity Theory

**2864** (COO–1198-300) LECTURES ON SPIN TEMPERATURE. Slichter, Charles P. (Illinois Univ., Urbana. Dept. of Physics. Illinois Univ., Urbana. Materials Research Lab.). [1965]. Contract AT(11-1)-1198. 31p. Dep. mn; CFSTI $2.00 cy, $0.50 mn.

The concept of spin temperature is discussed, and used to solve problems of a complex nature. The cases of static and time-varying magnetic fields are treated. Spin-lattice relaxation and magnetic resonance are studied. The problems are approached from statistical-mechanical and thermodynamic bases. (T.F.H.)

**2865** (JINR-P-2325) EKSPERIMENTAL'NOE OPREDELENIE VEROYATNOSTI RASPADA $K_2^0 \to 2\pi$ V NAKLONNOM PUCHKE $K_2^0$-MEZONOV. (An Experimental Determination of the $K_2^0 \to 2\pi$ Decay Probability in a Sloped $K_2^0$ Beam). Nyagu, D.; Okonov, E. O.; Petrov, N. I.; Rusakov, V. A.; Takhtamyshev, G. G.; Wu Tsun-fan (Joint Inst. for Nuclear Research, Dubna (USSR). Lab. of High Energy; Joint Inst. for Nuclear Research, Dubna (USSR). Lab. of Nuclear Problems). 1965. 7p. Dep. mn.

It is found that in the sloped and horizontal $K_2^0$ beams the magnitude of $K_2^0 \to 2\pi$ decay probability is the same within the experimental error. The result obtained shows that the gravitational masses of the $K^0$ and $\overline{K}^0$ have identical signs. (auth)

**2866** QUANTIZATION AND PHYSICAL INTERPRETATION OF THE GRAVITATIONAL FIELD. Rayski, Jerzy (Jagiellonian Univ., Krakow). Acta Phys. Pol., 28: 201-6(Aug. 1965).

A program of quantization of the gravitational field was presented. Now the problem of consistency of the commutation relations proposed previously is investigated in more detail. Some problems of interpretation are discussed. (auth)

**2867** EQUATIONS OF MOTION FOR A ONE-POINT MODEL OF ELEMENTARY PARTICLE IN AN EXTERNAL GRAVITATIONAL FIELD. Borelowski, Z. (Jagellonian Univ., Krakow). Acta Phys. Pol., 28: 349-60(Sept. 1965).

A point singularity is considered moving in Minkowski space in accordance with the variational principle $\delta \int_{\tau_1}^{\tau_2} L d\tau = 0$, where $\tau$ is the proper time of the particle and L – the Lagrange function, dependent not only on the four-velocity $u^\alpha$ but moreover on the four-acceleration $w^\alpha$. $L = -m_0(\sqrt{u_\lambda u^\lambda} + \Lambda w_\eta w^\eta)$, with $m_0$ denoting a multiplicative constant and $\Lambda$ – a constant involving a characteristic constant length $l_0$ rendering identical the dimensions of both term of L. It is well-known that the singularity considered can serve as model of an elementary particle whose bivector of spin $s^{\alpha\beta}$ is given by the formula $s^{\alpha\beta} = 2m_0\Lambda(u^\alpha w^\beta - u^\beta w^\alpha)$. Assuming it as a test particle (that is, neglecting its own gravitational field) its equations of motion are sought in an external gravitational field with metric tensor $g_{\mu\nu}$. In a first approach, the Euler-Lagrange equations implied by

the above stated variational principle are used, the Lagrangian now being given by the formula $L = -m_0(\sqrt{g_{\mu\nu}u^\mu u^\nu} + \Lambda g_{\mu\nu}w^\mu w^\nu)$, where $w^\nu \overset{df}{=} u^\lambda \nabla_\lambda u^\nu$. In a second approach the picture of an ideal liquid (assuming continuity equations is used with the well-known principle of least action assuming traditionally action of the field $S_p = \int \sqrt{-g}Rd^4x$ and action of matter $S_{int} = \int \sqrt{-g}Ld^4x$. Thus both the equations of motion and those of the field (the momentum-energy tensor is symmetric and involves higher derivatives of $u^\alpha$) are derived. The equations of motion derived by the two methods resemble those of a spin (dipolar) particle derived previously by Mathisson. The module of the particle's spin remains constant, and the Lagrangian is a first integral of the equations of motion. The constant M replacing the mass of the particle in the equations of motion consists of two terms the second of which is the counterpart of Mathisson's "acceleration energy" of the particle. (auth)

**2868** STUDY OF THE CHARACTERISTIC VARIETIES OF THE EQUATIONS OF ELASTICITY IN GENERAL RELATIVITY. Bennoun, Jean-Francois (Institut Henri Poincare, Paris). Bol. Univ. Parana, Fis. Teorica, No. 6, 1-26(Dec. 1963). (In Spanish).

The equations of elasticity in general relativity are studied for the purpose of determining the most natural hypothesis at the basis of a relativistic theory of elasticity and to show the differences in such a theory and the classical theory of elasticity. The study is limited to phenomena of propagation of elastic waves and to the transposition of the laws of classical mechanics. Only linear theories are considered. It is shown that a group of equations deduced from equations proposed by Rayner can be adopted as relativistic equations of elasticity. The characteristic varieties of these equations together with the equations of Singe are studied. This study leads to the conclusion that equations based on the Rayner equations more accurately describe elasticity in general relativity. (J.S.R.)

**2869** THE EINSTEIN-SCHROEDINGER THEORY AND ITS GENERALIZATIONS. Lenoir, Marcel (Faculte des Sciences, Clermont-Ferrand, France). Bol. Univ. Parana, Fis. Teorica, No. 7, 1-34(Sept. 1964). (In Spanish).

A bibliographic study is made of the Einstein-Schroedinger unified theory and its generalizations using a linear connection and maintaining a four-dimensional character. The equations of the electromagnetic field in general relativity and the Einstein-Schroedinger theory are given. Within the framework of the Einstein-Schroedinger theory approximate equations, the conservation identities, the solutions with spherical symmetry, the attempts at physical interpretation and the equations of motion are considered. It is shown that the Einstein-Schroedinger unitary theory does not give equations of motion for charged particles. Two extensions to the theory to permit the formulation of motion equations by modifying the lagrangian of the theory without changing its geometric framework are reported. (J.S.R.)

**2870** A NOTE ON BOUNCING PHOTONS. Pirani, F. A. E. (Brandeis Univ., Waltham, Mass.). Bull. Acad. Polon. Sci., Ser. Sci. Math. Astron. Phys., 13: 239-42(1965).

Synge's experiment (Relativity: the general theory. 125 1960)) is given an intrinsic geometrical description and a simple verification, since his verification of the characterization is rather long and complicated. This description makes manifest the conformal invariances of Fermi transport of direction. (J.F.P.)

**2871** SOME REMARKS ON THE CORRELATED WAVE FUNCTION METHOD. Jankowski, K.; Woznicki, W. (Nicholas Copernicus Univ., Torun, Poland). Bull. Acad. Polon. Sci., Ser. Sci. Math. Astron. Phys., 13: 249-54(1965).

It is shown that there exist many classes of correlation factors which eliminate the poles from the Schrödinger equation. An explicit equation which determines these factors is given, and some simple examples of them are also given. The N-electron Schrödinger equation is considered. (J.F.P.)

**2872** AN ABSTRACT FORMULATION OF QUANTUM DYNAMICS. Tulczyjew, W. M. (Univ. of Warsaw). Bull. Acad. Polon. Sci., Ser. Sci. Math. Astron. Phys., 13: 329-33 (1965).

A formulation is given of quantum dynamics which would fit the relativistic theory in a natural way and be equivalent to Dirac's formulation in the nonrelativistic case. Only the general formalism is considered. Two possible approaches are used for an abstract interpretation of the theory. (J.F.P.)

**2873** AN ABSTRACT FORMULATION OF NON-RELATIVISTIC QUANTUM DYNAMICS. Tulczyjew, W. M. (Univ. of Warsaw). Bull. Acad. Polon. Sci., Ser. Sci. Math. Astron. Phys., 13: 335-40(1965).

The general formalism developed by Tulczyjew (Bull. Acad. Polon. Sci., 13: 335) is applied to nonrelativistic dynamics. Results of this formalism and notation introduced there are used. It is shown that in this special case the general formalism reduces to Dirac's abstract formulation of nonrelativistic dynamics presented in Dirac's book on quantum mechanics. Nonrelativistic quantum dynamics is characterized by the existence of a distinguished pair of operators $\hat{t},\hat{E}$ canonically conjugate to each other and representing time and energy of the system, respectively. There is further an operator $\hat{H}$ commuting with time but not necessarily with energy and called the hamiltonian. Only vectors satisfying the equation $(\hat{E} - \hat{H}/\psi) = 0$ are considered. They represent dynamically admissible histories of the system. (J.F.P.)

**2874** LORENTZ INVARIANCE AND LINEARISATION OF THE RELATIVISTIC HAMILTONIAN. Kar, K. C. (Inst. of Theoretical Physics, Calcutta). Indian J. Theor. Phys., 11: 1-19(Mar. 1963).

Lorentz invariance of the electromagnetic equations and other fundamental equations were proved by a new method. It is shown incidentally that the charge density ($\rho$), the electric potential ($\phi$) and the electron mass ($m_0$) are vectors in the direction of time. It is also shown that, the magnetic intensity (H) and the acceleration are purely space vectors, whereas the electric intensity (E), the velocity (v) and the mechanical force on an electron (f) are both space and time vectors. (auth)

**2875** VECTORS IN THE THEORY OF RELATIVITY. Kar, K. C. (Inst. of Theoretical Physics, Calcutta). Indian J. Theor. Phys., 11: 75-80(Sept. 1963).

It is shown that dx, dy, dz and dt forming the four dimensional manifold, are contravariant vectors. $A_x$, $A_y$, $A_z$ and $\phi$ in electromagnetic theory are also contravariant four vectors. It is also shown that the charge density (p) and electronic mass (m) are contravariant vectors along time. The gradient of a scalar along any of the four axes is a covariant vector in the direction of the gradient. However, the gradient along time, of a space vector is a space-time contra-covariant double vector. The electric intensity (E) and velocity (v) are shown to be double vectors of this type. But as the time gradient of a time vector is a time-scalar, acceleration (f) = dv/dt is a space vector. However, force = mf is a space-time double vector. (auth)

**2876** A POSSIBLE GENERALIZATION OF EINSTEIN'S EQUATIONS. Gliner, E. B. (Ioffe Inst. of Physics and Tech., Leningrad). JETP Lett. (USSR) (Engl. Transl.), 2: 33-5(July 15, 1965).

The principle whereby physical media are described with the aid of a certain tensor and equations that relate the tensor with a metric is extended, within the framework of general relativity, to all media that differ from zero-curvature space-time and are characterized by tensor invariants. A tensor is considered with the properties that it is a rational function of a metric tensor and that its first and second derivatives are linear in the second derivatives, that it satisfies the conservation law, and vanishes if and only if space-time has no curvature. (J.F.P.)

**2877** GRAVITATIONAL RADIATION OF EXPLOSIVE ORIGIN. Ozernoi, L. M. (Lebedev Inst. of Physics,

Moscow). JETP Lett. (USSR) (Engl. Transl.), 2: 52-5 (July 15, 1965).

An estimation is made of the power of gravitational radiation produced by explosively scattered matter during the course of various natural cataclysms. The arguments are based on a model of asymmetrical scattering. Among the various natural sources of explosive gravitational radiation, a power estimation is made for the explosion of quasars, of galaxies, for radiation due to collision of stars in radiogalaxy cores, and for explosions of supernovas and novas. It is concluded that the explosive gravitational radiation in these processes is quite appreciable. It is noted that such an analysis may be a fundamentally new method of investigating processes occurring in the central regions of exploding cosmic objects. (J.F.P.)

**2878** THE PAULI PRINCIPLE AND THE LORENTZ GROUP. Jost, Res. Magy. Fiz. Folyoirat, 13: 207-28 (1965). (In Hungarian).

A historical review is given of Pauli's attempts to correlate the special theory of relativity with the requirements of the quantum theory. The development of the exclusion principle was the result of this effort. This relativistic concept, coordinating spin and statistics states that particles with ½ spin follow the exclusion principle while those with an integer spin number follow Bose–Einstein statistics. In collaboration with Heisenberg, Pauli developed the quantum electrodynamics within the framework of a general quantization theory of space; he was able to show that the canonic quantization is Lorentz invariant. Instead of the 4-dimensional system, used in his work with Jordan, he employed a 3-dimensional concept. The elimination of time later hindered the development of invariant perturbation calculation and that of the field theory. Discovery of the positron by Anderson and later proof of Dirac's hole theory clarified this situation. The Wightman scheme is reviewed, in order to place the CTP invariance in proper perspective. It is pointed out that the electromagnetic field interacting with charged particles cannot be adapted to the Wightman formalism. The vacuum values are invariant with respect to complex Lorentz transformation. (Historical review article, 37 references). (TTT)

**2879** THE EQUILIBRIUM OF A CHARGED SPHERE. Bonner, W. B. (London Univ.). Monthly Notices Roy. Astron. Soc., 129: 443-6(1965).

A relativistic model is presented for a sphere of charged dust in equilibrium under its own gravitation and electrical repulsion. The mass and radius are arbitrary. Equilibrium configurations of this sort suggest that electric repulsion may be able to halt the gravitational collapse of very large masses. (auth)

**2880** CONCERNING THE EXPERIMENTAL VERIFICATION OF THE THEORY OF RELATIVITY BY MEANS OF THE MOESSBAUER EFFECT. Bennewitz, F. (Institut fuer Theoretische Physik, Freiburg). Phys. Lett., 19: 282-3(Nov. 1, 1965).

In order to test the theory of relativity by means of the Mössbauer effect, the second order Doppler effect was measured on a rotating disc. The calculation is performed for emitter and absorber, but rotating with the same angular velocity around the common axis. The calculations are performed in the laboratory system, but only the Lorentz-invariant quantities are used. It is shown that the previous experiments on a rotating disc with small extended emitter and absorber can be extended to concentric circular cylinders or parts of them without affecting the frequency shift. This not only simplifies the measuring procedure, but increases the accuracy in measurement because of the much larger counting rates. (J.F.P.)

**2881** QUANTUM MECHANICAL MICROSCOPIC BROWNIAN MOTION. McKenna, J.; Frisch, H. L. (Bell Telephone Labs., Inc., Murray Hill, N. J.). Phys. Letters, 19: 112-14(Oct. 1, 1965).

From a strictly quantum mechanical formulation of the problem, using a density matrix description of the composite system, it is shown that in an appropriate classical limit the Fokker-Planck equation results. To the lowest order in $h/2\pi$, this technique gives the same expression for the friction coefficient obtained in previous work, and it also yields corrections to the Fokker-Planck equation to all orders in $h/2\pi$. It is assumed that the Brownian particle has charge, while the fluid particles are uncharged, the system has finite volume, and a constant electric field is assumed to act on the system. (J.F.P.)

**2882** LORENTZ-COVARIANT GRAVITATIONAL ENERGY-MOMENTUM LINKAGES. Winicour, J.; Tamburino, L. (Aerospace Research Labs., Wright-Patterson AFB, Ohio). Phys. Rev. Letters, 15: 601-5(Oct. 11, 1965).

A gravitational energy-momentum expression is presented with the transformation properties of a Lorentz free vector in asymptotically flat but radiative spaces. This expression and its transformation properties apply to finite regions as well as to the entire space. In the Bondi-van der Burg-Metzner (Proc. Roy. Soc. (London) A269, 21 (1962)) formulation of the characteristic initial-value problem, certain of the field equations need only be applied on a world tube. For world tubes of topology $S^2 \times E^1$, the equations are cast in the form of conservation conditions. (J.F.P.)

**2883** PROPOSAL FOR THE QUANTUM MECHANICAL ORBIT EQUATION. Nishiyama, Yoshio (Univ. of Osaka Prefecture). Progr. Theoret. Phys. (Kyoto), 34: 473-97 (Sept. 1965).

The orbit equation for the motion of a quantum in a potential is proposed by defining uniquely the quantum mechanical momentum from the Schroedinger wave equation of a one-particle system and using the Hamilton-Jacobi formalism. On this occasion it is necessary to introduce a new dynamical postulate, "initial condition", which is independent of the quantization condition as well as of the Schroedinger wave equation. The momentum is determined in such a way that it is approximately equal to the corresponding classical mechanical momentum in the classical region of validity of the coordinates. The momentum in the nonclassical region is in general very small in comparison with that in the classical region. The quantum-mechanical motion well corresponds to the classical motion. If a system is macroscopic, the motion of the particle is described by Newtonian mechanics and the quantization condition is of no validity. The "quantization of magnetic flux" derives from the quantization condition. It is closely related to the energy level structure of the atomic system. The above argument is applied to the scalar electromagnetic and sound wave equations to give the dynamical motion of a photon and a phonon without recourse to the so-called second quantization method. (auth)

**2884** GRAVITATIONAL RADIATION AND POSSIBILITIES OF DETECTING IT. Braginskii, V. B. Usp. Fiz. Nauk, 86: 433-46(July 1965). (In Russian).

Gravitational radiation and detection possibilities are reviewed. Emphasis is placed on sources and detectors of gravitational radiation. Binary stars, hypothetical sources, extraterrestrial high-frequency sources, and possible terrestrial sources are discussed. Restrictions imposed on detectors, limitations of such devices, and detectors utilizing bodies whose length exceeds its other dimensions, such as the apparatus being developed by J. Weber are discussed. It is suggested that detection by extended bodies may be conducted by means of phonon counters which can record minute deformations of the order $\Delta l/l \simeq 10^{-25}$. (ATD)

**2885** EFFECT OF ION GYRATION RADIUS ON THE MAGNETOGRAVITATIONAL INSTABILITY OF AN INFINITE HOMOGENEOUS MEDIUM. Surindar, Singh; Harikrishan, Hans (Univ. of Delhi). Z. Astrophys., 62: 12-14(1965).

Jeans' criterion for the gravitational instability of an infinite homogeneous medium in the presence of a magnetic field remains unaffected by taking into account a finite ion gyration radius although the modes of propagation of a wave are modified. (auth)

**2886** ON THE SELF-ENERGY AND CHARGE OF A PARTICLE STABILIZED BY GRAVITATIONAL ACTION IN A CURVED SPACE. Efinger, Helmut J. (Universitaet Vienna). Z. Physik, 188: 31-7(1965). (in German).

The problem of the self-energy and the charge of particles is discussed by solving Einstein's field-equations of general relativity. The mass and the charge of a particle are fixed by its radius. If the background is flat the specific charge $\epsilon/m$ is a universal constant, if the particle is embedded in a De-Sitter universe $\epsilon/m$ depends on the particle-radius. (auth)

**2887** ON THE EMPIRICAL AND MATHEMATICAL FOUNDATIONS OF QUANTUM MECHANICS [Thesis]. Prugovecki, Eduard Slavko. Princeton, N. J., Princeton Univ., 1965. 231p.

A critical reconsideration of the fundamental principles of quantum mechanics is undertaken. A certain attitude towards the measurement process, which is very well suited to the needs of microscopic physics but can be also adapted to any other branch of physics, is formulated by developing a semantics of measurement. In doing this a sharp distinction is made (following Margenau) between state-preparation and measurement. Next, the relation of theory to experiment, generally established by correlation rules, is investigated. Different fundamental concepts, like those of observable, state, etc. are analyzed. The results of such an analysis are applied on an investigation of the fundamental principles of quantum physics in an attempt to achieve a more precise formulation of the correspondence principle, wave-particle duality, etc. Some "gedanken" experiments are reconsidered and the question of simultaneous measurability of incompatible observables, like position and momentum, is analyzed in the light of preceding considerations. It is pointed out that there is a possibility of giving a theoretical treatment to simultaneous measurements of incompatible observables by generalizing the tools of mathematical statistics — mainly by introducing "complex probability measures." A system of axioms for a formalism that would be able to exploit in a most direct form the possibility of simultaneous measurements of incompatible observables is given by making use of the concept of complex probability measure. After showing that such a formalism represents a generalization of the conventional Hilbert space formalism, the question of the conditions for a complete logical equivalence of these two formalisms is closely examined. In doing this the tools of the theory of Lesbegue measure and of the theory of Banach algebras are extensively used. It is found that the addition of two hypotheses are necessary and sufficient conditions for such a complete logical equivalence. (Dissertation Abstr.)

**2888** WAVE MECHANICS OF A FREE PARTICLE. Fisher, Edward. North Hollywood, Calif., Western Periodicals Co., 1965. 113p.

The wave mechanics of a stable particle in the absence of force fields and other particles are derived. Neither operator nor wave concepts are used, and the usual macroscopic properties of a particle, that is, mass, energy, etc., are not assumed. Wave mechanics is synthesized directly from probability and relativity on the basis of following assumptions: the motion of a particle can be regarded as that of a point, which describes a trajectory that is one of a statistical ensemble. The free space in which the particle moves is homogeneous and isotropic, and has a uniform time scale, in the sense that, when all the trajectories of all possible ensembles are considered, then there is not preferred position, direction or point of time. And lastly the particle and space satisfy a relativity principle. (J.F.P.)

## Low Temperature Physics

*Refer also to abstracts 2383 and 3018.*

**2889** (AD-618203) SUPERCONDUCTIVITY IN ONE AND TWO DIMENSIONS. Rice, T. M. (California Univ., La Jolla, San Diego). July 13, 1965. Contract NONR-221611. 11p. (TR-32). CFSTI $1.00 cy, $0.50 mn.

The effects of thermodynamic fluctuations on off diagonal long range order (ODLRO) is discussed. The two particle Yang correlation function was calculated using the Ginzburg-Landau theory allowing such fluctuations. The behavior of the correlation function at large separation was examined and was found to be consistent with Yang's criterion for ODLRO only in three dimensions. In one and two dimensions Yang's criterion is not satisfied. (auth)

**2890** (AFML-TR-65-154) THE PROPERTIES OF SUPERCONDUCTING Mo-Re ALLOYS. Daunt, J. G.; Lerner, E. (Ohio State Univ. Research Foundation, Columbus). Aug. 1965. 32p.

Details of the research carried out and the results obtained therefrom on the low temperature properties of Mo-Re alloys in the superconducting and normal states are presented. Measurements were made on a variety of Mo-Re alloys in various states of anneal, the alloys being in the form of fine wires, as suitable for the winding of high-field superconducting solenoids. Micrograph studies were made to determine the percentage of the various phases present in each specimen. The low temperature measurements covered observations on the various specimens of the electrical resistivity as a function of temperature and of magnetic field, the magnetic moment as a function of temperature and magnetic field, and the thermal conductivity also as a function of temperature and magnetic field. The measurements yielded evaluations of the three critical magnetic fields, $H_{c1}$, $H_{c2}$, and $H_{c3}$ as a function of temperature and alloy constitution, the transition temperatures $T_c$ and the Landau-Ginsburg parameters $\kappa$. Detailed comparisons of the results are made with theoretical predictions and with results by previous authors on similar high-field superconducting alloys. (auth)

**2891** SUPERCONDUCTING $H_C$-$J_C$ CHARACTERISTICS OF NITRIDED Nb-Zr WIRE TO 130 kOe. Anderson, D. E.; Toth, L. E.; Rosner, L. G.; Yen, C. M. (Univ. of Minnesota, Minneapolis). Appl. Phys. Letters, 7: 90-2 (Aug. 15, 1965).

It was recently concluded that transition metal carbides and nitrides are unable to carry large supercurrents even in modest magnetic fields. It is pointed out that the low values obtained may be due to the metallurgical state of the samples and do not necessarily represent some intrinsic property of the materials. The $H_c$-$J_c$ properties of carbides and nitrides prepared by two different techniques are studied. One technique was the standard powder-metallurgy technique in which the $J_c$ values were low even though several high $H_c$ values were obtained. The other technique was that of nitriding Nb-Zr wires in which more reasonable $J_c$ values were observed even in magnetic fields as high as 130 kOe. The results on the nitrides of Nb-Zr are described, and a discussion of the differences in the metallurgical state which distinguish this result from those obtained by standard powder-metallurgy techniques is given. It is concluded that agreement was found with the previous result by the same method, but that more promising $J_c$ values can be obtained by different preparation techniques. (J.F.P.)

**2892** THE PROBLEM OF HEAT FLUXES IN SUPERCONDUCTING DEVICES. Kazovskii, E. A.; Kartsev, V. P. Inzh.-Fiz. Zh., 9: 96-101(July 1965). (In Russian).

An attempt was made to estimate, with the aid of simplifying assumptions, the value of heat fluxes entering into a cryostat with liquid helium through electrical leads in contact with leaving gaseous helium. Comparison of experimental and predicted values showed rather high accuracy of the latter. However, in order to get reliable results, the empirical coefficient introduced into the calculation should be modified for every particular case. (auth)

**2893** THERMAL CONDUCTIVITY OF SUPERCONDUCTING AND NORMAL LANTHANUM. Mamiya, Takayoshi (Tohoku Univ., Sendai); Fukuroi, Tadao; Tanuma, Seiichi. J. Phys. Soc. Jap., 20: 1559-67(Sept. 1965).

The thermal conductivity of superconducting and normal f.c.c. lanthanum was measured at the temperature range 1.7 to 7.0°K. The thermal conductivity of yttrium

was also measured to test the cryostat. The ratio of the energy gap of lanthanum at absolute zero to the transition temperature, $2\Delta(0)/kT_c$ is 2.9 to 3.0, where $T_c = 6.04°K$. The ratio obtained from the temperature dependence of the thermal conductivity in the superconducting state is in agreement with the value deduced from the ratio of the thermal conductivities of the superconducting to the normal state. Although the specimen employed in this experiment has the resistivity ratio of 44, the magnetization measurements indicate that the specimen is a second kind superconductor due to a trace of impurity contained. High critical fields and the wide range of the field transition can be interpreted in terms of a second kind superconductor. (auth)

**2894** SUPERCONDUCTING PROPERTIES OF Fe–Sn SUPERIMPOSED FILMS. Tsuya, Hideki (Nippon Electric Co., Ltd., Kawasaki, Japan). J. Phys. Soc. Jap., 20: 1734-5(Sept. 1965).

An abrupt drop in transition temperature was observed for increasing component thickness of superimposed Fe–Sn films. An empirical relation was obtained between the transition temperature and the film thickness. It was also observed that all transition curves had resistance maxima before entering the superconducting state. (L.B.S.)

**2895** INTERACTION OF THE ALTERNATING JOSEPHSON CURRENT WITH RESONANT MODES IN A SUPERCONDUCTING TUNNEL STRUCTURE. Dmitrenko, I. M.; Yanson, I. K.; Svistunov, V. M. (Physicotechnical Inst. of Low Temperatures, Academy of Sciences, Ukrainian SSR). JETP Lett. (USSR) (Engl. Transl.), 2: 10-13(July 1, 1965).

A simple model is proposed in which steps result from excitation of resonant electromagnetic oscillations in tunnel structures when alternating Josephson current flows between the films. This model is confirmed by the experimental data which is also presented. The occurrence of a step is treated as a consequence of the excitation of resonant oscillations of electromagnetic waves in the tunnel structure by alternating Josephson current. Also tunnel structures of the type Sn–I–Sn (where I is an insulator 10–20 Å thick), similar to those described previously, as well as more complicated structures are experimentally investigated. The discrete set of voltages obtained for each tunnel structure is in good agreement with theoretical predictions. Plots of the results are shown. It is concluded that unlike the Pb–I–Pb tunnel structure, a strong interaction between the alternating Josephson current and the resonant mode of the strip resonator formed by the tunnel junction occurs in the tunnel structures. This is the mechanism that causes an effective coupling between the alternating Josephson current and the electromagnetic field, and which made it possible to observe the photon emission in previous work. (J.F.P.)

**2896** LIGHT SCATTERING DETECTION OF THERMAL WAVES. Guyer, R. A. (Duke Univ., Durham, N. C.). Phys. Lett., 19: 261(Nov. 1, 1965).

An alternative but similar experiment to the light scattering experiment for detecting second sound in solids is proposed. The detection of the width of the first sound doublet as a function of velocity is suggested as a reasonable alternative to the previous experiment. A change in the width of the doublet by a factor of about 100 is expected since the angle of detection corresponds to acoustic wave velocities on and off resonance. Solid helium, which can be obtained with very high chemical and isotopic purity and which has highly anisotropic velocities in the hcp phase is suggested as a good subject for experimental investigation by either method. (J.F.P.)

**2897** A NEW KIND OF TRANSVERSE VOLTAGE IN A TYPE II SUPERCONDUCTOR. Druyvesteyn, W. F.; Staas, F. A. (Philips' Gloeilampenfabrieken, Eindhoven, Netherlands). Phys. Lett., 19: 262-3(Nov. 1, 1965).

A new type of transverse voltage is reported. This can occur when j is not perpendicular to H. These voltages change sign upon reversal of j but not upon reversal of H. Their magnitude can be greater than the earlier mentioned transverse voltages and can be the same order of magnitude as $E\|$. The experiments were performed on a Pb-15 at. % In alloy in the form of a sheet. The experimental results are given with the field perpendicular to the current plotted against the field parallel to it. No satisfactory theory is known to explain the behavior of the flux lines for high values of the electric field parallel to the current. (J.F.P.)

**2898** SUPERCONDUCTIVITY IN THE BERYLLIUM-RHENIUM SYSTEM. Bucher, E.; Heiniger, F.; Muller, J.; Spitzli, P. (Univ., Geneva). Phys. Lett., 19: 263-4 (Nov. 1, 1965).

Superconductivity is reported in the beryllium-rhenium system. These new superconducting alloys are characterized by some outstanding features such as low atomic mass and density, low specific heat, and high transition temperature. The magnetically observed transition temperatures are shown as a function of nominal composition. For arc-melted alloys in the quenched state, a flat maximum of $T = 9.75°K$ is observed at approximately 2 at.% rhenium, while annealed specimens show the maximum near a rhenium concentration of 4 at.%. In both cases the width of the transition was of the order of 0.1°K. Within the measurement precision no variation of the lattice constant, $a = 11.56 \pm 0.01$ Å, could be detected as a function of nominal composition. The electronic specific heat and Debye temperatures are also given. (J.F.P.)

**2899** CONDUCTION ELECTRON SPIN RESONANCE IN A SUPERCONDUCTOR. Kaplan, J. I. (Brown Univ., Providence). Phys. Lett., 19: 266-7(Nov. 1, 1965).

Since it is expected that ESR can be observed in aluminum, the possibility of experimentally observing this effect in a superconductor is considered. The model is a thin film superconductor where the London quasi-stationary relations and the modified Bloch equations are assumed to be valid. It is concluded that, subject to the omission of surface scattering, electron spin resonance can be observed in the normal state. (J.F.P.)

**2900** MAGNETIC FIELD PENETRATION AND BREAKDOWN OF SURFACE SUPERCONDUCTIVITY. II. Paskin, A.; Strongin, M.; Schweitzer, D. G.; Bertman, B. (Brookhaven National Lab., Upton, N. Y.). Phys. Lett., 19: 277-9(Nov. 1, 1965). (BNL-9569)

The effects of currents in surface layers on the magnetization of type II superconductors, and critical surface currents versus magnetic field calculations are considered, and previously reported susceptibility and magnetization results are explained. The picture of the surface used is one where the external critical current is a function of the external field. A curve is given for the sinusoidal a-c field superimposed on the d-c field, in this the peak to peak a-c amplitude is typically 0.04 Oe. Another curve is drawn for the expanded region of magnetization showing the equilibrium hysteresis loop. A third curve is shown for the expanded region of surface current versus the field curve. Hysteresis loops are indicated that show surface currents less than or equal to the critical surface current. It is found that the concept of a superconducting surface sheath and its associated hysteresis properties is sufficient to explain all the susceptibility and magnetization results. (J.F.P.)

**2901** SUPERCONDUCTIVITY OF BARIUM TUNGSTEN BRONZE. Sweedler, A. R.; Hulm, J. K.; Matthias, B. T.; Geballe, T. H. (Univ. of California, San Diego, La Jolla). Phys. Letters, 19: 82(Oct. 1, 1965).

It is reported that $Ba_xWO_3$ becomes superconducting at a temperature of 1.9°K. The sample had a nominal composition of x = 0.13 and was prepared by heating $BaCl_2$, $WO_3$, and $WO_2$ to 950°C for 24 hours. The sample showed a deep violet color with red crystals visible under the microscope. Superconductivity was measured magnetically by monitoring the self inductance of a coil containing the sample. The transition was broad and indicated that 35% of the sample became superconducting. This checked with the x-ray analysis which showed that $WO_3$ was present. It is noted that in the bronze systems studied thus far

superconductivity was only observed in the tetragonal I and hexagonal structures. (J.F.P.)

**2902** THE REESTABLISHMENT OF THE NORMAL STATE IN DIFFERENT SUPERCONDUCTING ALLOYS SUBJECTED TO VARIABLE MAGNETIC FIELDS. Vallier, J. C. (Centre de Recherches sur les Tres Basses Temperatures, Grenoble, France). Phys. Letters, 19: 83-4(Oct. 1, 1965).

After studying the mechanism of the mixed and normal transition states in a variable magnetic field, the drop in voltage along different wires of Nb–Zr and of Nb–Ti, with a diameter of 0.25 mm, was measured when they carry a current density previously adjusted to a value between 0 and $10^5$ amp/cm$^2$ in a pulsed longitudinal magnetic field. The latter had a maximum value of 110 kOe and a duration of 40 milliseconds. A preamplifier was used, allowing the detection of voltages equal to or greater than several tens of microvolts. The results shown correspond to the first appearance of detectable voltage in different samples, other than that induced directly by the variable field, for different values of the intensity. Other curves indicate that for each sample at a certain temperature there exists only one field corresponding to the first appearance of voltage. It is shown that the values of this field are equally influenced by thermal environment. (J.F.P.)

**2903** SURFACE STATES AND HIGH-TEMPERATURE SURFACE SUPERCONDUCTIVITY. Silvert, W. (Michigan State Univ., East Lansing). Phys. Letters, 19: 93-4 (Oct. 1, 1965).

A review is given of surface states and high-temperature surface superconductivity. It was previously suggested that the occurrence of surface superconductivity might be marked by transition temperatures on the order of $10^2$–$10^4$°K. But observed changes in the transition temperatures of thin films which were tentatively ascribed to surface superconductivity were on the order of one degree, and the effect was explained in terms of increased volume average of the electron–electron interaction. It was shown that there can also occur a form of localized superconductivity due to short-range correlation effects at the surface. This type of surface superconductivity may occur at room temperature or above. It is also pointed out that at the extremes of temperature, where the correlation length becomes comparable with the interatomic spacing, the concept of a coherent many-electron state is open to question. (J.F.P.)

**2904** THE MINIMUM PROPAGATING CURRENT OF A COMPOSITE SUPERCONDUCTOR. Williams, J. E. C. (Massachusetts Inst. of Tech., Cambridge). Phys. Letters, 19: 96-7(Oct. 1, 1965).

It was previously shown that it is possible to stabilize an inherently unstable superconductor at its short sample current by shunting it with sufficient normal material. Stable operation is also achieved at currents below the short sample value with less normal material. It is shown that this leads to an increased overall current density in some instances which should be considered in coil design. By solving the equations for the thermal equilibrium of a composite superconducting wire along which a stationary thermal gradient exists, an expression for the minimum propagating current can be evolved as a function of the amount of normal material in the composite. This minimum propagating current is that current at which quenching will just not propagate in the composite, under given conditions of field strength and thermal environment. This theory is offered as a basis for the optimization of coil design based on the minimum propagating current concept. (J.F.P.)

**2905** THE SPECIFIC HEAT OF SUPERCONDUCTING TRANSITION METALS. Sung, C. C. (Univ. of California, Berkeley); Shen, L. Yun Lung. Phys. Letters, 19: 101-2 (Oct. 1, 1965). (UCRL-16298).

A two-energy gap model which was proposed previously is used to obtain an expression for the specific heat of pure and impure superconductors. Data are fitted to the expression and the following parameters are determined: the small energy gap $\Delta_s$, $N_s/N_d$, (where $N_{s,(d)}$ is the density of states of s-(d-) band) and the magnitude of the interband interaction. This model gives a reasonable specific heat of pure niobium over the whole measured temperature range. The discrepancy between the experimental value and that calculated may be due to the fact that the pure sample is not 100% pure as it is assumed in the calculation. The effect of impurities is also calculated, assuming they are nonmagnetic. The results cannot fit the experimental data. It seems that the electronic structure of the impurities has to be taken into account to explain the experimental data. (J.F.P.)

**2906** GINZBURG-LANDAU PARAMETERS OF TYPE-II SUPERCONDUCTORS. McConville, T.; Serin, B. (Rutgers Univ., New Brunswick, N. J.). Phys. Rev., 140: A1169-77(Nov. 15, 1965).

Specific heats in a magnetic field were measured for three specimens of niobium, a 50% Nb–50% Ta specimen, and an In + 1.9% Bi specimen. These data were supplemented by magnetization measurements on one niobium specimen. From the data, two Ginzburg-Landau parameters are calculated: $K_1$, determined by the magnitude of the upper critical field, and $K_2$, determined by the slope of the magnetization curve at this field. For the niobium specimens, $K_2$ exceeds $K_1$ at all temperatures below the transition temperature, in qualitative agreement with the theory of pure type-II superconductors of Maki and Tsuzuki. The ratio $K_2/K_1$ at a given temperature is largest in the purest Nb and less in impure Nb. In the pure specimens, the temperature dependence of $K_1$ is more rapid than predicted by theory, the experimental value of $K_1(0)$ being about 25% larger than the theoretical value of 0°K. For the alloy specimens, $K_2 \sim K_1$, over the temperature range measured, and both parameters increase with decreasing temperature. This result contradicts the inequality $K_2 < K$ (where K is the Ginzburg-Landau parameter at $T_c$) derived by Maki for type-II superconductors of short electron mean free path. (auth)

**2907** SUPERCONDUCTING TECHNETIUM–TUNGSTEN ALLOYS. Autler, S. H. (Westinghouse Electric Corp., Pittsburgh); Hulm, J. K.; Kemper, R. S. Phys. Rev., 140: A1177-80(Nov. 15, 1965).

The transition temperatures, critical fields, electrical resistivities, and crystalline structures of a series of technetium–tungsten alloys containing up to 60 at. % technetium are reported. $T_c$ increases monotonically to 7.9°K and $H_{c2}$ (at 4.2°K) to 43.5 kG for 60 at. % technetium. The samples are single-phase solid solutions up to 40 at. % Tc, but a sigma phase is present at higher concentrations. The measured values of $H_{c2}$ are in good agreement with calculated values based on the BCS and Ginsberg-Landau-Abrikosov-Gor'kov theories and with our resistivity measurements. (auth)

**2908** THEORY OF THE MOTION OF VORTICES IN SUPERCONDUCTORS. Bardeen, John (Univ. of Illinois, Urbana); Stephen, M. J. Phys. Rev., 140: A1197-1207 (Nov. 15, 1965).

The theory of the motion of vortex lines in the mixed state of type II superconductors is derived on the basis of a local model that is a generalization of the London theory. It is believed the model simulates reasonably well the behavior of relatively pure superconductors ($l > \xi_0$), giving a vortex line with a normal core. It is found that if the force on a line is produced by a uniform transport current $J_T$, electric fields generated by the motion drive the current through the core, so that the total current flow is $J_T + J_0(r - v_L t)$, where $J_0(r)$ is the circulation of a stationary vortex and $V_L$ is the velocity of the line. In part $J_T$ represents superfluid flow and in part normal flow. Expressions derived for the viscosity and flow resistivity are nearly identical with empirical laws of Kim and co-workers. The Hall angle expected in the mixed state is the same as in the normal state for a magnetic field equal to that in the core. (auth)

**2909** GEOMETRICAL RESONANCE IN THE TUNNELING CHARACTERISTICS OF SUPERCONDUCTING Pb.

Tomasch, W. J. (North American Aviation, Canoga Park, Calif.). Phys. Rev. Lett., 15: 672-5(Oct. 18, 1965).

Relatively high-impedence film diodes of the form Al-$AlO_x$-Pb were prepared by standard methods and the voltage dependence of dV/dI and $d^2V/d^2I$ was investigated, using conventional modulation techniques. A damped oscillation was observed in $d^2V/d^2I$, which is periodic in V. The voltage period $h\nu$ was found to vary inversely with Pb thickness over the range 2.9 to 9.7 $\mu$. The linear relation between $h\nu$ and 1/d suggests that the Pb films exhibit geometrical resonances (standing wave modes), and that these serve as monochromatic or harmonic reservoirs to which tunneling electrons may lose energy. (L.B.S.)

**2910** GAPLESS SUPERCONDUCTIVITY INDUCED BY METALLIC CONTACTS. Fulde, Peter; Maki, Kazumi (Univ. of California, Berkeley). Phys. Rev. Lett., 15: 675-7(Oct. 18, 1965).

A theoretical investigation is made of the tunneling density of states for a superconducting film in contact with a nonmagnetic normal film, assuming that the mean free path in the metals is small compared with the coherence distance. The calculations show that the tunneling density of states is similar to that found for superconductors containing paramagnetic impurities, which reveal that the essential influence of a metallic contact on superconductivity is a tendency to break electron pairs. The calculations are extended to the case of contacts between superconducting films and paramagnetic metals. No qualitative difference was found, but quantitatively it was found that the pair-breaking effect of paramagnetic metal contacts is an order of magnitude larger than that of nonmagnetic normal metal contacts having the same dimensions. (L.B.S.)

**2911** EFFECT OF THE SUHL-ABRIKOSOV RESONANCE ON THE TRANSITION TEMPERATURE OF SUPERCONDUCTORS. Griffin, Allan (Univ. of California, San Diego, La Jolla). Phys. Rev. Lett., 15: 703-6(Oct. 25, 1965).

It was previously shown by Suhl and by Abrikosov that in a normal metal, the s–d interaction may give rise to a resonance in the electronic scattering amplitude (for antiferromagnetic coupling, $J < 0$). It was observed by Kondo that, to the third order in J, the scattering cross section seem to diverge logarithmically as the electronic energy approaches the Fermi energy $\epsilon_F$. A study is made of how the transition temperature $T_c$ of a superconducting paramagnetic alloy is affected by the anomalous scattering. Numerical calculations are discussed which are based on somewhat arbitrary values of J, $\epsilon_F$, and $T_{cp}$. (L.B.S.)

**2912** CALCULATIONS OF SOUND VELOCITIES IN CRYSTALLINE HELIUM AT ZERO TEMPERATURE. Nosanow, L. H.; Werthamer, N. R. (Bell Telephone Labs., Murray Hill, N. J.). Phys. Rev. Letters, 15: 618-21 (Oct. 11, 1965).

The problem of calculations of sound velocities in crystalline helium at zero temperature are treated by using the time-dependent Hartree approximation, together with the results of variational calculations of the ground-state energy using correlated trial wave functions. Calculations of sound velocities for various densities of crystalline helium at zero temperature are reported and an estimation of the Debye $\theta$ is made as a function of density. Despite many approximations made, agreement between theory and experiment is found to be quite good. But a few discrepancies are found, one of which is the calculated anisotropies of the order of 100 m/sec for the longitudinal modes, whereas anisotropies of this size were observed only in the transverse velocity of hcp $^4$He. (J.F.P.)

**2913** ELECTRONIC INTEGRATION TECHNIQUE FOR MEASURING MAGNETIZATION OF HYSTERETIC SUPERCONDUCTING MATERIALS. Fietz, W. A. (Cornell Univ., Ithaca, N. Y.). Rev. Sci. Instrum., 36: 1621-6 (Nov. 1965).

A simple system capable of continuously recording complete magnetization curves for hysteretic superconductors is described. The system allows the applied field to be cycled slowly in order to avoid transient effects in the specimen material. A voltage proportional to the differential susceptibility of the material is integrated by a chopper-stabilized solid state amplifier, and plotted on an X-Y recorder as a function of applied field. The system is capable of recording magnetization curves over periods of 15 min with an overall uncertainty of 5% or less. (auth)

**2914** QUANTUM EFFECTS IN SUPERCONDUCTORS. Parks, R. D. Sci. Am., 213: 57-67(Oct. 1965).

The Meissner effect in superconductors is discussed. This second basic property of the superconducting state is the converse of ferromagnetism. A superconducting body completely expels an externally applied magnetic field. A superconducting body pushes out the lines of force in a magnetic field whereas a ferromagnetic one concentrates them. A general explanation of the Meissner effect is that an external field sets up electron currents in a thin layer at the surface of a superconductor. These currents produce a magnetic field that is opposite to the applied field and just large enough to cancel the applied field within the body. But this explanation does not apply to special cases. It was suggested therefore that a long-range correlation exists between the electrons in a superconductor; that is, one electron cannot move independently of the others. Quantum states for such electrons were suggested. The vortices of type II superconductors are also discussed. (J.F.P.)

**2915** ON THE TRANSITION TEMPERATURES OF SUPERCONDUCTORS OF VARIOUS METALS UNDER THE INFLUENCE OF VERY THIN OXIDE LAYERS. Ruehl, W. (Physikalisch-Technische Bundesanstalt, Brunswick). Z. Physik, 186: 190-202(1965). (In German).

The superconducting transition of thin films of Al, In, Tl, Pb, Sn, and $Ga^+$ is investigated by resistance measurements before and after the low temperature oxidation of the surface. The films are condensed onto a crystalline quartz plate to a thickness of about 100 Å or less at a temperature of mostly 105°K. The oxidation process below 40°K was described previously. The experimental results show a shift of the transition to higher temperatures with the metals Al, In, and Tl, however, with the metals Sn, Pb, and $Ga^+$ to lower temperatures. These results agree qualitatively very well with direct measurements of the influence of surface charges on the superconducting transition of Sn and In by Glover and Sherrill. The $T_c$-shift depends clearly upon the film thickness and amounts to above 0.3 to 0.4°K for the thinnest films used. Some experiments are undertaken in order to prove the existence of the electric field. Removing the residual oxygen molecules on top of the oxide layer destroys the acceptor levels and causes a reduction of the transition temperature to the value observed with the oxygen free film. As expected, the thickness of the oxide layer is not important for the magnitude of the $T_c$ shift. (auth)

**2916** SUPERCONDUCTING LEAD FILMS WITH ADDITIONS OF TRANSITION METALS AND THEIR OXIDES. Wassermann, Eberhard (Universitaet, Gottingen, Ger.). Z. Physik, 187: 369-85(1965). (In German).

The influence of small additions of 3d-metals (Cr, Fe, Co) on the superconducting transition temperature of lead was studied. Both components are condensed simultaneously on a quartz substrate, held at 10°K. With the quench evaporation technique a statistical distribution of the impurity atoms in the lead matrix was obtained. As in early experiments on In and Sn the superconducting transition temperature of Pb decreases linearly with increasing 3d-metal content. This is in agreement with the theoretical results of Abrikosov-Gorkov and Skalski et al. For the first time an influence of 3d-metal oxides (Cr-, Mn- and Co-oxide) on the superconductivity of Pb was found. The transition temperature $T_c$ decreases linearly with increasing oxide content (c) as in the case of the pure metals. For Mn and Co the slopes $dT_c/dc$ are nearly equal for the pure metal and its oxide. In the case of Cr the influence of the oxide is about seven times greater than that of the pure metal. Further it is shown by annealing experiments that the degree of precipitation has also an influence on the transition temperature in the system of lead with Fe, Co and $Co_2O_3$. (auth)

**2917** COHERENCE EFFECT IN DOUBLE LAYERS OF DIFFERENT SUPERCONDUCTORS. Bergmann, G. (Universitaet, Goettingen, Ger.). Z. Physik, 187: 395-410(1965). (In German).

Films of lead are deposited on a superconducting substrate. The transition temperature $T_c$ of this sandwich is measured as a function of the lead thickness $D_{Pb}$. In different experiments the properties (thickness, transition temperature, mean free path of electrons) of the substrate are varied. It is especially interesting that the initial slope (small lead thickness) of the $T_c(D_{Pb})$-curve is independent of the electronic mean free path of the superconducting substrate and inversely proportional to its thickness. The results for different thicknesses of the components in the system indium–lead can be well described by a theory of de Gennes and Werthamer. (auth)

**2918** ON THE SPIN ORDERING OF PARAMAGNETIC STATES IN QUENCHED CONDENSED LAYERS ON SUPERCONDUCTORS. Korn, Dietrich (Universitaet, Goettingen, Ger.). Z. Physik, 187: 463-77(1965). (In German).

The susceptibility of the dilute alloys Pb–Mn, Cu–Mn, Sn–Mn, and La–Gd is measured in the temperature range from 2 to 300°K. The dilute alloys are produced by simultaneous evaporating of both components on a substrate at 14°K. In this way a statistic distribution of the paramagnetic impurities in the solvent was obtained. The Mn atoms, dissolved in Pb, obey Curie's law. The paramagnetic Curie temperature equals zero at every chosen concentration for the mentioned systems. Mn in Pb shows an effective magnetic moment of 3.9 Bohr magnetons in the concentration range from 2 to 10 at % Mn. At low temperature there exists a quasi-antiferromagnetic ordering among the spins of the Mn atoms. The temperature at which this ordering appears, linearly increases with the concentration of Mn. With regard to the systems of Cu–Mn, Sn–Mn, and La–Gd an antiferromagnetic spin ordering was also found. The transition temperature of superconductivity is depressed by adding Mn to Pb. The decrease disappears when the Pb–Mn films are annealed to 290°K. This agrees with the fact that Mn loses its magnetic moment after annealing the films to room temperature. (auth)

**2919** INVESTIGATIONS ON TIN AND INDIUM–TIN ALLOYS IN THE SUPERCONDUCTING STATE WITH THE HELP OF THE MOESSBAUER EFFECT. Pobell, Frank (Nebenstelle Reaktorstation, Garching, Ger.). Z. Physik, 188: 57-77(1965). (In German).

The recoilless nuclear resonance absorption of the 23.8 kev-$\gamma$-line of $^{119}$Sn was measured in a transmission experiment. The measurements were performed with tin and tin-indium alloys, as a function of temperature above and below the transition points of superconductivity ($2°K < T < 6°K$). The Lamb-Moessbauer-factors, the Debye-temperatures, and an upper limit of the quadrupole interaction were calculated from the data. Within the experimental accuracy there is no evidence for a difference of the quantities in the normal and super-conducting state down to $T = 0.6\ T_c$. The data for the isomeric shift yield a constant s-electron density within the nucleus in the two states within $2 \cdot 10^{-4}$ down to $T = 0.8\ T_c$. (auth)

**2920** SPECIFIC HEAT OF Gd NEAR THE CURIE POINT. Voronel, A. V.; Garber, S. R.; Simkina, A. P.; Charkina, I. A. (Inst. of Physico-Technological and Radiotechnical Measurements, USSR). Zh. Eksp. Teor. Fiz., 49: 429-32(Aug. 1965). (In Russian).

The specific heats of two Gd samples ($\rho(300°K)/\rho(4.2°K) = 12$ and 27) are measured near the Curie point. The effect of impurities on the singularity of the thermodynamic potential for transitions of the second kind is discussed, and it is shown that the singularity is apparently masked by imperfection of the samples. It is pointed out that determination of the Curie point according to the maximum of the nonmagnetic properties is erroneous, and an explanation is presented for the discrepancies encountered in the literature between the Curie points determined on the basis of various properties. (auth)

**2921** MAGNETIC FLUX JUMPS IN HARD SUPERCONDUCTORS IN PULSED MAGNETIC FIELDS. Borovik, E. S.; Fogel, N. Ya.; Litvinenko, Yu. A. (Inst. of Physics and Tech., Moscow). Zh. Eksp. Teor. Fiz., 49: 438-46 (Aug. 1965). (In Russian).

A large number of abrupt changes in the magnetic flux are observed on destruction of the superconductivity in $Nb_3Sn$ and NbZr samples. The magnitude of the changes and their duration are measured. The durations vary between $2 \cdot 10^{-5}$ and $5 \cdot 10^{-4}$ sec. Each change is connected with a partial penetration of the flux into the superconductor. (auth)

**2922** VISCOSITY OF HYDROGEN ISOTOPE SOLUTIONS. Rudenko, N. S.; Konareva, V. G. (Inst. of Physics and Tech., Kiev). Zh. Eksp. Teor. Fiz., 49: 447-8 (Aug. 1965). (In Russian).

The viscosity of hydrogen isotope solutions is measured. The viscosity coefficients are found to be smaller than their additive values. It is moreover found that the magnitude of the divergence of the viscosity coefficients from additivity depends on the mass of the solution components. (auth)

**2923** ELECTRON SPECTRUM OF THE INTERMEDIATE STATE OF SUPERCONDUCTORS. Andreev, A. F. (Inst. of Problems in Physics, Academy of Sciences, USSR). Zh. Eksp. Teor. Fiz., 49: 655-60(Aug. 1965). (In Russian).

It is shown that at energies of the order of v/a (v is the fermi velocity, a the thickness of the normal layers) quantization of the energy levels of electron excitations becomes important. As a result the temperature dependence of the thermodynamic quantities changes at temperatures of the order of 0.1°K. (auth)

**2924** LOCAL MAGNETIC FIELDS ON THE SURFACE OF A Nb–Zr SUPERCONDUCTOR IN THE MIXED STATE. Krivko, N. I.; Berger, M. M. (Ioffe Inst. of Physics and Tech., Leningrad). Zh. Eksp. Teor. Fiz., 49: 730-3(Sept. 1965). (In Russian).

Results are presented on the measurement of local magnetic fields on the surface of a Nb–Zr (60–40 wt %) superconductor in an external magnetic field of $\approx 3000$ Oe. The experiments revealed that the magnitude of the local field strength appreciably depends on the conditions of magnetization of the superconductor. The local field is apparently the field due to currents induced in the superconductor by a varying external magnetic field. (auth)

**2925** DETERMINATION OF THE CRITICAL TEMPERATURE OF A SUPERCONDUCTOR WITH AN IMPURITY IN THE TWO-BAND MODEL. Moskalenko, V. A.; Palistrant, M. E. (Moscow State Univ.; Inst. of Mathematics, Academy of Sciences, USSR). Zh. Eksp. Teor. Fiz., 49: 770-80(Sept. 1965). (In Russian).

The effect of a nonmagnetic impurity on the critical temperature $T_c$ of a superconductor with overlapping energy bands is investigated. It is shown that due to interband scattering of electrons on the impurity, a significant change in the magnitude of $T_c$ occurs. The extreme cases of small and large impurity concentrations are investigated. In the first limiting case increase of concentration is accompanied by a linear decrease of $T_c$. The definition of the critical temperature as the eigenvalue of the equation for bound pair production is exploited in the proof. The calculations are performed in the weak electron–phonon coupling approximation and by neglecting single particle Green function elements which are nondiagonal with respect to the band indices. (auth)

**2926** CRITICAL FIELDS OF THIN SUPERCONDUCTING FILMS. Shapoval, E. A. (Moscow State Univ.). Zh. Eksp. Teor. Fiz., 49: 930-40(Sept. 1965). (In Russian).

Critical fields for phase transitions of the second kind are found for thin films throughout the complete temperature range. Pure films as well as those containing various concentrations of impurities are considered. Reflection of electrons from the film surface is assumed to be diffuse. (auth)

**2927** FLUXOID CONSERVATION BY SUPERCONDUCTING THIN FILM RINGS [Thesis]. Hunt, Thomas Kintzing. Pasadena, Calif., California Inst. of Tech., 1964. 77p.

A torque method for measuring the persistent current in superconducting rings was used to investigate the conservation of the fluxoid originally predicted by F. London. The fluxoid through a superconducting ring is the action integral of the canonical angular momentum of the superconducting electrons taken around the ring. This is comprised of two parts, one describing the mechanical angular momentum of the electrons and the other describing the magnetic flux trapped by the ring. The mechanical angular momentum depends on the penetration depth ($\lambda$) and therefore on temperature. If the fluxoid is conserved, temperature variations should alter the balance between the mechanical and electromagnetic angular momenta. As a consequence, the amount of trapped flux, and hence the persistent current, should vary with temperature even though the ring remains at all times entirely within the pure superconducting state with zero resistance. Very thin films of tin showed experimentally a decrease in persistent current with increasing temperature and an increase with decreasing temperature, which agrees with that to be expected on the basis of the fluxoid conservation predicted by London. (Dissertation Abstr.)

**2928** THE NON-LINEAR THERMO-HYDRODYNAMICS OF He(II) IN WIDE CHANNELS [Thesis]. Tough, James Thomas. Seattle, Univ. of Washington, 1964. 123p.

Critical heat currents in He II thermal counterflow through wide channels of rectangular cross section were investigated by measuring the damping of small amplitude vibrations of a fine wire situated in the channel. The damping measured in the absence of a heat current is found to be consistent with that calculated from the accepted He II hydrodynamic equations, and is used to measure the viscosity of the liquid. An excess damping force is observed when the heat current W exceeds a critical value $W_c$, which is found to depend only on temperature and channel width. The lack of any dependence of $W_c$ on wire parameters (diameter and frequency of vibration) indicates that the wire acts as a probe of the thermal counterflow in the channel. Previous thermal counterflow measurements are discussed in terms of the mutual friction and normal fluid turbulence theories of the critical heat current. The observed excess damping of the vibrating wire is found to be in agreement with a calculation based on normal fluid turbulence. The calculation also indicates that a mutual friction would not provide an excess damping force. (Dissertation Abstr.)

**2929** TWO PROBLEMS IN THE THEORY OF SUPERCONDUCTIVITY [Thesis]. Skalski, Stanislaus. New Brunswick, N. J., Rutgers Univ., 1964. 125p.

The effects of paramagnetic impurities in superconductors are calculated, using the Abrikosov-Gor'kov theory and the Green's function of the system. The density of states in energy is computed for different values of the inverse collision time for exchange scattering $\Gamma$. The temperature-dependent order parameter is computed for different values of $\Gamma$, and the behavior of the excitation energy gap $\Omega_G(T)$ is determined. The thermodynamic properties follow from the density of states; the critical field and the discontinuity in the specific heat at the critical temperature are calculated. Expressions for the penetration depth and complex conductivity are obtained, and numerical results are presented for the case $T = 0°$. A pair wave function is defined, and the effect of impurities on the correlation distance is discussed. The role of spin-orbit coupling in explaining the observed finite Knight shift in the superconducting state is considered. A simplified version of the theory of Abrikosov and Gor'kov is presented which leads to a nonvanishing electron spin susceptibility. The vertex corrections are shown to be equivalent to an averaging over the orientation of the scattering plane in a spin-orbit interaction and result only in a redefinition of the collision frequency parameter. Thus, the nonvanishing susceptibility arises because the electron spin operator has only off-diagonal matrix elements in the presence of the spin-orbit interaction. (TCO)

# Neutron Physics

## See also REACTOR TECHNOLOGY — Criticality Studies

*Refer also to abstracts 1947, 3256, 3257, 3366, and 3423.*

**2930** (AD-614636) NUMERICAL RESULTS FOR THE AUXILIARY EQUATION OF RADIATIVE TRANSFER. Bellman, R.; Kagiwada, H.; Kalaba, R. (RAND Corp., Santa Monica, Calif.). Apr. 1965. Contract AF49(638)-700. 26p. (RM-4572-PR). CFSTI $2.00 cy, $0.50 mn.

A basic problem in astrophysics, meteorology, and neutron transport theory is the determination of the internal intensity produced when uniform parallel rays illuminate a slab of finite thickness which both absorbs and scatters radiation isotropically. One approach to this problem is through the intermediate step of determining the source function which represents the rate of production of scattered radiation per unit volume per unit solid angle as a function of the depth below the top surface. The results of extensive calculations of source functions in both graphical and tabular form are presented. (TAB)

**2931** (AD-616518) MEASUREMENT OF FAST NEUTRON SPECTRA IN AN INFINITE MEDIUM OF $CH_2$. Final Report, March 24-November 24, 1964. Profio, A. E.; Kirkbride, J. (General Atomic, San Diego, Calif.). Apr. 2, 1965. Contract AF 29(601)-6376. 140p. (WL-TR-64-180; GA-5973). CFSTI $4.00 cy, $1.00 mn.

Measurements of the fast neutron spectrum and angular distribution in a large assembly of paraffin wax ($CH_2$) were made. Two targets were irradiated with a pulsed electron beam from a Linear Accelerator, one as essentially point isotropic fission spectrum source and the other a narrow photoneutron source for small angle measurements. The time-of-flight technique was employed to measure the energy from approximately 0.3 to approximately 15 Mev with an energy resolution of 10 percent. Estimated error in the spectrum is ±20 percent outside this range. The source spectra were measured in air for input to calculations. Data were obtained at 0° up to 15 cm penetration with preliminary results to 45 cm. Angular flux measurements were made up to 60° at 30 cm, with preliminary data at 8° and 45 cm. The results, within the stated accuracy and resolution, should be suitable for testing analytical techniques and corresponding shielding codes. (auth)

**2932** (ORNL-3822(Vol.1)) DIFFERENTIAL FAST-NEUTRON ALBEDOS FOR CONCRETE. I. DESCRIPTIONS OF MONTE CARLO CALCULATION AND TSF EXPERIMENT AND COMPARISON OF CALCULATED AND EXPERIMENTAL RESULTS. Maerker, R. E.; Muckenthaler, F. J. (Oak Ridge National Lab., Tenn.). Oct. 1965. Contract W-7405-eng-26. 45p. Dep. mn; CFSTI $2.00 cy, $0.50 mn.

Monte Carlo calculations are carried out on the reflection properties of concrete for fast neutrons. Results are presented for the differential angular dose albedo for various incident-beam conditions, and some of the other distributions calculated are discussed. A comparison of the fast-neutron angular dose albedo calculations, weighted by an incident spectrum as measured at the Tower Shielding Facility, with the results of a series of dose albedo measurements performed at the TSF shows a root mean square deviation from 147 combinations of the incident and reflected angles of 3.1%, with the largest single deviation being 9%. This excellent agreement shows that existing cross sections are adequate to calculate differential albedos to a high precision. (auth)

**2933** (ORNL-3822(Vol.2)) DIFFERENTIAL FAST-NEUTRON ALBEDOS FOR CONCRETE. II. RESULTS OF MONTE CARLO CALCULATIONS FOR AN INCIDENT AN-

GLE OF 0 deg. Maerker, R. E. (Oak Ridge National Lab., Tenn.). July 1965. Contract W-7405-eng-26. 232p. Dep. mn; CFSTI $6.00 cy, $1.25 mn.

Experimental and calculated differential fast-neutron albedos are tabulated for concrete. The experiment consists of measuring neutrons reflected at various angles from a concrete slab, which is located in a highly collimated beam of neutrons from the TSR-II (four angles of incidence). Calculations are performed with the 05R Monte Carlo computer code, and cover six different source energy bands for each angle of incidence of a "gun barrel" source of monodirectional neutrons. Volumes II–IV present the machine output in detail, each volume representing a different angle of incidence: Vol. II, 0°; Vol. III, 45°; Vol. IV, 60°; Vol. V, 75°; and Vol. VI, 85°. (auth)

**2934** (ORNL–3822(Vol.3)) DIFFERENTIAL FAST-NEUTRON ALBEDOS FOR CONCRETE. III. RESULTS OF MONTE CARLO CALCULATIONS FOR AN INCIDENT ANGLE OF 45 deg. Maerker, R. E. (Oak Ridge National Lab., Tenn.). July 1965. Contract W-7405-eng-26. 230p. Dep. mn; CFSTI $6.00 cy, $1.25 mn.

**2935** (ORNL–3822(Vol.4)) DIFFERENTIAL FAST-NEUTRON ALBEDOS FOR CONCRETE. IV. RESULTS OF MONTE CARLO CALCULATIONS FOR AN INCIDENT ANGLE OF 60 deg. Maerker, R. E. (Oak Ridge National Lab., Tenn.). July 1965. Contract W-7405-eng-26. 230p. Dep. mn; CFSTI $6.00 cy, $1.25 mn.

**2936** (ORNL–3822(Vol.5)) DIFFERENTIAL FAST-NEUTRON ALBEDOS FOR CONCRETE. V. RESULTS OF MONTE CARLO CALCULATIONS FOR AN INCIDENT ANGLE OF 75 deg. Maerker, R. E. (Oak Ridge National Lab., Tenn.). July 1965. Contract W-7405-eng-26. 230p. Dep. mn; CFSTI $6.00 cy, $1.25 mn.

**2937** (ORNL–3822(Vol.6)) DIFFERENTIAL FAST-NEUTRON ALBEDOS FOR CONCRETE. VI. RESULTS OF MONTE CARLO CALCULATIONS FOR AN INCIDENT ANGLE OF 85 deg. Maerker, R. E. (Oak Ridge National Lab., Tenn.). July 1965. Contract W-7405-eng-26. 230p. Dep. mn; CFSTI $6.00 cy, $1.25 mn.

**2938** (UCRL–14245) INTERACTION IN ARRAYS OF FISSIONABLE MATERIALS. Kolar, O. C.; Morton III, J. R.; Pruvost, N. L. (Lawrence Radiation Lab., Univ. of California, Livermore). Oct. 5, 1965. Contract W-7405-eng-48. 32p. (CONF-651103–12). Dep. mn; CFSTI $2.00 cy, $0.50 mn.

From IAEA Symposium on Criticality Control of Fissile Materials, Stockholm.

The interaction effect is studied in arrays of fissionable materials. Both experimental and theoretical efforts are reported. The arrays studied experimentally are composed of Pu metal units. Array geometries are simple; the basic units are cylinders and the arrays are cubical. Bare arrays are studied, as well as those with internal moderation or external reflection. 130 basic units are available so that arrays up to $5 \times 5 \times 5$ in size can be studied. The purposes of the study are two-fold: to provide clean, critical data to use in the development and normalization of computational techniques; and the data as such are expected to be useful for interpolation and extrapolation for application to actual systems of interest. The basic array unit is a 3-kg cylinder of Pu metal, 4.62 cm high, 6.53 cm in diameter, and of density 19.54 g/cm$^3$. The height-to-diameter ratio is chosen so that a double unit consisting of two basic units, one on top of the other, will have the same shape factor as a single basic unit. A brief description of the canning, assembly equipment, and the experimental building is presented. A short discussion of the safety evaluation (startup accident, step insertion of reactivity) is also given. Pertinent calculations are performed using both the GEM and SORS neutron Monte Carlo electronic computer programs. Experimental results for arrays consisting of two units up to the maximum number are presented. (auth)

**2939** (WAPD-T-1710) FEW GROUP AND MULTIGROUP CALCULATIONS OF NEUTRON PENETRATION. Shure, K. (Bettis Atomic Power Lab., Pittsburgh, Pa.). Sept. 1964. Contract AT-11-1-GEN-14. 17p. Dep. mn; CFSTI $1.00 cy, $0.50 mn.

P3 few-group estimates and P3 multigroup estimates of thermal neutron flux distributions in water and iron–water are compared. The energy-group structure of the few-group technique is varied in order to find the structure that most nearly reproduces the multigroup results. (T.F.H.)

**2940** METHOD FOR SOLUTION OF THE NEUTRON TRANSPORT EQUATION WITHIN THE FRAMEWORK OF THE Sn APPROXIMATION. Pavelescu, M. (Inst. of Atomic Physics, Bucharest). Acad. Repub. Pop., Stud. Cercet. Fiz., 16: 625-33(1964). (In Rumanian).

The calculation method is presented of the neutron flux distribution by Sn approximation in spherical geometry. One starts from the neutron transport equation, one obtains Sn approximation of that equation and afterwards it is solved. All calculations are exposed and one gives the final form used in different applications. (auth)

**2941** ON THE USE OF RECURSION FORMULAS FOR THE LIE-SERIES METHOD. Mennig, J. Acta Phys. Austriaca, 19: 339-48(1965). (In German).

The Cap method for the use of the Lie-series in the analytical calculation of $\underline{n}$-group neutron fluxes in $\underline{m}$ zones of non-multiplying medium was described. The recursion formula method is then illustrated with an example. (J.S.R.)

**2942** NEUTRON SPECTRA IN HETEROGENEOUS MEDIA. Meier, K. (VEB Atomkraftwerk Rheinsberg, Berlin). At. Energ. (USSR), 19: 253-7(Sept. 1965). (In Russian).

The spectrum of neutrons in a heavy-atom medium consisting of two nonabsorbing components at different temperature is determined on the basis of transport theory. The results are compared with data obtained using the group model of Selengut. In those cases where the neutron spectra obtained by the exact solution of the initial equations can be represented by closed expressions containing only tabulated functions, a comparison of the numerical results is presented. It can be assumed that the error in the neutron temperature is 10%, it being smaller the smaller the slowing-down power of the components of the medium and the smaller the difference in their temperature. (tr-auth)

**2943** HEAVY MONOATOMIC GAS MODEL AND UNSTEADY THERMALIZATION OF NEUTRONS IN LEAD. Kenzhebaev, Sh. At. Energ. (USSR), 19: 296-7(Sept. 1965). (In Russian).

Neutron scattering in lead can satisfactorily be described in the framework of the heavy monoatomic gas model, since lead, having a large mass, has a low Debye temperature. Calculations are carried out of the average velocity of neutrons in lead in the range of slowing-down times where the spectrum is close to maxwellian, and results are compared with previous experiments. Deviations at small time values can be explained by the presence of higher energy harmonics; at larger times, discrete characteristic values are not present, even in the first harmonic. This result shows that the effect associated with the finiteness of the limit of the attenuation time constants is significant only at sufficiently large times. (M.J.T.)

**2944** PROPAGATION OF THERMAL NEUTRON BURSTS IN DIFFUSION MEDIA. Fleck, C. M.; Kopitsch, F. (Oesterreichische Hochschule, Vienna). Atomkernenergie, 8: 239-42(July-Aug. 1965). (In German).

The propagation of thermal neutron bursts was investigated in an infinite water geometry. The thermal neutron lifetime $l_0$ and the diffusion coefficient $D_0 = \overline{D \cdot v}$ can be derived from measurements of the time dependent neutron density at different spatial points. By chopping a thermal neutron beam, δ-source bursts were produced at a Ni-scattering target inside the diffusion medium. The results are compared with those obtained by different authors. A reasonable agreement can be stated. (auth)

**2945** NEUTRON SPECTRA OF COOLED MODERATORS. Rauch, H.; Schmidt, H. (Oesterreichische Hoch-

schule, Vienna). Atomkernenergie, 8: 243-6(July-Aug. 1965). (In German).

Thermal neutron spectra of paraffin, polyethylene, water, methanol and benzene were investigated at the boiling point of liquid nitrogen. The most favorable configuration for moderation was determined by variation of the geometrical form of the moderator. The efficiency of the different moderator materials will be discussed in terms of the effective neutron temperature and the gain factor for cold neutrons. In the case where best moderation was observed effective neutron temperature was about 28°K above the moderator temperature, the gain of cold neutrons was approximately 3.5. (auth)

**2946** SLABS OF AN 1/v-ABSORBER IN AN 1/E-NEUTRON FLUX. Bensch, F. (Oesterreichische Hochschule, Vienna). Atomkernenergie, 8: 247-8(July-Aug. 1965). (In German).

Slabs of a 1/v-absorber in a 1/E-neutron flux are considered. General solutions are given for the absorption rate per square unit in the case of a collimated neutron beam and an isotropic flux. (auth)

**2947** ON THE PROBLEM OF COMPARING NEUTRON EMITTERS OF VARIOUS SPECTRAL COMPOSITION. Fominykh, V. I. Izmeritel. Tekh., No. 6, 43-6(June 1965). (In Russian).

If neutron scattering in air is neglected, the following formula can be used to determine the neutron strengths of two sources having a different spectral composition: $N_0 = N_p + [Q\sigma\eta_0(E)S\alpha_0]/4\pi(R + \Delta r_0)^2$. Here $N_0$ is the neutron count of a standard source at a distance R. $N_0$ is a correction coefficient for the neutron scattering determined experimentally by using a paraffin cone containing 5% $B_2O_3$. The term $\eta_0$ is the counting efficiency. S is the area of the front surface of the counter. The asymmetry coefficient $\alpha_0$ is determined experimentally from the ratio of the count rate 90° to the count rate on an angle $\theta$ to the source. The effective center of the counter $\Delta r_0$ is determined experimentally from the neutron count rate as a function of the distance R. The unknown neutron source is then placed at the same distance R, and the whole cycle of measurements is again repeated for the new source in order to make a valid comparison. Thus, it is possible to compare a standard RaBe $(\alpha,n)$ source with a PuBe $(\alpha,n)$ source. An all-wave detector having $B_2O_3$ sides and a polyethylene layer 7 cm thick can be used as the neutron counter. (TTT)

**2948** KOHN ANOMALY AND COHERENT SCATTERING OF SLOW NEUTRONS IN LIQUID METALS. Singwi, K. S.; Andersson, Lars-Erik (Argonne National Lab., Ill.). Phys. Rev. Lett., 15: 693-4(Oct. 25, 1965).

It is shown that there exists a Kohn anomaly in liquid metals which is exhibited as a logarithmic singularity at $\kappa = 2k_F$ in the gradient of the fourth moment $\langle\omega_{coh}{}^4(\kappa)\rangle$ of the usual scattering function $S_{coh}(\vec{\kappa},\omega)$. It is also shown that the width $\Delta E(\kappa)$ of the quasielastic scattering also exhibits a similar anomalous behavior. (L.B.S.)

**2949** NEUTRON PRODUCTION BY THE $(\alpha,n)$ REACTION FROM HETEROGENEOUS ISOTOPIC SOURCES. Jordan, E. D. (Catholic Univ. of America, Washington, D. C.); Knuth, D. F. Trans. Amer. Nucl. Soc., 8: 317-18 (Nov. 1965).

**2950** EXPERIMENTAL INVESTIGATIONS OF FAST-NEUTRON DECAY TIMES IN LEAD ASSEMBLIES. Beghian, L. E.; Hofmann, F.; Wilensky, S. (Massachusetts Inst. of Tech., Cambridge). Trans. Amer. Nucl. Soc., 8: 431(Nov. 1965).

**2951** DIFFUSION PARAMETERS OF MIXTURES OF LIGHT AND HEAVY WATER AT SEVERAL TEMPERATURES. Jones, H. G.; Robeson, A.; Salaita, G. N. (Virginia Polytechnic Inst., Blacksburg). Trans. Amer. Nucl. Soc., 8: 431-2(Nov. 1965).

**2952** EFFECT OF SAMPLE GEOMETRY ON DECAY-CONSTANT MEASUREMENTS IN WATER USING THE PULSED-NEUTRON TECHNIQUE. Freed, DeBow; Whan, Glenn A. (Univ., New Mexico, Albuquerque). Trans. Amer. Nucl. Soc., 8: 433-4(Nov. 1965).

**2953** PULSED-NEUTRON MEASUREMENTS IN DIPHENYL AT 85 deg C AND 105 deg C. Reier, M. (Atomics International, Canoga Park, Calif.). Trans. Amer. Nucl. Soc., 8: 434(Nov. 1965).

**2954** PULSED MEASUREMENTS OF NEUTRON-DIFFUSION PARAMETERS IN $D_2O$. Parks, P. B.; Baumann, N. P. (E. I. duPont de Nemours, Aiken, S. C.). Trans. Amer. Nucl. Soc., 8: 436(Nov. 1965).

**2955** PULSE-PROPAGATION EXPERIMENTS USING A FAST-BURST REACTOR. Miley, G. H.; Doshi, P. K. (Univ. of Illinois, Urbana). Trans. Amer. Nucl. Soc., 8: 437(Nov. 1965).

**2956** ACCELERATOR-PULSED FAST-ASSEMBLY OPERATING EXPERIENCE. Russell, J. L. Jr.; Crosbie, K. L. (General Atomics Div., General Dynamics Corp., San Diego, Calif.). Trans. Amer. Nucl. Soc., 8: 437-8 (Nov. 1965).

**2957** MEASUREMENT OF DIFFUSION COEFFICIENT IN A HIGHLY ANISOTROPIC MEDIUM. Pilat, E. E.; Gueron, H.; Lanning, D. D. (Massachusetts Inst. of Tech., Cambridge). Trans. Amer. Nucl. Soc., 8: 446-7(Nov. 1965).

**2958** DOPPLER COEFFICIENTS OF FERTILE AND REFRACTORY MATERIALS. Mountford, L. A.; Carpenter, S. G.; Springer, T. H.; Tuttle, R. J. (Atomics International, Canoga Park, Calif.). Trans. Amer. Nucl. Soc., 8: 454(Nov. 1965).

**2959** DOPPLER-EFFECT MEASUREMENTS ON A DILUTE FAST-CARBIDE ASSEMBLY, ZPR-6 ASSEMBLY 4Z. Till, C. E.; Lewis, R. A.; Groh, E. F. (Argonne National Lab., Ill.). Trans. Amer. Nucl. Soc., 8: 454-5 (Nov. 1965).

**2960** EFFECT OF REVISIONS TO THE MULTIGROUP REPRESENTATIONS OF THE BERYLLIUM (n,2n) AND BERYLLIUM $(n,\alpha)$ REACTIONS. Ottewitte, E. H. (Atomics International, Canoga Park, Calif.). Trans. Amer. Nucl. Soc., 8: 456-7(Nov. 1965).

**2961** NEUTRON CROSS SECTIONS FOR TANTALUM AND TUNGSTEN. Prince, A. (General Electric Co., Cincinnati). Trans. Amer. Nucl. Soc., 8: 457-8(Nov. 1965).

**2962** THE INTERACTIONS OF 14.6-Mev NEUTRONS IN IRON, $^7$Li AND CARBON. Western, G. T.; Gibbons, F. L.; Williams, J. R.; Baird, R. C. (General Dynamics, Ft. Worth, Tex.). Trans. Amer. Nucl. Soc., 8: 458-9 (Nov. 1965).

**2963** DIFFERENTIAL NEUTRON SCATTERING FROM $D_2O$ AND $ZrH_{1.85}$. Beyster, J. R.; Young, J. C.; Neill, J. M. (General Atomics Div., General Dynamics Corp., San Diego, Calif.). Trans. Amer. Nucl. Soc., 8: 459-60(Nov. 1965).

**2964** SCATTERING OF NEUTRONS BY POLYETHYLENE. Whittemore, W. L. (General Atomics Div., General Dynamics Corp., San Diego, Calif.). Trans. Amer. Nucl. Soc., 8: 460-1(Nov. 1965).

**2965** THE USE OF INTEGRAL ACTIVATION TECHNIQUES TO EXPERIMENTALLY DETERMINE $H_2O$–$H_3BO_3$ THERMAL-NEUTRON SPECTRA. Ibarra, H.; Sher, R. (Stanford Univ., Calif.). Trans. Amer. Nucl. Soc., 8: 462-3(Nov. 1965).

**2966** NEUTRON SPECTRUM MEASUREMENTS IN $H_2O$ AS A FUNCTION OF TEMPERATURE. Young, J. C.; Houston, D. H.; Houghton, G. K.; Neill, J. M.; Beyster, J. R. (General Atomics Div., General Dynamics Corp., San Diego, Calif.). Trans. Amer. Nucl. Soc., 8: 463-4 (Nov. 1965).

**2967** FAST-NEUTRON SPECTRA IN LIQUID HYDROGEN. Trimble, G. D.; Houghton, G. K.; Audas, J. H.; Beyster, J. R. (General Atomics Div., General Dynamics Corp., San Diego, Calif.). Trans. Amer. Nucl. Soc., 8: 465(Nov. 1965).

**2968** NEUTRON SPECTRA IN BERYLLIUM METAL. Neill, J. M.; Young, J. C.; Brouwer, W. (General Atomics

Div., General Dynamics Corp., San Diego, Calif.). Trans. Amer. Nucl. Soc., 8: 465-6(Nov. 1965).

**2969** SPIN POLARIZATION AND THE AGE OF NEUTRONS IN WATER. Goldsmith, M. (Bettis Atomic Power Lab., Pittsburgh). Trans. Amer. Nucl. Soc., 8: 466-7(Nov. 1965).

**2970** THE AGE OF FISSION NEUTRONS TO INDIUM RESONANCE ENERGY IN ALUMINUM-WATER MIXTURES. Paschall, R. K. (Atomics International, Canoga Park, Calif.). Trans. Amer. Nucl. Soc., 8: 467-8(Nov. 1965).

**2971** THE MEASUREMENT OF RESONANCE NEUTRON FLUX AND SPECTRA BY AN ACTIVATION TECHNIQUE. Hogg, C. H.; Howes, B. W. (Phillips Petroleum Co., Idaho Falls, Idaho). Trans. Amer. Nucl. Soc., 8: 468(Nov. 1965).

**2972** ON GROUP CROSS SECTIONS OF FISSILE NUCLIDES IN THE UNRESOLVED ENERGY RANGE. Kelber, C. N.; Kier, P. H. (Argonne National Lab., Ill.). Trans. Amer. Nucl. Soc., 8: 469(Nov. 1965).

**2973** GEOMETRICAL EFFECTS ON NEUTRON RESONANCE ABSORPTION IN A HETEROGENEOUS SYSTEM. Ludewig, H.; Lurie, H. (California Inst. of Tech., Pasadena). Trans. Amer. Nucl. Soc., 8: 469-70 (Nov. 1965).

**2974** INTERMEDIATE RESONANCE ABSORPTION IN HETEROGENEOUS MEDIA INCLUDING MODERATOR SCATTERING. Sehgal, Bal Raj; Goldstein, Rubin (Brookhaven National Lab., Upton, N. Y.). Trans. Amer. Nucl. Soc., 8: 470-1(Nov. 1965).

**2975** STRUCTURE IN THE DOPPLER EFFECT AS A FUNCTION OF SURFACE. MASS RATIO IN $^{197}$Ag. Beller, L. S.; Farrar IV, H.; Otter, J. M. (Atomics International, Canoga Park, Calif.). Trans. Amer. Nucl. Soc., 8: 471-2(Nov. 1965).

**2976** MEASUREMENT OF THE EFFECTIVE RESONANCE INTEGRAL AND DOPPLER COEFFICIENT OF THORIUM-OXIDE RODS. Palowitch, B. L.; Hardy, J. Jr. (Bettis Atomic Power Lab., Pittsburgh). Trans. Amer. Nucl. Soc., 8: 472-3(Nov. 1965).

**2977** A GENERALIZED EQUIVALENCE PRINCIPLE FOR RESONANCE INTEGRAL CALCULATIONS. Suich, John E. (E. I. duPont de Nemours, Aiken, S. C.). Trans. Amer. Nucl. Soc., 8: 473-4(Nov. 1965).

**2978** VARIATIONAL VACUUM BOUNDARY CONDITIONS FOR A $P_N$ APPROXIMATION. Davis, James A. (Westinghouse Electric Co., Pittsburgh). Trans. Amer. Nucl. Soc., 8: 484-5(Nov. 1965).

**2979** HIGHER ORDER VARIATIONAL PRINCIPLES. Selengut, D. S. (General Electric Co., Schenectady, N. Y.). Trans. Amer. Nucl. Soc., 8: 485(Nov. 1965).

**2980** A NUMERICAL COMPARISON OF HIGHER ORDER VARIATIONAL PRINCIPLES. Schreiner, Sheldon (Univ. of California, Berkeley); Selengut, D. S. Trans. Amer. Nucl. Soc., 8: 485-6(Nov. 1965).

**2981** MOMENTS EQUATIONS AND EQUIVALENT DISCRETE ORDINATES EQUATIONS. PART I. GENERALIZED MOMENTS EQUATIONS. Carlson, B. G.; Lathrop, K. D. (Los Alamos Scientific Lab., N. Mex.). Trans. Amer. Nucl. Soc., 8: 487(Nov. 1965).

**2982** MOMENTS EQUATIONS AND EQUIVALENT DISCRETE ORDINATES EQUATIONS. PART II. EQUIVALENT DISCRETE ORDINATES EQUATIONS. Carlson, B. G.; Lathrop, K. D. (Los Alamos Scientific Lab., N. Mex.). Trans. Amer. Nucl. Soc., 8: 487-8(Nov. 1965).

**2983** A FLEXIBLE NUMERICAL APPROACH TO LINEAR TRANSPORT PROBLEMS. Pomraning, G. C. (General Atomic Div., General Dynamics Corp., San Diego, Calif.). Trans. Amer. Nucl. Soc., 8: 488-9(Nov. 1965).

**2984** NUMERICAL SOLUTIONS OF THE TRANSPORT EQUATION. Lucey, J. W.; Hansen, K. F. (Massachusetts Inst. of Tech., Cambridge). Trans. Amer. Nucl. Soc., 8: 489-90(Nov. 1965).

**2985** ENERGY-INDEPENDENT BIASING FUNCTIONS FOR MONTE CARLO TRANSPORT CALCULATIONS. Jordan, T. M. (Douglas Aircraft Co., Inc., Santa Monica, Calif.). Trans. Amer. Nucl. Soc., 8: 490-1(Nov. 1965).

**2986** CRITICALITY OF A BARE SLAB OF ARBITRARY SIZE WITH ANISOTROPIC SCATTERING. Paik, N. C.; Kaplan, I.; Travelli, A. (Massachusetts Inst. of Tech., Cambridge). Trans. Amer. Nucl. Soc., 8: 504-5 (Nov. 1965).

**2987** TIME-DEPENDENT MONOENERGETIC NEUTRON TRANSPORT IN TWO ADJACENT SEMI-INFINITE MEDIA. Erdmann, R. C.; Lurie, H. (California Inst. of Tech., Pasadena). Trans. Amer. Nucl. Soc., 8: 506-7 (Nov. 1965).

**2988** EXTRAPOLATION DISTANCE OF HIGHER VELOCITY MODES IN SLAB GEOMETRY. Copic, M. (Kansas State Univ., Manhattan). Trans. Amer. Nucl. Soc., 8: 507-8(Nov. 1965).

**2989** INVARIANT IMBEDDING SOLUTIONS FOR ENERGY-DEPENDENT NEUTRON TRANSPORT IN HETEROGENEOUS ANISOTROPICALLY SCATTERING SHIELDS. Mathews, D. R.; Hansen, K. F. (Massachusetts Inst. of Tech., Cambridge). Trans. Amer. Nucl. Soc., 8: 508-9 (Nov. 1965).

**2990** TRANSPORT SYNTHESIS. Davis, James A.; Kaplan, Stanley (Westinghouse Electric Corp., Pittsburgh). Trans. Amer. Nucl. Soc., 8: 509(Nov. 1965).

**2991** THE DISPERSION LAW OF A MODERATOR. Moore, M. N. (San Fernando Valley State Coll., Northridge, Calif.). Trans. Amer. Nucl. Soc., 8: 509-10(Nov. 1965).

**2992** HETEROGENEOUS ANALYSIS BY MULTIGROUP METHODS OF EPITHERMAL REACTIONS. Suich, John E. (E. I. duPont de Nemours and Co., Aiken, S. C.); Honeck, H. C. Trans. Amer. Nucl. Soc., 8: 511(Nov. 1965).

**2993** EFFECTIVE THERMAL-NEUTRON CROSS SECTIONS FOR MATERIALS WITH GRAIN STRUCTURE. Dyos, M. W.; Pomraning, G. C. (General Atomic Div., General Dynamics Corp., San Diego, Calif.). Trans. Amer. Nucl. Soc., 8: 516(Nov. 1965).

**2994** MEASUREMENT OF NEUTRON-FLUX SPECTRA USING A FERMI CHOPPER. Nunn, L. R. Jr.; Welt, M. A. (North Carolina State Coll., Raleigh). Trans. Amer. Nucl. Soc., 8: 536-7(Nov. 1965).

**2995** THE CRITICALITY OF $^{244}$Cm. Keshishian, Vahe; Ottewitte, Eric H.; Dunford, Charles L. (Atomics International, Canoga Park, Calif.). Trans. Amer. Nucl. Soc., 8: 549-50(Nov. 1965).

**2996** A DIGITAL COMPUTER CONTROLLED DATA-ACQUISITION AND PROCESSING SYSTEM FOR NUCLEAR EXPERIMENTS. Diaz, Hildebram; Uhrig, Robert E. (Univ. of Florida, Gainesville). Trans. Amer. Nucl. Soc., 8: 588-9(Nov. 1965).

**2997** DESIGN OF THE ARGONNE ISOTOPIC SOURCE NEUTRON FACILITY. Mohr, W. C.; Wahlgren, M. A.; Stewart, D. C. (Argonne National Lab., Ill.). Trans. Amer. Nucl. Soc., 8: 628(Nov. 1965).

**2998** PASSAGE OF POLARIZED NEUTRONS THROUGH A SUPERCONDUCTOR IN THE MIXED STATE. Mamaladze, Yu. G.; Kharadze, G. A.; Cheishvili, O. D. (Inst. of Physics, Academy of Sciences, Georgian SSR). Zh. Eksp. Teor. Fiz., 49: 925-9(Sept. 1965). (In Russian).

It is shown that when a beam of polarized neutrons passes through a superconductor of the second kind it becomes depolarized. The sharp dependence of the depolarization on the beam direction and the direct relation between the period of this dependence and the structure of the magnetic field can in principle be used for investigating

experimentally the two-dimensional lattice of the Abrikosov vortexes. (auth)

**2999** EIGENFUNCTION ANALYSIS OF HYDROGENOUS NEUTRON SPECTRA [Thesis]. Ohanian, Mihran J. Troy, N. Y., Rensselaer Polytechnic Inst., 1963. 142p.

The time dependent thermalization problem is solved using two methods. The first method is based upon the direct integration of the Boltzmann equation using a Taylor Series expansion, in the time variable, of the neutron-density function. The second method is a modal expansion of the neutron-density function in terms of the eigenvalues and eigenfunctions of the Boltzmann operator. The exact transport solution of the infinite medium problem as well as the finite medium problem, in the diffusion approximation, is considered. The medium is homogeneous, non-multiplying, and 1/v absorber. The numerical calculations are done for hydrogen in water using the Wigner-Wilkins hydrogen gas model and the Nelkin model for bound hydrogen, at 68°F. The numerical solutions are obtained using a discrete energy representation of the thermalization problem with 32 energy points between 0.00002 and 1.03 ev distributed at equal intervals in $z = [1 + (kT/E)^{1/2}]^{-1}$. The eigenvalues and eigenfunctions are computed using the Jacobi method of matrix diagonalization. Introducing an initial pulse at 1.03 ev, time-dependent spectra are computed. The steady-state spectrum is obtained by integrating the time dependent spectrum over time. The discrepancy between the results obtained by the two methods is less than 1% at each energy point. By use of perturbation theory approach the diffusion cooling coefficient predicted by the two kernels is computed from the infinite medium eigenvalues and eigenfunctions; it is noted that this coefficient is appreciably sensitive to the model used. A scheme is suggested for the comparison of experimentally obtained steady-state spectra with the predictions of theoretical models. The method is based upon extracting that part of the steady state spectrum that is sensitive to the scattering law and comparing this with the similar quantity predicted theoretically. An interpolation method is also presented to determine steady-state spectra for a given 1/v absorption using two computed universal functions. (A.G.W.)

**3000** SOLUTIONS OF THE ONE-SPEED NEUTRON TRANSPORT EQUATION IN PLANE GEOMETRY [Thesis]. Mendelson, Max Richard. Ann Arbor, Mich., Univ. of Michigan, 1964. 219p.

Case's method for solving the one-speed neutron transport equation with isotropic scattering is applied to two classes of problems in plane geometry. First, problems defined in two adjacent half-spaces which, in general, possess exact solutions are considered. Specifically, the Milne problem solution, the solution for a constant source in one half-space, the solution for a plane monodirectional source at the interface, and the Green's function solution are obtained. These problems have been solved previously by other methods, but the derivations given here are greatly simplified by using Case's method. Second, problems defined in several regions (i.e., problems with more than one boundary), which usually do not possess exact solutions in closed form are considered. However, by means of the analysis developed for the two half-space problem, Case's method may be used to obtain explicit "first order" solutions valid for sufficiently large region thickness. Specifically considered are the slab with infinite reflectors, the slab with finite reflectors, and the uniform infinite lattice. Computer analysis of the first order solutions of these problems shows that they compare very well with a double Gauss 10 numerical quadrature of the transport equation for region thickness of at least five mean free paths. Results are inconclusive for thinner regions because of the questionable accuracy of the numerical quadrature calculation. (Dissertation Abstr.)

**3001** NEUTRON TRANSPORT THEORY IN PULSED MULTIPLYING ASSEMBLIES [Thesis]. Judge, Frank D. Troy, N. Y., Rensselaer Polytechnic Inst., 1963. 175p.

The variational method is used to reduce the general time-dependent Boltzmann equation to a multigroup (with overlapping or non-overlapping) form. The variation of the fundamental decay rate with material properties is then studied. The relation between energy and space transients in pulsed multiplying and pulsed moderating systems is investigated. It is shown that the decay times for energy transients in hydrogen-moderated fueled assemblies are essentially the same as those in non-reproducing assemblies having the same moderating properties. Space transients are shown to decay more rapidly, relative to the fundamental, in fueled assemblies than in moderating systems. The variational method is then used to obtain a simple relationship for the fundamental eigenvalue of the monoenergetic transport operation in small assemblies. Quantitative results for slabs, spheres, and cylinders are presented. The failure of other transport approximations to handle properly the asymptotic time dependence of the neutron flux in small slabs is then quantitatively demonstrated. The limit of applicability of each calculated method is determined. The development of an improved calculational procedure ($DP_l$ multigroup overlapping or non-overlapping) for determining the space and time dependence of the neutron flux in pulsed multiplying system is described. This method is then applied to the analysis of recent pulsed measurements. The duration of the energy and spatial transients and the variation of the vector flux distribution from the center to the edge of an assembly are described quantitatively. It is demonstrated that spatial asymmetries in the flux could exist after the flux distribution appears asymptotic. Calculations of asymptotic spectra in pulsed water and polyethylene multiplying assemblies using various scattering kernels (Nelkin, free proton and Goldman polyethylene kernels) are compared with measured spectra. (Dissertation Abstr.)

**3002** THERMAL NEUTRON TRANSIENTS IN VARIOUS ORDER P-N APPROXIMATIONS [Thesis]. Travelli, Armando. Troy, N. Y., Rensselaer Polytechnic Inst., 1963. 196p.

The study of the distribution of the eigenvalue curves that arise in the analysis of experiments with pulsed sources of neutrons and in the measurement of diffusion lengths in poisoned moderators is shown to be reducible, in plane geometry, to the study of the eigenvalue curves of the Laplace-Fourier transform of the homogeneous Boltzmann equation. A numerical procedure is developed to investigate the distribution of these eigenvalue curves using multigroup spherical harmonics approximations of various orders and assuming the scattering to be linearly anisotropic. In the application of the P-N approximations to the case in which the moderator is water, the behavior of the fundamental eigenvalue curves shows the existence of a critical value for the geometric buckling beyond which only complex eigenvalues, corresponding to travelling waves, could be detected in the pulsed experiment. In high order P-N approximation this critical value is so large, however, that it is possible to conclude that a real eigenvalue with a correspondingly stable spatial mode is always present in any die-way experiment performed on a slab of water of whatever thickness. The diffusion parameters of water are obtained for the fundamental eigenvalue in the P-15 approximation with thirty-two groups using the free-gas model with unit mass and with the Radkowsky prescription, and they are found again using the Goldman modification of Nelkin's kernel with the Selengut-Goertzel approximation. The results agree qualitatively with the experimental data, but some discrepancies show that both scattering kernels could be considerably improved. The higher eigenvalue curves are also obtained in the multigroup P-N approximation, and they may be divided in two major categories: the group of the so-called "continuum" eigenvalues, and the group of the "discrete" ones. (Dissertation Abstr.)

**3003** TIME-, ENERGY- AND SPACE-DEPENDENT NEUTRON THERMALIZATION THEORY [Thesis]. Kunaish, Hassan H. Gainesville, Fla., Univ. of Florida, 1964. 170p.

The time-, energy- and space-dependent neutron ther-

malization theory in moderating assemblies is developed in the consistent $P_1$ approximation of the Boltzmann equation of neutron transport. In order to evaluate the scattering integral involved in this equation the neutron flux is analyzed into two components according to the expression: $\phi(\vec{r},E,t) = m(E)\,\psi(\vec{r},E,t)$. The Maxwellian function, m(E), represents the energy spectrum of neutrons in a non-absorbing infinite medium. In a finite medium with a small absorption cross section the energy spectrum of the neutron flux resembles a Maxwellian distribution. Therefore, the non-Maxwellian component, $\psi(\vec{r},E,t)$, is expected to be a smooth function of energy, E, and hence its value at a different energy, E', can be well approximated by a finite Taylor series expansion about E. This analysis and the detailed balance principle are used to evaluate the scattering integral. The resulting form of the transport equation is a fourth-order differential equation with respect to time, energy, and space. This theory is used in two applications of practical interest, the neutron waves and the pulsed neutrons experiments. Numerical computations are made for both applications using a heavy gas scattering kernel and a 1/v absorption cross section in graphite in order to test the applicability of this model and its compatibility with the $P_1$ approximation. The comparison of these results with the experimental ones confirms that this model is conveniently accurate in describing the pulsed neutron experiment in relatively large systems of buckling up to $3 \times 10^{-3}$ $cm^{-2}$. This model is also proven to provide accurate description of the neutron waves experiment with source frequencies up to 500 cycles per second which are equivalent to transients of periods down to about 2 milliseconds. (Dissertation Abstr.)

**3004** A NUMERICAL SOLUTION TO THE NEUTRON ONE-VELOCITY TIME-INDEPENDENT BOLTZMANN EQUATION IN SLAB GEOMETRY USING A HOMOGENEOUS GREEN'S FUNCTION AND ITS $P_n$ ANGULAR MOMENTS [Thesis]. Aswad, Adnan Ahmad. Gainesville, Fla., Univ. of Florida, 1964. 123p.

The one-speed time-independent neutron integro-differential equation is converted into an integral equation by the use of the homogeneous Green's function. The flux, the Green's function, and the source in the resultant integral equation are expanded in spherical harmonics. The integrations over the angular variables are carried out by the use of the orthogonal relation of the spherical harmonics. The net result is a set of coupled integral equations in the flux angular moments. Relations that give the Green's function angular moments are derived for any geometry and all boundary conditions applicable to the neutron transport equation. It is found that in a slab geometry the Green's function angular moments can be represented analytically by a combination of exponential integral functions. It is observed that if the macroscopic total cross section is the same in all regions of a cell and if the $n^{th}$ coefficient in the expansion of the scattering function is equal to zero, then the flux angular moments will be decoupled from the flux $n^{th}$ angular moment. A sample problem is studied to check the effect of the non-zeroth angular moments of the flux on the scalar flux in the case of isotropic scattering and an isotropic source. Sample problems solved by the TRANVAR and the TRANSANGULAR codes are solved by the method of this work. The results are in good agreement with those answers obtained by the TRANVAR code, but a disagreement with those obtained by the TRANSANGULAR code is found. (Dissertation Abstr.)

**3005** HIGH OUTPUT NEUTRON TUBES. Bounden, J. E.; Lomer, P. D.; Wood, J. D. L. H. (Electronics Research Lab., Baldock, Eng.). 12p. (CONF-650405-2). Gmelin, AED-CONF-65-040-29.

From International Conference on Modern Trends in Activation Analysis, College Station, Tex.

Sealed-off neutron tubes producing a steady output of $10^{10}$ n/sec were developed and used for fast neutron activation analysis. The design principles which lead to this high output with an associated long tube life are discussed. In particular the behavior of targets subjected to long periods of intense ion bombardment was studied and the sputtering rates were determined. Extensions of these principles to higher outputs are described with reference to a tube producing $10^{11}$ n/sec. Ultimate limits of sealed-off neutron generators for activation analysis are outlined. (auth)

## Nuclear Properties and Reactions

*Refer also to abstracts 2880 and 3374.*

**3006** (AD-618676) APPLICATION OF AN ANTI-COINCIDENCE-SHIELDED SCINTILLATION SPECTROMETER TO THE STUDY OF THE $N^{14}(p,\gamma)O^{15}$ REACTION. Evans, Albert E. Jr. (Naval Ordnance Lab., Corona, Calif.). May 11, 1965. 180p. (NOLTR-65-72). CFSTI $5.00 cy, $1.00 mn.

A gamma spectrometer was built using a liquid-scintillator anticoincidence shield for a 5 in. dia × 10 in. long NaI(Tl) crystal. The spectrometer was used to study radiation from the $^{14}N(p,\gamma)^{15}O$ reaction for proton energies of from 0.97 to 1.96 Mev. Decay schemes for the 8.29, 8.75, 8.92, and 8.98 Mev levels in $^{15}O$ were derived. (auth)

**3007** (CEA-Bib-32) LES ISOTOPES DU BERYLLIUM—REACTIONS NUCLEAIRES. (Beryllium Isotopes—Nuclear Reactions). Moulet, Elisee (Commissariat a l'Energie Atomique, Saclay (France). Centre d'Etudes Nucleaires). Oct. 1965. 151p. Dep. mn.

This annotated bibliography is a selection of documentary references on beryllium isotopes in the range from low energies to energies up to 100 Mev. The beryllium acts as target or as a product in these nuclear reactions. Certain generalities concerning nuclear reactions and thought to be of particular interest have been selected together with various characteristics of the nucleus. The period covered is 1933 to 1964. 1269 references. (auth)

**3008** (COO-1420-104) LARGE-SPIN ROTATIONAL STATES OF DEFORMED NUCLEI. Harris, Samuel M. (Columbia Univ., New York. Dept. of Physics. Purdue Univ., Lafayette, Ind. Dept. of Physics). [1964]. Contracts AT(30-1)-1934; AT 1420. 9p. Dep. mn; CFSTI $1.00 cy, $0.50 mn.

A simple explanation for the dependence of moment of inertia (I) on the degree of rotation is proposed, using comparison of calculated and measured values for W-174, W-176, Hf-166, Hf-168, Hf-170, Hf-172, Yb-164, and Yb-166 as a basis. (P.C.H.)

**3009** (GA-6685) UNPACK. A NEUTRON CROSS SECTION DATA RETRIEVAL PROGRAM. Smith, C. V.; Drake, M. K. (General Atomic, San Diego, Calif. John Jay Hopkins Lab. for Pure and Applied Science). Sept. 1, 1965. Contract AT(04-3)-167. 40p. Dep. mn; CFSTI $2.00 cy, $0.50 mn.

A program was written for the retrieval of neutron cross section data and related information from a Brookhaven National Laboratory SC/SRS data tape. This program, UNPACK, was written in FORTRAN IV and MAP machine language for the IBM-7044. The SC/SRS tape contains neutron cross section data in a packed format and the UNPACK code searches through these data for particular cross sections. The retrieved data are then printed and may also be punched on cards. (M.O.W.)

**3010** (IDO-14663) BURNUP DETERMINATION OF NUCLEAR FUELS. Project Report for the Quarter, April 1-June 30, 1965. Maeck, William J.; Rein, James E. (Phillips Petroleum Co., Idaho Falls, Idaho. Atomic Energy Div.). Sept. 1965. Contract AT(10-1)-205. 23p. Dep. mn; CFSTI $2.00 cy, $0.50 mn.

In the development of methods for the accurate determination of the burnup of nuclear fuels, the main emphasis was the measurement of $^{233}U$ thermal fission yields for many stable and long-lived fission products. A capsule containing a weighed quantity of highly enriched $^{233}U$, irradiated to 11.4 atom percent fission, was dissolved and analyzed for the number of atoms of each uranium isotope and for the number of atoms of various stable and long-lived fission product nuclides. From these data the cap-

ture-to-fission ratio ($\alpha$) and absolute fission yields were determined. The value for $\alpha_0$ is 0.0986 ± 0.0015. (auth)

**3011** (IFA-NR-22) GAMMA RAYS FROM $^{75}As(n,\gamma)^{76}As$ REACTION. Cristu, M. I.; Popa, M. S. (Institutul de Fizica Atomica, Academia R. P. R., Bucharest (Romania)). [1965]. 17p. Dep. mn,

By means of a gamma-gamma coincidence spectrometer using two NaI(Tl) crystals single and coincidence spectra from the $^{75}As(n,\gamma)^{76}As$ reaction were measured. More prominent gamma ray peaks appeared at 49.5, 89, 120, 136 and 163 kev in the single spectrum. The coincidence and sum-coincidence measurements revealed the following more intensive cascades: 120–163, 136–163, 163–220–275, 275–540 and 275–660 kev. The data obtained were used for derivation of the probable $^{76}As$ level scheme with level energies at 163, 283, 390, 480, 590, 660, 940, 1270, 1910, 2150, 2350, and 2550 kev. A discussion about the spins and parities of the lowest levels of $^{76}As$ nucleus is given. (auth)

**3012** (IKF-11) UNTERSUCHUNG DER REAKTIONEN $^{58}Ni(n,p)^{58}Co$ UND $^{27}Al(n,p)^{27}Mg$ BEI VERSCHIEDENEN NEUTRONENENERGIEN. (The Reactions $^{58}Ni(n,p)^{58}Co$ and $^{27}Al(n,p)^{27}Mg$ at Different Neutron Energies). Debertin, Klaus (Institut fuer Kernphysik, Universitaet Frankfurt (West Germany)). May 1965. 68p. Dep. mn.

A counter telescope consisting of a CsI(Tl) detector and two gaseous scintillation counters has been constructed in order to investigate (n,p) and (n,d) reactions at different neutron energies. The energy spectra and angular distributions of the protons from the reactions $^{58}Ni(n,p)^{58}Co$ and $^{27}Al(n,p)^{27}Mg$ at incident neutron energies of 8, 14, and 22 Mev are studied. The measurements at 8 Mev yield a nearly isotropic angular distribution, while at 22 Mev the angular distribution of the high energy protons is strongly peaked forward. For $^{58}Co$, level density parameters are evaluated. For both reactions absolute cross sections are given. At 22 Mev deuteron spectra are also recorded. (auth)

**3013** (JINR-P-2331) UGLOVOE RASPREDELENIE NEUPRUGO RASSEY ANNYKH SLOZHNYKH CHASTITS. (Angular Distribution of Inelastically Scattered Complex Particles). Kalinkin, B. N.; Grabovskii, Ya. (Joint Inst. for Nuclear Research, Dubna (USSR). Lab. of Theoretical Physics). 1965. 6p. Dep. mn.

The angular distribution in inelastic scattering of complex nuclei accompanied by an excitation of low-lying levels of the collective type is discussed. (auth)

**3014** (LA-DC-7386) ELASTIC SCATTERING OF POLARIZED NUCLEONS. Rosen, Louis (Los Alamos Scientific Lab., Univ. of California, N. Mex.). [1965]. Contract W-7405-eng-36. 52p. (CONF-650928-9). Dep. mn; CFSTI $3.00 cy, $0.50 mn.

From International Conference on Polarization Phenomena of Nucleons, Karlsruhe, Ger.

Los Alamos work with polarized protons is discussed. A survey of work done at other laboratories in the general domain of elastic scattering of polarized protons and neutrons from complex nuclei and for energies below 50 Mev is presented. Extensive data comparisons to the predictions of an optical model potential which were determined from polarized proton data at 10.5 and 14.5 Mev are included. (M.O.W.)

**3015** (NASA-SP-71, pp 357-62) SOME EXPERIMENTAL DATA ON THE NUCLEAR CASCADE IN THICK ABSORBERS. Shen, B. S. P. (New York Univ., N. Y.).

A series of survey experiments on the passage of high-energy protons in solid absorbers is reported. Some raw data suitable for comparison with nuclear-cascade calculations are given. (auth)

**3016** (NASA-TN-D-3020) EQUATION OF STATE OF MATTER AT SUPERNUCLEAR DENSITY. Harrison, E. R. (National Aeronautics and Space Administration, Greenbelt, Md. Goddard Space Flight Center). Oct. 1965. 7p. CFSTI $1.00 cy, $0.50 mn.

Using a vector meson model, Zel'dovitch has shown that at very high densities, the pressure tends to equal $\epsilon$, where $\epsilon$ is the energy density. By modifying Zel'dovitch's model to avoid certain unrealistic simplifications, and by assuming that the higher masses of the meson hierarchy progressively predominate in the interactions as the density increases, it is shown that the pressure, in fact, tends to equal $\epsilon/3$. (auth)

**3017** (NASA-TN-D-3067) ELASTIC AND INELASTIC SCATTERING OF 40-Mev ALPHA PARTICLES FROM EVEN TIN ISOTOPES. Baron, Norton; Leonard, Regis F.; Need, John L.; Stewart, William M. (National Aeronautics and Space Administration, Cleveland, Ohio. Lewis Research Center). Oct. 1965. 44p. CFSTI $2.00 cy, $0.50 mn.

Angular distributions were measured for alpha elastic and inelastic scattering by isotopically enriched targets of $^{116}Sn$, $^{118}Sn$, $^{120}Sn$, and $^{122}Sn$ using the 40-Mev alpha beam of the 60-inch cyclotron. In each isotope, only two strongly excited states were observed. Their energies were about 1.2 and 2.4 Mev above the ground state. The elastic angular distributions were analyzed using both the Blair-Fraunhofer black-disk method and the optical model. These analyses are consistent with the concept that the elastically scattered particles result from surface reactions of a direct nature. The inelastically scattered groups of alpha particles were analyzed using a distorted waves Born approximation (DWBA). The results of these calculations predict the first excited state of each isotope to have a spin of two and positive parity. Similarly, the second excited state of each isotope is predicted to have a spin of three and negative parity. In addition, the angular distributions of the ground state, first excited state, and second excited state of each isotope are observed to obey the Blair phase rule. Deformation parameters were extracted from the DWBA calculations and are found to be in agreement with those obtained by Coulomb excitation experiments. (auth)

**3018** (NYO-72-27) CINDA—AN INDEX TO THE LITERATURE ON MICROSCOPIC NEUTRON DATA. (Columbia Univ., New York; ENEA Neutron Data Compilation Centre, Gif-sur-Yvette (France)). May 1, 1965. Contract AT(30-1)-1808. 978p. (EANDC-46(U); CCDN-CI/1). CFSTI $12.78 cy, $4.00 mn.

Data on neutron cross sections of isotopes, elements, and compounds are tabulated cumulatively. (T.F.H.)

**3019** (ORNL-P-1657) CONVERSION COEFFICIENT MEASUREMENTS EMPLOYING MAGNETIC AND SOLID-STATE SPECTROMETERS. van Nooijen, B.; Ramayya, A. V.; Hamilton, J. H. (Vanderbilt Univ., Nashville, Tenn.); Pinajian, J. J.; Johnson, N. R. (Oak Ridge National Lab., Tenn.). [nd]. Contract W-7405-eng-26. 5p. (CONF-650563-3). Dep. mn; CFSTI $1.00 cy, $0.50 mn.

From International Conference on the Internal Conversion Process, Nashville.

A brief discussion of using $\beta$-ray spectrometers in conjunction with lithium-drifted germanium detectors for conversion coefficient measurements is presented. This method was used to calculate K-conversion coefficients for yttrium-86. The results are presented. (M.O.W.)

**3020** (ORNL-TM-1065) REACTOR NEUTRON CROSS SECTIONS FOR PRODUCTION OF $^{33}P$ FROM $^{36}Cl$ AND ENRICHED $^{33}S$ IN THE OAK RIDGE RESEARCH REACTOR. Lewis, R. E.; Butler, T. A. (Oak Ridge National Lab., Tenn.). Oct. 1965. Contract W-7405-eng-26. 12p. Dep. mn; CFSTI $1.00 cy, $0.50 mn.

Enriched $^{33}S$, prepared by electromagnetic separation techniques, and $^{36}Cl$, prepared by reactor irradiation of natural chlorine, were evaluated as targets for the production of $^{33}P$ by the $^{33}S(n,p)^{33}P$ and $^{36}Cl(n,\alpha)^{33}P$ reactions. The reactor neutron cross sections of these reactions and those of the $^{32}S(n,p)^{32}P$ and $^{35}Cl(n,\alpha)^{32}P$ reactions were measured in positions 1.5, 3.3, 5.0, and 33 cm from the fuel element in the Oak Ridge Research Reactor (ORR). The reactor neutron cross sections of the $^{33}S(n,p)^{33}P$ and $^{36}Cl(n,\alpha)^{33}P$ reactions were relatively higher than those of the $^{32}S(n,p)^{32}P$ and $^{35}Cl(n,\alpha)^{32}P$ reactions with increasing

distance from the fuel elements. Using target material containing mixtures of $^{33}S$ with $^{32}S$ and $^{36}Cl$ with $^{35}Cl$, it was necessary to age the $^{32,33}P$ mixture several months to prepare $^{33}P$ containing <5% $^{32}P$. The ORR position for irradiation of sulfur enriched in $^{33}S$, which gave the highest yield of $^{33}P$ containing 5% $^{32}P$ after several months' aging, was ~5 cm from the fuel element. In this position, the reactor cross section of the $^{33}S(n,p)^{33}P$ reaction was 11.3 mb, and of the $^{32}S(n,p)^{32}P$ reaction was 9.2 mb. The reactor position for irradiation of chlorine enriched in $^{36}Cl$ which gave the highest yield of 95% $^{33}P$ after aging several months was ~3.3 cm from the fuel element. In this position the reactor neutron cross section of the $^{36}Cl(n,\alpha)^{33}P$ reaction was 13.2 mb, and of the $^{35}Cl(n,\alpha)^{32}P$ reaction was 10.2 mb. Procedures for the separation and recovery of carrier-free $^{32,33}P$ from elemental sulfur and KCl are described. (auth)

**3021** (ORNL-TM-1238) ANALYSIS OF ELASTIC AND INELASTIC SCATTERING OF NEUTRONS FROM $^{206}Pb$, $^{208}Pb$, AND $^{209}Bi$ BELOW 4.5 Mev. Smith, William R. (Oak Ridge National Lab., Tenn.). Sept. 27, 1965. Contract W-7405-eng-26. 17p. Dep. mn; CFSTI $1.00 cy, $0.50 mn.

The Hauser–Feshbach compound-nucleus scattering theory has been applied to neutron elastic and inelastic scattering from $^{206}Pb$, $^{208}Pb$, and $^{209}Bi$ in the energy range of 0.8 to 4.5 Mev. The theory appears to work quite well both for the compound-elastic scattering and for the inelastic scattering, provided the imaginary potential W has the correct energy dependence. The results show that for the isotopes considered W should be constant as a function of bombarding-minus-excitation energy and nearly constant above 4 Mev as a function of bombarding energy, but should be made increasingly smaller as the bombarding energy is lowered below this amount. (auth)

**3022** (UCRL-16216) POLARIZATION IN p-$^{4}He$ SCATTERING BETWEEN 27 AND 63 Mev. Boschitz, E. T.; Chabre, M.; Conzett, H. E.; Shield, E.; Slobodrian, R. J. (Lawrence Radiation Lab., Univ. of California, Berkeley). Aug. 1965. Contract W-7405-eng-48. 7p. (CONF-650928-11). Dep. mn; CFSTI $1.00 cy, $0.50 mn.

From International Conference on Polarization Phenomena of Nucleons, Karlsruhe, Ger.

A preliminary phase-shift analysis for proton scattering by $^{4}He$ at 21 to 63.3 Mev is reported, using polarized protons. (T.F.H.)

**3023** (UCRL-16218) STUDY OF THE $^{4}He(p,d)^{3}He$ REACTION WITH POLARIZED PROTONS AT 55 AND 63 Mev. Boschitz, E. T.; Chabre, M.; Conzett, H. E.; Slobodrian, R. J. (Lawrence Radiation Lab., Univ. of California, Berkeley). Aug. 1965. Contract W-7405-eng-48. 5p. (CONF-650928-12). Dep. mn; CFSTI $1.00 cy, $0.50 mn.

From International Conference on Polarization Phenomena of Nucleons, Karlsruhe, Ger.

The component of the deuteron polarization parallel to the proton polarization is determined by measuring the asymmetry in the deuteron distributions from the $^{4}He(p,d)^{3}He$ reactions at 55 and 63 Mev. The data are compared with the results of a DWBA analysis and a diffraction-model analysis. (T.F.H.)

**3024** (UCRL-16324) NUCLEAR SPECTROSCOPIC STUDIES OF $^{204}Po$ [Thesis]. An, Jiann-min (Lawrence Radiation Lab., Univ. of California, Berkeley). Aug. 5, 1965. Contract W-7405-eng-48. 26p. Dep. mn; CFSTI $2.00 cy, $0.50 mn.

Sources of polonium-204 were derived from the electron capture decay of astatine-204 made by bombarding $^{197}Au$ with $^{12}C$ in the Heavy Ion Linear Accelerator at Berkeley. Physical and chemical methods were adjusted to make the sources as pure as possible for the measurements. Using scintillation crystals coupled to a 400 channel pulse-height analyzer, an investigation of some of the nuclear radiations of $^{204}Po$ was made. Gamma-rays from $^{204}Po$ were identified by their half life; their energies and relative intensities were carefully determined and the alpha branching ratio was measured. (auth)

**3025** ANGULAR CORRELATION BETWEEN PROMPT NEUTRONS AND FISSION FRAGMENTS. Diaconescu, Aurelian (Inst. of Atomic Physics, Bucharest). Acad. Repub. Pop. Rom., Stud. Ceret. Fiz., 16: 635-56(1964). (In Rumanian).

The fundamental experimental methods are outlined for the study of prompt neutron fission fragment angular correlation in fissions induced by low-energy neutrons, as well as the interpretation of results obtained in a series of fundamental works in this field. (auth)

**3026** DIFFRACTION SCATTERING OF DEUTERONS ON NON-SPHERICAL NUCLEI. III. SEMITRANSPARENT NUCLEUS WITH DIFFUSE EDGES. Borysowicz, Jerzy (Inst. for Nuclear Research, Warsaw). Acta Phys. Pol., 28: 239-46(Aug. 1965).

Diffraction scattering of deuterons on nuclei is considered. Elastic and inelastic scattering leading to excitation of the collective states in nuclei are investigated. Deuteron scattering is treated as a superposition of the diffraction scatterings of both the neutron and proton of the deuteron by applying the Achiezez-Sitenko method. The optical model is used to describe the nucleon-nucleus scattering, instead of the "black nucleus" model used in previous investigations. There is no evidence for the existence of the "universal curve" in the present approach. The results of numerical calculations presented agree better with experiment than in previous calculations. (auth)

**3027** ELECTRIC MULTIPOLE RELATIVISTIC RADIATIVE TRANSITIONS. Babushkin, F. A. (Kome State Pedagological Inst., USSR). Acta Phys. Pol., 28: 427-31(Sept. 1965). (In Russian).

An expression is obtained for the probability of electric multipole transitions in the one-electron relativistic approximation. It is proved that the probability is independent of an arbitrary constant appearing in the expression for the potential of a photon in a state of the electric type. (tr-auth)

**3028** HALF-LIFE OF $^{147}Sm$; COMPARISON OF IONIZATION CHAMBER AND LIQUID SCINTILLATION RESULTS. Valli, K.; Aaltonen, J.; Graeffe, G.; Nurmia, M.; Poeyhoenen, R. (Univ. of Helsinki). Ann. Acad. Sci. Fenn., Ser. A VI, 177: 1-20(1965).

A detailed study was made of the ionization chamber and the liquid scintillation methods in the determination of the half life of Sm-147. The ionization chamber method yielded $(1.083 \pm 0.020) \cdot 10^{11}$ years whereas the scintillation method gave $(1.075 \pm 0.015) \cdot 10^{11}$ years. Thus the previous discrepancy between the results of the two methods is eliminated. The final result for the half life of Sm-147 is given as $(1.08 \pm 0.02) \cdot 10^{11}$ years. The atomic stopping cross section of samarium for alpha particles was measured. (auth)

**3029** DISTRIBUTION OF THE SPECIFIC IONIZATION ALONG THE TRACK AS A FUNCTION OF THE INITIAL ENERGY OF THE $^{235}U$ FISSION FRAGMENTS. Nasyrov, F.; Rostovtsev, A. A.; Il'in, Yu. I.; Linev, S. V. At. Energ. (USSR), 19: 244-50(Sept. 1965). (In Russian).

The distribution along the track of specific energy losses in ionization was measured as a function of the initial energy of the fission fragments, using a telescope of 11 pulsed ionization chambers and a two-dimensional pulse amplitude analyzer. The fragments from $^{235}U$ fission by thermal neutrons were studied in the initial energy ranges of 78 to 115.5 Mev for light fragments and 34 to 88 Mev for heavy fragments. The data obtained allowed the variation of specific ionization with the velocity of the fission fragments to be found. These variations point to some differences in the character of ionization energy losses of light and heavy fragments. (tr-auth)

**3030** TOTAL NEUTRON CROSS SECTIONS OF $^{185}Re$ AND $^{187}Re$. Vertebnyi, V. P.; Vlasov, M. F.; Kirilyuk, A. L.; Kolotyi, V. V.; Pisanko, Zh. I.; Trofimova, N. A. At. Energ. (USSR), 19: 250-2(Sept. 1965). (In Russian).

The method is described and results are presented for measurements of the total neutron cross sections of the isotopes $^{185}Re$ and $^{187}Re$ in the resonance, thermal, and cold ranges of the neutron spectrum, performed on the VVR-M reactor. The cross sections for these isotopes below 0.08 ev obey the 1/v law with good accuracy; how-

ever, the positive levels of $^{185}$Re contribute only 56% of the total cross section in the thermal range, and of $^{187}$Re, only 3%. Analysis of the cross sections shows that the energy of the $^{187}$Re negative level closest to zero is 5 ev ≤ $|E_0|$ ≤ 10 ev; in $^{185}$Re, $|E_0|$ ≥ 10 ev. (tr-auth)

**3031** ON THE PROPAGATION OF RESONANCE NEUTRONS IN URANIUM. Stavisskii, Yu. Ya.; Sherman, L. E. At. Energ. (USSR), 19: 292-4(Sept. 1965). (In Russian).

A study was made of the diffusion of neutrons, slowed down in large thicknesses of copper, in depleted uranium metal. In the process of determining the neutron spectrum in uranium, the cross sections of capture for several elements were measured. The measured ratios $\sigma_f(^{235}U)/\sigma_f(^{238}U)$ and $\sigma_f(^{235}U)/\sigma_c(^{197}Au)$ are presented as functions of the thickness of uranium. Results of capture cross section measurements are given for $^{55}$Mn, $^{115}$In, $^{127}$I, $^{197}$Au, and $^{238}$U, and of fission cross section measurements for $^{235}$U and $^{239}$Pu. (M.J.T.)

**3032** CROSS SECTIONS OF 1- TO 50,000-ev NEUTRON RADIATIVE CAPTURE BY V, Zr, $^{90}$Zr, $^{91}$Zr, AND $^{94}$Zr NUCLEI. Kapchigashev, S. P. At. Energ. (USSR), 19: 294-6(Sept. 1965). (In Russian).

Radiative-capture cross sections were measured for natural V and Zr and for the separated isotopes $^{90}$Zr, $^{91}$Zr, and $^{94}$Zr in the energy range 1 to 50,000 ev. Graphs of the energy variation of the capture cross sections and a table of the absorption resonance integrals are given, and results are compared with those of previous calculations and experiments. (M.J.T.)

**3033** SPIN DETERMINATION ON $^{144}$Pr BY ANGULAR CORRELATION MEASUREMENTS. Reiser, W. (Univ., Giessen, Ger.). Atomkernenergie, 8: 307-10(July-Aug. 1965). (In German).

The nuclear spins of the ground state and the 134 kev level of $^{144}$Pr were determined by $\beta$(186 kev)-$\gamma$(134 kev) angular correlation measurements. The investigations were performed by a slow-fast-coincidence device. The measurement yields a small positive anisotropy, excluding the spin 0 for the 134 kev level; it must be 1. The resulting spin sequence then is 0(1) 1 (1)0 and the spin of the ground state is 0. (auth)

**3034** ABSOLUTE STANDARDIZATION OF THE ELECTRON-CAPTURING RADIONUCLIDE $^{54}$Mn BY 4$\pi$ X(PC)- AND 4$\pi$(X,$e_K$)-$\gamma$-MEASUREMENTS. Leistner, M.; Friedrich, K. (Angewandte Radioaktiviaet, Leipzig). Atomkernenergie, 8: 311-14(July-Aug. 1965). (In German).

Formulas are given for the absolute determination of the activity for the electron-capturing radionuclide $^{54}$Mn by 4$\pi$X(PC)- and 4$\pi$(X,$e_K$)-$\gamma$-measurements. In spite of an exact proof of the error sources an agreement of disintegration rates could not be obtained with $P_K w_K$-values reported by other authors. Measurements give $w_K$ = 0.27 ± 10% if the calculated $P_K$ = 0.90 is used. (auth)

**3035** ANGULAR DISTRIBUTIONS IN THE REACTIONS $^{11}$B(d,p)$^{12}$B AND $^{11}$B(d,$\alpha$)$^{9}$Be. Sargood, D. G.; Putt, G. D. (Univ. of Melbourne). Australian J. Phys., 18: 491-6(Oct. 1965).

The direct interaction technique was used to carry the investigation from a bombarding energy of 700 to 390 kev in the reactions $^{11}$B(d,$\alpha$)$^{9}$Be and $^{11}$B(d,p)$^{12}$B. The target consisted of a separated $^{11}$B isotope deposited on a thick nickel backing, and the target was bombarded by a deuteron beam from an electrostatic generator at energies of 700, 600, 490, and 390 kev. Charged particles resulting from this bombardment were detected with a silicon surface barrier detector. Angular distributions were extracted for the alpha particle groups leading to the ground state and 2.43-Mev state of $^{9}$Be, and for the proton group leading to the ground state of $^{12}$B. These angular distributions are shown, and also the three excitation functions measured in the 90° direction normalized to the same value at 550 kev. (J.F.P.)

**3036** ANALOGOUS ISOBARIC STATES OF $^{41}$Ar IN $^{41}$K. Dumazet, Gerard; Lambert, Michel (Institut d'-Etudes Nucleaires, Algiers). Compt. Rend., 261: 949-52(July 1965). (In French).

The existence of isobaric states in $^{41}$Ar analogous to excited states in $^{41}$K was investigated, using incident protons of energy from 1 to 3 Mev. The principal residences observed are tabulated. The analogous isobaric states observed are very pure and divide little of their force with few of the neighboring normal states. The high density of the normal states which cause very fast fluctuations in the excitation curve so that the very fine real structure could not be observed was noted. The resonances of 1088, 1589, 1860 and 2450 Kev correspond to excited states of $^{41}$K that appear to be the analogous isobaric states of the excited states of 517, 1035, 1354, and 1871 Kev. From this correspondence it results that the spins and parities of the 2nd, 4th, and 6th excited states of $^{41}$Ar are $3/2^-$, $3/2^-$ and $1/2^+$. (J.S.R.)

**3037** CONCERNING ONE EFFECT ACCOMPANYING NUCLEAR REACTIONS IN SINGLE CRYSTALS AND ITS USE IN DIFFERENT PHYSICAL INVESTIGATIONS. Tulinov, A. F. (Moscow State Univ.). Dokl. Akad. Nauk SSSR, 162: 546-8(May 21, 1965). (In Russian).

It was previously reported that when a single crystal of tungsten is bombarded by a beam of accelerated particles, a new effect arises which is connected with the ordering of the nuclei and the target. It is shown that the effect is not confined to thin films and can be observed also with a thick target. Inasmuch as the feasibility of observing this effect and using it for various purposes is connected with the angular distribution of the reaction products, the angular dimensions of the regions to which these products are confined were estimated theoretically, for crystals of magnesium, molybdenum, and tungsten. Results are also reported of an experiment aimed at observing this effect in the case of elastic scattering of protons by a thick sample of single-crystal tungsten. The tests were made using 3-Mev incident protons. The scattered protons were registered with a semiconductor counter. It is also shown that the method can be used as a means of investigating the rate of nuclear reactions by determining the lifetimes of nuclear systems such as a compound nucleus or a highly excited reaction product. It is also hoped that this effect will help to determine the correlation between the motion of an atom and a lattice. (auth)

**3038** USE OF THE COINCIDENCE METHOD FOR DETERMINATION OF TOTAL CONVERSION COEFFICIENTS. Baumgartner, E.; Walthert, A.; Huber, P. (Univ., Basel). Helv. Phys. Acta, 38: 514-22(Aug. 1965). (In German).

The total conversion coefficients for gamma-rays were determined by the following method. The source strength of the sample was measured by $\beta$-$\gamma$-coincidences, and the detection efficiency of the scintillation counter was calculated. From the knowledge of these two numbers and the counting rate in the detector, the relative intensity of $\gamma$-rays can be ascertained. For the transition from the first excited state to the ground state the following values were obtained: $^{129}$Xe: $\alpha$ = 21.0 ± 1.0, $^{141}$Pr: $\alpha$ = 0.45 ± 0.04, $^{198}$Hg: $\alpha$ = 0.047 ± 0.017, $^{203}$Tl: $\alpha$ = 0.222 ± 0.015. These values are compared with present theoretical and experimental values. (auth)

**3039** THE T(d,n)$^4$He REACTION WITH POLARIZED DEUTERONS. Traechslin, W.; Buergisser, H.; Huber, P.; Michel, G.; Striebel, H. R. (Univ., Basel). Helv. Phys. Acta, 38: 523-40(Aug. 1965). (In German).

The Basel source of polarized deuterons is combined with a 600 kev d-c-accelerator. The axis of alignment of the deuterons may be turned in any direction by a magnetic field at the place of ionization. The alignment axis is determined from the measurement of the angular distribution of the (d,T)-neutrons with polarized deuterons of 150 kev energy. The ratios of the differential cross-sections with polarized and unpolarized deuterons were measured at different angles of neutron emission and at energies of 0.36, 0.50 and 0.58 Mev. At energies of 0.15 and 0.58 Mev different states of polarization are used. The measurements showed that above 300 kev deuteron energy the reaction cannot be caused only

by a pure S-wave-resonance in the $3/2^+$-level of the compound nucleus. (auth)

**3040** ENERGIES AND RELATIVE INTENSITIES OF 2201, 2490, AND 2508 kev γ LINES IN THE SPECTRUM OF $^{72}$Ga. Vitman, V. D.; Dzhelepov, B. S.; Sergeev, A. G. (Ioffe Inst. of Physics and Tech., Leningrad). JETP Lett. (USSR) (Engl. Transl.), 2: 61(July 15, 1965).

The 2201, 2490, and 2508 kev γ lines of gallium-72 were measured in order to obtain more accurate values for previously found energies and intensities. The shape of the 2201-kev line was used to resolve the 2490 + 2508 kev doublet into its components, since it was already shown that the line shape is independent of the energy if $h\nu \geq 1.5$ Mev. The results are given. These results are compared with those of others. Since the 2462-kev line previously reported was not observed in the experiments, it is concluded that the existence of this line is doubtful. (J.F.P.)

**3041** LEVELS OF $^{56}$Ni FROM THE REACTION $^{58}$Ni(p,t)$^{56}$Ni AT 28 Mev. Hoot, Charles G.; Kondo, M.; Rickey, M. E. (Univ. of Colorado, Boulder). Nucl. Phys., 71: 449-58(1965).

Tritons were observed from the (p,t) reaction on $^{58}$Ni leading to the ground state of $^{56}$Ni with a Q of −13.987 ± 0.018 Mev and to excited states of $^{56}$Ni at excitations (±0.05 Mev) of 2.71, 3.94, 4.97, 5.35 and 6.62 Mev. The ground state results from L = 0 pickup by comparison with other angular distributions for known $0^+ \rightarrow 0^+$ (p,t) reactions. Angular distributions for the stronger excited state transitions were measured. (auth)

**3042** THE DEUTERON–DEUTERON INTERACTION AT 270 TO 507 Mev/c. Lys, J. E. A.; Lyons, L. (Nuclear Physics Lab., Oxford). Nucl. Phys., 74: 261-80 (1965).

A bubble chamber experiment was performed to study the deuteron-deuteron interaction in the momentum range 270 to 507 Mev/c. Results are presented for elastic scattering, the stripping reactions, and the inelastic reactions. The elastic scattering differential cross-section for the incident momentum range 433 to 507 Mev/c is compared with impulse approximation calculations. (auth)

**3043** GAMMA-RAY ENERGIES DETERMINED WITH A LITHIUM-DRIFTED GERMANIUM DETECTOR. Robinson, R. L.; Stelson, P. H.; McGowan, F. K.; Ford, J. L. C. Jr.; Milner, W. T. (Oak Ridge National Lab., Tenn.). Nucl. Phys., 74: 281-8(1965). (ORNL-P-1518).

The energies of gamma rays from about sixty nuclides have been determined to within a few tenths of a kev by means of a lithium-drifted germanium detector. They include values for the transitions resulting from the decay of $^{51}$Cr, $^{7}$Be, $^{207}$Bi, $^{54}$Mn, $^{88}$Y, $^{65}$Zn, and $^{22}$Na which are frequently used as calibration standards. The majority of energies are for transitions following Coulomb excitation. Previously unresolved gamma-ray doublets have been observed in the decay of the radioactive nuclei $^{102}$Rh and $^{106}$Rh and in Coulomb-excited $^{75}$As, $^{77}$Se, $^{117}$Sn, and $^{119}$Sn. From the relative intensities of the members of the $^{77}$Se doublet, new estimates have been made for the $B(E2)_{ex}$'s of the 239.3 and 250.1 kev states. They are, respectively, 1770 ± 160 and 94 ± 26 $e^2$ $fm^4$. (auth)

**3044** ELASTIC SCATTERING OF DEUTERONS FROM COMPLEX NUCLEI AT HIGH ENERGIES. Sawada, T. (Univ. of California, Los Angeles). Nucl. Phys., 74: 289-317(1965).

The high-energy elastic scattering of deuterons from complex nuclei is considered in terms of the impulse approximation for the deuteron. The results derived from either a many-body or a quasi two-body approach are identical to second order if simultaneous scattering via nuclear excited states is neglected. At high energies, the correction to the impulse approximation for the deuteron caused by simultaneous deuteron-nucleon scattering is smaller by a factor 1/N than the effect of simultaneous deuteron-nucleus scattering, where N is the number of target nucleons. Deuteron-nucleus scattering amplitudes are expressed in terms of nucleon-nucleus scattering amplitudes obtained from optical model potentials which yield optimum fits to the angular distributions and the reaction cross sections of nucleon-nucleus scatterings at half the deuteron incident energy. It is seen that simultaneous scattering strongly affects both the differential cross sections and the polarizations and greatly improves the results of the first order calculations. The theory gives a good agreement with experiment for energies above 156 Mev although the agreement becomes poor for lower energies. (auth)

**3045** MEAN LIVES OF EXCITED STATES IN $^{14}$N. Lonergan, J. A.; Donahue, D. J. (Univ. of Arizona, Tucson). Nucl. Phys., 74: 318-20(1965).

The Doppler-shift technique was used to measure the mean life $\tau = (8.3 \pm 3) \times 10^{-14}$ s for the 2.31-Mev level in $^{14}$N and to establish limits of $\tau \lesssim 2.5 \times 10^{-14}$ s and $\tau > 6 \times 10^{-13}$ s on the mean lives of the 3.95- and 5.10-Mev levels of $^{14}$N, respectively. These measurements are compared with predictions made on the basis of the shell model. (auth)

**3046** GENERALIZED QUASI-SPIN IN NEUTRON-PROTON SYSTEMS. Ginocchio, J. N. (Univ. of Rochester, N. Y.; The State Univ., New Brunswick, N. J.). Nucl. Phys., 74: 321-47(1965).

Using the fact that, in a $j^n$ configuration, the nucleon-number and isospin dependence for neutrons and protons in a seniority representation is incorporated in a R(5) quasi-spin group, the allowed values of isospin and the number of times it occurs for a given symplectic symmetry (seniority s and reduced isospin t) and nucleon number is derived. Also closed form expressions for the R(5) Clebsch-Gordan coefficients are derived in which one of the irreducible representations if the four-dimensional representation and the others have (a) reduced isospin one- and zero and (b) reduced isospin equal $\frac{1}{2}(2j + 1 - s)$. All others needed for $j \leq 7/2$ are calculated numerically. It is shown that these Clebsch-Gordan coefficients give the n, T dependence of the spectroscopic factors. A generalization is made immediately to mixed configurations. (auth)

**3047** INTERACTIONS OF 9 Gev PROTONS WITH LARGE ENERGY TRANSFER TO THE TARGET NUCLEI. Kaczarowski, R.; Makowska, E. (Univ. of Warsaw). Nucl. Phys., 74: 348-52(1965).

In a sample of interactions of 9-Bev protons with heavy nuclei in emulsion, accompanied by $^{8}$Li and $^{8}$B emission, 35 stars of large size ($N_h \geq 27$, $N_b \geq 20$) have been selected. The ranges of 769 black and black-grey tracks ($10\ \mu m < R \leq 10{,}000\ \mu m$) have been measured. The charge balance and the energy transfer to the target nuclei have been analyzed under plausible assumptions. It follows from the analysis that on the average there is no massive residual nucleus left in the interactions, that the Coulomb barrier of the particles emitted is drastically reduced, and the two-stage model (the cascade followed by the evaporation) seems to be not applicable for the considered class of interactions. (auth)

**3048** ELEMENTARY QUANTUM THEORY OF NUCLEAR COLLECTIVE ROTATION. Villars, Felix M. H. (Centre d'Etudes Nucleaires de Saclay, Gif-sur-Yvette, France). Nucl. Phys., 74: 353-67(1965).

A new, entirely quantal description of nuclear collective rotation is developed. The basic element is the explicit introduction of the pair (or pairs) of operators which describe the collective motion; in the case of rotation this is the total angular momentum J and a phase angle $\varphi$. A representation is then constructed, in which either J or $\varphi$ is diagonal. The non-collective degrees of freedom are described in a subspace of the set of antisymmetrized independent particle wave functions $\phi_n$; this subspace is obtained by using suitable projection operators. The formalism is developed for "nuclei" in two dimensional space only. It is shown that the $\varphi$-representation is particularly useful and leads to the construction of an operator $H^J = H^{(1)} + JH^{(c)} + \frac{1}{4}J^2Q$, whose eigenvalues are the set of all levels with angular momentum

J. These levels may be found by the usual HF and RPA procedures. It is shown that the moment of inertia of the ground state rotational band is given by the Thouless-Valatin formula. (auth)

**3049** SEMICLASSICAL THEORY OF POLARIZATION IN DIRECT NUCLEAR REACTIONS. II. Abul-Magd, A. Y.; El-Nadi, M. (Atomic Energy Establishment, Cairo). Nucl. Phys., 74: 368-76(1965).

The semiclassical theory of polarization in direct nuclear reactions is applied to stripping reactions from non-s-internal states of the projectile, and the results obtained for the polarization of the reaction products are found to be similar to those obtained for stripping reactions from s-states. The circular polarization of gamma-rays emitted after stripping reactions is discussed and is related to the polarization of the outgoing particles. Finally, the cross sections of direct reactions with polarized beams are evaluated and the derived expressions were found to agree with the quantal calculations. (auth)

**3050** $^{238}$U FISSION INDUCED BY LOW-ENERGY MONOCHROMATIC $\gamma$-RAYS. CROSS-SECTIONS BETWEEN 5 AND 8 Mev. Manfredini, A. (Istituto Nazionale di Fisica Nucleare, Rome; Univ., Rome); Muchnik, M.; Fiore, L.; Ramorino, C.; de Carvalho, H. G.; Lang, J.; Mueller, R. Nucl. Phys., 74: 377-84(1965).

The photofission cross section of $^{238}$U has been measured at six energies between 5.43 and 7.72 Mev, using nuclear emulsions and monochromatic $\gamma$ rays. The existence of minima in this energy region, suggested by previous workers, has been confirmed. (auth)

**3051** CIRCULAR POLARIZATION MEASUREMENTS OF GAMMA RAYS FOLLOWING THE BETA DECAY OF $^{124}$Sb AND $^{134}$Cs. Tirsell, Kenneth Glenn; Talbert, W. L. Jr. (Iowa State Univ., Ames). Nucl. Phys., 74: 385-402 (1965). (IS-1173).

Circular polarization measurements of gamma rays following allowed beta transitions in $^{134}$Cs and $^{124}$Sb were made using forward Compton scattering of the photons from partially polarized electrons available in magnetized iron. Stable fast-slow coincidence circuitry and an accurately timed 32 sec polarization analyzer magnet switching cycle were used. From the observed coincidence counting rates for opposite orientations of the magnet, the value obtained for the $^{134}$Cs circular polarization asymmetry parameter was $A = -0.077 \pm 0.013$. Measurements were performed relative to $^{60}$Co for which the theoretical value $A = -1/3$ was assumed. From the theoretical relation (computed assuming the (V−A) beta interaction) between A and the Fermi-to-Gamow-Teller matrix element ratio $Y = C_V M_F / C_A M_{GT}$, the corresponding matrix element ratio for the $^{134}$Cs beta transition was determined to be $Y = 0.220 \pm 0.019$. The asymmetry parameter measured for the allowed 0.621 Mev beta transition of $^{124}$Sb was $A = +0.356 \pm 0.030$ with the corresponding ratio $Y = -0.173 \pm 0.031$. The value obtained for the $^{124}$Sb asymmetry parameter agrees in sign with that of the only known measurement previously reported but is greater in magnitude. (auth)

**3052** THE LEVEL STRUCTURE OF $^{18}$O AND $^{19}$O BY STRIPPING REACTIONS. Moreh, R.; Daniels, T. (Manchester Univ., Eng.). Nucl. Phys., 74: 403-16(1965).

The (d,p) reactions on $^{16}$O, $^{17}$O, and $^{18}$O were investigated at a deuteron energy of 5.56 Mev, with a view to studying the $^{18}$O energy levels. The reaction Q values of the ground state transitions in $^{17}$O(d,p)$^{18}$O and $^{18}$O(d,p)$^{19}$O were determined to be $5.820 \pm 0.010$ and $1.734 \pm 0.010$ Mev, respectively. The positions of several energy levels in $^{18}$O and $^{19}$O were established. Angular distributions of proton groups leading to some levels in $^{17}$O, $^{18}$O, and $^{19}$O were measured. The experimental results were analyzed using the Butler-Born theory, and an estimate was obtained of the amplitudes of the simple shell model configurations and deformed states in several levels of $^{18}$O. The results compare fairly well with recent theoretical estimates by Federman and Talmi. (auth)

**3053** OPTICAL MODEL ANALYSIS OF 26 Mev DEUTERON SCATTERING. Tjin A Djie, H. R. E.; Brockman, K. W. Jr. (Instituut voor Kernphysisch Onderzoek, Amsterdam). Nucl. Phys., 74: 417-37(1965).

Elastic scattering data for 26- and 21.6-Mev deuterons were analyzed in terms of a surface absorption optical model. Although good fits to the experimental angular distributions could be obtained for the heavy nuclei, those for the lighter nuclei are less satisfactory in parts of the angular range. A refinement of the potential seems necessary. For most nuclei two or three potentials were found to fit the data. The potentials could be classified into three groups with the help of the wave number of the S-wave in the center of the nucleus. When the geometrical parameters were fixed to their average values for one group the real potential parameter was found to increase with the nuclear mass number. For Ni the potential parameter appeared to be independent of energy between 15 and 26 Mev. Good agreement was obtained with experimental values of the reaction cross section. (auth)

**3054** MEASUREMENT OF THE BETA-GAMMA DIRECTIONAL CORRELATION OF $^{22}$Na AND $^{56}$Co. Mueller, Heinz (Technische Hochschule and Kernforschungszentrum, Karlsruhe). Nucl. Phys., 74: 449-58(1965).

The anisotropy $A = [W(180°) - W(90°)]/W(90°)$ of the $\beta\gamma$ directional correlation has been measured for the strongly hindered allowed positron transitions of $^{22}$Na and $^{56}$Co. Special precautions have been taken to eliminate the anisotropy due to the accompanying strongly correlated annihilation quanta. The results for $^{22}$Na are $A = -0.0004 \pm 0.0007$ for the positron energy interval 250−480 kev and $A = -0.0005 \pm 0.0006$ for 140−250 kev. Other authors have reported anisotropic correlations. For the $\beta$(1.5 Mev) − $\gamma$(1.24 Mev) correlation of $^{56}$Co $A = +0.0104 \pm 0.0028$ for a positron energy interval from 1.0 to 1.5 Mev. This is in agreement with other measurements. The results show that in both transitions the twice forbidden matrix element $M(\alpha \times r)$ is reduced together with the allowed matrix element. (auth)

**3055** SHAPE OF THE 962 kev BETA SPECTRUM OF $^{198}$Au. Beekhuis, H.; de Waard, H. (Rijksuniversiteit Groningen, Nederland). Nucl. Phys., 74: 459-68(1965).

The shape of the 962 kev beta spectrum of $^{198}$Au has been measured by many investigators but the results do not agree very well. This shape was remeasured in the energy range 420−940 kev with some improvements in the experimental arrangement and with a careful analysis of the results. Using the NBS-Fermi function, the coefficient a in the expression $k(1 + aW)$ of the shape factor is found to be $-0.050 \pm 0.010$. The dependence of a on the value chosen for the maximum energy is discussed. The performance of the spectrometer was checked with a $^{24}$Na source, giving $a = +0.002 \pm 0.010$. (auth)

**3056** BACKWARD SCATTERING OF ALPHA PARTICLES BY $^{16}$O AT MEDIUM ENERGIES. Van Oers, W. T. H. (Instituut voor Kernphysisch Onderzoek, Amsterdam; Univ. of California, Los Angeles); Van Niftrik, G. J. C.; Jonkers, H. L.; Brockman, K. W. Jr. Nucl. Phys., 74: 469-80(1965).

The backward elastic scattering of $\alpha$ particles by $^{16}$O was measured at incident $\alpha$-particle energies of 41.9 and 49.7 Mev. The measurements at an incident energy of 49.7 Mev subtended the interval from 145° to 178° in the c.m. system, whereas the measurements at 41.9 Mev subtended the interval from 155° to 175°. The results are similar to those at lower energies, i.e., the phenomenon of a large peak at extremely backward scattering angles. Measurements at a fixed angle of 175° showed the differential cross section to be a smoothly decreasing function of increasing incident $\alpha$-particle energy. An expression for a second-order correction to the measured differential cross section for the effects of finite geometry is given. The experimental angular distributions are compared with predictions based upon the exchange-scattering model introduced by Honda et al. (auth)

**3057** ELASTIC SCATTERING OF 27.5 Mev DEUTERONS AND ITS OPTICAL MODEL ANALYSIS. Testoni, J.; Rosenblatt, J.; Mayo, S. (Comision Nacional de Energia Atomica, Buenos Aires). Nucl. Phys., 74: 491-6 (1965).

Absolute differential cross sections for elastic scattering of 27.5-Mev deuterons by Mg, V, Fe, $^{58}$Ni, Co, $^{65}$Cu, Ag, Au, and $^{208}$Pb were measured from 15 to 140°. The data were analyzed in terms of a surface absorption optical model. Some sets of parameters giving good fits to the data show definite dependence on mass number. (auth)

**3058** THE PROTON-THERMAL NEUTRON CAPTURE CROSS SECTION. Cox, A. E.; Wynchank, S. A. R.; Collie, C. H. (Oxford Univ.). Nucl. Phys., 74: 497-507(1965).

The proton thermal-neutron capture cross section $\sigma_a^H$ (2200 m/sec) was obtained from measurements of the lifetime of thermal neutrons from a pulsed neutron source in an essentially infinite tank of water. A plastic scintillator counter was used to detect the gamma rays from thermal neutron capture. Since capture was the only process contributing to the decay of the total number of thermal neutrons in the tank, the scintillator counter measurements could be analyzed to give the thermal neutron lifetime, which is inversely proportional to $\sigma_a^H$. The capture cross section was measured eight times, and a weighted mean was taken to yield a value of 334.2 ± 0.5 mb for $\sigma_a^H$. An investigation of the possible sources of systematic error showed them to be negligible, and the error quoted in the result was determined from purely random errors. (auth)

**3059** THE INTERACTION EFFECT IN n-p CAPTURE. Noyes, H. Pierre (Stanford Univ., Calif.). Nucl. Phys., 74: 508-32(1965).

The nonrelativistic prediction of the n−p capture cross section at a neutron laboratory velocity of 2200 m/sec is evaluated as 302.5 ± 4.0 mb assuming that $r_s^{np} = 2.73 \pm 0.03$ f as predicted by charge independence, or 308.5 ± 5.0 mb if $r_s^{np} = 2.44 \pm 0.11$ f. The smaller values for $r_s^{np}$, derived from the two most recent n−p total cross section measurements, raises serious difficulties with the hypothesis of charge independence, which are discussed. The prediction includes corrections for the shape dependence of the triplet effective range, the deuteron D-state probability, and the intermediate range behavior of the wave functions, which contribute half the quoted uncertainty; these corrections are model independent to within that uncertainty if the longest range part of the interaction is due to one-pion exchange. The experimental value of 334.2 ± 0.5 mb obtained by Cox, Wynchank, and Collie therefore shows an interaction effect of 9.5 ± 1.2% (or 7.7 ± 1.5%). A recently proposed approximation based on dispersion theory which would, if accepted, explain two-thirds of the effect, is shown to be quantitatively inadequate. Hence covariant calculations which reduce to this approximation must be rejected, except for those parts of the calculation which give meson current corrections. Stranahan predicts a 2.9% correction coming from the $\pi$ −N 33 resonance, while the calculation of Skolnick, interpreted as indicated, gives a nonresonant contribution of 2.2%. Even if these effects could be added, a substantial part of the meson current contribution remains unexplained. It is suggested that at least part of this residual effect might be due to the large $\pi$-$\gamma$-$\rho$ coupling recently invoked by Adler and Drell to account for the static magnetic moment of the deuteron and the large forward photopion production cross section in the multi-Bev region. (auth)

**3060** PHASE SHIFT ANALYSIS OF $^3$H(p,p), $^3$H(p,n) AND $^3$He(n,n) REACTIONS. Meyerhof, W. E.; McElearney, J. N. (Stanford Univ., Calif.). Nucl. Phys., 74: 533-50 (1965).

A least-squares phase shift analysis was made to experimental cross sections and angular distributions of the $^3$H(p,p), $^3$H(p,n), and $^3$He(n,n) reactions up to 1.5 Mev in the p + T cms. The energy variation of the phase shifts considered was parametrized as follows: $^1$S by the Breit-Wigner single level formalism, $^3$S, $^1$P, and $^3$P by an effective range approximation of Shaw and Ross. In agreement with earlier work of Werntz, evidence was found for a $0^+$ state in $^4$He, peaking at approximately 20.1-Mev excitation energy and having a total reduced width close to the single particle value. The P-wave phase shifts point to a p + T interaction which would appear experimentally as a state in $^4$He peaking around 22-Mev excitation energy. Recent $^3$H(p,n) polarization measurements are consistent with a spin $1^-$ for this state. An analysis by Tombrello of the $^3$He(p,p) reaction supports a tentative conclusion that both the $^4$He states have T = 0. It is shown also that the Wigner cusp phenomena in the T(p,p) reaction can be well explained over a wide range of energies by the reaction formalisms used in the analysis. (auth)

**3061** DIRECT REACTION ANALYSIS OF THE $^{15}$N(p,$\alpha_0$)$^{12}$C REACTION. Warsh, Kenneth L. (Jacksonville Univ., Fla.); Roy, Gerald; Edwards, Steve. Nucl. Phys., 74: 551-6(1965).

Thirty-nine angular distributions of the $^{15}$N(p,$\alpha_0$)$^{12}$C reaction over a 9-Mev range were analyzed using a plane-wave direct-reaction theory incorporating pick-up and exchange pick-up (or heavy-particle stripping) coherently mixed. The results of this analysis indicate that the reaction proceeds predominantly by a direct reaction mechanism. (auth)

**3062** EXPERIMENTAL RESULTS CONCERNED WITH THE PRODUCTION OF HYPERFRAGMENTS AND $^8$Li FRAGMENTS IN THE INTERACTION OF K$^-$-MESONS OF 5 Gev/c WITH NUCLEI OF NUCLEAR EMULSION. Baumann, G.; Gerber, J. P.; Bechdolff, A.; Braun, H.; Lonchamp, J. P.; Cueer, P. (Centre de Recherches Nucleaires, Strasbourg). Nucl. Phys., 74: 557-71(1965).

Some experimental results of hyperfragment and $^8$Li-fragment emission in 5-Bev/c K$^-$ interactions with nuclear-emulsion nuclei are given. They show an increase of the production rate of $^8$Li fragments and a decrease of hyperfragment production with increasing incident energy. The mean energy transferred is higher in the stars with hyperfragment or $^8$Li-fragment emission than in the stars without. The rate of intermediate-mass-number hyperfragments increases when the incident energy rises. (auth)

**3063** PRODUCTION OF HEAVY HYPERNUCLEI AND SCATTERING OF ARGON IONS IN PHOTOGRAPHIC EMULSION. Danysz, M.; Zakrzewski, J. (Univ. of Warsaw, Inst. for Nuclear Research, Warsaw). Nucl. Phys., 74: 572-6(1965).

Scattering of argon ions in photographic emulsion was examined in order to learn what is the minimum transfer of momentum to a heavy emulsion nucleus (bromine or silver) that is necessary for it to record a visible track in emulsion. The results indicate that this minimum momentum transfer is about 400 Mev/c. Since the average mass of the heavy spallation hypernuclei produced in the interactions of K$^-$ mesons of 800-Mev/c momentum is not much different from the masses of the heavy emulsion nuclei, a similar momentum cutoff should be applicable to the reactions in which such hypernuclei originate. (auth)

**3064** SEARCH FOR $Y_1^*$ PRODUCTION IN K$^-$ CAPTURES IN NUCLEI. Carlson, P. J.; Danielsson, O.; Ekspong, A. G.; Frisk, A. (Univ. of Stockholm). Nucl. Phys., 74: 642-56(1965).

An investigation of 128 K$^-$ interactions at rest in emulsions with a final state of a $\Sigma$ hyperon, a pion, and a recoiling nucleus is reported. The main emphasis is laid on the study of the momentum and invariant mass distributions of the $\Sigma\pi$ system in order to detect possible isobar Y* production. The distributions show, however, no features which can unambiguously be interpreted as due to resonance production. These results are at variance with results in an earlier experiment where a highly significant peak in the $\Sigma\pi$ momentum was reported. These results and collected data are compared with Adair's theoretical model without appeal to Y* production. Good agreement is obtained with both samples. (auth)

**3065** EFFECT OF RADIATION DAMAGE ON THE 23.8 kev MOESSBAUER TRANSITION IN $^{119}$Sn. Hannaford, P.; Howard, C. J.; Wignall, J. W. G. (Univ. of Melbourne). Phys. Lett., 19: 257-9(Nov. 1, 1965).

It was found that radiation damage sustained in the double oxide $^{118}SnO_2 \cdot 2MgO(Mg_2SnO_4)$ during the thermal neutron capture reaction $^{118}$Sn(s,$\gamma$)$^{119m}$Sn can produce a

weak but interpretable secondary line in the 23.8 kev $^{119}$Sn Mössbauer spectrum. The Mössbauer spectrum was obtained at room temperature using the irradiated $Mg_2{}^{119m}SnO_4$ source and a 30 mg/cm$^2$ absorber. The estimated parameters for the two observed lines are summarized. Upon annealing the source in air, one line reverted to the other in the temperature range 600 to 1,000°C. Assuming that the increase in this line is due solely to the recovery of $^{119m}$Sn atoms in the other line, the latter line represents about 25% of all $^{119m}$Sn. The estimate of the recoilless fraction for this line is also based on this assumption. This effect is discussed. (J.F.P.)

**3066** PAIRING FORCES WITH NEUTRONS AND PROTONS. Elliott, J. P.; Lea, D. A. (Univ. of Sussex, Brighton, Eng.). Phys. Lett., 19: 291-2(Nov. 1, 1965).

The problem of extending the simple B.C.S. treatment of pairing between like particles to the fully charge-independent pairing force between nn, pp, and np pairs is considered. It is shown how a solution may be deduced from the usual B.C.S. solutions for like particles by an isospin projection. The procedure is similar to the construction of rotational wave functions by an angular momentum projection from a simple intrinsic function. In calculating pairing force energies, the projection may be treated formally, without any explicit calculations. A comparison with some exact solutions derived for a simple system indicates that the accuracy of the method is similar to that of the usual B.C.S. procedure. (J.F.P.)

**3067** DALITZ DIAGRAMS AND DECAY OF $^{12}$C STATES. MacDonald, N. (The Univ., Glasgow). Phys. Lett., 19: 293-4(Nov. 1, 1965).

The kinematics of the system for the $p + {}^{11}B \rightarrow {}^{12}C^* \rightarrow 3\alpha$ reaction are studied by the symmetric Dalitz diagram. The $^{12}$C rest frame is used so that the momenta are coplanar. The first property discussed uses the facts that the $\alpha$ particles have zero spin and positive parity. The boundary of the diagram corresponds to collinear momenta. The second property makes use of the symmetry of the wavefunction under exchange of the $\alpha$ particles. (J.F.P.)

**3068** AN INTER-NUCLEON POTENTIAL DEDUCED FROM SHELL MODEL CALCULATIONS. Clark, J. M.; Elliott, J. P. (Univ. of Sussex, Brighton, Eng.). Phys. Lett., 19: 294-6(Nov. 1, 1965).

The results are reported of an attempt to deduce an effective potential from shell model calculations. This potential is then compared with a realistic one. It is initially assumed that the potential is mass-independent and has the same Gaussian shape and range for all components. The data were taken only from nuclei which are believed to have a reasonably pure j-j configuration or a mixture of just two configurations. The configurations and mass ranges considered are indicated. The values for the eight potential strengths which emerge from the least squares fit are given together with a statistical estimate for the standard deviation as a measure of the reliability of each value. With the aid of the F test, it is shown that the inclusion of noncentral forces in the potential makes a significant improvement in the fit obtained with central forces alone. (J.F.P.)

**3069** THE $^{24}Mg(\alpha,\alpha)^{24}Mg$ REACTION AND A $J^\pi = 10^+$ STATE OF $^{28}$Si. Kim, H. J. (Oak Ridge National Lab., Tenn.). Phys. Lett., 19: 296-98(Nov. 1, 1965).

The results are presented of an effort to explain some features of $\alpha$-particle scattering by including the contribution from an isolated resonance in addition to the scattering from an appropriate optical model potential. It is concluded that an optical model adequately describes alpha-particle scattering from $^{24}$Mg for the incident energy of approximately 20 Mev. A high spin resonance can be analyzed by adding a resonance term to the usual optical model term. It is found that a $J^\pi = 10^+$ state of $^{28}$Si exists with an excitation energy of 27.64 ± 0.1 Mev and a $\gamma\alpha/\gamma$ ratio of 0.151 ± 0.002 whose width is about 0.5 Mev. (J.F.P.)

**3070** DEUTERON STRIPPING AT LOW ENERGIES ACCORDING TO THE PRIOR FORMALISM. Goldfarb, L. J. B.; Hooper, M. B. (Manchester Univ., Eng.). Phys. Lett., 19: 299-301(Nov. 1, 1965).

To obtain further insight into the reaction mechanism of deuteron stripping at low energies, calculations were performed using the prior formalism. The relative magnitude of the principal polarizability corrections in post formations is found to be much smaller than that in prior formations, but it has greater intrinsic interest as a needed correction to what are currently the most accurate calculations of stripping reactions. Although the method used is crude, it gives quantitatively reasonable results. This suggests a similar approach for estimating related functions. (J.F.P.)

**3071** THE $h_{\frac{1}{2}}$ SINGLE PROTON HOLE STATE IN $^{207}$Tl. Eccleshall, D.; Yates, M. J. L. (Atomic Weapons Research Establishment, Berkshire, Eng.). Phys. Lett., 19: 301-3(Nov. 1, 1965).

The single proton hole states in $^{207}$Tl were determined by studying the $^{208}Pb(t,\alpha)^{207}Tl$ reaction. In order to confirm the $1h_{\frac{1}{2}}$ assignment of the 1.34-Mev level in $^{207}$Tl a search was made for delayed $\gamma$ rays from this level following the reaction. A thick natural lead target was irradiated with about 1.0 $\mu$ A of 12-Mev tritons for about a second. Then the beam was switched off and $\gamma$ rays were observed with a 7.6 × 7.6 cm$^2$ NaI(Tl) crystal. It was deduced that there were four $\gamma$ rays in the spectrum at 0.350, 0.570, 1.00, and 1.06-Mev. The 0.570 and 1.06 Mev $\gamma$ rays both had a half life of about 0.8 seconds, and were assumed to be the cascade $\gamma$ rays from the 1.634-Mev level in $^{207}$Pb, which has a known half life of 0.799 seconds. These served as a time calibration. The other two $\gamma$ rays are the cascade $\gamma$ rays from the 1.34-Mev level of $^{207}$Tl. The half life of this level was determined. It was found to be 1.33 ± 0.11 seconds, and the mean life was 1.92 ± 0.15 seconds. Thus the $h_{\frac{1}{2}}$ assignment for the 1.34-Mev state is strongly supported. (J.F.P.)

**3072** AN ISOBARIC-SPIN IMPURITY IN THE $^{170}$Lu GROUND STATE. Hansen, P. G. (Research Establishment Risoe, Roskilde, Den.); Nielsen, H. L.; Wilsky, K.; Treherne, Jacqueline. Phys. Lett., 19: 304-6(Nov. 1, 1965).

Data are presented for $\beta^+$ transitions observed in the decay of 2.0 d $^{170}$Lu, and another possible case is indicated. This is the transition $^{234}Np(0)(\beta^+)^{234}U(O)$. Arguments are given to support the assignment $O^+$ for the $^{170}$Lu ground state. These include that from the present investigation where it is established that the $\beta^+$ group to the 84-kev $2^+$ level in $^{170}$Yb is absent. High-energy positron radiations were observed from $^{170}$Lu with a six-gap beta spectrometer. A Fermi plot of the positron energy distribution shown yielded a prominent 2.39-Mev component, which from its half life, was found to originate from $^{170}$Lu. From the experimental evidence, which is shown, it is seen that the effective Coulomb matrix elements are only of the order of 5 kev, and it is thus concluded that the selection rule in isobaric spins holds well for Fermi transitions, even in the region of heavy nuclei. (J.F.P.)

**3073** STUDY OF LEVELS OF $^{63}$Cu BY INELASTIC SCATTERING OF 10 Mev DEUTERONS. Barloutaud, M.; Gastebois, J.; Laget, J. M.; Quidort, J. (Centre d'Etudes Nucleaires de Saclay, France). Phys. Lett., 19: 306-8 (Nov. 1, 1965). (In French).

The reaction $^{63}Cu(d,d')^{63}Cu$ was studied in order to clarify the still very controversial energy level diagram for this nucleus. Deuterons at 10 Mev from a Van de Graaff were scattered by the copper-63 target. The energy spectra of the scattered particles was obtained by a summation of the impulses from two detectors. There were 8 spectra of 512 channels obtained. The total energy resolution was about 70 kev. The excitation of at least 14 levels are established, and these are shown. Angular distributions of deuterons were obtained relative to 11 of these levels. The most strongly excited levels are the same as those from the inelastic scattering of alpha particles, and the classification of levels is identical for the distributions of each type of particle. Theoretical interpretations of these results are discussed, and the results are tabulated. (J.F.P.)

**3074** OBSERVATION OF THE DE-EXCITATION OF STATES OF THE GIANT DIPOLAR RESONANCE OF $^{16}O$ TO THE EXCITED LEVELS OF POSITIVE AND NEGATIVE PARITY OF $^{15}O$ AND $^{15}N$. Maison, J. M.; Langevin, M.; Loiseaux, J. M. (Faculte des Sciences, Orsay, France). Phys. Lett., 19: 308-10(Nov. 1, 1965). (In French).

Gamma rays emitted from excited states of oxygen-15 and nitrogen-15 produced by the emission of protons and neutrons from the states of the giant resonance of oxygen-16 were observed. A NaI(Tl) crystal detector with a resolution of 3.1% for the total absorption peaks for gamma rays of 4.43 Mev was used. The experimental spectra obtained gave evidence of a de-excitation from the giant resonance of oxygen-16 to negative parity states of oxygen-15 (6.16 Mev) and to those of nitrogen-15 (6.32 Mev). Evidence for a de-excitation to the states of positive parity of oxygen-15 (the doublet at 5.18 and at 5.24 Mev) and of nitrogen-15 (5.27 and 5.30 Mev) was also given. These spectra are shown and described. A maximum is shown at 23.5 Mev in the curve showing the variation of cross section with energy for the de-excitation to the negative parity states of oxygen-15 and nitrogen-15. The particle-hole model does not provide for a level at this energy, but the importance of the de-excitation to the positive parity states seems to indicate that the configurations are more complicated than those of a particle-hole. (J.F.P.)

**3075** ON THE DECAY OF $^{146}Eu$. Avotina, M. P.; Grigoriev, E. P.; Sergeyev, V. O.; Zolotavin, A. V. (Physical Inst. of Leningrad Univ.). Phys. Lett., 19: 310-12(Nov. 1, 1965).

The decay scheme of europium-146 was observed in order to determine the energy levels of samarium-146, and thus to resolve previous discrepancies in these levels. An investigation of the conversion electron spectrum was carried out using two $\pi/2$ double focusing $\beta$ spectrometers. The observed energies of $\gamma$ transitions in the $^{146}Eu \rightarrow {}^{146}Sm$ decay and the relative intensities of their K-conversion lines are given. It was established that there are two transitions of energies of 633.4 and 634.2 kev in the strong 634-kev transition. The 634.2-kev transition has E2 character and the 633.4-kev transition has E1 character. The 705- and 901-kev $\gamma$ transitions are also found to have doublet character. The improved $^{146}Sm$ level scheme is constructed and shown. The interpretation of its characteristics is discussed. (J.F.P.)

**3076** POLARIZATION-ASYMMETRY EQUALITY AND THE MEASUREMENT OF SPIN-FLIP IN INELASTIC SCATTERING FROM NUCLEI. Satchler, G. R. (Oak Ridge National Lab., Tenn.). Phys. Lett., 19: 312-13 (Nov. 1, 1965).

Use is made of the property that inelastic scattering amplitudes (in the adiabatic limit when computed in the distorted waves (DW) approximation) as well as elastic scattering amplitudes of particles with spin scattered from spin-zero nuclei produce a polarization equal to the asymmetry which would have been observed if the projectiles had been 100% polarized. It is also assumed that elastic scattering from the excited residual nucleus can be described by the same optical potential as the target ground state. A z axis is chosen normal to the scattering plane, and the x axis is chosen along the recoil direction, thus a simple rotation of $\pi$ about the x axis leads to the equality investigated; that is, $P_s = \epsilon_s$, and $P_{int} = \epsilon_{int}$, where P is the polarization and $\epsilon$ is the asymmetry. Thus polarization and asymmetry are equal if only one s contributes to the scattering, but differ if there is interference between s = 0 and s = 1. (J.F.P.)

**3077** NEW LEVELS IN $^{58}Co$. Gorodetzky, S. (Institut de Recherches Nucleaires, Strasbourg); Gehringer, C.; Chevallier, P.; Cottin, S.; Drouin, R. S.; Sutter, G.; Siffert, P.; Stab, L. Phys. Lett., 19: 313-16(Nov. 1, 1965). (In French).

In order to identify energy levels situated between 25 and 1055 kev, excitation curves from the reaction $^{58}Fe$ $(p,n\gamma)^{58}Co$ were studied. The agreement of neutrons method was used, and the spectra of gamma emission for each was studied separately. For this purpose separate detectors were used for the slow and fast neutrons. The excitation curve from the reaction studied showed three peaks which correspond to gamma energies of 115 ± 3, 365 ± 3, and 692 ± 3 kev. The regions where these peaks exist are shown. These seem to indicate the existence of three new levels. Both natural and enriched iron were used as a target, and good agreement was obtained between the results using each. (J.F.P.)

**3078** THE FIRST EXCITED STATE OF $^5He$. Assimakopoulos, P. A.; Gangas, N. H.; Kossionides, S.; Democritus, N. R. C. (Creek Atomic Energy Commission, Athens). Phys. Lett., 19: 316-18(Nov. 1, 1965).

Excited states of $^5He$ below 10 Mev are sought by means of a multiparameter experiment on the reaction $^7Li + d \rightarrow \alpha + \alpha + n$. This reaction may proceed to the three particle final state either via intermediate two-body stages or directly as a three-body break-up. A LiOH target on a carbon backing was bombarded with a beam of 380-kev deuterons from a Van de Graaff accelerator. The two alpha particles produced in the reaction were detected in two solid state detectors. The detectors and the deuteron beam axis were coplanar, one detector was fixed at 90° with respect to the beam, and the other placed successively at the angles 65, 77.5, and 97.5° with respect to the deuteron beam axis. For the contribution from the $^5He$ ground state at 77.5° the spectra obtained through a simple projection of the results on the two energy axes are shown together with the spectra, after the normalization through the available phase space for each channel was carried out. The experimental results seem to confirm the estimate of the reaction via the $^8Be^*$ nucleus being about 10% of that via the $^5He^*$ nucleus. (J.F.P.)

**3079** GROUND STATE ENERGY OF NUCLEAR MATTER WITH PURE HARD CORE INTERACTION WITH NEUTRON EXCESS. Dabrowski, J.; Hassan, M. Y. M. (Univ. of Warsaw). Phys. Lett., 19: 318-19(Nov. 1, 1965).

The result of the calculation of the ground state energy of nuclear matter with a pure hard core interaction with a neutron excess characterized by the parameter $\alpha = (N-Z)/A$ is given. The calculation includes terms proportional to $k_F c)^2$. Within this accuracy it is sufficient to consider the interaction in the S state only. The unperturbed state is considered in which neutrons and protons occupy all the spin up and spin down plane wave states below the respective Fermi momenta $k_{Fn}$ and $k_{Fp}$. (J.F.P.)

**3080** DOUBLE CHARGE EXCHANGE WITH NEGATIVE PIONS. SEARCH FOR TETRANEUTRON. Gilly, L.; Jean, M.; Meunier, R.; Spighel, M.; Stroot, J. P.; Duteil, P. (CERN, Geneva. Faculte des Sciences, Orsay, France). Phys. Lett., 19: 335-8(Nov. 1, 1965).

Eventual production of light nuclei such as tetraneutrons and hydrogen-7 was investigated in double charge exchange reactions with negative mesons ($\pi$). Since production of A(Z-2) in a two-body process would lead to a mono-energetic meson ($\pi$) emission, positive mesons ($\pi$) emitted forward were registered. The meson ($\pi^+$) detection equipment was the double spectrometer with DISC Cherenkov counters. A negative meson ($\pi$) beam over an energy range from 120 to 280 Mev was used. Data were taken at a fixed spectrometer velocity setting, the incident negative mesons ($\pi$) being varied in steps of 6 Mev. Liquid He, Li, Be, and C targets were investigated. In no case was a two-body reaction observed. Curves of the intensity distribution of about 180 Mev $\pi^+$ as a function of $\pi^-$ energy are given. For each target nucleus a binding energy scale was drawn for an eventual two-body channel. Double charge exchange cross section for all final states available increases with the atomic number. (J.F.P.)

**3081** MOMENTUM DISTRIBUTION OF RECOIL NUCLEI IN THE REACTION $^{12}C(p,2p)^{11}B$. Yuasa, T.; Hourany, E. (Universite de Paris, Orsay, France). Phys. Letters, 18: 146-9(Aug. 15, 1965). (In French).

A 4-$\pi$ study was made of the momentum distribution of

recoil nuclei in the reaction $^{12}C(p,2p)^{11}B$ ejecting a bound proton in the $^{12}C$ nucleus. The momentum distributions were calculated, and all the collisions classified in the three intervals $50 < E_0 < 70$ Mev, $70 < E_0 < 90$ Mev, and $900 < E_0 < 110$ Mev were studied. The results show an asymmetry of the distribution for $\theta_r < \frac{1}{2}\pi$ and $> \frac{1}{2}\pi$ due to kinematic limitation and the difference of the solid angles of detection. There is a peak at approximately 60 Mev/c in all of the curves. There is also a peak at approximately 200 Mev/c which is less pronounced for coplanar and symmetrical collisions. The 60 Mev/c peak corresponds to quasielastic collisions. The differential cross sections for the coplanar and symmetrical collisions were also calculated. It was observed that the valley peak is higher in the present study than in previous studies and agrees better with the theoretical value without too much distortion. (J.S.R.)

**3082** ON SPIN DEPENDENCE OF RAYLEIGH SCATTERING. Daniel, H.; Schmitt, H. (Max Planck Inst. of Nuclear Physics, Heidelberg). Phys. Letters, 19: 129-30 (Oct. 1, 1965).

An experiment is described from which the results can be most easily interpreted in terms of spin-dependent Rayleigh scattering. The experimental method consisted in forward scattering of circularly polarized $\gamma$ rays on magnetized iron in a cylindrical geometry. The mean scattering angle was 53°. The $\beta$ correlations of several isotopes with correlations known from $\beta$ decay theory and from experiments of other types were measured. A summary is given of the isotopes, $\gamma$-ray energies, asymmetry parameters, experimental efficiencies, and calculated efficiencies. The effect of plural scattering was investigated in two separate experiments. It is shown that the plurally scattered quanta gave rise to a lower experimental efficiency. When the spectra of the scattered gamma radiation were measured as a function of the iron-scatterer thickness, it was found that the intensity of plurally scattered quanta is always small compared with that of simply scattered quanta. The analyzer efficiency at high energies is well understood while at low energies the experimental values are definitely higher than the computed ones. The stated discrepancy is most easily interpreted in terms of spin-dependent Rayleigh scattering. (J.F.P.)

**3083** MICROSCOPIC MODELS FOR VIBRATIONAL STATES IN EVEN NICKEL ISOTOPES. Hsu, L. S.; French, J. B. (Univ. of Rochester, N. Y.; Oak Ridge National Lab., Tenn.). Phys. Letters, 19: 135-8(Oct. 1, 1965).

In order to study the relation between various microscopic models for low-lying states of vibrational nuclei, various methods (shell-model, seniority, T-D, and R.P.A. approximations) were used to calculate the low-lying spectra for even nickel isotopes ($^{58}Ni$, $^{60}Ni$, $^{62}Ni$, and $^{64}Ni$). The results for $^{62}Ni$ and $^{64}Ni$ are shown. The active orbits are $2p_{3/2}$, $1f_{5/2}$ $2p_{1/2}$ for neutrons only. The single particle energies were taken to be 0, 0.78, and 1.08 Mev respectively. The two-body interaction used was an S-state interaction produced, via a least-squares analysis to energy levels, using shell-model programs. It is concluded that the interaction used is a reasonable one, and that the conclusions drawn about the models are probably valid. (J.F.P.)

**3084** ISOBARIC ANALOGUE STATES VIA (p,p) AND (p,n) ON $^{144}Sm$. Moore, C. F.; Jolly, R. K. (Florida State Univ., Tallahassee). Phys. Letters, 19: 138-41 (Oct. 1, 1965).

The range of the applicability of the measurement of isobaric analog states as resonances in a highly excited compound nucleus for spectroscopic assignments of the states of the neutron plus target system are explored for heavy nuclei. The difficulties and limitations are mentioned. In the case of $^{144}Sm$ the energy of the incident particles was limited to 10.8 Mev at the time of the experiment. For elastic scattering, a well collimated beam of protons bombarded the target and the scattered protons were detected by solid state detectors. For (p,n) reactions an arrangement designed to minimize the neutron background was used. The results from both reactions are given. It is found that the (p,n) data are most suitable for extracting resonance energies. Other resonance parameters are best determined from the elastic scattering data. The excitation functions for both (p,p) and (p,n) reactions were measured up to 10.8 Mev. (J.F.R.)

**3085** NUCLEAR GROUND STATES IN THE RANDOM PHASE APPROXIMATION. Sanderson, E. A. (Univ. of Pittsburgh). Phys. Letters, 19: 141-3(Oct. 1, 1965).

It is shown that the coefficients derived by Goswami and Pal (Nucl. Phys. 44: 294(1963)) for first order correlations in the ground state determine as well higher order correlations in the random phase approximation, in accordance with an analytic expression of the form previously given, without proof, for the case of virtual quadrupole vibrations. In addition an implicit equation for these coefficients is derived which is suitable for calculation by iteration. The main advantage of the iterative equation lies in the fact that it involves directly the matrix elements of the quasi-particle or particle-hole interaction and does not require a complete knowledge of all the random phase approximation excited-state eigenvectors. This is important for shell-model calculations in which large matrices have to be diagonalized, since considerable economy of machine time can be achieved by using the random phase approximation for the lowest states only and using the symmetric approximation, or simply the Tamm-Dancoff approximation for all higher levels. (J.F.P.)

**3086** INELASTIC ELECTRON SCATTERING FROM THE ALPHA PARTICLE. Frosch, R.; Rand, R. E.; Yearian, M. R.; Crannell, H. L.; Suelzle, L. R. (Stanford Univ., Calif.). Phys. Letters, 19: 155-7(Oct. 1, 1965).

The use of liquid $^4He$ target and a detection system of 100 closely spaced scintillation counters in a ladder configuration permits the study of the spectrum of inelastically scattered electrons with a momentum resolution of about 25%. Experimental parameters were chosen to give the best compromise between counting rate and momentum resolution. A beam of 200-Mev electrons from a linear accelerator was focused upon a liquid helium target cell containing the helium at a temperature of 4.2°K. Both elastic and inelastic spectra were observed at scattering angles of 45, 60, 75, and 90°. No momentum shifts of the elastic peak greater than 0.05% (0.1 Mev) were detected. Two of the four inelastic spectra are shown. All four spectra show a narrow peak at $E \approx 20.5$ Mev and a step. The energy at which the step occurs appears to decrease monotonically from about 24.5 to 23 Mev as the scattering angle increases from 45 to 90°. The cross sections for the excitation of the narrow peak are given. It is suggested that the step in the spectra is due to the overlap of two or more broad resonances. (J.F.P.)

**3087** F CENTERS IN SrO AND THE QUADRUPOLE MOMENT OF $^{87}Sr$. Culvahouse, J. W. (Univ. of Kansas, Lawrence); Holroyd, Louis V.; Kolopus, James L. Phys. Rev., 140: A1181-8(Nov. 15, 1965).

The paramagnetic resonance spectrum of F centers in single crystals of SrO is reported. The isotropic part of the hyperfine interaction A is 14.65 ± 0.08 G for the nearest-neighbor $^{87}Sr$ nuclei, and the dipolar hyperfine interaction constant B is 1.55 ± 0.03 G. Quadrupole-moment effects are prominent in the spectrum and $Qqe^2/h = 46 \pm 4$ Mo. Without detailed calculation, a value for the electric field gradient is found which is sufficiently accurate to allow $Q = 0.15 \times 10^{-24}$ cm$^2$ for $^{87}Sr$ with an uncertainty of no more than 40%. The values of A and B are correlated rather well with the values measured in other II–VI compounds by an extension of the analysis used for F centers in the alkali halides. (auth)

**3088** EFFECT OF THE CHEMICAL STATE ON THE LIFETIME OF THE 24-SECOND ISOMER OF $^{90}Nb$. Cooper, J. A.; Hollander, J. M.; Rasmussen, J. O. (Univ. of California, Berkeley). Phys. Rev. Lett., 15: 680-3(Oct. 18, 1965). (UCRL-16319).

An experiment is described by which a large change in the decay constant of the 24-sec $^{90}$Nb isomer was observed following a change in the chemical state. Nb foils were bombarded by 50-Mev protons producing $^{90}$Mo by a (p,4n) reaction. The foils, which contained $^{90m}$Nb in equilibrium with the $^{90}$Mo, were rapidly dissolved in a mixture of hot concentrated $HNO_3$ and HF, thus changing the chemical environment of the metastable state from metallic to that of a fluoride complex. A four-point growth curve was obtained by recording the gamma-ray spectra from a Ge(Li) detector at 18-sec counting intervals after the chemical reaction. The results of a least-squares analysis showed that the decay constant of the metal is 3.6 ± 0.04% greater than the decay rate of the fluoride complex. The size of the effect indicates that the transition depopulating the 24-sec isomer state has a very low energy and decays by internal conversion in the outermost electron shells, where changes in the chemical state can be expected to affect most strongly the electron density at the nucleus. (L.B.S.)

**3089** HIGH-ENERGY (0.1-2 Mev) FISSION CROSS-SECTION STRUCTURE MEASURED USING A NUCLEAR EXPLOSION IN SPACE. Albert, Richard D. (Univ. of California, Livermore). Phys. Rev. Letters, 15: 637-9 (Oct. 11, 1965). (UCRL-14369-T).

An experiment to measure the fission cross sections of $^{233}$U and $^{235}$U was performed using a nuclear explosion as a source of neutrons. Details of the data obtained for the energy region above 100 kev where the fission cross section is characterized by large variations in amplitude as a function of incident neutron energy are reported. The data which were obtained with an experimental resolution of less than 1 nsec/m, are averaged over 10- to 30-kev energy intervals to reduce statistical errors and facilitate correlation analyses. The structure which is shown in both cross sections, although its features are more prominent in the $^{233}$U data, which exhibit variations of the order of three times the statistical error, is given. An autocorrelation analysis of the $^{233}$U data obtained below 1-Mev energy indicates that the points are strongly correlated over an energy width of about 45 kev. Visual inspection of the data indicates that this width increases to about 100 kev in the 2-Mev energy region. Many mechanisms were proposed to account for variations in nuclear cross sections which cannot be ascribed to compound-nucleus single-resonance behavior. These are discussed. (J.F.P.)

**3090** THE MEASUREMENT OF MATRIX ELEMENTS FOR SINGLY FORBIDDEN BETA TRANSITIONS. Subotowitz, Mieczyslaw (Cathedral of Experimental Physics UMCS, Lublin). Postepy Fiz., 16: 349-67(1965). (In Polish).

The present state of beta decay theory is reviewed, both for allowed and forbidden beta transitions with stress on the latter. The many approximations resorted to in formulating the theory quantitatively, and the degree of accuracy of the approximations are discussed. An example of this is the relativistic correction. After a review of the fundamentals, the measurement of matrix elements is discussed in terms of the observables to which the experimenter has access. These include the value of ft, the correction factor C(W) for the energy spectrum, the asymmetry coefficient for beta-gamma angular correlation, and the various beta-gamma polarization correlation coefficients. (TTT)

**3091** ON THE ANGULAR DISTRIBUTION OF NUCLEONS SCATTERED FROM $^{14}$N. IMPULSE APPROXIMATION. Takemiya, Toshinori (Kumamoto Univ., Japan). Progr. Theoret. Phys. (Kyoto), 34: 433-41(Sept. 1965).

The differential cross section and the polarization of the nucleons scattered elastically and inelastically by $^{14}$N are calculated by the use of the impulse approximation, for $E_n$ = 90, 156, and 310 Mev. The effect of D state in $^{14}$N is surveyed by these angular distributions. It was found that the influence of D state made no appearance in the angular distributions of the elastic differential cross sections, but in the angular distributions of the inelastic scattering to the first excited state of $^{14}$N. The polarizations of the nucleons both elastically and inelastically scattered by $^{14}$N were also calculated. (auth)

**3092** STUDY OF THE MECHANISM OF THE REACTION $^{26}$Mg(p,p′,γ) AT LOW ENERGY. Hulubel, H.; Martalogu, N.; Ivascu, M.; Scintei, N.; Berinde, A.; Neamu, I.; Franz, J. (Institut de Physique Atomique de l'Academie de la R.P. Roumaine, Bucharest). Rev. Roumaine Phys., 10: 253-5(1965). (In French).

The angular distributions and the p′-γ angular correlations of protons inelastically scattered by the first and second excited state of $^{26}$Mg was measured for incident proton energies between 5.67 and 6.46 Mev. The excitation functions obtained show the existence of a resonance at 5.92 Mev. The comparison of the experimental total excitation functions with the theoretical values, calculated by assuming the formation of the compound nucleus and the realization of the statistical hypothesis, shows a poor agreement for the first excited level but a satisfactory agreement for the second. The angular distributions obtained show a pronounced dependence on energy with respect to the value of the cross sections and the form of the angular distribution curves. For the second excited level the curves obtained at the same proton energies are almost isotropic. The p′-γ angular correlations measured for the excitation of the first level show that the angular correlation functions are less sensitive to interference terms than the angular distributions. The angular distributions of the protons inelastically scattered on the second excited state of $^{26}$Mg and the second γ ray of the $2^+ \rightarrow 2^+ \rightarrow 0^+$ are almost isotropic. (J.S.R.)

**3093** LIQUID HELIUM CRYOSTAT FOR MOESSBAUER SCATTERING EXPERIMENTS. Barrett, P. H.; Grodzins, L. (Massachusetts Inst. of Tech., Cambridge). Rev. Sci. Instrum., 36: 1607-10(Nov. 1965). (MIT-2098-112).

A simply constructed cryostat designed for Mössbauer scattering experiments is described. The sample volume is part of the transfer line from a liquid helium reservoir to a mechanical pump; the sample is thus cooled by helium flow. The helium vapor exiting from the sample volume cools the transfer line and radiation shield. The temperature of the sample is controlled by the helium flow rate determined by a needle valve at the pump. The operating range is from 9 to ~300°K. The liquid helium consumption in l/hr is 0.3 at 10°K, 0.2 at 16°K, and 0.1 at 34°K. Possible modifications to improve the operating characteristics are discussed. (auth)

**3094** PLASMA IMPEDANCE MEASURING TECHNIQUE. Christy, E. H. Jr. (Oak Ridge National Lab., Tenn.). Rev. Sci. Instrum., 36: 1659-60(Nov. 1965). (ORNL-P-1437).

A circuit is described, consisting of a sampling oscilloscope equipped with high-impedance cathode-follower probes and a constant-impedance adjustable coaxial transmission line. The circuit is designed for plasma impedance measurements in the 40- to 300-Mc range. The circuit used and its equivalent circuit are described. The device is reliable, gives reproducible results, is simple, can be used for remote measurements, and is almost as accurate as impedance-bridge instruments. (T.F.H.)

**3095** THE PRODUCTION OF TRITIUM AND $^3$He BY PROTON BOMBARDMENT OF METALS, SOLAR ORIGIN OF TERRESTRIAL TRITIUM. Ide, R. H. (Univ. of California, Livermore); Libby, W. F. Trans. Amer. Nucl. Soc., 8: 328(Nov. 1965).

**3096** NUCLEAR NOTATIONS. Weiss, Francis Joseph (Library of Congress, Arlington, Va.). Trans. Amer. Nucl. Soc., 8: 537-8(Nov. 1965).

**3097** INVESTIGATION OF THE $^{116*}$In DECAY. Vesna, V. A.; Voinova, N. A.; Kalinichev, Yu. V.; Sergeev, A. G. (Ioffe Inst. of Physics and Tech., Leningrad). Yadern. Fiz., 2: 3-9(July 1965). (In Russian).

The γ-spectrum of $^{116*}$In ($T_{½}$ = 54 min) is investigated. A magnetic Compton spectrometer was used, making it possible to determine the energies and intensities of γ-lines with high accuracy. Samples of $In_2O_3$ were irradiated by a $(3-4)\cdot 10^{13}$ neutron/cm$^2\cdot$ sec flux of thermal neutrons in a reactor and were transported to the spectrometer by

a pneumopost. The following energy levels and intensities were observed: 2113.2 ± 0.6 (16.3 ± 1.0); 1751.3 ± 0.8 (2.8 ± 0.2); 1507.9 ± 0.5 (9.1 ± 0.6); 1293.7 ± 0.5 (83.7 ± 2.0); 1098.5 ± 0.7 (56 ± 3); 820.1 ± 0.6 (11.2 ± 1.0); 416.9 ± 0.4 (27.5 ± 3.0). The upper limit of the intensity of the γ-transition with the energy ~445 kev is found to be 1.5%. The decay scheme of $^{116*}$In is discussed. (auth)

**3098** BINDING ENERGY ANOMALIES FOR THE LAST TWO NEUTRONS IN THE REGION N = 86–92. Demirkhanov, R. A.; Dorokhov, V. V.; Solov'ev, V. G. (Inst. of Theoretical and Experimental Physics, Moscow). Yadern. Fiz., 2: 10-13(July 1965). (In Russian).

The boundary between spherical and deformed nuclei in the rare earth region is determined by analyzing the values of the binding energy of the last two neutrons ($B_{2n}$). It is shown that an anomaly in the behavior of $B_{2n}$ appears at N = 88–91, both for even-even and even-odd nuclei. The magnitudes (~0.3–0.6 Mev) and approximate boundaries of this effect are determined. Spectroscopic data on the energies of the lowest rotational states confirm the conclusions based on exact mass measurements and an analysis of the nuclear binding energies. (auth)

**3099** ASYMPTOTIC PROPERTIES OF SOME MODEL HAMILTONIANS IN NUCLEAR PHYSICS; SINGLE-PARTICLE EXCITATIONS. Czerwonko, J. (Inst. of Theoretical and Experimental Physics, Moscow). Yadern. Fiz., 2: 14-23(July 1965). (In Russian).

The asymptotic properties of the mean energy and finite temperature single-particle excitations of a class of model hamiltonians are investigated. The case is considered where the number of particles tends to infinity leaving the density constant. A model interaction hamiltonian is used, in which there is one summation over one-particle degrees of freedom less than in the real case. (auth)

**3100** SINGLE-PARTICLE l-FORBIDDEN TRANSITIONS IN NUCLEI. Khodel', V. A. (Moscow Inst. of Physics and Tech.). Yadern. Fiz., 2: 24-7(July 1965). (In Russian).

The interacting quasiparticle method is applied to l-forbidden transitions. It is shown that the existence of single-particle l-forbidden transitions can be accounted for by the spin-spin interaction between quasiparticles. (auth)

**3101** ON β-DECAY IN NUCLEI. Migdal, A. B.; Khodel, V. A. (Inst. of Physics and Tech., Moscow). Yadern. Fiz., 2: 28-34(July 1965). (In Russian).

The interacting quasiparticle method is applied to β-transitions in nuclei. The probabilities of allowed β-transitions are calculated, taking the interaction between quasiparticles into account. It is shown that l-forbidden transitions are due to spin-spin interactions. (auth)

**3102** ON A RELATION BETWEEN NUCLEAR MASSES. Mikulinskii, M. A. Yadern. Fiz., 2: 35-9 (July 1965). (In Russian).

Relations between the masses of neighboring nuclei and interaction amplitudes are obtained from β-transition frequencies in mirror nuclei, using the Fermi-liquid theory for finite systems. (auth)

**3103** NUCLEAR ROTATIONAL SPECTRA AT HIGH MOMENTA. Grin', Yu. T.; Larkin, A. I. Yadern. Fiz., 2: 40-50(July 1965). (In Russian).

The dependence of the pairing correlation, moment of inertia and energy of the nucleus on the momentum of the system is calculated, without any assumption as to the smallness of the momentum in comparison with the magnitude of the nucleon pairing correlation. The critical nuclear momenta, at which the pairing correlation vanishes, are calculated, and are found to depend weakly on the deformation. The developed theory is compared with experiments. (auth)

**3104** GREEN FUNCTIONS AND TRANSITION PROBABILITIES IN ODD NUCLEI. Belyaev, S. T.; Zelevinskii, V. G. Yadern. Fiz., 2: 51-8(July 1965). (In Russian).

Expressions are obtained for various Green functions of odd nuclei, both for single-particle and collective excitations. Transition probabilities and mean values of physical quantities are derived for arbitrary low-lying states in odd nuclei. (auth)

**3105** ON THE PHOTODISINTEGRATION THEORY FOR THE LIGHTEST NUCLEI. Dzhibuti, R. I.; Mamasakhlisov, V. M.; Macharadze, T. S. (Inst. of Physics, Academy of Sciences, Georgian SSR). Yadern. Fiz., 2: 59-63(July 1965). (In Russian).

Cross-sections for the total and two-particle photodisintegration of the nuclei $^3$He and $^4$He are calculated in the Born approximation on the basis of the matrix element in the form $(JA)_{if}$. The results are compared with cross-sections calculated using a matrix element in the form $(ED)_{if}$. Considerable differences are found. It is shown that the main reason for the large contradiction between the existing theory and experimental data is the choice of the matrix element in the form $(ED)_{if}$. The results obtained with the help of the form $(JA)_{if}$ are in good agreement with the experimental data. (auth)

**3106** THE $^{12}$C(d,α)$^{10}$B REACTION AS A NUCLEON ASSOCIATION REPLACEMENT PROCESS. Melikov, Yu. V.; Tulinov, A. F. Yadern. Fiz., 2: 64-9(July 1965). (In Russian).

Angular distributions of α-particles from the reaction $^{12}$C(d,α)$^{10}$B corresponding to the formation of the final nucleus in the ground state and in three excited states, were measured for 13 Mev deuterons. The experimental results are analyzed from the point of view of a mechanism considering the replacement of nucleon associations on the basis of the shell model with intermediate coupling, using the plane wave Born approximation. The influence of the excited states of the $^8$Be core on the differential cross-section is considered. A theoretical analysis of the experimental data on the $^{12}$C(d,α)$^{10}$B reaction at higher deuteron energies is performed. (auth)

**3107** INVESTIGATION OF THE REACTION $^{16}$O(γ,p)$^{15}$N. Denisov, V. P.; Kul'chitskii, L. A. (Ioffe Inst. of Physics and Tech., Leningrad). Yadern. Fiz., 2: 70-81(July 1965). (In Russian).

Photoproton spectra from the $^{16}$O nucleus were measured with the help of telescopes, containing a proportional and a scintillation counter, for fourteen values of $E_{\gamma m}$ in the region from 21.3 to 43.7 Mev. Excitation functions of the reaction $^{16}$O(γ,p)$^{15}$N for transitions to the ground state, to the doublet positive parity state (5.28 and 5.30 Mev) and to the third excited state (6.33 Mev) of the $^{15}$N nucleus, were obtained from an analysis of the proton output curves in various regions of their spectrum, using the bremsstrahlung spectrum isochromas. The relative intensities of transitions to these states are equal to 45, 25 and 30%, for transitions from the 22.3 Mev dipole state of the $^{16}$O nucleus and to 42, 28 and 30% from the 24.4 Mev state. The total integral (γ,p) reaction cross-section is equal to 83 ± 8 mbn·Mev in the region 17 to 40 Mev. The cross-sections for various excited states in the $^{16}$O nucleus are determined. The positions of these states are in good agreement with the energies, obtained in other experiments ((γn), (e, e'p) and (p,$\gamma_0$) reactions). The results are compared with theoretical calculations and with experimental results concerning reactions on the $^{16}$O nucleus. (auth)

**3108** THE ANGULAR AND ENERGY DISTRIBUTIONS OF $^{18}$F RECOIL NUCLEI IN THE REACTION $^{19}$F(γ,n)$^{18}$F. Denisov, F. P.; Duisebaev, A.; Kosareva, K. V.; Cherenkov, P. A. (Lebedev Inst. of Physics, Moscow). Yadern. Fiz., 2: 82-3(July 1965). (In Russian).

Angular and energy distributions of recoil nuclei were measured, produced in the $^{19}$F(γ,n)$^{18}$F reaction by bremsstrahlung with the maximal energy 260 Hev. The angular distributions of recoil nuclei, the paths of which correspond to the widths ~0 and 0.186 mg/cm$^2$ of the absorber, are anisotropical in the laboratory system and correspond to the preferential emission of recoil nuclei in the direction of the beam. Recoil nuclei with paths corresponding to the absorber widths 0.566 and 0.841 mg/cm$^2$, demonstrate an angular distribution symmetrical with respect to 90° in the laboratory system. (auth)

**3109** THE γ-SPECTRUM FROM THE REACTION $^{54}Fe(n,\gamma)^{55}Fe$. Loskutova, N. G.; Rudak, E. A.; Firsov, E. I. (Inst. of Physics, Minsk). Yadern. Fiz., 2: 84–91 (July 1965). (In Russian).

Gamma rays from the reaction $^{54}Fe(n,\gamma)^{55}Fe$ with thermal neutrons were investigated with the help of a magnetic Compton γ spectrometer with 2% resolution and the lower boundary of the measured γ-ray energies equal to 0.3 Mev. The measured sample was prepared from iron, enriched up to 78.1% in the isotope $^{54}Fe$. Its weight was 72.06 g. γ-Rays with the following energies (in Mev) and intensities (given in parentheses) were found in the experiment: 9.31 (61), 8.98(12), the doublet 7.27(3.0), 6.82(2.0), 6.27(3.0), 5.75(2.5), 5.50(2.0), 5.37(1.3), doublet 4.73(3.0), 4.55(1.4), 4.46(1.5), 4.17*(1.5), 3.79*(1.7), 3.38*(1.5), doublet 3.07* (4.0), 2.90*(1.0), 2.67*(1.5), 2.63*(1.0), 2.47*(2.4), 2.05* (2.5), 1.92*(2.5), 1.63*(1.5), 1.5*(1.5), 1.32*(1.0), 1.24* (1.0); the group of lines—0.93*(10.0), 0.41*(29.0). A scheme for the decay of the $^{55}Fe$ isotope from the capture level is suggested on the basis of the data obtained and its principal characteristics are discussed. (A star indicates γ-rays found for the first time.) (auth)

**3110** KINETIC ENERGIES OF FRAGMENTS WITH VARIOUS MASSES IN THE FISSION OF $^{235}U$ BY THERMAL AND FAST NEUTRONS. D'yachenko, P. P.; Kuz'minov, B. D.; Smirnov, V. I.; Chernukhin, V. L.; Chubarov, S. I. Yadern. Fiz., 2: 92-6(July 1965). (In Russian).

The kinetic energy distributions of fragments with various masses were investigated in the fission of $^{235}U$ by thermal neutrons and neutrons with the mean energy 720 kev. The fragments were detected by surface-barrier counters. The amplitude analysis was performed by a two-dimensional 128 × 128-channel pulse analyzer. The mean total kinetic energies of the fission fragments for thermal and fast neutron fission are equal for all types of fission. This quantity is equal to 156 ± 2 Mev for fission into fragments with approximately equal masses. (auth)

**3111** THE ANGULAR DISTRIBUTION OF FRAGMENTS. Gorichev, P. A.; P'yanov, I. I. Yadern. Fiz., 2: 97-108(July 1965). (In Russian).

Formulas are obtained, connecting the energy and angular distributions of fragments and making it possible to find any angular characteristics of the fragments, from the energy spectrum. They are derived on the basis of a model in which fragments are emitted isotropically by excited moving nuclei. Various angular fragment characteristics, calculated according to this model, are compared with the large number of experimental data, for initial particle energies in the region from 76 Mev to 25 Bev. The agreement between the calculated and experimental values is satisfactory nearly in all cases. This suggests that such an approach could be applied to explain the fragmentation process. (auth)

**3112** DETERMINATION OF INTENSITIES AND MULTIPOLARITIES IN HIGH-ENERGY $^{182}Ta$ DECAY γ TRANSITIONS. Vitman, V. D.; Voinova, N. A.; Dzhelepov, B. S. (Ioffe Inst. of Physics and Tech., Leningrad; Mendeleev Inst. of Metrology, USSR). Yadern. Fiz., 2: 393-401(Sept. 1965). (In Russian).

Accurate intensity measurements of $^{182}Ta$ gamma transitions with energy above 900 kev were performed. Ta activated by neutrons served as the source. Twenty transitions were observed in all. Multipolarities and in some cases mixing of various multipolarities were determined. Multipolarities of transitions with energies 1342, 1372, 1386, 1410, (1435), and 1453 kev were determined for the first time. The level scheme of $^{182}W$ is discussed. The following quantum characteristics I, $J^\pi$: 0, $2^+$ (1222); 2, $2^+$ (1258); 2, $2^-$ (1289); 2, $3^+$ (1331); (1), $0^+$ (1410); and $J^\pi = 2^-$ (1435) were assigned to excited levels on the basis of the data. The data do not contradict the values of $J^\pi = 4^-$ for the 1488- and 1554-kev levels and $J^\pi = 4^+$ for the 1443-kev level. (auth)

**3113** INVESTIGATION OF THE RADIATION OF $^{117}Cd$. Baskova, K. A.; Vasil'ev, S. S.; Rudenko, N. P.; Sevastyanov, A. I.; Hamo-Leila, M. A.; Shavtvalov, L. Ya. (Moscow State Univ.). Yadern. Fiz., 2: 402-8(Sept. 1965). (In Russian).

$^{117}Cd$ was obtained in the reaction $^{116}Cd(d,p)$. Investigations showed that $^{117}Cd$ has a single half life equal to about 3 hours. The half life 50 minutes, previously erroneously ascribed to $^{117}Cd$, probably belongs to $^{116}In$, produced in the reaction $^{116}Cd(d,2n)$. The β spectrum of $^{117}Cd$ (3 hours) was investigated on a β spectrometer with a magnetic lens. The upper limits of the partial β spectra have the energies 670, 1250, 1800, and 2200 kev. The log ft values were found to be 4.9, 6.7, 6.9, and 7.6, respectively. The results and an investigation of the βγ coincidences made it possible to suggest a decay scheme for $^{117}Cd$, differing significantly from those in the literature. (auth)

**3114** MEAN WIDTHS FOR RADIATIVE TRANSITIONS IN HEATED NUCLEI. Kuklin, R. N. Yadern. Fiz., 2: 409-14(Sept. 1965). (In Russian).

A formula is obtained for the average width of a dipole transition in a heated nucleus, as a function of the emitted energy. The averaging in the initial state is performed with respect to the Gibbs ensemble, and the quantum summation in the final state—over all states allowed by energy conservation. The calculated mean width is in satisfactory agreement with experiment, and the energy characterizing the quasiparticle damping, which causes the radiative transitions, is equal to the imaginary part of the optical potential. (auth)

**3115** ON THE EFFECTIVE QUADRUPOLE CHARGE IN NUCLEI (MATRIX ELEMENTS). Kamerdzhiev, S. P. Yadern. Fiz., 2: 415-22(Sept. 1965). (In Russian).

An equation for the effective quadrupole charge is obtained and solved, using the method of interacting quasiparticles. The connection with calculations in the model "pairing + quadrupole forces" is demonstrated. The same method is used to calculate the probabilities of single-particle low-energy E2 transitions in several nuclei. (auth)

**3116** ON THE OPTICAL POTENTIAL FOR A NUCLEUS IN AN EXCITED STATE. Inopin, E. V. Yadern. Fiz., 2: 423-6(Sept. 1965). (In Russian).

The influence of the finite temperature of the nucleus on the imaginary part of the optical potential is calculated on the basis of the nucleon Fermi gas model. It is shown that the imaginary part of the potential for scattered nucleon energies of the order 1 Mev increases considerably for nonzero temperatures, i.e., for excited nuclear states. (auth)

**3117** SELECTION RULES FOR NUCLEAR REACTIONS INVOLVING NUCLEON ASSOCIATIONS IN THE SU(3) SCHEME. Zelenskaya, N. S.; Mailing, L.; Neudatchin, V. G.; Smirnov, Yu. F. (Moscow State Univ.). Yadern. Fiz., 2: 427-32(Sept. 1965). (In Russian).

Selection rules with respect to quantum numbers in the SU(3) scheme, extensively used in light nuclear spectroscopy, are formulated for nuclear reactions involving nucleon associations. In some cases these selection rules lead to very strong restrictions, so that it is easy to check them experimentally. For instance the quasi-elastic knockout of an α particle from the nucleus $^{16}O$ by a rapid particle a: $^{16}O(a,a\alpha)^{12*}C$, accompanied by the α decay of $^{12*}C \rightarrow 3\alpha$, is possible only through the 12-Mev level $|1s^4 1p^8 [444]\ 4^+\rangle$ of the $^{12}C$ nucleus. Further, in the stripping reaction $^{16}C(^6Li,d)^{20*}Ne$ the only levels of the configuration $(1d-2s)^4$ which can be excited are those of the lowest rotational series $0^+, 2^+, \ldots$, based on the ground state of $^{20}Ne$. (auth)

**3118** ON THE CALCULATION OF MAGNETIC MOMENTS OF SPHERICAL NUCLEI. Sapershtein, E. E.; Khodel, V. A. Yadern. Fiz., 2: 433-5(Sept. 1965). (In Russian).

Corrections to the expression for magnetic moments, calculated previously, are considered. It is shown that the maximum deviation from the calculated values is obtained for $j = l + \frac{1}{2}$. (auth)

**3119** ON THE THEORY OF THE ELECTROMAGNETIC FORM FACTORS IN THE THREE-NUCLEON SYSTEM. Kalade, Yu. A.; Pipiraite, P. P.; Shugurov, V. K. (Vilnius State Univ., USSR). Yadern. Fiz., 2: 436-40(Sept. 1965). (In Russian).

The energy of the ground state is calculated using the function describing the motion of the particles with respect to the center of mass. The parameter in the radial part of the wave function is found from the energy minimum. The obtained function is used to calculate the electromagnetic form factors. The agreement with experimental data is satisfactory. (auth)

**3120** THE SCATTERING OF NEUTRONS ON POLARIZED TARGETS. Baryshevskii, V. G.; Lyuboshits, V. L.; Pogdoretskii, M. I. (Joint Inst. of Nuclear Research, Dubna, USSR). Yadern. Fiz., 2: 441-4(Sept. 1965). (In Russian).

The scattering of neutrons on a polarized target in an external magnetic field is considered for the case of a quadrupole splitting of the target nuclei levels in an inhomogeneous intracrystalline electric field. It is shown that the particle intensities and polarizations change periodically in time, both in the scattered and in the transmitted beam. Effects due to the crossing of nuclear levels in the target nuclei are discussed. (auth)

**3121** TWO-NUCLEON TRANSFER IN DIRECT REACTIONS. Shapiro, I. S.; Timashev, S. F. (Inst. of Theoretical and Experimental Physics, Moscow). Yadern. Fiz., 2: 445-59(Sept. 1965). (In Russian).

The angular distributions in the direct (t,p) and (He-3,n) reactions on light nuclei are calculated. The results are in reasonable agreement with experimental data in the region of small momentum transfers. (auth)

**3122** THE ANGULAR ANISOTROPY OF FISSION BY SUB-BARRIER DEUTERONS. Nemilov, Yu. A.; Selitskii, Yu. A.; Solov'ev, S. M.; Eismont, V. P. Yadern. Fiz., 2: 460-5(Sept. 1965). (In Russian).

The angular distribution of fission products was measured for the fission of heavy nuclei by deuterons with various energies (below the Coulomb barrier). It was found that the distributions are anisotropic and that the energy dependence of the anisotropy for even old target nuclei has some significant features. E.g., for $^{238}$Pu the anisotropy increases as the deuteron energy decreases, whereas for $^{235}$U it decreases and goes into the region of negative values ($\sigma_f(0°)/\sigma_f(90°) < 1$). These features are interpreted as due to the specific character of the interaction of low-energy deuterons with heavy nuclei. The results are used to obtain additional information on the properties of nuclei at the saddle point. (auth)

**3123** THE ABSORPTION OF STOPPED $\pi^-$ MESONS BY CARBON NUCLEI. Fedotov, P. I. Yadern. Fiz., 2: 466-70(Sept. 1965). (In Russian).

The absorption of $\pi^-$ mesons by carbon nuclei was investigated on diamond samples placed in the layers of a photoemulsion chamber. It was found, after analyzing 520 $\pi^-$ meson captures by carbon nuclei, that the contribution of one-nucleon absorption is no more than 15%. The experimental data confirm the assumed two-nucleon mechanism of $\pi^-$ meson capture. The probability of the capture of mesons by np and pp pairs is estimated. (auth)

**3124** ON THE AMPLITUDE OF INELASTIC SCATTERING OF ELECTRONS BY NUCLEI. Petkov, I. (Joint Inst. for Nuclear Research, Dubna, USSR). Yadern. Fiz., 2: 485-6(Sept. 1965). (In Russian).

The amplitude of inelastic scattering of electrons by nuclei is considered in a high energy approximation. The calculated cross section for inelastic scattering of electrons with $0^+$ state excitation is compared with the corresponding cross section in the framework of the method of distorted waves. (auth)

**3125** THE REDUCTION OF DEUTERON STRIPPING CROSS SECTIONS BY A CHANGE OF DEFORMATION. Hebach, H. (Max-Planck-Institut fuer Chemie, Mainz). Z. Physik, 187: 338-50(1965).

The effect of a change in deformation on stripping cross sections is discussed near N = 88 to 90, where the nuclear deformations strongly depend on the neutron number. For a series of initial and final deformations a reduction factor is calculated by which the stripping cross section as given by Satchler and others has to be multiplied. For instance, differences in deformations of $\Delta\delta = 0.10$ which could be expected in this region should give a reduction factor of about 0.08. (auth)

**3126** YIELD OF THE (γ,t) REACTION IN OXYGEN WITH 50-Mev BREMSSTRAHLUNG. von Buttlar, H.; Goldmann, A. (Technische Hochschule, Darmstadt, Ger.). Z. Physik, 187: 355-8(1965). (In German).

Water was irradiated with 50 Mev bremsstrahlung, converted to hydrogen gas, and the triton yield was measured relative to the yield of the reaction $^{12}C(\gamma,n)^{11}C$. The ratio of the yields was found to be $(2.0 \pm 0.2) \cdot 10^{-2}$. The (γ,t)-reaction below 50 Mev carries 0.4% of the bremsstrahlung-weighted cross-section and less than 1% of the dipole sum for $^{16}$O. The reactions partially proceed through excited states of the daughter nucleus $^{13}$N. (auth)

**3127** NEUTRON CAPTURE GAMMA SPECTRUM AND LEVEL SCHEME OF $^{167}$Er. Koch, H. Ruediger (Technische Hochschule, Munich). Z. Physik, 187: 450-62 (1965). (In German).

The (n,γ)-spectrum of $^{167}$Er was investigated by means of the Riso bent crystal spectrometer. The energies and intensities of 47 transitions were measured. 22 of them were fitted into a level scheme. The rotational bands of the $K = 7/2^+$ [633], $K = 1/2^-$ [521], and $K = 5/2^-$ [512] states were found up to the spin values $I = 11/2^+$, $9/2^-$, and $7/2^-$. Gamma vibrational states of these Nilsson orbitals were determined or proposed. The energy of the $K = 5/2^-$ [523] state was suggested. Branching ratios of gamma transitions were compared with theoretical predictions. (auth)

**3128** ELECTRON CAPTURE IN THE DECAY OF $^{45}$Ti. Gfoeller, D.; Flammersfeld, A. (Universitaet, Goettingen, Ger.). Z. Physik, 187: 490-4(1965). (In German).

Electron capture to the 718-kev, 1238-kev, 1408-kev and 1665-kev excited states of $^{45}$Sc was observed in the decay of $^{45}$Ti. The branching ratios were determined to be (0.4 ± 0.04)%, (0.05 ± 0.02)%, (0.27 ± 0.03)% and (0.08 ± 0.01)% per decay of $^{45}$Ti respectively. (auth)

**3129** MEASUREMENT OF THE $\beta$-$\gamma$ ANGULAR CORRELATION FOR $^{198}$Au. Deinet, W.; Mueller, H.; Schopper, H. (Kernforschungszentrums, Karlsruhe, Ger.). Z. Physik, 188: 23-30(1965). (In German).

The energy dependence of the $\beta$-$\gamma$ asymmetry coefficient was measured. No anomaly at low $\beta$ energies as reported by other authors was found. The $\xi$-approximation holds and $\epsilon W/p^2\nu_{12} = 0.027 \pm 0.007$ was obtained. The matrix elements of the $\beta$ transition are discussed. (auth)

**3130** DELAYED NEUTRONS IN THE DECAY OF $^{9}$Li. Schoeneberg, R.; Hansen, H.; Weigmann, H.; Flammersfeld, A. (Universitaet, Goettingen, Ger.). Z. Physik, 188: 38-46(1965). (In German).

The neutron spectrum of the delayed-neutron-emitter $^{9}$Li was measured with a cooled $^{6}$Li J-crystal. Neutrons resulting from the decay of the 2.43 Mev level in $^{9}$Be revealed a continuum with endpoint-energy of 760 kev. The energy-region above this endpoint up to 7 Mev showed no evidence for deexcitation of higher excited levels of $^{9}$Be by monoenergetic neutrons. A discussion of the experimental results and the various models of the nuclear theory describing the $^{9}$Be-nucleus and its excited levels is given. (auth)

**3131** INVESTIGATIONS OF THE GAMMA RADIATION IN THE CAPTURE OF THERMAL NEUTRONS IN $^{143}$Nd BY MEANS OF THE SUM-COINCIDENCE METHOD. Zehender, Otto; Fleischmann, Rudolf (Universitaet, Erlangen-Nurnberg, Ger.). Z. Physik, 188: 93-8(1965). (In German).

2 two-step cascades from the capturing state to the groundstate of $^{143}$Nd and 6 two-step cascades from the capturing state to the 0.69 Mev excited state were found

by means of the sum-coincidence method. The relative intensities of the cascades were determined. (auth)

**3132** THE DECAY OF $^{55}$Co, $T_{\frac{1}{2}}$ = 18 hr. Haupt, W.; Lange, D.; Eckert, H. G.; Flammersfeld, A. (Univ., Goettingen, Ger.). Z. Physik, 188: 256-73(1965). (In German).

The $^{55}$Co($T_{\frac{1}{2}}$ = 18 hr) was produced by bombarding iron-foils with 9-Mev deuterons. The $\gamma$-spectra from the decay of $^{55}$Co were investigated using a scintillation fast-slow-coincidence circuit and a Li-drifted Ge-counter. Eighteen $\gamma$-transitions were observed having the following energies in kev and intensities per $^{55}$Co-decay: $\gamma_1$ = 95 (0.006), $\gamma_2$ = 413 (0.016), $\gamma_3$ = 475 (0.12), $\gamma_4$ = 645 (0.005), $\gamma_5$ = 750 (0.002), $\gamma_6$ = 810 (0.025), $\gamma_7$ = 900 (0.024), $\gamma_8$ = 940 (0.80), $\gamma_9$ = 985 (0.009), $\gamma_{10}$ = 1055 (0.005), $\gamma_{11}$ = 1210 (0.01), $\gamma_{12}$ = 1320 (0.065), $\gamma_{13}$ = 1375 (0.042), $\gamma_{14}$ = 1410 (0.13), $\gamma_{15}$ = 1600 (0.001), $\gamma_{16}$ = 1800 (0.0006), $\gamma_{17}$ = 2160 (0.001), $\gamma_{18}$ = 2310 (0.0042). (auth)

**3133** RADIATION WIDTHS OF INTERMEDIATE NUCLEI. Kim, Hi-sang; Pikelner, L. B.; Sirazhet, Kh.; Sharapov, E. I. (Joint Inst. for Nuclear Research, Dubna, USSR). Zh. Eksp. Teor. Fiz., 49: 410-13(Aug. 1965). (In Russian).

The radiation widths of a number of neutron resonances of zinc, molybdenum, niobium, and rubidium isotopes are investigated on the pulsed reactor of the Joint Institute for Nuclear Research. A maximum is observed in the dependence of the radiation widths on neutron number N of the nucleus at N = 43 − 44 and a minimum at N = 38 − 40. (auth)

**3134** ANGULAR DISTRIBUTION OF $^{238}$U PHOTOFISSION FRAGMENTS NEAR THE FISSION THRESHOLD. Bocharova, I. E.; Zolotukhin, V. G.; Kapitsa, S. P.; Smirenkin, G. N.; Soldatov, A. S.; Tsipeniuk, Yu. M. (Inst. of Problems in Physics, Academy of Sciences, USSR). Zh. Eksp. Teor. Fiz., 49: 476-84(Aug. 1965). (In Russian).

The angular distributions of fragments emitted in photofission of $^{238}$U near the threshold are measured by recording the fission events in glass. The $\gamma$ quanta were produced by electrons accelerated in the 12-Mev high-current microtron of the Institute for Physical Problems, USSR Academy of Sciences. The work was carried out with the aim of detecting the ~$\sin^2 2\theta$ component in the angular distribution which should be due to the $2^+$, K = 0 channel in quadrupole photon absorption. Quadrupole absorption has been detected only in an excitation region which is much lower than the barrier for dipole fission. This is in good agreement with the usual assumption that the quadrupole absorption cross section is much smaller than that for dipole absorption. The experimental data confirm Bohr's hypothesis regarding the similarity of the fission channel spectrum and lower excited level spectrum near the ground state of the equilibrium nucleus. The distance between the thresholds of the fission channels for $2^+$ and $1^-$, K = 0 as well as $1^-$, K = 0 and $1^-$, K = 1 is not less than 0.5 Mev. (auth)

**3135** ON THE ROLE OF ROTATIONAL STATES IN SCATTERING OF SLOW NEUTRONS BY GAS MOLECULES. Dzyub, I. P. (Inst. of Physics, Academy of Sciences, Ukrainian SSR). Zh. Eksp. Teor. Fiz., 49: 493-9(Aug. 1965). (In Russian).

The Zemach–Glauber formalism is employed for calculating the differential cross section for scattering of slow neutrons by gas molecules. The limits of applicability of the Krieger–Nelkin formula are considered. The differential cross section is calculated for scattering of neutrons involving small momentum transfer when the quasiclassical approximation is not valid. (auth)

**3136** AN ANALYSIS OF THE $^{119}$Sn NUCLEAR CHARGE RADIUS BASED ON THE MOESSBAUER SPECTRA. Bersuker, I. B.; Goldanskii, V. I.; Makarov, E. F. (Inst. of Chemical Physics, Academy of Sciences, USSR; Inst. of Chemistry, Academy of Sciences, USSR). Zh. Eksp. Teor. Fiz., 49: 699-706(Aug. 1965). (In Russian).

It has previously been assumed that the charge radius of the $^{119}$Sn nucleus in the 23.8-kev excited state is larger than that for the nucleus in the ground state ($\Delta R/R > 0$). This conclusion was drawn on basis of data pertaining to the chemical shifts in Mössbauer spectra of tin compounds and involves a very rough representation of the structure of the electron shell of these compounds and its interaction with the nucleus. The present analysis yields a general formula for the dependence of the chemical shift on the parameters of the molecular orbits and inner shell orbits. An appraisal of the orbits indicates that for tin tetrahalogenides $\Delta R/R < 0$. The results may be important for interpretation of many experimental data on Mössbauer spectra of tin compounds. (auth)

**3137** AN ATTEMPT TO DETECT DOUBLE $\beta$-DECAY IN $^{48}$Ca. Lazarenko, V. R.; Lukyanov, S. Yu. Zh. Eksp. Teor. Fiz., 49: 751-4(Sept. 1965). (In Russian).

The lower limit for the lifetime of $^{48}$Ca nuclei with respect to double $\beta$ decay is evaluated by employing the scintillation technique. A sample containing 3.8 g of pure $^{48}$Ca isotope was employed in the experiments. The lifetime is greater than $5 \cdot 10^{19}$ years for the non-neutrino decay scheme and greater than $3 \cdot 10^{18}$ years for the two-neutrino scheme. (auth)

**3138** ISOMER SHIFT AND THE STRUCTURE OF METASTABLE NUCLEAR STATES. Belyakov, V. A. Zh. Eksp. Teor. Fiz., 49: 832-40(Sept. 1965). (In Russian).

The difference between the mean square radii of the electric charge distributions of the excited and ground states of nuclei, $\Delta\langle R^2\rangle$, is calculated on basis of the theory of finite fermi systems. The volume isotopic shift constant is calculated for the same range of atomic weights. The nature of the excited states of nuclei is discussed. (auth)

**3139** LES MODELES EN SPECTROSCOPIE NUCLEAIRE. (Models in Nuclear Spectroscopy). Nataf, R. Paris, Dunod, 1965. 252p.

A textbook on models in nuclear spectroscopy is presented. It contains supplements from quantum mechanics. The empirical models are included without an attempt at "microscopic" justification in general. Shell models and collective models are considered. (J.S.R.)

**3140** INVESTIGATION OF THE $^6$Li(p,n)$^6$Be REACTION BY THE NEUTRON THRESHOLD TECHNIQUE [Thesis]. Honsaker, John Leonard. Pasadena, Calif., California Inst. of Tech., 1965. 103p.

The measurement of the reaction $Li^6(p,n)Be^6$ by slow-neutron methods is described with particular attention to the $Be^6$ ground-state threshold. The detector response was calculated by a Monte Carlo technique and verified with a measurement of the $Li^7(\alpha,n)B^{10}$ threshold. An analysis of the shape of the $Be^6$ threshold indicated that both s- and p-wave neutrons contribute significantly to the reaction. The results depend on what mode of decay is assumed for the ground state of $Be^6$. If a two-stage process is assumed, with either an alpha particle and an unbound diproton or $Li^5$ and a proton as intermediate state, the width is found to be 95 ± 28 kev and the Q-value obtained for the $Li^6(p,n)Be^6$ reaction is −5074 ± 13 kev. It was not possible to determine which process is predominant. No further states in $Be^6$ with excitation energy less than 4 Mev and width less than 1.5 Mev could be detected. Evidence suggesting other neutron-producing reactions from the proton bombardment of $Li^6$ at higher energies is discussed. (Dissertation Abstr.)

**3141** A STUDY OF COINCIDENCES BETWEEN INELASTICALLY SCATTERED 42-Mev ALPHA PARTICLES AND DE-EXCITATION GAMMA RAYS [Thesis]. Hendrie, David Lowery. Seattle, Univ. of Washington, 1964. 217p.

The angular correlation between an inelastically scattered alpha particle and a de-excitation gamma ray was measured for the 4.43-Mev $2^+$ level of $C^{12}$ and the 1.37-Mev $2^+$ level of $^{24}$Mg. For these $2^+ \rightarrow 0^+$ gamma transitions the correlation pattern in the scattering plane has the simple form $W(\theta) = A + B \sin^2 2(\theta - \theta_0)$, where $\theta$ is the gamma detection angle and $\theta_0$ defines a symmetry axis for the correlation. A, B, and $\theta_0$ are parameters determined by the nuclear reaction mechanism that causes the scattering. $\theta_0$ and the ratio A/B were measured for a number of forward scattering angles;

absolute values for A and B are provided by measurements of the inelastic differential cross sections. The adiabatic approximation predicts that A = 0 and that the symmetry axis lies in the direction of nuclear recoil from elastic scattering. Our data show that the symmetry axes deviate markedly from this prediction, especially near minima of the inelastic angular distributions. Upon comparing the data to other models, the results of these measurements seem particularly sensitive to the non-adiabatic contribution to the scattering amplitudes. It is also seen that such experiments may resolve the ambiguities in the optical potential that arise when scattering is treated in the distorted wave Born approximation. The above results are then applied in the resolution of a long-standing puzzle of nuclear spectroscopy. Experiments had succeeded in identifying all the low-lying levels expected from shell model calculations on $^{90}Zr$ with the exception of a heretofore missing $4^-$ level. Taken together with results of recent neutron scattering work, these results demonstrate that this level does in fact exist and that it forms an as-yet-unresolved doublet with a known $3^-$ collective level at about 2.75 Mev. (Dissertation Abstr.)

**3142** MEASUREMENT OF RESONANCE WIDTHS IN $^{27}Al(p,\gamma)^{28}Si$ REACTION [Thesis]. Ferry, James Allen. (Madison, Wis., Univ. of Wisconsin, 1965). 114p.

Measurements were made of the full widths at half maximum and the energies relative to a fixed point of several narrow resonances in the $^{27}Al(p,\gamma)^{28}Si$ reaction. This study was made possible by the correction of systematic imperfections in the gap of a 90° one-meter cylindrical electrostatic analyzer. The resolution achieved was determined for two different settings of the analyzer slits from an analysis of thick and thin target yield curves taken over the resonance of known width near 774 kev. The widths of the resonances near 992 and 1317 kev were found to be about 100 ev by an analysis of thick and thin target yield curves. By analyzing thin target yield curves, the energies of the resonances were found to be 773.7 ± 0.1 and 1316.8 ± 0.2 kev relative to the one at 991.82 ± 0.1 kev. Analysis of all yield curves was performed utilizing techniques that accounted for the discontinuous nature of the proton energy loss. Values found for the resonance widths agreed well with those found in previous measurements. Such agreement was unexpected and apparently occurred because in previous measurements the error made in the assumption of unattained high resolution compensated for the neglect of the Lewis effect. (Dissertation Abstr.)

**3143** A STUDY OF RATES OF RELAXATION AND DYNAMIC POLARIZATION OF NUCLEAR SPINS AT LOW TEMPERATURES [Thesis]. Karra, James Sundararao. New Brunswick, N. J., Rutgers Univ., 1964. 74p.

The observation of long proton polarization times close to the central electron resonance frequency, possibly due to the effective decrease in the electron correlation time resulting from the forced flipping of electron spins under the influence of an intense microwave field, was investigated in samples of polystyrene with 10% and 1% concentration of DPPH at 1.7°K using a triple-resonance technique. No change in the electron correlation time due to the forced flipping of electrons was observed. A further investigation using double resonance on the nature of the polarization and relaxation processes revealed that they are not simple exponentials. The quadratic dependence of magnetization on time is thought to be due to the spin diffusion barrier resulting from the large field gradient created by the electron moment of the paramagnetic impurity. A semiquantitative theory was developed to account for the general features of magnetization. The equation of continuity for the magnetization was solved for the transient region in an approximate way. A small shift of the zero enhancement point of the proton polarization towards the lower magnetic field was observed in the sample of polystyrene with 10% DPPH but not in the one with 1% DPPH. This shift is due to the superposition of Overhauser and solid-state-effect polarization. In a crystal of $(Ce,La)_2Mg_3(NO_3)_{12} \cdot 24H_2O$ with 5% cerium, at 4.2°K, Overhauser type polarization and at 1.7°K, a polarization due to the solid state effect were observed. (TCO)

**3144** PULSED NUCLEAR QUADRUPOLE RESONANCE SPECTROSCOPY [Thesis]. Gabriel, Cedric John. Berkeley, Calif., Univ. of California, 1964. 171p.

The three-pulse spin-echo double resonance technique with the $^{35}Cl$ nuclei as the indicator was used to measure the quadrupole resonance frequencies of deuterium for a single crystal of $Ba(ClO_3)_2 \cdot D_2O$. The quadrupole coupling constant $e^2qQ/\hbar$ and asymmetry parameter $\eta$ of the electric field gradient tensor were obtained for each of the two sites at 77°K and for the single site at 25°C. The results at 25°C were interpreted in terms of the results at 77°K by assuming a twofold hindered rotation of the $D_2O$ molecule about the bisector of the D-O-D angle. A method utilizing the relation between the roots and coefficients of the secular equation is outlined, whereby $e^2qQ/\hbar$ and $\eta$ are calculated from the measured frequencies and $H_0$. Double resonance measurements of the low frequency transition between Zeeman split energy levels (audio transition) of $^{135}Ba$ and $^{137}Ba$ were used to obtain the estimate $0.5 \leqq \eta \leqq 0.7$ (T = 77°K) at the Ba sites. An experimental and theoretical study based on a simple stochastic model of spin-echo formation and c-w double resonance in solids was carried out on the $^{35}Cl$ spin echo for a single crystal of $NaClO_3$ using the $^{23}Na$ audio transition as the means of investigation. A crossing effect utilizing the dependence of the resonance frequencies upon $H_0$ in a quadrupole system was introduced as a means of measuring quadrupole resonance parameters. (TCO)

**3145** THE MOESSBAUER EFFECT OF $^{57}Fe$ IN BERYLLIUM AND COPPER [Thesis]. Housley, Robert Melvin. Seattle, Univ. of Washington, 1964. 109p.

The design and construction of a Mössbauer spectrometer are described. A method for obtaining precise f values for $^{57}Fe$ in various hosts is discussed in detail. The f values as a function of temperature are presented for $^{57}Fe$ in Cu and Be. The interpretation of these f values in terms of lattice dynamics is discussed. The Mössbauer spectrometer uses a sinusoidally driven dual loudspeaker drive. The spectrum and a normalization spectrum are taken simultaneously on the multichannel analyzer. Pulses are formed from the velocity analog voltage at the input to the analyzer by using the coincidence mode of operation. Natural linewidth (.20 mm/sec) was obtained with this spectrometer using a $^{57}Co$ in Cu source and a thin natural Fe absorber. The technique of making f measurements is discussed in detail and the black absorber method is introduced. Its advantages and limitations are discussed. Techniques for making the necessary background corrections are also discussed. (Dissertation Abstr.)

**3146** MOESSBAUER EFFECT DATA INDEX. Issue 3. Muir, A. H. Jr.; Ando, K. J.; Coogan, H. M. Thousand Oaks, Calif., North American Aviation Science Center, 1965. 258p. (SCTR-65-2).

The Moessbauer data and references for each isotope are given and also the parent decay schemes and a simplified nuclear level scheme for the isotope, a tabulation of measured nuclear properties and a tabulation of the Moessbauer properties which were derived from these properties. Other data include the gamma ray transition energy, the host material in which the source atoms are embedded, the source temperature, the host material in which the absorber atoms are embedded, the absorber temperature, the line width and shift, dip of the absorption spectrum, quadrupole splitting, and the shape of the absorption spectrum, and additional remarks on experimental results. (J.F.P.)

**3147** NUCLEAR STRUCTURE AND ELECTROMAGNETIC INTERACTIONS. MacDonald, N. (ed.). New York, Plenum Press, 1965. 524p. $22.50.

Ten lectures are included; separate abstracts have been prepared for each. (L.B.S.)

*For abstracts of individual papers see: 2118, 2177, 2218, and 3148–3154.*

**3148** NUCLEAR MODELS AND ELECTROMAGNETIC PROPERTIES OF NUCLEI. de-Shalit, A. (Weizmann Inst. of Science, Rehovoth, Israel). pp 1-18 of Nuclear Structure and Electromagnetic Interactions. New York, Plenum Press, 1965.

The role of nuclear models is considered for constructing wave functions and operators in a semi-phenomenological approach to the description of nuclei. The problem of testing wave functions is discussed. The collective model and the core-excitation model are considered as examples for specific features which are sensitive to tests involving the electromagnetic properties of nuclei. (L.B.S.)

**3149** GENERAL PROPERTIES OF NUCLEAR MODELS. Bayman, B. F. (Univ. of Minnesota, Minneapolis). pp 19-60 of Nuclear Structure and Electromagnetic Interactions. New York, Plenum Press, 1965.

Some of the models that have been developed in an attempt to understand nuclear spectra are described within the framework of the independent-particle model. Hartree–Fock theory and approaches to shell model calculations are briefly discussed. Sample calculations of the pure configuration model applied to the $1f_{\frac{7}{2}}$ shell are described, and limitations of the pure configuration approach are discussed. Certain aspects of the independent-particle model are discussed, which include particle-hole states in $^{16}O$, excited-core model of odd-A nuclei, deformed self-consistent potential and rotating solution of the Hartree–Fock equations. The quasi-particle method, and the boson model for nuclear vibrational states are also discussed. (L.B.S.)

**3150** RADIATIVE TRANSITIONS FOLLOWING NUCLEAR REACTIONS. Litherland, A. E. (Atomic Energy of Canada Ltd., Chalk River, Ont.). pp 61-140 of Nuclear Structure and Electromagnetic Interactions. New York, Plenum Press, 1965.

The study of radiative transitions following nuclear reactions is described with particular emphasis on the determination of some of the important properties of isolated nuclear energy levels such as angular momenta, parities and lifetimes. Methods are described for measuring the lifetimes for electromagnetic decay of an unbound nuclear energy level; angular momenta, parities, and gamma-ray multipole admixtures; angular correlations of two gammas in coincidence; and for producing strongly aligned nuclei by a nuclear reaction. The Doppler shift attenuation method, and some recent studies of $^{20}Ne$ and the nuclear s-d shell are also described. (L.B.S.)

**3151** PHOTONUCLEAR REACTIONS. Hayward, Evans (National Bureau of Standards, Washington, D. C.). pp 141-209 of Nuclear Structure and Electromagnetic Interactions. New York, Plenum Press, 1965.

A brief discussion is given of the basic concepts for the treatment of photonuclear reactions, which includes the photonuclear cross section, the interaction hamiltonian, effective charges, and the electric dipole sum rule. Discussions are presented on scattering and absorption of photons by nuclei; photonuclear experiments; heavy nuclei and the hydrodynamic model; light nuclei and the independent-particle model; and the decay of the dipole state. (L.B.S.)

**3152** ELECTRON SCATTERING. Bishop, G. R. (Univ. of Glasgow). pp 211-286 of Nuclear Structure and Electromagnetic Interactions. New York, Plenum Press, 1965.

A detailed treatment is presented on electron scattering, with discussions on virtual photons, calculations in the Born approximation, radiative corrections, phase shift analysis, nuclear models, and continuum scattering. (L.B.S.)

**3153** COULOMB EXCITATION. Newton, J. O. (Univ. of Manchester, Eng.). pp 287-317 of Nuclear Structure and Electromagnetic Interactions. New York, Plenum Press, 1965.

A qualitative treatment of the theory of Coulomb excitation by heavy particles is presented. Semiclassical first-order theory, angular distribution of de-excitation gamma rays, and first-order results are discussed. Higher order processes are also considered. Experimental methods and typical results are outlined to illustrate the advantages and disadvantages of each method. (L.B.S.)

**3154** STRUCTURE OF THE TRANSITION STATE NUCLEUS IN NUCLEAR FISSION. Huizenga, J. R. (Argonne National Lab., Ill.). pp 319-74 of Nuclear Structure and Electromagnetic Interactions. New York, Plenum Press, 1965.

Methods for obtaining information about the low-lying levels of the transition state nucleus from fission-fragment angular distributions are treated. The following cases are considered for fission near the threshold: (n,f) on even targets; (d,pf) on even-even targets; $(\alpha,\alpha'f)$ on $^{238}U$; and (d,pf) fission on even-Z odd-N targets. Neutron and charged-particle induced fission at excitation energies well above the fission threshold are also treated in considerable detail. (L.B.S.)

**3155** DETERMINATION OF THE CONVERSION COEFFICIENT IN $^{170}Yb$ WITH SCINTILLATION METHODS. Jansen, J. F. W.; Wapstra, A. H. (Instituut voor Kernphysisch Onderzoek, Amsterdam). 17p. (CONF-650563-2). Gmelin, AED-CONF-65-117-4.

From International Conference on the Internal Conversion Process, Nashville.

The gamma-ray spectrum of $^{170}Tm$ was studied for the determination of the K-conversion coefficient of the 84 kev transition. A thin source and a collimated beam were used to minimize possible errors and uncertainties. The spectrum was measured with flat and well-type crystals, using different absorbers, both single and in coincidence with feeding beta-rays. $^{109}Cd$ and $^{32}P$ sources were used for the analysis of the spectrum. A 3% correction in the K X-ray intensity due to the presence of a weak electron capture decay to $^{170}Er$, was applied. The resulting value for $\alpha_K$ is $1.31 \pm 0.05$ in good agreement with theory. Values as obtained with the flat crystal and with larger collimators were consistently higher (average 1.47) indicating that back-scattering of photons could be a source of error in flat scintillation crystals. For the ratio $X_K/\gamma$ of $^{109}Cd$ we found a value $22.2 \pm 0.6$ using the same experimental arrangement. (auth)

**3156** $^{17}O$ AND $^{19}O$ LIFETIMES BY A PARTICLE-GAMMA COINCIDENCE TECHNIQUE. McDonald, R. E.; Fossan, D. B.; Chase, L. F. Jr.; Becker, J. A. (Lockheed Palo Alto Research Labs., Calif.). 17p. (CONF-650410-42). Gmelin, AED-CONF-65-073-72.

From American Physical Society, Washington, D. C.

Lifetimes of the 96-kev and 1.47-Mev levels in $^{19}O$ produced by the $^{18}O(d,p)^{19}O$ reaction were measured from the distribution of time delays between protons and the appropriate decaying gamma rays. A solid-state detector was used both as a timing and energy measuring device for the protons. The time-delay distributions were obtained with a time-to-height converter in the normal fast-slow coincidence arrangement. The measured half-lives of the 96-kev and 1.47-Mev levels in $^{19}O$ are $(1.39 \pm 0.05)$ nsec and $\leq 75$ psec, respectively. These results are compared with intermediate-coupling shell-model calculations. Using this particle-gamma coincidence technique a remeasurement of the lifetime for the 871-kev level in $O^{17}$ produced by the $^{16}O(d,p)^{17}O$ reaction resulted in a half-life of $(182 \pm 5)$ psec. (auth)

# Plasma Physics and Thermonuclear Processes

**See also Fluid Physics and Thermodynamics**

*Refer also to abstract 2858.*

**3157** (AD-614654) INTERACTION BETWEEN MICROWAVES AND PLASMAS IN GAS DISCHARGES AND SEMICONDUCTORS. Final Scientific Report. Agdur, B. (Kungliga Tekniska Hogskolan, Stockholm (Sweden)). Mar. 31, 1965. Contract AF61(052)-796. 154p. (RADC-TR-65-173). CFSTI $5.00 cy, $1.00 mn.

Information is included on: waves in hot anisotropic electron-plasmas; wave propagation in a parallel-plate waveguide partially filled with a hot and inhomogeneous plasma; the influence of collisions on whistler propagation; experiments on plasma microwave interaction; ion waves on bounded plasmas; and determination of electron drift

velocity in a gaseous discharge from Doppler shifts of plasma waves. An experimental investigation of coupling to slow waves in a plasma waveguide and an experiment on helicon waves in InSb are described. (TAB)

**3158** (AD-614923) STUDY OF COLLISION PROCESSES IN GASEOUS PLASMAS. Semiannual Technical Report No. 3, July 1964–January 1965. Oskam, H. J. (ed.) (Minnesota Univ., Minneapolis. Plasma Physics Lab.). Mar. 1965. Contract Nonr71037. 18p. CFSTI $1.00 cy, $0.50 mn.

A detailed description is given of the SLEMA II (Simultaneous Light Emission, Absorption and Mass Analysis) measuring system. The system is designed to measure simultaneously on the same gaseous plasma the time dependence of the number density of electrons, positive and negative ions, and metastable atoms and molecules, while also the intensity of spectral lines and bands can be determined. Summaries are given of results obtained with the SLEMA I system and of a redesign of the auxiliary electronics for an ion mobility measuring tube. (TAB)

**3159** (AD-618138) MHD OF A QUASINEUTRAL PLASMA WITH VANISHING INTERNAL FRICTION AND HEAT CONDUCTIVITY AND FINITE ELECTRICAL CONDUCTIVITY. Friedel, H. (Innsbruck Univ. (Austria)). Mar. 10, 1965. Contract AF61(052)-675. 23p. (AFOSR-65-1314). CFSTI $1.00 cy, $0.50 mn.

The MHD basic equations for a quasineutral plasma are considered in the 1-dimensional unsteady and 2-dimensional steady cases. If the displacement current is neglected, the 1-dimensional unsteady system is parabolic, and the 2-dimensional steady system is elliptic. The influence of electrical conductivity on MHD solutions was investigated, and 3 methods for solving the general MHD equations are given. (auth)

**3160** (AD-618503) AC BREAKDOWN IN GASES. Muehe, C. E. (Lincoln Lab., Massachusetts Inst. of Tech., Lexington). Feb. 26, 1965. Contract AF19(628)-500. 30p. (TR-380). CFSTI $1.00 cy, $0.50 mn.

The breakdown potential of helium, neon, argon and xenon was measured over the frequency range from dc to 1000 Mcps, and the pressure range from $10^{-8}$ to 600 mmHg employing a glass breakdown cell with 1-cm spacing. Graphs showing contours of constant breakdown potential as a function pf pd and d/gamma are presented. The graphs show three distinct breakdown regions: the diffusion-controlled region; the secondary-electron-emission (multipactor) region; and the low-frequency region. The breakdown mechanism in each of these regions is explained. An extensive bibliography on ac breakdown in gases is included. (auth)

**3161** (AD-618520) RADIATION FROM AN ELECTRIC DIPOLE IN AN INFINITE COLUMN OF WARM PLASMA. Seshadri, S. R. (Sylvania Electronic Systems, Waltham, Mass. Applied Research Lab.). June 1, 1965. Contract AF19(628)-2410. 33p. (AFCRL-65-409). CFSTI $2.00 cy, $0.50 mn.

The radiation characteristics of an axially oriented electric dipole situated at the center of an infinitely long, cylindrical column of warm plasma were investigated. Two types of surface waves were excited along the plasma column and their dispersion and power relations were examined. The radiation pattern in the far-zone and the radiation resistance arising from the space waves were evaluated and their dependence on the source frequency and the radius of the plasma column is discussed. (auth)

**3162** (AD-618683) AN INVESTIGATION OF WAVES OF IONIZATION IN A PULSED DISCHARGE [Thesis]. Johnson, Harold E. (Air Force Inst. of Tech., Wright-Patterson AFB, Ohio. School of Engineering). June 1965. 68p. (GGC/EE/65-7). CFSTI $3.00 cy, $0.75 mn.

Experiments were made in plasma physics to glean information about the time history of the initiation of a glow discharge in a low pressure gas. General characteristics of a specific glow lamp containing an admixture of mercury vapor and argon were determined. Subsequent experiments were performed spectrally by use of spectroscope, photomultiplier, and image converter methods, to evaluate the conditions of the plasma from initial breakdown through the initiation of the first striations. A novel and generally useful method of time resolved, spectrally resolved, absorption measurements is demonstrated with application to the investigation. (auth)

**3163** (CNAEM-26) PRE-KINETIC EQUATIONS FOR A PLASMA. Oezizmir, Ercuement; Imre, Kaya (Cekmece Nuclear Research Center, Atomic Energy Commission, Istanbul (Turkey)). Aug. 1965. 34p. Dep. mn.

Bogoliubov theory for a multicomponent plasma is generalized through relaxation of his assumptions regarding the functional dependence and the "initial condition" to obtain a theory within which the approach to the kinetic regime can be studied. It is assumed that the correlations $G_l (l > s)$ are functionals of $G_1, \ldots, G_s$ and $e^{\tau H} G_l (e^{-\tau H} G_1, \ldots, e^{-\tau H} G_s) \to 0$ as $\tau \to \infty$ where H is the Poisson bracket operator corresponding to the kinetic energy and $s(\geq 1)$ is a fixed but otherwise arbitrary integer. It is shown that the analytic solution of the resulting functional chain with respect to the parameters $\alpha = n\lambda^{1/s}$, $\beta = \lambda^{1/s}$ (where n is the density, and $\lambda$ is the interaction strength) is of order $\beta^{1-s}$ provided $G_1, \ldots, G_s$ are of order $\beta^0$. This property enables one to break the hierarchy in the expansion with respect to $\beta$, only. The case s = 2 which leads to the "pre-kinetic" equations is considered in some detail. The closed coupled set of equations for $G_1$ and $G_2$ obtained in this case differ from those studied in the literature through appearance of the double pair correlations in the equation for $G_2$ which makes the latter equation nonlinear. (auth)

**3164** (IPPJ-39) ON THE KINETIC STRUCTURE OF A PLASMA. Dawson, John M.; Nakayama, Toshio (Institute of Plasma Physics, Univ. of Nagoya (Japan)). July 1965. 42p. Dep. mn.

The kinetics of a plasma is investigated by expanding the motion in terms of the deflection of the particles from their noninteracting orbits. It is shown that this procedure leads to the following results. At the first stage, the dressed particle picture of Thompson and Hubbard, and of Rostoker for obtaining fluctuations in a plasma is obtained. Rostoker's principle for obtaining two particle correlations in terms of test particle results is also obtained at this stage. At the second stage, encounters between shielded particles appear, and the picture of Birmingham, Dawson and Oberman for computing bremsstrahlung emerges. The usual Fokker-Planck equation may also be obtained at this stage. The treatment applies to the full electromagnetic field. (auth)

**3165** (JINR-P-2352) O POVERKHNOSTNOI VOLNE V PLAZME S TOKOM OGRANICHENNOGO RADIUSA. (On Surface Wave in Plasma With Current of Limited Radius). Makhan'kov, V. G. (Joint Inst. for Nuclear Research, Dubna (USSR). Lab. of High Energy). 1965. 10p. Dep. mn.

For the plasma cord with a current the boundary conditions were obtained which take into account the surface currents. For one particular case the dispersion equation of the surface wave was obtained. The temperature effects are neglected. (auth)

**3166** (LA-DC-7252) THE LOS ALAMOS FLUX COMPRESSION PROGRAM FROM ITS ORIGIN. Fowler, C. M.; Caird, R. S.; Garn, W. B.; Thomson, D. B. (Los Alamos Scientific Lab., Univ. of California, N. Mex.). [1965]. Contract W-7405-eng-36. 37p. (CONF-650937-4). Dep. mn; CFSTI $2.00 cy, $0.50 mn.

From Conference on Megagauss Magnetic Field Generation by Explosives and Related Experiments, Frascati, Italy.

The development of the Los Alamos magnetic flux compression program is reviewed. Discussions are given concerning the explosive technique as applied to jet experiments and motion of materials. The current and possible future flux compression programs are discussed. (M.O.W.)

**3167** (MATT-374) THE STABILITY OF NEGATIVE V′ SYSTEMS. Kulsrud, Russell M. (Princeton Univ., N. J. Plasma Physics Lab.). July 1965. Contract AT (30-1)-1238. 17p. (CONF-650935-44). Dep. mn; CFSTI $1.00 cy, $0.50 mn.

From 2nd IAEA Conference on Plasma Physics and Controlled Nuclear Fusion Research, Culham, Eng.

The plasma containment systems proposed by Johnson and Leonard were analyzed for stability against the interchange instability. The normal mode equations are derived for the interchange in this system including resistivity. These equations are analyzed in the limit of large m. These results are applied to three cases: (1) zero resistivity for which a critical $\beta$, $\beta_c$ is given, (2) finite resistivity with $\beta < \beta_c$ and flow along the lines is neglected, and (3) finite resistivity with $\beta < \beta_c$ and flow along the lines is taken as infinitely fast. In each case an ordinary eigenvalue differential equation is derived; for case (1) the eigenvalue is $\beta_c$, for case (2) it is $\sigma_R$, while for case (3) no eigenvalue exists. These eigenvalues are estimated approximately by a Raleigh–Ritz technique, and the different results are compared. (M.O.W.)

**3168** (ML–1185) NUMERICAL SOLUTION OF THE COLLISIONLESS PLASMA-SHEATH EQUATION IN CYLINDRICAL GEOMETRY. Self, S. A. (Stanford Univ., Calif. Microwave Lab.). June 1964. Contract NAS 3-4100. 40p.

The collisionless plasma sheath equation was solved numerically for the case of cylindrical geometry. Results are presented which give the potential and several other quantities of interest as a function of radius for a cylindrical discharge column operating in the low pressure regime. (M.O.W.)

**3169** (NASA-CR-319) A MICROWAVE LENS SYSTEM FOR PLASMA DIAGNOSTICS. Bitzer, R. A.; Holt, E. H. (Rensselaer Polytechnic Inst., Troy, N. Y.). Oct. 1965. 13p. CFSTI $1.00 cy, $0.50 mn.

The use of lenses to provide plane waves at microwave frequencies for plasma probing is discussed. Based on the requirements dictated by an experimental objective of measuring the Faraday rotation of the polarization of an electromagnetic wave in a magnetoplasma, two types of lenses were designed. These were the dielectric lens and the Fresnel half-period zone plate. Tests were conducted on lenses built to these designs and the results obtained were close to the design figures. The superiority of the Fresnel plate over the dielectric lens for plasma diagnostics is demonstrated. The lenses were built for use at K-band frequencies (20 Gc) but improved diagnostics of a plasma can be expected if lenses built to these designs are used at higher frequencies. (auth)

**3170** (NASA-TN-D-3052) TWO-STREAM INSTABILITY IN GRAVITATING PLASMAS WITH MAGNETIC FIELD AND ROTATION. Talwar, S. P. (National Aeronautics and Space Administration, Greenbelt, Md. Goddard Space Flight Center). Oct. 1965. 17p. CFSTI $1.00 cy, $0.50 mn.

The problem of instability in contrastreaming streams of plasma or self-gravitating gas clouds is investigated for general propagation direction, using moment equations. A uniform rotation is also included in view of its astrophysical importance. Conditions for instability (monotonic or growing wave) are derived. It is found that the classical Jeans wavelength for fragmentation of interstellar medium is considerably diminished due to interstreaming speeds. For a non-gravitating plasma it is concluded that perturbations propagating normal to the interstreaming direction lead to a monotonic instability. Though characterized by a small growth rate, it should be possible to observe this instability in laboratory plasmas if dimensions are suitably chosen to eliminate the conventional electrostatic two-stream instability. (auth)

**3171** (NP–15562) ANNUAL REVIEW, APRIL 1964–MARCH 1965. (Institute of Plasma Physics, Univ. of Nagoya (Japan)). 92p. Dep. mn.

Experimental and theoretical plasma research carried out at the Institute of Plasma Physics is reported in five sections. Individual abstracts were prepared for each section. (M.O.W.)

*For abstracts of individual sections see: 3172–3176.*

**3172** (NP–15562, pp 4-19) EXPERIMENTAL DIVISION I (QP PROJECT). (Institute of Plasma Physics, Univ. of Nagoya (Japan)).

Experimental work carried out concerning the QP Project is presented. Discussions are presented on the control systems for the QP machine, field configurations and the stabilization of plasma in the PIG discharge tube, properties of the QP plasma, ion cyclotron resonance in low density plasma, ion cyclotron resonance heating by an induction coil, and on adiabatic compression of the QP plasma. (M.O.W.)

**3173** (NP–15562, pp 20-9) EXPERIMENTAL DIVISION II. MACETIE PROJECT (B.S.G. PROJECT). (Institute of Plasma Physics, Univ. of Nagoya (Japan)).

A brief review of the Multistage Adiabatic Compression and Equi-Temperature Irreversible Expansion (MACETIE) Program is given. Descriptions of the MACETIE I and II devices are given. A brief discussion of experiments performed with these devices is presented. (M.O.W.)

**3174** (NP–15562, pp 30-7) EXPERIMENTAL DIVISION III (HELIOTRON PROJECT). (Institute of Plasma Physics, Univ. of Nagoya (Japan)).

The design and construction of the Heliotron C magnetic mirror machine carried out from May 1964 to April 1965 is discussed. Discussions concern the magnetic field coils, Joule heating, vacuum system, operation, and plasma diagnostics. (M.O.W.)

**3175** (NP–15562, pp 38-79) EXPERIMENTAL DIVISION IV (FUNDAMENTAL EXPERIMENTS). (Institute of Plasma Physics, Univ. of Nagoya (Japan)).

An extensive discussion on the generation of a stable plasma suitable for long laboratory experiments is presented. Three methods for producing stable plasma are described. Various experimental results are presented for plasma research on oscillations in a plasma and its relevant phenomena, radiation from the magnetoplasma, plasma beam in a magnetic field, and beam-plasma interaction in a magnetic field. (M.O.W.)

**3176** (NP–15562, pp 80-4) THEORETICAL DIVISION. (Institute of Plasma Physics, Univ. of Nagoya (Japan)).

Brief theoretical discussions are given on several topics including propagation of hydromagnetic waves in collisionless plasmas, higher order correction to the Alfvén wave instability, plasma kinetics, unified theory of relaxations in plasma applied to electric conductivity in ideal turbulence, resonance phenomena and enhancement of cyclotron harmonics in magnetoplasma, radiation by longitudinal waves due to density discontinuity in magnetized plasma, negative absorption phenomena in partially ionized gases, and radiations from an oscillator in a rectangular waveguide. (M.O.W.)

**3177** (NP–15570) EXPERIMENTAL STUDIES OF J x B IONIZING FRONTS PROPAGATION OVER THE PRESSURE RANGE 10 TO 800 MILLITORR. Millar, D. D.; Watson-Munro, C. N. (Sydney Univ. (Australia). School of Physics). Aug. 1965. 18p. (ER–16). Dep. mn.

Experimental results of the properties of J × B ionizing fronts over the pressure range 10 to 800 millitorr of hydrogen are presented. It is concluded that the fractional ionization (which in our case ranged from close to unity down to 0.15 at the higher pressures) plays an important role in determining the azimuthal and front velocities. The results of experiments designed to collide two fronts rotating in opposite directions are also reported. (auth)

**3178** (ORNL-P–1513) DCX-2 SCANNING ENERGY SPECTROMETER. Culver, J. S. (Oak Ridge National Lab., Tenn.). [nd]. Contract W-7405-eng-26. 16p. (CONF-650512-8). Dep. mn; CFSTI $1.00 cy, $0.50 mn.

From Symposium on Engineering Problems of Controlled Thermonuclear Research, Livermore, Calif.

A collimated energy spectrometer is described that has a scanning ability. The spectrometer is designed to measure the angular distributions, radial positions, and spectra of particles in DCX-2. (T.F.H.)

**3179** (ORNL-P-1575) SIMPLE MOMENTUM PROBE FOR PLASMA STUDIES. Alexeff, Igor; Jones, W. D.; Montgomery, D.; Rankin, M. (Oak Ridge National Lab., Tenn.). [1965]. Contract W-7405-eng-26. 13p. (CONF-650806-15). Dep. mn; CFSTI $1.00 cy, $0.50 mn.

From 7th International Conference on Phenomena in Ionized Gases, Belgrade.

The momentum probe is simply a bare, current-carrying wire placed in the plasma. The magnetic field surrounding the wire tends to deflect charged particles away from the wire. The current of charged particles reaching the wire as a function of magnetic field gives information about the momentum distribution of the charged particles. Comparison of experimental measurements with detailed theoretical calculations demonstrates that the momentum probe behaves in the manner expected. An interesting modification is to electrically bias the probe so as to combine both the useful features of magnetic and electrostatic analysis. (auth)

**3180** (SEL-63-116) REFLEX IONIZATION IN A TORUS. Technical Report No. 0253-3. Pigache, D. R. (Stanford Univ., Calif. Stanford Electronics Labs.). Nov. 1963. Contract AT(04-3)-326. 19p. Dep. mn; CFSTI $1.00 cy, $0.50 mn.

The electron density obtained in the equilibrium of a toroidal reflex discharge was observed to be of the order of $10^{13}$ $cm^{-3}$. The density was measured with an 8-mm microwave interferometer placed in a straight section of the immediate vicinity of the anode–cathode structure. The research was carried out in a systematic fashion as a function of magnetic field and pressure for different positions of the interferometer with respect to the anode–cathode structure. (M.O.W.)

**3181** (SU-IPR-20) ABSOLUTE INSTABILITIES OF OBLIQUELY-PROPAGATING CYCLOTRON HARMONIC PLASMA WAVES. Crawford, F. W.; Tataronis, J. A. (Stanford Univ., Calif. Inst. for Plasma Research). July 1965. Contract AT(04-3)-326. 39p. Dep. mn; CFSTI $2.00 cy, $0.50 mn.

Studies were made of micro-instabilities associated with the dispersion relation for cyclotron harmonic waves in a warm magnetoplasma. A thorough study is made of the instabilities occurring for propagation oblique to the magnetic field, and series of computed dispersion curves are presented indicating the various regions of stability and wave growth. Even more violent instabilities are predicted for this case, over a very wide range of wave-numbers, and with a much lower instability threshold value of $(\omega_p^2/\omega_c^2)$ than for perpendicular propagation. The relevance of these instabilities to results from some fusion study plasmas and to noise generation in crossed-field electron devices is discussed. (auth)

**3182** (UCRL-12447) ELECTROSTATIC INSTABILITIES OF A PLASMA WITH MAGNETICALLY SUPPORTED VELOCITY-SPACE ANISOTROPY AT HIGH DENSITY. Hall, Laurence S.; Heckrotte, Warren (Lawrence Radiation Lab., Univ. of California, Livermore). Apr. 19, 1965. Contract W-7405-eng-48. 17p. (CONF-650806-1). Dep. mn; CFSTI $1.00 cy, $0.50 mn.

From 7th International Conference on Phenomena in Ionized Gases, Belgrade.

The electrostatic instabilities of a uniform anisotropic, magnetized plasma to modes of the form exp $\{i\underline{k}\cdot\underline{r} - i\omega t\}$ for which Re $(\omega)$ is zero or near a harmonic of the cyclotron frequency was the subject of a previous comprehensive study. In these cases the magnetic field plays an important resonant part in the interaction, and as well provides the support for the initial velocity-space anisotropy on which such instabilities feed. High densities are considered in which growth rates (characterized by the plasma frequency) are large compared to the cyclotron frequency, so that the magnetic field is important only in the latter capacity. Both ion–electron and ion–ion (electron–electron) interactions are treated. The first case, where both ions and electrons play a critical role, is essentially that treated by Rosenbluth and Post. Such modes, however, require that $k_\parallel^2 T_{\parallel e} < (m_e/m_i)k_1^2 T_{1i}$, and will often be suppressed by the finite length of an experimental assembly. Conversely, when particles of comparable mass interact, the instability may be longitudinally localizable. For example, if a cold plasma (plasma frequency $\omega_{pc}$) is present together with a hot plasma (frequency $\omega_{ph}$) whose transverse velocity distribution is proportional to $\delta(|v_\perp| - v_{\perp h})$, we may properly consider those waves propagating normal to the magnetic field, for which the dispersion relation reads $0 = 1 - \omega_{pc}^2\omega^{-2} - \omega_{ph}^2\omega^{-2}[1 - k_\perp^2 v_{\perp h}^2\omega^{-2}]^{-\frac{1}{2}}$. Unstable modes in this and other limits are found, and growth rates are given. (auth)

**3183** (UCRL-14275) DIFFUSION AND LOSSES OF ELECTRONS IN THE ASTRON E-LAYER. Nicholson, Richard B.; Heckrotte, Warren (Lawrence Radiation Lab., Univ. of California, Livermore). July 21, 1965. Contract W-7405-eng-48. 45p. Dep. mn; CFSTI $2.00 cy, $0.50 mn.

A quantitative description of the time-rate of loss of relativistic electrons from the Astron E-layer was developed. Qualitatively, the loss is ascribed to the small-angle scattering of the relativistic electrons by the neutral gas atoms to orbits not contained by the Astron fields. The diffusion theory to describe this is developed from the Boltzmann equation assuming axially symmetric magnetic fields. The reduction to a diffusion equation is accomplished by the application of multiple time perturbation theory. The limiting orbits for confinement are not known and are specified parametrically by two models. One is a radial loss model which states that an electron is lost if its radius of gyration is displaced more than a critical amount from the magnetic field axis; the other, an axial loss model which states that an electron is lost if its axial momentum reaches a specified critical value. The effect of the self-field of the E-layer on the diffusion is included and is shown to be unimportant at the current E-layer densities. The self-field may, however, be important in specifying the critical orbits. The solution of the diffusion equation is obtained in a standard manner as a series of modes, each with a characteristic exponential decay. The fundamental has the slowest decay rate. The initially trapped distribution determines the modal composition of the E-layer. The initially trapped distribution is not known, so several assumed distributions were taken for numerical calculations. The numerical results indicate that the radial loss model is inconsistent with the preliminary experimental data. There is no reasonable initial radial distribution that can give a sufficiently rapid decay arising from radial diffusion. The numerical results for the axial loss model are consistent with the preliminary data, but because of the freedom to vary initial conditions, no conclusions can be drawn about the validity of the model. (auth)

**3184** (UCRL-14310) HOT ELECTRON PLASMA STABILITY IN MIRROR AND MINIMUM B CONTAINMENT SYSTEMS. Hartman, Charles W. (Lawrence Radiation Lab., Univ. of California, Livermore). July 27, 1965. Contract W-7405-eng-48. 22p. (CONF-650653-10). Dep. mn; CFSTI $1.00 cy, $0.50 mn.

From American Physical Society, Summer Meeting, New York.

Experimental observations are reported on the containment of electron-cyclotron-heated plasma in magnetic mirror configurations possessing "saddle" in B, and minimum-B fields that may also possess shear. In all configurations that have "saddle" fields, independent of shear, a dominant cross-field loss is observed that can be suppressed by a cold-plasma background. In minimum-B fields, cross-field loss is suppressed independent of the cold plasma. (auth)

**3185** (TT-1193) ESTIMATION OF HEATING OF A PLASMA BY LASERS. Hora, H. (Institut fuer Plasma-

physik, Universitaet Frankfurt (West Germany)). Translated by D. A. Sinclair (National Research Council of Canada) from report IPP/6/23, 1964. 22p. Dep. mn; JCL $2.60 fs, $0.86 mf.

Earlier estimations of whether plasmas can be heated with brief laser impulses to temperatures which are of interest with respect to thermonuclear conditions are continued from the point of view that the high light field intensities produce a non-resonant ionization. Depending on whether the duration of this process is comparable with, or much greater than, the period of vibration of the light, some rough estimates are made of the extent to which a more favorable heating can be achieved with the greater densities that are then very probably attainable. In making these estimates the optical constants are explicitly computed for the hydrogen plasma, and the earlier results of Engelhardt are improved by numerical methods. (auth)

**3186** RUNAWAY ELECTRON COLLECTIVE INTERACTIONS WITH PLASMA IN THE STELLARATOR S-1. Blinov, P. I.; Zakatov, L. P. At. Energ. (USSR), 19: 233-8(Sept. 1965). (In Russian).

Collective interactions of runaway electrons with the plasma during ohmic heating in the S-1 stellarator were studied. The radio emission associated with this interaction was investigated in the frequency range from tens of kilocycles to $1.5 \times 10^{10}$ cps. Results are described of measurements of radio-wave polarization and of the variations in spectrum and intensity of the radio emission, electric field intensity, and magnetic field intensity. (M.J.T.)

**3187** AN EXACT SOLUTION IN THE THEORY OF THE DECAY OF A PULSE DISTURBANCE IN A ONE-DIMENSIONAL DIFFUSION PLASMA. Ruzicka, T.; Pekarek, L. (Physikalisches Institut der Tschechoslowakischen Akademie der Wissenschaften, Prague). Beitr. Plasmaphysik, 5: 161-79(1965). (In German).

A system of partial differential equations that describes a simple physical model of a weakly ionized plasma was solved exactly. The plasma was treated in the one-dimensional approximation. The solution for small deviations from the equilibrium values was obtained using the two-sided Laplace transformations. The initial disturbance was given in the form of a Dirac function. It was shown that the plasma can not react to an aperiodic disturbance with vibrational alterations. Limiting expressions of the solution both for a small time interval immediately after introduction of the disturbance (in the region of the free diffusion of the ions) and also for times that were sufficiently far removed from the time of the introduction of the disturbance (in the regime of antipolar diffusion) were found. A criterion was determined when the decay of the disturbance occurs through antipolar diffusion. The results of the theory were illustrated using numerical examples in which the basic plasma parameters were characterized for the column of a direct current low pressure discharge. For the time interval in which none of the approximation solutions could be used the solution was determined numerically. (J.S.R.)

**3188** THE APPROXIMATION OF THE VELOCITY DISTRIBUTIONS OF ELECTRONS IN A MAXWELL DISTRIBUTION IN THE REGION OF INELASTIC COLLISIONS. Wojaczek, K. (Physikalisch-Technisches Institut der Deutschen Akademie der Wissenschaften, Berlin). Beitr. Plasmaphysik, 5: 181-98(1965). (In German).

Under the assumption that the ratio of the excitation energy $U_\alpha$ of atoms to the mean kinetic energy $U_e$ of the electrons is sufficiently large, the velocity distribution of the electrons in the energy range above $U_\alpha$ was calculated for various conditions for the case of a non-isothermal plasma in a constant electric field on the basis of the Boltzmann kinetic equation with consideration of the electron interaction and inelastic collisions. As an integral measurement for an approximation to the Maxwell velocity distribution in this energy range, the excitation rate $Z_\alpha$ was used, for which in various forms of the excitation cross section closed expressions were given as functions of the electron concentration. The case was also treated where the constant electric field and the elastic atomic collisions cause small deviations from the Maxwell distribution under the excitation energy. In conclusion it was investigated how far collisions of the second type with excited atoms can favor the introduction of a Maxwell distribution of the electrons in the region of inelastic collisions. (tr-auth)

**3189** A STATIONARY STATE OF A CYLINDRICAL PLASMOID IN AN EXTERNAL LONGITUDINAL MAGNETIC FIELD. Kilimann, K. (Universitaet Rostock, Ger.). Beitr. Plasmaphysik, 5: 221-7(1965). (In German).

The analytical proof for the existence of a critical magnetic field value in dependence on the internal parameters of the system (temperature, concentration along the axis, etc.) was given. An expression for the radial site distribution for the particles in the plasma was given for the case of a homogeneous external magnetic field in the vicinity of the critical value. In an inhomogeneity of the external field $H_z^0$ caused by the self magnetic field of the beam, the site distribution for large distances of the Z axis was determined. (tr-auth)

**3190** ELECTROSTATIC SCREENING IN A THETA-PINCH COIL. Barrault, M. R.; McCartan, J. (Univ. of Liverpool). Brit. J. Appl. Phys., 16: 1535-42(Oct. 1965).

The theoretical and practical considerations involved in the design and construction of a resistive electrostatic screen, as used in certain theta-pinch experiments, are presented. The spatial and temporal variation of the total electric field within the shield is analyzed, and a generalized time constant is derived which describes the screening properties of such shields with good accuracy over a wide range of parameters. (auth)

**3191** PLASMA ION OSCILLATION IN PLASMA BEAM SYSTEM. Yoseri, Norihiro; Kato, Kiyoe. Denki Shikensho Iho, 29: 248-54(Mar. 1965). (In Japanese).

A series of experimental studies were performed on plasma ion oscillation in a plasma beam system. The plasma was formed with a hot cathode discharge tube containing mercury drops, and the oscillation was detected in the frequency range of 10 kc/s to 100 Mc/s with a super-heterodyne detector and a synchroscope. Two types of discharge tubes, i.e., the divergent beam type and the convergent beam type were used. In either case, plasma ion oscillations of two modes were detected. Especially, in the case of the experiment with the dispersed-beam type tube, it is confirmed that the oscillation of higher frequency (Mode I) is modulated by the oscillation of lower frequency (Mode II). Mode I has a frequency which increases with the discharge current, and Mode II has a frequency which decreases with the discharge current. A simple theory is given for qualitative interpretation of the two modes observed experimentally. (auth)

**3192** A CONTRIBUTION TO THE STATISTICAL THEORY OF THE ACCELERATION OF PARTICLES BY MAGNETOHYDRODYNAMIC WAVES IN SLIGHTLY TURBULENT RAREFIED PLASMA. Galeev, A. A. (Novosibirsk State Univ., USSR). Dokl. Akad. Nauk SSSR, 161: 802-5 (Apr. 1, 1965). (In Russian).

The statistical mechanism of particle acceleration was originally proposed by Fermi to explain problems involved in the passage of cosmic rays. The turbulent motion does not describe the movement of individual particle clusters; there is weak interaction between the collective motion of the particles and oscillations of the medium. Thus, acceleration of particles in a slightly turbulent plasma may be considered as the excitation of a large number of internal low-amplitude oscillations which interact with each other and with the particles of the plasma; this behavior may be studied by means of the perturbation theory. In this connection, the slightly turbulent stationary condition, involving low-frequency, long-wave Alfvén frequencies propagating in an unperturbed magnetic field was investigated more closely. In order to determined the polarization effects, it was assumed that there is a small wave vector

component transversal to the field and that the vector of the electric field is perpendicular to the plane; the Maxwell equation was used to determine the correlation between the electric and magnetic fields. For the acceleration of very fast particles by high phase-velocity Alfvén waves, the law of energy conservation permits only the simultaneous absorption of the 2 oscillations by two pulses of opposite signs. An expression, similar to that of Fermi (Phys. Rev 75, 1169 (1949)) was derived. (TTT)

**3193** ESTIMATE OF THE ELECTRON DENSITY IN A PLASMA AFTER-GLOW FROM A STUDY OF ELECTROMAGNETIC SCATTERING. Jones, A. R.; Wooding, E. R. (Univ. Coll. of Wales, Aberystwyth). Electron. Letters, 1: 171(Aug. 1965).

The decay of electron density in an argon-plasma afterglow was determined by analysis of the scattering of microwave radiation. The results are applicable to overdense plasmas and are in good agreement with a short-wavelength cutoff measurement; they lead to a reasonable value of the ambipolar diffusion coefficient. (auth)

**3194** DYNAMIC THEORY OF NOISE IN A MAGNETOPLASMA. Gold, Louis (Stevens Inst. of Tech., Hoboken, N. J.). Intern. J. Electron. (1), 18: 547-51(June 1965).

The characteristic equation describing the stability of a magnetoplasma in the realm where collisions play a dominant role was found. Instability ordinarily associated with collective plasma oscillations cannot manifest itself. However, instability is nonetheless mirrored in the characteristic equation by the possible occurrence of complex roots. This variety of instability associated with complex transit times is believed to be noise and is ruled out in the cold plasma limit; not only are collisions needed to bring on noise, but also the thermal velocity must dominate over the directed electronic motion. In such an environment, a magnetic field can act to suppress or favor noise output. Where stable operation is in effect at sufficiently high anode voltages, imposition of a magnetic field can bring on noise. (auth)

**3195** SLOW SURFACE WAVE ALONG A COMPRESSIBLE PLASMA SLAB. Mukherjee, S. (Philbrick Researches, Inc., Boston). Intern. J. Electron. (1), 18: 553-67(June 1965).

Slow surface wave phenomena are studied in a compressible plasma–dielectric interface, the structure being rectangular. Cases with plasma dielectric constant $\epsilon_p$ positive (i.e., plasma frequency is less than excitation frequency) and negative (i.e., plasma frequency is greater than excitation frequency) are both considered. The existence of the "forward" surface wave is observed in all cases. The Philbrick repetitive SK5-Analog Computer was used for computation. Limiting case of incompressible plasma slab is also discussed. (auth)

**3196** THERMONUCLEAR POWER. Roderick, Hilliard; Ruark, Arthur E. Intern. Sci. Technol., No. 45, 18-34(Sept. 1965).

A review is given of thermonuclear power research. The fusion reaction, plasma confinement, production, turbulence, diffusion and instabilities — especially the flute instability — are discussed. Fusion reactor engineering, the DCX-1, and the Model C Stellarator are also discussed. Four current questions are considered. These are the maximum density to which a simple mirror system or a complex minimum B system can confine a plasma without major loss, and the instability that causes the loss. Also considered is the possible use of magnetic shear in a torus to prevent rapid radial leakage. The possible sharp reduction of plasma loss out the ends of a theta-pinch configuration without causing a large increase in the radial loss of plasma is another question. Lastly, means are considered for preventing the rapid cooling of hot confined plasma by cold neutral particles coming from the walls of the vessel. Future developments are also discussed. (J.F.P.)

**3197** SYSTEM OF EQUATIONS FOR A PLASMA JET WITH ACCOUNT OF THE REACTION OF THE DECOMPOSITION OF METHANE IN IT. Polak, L. S.; Mukhtarova, T. A. Izv. Akad. Nauk Azerbaidzh. SSR, Ser. Fiz.-Tekhn. Mat. Nauk, No. 6, 93-101(1964). (In Russian).

An attempt was made to find the optimal conditions of acetylene yield during craeking of methane in a plasma jet by analyzing the system of hydrodynamic equations of a plasma jet in which thermal decomposition of methane takes place. The analysis is limited to one-dimensional stationary jet flow, which is assumed to be laminar; the external forces are disregarded. Methane at room temperature is assumed to be introduced uniformly at an arbitrary point into a jet of hydrogen at high temperature (~3000°K). A system of differential equations for this process is written out taking into account the boundary conditions and the conservation laws. The transport coefficients which are involved in these equations are determined from approximate formulas. It is shown that thermal diffusion can be neglected. The dissipative terms in the transport equations are estimated. The zeroth and first approximation to the system of equations are obtained, making it possible to solve the system by successive approximations. (ATD)

**3198** ON THE RADIATION OF FAST-MOVING CHARGES IN A WAVE-DAMPING MEDIUM IN A NONHOMOGENEOUS PLASMA. Eidman, V. Ya. (Gor'kii State Univ., USSR). Izv. Vyssh. Ucheb. Zaved., Radiofiz., 8: 655-8(1965). (In Russian).

Cherenkov radiation is shown to decease for a charge moving with acceleration in a medium. This effect leads to the reduction of Landau damping in a weak nonhomogeneous plasma. (auth)

**3199** ON THE POSSIBILITY OF STATISTICAL ACCELERATION OF PHOTONS IN TURBULENT PLASMA. Tsytovich, V. N. (Lebedev Inst. of Physics, Moscow). Izv. Vyssh. Ucheb. Zavedenii, Radiofiz., 8: 622-5(1965). (In Russian).

Effects of induced photon decay — plasmon emission — and induced combination of photons with plasmons are studied. It is shown that, in a turbulent plasma, these processes can lead to an increase of the average energy of the photons. Possibilities of the application of this mechanism in astrophysical processes are considered. (M.J.T.)

**3200** PLASMA BREMSSTRAHLUNG. Pataraya, A. D.; Svimonishvili, V. I. (Inst. of Physics, Academy of Sciences, Georgian SSR). Izv. Vyssh. Ucheb. Zavedenii, Radiofiz., 8: 628-9(1965). (In Russian).

Bremsstrahlung from a plasma is studied, taking into account the thermal motion of electrons and ions and the direction of electron motion. The bremsstrahlung intensity is calculated as a function of the temperature, mass, and density of the electrons and ions for the nonrelativistic case and for the case of a relativistic electron beam in a plasma. (M.J.T.)

**3201** ON IONIZING SHOCK WAVES IN A CYLINDRICAL PLASMA. Woods, L. C. (Oxford Univ.). J. Fluid Mech., 22: 689-99(Aug. 1965).

The "switch-on" ionizing shock wave, initiated by a strong radial discharge between electrodes at one end of a cylindrical tube placed in a solenoid, moves along the tube with a speed that depends principally on the parameter $\xi = B_\theta B_0/(2e_0\rho_1)$, where $B_\theta$ is the jump in the transverse magnetic field caused by the discharge current, $B_0$ is the applied axial field, $\rho_1$ is the upstream (neutral) gas density, and $e_0$ is the ionization energy. This simple result, established by Kunkel & Gross (1962) with the aid of the Chapman-Jouguet hypothesis and for fully ionizing shocks in an infinite-slab plasma, is here extended to cylindrical plasmas and to partially ionizing shocks. The effect of dissociation energy is also taken into account. The degree of ionization is determined by applying the Saha equation downstream of the shock. Most reported experiments fall into the partially ionized region, and are found to be in good agreement with the theory given. (auth)

**3202** DISCHARGES BETWEEN COAXIAL CYLINDERS IN A MAGNETIC FIELD. Hayakawa, Shigeru; Wasa, Kiyotaka (Matsushita Electric Industrial Co., Ltd., Kadoma, Japan). J. Phys. Soc. Jap., 20: 1692-8(Sept. 1965).

The discharge in the crossed field is divided into three types under the condition of which the current is 0.1 ~ 30 mA, pressure is 0.01 ~ 10 mm Hg and magnetic field is 50 ~ 13500 gauss. In strong magnetic fields a new type of stable discharge exists in which the electron sheath forms the large anode fall and gas atoms are mainly ionized by electron impact in the anode fall region. With an increase in the current, stable discharge transits into an intermittent discharge accompanied with the spontaneous oscillation. The oscillation is induced in the region of plasma in which space charge distributes uniformly. In weak magnetic fields, another stable discharge exists that is an unusual glow discharge. (auth)

**3203** STRIATED COLUMN APPEARING IN HIGH-FREQUENCY GAS DISCHARGE. Nakata, Junji; Takenaka, Eiji; Masutani, Takaya (Nihon Univ., Tokyo). J. Phys. Soc. Jap., 20: 1698-1705(Sept. 1965).

Stationary striations appearing in the plasma column of low pressure argon h-f discharge brought about in cylindrical discharge tube of diameter from 5.8 to 18 mm are investigated experimentally for the pressure range from 0.07 to 8 mm Hg. Their spatial intervals (so-called "wave length") are proportional to the electrodes distance within a limited range of the wave length. The relation between the wave length and the electrodes distance is shown by sawteeth-like characteristics. The wave length increases linearly as the radius of the discharge tube increases. But it decreases exponentially as the gas pressure increases. The influence of the frequency of the h-f source does not exist over a range from 5 mc to 53 mc. The wave length, however, increases as the h-f power increases. When a d-c voltage is superposed on the h-f field through another pair of electrodes, striations move from positive side to negative side at a velocity proportional to the d-c current. These results indicate that the stationary striations appearing in h-f discharge can be regarded as a special state of moving striations. (auth)

**3204** NEGATIVE ABSORPTION OF MICROWAVE RADIATION IN A WEAKLY IONIZED XENON PLASMA IN MAGNETIC FIELD. Terumichi, Yasushi; Idehara, Toshitaka; Takahashi, Isao; Kubo, Hiroshi; Mitani, Kenji (Kyoto Univ.). J. Phys. Soc. Jap., 20: 1705-10(Sept. 1965).

The negative absorption of microwave radiation was confirmed at the electron cyclotron frequency in a weakly ionized xenon plasma. The gain was about 11 db for the input power in the range between about $10^{-11}$ and $10^{-9}$ w. Using an expression for the Q of plasma in a plasma-cavity system, the experimental results were analyzed and $-10^2$ per meter was obtained for the energy absorption coefficient $\alpha_\omega$, under the assumption that the velocity distribution of plasma electrons is a δ- function. (auth)

**3205** INFLUENCE OF TOROIDAL DRIFT ON PLASMA INJECTION TRANSVERSELY TO THE MAGNETIC FIELD. Fedyanin, O. I.; Khokhlov, Yu. V. (Lebedev Inst. of Physics, Moscow). JETP Lett. (USSR) (Engl. Transl.), 2: 50-2 (July 15, 1965).

An investigation is made of the validity of the toroidal drift effects on plasma jet motion in a transverse magnetic field, with resulting plasma distribution through the trap volume depending on the initial conditions, namely, on the direction of the plasma-current velocity vector relative to the magnetic-field gradient. This plasma motion was observed by means of a toroidal stainless-steel vacuum chamber placed in the magnetic system of a sectionalized solenoid, which produced a quasi-stationary field. The plasma was injected by two spark sources, with the internal and external injectors located such that they produced an initial plasma-current velocity parallel and antiparallel to $H^2$, respectively. The plasma current captured in the trap was measured with local screened electric probes. The radial distribution of the ions is shown with the externally injected plasma having a bell-shaped distribution, and an ordinary plasma distribution for the internal injection. It is concluded that the model proposed for the resultant plasma drift is correct. (J.F.P.)

**3206** SCIENTIFIC PROGRAM OF THE LABORATORY FOR RESEARCH ON PLASMA PHYSICS. Keller, R. (Laboratoire de Recherches sur la Physique des Plasmas, Lausanne, Switzerland). Neue Tech., 7: 174-8(Aug. 1965). (In French).

Research directed toward the production of plasmas, confined and heated by means of high frequency fields is discussed. The work is related to current results obtained at other research centers which are working toward the liberation of fusion energy. (auth)

**3207** MHD THEORY OF STATIONARY INTERACTION BETWEEN A HIGH-FREQUENCY FIELD AND A PLASMA IN NON-HOMOGENEOUS FIELDS. Teichmann, Jiri (Inst. of Plasma Physics, Prague). Nucl. Fusion, 5: 107-20 (June 1965).

Using the MHD model of the three-component plasma, the forces affecting unit volume of an unbounded plasma in a space occupied by generally nonuniform high-frequency and magnetostatic fields are discussed. In the metric defined by the geometry of the magnetic field lines, the forces affecting the three-fluid plasma arising from a high-frequency field with a high $^1E/^1H$ ratio were derived. Effects of collisions among plasma components and viscosity are included. The solution was obtained by applying the method of successive approximations. Similarly, anisotropic plasma is studied in the collision-free approximation. Stationary h-f forces in fundamental field configurations are quantitatively discussed; there are some characteristic effects in fields with curved field lines. The role of the temperature correction is discussed. The h-f forces, especially near the cyclotron frequencies, can be used for the limitation of plasma escape along magnetic lines and for the acceleration and injection of plasma in nonuniform magnetostatic fields. The possibilities of the application in magnetic traps are demonstrated by some examples. (auth)

**3208** DRIFT CYCLOTRON INSTABILITY OF A PLASMA WITH HOT IONS. Mikhailovskii, A. B. (Kurchatov Inst. of Atomic Energy, Moscow). Nucl. Fusion, 5: 125-43(June 1965). (In Russian).

The role of drift cyclotron instability in a spatially inhomogeneous plasma is analyzed. The instability can occur in a not-too-dilute plasma with a finite Larmor radius of the ions $(Q/a)^2 > (C_A/C)^2$($C_A$ is the Alfvén velocity, Q is the Larmor radius of the ions, and a is the characteristic dimension of the inhomogeneity). A detailed investigation was made of the effects on the instability criterion of various factors: the curvature of the lines of force and the inhomogeneity of the magnetic field, the form of the equilibrium particle velocity distribution function, the relationship between the transverse and longitudinal dimensions of the system, and the ratio of electron to ion temperature. It is concluded that, if the flute (hydrodynamic) instability is stabilized, the drift cyclotron instability is the most dangerous for a system with a finite Larmor radius of the ions. The instability may be overcome by creating a system with finite intersection of the magnetic lines of force (shear). In short systems the instability need not occur if there is cold plasma of finite density between the hot plasma and the conducting ends of the apparatus. (auth)

**3209** PLASMA CONFINEMENT IN A TOROIDAL MAGNETIC FIELD AND WITH A CONDUCTING DIAPHRAGM. Shafranov, V. D. (Kurchatov Inst. of Atomic Energy, Moscow). Nucl. Fusion, 5: 150-1(June 1965). (In Russian).

A plasma column is considered that is maintained in equilibrium in a toroidal magnetic field and its shape defined by a diaphragm. The maximally admissible value of $\beta = 8\pi p/B^2$ for such a retention is $\beta_{max} = 4b/\pi^2R$ in which b is the small radius and R the large radius of the toroidal chamber containing the plasma. (auth)

**3210** FLUTE INSTABILITY OF A DILUTE INHOMOGENEOUS PLASMA IN AN INHOMOGENEOUS ELECTRIC FIELD. Arsenin, V. V. (Moscow Inst. of Engineering and Physics). Nucl. Fusion, 5: 152-5(June 1965). (In Russian).

Flute perturbations of a strongly inhomogeneous dilute plasma in an inhomogeneous electric field are discussed. An inhomogeneous electric field, appearing at weak charge separation in a region with a width the order of an ion Lar-

mor radius in which plasma is inhomogeneous, does not affect the stability of long-wave oscillations of low frequency. The case of a very strong inhomogeneity is also examined in which the characteristic dimension at which the electric field changes is the order of an electron Debye length. In this case perturbations with a wavelength the order of an inhomogeneity dimension can be unstable. (auth)

**3211** NECESSITY OF THE ENERGY PRINCIPLES FOR MAGNETOSTATIC STABILITY. Laval, G.; Mercier, C.; Pellat, R. (EURATOM-CEA, Fontenay-aux-Roses, France). Nucl. Fusion, 5: 156-8(June 1965).

Three energy principles for magnetostatic stability are known that are supposed to give necessary and sufficient conditions. For this reason their minimization has been the subject of a lot of work in plasma physics. Indeed one can easily justify the sufficiency of the conditions of stability devised from these energy principles. But to demonstrate their necessity it is usually assumed that the operators of the perturbed linearized motions have a complete spectrum of eigenfunctions in the space of square integrable functions. The weakness of that assumption is shown and two new demonstrations are proposed of the necessity of energy principles for stability that require less stringent assumptions. The first demonstration involves some properties of the Laplace transform. In the second one the integral invariants of the linearized motion are used. The conclusions in both cases are identical: if a trial function is found which makes the potential energy negative, the equilibrium is unstable. Lower and upper bounds for the growth rate of the unstable perturbation are given. (auth)

**3212** END LOSSES FROM A THETA PINCH. Taylor, J. B.; Wesson, J. A. (United Kingdom Atomic Energy Authority, Abingdon, Eng.). Nucl. Fusion, 5: 159-61(June 1965).

A simple model for the flow of plasma from the ends of a theta pinch is used to calculate the steady state plasma loss rate. The flow is similar to hydrodynamic flow in a flexible nozzle; special attention must be paid to the conditions in the "throat" of the nozzle. The plasma loss rate is then a function of the plasma parameters and the mirror ratio of the coil—when this is appropriately defined. Graphs and convenient formulas for the loss are provided. (auth)

**3213** LORENTZ DISSOCIATION OF $H_3^+$ IN DCX-1. Haste, G. R.; Dunlap, J. L.; Postma, H.; Reber, L. H. (Oak Ridge National Lab., Tenn.). Nucl. Fusion, 5: 164-5(June 1965). (ORNL-P-1161).

Evidence was found for proton trapping resulting from Lorentz dissociation of the triatomic ion $H_3^+$. The $H_3^+$ ions were extracted at 60 kev directly from a duoplasmatron source, accelerated to 400 kev, and injected into the median plane of a 2:1 magnetic mirror field. It was verified, by measurements of the energy distributions of escaping charge-exchange neutrals and considerations of the cross sections, that the trapped energetic ions are predominantly protons of approximately 133 kev. (L.B.S.)

**3214** OPTICAL INTERFEROMETRIC AND SPECTROSCOPIC MEASUREMENTS OF ELECTRON DENSITY IN A PLASMA. McLean, E. A.; Ramsden, S. A. (Naval Research Lab., Washington, D. C.). Phys. Rev., 140: A1122-9(Nov. 15, 1965).

A Mach-Zehnder interferometer is used to determine the electron density ($\sim 2 \times 10^{17}$ cm$^{-3}$) behind the reflected shock wave in an electromagnetic, T-type shock tube filled with hydrogen to 2 Torr. The results are compared with simultaneous measurements of electron density from Stark broadening of the $H_\beta$ line and the absolute continuum intensity. Using two-wavelength interferometry, agreement is found to be within the experimental accuracy of about 6%, thus showing the validity of the theory for these three methods of density measurement. Although spectroscopic methods indicate that the plasma is highly ionized (~90%) so that the refractivity is determined primarily by free electrons, single-wavelength interferometry yields results which are 10–15% too low. This is taken to indicate the presence of a boundary layer of cold, high-density neutral gas near the walls of the shock tube. In addition, it is concluded on the basis of this experimental data that the Griem asymptotic wing formulas for Stark-broadened hydrogen lines is more accurate than the earlier asymptotic wing formulas of Griem, Kolb, and Shen. (auth)

**3215** MEASUREMENT OF STARK PROFILES OF SINGLY IONIZED NITROGEN LINES FROM A T-TUBE PLASMA. Day, R. A.; Griem, H. R. (Univ. of Maryland, College Park). Phys. Rev., 140: A1129-32(Nov. 15, 1965).

A hot plasma composed of helium and ionized nitrogen was created by reflecting the shock wave produced in an electromagnetic T tube. The plasma temperature was measured by monitoring three nitrogen-ion lines whose intensities are strong functions of temperature. The profiles of various lines emitted in the plasma were obtained by scanning with a monochromator from shot to shot. The half-width of He I 3889 Å was compared with empirically corrected calculations to determine the electron density. Half-widths of various nitrogen-ion lines were measured from the impact-broadened profiles; their shifts were obtained by comparing these profiles with unshifted lines from a pulsed capillary discharge. The results indicate agreement between experiment and recent Stark-broadening calculations within 20%, except for lines originating from the 4f level where Debye screening effects are important. No evidence was found for plasma polarization shifts. (auth)

**3216** SELF-CONSISTENT EQUATIONS INCLUDING EXCHANGE AND CORRELATION EFFECTS. Kohn, W.; Sham, L. J. (Univ. of California, San Diego, La Jolla). Phys. Rev., 140: A1133-8(Nov. 15, 1965).

From a theory of Hohenberg and Kohn, approximation methods for treating an inhomogeneous system of interacting electrons are developed. These methods are exact for systems of slowly varying or high density. For the ground state, they lead to self-consistent equations analogous to the Hartree and Hartree-Fock equations, respectively. In these equations the exchange and correlation portions of the chemical potential of a uniform electron gas appear as additional effective potentials. (The exchange portion of the effective potential differs from that due to Slater by a factor of $\frac{2}{3}$.) Electronic systems at finite temperatures and in magnetic fields are also treated by similar methods. An appendix deals with a further correction for systems with short-wavelength density oscillations. (auth)

**3217** THEORY OF WING BROADENING OF THE HYDROGEN LYMAN-$\alpha$ LINE BY ELECTRONS AND IONS IN A PLASMA. Griem, Hans R. (Univ. of Maryland, College Park; Naval Research Lab., Washington, D. C.) Phys. Rev., 140: A1140-54(Nov. 15, 1965).

The frequency distribution of the absorption and emission coefficients on the wings of the hydrogen Lyman-$\alpha$ line broadened by local fields of both electrons and (quasistatic) ions in a plasma is calculated in the classical path approximation for regions well outside the half-intensity points. Depending on velocities and frequency separations from the line center, electron collisions are treated by an impact theory, which accounts both for Debye shielding and for the finite duration of the collisions, or by the quasistatic theory. Quadrupole interactions are considered in addition to the usual dipole interactions, and the (dominant) contribution of dipole interactions to the impact broadening is calculated to higher orders in the iterated solution of the time-dependent Schrödinger equation. Asymmetries introduced by quadratic Stark effect, by quadrupole interactions, by field-strength dependence of the oscillator strengths, and by the ion broadening of the central component through quadratic-Stark-effect and quadrupole interactions are evaluated. Also considered are asymmetries from the variation of factors usually assumed to be constant (frequencies and Boltzmann factors), and from the transformation from frequency to wavelength increments. Remaining theoretical uncertainties in the absolute values of absorption or emission coefficients for typical plasma conditions are estimated to be less than 10% over ranges in which

these coefficients vary by three orders of magnitude. (auth)

**3218** KINETIC EQUATION WITH A RELATIVISTIC INTERACTION CORRECTIONS FOR A PLASMA. Krizan, John E. (Univ. of Vermont, Burlington). Phys. Rev., 140: A1155-60(Nov. 15, 1965).

Using the formalism of Weinstock, a master equation for a momentum-dependent interaction is given. An exact kinetic equation (to lowest order in $e^2$) for a homogeneous plasma in which relativistic interaction corrections to order $(v/c)^2$ are included is also given. It is readily shown that with the relativistic approximation the well-known divergences of the kinetic equation are removed without invoking cutoffs (as is also true in the nonrelativistic case given by Weinstock). (auth)

**3219** PERTURBATION OF DISK-LOADED WAVEGUIDE MODES BY AN ANISOTROPIC PLASMA. Gilson, V. A.; Johnson, C. C. (Univ. of Utah, Salt Lake City). Proc. IEEE (Inst. Elec. Electron. Eng.), 53: 1639(Oct. 1965).

Experimental tests were carried out on theoretically predicted propagation characteristics in a plasma-filled disk-loaded waveguide. The entire plasma medium was immersed in a uniform axial static magnetic field. The geometric dimensions of the experimental circuit are given. The radiofrequency energy was coupled to the circuit by magnetic loops located near the outside wall at each end. Cesium contact ionization was used as the plasma generation mechanism. Experiments were successfully conducted with both glass and metal-wall tubes, and equivalent plasma densities were obtained. The propagation characteristics were obtained by observing the resonances of the slow wave structure. The $\omega$-$\beta$ plots are shown, and theoretical predictions are given for comparison. (J.F.P.)

**3220** REMARK ON THE KINETIC EQUATION IN AN UNSTABLE PLASMA. Yamada, Kazuo (Nagoya Univ., Japan); Watabe, Mitsuo; Ichikawa, Yoshihiko. Progr. Theoret. Phys. (Kyoto), 34: 383-98(Sept. 1965).

The kinetic equation in the inhomogeneous plasma is investigated for weakly stable and unstable cases according to the B-B-G-K-Y method to clarify the interrelation of the existing theories. With consideration for the initial value problem, the equation of motion for the spacially uniform one particle velocity distribution function is expressed by means of the collision terms between particles and collective motions, i.e., the optical and the acoustical modes in an electron-ion system. Generally, in the inhomogeneous system, it is necessary to take account of both the Vlasov term and the two particle correlation term for the collision terms. If the R.P.A. is adopted, it is seen that the collision terms are a simple sum of each result in two independent approaches, that is, one is the result in the quasi-linear theory for the Vlasov term, the other the correlation effect in the homogeneous plasma. Comparison of the calculation with the Pines-Schrieffer approach is made lastly. (auth)

**3221** ON THE HIGHER ORDER CORRECTIONS TO THE ALFVEN WAVE INSTABILITY. Sato, Masatomo (Nihon Univ., Tokyo). Progr. Theoret. Phys. (Kyoto), 34: 417-23(Sept. 1965).

The higher order corrections to the instability of an Alfvén wave, propagating along an external magnetic field in a plasma of anisotropic pressure components, are considered on the basis of the Vlasov equations. It is shown that terms of the order of $1/\Omega_i^2$, besides those of $1/\Omega_i$ ($\Omega_i$ = the gyro-frequency of an ion), should be retained as correction terms to the lowest order (Chew-Goldberger-Low) dispersion relation to obtain a correct criterion of stability. The result is to expand slightly the region of instability, and there is no "finite Larmor radius stabilization effect" as obtained from the modified C.G.L. approximation. (auth)

**3222** LOW FREQUENCY OSCILLATIONS IN THE PLASMA OF A REFLEX DISCHARGE. Kucherenko, E. T.; Saenko, V. A. (Kiev State Univ.). Ukr. Fiz. Zh., 10: 838-43(Sept. 1965). (In Ukrainian).

Investigation of the l-f oscillations in a reflex discharge with a hot cathode in a weak external magnetic field and at low pressure ($P < 1.10^{-3}$ mm Hg) showed that the oscillations are ionic sound waves in the discharge plasma. The amplitude and frequency vs magnetic field are connected with the specific motion of the fast electrons emitted from the cathode. (auth)

**3223** POPULATION DENSITIES OF EXCITED HYDROGEN LEVELS IN STATIONARY PLASMAS WITH REGARD TO THE DIFFUSION OF NEUTRAL PARTICLES. Drawin, H. W. (Euratom-C.E.A., Fontenay-aux-Roses, France). Z. Physik, 186: 99-107(1965). (In German).

When strong diffusion of neutral particles from outer zones of the plasma into the inner region of a plasma column takes place the population densities of the excited atoms will deviate from those obtained without a diffusion current of neutral particles. By solving the corresponding rate equations the population densities of the hydrogen levels in a non-thermal, optically thin plasma with a superposed diffusion current hydrogen atoms were calculated. Numerical values are given for electron temperatures $T_e = 5$ ev, $T_e = 10$ ev, and $T_e = 30$ ev, and for electron densities varying from $n_e = 10^8$ cm$^{-3}$ to $n_e = 10^{14}$ cm$^{-3}$. (auth)

**3224** HYDROMAGNETIC STABILITY OF TWO SUPERPOSED PLASMA COLUMNS WITH ANISOTROPIC PRESSURE. Tandon, J. N.; Bajaj, N. K. (Univ. of Delhi). Z. Physik, 187: 351-4(1965).

The problem of hydromagnetic stability of the interface formed by two superposed columns of dilute plasmas was investigated. The plasmas are assumed to be pervaded by magnetic fields strong enough to render the plasma pressure anisotropic and to justify the fluid description of the plasmas obeying the double adiabatic invariant relation of Chew, Goldberger and Low. It is shown that the interface remains stable in spite of anisotropy in the plasma pressure. (auth)

**3225** A MAGNETIC MIRROR TRAP FOR PROLONGED CONFINEMENT OF ELECTRONS. Dubinina, A. N.; Trainin, L. Ya.; Chirikov, B. V. (Inst. of Nuclear Physics, Academy of Sciences, Siberian SSR). Zh. Eksp. Teor. Fiz., 49: 373-8(Aug. 1965). (In Russian).

A magnetic mirror trap with a simple system for external injection by an electron gun with a vacuum $\sim 8.10^{-10}$ mm Hg and electron confinement time up to 40 sec is described. Electron capture by the trap is based on fast variation of the electric field. The arrangement will be used for a detailed study of prolonged motion of electrons in a magnetic trap and also for a study of the behavior of a rarefied plasma. (auth)

**3226** DAMPING OF LONGITUDINAL WAVES IN AN INHOMOGENEOUS PLASMA. Eidman, V. Ya. (Gor'kii State Univ., USSR). Zh. Eksp. Teor. Fiz., 49: 529-37(Aug. 1965). (In Russian).

It is taken into account that in a weakly inhomogeneous medium for which the geometrical optics approximation is valid, the number of resonance particles interacting with a longitudinal wave may vary considerably with the distance. As a result, in some cases the wave absorption coefficient in a certain region of the plasma may oscillate in space. (auth)

**3227** CONFINEMENT OF SLOW IONS IN A MIRROR TRAP IN A PLASMA WITH A POSITIVE POTENTIAL. Yushmanov, E. E. Zh. Eksp. Teor. Fiz., 49: 588-98 (Aug. 1965). (In Russian).

The magnitude of the effective mirror ratio for comparatively slow ions (with energies of the order of $T_e$) confined by a magnetic trap with a small mirror ratio ($R = 1.5$ to 2.0) is determined for the case when the plasma is charged to a considerable positive potential ($\varphi_0 \gg T_e$). It is assumed that the ion component of the plasma consists almost wholly or partially of ions with a high energy which significantly exceeds the plasma potential. The potential distribution along the trap, the minimal energy of the confined ions, the magnitude of the effective mirror ratio for ions with an energy near the minimal value and finally the limiting possible density of such ions as compared with that of fast ions are considered. It is shown that due to concentration of the

largest potential drop in a narrow region near the mirror traps, the minimal energy of the confined ions does not depend on $\varphi_0$ and is of the order of $T_e$. In this case the effective mirror ratio for ions with an energy above the minimal value may not differ strongly from the initial ratio, whereas the critical density of accumulated slow ions may exceed by several times the fast ion density. It is concluded that the presence of a group of fast ions and the consequent small potential drop in the major volume of the trap may be a favorable factor in the ambipolar plasma losses through the magnetic mirror traps. (auth)

**3228** AUTOMODEL MOTION OF A RAREFIED PLASMA. Gurevich, A. V.; Pariskaya, L. V.; Pitaevskii, L. P. (Lebedev Inst. of Physics, Moscow; Inst. of Problems in Physics, Academy of Sciences, USSR). Zh. Eksp. Teor. Fiz., 49: 647-54(Aug. 1965). (In Russian).

A nonlinear kinetic equation is deduced for the automodel motion of an electron-ion plasma in the absence of collisions. The problem of expansion of the plasma in vacuum is solved. The distribution of the concentration and velocities of the ions is determined. It is shown that as the rarefied semi-space is filled up, the electric field thus produced accelerates part of the ions to velocities up to those of the order of thermal electron velocities. Simultaneously, the effective ion temperature sharply drops. It turns out to be many times smaller than the electron temperature (for identical temperatures in the initial plasma). Results of a numerical calculation are presented. (auth)

**3229** ION ESCAPE FROM A MAGNETIC MIRROR TRAP DUE TO DEVELOPMENT OF INSTABILITY CONNECTED WITH THE LOSS CONE. Galeev, A. A. Zh. Eksp. Teor. Fiz., 49: 672-81(Aug. 1965). (In Russian).

The nonlinear stage of development of microinstability in a plasma in magnetic mirror traps caused by the loss cone in the ion velocity distribution is considered. The oscillations which arise as result of the instability leads to fast diffusion of the ions in velocity space to the loss cone and to their subsequent escape from the trap. (auth)

**3230** ON THE THEORY OF NONLINEAR INTERACTION OF WAVES IN A MAGNETOACTIVE ANISOTROPIC PLASMA. Tsytovich, V. N.; Shvartsburg, A. B. (Lebedev Inst. of Physics, Moscow). Zh. Eksp. Teor. Fiz., 49: 797-806(Sept. 1965). (In Russian).

General equations are obtained which describe nonlinear interactions of waves in a magnetoactive anisotropic plasma. Explicit expressions are derived for the probabilities of scattering of normal waves on plasma electrons and ions and for the probabilities of decay processes. (auth)

**3231** THE EXISTENCE OF ELECTROMAGNETIC SURFACE WAVES ON A PLANAR PLASMA SLAB WITH A FINITE TRANSVERSE MAGNETIC FIELD [Thesis]. White, David Parker. Ithaca, N. Y., Cornell Univ., 1965. 112p.

The class of wave solutions of Maxwell's equations that propagate along the interfaces, namely the electromagnetic surface waves, are investigated. The models consist of an infinite planar slab of homogeneous, anisotropic plasma of finite thickness. On one side of the plasma slab is an infinite half space of vacuum and the other side is terminated by either a perfect electric conducting or magnetic conducting sheet. A finite magnetic field B is oriented perpendicular to these interfaces. The plasma boundaries are assumed to remain unperturbed. The plasma is assumed to be "cold," allowing only the two electromagnetic modes to propagate. The solutions, for the electric and magnetic line sources, are accomplished through a modal analysis and synthesis, utilizing classical waveguide techniques. The solutions for the field quantities at first are expressed in terms of integral equations. Complex function techniques are used to extract the relevant surface wave fields. The surface wave modes belong to the discrete spectrum associated with the poles of the kernel of the integral equations for the fields. The locations of these poles are found by solving for the roots of complicated transcendental dispersion equations. A simple method of finding these roots, provided the geometrical and plasma parameters are given, is outlined. The use of various approximations to these transcendental dispersion equations is discussed. After the roots are found, a simple residue calculation gives the surface wave field. The surface wave behavior for the limiting case of $B_0 \rightarrow 0$ is discussed in detail. The general nature of the solution permits an easy extension to the determination of the radiation field and of other discrete mode phenomena. (Dissertation Abstr.)

**3232** PLASMA DIAGNOSIS BY MEANS OF PHOTON-ELECTRON SCATTERING [Thesis]. Schwarz, Steven Emanuel. Pasadena, Calif., California Inst. of Tech., 1964. 110p.

When a pulse of intense light from a giant-pulse laser passes through a plasma, a very small fraction of the light is scattered out of the beam as a result of ("Thomson") scattering by free electrons. Under suitable conditions the intensity of the scattered light is proportional to the density of free electrons, while its spectral distribution is related to the velocity distribution of the free electrons through the Doppler formula. Theoretical considerations, relating to the conditions of validity of the method, are discussed. Various mechanisms that could interfere with the diagnostic technique are mentioned and their importance is considered. Design considerations for diagnostic experiments are then taken up, and signal-to-noise ratios calculated. An apparatus for conducting scattering experiments was constructed. Phenomenological checks indicate that the observed scattering is by free electrons. Measurements conducted at various times in the development of an afterglow plasma indicate Doppler broadening of the scattered light; the broadening disappears as the electrons cool during the first three microseconds of the afterglow. Measurements of electron density as a function of time are made in the afterglow, and are calibrated by means of Rayleigh scattering from gas at a known pressure. Two unexpected laser-plasma interactions were observed. The first is designated as "induced plasma luminosity" and the second as "giant scattering." Both effects appear to be related to the presence of hydrocarbon impurities in the gas. (Dissertation Abstr.)

**3233** NON-EQUILIBRIUM IONIZATION AND MAGNETOHYDRODYNAMIC FLOW PHENOMENA [Thesis]. Sherman, Arthur. Philadelphia, Univ. of Pennsylvania, 1964. 128p.

The interaction between nonequilibrium ionization phenomena in a plasma and the nonuniform flow of that plasma was studied. The simple case for which the plasma is stationary and only an electric field is applied is considered first. It is shown that the electron distribution function is Maxwellian and that the average electron temperature can be calculated from an energy balance. The same phenomenon is next considered in a moving plasma in the presence of electric and magnetic fields and the macroscopic equations for a "single fluid" are derived. These equations are used to study the classical Hartmann Channel flow with and without the Hall effect. For particularly simple assumptions about the influence on plasma electrical conductivity of the nonequilibrium effect, solutions are obtained. It is shown that the problem becomes essentially nonlinear, and that for some choices of the parameters no solution can exist. It was shown that the nonequilibrium phenomenon can be incorporated into a "single fluid theory." This theory is sufficiently simple that magnetohydrodynamic flow problems can be treated, and some simple solutions obtained. For the present work only Hartmann flow was treated. Other equally simple flows can be considered in the same way. (Dissertation Abstr.)

**3234** ELECTRON DENSITIES DETERMINED BY MEASUREMENT OF THOMSON SCATTERING OF LASER LIGHT FROM A PLASMA [Thesis]. Sigman, Donald Ray. Columbus, Ohio, Ohio State Univ., 1964. 64p.

Work was done on the development of the laser technique for measurement of electron densities of a plasma confined in a magnetic mirror system and heated by two-phase radio-frequency power. The general theory of Thomson scattering of polarized laser light from a free electron is presented, and the effects of a pulsed laser beam on the

steady-state conditions of the plasma are discussed. The main problem encountered was that of reducing stray laser light from walls and windows of the plasma bottle. This was done to the extent that it was possible to measure electron densities as low as $10^{13}$ $cm^{-3}$. It is also shown that at low electron temperatures little advantage could be taken of the fact that properly scattered laser light is Doppler shifted. Finally, the relative Rayleigh scattering cross section for laser light between air and hydrogen was examined and found to be in agreement with previous measurements on the refractive index of these two gases. (Dissertation Abstr.)

**3235** DATA FOR PLASMAS IN LOCAL THERMODYNAMIC EQUILIBRIUM. Drawin, Hans-Werner; Felenbok, Paul. Paris, Gauthier-Villars, 1965. 503p. 64 F.

Numerical values are presented for formulas often used in quantitative and in qualitative spectroscopy, as well as in general plasma physical problems, when the state of the plasma can be described by local thermodynamic equilibrium. Often-used conversion factors and numerical values for fundamental constants are also listed. Other useful values, such as the emissivity of the d-c carbon arc, and emission coefficients for hydrogen continua, etc. are given. (J.F.P.)

**3236** PLASMA TURBULENCE. Kadomtsev, B. B. New York, Academic Press, 1965. 154p. $6.50.

Translated from the Russian by L. C. Ronson.

Quasi-linear approximations are considered for instability, turbulence, laminar plasma convection, and kinetics. The kinetic equation for wave interactions with weak turbulence, and these wave interactions in plasma are given considering the thermal motion of the particles. The weak coupling approximation for strong turbulence and the phenomenological approach to a description of strong turbulence are also given. Turbulence in plasma is discussed for nonlinear damping of Langmuir waves, excitation of ion oscillations by an electric current, and drift instability; the turbulent plasma under experimental conditions is also considered. (J.F.P.)

**3237** TWO-PHASE RADIO FREQUENCY HEATING OF A PLASMA CONFINED IN A MAGNETIC MIRROR SYSTEM [Thesis]. Hagenlocker, Edward Emerson. Columbus, Ohio, Ohio State Univ., 1964. 72p.

The theory of an ion moving in phase with a rotating electric field and revolving magnetic field was presented. In a properly phased revolving magnetic field and rotating electric field, it was shown that an ion in phase with the rotating electric field will drift toward the axis about which the electric field is rotating. Experimental observations supported this theory. Mathematically it was shown that a uniform rotating magnetic field alone does not enhance the confinement of the plasma. Also, a radial nonuniformity in the axial magnetic field will introduce a phase difference between the ion motion and the rotating electric field. A radio-frequency coil configuration, which incorporated the properties of a rotating electric field, revolving magnetic field, and rotating magnetic field, was described. This coil configuration was used in conjunction with a magnetic mirror system capable of confining 30-kev deuterons. The proper phasing of this two-phase system made a considerable difference in the properties of the plasma generated. The observed electron densities at a deuterium gas pressure of 1 and 14 microns indicated ion cyclotron resonance. Ion cyclotron resonance was not indicated by a change in the loading of the r-f power supplies at either of these gas pressures. For a deuterium gas pressure of 14 microns, the electron density and light emitted increased as the axial magnetic field was decreased because of increased heating of the free electrons. (Dissertation Abst.)

## Shielding

*Refer also to abstracts 2552–2555, 2557–2559, 2932–2937, 2939, 2962, 2968, 2989, 3348, and 3647.*

**3238** (JINR-P-2354) OSLABLENIE PUCHKOV μ-MEZONOV VYSOKIKH ENERGII V ZASHCHITE. (Weakening of High Energy μ Beams in Shielding). Sychev, B. S.; Cherevatenko, A. P. (Joint Inst. for Nuclear Research, Dubna (USSR)). 1965. 9p. Dep. mn.

Ionization energy losses of muons in different types of concrete are calculated. A method is suggested to calculate a shield form for a filament-like muon beam. (auth)

**3239** (NASA-SP-71) SECOND SYMPOSIUM ON PROTECTION AGAINST RADIATIONS IN SPACE, GATLINBURG, TENNESSEE, OCTOBER 12–14, 1964. Reetz, Arthur Jr. (ed.) (National Aeronautics and Space Administration, Washington, D. C. Scientific and Technical Information Div.). 1965. 518p. (CONF-720). GPO $3.25.

Fifty-eight papers are included; separate abstracts have been prepared for 24. One of the papers not abstracted separately is a review article on radiation effects on semiconductors. The remaining 33 papers were previously abstracted in NSA, see 19:2184, 3457, 9492, 14535, 14536, 15018, 15215, 16242, 16365, 16762, 16763, 16856, 17161, 17162, 17172, 17173, 17491, 19336, 19616, 20019, 21244, 21992, 22390, 22651, 23341, 23944, 23945, 23946, 23947, 23949, 25547, 25618, and 43879. (T.F.H.)

*For abstracts of individual papers see: 1614–1616, 2133, 2652–2658, 3015, and 3240–3251.*

**3240** (NASA-SP-71, pp 183-8) COSMIC-RAY SHOWER PRODUCTION IN MANNED SPACE VEHICLES—COPPER. More, K. A.; Tiffany, O. L. (Bendix Systems Div., Bendix Corp., Ann Arbor, Mich.).

The generation of cosmic ray showers in a Cu-walled space vehicle is calculated by a three-dimensional Monte Carlo technique. Data on neutron and pion production are of particular interest, since only a model including shower production can give an estimate of these products. The proton results are compared with the simpler calculations using ionization only or ionization and exponential absorption. (auth)

**3241** (NASA-SP-71, pp 199-209) MAGNETIC RADIATION SHIELDING USING SUPERCONDUCTING COILS. Bernert, R. E.; Stekly, Z. J. J. (Avco-Everett Research Lab., Everett, Mass.).

Superconducting magnetic shield systems are analyzed, in order to determine the total weight of this type of active shield. The major components of the superconducting magnet considered are superconducting wire, support structure, and cryogenic environment. An optimum system mass is determined as a function of shielded volume and shielding level. Of three magnetic field geometries analyzed, the best configuration on the basis of weight was found to be a spherically shaped shield consisting of a set of nested toroidal windings having a confined magnetic field and a field-free shielded cavity in the center of the sphere. The shielding values of magnetic and passive shields are compared on a dose rate basis. The general results of this comparison show that as shielded volumes and shielding levels increase, the advantage of using magnetic shields also increases. A preliminary study of mission requirements was conducted, and is summarized by presenting a design of a Mars class solar flare storm cellar. The study shows that the system is feasible and compatible with the spacecraft and that, with design improvements, the indicated weight savings of 4000 kg for the 10-man 200-Mev-equivalent-threshold storm cellar may be exceeded. (auth)

**3242** (NASA-SP-71, pp 225-8) SYNTHESIS OF SPHERICAL MINIMUM-WEIGHT PROTON SHIELDS. Celnik, J.; Krumbein, A. D.; Nakache, F. R. (United Nuclear Corp., White Plains, N. Y. Development Div.).

A systematic method is developed for minimizing spherical shield weights for protection against proton radiation, including secondary neutron production, subject to various specified dose constraints. Variational methods are applied to a radiation model yielding the choice of optimum shielding materials and their mixtures, together with a prescription for their disposition in a multi-layer spherical shield. An extension of the general synthesis theory shows that, neglecting secondary neutron production, the optimum materials are polyethylene, carbon, nickel, and tungsten. (T.F.H.)

**3243** (NASA-SP-71, pp 229-34) QUALITY FACTORS FOR DEGRADED PROTON SPECTRA. Madey, Richard; Stephenson, Thomas E. (Republic Aviation Corp., Farmingdale, N. Y.).

Quality factors for degraded proton spectra may be obtained by evaluating the ratio of the dose equivalent (rem) to the absorbed dose (rad). For a monoenergetic proton, the dose equivalent is given by the product of the absorbed dose and a monoenergetic quality factor. For a spectral distribution of protons incident omnidirectionally on a spherical shell shield, the quality factor for the proton dose absorbed at the center of the shield may be represented by an analytic formula. Numerical values for use in this formula are presented. (auth)

**3244** (NASA-SP-71, pp 365-75) APOLLO SPACECRAFT NUCLEAR RADIATION PROTECTION STATUS REPORT. Raymes, Frederick (North American Aviation, Inc., Downey, Calif.).

Space radiation protection considerations are discussed with regard to the Command/Service Module (CSM) of the Apollo vehicle. Shielding and dose calculations for particular environmental situations are discussed, and compared with present standards. It is concluded that the astronauts' radiation protection in the CSM is adequate. (T.F.H.)

**3245** (NASA-SP-71, pp 407-14) THE IMPORTANCE OF SPACE RADIATION SHIELDING WEIGHT. Beever, E. R.; Rusling, D. H. (North American Aviation, Inc., Downey, Calif.).

The shielding weights required to protect astronauts against space radiation should be considered in relation to the weights of the meteoroid shielding and the life support systems. Comparisons have been carried out for a variety of crew sizes and mission durations. The radiation shield weights were based upon a 1% probability and were obtained from data on solar proton events. A mission dose of 100 rad was used as the allowed limit. The doses allowed from solar events were reduced by 45 mrad/day due to galactic radiation and by the amount of radiation expected for two high-thrust trips through the earth's trapped radiation belts. In the calculation of the shield weights, the "storm cellar" concept was employed, allotting 50 $ft^3$ per man. The meteoroid shield weights were taken into account. The single shield thicknesses calculated were modified to take into account the reduced penetration where two facing sheets with space between them are used as the meteoroid shield. A 1% probability of penetration was assumed in the calculations. The weights of the life support system are dependent upon the assumptions made regarding the particular subsystems to use for a specific mission. Two systems were used for this comparison. The system selected for the 30-day mission provides for body waste storage rather than reprocessing. Each system assumes a cabin leakage rate of 10 lbs/day and a power penalty weight of 320 lbs/kwe. (auth)

**3246** (NASA-SP-71, pp 437-48) RESULTS OF SOME RECENT TRANSPORT CALCULATIONS FOR ELECTRONS AND BREMSSTRAHLUNG. Berger, M. J.; Seltzer, S. M. (National Bureau of Standards, Washington, D. C.).

Illustrative results are given for three types of problems: the transmission of electrons through thin and thick foils, with emphasis on the effect of energy loss straggling; the energy dissipation by electrons in a semi-infinite water phantom, for an incident broad beam (depth dose distribution), and for an incident pencil beam (distribution as function of two spatial variables); and the production of bremsstrahlung in thick targets. The data presented for the first two problems are entirely theoretical and result from a Monte Carlo calculation. Similar calculations for the third problem are compared with experiments. (auth)

**3247** (NASA-SP-71, pp 449-53) BREMSSTRAHLUNG PRODUCTION IN THICK ALUMINUM AND IRON TARGETS BY 0.5- TO 3.0-Mev ELECTRONS. Baggerly, L. L.; Dance, W. E.; Farmer, B. J.; Johnson, J. H. (Ling-Temco-Vought, Inc., Dallas, Tex.).

The intensity of bremsstrahlung produced by bombarding thick targets of aluminum and iron is measured as a function of incident electron energy, photon energy, and angle of photon emission. The energy of the incident electrons is 0.5 to 3.0 Mev. The electron beam from a 3-Mev Van de Graaff accelerator is incident normally on targets of sufficient thickness to stop the electrons. The total integrated intensities are computed from these measurements and the results from aluminum and iron are compared. (auth)

**3248** (NASA-SP-71, pp 455-63) SPACE ELECTRON RADIATION SHIELDING—BREMSSTRAHLUNG AND ELECTRON TRANSMISSION. Magnuson, G. D.; McReynolds, A. W. (General Dynamics/Astronautics, San Diego, Calif.).

Curves of transmission versus incident electron energy are measured over the energy range 0.2 to 2.5 Mev for a number of thicknesses of aluminum and polyethylene from about 0.07 to 1.3 $g/cm^2$. Generally, for equal $g/cm^2$, transmission starts at higher energy for polyethylene but the curve rises more steeply, crossing the aluminum transmission curve. Thus, the relative shielding effectiveness depends on the incident energy. At larger angles of incidence, for either material, the curves rise less steeply, as a result of angular deviations of the electrons in transmission. For equal $g/cm^2$ measured along the incident direction, transmission starts at lower energy for larger angle of incidence, and the transmission curve crosses the curve for normal incidence. Transmission coefficient versus angle of incidence curves for aluminum agree with Monte Carlo calculations up to material thicknesses of about 0.3 maximum range, but diverge substantially from the calculations at greater thicknesses. Bremsstrahlung intensities behind laminar aluminum-polyethylene-aluminum structures show a broad angular distribution at 0.5 Mev incident energy, increasingly forward peaked at 1.0 and 2.0 Mev in accordance with theory. Energy distributions of the transmitted electrons are measured behind the target panels by solid state detectors. (T.F.H.)

**3249** (NASA-SP-71, pp 473-6) AN EVALUATION OF RADIATION SHIELDING BY VEHICLE ORIENTATION. Mar, B. W. (Boeing Co., Seattle, Wash.).

An elementary analysis was performed to determine the decrease in shield weight obtained by selective orientation of a vehicle in an anisotropic flux of geomagnetically trapped charged particles. Study results indicated a minor decrease in proton shield weight and electron shield weight. The study was limited to cylindrical and conical geometries; the energy spectra were assumed to be independent of pitch angle, whereas angular distribution was a function of pitch angle (maximum cutoff angle of 60 degrees). (auth)

**3250** (NASA-SP-71, pp 493-505) THE CALCULATION OF PROTON PENETRATION AND DOSE RATES. Burrell, Martin O. (National Aeronautics and Space Administration, Huntsville, Ala. George C. Marshall Space Flight Center).

A method is presented for calculating the energy degradation and flux attenuation of protons, as functions of the penetration depths in various materials. The straight-ahead approximation is used. The objective of the calculation is the determination of the energy deposition at a given depth or on a given surface. (T.F.H.)

**3251** (NASA-SP-71, pp 507-12) LOCAL DOSE FROM PROTON AND ALPHA PARTICLE ENDERS BEHIND COMPLEX SHIELD SYSTEMS. Schaefer, Hermann J. (Naval School of Aviation Medicine, Pensacola, Fla.).

Flux ratios as high as 1 for protons/alpha particles in the integral rigidity spectra of some flare-produced solar particle beams have been reported. Evaluation of tissue depth doses for the shield configuration of the Apollo vehicle shows that the alpha component contributes significantly to total exposure only for low shielding and only in the superficial layers of a tissue target. The fractional high LET dose due to alpha enders, however, is substantially larger than the corresponding dose from proton enders even at greater depths. Separate measurement of the high LET fraction of total dose and proper determination of RBE and $Q^F$ factors, therefore, seems of even greater importance for the alpha component than for protons. (auth)

**3252** (NP–15578) THE DIOCOTRON INSTABILITY IN A QUASI-TOROIDAL GEOMETRY. Research Report 228. Levy, R. H.; Callen, J. D. (Avco-Everett Research Lab., Everett, Mass.). Sept. 1965. Contract NASw-1101. 22p.

The diocotron (or slipping stream) instability of low density ($\omega_p \ll \omega_c$) electron beams in crossed electric and magnetic fields is considered for a cylindrical geometry with a radial electric field and an azimuthal magnetic field. In the analysis the electrons are assumed to have no thermal energy, collisional effects are neglected, the quasi–static approximation is made, and perturbations of the electric field along the magnetic field are ignored. For a simple density distribution the important normal modes of the electron beam correspond to two discrete eigenvalues. A condition for the stability of these modes is derived. This condition shows that, within the approximations of the analysis, the electron beam can be stabilized against diocotron modes of all wavelengths by proper selection of dimensions. The application of this theory to a proposed toroidally-shaped space radiation shield is discussed. Assuming the long straight cylinder geometry to be a reasonable approximation to a torus with a large radius ratio, it is shown that the crossed field electron beam surrounding a space radiation shield will, within the same approximations, be stable against diocotron instabilities when the beam is sufficiently thick. (auth)

**3253** SHIELDING PARAMETERS OF CONCRETES. Zaitsev, L. N.; Lavdanskii, P. A.; Mal'kov, V. V.; Sychev, B. S. At. Energ. (USSR), 19: 303-7(Sept. 1965). (In Russian).

Data from previous works are summarized on the chemical composition and shielding parameters of materials used as aggregates for concretes and on the shielding parameters of the separate elements for fission-spectrum neutrons and gamma radiation to 10 Mev. Results of calculations are presented for macroscopic removal cross sections of 10- to 100-Mev neutrons for the separate elements. The variation of the fast-neutron removal cross sections of concretes containing water is given. Results are graphed of the dependence of the neutron inelastic cross section on the iron content and of the dependence of the thermal-neutron absorption cross section on the boron and iron content in concretes. (M.J.T.)

**3254** SHIELDING FOR RADIOISOTOPE BREMSSTRAHLUNG SOURCES $^{90}Sr + ^{90}Y$. Naumann, H. H.; Waechter, K. H. (Frieseke and Hoepfner GmbH, Erlangen, Ger.). Int. J. Appl. Radiat. Isotop., 16: 613-15(Oct. 1965).

The experimental values of the attenuation factors for bremsstrahlung in lead were determined by means of Geiger counters calibrated with a Ra source. Attenuation curves in lead for a bremsstrahlung source of $^{90}Sr + ^{90}Y$ are shown. The error in the measurements was estimated to be ± 5%. The experimental values showed better agreement with the theoretical values than previous experimental results. (F.J.H.)

**3255** FISSION NEUTRON AGE AND THERMAL DIFFUSION LENGTH IN ORDINARY CONCRETE. Lim, M. Gene; Johnson, W. Reed; Williamson, T. G. (Univ. of Virginia, Charlottesville). Trans. Amer. Nucl. Soc., 8: 450(Nov. 1965).

**3256** DIRECT-INTERACTION INELASTIC SCATTERING OF ENERGETIC NEUTRONS. Carter, H. G.; Baird, R. C. (General Dynamics, Ft. Worth, Tex.). Trans. Amer. Nucl. Soc., 8: 459(Nov. 1965).

**3257** FAST-NEUTRON SPECTRA IN PARAFFIN SHIELDS. Profio, A. E.; Trimble, G. D.; Houghton, G. K.; Russell, J. L. Jr. (General Atomics Div., General Dynamics Corp., San Diego, Calif.). Trans. Amer. Nucl. Soc., 8: 464-5(Nov. 1965).

**3258** CALCULATION OF THE NUCLEON-MESON CASCADE IN IRON INITIATED BY 1- AND 3-Gev PROTONS AND COMPARISON WITH EXPERIMENT. Alsmiller, R. G. Jr.; Barish, J. (Oak Ridge National Lab., Tenn.). Trans. Amer. Nucl. Soc., 8: 632(Nov. 1965).

**3259** EMPIRICAL FORMULAE FOR SECONDARY NUCLEON-PRODUCTION CROSS SECTIONS. Yucker, W. R. (Douglas Aircraft Co., Inc., Santa Monica, Calif.). Trans. Amer. Nucl. Soc., 8: 632-3(Nov. 1965).

**3260** ENERGY SPECTRA FROM INELASTIC NUCLEAR REACTIONS AT ENERGIES BELOW 450 Mev. Bertini, Hugo W. (Oak Ridge National Lab., Tenn.). Trans. Amer. Nucl. Soc., 8: 634(Nov. 1965).

**3261** ELECTRON-PHOTON CASCADE CALCULATIONS AND NEUTRON YIELDS FROM ELECTRONS IN THICK TARGETS. Alsmiller, R. G. Jr.; Moran, H. S. (Oak Ridge National Lab., Tenn.). Trans. Amer. Nucl. Soc., 8: 634-5(Nov. 1965).

**3262** CALCULATED FLUXES OF LESS THAN 50-Mev NEUTRONS DIFFUSING BENEATH THE SHIELD OF A MESON PRODUCTION FACILITY. Kinney, W. E. (Oak Ridge National Lab., Tenn.). Trans. Amer. Nucl. Soc., 8: 635-6(Nov. 1965).

**3263** INDUCED RADIOACTIVITY DATA COMPUTED FOR VARIOUS MATERIALS AND COMPARISON WITH IRRADIATED SAMPLES. Barbier, M. (CERN, Geneva). Trans. Amer. Nucl. Soc., 8: 637(Nov. 1965).

**3264** PROBLEMS ASSOCIATED WITH A 14-Mev NEUTRON SOURCE IN A CONCRETE ENCLOSURE. Groce, David E. (General Atomic Div., General Dynamics Corp., San Diego, Calif.). Trans. Amer. Nucl. Soc., 8: 637-8(Nov. 1965).

**3265** FAST-NEUTRON SCATTERING FROM SMALL CYLINDERS OF STEEL, ALUMINUM, GRAPHITE, CONCRETE AND LITHIUM HYDRIDE. Courtney, J. C.; Verbinski, V. V.; Betz, N. A. (Oak Ridge National Lab., Tenn.). Trans. Amer. Nucl. Soc., 8: 647(Nov. 1965).

**3266** SINGLE-VELOCITY CALCULATION AND MEASUREMENT OF DIFFERENTIAL ANGULAR THERMAL-NEUTRON ALBEDOS FOR CONCRETE. Maerker, R. E.; Muckenthaler, F. J. (Oak Ridge National Lab., Tenn.). Trans. Amer. Nucl. Soc., 8: 647-8(Nov. 1965).

**3267** ON THE LOW-ENERGY COMPONENT OF THE TOTAL DOSE FOR DEEP-GAMMA PENETRATIONS. Garrett, Charles W. (Armed Forces Radiobiology Research Inst., Bethesda, Md.). Trans. Amer. Nucl. Soc., 8: 648-9(Nov. 1965).

**3268** INFINITE MEDIUM SPECTRUM-WEIGHTED GROUP CONSTANTS FOR GAMMA HEATING CALCULATIONS. Dudley, T. E.; Mendelson, M. R. (General Electric Co., Schenectady, N. Y.). Trans. Amer. Nucl. Soc., 8: 649-50(Nov. 1965).

**3269** HEATING IN INFINITE CYLINDERS BY UNIFORM GAMMA SOURCES. Claiborne, H. C.; Nestor, C. W. Jr. (Oak Ridge National Lab., Tenn.). Trans. Amer. Nucl. Soc., 8: 650-1(Nov. 1965).

**3270** DIFFERENTIAL DOSE ALBEDOS FOR $^{60}Co$ RADIATION AT GRAZING INCIDENCE ON CONCRETE AND STEEL. Clarke, E. T. (Technical Operation Research, Burlington, Mass.). Trans. Amer. Nucl. Soc., 8: 653(Nov. 1965).

**3271** ATTENUATION OF RADIATION FROM A FINITE PLANE SOURCE BY HORIZONTAL CONCRETE SLABS. Little, R.; Velletri, J. (Conesco, Springfield, Va.). Trans. Amer. Nucl. Soc., 8: 653-4(Nov. 1965).

**3272** BASEMENT RADIATION FROM AN INFINITE-PLANE GAMMA SOURCE. Kaplan, Arthur L. (Technical Operation Research, Burlington, Mass.). Trans. Amer. Nucl. Soc., 8: 654-5(Nov. 1965).

**3273** EXPERIMENTAL DIFFERENTIAL NUMBER, ENERGY AND DOSE ALBEDOS FOR SEMI-INFINITE MEDIA, FOR NORMALLY-INCIDENT GAMMA RADIATION. Andrews, D. G.; Steyn, J. J. (Univ. of Toronto). Trans. Amer. Nucl. Soc., 8: 655-6(Nov. 1965).

**3274** PARAMETERS FOR C-H ALBEDO FORMULA FOR GAMMA RAYS REFLECTED FROM WATER, CONCRETE, IRON AND LEAD. Chilton, A. B. (Univ. of

Illinois, Urbana); Davisson, Charlotte M.; Beach, L. A. Trans. Amer. Nucl. Soc., 8: 656-7(Nov. 1965).

**3275** MONTE CARLO TECHNIQUE APPLIED TO A COMPARTMENTED STRUCTURE. Haggmark, L. G. (Naval Research Lab., Washington, D. C.). Trans. Amer. Nucl. Soc., 8: 657-8(Nov. 1965).

**3276** INITIAL RADIATION SHIELD REQUIREMENTS FOR HARDENED STRUCTURES. Karcher, R. H.; Wilson, J. H. (Holmes and Narver, Inc., Los Angeles). Trans. Amer. Nucl. Soc., 8: 658-9(Nov. 1965).

# Solid State Physics

**See also CHEMISTRY — Inorganic and Physical Chemistry**
**METALS, CERAMICS, AND OTHER MATERIALS — Properties and Structure**

*Refer also to abstract 3087.*

**3277** (BLG-328) A NEW APPROACH TO CONTINUUM POLARON THEORY. Evrard, R.; Kartheuser, E.; Devreese, J. (Centre d'Etude de l'Energie Nucleaire, Brussels (Belgium)). Jan. 1965. 6p. (CONF-65117-1). Dep. mn.

From 2nd Conference on Solid State Physics, Bristol, Eng.

The polaron problem is treated in the Heisenberg representation. After the elimination of the phonon variables from the equations an harmonic approximation is made on the motion of the electron. For the first time nondivergent results for the energy of the polaron in the classical case are obtained. (auth)

**3278** (COO-1198-222) INFLUENCE OF DISLOCATION DIPOLES ON PHYSICAL PROPERTIES. Gilman, J. J. (Illinois Univ., Urbana). [1964]. Contracts AT(11-1)-1198; Nonr-3985(06). 37p. Dep. mn; CFSTI $2.00 cy, $0.50 mn.

A survey was made on the effects that edge dislocation dipoles can be expected to have on the physical properties of plastically deformed crystals. It is believed that some effects previously attributed to monopoles are more closely associated with dipoles. Various properties of dipoles are reviewed. (P.C.H.)

**3279** (ORNL-P-1704) X-RAY TOPOGRAPH EXAMINATION OF VACANCY CLUSTERS IN NEARLY PERFECT COPPER CRYSTALS. Young, F. W. Jr.; Baldwin, T. O.; Sherrill, F. A. (Oak Ridge National Lab., Tenn.). [1965]. Contract W-7405-eng-26. 22p. (CONF-650927-4). Dep. mn; CFSTI $1.00 cy, $0.50 mn.

From American Physical Society, Honolulu, Hawaii.

Vacancies present at temperatures near the melting point in nearly perfect 99.999% copper crystals with dimensions of order centimeters cluster upon cooling the crystal, and the clusters are visible as black spots in Borrmann x-ray topographs. Phenomenological evidence that the black spots correspond to some form of vacancy cluster is presented. The diffraction contrast of the black spot images was examined in a series of 111, 220, 200, and 222 topographs taken with Ag, Mo, Cu, and Cr $K_{\alpha_1}$ radiation. Some of the images show the proper contrast for prismatic dislocation loops. Many of the images appear in all topographs. Images of defects that intersect the exit surface for the x rays show a black-white contrast which can be interpreted in terms of vacancy loops. It was concluded that the evidence from diffraction contrast supports the assumption that the black spots correspond to vacancy clusters of various forms. (auth)

**3280** (ORNL-P-1737) THE MAGNETIC FORM FACTOR OF CHROMIUM. Moon, R. M.; Koehler, W. C.; Trego, A. L. (Oak Ridge National Lab., Tenn.). Oct. 1965. Contract W-7405-eng-26. 9p. (CONF-651106-3). Dep. mn; CFSTI $1.00 cy, $0.50 mn.

From Conference on Magnetism and Magnetic Materials, San Francisco.

Neutron diffraction measurements of the magnetic Bragg peaks from single crystals of chromium with small additions of manganese were used to determine the magnetic form factor of chromium. The addition of manganese simplifies the experimental problem by stabilizing the simple antiferromagnetic structure. A single magnetic peak was observed at reciprocal lattice positions, rather than a group of six satellite peaks as in pure chromium. Also, manganese increases the Néel point so that the measurements were performed at room temperature. The results are in good agreement with free atom Hartree-Fock calculations for the chromium 3d electrons. A definite indication of nonspherical symmetry was obtained by comparing the (221) and (300) reflections. These reflections come at the same scattering angle, yet the (221) intensity is larger by about a factor of six. This indicates a $t_{2g}$ population of 79%, compared to 60% for a spherical spin distribution. The results are independent of manganese concentration over a range from 1.7 to 4.1 atomic percent. (auth)

**3281** (MLM-1276(tr)) INTERNAL FRICTION AT HIGH TEMPERATURES AND DIFFUSION OF VACANCIES BETWEEN DISLOCATIONS. Escaig, B. Translated by J. E. Selle (Mound Lab., Miamisburg, Ohio) from Acta Met., 10: 829-34(1962). 16p. Dep. mn; JCL $1.60 fs, $0.80 mf.

A theory is given of amplitude independent internal friction by diffusion of vacancies between dislocations of the lattice which emit or absorb them. The case of the polygonized structure and the Frank array are discussed. Both cases are treated with the Nabarro creep formalism. The equations of diffusion are resolved, assuming that dislocations emit or absorb vacancies easily (small jog energies). The internal friction is found for any frequency of applied stress. Two simplified expressions are derived for internal friction, at high or low frequencies, and are compared with experiment. At low frequencies, the calculated activation energy, i.e., the self-diffusion energy, is in good agreement with experiment. At high frequencies, however, the experiment seems to show an activation energy much smaller than that predicted by this model. (auth)

**3282** THE PHOTOLUMINESCENCE OF SILVER-CONTAINING QUARTZ. PART II. Gross, F. (Universitaet Graz). Acta Phys. Austriaca, 19: 308-24(1965). (In German).

The description of the experimental results obtained in the study of the photoluminescence of silver-containing quartz is completed. The significance of these results is discussed with respect to the coagulation tendencies, electron yield and colloidal germs, band assignment, luminescence of quartz glass, and kinetics of the centers. (J.S.R.)

**3283** STIMULATED EMISSION FROM 4.3 percent ABUNDANT $^{50}Cr$ IONS IN RUBY. Riley, L. W.; Bass, M.; Hahn, E. L. (Univ. of California, Berkeley). Appl. Phys. Letters, 7: 88-90(Aug. 15, 1965).

Stimulated emission was observed from chromium-50 ions in a Q-spoiled ruby laser. The $R_1$ stimulated emission from a 0.05%-concentration, 3-in. by ¼-in., 90°-orientation ruby rod at temperatures below 100°K in both burst and Q-spoiled operation is discussed. In Q-spoiled operation one or two 25-kw pulses were obtained by using a rotating 55% dielectric mirror in conjunction with a phthalocyanine in chloronaphthalene saturable filter solution. The spectroscopic data were obtained using a plane grating monochromator. At threshold input energy, about 400 J, two lines were observed in the Q-spoiled laser's output. They correspond to the $R_1$ lines of $^{52}Cr$. When the input energy was increased to about 1½ times threshold, a third line was observed in the laser's spectrum. This line was much weaker than the first two, has a threshold well above either of them, and is shifted by 0.13 Å towards longer wavelengths from the long wavelength component of the $^{52}Cr$ line. This third line is the long wavelength component of the $R_1$ line of the $^{50}Cr$ ions. These lines are all shown. Also the relative intensities of the $^{52}Cr$ $R_1$ lines

were measured in both the burst and the Q-spoiled operation. These results are also shown. (J.F.P.)

**3284** ENERGY LEVELS AND RELATIVE INTENSITIES OF NQR LINES FOR SOME INTEGRAL SPINS. Ainbinder, N. E.; Grechishkin, V. S. (Perm State Univ., USSR). Izv. Vysshikh Uchebn. Zavedenii, Radiofiz., 8: 416-20(1965). (In Russian).

Equations were obtained for energy levels and nuclear quadrupole resonance line intensities for integral spins of $J \geq 2$ and $J \geq 3$ and for relative line intensities which hold for any arbitrary asymmetry parameters. The obtained formulas can be used for determining asymmetry parameters and absorption lines in monocrystals. (R.V.J.)

**3285** SCATTERING OF LONG WAVELENGTH NEUTRONS BY PRECIPITATIONS IN $Al_{99.5}Cu_{0.5}$ ALLOYS. Sakamoto, Masanobu; Kunitomi, Nobuhiko (Japan Atomic Energy Research Inst., Tokyo). J. Phys. Soc. Jap., 20: 1723(Sept. 1965).

Cross sections for neutron scattering by precipitation clusters in $Al_{99.5}Cu_{0.5}$ were obtained by subtracting the cross sections measured for specimens quenched from 500°C from those annealed at 200°C for 245 hours. The excess scattering is attributed to the precipitation of copper atoms. Preliminary calculations were performed, assuming that the cluster contains nine copper and four aluminum atoms in the tetragonal structure; poor agreement was found for wavelength dependence of the excess scattering cross section. (L.B.S.)

**3286** THE EFFECT OF STRAIN RATE ON DISLOCATION MULTIPLICATION IN POLYCRYSTALLINE MOLYBDENUM. Gilbert, A.; Wilcox, B. A.; Hahn, G. T. (Battelle-Columbus Labs., Columbus, Ohio). Phil. Mag. (8), 12: 649-53(Sept. 1965).

Dislocation densities were measured as a function of plastic strain in recrystallized molybdenum tested at strain rates of $2 \times 10^{-5}$ and approximately $2 \times 10^{3}$ $sec^{-1}$. Only a small difference in total dislocation density was observed for the two rates, indicating that an increase in strain rate by $10^8$ was accommodated mainly by an increase in the average dislocation velocity rather than in the number of mobile dislocations. (auth)

**3287** BAND STRUCTURE OF GALLIUM ARSENIDE: SPIN-ORBIT SPLITTING. Cardona, M. (Brown Univ., Providence); Pollak, F. H.; Broerman, J. G. Phys. Lett., 19: 276-7(Nov. 1, 1965).

The effect of the spin-orbit interaction on the band structure of gallium arsenide is presented. This is calculated by perturbation theory using the eigenvectors of the $k \cdot p$ hamiltonian of GaAs. The effect of the spin-orbit interaction on the valence bands and lowest conduction bands of germanium can be calculated using only two matrix elements of the spin-orbit hamiltonian. The valence bands in the [111] and [100] directions including the spin-orbit interaction are shown. The spin-orbit splitting of the upper valence bands and lowest conduction band of GaAs is shown in the [110] direction. (J.F.P.)

**3288** MICROWAVE ABSORPTION AND MAGNETIC TRANSITION IN $GdCl_3$. Becker, E.; Bonrath, H.; Hellwege, K. H.; Kuech, F.; Schinkmann, M.; Unger, B. (Technische Hochschule Darmstandt, Ger.). Phys. Letters, 19: 86-7(Oct. 1, 1965).

It is shown that the change of the magnetization due to microwave absorption is a very sensitive indicator for the detection of magnetic transition temperatures. This method is particularly suitable for the determination of the line shape functions of levels in diamagnetic diluted and undiluted crystals. The temperature region within which the ordering process takes place can be carefully investigated. This method was previously applied to the ferromagnetic ordering process of $GdCl_3$. This substance was chosen because of its simple S-ground state and the relative high Curie temperature of 2.20°K. Results are shown, and it is seen that the ordering process takes place within a temperature region less than 0.01°K. An ordering temperature of $2.20 \pm 0.01$°K is derived in good agreement with previous results. (J.F.P.)

**3289** MOESSBAUER EFFECT OF $^{57}Fe$ DOPED IN $V_2O_3$. Shinjo, T.; Kosuge, K.; Shiga, M.; Nakamura, Y.; Kachi, S.; Takaki, H. (Kyoto Univ.). Phys. Letters, 19: 91-2(Oct. 1, 1965).

The existence of antiferromagnetism in the low temperature phase of $V_2O_3$ is confirmed by the Mössbauer effect in doped $^{57}Fe$. A sample was prepared in which a small quantity of V atoms was substituted by $^{57}Fe$ atoms and heated at 1200°C for 20 hours in an evacuated silica tube and quenched from 800°C. Mössbauer experiments were made at 300 and 110°K, and the results are shown. At 110°K, which is well below the transition temperature, a clear magnetic hyperfine splitting appeared. The splitting corresponds to 330 kOe and apparently is originated from an antiferromagnetic ordering. The co-existing quadrupole interaction must be due to the crystalline distortion. The precise temperature dependence of the internal field will clarify the character of the transition by showing whether Néel temperature agrees exactly with the transition temperature. (J.F.P.)

**3290** MOESSBAUER EFFECT IN Sn–Pt ALLOYS. Kanekar, C. R.; Rao, K. R. P. Mallikarjuna; Rao, V. Udaya Shankar (Tata Inst. of Fundamental Research, Bombay). Phys. Letters, 19: 95-6(Oct. 1, 1965).

The Mössbauer effect was observed in tin–platinum alloys, using a conventional constant velocity loudspeaker drive for moving the source. The data for isomer shifts and quadrupole splittings observed are given. These isomer shifts are found to be negative with reference to $^{119}Sn$ in tin metal and to increase systematically with the decrease in the concentration of tin in the alloys. This indicates that in these alloys the s-electron density at the tin site is smaller than that in white tin and it decreases with a decrease in the tin concentration in the alloy. The number of 5 s-electrons at the tin site in the various alloys is also given. The Knight shift for $^{119}Sn$ in $Nb_3Sn$ is negative, large, and temperature dependent, whereas in $Pt_3Sn$ it is only slightly negative and temperature dependent. It is noted that a quadrupole splitting was observed in $Pt_3Sn$ although its structure is cubic and the local symmetry is also cubic. On the other hand, the structure of PtSn is hexagonal and a quadrupole splitting is expected, although no resolvable splitting could be observed. For the other alloys, the local symmetry is non-cubic and the splitting could be observed as expected. (J.F.P.)

**3291** STRAIN EFFECTS IN RARE EARTH TRANSITIONS. Burns, G.; Axe, J. D. (IBM Watson Research Center, Yorktown Heights, N. Y.). Phys. Letters, 19: 98-9(Oct. 1, 1965).

The pressure dependence of the crystal field of the rare earth $Tm^{2+}:CaF_2$ is reported. The result is about 30% larger than that predicted by an ionic model. Measurements of the $\Gamma_7' \rightarrow \Gamma_7$ line of $Tm^{2+}:CaF_2$ were made with uniaxial stress applied along the ⟨111⟩, ⟨110⟩, and ⟨100⟩ directions. Stresses as high as $4.05 \times 10^9$ dyn/cm were applied. The fluorescence measurements were made, usually at 4.2°K on a one meter grating monochromator with a cooled PbS detector. Linewidths of about 0.12 $cm^{-1}$ were observed and shifts up to six linewidths were measured. The line shifts were accurately found to be independent of direction, and linear with the applied stress. An experimental result of $\Delta(W_4 - W_1)/\beta = -499$ $cm^{-1}$ was found. The strain effect on the $\Gamma_7'$ to $\Gamma_7$ transition is predicted to be about 30% smaller than measured. Preliminary measurements on $Tm^{2+}:SrF_2$ confirm this discrepancy. (J.F.P.)

**3292** INVESTIGATIONS OF THE ORDERING TRANSFORMATION IN THE $Fe_3Al$ ALLOY BY MOESSBAUER EFFECT. Cser, L.; Dezsi, I.; Keszthelyi, L.; Ostanevich, J.; Pal, L. Phys. Letters, 19: 99-100(Oct. 1, 1965).

The effect of the atomic ordering on the local magnetization is observed by the Mössbauer effect. The experiments were performed using as absorbent $Fe_3Al$ foil of 14.8 mg/$cm^2$ thickness with 24.8 atomic percent aluminum content. The absorbent was placed in a vacuum furnace and sandwiched between two beryllium plates to minimize the radial inhomogeneity of the absorbent temperature. The maximum of the relative deviation in the temperature within the irradiated foil surface was within $(\Delta T/T)_{max} < 4 \times 10^{-3}$. It was

found that the paramagnetic and hyperfine peaks coexist below the Curie temperature of the disordered alloy within a rather large temperature interval. The temperature dependence of the internal magnetic field in the disordered (or pseudo ordered) alloy and the temperature dependence of the area ratio of the central to the resolved hyperfine peaks are shown. The temperature dependence of the isomer shift, which has a break near the Curie point, is also shown. The results confirm those obtained in the earlier macroscopic magnetic measurements; and it is shown that the $D_2O$ type ordered alloy at the initial stage of the ordering process exhibits a well expressed paramagnetic behavior. (J.F.P.)

**3293** NEUTRON DIFFRACTION STUDIES ON THE $(1-x)Fe_2O_3$–$xRh_2O_3$ SYSTEM. Kren, E.; Szabo, P.; Konczos, G. (Central Research Inst. for Physics, Budapest). Phys. Letters, 19: 103-4(Oct. 1, 1965).

Magnetic and crystallographic structure properties of the $(1-x)Fe_2O_3-xRh_2O_3$ system are reported. The neutron diffraction measurements were carried out in this temperature range from 77 to 1000°K. Super-reflections characteristic of the hematite magnetic order appeared but other magnetic or atomic super-reflections were not detected. The magnetic moments were measured at 77°K and given for the average ion of the sublattice and for one Fe ion. The Néel temperature $T_N$ and the Morrin temperature $T_S$ at which the spins turn from the direction [111] into the plane [111] and where a weak ferromagnetism sets in were determined from the temperature dependence of the [111] and [100] reflections. The results are summarized, and the temperature ranges are also shown at the values of $T_S$. It is clearly apparent from the measured data that the addition of Rh cations results simply in magnetic dilution. The linear decrease indicates the magnetization of the sublattice to be due exclusively to Fe cations and the value of the magnetic moment per Fe ion to be the same as in pure hematite. The most striking feature of the system is the increase of the transformation temperature $T_S$ with the concentration. (J.F.P.)

**3294** DISPERSION OF LATTICE WAVES IN TUNGSTEN. Pal, S.; Sharma, P. K. (Allahabad Univ., India). Phys. Letters, 19: 105-6(Oct. 1, 1965).

The validity of a model for the dispersion of lattice waves in tungsten is tested comparing the dispersion curves deduced from the theory with the neutron scattering data. The dispersion curves for tungsten along symmetry directions [100], [110], and [111] are computed using the dispersion relations for body-centered cubic metals, and the calculated dispersion curves are shown. It is seen that the relations for tungsten deduced from the model are in broad agreement with the neutron spectroscopic data. At the zone boundary for [100] and [111] directions, the model slightly violates the symmetry requirements of the bcc structure. Along [110] direction, the calculated transverse branches are degenerate due to the isotropy relation between the elastic constants of tungsten. (J.F.P.)

**3295** $^{55}$Mn ZERO-FIELD NUCLEAR MAGNETIC RESONANCE IN THE ANTIFERROMAGNET MnSe. Jones, E. D. (Sandia Lab., Albuquerque, N. Mex.). Phys. Letters, 19: 106-7(Oct. 1, 1965).

Observations of the $^{55}$Mn zero-field nuclear magnetic resonance in the antiferromagnetic state of MnSe are reported. Also a summary of the current data for the $^{55}$Mn hyperfine interaction in the three isomorphic antiferromagnetic salts MnO, $\alpha$-MnS, and MnSe is included. These data indicate an apparent increase in the $^{55}$Mn hyperfine coupling constant in the concentrated salts over the value determined by electron spin resonance measurements in nonmagnetic host crystals. The $^{55}$Mn zero-field nuclear magnetic resonance in antiferromagnetic MnSe was observed between 1.5 and 4.0°K using a frequency-modulated superregenerative u-h-f oscillator at a frequency of $^{55}\nu = 554.6 \pm 0.2$ Mc. From the sideband response of the superregenerative spectrum the $^{55}$Mn nuclear magnetic resonance linewidth is $\delta H = 1000$ Oe. It is found that the hyperfine coupling constant increases to about $-77 \times 10^{-4}$/cm, taking into account the expected zero point spin reduction of about 3%. (J.F.P.)

**3296** MOESSBAUER SPECTRA OF ALKALINE FERROCYANIDES. Matas, J.; Zemcik, T. (Czechoslovak Academy of Sciences, Rez). Phys. Letters, 19: 111-12 (Oct. 1, 1965).

Mössbauer spectra of alkaline ferrocyanides and analogous compounds of type $M_4Fe(CN)_6 \cdot aq$(M = H, Li, Na, K, Rb, Cs, $NH_4$) were measured. They are very similar to the previous measurements of $K_4Fe(CN_6) \cdot 3H_2O$ and of $Na_4Fe(CN_6) \cdot 10H_2O$, that is, they consist of simple lines without magnetic and measurable quadrupole splitting. All spectra were measured by means of the cam-valve constant-velocity Mössbauer spectrometer. For each run the data were fitted to a spectrum of either Lorentzian or Gaussian shape by means of a least squares analysis of an ELLIOTT 803 computer. The analysis of the spectra shows better fits with the Lorentzian than with the Gaussian shape. The results are plotted in the dependence on the electronegativity of cations. It is seen that with the increase of atomic number, that is, with the decreasing of electronegativity the center of line shift shows a systematic trend, and it is possible that the same trend shows the line width. The value of the resonance effect is approximately constant. These effects are explained. (J.F.P.)

**3297** g FACTOR OF CONDUCTION ELECTRONS IN METALLIC LITHIUM. Pressley, R. J.; Berk, H. L. (Princeton Univ., N. J.). Phys. Rev., 140: A1207-10 (Nov. 15, 1965).

The electron spin resonance of metallic lithium particles immersed in mineral oil has been carefully examined in order to determine the g shift of the conduction electrons with respect to the free-electron value. By comparing the ESR frequency with the proton nuclear-spin frequency of the mineral oil, and extending Dyson's line-shape theory to apply to intermediate-size metallic particles, the shift at room temperature was found to be $\Delta g = -2 \times 10^{-6}$. This small g shift indicates that the inherent linewidth of the ESR in metallic lithium may well be only 4 mG in a 3000-G field. In addition, an Overhauser enhancement of over 750 was measured when the lithium NMR was monitored and the ESR saturated. The shift in the lithium NMR arising from ESR saturation demonstrated that at least 75% of the measured Knight shift is due to electron-gas paramagnetism. (auth)

**3298** BLOCH ELECTRONS IN EXTERNAL ELECTRIC AND MAGNETIC FIELDS. Praddaude, H. C. (Massachusetts Inst. of Tech., Cambridge). Phys. Rev., 140: A1292-6(Nov. 15, 1965).

The Schrödinger equation for a Bloch electron in external electric and magnetic fields is rewritten with the help of redundant variables, the wave function being obtained when a limiting process is carried out. The connection with the standard effective-mass approximation is discussed, and an application to the case of crossed electric and magnetic fields is carried out for the simple case of two parabolic bands in order to examine the singularity $\frac{1}{2}m^*(E/B)^2$ that appears in the energy in the effective-mass approximation when $B \to 0+$. It is concluded that below a certain value of E/B the character of the solution changes and the effective-mass formula is then not applicable. (auth)

**3299** NUCLEAR ELECTRIC-FIELD GRADIENT DETERMINATION UTILIZING THE MOESSBAUER EFFECT ($^{57}$Fe). Zory, Peter (Carnegie Inst. of Tech., Pittsburgh). Phys. Rev., 140: A1401-7(Nov. 15, 1965).

If a compound containing $^{57}$Fe exhibits a two-line Mössbauer absorption spectrum, as is the case for most paramagnetic ferrous salts, then this spectrum may usually be attributed to the electrostatic interaction between an electric-field gradient (EFG) and the quadrupole moment of the first excited state of the $^{57}$Fe. Since the EFG may be represented as a traceless, symmetric tensor of the second rank, it is completely specified by five independent parameters. If the absorber is a single crystal, the two absorption peaks will generally have different intensities,

the ratio of the intensities depending upon the orientation of the incident, unpolarized radiation relative to the crystal axes. In this paper, a general method is developed which utilizes this intensity ratio to determine the five EFG parameters. The possibility of an anisotropic recoilless factor is also considered. The method is then applied to $FeCl_2 \cdot 4H_2O$. (auth)

**3300** de HAAS-van ALPHEN EFFECT IN PYROLYTIC AND SINGLE-CRYSTAL GRAPHITE. Williamson, S. J. (Massachusetts Inst. of Tech., Cambridge); Foner, S.; Dresselhaus, M. S. Phys. Rev., 140: A1429-47(Nov. 15, 1965).

The de Haas–van Alphen (DHVA) oscillations have been observed in the differential susceptibility of well-annealed pyrolytic graphite (PG) with the low-frequency field-modulation technique. The results for PG are compared with similar studies of natural single crystal (SCG) by Soule et al., and by the present authors. Majority-electron and majority-hole DHVA periods in PG are resepctively equal to the periods in SCG for $0° \leq \theta \lesssim 50°$, where $\theta$ is the angle between the applied field and the c axis of the sample. Observation of a long-period, minority-carrier DHVA oscillation in PG and SCG confirms Soule's discovery of such an oscillation in SCG and provides a sensitive test for the Slonczewski-Weiss band model. The minority-carrier oscillation in PG is qualitatively but not quantitatively similar to the one in SCG. This oscillation is attributed to magnetic energy levels passing through the Fermi level near the Brillouin-zone corner at $k_z = \pi/c_0$, where for $\theta = 0°$ there is no extremal area of the Fermi surface at zero field, when spin-orbit interactions are neglected. This interpretation is supported by the calculation of an oscillatory free energy and by the excellent agreement for PG between the predicted values and experimental results for the period, effective mass, period anisotropy, and phase. The phase is not the value which would be predicted from a free-electron model for either a maximal or a minimal cross-sectional area. The existence of minority-carrier oscillations in PG indicates that the hole and electron Fermi surfaces are closed and that the electron surface intersects the hexagonal face of the Brillouin zone. The band parameters of the Slonczewski-Weiss model for PG were evaluated from the DHVA data and the preliminary magnetoreflection measurements of Dresselhaus and Mavroides. A similar analysis for SCG was carried out successfully for the majority-carrier pockets, but did not provide a consistent picture for the minority-carrier surface. The effects of spin-orbit interaction on the Fermi surface are discussed. Neutron and x-ray diffraction studies show that the c axes of the individual crystallites in a PG sample are aligned to no better than ~1°. The effects of this misalignment as well as of the finite crystallite size on the DHVA oscillations are considered. (auth)

**3301** NEUTRON-DIFFRACTION STUDY OF ANTIFERROMAGNETISM IN $UO_2$. Frazer, B. C. (Brookhaven National Lab., Upton, N. Y.); Shirane, G.; Cox, D. E.; Olsen, C. E. Phys. Rev., 140: A1448-52(Nov. 15, 1965). (BNL-9318).

Antiferromagnetism in $UO_2$ has been investigated in a detailed single-crystal neutron-diffraction study. Work on this material was prompted by a general interest in unpaired 5f and 6d electron distributions for different valence states of uranium in simple compounds. The form factor determined in the present case indicates a $5f^2$ electronic configuration with an effective moment slightly less than $1.8\mu_B$ for the $U^{4+}$ ion. The magnetic ordering of the first kind, reported earlier by Henshaw and Brockhouse, is confirmed, but their proposed [111] orientation for the magnetization axis is not. The axis is found to be within the alternating ferromagnetic sheets. In the course of the diffraction study it was found that the paramagnetic-to-antiferromagnetic transition is an unusually sharp one, especially for such a simple magnetic system. Accordingly, the temperature dependence of magnetic neutron intensities was investigated through the Néel point. From the sharpness of the transition (50% of the magnetization is established within 0.03° below the Néel temperature), and the absence of a critical scattering peak, it is concluded that the transition is of the first order. (auth)

**3302** OBSERVATION OF RESONANT LATTICE MODES BY INELASTIC NEUTRON SCATTERING. Moeller, H. Bjerrum (Research Establishment Risoe, Roskilde, Denmark); Mackintosh, A. R. Phys. Rev. Letters, 15: 623-5(Oct. 11, 1965). (IS-1201).

The observation by inelastic neutron scattering of resonant lattice modes due to a small concentration of W atoms in a Cr host crystal is reported. Since tungsten is a very heavy atom, the resonant modes should be well developed. Therefore the lower transverse [110] phonon branch was studied in single crystals of Cr and a Cr-3.0-at. % W alloy by inelastic neutron scattering, using the constant-$\vec{q}$ method. The observed neutron groups, and the energy shifts plotted as a function of the phonon energies in pure Cr are shown. There is clear evidence of a resonant mode near 21 Mev. There is a large change in the frequency shift, of the right order of magnitude, while the neutron groups broaden perceptibly near q = 0.694. The predicted maximum width of about 3 Mev is also observed. The discrepancies noted are ascribed to the relatively large concentration of impurities and changes in the force constants near them. The resonant mode occurs at approximately one-half of the maximum phonon energy of 42 Mev in Cr. (J.F.P.)

**3303** OBSERVATIONS ON THE FERMI SURFACE OF ALUMINUM BY NEUTRON SPECTROMETRY. Stedman, R.; Nilsson, G. (Aktiebolaget Atomenergi, Studsvik, Sweden). Phys. Rev. Letters, 15: 634-7(Oct. 11, 1965).

The dispersion relations for phonons are determined in aluminum at 80 and 300°K by slow neutron spectrometry, using a three-axis spectrometer. The expected sites of Kohn anomalies in aluminum are shown. The expected positions and relative sizes of these anomalies in aluminum are also shown. The slope versus g for the (1,1,1) L and T curves and for the (2,0,0) L and T curves are given and discussed. Points on the Fermi surface corresponding to six of the anomalies discussed are shown as a section through the Fermi surface. A rough estimate of the magnitude of anomalies in aluminum may be made from three of them which correspond to points on the Fermi surface far from the Bragg planes, and for which the given estimates may be reasonable. In frequency units of $10^{13}$ rad/sec the resulting figure is $(0.3 \pm 0.15)$ times the estimated relative strength given. (J.F.P.)

**3304** METHODS FOR DETERMINING THE ISOTOPIC DIFFUSION EFFECT IN A SOLID. Naumov, A. N.; Ptashnik, V. B. (Ioffe Inst. of Physics and Tech., Leningrad). Soviet Phys.-Solid State (English Transl.), 7: 543-6(Sept. 1965).

Translated from Fiz. Tverd. Tela, 7: 677-82(Mar. 1965).

Exact and approximate formulas are deduced, relating the experimentally determined separation factor to the magnitude of the isotopic diffusion effect in a solid. A comparison is made of the effectiveness of some diffusion systems from the point of view of obtaining a maximum separation factor. (auth)

**3305** ISOTOPIC EFFECT IN THE DIFFUSION OF LITHIUM IN SODIUM. Naumov, A. N.; Ryskin, G. Ya. (Ioffe Inst. of Physics and Tech., Leningrad). Soviet Phys.-Solid State (English Transl.), 7: 558-9(Sept. 1965).

Translated from Fiz. Tverd. Tela, 7: 695-6(Mar. 1965).

A study was made of the isotopic effect in the diffusion of Li in polycrystalline Na at 80°C. The ratio of the diffusion coefficients of the isotopes, $^6Li$ and $^7Li$, was $1.073 \pm 0.006$, in good agreement with the theoretical value of 1.08 (the square root of the ratio of the isotope masses). (auth)

**3306** THE MECHANISM OF FORMATION OF GROWTH TEXTURES IN BERYLLIUM CONDENSATES. Palatnik, L. S.; Fedorenko, A. I. (Lenin Kharkov Polytechnic Inst., USSR). Soviet Phys.-Solid State (English Transl.), 7: 653-6(Sept. 1965).

Translated from Fiz. Tverd. Tela, 7: 819-22(Mar. 1965).

X-ray diffraction, electron diffraction, and optical and electron microscopy were used to investigate the mechanism of formation of growth textures and growth forms in

beryllium films condensed on a polycrystalline substrate. The initial stage of formation of the growth texture is observed at some thickness $h_t$ of the condensate which increases with increase in the temperature $T_s$ of the substrate. The effect is related to the degree of dispersion of the condensate crystals. (auth)

**3307** ISOTOPIC EFFECT IN THE VALUES OF THE MOLAR VOLUMES OF LiF AND LiH. Kogan, V. S.; Omarov, T.G. (Inst. of Physics and Tech., Academy of Sciences, Khar'kov; Physics Inst., Academy of Sciences, Baku). Soviet Phys.-Solid State (English Transl.), 7: 747-8(Sept. 1965).

Translated from Fiz. Tverd. Tela, 7: 933-4(Mar. 1965).

$^6$LiF and $^7$LiF samples were studied using Co radiation in an x-ray camera; samples of lithium hydrides were studied using Cu$K_\alpha$ radiation in the same camera. Values of the isotopic effect in the molar volume ($\Delta V/V$), average linear expansion coefficient, and lattice parameters at 78 and 300°K are tabulated, which were obtained from analysis of the x-ray diffraction patterns. (L.B.S.)

**3308** THE DETERMINATION OF THE INTERPLANAR SPACINGS IN POLYMERS USING SINGLE-NEUTRON DIFFRACTION. Akin, Erol; Duffey, Dick (Univ. of Maryland, College Park). Trans. Amer. Nucl. Soc., 8: 370(Nov. 1965).

**3309** QUASI FERMI LEVEL ANALYSIS OF RADIATION-INDUCED CONDUCTIVITY IN CERAMIC INSULATORS. Bohren, Craig F.; Davis, Monte V. (Univ. of Arizona, Tucson). Trans. Amer. Nucl. Soc., 8: 370-1 (Nov. 1965).

**3310** ELECTRON DIFFRACTION BY CRYSTALLINE HYDROGEN. Bostanjoglo, O. (Technische Universitaet, Berlin). Z. Physik, 187: 444-9(1965). (In German).

The crystalline structure of polycrystalline n-, p-hydrogen and n-deuterium layers were examined by electron diffraction. Five of the seven Debye-Scherrer rings found in the diffraction pattern were ascribed to a face-centered cubic lattice with $a = 5.35 \pm 0.02$ Å for hydrogen and $5.08 \pm 0.03$ Å for deuterium. The remaining two diffraction rings could arise either from diffraction by crossgratings and double diffraction by twinned crystals or from a hexagonal lattice. The first explanation is however more probable since the relative intensities of the rings are wrong according to the kinematical theory of electron diffraction if a hexagonal lattice is supposed, and they respond differently to changes of the substrate temperature. (auth)

**3311** DYNAMIC POLARIZATION OF PROTONS IN A ROTATING LANTHANUM–MAGNESIUM NITRATE CRYSTAL. Lushchikov, V. I.; Neganov, B. S.; Parfenov, L. B.; Taran, Yu. V. (Joint Inst. for Nuclear Research, Dubna, USSR). Zh. Eksp. Teor. Fiz., 49: 406-9(Aug. 1965). (In Russian).

A new possibility of polarization of nuclei in anisotropic crystals by rotating them in a stationary magnetic field and weak radiofrequency field is reported. A proton polarization amplification coefficient of about 70 has been obtained in a field of 5 kOe and frequency of 165 Mc/s. An advantage of the method is the very low uniformity and stability required of the magnetic field and the use of radio frequencies in the meter range instead of ultra high frequencies. (auth)

**3312** MAGNETOSTRICTION IN A GADOLINIUM CRYSTAL. Belov, K. P.; Ergin, Yu. V.; Ped'ko, A. A. (Moscow State Univ.). Zh. Eksp. Teor. Fiz., 49: 414-19 (Aug. 1965). (In Russian).

The magnetostriction of a gadolinium crystal is measured for various crystallographic directions as a function of the magnetic field strength and temperature. It is found that magnetostriction of the paraprocess along the hexagonal axis is not only great near the Curie temperature but also at lower temperatures (beginning at 180°). The spontaneous magnetostriction $\lambda_s'$ due to change in the exchange energy on transition through the Curie point as calculated by the thermodynamic coefficient method is found to be sharply anisotropic. The curve of the temperature dependence of saturation magnetostriction $\lambda_s$, which is obtained after separation of magnetostriction of the paraprocess, is found to possess a complicated form. Some of the curves have maxima in the 200–250°K temperature range. (auth)

**3313** EFFECT OF UNIFORM COMPRESSION ON THE CURIE TEMPERATURE OF THE FERROMAGNETIC COMPOUND EuO. Sokolova, G. K.; Demchuk, K. M.; Rodionov, K. P.; Samokhvalov, A. A. (Inst. of Physics of Metals, Academy of Sciences, USSR). Zh. Eksp. Teor. Fiz., 49: 452-5(Aug. 1965). (In Russian).

The dependence of the Curie temperature of EuO on uniform compression is investigated at pressures up to 12 katm. It is shown that in this pressure range the Curie temperature of EuO linearly increases with the pressure, $d\Theta/dp = (4 \pm 1) \cdot 10^{-4}$ degree · atm$^{-1}$. (auth)

**3314** POSITRON ANNIHILATION IN THE $e^+$Li SYSTEM. Hoang, Dinh Van (Belorussian State Univ., USSR). Zh. Eksp. Teor. Fiz., 49: 630-4(Aug. 1965). (In Russian).

The $e^+$ Li atomic system is investigated by a variational method. The value ~2.13 ev is obtained for the positron binding energy and $3.2 \cdot 10^{-10}$ sec for the positron lifetime with respect to annihilation by an optical electron of Li. These values are exactly the same as those found experimentally by Bell and Jørgensen. (auth)

**3315** MEASUREMENT OF THE PHONON FREQUENCY DISTRIBUTION FOR POLYETHYLENE BY NEUTRON SCATTERING [Thesis]. Donovan, John Leo. Ann Arbor, Mich., Univ. of Michigan, 1964. 139p.

Neutron inelastic scattering experiments were used to investigate low frequency (0 – 800 cm$^{-1}$) vibrational motions in highly crystalline polyethylene. Warm neutrons (0.025–0.15 ev) were downscattered from polyethylene targets at 298, 125, and 90°K. Phonon excitation corresponding to neutron energy loss was determined. The measured inelastic cross section data were analyzed using the one-phonon incoherent approximation to determine the phonon frequency distribution. The corrections to the observed data necessary to obtain the cross section are discussed. The design features of the spectrometer which provide sufficient intensity for inelastic scattering experiments with a two megawatt reactor source are presented. The four low frequencies seen in previous neutron experiments at 100°K (60, 130, 190 and 340 cm$^{-1}$) are confirmed but some additional frequencies were observed. These frequency values are compared with models that attempt to account for intermolecular effects in the crystalline molecular structure. Frequency spectra at 90° are reported for two target thicknesses (29.5 and 16.1 mils). The spectra indicate that multiple scattering effects are small. Good agreement between these spectra and the cold neutron spectrum at 100°K is found for the frequency range below 200 cm$^{-1}$. Above 330 cm$^{-1}$ the agreement is poor; both sets of experiments are less reliable above about 450 cm$^{-1}$. Both the cold and warm spectra show much larger amplitude in the frequency region 250–450 cm$^{-1}$ than the spectrum calculated by Wunderlich using specific heat data. The effect of multiphonon interference on the measured scattering data apparently does not produce a major difference between the cold and warm neutron techniques for low temperature polyethylene. An important intensity advantage occurs with low temperature targets which makes the warm neutron downscatter method attractive. (A.G.W.)

**3316** NUCLEAR MAGNETIC RESONANCE AND RELAXATION IN SOLIDS. Proceedings of the XIIIth Colloque Ampere, University of Leuven, 1–5 September 1964. Van Gerven, Lieven (ed.). Amsterdam, North-Holland Publishing Company, 1965. 457p. $12.50. (CONF-608).

The proceedings of the international radio-spectroscopic conference are presented on nuclear magnetic resonance and relaxation in solids. The papers on liquids and gases, which were discussed in parallel sessions during the same conference, are also included. (L.B.S.)

**3317** THE MOESSBAUER EFFECT IN IRON COMPOUNDS WITH MARCASITE TYPE STRUCTURE [Thesis]. Temperley, Archibald Angus. Eugene, Ore., Univ. of Oregon, 1964. 117p.

The line shifts and electric quadrupole splittings of the 14.4-kev level of $^{57}Fe$ were measured in the marcasite-structure compounds $FeS_2$, $FeSe_2$, $FeTe_2$, and $FeSb_2$ and in the pyrite structure of $FeS_2$ by use of the Mössbauer effect. Measurements were made with polycrystalline absorbers at temperatures of 81°K and 300°K for the marcasites and at temperatures from 81°K to 600°K for $FeS_2$ (pyrite). The source consisted of $^{57}Co$ nuclei diffused into a copper matrix. All measurements were made with the source at room temperature. A velocity drive was constructed to measure the transmission of the Mössbauer gamma ray as a function of the Doppler shift in its energy. Results of the measurements of quadrupole splittings and isomer shifts are discussed. (TCO)

**3318** LOW TEMPERATURE MAGNETIC SUSCEPTIBILITIES OF SIX RARE EARTH OXIDES [Thesis]. Hacker, Herbert Jr. Ann Arbor, Mich., Univ. of Michigan, 1964. 148p.

A study of the temperature dependence of the magnetic susceptibilities of the sesquioxides of neodymium, gadolinium, dysprosium, holmium, erbium, and ytterbium was conducted throughout the range from 4 to 300°K. Each of these compounds, with the exception of $Gd_2O_3$, shows an anomaly of the type characteristic of crystalline field splitting of the ground state degeneracy of the free rare earth ion. In the case of gadolinium oxide the magnetic susceptibility obeys a Curie-Weiss Law throughout the range from 4 to 300°K. Descriptions of the susceptibility measurement system, which is based on the mutual inductance principle, and other experimental details, including thermometry and cryostat design, are included. Theoretical analyses of the behavior of the rare earth ions were carried out, where practical, using the techniques of crystalline field theory. The experimental data on $Yb_2O_3$ agree very well with the theoretical susceptibility calculated in terms of a cubic crystalline field. The associated energy level scheme, which results from the splitting of the eight-fold degenerate ground term of the $Yb^{+++}$ ion, consists of a doublet at 0, a quartet level at 600, and another doublet at 960 $cm^{-1}$. The experimental data on $Nd_2O_3$ are reasonably well described by a susceptibility calculated under the assumption of a cubic field. The energy level pattern associated with the susceptibility data consists of a doublet at 0, a quartet level at 180, and another quartet level at 615 $cm^{-1}$. Additional calculations are described, which involve tetragonal and orthorhombic fields, but agreement between experimental and theoretical susceptibilities is not satisfactory. This result indicates that further calculations involving crystalline fields of lower symmetry are desirable. (Dissertation Abstr.)

# REACTOR TECHNOLOGY

## General

*Refer also to abstracts 1977, 1993, 1994, and 3647.*

**3319** (ANL–7082) REACTOR DEVELOPMENT PROGRAM PROGRESS REPORT, JULY 1965. (Argonne National Lab., Ill.). Aug. 24, 1965. Contract W-31-109-eng-38. 82p. Dep. mn; CFSTI $3.00 cy, $0.75 mn.

Research and development is reported in 4 sections. Separate abstracts were prepared for each section. (J.R.D.)

*For abstracts of individual sections see: 2221, 3320, 3321, and 3579.*

**3320** (ANL–7082, pp 1-28) LIQUID-METAL-COOLED REACTORS. (Argonne National Lab., Ill.).

Development and operation of EBR-II and FARET are summarized. Progress is reported on Doppler measurements with ZPR-6, central-rod calibration in ZPR-9 using on-line computer methods, and design of ZPPR. Development work on metallic fuels, jacket materials, fuel for zero-power reactors, carbide fuel elements, and EBR-II test fuel elements is reported along with work on skull reclamation, and pyrochemical fuel recovery processes. (J.R.D.)

**3321** (ANL–7082, pp 29-53) GENERAL REACTOR TECHNOLOGY. (Argonne National Lab., Ill.).

Calibration of neutron sources using $^{56}Mn$ is described along with methods for determining capture-to-fission ratios of $^{239}Pu$ and $^{241}Pu$. ZPR-7 data are analyzed. Development work on Th-Pu-U phosphides and sulfides is reported, and anelasticity measurements of U compounds are summarized. Polarization studies of Zr corrosion by liquid Na are described along with tests of Li corrosion of Ta alloys, Mo alloys, and unalloyed Mo and Ta. Irradiation testing of vibratorily compacted UC-PUC is summarized. Development of neutron image-intensification systems and infrared systems for nondestructive testing is reported along with fabrication of an Nb-Zr liquid metal loop. Engineering experiments on heat transfer are summarized along with work on chemical separation of fuels by fluidization and volatility, Na coolant chemistry, and Pu recycle reactors. (J.R.D.)

**3322** (EUR-2448.f) PRINCIPALES CARACTERISTIQUES TECHNIQUES DES CENTRALES NUCLEAIRES DES TYPES GRAPHITE–GAZ ET EAU LEGERE BOUILLANTE OU PRESSURISEE. (Main Technical Characteristics of the Graphite–Gas and Light Boiling- or Pressurized-Water Type Plants). Pleinevaux, C.; Van Bockstael, G. (European Atomic Energy Community). July 1965. 33p. Dep. mn.

The main mechanical, thermal, hydraulic and nuclear characteristics of graphite-gas and light boiling- or pressurized-water type plants are discussed. (auth)

**3323** (GAMD–6644) BLOOST-5: A COMBINED REACTOR KINETICS-HEAT TRANSFER CODE FOR THE IBM-7044. PRELIMINARY DESCRIPTION. Merrill, M. (General Atomic, San Diego, Calif. John Jay Hopkins Lab. for Pure and Applied Science). Aug. 17, 1965. Contract AT(04-3)-167. 29p. Dep. mn; CFSTI $2.00 cy, $0.50 mn.

BLOOST-5 is a combined reactor kinetics-heat transfer code written in FORTRAN IV for IBM-7044. It is essentially a combination of two previous codes, and is applicable to problems for which the space-independent form of the reactor kinetics equation is valid. Considerable flexibility in fuel element geometry is possible in the heat transfer subroutines. The program operations and input are described. (M.O.W.)

**3324** (IITRI–578P21-13) STUDIES OF REACTOR CONTAINMENT. Progress Report, October 1, 1964–July 31, 1965. Eichler, J. B.; Gallagher, E. V.; Lieberman, P.; Singer, T. (comps.) (IIT Research Inst., Chicago, Ill.). Contract AT(11-1)-578. 81p. (IITRI–T6042-13). Dep. mn; CFSTI $3.00 cy, $0.75 mn.

Work on the following three main tasks is reported; (1) crushable shield, analysis and design, (2) shock impingement experiments on crushable shields, and (3) coolant decompression experiments and analysis. Task (1) is discussed in terms of the formulation of tentative shield design trends through a series of computer runs. Shock impingement experiments on styrofoam were carried out under Task (2). Work reported under Task (3) deals with: (a) one-dimensional water shock tube experiments and analysis with various amounts of vapor present initially in the driver section, in conjunction with various orifice sizes; and (b) three-dimensional water shock tube experiments, both with and without vapor present initially in the driver section, with various orifice sizes. (M.O.W.)

**3325** (ORNL-P-1480) HEATING IN INFINITE CYLINDERS BY UNIFORM GAMMA SOURCES. Claiborne, H. C.; Nestor, C. W. Jr. (Oak Ridge National Lab., Tenn.). [1962]. Contract W-7405-eng-26. 7p. Dep. mn; CFSTI $1.00 cy, $0.50 mn.

As an aid to the reactor designer concerned with gamma heating in elements that may be approximated by long cylinders, the point kernel describing the transfer of gamma energy for the case of sources distributed uniformly throughout a right circular cylinder of infinite length was integrated. (M.O.W.)

**3326** (WAPD-T-1732) CONTROL-INDUCED XENON OSCILLATIONS. Margolis, S. G.; Curlee, N. J. Jr. (Bettis Atomic Power Lab., Pittsburgh, Pa.). July 1964. Contract AT-11-1-GEN-14. 21p. Dep. mn; CFSTI $1.00 cy, $0.50 mn.

Spatial oscillations of Xe concentrations in large reactor cores are studied. The effects of control rod motion on these oscillations are discussed. The stability of the oscillations is investigated in the vicinity of equilibrium. (T.F.H.)

**3327** DISTRIBUTION OF GASEOUS IMPURITIES AND CARBON TRANSPORT IN GAS COOLED ATOMIC REACTORS. Thrun, E. Atomkernenergie, 8: 278-84(July-Aug. 1965). (In German).

High-temperature gas-cooled reactors are suffering from graphite corrosion in the core and from carbon deposition in the heat exchangers. It is shown quantitatively that this carbon transport depends on the following layout of a reactor, reaction rates, reactor materials, and the concentrations of water and other impurities within the primary circuit. Carbon transport is caused by several independent chemical reactions. Recently published experimental works referring to temperature dependent rates of these partial reactions involve activation energies, frequency factors, and orders of the reactions. The differential changes of gaseous impurities have been developed. It is shown that the calculated distribution of the gaseous impurities vary with layout data, physical chemical constants of the reactor materials, and leak rate. The influence of radiation is considered to be dependent on the frequency factors of the reactions. The distribution of the concentrations and the maximum change of the concentrations are demonstrated. (auth)

**3328** A SOLUTION OF NONLINEAR VIBRATION PROBLEMS IN REACTOR COMPONENTS. Nahavandi, Amir N.; Bohm, George J. (Westinghouse Electric Corp., Pittsburgh). Trans. Amer. Nucl. Soc., 8: 491-2(Nov. 1965).

**3329** APPLICATIONS OF NUCLEAR ENERGY—A NEW COURSE FOR THE HUMANITIES. Ruby, Lawrence (Univ. of California, Berkeley). Trans. Amer. Nucl. Soc., 8: 534(Nov. 1965).

**3330** OPTIMIZATION THEOREMS IN REACTOR PHYSICS. Lewins, Jeffery (Univ. of Washington, Seattle). Trans. Amer. Nucl. Soc., 8: 534-5(Nov. 1965).

**3331** AN ANALOGY BETWEEN THE VARIATIONAL PRINCIPLES OF REACTOR THEORY AND THOSE OF CLASSICAL MECHANICS. Kaplan, S. (Westinghouse Electric Corp., Pittsburgh). Trans. Amer. Nucl. Soc., 8: 535-6(Nov. 1965).

**3332** METHOD FOR THE CALCULATION OF CORE TEMPERATURE FOLLOWING LOSS OF COOLANT. Stanek, L. J. (Babcock and Wilcox Co., Lynchburg, Va.). Trans. Amer. Nucl. Soc., 8: 539(Nov. 1965).

**3333** ANNULAR-RING MODEL FOR LOFT MELT-DOWN STUDIES. Hyer, F. K.; Rose, R. P. (Phillips Petroleum Co., Idaho Falls, Idaho). Trans. Amer. Nucl. Soc., 8: 539-40(Nov. 1965).

**3334** THE INFLUENCE OF ZIRCONIUM CLADDING ON THE LOFT LOSS-OF-COOLANT TEST. Jensen, S. E.; Finnegan, L. J. (Phillips Petroleum Co., Idaho Falls, Idaho). Trans. Amer. Nucl. Soc., 8: 540-1(Nov. 1965).

**3335** BLOWDOWN MODELS APPLICATION TO THE LOSS-OF-FLUID TEST FACILITY (LOFT) EVALUATION. Parks, Charles E. (Babcock and Wilcox Co., Lynchburg, Va.). Trans. Amer. Nucl. Soc., 8: 541-2(Nov. 1965).

**3336** LOFT SEMI-SCALE BLOWDOWN TESTS. Rose, R. P.; Ahrens, F. W. (Phillips Petroleum Co., Idaho Falls, Idaho). Trans. Amer. Nucl. Soc., 8: 542-3 (Nov. 1965).

**3337** AN ANALYTICAL MODEL FOR PREDICTING THE PRESSURE-TEMPERATURE HISTORY WITHIN A CONTAINMENT VESSEL IN RESPONSE TO A LOSS-OF-COOLANT ACCIDENT. Wagner, R. J.; Finnegan, L. J. (Phillips Petroleum Co., Idaho Falls, Idaho). Trans. Amer. Nucl. Soc., 8: 543-4(Nov. 1965).

**3338** FIXED-VOLUME EXPERIMENTS ON TRANSIENT THERMAL PRESSURE PRODUCTION IN WATER. Wentz, L. B.; Wright, R. W. (TRW Systems, Redondo Beach, Calif.). Trans. Amer. Nucl. Soc., 8: 561-2(Nov. 1965).

**3339** POST-ACCIDENT RECOVERY PROGRAM. McKinley, John C. (Atomic Energy Commission, Washington, D. C.); Lewis, Robert H. Trans. Amer. Nucl. Soc., 8: 563-4(Nov. 1965).

**3340** MEASUREMENT OF FILTER EFFICIENCY WITH A CONDENSATION NUCLEI COUNTER. Smith, M. L. (General Electric Co., Richland, Wash.). Trans. Amer. Nucl. Soc., 8: 564(Nov. 1965).

**3341** DIMENSIONAL LOCATION OF REACTOR COMPONENTS BY OPTICAL TOOLING. Abbatiello, A. A. (Oak Ridge National Lab., Tenn.). Trans. Amer. Nucl. Soc., 8: 582-4(Nov. 1965).

**3342** USE OF EXPONENTIAL COSINE AUTOCORRELATION FUNCTIONS IN PROCESSING NUCLEAR-SYSTEM TEST DATA. Uhrig, Robert E. (Univ. of Florida, Gainesville). Trans. Amer. Nucl. Soc., 8: 586-7(Nov. 1965).

## Auxiliaries and Components

*Refer also to abstracts 2408, 2419, 3265, 3267, and 3268.*

**3343** THE CLOSED-CYCLE GAS TURBINE FOR NUCLEAR POWER PLANTS. Keller, C. (Escher Wyss AG, Zurich). Neue Tech., 7: 153-63(Aug. 1965). (In German).

Design and applications of the closed cycle gas turbine combined with high temperature reactors are discussed. Compared with water reactors and steam turbines, the direct cycle gas system—preferably helium—under elevated pressure opens possibilities to lower capital costs as well as better fuel economy by higher efficiency. With helium as working medium not only small and medium size plants can be built with todays technology but also machine sets up to 250 Mw(e) and more. (auth)

**3344** THEORETICAL INVESTIGATIONS OF FISSION-PRODUCT DEPOSITION FROM FLOWING GAS STREAMS. Venerus, Ernest R.; Ozisik, M. Necati (North Carolina State Univ., Raleigh). Trans. Amer. Nucl. Soc., 8: 337-8 (Nov. 1965).

**3345** FRACTURE MECHANICS IN DESIGN AGAINST BRITTLE FAILURE. Johnson, Richard E.; Parrish, Marvin L. (Bettis Atomic Power Lab., Pittsburgh). Trans. Amer. Nucl. Soc., 8: 367-8(Nov. 1965).

**3346** OPTIMUM SHIELDING THEORY. Lewins, Jeffery (Univ. of Washington, Seattle). Trans. Amer. Nucl. Soc., 8: 492-3(Nov. 1965).

**3347** THE DEVELOPMENT OF A SMALL INTEGRAL LOOP FOR IN-PILE FUEL-FAILURE STUDIES IN THE PRESENCE OF FLOWING SODIUM. Sowa, E. S.; Heap, J. C. (Argonne National Lab., Ill.). Trans. Amer. Nucl. Soc., 8: 559(Nov. 1965).

**3348** A COMPARISON OF SHIELD LEAKAGE OBTAINED FROM 3-D CALCULATIONS AND MEASUREMENTS. Grochowski, G.; Schamberger, R. (United Nuclear Corp., White Plains, N. Y.). Trans. Amer. Nucl. Soc., 8: 644-5(Nov. 1965).

**3349** IMPROVEMENTS IN CONCRETE PRESSURE VESSELS. Measor, Ernest Oliver; Williams, Geoffrey Milson John. British Patent 1,004,482. Sept. 15, 1965. Filed Jan. 30, 1962.

An end wall for a cylindrical prestressed concrete pressure vessel is patented. The wall is in the form of a block of concrete and includes means for applying inwardly directed forces [to the sides of the block to prestress the block so as to offset tensile stresses produced by the working pressure in the vessel]. The prestressing means may be a collar of steel, reinforced concrete, or other suitable material extending around the end block with prestressing forces being applied by jacks or wedges between the collar and the vessel. Alternatively, the prestressing means may be straight tendons of steel or other suitable material passing through the end block and anchored and applying forces to the concrete at their ends. (A.G.W.)

**3350** IMPROVEMENTS IN CONCRETE PRESSURE VESSELS. Measor, Ernest Oliver; Williams, Geoffrey Milson John. British Patent 1,004,483. Sept. 15, 1963. Filed Jan. 30, 1962.

The body portion of a prestressed concrete pressure vessel is provided with a set of prestressing tendons extending longitudinally of the vessel and spaced around it. Each tendon lies substantially in a plane containing the longitudinal axis of the vessel and follows a predetermined outwardly curved path designed to exert forces both parallel to and perpendicular to the longitudinal and thus reduce or eliminate the need for circumferential tendons. The majority of the tendons are arranged to be accessible on the exterior of the vessel. Means are provided for resisting outward forces on the vessel near the tendon anchorage points. (A.G.W.)

**3351** MOUNTING ARRANGEMENTS FOR CASING-ENCLOSED APPARATUS. Geiger, Wallace Aime; Kudlacik, Louis (to United Aircraft Corp.). British Patent 1,004,546. Sept. 15, 1965. Filed Feb. 21, 1964.

A mounting arrangement for a pressure casing includes a mounting ring surrounding the casing and having in general the same peripheral shape as the side wall of the casing. The casing is supported from the ring by peripherally spaced lugs fixed to the side wall of the casing and hanger strips secured at their upper ends to the mounting ring, each hanger strip having a lug at its free end receivable between a pair of adjacent lugs on the casing. (A.G.W.)

**3352** IMPROVEMENTS IN OR RELATING TO DEVICES FOR LOADING AND UNLOADING FUEL ELEMENTS FROM NUCLEAR REACTORS. (to Societe Indatom). British Patent 1,004,755. Sept. 15, 1965. Priority date Jan. 19, 1962, France.

A device for loading and unloading fuel elements is designed for a nuclear reactor whose biological shield at the end above the core is provided by two protective walls separated by a chamber. The outer wall has, opposite the

reactor core, a cylindrical hole shut off by a rotatable plug. Located inside the chamber is a storage and handling arrangement supported on a trolley framework and a network of rails partly on the lower surface of the rotatable plug and partly on the lower surface of the outer wall. The storage and handling arrangement can be moved over the rails to take up a desired position above any channel that is to be loaded or unloaded. (A.G.W.)

**3353** ELECTRICAL CONDUCTOR. (to Groupement Atomique Alsacienne Atlantique). British Patent 1,004,993. Sept. 22, 1965. Priority date June 15, 1961, France.

A resilient member for supporting and supplying electrical current to a mobile element, such as an electromagnet holding the control rods of a reactor, consists of two helical springs of opposite twist connected by an intermediate ring. At their ends remote from the intermediate ring the springs are connected, one to a stationary element such as an electrical connection box and the other to the mobile element. The springs are U-shaped in cross section and support at least one electrical conductor in their U-shaped channels. (A.G.W.)

**3354** LIQUID-MODERATED NUCLEAR REACTORS. Green, Albert; Bradley, Norman (to United Kingdom Atomic Energy Authority). British Patent 1,005,133. Sept. 22, 1965. Filed July 4, 1963.

A liquid-moderated nuclear reactor is designed to reduce the required volume of moderating liquid. The moderator is contained by a calandria vessel in which the calandria tubes are arranged on two superimposed geometrical lattices of equal pitch. The corresponding coordinates of the lattices are parallel and are displaced from each other by one half pitch. The pressure tubes of the reactor are all within the calandria tubes of one of the lattices, and reactor control equipment can be located in the tubes of the second lattice. (A.G.W.)

**3355** IMPROVEMENTS IN OR RELATING TO REFUELLING MACHINES FOR NUCLEAR REACTORS. Anderson, Douglas Edward; Gartside, Colin; Wright, Robert Andrew (to General Electric Co. Ltd.). British Patent 1,005,416. Sept. 22, 1965. Filed Aug. 30, 1963.

A nuclear reactor refuelling machine capable of servicing a fluid-cooled reactor while the reactor is in an operating condition has fluid circuits for operating internal mechanisms of the machine. The fluid in the mechanism fluid circuit is the same as the fluid used in the reactor coolant circuit but is arranged to have a higher pressure than the reactor coolant circuit. A substantial part of the servicing machine is included in the containment area for the reactor core, but a winch unit may be provided with its own containment vessel. The two containment vessels communicate when the winch unit is in operation but can be separated, and sealing for the reactor containment area is provided when the winch unit is separated from it. (A.G.W.)

**3356** DRIVE MECHANISM FOR NUCLEAR REACTOR CONTROL RODS. Lechevallier, Maurice (to Groupement Atomique Alsacienne Atlantique). British Patent 1,005,514. Sept. 22, 1965. Priority date Nov. 12, 1962, France.

A drive mechanism for reactor control rods includes a chain passing over a pulley to form two downcoming vertical lengths, one of which is secured to a control rod and the other of which is secured in a storage section. Two locking systems, one for locking each length of chain, are mounted on the same frame. A pneumatic system produces movement of the pulley in relation to the frame. In this arrangement, coarse or fine control of the reactor can be effected by displacement of the control rod at different speeds when one of the locking devices is released. When both locking devices are released, the rod can be speedily inserted to perform a safety function. (A.G.W.)

**3357** IMPROVEMENTS IN AND RELATING TO NUCLEAR REACTOR PLANT. (to Sulzer Brothers Ltd.). British Patent 1,005,850. Sept. 29, 1965. Priority date Sept. 13, 1963, Switzerland.

A method is patented for control of a nuclear reactor plant that includes a nuclear reactor and two load medium circuits arranged to receive heat from a coolant that is heated as it flows through the reactor. The total rate of feed of load medium to the two load circuits is controlled in dependence upon the temperature of the coolant entering the reactor. The individual rates of feed of load medium to the two circuits are adjusted simultaneously in dependence upon a comparison of the live vapor pressures in the two circuits to tend to equalize the two live vapor pressures. Preferably the load medium supplied to each circuit is additionally controlled in dependence upon the output requirements of that circuit, and the reactor output is controlled by variation of the position of at least one control rod in the reactor core in dependence upon the sum of the live vapor pressures in the circuits. (A.G.W.)

**3358** IMPROVEMENTS IN AND RELATING TO NUCLEAR REACTORS. (to Sulzer Brothers Ltd.). British Patent 1,005,940. Sept. 29, 1965. Priority date Sept. 19, 1963, Switzerland.

A method for controlling the heat generated by a nuclear reactor makes use of neutron flux measurement at a point in the reactor and of heat output measurement. Signals dependent on these two measurements are multiplied together, and the resultant signal is supplied to a mechanism for adjusting the reactor control rods. (A.G.W.)

**3359** IMPROVEMENTS IN NUCLEAR REACTORS. (to Societe Anglo-Belge Vulcain). British Patent 1,006,187. Sept. 29, 1965. Priority date Feb. 13, 1962, Luxembourg.

A method for automatically compensating for variations of the poisoning due to $^{135}Xe$ is intended for use in nuclear reactors in which a primary fluid flows through a circuit of which at least a part passes through the core and/or reflector. A neutron-absorbing substance is added to the primary fluid by any known means in amounts sufficient to maintain the total reactivity effect of the $^{135}Xe$ and the neutron-absorbing substance substantially equal to that due to the equilibrium concentration of $^{135}Xe$ at full reactor power. As the $^{135}Xe$ concentration increases, the neutron-absorbing substance is removed from the system. In the example described, boric acid is used as neutron absorber and is removed from the system by distillation. (A.G.W.)

**3360** IMPROVEMENTS IN MACHINES FOR THE LOADING AND UNLOADING OF THE CHANNELS OF A NUCLEAR REACTOR. Forey, Francois (to Commissariat a l'Energie Atomique). British Patent 1,006,322. Sept. 29, 1965. Priority date Aug. 7, 1963, France.

A machine for loading and unloading the horizontal channels of a nuclear reactor is designed for greater efficiency in extracting plugs from the channels when the plugs are jammed. The machine is of the type that utilizes a poker sliding in a guide tube for introducing and extracting elements. The control means for the sliding movement includes an auxiliary traction device for applying increased force to the poker for releasing jammed elements. (A.G.W.)

**3361** METHOD OF OPERATING A REACTOR DURING START-UP OR SHUT-DOWN. McGrath, Robert G. (to Westinghouse Electric Corp.). U. S. Patent 3,206,371. Sept. 14, 1965. Filed Dec. 28, 1962.

A method is described for controlling a reactor by controlling the quantity of fissile material that is contained in a moderating vehicle within the reactor at any one time. The method is particularly applicable to a slurry type homogeneous reactor. The reactor system is filled with the vehicle or fuel material fluidized in the vehicle at a concentration below the low critical fuel concentration. A quantity of fuel is added to the vehicle contained within the reactor and at the same time a quantity of the vehicle including the fuel material is bled from the reactor. The bled quantity is separated into dilute and concentrated fractions of fuel material and the concentrated fraction is returned to the reactor system until the low critical fuel concentration is attained and until the reactor begins to operate. The reactor is operated for a period of time sufficient to build up a substantial quantity of fission products, and then the temperature is increased sufficiently to shut down the reactor. A substantial portion of the heat of radioactive decay of the

fission products is retained within the reactor in the shutdown condition to maintain the system in a subcritical condition until high critical fuel concentration can be attained by the further addition of fuel to the fluidizing medium. (B.L.M.)

**3362** METHOD AND APPARATUS TO DETERMINE REACTOR FLUX DISTRIBUTION. Campbell, Ronald Hugh (to United Kingdom Atomic Energy Authority). U. S. Patent 3,207,667. Sept. 21, 1965. Priority date June 12, 1959, Great Britain.

A method of nuclear reactor flux scanning includes the steps of passing a filament of gas along a passage extending through the core of the reactor and monitoring its activity at the outlet to determine the integrated flux through the core. Then, the flow rate of the filament of fluid is changed in its passage through the core, and the monitoring of its activity at the outlet is continued as the flow rate is changed to obtain readings of activity level, which are firstly transitional and then steady as the new flow rate becomes established through the core. The transitional readings are differentiated to obtain the distribution of flux in the core. (B.L.M.)

**3363** PRESSURE RELEASE DEVICE TO DRENCH REACTOR CORE. Kornbichler, Heinz (to Licentia Patent-Verwaltungs-G.m.b.H.). U. S. Patent 3,207,671. Sept. 21, 1965. Priority date Nov. 24, 1959, Germany.

A protective device is provided for a boiling water reactor. The entire pressure system, including the reactor, a heat exchanger, and a primary circuit connecting the heat exchanger to the reactor is enclosed in a casing. A wall surrounds the pressure system and divides the casing horizontally during normal operation of the reactor. The wall is provided with a large number of holes, normally covered, that open if a predetermined pressure difference is built up between the two sides of the wall. A water pool at the top of the wall has a free surface and an emergency condenser communicating with the pressure system of the reactor. The condenser is inside the pool, and an auxiliary circuit connects the primary circuit with the condenser through a pressure relief valve. (B.L.M.)

**3364** FIRE EXTINGUISHING SYSTEM FOR NUCLEAR REACTORS. Costes, Didier (to Commissariat a l'Energie Atomique). U. S. Patent 2,207,672. Sept. 21, 1965. Priority Aug. 7, 1962, France.

Emergency means are described for extinguishing a fire occurring in the vertical fuel channel of a heterogeneous reactor. A finely divided, non-combustible material is released into an upper section of the channel in which the fire has commenced. The material is retained in the channel in order to obstruct the flow of coolant gas through the channel, to cool the hot areas of the combustion zone, and to damp the combustion reaction. The material is stored in a magazine supported at a level above the upper ends of the channels, and the magazine may be connected to any selected one of the reactor channels by a network of flow passages. (B.L.M.)

**3365** TEMPERATURE FLOW CONTROL OF COOLANT IN A REACTOR. Hennig, Robert J. (to Atomic Power Development Associates, Inc.). U. S. Patent 3,208,913. Sept. 28, 1965. Filed Apr. 17, 1963.

In a reactor having a number of subassemblies with coolant flowing through the assemblies, means are provided for regulating the volumetric flow of coolant through each assembly individually to control and limit the temperature of each assembly. The control means includes a throttling type arrangement including means located in the coolant being discharged from each subassembly and actuatable responsive to varying temperature of the discharging coolant to change the degree of such throttling. The throttling means comprises a pair of slotted grids adjacent to each other in the discharge coolant stream and so adapted that the slots register one with the other in response to the temperature of the coolant passing by them. (B.L.M.)

## Criticality Studies

*Refer also to abstracts 2957, 2965, 2966, 2972, 2978–2980, 2986, 2992, 3001, and 3010.*

**3366** (ANL–7052) DEL—A PERTURBATION PROGRAM WRITTEN IN FORTRAN. Kvitek, Louis C. (Argonne National Lab., Ill.). June 1965. Contract W-31-109-eng-38. 47p. Dep. mn; CFSTI $2.00 cy, $0.50 mn.

DEL is a perturbation theory code which determines the fractional change in $k_{eff}$ due to a perturbation in macroscopic cross sections and/or in the buckling. It is written in FORTRAN for the IBM-704 computer with 32K core storage and at least six tape drives, including one for the FORTRAN Subroutine Library. The analysis assumes the input of the radial distributions of sources and fluxes to result from a one-dimensional diffusion-theory calculation. Preparation of the cross-section tape is described. (auth)

**3367** (BNWL–156) THE STATIONARY CALCULATION OF RATIOS IN REACTOR STATICS. Lewins, Jeffery (Battelle-Northwest, Richland, Wash. Pacific Northwest Lab.). Oct. 1965. Contract AT(45-1)-1830. 25p. Dep. mn; CFSTI $2.00 cy, $0.50 mn.

Expressions are given for the stationary calculations of arbitrary ratios of interest in critical systems and in steady-state sub-critical systems having a source. Emphasis is placed on the calculation of the adjoint functions by iterative methods already used in standard reactor codes and on the reduction in computing time offered by stationary methods compared to direct computation. Both variational principles and perturbation expressions are provided. (auth)

**3368** (BNWL-SA–214) CRITICALITY RESEARCH ON PLUTONIUM. Clayton, E. D.; Richey, C. R.; Lloyd, R. C.; Bierman, S. R.; Carter, L. L. (Battelle-Northwest, Richland, Wash. Pacific Northwest Lab.). Aug. 12, 1965. Contract AT(45-1)-1830. 26p. (CONF-651103–10). Dep. mn; CFSTI $2.00 cy, $0.50 mn.

From IAEA Symposium on Criticality Control of Fissile Materials, Stockholm.

Included are significant results obtained from criticality experiments with plutonium solutions and compounds and the analyses of the obtained data. Previously estimated curves for critical dimensions of homogeneous water moderated $^{239}Pu$ in the undermoderated range were revised. Computed curves are also given which show the effect of $^{240}Pu$ on criticality, together with experimental data points at 2.2 and 8% $^{240}Pu$. Measured decay constants from experiments on critical and subcritical systems are compared with computed values for H/Pu atomic ratios of 15–1060. An analysis of critical data on Pu solutions was made showing the effect of nitrate on criticality for reflected spheres with nitrate and Pu concentrations extending to several hundred grams per liter. The results from a subcritical neutron interaction experiment performed with cans of dry $PuO_2$ powder in a low density reflected cubic array are also presented. Aspects of the current criticality research on plutonium and of planned experiments are discussed. (M.O.W.)

**3369** (CEA-R–2814) ALECTO—RESULTATS DES EXPERIENCES CRITIQUES HOMOGENES REALISEES SUR LE $^{239}Pu$, $^{235}U$ ET $^{233}U$. (ALECTO—Results Obtained with Homogeneous Critical Experiments on $^{239}Pu$, $^{235}U$ and $^{233}U$). Bruna, Jean-Georges; Brunet, Jean-Paul; Caizergues, Robert; Clouet D'Orval, Christian; Kremser, Jacques; Tellier, Henry; Verriere, Philippe (Commissariat a l'Energie Atomique, Saclay (France). Centre d'Etudes Nucleaires). 1965. 130p. Dep. mn.

The results of the homogeneous critical experiments ALECTO, made on plutonium-239, uranium-235, and -233 are given. After a brief description of the equipment, the critical masses for cylinders of diameters varying from 25 to 42 cms are given and compared with other values (foreign results, criticality guide). Experiments relating to cross sections and constants to be used on these materials are presented. Lastly, kinetic experiments allow a comparison of pulsed neutron and fluctuation methods. (auth)

**3370** (CONF-651103–2) NUCLEAR SAFETY COORDINATION WITHIN OAK RIDGE OPERATIONS FACILITIES. Johnson, Wiley A.; Pryor, William A. (Oak Ridge

Operations Office (AEC), Tenn. Research and Development Div.). [1965]. 20p. (SM–70/38). Dep. mn; CFSTI $1.00 cy, $0.50 mn.

From IAEA Symposium on Criticality Control of Fissile Materials, Stockholm.

The role of the AEC Oak Ridge Operations Office in nuclear safety coordination among its many contractors is discussed. The broad spectrum of nuclear safety applications for the manifold operations involved is reviewed. Topics discussed include the approval of shipping containers and methods for fissile materials; support of criticality research and the compilation of criticality data; the bulk transport of $UF_6$; the bulk transport of low $^{235}U$ enriched metal; $^{233}U$ processing; and the use of fixed neutron absorbers as primary and secondary criticality control devices; and batch and concentration monitoring of fissile materials. (C.H.)

**3371** (EUR–2492.e) KINETIC THEORY AND CALCULATIONS FOR AN ACCELERATOR BOOSTER WITH PERIODICALLY VARYING MULTIPLICATION FACTOR. Misenta, R. (European Atomic Energy Community, Ispra (Italy). Joint Nuclear Research Center). 1965. 44p. Dep. mn.

The relation for the mean power of a periodically pulsed reactor and accelerator system was derived using the multiplication factor $\chi$ for the mean power of a periodically pulsed reactor. The relation shows that the power produced in the reactor by the accelerator pulse is multiplied by a factor $1/1 - \chi$), due to the presence of delayed neutron emitters. In analogy to normal reactors the operation of a periodically pulsed reactor in connection with an accelerator is called "pulsed subcritical." The pulsed subcritical mode of operation offers the possibility of shaping the resulting pulse according to the requirements of the experiments by varying the maximum value of the effective multiplication factor k or the point of time for the injection of the accelerator pulse. For an assumed accelerator source strength of $10^{17}$ n/sec pulse characteristics as a function of the mean power density of the reactor are calculated for two cases which differ by the maximum value of the effective multiplication factor. (auth)

**3372** (EUR–2506.e) REACTOR POWER REDUCTION IN MINIMUM TIME INCLUDING RESTRICTION OF XENON POISONING. De Backer, W. (European Atomic Energy Community, Ispra (Italy). Joint Nuclear Research Center; European Atomic Energy Community, Ispra (Italy). European Scientific Data Processing Center). June 18, 1965. 24p. (CONF-650564–1). Dep. mn.

From Theoretical Automatics Congress, Saclay, France.

Some typical difficulties, non-linearities and state constraints, render this problem an interesting case for testing, optimization methods. In the framework of Prontryagin's Maximum Principle the Gamkrelidze conditions and the method of penalty functions for the state constraints are analyzed. The influence of the optimization criterion, the limit conditions and the fundamental parameters on the numerical results are discussed. (auth)

**3373** (EURAEC–1353) STABILITY INVESTIGATIONS FOR BOILING WATER REACTORS. Quarterly Report No. 4, January 1–March 31, 1965. (Kernenergieanlagen, Allgemeine Elektricitaets-Gesellschaft, Frankfurt am Main (West Germany)). Contract 020-64-4 TEED. 60p. (EUR–2328). Dep. mn; CFSTI $3.00 cy, $0.75 mn.

Work Performed under United States–Euratom Joint Research and Development Program.

The simulated control system for the velocity modulator was constructed after the control devices could be obtained. Experimental investigations of this test assembly, which are still under way, yielded first results. The calibration of the density measuring device was terminated at the measuring section with annular gap geometry. This makes available a measuring process which explores the entire measuring cross section by means of a wide gamma beam and so enables the determination of steam bubble fractions which are variable with time, in the range of time constants from 10 to 20 ms and with a 1% dissolving power of density variation. Following these calibrations, the frequency response of the power/steam-bubble-content was measured and evaluated at average heat-flux densities of 120 and 145 $W/cm^2$ and a rate of flow of $5.71 \times 10^6$ $kg/m^2h$. Work was spent in solving the integrals occurring in the transfer functions for determining the variation of the local steam bubble fraction while taking due account of the way in which the steam bubble velocity depends on location. For some special functions of the average local steam bubble velocity, analytical solutions were obtained. The general assumptions of the model on which the work was based were retained. The preparation of the formula schedule of the final calculation program is nearly ready. (auth)

**3374** (IA–1053) TWO FAST REACTOR STUDIES. 1. STUDY OF DOPPLER COEFFICIENT BY SINUSOIDAL FUEL HEATING. 2. MULTI-LEVEL MODEL FOR HEAVY FISSION AND TOTAL CROSS SECTIONS. Ash, M. (Israel Atomic Energy Commission, Yavne. Soreq Nuclear Research Center). July 1965. 16p. Dep. mn.

An experiment is suggested to investigate the nature of the temperature Doppler coefficient of dilute fast reactor assemblies, by heating a fuel sample sinusoidally, and measuring the subsequent fuel sample temperature spectrum and/or the neutron density fluctuation spectrum. Such an experiment should be more accurate than physically reciprocating cold and heated samples, because in the suggested experiment there is no movement of the sample in and out of regions of varying neutron importance. A formula for fission and total cross sections of heavy isotopes embodying the multi-level model of Reich and Moore is presented. It is applicable to either one or two fission channels. (auth)

**3375** (IDO–17120) TOPICS IN NUCLEAR REACTOR THEORY. Solbrig, A. W. Jr. (Phillips Petroleum Co., Idaho Falls, Idaho. Atomic Energy Div.). Sept. 1965. Contract AT(10-1)-205. 36p. Dep. mn; CFSTI $2.00 cy, $0.50 mn.

Derivations of several known results are presented. The discussion modifies and extends existing work in an attempt to make the presentation more direct and simple. The principal known results are formulas for Doppler broadening of neutron cross sections by motion of target nuclei, the P-1 approximation to the Boltzmann equation for neutron transport, and a relation between the neutron scattering cross sections for a free nucleus and for an identical nucleus bound in a molecule. Appendixes contain a derivation of a property of the Doppler broadening integral, proofs of a lemma used in deriving the P-1 equations without spherical harmonics, and some remarks about derivation of a form of the B-1 equations. (auth)

**3376** (NP–15573) JAPAN FAST CRITICAL EXPERIMENT PROGRAM. (Japan Atomic Energy Research Inst., Tokyo). Sept. 25, 1965. 6p. Dep. mn.

Developments in the Fast Critical Facility Program are briefly discussed and the preliminary design of the Fast Critical Assembly is given. (M.O.W.)

**3377** (ORNL-P–1482) FREQUENCY RESPONSE SENSITIVITIES IN REACTOR DYNAMICS STUDIES. Kerlin, T. W. (Oak Ridge National Lab., Tenn.); Lucius, J. L. (Oak Ridge Gaseous Diffusion Plant, Tenn.). [1964]. Contract W-7405-eng-26. 5p. Dep. mn; CFSTI $1.00 cy, $0.50 mn.

It is common practice to include theoretical frequency response analysis in the design and evaluation of reactor systems. An analytical procedure for calculating the frequency response is presented. This procedure simultaneously evaluates the effects of individual changes in several reactor design parameters. (M.O.W.)

**3378** (ORNL–P–1680) EXPERIMENTAL AND CALCULATED SYSTEM CRITICALITY. Thomas, J. T. (Oak Ridge National Lab., Tenn.). [1965]. Contract W-7405-eng-26. 38p. (CONF-651103–11). Dep. mn; CFSTI $2.00 cy, $0.50 mn.

From IAEA Symposium on Criticality Control of Fissile Materials, Stockholm.

Criticality parameter measurements on various combinations of fissile, moderating, and scattering materials are reported. The systems studied have simple geometrical configurations. The performance of various computational methods for predicting the criticality of these systems is evaluated. (T.F.H.)

**3379** (ORNL-TM-1207) CRITICAL EXPERIMENTS WITH SPERT-D FUEL ELEMENTS. Johnson, E. B.; Reedy, R. K. Jr. (Oak Ridge National Lab., Tenn.). July 14, 1965. Contract W-7405-eng-26. 17p. Dep. mn; CFSTI $1.00 cy, $0.50 mn.

The critical dimensions of lattices of SPERT-D fuel elements in several non-reactor environments were determined to establish specifications for use in storage, transportation, and chemical processing operations. Each fuel element contained about 300 g of $^{235}U$ in 22 aluminum-clad flat plates. In addition to lattices with water moderator and reflector, a dilute aqueous solution of uranyl nitrate was used in some experiments to simulate a dissolver. In still other experiments, varying amounts of boron were added to the uranyl nitrate solution to determine its effect as a soluble neutron absorber in chemical process equipment. It was shown, for example, that a minimum of about 3.5 kg of $^{235}U$ is required in a critical lattice moderated and reflected by water. This mass is reduced to 2.8 kg (contained in the elements) when U(92.6) solution having a $^{235}U$ concentration of 3.99 g/liter was substituted for water. It was increased to 13.6 kg when 1.118 g of natural boron was added to each liter of the uranyl nitrate solution. (auth)

**3380** (ORNL-TM-1305) FREQUENCY RESPONSE SENSITIVITIES IN REACTOR DYNAMICS STUDIES. Kerlin, T. W.; Lucius, J. L. (Oak Ridge National Lab., Tenn.). Oct. 22, 1965. Contract W-7405-eng-26. 13p. (CONF-651101-36). Dep. mn; CFSTI $1.00 cy, $0.50 mn.

From 13th Conference on Remote Systems Technology, Washington, D. C.

The value of a frequency response analysis of a dynamic system is increased if the sensitivity of the frequency response to parameter changes is also available. Sensitivity information is helpful in interpreting calculated results and in assessing the effects of uncertainties in system design parameters. A method is described that permits the analytical determination of the sensitivities, along with the usual frequency response. The method is implemented with a digital computer program, which is used to provide the solution of an illustrative problem. (auth)

**3381** (UJV-1309b/65) VYPOCET FYSIKALNICH PARAMETRU MRIZE TEZKOVODNIHO REAKTORU S PRIRODNIM URANEM CHLAZENEHO PLYNEM. POPIS PROGRAMU PARAMETRY II. (Calculation of Physical Parameters of a Gas Cooled Heavy-Water Natural Uranium Reactor. Description of the Program PARAMETRY II). Sulc, P.; Markvart, J.; Pfann, J.; Straka, J. (Ustav Jaderneho Vyzkumu, Ceskoslovenska Akademie Ved, Rez). [1965]. 63p. Dep. mn.

A description of a new version of the program PARAMETRY II, for physical lattice parameters calculations of a heavy water gas-cooled metal uranium reactor, is presented. A detailed description of the calculational algorithm, the ways of program utilization and some of its further possibilities are given. In conclusion illustrative examples calculated by this program are added. (auth)

**3382** (WAPD-TM-532) WIGL2. A PROGRAM FOR THE SOLUTION OF THE ONE-DIMENSIONAL, TWO-GROUP, SPACE-TIME DIFFUSION EQUATIONS ACCOUNTING FOR TEMPERATURE, XENON, AND CONTROL FEEDBACK. Henry, A. F.; Vota, A. V. (Bettis Atomic Power Lab., Pittsburgh, Pa.). Oct. 1965. Contract AT(11-1)-Gen-14. 54p. Dep. mn; CFSTI $3.00 cy, $0.50 mn.

A description is given of WIGL2, a one-dimensional, two-group, space-time diffusion theory program with zero, one, or six delayed neutron groups. The program will treat slab, cylindrical and spherical geometries and includes non-boiling heat transfer. Xenon feedback and feedback effects due to fuel and coolant temperature are accounted for. Control rod motion and control system feedback based on total core power or outlet coolant temperature can be simulated. Transients may be excited by prescribed changes in inlet coolant temperature, coolant flow rate, or rod position. The governing equations and a description of the input and edit features of the program are included. (auth)

**3383** (WCAP-3269-48) XENON INDUCED CORE INSTABILITIES. Strawbridge, L. E.; Allard, E. C.; Bhalla, C. P. (Westinghouse Electric Corp., Pittsburgh, Pa. Atomic Power Div.). Feb. 1965. Contract AT(30-1)-3269. 98p. Dep. mn; CFSTI $3.00 cy, $0.75 mn.

An extensive analysis of axial xenon oscillations in a pressurized water reactor was made. It has been shown that the properties of xenon oscillations can be determined by straightforward calculations using readily available computer codes. Using a one-dimensional diffusion theory analysis, the effect of core height, power distribution, Doppler coefficient, and moderator coefficient on xenon oscillations was evaluated. The results indicate: stability to xenon oscillations definitely decreases with increasing core size; stability is quite sensitive to the power distribution with flat or dished power shapes tending to be less stable than normal cosine distributions; the Doppler coefficient is extremely important and is the principal damping mechanism in slightly enriched pressurized water reactors; and the moderator temperature coefficient has a relatively small effect on xenon oscillations. Threshold analyses using the procedures of Randall and St. John were performed. A revised threshold calculation was developed during the program. The revised procedure eliminates certain approximations in the previous procedure and produces results in substantial agreement with the diffusion theory results. Methods of controlling reactors to prevent xenon oscillations were studied. It was demonstrated that either partial length or full length control rods can satisfactorily be used to maintain stability in cores that would otherwise be unstable. Based on these studies, it is concluded that the Doppler coefficient is sufficiently negative to prevent divergent axial xenon oscillations in a 10 ft. pressurized water reactor. Nevertheless, if a xenon oscillation should be initiated, it was demonstrated that the control system is capable of controlling the reactor without sacrificing power capability. (auth)

**3384** NUCLEAR REACTIVITY MEASUREMENTS OF IRRADIATED URANIUM DIOXIDE. Guon, J. (Atomics International, Canoga Park, Calif.). Trans. Amer. Nucl. Soc., 8: 384-5(Nov. 1965).

**3385** ASYMPTOTIC REACTOR-THEORY ANALYSIS OF THE GARELIS-RUSSELL EXPERIMENT. Cady, K. B.; Masters, Christopher F.; Zolotar, B. A. (Cornell Univ., Ithaca, N. Y.). Trans. Amer. Nucl. Soc., 8: 432-3(Nov. 1965).

**3386** MEASUREMENTS OF GENERATION-TIME VARIATIONS. Gozani, T. (Rensselaer Polytechnic Inst., Troy, N. Y.); Demarmels, P.; Huerlimann, T. Trans. Amer. Nucl. Soc., 8: 434-5(Nov. 1965).

**3387** CONSIDERATION OF FINITE CORRELATION TIMES IN PSEUDO-RANDOM-IMPULSE RESPONSE METHODS. Garelis, Edward (General Electric Co., Pleasanton, Calif.). Trans. Amer. Nucl. Soc., 8: 435-6(Nov. 1965).

**3388** CALORIMETRIC AND SPECTROMETRIC TECHNIQUES TO RELATE ZONEWISE POWER DISTRIBUTIONS IN Pu-U MULTIZONED CORES. Hamilton, G. N.; Nath, R. J.; Leamer, R. D.; Corbett, J. A. (Westinghouse Electric Co., Pittsburgh). Trans. Amer. Nucl. Soc., 8: 439(Nov. 1965).

**3389** A COMPARISON OF ANALYSIS WITH EXPERIMENT FOR THE SAXTON PLUTONIUM CRITICAL EXPERIMENTS. Orr, W. L. (Westinghouse Electric Co., Pittsburgh); Sternberg, H. I.; Deramix, P. Trans. Amer. Nucl. Soc., 8: 439-41(Nov. 1965).

**3390** NEUTRONIC ISOLATION CHARACTERISTICS OF CONCRETE, LEAD, WOOD, POLYETHYLENE AND BERYLLIUM. McCreless, Thomas G. (U. S. Atomic Energy Commission, Washington, D. C.); Smith, David R.; Jarvis, George A.; Duffey, Dick. Trans. Amer. Nucl. Soc., 8: 441(Nov. 1965).

**3391** NEUTRON INTERACTION BETWEEN MULTIPLYING MEDIA SEPARATED BY VARIOUS MATERIALS. White, J. D.; Richey, C. R. (Battelle-Northwest, Richland, Washington). Trans. Amer. Nucl. Soc., 8: 441-2 (Nov. 1965).

**3392** CRITICAL URANIUM-METAL ANNULI REFLECTED WITH POLYETHYLENE AND GRAPHITE. Mihalczo, John T. (Oak Ridge National Lab., Tenn.). Trans. Amer. Nucl. Soc., 8: 442-3(Nov. 1965).

**3393** RECENT EXPONENTIAL AND CRITICAL APPROACH EXPERIMENTS WITH SLIGHTLY ENRICHED URANIUM METAL TUBES IN LIGHT WATER. Brown, C. L.; Lloyd, R. C. (Battelle-Northwest, Richland, Wash.). Trans. Amer. Nucl. Soc., 8: 443-4(Nov. 1965).

**3394** CALCULATIONAL CHECKS OF PLUTONIUM CROSS SECTIONS BY COMPARISON WITH CRITICAL-ASSEMBLY RESULTS. Meneley, D. A.; White, J. R. (Argonne National Lab., Ill.). Trans. Amer. Nucl. Soc., 8: 444(Nov. 1965).

**3395** CRITICALITY STUDIES WITH PLUTONIUM SOLUTIONS. Lloyd, R. C.; Richey, C. R.; Clayton, E. D.; Skeen, D. R. (Battelle-Northwest, Richland, Wash.). Trans. Amer. Nucl. Soc., 8: 444-5(Nov. 1965).

**3396** MEASUREMENT OF FAST ADVANTAGE FACTORS AND INTRA-CELL FLUX SHAPES IN SEVERAL LIGHT-WATER-MODERATED SLIGHTLY ENRICHED URANIUM LATTICES. Hardy, J. Jr.; Klein, D. (Bettis Atomic Power Lab., Pittsburgh). Trans. Amer. Nucl. Soc., 8: 446(Nov. 1965).

**3397** REACTOR PHYSICS MEASUREMENTS IN SLIGHTLY ENRICHED URANIUM $D_2O$ LATTICES. D'Ardenne, W. H.; Kaplan, I.; Lanning, D. D.; Thompson, T. J. (Massachusetts Inst. of Tech., Cambridge). Trans. Amer. Nucl. Soc., 8: 447-8(Nov. 1965).

**3398** ANALYSIS AND MEASUREMENT OF PuAl–POLYETHYLENE SYSTEMS IN THE PCTR. Albertson, D. G.; Busselman, G. J. (Battelle-Northwest, Richland, Wash.). Trans. Amer. Nucl. Soc., 8: 448-9(Nov. 1965).

**3399** BUCKLING MEASUREMENTS BY SUCCESSIVE SUBSTITUTION IN A SUBCRITICAL ASSEMBLY. Rogers, W. B.; Vandervelde, V. D.; Basumann, N. P. (E. I. duPont de Nemours, Aiken, S. C.). Trans. Amer. Nucl. Soc., 8: 449-50(Nov. 1965).

**3400** EFFECTIVENESS OF LINEAR ARRAYS OF ABSORBER TUBES AS CONTROL-ROD BLADES. Duffy, D. (Univ. of Maryland, College Park); Fisher, J. R. Trans. Amer. Nucl. Soc., 8: 450-1(Nov. 1965).

**3401** EQUIPMENT AND TECHNIQUES FOR DOPPLER-EFFECT MEASUREMENTS ON FAST CRITICAL ASSEMBLIES. Till, C. E.; Groh, E. F.; Lewis, R. A. (Argonne National Lab., Ill.). Trans. Amer. Nucl. Soc., 8: 455-6(Nov. 1965).

**3402** DISCREPANCIES IN IMPORTANCE AND NEUTRON LIFETIME IN FAST AND THERMAL SPECTRA. Brown, P. S.; Haling, R. K. (General Electric, Pleasanton, Calif.). Trans. Amer. Nucl. Soc., 8: 462(Nov. 1965).

**3403** ANALYTICAL DETERMINATION OF THE EFFECT OF TANTALUM RODS IN AN INTERMEDIATE SPECTRUM REACTOR. Hill, D. J. (Westinghouse Astronuclear Lab., Pittsburgh). Trans. Amer. Nucl. Soc., 8: 473(Nov. 1965).

**3404** CONDITIONS FOR PROBABILISTIC BOUNDEDNESS OF REACTORS WITH RANDOM MACROSCOPIC CROSS SECTIONS. Wade, David C. (General Electric Co., Schenectady, N. Y.); Gyftopoulos, Elias P. Trans. Amer. Nucl. Soc., 8: 475(Nov. 1965).

**3405** TWO CRITERIA FOR LAGRANGE STABILITY. Akcasu, A. Ziya (Brookhaven National Lab., Upton, N. Y.). Trans. Amer. Nucl. Soc., 8: 476(Nov. 1965).

**3406** EXPERIMENTAL INTERPRETATION OF A CRITERION OF NONLINEAR STABILITY. Gyftopoulos, Elias P.; Green, Michael (Massachusetts Inst. of Tech., Cambridge). Trans. Amer. Nucl. Soc., 8: 476-7(Nov. 1965).

**3407** A LIAPUNOV FUNCTION FOR THE PROMPT-JUMP APPROXIMATION IN REACTOR DYNAMICS. Hetrick, David L. (Univ. of Arizona, Tucson). Trans. Amer. Nucl. Soc., 8: 477-8(Nov. 1965).

**3408** AUTONOMOUS POWER OSCILLATIONS IN REACTORS. Akcasu, A. Ziya; Shotkin, Louis M. (Brookhaven National Lab., Upton, N. Y.). Trans. Amer. Nucl. Soc., 8: 478(Nov. 1965).

**3409** INPUT-OUTPUT APPROACH TO OPTIMAL CONTROL. Kyong, Sang H.; Gyftopoulos, Elias P. (Massachusetts Inst. of Tech., Cambridge). Trans. Amer. Nucl. Soc., 8: 479-80(Nov. 1965).

**3410** LIMITATIONS TO THE APPLICABILITY OF THE RESTRICTED SPACE, TIME-OPTIMAL XENON SHUTDOWN PROBLEM. Fleming, Ronald F.; Roberts, John J.; Smith, Harold P. Jr. (Univ. of California, Berkeley). Trans. Amer. Nucl. Soc., 8: 480-1(Nov. 1965).

**3411** ANALYTIC ERROR ESTIMATES FOR INTEGRAL-EQUATION EIGENVALUE PROBLEMS. Sargis, D. A. (Argonne National Lab., Ill.); Grossman, L. M. Trans. Amer. Nucl. Soc., 8: 482-3(Nov. 1965).

**3412** A UNIFIED COMPUTATIONAL METHOD FOR THERMAL-NEUTRON SCATTERING. Triplett, John R.; Koppel, Juan U.; Naliboff, David (General Atomic Div., General Dynamics Corp., San Diego, Calif.). Trans. Amer. Nucl. Soc., 8: 483(Nov. 1965).

**3413** TIME-DEPENDENT PERTURBATION THEORY APPROACH TO THE NON-LINEAR KINETICS PROBLEM. Jason, R. H. (Argonne National Lab., Ill.). Trans. Amer. Nucl. Soc., 8: 483-4(Nov. 1965).

**3414** CALCULATIONAL STUDIES OF EFFECTS OF THIN-SLAB HETEROGENEITIES UPON SPECTRAL REACTIVITY COMPONENT OF Na-VOIDING. Meneghetti, David (Argonne National Lab., Ill.). Trans. Amer. Nucl. Soc., 8: 493-4(Nov. 1965).

**3415** REACTOR EXCURSIONS WITH RAMP REACTIVITY INSERTION. Canosa, Jose (General Electric Co., Pleasanton, Calif.). Trans. Amer. Nucl. Soc., 8: 495-6(Nov. 1965).

**3416** FREQUENCY RESPONSE SENSITIVITIES IN REACTOR DYNAMICS STUDIES. Kerlin, T. W.; Lucius, J. L. (Oak Ridge National Lab., Tenn.). Trans. Amer. Nucl. Soc., 8: 496-7(Nov. 1965).

**3417** USE OF THE ADIABATIC APPROXIMATION IN PROMPT-CRITICAL, LARGE-CORE REACTOR-EXCURSION ANALYSES. West, D. L.; Kalman, M. P.; Boyden, J. E.; Stirn, R. C.; Barth, J. J. (General Electric Co., San Jose, Calif.). Trans. Amer. Nucl. Soc., 8: 497-8 (Nov. 1965).

**3418** A TIME-INTEGRATED MODEL FOR REACTOR-EXCURSION CALCULATIONS. Gyorey, Geza L.; Keck, Carolyn A. (General Electric Co., San Jose, Calif.). Trans. Amer. Nucl. Soc., 8: 498-9(Nov. 1965).

**3419** SPATIAL KINETICS IN LARGE REACTORS. Hamric, J. P. (General Electric Co., Richland, Wash.). Trans. Amer. Nucl. Soc., 8: 499-500(Nov. 1965).

**3420** THE IMPORTANCE OF SPACE AND ENERGY EFFECTS IN NEUTRON-FLUCTUATION EXPERIMENTS. Natelson, M.; Osborn, R. K.; Shure, F. (Univ. of Michigan, Ann Arbor). Trans. Amer. Nucl. Soc., 8: 500-1(Nov. 1965).

**3421** CALCULATING SPACE-DEPENDENT REACTOR TRANSFER FUNCTIONS USING STATICS TECHNIQUES.

MacDonald, R. N.; Johnson, R. J. (Georgia Inst. of Tech., Atlanta). Trans. Amer. Nucl. Soc., 8: 501-2(Nov. 1965).

**3422** APPROXIMATE TRANSFER FUNCTIONS FOR COUPLED-CORE REACTOR DYNAMICS. Gage, Stephen J. (Purdue Univ., Lafayette, Ind.); Adler, F. T. Trans. Amer. Nucl. Soc., 8: 502-3(Nov. 1965).

**3423** SOLUTIONS TO THE MONOENERGETIC TRANSPORT EQUATION FOR A CRITICAL SLAB BY PERTURBATION THEORY. Hendry, W. L. (Massachusetts Inst. of Tech., Cambridge). Trans. Amer. Nucl. Soc., 8: 505-6(Nov. 1965).

**3424** A NEW LATTICE CALCULATION METHOD FOR ORGEL-TYPE REACTORS. Amyot, L.; Casini, G.; Cuniberti, R.; DeHaan, W.; Kind, A. (EURATOM, Ispra, Italy). Trans. Amer. Nucl. Soc., 8: 511-12(Nov. 1965).

**3425** EVALUATION OF CALCULATIONAL MODELS AND THERMAL CROSS-SECTION DATA IN THE ANALYSIS OF $PuO_2$–$UO_2$–$H_2O$ LATTICES. Bindler, L. (Westinghouse Electric Corp., Pittsburgh; CEN, Mol, Belg.); Poncelet, C. G. Trans. Amer. Nucl. Soc., 8: 512-13(Nov. 1965).

**3426** AN APPROXIMATION TO SPACE-ENERGY SLOWING DOWN THROUGH USE OF MULTIGROUP THERMAL SELF-SHIELDING FACTORS IN $PuO_2$–$UO_2$ LATTICE CALCULATIONS. Tomonto, James R.; Kazi, A. Halim (United Nuclear Corp., White Plains, N. Y.). Trans. Amer. Nucl. Soc., 8: 513-14(Nov. 1965).

**3427** CALCULATION OF THE FAST-FLUX FINE STRUCTURE IN THE CYLINDRICAL-CELL APPROXIMATION. Cohen, S. C. (General Atomic Div., General Dynamics Corp., San Diego, Calif.). Trans. Amer. Nucl. Soc., 8: 514-15(Nov. 1965).

**3428** PRESCRIPTION FOR DIFFUSION-THEORY REPRESENTATION OF FUEL CLUSTERS CONTAINING CONTROL RODS BASED ON MONTE CARLO CORRELATION OF CAPTURE PROBABILITIES. Flanagan, Charles A. (Westinghouse Electric Corp., Pittsburgh). Trans. Amer. Nucl. Soc., 8: 515-16(Nov. 1965).

**3429** WANL EXPERIENCE WITH r-θ CALCULATIONS. Ravets, J. M.; Brevard, D. G. (Westinghouse Astronuclear Lab., Pittsburgh). Trans. Amer. Nucl. Soc., 8: 517-18(Nov. 1965).

**3430** DIRECT MEASUREMENT OF EFFECTIVE CAPTURE-TO-FISSION RATIO AT LOW FLUX. Redman, W. C.; Bretscher, M. M. (Argonne National Lab., Ill.). Trans. Amer. Nucl. Soc., 8: 531-2(Nov. 1965).

**3431** ON THE INTERPRETATION OF REACTIVITY MEASUREMENTS OF REACTOR MEDIA. Heineman, R. E. (Battelle-Northwest, Richland, Wash.). Trans. Amer. Nucl. Soc., 8: 532-3(Nov. 1965).

**3432** STUDIES OF SUBCRITICAL LATTICES WITH DISTRIBUTED NEUTRON ABSORBER BY MEANS OF THE PULSED-NEUTRON SOURCE TECHNIQUE. Bliss, Henry E.; Lanning, D. D.; Harrington, Joseph; Kaplan, I.; Malaviya, B. K.; Thompson, T. J. (Massachusetts Inst. of Tech., Cambridge). Trans. Amer. Nucl. Soc., 8: 533 (Nov. 1965).

**3433** INITIAL USAGE OF A COMPUTER FOR ON-LINE DATA REDUCTION IN REACTOR PHYSICS EXPERIMENTS. Cohn, Charles E. (Argonne National Lab., Ill.). Trans. Amer. Nucl. Soc., 8: 585(Nov. 1965).

**3434** THE LATTICES OF GRAPHITE MODERATED REACTORS. Zamparo, Giuseppe (A.C.F. Industries, Inc., Washington, D. C.). Termotecnica (Milan), 18: 240-53(1964). (In Italian).

The lattices of a graphite-moderated, gas-cooled reactor using metallic bars of natural U were calculated. The effects of the substitution of natural uranium oxide as the fuel and of enriched metallic uranium on the lattice parameters are investigated. (J.S.R.)

**3435** SCATTERING KERNELS AND THEIR TEMPERATURE DEPENDENCE [Thesis]. Dahlberg, Richard Craig. Troy, N. Y., Rensselaer Polytechnic Inst., 1964. 159p.

The temperature dependence of the elastic and inelastic components of the differential cross section is studied. A brief derivation of the incoherent formulation for $\sigma(E_0/E,\Omega)$ is given and it is pointed out that only one factor in this cross section, the average number of phonons per oscillator, is usually assumed to be temperature-dependent. An outline of the frequently used physical models and numerical approximations is then presented with specific attention given to the free gas type models, phonon expansion, short collision time approximation, mass expansion, and a model that combines a free-gas and an Einstein oscillator. The temperature characteristics of these models are considered. Emphasis is placed on both the temperature derivative of the cross section and on its scaling properties. It is shown that the temperature dependence of the bound atom kernels are significantly different from those of the free gas type kernels. The difference between Debye and Einstein solids is often significant, but usually the differences between bound atom kernels with respect to their temperature dependence is not large. The case for large energy transfers is treated explicitly. Nelkin's water model is also treated separately. Figures are presented showing the energy dependence of the temperature coefficients for the various scattering kernels examined. The effect of the scattering kernel on the (thermal) reactor flux is studied. The temperature dependence of various reactor physics parameters is considered. The power spike at the core-reflector interface of a beryllium reflected fast reactor is shown to be sensitive in some cases to whether a crystalline kernel or a free gas kernel is used for beryllium. And in hydrogenous systems, the thermal utilization, eta, $\sigma_a$ ($Pu^{239}$), and water gap peaking are shown to be temperature-dependent, but this dependency does not appear to be too sensitive to the scattering kernel. Finally, the effect of the kernel on neutron moderation is examined. (Dissertation Abstr.)

**3436** A GENERAL TIME-DEPENDENT PERTURBATION THEORY FOR REACTOR PHYSICS [Thesis]. Munno, Frank J. Gainesville, Fla., Univ. of Florida, 1964. 105p.

Techniques for the approximate solution of a set of space- and time-dependent differential equations of the following form are described: $[H_0(r) + H(r,t)]\psi(r,t) = (\partial/\partial t)\psi(r,t)$ + associated boundary conditions. Equations of this type are important in the study of neutron chain reactor kinetics. The approaches involved follow lines developed in the quantum mechanics and quantum field theories. The so-called period eigenfunctions are employed in these techniques. Examples of neutron reactor oscillators are presented, including spatial effects, oscillator localization effects, and reflector effects. (Dissertation Abstr.)

**3437** APPLICATION OF THE PROMPT-JUMP APPROXIMATION TO PROBLEMS IN REACTOR STABILITY. Hetrick, David L. (Univ. of Arizona, Tucson). 17p. (CONF-650602-63). Gmelin, AED-CONF-65-125-35.

From American Nuclear Society, 11th Annual Meeting, Gatlinburg, Tenn.

The prompt-jump approximation is used for reducing a third-order non-linear reactor dynamic model to second-order for three examples: (1) the adiabatic model, (2) the constant power-removal model, and (3) Newton's law of cooling, thus permitting standard phase-plane analysis. Case (3) is the simplest reactor model having realistic treatment of both delayed neutrons and heat transfer. Limits of validity and artificial initial conditions for the prompt-jump approximation are discussed, and the possibility of three dimensional stability studies is pointed out for fourth-order nonlinear systems (e.g., delayed neutrons plus two reactivity feedbacks). (auth)

**3438** NEAR-OPTIMUM SHUTDOWNS FOR NUCLEAR REACTORS. Fredsall, J. R. (Australian Atomic Energy Commission). 15p. (CONF-650602-61). Gmelin, AED-CONF-65-125-42.

From American Nuclear Society, 11th Annual Meeting, Gatlinburg, Tenn.

The general problem of determining the optimum power reduction function is a complex one that depends on the desired startup time, the xenon and iodine concentrations, the variations of reactor reactivity, and the purpose of the reactor in question. An analysis method embodied in the digital computer code SHUTDOWN makes possible the determination of near-optimum shutdown modes for most reactors. Determined functions compare favorably with available data for the Canadian NRU reactor, and solutions for the minimization of peak xenon problem found using Pontryagin's Maximum Principle. (auth)

**3439** LINEAR RELATIONSHIP BETWEEN CADMIUM RATIO AND REACTOR CORE MODERATING RATIO. Stanford, G. S.; Plumlee, K. E.; Robinson, W. R. 16p. (CONF-650602-68). Gmelin, AED-CONF-64-219-135.

From American Nuclear Society, 11th Annual Meeting, Gatlinburg, Tenn.

Cadmium ratios for several materials were measured in a number of different thermal critical assemblies, covering a wide range of fuel-to-moderator ratios, with emphasis on undermoderated systems. It has been found, for the cores and detector materials investigated, that the cadmium ratio for a given material is primarily a function of the moderating ratio of the core, with only secondary dependence on the actual materials or configuration of the lattice. (auth)

## Design and Feasibility

**3440** (RT/ING(65)16) REATTORE "TANK TYPE" MODERATO E REFRIGERATO AD ORGANICO. ESAME PRELIMINARE DI UN PROTOTIPO DA 50 MWt. (Tank Type Organic Cooled and Moderated Reactor. Preliminary Investigation of a 50-MWt Prototype). Merli, E. (Comitato Nazionale per l'Energia Nucleare, Rome (Italy)). Sept. 1965. 51p. Dep. mn.

The nuclear plant description included is a conceptual design of a prototype plant utilizing an organic moderated and cooled reactor. The plant design includes features that have the objective of improving the economic characteristic of the plant over that of previous organic moderated and cooled reactor designs. (auth)

**3441** VERIFICATION OF A METHOD FOR CALCULATIONS OF GAS-COOLED AND GRAPHITE-MODERATED REACTORS. Zamparo, Giuseppe (A.C.F. Industries, Inc., Washington, D. C.). Termotecnica (Milan), 18: 254-8(1964). (In Italian).

A method is presented for doing design calculations on gas-cooled and graphite moderated reactors. The method is verified by comparison with experimental data obtained from the Calder Hall reactor. (J.S.R.)

**3442** PRESSURE TUBE NEUTRONIC REACTOR. Campbell, Ronald M.; Jones, Stuart M. (to Canadian Westinghouse Co., Ltd.). U. S. Patent 3,208,915. Sept. 28, 1965. Priority date Aug. 30, 1958, Canada.

A pressure tube reactor, fuel transport, refueling, and manipulating arrangements for the reactor and flow regulating and port closure devices for the individual pressure tubes of the reactor are patented. The reactor includes an elongated moderator tank and a pair of shielding tanks. The shielding tanks are joined to and close the ends of the moderator tank. A number of the pressure tubes extend through the moderator tank and have their end portions passing through and secured to the shielding tanks so that the tubes are suspended in the moderator tank. The fuel is contained in tandem arrangement within the pressure tubes. Means are provided for circulating coolant through the tubes. A number of radially reinforcing ribs are secured to the outer surface of the moderator tank, and a generally tubular reflecting and shielding tank surrounding the moderator tank is sealed to the outermost ribs to enclose a shielding and reflecting space between the two tanks. (B.L.M.)

## Fuels

*Refer also to abstracts 1978, 2022, 2231, 2469, and 3511.*

**3443** (EURAEC-1356) NUCLEAR VAPOTRON. Quarterly Report No. 8, January 1–March 31, 1964. (Compagnie Francaise Thomson-Houston, Paris. Societe Alsthom, Paris (France). Allgemeine Elektrizitaetsgesellschaft, Frankfurt am Main (West Germany)). Feb. 12, 1965. Contract 034-63-11 TEEC(RD). 38p. (EUR-2331). Dep. mn; CFSTI $2.00 cy, $0.50 mn.

Work Performed under United States–Euratom Joint Research and Development Program.

The design of a test cell, instrumentation for flow and electric-property measurements, and instruments for observing the phenomena under study are described, for a facility whose purpose is the thermal testing of nuclear-vapotron fuel cans. (T.F.H.)

**3444** (EURAEC-1357) NUCLEAR VAPOTRON. Quarterly Report No. 9, April–June 1964. (Compagnie Francaise Thomson-Houston, Paris. Societe Alsthom, Paris (France). Allgemeine Elektrizitaetsgesellschaft, Frankfurt am Main (West Germany)). Feb. 12, 1965. Contract 034-63-11-TEEC(RD). 48p. (EUR-2332). Dep. mn; CFSTI $2.00 cy, $0.50 mn.

Work Performed under United States–Euratom Joint Research and Development Program.

Nuclear-vapotron fuel-can configurations are studied in a test system. The operation of a test loop and test cell are described. The safety and control systems for the test facility are noted. Instrumentation for obtaining measurements and for observing and recording processes in the test area is described. Measurements are reported of flow rates, static pressures, and temperatures. (T.F.H.)

**3445** (EURAEC-1358) NUCLEAR VAPOTRON. Quarterly Report No. 10, July–September 1964. (Compagnie Francaise Thomson-Houston, Paris. Societe Alsthom, Paris (France). Allgemeine Elektrizitaetsgesellschaft, Frankfurt am Main (West Germany)). Feb. 15, 1965. Contract 034-63 TEEC(RD). 14p. (EUR-2333). Dep. mn; CFSTI $1.00 cy, $0.50 mn.

Work Performed under United States–Euratom Joint Research and Development Program.

Burnout measurements are reported on several nuclear-vapotron fuel-can configurations. (T.F.H.)

**3446** (GEST-2045) RESEARCH PROGRAM FOR THE LONG TERM TESTING OF CYLINDRICAL DIODES AND THE IRRADIATION OF FUEL AND INSULATOR. Sixth Quarterly Progress Report, September 18–December 17, 1964. (General Electric Co., Pleasanton, Calif. Special Purpose Nuclear Systems Operation). Dec. 17, 1964. Contract NAS 3-2544. 82p. (NASA-CR-54384).

Experimental and analytical work in nuclear thermionics is presented. (auth)

**3447** NUCLEAR FUELS AND NUCLEAR ELEMENTS. Wirths, Guenter (Nukem, Nuklear-Chemie und -Metallurgie GmbH, Hanau, Ger.). At. Strom., 11: 94-101(Sept.-Oct. 1965). (In German).

The state of development in the Federal Republic for processing nuclear fuels and for manufacturing fuel elements for reactors is reported. (L.B.S.)

**3448** THE PRESENT STATE OF FUEL COSTS FOR HIGH-TEMPERATURE REACTORS WITH SPHERICAL FUEL ELEMENTS. Cautius, Werner (Arbeitsgemeinschaft Versuchs-Reaktor (AVR) GmbH, Duesseldorf, Ger.). At. Strom., 11: 102-5(Sept.-Oct. 1965). (In German).

Fifa values are determined for the fuel system of a high-temperature reactor from a solution of the burn-up equation, on the basis of the burn-up performance of the uranium–thorium charge. Fuel costs are determined from the fifa values with certain assumptions. Possibilities of a reduction in the calculated values are outlined as a future task; recent data from the American literature are used for comparison. (auth)

**3449** FUTURE REACTOR FUELS COULD BE Pu OR Th. Can. Chem. Process., 49: 49-51(Aug. 1965).

A fuel reprocessing plant for plutonium extraction and more refining of thorium are prospects in the 1970's for Canada's chemical industry supporting nuclear power gen-

eration within the country and elsewhere. Plutonium extraction in the U.S. and U.K. is examined and the economic aspects are considered for CANDU-type reactors. Fabrication aspects and flexibility of U, Th and Pu fuels are discussed. (F.S.A.)

**3450** TEMPERATURE DISTRIBUTION AND HEAT TRANSFER IN A ROD OF A BUNDLE FUEL ELEMENT FOR NUCLEAR REACTORS. Markoczy, G.; Stiefel, U. (Eidgenoessisches Institut fuer Reaktorforschung, Wuerenlingen, Switzerland). Neue Tech., 7: 163-73(Aug. 1965). (In German).

A method was developed for thermal calculations of rod-cluster fuel-elements for nuclear reactors. Computer calculations of the temperature distributions in a fuel rod were carried out. Approximate equations used in the cluster calculations were developed for the heat transferred through the rod and for the surface temperature distribution. The accuracy of the approximation was checked by comparison with the computer results. (auth)

**3451** THE ONTARIO ECONOMIC AND NUCLEAR MISSION. McRae, I. F. Nucl. Energy, 213-15(July 1965).

A comparison is made of the fuel through-put economy for the heavy-water, light-water, and graphite moderated reactor types. Some advantages of the heavy-water reactor system are pointed out. (L.B.S.)

**3452** DEVELOPMENT FUEL ASSEMBLY IRRADIATION TESTING IN THE BIG ROCK POINT REACTOR. Duncan, R. N.; Arlt, W. H.; Pashos, T. J. (General Electric Co., San Jose, Calif.). Trans. Amer. Nucl. Soc., 8: 363-5(Nov. 1965).

**3453** STRUCTURAL ANALYSIS OF FUEL GROWTH IN FUEL PLATES. Scavuzzo, R. J. (Univ. of Toledo). Trans. Amer. Nucl. Soc., 8: 386(Nov. 1965).

**3454** FEW LONG-TIME-INCREMENT DEPLETION CALCULATIONS FOR APPROXIMATING BY SYNTHESIS A MANY SHORT-TIME-INCREMENT DEPLETION CALCULATION. Flanagan, Charles A. (Westinghouse Electric Corp., Pittsburgh). Trans. Amer. Nucl. Soc., 8: 518-19 (Nov. 1965).

**3455** THE CALIBRATION OF A HIGH-SPEED BURNUP CODE FOR NUCLEAR FUEL SURVEYS. Deonigi, Duane E.; Merrill, E. T.; Porath, W. W. (Battelle-Northwest, Richland, Wash.). Trans. Amer. Nucl. Soc., 8: 522-3(Nov. 1965).

**3456** MONTE CARLO CALCULATION OF OPTIMUM LOADING OF PLUTONIUM IN FUELS. Merrill, E. T. (Battelle-Northwest, Richland, Wash.). Trans. Amer. Nucl. Soc., 8: 573-4(Nov. 1965).

**3457** A NEW FUEL CONFIGURATION TO INCREASE PLUTONIUM VALUE IN THERMAL REACTORS. Deonigi, Duane E.; Nail, James H. (Battelle-Northwest, Richland, Wash.). Trans. Amer. Nucl. Soc., 8: 575-6(Nov. 1965).

**3458** CONSERVATION ECONOMICS AND REACTOR TECHNOLOGY. Neef, W. I.; Jones, E. D. Jr. (Battelle-Northwest, Richland, Wash.). Trans. Amer. Nucl. Soc., 8: 576-8(Nov. 1965).

**3459** POST-BUCKLING BEHAVIOR OF HYDRAULICALLY COLLAPSED ASSEMBLY FUEL PLATES. Scavuzzo, R. J. (Univ. of Toledo, Ohio). Trans. Amer. Nucl. Soc., 8: 591-2(Nov. 1965).

**3460** OPERATION OF A SODIUM LOOP WITH CIRCULATION OF STAINLESS-STEEL PASTE. Chamberlain, Harry V.; Moore, Charles R.; Chase, Wayne L. (Atomic Power Development Associates, Inc., Detroit). Trans. Amer. Nucl. Soc., 8: 598(Nov. 1965).

**3461** HYDRAULIC STUDIES WITH RANDOM-PACKED BEDS APPLICABLE TO THE PASTE-FUEL CONCEPT. Moore, Charles R.; Kovacic, Evan C.; Chamberlain, Harry V. (Atomic Power Development Associates, Inc., Detroit). Trans. Amer. Nucl. Soc., 8: 598-9(Nov. 1965).

**3462** FUELS FOR GASEOUS-CORE NUCLEAR ROCKETS. Holl, R. J.; Plunkett, T. F. (Douglas Aircraft Co., Inc., Santa Monica, Calif.). Trans. Amer. Nucl. Soc., 8: 609-10(Nov. 1965).

**3463** TRANSIENT THERMAL STRESSES IN LIQUID METAL COOLED REACTOR FUEL ELEMENTS [Thesis]. Reuscher, Jon Arthur. College Station, Tex., Texas Agricultural and Mechanical Univ., 1965. 312p.

A numerical solution for two-dimensional transient thermal stresses in a liquid-metal-cooled nuclear reactor fuel element is presented. The method consists of first determining the two-dimensional transient temperature field across a fuel element and its adjacent coolant channel by a finite difference solution to a set of partial differential equations for a given time variation of both reactor power and coolant flow rate. The determination of the temperature field solution takes into account a heat source term and conduction in the fuel element in the direction perpendicular to the direction of coolant flow, convection and conduction perpendicular to the coolant flow in the coolant channel, and convection only in the direction of coolant flow in the channel. After the transient temperature field is determined, values of the components of the stress tensor are calculated using a variational type solution to an inhomogeneous biharmonic equation for the Airy stress function in uncoupled, linear, quasi-static thermoelastic theory. Results are presented for temperatures and thermal stresses in plate and cylindrical fuel elements for a variety of power level and coolant flow transients, including the loss of pumping power accident. The computer programs used to calculate these results are also included. (Dissertation Abstr.)

**3464** PRACTICAL GAMMA COUNTING OF UNIRRADIATED $^{235}U$. Colsmann, P. (Brookhaven National Lab., Upton, N. Y.). Vienna, International Atomic Energy Agency, 1965, Preprint No. SM-67/47, 17p. (CONF-650803-15). ORINS.

From IAEA Symposium on Nuclear Materials Management, Vienna.

The particular method described was used for checking fuel cores of nominal 30 wt % enriched uranium in aluminum measuring about two inches square by .080 and .160 in. thick. The equipment was a basic NaI scintillation counter equipped with a single channel analyzer. The analyzer, however, was operated with a wide window covering both the 90 and 184 kev peaks characteristic of $^{235}U$. In practice, the threshold level and the window opening were adjusted to give the optimum maximum count rate as indicated by a rate-meter. The counting of a fuel core was then performed with the NaI crystal essentially unshielded and located several inches above the fuel core. The counting time was adjusted to yield a total count in the range of $10^5$ to $10^6$ in order to minimize the counting error. Effects due to variations in the counting geometry and to non-uniform uranium distribution were minimized by the relatively large separation of the crystal from the fuel core. Effects due to shifting of analyzer window were minimized by use of a wide opening. To compensate for possible non-uniform uranium distribution through the thickness of a fuel core, each core was counted on both sides. The total count obtained in this manner was directly proportioned to the $^{235}U$ content of the fuel core. (auth)

**3465** IMPROVEMENTS RELATING TO NUCLEAR REACTORS. Currell, Kenneth Richard; Rout, Reginald Harold (English Electric Co. Ltd.). British Patent 1,005,541. Sept. 22, 1965. Filed Jan. 10, 1961.

A fuel element for a nuclear reactor includes a cylindrical graphite sleeve and a cluster of fuel cans, each can containing nuclear fuel and supported in the sleeve by an end support member. Each support member is attached independently to the sleeve, preferably by rivets passing through axially extending tabs on the supports. Each fuel can has a radially protecting portion adjacent each end to limit axial movement of the can between support members. Each sleeve is provided with an arrangement of projections and recesses for engaging adjacent sleeves. (A.G.W.)

**3466** IMPROVEMENTS IN OR RELATING TO NUCLEAR REACTOR FUEL ELEMENTS. Griffiths, Jack

Jones (to United Kingdom Atomic Energy Authority). British Patent 1,005,881. Sept. 29, 1965. Filed Jan. 26, 1961.

A brace is described for splitter fins loosely fitted in longitudinal slots in heat transfer fins on the tubular sheath of a reactor fuel element. The brace consists of an endless hoop, which is a near fit around the heat transfer fins and which has pairs of locating plates integral with and projecting radially outward from it. The outwardly projecting part of each splitter fin is located between a pair of the locating plates, which are wide enough to extend from the hoop to the outer edges of the fins. The hoop passes through a transverse slot in the splitter fin. (A.G.W.)

**3467** NUCLEAR REACTOR FUEL ELEMENT HAVING IMPROVED FIN STRUCTURE. Bowden, Andrew T. (to C. A. Parsons and Co. Ltd.). U. S. Patent 3,207,673. Sept. 21, 1965. Priority date Sept. 27, 1957, Great Britain.

A fuel element consists of a nuclear fuel housed in a container having fins on its outer surface. The fins are helically disposed with respect to the central axis of the container, and baffles extend along the axis of the container to interrupt the channels formed between the fins. The baffles extend outwardly beyond the tips of the fins, and the part that is located beyond the helical fins is corrugated transverse to the axis of the element. (B.L.M.)

**3468** FUEL ELEMENT FOR A NUCLEAR REACTOR. Bosshard, Ernst (to Sulzer Freres). U. S. Patent 3,208,917. Sept. 28, 1965. Priority date Mar. 15, 1960, Switzerland.

A fuel element for a nuclear reactor is made up of an oblong casing closed at one end containing a number of tubes made substantially of fissionable material. A pipe is connected to the open end of the casing and extends coaxially of the casing. Oblong spaces exist between the tubes and between the tubes and casing, and a coolant flows under pressure through some of the spaces in one direction and through the fuel tubes in the opposite direction. (B.L.M.)

## Power and Power-Breeder Reactors

*Refer also to abstracts 2093, 2116, 2230, 2297, 2386, 2670, and 3553.*

**3469** (CVNA–242) RESEARCH AND DEVELOPMENT PROGRAM QUARTERLY PROGRESS REPORT, JANUARY–MARCH 1965. (Westinghouse Electric Corp., Pittsburgh, Pa. Atomic Power Div.). Contract AT(30-1)-3269. 74p. Dep. mn; CFSTI $3.00 cy, $0.75 mn.

For Carolinas Virginia Nuclear Power Associates, Inc., Parr, S. C.

Results are presented for investigations on the primary system pressure drops, reactor transients, radiation analysis, chemistry program, thermal and hydraulic cores, nuclear evaluation of the plant, ultrasonic inspection of pressure tubes, metallurgical examination of CVTR components, high power-high burnup evaluation tests, and a hazards analysis. (M.O.W.)

**3470** (GA–5499) EXPERIMENTAL BERYLLIUM OXIDE REACTOR PROGRAM. Quarterly Progress Report for the Period Ending June 30, 1964. (General Atomic, San Diego, Calif. John Jay Hopkins Lab. for Pure and Applied Science). Aug. 28, 1964. Contract AT(04-3)-187. 42p. Dep. mn; CFSTI $2.00 cy, $0.50 mn.

Component design modifications, fabrication, and testing are described. (W.L.G.)

**3471** (GEAP–4861) NUCLEAR SUPERHEAT PROJECT TWENTY-THIRD QUARTERLY REPORT, FEBRUARY 1965–APRIL 1965. (General Electric Co., San Jose, Calif. Atomic Power Equipment Dept.). May 1965. Contract AT(04-3)-189. 92p. Dep. mn; CFSTI $3.00 cy, $0.75 mn.

Topics reviewed include: testing and evaluation of Incoloy 800, Incoloy 2, Inconel, boron-rich 304 stainless steel, Ni–Cr alloys, Inconel 625, Hastelloy F, Inconel 718, Rene 62, 310 stainless steel, and Hf for fast superheat reactor uses; heat transfer in rod bundles having turbulence promoters; operations of the Mixed Spectrum Superheat Critical Experiment Facility; the use of this critical facility to conduct experimental and analytic studies of reactivity distribution, flooding, Doppler effects, heterogeneous effects, neutron spectra, fission and conversion ratios, danger coefficients, plutonium characteristics, reactivity effects of structural materials, and kinetics of mixed-spectrum superheat reactors; studies of the feasibility of a mixed-spectrum superheat power reactor; and the performance of $PuO_2-UO_2$ fuel mixtures in this type of reactor. (T.F.H.)

**3472** (GEAP–4891) EVESR-NUCLEAR SUPERHEAT FUEL DEVELOPMENT PROJECT. Twelfth Quarterly Report, March–May 1965. Murray, J. L. (General Electric Co., San Jose, Calif. Atomic Power Equipment Dept.). June 1965. Contract AT(04-3)-189. 128p. Dep. mn; CFSTI $4.00 cy, $1.00 mn.

The EVESR power level was increased from 12.5 Mw(t) to the new license limit of 17 Mw(t). This increase was made possible by a combination of changes which resulted in greater steam production by the gas-fired boiler, and by more detailed analysis of the steam flow requirements of the core for the actual existing power distribution. Shortly after reaching 17 Mw(t), a cladding failure occurred in the Mark III fuel bundle which contains 8-mil-thick Incoloy-800 clad fuel elements. Tests are being conducted to evaluate the fission product release characteristics. The early part of May was spent evaluating and controlling the iodine-131 release. The iodine-131 problem was resolved satisfactorily, and since then the primary concern has been the buildup of fission product activity in the superheat steam piping and components. Operation with the fuel defect will continue before removing the fuel bundle for RML examination. Prior to occurrence of the natural defect in the Mark III fuel bundle, plans were made to insert artificial defects in the core. A small slit was made in the cladding of one fuel element in spare Mark II fuel bundle KB-35. Consideration is being given to inserting this defect in the core after evaluation of the natural defect is completed. A three-dimensional physics analysis of the Mark III core was completed, and is reported in some detail. This analysis made possible the last incremental power increase in going to 17 Mw(t). Work continued on operation of the Mark III core with a reversed control rod pattern. Fabrication of the Mark IV bundle hardware is 90% complete, and all but 2 of the 16 fuel rods are complete. Design work and selection of test variables progressed well for the Mark V fuel bundles. Design work was initiated for the fabrication of Mark IV spare fuel rods. Detailed design for the EVESR irradiation of two Advanced BONUS Core fuel assemblies was initiated. (auth)

**3473** (GEAP–4903) A SURVEY FOR A HIGH TEMPERATURE SENSOR FOR SEFOR. Asamoto, R. R.; Novak, P. E. (General Electric Co., San Jose, Calif. Atomic Power Equipment Dept.). Apr. 30, 1965. Contract AT (04-3)-540. 28p. Dep. mn; CFSTI $2.00 cy, $0.50 mn.

Measurements of reactor fuel temperatures in the Southwest Experimental Fast Oxide Reactor, under both steady-state and transient operating conditions, are desirable in order to correlate and evaluate reactor physics parameters, primarily the Doppler effect. An extensive literature search was undertaken to investigate temperature sensing devices usable up to 4700°F in a $(Pu, U)O_2$ environment. Conclusions from this survey are presented. (M.O.W.)

**3474** (GNEC–364) BONUS NUCLEAR POWER PLANT. DRL Monthly Report No. 44, July 1964. (General Nuclear Engineering Corp., Dunedin, Fla.; Puerto Rico Water Resources Authority, San Juan). Aug. 25, 1964. Contract AT(30-1)-143. 47p. Dep. mn; CFSTI $2.00 cy, $0.50 mn.

Developments in the BONUS reactor for July 1964 are presented. Summaries are given for the total hours of operation and total power generated, number of shutdowns with a brief explanation of each, operating experience including malfunctions in the control and safety systems,

measurements and tests performed and the results thereof, principle maintenance performed, and the kind and quantity of radioactive material released to the environment. (M.O.W.)

**3475** (NP–15458) ATOMNAYA STANTSIYA BN-350. (The BN-350 (Fast Neutron) Atomic Power Station). Leipunskii, A. I.; Kazachkovskii, O. D.; Pinkhasik, M. S.; Krasnoyarov, N. V.; Bagdasarov, Yu. E.; Troyanov, M. F.; Milovidov, I. V.; Afrikantov, I. I.; Poido, M. S.; Stekol'nikov, V. V. (Gosudarstevnnyi Komitet po Ispol'zovaniyu Atomnoi Energii SSSR, Obninsk. Fiziko-Energeticheskii Institut). 1965. 30p. Dep. mn.

The projected BN-350 fast sodium-cooled power-breeder reactor is described. Design power is 1000 Mw(t) and 350 Mw(e). The selection of the $UO_2$ and $PuO_2$ fuel, the reactor-core configuration, and the enrichment of the various zones are discussed. Control and shielding systems are considered, including measurement and regulation of the power and period, automatic control, reactivity compensation, and emergency shielding. Selection and testing of reactor materials—for the reactor vessel, coolant loops, steam generators, and coolant—are briefly discussed. The heat-removal system, including the primary and secondary coolant loops, equipment layout, emergency procedures, and intermediate heat exchanger, is described. The steam generator and pump are described. Work on design improvements is surveyed, including increasing the burnup depth and the use of carbide fuel elements. Diagrams of the various reactor parts are included. (M.J.T.)

**3476** (NP–15538(Vol.1)) DRESDEN NUCLEAR POWER STATION. UNIT 2. PLANT DESIGN AND ANALYSIS REPORT. VOLUME I. (Commonwealth Edison Co., Chicago, Ill.). [nd]. 286p. Dep. mn; CFSTI $6.00 cy, $1.50 mn.

Preliminary information on a nuclear power plant for operating at power levels up to approximately 2300 Mw(t) is given. Information is given in separate sections on the reactor design, plant safeguards features, radioactive waste control systems, plant electrical system, process, area, and health monitoring, other plant features, general plant control and instrumentation, safety analysis, and plant management. (M.O.W.)

**3477** (NP–15538(Vol.2)) DRESDEN NUCLEAR POWER STATION. UNIT 2. PLANT DESIGN AND ANALYSIS REPORT. VOLUME II. DRAWINGS. (Commonwealth Edison Co., Chicago, Ill.). [nd]. 113p. Dep. mn; CFSTI $4.00 cy, $0.75 mn.

Included are the applicable pictures, drawings, plot and building elevation plans, sketches, and electrical and piping diagrams of the Dresden Nuclear Power Station Unit 2. (M.O.W.)

**3478** (NP–15538(Vol.3)) DRESDEN NUCLEAR POWER STATION. UNIT 2. PLANT DESIGN AND ANALYSIS REPORT. VOLUME III. PLANT SITE AND ENVIRONS. (Commonwealth Edison Co., Chicago, Ill.). [nd]. 274p. Dep. mn; CFSTI $6.00 cy, $1.50 mn.

Information on the site and environs of the proposed Unit 2 of the Dresden Nuclear Power Station is given. Sections are given concerning the geology, land usage and population in the environs, seismology, hydrology, regional meteorological characteristics, and site atmospheric diffusion characteristics. (M.O.W.)

**3479** (NP–15556) PRELIMINARY DESIGN WORK OF THE 2 MW Na LOOP. Nozawa, Masao; Sako, Kiyoshi; Ueda, Hiroshi (Japan Atomic Energy Research Inst., Tokyo). Sept. 1, 1965. 11p. Dep. mn.

The preliminary design of a 2-Mw sodium loop for use with the experimental fast reactor to be built in 1971 is given. Engineering drawings are given on the piping and instrumentation, general arrangement of the loop, and the heater tube bundle and heat exchanger for a heat transfer experiment. (M.O.W.)

**3480** (ORNL-P–1679) A CONTROL SYSTEM FOR A GAS-COOLED NUCLEAR POWER PLANT. O'Brien, H. G.; Ditto, S. J. (Oak Ridge National Lab., Tenn.). [1965]. Contract W-7405-eng-26. 17p. (CONF-651001–7). Dep. mn; CFSTI $1.00 cy, $0.50 mn.

From IEEE Nuclear Science Symposium, San Francisco.

A major consideration in the control of a nuclear power plant such as the Experimental Gas Cooled Reactor is the regulation of both the temperature and pressure of the steam entering the turbine. A control system is described that varies the primary coolant flow and reactor power to make the plant produce steam at the required conditions of temperature and pressure over a wide range of steam flows. Analog computer studies show that the control system is able to make the simulated plant smoothly follow both large changes of turbine load (changing at a rate of 10% per minute) and small rapid changes of load (1% per second), while limiting the transient variations in steam conditions to acceptable values. (auth)

**3481** (SC-RR–65-121A) NUCLEAR ELECTRICAL POWER FOR SEA-LEVEL CANAL CONSTRUCTION. McDonald, G. Corry (Sandia Corp., Albuquerque, N. Mex.). Oct. 1965. Contract AT(29-1)-789. 26p. Dep. mn; CFSTI $2.00 cy, $0.50 mn.

Nuclear power reactors, government owned, can be used to advantage to furnish a portion of the electrical power required for sea-level isthmian canal construction. The possibility is suggested of developing 20 to 30-Mw portable reactor sources, nationally owned, for disaster area use and temporary construction projects. The interactions of nuclear and electrical power with mining processes are described. The various construction methods discussed are ranked by cost. Slide inducement as a mining method is detailed, and the necessity of post-slide slope stabilization after construction, even after nuclear excavation, is explained. Nonnuclear power-plant fuel quantities and costs which are of such magnitude as to demand optimum solutions are examined as well as the proposition that use of electrical power from any source can reduce work force size and promote health and safety. A pilot program and a preshipment equipment qualification plan are recommended. (auth)

**3482** (SWRI–1228-75) EVALUATION OF THE SERVICEABILITY OF THE ELK RIVER REACTOR PRESSURE VESSEL. Progress Report No. 12, May 1, 1965–July 31, 1965. Gunkel, W. A.; Lautzenheiser, C. E.; Lowenberg, A. L.; Norris, E. B. (Southwest Research Inst., San Antonio, Tex.). Sept. 29, 1965. Contract AT(11-1)-1228. 31p. Dep. mn; CFSTI $2.00 cy, $0.50 mn.

Work is reported on three phases of the program for the evaluation of the serviceability of the ERR pressure vessel. The three phases under study are the fatigue properties of steels and weldments, neutron irradiation on the nil ductility transition temperature, and the development of remote nondestructive testing procedures for critical locations in the pressure vessel. Results from the tests are presented. (M.O.W.)

**3483** (TID–22201) GARIGLIANO NUCLEAR POWER PLANT. Operation Report for the 1st Quarter of 1965. Technical Report, March 31, 1965. (Ente Nazionale per l'Energia Elettrica, Rome (Italy)). 7p. Dep. mn; CFSTI $1.00 cy, $0.50 mn.

The operations, maintenance, and waste and coolant chemistry data for Garigliano Power Reactor are summarized. (T.F.H.)

**3484** (TID–22329) ARDENNES NUCLEAR POWER PLANT QUARTERLY REPORT NO. 12, APRIL 1–JUNE 30, 1965. SUMMARY. I. DESIGN STUDIES. II. PREFABRICATED COMPONENTS. III. ON-SITE WORK. (Societe d'Energie Nucleaire Franco-Belge des Ardennes, Chooz-lez-Givet (France)). Aug. 2, 1965. 60p. Dep. mn; CFSTI $3.00 cy, $0.75 mn.

Includes original.

Summaries are presented on civil-engineering design, design studies on the conventional and nuclear parts, startup test, status of major components, and a general view of on-site work. (M.O.W.)

**3485** (WCAP–2120) 1000 MWe SUPERCRITICAL PRESSURE NUCLEAR REACTOR PLANT STUDY. Quar-

terly Progress Report No. 3, July 1, 1962–September 30, 1962. Kellogg, H. B.; Frain, J. F. (eds.) (Westinghouse Electric Corp., Pittsburgh, Pa. Atomic Power Div.). Nov. 1962. Contract AT(30-1)-2948. 96p. Dep. mn; CFSTI $2.00 cy, $0.75 mn.

The scope of work accomplished covers two general areas: supercritical pressure heat transfer loop design and procurement, and the design and evaluation of two 1000 Mw(e) supercritical pressure once-thru reactors. The supercritical pressure heat transfer loop basic design is complete, procurement was completed, and operation began as scheduled on August 15, 1962. Test pressures and heat fluxes will vary from 2400 to 4000 psia and from 0.2 to $1.5 \times 10^6$ Btu/hr-ft$^2$, respectively. Although the loop is designed for 600 kw test section heat input capability, initial testing will be limited to heat inputs of 250 kw. Details of the program progress are given. (auth)

**3486** STUDIES OF STARTUP CONDITIONS OF I. V. KURCHATOV BELOYARSK NUCLEAR POWER STATION PERFORMED AT THE TEST RIG. Smolin, V. N.; Polyakov, V. K.; Esikov, V. I.; Shuinov, Yu. N. At. Energ. (USSR), 19: 261-8(Sept. 1965). (In Russian).

Results are presented of an experimental study of the hydrodynamic stability of coolant flow in the first and second loops of the Beloyarsk atomic power station reactors at the test rig. The conclusion is substantiated on the methods of startup of the units of the power station adopted to the experimental utilization, development. Results are given of a study of startup regimes. (tr-auth)

**3487** NUCLEAR POWER PLANTS AND INSULATING PROBLEMS. Hempel, Rudolf (Rheinhold and Mahla GmbH, Mannheim, Ger.). At. Strom, 11: 71-3(July 1965). (In German).

In the design and construction of nuclear power plants there is need for insulating construction of various kinds — roofing and external shell installations for the reactor building, insulation constructions for air-conditioning plants and cooling systems, heat shields for the secondary coolant, and sound proofing. The constructional materials and techniques used in each of these areas are briefly indicated. (J.S.R.)

**3488** THE OBRIGHEIM NUCLEAR POWER STATION. Kallenbach, Reinhard (Kernkraftwerk Obrigheim GmbH, Stuttgart). At. Strom, 11: 121-32(Sept.-Oct. 1965). (In German).

The development and technical details of the nuclear power station are compared with a conventional steam power station. A short comparison of the characteristic data for other nuclear stations, and economic questions are also given. (auth)

**3489** THE OBRIGHEIM NUCLEAR POWER STATION. Brennstoff-Waerme-Kraft, 17: 310-15(June 1965). (In German).

The technical characteristics of the Obrigheim pressurized water reactor, which is scheduled for operation in 1968, are described. The planning and design of the reactor are discussed from the viewpoint of the operator. (J.S.R.)

**3490** THE COMPUTER ALARM, MONITORING, LOGGING, AND ANALYSIS SYSTEM FOR OLDBURY NUCLEAR POWER STATION. Westhead, J. M. Euro Nucl., 2: 489-92(Oct. 1965).

A computer system for assistance in the presentation and analysis of alarms at the 600-Mw(e) Oldbury-on-Severn power station is described. There are 2700 alarm contacts to be scanned using an AEI 1040 computer, two burst-cartridge-detector computers, and two temperature alarm scanners. It is shown that the computer's analysis feature suppresses uninformative intermediate "dependent alarms", sorts out interrelated alarm situations, and identifies "deduced alarms". The temperature-monitoring equipment, burst-cartridge-detection equipment, and computer displays are described. (M.C.G.)

**3491** BREEDER REACTORS—TOMORROW'S POWER PLANTS. Madell, John T. (Argonne National Lab., Ill.). Ind. Res., 7: No. 8, 58-63(July 1965).

Due to the high consumption of fossil fuels and the fact that uranium-235 does not provide a significant increase in energy reserves, breeder reactors are important for the production of fissile from fertile material, which exists more abundantly in nature. The development of breeder reactors is discussed. Other topics considered include the international interest in breeder reactors, some problems encountered in the development of these reactors including the development of a low-cost fuel element for economic operation, study of large fast reactor dynamic response characteristics to aid in safe plant design, and the extension of liquid sodium technology to the point where all components of the power plant will be compatible and highly reliable. Testing facilities are also discussed. (J.F.P.)

**3492** THE UNITED STATES NUCLEAR POWER PROGRAMME. Nordlinger, S. G. (U. S. Atomic Energy Commission, London). Nucl. Energy, 208-13(July 1965).

The roles of the U. S. Atomic Energy Commission and American private industry in developing competitive nuclear power are described, and the course of this development is outlined from water-cooled reactors through advanced converter and fast breeder reactors. The economics of nuclear reactors for central-station power generation is briefly considered; and a summary is presented of the AEC's international program of assistance and co-operation in the nuclear power field. (L.B.S.)

**3493** PHASE RELATIONS IN THE PSEUDO-TERNARY URANIUM–PLUTONIUM–FISSIUM SYSTEM. Kruger, O. L. (Argonne National Lab., Ill.). Trans. Amer. Nucl. Soc., 8: 350-1(Nov. 1965).

**3494** FUEL ELEMENTS FOR THE ARBEITSGEMEINSCHAFT VERSUCHS REAKTOR (AVR). Reuter, R. A.; Howard, R. A.; Green, F. P.; Kellar, A. A. (Union Carbide Corp., Lawrenceburg, Tenn.). Trans. Amer. Nucl. Soc., 8: 356(Nov. 1965).

**3495** BEHAVIOR OF BLANKET $UO_2$ FUEL RODS IN PWR CORE I. Rubin, B.; Lynam, L. (Bettis Atomic Power Lab., Pittsburgh). Trans. Amer. Nucl. Soc., 8: 359-61(Nov. 1965).

**3496** CANDU FUEL PERFORMANCE IN NPD. Pawliw, J. (Canadian General Electric Co., Ltd., Peterborough, Ontario); Chalder, G. H.; Popple, R. T. Trans. Amer. Nucl. Soc., 8: 361-2(Nov. 1965).

**3497** FUEL PERFORMANCE IN BOILING-WATER REACTORS. Pashos, T. J.; Williamson, H. E.; Duncan, R. N. (General Electric Co., San Jose, Calif.). Trans. Amer. Nucl. Soc., 8: 362-3(Nov. 1965).

**3498** NUCLEAR AND FUEL-CYCLE PERFORMANCE OF MOLTEN-SALT BREEDER REACTORS. Kasten, Paul R.; Bauman, Howard F. (Oak Ridge National Lab., Tenn.). Trans. Amer. Nucl. Soc., 8: 520-2(Nov. 1965).

**3499** ELK RIVER LIFETIME—PREDICTED AND OBSERVED. Kendrick, E. D.; Fisher, J. R. (Allis-Chalmers Mfg. Co., Bethesda, Md.). Trans. Amer. Nucl. Soc., 8: 523-4(Nov. 1965).

**3500** A NON-ITERATIVE NUCLEAR-THERMAL INTERACTION METHOD. Sha, William T. (Westinghouse Electric Corp., Pittsburgh). Trans. Amer. Nucl. Soc., 8: 524-5(Nov. 1965).

**3501** ADEQUACY OF A ONE-GROUP THREE-DIMENSIONAL MODEL IN A CORE-FOLLOWING PROGRAM. Fisher, J. R.; Kendrick, E. D. (Allis-Chalmers Mfg. Co., Bethesda, Md.). Trans. Amer. Nucl. Soc., 8: 525-6(Nov. 1965).

**3502** EVALUATION OF BEGINNING-OF-LIFE MEASURED AND CALCULATED REACTIVITY CHARACTERISTICS OF PWR CORE-2 SEED-1. Stuart, Malcolm R.; Taylor, Edward J. (Westinghouse Electric Corp., Pittsburgh). Trans. Amer. Nucl. Soc., 8: 527-8(Nov. 1965).

**3503** MEASUREMENT AND ANALYSIS OF SM-1A CORE-3. Rahe, E. P. Jr.; Clark, W. S.; Batch, M. L.; Ball, R. M.; Deutsch, R. W. Trans. Amer. Nucl. Soc., 8: 528-9(Nov. 1965).

**3504** COMPARISON OF CALCULATED AND MEASURED BURNUP DISTRIBUTIONS AND ISOTOPIC INVENTORY IN THE YANKEE CORE. Lacey, P. G.; Nodvik, R. J.; Radcliffe, R. E. (Westinghouse Electric Corp., Pittsburgh). Trans. Amer. Nucl. Soc., 8: 529-30(Nov. 1965).

**3505** PREDICTED AND OBSERVED NUCLEAR CHARACTERISTICS OF THE MOLTEN SALT REACTOR EXPERIMENT. Engel, J. R.; Haubenreich, P. N.; Prince, B. E. (Oak Ridge National Lab., Tenn.). Trans. Amer. Nucl. Soc., 8: 530-1(Nov. 1965).

**3506** FAST REACTOR SAFETY EXPERIMENTS ON EBR-II SAMPLES IN FLOWING SODIUM ENVIRONMENT. Dickerman, C. E.; Robinson, L. E.; Stephany, W.; Willis, L. (Argonne National Lab., Ill.). Trans. Amer. Nucl. Soc., 8: 559-60(Nov. 1965).

**3507** AN ANALYSIS OF REACTOR EXCURSIONS INITIATED AT HIGH POWER IN THE SPERT-III PWR. Condit, C. M.; Garner, R. W. (Phillips Petroleum Co., Idaho Falls, Idaho). Trans. Amer. Nucl. Soc., 8: 562-3 (Nov. 1965).

**3508** ECONOMIC POTENTIAL OF DIRECT NUCLEAR SUPERHEAT. McLeod, N. B.; Reed, G. L.; Schwoerer, F. (Nuclear Utility Services, Washington, D. C.). Trans. Amer. Nucl. Soc., 8: 570(Nov. 1965).

**3509** UC FABRICATION COST DATA FOR THE HALLAM SECOND CORE. Magnus, D. K. (Atomics International, Canoga Park, Calif.). Trans. Amer. Nucl. Soc., 8: 570-1(Nov. 1965).

**3510** COST OF REMOTE FABRICATION OF METAL-CLAD METAL-FUEL FAST-REACTOR FUEL ELEMENTS. Ayer, J. E.; Jones, D. A. (Argonne National Lab., Ill.). Trans. Amer. Nucl. Soc., 8: 571-2(Nov. 1965).

**3511** DIRECT SUBSTITUTE PLUTONIUM FUEL FOR COMMERCIAL WATER REACTORS. McLeod, N. B. (Nuclear Utility Services, Washington, D. C.); Uematsu, K.; Yumoto, R.; Yasukawa, S. Trans. Amer. Nucl. Soc., 8: 572-3(Nov. 1965).

**3512** A COMPARISON OF FUEL CYCLES FOR CROSSED-PROGENY FUELS IN CONVENTIONAL AND NOVEL CONFIGURATIONS. Deonigi, D. E. (Battelle-Northwest, Richland, Wash.). Trans. Amer. Nucl. Soc., 8: 574-5(Nov. 1965).

**3513** NUCLEAR FUEL UTILIZATION AND ECONOMIC INCENTIVES. Kasten, Paul R. (Oak Ridge National Lab., Tenn.). Trans. Amer. Nucl. Soc., 8: 578(Nov. 1965).

**3514** EBR-II SELF-EXCITED OSCILLATIONS. Hyndman, R. W. (Argonne National Lab., Ill.); Kirn, F. S.; Smith, R. R.; Kuroi, H. Trans. Amer. Nucl. Soc., 8: 590(Nov. 1965).

**3515** EFFECT OF NATURAL CONVECTION UPON THE TEMPERATURE TRANSIENT FOLLOWING A LOSS-OF-COOLANT ACCIDENT. Omberg, R. P.; Olander, D. R.; Schrock, V. E. (Univ. of California, Berkeley). Trans. Amer. Nucl. Soc., 8: 596-7(Nov. 1965).

**3516** HYDRODYNAMIC STABILITY OF NATURAL-CIRCULATION BOILING-WATER REACTORS—A COMPARATIVE STUDY OF ANALYTICAL MODELS AND EXPERIMENTAL DATA. Neal, L. G.; Zivi, S. M. (TRW Systems, Redondo Beach, Calif.). Trans. Amer. Nucl. Soc., 8: 597-8(Nov. 1965).

**3517** MONITORING REACTOR KINETICS OF EBR-II. Kirn, F. S. (Argonne National Lab., Idaho Falls, Idaho); Hyndman, R.; Smith, R. R.; Kuroi, H. Trans. Amer. Nucl. Soc., 8: 602(Nov. 1965).

**3518** FUEL-ELEMENT FAILURE DETECTION IN EBR-II. Smith, R. R. (Argonne National Lab., Idaho Falls, Idaho); Doe, C. B.; Porges, K. Trans. Amer. Nucl. Soc., 8: 602-3(Nov. 1965).

**3519** PWR-2 FLUX WIRE MEASUREMENTS AND COMPARISON TO CALCULATIONS. Barr, Kenneth P.; Rutherford, Charles H. (Westinghouse Electric Corp., Pittsburgh). Trans. Amer. Nucl. Soc., 8: 604(Nov. 1965).

**3520** BONUS REACTOR-OPERATING PERFORMANCE. Gerken, W. W. (Combustion Engineering, Inc., Windsor, Conn.); West, J. M.; Jameson, A. S.; Withers, W. T.; Fragoso, J. H. Trans. Amer. Nucl. Soc., 8: 604-5 (Nov. 1965).

**3521** SHIPPINGPORT ATOMIC POWER STATION DISPOSITION OF RADIOACTIVE WASTE. Suchoza, B. P. (Westinghouse Electric Corp., Pittsburgh). Trans. Amer. Nucl. Soc., 8: 605-6(Nov. 1965).

**3522** STARTUP EXPERIENCE WITH THE EBR-II FUEL CYCLE FACILITY. I. MANIPULATORS AND PROCESS AUXILIARIES. Stevenson, C. E.; Paige, D. M.; Holcomb, W. F.; Kleffner, J. O. (Argonne National Lab., Idaho Falls, Idaho). Trans. Amer. Nucl. Soc., 8: 612 (Nov. 1965).

**3523** STARTUP EXPERIENCE WITH THE EBR-II FUEL CYCLE FACILITY. II. FUEL PROCESSING. Hampson, D. C.; Mitchell, D. L.; Fryer, R. M. (Argonne National Lab., Idaho Falls, Idaho). Trans. Amer. Nucl. Soc., 8: 612-13(Nov. 1965).

**3524** LOW-POWER SHIELD MEASUREMENTS ON THE ENRICO FERMI REACTOR. Beaudry, R. J. (Atomic Power Development Associates, Inc., Detroit); Horne, R. E.; Feldes, J. G. Trans. Amer. Nucl. Soc., 8: 644(Nov. 1965).

**3525** ML-1 SHIELD STUDY. Whittum, H. O.; Witthaus, J. K. (Aerojet-General Nucleonics, San Ramon, Calif.). Trans. Amer. Nucl. Soc., 8: 645-6(Nov. 1965).

**3526** BERKELEY AND BRADWELL NUCLEAR POWER STATIONS. Proceedings of the Symposium, 27th June 1963. London, The Institution of Mechanical Engineers, 1964. 138p. (CONF-630603).

The conference included 5 papers. Separate abstracts were prepared for each. (J.F.P.)

*For abstracts of individual papers see: 3527–3531.*

**3527** BRADWELL NUCLEAR POWER STATION. Vaughan, R. D. (The Nuclear Power Group, Knutsford, Cheshire, Eng.). pp 1-39 of Berkeley and Bradwell Nuclear Power Stations. London, The Institution of Mechanical Engineers, 1964.

The Bradwell Power Station is designed for a net output of 300 Mw(e). It incorporates two identical reactors of the graphite-moderated gas-cooled type. The design of the reactors and power station is discussed including plant configuration, reactor core dimensions, fuel element parameters, the choice of reactor gas temperatures, the steam cycle, the fuel element, the reactor core, fuel handling, and burst cartridge equipment. Other topics include reactor vessel and gas circuits, the main blowers, control and instrumentation, and turbo-alternators. Although Bradwell is not yet operated at design temperature levels, a brief review is given of the performance of the various components. Diagrams are included, and a list of design parameters is given. (J.F.P.)

**3528** BERKELEY NUCLEAR POWER STATION. Southwood, J. R. M. (The Nuclear Power Group, Knutsford, Cheshire, Eng.). pp 40-70 of Berkeley and Bradwell Nuclear Power Stations. London, The Institution of Mechanical Engineers, 1964.

A number of the major features of the Berkeley Nuclear Power Station are discussed. These illustrate the experience gained as the work progressed and indicate how changes prompted by new data were included in the design where essential or where considered practical within the construction program. The topics include a brief description of the plant, design considerations, fuel elements, station performance, the core performance including graphite cores, shielding, and a pressure vessel description. Also discussed are blowers, boilers, burst cartridge detection gear, fueling handling, the turbine house, circulating water, and the electric system. The control of the reactor and the commissioning program are also discussed. (J.F.P.)

**3529** COMMISSIONING PROGRAMMES AND PROCEDURES. Peddie, R. A.; Farkasch, G.; Rutter, R. L.

pp 89-102 of Berkeley and Bradwell Nuclear Power Stations. London, The Institution of Mechanical Engineers, 1964.

A description of the commissioning programs and procedures is given. A brief history is given of the Central Electricity Generating Board. Other topics include the scope and work of the station commissioning committee, the value of commissioning documentation, and management control during commissioning. The technical aspects of the commissioning of the Berkely and Bradwell power stations are also considered. These commissioning processes were divided into three phases. The first phase comprised combined engineering tests on the complete reactor pressure circuit and the pressurized equipment associated with it, such as the charge-discharge equipment. The second phase started with fuel loading, included absorber and control rod calibrations, channel flow tests and sensitivity tests for burst cartridge detection, and concluded with the reactor ready for startup. The third phase included the approach to criticality, power raising, and operational tests at power. (J.F.P.)

**3530** NUCLEAR FUEL MANAGEMENT. Exley, J. pp 103-12 of Berkeley and Bradwell Nuclear Power Stations. London, The Institution of Mechanical Engineers, 1964.

Aspects of fuel management are considered which relate to the fuel from the time of delivery to a nuclear power station until its safe disposal at the United Kingdom Atomic Energy Authority. After giving the fuel element route including a diagram, the stock control is considered including requirements of a fuel record system, and the punched card system for fuel and document movement. Operational control is discussed including fuel element inspection before loading, testing the initial fuel charge after loading, handling and testing replacement fuel, and the care of fuel within the reactor. The disposal of irradiated fuel, and the post irradiation examination are also considered. (J.F.P.)

**3531** OPERATIONAL PERFORMANCE. Weeks, R. J. pp 113-19 of Berkeley and Bradwell Nuclear Power Stations. London, The Institution of Mechanical Engineers, 1964.

The reliability and performance of the stations are described and the reactor performance and control are discussed. The main features of the reactor core and their observed changes in the initial period of operation at power are presented. (auth)

**3532** COMPARISON OF RESULTS OF ANALYSIS OF BOILING SYSTEM DYNAMICS BY ANALOG AND DIGITAL METHODS. Bogaardt, M. (Technical Univ., Eindhoven, The Netherlands); Spigt, C. L.; Dijkman, F. J. M.; Verheugen, A. N. J. Paper 1-1 of Eighth National Power Instrumentation Symposium. Pittsburgh, Instrument Society of America, 1965.

Experimental and theoretical results of analysis of boiling water system dynamics are described in terms of transfer functions and transients obtained by direct analog and digital computations, on the basis of either noise analysis or of direct transfer function measurements on a high pressure boiling system. A description is given of the measuring and analyzing equipment. (auth)

**3533** SOME CONTROL FEATURES OF CANADIAN NUCLEAR GENERATING STATIONS. Elston, K. E. (Central Nuclear Operations, Toronto). Paper 3-2 of of Eighth National Power Instrumentation Symposium. Pittsburgh, Instrument Society of America, 1965.

Canada's first nuclear generating station, the Nuclear Power Demonstration Station, NPD, is fully automatic during normal operation, except for fuel changing. The stations presently being built, Douglas Point and Pickering, will employ a greater degree of automation during start-up than NPD and will also use digital computers for many of the regulating and monitoring functions. Some of the main control features of these stations are described and protective and regulating system experience at NPD are reviewed. (auth)

**3534** INSTRUMENTATION, CONTROL AND AUTOMATION IN THE FIRST CZECHOSLOVAK NUCLEAR POWER PLANT A 1 NOW UNDER CONSTRUCTION. Stirsky, Pavel (Power Research Inst., Prague). Paper 5-2 of Eighth National Power Instrumentation Symposium, Pittsburgh, Instrument Society of America, 1965.

A brief description is given of the technological scheme of the first Czechoslovak nuclear power station with a heavy-water gas-cooled reactor. Descriptions are also given of the following: the control system of the power station and its main features; the extent of the control system analyses, with some results; the design of the control system of the reactor and the main problems which had to be solved during its development; the measuring system of the reactor and the special instruments developed for it; the basic philosophy of measuring and control and the design of the main control room; and the automation of the power station and the design and testing of automation devices. Experimental work in the field of regulation and control and a perspective of further development are briefly outlined. (auth)

**3535** PLUTONIUM PRODUCTION AND BURNUP CALCULATION METHODS FOR LIGHT WATER MODERATED REACTORS. Sofer, G. A.; Kazi, A. H.; Tomonto, J. R.; Buck, P. (United Nuclear Corp., White Plains, N. Y.). Vienna, International Atomic Energy Agency, 1965, Preprint No. SM-67/42, 43p. (CONF-650803-45). ORINS.

From IAEA Symposium on Nuclear Materials Management, Vienna.

Results are summarized of calculations at United Nuclear of plutonium loaded criticals for light water power reactors, and plutonium burnup and production. The emphasis is on evaluation of various methods used in industry for calculating plutonium-fueled reactors, and assessment of the error inherent in relatively simple calculation techniques. (auth)

**3536** SPECIAL NUCLEAR MATERIAL CONTROL BY THE POWER REACTOR OPERATOR. Cordin, R. A. (Yankee Atomic Electric Co., Boston). Vienna, International Atomic Energy Agency, 1965, Preprint No. SM-67/40, 18p. (CONF-650803-16). ORINS.

From IAEA Symposium on Nuclear Materials Management, Vienna.

The reactor operator must have adequate controls for the special nuclear material used. Nuclear material management must be as modern and efficient as is humanly possible, requiring complete and informative records by the reactor operator. These records need not be complex to satisfy the criteria of completeness and adequacy. In fact, simplicity is extremely desirable. Nuclear material control is not limited to simple inventory work but it is the basis for a great deal of other activity such as irradiated fuel shipment and reprocessing and the maintenance of an adequate insurance program. (auth)

**3537** COOLING APPARATUS FOR A NUCLEAR REACTOR. Devidas, Roger (to Groupement Atomique Alascienne Atlantique). British Patent 1,005,489. Sept. 22, 1965. Priority date Apr. 30, 1963, France.

A reactor cooling apparatus, which includes primary and secondary cooling fluid circuits, is designed for improved compactness and reduction in equipment needed. The apparatus utilizes a tank divided into two sections, one section for collecting primary fluid and the other for heat exchange between the primary fluid and the heat extracting fluid. A control pump for the circulation of the primary fluid is fixed on the wall common to the two sections. A control pump for the secondary fluid is mounted below the primary pump. The apparatus is particularly suited for power reactors cooled by a liquid metal. (A.G.W.)

**3538** NUCLEAR REACTORS. Long, Everett (to English Electric Co. Ltd.). British Patent 1,006,471. Oct. 6, 1965. Filed July 10, 1963.

In the reactor patented some of the fuel is arranged for heating a portion of the coolant to a first temperature, and the remainder of the fuel is arranged for heating the remainder of the coolant fluid to a second lower temperature. The heat exchanger includes a first portion arranged to receive only the hotter portion of the coolant and to cool it

to the lower temperature. The coolant portions are then mixed and further cooled together. Preferably two different fuels such as uranium oxide and natural uranium are used. (A.G.W.)

## Process Heat Reactors

**3539** (ACNP-65558(Rev.1)) SURVEY OF HIGH-TEMPERATURE DEMINERALIZATION FOR DUAL-PURPOSE BWR PLANTS. Lang, Peter M. (Allis-Chalmers Mfg. Co., Bethesda, Md. Atomic Energy Div.). Aug. 1965. Contract W-7405-eng-26; Subcontract No. 2504. 45p. Dep. mn; CFSTI $2.00 cy, $0.50 mn.

For Oak Ridge National Lab., Tenn.

A preliminary conceptual design of a mixed-bed ion-exchange unit was evolved in which the ratio of cation to anion resin was set at over 100. This ratio was chosen because the normal corrosion-product removal duty is predominantly cationic and also in order to keep the anion-resin replacement cost reasonable. If a major brine-heater leak occurs (assumed to be one completely ruptured tube), this system would give protection for about 2 min. For small leaks the protection period is, of course, much longer. High-temperature ion exchange should not be relied upon as the only protection against such leakage. It is useful, however, in combination with one or more of a number of suggested alternate schemes for coping with brine-heater leakage and is in any case needed for removal of primary-system corrosion products. A rough operating cost comparison was made of the conceptual design vs. the Powdex process, a commercially available high-temperature ion-exchange and filtration process. The operating cost of Powdex is estimated to be at least three times that of the conventional demineralizer unit used in the conceptual design. (auth)

**3540** (ACNP-65573) FLEXIBILITY STUDY OF BACK-PRESSURE TURBINES FOR DUAL-PURPOSE PLANTS. (Allis-Chalmers Mfg. Co., Bethesda, Md. Atomic Energy Div.). Aug. 1965. Contract W-7405-eng-26; Subcontract No. 2504. 48p. Dep. mn; CFSTI $2.00 cy, $0.50 mn.

For Oak Ridge National Lab., Tenn.

Back-pressure turbine-generator units rated at 500 Mw and exhausting at 35.4 psia (260°F) were studied for turbine throttle pressures of 600 psig and 1000 psig. For both throttle pressures, the turbine is a double flow, 1800 rpm, stright reaction machine. The steam cycle for the 600 psig throttle pressure uses a single open feedwater heater, and the cycle for the 1000 psig pressure uses an open heater plus a second closed heater. For each throttle pressure, plots are presented giving part-load and stretch-load performance for throttle flows up to the design value and for exhaust pressures from 15 psia to 80 psia. These plots show the electrical output, the heat exhausted to the water plant, and the temperature of the feedwater returned to the reactor. Other plots showing turbine expansion lines on Mollier diagrams, turbine heat rates, turbine exhaust enthalpies and flows, and gland-sealing steam requirements are also included. For operation at either increased or decreased exhaust pressure, certain turbine modifications are necessary, and the corresponding additional turbine costs were estimated. Similar differential costs to enable the generator to attain outputs in excess of 500 Mw are also given. (auth)

## Production Reactors

**3541** (RL-NRD-81(Suppl.1)) OPERATIONAL MODES ANTICIPATED FOR THE CONVERTED N-REACTOR INTER-PLANT OPERATING RESTRICTIONS (PRELIMINARY). Ebens, A. J.; Hall, R. E. (General Electric Co., Richland, Wash. Hanford Atomic Products Operation). Mar. 15, 1965. Contract AT(45-1)-1350. 9p. Dep. mn; CFSTI $1.00 cy, $0.50 mn.

Reliance of the 185 export generating plant upon the N-Reactor Plant for steam and startup electric supplies, and reliance of the reactor plant upon the generating plant for condensate return, requires the generation of limitations upon both plants to assure safe and reliable joint operation. A listing of specific inter-plant operating restrictions is presented. (M.O.W.)

**3542** CLEAN $^{233}U$ PRODUCTION-METHODS AND PARAMETERS. Meichle, R. H. (General Electric Co., Richland, Wash.). Trans. Amer. Nucl. Soc., 8: 520(Nov. 1965).

**3543** CONTROL-ROD SYSTEMS FOR THE HFIR. Collins, C. W.; Jones, J. E.; Oakes, L. C. (Oak Ridge National Lab., Tenn.). Trans. Amer. Nucl. Soc., 8: 590-1(Nov. 1965).

**3544** COMPARISON OF MEASURED AND CALCULATED NEUTRON FLUX AND GAMMA-RAY DOSE DISTRIBUTIONS IN THE NPR REFLECTOR AND TOP SHIELD. Greenborg, J. (Battelle-Northwest, Richland, Wash.). Trans. Amer. Nucl. Soc., 8: 646-7(Nov. 1965).

## Propulsion and Space

### *See also* ENGINEERING — Space Propulsion

*Refer also to abstracts 2242 and 3462.*

**3545** (CNLM-5729) SNAP-50/SPUR NUCLEAR TEST FACILITY INITIAL DESIGN REQUIREMENTS, CANEL SITE, MIDDLETOWN, CONNECTICUT. (Pratt and Whitney Aircraft, Middletown, Conn. Connecticut Advanced Nuclear Engineering Lab.). June 1, 1964. Contract AT(30-1)-2789. 78p. Dep. mn; CFSTI $3.00 cy, $0.75 mn.

The nuclear test facility for demonstrating the feasibility of SNAP-50 reactor technology is discussed. A preliminary plan regarding the extent of the facility, test related systems, and associated service systems was developed. Descriptive material and functional requirements pertaining to these areas are presented. A brief description of existing facilities at CANEL, which will be used in support of the nuclear test facility, is presented. (M.O.W.)

**3546** (GE-TM-64-12-12) THE 630A - MARK IV. A NUCLEAR FUELED STEAM GENERATOR-SUPERHEATER FOR MERCHANT SHIP PROPULSION. Delson, E. B.; Hunt, E. C. (General Electric Co., Cincinnati, Ohio. Nuclear Materials and Propulsion Operation). Dec. 15, 1964. Contract AT(40-1)-2847. 74p. (CONF-641220-1). Dep. mn; CFSTI $3.00 cy, $0.75 mn.

From Society of Naval Architects and Marine Engineers, Southern California Section, Los Angeles.

A brief discussion on the evolution of the 630A design is presented. The design and development of the 630A Mark IV are discussed. Further discussions are presented on safety and fuel costs of the Mark IV. An economic analysis is presented. (M.O.W.)

**3547** (NAA-SR-Memo-7581) A 1.5 MWE THERMIONIC REACTOR SPACE POWER SYSTEM. Smith, C. K.; Parkinson, R. Y. (Atomics International, Canoga Park, Calif.). [nd]. Contract AT-11-1-GEN-8. 28p. Dep. mn; CFSTI $2.00 cy, $0.50 mn.

A brief review of the thermionic fuel element concept is presented. The performance potential of nuclear reactor power system concepts employing direct-nuclear heated thermionic converters within the reactor fuel elements is discussed in some detail. (M.O.W.)

**3548** (SC-DC-65-1752) AEROSPACE NUCLEAR SAFETY. Blake, V. E. Jr. (Sandia Corp., Albuquerque, N. Mex.). Sept. 22, 1965. Contract AT(29-1)-789. 13p. (CONF-651026-1). Dep. mn; CFSTI $1.00 cy, $0.50 mn.

From 1st AIAA Rankine Circle Space Power System Specialists Conference, Cleveland.

A brief history of the introduction of nuclear power into space and the results of early flights are presented. The problem of safety is discussed, as well as the direction taken by early designers to achieve safety. The discussions

also cover alternate approaches to safety which were initially considered. There is a discussion of power supplies currently under development, and the approaches being followed to achieve safety. A series of charts is presented which categorize the main safety approaches, and will provide the basis for a systematic safety assessment. Finally, a safety philosophy for future design is presented. It is shown that safety is not the responsibility of any one agency but rather a problem of all. (M.O.W.)

**3549** (SC-RR-65-417) AEROSPACE NUCLEAR SAFETY: PROBABILITY ANALYSIS OF REACTOR POWER LEVEL AND DOSE RATE. Kitzinger, D. G. (Sandia Corp., Albuquerque, N. Mex.). Oct. 1965. Contract AT(29-1)-789. 12p. Dep. mn; CFSTI $1.00 cy, $0.50 mn.

The probability spaces of power versus time and of dose rate versus time for a reactor operated in space are quantized. These probability functions aid in the determination of safety. (auth)

**3550** (TID-21994) TITLE 1 REPORT. PRELIMINARY SERVICES FOR SNAP 8, FLIGHT PROTOTYPE TEST FACILITY, BUILDING 056, SANTA SUSANA, CALIFORNIA. (Bechtel Corp., San Francisco, Calif.). Aug. 1964. Contract AT(11-1)-708. 227p. Dep. mn; CFSTI $6.00 cy, $1.25 mn.

Design data, outline specifications, reliability procedures, schedules, and drawings are presented for the SNAP 8 Flight Prototype Test Facility. The facility is designed for testing the startup capability, control stability, thermal and nuclear capabilities, performance, and endurance of the SNAP 8 Flight Prototype. (T.F.H.)

**3551** (TID-22316) N. S. SAVANNAH CONTAINMENT INTEGRITY—ITS MEASUREMENT AND IMPROVEMENT. Taylor, J. H. (Babcock and Wilcox Co., Galveston, Tex.). Feb. 1964. Contract AT(11-1)-766. 52p. (STS-3). Dep. mn; CFSTI $3.00 cy, $0.50 mn.

Containment leak tests were performed on the N. S. Savannah. The reactor plant conditions, the equipment and instrumentation, and the various procedures and methods used to conduct a test and determine leak rates are discussed. Four sets of tests were performed and results are given for each. Results and a discussion of tests performed on seven individual electrical penetrations are presented. (M.O.W.)

**3552** CONSOLIDATED NUCLEAR STEAM GENERATOR III (CNSG III) A NUCLEAR SHIPS-PROPULSION. Junkermann, W. (Babcock and Wilcox, Oberhausen, Ger.). Atomkernenergie, 8: 273-7(July-Aug. 1965). (In German).

A review is presented of the development by the Babcock-Societies in the field of ship reactors, and of the recent stage of technics with the Consolidated Nuclear Steam Generator III of the Babcock and Wilcox Company in USA. Exceeding the improvements of the advanced PWR resulting from a federal German design and now being built, this reactor represents a further essential development progress in nuclear ships propulsion. Compared to former designs the CNSG III is marked by an improved heat efficiency, smaller dimensions, and an essential lower weight per unit of power. All these improvements effect better economy. (auth)

**3553** POWER FOR DEEP SPACE. Stambler, Irwin. New Scientist, 27: 620-3(Sept. 9, 1965).

Sources of electric power for deep space are discussed. The system for Nuclear Auxiliary Power and the Space Power Unit Reactor development is considered. A diagram of the SNAP 50/SPUR is given. This diagram shows three main subsystems a lithium reactor loop heating a potassium Rankine-cycle power-conversion loop, from which a sodium–potassium loop removes waste. The design of the potassium turbo-generator is also given. These power sources are considered for use in supplying power to a moon base and for spacecraft propulsion. (J.F.P.)

**3554** SNAP-50/SPUR BOILER DEVELOPMENT. Van Hagan, Thomas H. (AiResearch Manufacturing Co., Los Angeles). Trans. Amer. Nucl. Soc., 8: 400(Nov. 1965).

**3555** BEARING MATERIALS FOR USE IN RANKINE-CYCLE SPACE POWER SYSTEMS. Frank, R. G. (General Electric Co., Cincinnati). Trans. Amer. Nucl. Soc., 8: 403-5(Nov. 1965).

**3556** MATERIAL AND GEOMETRY ASPECTS OF SPACE RADIATORS. Lieblein, S. (National Aeronautics and Space Admin., Cleveland). Trans. Amer. Nucl. Soc., 8: 406-7(Nov. 1965).

**3557** DYNAMIC MEASUREMENTS OF SNAP-8ER FEEDBACK COEFFICIENTS. Pekrul, P. J. (Atomics International, Canoga Park, Calif.). Trans. Amer. Nucl. Soc., 8: 452-3(Nov. 1965).

**3558** ANALYSIS OF SNAP-10A/2 KINETIC BEHAVIOR USING PULSE REACTIVITY EXCITATIONS. Kessler, W. E. (Phillips Petroleum Co., Idaho Falls, Idaho). Trans. Amer. Nucl. Soc., 8: 495(Nov. 1965).

**3559** STATIC CONTROL OF SNAP REACTORS. Johnson, R. A.; McGoff, D. J. (Atomics International, Canoga Park, Calif.). Trans. Amer. Nucl. Soc., 8: 527 (Nov. 1965).

**3560** RE-ENTRY BURNUP OF SNAP-10A REACTOR FUEL ELEMENTS. Barsell, A. W.; Eng, K. Y. (Atomics International, Canoga Park, Calif.). Trans. Amer. Nucl. Soc., 8: 545-6(Nov. 1965).

**3561** SNAPTRAN-2 DESTRUCTIVE TEST PREDICTIONS. Rose, R. P.; Prael, R. E. (Phillips Petroleum Co., Idaho Falls, Idaho). Trans. Amer. Nucl. Soc., 8: 546-7(Nov. 1965).

**3562** FISSION-PRODUCT RELEASE FROM IRRADIATED URANIUM–ZIRCONIUM–HYDRIDE SNAP FUEL. Cegelski, W. M. (Atomics International, Canoga Park, Calif.). Trans. Amer. Nucl. Soc., 8: 547(Nov. 1965).

**3563** MEASUREMENTS AND CALCULATIONS OF HYDROGEN LOSS FROM HYDRIDED ZIRCONIUM–URANIUM FUEL ELEMENTS DURING TRANSIENT HEATING TO TEMPERATURES NEAR THE MELTING POINT. Leadon, Bernard M. (Univ. of Florida, Gainesville); Gallaher, William H.; Rayfield, George T.; Obermeyer, Ronald W. Trans. Amer. Nucl. Soc., 8: 547-8(Nov. 1965).

**3564** POST-IRRADIATION CHEMICAL ANALYSIS OF SNAP-8 EXPERIMENTAL REACTOR COOLANT. Broom, Knox M. Jr.; Bingham, Carleton D.; Crockett, Thomas B.; Trahey, Nancy M. (Atomics International, Canoga Park, Calif.). Trans. Amer. Nucl. Soc., 8: 548-9 (Nov. 1965).

**3565** NERVA REACTOR EXPERIMENT (NRX) REACTOR TESTING. Davison, P. W. (Westinghouse Astronuclear Lab., Pittsburgh); Ney, E. J.; Neal, P. E. Trans. Amer. Nucl. Soc., 8: 551-2(Nov. 1965).

**3566** KIWI TEMPERATURE COEFFICIENT. Mills, C. B. (Los Alamos Scientific Lab., N. Mex.). Trans. Amer. Nucl. Soc., 8: 552-3(Nov. 1965).

**3567** COMPARISON OF ANALYTICAL AND EXPERIMENTAL OPERATING REACTIVITY OF NERVA REACTORS. Ortenberg, L. I.; Mowery, A. L.; Hill, D. J. (Westinghouse Astronuclear Lab., Pittsburgh). Trans. Amer. Nucl. Soc., 8: 553-4(Nov. 1965).

**3568** COMPARISON OF ANALYTICAL AND EXPERIMENTAL POWER DISTRIBUTION OF NERVA REACTORS. Doncals, R.; McCutchan, D. A.; Ortenberg, L.; Ravets, J. (Westinghouse Astronuclear Lab., Pittsburgh). Trans. Amer. Nucl. Soc., 8: 554-5(Nov. 1965).

**3569** NERVA REACTOR CONTROL. Kirschbaum, H. S.; Morris, W. R. (Westinghouse Astronuclear Lab., Pittsburgh). Trans. Amer. Nucl. Soc., 8: 555(Nov. 1965).

**3570** DYNAMIC PERFORMANCE OF CLUSTERED NUCLEAR ENGINES. Woyski, Jan S. (Douglas Aircraft Co., Inc., Santa Monica, Calif.). Trans. Amer. Nucl. Soc., 8: 555-7(Nov. 1965).

**3571** TUNGSTEN WATER-MODERATED ROCKET CRITICAL ASSEMBLY, ANALYTICAL METHOD AND EXPERIMENTAL RESULTS. Peak, J. C.; Bardes, R. G.

(General Atomic Div., General Dynamics Corp., San Diego, Calif.). Trans. Amer. Nucl. Soc., 8: 558(Nov. 1965).

**3572** SOME FEASIBILITY STUDIES OF THE NUCLEAR DESTRUCT CONCEPT FOR ROVER REACTOR DISPOSAL. King, L. D. P.; Mills, C. B. (Los Alamos Scientific Lab., N. Mex.). Trans. Amer. Nucl. Soc., 8: 565-6(Nov. 1965).

**3573** AEROSPACE SAFETY RESULTS FROM A NERVA POST-OPERATIONAL DESTRUCT TEST. Clark, A. J. Jr.; Berry, R. E. (Sandia Corp., Albuquerque, N. Mex.). Trans. Amer. Nucl. Soc., 8: 566(Nov. 1965).

**3574** PARTICLE-SIZE DISTRIBUTIONS FROM ROVER FUEL-ELEMENT FRAGMENTATION STUDIES. Campbell, E. E.; Ide, H. M.; Moss, W. D.; Reithel, R. J. (Los Alamos Scientific Lab., N. Mex.). Trans. Amer. Nucl. Soc., 8: 566-7(Nov. 1965).

**3575** AN ANALYSIS FOR CORRELATING GROUND DESTRUCT TESTS WITH IN-FLIGHT DESTRUCT OF NUCLEAR ROCKETS. Hargrove, H. G.; Trammell, M. R. (Westinghouse Astronuclear Lab., Pittsburgh). Trans. Amer. Nucl. Soc., 8: 567-8(Nov. 1965).

**3576** THE DESIGN AND ANALYSIS OF A POISSON SYSTEM FOR SAFE SHIPPING THE NERVA REACTOR. Speis, T. P.; Ortenberg, L. I.; Mowery, A. I. (Westinghouse Astronuclear Lab., Pittsburgh). Trans. Amer. Nucl. Soc., 8: 568-9(Nov. 1965).

**3577** DESIGN STUDY OF A FISSION-ELECTRIC CELL REACTOR FOR SPACE POWER. Shapiro, J. L.; Heindl, C. J. (California Inst. of Tech., Pasadena). Trans. Amer. Nucl. Soc., 8: 610-11(Nov. 1965).

**3578** NUCLEAR REACTOR WITH IMPROVED CORE ARRANGEMENT FACILITATING LOADING AND UNLOADING OF FUEL ASSEMBLIES AND CONTROL ROD ASSEMBLIES. Dickson, James J. (to Allis-Chalmers Manufacturing Co.). U. S. Patent 3,208,914. Sept. 28, 1965. Filed Jan. 5, 1961.

A nuclear reactor affording a source of propelling power as for a submarine has an elongated horizontally positioned pressure vessel mounted to extend lengthwise in the direction of propulsion. Access to the compactly arranged fuel elements is afforded through a top opening between the opposite ends of the reactor vessel, and the fuel elements are constructed and arranged so that they may be moved generally endwise through the top opening for loading and may be placed into lengthwise operative position in the vessel. The control rods are movable axially of the vessel to different positions of adjustment including a scram position, various regulating positions, and a core unloading position where the control portions of the rods are entirely withdrawn from the active core region to facilitate the installation of fuel elements. The control rods are actuated by two different type power sources, e.g., an electric motor and pneumatic cylinder, one for the regulating positions and one for the scram position. (B.L.M.)

## Research and Test Reactors

*Refer also to abstracts 2175, 2282, 2290, 2520, and 2994.*

**3579** (ANL-7082, pp 54-61) ADVANCED SYSTEMS RESEARCH AND DEVELOPMENT. (Argonne National Lab., Ill.).

Research and development of the Argonne Advanced Research Reactor are reported. (J.R.D.)

**3580** (BNL-9591) HFBR PHYSICS STARTUP MANUAL. Sastre, C. (Brookhaven National Lab., Upton, N. Y.). Oct. 1965. Contract AT(30-2)-Gen-16. 46p. Dep. mn; CFSTI $2.00 cy, $0.50 mn.

Procedures for startup of the HFBR are given. Reactivity behavior is analyzed for initial loading and criticality, control rod calibration, helium pressure variation, and coolant flow effects. Neutron lifetimes, temperature coefficient of reactivity, reactivity effects of thimbles and samples, partial core loadings, reactor noise, and xenon effects are considered. (M.O.W.)

**3581** (BNWL-SA-340) SAFETY AND NUCLEAR CONSIDERATIONS IN THE DESIGN OF THE FTR. Astley, E. R.; de Halas, D. R.; Finch, L. M.; Hofmann, P. L.; Little, W. W. Jr. (Battelle-Northwest, Richland, Wash. Pacific Northwest Lab). Sept. 27, 1965. Contract AT(45-1)-1830. 35p. (CONF-651009-2) Dep. mn; CFSTI $2.00 cy, $0.50 mn.

From the Conference on Safety, Fuels and Core Design in Large Fast Power Reactors, Argonne, Ill.

A conceptual design for the Fast Flux Test Reactor (FTR) was formulated. Steel cermets were chosen to be the FTR reference fuel because of their expected reliability and desirable safety features. Plutonium was chosen to be the reference fissile fuel, because it yields the highest flux achievable for a given power density. In-core poison rod control was selected, because it can supply the large control margins necessary for the operation of a test reactor. (M.O.W.)

**3582** (CEA-R-2482) RESULTATS ET INTERPRETATION DE MESURES D'INDICES DE SPECTRE DANS AQUILON. (Results and Interpretation of Spectral Indices Measurements Made with Aquilon). Frichet, Jean-Pierre; Mougey, Jean; Naudet, Roger; Taste, Jean (Commissariat a l'Energie Atomique, Saclay (France). Centre d'Etudes Nucleaires). Aug. 1965. 50p. Dep. mn.

A set of spectral indices measurements made in the heavy water reactor Aquilon on lattices constituted by massive fuel elements of dia. 29.2 mm are discussed. The fuel elements were made either of natural uranium or of slightly depleted or slightly enriched uranium, or of a uranium–plutonium alloy. The measurements were carried out for various lattice pitches (square pitch from 110 to 210 mm) and in certain cases for various temperatures (from 20 to 80°C). The results are compared to calculated values obtained by using the latest advances of the thermalization theory developed at Saclay applied to the moderation by heavy water. (auth)

**3583** (CRT-1187 B) CARIBOU—A PROGRAM FOR COMPUTING THE ISOTOPIC COMPOSITION OF NRX URANIUM METAL RODS. Halsall, M. J. (Atomic Energy of Canada Ltd., Chalk River (Ontario)). Aug. 1965. 27p. (AECL-2296). Dep.; AECL $1.00.

The computer program used to integrate the burnup equations is described. (M.O.W.)

**3584** (EUR-2433.e) TESI—AN ADVANCED POWER EXCURSION REACTOR FOR RESEARCH IN REACTOR SAFETY. Preliminary Studies. Rinaldini, C.; Coen, V.; Foggi, C.; Gall de Paratesi, S.; Lanza, F.; Ricchena, R.; Riebold, W.; Volta, G. (European Atomic Energy Community, Ispra (Italy). Joint Nuclear Research Center). June 1965. 196p. Dep. mn.

The TESI power excursion reactor is described in detail. Design features are discussed in terms of fuel materials, reactor physics, thermomechanical studies, heat transfer, reactor control and instrumentation, and shielding. A brief discussion of the operational characteristics is given in terms of transient operation kinetics and specimen irradiation. (M.O.W.)

**3585** (JUL-259-RE) DAS VERHALTEN DES FRJ-1 (MERLIN) BEIM AUSFALL DER ZWANGSKUEHLUNG. (The Behavior of the FRJ-1(MERLIN) as a Result of Forced Cooling). Muench, E. (Kernforschungsanlage, Juelich (West Germany)). May 1965. 45p. Dep. mn.

The special effects in the break-down of the primary coolant pumps of the FRJ-1(MERLIN) was investigated for two nuclear configurations using fuel elements provided with thermoelements. The time for the transition of the coolant flow from forced circulation to natural convection was determined. The conversion time was shorter with increasing power and was 7.5 sec at 5 Mw. The measurements make possible an explanation of oscillations of the fuel element temperatures during the break-down of forced cooling. These are seen as a result of the flow transition and the beginning of bubble vaporization. In addition to fuel element and coolant temperatures the power pattern was also investigated. Here a stronger decay

limited by the temperature effect was observed on which uncontrolled oscillations were superposed at higher out-puts. The oscillations could be established as subcritical reactivity variations through bubble formation. Within 30 min after pump failure no new power increase could be observed. (tr-auth)

**3586** (ORNL-TM-1291) THE RELEASE AND ADSORPTION OF METHYL IODIDE IN THE HFIR MAXIMUM CREDIBLE ACCIDENT. Adams, R. E.; Browning, W. E. Jr.; Cottrell, Wm. B.; Parker, G. W. (Oak Ridge National Lab., Tenn.). Oct. 1, 1965. Contract W-7405-eng-26. 41p. Dep. mn; CFSTI $2.00 cy, $0.50 mn.

This study was undertaken to establish both the maximum percentage of the iodine inventory which could exist in the containment vessel as methyl iodide, and the efficiency of the HFIR–SBHE system filter for methyl iodide. Review of all known existing relevant data has led to the conclusion that 5% of the iodine is the upper limit which can exist as $CH_3I$. The removal efficiency of Barneby-Cheney Type 513 coconut charcoal heretofore proposed for use in the HFIR filters was determined for a number of conditions of humidity, flow rate, flow time, and bed depth. At the 70% relative humidity, the removal efficiency of 1-in. charcoal, 50 $ft^3\ min^{-1}$ flow is only 85% after two hours and decreases with continued flow time. Under similar conditions, MSA-85851 charcoal—an activated impregnated coconut charcoal—has an efficiency of 92% after 28 hours. Although investigation of methyl iodide absorption on charcoal is still continuing, it is recommended that the HFIR filter employ a 2-in. bed of the MSA charcoal. (auth)

**3587** (RT/ING(65)–3) IL SISTEMA DI CONTROLLO AUTOMATICO DEL REATTORE ISPRA-1. (An Automatic Control System for the ISPRA-1 Reactor). Galli de'Paratesi, S.; Pulacci, A. (Comitato Nazionale per l'Energia Nucleare, Rome (Italy)). Mar. 1965. 45p. Dep. mn.

The control system of the ISPRA-1 research reactor is described. This system is provided with a fully automatic start-up device from five decades below the maximum flux level and permits the automatic control above the range of the three upper decades. Two channels with dead zones attenuate the noise effects, permitting high regulating precision. (auth)

**3588** FFTF DRIVER FUEL—$PuO_2$ STAINLESS-STEEL CERMET. Bailey, W. J.; Hennig, R. J.; de Halas, D. R.; Skavdahl, R. E. (Battelle-Northwest, Richland, Wash.). Trans. Amer. Nucl. Soc., 8: 345-6(Nov. 1965).

**3589** EFFECTS OF REFLECTORS ON THE BURST CHARACTERISTICS OF THE WSMR FAST-BURST REACTOR. Long, Robert L. (White Sands Missile Range, N. Mex.). Trans. Amer. Nucl. Soc., 8: 451-2(Nov. 1965).

**3590** EBR-II DYNAMICS. Smith, R. R.; DeForest, R. D.; Just, F.; Kirn, F. S. (Argonne National Lab., Idaho Falls, Idaho). Trans. Amer. Nucl. Soc., 8: 478-9(Nov. 1965).

**3591** APPLICATION OF AN ON-LINE DIGITAL COMPUTER TO A REACTOR EXPERIMENT. Engel, J. R. (Oak Ridge National Lab., Tenn.). Trans. Amer. Nucl. Soc., 8: 585-6(Nov. 1965).

**3592** THERMO-MECHANICAL INERTIA FORCES AND THEIR CONTROL IN THE SANDIA PULSED REACTOR. Arasim, Kenneth W. (Sandia Corp., Albuquerque, N. Mex.). Trans. Amer. Nucl. Soc., 8: 592(Nov. 1965).

**3593** PERFORMANCE OPTIMIZATION OF A FAST-BURST REACTOR CORE. Stathoplos, A.; Goldman, A. J.; Breidenbach, G. (United Nuclear Corp., White Plains, N. Y.). Trans. Amer. Nucl. Soc., 8: 592-3(Nov. 1965).

**3594** REPORT OF REACTOR EXCURSION DURING TEST OF MODIFIED WSMR FAST-BURST REACTOR CORE. Long, Robert L. (White Sands Missile Range, N. Mex.). Trans. Amer. Nucl. Soc., 8: 603(Nov. 1965).

**3595** MODIFICATION OF THE SHIELD TEST AND IRRADIATION REACTOR FOR ONE-MEGAWATT OPERATION. Randen, K. G. (Atomics International, Canoga Park, Calif.). Trans. Amer. Nucl. Soc., 8: 605(Nov. 1965).

**3596** THE FAST-FLUX TEST FACILITY DESIGN CONCEPT. Astley, E. R.; Finch, L. M.; Hennig, R. J. (Battelle-Northwest, Richland, Wash.). Trans. Amer. Nucl. Soc., 8: 607(Nov. 1965).

**3597** PHYSICS ASPECTS OF THE FAST-FLUX TEST REACTOR. Little, W. W.; Hofmann, P. L. (Battelle-Northwest, Richland, Wash.). Trans. Amer. Nucl. Soc., 8: 608(Nov. 1965).

**3598** ROTATING FLUIDIZED-BED RESEARCH REACTOR. Hoffman, K. C.; Epel, L. G.; Green, L.; Chernick, J. (Brookhaven National Lab., Upton, N. Y.). Trans. Amer. Nucl. Soc., 8: 608-9(Nov. 1965).

**3599** CHEMONUCLEAR LOOP REMOVAL FROM THE BGRR USING A SEMI-REMOTE CUTTING TECHNIQUE. Waide, C. H.; Klein, J. H. (Brookhaven National Lab., Upton, N. Y.). Trans. Amer. Nucl. Soc., 8: 620 (Nov. 1965).

**3600** NEUTRON SPECTRUM MEASUREMENTS IN HETEROGENEOUS MEDIA [Thesis]. Salah, Sagid. Gainesville, Fla., Univ. of Florida, 1964. 145p.

Neutron spectra were measured both integrally and differentially and then compared with theoretical calculations. Measurements were made in highly absorbing media in the University of Florida Training Reactor (UFTR) thermal column, in the UFTR core, and in the subcritical assembly sitting on top of the graphite pedestal of the UFTR. The subcritical assembly contained some typical $D_2O$-moderated natural uranium lattices. In the thermal column of the UFTR, thermal neutron spectra were measured integrally using activation detectors such as $^{197}Au$, $^{164}Dy$, $^{175}Lu$, $^{176}Lu$, and $^{239}Pu$. The measurements were made in a stainless steel rod, a natural uranium slab, and an Al can filled with borated water, and results were interpreted using Westcott's formulation. The effective neutron temperature and the epithermal index, $r\sqrt{T/T_0}$, were measured by using activation detectors in the UFTR core between the two fuel boxes in the North-South center line. The result of the effective neutron temperature measurement was compared with the open-beam differential spectrum and found to be in good agreement. A crystal diffraction spectrometer for differential spectrum measurements in the subcritical assembly was used. The neutron spectrum out of the subcritical assembly was measured for two different lattice pitches using Mark I and Mark V-B natural U fuel elements in $D_2O$. A neutron beam was extracted from the cell boundary and from the center of the cell for each of the three lattice arrangements. The results were compared with the theoretical spectra calculated with the THERMOS code and found to be in excellent agreement. Integral measurements were also made in the subcritical using $^{176}Lu$ and $^{197}Au$ detectors. The experimental activation measurements were compared with the THERMOS calculations and were also found to be in excellent agreement. Finally, the effective neutron temperature change in a unit cell for four U–$D_2O$ lattice arrangements was measured differentially and integrally and compared with the theoretical calculations. The results were in good agreement. (A.G.W.)

**3601** BURNUP CALCULATIONS FOR THE BROOKHAVEN GRAPHITE RESEARCH REACTOR FUEL ELEMENTS. Colsmann, P. (Brookhaven National Lab., Upton, N. Y.). Vienna, International Atomic Energy Agency, 1965, Preprint No. SM-67/36, 15p. (CONF-650803–14). ORINS.

From IAEA Symposium on Nuclear Materials Management, Vienna.

Fuel burnup calculations involve a distribution of the thermal megawatt days of operations to the fuel elements in proportion to the average thermal neutron flux at their location in the reactor. The megawatt days so assigned can be converted to equivalent $^{235}U$ consumption when needed. The original fuel loading was natural uranium, and a single calculation was performed on each fuel element upon dis-

charge. A subsequent change to a fully enriched $^{235}U$ fuel element, however, introduced complications. The average loading of enriched uranium involves about 4800 individual elements, each occupying four different reactor positions during its term in the reactor. The total term for a central channel element is about one year as against six to eight years for an element in a peripheral channel. With the large number of individual fuel elements involved and the approximately monthly small changes needed for operation, it was necessary to resort to a computer program to continuously follow the burnup of all the elements in the reactor. This program, in addition to updating the burnup of all fuel elements, also records the charging, shifting, and discharging of fuel elements so as to reflect the correct positions of all the elements. Printed outputs from a computer run are listings of all elements charged, shifted, and discharged as well as a list of those elements exceeding any desired burnup criteria. There is also a summary sheet which totalizes the operations performed and which summarizes the amount of fuel in the reactor and the amounts discharged. (auth)

**3602** IMPROVEMENTS IN OR RELATING TO IRRADIATION ENCLOSURES FOR SWIMMING POOL TYPE REACTORS. Bochirol, Louis; Doulat, Jacques; Weil, Louis (to Commissariat a l'Energie Atomique). British Patent 1,005,551. Sept. 22, 1965. Priority date Dec. 28, 1962, France.

An irradiation enclosure for a swimming-pool reactor consists of a lower tube for containing a capsule or sample to be irradiated and an upper tube in communication with the lower tube but not in alignment with it. The upper tube rises out of the water of the pool and contains any fluid channels or electrical conductors necessary to effect the desired experimental conditions. The upper end of the lower tube is closed by a sealed stopper and is provided with an axial sleeve rising out of the water and permitting direct access to the stopper. The sample can thus be replaced without breaking of connections. (A.G.W.)

# WASTE DISPOSAL AND PROCESSING

**See also BIOLOGY AND MEDICINE — Ecology**
**CHEMISTRY — Radiochemistry**
**CHEMISTRY — Separation Processes and Procedures**
**HEALTH AND SAFETY**

*Refer also to abstracts 1940, 1989, and 3521.*

**3603** (LA-DC-7249) OPERATIONAL PRACTICES IN THE TREATMENT OF LOW AND INTERMEDIATE LEVEL RADIOACTIVE WASTES—ARGONNE AND LOS ALAMOS LABORATORIES, U.S.A. Emelity, L. A.; Christenson, C. W. (Los Alamos Scientific Lab., Univ. of California, N. Mex.); Kline, W. (Argonne National Lab., Ill.). [1965]. Contract W-7405-eng-36. 18p. (SM/71-24; CONF-651202-3). Dep. mn; CFSTI $1.00 cy, $0.50 mn.

For Presentation at Symposium on Practices in the Treatment of Low and Intermediate Level Radioactive Waste, Vienna.

Several fundamental differences exist between waste disposal practices at Argonne and Los Alamos, but the basic "concentrate and contain" philosophy is identical. There is also complete agreement between the laboratories as to the primary responsibility for protection of operating personnel and the public in pursuing the established practices. Environmental surveys provide witness to the fact that precautionary attitudes are successful. (auth)

**3604** (RT/PROT(65)-12) ASPETTI TECNICO-IGIENISTICI DELLO SMALTIMENTO DEI RIFIUTI RADIOATTIVI IN ITALIA. (Technological-Hygienic Aspects of Radioactive Waste Disposal in Italy). Branca, G. (Comitato Nazionale per l'Energia Nucleare, Rome (Italy)). Apr. 1965. 54p. (CONF-631005-1). Dep. mn.

From 23rd Congress of the Italian National Assn. for Hygiene and Public Health, Catania, Italy.

The most important technical procedures giving rise to liquid, solid, and gaseous radioactive wastes are described. Particular reference is made to typical situations which exist or will be set up in Italy in the near future. Measures taken in the different Italian nuclear research centers to solve the problem of contamined waste treatment and disposal are examined. Finally, a description of the waste discharge philosophy applied in some particular cases is given. This philosophy is established taking into account the environmental characteristics and the possible influence of the radioisotopes dispersed in the ecosystem. (auth)

**3605** HEAT GENERATION BY RADIOACTIVE WASTES. Bradshaw, R. Louis (Oak Ridge National Lab., Tenn.). J. Sanit. Eng. Div. Amer. Soc. Civil Eng., 90: 55-7(Oct. 1964).

A discussion is given of an article by Gloyna, et al. (ibid., 90: 43-66(Feb. 1964)), concerning the storage of radioactive wastes in salt mines, and additional data on the subject are provided, particularly of temperatures of such stored wastes. Equations have been developed which allow the calculation of temperature rises for the case of an infinite array of finite length cylindrical sources, an array of seven finite length cylindrical sources, and an isolation finite cylinder. These equations assume a line source to obtain the temperature rise in the medium (rock salt in this case) and at the wall of the hole containing the cylinder, and assume a constant salt wall temperature (400°F, typically) to obtain the temperature rise at the center of the waste cylinder. By these equations, it was possible to calculate the spacing required between waste cylinders to meet the criteria for both maximum allowable waste temperature and salt temperature. Calculations were performed for storage of wastes of various ages and compositions in 10-ft long cylinders of 6- to 24-in. in 50 by 300-ft rooms in a salt mine. The maximum allowable temperature at the center-line of the waste cylinder was taken to be 1650°F, and the maximum allowable salt temperature was taken as 400°F. For wastes less than 3 to 6 yr old at the time of storage, peak salt temperatures were reached in a few hundred to a few thousand hours, but, for older wastes, the peak salt temperatures were not reached for several years, and, in some cases, for several decades. Of the estimated costs for processing and ultimate disposal of high-activity power reactor wastes in a salt mine, total costs were found to be higher for disposal of the wastes in a form that produced a larger volume of solids per unit of fission-product activity. (TCO)

**3606** FIXATION OF HIGH-LEVEL RADIOACTIVE WASTE IN PHOSPHATE GLASS. Upson, U. L. (Battelle-Northwest, Richland, Washington); Weth, George. Trans. Amer. Nucl. Soc., 8: 336-7(Nov. 1965).

**3607** DRYING PROCESS AND APPARATUS THEREFOR FOR REMOVING SOLIDS FROM LIQUID MIXTURES. Oetjen, Georg-Wihelm; Nerge, Wilhelm; Eilenberg, Hanns; Fauser, Friedrich (to Leybold-Anlagen Holding A.G.). U. S. Patent 3,205,588. Sept. 14, 1965. Priority date Oct. 21, 1960, Germany.

A process for converting filterable radioactive waste products included in a liquid into a permanent form capable of being stored and transported consists of first filtering the liquid within an evacuable drying chamber to separate the waste products from the liquid in the form of a filter residue. The residue is then vacuum freeze dried in situ forming a product that may be easily handled. The apparatus for carrying out the process is described. (B.L.M.)

**3608** RADIOACTIVE GAS DISPOSAL. Maue, Marilyn J. (to Pullman Inc.). U. S. Patent 3,206,409. Sept. 14, 1965. Filed Sept. 10, 1959.

A process for the production of water-unleachable rock containing radioactive components is proposed as a process for the disposal of radioactive gases, such as halogens and the noble gases. A solid inorganic oxide of a metal, which is polyvalent in the oxide composition, is reacted with a solid elemental metal in the presence of the gaseous radioactive component. The elemental metal is characterized as being polyvalent in a combined state and as having a higher exothermic heat of oxide formation per oxygen atom than the monoxide of the metal oxide reactant and is selected from the group of metals consisting of Al, Si, Zr, and Mg. The metal oxide is selected from the group consisting of the oxides of Cr, V, Cd, Fe, Cu, Ti, Mn, Pb, W, In, Ga, Bi, Ni, Sn, Co, and Mo. The reaction is initiated at a temperature above 200°C, and the exothermic reaction is allowed to proceed to completion after which the reactor and contents are gradually cooled to form a water-unleachable rock-like product containing the gaseous radioactive components in the interstices of the crystalline lattice. (B.L.M.)

# GENERAL AND MISCELLANEOUS

**3609** (ACF-11) METALLURGICAL CHARACTERISTICS OF WELDMENTS IN 0.750-INCH-THICK 6061 ALUMINUM. Kish, A. J.; Erickson, R. B. (ACF Industries, Inc., Albuquerque, N. Mex.). Aug. 14, 1965. Contract AT(29-1)-1352. 27p. (ACF-412-253). Dep. mn; CFSTI $2.00 cy, $0.50 mn.

Techniques and weld procedures were developed for producing acceptable weldments in 3/4 in. thick 6061 Al. Strength levels (crossweld) of 15 ksi yield and 27 ksi ultimate were typical in the as-welded condition (welded in T6 temper). Weld metal elongations as-deposited were typically 18% in 1 in. Aging of weldments for 4 hr at 350°F increased cross-weld strength and reduced weld-metal elongations 7 to 10 %. (P.C.H.)

**3610** (AD-622333) TRAJECTORY ANALYSIS FOR STRUCTURAL FRAGMENTS. Addendum to Final Report: DEBRIS CLEARANCE STUDY. Ahlers, Edward B. (IIT Research Inst., Chicago, Ill.). Aug. 1, 1965. Contract OCD-OS-62-202. 103p. (SRM-65-1). CFSTI $4.00 cy, $0.75 mn.

Trajectories of structural fragments subject to nuclear blast winds are analyzed. Trajectory computations are made for spherical masonry fragments, and are compiled for the following range of parameters: 2- to 24-in. dia fragments, initial fragment elevations from grade to 280 ft above grade, nuclear weapon yields 100 kt to 50 Mt, and peak overpressures 7 to 250 psi. (D.L.C.)

**3611** (BNWL-113-8) PLUTONIUM ABSTRACTS. VOLUME 5, NUMBER 8. (Battelle-Northwest, Richland, Wash. Pacific Northwest Lab.). Sept. 30, 1965. Contract AT(45-1)-1830. 37p. Dep. mn; CFSTI $2.00 cy, $0.50 mn.

Seventy-seven references to all areas of plutonium technology, including biology and medicine, chemistry, health and safety, metallurgy, miscellaneous, physics, and reactor technology are given to reports and journals published from 1964 through Sept. 1965. (P.C.H.)

**3612** (CONF-651001-6) NEW TECHNIQUES FOR SUPERCONDUCTING CABLES. Cummings, A. J.; Wilson, A. R. (Edgerton, Germeshausen and Grier, Inc., Las Vegas, Nev.). Oct. 19, 1965. Contract AT(29-1)-1183. 19p. Dep. mn; CFSTI $1.00 cy, $0.50 mn.

From IEEE Nuclear Science Symposium, San Francisco.

Techniques are tested for constructing superconducting cables, including those fabricated from braided elemental and high-field alloying superconductors. Braided superconducting cables are feasible for small size, packaged delay lines. Tests are facilitated by the use of a tunnel diode pulse generator operating at 4.2°K. Cables fabricated with a braided niobium outer conductor and a solid niobium inner conductor, having lengths of 200 to 1500 feet, show an output 10 to 90% risetime of less than 3 nsec at 4.2°K. When compared to the same length of RG-213/U a marked improvement is observed. Similar cables constructed of a solid Nb–25% Zr inner conductor, having lengths of 263 and 900 feet, exhibit an output 10 to 90% risetime of 0.65 nsec. These results indicate that the risetime is not a function of length as is the case in ordinary cables. (auth)

**3613** (CONF-651016-1) VIBRATION ISOLATION THROUGH PNEUMATIC SPRING AND DAMPING. Hall, Russel L. (Edgerton, Germeshausen and Grier, Inc., Las Vegas, Nev.). Oct. 11, 1965. Contract AT(29-1)-1183. 24p. Dep. mn; CFSTI $1.00 cy, $0.50 mn.

From 35th Symposium on Shock and Vibration, New Orleans.

The passive isolation of harmful shock and vibrations as applied to a relatively large package containing fragile data acquisition equipment is discussed. The shock isolator was comprised of a lightweight cylinder containing compressed air and a piston which is fully extended at steady state. The air cylinder isolator functions as zero deflection support, spring and damper. The package resembles a large commercial trailer. The trailer package was designed to be temporarily located at ground level in areas subjected to severe jolting earth movements. Efficient isolation through air spring damper appeared to require that the nonlinearities associated with the air spring offset the nonlinearities associated with the air damper. Linear nodal force balance equations were written, describing one degree of freedom, lumping all vibration control into one isolator. (M.O.W.)

**3614** (COO–1149-16) 2,5-DIMETHYLTHIOPHENE. HEAT CAPACITIES AND THERMODYNAMIC PROPERTIES FROM 5 TO 300 DEG K AND FUSION OF STABLE AND METASTABLE PHASES. Carlson, H. Gary; Westrum, Edgar F. Jr. (Michigan Univ., Ann Arbor). [1965]. Contract AT(11-1)-1149. 32p. Dep. mn; CFSTI $2.00 cy, $0.50 mn.

Heat capacities of both the stable crystalline form ($T_m$ = 210.55°K, $\Delta$Hm = 1958 cal/mole) and a metastable form ($T_m$ = 204.87°K, $\Delta$Hm = 1769 cal/mole) of 2,5-dimethylthiophene were determined by adiabatic calorimetry. The derived thermodynamic properties of the liquid at 298.15°K. are 42.62, 58.49, and 27.91 cal/(mole °K) for the heat capacity ($C_p$), entropy ($S^0$), and Gibbs energy function $[-(G^0 - H^0_0)/T]$, respectively. (auth)

**3615** (COO–1149-17) 2-METHYLFURAN: HEAT CAPACITY AND THERMODYNAMIC PROPERTIES FROM 5 to 350 DEG K. Carlson, H. Gary; Westrum, Edgar F. Jr. (Michigan Univ., Ann Arbor). [1965]. Contract AT(11-1)-1149. 13p. Dep. mn; CFSTI $1.00 cy, $0.50 mn.

The heat capacity of 2-methylfuran was measured over the low temperature range by adiabatic calorimetry. A fractional melting study applied over the premelting region indicated an enthalpy of melting ($\Delta$Hm) of 2044 cal/mole and temperature of melting ($T_m$) of 181.90°K. Values of the heat capacity at saturation ($C_s$), entropy ($S^0$), and Gibbs function $[-(G^0 - H^0_0)/T]$ are 34.35, 51.12, and 24.26 cal/(mole °K), respectively, at 298.15°K. (auth)

**3616** (COO–1149-22) HEAT CAPACITIES AND THERMODYNAMIC PROPERTIES OF GLOBULAR MOLECULES. XIII. TRANSITION AND FUSION OF PENTAERYTHRITYL CHLORIDE AND BROMIDE, TRANSITION OF PENTAERYTHRITYL IODIDE. Clever, H. Lawrence; Wong, Wen-Kuei; Westrum, Edgar F. Jr. (Michigan Univ., Ann Arbor. Dept. of Chemistry). Sept. 1964. Contract AT(11-1)-1149. 25p. Dep. mn; CFSTI $1.00 cy, $0.50 mn.

The heat capacities of crystalline pentaerythrityl iodide, and of crystalline and liquid pentaerythrityl chloride and bromide above 290°K were determined by adiabatic calorimetry. The high entropies of fusion, 14.45 and 15.42 cal/(mole °K) found for pentaerythrityl chloride and bromide, respectively, indicate that these halides have no plastic crystal phase at atmospheric pressure. However, at temperatures corresponding to the same fraction of their respective melting points all three compounds show broad lambda anomalies in their heat capacity curves. These involve excess entropies of less than one cal/(mole °K). (auth)

**3617** (COO–1149-23) HEAT CAPACITIES AND THERMODYNAMIC PROPERTIES OF GLOBULAR MOLECULES. XIV. TETRAPHOSPHORUS TRISULFIDE, TETRAPHOSPHORUS TRISELENIDE, AND TETRAPHOSPHORUS DECASULFIDE BETWEEN 5 AND 350°K Clever, H. Lawrence; Westrum, Edgar F. Jr.; Cordes, A. W. (Michigan Univ., Ann Arbor). Oct. 1964. Contract AT(11-1)-1149. 26p. Dep. mn; CFSTI $2.00 cy, $0.50 mn.

Thermal properties of three phosphorus chalcogenides were determined by adiabatic calorimetry and yielded entropies at 298.15°K for $P_4S_3$, $P_4Se_3$, and $P_4S_{10}$ of 48.60, 57.26, and 91.24 cal/(mole °K). The $P_4S_3$ has transits to a plastically crystalline state at 313.90°K with $\Delta$St = 7.89 cal/(mole °K) and $P_4Se_3$ shows an anomalous increase in

heat capacity suggesting such an effect slightly above 350°K. Diffraction data on $P_4S_3$ provided coefficients of thermal expansion on both phases and confirmation of the plastically crystalline nature of the Crystal I phase. (auth)

**3618** (COO–1149-25) THE SYSTEM TETRAMETHYLMETHANE–TETRACHLOROMETHANE. THERMODYNAMICS OF MIXING IN THE PLASTICALLY CRYSTALLINE REGION. Chang, Elfreda T.; Westrum, Edgar F. Jr. (Michigan Univ., Ann Arbor. Dept. of Chemistry). Oct. 1964. Contract AT(11-1)-1149. 27p. Dep. mn; CFSTI $2.00 cy, $0.50 mn.

Heat capacities of five different compositions (mole fraction $CCl_4$ of 0.200, 0.334, 0.501, 0.666, and 0.826) of the system tetramethylmethane–tetrachloromethane were determined by adiabatic calorimetry from 5 to 300°K. Thermodynamic functions calculated by integration of the data together with similar values for the pure components and mixing data for the liquid solutions, yield the excess enthalpies of mixing in the solid state (i.e., for the plastically crystalline solid solution) and the temperature dependence of this quantity. The excess enthalpy of the equimolal solution was compared with the values predicted by theory. (auth)

**3619** (COO–1149-26) HEAT CAPACITIES AND THERMODYNAMIC PROPERTIES OF GLOBULAR MOLECULES. XV. THE BINARY SYSTEM TETRAMETHYLMETHANE–TETRACHLOROMETHANE. Chang, Elfreda T.; Westrum, Edgar F. Jr. (Michigan Univ., Ann Arbor. Dept. of Chemistry). Oct. 1964. Contract AT(11-1)-1149. 45p. Dep. mn; CFSTI $2.00 cy, $0.50 mn.

Heat capacities and derived thermal properties on five compositions of the system tetramethylmethane–tetrachloromethane (mole fraction $CCl_4$ = 0.200, 0.334, 0.501, 0.666, and 0.826) were determined by adiabatic calorimetry from 5 to 300°K. The temperature, enthalpy, and entropy increments of each of the transitions, including fusion, in each composition were determined. The results indicated the effects on the reorientational-rotation transitions of the pure components due to the change of molecular environment and provide a tentative partial phase diagram for this system below room temperature. (auth)

**3620** (COO–1149-27) AMERICAN DOCUMENTATION INSTITUTE DOCUMENT NO. 0000. SUPPLEMENTING: "THE SYSTEM TETRAMETHYLMETHANE–TETRACHLOROMETHANE. THERMODYNAMICS OF MIXING IN THE PLASTICALLY CRYSTALLINE REGION." AND "HEAT CAPACITIES AND THERMODYNAMIC PROPERTIES OF GLOBULAR MOLECULES. XV. THE BINARY SYSTEM TETRAMETHYLMETHANE–TETRACHLOROMETHANE." Chang, Elfreda T.; Westrum, Edgar F. Jr. (Michigan Univ., Ann Arbor. Dept. of Chemistry). Oct. 1964. Contract AT(11-1)-1149. 47p. Dep. mn; CFSTI $2.00 cy, $0.50 mn.

An extensive tabulation of thermodynamic functions of tetrachloromethane–tetramethylmethane is presented. This includes data on enthalpy and enthalpy of transition, heat capacities, equilibrium temperatures, liquidus temperatures, and physical properties for theoretical calculation of excess enthalpy of mixing. (P.C.H.)

**3621** (IS–1261) THERMAL DIFFUSIVITY OF PLATINUM. Martin, J. J.; Sidles, P. H.; Danielson, G. C. (Iowa State Univ. of Science and Tech., Ames). Oct. 14, 1965. Contract W-7405-eng-82. 11p. (CONF-651020–2). Dep. mn; CFSTI $1.00 cy, $0.50 mn.

From 5th Thermal Conductivity Conference, Denver.

The thermal diffusivity of four platinum samples with resistivity ratios of 34, 100, 900, and 5000 was measured from 300 to 1200°K. The thermal diffusivity was not sensitive to small amounts of impurities. Thermal conductivity values were calculated from these results and compared with the thermal conductivity results of other investigators. At room temperature most results are in good agreement, but at high temperatures the agreement among different investigators is unsatisfactory. The data from these four specimens indicate that platinum would be suitable for a thermal conductivity standard, but additional measurements should be made by other absolute methods. (auth)

**3622** (IS–1266) THERMAL DIFFUSIVITY OF ARMCO IRON BY THREE METHODS. Klein, A. H.; Shanks, H. R.; Danielson, G. C. (Ames Lab., Iowa State Univ. of Science and Tech.). Oct. 14, 1965. Contract W-7405-eng-82. 8p. (CONF-651020–3). Dep. mn; CFSTI $1.00 cy, $0.50 mn.

From 5th Thermal Conductivity Conference, Denver.

The thermal diffusivity of Armco iron was measured by three different methods in the temperature range 25 to 1100°C. The methods were the finite rod method, the radial method, and the modified Angstrom method. The data obtained by the three methods are in good agreement. The results were used to calculate thermal conductivity values which were compared with the results of others. (auth)

**3623** (IS–T–36) SPECTROPHOTOMETRIC STUDY OF THE REDUCTION OF MELTS CONTAINING Cd(II) SALTS [Thesis]. Barnes, Richard David (Ames Lab., Iowa State Univ. of Science and Tech.). Nov. 1965. Contract W-7405-eng-82. 56p. Dep. mn; CFSTI $3.00 cy, $0.50 mn.

The visible and uv absorption spectra of a series of molten salts of general type $Cd(II)Cl_x(AlCl_4)_{2-x}$ where $0 < x < 2$ were obtained at temperatures of 300–600°C. Absorption spectra of the same salts to which small amounts of Cd had been added were obtained at the same temperatures. These studies were undertaken in an effort to learn more about the state of the solute in metal–metal halide melts and the reason for the change in color on going from Cd–$CdCl_2$ (deep red) to Cd–Cd $(AlCl_4)_2$ (pale green-yellow). The spectra were recorded using a Cary 12 spectrophotometer with a furnace block-cell holder. Very short path lengths, down to 0.0073 cm, were achieved by using an insert in the standard 1 $cm^2$ cell. Concentrations of dissolved metal were in the range 0.00399–0.0160 M. The spectra of the unreduced melts consist of the steeply rising tail of an intense band extending to shorter wave lengths. The absorbance of this tail is 1.0 at 2570 Å for $Cd(AlCl_4)_2$ at 300°C, moving out to 3470 Å in $CdCl_2$ at 600°C. The reduced melts show (in addition to the solvent edge) a single intense band at 2900 Å ($\epsilon$ = 44,200) for reduced $Cd(AlCl_4)_2$ at 300° changing to 3125 Å ($\epsilon$ = 16,700) for the salt of composition $AlCl_3/CdCl_2$ = 0.92 at 550°. In $CdCl_2$ melts the solvent cut-off overlaps the solute band making resolution impossible. Both solvent and solute bands shift to the red with increasing temperature or with increasing chloride concentration. An electronic charge transfer process from the anion to the cation is postulated for the solvent band. (P.C.H.)

**3624** (LA-DC-7088) QUANTITATIVE REDUCTION OF DATA FROM HIGH-SPEED STEREOSCOPIC PHOTOGRAPHS. Taylor, J. W.; Hughes, D. S. (Los Alamos Scientific Lab., Univ. of California, N. Mex.). [nd.]. Contract W-7405-eng-36. 18p. (CONF-650934-1). Dep. mn; CFSTI $1.00 cy, $0.50 mn.

From 7th International Congress on High-Speed Photography, Zurich.

An integrated photographic and data-reduction technique is described that uses a high-speed framing camera and stereoscopic methods. The use of the technique in the analysis of explosions is shown as an example. (T.F.H.)

**3625** (NYO–3282-1) BIOELECTRIC EFFECTS IN CALCIFIED TISSUES. Progress Report for Period September 1, 1964 to date. Lavine, Leroy S. (Long Island Jewish Hospital, New Hyde Park, N. Y.). June 1965. Contract AT(30-1)-3282. 11p. Dep. mn; CFSTI $1.00 cy, $0.50 mn.

Progress is reported in the development of methods and equipment for use in making piezoelectric measurements in bone and other materials. Preliminary results indicate that the piezoelectric effect may not be confined to calcified tissues but may be a general property of practically all tissue and may play a vital role as the initiating mechanism in tactile responses. Data are included from piezoelectric measurements on bone, tendon, ivory, and bamboo.

A technique was developed for studying the uptake and deposition of $^{45}Ca$ by clams while portions of their shells are under local stress. (C.H.)

**3626** (ORNL-P-1722) GRAIN BOUNDARY MIGRATION. Gordon, Paul; Vandermeer, R. A. (Oak Ridge National Lab., Tenn.). [1965]. Contract W-7405-eng-26. 122p. (CONF-651031-2). Dep. mn; CFSTI $4.00 cy, $0.75 mn.

From American Society of Metals Meeting, Detroit.

The effects of orientation and boundary structure factors and their interdependence with impurity effects are considered, and investigations aimed at the quantitative understanding of the drastic effect dissolved impurities have on boundary migration are examined. The results of the investigations are compared with the predictions of migration rate theories designed to account quantitatively for the impurity effect. Special attention is given to results on zone-refined Al, Ni, Pb, and Sn. 84 references are cited. (P.C.H.)

**3627** (RFP-670) MACHINE GAGING PHILOSOPHY ON INSTRUMENTATION. Grote, L. W. (Rocky Flats Div., Dow Chemical Co., Golden, Colo.). Sept. 30, 1965. Contract AT(29-1)-1106. 5p. (CONF-651011-2). Dep. mn; CFSTI $1.00 cy, $0.50 mn.

From IMOG and Metrology Subgroup Meeting, Las Vegas, Nev.

A discussion is presented on the use of high-precision fabrication machines of known reliability equipped with feedback devices and servosystems for both fabrication and inspection. Several economic aspects are considered, and it is proposed that separate machine and gage systems are more advantageous for both fabrication and inspection. (M.O.W.)

**3628** (RPI-1044-1) THERMAL DIFFUSION OF PLATINUM IN A TEMPERATURE GRADIENT. Ho, S. C.; Hehenkamp, Th.; Huntington, H. B. (Rensselaer Polytechnic Inst., Troy, N. Y. Dept. of Physics). Apr. 1, 1964. Contract AT(30-1)-1044. 22p. Dep. mn; CFSTI $1.00 cy, $0.50 mn.

Thermal diffusion of Pt in a temperature gradient was followed by a marker motion technique. Observation of different runs with various temperatures showed a clear and reproducible effect. Marker motion of 1 micron per day was measured at about 1600°C in a temperature gradient of 400°C/cm. The heat of transport was found to be $+0.68 \pm .09$ ev. This quantity is considerably larger than $E_m - E_f$, the difference between migration and formation energy, with which the heat of transport has frequently in the past been correlated. Discrepancies in this direction are not easily explained. (auth)

**3629** (SC-DC-64-288) ON SYMMETRY IN SUMMABILITY THEORY. Brannen, J. P. (Sandia Corp., Albuquerque, N. Mex.). [Jan. 23, 1963]. Contract AT(29-1)-789. 8p. Dep. mn; CFSTI $1.00 cy, $0.50 mn.

Symmetry properties of certain semi-infinite and infinite matrices of summability theory are derived. Examples are given of uses of the derived results. (T.F.H.)

**3630** (SC-DC-65-1697) ANALOG MODEL OF WAVE PROPAGATION IN AN OPEN-END CYLINDER. PHASE I OF INVESTIGATION IN ANALOG STUDY OF IMPACT FRACTURE OF CLOSED-END CYLINDERS. Ju, F. D.; Wambold, J. C. (New Mexico Univ., Albuquerque). June 1965. Contract AT(29-1)-789. 50p. Dep. mn; CFSTI $2.00 cy, $0.50 mn.

For Sandia Corp., Albuquerque, N. Mex.

Analog computer techniques were applied to the problem of elastic wave propagation in an open-end hollow cylinder. A mathematical model of the cylinder was formulated and converted to the analog computer to test its feasibility. Results of a few runs were checked against theory and tests. (D.L.C.)

**3631** (SC-DC-65-1723) USE OF THE SHOCK SPECTRUM TECHNIQUE FOR NON-LINEAR SYSTEMS. Murfin, Walter B. (Sandia Corp., Albuquerque, N. Mex.). Sept. 14, 1965. Contract AT(29-1)-789. 27p. (CONF-651013-2). Dep. mn; CFSTI $2.00 cy, $0.50 mn.

From Shock and Vibration Symposium, New Orleans.

Because the shock spectrum technique is dependent on linear simple oscillators, application of the method to non-linear systems may be of dubious value. Several types of nonlinearities are briefly discussed. Applications of shock spectra to some specific systems are investigated. The specific non-linear systems chosen are: an elastic-plastic, strain hardening system; a system with dead zone; and a system with bilinear stiffness. The spectra of the responses of these systems to simple geometric pulses are examined and compared with the spectra of the corresponding linear systems. It is shown that the spectra may differ widely. Complex environmental shock pulses are investigated. Again, it is shown that the responses of linear and non-linear systems (i.e., their shock spectra) are markedly different. The linear response spectrum is widely used to derive realizable "equivalent" test pulses from complex environmental pulses. The derived pulses for the linear and non-linear systems are compared, and it is discovered that the test pulse derived for the linear system is also applicable to the non-linear system. (auth)

**3632** (SC-DR-65-459) FRESHWATER PROPAGATION TESTS. Caffey, Thurlow W. H. (Sandia Corp., Albuquerque, N. Mex.). Oct. 1965. Contract AT(29-1)-789. 15p. Dep. mn; CFSTI $1.00 cy, $0.50 mn.

Field strengths in air generated by underwater transmitters were measured at two freshwater lakes to evaluate Moore's propagation theory as a means of predicting field strength, and to compare cylindrical loop and spherical antennas. Results are reported for Lake Mead and Lake Roosevelt. (auth)

**3633** (SC-TM-64-1686) WEIGHT, CENTER OF GRAVITY, AND MOMENT OF INERTIA OF GEOMETRIC SOLIDS. Letourneau, R. O.; Flury, R. L. (Sandia Corp., Albuquerque, N. Mex.) Nov. 1964. Contract AT(29-1)-789. 27p. Dep. mn; CFSTI $2.00 cy, $0.50 mn.

A 7090 electronic computer program is prepared for obtaining the weights, centers of gravity, and moments of inertia of geometric solids. These solids may be oriented with or without symmetry to a chosen set of reference axes. (auth)

**3634** (SC-TM-65-462) MOLDING PRECISION MICROBALLOON-FILLED EPOXY PARTS IN PLASTISOL MOLDS. (Sandia Corp., Albuquerque, N. Mex.). Sept. 1965. Contract AT(29-1)-789. 9p. Dep. mn; CFSTI $1.00 cy, $0.50 mn.

A low-cost method for producing high-quality electronic packages of solid honeycomb is described. The molded parts are composed of a glass microballoon-filled epoxy resin, cast in a flexible plastisol mold. The procedures for making and filling the mold are fully described. (auth)

**3635** (SC-TM-65-544) "ACCEL" AUTOMATED CIRCUIT CARD ETCHING LAYOUT. Fisk, C. J.; Isett, D. D. (Sandia Corp., Albuquerque, N. Mex.). Oct. 1965. Contract AT(29-1)-789. 30p. Dep. mn; CFSTI $2.00 cy, $0.50 mn.

Printed circuit board design time can be greatly reduced by the use of a computer program called ACCEL developed jointly by Sandia Corporation and the Thomas Bede Foundation under contract to Sandia. ACCEL is a program which designs printed circuit boards and produces the drawings for their construction. The input is encoded from an engineer's schematic diagram by a clerk with no knowledge of electronics. The outputs of the program are a schematic, parts list, printed circuit negative, assembly drawing, and a hole drilling list. ACCEL is written in Fortran II for the IBM-7090 computer and the drawings are produced on the Stromberg Carlson 4020 cathode ray tube plotter. (auth)

**3636** (TID-22319) THE TRANSMISSION OF LIGHT BY CRYSTAL AGGREGATES BETWEEN POLARIZERS. II. TRANSMISSION OF TWO-DIMENSIONAL SPHERU-

LITES. ONR Technical Report No. 75. Clough, S.; Stein, R. S. (Massachusetts Univ., Amherst. Polymer Research Inst.). Aug. 26, 1965. Contracts AT(30-1)-3003-3; Nonr 3357(01). 47p. Dep. mn; CFSTI $2.00 cy, $0.50 mn.

The transmission of light by crystalline polymer films is discussed. For light coherent over the area of an ideal spherulite, the transmittance between crossed polaroids is zero. The intensity measured in the transmission experiment is actually the low-angle light scattering. The equation is presented for the intensity of scattered light integrated out to the maximum angle collected by the detector. Also presented is the correlation function for scattering by a two-dimensional spherulite. (auth)

**3637** (UCLA-12-534) THE LIPIDS OF RUVETTUS PRETIOSUS MUSCLE AND LIVER. Nevenzel, Judd C.; Rodegker, Waldtraut; Mead, James F. (California Univ., Los Angeles. Lab. of Nuclear Medicine and Radiation Biology). [1964]. Contract AT(04-1)-Gen-12. 19p. Dep. mn; CFSTI $1.00 cy, $0.50 mn.

The muscle of the gempylid fish, Ruvettus pretiosus, contains 14.7% (wet weight) of lipid, which is predominantly wax esters of 34 and 36 carbon atoms with one and two double bonds. The liver lipids contain only about 2% wax esters. Contrary to a previous report, the muscle lipid does not contain hydroxy fatty acids. Gas-liquid chromatographic analyses are reported for the fatty acids of several lipid fractions, including the muscle wax esters, for the long-chain alcohols of the muscle wax esters, and for the unhydrolyzed wax esters. (auth)

**3638** (UCRL-7873) SOME ANALYTICAL METHODS FOR EXPLOSIVES AND EXPLOSIVE SIMULANTS. Selig, Walter (Lawrence Radiation Lab., Univ. of California, Livermore). May 1964. Contract W-7405-eng-48. 68p. Dep. mn; CFSTI $3.00 cy, $0.75 mn.

The nonaqueous titration of RDX and HMX as acids with tetrabutylammonium hydroxide ($Bu_4NOH$) is described. HMX is determined in dimethylformamide (DMF); RDX may be determined in either DMF, methylisobutyl ketone (MIBK), or cyclohexanone, although the latter two solvents are preferred. The total amount of RDX and HMX in mixtures may be estimated in DMF. Sample size is about 30 mg and a single determination takes about 25 minutes. (auth)

**3639** (UCRL-11194) THE MECHANICAL BEHAVIOR OF THE INTERNALLY OXIDIZED SINGLE CRYSTALS OF SILVER AND SILVER BASE ALLOYS [Thesis]. Gupta, Subhash (Lawrence Radiation Lab., Univ. of California, Berkeley). Aug. 1965. Contract W-7405-eng-48. 60p. Dep. mn; CFSTI $3.00 cy, $0.50 mn.

The presence of oxygen in the amount of 70 ppm in high-purity silver single crystals was found to strengthen the matrix. Oxygen, which is known to dissolve interstitially in the silver lattice, affects the mechanical behavior of these crystals in a manner analogous to that of substitutional solutes. A yield drop phenomenon, observed in oxygen-bearing silver crystals oriented for single slip, is explained on the basis of "Dislocation Multiplication Mechanism" proposed by Gilman and Johnston (J. Appl. Phys. 31, 632 (1962)). It is suggested that dislocations are pinned by oxygen atoms and this results in the reduction of the number of mobile dislocations. A considerable increase in strength which occurs on internal oxidation of silver-magnesium and silver-cadmium alloy single crystals is attributed to the increase in number of dislocation-dislocation interactions. The high work hardening rate exhibited by these materials in the early stages of a deformation is attributed to the high initial dislocation density and its subsequent rapid increase with strain. (P.C.H.)

**3640** (UCRL-11488) THE STRUCTURE OF THE SO-CALLED "ETHYLMETAPHOSPHATE" (LANGHELD ESTER). Burkhardt, Gottfried; Klein, Melvin; Calvin, Melvin (Lawrence Radiation Lab., Univ. of California, Berkeley). June 1964. Contract W-7405-eng-48. 18p. Dep. mn; CFSTI $1.00 cy, $0.50 mn.

Phosphorus pentoxide reacts with ether to form bicyclotetraphosphate ester (II), cyclotetraphosphate ester (III), isocyclotetraphosphate ester (IV), and tetraphosphate ester (V). Phosphorus nmr measurements show the content of the mixtures. The so-called ethyl metaphosphate (Langheld ester) was determined to be a mixture of III (50% to 45%), IV (36% to 25%), and V (14% to 30%). (auth)

**3641** (UCRL-11512(Rev.)) THE EFFECT OF TEMPERATURE, STRAIN RATE AND STRUCTURE ON THE FLOW STRESS OF AN IRON-2 PERCENT MANGANESE ALLOY. Wynblatt, P.; Rosen, A.; Dorn, J. E. (Lawrence Radiation Lab., Univ. of California, Berkeley). Sept. 15, 1964. Contract W-7405-eng-48. 21p. Dep. mn; CFSTI $1.00 cy, $0.50 mn.

The temperature, strain rate, and structure dependence of the flow stress in a polycrystalline iron-2% manganese alloy was investigated between 77 and 370°K. It was possible to identify the low temperature data from 77 to 160°K with Dorn and Rajnak's theory of the Peierls mechanism of plastic deformation. Above 160°K one or more thermally activated mechanisms must be operative, however, these were not identified. (auth)

**3642** (UCRL-11639) THE ELECTRICAL RESISTANCE OF BISMUTH FROM 25 TO 80 KILOBARS. Phillips, David; Jura, George (Lawrence Radiation Lab., Univ. of California, Berkeley). Aug. 1964. Contract W-7405-eng-48. 7p. Dep. mn; CFSTI $1.00 cy, $0.50 mn.

The electrical resistance of bismuth was carefully investigated in the pressure region between 30 and 90 kbars. No discontinuities were found in the electrical resistance in this region. However, this does not necessarily mean that the phase changes found by Bridgman (Proc. Amer. Acad. Arts and Sci., 79; 425(1942)) at 45 and 64 Kg $cm^{-2}$ do not exist. (auth)

**3643** (UCRL-11685) PARAMAGNETIC RESONANCE OF $Fe^{3+}$ IN POLYCRYSTALLINE FERRICHROME A. Wichman, H. Hollis; Klein, Melvin P.; Shirly, D. A. (Lawrence Radiation Lab., Univ. of California, Berkeley). Sept. 1964. Contract W-7405-eng-48. 18p. Dep. mn; CFSTI $1.00 cy, $0.50 mn.

Polycrystalline samples of iron-containing Ferrichrome A, a cyclic hexapeptide obtained from the fungus Ustillago sphaerogena, were investigated by paramagnetic resonance. Spectra were obtained at several temperatures between 300 and 1°K; a prominent line of 400 0e. width located at $g = 4.3$ was observed at all temperatures, while at 1°K additional resonances at g values of 9.6, 1.3, and 1.0 were observed. The spectra were interpreted by assuming a spin Hamiltonian containing large crystal field terms compared with the Zeeman splittings; the crystal field situation is intermediate between the case of axial symmetry, with $\mathcal{H} = D[S_z^2 - \frac{1}{3} S(S+1)] + g\beta \vec{S} \cdot \vec{H}$ and a model proposed by Castner, et al (J. Chem. Phys. 32, 668 (1960)) to explain certain iron resonances occurring at $g = 4.3$, with $\mathcal{H} = E(S_x^2 - S_y^2) + g\beta \vec{S} \cdot \vec{H}$. Energy eigenvalues, g values, and eigenfunctions to be expected for the region between these two extremes were computed, and the results should be useful in interpreting similar spectra due to iron situated in strong crystal fields of low symmetry. (auth)

**3644** (UCRL-16199) TRIST—A TRI-LEVEL MULTIPROGRAMMING EXECUTIVE INVOLVING REAL-TIME CALCULATIONS AND AN ASYNCHRONOUS ON-LINE DATA SOURCE. Osborne, Carol; Larson, Robert; Oliver, Thomas; Stekler, Joan; White, Howard S. (Lawrence Radiation Lab., Univ. of California, Berkeley). June 15, 1965. Contract W-7405-eng-48. 15p. (CONF-651104-1). Dep. mn; CFSTI $1.00 cy, $0.50 mn.

From Joint Computer Conference, Las Vegas, Nev.

TRIST is a TRI-level multiprogramming SysTem executive written at Lawrence Radiation Laboratory. The TRIST executive is designed to coordinate computer operations with a real-time asynchronous device attached on-line to an IBM 7094-II and to make the computer time between real-time demands available for other uses. The asynchronous device operation requires that the computer be available to accept data when the device is transmitting. Data are transmitted to alternate core buffers. The com-

puter must immediately interchange buffers and process data from one buffer while the other buffer is being filled; however, a large portion of the computer time is also available for processing general programs. Real-time demands for CPU control are met within 500 microseconds. The three priority levels of programs controlled by TRIST are: the A-level or real-time program, which receives data from the on-line device; the B-level programs, which process the data produced by the A level; and the C-level programs, which are general production and debug. (auth)

**3645** (UCRL–16344) IMPROVED TECHNIQUES FOR THE ANALYSIS OF NUCLEAR MAGNETIC RESONANCE SPECTROSCOPIC DATA: ANALYSIS OF FOUR-MEMBERED RING COMPOUNDS [Thesis]. Lusebrink, T. R. (Lawrence Radiation Lab., Univ. of California, Berkeley). Aug. 1965. Contract W-7405-eng-48. 200p. Dep. mn; CFSTI $5.00 cy, $1.25 mn.

Two computer programs were written which substantially aid the analysis of complex NMR spectra. One program, DECOMP, allows the decomposition of superimposed groups of peaks so that peak positions in an unresolved group can be determined nearly as accurately as resolved peaks. The second program, ASSIGN, calculates all possible sets of energy levels which are consistent with the observed frequencies and intensites of the completely resolved spectrum. This system of programs was utilized in the complete spectral analysis of two four-membered ring compounds; a class of compounds which have not previously been analyzed. The compounds are 3-chlorothietane and 3-thietanyl acetate, two highly mixed five-spin systems of the $A_2B_2X$ type. Details of the analyses and listings of the computer programs are given. Extension of the method to six nuclei $A_2B_4$ systems, occurring in four membered rings, is also indicated. (M.O.W.)

**3646** RESEARCH CENTRES IN EUROPE – NO. 10. RISOE. Euro Nucl., 2: 497-504(Oct. 1965).

Studies at the Risö research center are discussed. Reactor development, facilities for handling radioactive materials, waste treatment, metallurgical studies, chemistry research, theoretical studies, research in plasma physics, applied radiation studies, and the linear accelerator are described. (M.C.G.)

**3647** TRANSACTIONS OF THE AMERICAN NUCLEAR SOCIETY 1965 ANNUAL MEETING, WASHINGTON, D. C., NOVEMBER 15–18, 1965. Trans. Amer. Nucl. Soc., 8: 313-659(Nov. 1965). (CONF-651101).

*For abstracts of individual papers see: 1586, 1691, 1694, 1695, 1786–1792, 1864, 1924–1929, 1970, 1971, 1977, 1978, 1993–2001, 2021, 2022, 2030–2033, 2038, 2055, 2056, 2091, 2092, 2113–2117, 2164–2175, 2189–2191, 2194, 2195, 2201, 2202, 2206, 2207, 2210–2212, 2217, 2227–2247, 2268–2275, 2288–2299, 2386–2393, 2448–2469, 2551–2559, 2730, 2731, 2949–2997, 3095, 3096, 3255–3276, 3308, 3309, 3328–3342, 3344–3348, 3384–3433, 3452–3462, 3493–3525, 3542–3544, 3554–3577, 3588–3599, and 3606.*

**3648** ECONOMIE ET PERSPECTIVES DE L'ENERGIE ATOMIQUE. (Economy and Perspectives of Atomic Energy). Andriot, J. l'Energie et ses Problemes. Paris, Dunod, 1964. 287p.

The economy and probable future development of nuclear energy is discussed. Nuclear energy and its economic aspects, scientific and technical data on nuclear energy, the economy of primary nuclear materials, electricity production by nuclear power plants, development programs of nuclear energy, and the uses of nuclear energy other than for production of electricity are topics discussed. (J.S.R.)

# CORPORATE AUTHOR INDEX

This index contains entries for this period for all report literature and, in addition, for certain published literature items for which it is felt that a corporate approach is especially desirable, e.g., symposia, conference proceedings, and meetings.

Each entry under a corporate author is a shortened version of the title of the publication, followed by the *NSA* volume and abstract number. Report numbers are given in parentheses.

The phrase "Progress report" is abbreviated as "Prog. rpt.," permitting a more rapid and complete alphabetical arrangement of the titles without changing the location of the progress report titles in relation to the other titles.

## A


**ACF INDUSTRIES, INC., ALBUQUERQUE, N. MEX.**
Metallurgical characteristics of weldments in 0.750-inch-thick 6061 aluminum, 20: 3609 (ACF-11)

**ADELPHI UNIV., GARDEN CITY, N. Y.**
Sensitivity of incremental derivative polarography, 20: 1746 (TID-22199)

**AERONUTRONIC DIV., PHILCO CORP., NEWPORT BEACH, CALIF.**
Prog. rpt. on fabrication and properties of W single crystals, final, 3/64–2/65, 20: 2284 (NP-15093)

**AEROSPACE CORP., EL SEGUNDO, CALIF.**
The effect of charged-particle environments on manned military space systems, 20: 2656 (NASA-SP-71, pp 265-86)
Updating and dissemination of knowledge of trapped radiation—model environments, 20: 2654 (NASA-SP-71, pp 47-55)

**AGRICULTURAL RESEARCH SERVICE, ALBANY, CALIF. WESTERN REGIONAL RESEARCH LAB.**
Bulgur wafer and adjuncts for fallout shelter rations, 20: 2067 (AD-614824)

**AIR FORCE CAMBRIDGE RESEARCH LABS., L. G. HANSCOM FIELD, MASS.**
Sunspot cycle and ionospheric storms, 20: 2848 (AD-615111)

**AIR FORCE INST. OF TECH., WRIGHT-PATTERSON AFB, OHIO. SCHOOL OF ENGINEERING.**
Combined convection and radiation in radioisotope thrustors, 20: 2007 (AD-618026)
Investigation of waves of ionization in pulsed discharge, 20: 3162 (AD-618688)

**AIR FORCE MATERIALS LAB., WRIGHT-PATTERSON AFB, OHIO.**
Refractory metals—an assessment, 20: 2307 (AD-613023)

**AIR FORCE WEAPONS LAB., KIRTLAND AFB, N. MEX.**
Radiobiological consequences of dose distributions produced by solar-flare-type spectra, 20: 2655 (NASA-SP-71, pp 85-96)
Simulation of air-blast-induced ground motion, phase I, 20: 1980 (AD-614990)

**AKRON UNIV., OHIO. INST. OF RUBBER RESEARCH.**
Prog. rpt. on low-temperature polymerization, 4–6/65, 20: 1893 (AD-618228)

**AKTIEBOLAGET ATOMENERGI, STOCKHOLM (SWEDEN).**
Bibliography on preventive maintenance in chemical and mining industries, 20: 1976 (VDDIT-94)
Calculation of pressure drop in ducts and fuel elements with shroud, 20: 2010 (IPV-19)

**ALLGEMEINE ELEKTRIZITAETSGESELLSCHAFT, FRANKFURT AM MAIN (WEST GERMANY).**
Prog. rpt. on nuclear vapotron, 1–3/64, 20: 3443 (EURAEC-1356)
Prog. rpt on nuclear vapotron, 4–6/64, 20: 3444 (EURAEC-1357)
Prog. rpt. on nuclear vapotron, 7–9/64, 20: 3445 (EURAEC-1358)

**ALLIS-CHALMERS MFG. CO., BETHESDA, MD. ATOMIC ENERGY DIV.**
Flexibility study of back-pressure turbines for dual-purpose plants, 20: 3540 (ACNP-65573)
Survey of high-temperature demineralization for dual-purpose BWR plants, 20: 3539 (ACNP-65558(Rev.1))

**AMES LAB., IOWA STATE UNIV. OF SCIENCE AND TECH.**
Electronics in mass spectrometry, 20: 2100 (IS-1193)
Magnetoresistance of thallium, 20: 2329 (IS-T-35)
Prediction of approach to steady-state of a mixer-settler extractor, 20: 1953 (IS-T-34)
Preparation of vanadium metal by aluminum reduction of $V_2O_5$, 20: 2225 (IS-T-40)
Recoil chemistry of $^{11}C$ in liquid hydrocarbons, 20: 1896 (IS-T-23)
Spectrophotometric study of reduction of melts containing Cd(II) salts, 20: 3623 (IS-T-36)
Thermal diffusivity of armco iron by three methods, 20: 3622 (IS-1266)

**ARGONNE NATIONAL LAB., ILL.**
Advanced systems research and development, 20: 3579 (ANL-7082, pp 54-61)
Current magnet design practice in the U.S.A., 20: 2533 (BNL-9536)
Engineering development of fluid-bed fluoride volatility processes. IV., 20: 1952 (ANL-6859)
General reactor technology, 20: 3321 (ANL-7082, pp 29-53)
Laboratory investigations in support of fluid-bed fluoride volatility processes. VIII., 20: 2076 (ANL-7068)
Liquid-metal-cooled reactors, 20: 3320 (ANL-7082, pp 1-28)
Neutron monitor for simultaneous measurement of fluence and dose equivalent, 20: 2123 (ANL-7085)
Nuclear safety (Argonne National Lab., Ill.), 20: 2221 (ANL-7082, pp 62-73)
Operational practices in treatment of low and intermediate level radioactive wastes—Argonne and Los Alamos laboratories, U.S.A., 20: 3603 (LA-DC-7249)
Optimum design of high-pressure, large-diameter, direct-nuclear-pumped, gas lasers, 20: 2591 (ANL-7030)
Perturbation program written in fortran, 20: 3366 (ANL-7052)
Preparation of metals by Mg–Zn reduction. III., 20: 2220 (ANL-7959)
Prog. rpt. on reactor development, 7/65, 20: 3319 (ANL-7082)

**ARMY ELECTRONICS LABS., FORT MONMOUTH, N. J.**
Pulsed nuclear radiation induced transients in electrical cables, 20: 2186 (ECOM-2415)
Pulsed nuclear radiation effects on resistors and cables, 20: 2187 (ECOM-2545)

**ARMY ENGINEER NUCLEAR CRATERING GROUP, LIVERMORE, CALIF.**
Isthmian canal studies, 1964. Annex III. Appendix 1. Nuclear excavation plan, 20: 1983 (PNE-2000)
Isthmian canal studies, 1964. Annex III. Appendix 1. Inclosure A. Excavation with nuclear explosions, 20: 1984 (PNE-2001)

**ARMY MATERIALS RESEARCH AGENCY, WATERTOWN ARSENAL, MASS.**
Effect of deformation and heat treatment on mechanical properties of Ti-6Al-6V-2Sn-4Zr-1Fe-1Cu alloy, 20: 2309 (AD-615024)
Formability characteristics of polyphase titanium alloy Ti-6Al-6V-2Sn-4Zr, 20: 2308 (AD-614637)

**ATOMIC ENERGY OF CANADA LTD., CHALK RIVER (ONTARIO).**
Abstracts of Canadian patents on production of heavy water, 20: 1951 (AECL-2279)
CARIBOU—program for computing isotopic composition of NRX uranium metal rods, 20: 3583 (CRT-1187 B)
Effect of neutron irradiation and hydrogen concentration on tensile properties of CANDU coolant tube spacer alloy, 20: 2414 (AECL-2272)
High-sensitivity heavy water leak detector, 20: 2099 (AECL-2291)
Highly rated hollow $UO_2$ pellets irradiated in collapsible sheathing—dimensional stability, metallography and autoradiography, 20: 2415

(AECL-2276)
Melting of $UO_2$ during irradiations of short duration, 20: 2416(AECL-2289)
Re-irradiation of a high burnup $UO_2$—zircaloy fuel element at an increased heat rating, 20: 2421 (EXP-NRX-22902)

**ATOMIC ENERGY OF CANADA LTD., CHALK RIVER (ONTARIO). CHALK RIVER NUCLEAR LABS.**
Nucleation and growth of hydrides in zirconium alloys, 20: 2253 (AECL-2297)

**ATOMIC ENERGY RESEARCH ESTABLISHMENT, HARWELL (ENGLAND).**
Radiolytic reaction between graphite and carbon dioxide. VI., 20: 1895 (AERE-R-4988)

**ATOMIC WEAPONS RESEARCH ESTABLISHMENT, ALDERMASTON (ENGLAND).**
Investigation of the pressure wave propagated from open end of a 30 × 18 in. shock tube, 20: 2822 (AWRE-O-60/65)
Sodium flame photometer test for high-efficiency filters, 20: 2077 (AWRE-O-41/65)
Sorption of methanol by corroded uranium, 20: 1805 (AWRE-O-69/65)
Uranium corrosion studies. II., 20: 1804 (AWRE-O-68/65)

**ATOMICS INTERNATIONAL, CANOGA PARK, CALIF.**
Pressure drop for flowing vapors condensing in a straight horizontal tube, 20: 1814 (NAA-SR-6333)
Thermoelectromagnetic pump for the 3-kwe Hg Rankine system, 20: 1988 (NAA-SR-11198)
1.5 Mwe thermionic reactor space power system, 20: 3547 (NAA-SR-Memo-7581)

**AUSTRALIAN ATOMIC ENERGY COMMISSION, COOGEE.**
Radioisotopes catalog, 20: 2208 (NP-15575)

**AUTHORITY HEALTH AND SAFETY BRANCH, UNITED KINGDOM ATOMIC ENERGY AUTHORITY, HARWELL (ENGLAND).**
Computed deposition rates per unit release rate of windborne material, 20: 2074 (AHSB(RP)M-40)

**AUTHORITY HEALTH AND SAFETY BRANCH, UNITED KINGDOM ATOMIC ENERGY AUTHORITY, LONDON (ENGLAND).**
Review of UKAEA criticality detection and alarm systems 1963/64. I., 20: 2075 (AHSB(S)R-92)

**AVCO-EVERETT RESEARCH LAB., EVERETT, MASS.**
Diocotron instability in quasi-toroidal geometry, 20: 3252 (NP-15578)
Magnetic radiation shielding using superconducting coils, 20: 3241 (NASA-SP-71, pp 199-209)

## B

**BABCOCK AND WILCOX CO., GALVESTON, TEX.**
N. S. Savannah containment integrity—its measurement and improvement, 20: 3551 (TID-22316)

**BARTOL RESEARCH FOUNDATION, SWARTHMORE, PA.**
Prog. rpt. on solid state investigations utilizing electron-bombardment phenomena, annual, 1965, 20: 2434 (TID-22342)

**BATTELLE INSTITUT E. V., FRANKFURT AM MAIN (WEST GERMANY).**
Bibliography on direct conversion of nuclear energy into electric energy, 20: 2669 (AED-C-15-07)

**BATTELLE MEMORIAL INST., COLUMBUS, OHIO.**
Hot isostatic compaction of graphite, 20: 2278 (BMI-1746)

**BATTELLE-NORTHWEST, RICHLAND, WASH. PACIFIC NORTHWEST LAB.**
Age related changes in hematological and serum biochemical parameters in miniature swine, 20: 1581 (BNWL-SA-341)
Applications of eddy current testing at Battelle-Northwest, 20: 2025 (BNWL-SA-349)
Criticality research on plutonium, 20: 3368 (BNWL-SA-214)
High-temperature graphite irradiations: 800 to 1200°C, 20: 2417 (BNWL-112)
Plutonium abstracts. Volume 5, Number 8, 20: 3611 (BNWL-113-8)
Safety and nuclear considerations in design of FTR, 20: 3581 (BNWL-SA-340)
Stationary calculation of ratios in reactor statics, 20: 3367 (BNWL-156)

**BECHTEL CORP., SAN FRANCISCO, CALIF.**
Title 1 report. Preliminary services for SNAP 8, flight prototype test facility, building 056, Santa Susana, California, 20 3550 (TID-21994)

**BENDIX CORP., SOUTHFIELD, MICH. RESEARCH LABS. DIV.**
Prog. rpt. on development of Q-factor technique, 1–3/65, 20: 2184 (AD-614618)
Prog. rpt. on development of Q-factor technique, 4–6/65, 20: 2185 (AD-618194)

**BENDIX SYSTEMS DIV., BENDIX CORP., ANN ARBOR, MICH.**
Cosmic-ray shower production in manned space vehicles—copper, 20: 3240 (NASA-SP-71, pp 183-8)

**BETTIS ATOMIC POWER LAB., PITTSBURGH, PA.**
A program for the solution of the one-dimensional, two-group, space-time diffusion equations accounting for temperature, xenon, and control feedback, 20: 3382 (WAPD-TM-532)
Control-induced xenon oscillations, 20: 3326 (WAPD-T-1732)
Fatigue and burst tests on irradiated in-pile stainless steel pressure tubes, 20: 2435 (WAPD-T-1720)
Few group and multigroup calculations of neutron penetration, 20: 2939 (WAPD-T-1710)

**BETTIS ATOMIC POWER LAB., WEST MIFFLIN, PA.**
Hydride habit in Zr in unstressed and stressed Zircaloy-4, 20: 2355 (WAPD-T-1757(Rev.))

**BOEING CO., SEATTLE, WASH.**
Evaluation of radiation shielding by vehicle orientation, 20: 3249 (NASA-SP-71, pp 473-6)
Fractional cell lethality approach to space radiation hazards, 20: 1616 (NASA-SP-71, pp 219-23)

**BROOKHAVEN NATIONAL LAB., UPTON, N. Y.**
Biological interactions associated with spruce budworm infestations, 20: 1589 (BNL-917, pp 61-8)
Brookhaven radiofrequency beam separator, 20: 2532 (BNL-9505)
Current magnet design practice in the U.S.A., 20: 2533 (BNL-9536)
Ecological effects of nuclear war, 20: 1588 (BNL-917)
Effects of fire on major ecosystems, 20: 2079 (BNL-917, pp 11-19)
Effects of ionizing radiation on ecological systems, 20: 2080 (BNL-917, pp 20-38)
Evaluation of phase-space density measurement techniques, 20: 2534 (BNL-9587)
Gamma radiation source and irradiator design, 20: 1937 (BNL-9281)
HFBR physics startup manual, 20: 3580 (BNL-9591)
Ionizing radiation and homeostasis of ecosystems, 20: 2081 (BNL-917, pp 39-60)
Megachannel analyzers, 20: 2124 (BNL-9590)
Physical damage from nuclear explosions, 20: 2078 (BNL-917, pp 1-10)
Radiosensitivity of Marchantia thalli as related to nuclear and interphase chromosome volumes, 20: 1610 (BNL-9611)
Refinement in methods of neutron activation analysis of ancient glass objects, 20: 1731 (BNL-9614)
Response of skin of swine to increasing exposures of 250 kvp x rays, 20: 1609 (BNL-9477)
Role of computers in processing scanning data, 20: 2213 (BNL-9609)
Size of ribosomal site for messenger RNA binding, 20: 1592 (BNL-7903)
Technetium-99m generator, 20: 1730 (BNL-9601)

**BROWN UNIV., PROVIDENCE, R. I. DEPT. OF PHYSICS.**
Survey and classification of soluble field theory models, 20: 2757 (NYO-2262-98)

**BROWN UNIV., PROVIDENCE, R. I. DIV. OF ENGINEERING.**
Linear dislocation arrays in heterogeneous materials, 20: 2335 (NYO-2394-9)

**BRUSSELS UNIV. (BELGIUM). FACULTE DES SCIENCES.**
Thermodynamic study of the uranium–oxygen system by mass spectrometry. Heat of sublimation of uranium, 20: 1810 (EUR-2458.f)

**BUREAU OF MINES, ALBANY, OREG. ALBANY METALLURGY RESEARCH CENTER.**
Cold-mold induction melting, 20: 2352 (USBM-RC-1205, pp 9-10)
High-melting point carbides (HfC), 20: 2351 (USBM-RC-1205, pp 3-7)
Investigation of the system UC-UN-UO, 20: 2353 (USBM-RC-1205, pp 11-14)
Prog. rpt. on metallurgy, 8–9/65, 20: 2350 (USBM-RC-1205)
W-Re-Mo alloy development, 20: 2354 (USBM-RC-1205, pp 15-19)

**BUREAU OF MINES, COLLEGE PARK, MD. COLLEGE PARK METALLURGY RESEARCH CENTER.**
Stress-corrosion cracking of vanadium, molybdenum, and a titanium–vanadium alloy, 20: 2254 (BM-RI-6680)

**BUREAU OF MINES, RENO, NEV. RENO METALLURGY RESEARCH CENTER.**
Heat of formation of neodymium trichloride, 20: 1806 (BM-RI-6697)

## C

**CALIFORNIA UNIV., BERKELEY. DONNER LAB.**
Biological effects of heavy ions, 20: 1615 (NASA-SP-71, pp 105-14)

**CALIFORNIA UNIV., BERKELEY. INST. OF ENGINEERING RESEARCH.**
Scattered light in photothermo-elasticity, 20: 2026 (UCRL-13188)

**CALIFORNIA UNIV., LA JOLLA, SAN DIEGO.**
Superconductivity in one and two dimensions, 20: 2889 (AD-618203)

**CALIFORNIA UNIV., LOS ANGELES. LAB OF NUCLEAR MEDICINE AND RADIATION BIOLOGY.**
Lipids of Ruvettus pretiosus muscle and liver, 20: 3637 (UCLA-12-534)

**CAROLINAS VIRGINIA NUCLEAR POWER ASSOCIATES, INC., PARR, S. C.**
Prog. rpt. on CVTR, 1–2/65, 20: 3469 (CVNA-242)

**CASE INST. OF TECH., CLEVELAND, OHIO.**
Positron spectrum from fission antineutrinos on protons, 20: 2680 (COO-818-58)

**CEKMECE NUCLEAR RESEARCH CENTER, ATOMIC ENERGY COMMISSION, ISTANBUL (TURKEY).**

Pre-kinetic equations for plasma, 20: 3163 (CNAEM-26)
**CENTRE D'ETUDE DE L'ENERGIE NUCLEAIRE, BRUSSELS (BELGIUM).**
New approach to continuum polaron theory, 20: 3277 (BLG-328)
Preparation of Zr and U–Mo alloys, 20: 2222 (EURAEC-1390)
Working conditions and safety in laboratories of Department of Radioisotopes at Mol, 20: 2192 (BLG-68-11)
**CHICAGO UNIV., ILL.**
Prog. rpt. on expansion of H(II) regions, final, 10/63–12/64, 20: 2562 (AD-614715)
**COAST AND GEODETIC SURVEY, ROCKVILLE, MD. WASHINGTON SCIENCE CENTER.**
Strong-motion seismic measurements. Project Dugout, 20: 1981 (PNE-605F)
**COLORADO STATE UNIV., FORT COLLINS.**
Prog. rpt. on x irradiation of developing avian embryo as factor of aging, 9/20/64–9/10/65, 20: 1611 (COO-1119-4)
**COLUMBIA UNIV., NEW YORK.**
Index to literature on microscopic neutron data, 20: 3018 (NYO-72-27)
**COLUMBIA UNIV., NEW YORK. DEPT. OF PHYSICS.**
Large-spin rotational states of deformed nuclei, 20: 3008 (COO-1420-104)
**COMISION NACIONAL DE ENERGIA ATOMICA, BUENOS AIRES (ARGENTINA).**
Preparation of a $^{99m}$Tc labeled colloid. Note No. 152, 20: 1696 (CONF-641126-1)
Preparative chromatography of moving-gas phases, 20: 1886 (CONF-641123-1)
Properties of copper alloys of high resistance and high conductivity, 20: 2334 (NP-15530)
Tritiation of furfural, 20: 1887 (NP-15523)
**COMITATO NAZIONALE PER L'ENERGIA NUCLEARE, ROME (ITALY).**
Automatic control system for ISPRA-1 reactor, 20: 3587 (RT/ING(65)-3)
Data on environmental radioactivity collected in Italy, July–December 1963, 20: 2046 (BIO/04/64)
Method of gas-chromatographic analysis of polyphenyls in lithium chloride columns, 20: 1745 (RT/CHI(65)-25)
Preparation of uranium dioxide and carbide particles by sol-gel methods, 20: 2226 (RT/CHI(65)-30)
Tank type organic cooled and moderated reactor. Preliminary investigation of 50-MWt prototype, 20: 3440 (RT/ING(65)16)
Technological-hygienic aspects of radioactive waste disposal in Italy, 20: 3604 (RT/PROT(65)–12)
**COMMISSARIAT A L'ENERGIE ATOMIQUE, FONTENAY-AUX-ROSES (FRANCE). CENTRE D'ETUDES NUCLEAIRES.**
Computer processing of $\gamma$ spectra and determination of radioelements, 20: 1732 (CEA-R-2850)
Mechanical time shutter for spectrograph with exposure times from 1.5 $\mu$s to 3 ms, 20: 2125 (CEA-R-2816)
**COMMISSARIAT A L'ENERGIE ATOMIQUE, GRENOBLE (FRANCE). CENTRE D'ETUDES NUCLEAIRES.**
General views about sample irradiations in reactors, 20: 2418 (CEA-R-2801)
**COMMISSARIAT A L'ENERGIE ATOMIQUE, SACLAY (FRANCE). CENTRE D'ETUDES NUCLEAIRES.**
ALECTO—results obtained with homogeneous critical experiments on $^{239}$Pu, $^{235}$U and $^{233}$U, 20: 3369 (CEA-R-2814)
Anisotropy of the fluorine chemical shift tensor in $UF_6$, 20: 1807 (CEA-R-2827)
Bibliography on Be isotopes—nuclear reactions, 20: 3007 (CEA-Bib-32)
Bibliography on radiohydrology, 20: 2082 (CEA-Bib.-59)
Low-temperature oxidation of uranium powders and application to sintering of uranium oxide powders, 20: 2279 (CEA-R-2828)
Results and interpretation of spectral indices measurements made with aquilon, 20: 3582 (CEA-R-2482)
**COMMONWEALTH EDISON CO., CHICAGO, ILL.**
Dresden nuclear power station. Unit 2. Plant design and analysis report, I., 20: 3476 (NP-15538(Vol.1))
Dresden nuclear power station. Unit 2. Plant design and analysis report. II., 20: 3477 (NP-15538(Vol.2))
Dresden nuclear power station. Unit 2. Plant design and analysis report. III., 20: 3478 (NP-15538(Vol.3))
**COMPAGNIE DES ATELIERS ET FORGES DE LA LOIRE, PARIS (FRANCE). DEPARTEMENT DES RECHERCHES.**
Prog. rpt. on failure of stainless steel cladding fuel rods, 4–6/65, 20: 2256 (EURAEC-1449)
**COMPAGNIE FRANCAISE THOMSON-HOUSTON, PARIS.**
Prog. rpt. on nuclear vapotron, 1–3/64, 20: 3443 (EURAEC-1356)
Prog. rpt. on nuclear vapotron, 4–6/64, 20: 3444 (EURAEC-1357)
Prog. rpt. on nuclear vapotron, 7–9/64, 20: 3445 (EURAEC-1358)
**CONTINENTAL ELECTRONICS CORP., COLUMBUS, OHIO.**
High-sensitivity fast neutron dosimeter, 20: 2134 (TID-22335)
**CONTROLS FOR RADIATION, INC., CAMBRIDGE, MASS.**
Development of radiac set AN/TDQ-2 for detection of pulsed x radiation from high-powered electronic equipment, 20: 2121 (AD-614832)
Radiation facility support and solid-state studies, 20: 2531 (AD-618304)
**CRUFT LAB., HARVARD UNIV., CAMBRIDGE, MASS.**
Antenna inside a magneto-plasma-filled parallel-plate waveguide, 20: 2096 (AD-617928)

## D

**DIVISION OF BIOLOGY AND MEDICINE (AEC), WASHINGTON, D. C.**
Genetic effects of fast neutrons from nuclear detonations, 20: 1622 (WT-820)
**DIVISION OF TECHNICAL INFORMATION EXTENSION, (AEC), OAK RIDGE, TENN.**
Bibliography on hot laboratories, 20: 1990 (TID-3545(Rev.1))
**DU PONT DE NEMOURS (E. I.) & CO., AIKEN, S. C. SAVANNAH RIVER LAB.**
Depletion of deionizer resin in an SRP reactor system, 20: 2419 (DP-973)
Leak testing of HWCTR containment building, 20: 2037 (DP-968)
Process-scale separation of hydrogen isotopes by gas chromatography, 20: 1733 (DP-979)
Prog. rpt. on USAEC-AECL cooperative program, 8/65, 20: 2420 (DPST-65-83-8)
Uranium dioxide fuel tubes for irradiation in VBWR, 20: 2280 (DP-989)
**DYNATECH CORP., CAMBRIDGE, MASS.**
Prog. rpt. on boiling flow regimes and critical heat flux, 6/16–9/15/65, 20: 2012 (NYO-3304-6)

## E

**EDGERTON, GERMESHAUSEN AND GRIER, INC., LAS VEGAS, NEV.**
New techniques for superconducting cables, 20: 3612 (CONF-651001–6)
Vibration isolation through pneumatic spring and damping, 20: 3613 (CONF-651016–1)
**EMORY UNIV., ATLANTA, GA.**
Ionizing radiation and homeostasis of ecosystems, 20: 2081 (BNL-917, pp 39-60)
**ENEA NEUTRON DATA COMPILATION CENTRE, GIF-SUR-YVETTE (FRANCE).**
Index to literature on microscopic neutron data, 20: 3018 (NYO-72-27)
**ENTE NAZIONALE PER L'ENERGIA ELETTRICA, ROME (ITALY).**
Prog. rpt on Garigliano nuclear power plant, 3/31/65, 20: 3483 (TID-22201)
**EUROPEAN-AMERICAN NUCLEAR DATA COMMITTEE.**
Index to literature on microscopic neutron data, 20: 3018 (NYO-72-27)
**EUROPEAN ATOMIC ENERGY COMMUNITY.**
Bibliography concerning transplutonium elements, 20: 1726 (EUR-2508.e)
Electrochemical labeling of proteins, 20: 1939 (EUR-2476.i)
Environmental radioactivity, Ispra 1964, 20: 2047 (EUR-2509.e)
Feasibility of new procedure for biological dosimetry, 20: 1612 (EUR-2505.e)
Forced convection burnout and hydrodynamic instability experiments for water at high pressure. I., 20: 2009 (EUR-2490.e)
Identification chart for $\gamma$-emitting radionuclides formed by (n,$\gamma$) reactions, 20: 1735 (EUR-2408.e)
Kinetic theory and calculations for accelerator booster with periodically varying multiplication factor, 20: 3371 (EUR-2492.e)
Main technical characteristics of graphite-gas and light boiling- or pressurized-water type plants, 20: 3322 (EUR-2448.f)
Precise determination $\alpha$ $P_K\omega_K$ value and fluorescence yield of Cr, 20: 2593 (EUR-2524.e)
Reactor power reduction in minimum time including restriction of xenon poisoning, 20: 3372 (EUR-2506.e)
Self-radiolysis and methods for storage of tritiated organic compounds, 20: 1938 (EUR-2452.e)
TESI—advanced power excursion reactor for research in reactor safety, 20: 3584 (EUR-2433.e)
Thermal and mechanical studies of solid-solid contacts, 20: 1811 (EUR-2486.e)
Thermodynamic study of the uranium–oxygen system by mass spectrometry. Heat of sublimation of uranium, 20: 1810 (EUR-2458.f)
Water solubility in molten alkali nitrates, 20: 1812 (EUR-2495.e)
**EUROPEAN ATOMIC ENERGY COMMUNITY, GEEL (BELGIUM). CENTRAL NUCLEAR MEASUREMENTS BUREAU.**
Precise determination $\alpha$ $P_K\omega_K$ value and fluorescence yield of Cr, 20: 2593 (EUR-2524.e)
**EUROPEAN ATOMIC ENERGY COMMUNITY, ISPRA (ITALY). EUROPEAN SCIENTIFIC DATA PROCESSING CENTER.**
Reactor power reduction in minimum time including restriction of xenon poisoning, 20: 3372 (EUR-2506.e)
**EUROPEAN ATOMIC ENERGY COMMUNITY, ISPRA (ITALY). JOINT NUCLEAR RESEARCH CENTER.**
Environmental radioactivity, Ispra 1964, 20: 2047 (EUR-2509.e)

Feasibility of new procedure for biological dosimetry, 20: 1612 (EUR-2505.e)
Identification chart for γ-emitting radionuclides formed by (n,γ) reactions, 20: 1735 (EUR-2408.e)
Interaction of krypton with uranium oxide surfaces, 20: 1813 (EUR-2515.e)
Kinetic theory and calculations for accelerator booster with periodically varying multiplication factor, 20: 3371 (EUR-2492.e)
Reactor power reduction in minimum time including restriction of xenon poisoning, 20: 3372 (EUR-2506.e)
TESI—advanced power excursion reactor for research in reactor safety, 20: 3584 (EUR-2433.e)
Thermal and mechanical studies of solid-solid contacts, 20: 1811 (EUR-2486.e)
Water solubility in molten alkali nitrates, 20: 1812 (EUR-2495.e)

**EUROPEAN COMPANY FOR THE CHEMICAL PROCESSING OF IRRADIATED FUELS, MOL (BELGIUM).**
Eurochemic sampling system, 20: 1955 (NP-15403)

**EUROPEAN ORGANIZATION FOR NUCLEAR RESEARCH, GENEVA (SWITZERLAND).**
Missing bunch phase-lock system for proton storage rings, 20: 2535 (CERN-65-31)

## F

**FIAT, TURIN (ITALY). SEZIONE ENERGIA NUCLEARE.**
Forced convection burnout and hydrodynamic instability experiments for water at high pressure. I., 20: 2009 (EUR-2490.e)

**FOREST ENTOMOLOGY AND PATHOLOGY LAB., FREDERICTON (NEW BRUNSWICK).**
Biological interactions associated with spruce budworm infestations, 20: 1589 (BNL-917, pp 61-8)

**FOREST SERVICE, BERKELEY, CALIF. PACIFIC SOUTHWEST FOREST AND RANGE EXPERIMENT STATION.**
Effects of fire on major ecosystems, 20: 2079 (BNL-917, pp 11-19)

**FORSVARETS FORSKNINGSINSTITUTT, KJELLER (NORWAY).**
Particulate nuclear bomb debris as a meteorological tracer, 20: 2044 (NDRE-51)

**FRANKFORD ARSENAL, PHILADELPHIA, PA.**
Determination of Zr in Zr metal and Zr powder, 20: 1729 (AD-619244)

## G

**GENERAL ATOMIC, SAN DIEGO, CALIF.**
Measurement of fast neutron spectra in infinite medium of $CH_2$, 20: 2931 (AD-616518)

**GENERAL ATOMIC, SAN DIEGO, CALIF. JOHN JAY HOPKINS LAB. FOR PURE AND APPLIED SCIENCE.**
Combined reactor kinetics-heat transfer code for IBM-7044. Preliminary description, 20: 3323 (GAMD-6644)
Neutron cross section data retrieval program, 20: 3009 (GA-6635)
Prog. rpt. on advanced, graphite-matrix, dispersion-type fuel systems and research on graphite, 8/15-11/14/64, 20: 2318 (GA-5918(Pt.I))
Prog. rpt. on applications of neutron-activation analysis to scientific crime detection, 7/62, 20: 1736 (GA-3491)
Prog. rpt. on applications of neutron-activation analysis to scientific crime detection, 10/62, 20: 1737 (GA-3664)
Prog. rpt. on applications of neutron-activation analysis to scientific crime detection, 11/62–1/63, 20: 1738 (GA-4041)
Prog. rpt. on applications of neutron-activation analysis to scientific crime detection, 2–4/63, 20: 1739 (GA-4297)
Prog. rpt. on application of neutron-activation analysis to scientific crime detection, 5–7/63, 20: 1740 (GA-4576)
Prog. rpt. on experimental beryllium oxide reactor program, 4–6/65, 20: 3470 (GA-5499)
SNAP-15A—radioisotope thermoelectric generator, 20: 2204 (GA-6695)

**GENERAL DYNAMICS/ASTRONAUTICS, SAN DIEGO, CALIF.**
Space electron radiation shielding—bremsstrahlung and electron transmission, 20: 3248 (NASA-SP-71, pp 455-63)

**GENERAL DYNAMICS/FORT WORTH, TEX.**
Prog. rpt. on atmospheric diffusion at NARF site, 10/63–9/64, 20: 2073 (AD-618101)

**GENERAL ELECTRIC CO., CINCINNATI, OHIO. NUCLEAR MATERIALS AND PROPULSION OPERATION.**
Effect of radiation on refractory metals and alloys, 20: 2422 (GEMP-52A, pp 11-21)
Effect of radiation on heat-resistant metals and alloys, 20: 2423 (GEMP-52A, pp 27-35)
Evaluations of plastic fatigue properties of heat-resistant alloys, 20: 2320 (GEMP-52A, pp 23-5)
Fission product transport processes in refractory-metal fuel systems, 20: 2321 (GEMP-52A, pp 43-5)
Mechanism of rhenium-alloying effect in group VI-A metals, 20: 2323 (GEMP-314)
Physico-chemical studies of clad $UO_2$ in potential meltdown environments, 20: 2257 (GEMP-52A, pp 47-52)
Physico-chemical studies of Fe-Cr-Al-clad fuel systems, 20: 2322 (GEMP-52A, pp 53-4)
Prog. rpt. on high-temperature materials, 10/20/65, 20: 2224 (GEMP-52A)
Prog. rpt. on high-temperature materials, 6/15–8/15/65, 20: 2223 (GEMP-51A)
Radiation effects in BeO, 20: 2424 (GEMP-52A, pp 37-42)
Thermodynamic behavior of hypostiochiometric $UO_2$, 20: 2319 (GE-TM-65-6-13)
630A-Mark IV. A nuclear fueled steam generator-superheater for merchant ship propulsion, 20: 3546 (GE-TM-64-12-12)

**GENERAL ELECTRIC CO., PLEASANTON, CALIF. SPECIAL PURPOSE NUCLEAR SYSTEMS OPERATION.**
Prog. rpt. on testing of cylindrical diodes and irradiation of fuel and insulator, 9/18–12/17/64, 20: 3446 (GEST-2045)

**GENERAL ELECTRIC CO., RICHLAND, WASH. HANFORD ATOMIC PRODUCTS OPERATION.**
Fast neutron effects on productivity of young and old flour beetles, 20: 1613 (HW-SA-3537)
Influence of finely dispersed second phase on recrystallization, 20: 2325 (HW-SA-3767)
Operational modes anticipated for converted N-reactor interplant operating restrictions (preliminary), 20: 3541 (RL-NRD-81(Suppl.1))
Remote refabrication of reactor fuels, 20: 2282 (HW-SA-3755)
Structure of deformed internally oxidized alloys, 20: 2324 (HW-SA-3765)

**GENERAL ELECTRIC CO., SAN JOSE, CALIF. ATOMIC POWER EQUIPMENT DEPT.**
Prog. rpt. on EVESR fuel development, 3–5/65, 20: 3472 (GEAP-4891)
Prog. rpt. on nuclear superheat project, 2–4/65, 20: 3471 (GEAP-4861)
Survey for high temperature sensor for SEFOR, 20: 3473 (GEAP-4903)

**GENERAL NUCLEAR ENGINEERING CORP., DUNEDIN, FLA.**
Prog. rpt. on BONUS nuclear power plant, 7/64, 20: 3474 (GNEC-364)

**GEORGIA UNIV., ATHENS.**
Shelter occupancy studies at University of Georgia, 20: 2069 (AD-615003)
Shelter occupancy studies at University of Georgia, 20: 2070 (AD-615004)
Shelter occupancy studies at University of Georgia, 20: 2071 (AD-615005)

**GOSUDARSTVENNYI KOMITET PO ISPOL'ZOVANIYU ATOMNOI ENERGII SSSR, OBNINSK. FIZIKO-ENERGETICHESKII INSTITUT.**
The BN-350 (fast neutron) atomic power station, 20: 3475 (NP-15458)

## H

**HAHN-MEITNER-INSTITUT FUER KERNFORSCHUNG, BERLIN (WEST GERMANY).**
Influence of traps on diffusion (rare gas diffusion in solids), 20: 2360 (ORNL-tr-814)
Prog. rpt. on diffusion of rare gases in solids, 1-3/65, 20: 2317 (EURAEC-1380)

**HARVARD SCHOOL OF PUBLIC HEALTH, BOSTON, MASS.**
Performance of air cleaning system for U. S. Bureau of Mines Bomaec-30 incinerator, 20; 1989 (NYO-841-2)

**HOWARD UNIV., WASHINGTON, D. C. DEPT. OF BIOCHEMISTRY.**
Prog. rpt. on chemical effects of ionizing radiation on individual amino acids, 10/65, 20: 1604 (TID-22291)

**HUGHES AIRCRAFT CO., NEWPORT BEACH, CALIF. RESEARCH, DEVELOPMENT AND ENGINEERING DEPT.**
Prog. rpt. on semiconductor design effects on radiation resistance, 12/15/64–3/15/65, 20: 2411 (AD-618078)

**HUGHES RESEARCH LABS., MALIBU, CALIF.**
Lattice models for cooperative phenomena. I., 20: 1819 (UCRL-14287)

## I

**IIT RESEARCH INST., CHICAGO, ILL.**
Prog. rpt. on reactor containment, 10/64–7/65, 20: 3324 (IITRI-578P21-13)
Trajectory analysis for structural fragments, 20: 3610 (AD-622333)

**ILLINOIS UNIV., URBANA.**
Influence of dislocation dipoles on physical properties, 20: 3278 (COO-1198-222)

**ILLINOIS UNIV., URBANA. DEPT. OF PHYSICS.**
Lectures on spin temperature, 20: 2864 (COO-1198-300)

**ILLINOIS UNIV., URBANA. MATERIALS RESEARCH LAB.**
Lectures on spin temperature, 20: 2864 (COO-1198-300)
Semiconductivity in glass systems $V_2O_3$–$P_2O_5$ and $V_2O_5$–$P_2O_5$, 20: 2316 (COO-1198-220)

**INNSBRUCK UNIV. (AUSTRIA).**
MHD of quasineutral plasma with vanishing internal friction and heat conductivity and finite electrical conductivity, 20: 3159 (AD-618138)

**INSTITUT FUER KERNPHYSIK, UNIVERSITAET FRANKFURT (WEST GERMANY).**
Optical properties of $TiO_2$ as reflector for plastic sciatillators, 20: 2327 (IKF-12)
Reactions $^{58}Ni(n,p)^{58}Co$ and $^{27}Al(n,p)^{27}Mg$ at different neutron energies, 20: 3012 (IKF-11)
**INSTITUT FUER PLASMAPHYSIK, G.M.B.H. GARCHING (WEST GERMANY).**
Estimation of heating of plasma by lasers, 20: 3185 (TT-1193)
**INSTITUTE OF NUCLEAR RESEARCH, WARSAW (POLAND).**
Interdiffusion in nickel-uranium system, 20: 2328 (INR-625/XIV/R)
Possible occurrence of very high Lorentz factor calculated using Castagnoli's formula in secondary jets of ultra high energy, 20: 2651 (INR-608/VI/PH)
Removal of radioisotopes from the water solutions by use of silica gel, 20: 1742 (INR-636/XIII/J)
**INSTITUTE OF PLASMA PHYSICS, UNIV. OF NAGOYA (JAPAN).**
Experimental division I (QP project), 20: 3172 (NP-15562, pp 4-19)
Experimental division II., 20: 3173 (NP-15562, pp 20-9)
Experimental division III (Heliotron Project), 20: 3174 (NP-15562, pp 30-7)
Experimental division IV (fundamental experiments), 20: 3175 (NP-15562, pp 38-79)
Kinetic structure of plasma, 20: 3164 (IPPJ-39)
Prog. rpt. on plasma physics, annual, 4/64–3/65, 20: 3171 (NP-15562)
Theoretical division, 20: 3176 (NP-15562, pp 80-4)
**INSTITUTUL DE FIZICA ATOMICA, ACADEMIA R. P. R., BUCHAREST (ROMANIA).**
Gamma rays from $^{75}As(n,\gamma)^{76}As$ reaction, 20: 3011 (IFA-NR-22)
Study of liquidus diagrams and thermodynamic properties of $SiO_2$–$ThO_2$ and $SiO_2$–$ThO_2$ –$UO_2$ systems, 20: 2326 (IFA-FR-39)
Transverse momentum distribution in high-energy meson production, 20: 2681 (IFA-CR-55)
**INTERNATIONAL CENTRE FOR THEORETICAL PHYSICS, TRIESTE (ITALY).**
Mass formulae in U(6) ⊗ U(6) theory, 20: 2752 (IC/65/77)
Remark on crossing symmetry and parastatistics, 20: 2751 (IC/65/51)
**INTERNATIONAL RESEARCH AND DEVELOPMENT CO. LTD., NEWCASTLE-UPON-TYNE (ENGLAND).**
Feasibility study on use of powders as heat transfer media in irradiation capsules, 20: 2018 (TRG-Report-920)
**IOWA STATE UNIV. OF SCIENCE AND TECH., AMES.**
Recoil chemistry of $^{11}C$ in liquid hydrocarbons, 20: 1896 (IS-T-23)
Thermal diffusivity of platinum, 20: 3621 (IS-1261)
**IOWA STATE UNIV. OF SCIENCE AND TECH., AMES. COLL. OF VETERINARY MEDICINE.**
Inhalation study of pathogenesis of neodymium oxide in mice and guinea pigs, 20: 1593 (COO-1170-4)
**IOWA STATE UNIV. OF SCIENCE AND TECH., AMES. INST. FOR ATOMIC RESEARCH.**
Inhalation study of pathogenesis of neodymium oxide in mice and guinea pigs, 20: 1593 (COO-1170-4)
**ISRAEL ATOMIC ENERGY COMMISSION, YAVNE. SOREQ RESEARCH ESTABLISHMENT.**
Prog. rpt., semiannual, 7–12/63, 20: 2520 (IA-020)
**ISRAEL ATOMIC ENERGY COMMISSION, YAVNE. SOREQ NUCLEAR RESEARCH CENTER.**
Solvent extraction, 20: 1741 (IA-1031)
Two fast reactor studies, 20: 3374 (IA-1053)
**ISTITUTO SUPERIORE DI SANITA', ROME (ITALY). LABORATORI DI FISICA.**
Criteria for choice of best working conditions in measurements of radioactive sources, 20: 2127 (ISS-64/15)

## J

**JAPAN ATOMIC ENERGY RESEARCH INST., TOKYO.**
Japan fast critical experiment program, 20: 3376 (NP-15573)
Preliminary design work of 2 MW Na loop, 20: 3479 (NP-15556)
**JOHNS HOPKINS UNIV., BALTIMORE, MD.**
Precision x-ray spectroscopy, 20: 2126 (CONF-650657-1)
**JOINT INST. FOR NUCLEAR RESEARCH, DUBNA (USSR).**
Weakening of high energy $\mu$ beams in shielding, 20: 3238 (JINR-P-2354)
**JOINT INST. FOR NUCLEAR RESEARCH, DUBNA (USSR). LAB OF HIGH ENERGY.**
An experimental determination of $K_2^0 \to 2\pi$ decay probability in sloped $K_2^0$ beam, 20: 2865 (JINR-P-2325)
Elastic $\pi^+$-p scattering at 180° and high energies, 20: 2683 (JINR-P-2327)
Radiative kaon decays, 20: 2684 (JINR-P-2374)
Semi-automatic device for scanning and measuring spark chamber photographs, 20: 2130 (JINR-P-2340)
Surface wave in plasma with current of limited radius, 20: 3165 (JINR-P-2352)
Symmetric system of wire electrodes for an isotropic spark chamber, 20: 2129 (JINR-P-2312)
Wire spark chamber with external acoustic transducers, 20: 2132 (JINR-P-2368)
**JOINT INST. FOR NUCLEAR RESEARCH, DUBNA (USSR). LAB. OF NEUTRON PHYSICS.**
Account of the pulsed mode in intermediate memories, 20: 2101 (JINR-P-2319)
**JOINT INST. FOR NUCLEAR RESEARCH, DUBNA (USSR). LAB OF NUCLEAR PROBLEMS.**
An experimental determination of $K_2^0 \to 2\pi$ decay probability in sloped $K_2^0$ beam, 20: 2865 (JINR-P-2325)
Analyses of $\pi^- + p \to \pi^- + \pi^+ + n$ and $\pi^- + p \to \pi^- + \pi^0 + p$ at 338 Mev, 20: 2682 (JINR-P-2320)
Displacement of spark chamber discharges in a magnetic field, 20: 2131 (JINR-P-2344)
Ionization measurement in a streamer chamber, 20: 2128 (JINR-E-2324)
Possibility of stabilization of synchrocyclotron intensity, 20: 2536 (JINR-P-2341)
Semi-automatic device for scanning and measuring spark chamber photographs, 20: 2130 (JINR-P-2340)
**JOINT INST. FOR NUCLEAR RESEARCH, DUBNA (USSR). LAB OF THEORETICAL PHYSICS.**
Algebra of the currents and dispersion relations, 20: 2755 (JINR-E-2329)
Angular distribution of inelastically scattered complex particles, 20: 3013 (JINR-P-2331)
Investigation of infrared singularities in cross sections by functional integration method, 20: 2754 (JINR-P-2309)
Mass formula in SU(12) contains $Sp(6) \times SU(2)$ symmetry, 20: 2756 (JINR-P-2342)
Meson current in broken symmetry U(12) and experiments with colliding beams, 20: 2753 (JINR-P-2300)

## K

**KERNENERGIEANLAGEN, ALLGEMEINE ELEKTRICITAETS-GESELLSCHAFT, FRANKFURT AM MAIN (WEST GERMANY).**
Prog. rpt. on stability investigations for BWR, 1–3/65, 20: 3373 (EURAEC-1353)
**KERNFORSCHUNGSANLAGE, JUELICH (WEST GERMANY).**
Behavior of FRJ-1(MERLIN) as result of forced cooling, 20: 3585 (JUL-259-RE)
**KERNFORSCHUNGSANLAGE, JUELICH (WEST GERMANY). INSTITUT FUER PLASMAPHYSIK.**
Crowbar and power crowbar circuits and their calculation, 20: 2102 (JUL-273-PP)
**KERNFORSCHUNGSANLAGE, JUELICH (WEST GERMANY). INSTITUT FUER REAKTORWERKSTOFFE.**
Physico-chemical analysis methods for study of reactor materials and nuclear fuels, 20: 1743 (JUL-216-RW)
**KNOLLS ATOMIC POWER LAB., SCHENECTADY, N. Y.**
CURFIT. Curve fitting program, 20: 2214 (KAPL-M-6483)
Electron-beam tube-to-tubesheet welding, 20: 2283 (KAPL-3110)
Primary and secondary recrystallization of alpha Zircaloy-4, 20: 2330 (KAPL-3091)
Primary and secondary recrystallization of beta-quenched Zircalloy-4, 20: 2331 (KAPL-3103)
**KUNGLIGA TEKNISKA HOGSKOLAN, STOCKHOLM (SWEDEN).**
Interaction between microwaves and plasmas in gas discharges and semiconductors, 20: 3157 (AD-614654)

## L

**LABORATORI NAZIONALI DI FRASCATI, COMITATO NAZIONALE PER L'ENERGIA NUCLEARE (ITALY).**
Activity at the national laboratories of Frascati, July 1, 1964–June 30, 1965, 20: 2521 (LNF-65/28)
Possible experiment with a proton polarized target, 20: 2686 (LNF-65/22)
Theoretical aspects of colliding-beam experiments, 20: 2687 (LNF-65/25)
**LAWRENCE RADIATION LAB., UNIV. OF CALIFORNIA, BERKELEY.**
Analysis of nuclear magnetic resonance spectroscopic data: four-membered ring compounds, 20: 3645 (UCRL-16344)
Aspects of alloy thermochemistry: A and B, 20: 2349 (UCRL-16320)
Cost estimating magnet systems with the aid of a computer, 20: 2545 (UCRL-16386)
Current magnet design practice in the U.S.A., 20: 2533 (BNL-9536)
Design of experimental facilities at proposed 200-Bev accelerator, 20: 2540 (UCRL-16223)
Design problems associated with high-current-density water-cooled septum magnets, 20: 2544 (UCRL-16309)

Design study for a 200-Bev accelerator facility, 20: 2543 (UCRL-16238)
Effect of high energy protons and $\alpha$ particles on small mammals, 20: 1614 (NASA-SP-71, pp 97-103)
Effect of temperature strain rate and structure on flow stress of an iron-2 percent manganese alloy, 20: 3641 (UCRL-11512(Rev.))
Electrical resistance of bismuth from 25 to 80 kilobars, 20: 3642 (UCRL-11639)
Extraction of $HClO_4$ by trilauryl amine. I., 20: 1747 (UCRL-11616(Rev.))
Grain boundary energy, 20: 2348 (UCRL-16051)
Improved Bevatron and its performance at high intensity, 20: 2541 (UCRL-16228)
Magnet design applications of magnetostatic computer program called SIBYL, 20: 2546 (UCRL-16389)
Mechanical behavior of internally oxidized single crystals of silver and silver base alloys, 20: 3639 (UCRL-11194)
Nuclear spectroscopic studies of $^{204}$Po, 20: 3024 (UCRL-16324)
Optical pumping transients in $^{87}$Rb and application to disorientation cross sections, 20: 2596 (UCRL-16241)
Paramagnetic resonance of $Fe^{3+}$ in polycrystalline ferrichrome A, 20: 3643 (UCRL-11685)
Polarization in p-$^4$He scattering between 27 and 63 Mev, 20: 3022 (UCRL-16216)
Resistance measurements at high pressures, 20: 2345 (UCRL-11030)
Results of computations of depth dose in tissue irradiated by protons, 20: 1620 (UCRL-16154)
Spectroscopic investigation of high-temperature species isolated in inert gas matrices, 20: 1818 (UCRL-11976)
Structure of socalled "ethylmetaphosphate" (Langheld ester), 20: 3640 (UCRL-11488)
Studies of vicia faba root meristems irradiated with a $\pi^-$ beam, 20: 1621 (UCRL-16387)
Study of $^4$He(p,d)$^3$He reaction with polarized protons at 55 and 63 Mev, 20: 3023 (UCRL-16218)
Superconductivity of the cubic modification of MoC, 20: 2346 (UCRL-11471)
Techniques of magnetic-field measurement, 20: 2105 (UCRL-16357(Rev.))
Total and differential cross sections for reaction $\pi^- p \to \eta n$, 20: 2689 (UCRL-16149)
TRIST—tri-level multiprogramming executive involving real-time calculations and asynchronous on-line data source, 20: 3644 (UCRL-16199)
200-Bev accelerator handling systems in regions of high residual radioactivity, 20: 2542 (UCRL-16236)

**LAWRENCE RADIATION LAB., UNIV. OF CALIFORNIA, LIVERMORE.**
Cryogenic air sampler for high altitude application, 20: 2045 (UCRL-13162)
Crystal structure of tetramethyl ammonium hexahydrohexaborate, 20: 2347 (UCRL-12146)
Diffusion and losses of electrons in astron E-layer, 20: 3183 (UCRL-14275)
Electrostatic instabilities of plasma with magnetically supported velocity-space anisotropy at high density, 20: 3182 (UCRL-12447)
Hot electron plasma stability in mirror and minimum B containment systems, 20: 3184 (UCRL-14310)
Inelastic proton-proton scattering at 5.10 Bev, 20: 2688 (UCRL-14335)
Interaction in arrays of fissionable materials, 20: 2938 (UCRL-14245)
Isthmian canal studies, 1964. Annex III. Appendix 1. Nuclear excavation plan, 20: 1983 (PNE-2000)
Isthmian canal studies, 1964. Annex III. Appendix 1. Inclosure C. Safety evaluation for air blast, ground shock, throwout, and dust, 20: 1985 (PNE-2003)
Lattice models for cooperative phenomena. I., 20: 1819 (UCRL-14287)
Some analytical methods for explosives and explosive simulants, 20: 3638 (UCRL-7873)
Weapons effects display system study, 20: 1987 (UCRL-13189)

**LINCOLN LAB., MASSACHUSETTS INST. OF TECH., LEXINGTON.**
AC breakdown in gases, 20: 3160 (AD-618503)

**LINDE DIV., UNION CARBIDE CORP., INDIANAPOLIS, IND.**
Prog. rpt. on fabrication and properties of W single crystals, final, 3/64–2/65, 20: 2284 (NP-15093)

**LING-TEMCO-VOUGHT, INC., DALLAS, TEX.**
Bremsstrahlung production in thick aluminum and iron targets by 0.5- to 3.0-Mev electrons, 20: 3247 (NASA-SP-71, pp 449-53)

**LOCKHEED MISSILES AND SPACE CO., PALO ALTO, CALIF.**
Nuclear environmental effects on spacecraft thermal control coatings, 20: 2428 (NASA-SP-55, pp 365-79)

**LOCKHEED MISSILES AND SPACE CO., SUNNYVALE, CALIF.**
Environmental effects on space structures, 20: 2036 (AD-618030)
Tables of capacitor discharge in transient $\gamma$ radiation environments, 20: 2410 (AD-617918)

**LONG ISLAND JEWISH HOSPITAL, NEW HYDE PARK, N. Y.**
Prog. rpt. on bioelectric effects in calcified tissues, 9/64–6/65, 20: 3625 (NYO-3282-1)

**LOS ALAMOS SCIENTIFIC LAB., UNIV. OF CALIFORNIA, N. MEX.**
Analytical model for study of thermocouple error attributed to electrical conduction in insulation, 20: 2103 (LA-DC-7055)
Compatibility of refractory metals with solid solution (UC)(ZrC) at elevated temperatures, 20: 2332 (LA-3307)
Design of source of negative polarized hydrogen ions using charge exchange in cesium and argon, 20: 2537 (LA-DC-7268)
Elastic scattering of polarized nucleons, 20: 3014 (LA-DC-7386)
High-energy proton linear accelerators, 20: 2538 (LA-DC-7281)
Los Alamos flux compression program from its origin, 20: 3166 (LA-DC-7252)
Measurement of $C_{NN}$ in neutron-proton scattering at 23 Mev, 20: 2685 (LA-DC-7250)
Moving picture computer output, 20: 2011 (LA-DC-7189)
Operational practices in treatment of low and intermediate level radioactive wastes—Argonne and Los Alamos laboratories, U.S.A., 20: 3603 (LA-DC-7249)
Prospects for reactor-MHD commercial power production, 20: 2670 (LA-DC-7330)
Quantitative reduction of data from high-speed stereoscopic photographs, 20: 3624 (LA-DC-7088)
Radiation damage to alkali halides and other simple ionic crystals, 20: 2426 (LA-3387)
Synchronized mammalian cells. II., 20: 1594 (LA-DC-6507)

**LOVELACE FOUNDATION FOR MEDICAL EDUCATION AND RESEARCH, ALBUQUERQUE, N. MEX.**
Biological tolerance to air blast and related biomedical criteria, 20: 2083 (CEX-65.4)
Radiobiological consequences of dose distributions produced by solar-flare-type spectra, 20: 2655 (NASA-SP-71, pp 85-96)

## M

**MALAKER LABS., INC., HIGH BRIDGE, N. J.**
Kinetic study of rocket exhaust gases, 20: 2668 (AD-615124)

**MARBURG UNIV. (WEST GERMANY). INSTITUT FUER THEORETISCHE PHYSIK.**
Approach to electron-pion scattering, 20: 2678 (AD-614843)

**MARTIN CO., BALTIMORE, MD. NUCLEAR DIV.**
SNAP-19 support structure design development and qualification tests, 20: 2205 (MND-3169-52)

**MASSACHUSETTS INST. OF TECH., CAMBRIDGE. DEPT. OF CIVIL ENGINEERING.**
Non-linear response of reinforced concrete spherical domes to air blast loading, 20: 2035 (AD-615017)

**MASSACHUSETTS INST. OF TECH., CAMBRIDGE. DEPT. OF MECHANICAL ENGINEERING.**
Prog. rpt. on effect of surface conditions on pool boiling heat transfer of Na, 3–10/65, 20: 2017 (TID-22312)

**MASSACHUSETTS UNIV., AMHERST. DEPT. OF FOOD AND NUTRITION.**
Bibliography on wholesomeness of irradiated food, 20: 2196 (AD-614910)

**MASSACHUSETTS UNIV., AMHERST. POLYMER RESEARCH INST.**
Scattering of light by anisotropic discs with their principal polarizability direction at an angle to the radius, 20: 1817 (TID-22323)
Transmission of light by crystal aggregates between polarizers. II., 20: 3636 (TID-22319)

**MATERIALS RESEARCH LAB., INC., RICHTON PARK, ILL.**
Use of strain softening to improve properties of refractory metals, 20: 2311 (AD-618925)

**MAX-PLANCK-INSTITUT FUER BIOPHYSIK, FRANKFURT AM MAIN (WEST GERMANY).**
Bibliography on radiation effects on living tissues and organisms, 20: 1607 (AED-C-04-18)
Bibliography on radiation effects on living tissues and organisms, 20: 1608 (AED-C-04-19)

**METALLGESELLSCHAFT A. G., FRANKFURT AM MAIN (WEST GERMANY).**
Prog. rpt. on development of $ZrNb_2Sn_1$ for use as cladding material, 20: 2255 (EURAEC-1323)

**MICHIGAN STATE UNIV., EAST LANSING. DEPT. OF CHEMISTRY.**
Correlated EPR-optical spectra of potassium in ethylamine–ammonia mixtures, 20: 1808 (COO-958-5)

**MICHIGAN UNIV., ANN ARBOR.**
Heat capacities and thermodynamic properties of globular molecules. XIV., 20: 3617 (COO-1149–23)
2-Methylfuran: heat capacity and thermodynamic properties from 5 to 350°K, 20: 3615 (COO-1149-17)
2,5-dimethylthiophene. Heat capacities and thermodynamic properties from 5 to 300°K and fusion of stable and metastable phases, 20: 3614 (COO-1149–16)

**MICHIGAN UNIV., ANN ARBOR. DEPT. OF CHEMISTRY.**
Heat capacities and thermodynamic properties of globular molecules. XV., 20: 3620 (COO-1149-27)
Heat capacities and thermodynamic properties of globular molecules. XIII.,

20: 3616 (COO-1149-22)
Heat capacities and thermodynamic properties of globular molecules. XV., 20: 3619 (COO-1149-26)
Heat capacity and thermodynamic properties of $ZrF_4$ from 5 to 307°K, 20: 1809 (COO-1149-30)
System tetramethyl-methane-tetrachloromethane. Thermodynamics of mixing in plastically crystalline region, 20: 3618 (COO-1149-25)

**MICHIGAN UNIV., ANN ARBOR. LIQUID METALS LAB.**
Prog. rpt. on liquid metal boiling heat transfer, 5–8/65, 20: 2008 (AD-622825)

**MINNESOTA UNIV., MINNEAPOLIS. PLASMA PHYSICS LAB.**
Prog. rpt. on collision processes in gaseous plasmas, semiannual, 7/64–1/65, 20: 3158 (AD-614923)

**MSA RESEARCH CORP., CALLERY, PA.**
Prog. rpt. on effect of high-temperature Na on steels, 7–9/65, 20: 2258 (MSAR-65-149)

# N

**NATIONAL ACADEMY OF SCIENCES–NATIONAL RESEARCH COUNCIL, WASHINGTON, D. C. COMMITTEE ON NUCLEAR SCIENCE.**
Radiochemistry of selenium, 20: 1744 (NAS-NS-3030(Rev.))

**NATIONAL AERONAUTICS AND SPACE ADMINISTRATION, CLEVELAND, OHIO. LEWIS RESEARCH CENTER.**
Elastic and inelastic scattering of 40-Mev alpha particles from even tin isotopes, 20: 3017 (NASA-TN-D-3067)

**NATIONAL AERONAUTICS AND SPACE ADMINISTRATION, GREENBELT, MD. GODDARD SPACE FLIGHT CENTER.**
Equation of state of matter at supernuclear density, 20: 3016 (NASA-TN-D-3020)
Partial wave calculation of diatomic molecule $(HeH)^{++}$, 20: 2595 (NASA-TN-D-3050)
Review of galactic and solar cosmic rays, 20: 2653 (NASA-SP-71, pp 19-29)
Two-stream instability in gravitating plasmas with magnetic field and rotation, 20: 3170 (NASA-TN-D-3052)

**NATIONAL AERONAUTICS AND SPACE ADMINISTRATION, HUNTSVILLE, ALA. GEORGE C. MARSHALL SPACE FLIGHT CENTER.**
Calculation of proton penetration and dose rates, 20: 3250 (NASA-SP-71, pp 493-505)
Man-made radiations in space, 20: 2652 (NASA-SP-71, pp 1-4)

**NATIONAL AERONAUTICS AND SPACE ADMINISTRATION, LANGLEY STATION, VA. LANGLEY RESEARCH CENTER.**
Ionizing radiations in supersonic transport flights, 20: 2657 (NASA-SP-71, pp 287-99)
Transient effects in dielectric materials caused by electron irradiation, 20: 1897 (NASA-TN-D-3032)

**NATIONAL AERONAUTICS AND SPACE ADMINISTRATION, WASHINGTON, D. C.**
Conference on thermal radiation of solids, San Francisco, Calif., 3/64, 20: 2427 (NASA-SP-55)
Nuclear environmental effects on spacecraft thermal control coatings, 20: 2428 (NASA-SP-55, pp 365-79)

**NATIONAL AERONAUTICS AND SPACE ADMINISTRATION, WASHINGTON, D. C. SCIENTIFIC AND TECHNICAL INFORMATION DIV.**
Apollo spacecraft nuclear radiation protection status report, 20: 3244 (NASA-SP-71, pp 365-75)
Application of the generalized concept of dosimetry to space radiations, 20: 2133 (NASA-SP-71, pp 245-50)
Biological effects of heavy ions, 20: 1615 (NASA-SP-71, pp 105-14)
Bremsstrahlung production in thick aluminum and iron targets by 0.5- to 3.0-Mev electrons, 20: 3247 (NASA-SP-71, pp 449-53)
Calculation of proton penetration and dose rates, 20: 3250 (NASA-SP-71, pp 493-505)
Conference on protection against radiations in space, Gatlinburg, 10/64, 20: 3239 (NASA-SP-71)
Cosmic-ray shower production in manned space vehicles—copper, 20: 3240 (NASA-SP-71, pp 183-8)
Effect of high-energy protons and $\alpha$ particles on small mammals, 20: 1614 (NASA-SP-71, pp 97-103)
Evaluation of radiation shielding by vehicle orientation, 20: 3249 (NASA-SP-71, pp 473-6)
Examination of relative merits of stochastic and nonstatistical methods of computing primary ionization doses, 20: 2658 (NASA-SP-71, pp 527-33)
Fractional cell lethality approach to space radiation hazards, 20: 1616 (NASA-SP-71, pp 219-23)
Importance of space radiation shielding weight, 20: 3245 (NASA-SP-71, pp 407-14)
Ionizing radiations in supersonic transport flights, 20: 2657 (NASA-SP-71, pp 287-99)
Local dose from proton and alpha particle enders behind complex shield systems, 20: 3251 (NASA-SP-71, pp 507-12)
Magnetic radiation shielding using superconducting coils, 20: 3241 (NASA-SP-71, pp 199-209)
Man-made radiations in space, 20: 2652 (NASA-SP-71, pp 1-4)
Quality factors for degraded proton spectra, 20: 3243 (NASA-SP-71, pp 229-34)
Radiobiological consequences of dose distributions produced by solar-flare-type spectra, 20: 2655 (NASA-SP-71, pp 85-96)
Results of recent transport calculations for electrons and bremsstrahlung, 20: 3246 (NASA-SP-71, pp 437-48)
Review of galactic and solar cosmic rays, 20: 2653 (NASA-SP-71, pp 19-29)
Some experimental data on nuclear cascade in thick absorbers, 20: 3015 (NASA-SP-71, pp 357-62)
Space electron radiation shielding—bremsstrahlung and electron transmission, 20: 3248 (NASA-SP-71, pp 455-63)
Synthesis of spherical minimum-weight proton shields, 20: 3242 (NASA-SP-71, pp 225-8)
The effect of charged-particle environments on manned military space systems, 20: 2656 (NASA-SP-71, pp 265-86)
Updating and dissemination of knowledge of trapped radiation—model environments, 20: 2654 (NASA-SP-71, pp 47-55)

**NATIONAL BUREAU OF STANDARDS, WASHINGTON, D. C.**
Results of recent transport calculations for electrons and bremsstrahlung, 20: 3246 (NASA-SP-71, pp 437-48)

**NATIONAL ENGINEERING SCIENCE CO., PASADENA, CALIF.**
Cryogenic air sampler for high altitude application, 20: 2045 (UCRL-13162)

**NATIONAL MAGNET LAB., MASSACHUSETTS INST. OF TECH., CAMBRIDGE.**
Electronic band structure and optical properties of rare-earth metals, 20: 2592 (BNL-9556)
Prog. rpt. on solid state research using high magnetic fields, 7/60–10/64, 20: 2519 (AD-615152)

**NATIONAL MARINE CONSULTANTS, ANAHEIM, CALIF.**
Prog. rpt. on absolute pressure sensors, 20: 2059 (NVO-98-11)
Prog. rpt. on Hawaiian Run-Up Program, 10/15/65, 20: 2058 (NVO-98-10)

**NAVAL ORDNANCE LAB., WHITE OAK, MD.**
Application of anticoincidence-shielded scintillation spectrometer to study of $^{14}N(p,\gamma)^{15}O$ reaction, 20: 3006 (AD-618676)
Effects of alloying upon certain properties of 55.1 Nitinol, 20: 2310 (AD-618681)
Micrometeorological phenomena of underwater nuclear explosions, 20: 1979 (AD-614814)

**NAVAL RADIOLOGICAL DEFENSE LAB., SAN FRANCISCO, CALIF.**
Compendium of radiochemical procedures for determination of selected fission products in sea water, 20: 1749 (USNRDL-TR-912)
Gamma-emission data for calculation of exposure rates from nuclear debris. II., 20: 2048 (USNRDL-TR-888)
Low-dose measurements with modified silver-phosphate glass dosimeter reader, 20: 2122 (AD-622626)
Radiation-induced decomposition of millimolar concentrations of hydrogen peroxide in aerated pure water, 20: 1894 (AD-623095)
Urethan-induced lung tumors in mice: X-radiation dose dependent inhibition, 20: 1606 (AD-623079)

**NAVAL RESEARCH LAB., WASHINGTON, D. C.**
High-temperature properties of sodium, 20: 1815 (NRL-6241)
Prog. rpt. on irradiation effects on reactor structural materials, 11/64–1/65, 20: 2408 (AD-614899)
Prog. rpt. on irradiation effects on reactor structural materials, 2–4/65, 20: 2409 (AD-617319)

**NAVAL SCHOOL OF AVIATION MEDICINE, PENSACOLA, FLA.**
Local dose from proton and alpha particle enders behind complex shield systems, 20: 3251 (NASA-SP-71, pp 507-12)

**NEVADA OPERATIONS OFFICE (AEC), LAS VEGAS.**
Isthmian canal studies, 1964. Annex III. Appendix 1. Inclosure D. Nuclear operations, 20: 1986 (PNE-2004)

**NEW MEXICO UNIV., ALBUQUERQUE.**
Analog model of wave propagation in open-end cylinder. Phase I of investigation in analog study of impact fracture of closed-end cylinders, 20: 3630 (SC-DC-65-1697)

**NEW MEXICO UNIV., ALBUQUERQUE. BUREAU OF ENGINEERING RESEARCH.**
Heat transfer and temperature distribution in finned radiators, 20: 2016 (SC-DC-65-1765)

**NEW YORK UNIV., N. Y.**
Some experimental data on nuclear cascade in thick absorbers, 20: 3015 (NASA-SP-71, pp 357-62)

**NORTH AMERICAN AVIATION, INC., DOWNEY, CALIF.**
Apollo spacecraft nuclear radiation protection status report, 20: 3244 (NASA-SP-71, pp 365-75)
Examination of relative merits of stochastic and nonstatistical methods of computing primary ionization doses, 20: 2658 (NASA-SP-71, pp 527-33)

Importance of space radiation shielding weight, 20: 3245 (NASA-SP-71, pp 407-14)

**NORTHERN ILLINOIS UNIV., DEKALB. DEPT. OF BIOLOGICAL SCIENCES.**
Prog. rpt. on chemical protection against radiation-induced chromosome aberrations, final, 9/61–8/65, 20: 1619 (TID-22293)

**NORTHROP CORP., VAN NUYS, CALIF.**
Prog. rpt. on semiconductor radiation response prediction, 12/15/64–3/15/65, 20: 2412 (AD-618079)

## O

**OAK RIDGE NATIONAL LAB., TENN.**
Acoustic instrument for measuring subcooling in boiling systems, 20: 2014 (ORNL-P-1678)
Analysis of elastic and inelastic scattering of neutrons from $^{206}Pb$, $^{208}Pb$, and $^{209}Bi$ below 4.5 Mev, 20: 3021 (ORNL-TM-1238)
Application of the generalized concept of dosimetry to space radiations, 20: 2133 (NASA-SP-71, pp 245-50)
Comparative creep-rupture properties of D-43 and B-66 alloys, 20: 2336 (ORNL-P-1634)
Control system for gas-cooled nuclear power plant, 20: 3480 (ORNL-P-1679)
Conversion coefficient measurements employing magnetic and solid-state spectrometers, 20: 3019 (ORNL-P-1657)
Critical experiments with SPERT-D fuel elements, 20: 3379 (ORNL-TM-1207)
DCX-2 scanning energy spectrometer, 20: 3178 (ORNL-P-1613)
Deformation, creep, and fracture in alpha-zirconium alloys, 20: 2339 (ORNL-P-1753)
Development of the Excer Process. I., 20: 1956 (ORNL-1696)
Differential fast-neutron albedos for concrete. I., 20: 2932 (ORNL-3822(Vol.1))
Differential fast-neutron albedos for concrete. II., 20: 2933 (ORNL-3822(Vol.2))
Differential fast-neutron albedos for concrete. III., 20: 2934 (ORNL-3822(Vol.3))
Differential fast-neutron albedos for concrete. IV., 20: 2935 (ORNL-3822(Vol.4))
Differential fast-neutron albedos for concrete. V., 20: 2936 (ORNL-3822(Vol.5))
Differential fast-neutron albedos for concrete. VI., 20: 2937 (ORNL-3822(Vol.6))
Equilibrium solid solutions of nitrogen in Cb-1% Zr between 1200-1800°C, 20: 2337 (ORNL-P-1677)
Evaluation of niobium-vanadium alloys for application in high-temperature reactor systems, 20: 2340 (ORNL-TM-1131)
Experiences and developments in instrumentation for liquid metal experiments, 20: 2013 (ORNL-P-1661)
Experimental and calculated system criticality, 20: 3378 (ORNL-P-1680)
Flexibility study of back-pressure turbines for dual-purpose plants, 20: 3540 (ACNP-65573)
Frequency response sensitivities in reactor dynamics studies, 20: 3377 (ORNL-P-1482)
Frequency response sensitivities in reactor dynamics studies, 20: 3380 (ORNL-TM-1305)
Grain boundary migration, 20: 3626 (ORNL-P-1722)
Heating in infinite cylinders by uniform gamma sources, 20: 3325 (ORNL-P-1480)
Irradiation behavior of high-burnup $ThO_2$-4.45% $UO_2$ fuel rods, 20: 2429 (ORNL-3837)
Irradiation effects in stainless steels at high temperatures, 20: 2430 (ORNL-P-1713)
Irradiation experiment to study compatibility of BeO with graphite at 1500°C, 20: 2431 (ORNL-TM-1255)
Magnetic form factor of chromium, 20: 3280 (ORNL-P-1737)
Magnetic structure properties of Tb-Sc alloys, 20: 2338 (ORNL-P-1735)
Pressure drop with forced-convection boiling of potassium, 20: 2015 (ORNL-P-1681)
Problems in design of an 8th order power optimized coil, 20: 2522 (ORNL-P-1516)
Reaction of $U_3O_8$ with $CCl_4$ and mixtures of $CCl_4$ and $Cl_2$, 20: 1816 (ORNL-TM-1258)
Reactor neutron cross sections for production of $^{33}P$ from $^{36}Cl$ and enriched $^{33}S$ in Oak Ridge research reactor, 20: 3020 (ORNL-TM-1065)
Release and adsorption of methyl iodide in HFIR maximum credible accident, 20: 3586 (ORNL-TM-1291)
Simple momentum probe for plasma studies, 20: 3179 (ORNL-P-1575)
Survey of high-temperature demineralization for dual-purpose BWR plants, 20: 3539 (ACNP-65558(Rev.1))
X-ray topograph examination of vacancy clusters in nearly perfect copper crystals, 20: 3279 (ORNL-P-1704)

**OAK RIDGE OPERATIONS OFFICE (AEC), TENN. RESEARCH AND DEVELOPMENT DIV.**
Nuclear safety coordination within Oak Ridge operations facilities, 20: 3370 (CONF-651103-2)

**OESTERREICHISCHE STUDIENGESELLSCHAFT FUER ATOMENERGIE G.M.B.H., SEIBERSDORF. PHYSIK-INSTITUT.**
Numerical method for calculation of image aberrations of inhomogeneous magnetic sector fields between conical pole faces, 20: 2209 (SGAE-PH-26/1965)

**OHIO STATE UNIV., COLUMBUS.**
Enrichment and determination of tritium in water, 20: 1728 (AD-618552)

**OHIO STATE UNIV. RESEARCH FOUNDATION, COLUMBUS.**
Properties of superconducting Mo–Re alloys, 20: 2890 (AFML-TR-65-154)

**OSLO UNIV. (NORWAY). DEPT. OF ASTROPHYSICS.**
Sensitivity to irradiation damage—pressure vessel steels. III., 20: 2437 (WERL-3844-6)

**OWENS-ILLINOIS TECHNICAL CENTER, TOLEDO, OHIO.**
Studies on monoclinic zirconium dioxide from room temperature to 1095°C, 20: 2314 (ARL-65-140)

## P

**PADUA UNIV. (ITALY). ISTITUTO DI ZOOLOGIA E ANATOMIA COMPARATA.**
Prog. rpt. on cell survival as function of radiation dose, final 1959–62, 20: 1617 (NP-15149)

**PADUCAH GASEOUS DIFFUSION PLANT, KY.**
Electrolytic generation of fluorine from uranium hexafluoride, 20: 1954 (KY-287)

**PARIS UNIV. (FRANCE).**
Low-temperature oxidation of uranium powders and application to sintering of uranium oxide powders, 20: 2279 (CEA-R-2828)

**PENNSYLVANIA UNIV., PHILADELPHIA.**
Anisotropy of exchange in ytterbium iron garnet, 20: 1802 (AD-618038)

**PERKIN-ELMER CORP., NORWALK, CONN.**
Prog. rpt. on $CeO_2$ as laser host, 1965, 20: 2312 (AD-619197)

**PHILLIPS PETROLEUM CO. IDAHO FALLS, IDAHO., ATOMIC ENERGY DIV.**
Measurement of heat generation rate of highly radioactive calcined alumina, 20: 2425 (IDO-14665)
Prog. rpt. on burnup determination of nuclear fuels, 4–6/65, 20: 3010 (IDO-14663)
Topics in nuclear reactor theory, 20: 3375 (IDO-17120)

**PICATINNY ARSENAL, DOVER, N. J. NUCLEAR ENGINEERING DIRECTORATE.**
Laboratory experimental analysis of $\gamma$ radiation effects on silicon alloy junction semiconductor diodes, 20: 2413 (AD-618688)

**PRATT AND WHITNEY AIRCRAFT, MIDDLETOWN, CONN. CONNECTICUT ADVANCED NUCLEAR ENGINEERING LAB.**
SNAP-50/SPUR nuclear test facility initial design requirements, Canel Site, Middletown, Connecticut, 20: 3545 (CNLM-5729)

**PRINCETON UNIV., N. J. PLASMA PHYSICS LAB.**
A ferromagnetic resonance magnetometer, 20: 2104 (MATT-362)
Stability of negative V'' systems, 20: 3167 (MATT-374)

**PUERTO RICO WATER RESOURCES AUTHORITY, SAN JUAN.**
Prog. rpt. on BONUS nuclear power plant, 7/64, 20: 3474 (GNEC-364)

**PURDUE UNIV., LAFAYETTE, IND. DEPT. OF PHYSICS.**
Large-spin rotational states of deformed nuclei, 20: 3008 (COO-1420-104)

**PURDUE UNIV., LAFAYETTE, IND. SCHOOL OF AERONAUTICAL AND ENGINEERING SCIENCES.**
Quantum theory of vibrational energy exchange and effect of an attractive potential, 20: 2594 (N64-23208)

## Q

**QUARTERMASTER RESEARCH AND ENGINEERING COMMAND, NATICK, MASS.**
Feasibility study of filtration unit for removal by the individual of CBR agents from water, 20: 2072 (AD-618006)

## R

**RADIATION EFFECTS INFORMATION CENTER, BATTELLE MEMORIAL INST., COLUMBUS, OHIO.**
Bibliography on radiation effects on glass, 20: 2432 (REIC-Memo-26)
Compilation of nuclear, pulsed, and space radiation effects projects, 20: 2433 (REIC-Memo-27)

**RADIATION RESEARCH LABS., MELLON INST., PITTSBURGH, PA.**
Prog. rpt. on radiation research, 7–8/65, 20: 1898 (RRL-2310-164)

**RAND CORP., SANTA MONICA, CALIF.**
Chinese nuclear explosion, N-nation nuclear development and civil defense, 20: 2068 (AD-614895)
Estimation of fire damage to non-urban areas from nuclear attack,

20: 1590 (RM-3902-TAB)
Numerical results for auxiliary equation of radiative transfer, 20: 2930 (AD-614636)
**REACTOR GROUP, UNITED KINGDOM ATOMIC ENERGY AUTHORITY, RISLEY (ENGLAND).**
Comparison of procedures for dissolving ignited plutonium oxides for analysis, 20: 2344 (TRG-Report-1072)
**RENSSELAER POLYTECHNIC INST., TROY, N. Y.**
Microwave lens system for plasma diagnostics, 20: 3169 (NASA-CR-319)
**RENSSELAER POLYTECHNIC INST., TROY, N. Y. DEPT. OF PHYSICS.**
Thermal diffusion of platinum in temperature gradient, 20: 3628 (RPI-1044-1)
**REPUBLIC AVIATION CORP., FARMINGDALE, N. Y.**
Quality factors for degraded proton spectra, 20: 3243 (NASA-SP-71, pp 229-34)
**ROCHESTER UNIV., N. Y. DEPT. OF PHYSICS AND ASTRONOMY.**
Field-theoretic models of elementary particles, 20: 2758 (UR-875-100)
Muon and antiproton trap at SLAC, 20: 2547 (UR-375-98)
Present status of weak interactions, 20: 2759 (UR-875-102)
**ROCKETDYNE, CANOGA PARK, CALIF.**
Radiative properties of gases. I., 20: 1803 (AD-619266)
**ROCKY FLATS DIV., DOW CHEMICAL CO., GOLDEN, COLO.**
Aqueous radioactive waste treatment plant at rocky flats, 20: 1940 (RFP-638)
Machine gaging philosophy on instrumentation, 20: 3627 (RFP-670)
**ROME UNIV. (ITALY). ISTITUTO DI CHIMICA FARMACEUTICA.**
Self-radiolysis and methods for storage of tritiated organic compounds, 20: 1938 (EUR-2452.e)

## S

**SANDIA CORP., ALBUQUERQUE, N. MEX.**
"Accel" automated circuit card etching layout, 20: 3635 (SC-TM-65-544)
Aerospace nuclear safety, 20: 3548 (SC-DC-65-1752)
Aerospace nuclear safety: probability analysis of reactor power level and dose rate, 20: 3549 (SC-RR-65-417)
Analog model of wave propagation in open-end cylinder. Phase I of investigation in analog study of impact fracture of closed-end cylinders, 20: 3630 (SC-DC-65-1697)
Behavior of beryllium metal in simulated launch pad abort environments, 20: 2341 (SC-DC-65-1637)
Dendritic erosion in dielectrics, 20: 2259 (SC-DC-65-1789)
Freshwater propagation tests, 20: 3632 (SC-DR-65-459)
Heat transfer and temperature distribution in finned radiators, 20: 2016 (SC-DC-65-1765)
Ion-plated coatings for corrosion protection of uranium, 20: 2260 (SC-DR-65-519)
Isthmian canal studies, 1964. Annex III. Appendix 1. Inclosure C. Safety evaluation for air blast, ground shock, throwout, and dust, 20: 1985 (PNE-2003)
Mathematical models of magnetic flux compression, 20: 2523 (SC-RR-65-449)
Mechanical properties of wrought depleted uranium and of welds joining this material, 20: 2342 (SC-DR-58-61)
Molding precision microballoon-filled epoxy parts in plastisol molds, 20: 3634 (SC-TM-65-462)
Nuclear electrical power for sea-level canal construction, 20: 3481 (SC-RR-65-121A)
Safety as a design feature in systems, 20: 2085 (SC-R-65-991)
Symmetry in summability theory, 20: 3629 (SC-DC-64-288)
Thermal properties of selected metals at ambient temperature, 20: 2343 (SC-TM-65-242)
Use of shock spectrum technique for non-linear systems, 20: 3631 (SC-DC-65-1723)
Weight, center of gravity, and moment of inertia of geometric solids, 20: 3633 (SC-TM-64-1686)
**SCHWEISSTECHNISCHE LEHR- UND VERSUCHSANSTALT, DUISBURG (WEST GERMANY).**
Prog. rpt. on electro-slag welding of reactor steels, final, 2/65, 20: 2281 (EURAEC-1408)
**SOCIETA RICERCHE IMPIANTI NUCLEARI, SLUGGIA (ITALY). CENTRO RICERCHE NUCLEARI.**
Electrochemical labeling of proteins, 20: 1939 (EUR-2476.i)
**SOCIETE ALSTHOM, PARIS (FRANCE).**
Prog. rpt. on nuclear vapotron, 1–3/64, 20: 3443 (EURAEC-1356)
Prog. rpt. on nuclear vapotron, 4–6/64, 20: 3444 (EURAEC-1357)
Prog rpt. on nuclear vapotron, 7–9/64, 20: 3445 (EURAEC-1358)
**SOCIETE BELGE POUR L'INDUSTRIE NUCLEAIRE, BRUSSELS.**
Preparation of Zr and U–Mo alloys, 20: 2222 (EURAEC-1390)
**SOCIETE D'ENERGIE NUCLEAIRE FRANCO-BELGE DES ARDENNES, CHOOZ-LEZ-GIVET (FRANCE).**
Prog. rpt. on Ardennes nuclear power plant, 4–6/65, 20: 3484 (TID-22329)
**SOUTHERN RESEARCH INST., BIRMINGHAM, ALA.**
Lateral strain behavior of graphite—an anisotropic material, 20: 2315 (CONF-650632-3)
**SOUTHWEST RESEARCH INST., SAN ANTONIO, TEX.**
Prog. rpt. on evaluation of serviceability of Elk River reactor pressure vessel, 5–7/65, 20: 3482 (SWRI-1228-75)
**STANFORD LINEAR ACCELERATOR CENTER, STANFORD UNIV., CALIF.**
Current magnet design practice in the U.S.A., 20: 2533 (BNL-9536)
Properties of symmetric quadrupole magnet triplets, 20: 2539 (SLAC-47)
**STANFORD RESEARCH INST., MENLO PARK, CALIF.**
Physical damage from nuclear explosions, 20: 2078 (BNL-917, pp 1-10)
**STANFORD UNIV., CALIF. DEPT. OF AERONAUTICS AND ASTRONAUTICS.**
Hydromagnetic stability of a liquid layer under the action of a magnetic field and a gravitational force, 20: 2820 (AD-614645)
**STANFORD UNIV., CALIF. DEPT. OF MATERIALS SCIENCE.**
Influence of finely dispersed second phase on recrystallization, 20: 2325 (HW-SA-3767)
Structure of deformed internally oxidized alloys, 20: 2324 (HW-SA-3765)
**STANFORD UNIV., CALIF. HIGH-ENERGY PHYSICS LAB.**
Empirical mass formula involving the electron mass, 20: 2750 (AD-618659)
Polarization measurements on recoil proton from $\pi^0$ photoproduction, 20: 2679 (AD-618664)
**STANFORD UNIV., CALIF. INST. FOR PLASMA RESEARCH.**
Absolute instabilities of obliquely-propagating cyclotron harmonic plasma waves, 20: 3181 (SU-IPR-20)
**STANFORD UNIV., CALIF. MICROWAVE LAB.**
Numerical solution of collisionless plasma-sheath equation in cylindrical geometry, 20: 3168 (ML-1185)
**STANFORD UNIV., CALIF. STANFORD ELECTRONICS LABS.**
Reflex ionization in toma, 20: 3180 (SEL-63-116)
**STANRAY CORP., CHICAGO, ILL.**
Design and economic study of spent fuel shipping, 20: 2084 (EURAEC-374(Vol.2))
**STATE UNIV. OF IOWA, IOWA CITY.**
Method of determining $\alpha = n(H+)/n_e$ ion temperature from measurement of proton-whistlers, 20: 2847 (AD-614716)
**STATE UNIV. OF NEW YORK, BUFFALO. DEPT. OF BIOLOGY.**
Radiation sensitization of bacteria by p-hydroxymercuribenzoate, 20: 1618 (NYO-3319-6)
**STRATHCLYDE UNIV., GLASGOW (SCOTLAND). DEPT. OF MATHEMATICS.**
Research on magnetogasdynamics, 20: 2821 (AD-618296)
**SYDNEY UNIV. (AUSTRALIA). SCHOOL OF PHYSICS.**
Experimental studies of J × B ionizing fronts propagation over pressure range 10 to 800 millitorr, 20: 3177 (NP-15570)
**SYLVANIA ELECTRONIC SYSTEMS, WALTHAM, MASS. APPLIED RESEARCH LAB.**
Propagation constant along a cylindrical antenna immersed in a warm plasma. I and II., 20: 2097 (AD-618396)
Radiation from electric dipole in column of warm plasma, 20: 3161 (AD-618520)
Waveguide admittance for radiation into plasma layers—theory and experiment, 20: 2098 (AD-618398)
**SYRACUSE UNIV., N. Y. DEPT. OF BACTERIOLOGY AND BOTANY.**
Prog. rpt. on production and study of asporogenic mutants, annual, 1965, 20: 1582 (NYO-2038-2)
**SYSTEM DEVELOPMENT CORP., SANTA MONICA, CALIF.**
Weapons effects display system study, 20: 1987 (UCRL-13189)

## T

**TEMPLE UNIV., PHILADELPHIA, PA. RESEARCH INST.**
Handling hazardous materials, 20: 1727 (NASA-SP-5032)
**TRW EQUIPMENT LABS., THOMPSON RAMO WOOLDRIDGE INC., CLEVELAND, OHIO.**
Prog. rpt. on creep of refractory alloys at elevated temperatures, 3/26-6/26/65, 20: 2333 (NASA-CR-54457)
**TRW SYSTEMS, REDONDO BEACH, CALIF.**
Behavior of beryllium metal in simulated launch pad abort environments, 20: 2341 (SC-DC-65-1637)

## U

**UNION CARBIDE CORP., TUXEDO, N. Y. MINING AND METALS DIV.**
Radiochemistry of selenium, 20: 1744 (NAS-NS-3030(Rev.))
**UNION CARBIDE RESEARCH INST., TARRYTOWN, N. Y.**
Prog. rpt. on behavior of solid materials in high-temperature environments, 7–9/65, 20: 2261 (UCRI-326)
**UNITED AIRCRAFT CORP., EAST HARTFORD, CONN. RESEARCH LABS.**

Phase-reinforced high-temperature alloys produced directly from the melt, 20: 2219 (AMRA-CR-64-05/4)

**UNITED KINGDOM ATOMIC ENERGY AUTHORITY, RISLEY (ENGLAND). ENGINEERING GROUP.**

On-line gas analysis, 20: 1734 (EG-Report-36)

**UNITED NUCLEAR CORP., WHITE PLAINS, N. Y. DEVELOPMENT DIV.**

Synthesis of spherical minimum-weight proton shields, 20: 3242 (NASA-SP-71, pp 225-8)

**UNITED STATES–EURATOM JOINT RESEARCH AND DEVELOPMENT PROGRAM.**

Design and economic study of spent fuel shipping, 20: 2084 (EURAEC-374(Vol.2))

Preparation of Zr and U–Mo alloys, 20: 2222 (EURAEC-1390)

Prog. rpt. on development of $ZrNb_3Sn_1$ for use as cladding material, 20: 2255 (EURAEC-1323)

Prog. rpt. on diffusion of rare gases in solids, 1–3/65, 20: 2317 (EURAEC-1380)

Prog. rpt. on electro-slag welding of reactor steels, final, 2/65, 20: 2281 (EURAEC-1408)

Prog. rpt. on failure of stainless steel cladding fuel rods, 4–6/65, 20: 2256 (EURAEC-1449)

Prog. rpt. on nuclear vapotron, 1–3/64, 20: 3443 (EURAEC-1356)

Prog. rpt. on nuclear vapotron, 4–6/64, 20: 3444 (EURAEC-1357)

Prog. rpt. on nuclear vapotron, 7–9/64, 20: 3445 (EURAEC-1358)

Prog. rpt. on stability investigations for BWR, 1–3/65, 20: 3373 (EURAEC-1353)

**USTAV JADERNEHO VYZKUMU, CESKOSLOVENSKA AKADEMIE VED, REZ.**

Discovery of damage in uranium fuel elements in nonactive test in $CO_2$, 20: 1748 (UJV-1369/65)

Electronic devices for microwave spectrometers, 20: 2106 (UJV-1346/65)

PARAMETRY II for calculation of physical parameters of gas cooled heavy-water reactor, 20: 3381 (UJV-1309b/65)

## V

**VIENNA UNIV. (AUSTRIA). INSTITUT FUER PHYSIKALISCHE CHEMIE.**

Numerical method for calculation of image abberrations of inhomogeneous magnetic sector fields between conical pole faces, 20: 2209 (SGAE-PH-26/1965)

## W

**WEATHER BUREAU RESEARCH STATION, LAS VEGAS, NEV.**

Project Handcar, radiological surveillance, 20: 1982 (PNE-807F)

**WESTINGHOUSE ELECTRIC CORP., BLOOMFIELD, N. J.**

Recrystallization variables of flat-rolled molybdenum-cobalt alloys, 20: 2313 (AD-619208)

**WESTINGHOUSE ELECTRIC CORP., PITTSBURGH, PA. ATOMIC POWER DIV.**

High-temperature supercritical pressure water loop—corrosion tests, 20: 2262 (WCAP-2056(Pt.6))

Prog. rpt. on CVTR, 1–2/65, 20: 3469 (CVNA-242)

Prog. rpt. on supercritical reactor, 7/9/62, 20: 3485 (WCAP-2120)

Xenon induced core instabilities, 20: 3383 (WCAP-3269-48)

**WESTINGHOUSE RESEARCH LABS., PITTSBURGH, PA.**

Embrittlement of irradiated pressure vessel steels. I., 20: 2436 (WERL-8844-4)

**WILLIAMS (CLYDE) AND CO., COLUMBUS, OHIO.**

Handling hazardous materials, 20: 1727 (NASA-SP-5032)

**WRIGHT AERONAUTICAL DIV., CURTISS-WRIGHT CORP., WOOD-RIDGE, N. J.**

Prog. rpt. on slender-channel electrogasdynamics, 2/63–8/64, 20: 2667 (AD-614907)

# PERSONAL AUTHOR INDEX

Each entry after an author's name is a shortened version of the title of the report or article, followed by the *NSA* volume and abstract number. Report numbers are given in parentheses.

The phrase "Progress report" is abbreviated as "Prog. rpt.," permitting a more rapid and complete alphabetical arrangement of the titles without changing the location of the progress report titles in relation to the other titles.

Because of problems involving the mechanical preparation of this index, all accent marks are omitted. The following changes in spelling have been introduced to reduce some of the confusion which might result from omitting the accents:

| | | |
|---|---|---|
| ä | becomes | ae |
| ö | | oe |
| ø | | oe |
| ü | | ue (except in transliterated Chinese names) |

## A


**AALTONEN, J.**, Half-life of $^{147}Sm$; comparison of ionization chamber and liquid scintillation results, 20: 3028

**ABARENKOV, I. V.**, Model potential for positive ions, 20: 2611

**ABBATIELLO, A. A.**, Dimensional location of reactor components by optical tooling, 20: 3341

**ABDEL-WAHAB, M. F.**, Preparation of $^{131}I$-labeled insulin and isolation by gel filtration, 20: 1890

**ABE, Shiro**, Design and construction of $\alpha$ emitter laboratory, 20: 2089

**ABUL-MAGD, A. Y.**, Semiclassical theory of polarization in direct nuclear reactions. II., 20: 3049

**ACCARY, Andre**, Improvements in refractory uranium compounds, 20: 2250

**ADAMOVICH, M. I.**, Determination of isotopical components of the $\gamma + N \rightarrow N + \pi$ amplitude at $\gamma$ threshold, 20: 2737

**ADAMS, Duane E.**, Radiobiological consequences of dose distributions produced by solar-flare-type spectra, 20: 2655 (NASA-SP-71, pp 85-96)

**ADAMS, G. E.**, Rate constant for reaction of $O^-$ with oxygen, 20: 1917

**ADAMS, R. E.**, Release and adsorption of methyl iodide in HFIR maximum credible accident, 20: 3586 (ORNL-TM-1291)

**ADLER, F. T.**, Approximate transfer functions for coupled-core reactor dynamics, 20: 3422

**AFRIKANTOV, I. I.**, The BN-350 (Fast Neutron) Atomic Power Station, 20: 3475 (NP-15458)

**AGABEKYAN, A. S.**, Spontaneous particle radiation in resonator with several coupled modes, 20: 2527

**AGDUR, B.**, Interaction between microwaves and plasmas in gas discharges and semiconductors, 20: 3157 (AD-614654)

**AHLERS, Edward B.**, Trajectory analysis for structural fragments, 20: 3610 (AD-622333)

**AHRENS, F. W.**, Loft semi-scale blowdown tests, 20: 3336

**AIGAES, N. S.**, Mutants induced by ionizing radiations and ethyleneimine in winter wheat, 20: 1655

**AINBINDER, N. E.**, Energy levels and relative intensities of NQR lines for some integral spins, 20: 3284

**AIRAPETYANTS, M. G.**, Changes in higher nervous activity of dogs after irradiation, 20: 1627

**AITKEN, E. A.**, High-temperature studies of urania in a thermal gradient, 20: 2233

**AITKEN, E. A.**, Thermodynamic behavior of hypostoichiometric $UO_2$, 20: 2319 (GE-TM-65-6-13)

**AITZETMUELLER, K.**, Electrophoresis of $^{227}Ac$, 20: 1756

**AITZETMUELLER, K.**, Electrophoresis of radioactive rare earths, 20: 1961

**AKASOFU, S.-I.**, Auroral morphology as shown by all-sky photographs, 20: 2852

**AKCASU, A. Ziya**, Autonomous power oscillations in reactors, 20: 3408

**AKCASU, A. Ziya**, Two criteria for Lagrange stability, 20: 3405

**AKIN, Erol**, Determination of interplanar spacings in polymers using single-neutron diffraction, 20: 3308

**ALBANY, H. J.**, Effects of fast neutrons on the thermal conductivity of silicon, 20: 2487

**ALBERG, M.**, Stray neutron spectra at large pulsed-particle accelerator sites, 20: 2553

**ALBERT, Richard D.**, High-energy (0.1-2 Mev) fission cross-section structure measured using nuclear explosion in space, 20: 3089

**ALBERTSON, D. G.**, Analysis and measurement of PuAl–polyethylene systems in PCTR, 20: 3398

**ALEKSANDROV, S. N.**, Pathogenesis of late consequences of radiation therapy, 20: 1716

**ALEXEFF, Igor**, Simple momentum probe for plasma studies, 20: 3179 (ORNL-P-1575)

**ALFREDSON, P. G.**, Fluorination of $UO_2$–$PuO_2$ fission-product oxide pellets in a fluidized-bed reactor, 20: 1970

**ALI, A. W.**, Theory of resonance broadening of spectral lines by atom-atom impacts, 20: 2620

**ALIKHANOV, A. I.**, Elastic backward scattering of $\pi^-$ by neutrons, 20: 2700

**ALIKHANOV, A. I.**, $\pi^-$ meson-neutron elastic backward scattering at 1.4 to 4.0 Bev, 20: 2713

**ALLABY, J. V.**, Polarization measurements on recoil proton from $\pi^0$ photoproduction, 20: 2679 (AD-618664)

**ALLAIN, Y.**, Space explorations and the radiation belts, 20: 2663

**ALLARD, E. C.**, Xenon induced core instabilities, 20: 3383 (WCAP-3269-48)

**ALLEN, C. M.**, Materials development for sliding-contact applications in 1000°F potassium space power systems, 20: 2242

**ALLEN, R. T.**, Quantum theory of vibrational energy exchange and effect of an attractive potential, 20: 2594 (N64-23208)

**ALLIO, R. J.**, Fuel-element performance in pressurized water reactors, 20: 2231

**AL'PERT, Ya. L.**, Space physics with artificial satellites, 20: 2863

**ALSMILLER, R. G. Jr.**, Calculation of nucleon-meson cascade in iron initiated by 1- and 3-Bev protons and comparison with experiment, 20: 3258

**ALSMILLER, R. G. Jr.**, Electron-photon cascade calculations and neutron yields from electrons in thick targets, 20: 3261

**ALTAMARI, L. A.**, Modification of KAPL remote annealing facility, 20: 2299

**ALVAREZ, M. R.**, Reproductive integrity in the stamen hair and root meristem of Tradescantia paludosa following acute $\gamma$ irradiation, 20: 1668

**AMANO, E.**, Mutations induced by ethyl methane-sulfonate in maize, 20: 1656

**AMBRO, P.**, Wire spark chamber with external acoustic transducers, 20: 2132 (JINR-P-2368)

**AMBROSIANI, Vincent F.**, Decomposition of water vapor induced by $\alpha$ radiation, 20: 1936

**AMBROSINO, C.**, Electrochemical labeling of proteins, 20: 1939 (EUR-2476.i)

**AMENU-KPODO, Kwasi**, Color centers in sodium fluoride, 20: 1908

**AMIEL, J. L.**, Adoptive immunotherapy of acute leukemia: experimental and clinical results, 20: 1701

**AMMERLAAN, C. A. J.**, Gamma irradiation of lithium-drifted p-i-n junctions in silicon, 20: 2510

**AMMON, R. L.**, Tantalum-base alloys for alkali metal containment, 20: 2241
**AMMON, Robert L.**, Niobium alloys, 20: 2407
**AMORETTY, Stephen**, Global fallout of nuclear explosion products, 20: 2086 (BNL-tr-42)
**AMORETTY, Stephen**, Radiochemical processes taking place during radiolysis of carbon tetrafluorides, 20: 1899 (BNL-tr-23)
**AMPELOGOVA, N. I.**, Behavior of polonium in ketones and mixed aqueous-acetone solutions, 20: 1946
**AMPELOGOVA, N. I.**, Effects of ketones on polonium behavior in hydrochloric solutions, 20: 1777
**AMYOT, L.**, New lattice calculation method for ORGEL-type reactors, 20: 3424
**AN, Jiann-min**, Nuclear spectroscopic studies of $^{204}$Po, 20: 3024 (UCRL-16324)
**ANASTASIA, L. J.**, Fluorination of $UO_2$–$PuO_2$ fission-product oxide pellets in a fluidized-bed reactor, 20: 1970
**ANDELIN, R. L.**, High-temperature compatibility testing of molten plutonium fuel-container systems, 20: 2228
**ANDERSON, D. E.**, Superconducting $H_c$-$J_c$ characteristics of nitrided Nb–Zr wire to 130 kOe, 20: 2891
**ANDERSON, Douglas Edward**, Improvements in or relating to refuelling machines for nuclear reactors, 20: 3355
**ANDERSON, E. C.**, Synchronized mammalian cells. II., 20: 1594 (LA-DC-6507)
**ANDERSON, William E.**, Effects of high-radiation fields on electrical conductivity of metal oxides, 20: 2460
**ANDERSSON, Bo**, Boundaries of the singularity manifold associated with an arbitrary Feynman graph, 20: 2780
**ANDERSSON, Lars-Erik**, Kohn anomaly and coherent scattering of slow neutrons in liquid metals, 20: 2948
**ANDO, K. J.**, Moessbauer effect data index, 20: 3146
**ANDREEN, C. J.**, Channeling of 13-kev $D^+$ ions in gold crystals, 20: 2616
**ANDREEV, A. F.**, Electron spectrum of intermediate state of superconductors, 20: 2923
**ANDREWS, D. G.**, Experimental differential number, energy and dose albedos for semi-infinite media, for normally-incident gamma radiation, 20: 3273
**ANDREWS, Howard L.**, An organic plastic localizing whole-body counter, 20: 1710
**ANDREWS, P. A.**, Radiation-induced fluctuations in base resistance and emitter efficiency of Si transistors, 20: 2188
**ANDRIOT, J.**, Economy and perspectives of atomic energy, 20: 3648
**ANGERMAN, C. L.**, Irradiation behavior of zirconium–uranium alloy fuel tubes, 20: 2466
**ANGHILERI, L. J.**, In vivo distribution of radioactive chromic phosphate, 20: 1598
**ANISOVICH, V. V.**, Certain mass formulas in Quark model, 20: 2807
**ANISOVICH, V. V.**, Mass spectra of system $\pi + \Delta_{1238}$, $\pi + \Sigma_{1385}$, and $\pi + \phi$, 20: 2741
**ANSEL'M, A. A.**, Certain mass formulas in Quark model, 20: 2807
**ANSELM, A. A.**, Three-particle partial amplitudes and unitarity conditions for complex values of angular momenta, 20: 2811
**ANTILL, J. E.**, Oxidation of irradiated beryllium in carbon dioxide, 20: 2442
**APOSTOL, A.**, Preparation and characteristics of the IFA $EN_2$ nuclear emulsion, 20: 2158
**APTE, B. G.**, Ion exchange behaviour of U(VI) in aqueous sodium triphosphate and its separation from rare earths, 20: 1762
**ARAGONES, M.**, Melting of $UO_2$ during irradiations of short duration, 20: 2416 (AECL-2289)
**ARASIM, Kenneth W.**, Thermo-mechanical inertia forces and their control in Sandia pulsed reactor, 20: 3592
**ARCHAMBEAU, J. O.**, Response of skin of swine to increasing exposures of 250 kvp x rays, 20: 1609 (BNL-9477)
**ARCHER, Jacques**, Device for the leak-tight transmission of movement through a wall, 20: 2005
**ARDRAN, G. M.**, Measurement of patient dose, 20: 1697
**ARKHANGEL'SKII, A. A.**, Sensitivity of scintillation method in $\gamma$ defectoscopy, 20: 2027
**ARLASHCHENKO, N. I.**, Destruction of the otolith apparatus by ionizing radiation, 20: 1628
**ARLT, W. H.**, Development fuel assembly irradiation testing in Big Rock Point Reactor, 20: 3452
**ARLT, W. H.**, Performance of defected low-density powder $UO_2$ fuels in reactor service, 20: 2232
**ARMENTEROS, R.**, Spin, parity and isospin of Y*(1760), 20: 2711
**ARMSTRONG, F. S.**, Abstracts of Canadian patents on production of heavy water, 20: 1951 (AECL-2279)
**ARMSTRONG, R. W.**, Sensitivity to irradiation damage—pressure vessel steels. III., 20: 2437 (WERL-8844-6)
**ARNETT, Edward M.**, Analyzing water samples for deuterium content, 20: 1801
**ARNETT, L. M.**, Leak testing of HWCTR containment building, 20: 2037 (DP-968)
**ARSENIN, V. V.**, Flute instability of dilute inhomogeneous plasma in inhomogeneous electric field, 20: 3210
**ASAMOTO, R. R.**, Effective axial and radial thermal expansion of $UO_2$ with a radial thermal gradient, 20: 2234
**ASAMOTO, R. R.**, Evaluation of thermocouples for use to 2600°C in mixed-oxide fuel, 20: 2114
**ASAMOTO, R. R.**, Survey for high temperature sensor for SEFOR, 20: 3473 (GEAP-4903)
**ASATIANI, T. L.**, Ionization measurement in a streamer chamber, 20: 2128 (JINR-E-2324)
**ASH, M.**, Two fast reactor studies, 20: 3374 (IA-1053)
**ASHTON, Thomas**, Dependence of build-up ratio on field size and source-surface distance, 20: 1721
**ASPINALL, K. J.**, Review of UKAEA criticality detection and alarm systems 1963/64. I., 20: 2075 (AHSB(S)R-92)
**ASSIMAKOPOULOS, P. A.**, First excited state of $^5$He, 20: 3078
**ASTLEY, E. R.**, Fast-flux test facility design concept, 20: 3596
**ASTLEY, E. R.**, Safety and nuclear considerations in design of FTR, 20: 3581 (BNWL-SA-340)
**ASWAD, Adnan Ahmed**, Solution to neutron one-velocity time-independent Boltzmann equation, 20: 3004
**ATKINSON, J. S.**, Remotely operable fuel-rod profilometer, 20: 1993
**ATTRILL, J. E.**, Gas chromatographic determination of permanent gases in helium at reduced sample pressures, 20: 1751
**AUDAS, J. H.**, Fast-neutron spectra in liquid hydrogen, 20: 2967
**AULD, Harry E.**, Simulation of air-blast-induced ground motion, phase I, 20: 1980 (AD-614990)
**AUMAN, J. R.**, Structure and evolution of medium-mass stars. IV., 20: 2567
**AURAND, K.**, Evaporator collector, a simple apparatus for continuous sampling with simultaneous concentration of the sample, 20: 1757
**AUSLAENDER, J. S.**, Radioisotope viscometer, 20: 2200
**AUTHIER, A.**, Effects of proton irradiation on silicon, 20: 2489
**AUTLER, S. H.**, Superconducting technetium–tungsten alloys, 20: 2907
**AVDONINA, E. N.**, Reactions of tritium recoil atoms and $^{14}$C with heterocyclic amines, 20: 1921
**AVEN, M.**, Some electrical transport studies on n-type II-VI semiconductors, 20: 2499
**AVOGADRO, A.**, Purification of uranium from fission products by means of fractional precipitation of $UO_2$ by reduction of $UO_2Cl_2$ from alkali chloride melt, 20: 1962
**AVOTINA, M. P.**, Decay of $^{146}$Eu, 20: 3075
**AVRETT, E. H.**, Temperature structure of early-type model stellar atmospheres. II., 20: 2564
**AXE, J. D.**, Strain effects in rare earth transitions, 20: 3291
**AYER, J. E.**, Cost of remote fabrication of metal-clad metal-fuel fast-reactor fuel elements, 20: 3510
**AYVAZIAN, Arthur M.**, Formability characteristics of polyphase titanium alloy Ti–6Al–6V–2Sn–4Zr, 20: 2308 (AD-614637)
**AZHAZHA, V. M.**, Change of beryllium properties after aging treatment, 20: 2363
**AZIMOV, Ya. I.**, Certain mass formulas in Quark model, 20: 2807
**AZIMOV, Ya. I.**, Three-particle partial amplitudes and unitarity conditions for complex values of angular momenta, 20: 2811

## B

**BABIKOV, Yu. M.**, Effects of reactor radiation on thermophysical properties of monoisopropyldiphenyl, 20: 1923
**BABUSHKIN, F. A.**, Electric multipole relativistic radiative transitions, 20: 3027
**BABYAK, W. J.**, Hydride habit in Zr in unstressed and stressed Zircaloy-4, 20: 2355 (WAPD-T-1757(Rev.))
**BACCA, J. P.**, Startup experience with the EBR-II fuel cycle facility. III., 20: 2297
**BAGDASAROV, Yu. E.**, The BN-350 (Fast Neutron) Atomic Power Station, 20: 3475 (NP-15458)
**BAGGERLY, L. L.**, Bremsstrahlung production in thick aluminum and iron targets by 0.5- to 3.0-Mev electrons, 20: 3247 (NASA-SP-71, pp 449-53)
**BAIER, V. N.**, Two-photon emission in electron collisions, 20: 2743
**BAILEY, B. M.**, 150-kOe liquid nitrogen cooled pulsed flux-concentrator magnet, 20: 1991
**BAILEY, W. J.**, FFTF driver fuel—$PuO_2$ stainless-steel cermet, 20: 3588
**BAILEY, W. J.**, Irradiation of impacted $UO_2$–$PuO_2$, 20: 2461
**BAILY, W. E.**, High-power operation of $PuO_2$–$UO_2$ fast reactor fuel, 20: 2448
**BAILY, W. E.**, Melting point of plutonia–urania mixed-oxide fuels, 20: 2391
**BAILY, W. E.**, Observations on microstructural changes with burnup in mixed-oxide fuels, 20: 2451
**BAILY, W. E.**, Relative in-pile thermal conductivity of stoichiometric and hypostoichiometric mixed oxides of plutonia and urania, 20: 2453
**BAIN, A. S.**, Highly rated hollow $UO_2$ pellets irradiated in collapsible

sheathing—dimensional stability, metallography and autoradiography, 20: 2415 (AECL-2276)
JAIN, A. S., Highly rated hollow $UO_2$ pellets irradiated in collapsible sheathing, 20: 2463
BAIN, A. S., Melting of $UO_2$ during irradiations of short duration, 20: 2416 (AECL-2289)
BAIRD, R. C., Direct-interaction inelastic scattering of energetic neutrons, 20: 3256
BAIRD, R. C., Interactions of 14.6-Mev neutrons in iron, $^{7}Li$, and carbon, 20: 2962
BAJAJ, N. K., Hydromagnetic stability of two superposed plasma columns with anisotropic pressure, 20: 3224
BAKER, M. B., Geomagnetically trapped radiation, 20: 2849
BAKUMENKO, V. L., Stepwise excitation of fluorescence of $CaWO_4$ activated with $Er^{3+}$, 20: 1842
BALANDIN, A. A., Isotopic exchange of cyclohexane with deuterium over evaporated films of germanium and silicon, 20: 1838
BALCIUS, Joseph F., The determination of iodinated compounds by neutron activation of $^{129}I$-description of the technique, 20: 1790
BALDWIN, T. O., X-ray topograph examination of vacancy clusters in nearly perfect copper crystals, 20: 3279 (ORNL-P-1704)
BALKWELL, W. R., Radiation-induced decomposition of millimolar concentrations of hydrogen peroxide in aerated pure water, 20: 1894 (AD-623095)
BALL, R. M., Experimental evaluation of self-powered neutron-flux monitors for PWR in-core use, 20: 2174
BALL, R. M., Measurement and analysis of SM-1A core-3, 20: 3503
BALLANTINE, D. S., Effect of pressure on solid-state polymerization of trioxane, 20: 1926
BALZHISER, R. E., Critical heat flux for boiling liquid metal systems, 20: 2023
BALZHISER, Richard E., Prog. rpt. on liquid metal boiling heat transfer, 5–8/65, 20: 2008 (AD-622825)
BAMBYNEK, W., Precise redetermination of $P_K\omega_K$ value and fluorescence yield of Cr, 20: 2593 (EUR-2524.e)
BAMFORD, C. H., Electron spin resonance of irradiated methacrylic acid, 20: 1916
BANNYKH, O. A., Effect of electron irradiation on mechanical properties of steel subjected to thermal mechanical treatment, 20: 2438
BANSLABEN, A. J., Alpha-gamma facility for fuel studies, 20: 2001
BARANETSKAIA, N. K., Isotopic exchange of hydrogen atoms in cyclopentadienyl rings of cobalticinium compounds, 20: 1828
BARANOVSKII, I. B., Reactions of tritium recoil atoms and $^{14}C$ with heterocyclic amines, 20: 1921
BARBASHOV, B. M., Investigation of infrared singularities in cross sections by functional integration method, 20: 2754 (JINR-P-2309)
BARBIER, M., Induced radioactivity data computed for various materials and comparison with irradiated samples, 20: 3263
BARCHUK, V. T., Behavior of $ZrCl_2$ in molten mixtures of alkali and alkali earth metals, 20: 1822 (ANL-Trans-233)
BARDEEN, John, Theory of motion of vortices in superconductors, 20: 2908
BARDEN, J. L., Remotely operable fuel-rod profilometer, 20: 1993
BARDES, R. G., Tungsten water-moderated rocket critical assembly, analytical method and experimental results, 20: 3571
BARISH, J., Calculation of nucleon-meson cascade in iron initiated by 1- and 3-Bev protons and comparison with experiment, 20: 3258
BARKALOV, I. M., Calorimetric analysis of kinetics of radiation polymerization, 20: 1904
BARKALOV, I. M., Radiation polymerization of hexamethylcyclotrisiloxane in solid phase, 20: 1903
BARLOUTAUD, M., Study of levels of $^{63}Cu$ by inelastic scattering of 10 Mev deuterons, 20: 3073
BARMORE, Willis L., High-temperature plastic deformation of polycrystalline BeO, 20: 2371
BARNES, C. E., Effect of neutron irradiation on electrical properties of $Mg_2Ge_{.8}Si_{.2}$, 20: 2502
BARNES, R. S., Mechanisms of radiation-induced mechanical property changes, 20: 2471
BARNES, Richard David, Spectrophotometric study of reduction of melts containing Cd(II) salts, 20: 3623 (IS-T-36)
BAROCZY, C. J., Pressure drop for flowing vapors condensing in a straight horizontal tube, 20: 1814 (NAA-SR-6333)
BARON, Norton, Elastic and inelastic scattering of 40-Mev alpha particles from even tin isotopes, 20: 3017 (NASA-TN-D-3067)
BARR, Kenneth P., PWR-2 flux wire measurements and comparison to calculations, 20: 3519
BARRAULT, M. R., Electrostatic screening in theta-pinch coil, 20: 3190
BARRETT, Matthew J., Shielding of bremsstrahlung from an electron accelerator target, 20: 2557
BARRETT, P. H., Liquid helium cryostat for Moessbauer scattering experiments, 20: 3093
BARRY, Robert E., Prog. rpt. on liquid metal boiling heat transfer, 5–8/65, 20: 2008 (AD-622825)
BARSELL, A. W., Re-entry burnup of SNAP-10A reactor fuel elements, 20: 3560
BARTH, J. J., Use of adiabatic approximation in prompt-critical, large-core reactor-excursion analyses, 20: 3417
BARUCH, P., Drift mobility of radiation-induced defects in silicon, 20: 2507
BARUT, A. O., Remark on crossing symmetry and parastatistics, 20: 2751 (IC/65/51)
BARYSHEVSKII, V. G., Scattering of neutrons on polarized targets, 20: 3120
BASHAM, S. J., Materials development for sliding-contact applications in 1000°F potassium space power systems, 20: 2242
BASKOVA, K. A., Investigation of radiation of $^{109}Cd$, 20: 3113
BASS, M., Stimulated emission from 4.3 percent abundant $^{50}Cr$ ions in ruby, 20: 3283
BASS, R. F., Nature and yield of photon- and neutron-induced defects in semiconductors, 20: 2516
BASTIN, E. I., Purities of some commercially available $^{14}C$-labeled hydrocarbons, 20: 1764
BASU, D., Solar-terrestrial events in relation to phase of the solar cycle, 20: 2855
BATCH, M. L., Measurement and analysis of SM-1A core-3, 20: 3503
BATES, W., Examination of heavy steel castings with the betatron, 20: 2028
BATTER, John F., Attenuation of in-and-down scattered radiation, 20: 2038
BAUER, Ernest, Inelastic collisions of slow atoms, 20: 2624
BAUGNET-MAHIEU, L., Isotopic effect of tritium in the form of tritiated thymidine on the activity of ATP, 20: 1583
BAUM, B., The use of organometallic compounds in plastic scintillators for detection and resolution of $\gamma$ rays, 20: 1905
BAUMAN, Howard F., Nuclear and fuel-cycle performance of molten-salt breeder reactors, 20: 3498
BAUMANN, Elizabeth W., Depletion of deionizer resin in an SRP reactor system, 20: 2419 (DP-973)
BAUMANN, G., Production of hyperfragments and $^{8}Li$ fragments, 20: 3062
BAUMANN, N. P., Buckling measurements by successive substitution in subcritical assembly, 20: 3399
BAUMANN, N. P., Pulsed measurements of neutron-diffusion parameters in $D_2O$, 20: 2954
BAUMGARTNER, E., Energy loss per ion pair in various gases for nitrogen and oxygen ions from 0.14 to 0.7 Mev, 20: 2602
BAUMGARTNER, E., Use of coincidence method for determination of total conversion coefficients, 20: 3038
BAUMGARTNER, Kurt, Waterproof nuclear radiation screening substance, 20: 2248
BAYATYAN, G. L., Elastic backward scattering of $\pi^-$ by neutrons, 20: 2700
BAYATYAN, G. L., $\pi^-$ meson-neutron elastic backward scattering at 1.4 to 4.0 Bev, 20: 2713
BAYLES, B. J., Phase-reinforced high-temperature alloys produced directly from the melt, 20: 2219 (AMRA-CR-64-05/4)
BAYLY, J. G., High-sensitivity heavy water leak detector, 20: 2099 (AECL-2291)
BAYMAN, B. F., General properties of nuclear models, 20: 3146
BEACH, L. A., Parameters for C-H albedo formula for gamma rays reflected from water, concrete, iron and lead, 20: 3274
BEALL, R. A., Cold-mold induction melting, 20: 2352 (USBM-RC-1205, pp 9-10)
BEALL, R. A., High-melting point carbides (HfC), 20: 2351 (USBM-RC-1205, pp 3-7)
BEARDEN, J. A., Precision x-ray spectroscopy, 20: 2126 (CONF-650657-1)
BEAUDRY, R. J., Low-power shield measurements on Enrico Fermi reactor, 20: 3524
BEAVER, J. E., Cyclotron isotope production and other service irradiations, 20: 2212
BEAVERS, Darrell V., Bulgur wafer and adjuncts for fallout shelter rations, 20: 2067 (AD-614824)
BECHDOLFF, A., Production of hyperfragments and $^{8}Li$ fragments, 20: 3062
BECKER, E., Microwave absorption and magnetic transition in $GdCl_3$, 20: 3288
BECKER, J. A., $^{17}O$ and $^{18}O$ lifetimes by particle-gamma coincidence technique, 20: 3156
BECKER, Lothar, Mechanical time shutter for spectrograph with exposure times from 1.5 $\mu$s to 3 ms, 20: 2125 (CEA-R-2816)
BEEKHUIS, H., Shape of 962 kev beta spectrum of $^{198}Au$, 20: 3055
BEELER, J. R. Jr., Computer studies of neutron irradiation and annealing in finite bcc iron specimens, 20: 2473
BEESTON, J. M., Gas formation and compression fractures in irradiated beryllium, 20: 2478
BEEVER, E. R., Importance of space radiation shielding weight, 20: 3245 (NASA-SP-71, pp 407-14)
BEGHIAN, L. E., Experimental investigations of fast-neutron decay times

in lead assemblies, 20: 2950
**BEGLEY, Richard T.**, Niobium alloys, 20: 2407
**BEGLEY, T.**, Tantalum-base alloys for alkali metal containment, 20: 2241
**BEHRENS, H.**, Evaporator collector, a simple apparatus for continuous sampling with simultaneous concentration of the sample, 20: 1757
**BELARDI, Richard J.**, Prog. rpt. on semiconductor design effects on radiation resistance, 12/15/64–3/15/65, 20: 2411 (AD-618078)
**BELCHER, Ralph L.**, Absolute efficiencies and radiation damage in polycrystalline phosphors irradiated with high-energy electrons, 20: 2164
**BELINSKAYA, N. T.**, Effects of reactor radiation on thermophysical properties of monoisopropyldiphenyl, 20: 1923
**BELITZ, H.-J.**, Crowbar and power crowbar circuits and their calculation, 20: 2102 (JUL-273-PP)
**BELLANCA, Sandra C.**, Prog. rpt. on applications of neutron-activation analysis to scientific crime detection, 11/62–1/63, 20: 1738 (GA-4041)
**BELLER, L. S.**, Structure in Doppler effect as a function of surface, mass ratio in $^{197}Ag$, 20: 2975
**BELLETTINI, G.**, Real part of proton-neutron scattering amplitude at 19.3 Bev, 20: 2712
**BELLMAN, R.**, Numerical results for auxiliary equation of radiative transfer, 20: 2930 (AD-614636)
**BELOOZEROV, N. N.**, Solution of equation for high-energy neutron-deuteron scattering, 20: 2740
**BELOV, K. P.**, Magnetostriction in gadolinium crystal, 20: 3312
**BELTRAM, C.**, Development of $ThO_2$-pellet fabrication, 20: 2291
**BELY, Oleg**, Calculation of collision [cross] sections of $2s \rightarrow np$ type in ions of isoelectronics series of lithium, 20: 2598
**BELYAEV, S. T.**, Green functions and transition probabilities in odd nuclei, 20: 3104
**BELYAKOV, V. A.**, Isomer shift and structure of metastable nuclear states, 20: 3138
**BENDT, P. J.**, Measurement of $C_{NN}$ in neutron-proton scattering at 23 Mev, 20: 2685 (LA-DC-7250)
**BENESOVSKY, Friedrich**, High-temperature nuclear fuel structures and their production, 20: 2305
**BENNETT, G. A.**, Corrosion of refractory metals by zinc–magnesium–uranium and halide salt systems, 20: 2266
**BENNETT, M. J.**, Oxidation of irradiated beryllium in carbon dioxide, 20: 2442
**BENNEWITZ, F.**, Experimental verification of theory of relativity, 20: 2880
**BENNOUN, Jean-Francois**, Characteristic varieties of equations of elasticity in general relativity, 20: 2868
**BENSCH, F.**, Slabs of 1/v-absorber in 1/E-neutron flux, 20: 2946
**BENSON, E. M.**, ZPR-III fuel fabrication, 20: 2290
**BENSON, G. C.**, Some heats of solution in light and heavy water, 20: 1825
**BENSTON, Margaret Lowe**, Distomic forces and force constants from the Hellmann-Feynman theorem; application to $H_2$, 20: 2650
**BERGER, M. J.**, Dose models for evaluating the radiation hazard from reactor debris, 20: 2091
**BERGER, M. J.**, Results of recent transport calculations for electrons and bremsstrahlung, 20: 3246 (NASA-SP-71, pp 437-48)
**BERGER, M. M.**, Local magnetic fields on surface of Nb–Zr superconductor in mixed state, 20: 2924
**BERGLES, A. E.**, Prog. rpt. on boiling flow regimes and critical heat flux, 6/16–9/15/65, 20: 2012 (NYO-3304-6)
**BERGMANN, G.**, Coherence effect in double layers of different superconductors, 20: 2917
**BERINDE, A.**, Mechanism of reaction $^{26}Mg(p,p',\gamma)$ at low energy, 20: 3092
**BERK, H. L.**, Factor of conduction electrons in metallic lithium, 20: 3297
**BERLEY, D.**, Observation of a peak in $K^- + p \rightarrow \Lambda + \eta$ near threshold, 20: 2724
**BERNERT, R. E.**, Magnetic radiation shielding using superconducting coils, 20: 3241 (NASA-SP-71, pp 199-209)
**BERNSTEIN, Bruce S.**, Radiation crosslinking of nylon 66 and poly(vinyl alcohol), 20: 1909
**BERNSTEIN, Ira B.**, Explosion of a supernova into the interstellar magnetic field. I., 20: 2569
**BERNSTEIN, Ira B.**, Explosion of a supernova into the interstellar magnetic field. II., 20: 2570
**BERRY, R. E.**, Aerospace safety results from a NERVA post-operational destruct test, 20: 3573
**BERSUKER, I. B.**, Analysis of $^{119}Sn$ nuclear charge radius based on Moessbauer spectra, 20: 3136
**BERTINI, Hugo W.**, Energy spectra from inelastic nuclear reactions at energies below 450 Mev, 20: 3260
**BERTMAN, B.**, Magnetic field penetration and breakdown of surface superconductivity. II., 20: 2900
**BERTOZZI, G.**, Water solubility in molten alkali nitrates, 20: 1812
(EUR-2495.e)
**BETIN, Yu. P.**, Efficiency of $^3H/Zr$ sources in nondispersive x-ray spectrometric analysis, 20: 2136
**BETZ, N. A.**, Fast-neutron scattering from small cylinders of steel, aluminum, graphite, concrete and lithium hydride, 20: 3265
**BEVARD, D. G.**, WANL experience with $r$-$\theta$ calculations, 20: 3429
**BEVIS, H. A.**, Low-temperature adsorption and $\gamma$ scintillation spectrometry for measuring $^{41}Ar$, 20: 1763
**BEYSTER, J. R.**, Differential neutron scattering from $D_2O$ and $ZrH_{1.85}$, 20: 2963
**BEYSTER, J. R.**, Fast-neutron spectra in liquid hydrogen, 20: 2967
**BEYSTER, J. R.**, Neutron spectrum measurements in $H_2O$ as a function of temperature, 20: 2966
**BEZHAN, I. P.**, Investigations of polymerization radiation. V., 20: 1930
**BHALLA, C. P.**, Xenon induced core instabilities, 20: 3383 (WCAP-3269-48)
**BIANCONE, F.**, Forced convection burnout and hydrodynamic instability experiments for water at high pressure. I., 20: 2009 (EUR-2490.e)
**BIERMAN, S. R.**, Criticality research on plutonium, 20: 3368 (BNWL-SA-214)
**BIERMANN, Wendell Joseph**, Thiocyanate extraction of beryllium, 20: 1974
**BIGEON, Marie-Claude**, Radiative life of the $6\,^3P_0$ state of $^{199}Hg$ and $^{201}Hg$, 20: 2599
**BINDLER, L.**, Evaluation of calculational models and thermal cross-section data in analysis of $PuO_2$–$UO_2$–$H_2O$ lattices, 20: 3425
**BING, Richard J.**, Use of positron emitter in determination of coronary blood flow in man, 20: 1709
**BINGHAM, Carleton D.**, Post-irradiation chemical analysis of SNAP-8 experimental reactor coolant, 20: 3564
**BISHOP, G. R.**, Electron scattering, 20: 3152
**BISHOP, V. S.**, Effects of external irradiation of the heart on cardiac output, venous pressure and arterial pressure, 20: 1652
**BITTEL, Robert**, Bibliography on radiohydrology, 20: 2082 (CEA-Bib-59)
**BITTER, Francis**, Prog. rpt. on solid state research using high magnetic fields, 7/60–10/64, 20: 2519 (AD-615152)
**BITZER, R. A.**, Microwave lens system for plasma diagnostics, 20: 3169 (NASA-CR-319)
**BLACK, R. M.**, Comparison of procedures for dissolving ignited plutonium oxides for analysis, 20: 2344 (TRG-Report-1072)
**BLAHO, Dusan**, Electronic devices for microwave spectrometers, 20: 2106 (UJV-1346/65)
**BLAKE, V. E. Jr.**, Aerospace nuclear safety, 20: 3548 (SC-DC-65-1752)
**BLAND, R. D.**, Ion-plated coatings for corrosion protection of uranium, 20: 2260 (SC-DR-65-519)
**BLASIUS, E.**, Separation of cations on a paper-chromatographic basis, 20: 1750 (UCRL-Trans-1245(L))
**BLESHINSKII, S. V.**, Reactions of yttrium group rare earth chlorides with sodium fluosilicon, 20: 1870
**BLICKENSDERFER, Robert**, Investigation of the system UC–UN–UO, 20: 2353 (USBM-RC-1205, pp 11-14)
**BLINOV, P. I.**, Runaway electron collective interactions with plasma in stellarator S-1, 20: 3186
**BLISS, Henry E.**, Studies of subcritical lattices with distributed neutron absorber by means of pulsed-neutron source technique, 20: 3432
**BLOKHINTSEVA, T. D.**, Analysis of $\pi^- + p \rightarrow \pi^- + \pi^+ + n$ and $\pi^- + p \rightarrow \pi^- + \pi^0 + p$ at 338 Mev, 20: 2682 (JINR-P-2320)
**BLOOMER, J. L.**, Nitration and succinoylation of tritium-labeled toluene, 20: 1950
**BLUE, Robert D.**, Cesium production, 20: 1883
**BLUM, Pierre L.**, System uranium–uranium monocarbide, 20: 2366
**BLUMENTHAL, B.**, Improved metallic fast power breeder fuels, 20: 2386
**BLUMENTHAL, B.**, Thorium–uranium–plutonium alloys as potential fast power breeder fuels, 20: 2230
**BLUMENTHAL, J. L.**, Behavior of beryllium metal in simulated launch pad abort environments, 20: 2341 (SC-DC-65-1637)
**BLYTHE, P. C.**, Oxidation of irradiated beryllium in carbon dioxide, 20: 2442
**BOAG, J. W.**, Rate constant for reaction of $O^-$ with oxygen, 20: 1917
**BOATMAN, James Claude**, Equilibrium phase diagrams for tantalum–tantalum bromide and tantalum–tantalum iodide systems, 20: 2403
**BOBLETER, O.**, Diffusion of fission-product $^{147}Pm$ in aluminum oxide, 20: 2364
**BOCHAROVA, I. E.**, Angular distribution of $^{238}U$ photofission fragments near fission threshold, 20: 3134
**BOCHIROL, Louis**, Improvements in or relating to irradiation enclosures for swimming pool type reactors, 20: 3602
**BOCHVAR, I. A.**, Measurement of the background expternal radiation exposure or urban population in the USSR, 20: 2087
**BOCK-WERTHMANN, W.**, Determination of chlorine and sodium in selenium by non-destructive neutron activation analysis, 20: 1769
**BODENHEIMER, Peter**, Lithium isotope ratio in two Hyades F stars, 20: 2577

**BODENHEIMER, Peter,** Studies in stellar evolution. II., 20: 2566
**BOGAARDT, M.,** Analysis of boiling system dynamics, 20: 3532
**BOGANOV, A. G.,** Irreversible polymorphic transformations of rare earth oxides, 20: 1827
**BOHLANDER, K. M.,** Internal conversion BeO-base fuel element, 20: 2467
**BOHN, George J.,** Solution of nonlinear vibration problems in reactor components, 20: 3328
**BOHN, S. W.,** Development of photogrammetric techniques for measuring surface contours of small samples, 20: 2033
**BOHREN, Craig F.,** Quasi Fermi level analysis of radiation-induced conductivity in ceramic insulators, 20: 3309
**BOIRON, Pierre,** Device for the leak-tight transmission of movement through a wall, 20: 2005
**BOKROS, J. C.,** Prog. rpt. on advanced, graphite-matrix, dispersion-type fuel systems and research on graphite, 8/15–11/14/64, 20: 2318 (GA-5918(Pt.1))
**BOLLIGER, Theodore T.,** Demonstration of extracranial neoplasms with $^{99m}$Tc pertechnetate, 20: 1712
**BOLOTIN, A. B.,** Field form of perturbation theory for symmetrical molecules. I., 20: 2607
**BOLOTIN, A. B.,** Field form of perturbation theory for symmetrical molecules. II., 20: 2608
**BONARD, Rostum T.,** Preparative chromatograph of moving-gas phases, 20: 1886 (CONF-641123-1)
**BONNER, W. B.,** Equilibrium of charged sphere, 20: 2879
**BONRATH, H.,** Microwave absorption and magnetic transition in $GdCl_3$, 20: 3288
**BOOTH, Lawrence A.,** Prospects for reactor-MHD commercial power production, 20: 2670 (LA-DC-7330)
**BORDONALI, C.,** Method of gas-chromatographic analysis of polyphenyls in lithium chloride columns, 20: 1745 (RT/CHI(65)-25)
**BORELOWSKI, Z.,** Equations of motion for one-point model of elementary particle in external gravitational field, 20: 2867
**BORING, J. W.,** Total ionization in nitrogen by heavy ions of energies 25 to 50 kev, 20: 2623
**BOROVIK, E. S.,** Magnetic flux jumps in hard superconductors in pulsed magnetic fields, 20: 2921
**BORYSOWICZ, Jerzy,** Diffraction scattering of deuterons on non-spherical nuclei. III., 20: 3026
**BOSCH, J.,** Automation in radiation measurement techniques, 20: 2141
**BOSCHITZ, E. T.,** Polarization in p-$^4$He scattering between 27 and 63 Mev, 20: 3022 (UCRL-16216)
**BOSCHITZ, E. T.,** Study of $^4$He(p,d)$^3$He reaction with polarized protons at 55 and 63 Mev, 20: 3023 (UCRL-16218)
**BOSSHARD, Ernst,** Fuel element for a nuclear reactor, 20: 3468
**BOST, William E.,** Bibliography on hot laboratories, 20: 1990 (TID-3545(Rev.1))
**BOSTANJOGLO, O.,** Electron diffraction by crystalline hydrogen, 20: 3310
**BOULENGER, Bernard,** Improvements in remote control and automation devices for plant in radioactive surroundings, 20: 2003
**BOUNDEN, J. E.,** High output neutron tubes, 20: 3005
**BOUNIN, P.,** Possible experiment with a proton polarized target, 20: 2686 (LNF-65/22)
**BOURDEAU, Ph.,** Radiosensitivity of rice seed in relation to water content and free radicals, 20: 1669
**BOURGEOIS, Michel,** Preparation of uranium compounds from uranium–molybdenum alloys, 20: 1885
**BOURNE, J. G.,** Prog. rpt. on boiling flow regimes and critical heat flux, 6/16–9/15/65, 20: 2012 (NYO-3304-6)
**BOWDEN, Andrew T.,** Nuclear reactor fuel element having improved fin structure, 20: 3467
**BOWEN, I. Gerald,** Biological tolerance to air blast and related biomedical criteria, 20: 2083 (CEX-65.4)
**BOWEN, P. H.,** Polarization in neutron-proton scattering, 20: 2701
**BOYD, A. W.,** Temperature, dose-rate and track-density effects in radiolysis of ortho- and meta-terphenyl, 20: 1928
**BOYD, C. M.,** Gas chromatographic determination of permanent gases in helium at reduced sample pressures, 20: 1751
**BOYDEN, J. E.,** Use of adiabatic approximation in prompt-critical, large-core reactor-excursion analyses, 20: 3417
**BOYLE, R. F.,** Fission-product and heavy-element distributions in high-performance $UO_2$ fuel rods, 20: 2450
**BOYLING, J. B.,** Proof of Nakanishi's inequality, 20: 2767
**BRAAMS, R.,** Molecular weight of Factor XII (Hageman factor) estimated with ionizing radiation, 20: 1673
**BRABSON, G. D.,** Spectroscopic investigation of high-temperature species isolated in inert gas matrices, 20: 1818 (UCRL-11976)
**BRADBURY, N. G.,** Prog. rpt. on atmospheric diffusion at NARF site, 10/63–9/64, 20: 2073 (AD-618101)
**BRADLEY, J. M.,** Radiotherapy of pituitary tumours, 20: 1708
**BRADLEY, Norman,** Liquid-moderated nuclear reactors, 20: 3354
**BRADSHAW, R. Louis,** Heat generation by radioactive wastes, 20: 3605
**BRAETTER, P.,** Determination of chlorine and sodium in selenium by non-destructive neutron activation analysis, 20: 1769
**BRAGINSKII, V. B.,** Gravitational radiation and possibilities of detecting it, 20: 2884
**BRAIER, H. A.,** Bromine-82 tagged bromobenzene as an industrial tracer, 20: 2202
**BRAIER, H. A.,** Radiotracer study of product contamination by catalytic nickel, 20: 1889
**BRAKHMAN, E. V.,** Elastic backward scattering of $\pi^-$ by neutrons, 20: 2700
**BRAKHMAN, E. V.,** $\pi^-$ meson-neutron elastic backward scattering at 1.4 to 4.0 Bev, 20: 2713
**BRANCA, G.,** Technological-hygienic aspects of radioactive waste disposal in Italy, 20: 3604 (RT/PROT(65)-12)
**BRANDON, C. A.,** Irradiation experiment to study compatibility of BeO with graphite at 1500°C, 20: 2431 (ORNL-TM-1255)
**BRANNEN, J. P.,** Symmetry in summability theory, 20: 3629 (SC-DC-64-288)
**BRASSFIELD, H. C.,** Thermodynamic behavior of hypostoichiometric $UO_2$, 20: 2319 (GE-TM-65-6-13)
**BRAUN, H.,** Production of hyperfragments and $^8$Li fragments, 20: 3052
**BRECHNA, H.,** Current magnet design practice in the U.S.A., 20: 2533 (BNL-9536)
**BRECHNA, H.,** 150-kOe liquid nitrogen cooled pulsed flux-concentrator magnet, 20: 1991
**BRECKENRIDGE, W.,** Abstraction of H atoms by energetic recoil tritium atoms, 20: 1907
**BREGADZE, Yu. I.,** Impairment of ionization chamber homogeneity by conducting covering, 20: 2137
**BREGAR, John F.,** Effects of high-radiation fields on electrical conductivity of metal oxides, 20: 2460
**BREIDENBACH, G.,** Performance optimization of fast-burst reactor core, 20: 3593
**BRETSCHER, M. M.,** Direct measurement of effective capture-to-fission ratio at low flux, 20: 3430
**BREUCH, R. A.,** Nuclear environmental effects on spacecraft thermal control coatings, 20: 2428 (NASA-SP-55, pp 365-79)
**BREUER, H.,** Small NMR probe for use in inhomogeneous fields, 20: 2112
**BREWER, W. D.,** Deuterium isotope effects in decompositions of acetyl peroxide and two t-butyl peresters, 20: 1891
**BREZHNEVA, N. E.,** Preparation of specimens and corrections for self-absorption during measurement of activity of soft $\beta$ emitters, 20: 1780
**BRICKLEY, S. G.,** Behavior of krypton and xenon in uranium metal, 20: 2358 (AERE-Trans-1034)
**BRIGGS, B. H.,** Relation of spread-F echoes to magnetic disturbances, 20: 2854
**BRIMHALL, J. L.,** Influence of finely dispersed second phase on recrystallization, 20: 2325 (HW-SA-3767)
**BRIMHALL, J. L.,** Structure of deformed internally oxidized alloys, 20: 2324 (HW-SA-3765)
**BRISI, Cesare,** Investigations on the $UO_2$–$ThO_2$–$ZrO_2$, 20: 2361 (WAPD-Trans-21)
**BRITTON, W. R.,** SNAP-19 support structure design development and qualification tests, 20: 2205 (MND-3169-52)
**BROCKMAN, K. W. Jr.,** Backward scattering of alpha particles by $^{16}$O at medium energies, 20: 3056
**BROCKMAN, K. W. Jr.,** Optical model analysis of 26 Mev deuteron scattering, 20: 3053
**BROCKWELL, P. J.,** Multiple Compton scattering of low-energy $\gamma$ radiation, 20: 2705
**BRODY, T. A.,** Recursion relations for Wigner coefficients of unitary groups, 20: 2770
**BROERMAN, J. G.,** Band structure of gallium arsenide: spin-orbit splitting, 20: 3287
**BROHEE, H.,** Feasibility of new procedure for biological dosimetry, 20: 1612 (EUR-2505.e)
**BROIDA, H. P.,** Charge-transfer excitation of $(Co)^+$ comet-tail bands by slow $N_2^+$ ions, 20: 2631
**BROIDO, A.,** Effects of fire on major ecosystems, 20: 2079 (BNL-917, pp 11-19)
**BROOKE, C. O. S. Blyth,** Radon concentration in different environments and the factors influencing it, 20: 2090
**BROOM, Knox M. Jr.,** Post-irradiation chemical analysis of SNAP-8 experimental reactor coolant, 20: 3564
**BROUWER, W.,** Neutron spectra in beryllium metal, 20: 2968
**BROWN, C. L.,** Recent exponential and critical approach experiments with slightly enriched uranium metal tubes in light water, 20: 3393
**BROWN, G. W.,** Scattered light in photothermo-elasticity, 20: 2026 (UCRL-13188)
**BROWN, K. L.,** Properties of symmetric quadrupole magnet triplets, 20: 2539 (SLAC-47)
**BROWN, P. S.,** Discrepancies in importance and neutron lifetime in fast and thermal spectra, 20: 3402
**BROWN, R. L. Jr.,** Applications of eddy current testing at Battelle-

Northwest, 20: 2025 (BNWL-SA-349)
**BROWNELL, Gordon L.**, The determination of iodinated compounds by neutron activation of $^{129}$I-description of the technique, 20: 1790
**BROWNING, W. E. Jr.**, Release and adsorption of methyl iodide in HFIR maximum credible accident, 20: 3586 (ORNL-TM-1291)
**BRUCE, A. K.**, Radiation sensitization of bacteria by p-hydroxymercuribenzoate, 20: 1618 (NYO-3319-6)
**BRUGGEMAN, L. D.**, ZPR-III fuel fabrication, 20: 2290
**BRUNA, Jean-Georges**, ALECTO—results obtained with homogeneous critical experiments on $^{239}$Pu, $^{235}$U and $^{233}$U, 20: 3369 (CEA-R-2814)
**BRUNET, Jean-Paul**, ALECTO—results obtained with homogeneous critical experiments on $^{239}$Pu, $^{235}$U and $^{233}$U, 20: 3369 (CEA-R-2814)
**BRUSH, E. G.**, Partially selective corrosion of type-316 stainless steel in high-temperature sodium, 20: 2274
**BRUSH, Stephen G.**, Lattice models for cooperative phenomena. I., 20: 1819 (UCRL-14287)
**BRYANT, Pamela M.**, Computed deposition rates per unit release rate of windborne material, 20: 2074 (AHSB(RP)M-40)
**BUBERNAK, Joseph**, Determination of $^{155}$Eu in fission products using reduction by lithium amalgam, 20: 1752
**BUCHANAN, J. D.**, Prog. rpt. on applications of neutron-activation analysis to scientific crime detection, 10/62, 20: 1737 (GA-3664)
**BUCHER, E.**, Superconductivity in beryllium–rhenium system, 20: 2898
**BUCHER, J. J.**, Extraction of $HClO_4$ by trilauryl amine. I., 20: 1747 (UCRL-11616(Rev.))
**BUCHTELA, K.**, Electrophoresis of $^{227}$Ac, 20: 1756
**BUCHTELA, K.**, Electrophoresis of radioactive rare earths, 20: 1961
**BUCK, P.**, Plutonium production and burnup calculation methods for light water moderated reactors, 20: 3535
**BUCKMAN, R. W., Jr.**, Tantalum-base alloys for alkali metal containment, 20: 2241
**BUCKMAN, Raymond W. Jr.**, Niobium alloys, 20: 2407
**BUCKMAN, Trent D.**, Isotope effect on paramagnetic resonance of triplet excitons, 20: 1841
**BUDAK, E. A.**, $\gamma$-Spectrum from the reaction $^{54}$Fe(n,$\gamma$)$^{55}$Fe, 20: 3109
**BUDICK, B.**, Level-crossing spectroscopy with an electric field, 20: 2619
**BUECHI, J.**, Influence of radioactive rays on pharmaceuticals, 20: 1918
**BUEHLER, W. J.**, Effects of alloying upon certain properties of 55.1 Nitinol, 20: 2310 (AD-618681)
**BUEHRING, Wolfgang**, Computational improvements in phase shift calculations of elastic electron scattering, 20: 2635
**BUERGISSER, H.**, T(d,n)$^{4}$He reaction with polarized deuterons, 20: 3039
**BULANOVA, I. D.**, Determination of $^{233}$Pa in the air, 20: 1759
**BUMBA, V.**, Development of solar flares within the calcium network, 20: 2578
**BURBIDGE, E. Margaret**, Synthesis and destruction of elements in peculiar stars of types A and B, 20: 2565
**BURBIDGE, G. R.**, Synthesis and destruction of elements in peculiar stars of types A and B, 20: 2565
**BURKHARDT, Gottfried**, Structure of socalled "ethylmetaphosphate" (langheld ester), 20: 3640 (UCRL-11488)
**BURKHART, L. E.**, Design evaluation of fused-salt molten-metal extractor, 20: 2245
**BURLANT, W.**, Divinyl copolymerization initiated by high-intensity, low-energy electrons, 20: 1910
**BURLESON, G. R.**, Evidence for $\kappa^0$(725) in $\pi^-$ p reactions, 20: 2715
**BURNETT, J. L.**, Melting points of curium and americium trifluorides, 20: 1864
**BURNS, G.**, Strain effects in rare earth transitions, 20: 3291
**BURNS, Ralph William Jr.**, Enrichment and determination of tritium in water, 20: 1728 (AD-618552)
**BURNSTEIN, R. A.**, Absorption time of $\Sigma^-$ hyperons in liquid hydrogen, 20: 2723
**BURRELL, Martin O.**, Calculation of proton penetration and dose rates, 20: 3250 (NASA-SP-71, pp 493-505)
**BURRILL, E. Alfred**, Radiation shielding considerations for tandem accelerators, 20: 2558
**BURRIS, L. Jr.**, Corrosion of refractory metals by zinc–magnesium–uranium and halide salt systems, 20: 2266
**BURRIS, L. Jr.**, Diffusivity of uranium in liquid metal solutions, 20: 2368
**BURRIS, Leslie Jr.**, Corrosion of steels and tantalum by molten cadmium–magnesium–zinc systems, 20: 2265
**BURSUKOVA, M. I.**, Efficiency of $^{3}$H/Zr sources in nondispersive x-ray spectrometric analysis, 20: 2136
**BURTE, Harris M.**, Refractory metals—an assessment, 20: 2307 (AD-613023)
**BUSBOOM, H. J.**, Radiation damage in Incoloy-800, 20: 2458
**BUSSELMAN, G. J.**, Analysis and measurement of PuAl–polyethylene systems in PCTR, 20: 3398
**BUTLER, T. A.**, Reactor neutron cross sections for production of $^{33}$P from $^{36}$Cl and enriched $^{33}$S in Oak Ridge research reactor, 20: 3020 (ORNL-TM-1065)
**BUTOMO, S. V.**, Synthesis of trimethylbenzenes for measuring natural radiocarbon by means of scintillation method, 20: 2062
**BYATT, William J.**, Mathematical models of magnetic flux compression, 20: 2523 (SC-RR-65-449)
**BYCKLING, Eero**, Calculation of the Yang-Lee distribution of zeros, 20: 2845
**BYKHOVSKII, A. V.**, Problem of hot particles in atmospheric air (a survey), 20: 2053
**BYSTROV, L. N.**, Effect of electron irradiation on mechanical properties of steel subjected to thermal mechanical treatment, 20: 2438

## C

**CABICAR, J.**, Influence of physiological inoculum age on growth of microbe culture in $H_2O$ and 50% $D_2O$, 20: 1601
**CADY, K. B.**, Asymptotic reactor-theory analysis of Garelis-Russell experiment, 20: 3385
**CAFFEY, Thurlow W. H.**, Freshwater propagation tests, 20: 3632 (SC-DC-65-459)
**CAILLAT, Roger**, Improvements in beryllium–magnesium alloys, 20: 2277
**CAIRD, R. S.**, Los Alamos flux compression program from its origin, 20: 3166 (LA-DC-7252)
**CAIZERGUES, Robert**, ALECTO—results obtained with homogeneous critical experiments on $^{239}$Pu, $^{235}$U and $^{233}$U, 20: 3369 (CEA-R-2814)
**CALABRESI, P.**, Effects of 1-$\beta$-D-arabinofuranosylcytosine hydrochloride on regenerating bone marrow, 20: 1687
**CALDARELLA, Gerald J.**, High-energy electron irradiation of trihydroperfluoroalkyl acrylate monomers, 20: 1911
**CALLAWAY, Joseph**, Inelastic collisions of slow atoms, 20: 2624
**CALLCOTT, T. A.**, Application of hot carrier techniques to study of radiation damage in germanium, 20: 2483
**CALLEN, J. D.**, Diocotron instability in quasi-toroidal geometry, 20: 3252 (NP-15578)
**CALVIN, Melvin**, Structure of socalled "ethylmetaphosphate" (langheld ester), 20: 3640 (UCRL-11488)
**CAMPANA, R. J.**, SNAP-15A—radioisotope thermoelectric generator, 20: 2204
**CAMPANILE, A.**, Forced convection burnout and hydrodynamic instability experiments for water at high pressure. I., 20: 2009 (EUR-2490.e)
**CAMPBELL, E. E.**, Particle-size distributions from Rover fuel-element fragmentation studies, 20: 3574
**CAMPBELL, E. M.**, Device to facilitate threading of $^{60}$Co beads, 20: 1722
**CAMPBELL, J. C.**, Weapons effects display system study, 20: 1987 (UCRL-13189)
**CAMPBELL, Ronald Hugh**, Method and apparatus to determine reactor flux distribution, 20: 3362
**CAMPBELL, Ronald M.**, Pressure tube neutronic reactor, 20: 3442
**CAMPERO, A.**, Activation analysis simultaneous determination of manganese, copper and zinc in blood serum, 20: 1586
**CAMPION, P. J.**, Relative time distribution of pulses in $4\pi$ $\beta$-$\gamma$ coincidence technique, 20: 2146
**CANOSA, Jose**, Reactor excursions with ramp reactivity insertion, 20: 3415
**CARDONA, M.**, Band structure of gallium arsenide: spin-orbit splitting, 20: 3287
**CARLEY, D. D.**, Recent sutdies of the classical electron gas, 20: 2830
**CARLSON, B. G.**, Moments equations and equivalent discrete ordinates equations. I., 20: 2981
**CARLSON, B. G.**, Moments equations and equivalent discrete ordinates equations. II., 20: 2982
**CARLSON, H. Gary**, 2-Methylfuran: heat capacity and thermodynamic properties from 5 to 350°K, 20: 3615 (COO-1149-17)
**CARLSON, H. Gary**, 2, 5-Dimethylthiophene, heat capacities and thermodynamic properties from 5 to 300°K and fusion of stable and metastable phases, 20: 3614 (COO-1149-16)
**CARLSON, P. J.**, Search for Y$^{\ast}_{1}$ production in K$^-$ captures in nuclei, 20: 3064
**CARLSON, Thomas A.**, Electron shake-off resulting from K-shell ionization in Ne, 20: 2622
**CARLSTON, C. E.**, Secondary-electron emission from molybdenum due to positive and negative ions of atmospheric gases, 20: 2628
**CARMICHAEL, Donald C.**, Hot isostatic compaction of graphite, 20: 2278 (BMI-1746)
**CARPENTER, S. G.**, Doppler coefficients of fertile and refractory materials, 20: 2958
**CARRIGAN, Anne**, Auroral spectrograph data, 20: 2851
**CARTER, H. E.**, Detection of phospholipids on paper chromatograms by neutron activation, 20: 1771
**CARTER, H. G.**, Direct-interaction inelastic scattering of energetic neutrons, 20: 3256
**CARTER, J. P.**, Stress-corrosion cracking of vanadium, molybdenum, and a titanium–vanadium alloy, 20: 2254 (BM-RI-6680)
**CARTER, L. L.**, Criticality research on plutonium, 20: 3368 (BNWL-SA-214)
**CARTER, Robert L.**, Thermal conductivity of graphite, 20: 2387

**CASINI, G.,** New lattice calculation method for ORGEL-type reactors, 20: 3424
**CASKEY, G. R. Jr.,** Irradiation behavior of zirconium–uranium alloy fuel tubes, 20: 2466
**CASON, Neal Martin,** Reaction $\pi^- + p \rightarrow \pi^- + \rho^0 + p$ at 7.0 Bev, 20: 2746
**CASWELL, B. F.,** Critical heat flux for boiling liquid metal systems, 20: 2023
**CASWELL, Bruce F.,** Prog. rpt. on liquid metal boiling heat transfer, 5–8/65, 20: 2008 (AD-622825)
**CATTAN, A.,** Adoptive immunotherapy of acute leukemia: experimental and clinical results, 20: 1701
**CAUTHEN, Lewis J. Jr.,** Isthmian canal studies, 1964, 20: 1983 (PNE-2000)
**CAUTHEN, Lewis J. Jr.,** Isthmian canal studies, 1964, 20: 1985 (PNE-2003)
**CAUTIUS, Werner,** Present state of fuel costs for high-temperature reactors with spherical fuel elements, 20: 3448
**CEGELSKI, W. M.,** Fission-product release from irradiated uranium–zirconium–hydride SNAP fuel, 20: 3562
**CELNIK, J.,** Synthesis of spherical minimum-weight proton shields, 20: 3242 (NASA-SP-71, pp 225-8)
**CHABBAL, Robert,** Relative isotopic displacements in the spectrum of neodymium. Specific mass effect, 20: 1826
**CHABRE, M.,** Polarization in p-$^4$He scattering between 27 and 63 Mev, 20: 3022 (UCRL-16216)
**CHABRE, M.,** Study of $^4$He(p,d)$^3$He reaction with polarized protons at 55 and 63 Mev, 20: 3023 (UCRL-16218)
**CHALDER, G. H.,** CANDU fuel performance in NPD, 20: 3496
**CHALOVA, E. P.,** Reactions of yttrium group rare earth chlorides with sodium fluosilicon, 20: 1870
**CHAMBERLAIN, Harry V.,** Hydraulic studies with random-packed beds applicable to paste-fuel concept, 20: 3461
**CHAMBERLAIN, Harry V.,** Operation of sodium loop with circulation of stainless-steel paste, 20: 3460
**CHANDLER, James G.,** Effect of allogeneic bone marrow on lethally irradiated thymectomized mice, 20: 1660
**CHANG, Elfredo T.,** American Documentation Institute Document No. 0000. Supplementing: "The system tetramethylmethane–tetrachloromethane. Thermodynamics of mixing in the plastically crystalline region." and "Heat capacities and thermodynamic properties of globular molecules. XV., 20: 3620 (COO-1149-27)
**CHANG, Elfredo T.,** Heat capacities and thermodynamic properties of globular molecules. XV., 20: 3619 (COO-1149-26)
**CHANG, Elfredo T.,** System tetramethylmethane–tetrachloromethane. Thermodynamics of mixing in plastically crystalline region, 20: 3618 (COO-1149-25)
**CHANG, William W.,** Prog. rpt. on semiconductor radiation response prediction, 12/15/64–3/15/65, 20: 2412 (AD-618079)
**CHANGE, I-Dee,** Hydromagnetic stability of a liquid layer under the action of a magnetic field and a gravitational force, 20: 2820 (AD-614645)
**CHARKINA, I. A.,** Specific heat of Gd near Curie point, 20: 2920
**CHASE, B. H.,** High-sensitivity fast neutron dosimeter, 20: 2134 (TID-22335)
**CHASE, L. F. Jr.,** $^{17}$O and $^{19}$O lifetimes by particle-gamma coincidence technique, 20: 3156
**CHASE, Wayne L.,** Operation of sodium loop with circulation of stainless-steel paste, 20: 3460
**CHAWLA, A. S.,** Labeling of glycine by direct exchange with heavy water, 20: 1833
**CHEBOTAREV, N. T.,** Physico-chemical properties of crystal hydrates of terbium subgroup rare earth sulfates, 20: 1868
**CHECHERNIKOV, V. I.,** Magnetic properties of Ni–Eu alloys, 20: 2369
**CHEISHVILI, O. D.,** Passage of polarized neutrons through superconductor in mixed state, 20: 2998
**CHEN, S. H.,** Cooperative modes of motion in simple liquids, 20: 2837
**CHENG, L. J.,** High-energy electron (10–60 Mev) and proton (20–130 Mev) radiation damage in silicon and germanium, 20: 2517
**CHERENKOV, P. A.,** Angular and energy distributions of $^{18}$F recoil nuclei in reaction $^{19}$F(γ,n)$^{18}$F, 20: 3108
**CHEREVATENKO, A. P.,** Weakening of high energy μ beams in shielding, 20: 3238 (JINR-P-2354)
**CHERNAVSKII, D. S.,** Possible connection between $K_2^0$ decay and statistical irreversibility, 20: 2699
**CHERNICK, C.,** Cleaning blocked coolant passages in water-cooled magnets, 20: 1992
**CHERNICK, J.,** Rotating fluidized-bed research reactor, 20: 3598
**CHERNUKHIN, V. L.,** Kinetic energies of fragments with various masses in fission of $^{235}$U by thermal and fast neutrons, 20: 3110
**CHERNYAEV, V. A.,** Biphenyl thermal turbines and their maximum power, 20: 2019
**CHEVALLIER, P.,** New levels in $^{58}$Co, 20: 3077
**CHIBISOV, M. I.,** Attachment of electrons to atoms in triple collisions, 20: 2647
**CHIBISOV, M. I.,** Destruction of atomic particles by an electric field and by electron impact, 20: 2646
**CHILD, H. R.,** Magnetic structure properties of Tb–Sc alloys, 20: 2338 (ORNL-P-1735)
**CHILENSKAS, A. A.,** Fluid-bed fluoride volatility processing of irradiated fuels in hot cells, 20: 1971
**CHILTON, A. B.,** Parameters for C-H albedo formula for gamma rays reflected from water, concrete, iron and lead, 20: 3274
**CHIRIKOV, B. V.,** Magnetic mirror trap for prolonged confinement of electrons, 20: 3225
**CHIU, Charles B.,** Total and differential cross sections for reaction $\pi^- p \rightarrow \gamma n$, 20: 2689 (UCRL-16140)
**CHODIL, G.,** X-ray spectra from Scorpius (SCO-XR-1) and the sun observed above the atmosphere, 20: 2585
**CHOHAN, V. S.,** Spurious scattering in nuclear emulsions, 20: 2145
**CHOU, Y. T.,** Linear dislocation arrays in heterogeneous materials, 20: 2335 (NYO-2394-9)
**CHOW, J. G. Y.,** Alpha-gamma facility for fuel studies, 20: 2001
**CHOY, T.,** The determination of vanadium in blood by neutron activation analysis with preirradiation separation, 20: 1791
**CHRISTENSON, C. W.,** Operational practices in treatment of low and intermediate level radioactive wastes—Argonne and Los Alamos Laboratories, U. S. A., 20: 3603 (LA-DC-7249)
**CHRISTENSON, James Harlowe,** Regeneration of $K_2^0$ mesons and the $K_1^0$–$K_2^0$ mass difference, 20: 2748
**CHRISTY, E. H. Jr.,** Plasma impedance measuring technique, 20: 3094
**CHUBAROV, S. I.,** Kinetic energies of fragments with various masses in fission of $^{235}$U by thermal and fast neutrons, 20: 3110
**CHUDINOV, E. G.,** Neptunium(V) complex ability, 20: 1848
**CHUPP, W. W.,** Improved Bevatron and its performance at high intensity, 20: 2541 (UCRL-16228)
**CHUVILO, I. V.,** Radiative kaon decays, 20: 2684 (JINR-P-2374)
**CHWASZCZEWSKA, Janina,** Semiconductor nuclear radiation detectors and their applications, 20: 2155
**CIRANNI, G.,** Self-radiolysis and methods for storage of tritiated organic compounds, 20: 1938 (EUR-2452.e)
**CLAIBORNE, H. C.,** Heating in infinite cylinders by uniform gamma sources, 20: 3269
**CLAIBORNE, H. C.,** Heating in infinite cylinders by uniform gamma sources, 20: 3325 (ORNL-P-1480)
**CLARK, A. J. Jr.,** Aero heating results from the RFD-2 flight test, 20: 2207
**CLARK, A. J. Jr.,** Aerospace safety results from a NERVA post-operational destruct test, 20: 3573
**CLARK, Colin H.,** Investigations on reversions to methionine independence induced by mutagens in Schizosaccharomyces pombe, 20: 1654
**CLARK, Donald Eldon,** Recoil chemistry of $^{11}$C in liquid hydrocarbons, 20: 1896 (IS-T-23)
**CLARK, J. M.,** Inter-nucleon potential deduced from shell model calculations, 20: 3068
**CLARK, K. C.,** Vibration and rotation of $N_2^+$ excited by 10- to 65-kev ions, 20: 2618
**CLARK, W. S.,** Measurement and analysis of SM-1A core-3, 20: 3503
**CLARKE, E. T.,** Differential dose albedos for $^{60}$Co radiation at grazing incidence on concrete and steel, 20: 3270
**CLAUSNITZER, G.,** Proposal for source of completely polarized deuterons, 20: 2528
**CLAWSON, L. G.,** Prog. rpt. on boiling flow regimes and critical heat flux, 6/16–9/15/65, 20: 2012 (NYO-3304-6)
**CLAYTON, E. D.,** Criticality research on plutonium, 20: 3368 (BNWL-SA-214)
**CLAYTON, E. D.,** Criticality studies with plutonium solutions, 20: 3395
**CLAYTON, Frances E.,** Genetic effects from simultaneous irradiation of immature and mature Drosophila virilis males, 20: 1644
**CLEAVER, J. E.,** Effects of uv light on rate of DNA synthesis in mammalian cells, 20: 1625
**CLELAND, J. W.,** Nature and yield of photon- and neutron-induced defects in semiconductors, 20: 2516
**CLEMENT, J. M.,** Eurochemic sampling system, 20: 1955 (NP-15403)
**CLEVER, H. Lawrence,** Heat capacities and thermodynamic properties of globular molecules. XIII., 20: 3616 (COO-1149-22)
**CLEVER, H. Lawrence,** Heat capacities and thermodynamic properties of globular molecules. XIV., 20: 3617 (COO-1149-23)
**CLINE, David Bruce,** Study of rare decay modes of the $K^+$ meson, 20: 2749
**CLITES, P. G.,** Cold-mold induction melting, 20: 2352 (USBM-RC-1205, pp 9-10)
**CLOUET D'ORVAL, Christian,** ALECTO—results obtained with homogeneous critical experiments on $^{239}$Pu, $^{235}$U and $^{233}$U, 20: 3369 (CEA-R-2814)
**CLOUGH, S.,** Transmission of light by crystal aggregates between polarizers. II., 20: 3636 (TID-22319)
**CLOUGH, Stuart B.,** Scattering of light by anisotropic discs with their

principal polarizability direction at an angle to the radius, 20: 1817 (TID-22323)
**CLOYD, D. R.**, Handling hazardous materials, 20: 1727
**COCCONI, G.**, Real part of proton-neutron scattering amplitude at 19.3 Bev, 20: 2712
**COCHRAN, D. R. F.**, Shielding considerations for proposed Los Alamos meson physics facility, 20: 2559
**COEN, V.**, TESI—advanced power excursion reactor for research in reactor safety, 20: 3584 (EUR-2433. e)
**COGLIATI, G.**, Preparation of uranium dioxide and carbide particles by sol-gel methods, 20: 2226 (RT/CHI(65)-30)
**COHEN, Alberto**, Use of positron emitter in determination of coronary blood flow in man, 20: 1709
**COHEN, L.**, The positive excess of $\mu$ mesons at high energies, 20: 2702
**COHEN, S. C.**, Calculation of fast-flux fine structure in cylindrical-cell approximation, 20: 3427
**COHN, Charles E.**, Initial usage of computer for on-line data reduction in reactor physics experiments, 20: 3433
**COJAN, Jean-Louis**, Radiative life of the 6 $^3P_0$ state of $^{199}$Hg and $^{201}$Hg, 20: 2599
**COJOCARU, V.**, Argon gas scintillation detector, 20: 2163
**COLE, L. J.**, Urethan-induced lung tumors in mice: x-radiation dose dependent inhibition, 20: 1606 (AD-623079)
**COLEMAN, L. F.**, Inert-atmosphere enclosure for environmental testing, 20: 2246
**COLEMAN, S.**, Method of Dashen and Gellman, 20: 2787
**COLER, M. A.**, Nondestructive electrical method of studying density distribution of a randomly packed bed, 20: 1977
**COLLETT, J. G.**, ZPR-III fuel fabrication, 20: 2290
**COLLEY, D. C.**, $\Omega^-$ particle produced by 6-Bev $K^-$ meson in hydrogen, 20: 2717
**COLLIE, C. H.**, Proton-thermal neutron capture cross section, 20: 3058
**COLLINS, C. W.**, Control-rod systems for HFIR, 20: 3543
**COLLINS, H. A.**, Relative toxicity of angiographic contrast media, 20: 1724
**COLLINSON, A. J. L.**, Radon concentration in different environments and the factors influencing it, 20: 2090
**COLOMBO, G.**, Prog. rpt. on cell survival as function of radiation dose, final 1959-62, 20: 1617 (NP-15149)
**COLSMANN, P.**, Burnup calculations for Brookhaven graphite research reactor fuel elements, 20: 3601
**COLSMANN, P.**, Practical gamma counting of unirradiated $^{238}$U, 20: 3464
**COLTON, Robert M.**, Formability characteristics of polyphase titanium alloy Ti–6Al–6V–2Sn–4Zr, 20: 2308 (AD-614637)
**COLVETT, Robert**, Skyshine consideration for accelerator shielding design, 20: 2552
**COMMERFORD, S. L.**, Response of skin of swine to increasing exposure of 250 kvp x rays, 20: 1609 (BNL-9477)
**COMPRELLI, F. A.**, Radiation damage in Incoloy-800, 20: 2458
**COMPRELLI, R. A.**, Observations concerning localized corrosion in pumped sodium systems, 20: 2296
**CONDIT, C. M.**, Analysis of reactor excursions initiated at high power in SPERT-III PWR, 20: 3507
**CONDON, W. J.**, Direct-field $\gamma$ spectrometry for rapid quantitative assessment of environmental contamination, 20: 2171
**CONNOLLY, P. L.**, Observation of a peak in $K^- + p \rightarrow \Lambda + \eta$ near threshold, 20: 2724
**CONNOR, H. W. J.**, Temperature, dose-rate and track-density effects in radiolysis of ortho- and meta-terphenyl, 20: 1928
**CONRAD, Raymond Walter**, A light-scattering study of the nature of niobium(V) in aqueous solution, 20: 1875
**CONSTANT, R.**, Working conditions and safety in laboratories of Department of Radioisotopes at Mol, 20: 2192 (BLG-68-11)
**CONTE-ALBERT, Madeleine**, Low-temperature oxidation of uranium powders and application to sintering of uranium oxide powders, 20: 2279 (CEA-R-2828)
**CONZETT, H. E.**, Polarization in p-$^4$He scattering between 27 and 63 Mev, 20: 3022 (UCRL-16216)
**CONZETT, H. E.**, Study of $^4$He(p,d)$^3$He reaction with polarized protons at 55 and 63 Mev, 20: 3023 (UCRL-16218)
**COOGAN, H. M.**, Moessbauer effect data index, 20: 3146
**COOGLER, A. L.**, Evolution of high-level caves at the Savannah River Laboratory, 20: 2000
**COOK, G. B.**, Determination of some impurities in nuclear-grade U, 20: 1784
**COOPER, J. A.**, Effect of chemical state on lifetime of 24-second isomer of $^{90}$Nb, 20: 3088
**COOPER, Thomas D.**, Refractory metals—an assessment, 20: 2307 (AD-613023)
**COOPS, M. S.**, Livermore slug fabrication facility, 20: 2298
**COPE, Lawrence H.**, Mechanical properties of nuclear cermets, 20: 2381
**COPIC, M.**, Extrapolation distance of higher velocity modes in slab geometry, 20: 2988
**CORBETT, J. A.**, Calorimetric and spectrometric techniques to relate zone-wise power distributions in Pu–U multizoned cores, 20: 3388
**CORDES, A. W.**, Heat capacities and thermodynamic properties of globular molecules. XIV., 20: 3617 (COO-1149-23)
**CORDIN, R. A.**, Special nuclear material control by power reactor operator, 20: 3536
**CORELLI, J. C.**, High-energy electron (10–60 Mev) and proton (20–130 Mev) radiation damage in silicon and germanium, 20: 2517
**CORMIER, Raymond J.**, Sunspot cycle and ionospheric storms, 20: 2848 (AD-615111)
**CORNISH, J. J.**, Study of diffusion of carbon and molybdenum in chromium, 20: 2357 (AERE-Trans-1032)
**CORNISH, J. J.**, Value of self-diffusion parameters of zirconium, 20: 2356 (AERE-Trans-1030)
**CORTI, F.**, Criteria for choice of best working conditions in measurements of radioactive sources (a review), 20: 2127 (ISS-64/15)
**COSTES, Didier**, Fire extinguishing system for nuclear reactors, 20: 3364
**COTTIN, S.**, New levels in $^{58}$Co, 20: 3077
**COTTRELL, Wm. B.**, Release and adsorption of methyl iodide in HFIR maximum credible accident, 20: 3586 (ORNL-TM-1291)
**COULOMB, Rene**, Computer processing of $\gamma$ spectra and determination of radioelements, 20: 1732 (CEA-R-2850)
**COURTNEY, J. C.**, Fast-neutron scattering from small cylinders of steel, aluminum, graphite, concrete and lithium hydride, 20: 3265
**COUTURE, Jacques**, Improvements in remote control and automation devices for plant in radioactive surroundings, 20: 2003
**COX, A. E.**, Proton-thermal neutron capture cross section, 20: 3058
**COX, D. E.**, Neutron-diffraction study of antiferromagnetism in $UO_2$, 20: 3301
**COX, G. C.**, Polarization in neutron-proton scattering, 20: 2701
**CRAIG, C. N.**, Observations on microstructural changes with burnup in mixed-oxide fuels, 20: 2451
**CRAIG, C. N.**, Relative in-pile thermal conductivity of stoichiometric and hypostoichiometric mixed oxides of plutonia and urania, 20: 2453
**CRANNELL, H. L.**, Inelastic electron scattering from alpha particle, 20: 3086
**CRAWFORD, F. W.**, Absolute instabilities of obliquely-propagating cyclotron harmonic plasma waves, 20: 3181 (SU-IPR-20)
**CRAWFORD, J. H. Jr.**, Arsenic impurity defect interactions in $\gamma$-irradiated germanium, 20: 2494
**CRAWFORD, J. H. Jr.**, Nature and yield of photon- and neutron-induced defects in semiconductors, 20: 2516
**CRICK, N. W.**, Oxidation of irradiated beryllium in carbon dioxide, 20: 2442
**CRISTU, M. I.**, Gamma rays from $^{75}$As(n,$\gamma$)$^{76}$As reaction, 20: 3011 (IFA-NR-22)
**CROCKER, G. R.**, Gamma-emission data for calculation of exposure rates from nuclear debris. II., 20: 2048 (USNRDL-TR-888)
**CROCKETT, Thomas B.**, Post-irradiation chemical analysis of SNAP-8 experimental reactor coolant, 20: 3564
**CROITORU, Zicu**, Improvements in magnetohydrodynamic generators, 20: 2677
**CROMPTON, R. W.**, Precision measurements of the Townsend energy ratio for electron swarms in highly uniform electric fields, 20: 2825
**CROOKS, H. E.**, Measurement of patient dose, 20: 1697
**CROSBIE, K. L.**, Accelerator-pulsed fast-assembly operating experience, 20: 2956
**CSER, L.**, Investigations of ordering transformation in $Fe_3Al$ alloy by Moessbauer effect, 20: 3292
**CUEER, P.**, Production of hyperfragments and $^8$Li fragments, 20: 3062
**CULVAHOUSE, J. W.**, F centers in SrO and quadrupole moment of $^{87}$Sr, 20: 3087
**CULVER, J. S.**, DCX-2 scanning energy spectrometer, 20: 3178 (ORNL-P-1513)
**CUMMING, J.**, Unstable boson exchange interactions and pole approximation for resonance particles, 20: 2779
**CUMMINGS, A. J.**, New techniques for superconducting cables, 20: 3612 (CONF-651001-6)
**CUNIBERTI, R.**, New lattice calculation method for ORGEL-type reactors, 20: 3424
**CUNNINGHAM, C. W.**, Screening tests of turbine nozzle and blade materials, 20: 2240
**CURLEE, N. J. Jr.**, Control-induced xenon oscillations, 20: 3326 (WAPD-T-1732)
**CURRELL, Kenneth Richard**, Improvements relating to nuclear reactors, 20: 3465
**CURTIS, O. L. Jr.**, Arsenic impurity defect interactions in $\gamma$-irradiated germanium, 20: 2494
**CURTIS, S. B.**, Fractional cell lethality approach to space radiation hazards, 20: 1616 (NASA-SP-71, pp 219-23)
**CUTLER, J. A.**, Nondestructive electrical method of studying density distribution of a randomly packed bed, 20: 1977
**CZACHOWSKA, Z.**, Possible occurrence of very high Lorentz factor calculated using Castagnoi's formula in secondary jets of ultra high energy,

20: 2651 (INR-608/VI/PH)
**CZERWONKO, J.**, Asymptotic properties of some model Hamiltonians in nuclear physics; single-particle excitations, 20: 3099
**CZYZAK, S. J.**, Atomic wave functions, collision cross sections, and transition probabilities of Fe ions, 20: 2609

# D

**DABROWSKI, J.**, Ground state energy of nuclear matter, 20: 3079
**DAHL, Poul**, Large-angle collisions in an aluminum surface bombarded by 50-kev argon ions, 20: 2629
**DAHLBERG, Richard Craig**, Scattering kernels and their temperature dependence, 20: 3435
**DAKOWSKI, Miroslaw**, Semiconductor nuclear radiation detectors and their applications, 20: 2155
**DALGARNO, A.**, Corpuscular bombardment and $N_2^+$ radiation, 20: 2859
**DALTON, L. R.**, Correlated EPR-optical spectra of potassium in ethylamine–ammonia mixtures, 20: 1808 (COO-958-5)
**DANAHY, Daniel T.**, Accumulation of radioactive fission products in hair, 20: 1695
**DANCE, W. E.**, Bremsstrahlung production in thick aluminum and iron targets by 0.5- to 3.0-Mev electrons, 20: 3247 (NASA-SP-71, pp 449-53)
**DANIEL, H.**, Spin dependence of Rayleigh scattering, 20: 3082
**DANIELS, J. T.**, Review of UKAEA criticality detection and alarm systems 1963/64. I., 20: 2075 (AHSB(S)R-92)
**DANIELS, T.**, Level structure of $^{18}O$ and $^{19}O$ by stripping reactions, 20: 3052
**DANIELSON, G. C.**, Thermal diffusivity of platinum, 20: 3621 (IS-1261)
**DANIELSON, G. C.**, Thermal diffusivity of armco iron by three methods, 20: 3622 (IS-1266)
**DANIELSSON, O.**, Search for $Y_0^0$ production in K⁻ captures in nuclei, 20: 3064
**DANILIN, V. S.**, Biphenyl thermal turbines and their maximum power, 20: 2019
**DANILOV, G. S.**, Certain mass formulas in Quark model, 20: 2807
**DANILOV, G. S.**, Three-particle partial amplitudes and unitarity conditions for complex values of angular momenta, 20: 2811
**DANILOV, V. I.**, Duty cycle improvement of particle beams at 680-Mev JINR synchrocyclotron, 20: 2548
**DANILOV, V. I.**, Possibility of stabilization of synchrocyclotron intensity, 20: 2536 (JINR-P-2341)
**DANNIN, J.**, The use of organometallic compounds in plastic scintillators for detection and resolution of $\gamma$ rays, 20: 1905
**DANYSZ, M.**, Scattering of Ar ions in photographic emulsion, 20: 3063
**D'ARCY, Gerald P.**, Simulation of air-blast-induced ground motion, phase I, 20: 1980 (AD-614990)
**D'ARDENNE, W. H.**, Reactor physics measurements in slightly enriched uranium $D_2O$ lattices, 20: 3397
**DARRAS, Raymond**, Improvements in beryllium–magnesium alloys, 20: 2277
**DAS GUPTA, M. K.**, Solar-terrestrial events in relation to phase of the solar cycle, 20: 2855
**DATTA, Bhagwat**, Spurious scattering in nuclear emulsions, 20: 2145
**DAUNT, J. G.**, Properties of superconducting Mo–Re alloys, 20: 2890 (AFML-TR-65-154)
**DAUTREPPE, D.**, Neutron and gamma irradiations of indium antimonide at 70°K. Annealing of defects, 20: 2500
**DAVIDSON, K. V.**, Compatibility of refractory metals with solid solution (UC)(ZrC) at elevated temperatures, 20: 2332 (LA-3307)
**DAVIES, D. H.**, Some heats of solution in light and heavy water, 20: 1825
**DAVIES, J. H.**, Fission-product and heavy-element distributions in high-performance $UO_2$ fuel rods, 20: 2450
**DAVIS, Dorothy**, Bibliography on wholesomeness of irradiated food, 20: 2196 (AD-614910)
**DAVIS, J. A.**, Effects of external irradiation of the heart on cardiac output, venous pressure and arterial pressure, 20: 1652
**DAVIS, J. M.**, Central laboratory for hot chemistry at KFA-Juelich, 20: 1996
**DAVIS, James A.**, Transport synthesis, 20: 2990
**DAVIS, James A.**, Variational vacuum boundary conditions for $P_N$ approximation, 20: 2978
**DAVIS, Monte V.**, Effects of high-radiation fields on electrical conductivity of metal oxides, 20: 2460
tivity in ceramic insulators, 20: 3309
**DAVIS, Monte V.**, Quasi Fermi level analysis of radiation-induced conduc-
**DAVISON, Fred C.**, Inhalation study of pathogenesis of neodymium oxide in mice and guinea pigs, 20: 1593 (COO-1170-4)
**DAVISON, P. W.**, NERVA reactor experiment (NRX) reactor testing, 20: 3565
**DAVISSON, Charlotte M.**, Parameters for C-H albedo formula for gamma rays reflected from water, concrete, iron and lead, 20: 3274
**DAVOUST-SALTIEL, E.**, Drift mobility of radiation-induced defects in silicon, 20: 2507
**DAVYDOV, Yu. P.**, State of Pu(IV) at pH 1.0 to 12.0 and plutonium concentration $2 \times 10^{-5}$ M, 20: 1849
**DAWSON, John M.**, Kinetic structure of plasma, 20: 3164 (IPPJ-39)
**DAY, R. A.**, Measurement of Stark profiles of singly ionized nitrogen lines from T-tube plasma, 20: 3215
**DE BACKER, W.**, Reactor power reduction in minimum time including restriction of xenon poisoning, 20: 3372 (EUR-2506.e)
**DEBERTIN, Klaus**, Reactions $^{58}Ni(n,p)^{58}Co$ and $^{27}Al(n,p)^{27}Mg$ at different neutron energies, 20: 3012 (IKF-11)
**DEBOIS, Jean M.**, Proton radiobiology, 20: 1707
**DE BORTOLI, M.**, Environmental radioactivity, Ispra 1964, 20: 2047 (EUR-2509.e)
**DE CARLO, V. A.**, Irradiation evaluation of fuel elements for PBRE and AVR reactors, 20: 2464
**DE CARVALHO, H. G.**, $^{238}U$ fission induced by low-energy monochromatic $\gamma$-rays, 20: 3050
**DEELEY, T. J.**, Exit doses for lung fields measured by LiF thermoluminescence, 20: 1699
**DE FORCRAND, M.**, Dehydration and decomposition of hydrates of uranyl nitrate. Formation of a monohydrate, 20: 1821 (AEC-tr-6620)
**DE FOREST, R. D.**, EBR-II dynamics, 20: 3590
**DEGERING, Ed. F.**, High-energy electron irradiation of trihydroperfluoroalkyl acrylate monomers, 20: 1911
**DE HAAN, W.**, New lattice calculation method for ORGEL-type reactors, 20: 3424
**DE HALAS, D. R.**, FFTF driver fuel—$PuO_2$ stainless-steel cermet, 20: 3588
**DE HALAS, D. R.**, Safety and nuclear considerations in design of FTR, 20: 3581 (BNWL-SA-340)
**DEICHSEL, H.**, Angular dependence of polarization of 3.5 ev electrons on free Hg atoms, 20: 2615
**DEILY, G. J.**, Evolution of high-level caves at the Savannah River Laboratory, 20: 2000
**DEINET, W.**, Measurement of $\beta$-$\gamma$ angular correlation for $^{198}Au$, 20: 3129
**DEISS, J. L.**, Effects of neutron and proton bombardments on the exciton spectrum of $Cu_2O$, 20: 2505
**DELAHAYE, R. P.**, Space explorations and the radiation belts, 20: 2663
**DELBOURGO, R.**, Mass formulae in U(6) ⊗ U(6) theory, 20: 2752 (IC/65/77)
**DEL GROSSO, Anthony**, Brazed graphite-metal composites for space radiators, 20: 2294
**DELSON, E. B.**, 630A–Mark IV. A nuclear fueled steam generator-superheater for merchant ship propulsion, 20: 3546 (GE-TM-64-12-12)
**DE MARIA, R.**, Isochronal recovery of work hardening in aluminum–alumina alloys, 20: 2375
**DEMARMELS, P.**, Measurements of generation-time variations, 20: 3386
**DE MASTRY, John A.**, Corrosion studies of tungsten, molybdenum and rhenium in lithium, 20: 2269
**DE MASTRY, John A.**, Preparation of ceramic-refractory metal seals for space power systems, 20: 2292
**DEMCHUK, K. M.**, Effect of uniform compression on Curie temperature of ferromagnetic compound EuO, 20: 3313
**DEMIDOV, V. S.**, Production of slow $\pi$ mesons on light nuclei and the $\pi$-$\pi$ interaction, 20: 2739
**DEMINE, O.**, Bibliography concerning transplutonium elements, 20: 1726
**DEMINT, Robert J.**, Radiochemical determination of $^{90}Sr$ in water using ion exchange, 20: 1754
**DEMIRKHANOV, R. A.**, Binding energy anomalies for last two neutrons in region N = 86–92, 20: 3098
**DEMKOV, Yu. N.**, Electron detachment in slow collisions between negative ions and atoms. II., 20: 2648
**DEMOCRITUS, N. R. C.**, First excited state of $^5He$, 20: 3078
**DEMYOKHIN, V. F.**, Satellites of x-ray spectra, 20: 2645
**DENAYER, M.**, Effect of fast neutron bombardment on electrical properties of p- and n-type silicon carbide, 20: 2503
**DENISOV, F. P.**, Angular and energy distributions of $^{18}F$ recoil nuclei in reaction $^{19}F(\gamma,n)^{18}F$, 20: 3108
**DENISOV, V. P.**, Investigation of reaction $^{16}O(\gamma,p)^{15}N$, 20: 3107
**DENNIS, Richard**, Performance of air cleaning system for U. S. Bureau of Mines Bomaec-30 incinerator, 20: 1989 (NYO-841-2)
**DEONIGI, D. E.**, Comparison of fuel cycles for crossed-progeny fuels in conventional and novel configurations, 20: 3512
**DEONIGI, Duane E.**, Calibration of high-speed burnup code for nuclear fuel surveys, 20: 3455
**DEONIGI, Duane E.**, New fuel configuration to increase plutonium value in thermal reactors, 20: 3457
**DE PLANO, A.**, Purification of uranium from fission products by means of fractional precipitation of $UO_2$ by reduction of $UO_2Cl_2$ from alkali chloride melt, 20: 1962
**DERAMIX, P.**, Comparison of analysis with experiment for Saxton plutonium critical experiments, 20: 3389
**DERBENEV, Yu. S.**, Effects in electromagnetic interactions of particles with colliding clusters, 20: 2529

**DEROME, JeanRobert,** Racah algebra for an arbitrary group, 20: 2775
**DE ROOST, E.,** Precise redetermination of $P_K\omega_K$ value and fluorescence yield of Cr, 20: 2593 (EUR-2524.e)
**DES HAIES, R.,** Fission-product gas pressures in $UO_2$ fuel elements during irradiation, 20: 2462
**DE-SHALIT, A.,** Nuclear models and electromagnetic properties of nuclei, 20: 3148
**DE SHONG, James A. Jr.,** Optimum design of high-pressure, large-diameter, direct-nuclear-pumped, gas lasers, 20: 2591 (ANL-7030)
**DE STAEBLER, H.,** Semi-empirical shielding method for high-energy electron accelerators, 20: 2555
**DEUTSCH, R. V.,** Relativistic generalization of plasma waves theory in magnetohydrodynamic approximation of two fluids, 20: 2838
**DEUTSCH, R. W.,** Measurement and analysis of SM-1A core-3, 20: 3503
**DE VAN, J. H.,** Compatibility of refractory metals with boiling alkali metals, 20: 2236
**DE VAN, J. H.,** Compatibility of some refractory alloys in flowing nonisothermal lithium, 20: 2238
**DE VAN, J. H.,** Screening tests of turbine nozzle and blade materials, 20: 2240
**DEVIDAS, Roger,** Cooling apparatus for nuclear reactor, 20: 3537
**DEVLIN, James J.,** Auroral spectrograph data, 20: 2851
**DEVREESE, J.,** New approach to continuum polaron theory, 20: 3277 (BLG-328)
**DE WAARD, H.,** Shape of 962 kev beta spectrum of $^{198}Au$, 20: 3055
**DE WITT, Landis,** Tables of capacitor discharge in transient $\gamma$ radiation environments, 20: 2410 (AD-617918)
**DEY, Arun K.,** Chromotrope 2B in photometric determination of rare earths, 20: 1772
**DEZSI, I.,** Investigations of ordering transformation in $Fe_3Al$ alloy by Moessbauer effect, 20: 3292
**DHANESWAR, M. R.,** Extraction of thorium, protactinium, uranium, ruthenium, and zirconium by long-chain amines, 20: 1761
**DIACONESCU, Aurelian,** Angular correlation between prompt neutrons and fission fragments, 20: 3025
**DIAMOND, R. M.,** Extraction of $HClO_4$ by trilauryl amine. I., 20: 1747 (UCRL-11616(Rev.))
**DIAZ, Hildebran,** Digital computer controlled data-acquisition and processing system for nuclear experiments, 20: 2996
**DIBIASE, James A.,** Combined convection and radiation in radioisotope thrustors, 20: 2007 (AD-618026)
**DICKERMAN, C. E.,** Fast reactor safety experiments on EBR-II samples in flowing sodium environment, 20: 3506
**DICKSON, James J.,** Nuclear reactor with improved core arrangement facilitating loading and unloading of fuel assemblies and control rod assemblies, 20: 3578
**DIDDENS, A. N.,** Real part of proton-neutron scattering amplitude at 19.3 Bev, 20: 2712
**DIGESU, F. J.,** Lateral strain behavior of graphite—an anisotropic material, 20: 2315 (CONF-650632-3)
**DI GREGORIO, Ronald F.,** Techniques of magnetic-field measurement, 20: 2105 (UCRL-16357(Rev.))
**DIJKMAN, F. J. M.,** Analysis of boiling system dynamics, 20: 3532
**DI LEONE, Gilbert Robert,** Nature of recognition of antigenic determinants, 20: 1680
**DIMITROV, M.,** Concentrated serial irradiation method for treating carcinoma of the skin, 20: 1718
**DIMMOCK, J. O.,** Electronic band structure and optical properties of rare-earth metals, 20: 2592 (BNL-9556)
**DIMOND, W. J.,** Development of photogrammetric techniques for measuring surface contours of small samples, 20: 2033
**DI STEFANO, J. R.,** Compatibility of refractory metals with boiling alkali metals, 20: 2236
**DISTENFELD, Carl,** Skyshine consideration for accelerator shielding design, 20: 2552
**DITTO, S. J.,** Control system for gas-cooled nuclear power plant, 20: 3480 (ORNL-P-1679)
**DIXON, C. E.,** Radiation effects on materials at liquid-hydrogen temperature, 20: 2459
**DMITIRIEVSKII, V. P.,** Strong-current high-energy particle accelerators—meson factories, 20: 2560
**DMITRENKO, I. M.,** Interaction of alternating Josephson current with resonant modes in superconducting tunnel structure, 20: 2895
**DMITRIEV, I. S.,** Calculation of effective cross section for loss of K-electrons by fast hydrogen-like ions during encounters with hydrogen and helium atoms, 20: 2642
**DODD, W. P.,** $\Omega^-$ particle produced by 6-Bev $K^-$ meson in hydrogen, 20: 2717
**DOE, C. B.,** Fuel-element failure detection in EBR-II, 20: 3518
**DOEBNER, H. D.,** Approach to electron-pion scattering, 20: 2678 (AD-614843)
**DOLGOV, A. S.,** Profound stripping and scattering of $Kr^+$ ions in single collisions with Ne, Ar, Kr and Xe atoms, 20: 2644
**DOMINEY, D. A.,** Radiolytic reaction between graphite and carbon dioxide. VI., 20: 1895 (AERE-R-4988)
**DONAHUE, D. J.,** Mean lives of excited states in $^{14}N$, 20: 3045
**DONATO, L.,** Electrochemical labeling of proteins, 20: 1939 (EUR-2476.i)
**DONCALS, R.,** Comparison of analytical and experimental power distribution of NERVA reactors, 20: 3568
**DONER, J. E.,** Estimation of fire damage to non-urban areas from nuclear attack, 20: 1590 (RM-3902-TAB)
**DONNACHIE, A.,** Evidence for pion-nucleon inelastic $S_{31}$ resonance, 20: 2716
**DONOVAN, John Leo,** Measurement of phonon frequency distribution for polyethylene by neutron scattering, 20: 3315
**DORN, J. E.,** Effect of temperature, strain rate and structure on flow stress of an iron–2 percent manganese alloy, 20: 3641 (UCRL-11512(Rev.))
**DOROKHOV, V. V.,** Binding energy anomalies for last two neutrons in region N = 86–92, 20: 3098
**DORST, Joseph H.,** Magnet design applications of magnetostatic computer program called SIBYL, 20: 2546 (UCRL-16389)
**DOSCH, H. G.,** Low energy baryon-nucleon scattering, 20: 2707
**DOSCHENKO, N. M.,** Radiation-induced brain necrosis (clinical observation), 20: 1713
**DOSHI, P. K.,** Pulse-propagation experiments using fast-burst reactor, 20: 2955
**DOSORTSEVA, R. L.,** Effect of space flight factors on Evonymys europaea seeds, 20: 1649
**DOULAT, Jacques,** Improvements in or relating to irradiation enclosures for swimming pool type reactors, 20: 3602
**DOUMAS, M.,** Fatigue and burst tests on irradiated in-pile stainless steel pressure tubes, 20: 2435 (WAPD-T-1720)
**DOYLE, R. J.,** Glucose control of an x-radiation-induced difference in $CO_2$ production by yeast cells, 20: 1653
**DRAKE, M. K.,** UNPACK. Neutron cross section data retrieval program, 20: 3009 (GA-6685)
**DRAWIN, H. W.,** Population densities of excited hydrogen levels in stationary plasmas with regard to diffusion of neutral particles, 20: 3223
**DRAWIN, Hans-Werner,** Data for plasmas in local thermodynamic equilibrium, 20: 3235
**DRAWIN, Hans-Werner,** Mechanical time shutter for spectrograph with exposure times from 1.5 $\mu$s to 3 ms, 20: 2125 (CEA-R-2861)
**DRESSELHAUS, M. S.,** de Haas-van Alphen effect in pyrolytic and single-crystal graphite, 20: 3300
**DRESSLER, S.,** Late changes of skin after irradiation of haemangiomas, 20: 1719
**DROBNJAK, DJ.,** Surface structure in beta-quenched uranium, 20: 2377
**DROBOT, D. V.,** System $YCl_3$–NaCl–KCl, 20: 1872
**DROUIN, R. S.,** New levels in $^{58}Co$, 20: 3077
**DROWART, J.,** Thermodynamic study of the uranium–oxygen system by mass spectrometry. Heat of sublimation of uranium, 20: 1810 (EUR-2458.f)
**DRUMHELLER, K.,** Remote refabrication of reactor fuels, 20: 2282 (HW-SA-3755)
**DRUMMOND, J. L.,** Comparison of procedures for dissolving ignited plutonium oxides for analysis, 20: 2344 (TRG-Report-1072)
**DRUYVESTEYN, W. F.,** New kind of transverse voltage in type II superconductor, 20: 2897
**DUBASOV, Yu. V.,** Physico-chemical studies of some Ra compounds. I., 20: 1852
**DUBININA, A. N.,** Magnetic mirror trap for prolonged confinement of electrons, 20: 3225
**DUBOVIK, V. M.,** Scattering of electrons on particles with higher spins, 20: 2799
**DUBUISSON, Jacques,** Improvements in refractory uranium compounds, 20: 2250
**DUDLEY, T. E.,** Infinite medium spectrum-weighted group constants for gamma heating calculations, 20: 3268
**DUEREN, R.,** Measurement of velocity dependence of total scattering cross sections for scattering of He, $H_2$, and $D_2$ molecular beams on rare gases, 20: 2614
**DUFFEY, Dick,** Determination of interplanar spacings in polymers using single-neutron diffraction, 20: 3308
**DUFFEY, Dick,** Neutronic isolation characteristics of concrete, lead, wood, polyethylene and beryllium, 20: 3390
**DUFFY, D.,** Effectiveness of linear arrays of absorber tubes as control-rod blades, 20: 3400
**DUISEBAEV, A.,** Angular and energy distributions of $^{18}F$ recoil nuclei in reaction $^{19}F(\gamma,n)^{18}F$, 20: 3108
**DULLOW, R. J.,** Thermal resistance due to microcracking in neutron-irradiated beryllium oxide, 20: 2443
**DUMAZET, Gerard,** Analogous isobaric states of $^{41}Ar$ in $^{41}K$, 20: 3036
**DUNAVANT, B. G.,** Low-temperature adsorption and $\gamma$ scintillation spectrometry for measuring $^{41}Ar$, 20: 1763
**DUNCAN, I.,** Correlation of ESR centers and optical absorption bands in electron-irradiated diamond, 20: 2493

**DUNCAN, R. N.,** Development fuel assembly irradiation testing in Big Rock Point Reactor, 20: 3452
**DUNCAN, R. N.,** Fuel performance in boiling-water reactors, 20: 3497
**DUNCAN, R. N.,** Performance of defected low-density powder $UO_2$ fuels in reactor service, 20: 2232
**DUNCAN, R. N.,** Remotely operable fuel-rod profilometer, 20: 1993
**DUNFORD, Charles L.,** Criticality of $^{244}Cm$, 20: 2995
**DUNLAP, J. L.,** Lorentz dissociation of $H_I^+$ in DCX-1, 20: 3213
**DUNN, Gordon H.,** Dissociation of $H_2^+$ by electron impact, 20: 2632
**DUNSWORTH, R. J.,** Improved metallic fast power breeder fuels, 20: 2386
**DUPZYK, R. J.,** Use of $^{14}C$ to measure $CO_2$ removal in a synthetic ammonia plant, 20: 1836
**DUTEIL, P.,** Double charge exchange with negative pions. Search for tetraneutron, 20: 3080
**DVORAK, Robert F.,** Neutron monitor for simultaneous measurement of fluence and dose equivalent, 20: 2123 (ANL-7085)
**DVORIANTSEVA, G. G.,** Isotopic exchange of hydrogen atoms in cyclopentadienyl rings of cobalticinium compounds, 20: 1828
**D'YACHENKO, P. P.,** Kinetic energies of fragments with various masses in fission of $^{235}U$ by thermal and fast neutrons, 20: 3110
**D'YAKOV, I. G.,** Change of beryllium properties after aging treatment, 20: 2363
**DYATLOV, I. T.,** Certain mass formulas in Quark model, 20: 2807
**DYATLOV, I. T.,** Three-particle partial amplitudes and unitarity conditions for complex values of angular moments, 20: 2811
**DYE, D. L.,** Fractional cell lethality approach to space radiation hazards, 20: 1616 (NASA-SP-71, pp 219-23)
**DYE, J. L.,** Correlated EPR-optical spectra of potassium in ethylamine–ammonia mixtures, 20: 1808 (COO-958-5)
**DYER, Norman C.,** Neutron monitor for simultaneous measurement of fluence and dose equivalent, 20: 2123 (ANL-7085)
**DYMENT, J.,** Sodium flame photometer test for high-efficiency filters, 20: 2077 (AWRE-O-41/65)
**DYOS, M. W.,** Effective thermal-neutron cross sections for materials with grain structure, 20: 2993
**DZANTIEV, B. G.,** Formation of polymers labeled with $^{14}C$ during ethylene-ammonia irradiated in nuclear reactor, 20: 1922
**DZHELEPOV, B. S.,** Determination of intensities and multipolarities in high-energy $^{182}Ta$ decay $\gamma$ transitions, 20: 3112
**DZHELEPOV, B. S.,** Energies and relative intensities of 2201, 2490, and 2508 kev $\gamma$ lines in spectrum of $^{72}Ga$, 20: 3040
**DZHELEPOV, V. P.,** Scattering of $p\mu$ atoms on protons, 20: 2640
**DZHELEPOV, V. P.,** Strong-current high-energy particle accelerators—meson factories, 20: 2560
**DZHIBUTI, R. I.,** Photodisintegration theory for lightest nuclei, 20: 3105
**DZHIKIDZE, E. K.,** Immunological reactivity in monkeys after recovery from acute radiation sickness, 20: 1631
**DZYUB, I. P.,** Role of rotational states in scattering of slow neutrons by gas molecules, 20: 3135

# E

**EASTHAM, J. F.,** Nitration and succinoylation of tritium-labeled toluene, 20: 1950
**EBENS, A. J.,** Operational modes anticipated for converted n-reactor interplant operating restrictions (preliminary), 20: 3541 (RL-NRD-81(Suppl. 1))
**ECCLESHALL, D.,** $h_{11/2}$ Single proton hole state in $^{207}Tl$, 20: 3071
**ECH, F. A.,** Elastic backward scattering of $\pi^-$ by neutrons, 20: 2700
**ECKERT, H. G.,** Decay of $^{58}Co$, $T_{1/2}$ = 18hr, 20: 3132
**ECKHAUSE, M.,** New measurement of lifetime of the positive pion, 20: 2714
**EDER, O. J.,** Cooperative modes of motion in simple liquids, 20: 2837
**EDWARDS, G. W.,** Prog. rpt. on fabrication and properties of W single crystals, final, 3/64–2/65, 20: 2284 (NP-15093)
**EDWARDS, Steve,** Direct reaction analysis of $^{15}N(p,\alpha_0)^{12}C$ reaction, 20: 3061
**EFINGER, Helmut J.,** Self-energy and charge of particle stabilized by gravitational action in curved space, 20: 2886
**EFREMOV, A. V.,** Algebra of the currents and dispersion relations, 20: 2755 (JINR-E-2329)
**EGELSTAFF, P. A.,** Cooperative modes of motion in simple liquids, 20: 2837
**EGOROV, Yu. V.,** Radiocolloids in sorption systems. II., 20: 1968
**EHMANN, W. D.,** Automated system for rapid and precise fast neutron activation analysis, 20: 1765
**EICHELBERGER, T. W.,** Embrittlement of irradiated pressure vessel steels. I., 20: 2436 (WERL-8844-4)
**EICHELBERGER, T. W.,** Sensitivity to irradiation damage—pressure vessel steels. III., 20: 2437 (WERL-8844-6)
**EICHLER, J. B.,** Prog. rpt. on reactor containment, 10/64–7/65, 20: 3324 (IITRI-578P21-13)
**EIDMAN, V. Ya.,** Damping of longitudinal waves in inhomogeneous plasma, 20: 3226
**EIDMAN, V. Ya.,** Radiation of fast-moving charges in wave-damping medium in non-homogeneous plasma, 20: 3198
**EILENBERG, HANNS,** Drying process and apparatus therefor for removing solids from liquid mixtures, 20: 3607
**EINHORN, F.,** Influence of physiological inoculum age on growth of microbe culture in $H_2O$ and 50% $D_2O$, 20: 1601
**EISBERG, R. M.,** Polarization in elastic scattering at backward angles of 30-Mev protons from deuterons, 20: 2706
**EISEN, F. H.,** Radiation damage in semiconducting III-V compounds, 20: 2497
**EISMONT, V. P.,** Angular anisotropy of fission by sub-barrier deuterons, 20: 3122
**EKSPONG, A. G.,** Search for $Y_8^8$ production in K⁻ captures in nuclei, 20: 3064
**ELBAUM, Jerome K.,** Refractory metals—an assessment, 20: 2307 (AD-613023)
**ELBEL, M.,** Cross section of spin exchange between $^{85}Rb$ and $^{87}Rb$, 20: 2613
**ELFORD, M. T.,** Precision measurements of the Townsend energy ratio for electron swarms in highly uniform electric fields, 20: 2825
**ELIOFF, T.,** Improved Bevatron and its performance at high intensity, 20: 2541 (UCRL-16228)
**ELISEEV, G. P.,** Elastic backward scattering of $\pi^-$ by neutrons, 20: 2700
**ELISEEV, G. P.,** $\pi^-$ meson-neutron elastic backward scattering at 1.4 to 4.0 Bev, 20: 2713
**EL-KINAWI, S. A.,** Preparation of $^{131}I$-labeled insulin and isolation by gel filtration, 20: 1890
**ELLETT, W. H.,** Dose models for evaluating the radiation hazard from reactor debris, 20: 2091
**ELLIOTT, J. P.,** Inter-nucleon potential deduced from shell model calculations, 20: 3068
**ELLIOTT, J. P.,** Pairing forces with neutrons and protons, 20: 3066
**ELLIS, John G.,** System design in low background internal gas sample counting of $^{14}C$ and tritium, 20: 2179
**ELLS, C. E.,** Effect on neutron irradiation and hydrogen concentration on tensile properties of CANDU coolant tube spacer alloy, 20: 2414 (AECL-2272)
**EL-NADI, M.,** Semiclassical theory of polarization in direct nuclear reactions. II., 20: 3049
**ELSTON, K. E.,** Control features of Canadian nuclear generating stations, 20: 3533
**EL-WAKIL, M. M.,** Visual and frictional pressure-drop study of natural-circulation single-component two-phase flow at low pressures, 20: 2021
**ELY, Richard,** Strength of graphite tube specimens under combined stresses, 20: 2372
**EMELITY, L. A.,** Operational practices in treatment of low and intermediate level radioactive wastes—Argonne and Los Alamos Laboratories, U. S. A., 20: 3603 (LA-DC-7249)
**ENCHEVICH, I. B.,** Duty cycle improvement of particle beams at 680-Mev JINR synchrocyclotron, 20: 2548
**ENCHEVICH, I. B.,** Possibility of stabilization of synchrocyclotron intensity, 20: 2536 (JINR-P-2341)
**ENG, K. Y.,** Re-entry burnup of SNAP-10A reactor fuel elements, 20: 3560
**ENGEL, J. R.,** Application of on-line digital computer to reactor experiment, 20: 3591
**ENGEL, J. R.,** Predicted and observed nuclear characteristics of Molten Salt Reactor Experiment, 20: 3505
**EPEL, L. G.,** Rotating fluidized-bed research reactor, 20: 3598
**EPSTEIN, R. B.,** Bone marrow transplantation in acute leukemia, 20: 1700
**ERDMAN, Howard E.,** Fast neutron effects on productivity of young and old flour beetles, 20: 1613 (HW-SA-3537)
**ERDMANN, R. C.,** Time-dependent monoenergetic neutron transport in two adjacent semi-infinite media, 20: 2987
**EREMENKO, V. N.,** Capillary phenomena in densification process during sintering in presence of liquid phase, 20: 2286
**ERGIN, Yu. V.,** Magnetostriction in gadolinium crystal, 20: 3312
**ERICKSON, Nils Eric,** Study of bonding in iron compounds using the Moessbauer effect, 20: 1874
**ERICKSON, R. B.,** Metallurgical characteristics of weldments in 0.750-inch-thick 6061 aluminum, 20: 3609 (ACF-11)
**ERMOLOV, P. F.,** Scattering of $p\mu$ atoms on protons, 20: 2640
**ERNST, W. P.,** A ferromagnetic resonance magnetometer, 20: 2104 (MATT-362)
**ERWALL, L. G.,** Radiotracer studies of industrial processes and waste discharges, 20: 2201
**ESCAIG, B.,** Internal friction at high temperatures and diffusion of vacancies between dislocations, 20: 3281(T) (MLM-1276(tr))
**ESCAVIS, Armand,** Automatic tilting device for radioactive articles, 20: 2002
**ESCHEN, V. G.,** Startup experience with the EBR-II fuel cycle facility. III., 20: 2297
**ESIKOV, V. I.,** Studies of startup conditions of I. V. Kurchatov Beloyarsk

Nuclear Power Station performed at test rig, 20: 3486
**ESKREYS, A.,** Interaction of $\pi$ mesons with nucleons in the accelerator energy region, 20: 2725
**EVANGELISTI, Roberto,** Thermal conductivity of sodium from 90 to 850°C, 20: 2370
**EVANS, Albert E. Jr.,** Application of anticoincidence-shielded scintillation spectrometer to study of $^{14}N(p,\gamma)^{15}O$ reaction, 20: 3006 (AD-618676)
**EVANS, Hilton B.,** Factors influencing permeability and diffusion of radon in synthetic sandstones, 20: 1878
**EVANS, J. L.,** Feasibility study on use of powders as heat transfer media in irradiation capsules, 20: 2018 (TRG-Report-920)
**EVANS, Robley D.,** Application of Li-drifted Ge detectors to neutron activation analysis—studies in geochemistry and of 15th century printing, 20: 2166
**EVRARD, R.,** New approach to continuum polaron theory, 20: 3277 (BLG-328)
**EVSYUKOV, V. I.,** Effect of x rays on regenerative capacity of irradiated nerves, 20: 1635
**EWING, C. T.,** High-temperature properties of sodium, 20: 1815 (NRL-6241)
**EXLEY, J.,** Nuclear fuel management, 20: 3530
**EYRE, B. L.,** Effects of irradiation in iron and steels, 20: 2474
**EYRE, B. L.,** Nature and annealing behavior of irradiation damage in molybdenum, 20: 2476

## F

**FAHMY, A. R.,** Effect of radiation on nuclear phosphorylation in human malignant tumors, 20: 1626
**FAIRCHILD, R. G.,** Development and dosimetry of an epithermal neutron beam. I., 20: 1714
**FAIRCHILD, R. G.,** Response of skin of swine to increasing exposures of 250 kvp x rays, 20: 1609 (BNL-9477)
**FAKIROV, D. G.,** Mass formula in SU(12) contains Sp(6) × SU(2) symmetry, 20: 2756 (JINR-P-2342)
**FAM-K'UI-TU,** Asymptotic equality of the cross section of $\pi^{\pm}$ meson generation from the neutrino and antineutrino, 20: 2733
**FAN, H. Y.,** Radiation damage in semiconductors, 20: 2481
**FANG, P. H.,** Field and charge dependence of radiation damage in silicon, 20: 2511
**FANUCCI, Jerome,** Explosion of a supernova into the interstellar magnetic field. II., 20: 2570
**FARKASCH, G.,** Commissioning programmes and procedures, 20: 3529
**FARMER, B. J.,** Bremsstrahlung production in thick aluminum and iron targets by 0.5- to 3.0-Mev electrons, 20: 3247 (NASA-SP-71, pp 449-53)
**FARQUHAR, R. M.,** Lead isotope ratios from the Cobalt-Noranda Area, Canada, 20: 2051
**FARRAR IV, H.,** Structure in Doppler effect as a function of surface, mass ratio in $^{107}Ag$, 20: 2975
**FAUDROWICZ, Adam,** High-energy $\gamma$-ray astronomy, 20: 2586
**FAUGERAS, Pierre,** Improvements in remote control and automation devices for plant in radioactive surroundings, 20: 2003
**FAUGERAS, Pierre,** Preparation of uranium compounds from uranium–molybdenum alloys, 20: 1885
**FAULKNER, J.,** Surface boundary condition for stars, 20: 2581
**FAUSER, Friedrich,** Drying process and apparatus therefor for removing solids from liquid mixtures, 20: 3607
**FAVORIN, V. N.,** Stepwise excitation of fluorescence of $CaWO_4$ activated with $Er^{3+}$, 20: 1842
**FAVORSKAYA, M. P.,** Devices for spectral-isotopic determination of gases in metals, 20: 1793
**FAW, R. E.,** Charged-particle slowing-down spectra for fast-neutron irradiation of water, 20: 1924
**FEDEROV, G. B.,** Value of self-diffusion parameters of zirconium, 20: 2356 (AERE-Trans-1030)
**FEDORENKO, A. L.,** Mechanism of formation of growth textures in beryllium, 20: 3306
**FEDORENKO, N. V.,** Ionization produced in collisions between alkali metal atoms and gas molecules, 20: 2639
**FEDOSEEV, V. M.,** Action of protective agents following irradiation with sublethal doses, 20: 1688
**FEDOTOV, P. I.,** Absorption of stopped $\pi^-$ mesons by carbon nuclei, 20: 3123
**FEDYANIN, O. I.,** Influence of toroidal drift on plasma injection transversely to magnetic field, 20: 3205
**FEHSENFELD, F. C.,** A new speculation on terrestrial helium loss, 20: 2857
**FEINBERG, E. L.,** Cosmic rays and the physics of elementary particles, 20: 2665
**FEISEL, Lyle Dean,** Conduction characteristics of tantalum oxide films, 20: 2405
**FELDES, J. G.,** Low-power shield measurements on Enrico Fermi reactor, 20: 3524
**FELDMAN, M. J.,** Remote determination of gas pressure and volume for encapsulated fuel elements, 20: 2116
**FELDMAN, M. J.,** Startup experience with the EBR-II fuel cycle facility. III., 20: 2297
**FELENBOK, Paul,** Data for plasmas in local thermodynamic equilibrium, 20: 3235
**FELT, R. E.,** Design evaluation of fused-salt molten-metal extractor, 20: 2245
**FELTGEN, R.,** Measurement of velocity dependence of total scattering cross sections for scattering of He, $H_2$, and $D_2$ molecular beams on rare gases, 20: 2614
**FERGUSON, A. T. G.,** Recent advances in radiation detectors, 20: 2177
**FERGUSON, E. E.,** A new speculation on terrestrial helium loss, 20: 2857
**FERRARA, Anthony S.,** Uranium dioxide fuel tubes for irradiation in VBWR, 20: 2280 (DP-989)
**FERRARI, H. M.,** Behavior of water vapor in $UO_2$ during irradiation, 20: 2468
**FERREIRA, Carlos P.,** Fractionation of U isotopes and daughter products in U-bearing sandstone, 20: 2057
**FERREL, Robert E.,** Bulgur wafer and adjuncts for fallout shelter rations, 20: 2067 (AD-614824)
**FERRIER, Charles,** System for mechanically mounting a radioactive sample, 20: 2006
**FERRO-LUZZI, M.,** Spin, parity and isospin of Y*(1760), 20: 2711
**FERRY, James Allen,** Measurement of resonance widths in $^{27}Al(p,\gamma)^{28}Si$, reaction, 20: 3142
**FETT, Walter,** Initial analysis of fission products over Berlin from Chinese test of October 16, 1964, 20: 2050
**FEUER, P.,** Quantum theory of vibrational energy exchange and effect of an attractive potential, 20: 2594 (N64-23208)
**FIEDLER, W.,** Diffusion of fission-product $^{147}Pm$ in aluminum oxide, 20: 2364
**FIELD, George B.,** Statistical model of formation of stars and interstellar clouds, 20: 2574
**FIELD, George B.,** Thermal instability, 20: 2573
**FIETZ, W. A.,** Electronic integration technique for measuring magnetization of hysteretic superconducting materials, 20: 2913
**FIKS, M. M.,** Acceleration of particles with variables charges in an electrostatic field, 20: 2561
**FILCHENKOV, V. V.,** Scattering of $p\mu$ atoms on protons, 20: 2640
**FILIPPOV, A. P.,** Kinetics of $UO_2$ and Fe(III) reactions in perchloric acids, 20: 1851
**FILIPPOV, E. A.,** Extraction of U(VI) from carbonate solutions by quaternary phosphonium and arsonium bases, 20: 1782
**FINCH, L. M.,** Fast-flux test facility design concept, 20: 3596
**FINCH, L. M.,** Safety and nuclear considerations in design of FTR, 20: 3581 (BNWL-SA-340)
**FINER, S.,** Interactive effects of x irradiation and barbiturates, 20: 1662
**FINN, R.,** Symposium on applied mathematics, New York City, 4/64, 20: 2530
**FINNEGAN, L. J.,** Analytical model for predicting pressure-temperature history within containment vessel in response to loss-of-coolant accident, 20: 3337
**FINNEGAN, L. J.,** Influence of zirconium cladding on loft loss-of-coolant test, 20: 3334
**FINZI, Arrigo,** Vibrational energy of neutron stars and exponential light curves of type-I supernovae, 20: 2584
**FIORE, L.,** $^{238}U$ fission induced by low-energy monochromatic $\gamma$-rays, 20: 3050
**FIRSOV, E. I.,** $\gamma$-Spectrum from the reaction $^{54}Fe(n,\gamma)^{55}Fe$, 20: 3109
**FIRSOV, V. G.,** Effect of complex formation on reactions between positronium and inorganic ions, 20: 1844
**FISHER, D. E.,** Nondestructive activation analysis of cobalt in iron meteorites, 20: 2055
**FISHER, Edward,** Wave mechanics of free particle, 20: 2888
**FISHER, J. R.,** Adequacy of one-group three-dimensional model in core-following program, 20: 3501
**FISHER, J. R.,** Effectiveness of linear arrays of absorber tubes as control-rod blades, 20: 3400
**FISHER, J. R.,** Elk River lifetime—predicted and observed, 20: 3499
**FISK, C. J.,** "Accel" automated circuit card etching layout, 20: 3635 (SC-TM-65-544)
**FISKE, Susan,** Autoradiography of incorporation of tritiated leucine, 20: 1597
**FLAKS, I. P.,** Ionization produced in collisions between alkali metal atoms and gas molecules, 20: 2639
**FLAMMERSFELD, A.,** Decay of $^{55}Co$, $T_{1/2}$ = 18hr, 20: 3132
**FLAMMERSFELD, A.,** Delayed neutrons in decay of $^{9}Li$, 20: 3130
**FLAMMERSFELD, A.,** Electron capture in decay of $^{48}Ti$, 20: 3128
**FLANAGAN, Charles A.,** Few long-time-increment depletion calculations for approximating by synthesis many short-time-increment depletion calculation, 20: 3454
**FLANAGAN, Charles A.,** Prescription for diffusion-theory representation of fuel clusters containing control rods based on Monte Carlo correlation of

capture probabilities, 20: 3428
**FLANAGAN, T. M.,** Electron irradiation of p-type Ge at 0°C, 20: 2485
**FLATAU, Carl R.,** Development of servo-manipulators for high-energy accelerator requirements, 20: 2551
**FLECK, C. M.,** Low-level device for measurement of high-energy $\beta$-radioactive gases, 20: 2139
**FLECK, C. M.,** Propagation of thermal neutron bursts in diffusion media, 20: 2944
**FLEISCHMANN, Rudolf,** Gamma radiation in capture of thermal neutrons in $^{149}Nd$ by means of sum-coincidence method, 20: 3131
**FLEITMAN, A. H.,** Relative aggressiveness of Li, Na, K, Rb and Cs boiling and condensing in Nb–1Zr capsules, 20: 2268
**FLEMING, Ronald F.,** Limitations to applicability of restricted space, time-optimal xenon shutdown problem, 20: 3410
**FLESCH, Gerald D.,** Electronics in mass spectrometry, 20: 2100 (IS-1193)
**FLORES, J. Merlo,** Formation of defects at low temperature in Si irradiated by $^{60}Co$ $\gamma$ rays, 20: 2496
**FLURY, R. L.,** Weight, center of gravity, and moment of inertia of geometric solids, 20: 3633 (SC-TM-64-1686)
**FOELSCHE, H. W. J.,** Brookhaven radiofrequency beam separator, 20: 2532 (BNL-9505)
**FOELSCHE, Trutz,** Ionizing radiations in supersonic transport flights, 20: 2657 (NASA-SP-71, pp 287-99)
**FOGEL, N. Ya.,** Magnetic flux jumps in hard superconductors in pulsed magnetic fields, 20: 2921
**FOGGI, C.,** TESI—advanced power excursion reactor for research in reactor safety, 20: 3584 (EUR-2433.e)
**FOLEY, W. A.,** Urethan-induced lung tumors in mice: x-radiation dose dependent inhibition, 20: 1606 (AD-623079)
**FOLWELL, Philip A.,** Prog. rpt. on absolute pressure sensors, 20: 2059 (NVO-98-11)
**FOMIN, V. V.,** Mass spectra of system $\pi + \Delta_{1238}$, $\pi + \Sigma_{1385}$, and $\pi + \phi$, 20: 2741
**FOMINYKH, V. I.,** Problem of comparing neutron emitters of various spectral composition, 20: 2947
**FONER, S., de Haas-van Alphen effect in pyrolytic and single-crystal graphite,** 20: 3300
**FORD, J. L. C. Jr.,** Gamma-ray energies determined with lithium-drifted germanium detector, 20: 3043
**FORD, Leonard A.,** Relationship of wavelength of transfer system to quenching of radioisotopes in dyes, 20: 2189
**FOREY, Francois,** Improvements in machines for loading and unloading of the channels of nuclear reactor, 20: 3360
**FORSCHER, F.,** Development of $ThO_2$–pellet fabrication, 20: 2291
**FORTIN, Antoine,** Device for the transmission of movements and application of said device to remote-handling appliances, 20: 2004
**FORTIN, Marcel,** Device for the transmission of movements and application of said device to remote-handling appliances, 20: 2004
**FOSSAN, D. B.,** $^{17}O$ and $^{19}O$ lifetimes by particle-gamma coincidence technique, 20: 3156
**FOSTER, J. H.,** Relative toxicity of angiographic contrast media, 20: 1724
**FOSTER, James Sheridan,** Thermodynamics of Re–O and Mo–O systems and defect structure of alpha $Ta_2O_5$, 20: 1880
**FOULQUIER, Henri,** Apparatus for treating interior of a tubular element, 20: 2304
**FOWLER, C. M.,** Los Alamos flux compression program from its origin, 20: 3166 (LA-DC-7252)
**FOWLER, G. N.,** The positive excess of $\mu$ mesons at high energies, 20: 2702
**FOWLER, J. F.,** Exit doses for lung fields measured by LiF thermoluminescence, 20: 1699
**FOWLER, R. G.,** Lifetime of the $3^1P$ state of helium, 20: 2621
**FOWLER, William A.,** Synthesis and destruction of elements in peculiar stars of types A and B, 20: 2565
**FRAGOSO, J. H.,** BONUS reactor-operating performance, 20: 3520
**FRAIN, J. F.,** Prog. rpt. on supercritical reactor, 7–9/62, 20: 3485 (WCAP-2120)
**FRANC, Z.,** Measurement of soft $\beta$ radiation in biological material with aid of liquid scintillators. III., 20: 1758
**FRANCIS, J. M.,** Effect of Y on oxidation resistance of Fe–Cr base alloys, 20: 2263
**FRANCOIS, B.,** Grain growth in porous compacts, 20: 2373
**FRANK, A. L.,** Gamma radiation characteristics—angular distribution over a desert-terrain fallout field, 20: 2092
**FRANK, Burton V.,** Laboratory experimental analysis of $\gamma$ radiation effects on silicon alloy junction semiconductor diodes, 20: 2413 (AD-618688)
**FRANK, Clifford S.,** Transient effects in dielectric materials caused by electron irradiation, 20: 1897 (NASA-TN-D-3032)
**FRANK, Max,** Prog. rpt. on development of Q-factor technique, 1–3/65, 20: 2184 (AD-614618)
**FRANK, Max,** Prog. rpt. on development of Q-factor technique, 4–6/65, 20: 2185 (AD-618194)
**FRANK, P.,** Generation and prevention of severe radiation lesions, 20: 1717
**FRANK, R. G.,** Bearing materials for use in Rankine-cycle space power systems, 20: 3555
**FRANKE, H. G.,** Propagation of discharges in self-extinguishing counters. IV., 20: 2176
**FRANKEVICH, D. P.,** New compounds of $MgCu_2$ type in alloys of rare-earth metals with Fe, Co, and Ni, 20: 2385
**FRANKFURT, L. L.,** Calculation of the $\bar{\nu} + p \rightarrow n + \mu^+ + \gamma$ cross section, 20: 2736
**FRANKLIN, Allen David,** Photoproduction of rho mesons, 20: 2747
**FRANKLIN, E. W.,** Studies on monoclinic zirconium dioxide from room temperature to 1095°C, 20: 2314 (ARL-65-140)
**FRANZ, J.,** Mechanism of reaction $^{26}Mg(p,p',\gamma)$ at low energy, 20: 3092
**FRAZER, B. C.,** Neutron-diffraction study of antiferromagnetism in $UO_2$, 20: 3301
**FREDSALL, J. R.,** Near-optimum shutdowns for nuclear reactors, 20: 3438
**FREED, DeBow,** Effect of sample geometry on decay-constant measurements in water using pulsed-neutron technique, 20: 2952
**FREEMAN, A. J.,** Electronic band structure and optical properties of rare-earth metals, 20: 2592 (BNL-9556)
**FREEMAN, John R.,** Mathematical models of magnetic flux compression, 20: 2523 (SC-RR-65-449)
**FRENLING, Jean,** Apparatus for treating interior of a tubular element, 20: 2304
**FRENCH, J. B.,** Microscopic models for vibrational states in even nickel isotopes, 20: 3083
**FRESHLEY, M. D.,** Irradiation of $UO_2$–$PuO_2$ high-power-density fuel elements in PRTR, 20: 2449
**FREY, K. J.,** Recurrent irradiation for oat breeding, 20: 1665
**FRICHET, Jean-Pierre,** Results and interpretation of spectral indices measurements made with aquilon, 20: 3582 (CEA-R-2482)
**FRIED, H. M.,** $\phi$ suppression in K⁻p reactions, 20: 2719
**FRIED, H. M.,** Survey and classification of soluble field theory models, 20: 2757 (NYO-2262-98)
**FRIEDBERG, A. L.,** Semiconductivity in glass systems $V_2O_3$–$P_2O_5$ and $V_2O_5$–$P_2O_5$, 20: 2316 (COO-1198-220)
**FRIEDBERG, Felix,** Prog. rpt. on chemical effects of ionizing radiation on individual amino acids, 10/65, 20: 1604 (TID-22291)
**FRIEDEL, H.,** MHD of quasineutral plasma with vanishing internal friction and heat conductivity and finite electrical conductivity, 20: 3159 (AD-618138)
**FRIEDLAENDER, E.,** Transverse momentum distribution in high-energy meson production, 20: 2681 (IFA-CR-55)
**FRIEDRICH, K.,** Absolute standardization of electron-capturing radionuclide $^{54}Mn$ by $4\pi X(PC)$- and $4\pi(X,e_K)$-$\gamma$-measurements, 20: 3034
**FRIES, B. A.,** Use of $^{14}C$ to measure $CO_2$ removal in a synthetic ammonia plant, 20: 1836
**FRIES, N.,** Thermosensitizing effect of uv and x irradiation on cells of ophiostoma and rhodotorula, 20: 1640
**FRISCH, H. L.,** Quantum mechanical microscopic Brownian motion, 20: 2881
**FRISK, A.,** Search for $Y\bar{\beta}$ production in K⁻ captures in nuclei, 20: 3064
**FRITTS, Martin,** Radiation facility support and solid-state studies, 20: 2531 (AD-618304)
**FRONTASEV, V. P.,** Water solubility of complex compounds of lanthanum, cerium, praseodymium, neodymium, and samarium acetates with thiourea, 20: 1869
**FROSCH, R.,** Inelastic electron scattering from alpha particle, 20: 3086
**FROSCH, Reinhart,** Empirical mass formula involving the electron mass, 20: 2750 (AD-618659)
**FROST, D. C.,** Photoelectron spectroscopy with a spherical analyzer. Vibrational energy levels of $H_2^+$, 20: 2633
**FRUH, Erwin Gustav,** Cesium sorption by hydrobiotite, 20: 1879
**FRYER, R. M.,** Startup experience with the EBR-II fuel cycle facility. II., 20: 3523
**FRYXELL, R. E.,** Determination of melting point of $UO_{2+x}$, 20: 2390
**FRYXELL, R. E.,** High-temperature studies of urania in a thermal gradient, 20: 2233
**FRYXELL, R. E.,** Thermodynamic behavior of hypostoichiometric $UO_2$, 20: 2319 (GE-TM-65-6-13)
**FUIA, H. N.,** Radioisotope viscometer, 20: 2200
**FUKUI, Yoshihiko,** Collective description of a system of interacting Bose particles, 20: 2792
**FUKUROI, Tadeo,** Thermal conductivity of superconducting and normal lanthanum, 20: 2893
**FULDE, Peter,** Gapless superconductivity induced by metallic contacts, 20: 2910
**FULLER, L. E.,** Screening tests of turbine nozzle and blade materials, 20: 2240
**FUNK, C. W.,** Radiation effects on materials at liquid-hydrogen temperature, 20: 2459
**FUZELLIER, Jean,** Improvements in remote control and automation devices for plant in radioactive surroundings, 20: 2003

# G


**GABOR, John D.,** Engineering development of fluid-bed fluoride volatility processes. IV., 20: 1952 (ANL-6859)

**GABRIEL, Cedric John,** Pulsed nuclear quadrupole resonance spectroscopy, 20: 3144

**GABRYTSKI, S.,** Interdiffusion in nickel–uranium system, 20: 2328 (INR-625/XIV/R)

**GAGE, Stephen J.,** Approximate transfer functions for coupled-core reactor dynamics, 20: 3422

**GAGLIONE, P.,** Environmental radioactivity, Ispra 1964, 20: 2047 (EUR-2509.e)

**GAHMAN, Robert L.,** Prog. rpt. on liquid metal boiling heat transfer, 5–8/65, 20: 2008 (AD-622825)

**GAIDE, W.,** Measurement of velocity dependence of total scattering cross sections for scattering of He, $H_2$, and $D_2$ molecular beams on rare gases, 20: 2614

**GALAKTIONOV, $\pi^-$** meson-neutron elastic backward scattering at 1.4 to 4.0 Bev, 20: 2713

**GALAKTIONOV, Ye. V.,** Elastic backward scattering of $\pi^-$ by neutrons, 20: 2700

**GALANTER, Leonard,** Calorimetric calibrations of high-specific-activity $\gamma$ sources, 20: 2195

**GALASSO, G. J.,** Effect of particle aggregation on survival of irradiated Vaccinia virus, 20: 1651

**GALEEV, A. A.,** Ion escape from magnetic mirror trap due to development of instability connected with loss cone, 20: 3229

**GALEEV, A. A.,** Theory of acceleration of particles by MHD waves in slightly turbulent rarefied plasma, 20: 3192

**GALEJS, J.,** Propagation constant along a cylindrical antenna immersed in a warm plasma. I and II., 20: 2097 (AD-618396)

**GALEJS, Janis,** Waveguide admittance for radiation into plasma layers—theory and experiment, 20: 2098 (AD-618398)

**GALIMI, G.,** Forced convection burnout and hydrodynamic instability experiments for water at high pressure. I., 20: 2009 (EUR-2490.e)

**GALITSKII, V. M.,** Two-photon emission in electron collisions, 20: 2743

**GALLAGHER, E. V.,** Prog. rpt. on reactor containment, 10/64–7/65, 20: 3324 (IITRI-578P21-13)

**GALLAHER, William H.,** Measurements and calculations of hydrogen loss from hydrided zirconium–uranium fuel elements during transient heating to temperatures near melting point, 20: 3563

**GALL DE PARATESI, S.,** TESI—advanced power excursion reactor for research in reactor safety, 20: 3584 (EUR-2433.e)

**GALLI DE'PARATESI, S.,** Automatic control system for ISPRA-1 reactor, 20: 3587 (RT/ING(65)-3)

**GANGAS, N. H.,** First excited state of $^5$He, 20: 3078

**GANOUNA-COHEN, Gilbert,** Improvements in and relating to electrometer systems, 20: 2183

**GARARDI, F.,** Identification chart for $\gamma$-emitting radionuclides formed by (n,$\gamma$) reactions, 20: 1735 (EUR-2408.e)

**GARBER, S. R.,** Specific heat of Gd near Curie point, 20: 2920

**GARD, Gary Lee,** Studies in F chemistry. I and II., 20: 1881

**GARELIS, Edward,** Consideration of finite correlation times in pseudo-random-impulse response methods, 20: 3387

**GARN, W. B.,** Los Alamos flux compression program from its origin, 20: 3166 (LA-DC-7252)

**GARNER, R. W.,** Analysis of reactor excursions initiated at high power in SPERT-III PWR, 20: 3507

**GARRETT, Charles W.,** Low-energy component of total dose for deep-gamma penetrations, 20: 3267

**GARTSIDE, Colin,** Improvements in or relating to refuelling machines for nuclear reactors, 20: 3355

**GARTSIDE, J. M.,** Tumor uptake and distribution of niobium isotopes in rats, 20: 1595

**GARZON, O. L.,** Preparation of a $^{99m}$Tc labeled colloid, 20: 1696 (CONF-641126-1)

**GASCOIGNE, J.,** Precision measurements of the Townsend energy ratio for electron swarms in highly uniform electric fields, 20: 2825

**GASSER, M.,** Some measurements on hot particles during 1962 and 1963, 20: 2049

**GASTEBOIS, J.,** Study of levels of $^{63}$Cu by inelastic scattering of 10 Mev deuterons, 20: 3073

**GATTO, R.,** Theoretical aspects of colliding-beam experiments, 20: 2687 (LNF-65/25)

**GAUS, H.,** Influence of traps on diffusion (rare gas diffusion in solids), 20: 2360 (ORNL-tr-814)

**GAUTSCH, O.,** Interaction of krypton with uranium oxide surfaces, 20: 1813 (EUR-2515.e)

**GAYDOS, H. F.,** Weapons effects display system study, 20: 1987 (UCRL-13189)

**GAZARYAN, K. A.,** Ionization measurement in a streamer chamber, 20: 2128 (JINR-E-2324)

**GAZAZYAN, E. D.,** Cherenkov radiation of charged particles in circular waveguide with gyrotropic ferrite filing, 20: 2550

**GEBALLE, T. H.,** Superconductivity of barium tungsten bronze, 20: 2901

**GEBAUER, H.,** Method to compensate natural air radioactivity by means of $\beta$-$\alpha$ pseudocoincidences, 20: 2151

**GEDALIN, E. V.,** Parity conserving amplitudes of hadron decays of baryons in the U(12) symmetry scheme, 20: 2697

**GEDEONOV, L. I.,** Determination of $^7$Be in samples of atmospheric aerosols and atmospheric precipitation in presence of fission fragments, 20: 1778

**GEHRINGER, C.,** New levels in $^{58}$Co, 20: 3077

**GEIGER, J.,** Effective cross section for excitation of molecular vibrations by fast electrons, 20: 2638

**GEIGER, Wallace Aime,** Mounting arrangements for casing-enclosed apparatus, 20: 3351

**GELETSEANU, I.,** Complexing of actinide elements, 20: 1855

**GEL'MAN, V. A.,** Development of $ZrO_2$-base refractory materials, 20: 2382

**GENS, T. A.,** Reaction of $U_3O_8$ with $CCl_4$ and mixtures of $CCl_4$ and $Cl_2$, 20: 1816 (ORNL-TM-1258)

**GEORGE, G. G.,** Measurement of anisotropy of displacement energy in silicon, 20: 2515

**GEORGOPOULOS, C.,** Neutron and gamma irradiations of indium antimonide at 70°K. Annealing of defects, 20: 2500

**GERARD, Victor,** Automatic tilting device for radioactive articles, 20: 2002

**GERASIMOV, V. V.,** Influence of thermal neutron radiation on potential of oximercury electrode, 20: 1932

**GERBER, J. P.,** Production of hyperfragments and $^8$Li fragments, 20: 3062

**GERKEN, W. W.,** BONUS reactor-operating performance, 20: 3520

**GERRISH, R. W., Jr.,** ZPR-III fuel fabrication, 20: 2290

**GERSTENKORN, Simon,** Relative isotopic displacements in the spectrum of neodymium. Specific mass effect, 20: 1826

**GFOELLER, G.,** Electron capture in decay of $^{45}$Ti, 20: 3128

**GHIKA, G.,** Remark on crossing symmetry and parastatistics, 20: 2751 (IC/65/51)

**GIBBONS, F. L.,** Interactions of 14.6-Mev neutrons in iron, $^7$Li, and carbon, 20: 2962

**GIBSON, G. W.,** Controlled irradiation testing of uranium–aluminum fuels for the Advanced Test Reactor, 20: 2465

**GIBSON, James O.,** Synthesis of spherical nuclear fuels in a 4000°K plasma, 20: 2288

**GIBSON, W. R.,** Polarization in elastic scattering at backward angles of 30-Mev protons from deuterons, 20: 2706

**GILBERT, A.,** Effect of strain rate on dislocation multiplication in polycrystalline molybdenum, 20: 3286

**GILCHRIST, Ed,** Cryogenic irradiation of resistance temperature transducers for NERVA, 20: 2191

**GILCHRIST, Ed,** Fission-product behavior in fuel-element cladding materials, 20: 2389

**GILLESPIE, F. C.,** Xenon-133 partition coefficients, 20: 1599

**GILLY, L.,** Double charge exchange with negative pions. Search for tetraneutron, 20: 3080

**GILMAN, J. J.,** Influence of dislocation dipoles on physical properties, 20: 3278 (COO-1198-222)

**GILMAN, Peter A.,** Structure and energetics of large-scale hydromagnetic disturbances in the solar photosphere, 20: 2589

**GILMOUR, B. A.,** Bibliography on radiation effects on glass, 20: 2432 (REIC-Memo-26)

**GILSON, V. A.,** Perturbation of disk-loaded waveguide modes by anisotropic plasma, 20: 3219

**GINELL, W. S.,** Determination of solubility of several transition metals in molten potassium, 20: 2237

**GINOCCHIO, J. N.,** Generalized quasi-spin in neutron–proton systems, 20: 3046

**GINZBURG, E. I.,** Influence of negative ions on diffusion of charged particles in lower ionosphere, 20: 2853

**GINZBURG, V. L.,** Relativistic oscillator models of elementary particles, 20: 2778

**GIRARDEAU, M. D.,** Statistical mechanics of an assembly of quasi-particles, 20: 2843

**GIRARDI, Francesco,** Recent developments in radioactivation analysis, 20: 1785

**GIRAUD-HERAUD, Francois,** Dissolution and precipitation of uranium carbides, 20: 2285

**GIULIANI, S.,** Thermal and mechanical studies of solid-solid contacts, 20: 1811 (EUR-2486.e)

**GLASSBRENNER, Charles J.,** Radiation facility support and solid-state studies, 20: 2531 (AD-618304)

**GLAUERT, Audrey M.,** Fine structure of Micrococcus radiodurans, 20: 1584

**GLIDDON, J. E. C.,** Ambipolar diffusion and drift motions in the F2 region, 20: 2858

**GLINER, E. B.,** Possible generalization of Einstein's equations, 20: 2876

**GOBRECHT, H.**, Determination of chlorine and sodium in selenium by non-destructive neutron activation analysis, 20: 1769
**GODWARD, M. B. E.**, Invisible radiations, 20: 1681
**GOEDDEL, W. V.**, Prog. rpt. on advanced, graphite-matrix, dispersion-type fuel systems and research on graphite, 8/15–11/14/64, 20: 2318 (GA-5918(Pt. I))
**GOFFI, M.**, Forced convection burnout and hydrodynamic instability experiments for water at high pressure. I., 20: 2009 (EUR-2490.e)
**GOLD, Louis**, Dynamic theory of noise in magnetoplasma, 20: 3194
**GOLDANSKII, V. I.**, Analysis of $^{119}Sn$ nuclear charge radius based on Moessbauer spectra, 20: 3136
**GOL'DANSKII, V. I.**, Calorimetric analysis of kinetics of radiation polymerization, 20: 1904
**GOLDANSKII, V. I.**, Effect of complex formation on reactions between positronium and inorganic ions, 20: 1844
**GOL'DANSKII, V. I.**, Radiation polymerization of hexamethylcyclotrisiloxane in solid phase, 20: 1903
**GOLDBERG, P.**, Prog. rpt. on boiling flow regimes and critical heat flux, 6/16–9/15/65, 20: 2012 (NYO-3304-6)
**GOLDEN, S. A.**, Radiative properties of gases. I., 20: 1803 (AD-619266)
**GOL'DENFEL'D, I. V.**, Mass spectra of water ionized in a strong electrical field, 20: 1829
**GOLDFARB, L. J. B.**, Deuteron stripping at low energies according to prior formalism, 20: 3070
**GOLDMAN, A. E.**, Irradiation behavior of high-burnup $ThO_2$–4.45% $UO_2$ fuel rods, 20: 2429 (ORNL-3837)
**GOLDMAN, A. J.**, Performance optimization of fast-burst reactor core, 20: 3593
**GOLDMANN, A.**, Yield of $(\gamma,t)$ reaction in oxygen with 50-Mev Bremsstrahlung, 20: 3126
**GOLDMANN, K.**, Carbon and nitrogen transfer in type-316 stainless-steel Cb–1% Zr, liquid-potassium system, 20: 2239
**GOLDSMITH, M.**, Spin polarization and age of neutrons in water, 20: 2969
**GOLDSTEIN, D. M.**, Effects of alloying upon certain properties of 55.1 Nitinol, 20: 2310 (AD-618681)
**GOLDSTEIN, Rubin**, Intermediate resonance absorption in heterogeneous media including moderator scattering, 20: 2974
**GOLDSZTEIN, Marcel**, Computer processing of $\gamma$ spectra and determination of radioelements, 20: 1732 (CEA-R-2850)
**GOLLAN, Frank**, Cerebral blood flow monitoring by external detection of inhaled radioactive xenon, 20: 1711
**GONCHARENKO, G. I.**, Extraction of U(VI) from carbonate solutions by quaternary phosphonium and arsonium bases, 20: 1782
**GONZALEZ, O. D.**, Thermal diffusion of dissolved hydrogen isotopes in iron and nickel, 20: 2397
**GORDON, B. E.**, Purities of some commercially available $^{14}C$-labeled hydrocarbons, 20: 1764
**GORDON, Milton P.**, Photoreactivation of tobacco mosaic virus RNA following near uv irradiation, 20: 1659
**GORDON, Paul**, Grain boundary migration, 20: 3626 (ORNL-P-1722)
**GORENSTEIN, P.**, Positive pion photoproduction with coherent bremsstrahlung, 20: 2718
**GORICHEV, P. A.**, Angular distribution of fragments, 20: 3111
**GORODETZKY, S.**, New levels in $^{58}Co$, 20: 3077
**GORRELL, T. C.**, Leak testing of HWCTR containment building, 20: 2037 (DP-968)
**GOTSMAN, E.**, Bookstrap calculation for mass of the intermediate vector boson, 20: 2721
**GOTTLING, W.**, Separation of cations on a paper-chromatographic basis, 20: 1750 (UCRL-Trans-1245(L))
**GOUTIER, R.**, Isotopic effect of tritium in the form of tritiated thymidine on the activity of ATP, 20: 1583
**GOYA, H. A.**, Compendium of radiochemical procedures for determination of selected fission products in sea water, 20: 1749 (USNRDL-TR-912)
**GOZANI, T.**, Measurements of generation-time variations, 20: 3386
**GRABER, F.**, Neutron activation determination of rare-earth elements in silicate ores, 20: 2056
**GRABOVSKII, Ye.**, Angular distribution of inelastically scattered complex particles, 20: 3013 (JINR-P-2331)
**GRACHEVA, L. N.**, Certain polonium $\pi$-anisyl derivatives, 20: 1854
**GRADE, Maria Regina Soles**, Behavior of thorium nitrate solutions in amberlite IR-120, 20: 1783
**GRAEFFE, G.**, Half-life of $^{147}Sm$; comparison of ionization chamber and liquid scintillation results, 20: 3028
**GRANOVSKII, Ya. I.**, Relativistic generalization of SU(3) symmetry. Baryon current, 20: 2777
**GRASHIN, A. F.**, Production of slow $\pi$ mesons on light nuclei and the $\pi$-$\sigma$ interaction, 20: 2739
**GRASS, F.**, Diffusion of fission-product $^{147}Pm$ in aluminum oxide, 20: 2364
**GRASS, F.**, Electrophoresis of $^{227}Ac$, 20: 1756
**GRASS, F.**, Electrophoresis of radioactive rare earths, 20: 1961
**GRASYUK, A. Z.**, Spontaneous particle radiation in resonator with several coupled modes, 20: 2527
**GRAVES, Ernest Jr.**, Isthmian canal studies, 1964, 20: 1983 (PNE-2000)
**GREBENSHCHIKOVA, V. I.**, State of Pu(IV) at pH 1.0 to 12.0 and plutonium concentration $2 \times 10^{-5}$ M, 20: 1849
**GREBINNIK, V. G.**, Analysis of $\pi^- + p \rightarrow \pi^- + \pi^+ + n$ and $\pi^- + p \rightarrow \pi^- + \pi^0 + p$ at 338 Mev, 20: 2682 (JINR-P-2320)
**GRECHISHKIN, V. S.**, Energy levels and relative intensities of NQR lines for some integral spins, 20: 3284
**GREEN, Albert**, Liquid-moderated nuclear reactors, 20: 3354
**GREEN, F. P.**, Fuel elements for Arbeitsge-Meinschaft Versuchs reaktor (AVR), 20: 3494
**GREEN, L.**, Rotating fluidized-bed research reactor, 20: 3598
**GREEN, Michael**, Experimental interpretation of criterion of nonlinear stability, 20: 3406
**GREEN, Michael A.**, Design problems associated with high-current-density water-cooled septum magnets, 20: 2544 (UCRL-16309)
**GREEN, W. V.**, High-temperature creep of tantalum, 20: 2394
**GREENBERG, A. E.**, Simultaneous assay of $^{90}Sr$ and $^{90}Y$ by liquid scintillation spectrometry, 20: 1766
**GREENBORG, J.**, Comparison of measured and calculated neutron flux and gamma-ray dose distributions in NPR reflector and top shield, 20: 3544
**GREENE, D.**, Muon and antiproton trap at SLAC, 20: 2547 (UR-875-98)
**GREENE, R. L.**, Energy transfer mechanisms between rare-earth impurity ions, 20: 2627
**GREENHOW, W. A.**, Cryogenic irradiation of resistance temperature transducers for NERVA, 20: 2191
**GRENIS, Albert F.**, Infrared radiation of solids refractory materials, 20: 1823
**GRIB, A. A.**, Violation of CP invariance in $K^0$ meson decays and the non-invariant vacuum, 20: 2698
**GRIBOV, V. N.**, Three-particle partial amplitudes and unitarity conditions for complex values of angular moments, 20: 2811
**GRIEM, H. R.**, Measurement of Stark profiles of singly ionized nitrogen lines from T-tube plasma, 20: 3215
**GRIEM, H. R.**, Theory of resonance broadening of spectral lines by atom-atom impacts, 20: 2620
**GRIEM, Hans R.**, Theory of wing broadening of hydrogen Lyman-$\alpha$ line by electrons and ions in plasma, 20: 3217
**GRIESENAUER, Neal M.**, Preparation of ceramic-refractory metal seals for space power systems, 20: 2292
**GRIFFIN, Allan**, Effect of Suhl-Abrikosov resonance on the transition temperature of superconductors, 20: 2911
**GRIFFITH, O. Hayes**, Electron spin resonance of several molecules in the solid state, 20: 1935
**GRIFFITH, O. Hayes**, Isotope effect on paramagnetic resonance of triplet excitons, 20: 1841
**GRIFFITHS, Jack Jones**, Improvements in or relating to nuclear reactor fuel elements, 20: 3466
**GRIFFITHS, K.**, Surface boundary condition for stars, 20: 2581
**GRIFFITHS, R. J.**, Polarization in elastic scattering at backward angles of 30-Mev protons from deuterons, 20: 2706
**GRIFFITHS, Robert B.**, Microcanonical ensemble in quantum statistical mechanics, 20: 2832
**GRIGOR'EV, V. K.**, Analysis of $\pi^- + p$ reactions, 20: 2690 (AEC-tr-6591)
**GRIGOR'EV, Yu. G.**, Destruction of the otolith apparatus by ionizing radiation, 20: 1628
**GRIGORIEV, E. P.**, Decay of $^{146}Eu$, 20: 3075
**GRILLET, Leon**, Functional performance of a G-M counter, 20: 2144
**GRILLI, M.**, Positive pion photoproduction with coherent bremsstrahlung, 20: 2718
**GRIMES, J. H.**, Uranium corrosion studies. II., 20: 1804 (AWRE-O-68/65)
**GRIMSHAW, J. A.**, Effects of electron irradiation on mobility of electrons in gallium arsenide, 20: 2514
**GRIN', Yu. T.**, Nuclear rotational spectra at high moments, 20: 3103
**GRISHIN, A. P.**, Analysis of $\pi^- + p$ reactions, 20: 2690 (AEC-tr-6591)
**GRISOLI, J. J.**, Current magnet design practice in the U.S.A., 20: 2533 (BNL-9536)
**GROCE, David E.**, Problems associated with 14-Mev neutron source in concrete enclosure, 20: 3264
**GROCHOWSKI, G.**, Comparison of shield leakage obtained from 3-D calculations and measurements, 20: 3348
**GRODZINS, L.**, Liquid helium cryostat for Moessbauer scattering experiments, 20: 3093
**GROH, E. F.**, Doppler-effect measurements on dilute fast-carbide assembly, ZPR assembly 4Z, 20: 2959
**GROH, E. F.**, Equipment and techniques for Doppler-effect measurements on fast critical assemblies, 20: 3401
**GROMOVA, A. I.**, Influence of thermal neutron radiation on potential of oximercury electrode, 20: 1932
**GROSMANN, M.**, Effects of neutron and proton bombardments on the exciton spectrum of $Cu_2O$, 20: 2505
**GROSS, F.**, Photoluminescence of silver-containing quarts. Part II., 20: 3282

**GROSSMAN, L. M.,** Analytic error estimates for integral-equation Eigenvalue problems, 20: 3411
**GROTE, L. W.,** Machine gaging philosophy on instrumentation, 20: 3627 (RFP-670)
**GRUETER, H.,** Simple oscillographic $\gamma$ spectrometer with linear or parabolic energy scale, 20: 2149
**GRUZIN, P. L.,** Study of diffusion of carbon and molybdenum in chromium, 20: 2357 (AERE-Trans-1032)
**GRYCZ, B.,** Experimental investigations on boundary between flowing plasma and cooled metal electrodes, 20: 2672
**GUARINO, A.,** Self-radiolysis and methods for storage of tritiated organic compounds, 20: 1938 (EUR-2452.e)
**GUBEL'BANK, S. M.,** Polarographic determination of europium and ytterbium in presence of potassium chloride, 20: 1795
**GUBLER, W.,** Spontaneous radiation-emission fluctuations of gas discharges and their measurement using a suitable radiation detector, 20: 2828
**GUDECHEK, M.,** Discovery of damage in uranium fuel elements in nonactive test in $CO_2$, 20: 1748 (UJV-1369/65)
**GUDKOV, B. S.,** Isotopic exchange of cyclohexane with deuterium over evaporated films of germanium and silicon, 20: 1838
**GUERNSEY, Edwin Owens,** Production of heavy water, 20: 1884
**GUERON, H.,** Measurement of diffusion coefficient in highly anisotropic medium, 20: 2957
**GUERRERO, H.,** Melting of $UO_2$ during irradiations of short duration, 20: 2416 (AECL-2289)
**GUINET, Philippe,** System uranium–uranium monocarbide, 20: 2366
**GUINN, V. P.,** Prog. rpt. on applications of neutron-activation analysis to scientific crime detection, 7/62, 20: 1736 (GA-3491)
**GUINN, V. P.,** Prog. rpt. on applications of neutron-activation analysis to scientific crime detection, 11/62–1/63, 20: 1738 (GA-4041)
**GUINN, V. P.,** Prog. rpt. on applications of neutron-activation analysis to scientific crime detection, 2–4/63, 20: 1739 (GA-4297)
**GUINN, V. P.,** Prog. rpt. on application of neutron-activation analysis to scientific crime detection, 5–7/63, 20: 1740 (GA-4576)
**GUNKEL, W. A.,** Prog. rpt. on evaluation of serviceability of Elk River reactor pressure vessel, 5–7/65, 20: 3482 (SWRI-1228-75)
**GUNNERSEN, E. M.,** Measurement of anisotropy of displacement energy in silicon, 20: 2515
**GUON, J.,** Nuclear reactivity measurements of irradiated uranium dioxide, 20: 3384
**GUPTA, J.,** Ion exchange behaviour of U(VI) in aqueous sodium triphosphate and its separation from rare earths, 20: 1762
**GUPTA, Subhash,** Mechanical behavior of internally oxidized single crystals of silver and silver base alloys, 20: 3639 (UCRL-11194)
**GUREVICH, A. V.,** Automodel motion of rarefied plasma, 20: 3228
**GUREVICH, A. V.,** Space physics with artificial satellites, 20: 2863
**GURNETT, Donald A.,** Method of determining $\alpha = n(H+)/n_e$ and ion temperature from measurement of proton-whistlers, 20: 2847 (AD-614716)
**GUSEINOVA, E. S.,** X-ray and $\gamma$ conductivity of GaSe single crystals, 20: 2439
**GUS'KOV, B. N.,** Elastic $\pi^+$-p scattering at 180° and high energies, 20: 2683 (JINR-P-2327)
**GUYER, R. A.,** Light scattering detection of thermal waves, 20: 2896
**GUZZI, G.,** Identification chart for $\gamma$-emitting radionuclides formed by (n,$\gamma$) reactions, 20: 1735 (EUR-2408.e)
**GYFTOPOULOS, Elias P.,** Conditions for probabilistic boundedness of reactors with random macroscopic cross sections, 20: 3404
**GYFTOPOULOS, Elias P.,** Experimental interpretation of criterion of nonlinear stability, 20: 3406
**GYFTOPOULOS, Elias P.,** Input-output approach to optimal control, 20: 3409
**GYOREY, Geza L.,** Time-integrated model for reactor-excursion calculations, 20: 3418

## H

**HAANEN, C.,** Molecular weight of Factor XII (Hageman factor) estimated with ionizing radiation, 20: 1673
**HACKER, Herbert Jr.,** Low temperature magnetic susceptibilities of six rare earth oxides, 20: 3318
**HAGENLOCKER, Edward Emerson,** Two-phase radio frequency heating of plasma confined in magnetic mirror system, 20: 3237
**HAGGMARK, L. G.,** Monte Carlo technique applied to compartmented structure, 20: 3275
**HAGUE, A. K. M. M.,** Radon concentration in different environments and the factors influencing it, 20: 2090
**HAGUENAU, Francoise,** Autoradiography of incorporation of tritiated leucine, 20: 1597
**HAHN, E. L.,** Stimulated emission from 4.3 percent abundant $^{50}Cr$ ions in ruby, 20: 3283
**HAHN, G. T.,** Effect of strain rate on dislocation multiplication in polycrystalline molybdenum, 20: 3286
**HAHN, H.,** Brookhaven radiofrequency beam separator, 20: 2532 (BNL-9505)
**HAHS, C. A.,** Contaminated filter removal equipment, 20: 1995
**HAINES, George H.,** High-energy electron irradiation of trihydroperfluoroalkyl acrylate monomers, 20: 1911
**HALAMA, H. J.,** Brookhaven radiofrequency beam separator, 20: 2532 (BNL-9505)
**HALE, R. J.,** Evolution of high-level caves at the Savannah River Laboratory, 20: 2000
**HALING, R. K.,** Discrepancies in importance and neutron lifetime in fast and thermal spectra, 20: 3402
**HALL, Laurence S.,** Electrostatic instabilities of plasma with magnetically supported velocity-space anisotropy at high density, 20: 3182 (UCRL-12447)
**HALL, R. E.,** Operational modes anticipated for converted n-reactor interplant operating restrictions (preliminary), 20: 3541 (RL-NRD-81(Suppl. I))
**HALL, Russel L.,** Vibration isolation through pneumatic spring and damping, 20: 3613 (CONF-651016-1)
**HALL, William C.,** Radiation shielding composition comprising carbon and lead dispersed in cement, 20: 2306
**HALLIGAN, James Edmund,** Prediction of approach to steady-state of a mixer-settler extractor, 20: 1953 (IS-T-34)
**HALMSHAW, R.,** Diffraction effects in $\gamma$ radiography, 20: 2029
**HALSALL, M. J.,** Caribou—program for computing isotopic composition of NRX uranium metal rods, 20: 3583 (CRT-1187 B)
**HALTER, J.,** Some measurements on hot particles during 1962 and 1963, 20: 2049
**HAMA, Yogiro,** Range of validity of the one-boson-exchange model, 20: 2726
**HAMILL, William H.,** Ionic processes in $\gamma$-irradiated organic solids, 20: 1906
**HAMILTON, G. N.,** Calorimetric and spectrometric techniques to relate zonewise power distributions in Pu–U multizoned cores, 20: 3388
**HAMILTON, J. H.,** Conversion coefficient measurements employing magnetic and solid-state spectrometers, 20: 3019 (ORNL-P-1657)
**HAMMER, C. L.,** Time-dependent perturbation theory, 20: 2776
**HAMMES, John A.,** Shelter occupancy studies at University of Georgia, 20: 2070 (AD-615004)
**HAMMES, John A.,** Shelter occupancy studies at University of Georgia, 20: 2071 (AD-615005)
**HAMO-LEILA, M. A.,** Investigation of radiation of $^{113}Cd$, 20: 3113
**HAMPSON, D. C.,** Startup experience with the EBR-II fuel cycle facility. II., 20: 3523
**HAMRIC, J. P.,** Spatial kinetics in large reactors, 20: 3419
**HANLIN, H. H.,** Thermoelectromagnetic pump for the 3-kwe Hg Rankine system, 20: 1988 (NAA-SR-11198)
**HANNAFORD, P.,** Effect of radiation damage on 23.8 kev Moessbauer transition in $^{119}Sn$, 20: 3065
**HANSEN, E. M.,** Correlated EPR-optical spectra of potassium in ethylamine–ammonia mixtures, 20: 1808 (COO-958-5)
**HANSEN, H.,** Delayed neutrons in decay of $^{9}Li$, 20: 3130
**HANSEN, K. F.,** Invariant imbedding solutions for energy-dependent neutron transport in heterogeneous anisotropically scattering shields, 20: 2989
**HANSEN, K. F.,** Numerical solutions of transport equation, 20: 2984
**HANSEN, P. G.,** Isobaric-spin impurity in $^{170}Lu$ ground state, 20: 3072
**HANSEN, Robert J.,** Non-linear response of reinforced concrete spherical domes to air blast loading, 20: 2035 (AD-615017)
**HANSON, I. G.,** Recovery and strain-hardening of alpha-phase plutonium, 20: 2380
**HANSON, J. E.,** Response of low-burnup-irradiated mixed oxide ($PuO_2$–$UO_2$) fuel to transient overpower, 20: 2469
**HANUS, J. F.,** Fission-product and heavy-element distributions in high-performance $UO_2$ fuel rods, 20: 2450
**HAQUE, M. M.,** $\Omega^-$ particle produced by 6-Bev $K^-$ meson in hydrogen, 20: 2717
**HARBINSON, E. N.,** A device for outpile thermal simulation of reactor-fuel microstructures, 20: 2393
**HARDIE, D.,** Effect of oxygen on precipitation of hydrogen from zirconium, 20: 2267
**HARDY, Gyula,** Gamma-initiated polymerization of N-vinylsuccinimide in the liquid phase, 20: 1912
**HARDY, J. Jr.,** Measurement of fast advantage factors and intra-cell flux shapes in several eight-water-moderated slightly enriched uranium lattices, 20: 3396
**HARDY, J. Jr.,** Measurement of effective resonance integral and Doppler coefficient of thorium–oxide rods, 20: 2976
**HARDY, W. R.,** Scintillation decay in calcium tungstate, 20: 1900
**HARGROVE, H. G.,** Analysis for correlating ground destruct tests with in-flight destruct of nuclear rockets, 20: 3575
**HARIKRISHAN, Hons,** Effect of ion gyration radius on magnetogravitational instability of infinite homogeneous medium, 20: 2885
**HARLE, J. R.,** RBE of 14-Mev neutrons in dry barley seeds, 20: 1667
**HARRIES, D. R.,** Effects of irradiation in iron and steels, 20: 2474
**HARRINGTON, Joseph,** Studies of subcritical lattices with distributed

neutron absorber by means of pulsed-neutron source technique, 20: 3432
HARRIS, R. J. Jr., New measurement of lifetime of the positive pion, 20: 2714
HARRIS, R. L., Electrolytic generation of fluorine from uranium hexafluoride, 20: 1954 (KY-287)
HARRIS, Samuel M., Large-spin rotational states of deformed nuclei, 20: 3008 (COO-1420-104)
HARRISON, E. R., Equation of state of matter at supernuclear density, 20: 3016 (NASA-TN-D-3020)
HARRISON, Robert W., Alkali-metal corrosion studies on materials for advanced space power systems, 20: 2270
HARRITY, J. W., Carrier lifetime studies in high-energy electron-irradiated silicon, 20: 2518
HART, E. L., Observation of a peak in $K^- + p \to \Lambda + \eta$ near threshold, 20: 2724
HARTLEY, H. O., Improved model for least-squares analysis of $\gamma$ spectra in activation analysis, 20: 1787
HARTMAN, Charles W., Hot electron plasma stability in mirror and minimum B containment systems, 20: 3184 (UCRL-14310)
HARVEY, A., An in-pile study of the thermal conductivity and electrical properties of $UO_2$ and $UO_{2-x}$, 20: 2452
HARVEY, H. W., 160,000-Curie $^{60}Co$ facility, 20: 1929
HASHIZUME, A., Correlations between tests of aging in Hiroshima subjects—attempt to define physiologic age, 20: 1587
HASIGUTI, R. R., Defect mobility and annealing in irradiated germanium and silicon, 20: 2506
HASSAN, M. Y. M., Ground state energy of nuclear matter, 20: 3079
HASTE, G. R., Lorentz dissociation of $H_2^+$ in DCX-1, 20: 3213
HASTINGS, I. J., Helium gas precipitation in irradiated Cu–B alloys, 20: 2441
HAUBENREICH, P. N., Predicted and observed nuclear characteristics of Molten Salt Reactor Experiment, 20: 3505
HAUG, H., Mixed systems of lanthanide and actinide elements. III., 20: 2379
HAUPT, W., Decay of $^{58}Co$, $T_{1/2}$ = 18hr, 20: 3132
HAUSNER, H., New evidence to delineate the $UO_2$ molten boundary, 20: 2392
HAWKING, S. W., Occurrence of singularities in open universes, 20: 2583
HAWTHORNE, J. R., Prog. rpt. on irradiation effects on reactor structural materials, 2–4/65, 20: 2409 (AD-617319)
HAWTHORNE, J. R., Prog. rpt. on irradiation effects on reactor structural materials, 11/64–1/65, 20: 2408 (AD-614899)
HAYAKAWA, Shigeru, Discharges between coaxial cylinders in magnetic field, 20: 3202
HAYASHI, Koichiro, Gamma-induced polymerization of formaldehyde, 20: 1914
HAYES, Edward J., Radiation shelter, 20: 2040
HAYES, Edward J., Roof structure for radiation shelter, 20: 2039
HAYMES, R. C., Detectability of lunar x rays, 20: 2666
HAYWARD, Evans, Photonuclear reactions, 20: 3151
HAYWOOD, B. C. G., Cooperative modes of motion in simple liquids, 20: 2837
HEAP, J. C., Development of small integral loop for in-pile fuel-failure studies in presence of flowing sodium, 20: 3347
HEBACH, H., Reduction of deuteron stripping cross sections by change of deformation, 20: 3125
HECKROTTE, Warren, Diffusion and losses of electrons in astron E-layer, 20: 3183 (UCRL-14275)
HECKROTTE, Warren, Electrostatic instabilities of plasma with magnetically supported velocity-space anisotropy at high density, 20: 3182 (UCRL-12447)
HEENAN, W. F., Bibliography on radiation effects on glass, 20: 2432 (REIC-Memo-26)
HEFFERNAN, B. J., Measurement of helium content in neutron-irradiated copper–boron alloys, 20: 2444
HEGEWALD, H., Dosimetry of conventional and high-energy radiation with scintillation dosimeter, 20: 2157
HEHENKAMP, Th., Thermal diffusion of platinum in temperature gradient, 20: 3628 (RPI-1044-1)
HEINDL, C. J., Design study of fission-electric cell reactor for space power, 20: 3577
HEINE, V., Model potential for positive ions, 20: 2611
HEINEMAN, R. E., Interpretation of reactivity measurements of reactor media, 20: 3431
HEINIGER, F., Superconductivity in beryllium–rhenium system, 20: 2898
HEISER, W. H., Demonstration of the Hartmann layer, 20: 2831
HELBERT, Jean-Marie, Relative isotopic displacements in the spectrum of neodymium. Specific mass defect, 20: 1826
HELBING, R., Measurement of velocity dependence of total scattering cross sections for scattering of He, $H_2$, and $D_2$ molecular beams on rare gases, 20: 2614
HELCKE, G., Radiosensitivity of rice seed in relation to water content and free radicals, 20: 1669
HELCZ, Attila, Gamma-initiated polymerization of N-vinylsuccinimide in the liquid phase, 20: 1912
HELD, F., Examinations of radioiodine uptake of human fetuses, 20: 1600
HELLWEGE, K. H., Microwave absorption and magnetic transition in $GdCl_3$, 20: 3288
HELM, J. W., High-temperature graphite irradiations: 800 to 1200°C, 20: 2417 (BNWL-112)
HEMPEL, Rudolf, Nuclear power plants and insulating problems, 20: 3487
HENDERSHOTT, D., Pulsed nuclear irradiation effects on electronic parts, 20: 2190
HENDERSON, R. L., Weapons effects display system study, 20: 1987 (UCRL-13189)
HENDRICKSON, Wayne A., Compact versatile x-ray collimator with adjustable pinholes, 20: 2162
HENDRIE, David Lowery, Coincidences between scattered alpha particles and de-excitation gamma rays, 20: 3141
HENDRY, W. L., Solutions to monoenergetic transport equation for critical slab by perturbation theory, 20: 3423
HENNIG, R. J., Fast-flux test facility design concept, 20: 3596
HENNIG, R. J., FFTF driver fuel—$PuO_2$ stainless-steel cermet, 20: 3588
HENNIG, Robert J., Temperature flow control of coolant in reactor, 20: 3365
HENRY, A. F., WIGL2. A program for the solution of the one-dimensional, two-group, space-time diffusion equations accounting for temperature, xenon, and control feedback, 20: 3382 (WAPD-TM-532)
HENRY, Jack L., Investigation of the system UC–UN–UO, 20: 2353 (USBM-RC-1205, pp 11-14)
HERNANDEZ, H. P., Cost estimating magnet systems with the aid of a computer, 20: 2545 (UCRL-16386)
HERNANDEZ, H. P., Current magnet design practice in the U.S.A., 20: 2533 (BNL-9536)
HERRIOTT, Joe R., Compact versatile x-ray collimator with adjustable pinholes, 20: 2162
HESS, D. C., Proposal for source of completely polarized deuterons, 20: 2528
HESSON, J. C., Diffusivity of uranium in liquid metal solutions, 20: 2368
HESSON, J. C., Static and dynamic corrosion by tin, bismuth, and bismuth–sodium alloy up to 1000°C, 20: 2275
HETRICK, David L., Application of the prompt-jump approximation to problems in reactor stability, 20: 3437
HETRICK, David L., Liapunov function for prompt-jump approximation in reactor dynamics, 20: 3407
HETZLER, F. J., Effect of carbon-contaminated sodium on austenitic stainless steel, 20: 2244
HETZLER, F. J., Observations concerning localized corrosion in pumped sodium systems, 20: 2296
HEYDORN, K., The determination of vanadium in blood by neutron activation analysis with preirradiation separation, 20: 1791
HEYWOOD, John B., MHD channel flow with temperature-dependent electrical conductivity, 20: 2824
HICKMAN, B. S., X-ray line broadening in neutron-irradiated magnesium oxide, 20: 2445
HIGGINS, I. R., Development of the Excer Process. I., 20: 1956 (ORNL-1696)
HIGNETT, K. C., On-line gas analysis, 20: 1734 (EG-Report-36)
HILBORN, H. S., Prog. rpt. on USAEC–AECL cooperative program, 8/65, 20: 2420 (DPST-65-83-8)
HILL, D. A., 150-kOe liquid nitrogen cooled pulsed flux-concentrator magnet, 20: 1991
HILL, D. J., Analytical determination of effect of tantalum rods in intermediate spectrum reactor, 20: 3403
HILL, D. J., Comparison of analytical and experimental operating reactivity of NERVA reactors, 20: 3567
HINDMARSH, A. C., Properties of symmetric quadrupole magnet triplets, 20: 2539 (SLAC-47)
HINES, R. L., Channeling of 13-kev $D^+$ ions in gold crystals, 20: 2616
HINS, A. G., Nonremote fabrication of $^{233}U$ fuel elements, 20: 2289
HINSCH, J., Divinyl copolymerization initiated by high-intensity, low-energy electrons, 20: 1910
HNATZSCHE, E., Plasma effects, multiplication and secondary emission of anomalous hydrogen glow discharges, 20: 2826
HO, S. C., Thermal diffusion of platinum in temperature gradient, 20: 3628 (RPI-1044-1)
HOANG, Dinh Van, Positron annihilation in e⁺Li system, 20: 3314
HODGE, Edwin S., Hot isostatic compaction of graphite, 20: 2278 (BMI-1746)
HOFFMAN, E. E., Alkali metal. Refractory alloy component and compatibility evaluation tests, 20: 2271
HOFFMAN, E. E., Design and operation of an alkali metal. Refractory alloy corrosion test facility, 20: 2272
HOFFMAN, H. W., Acoustic instrument for measuring subcooling in boiling systems, 20: 2014 (ORNL-P-1678)
HOFFMAN, H. W., Pressure drop with forced-convection boiling of

potassium, 20: 2015 (ORNL-P-1681)
**HOFFMAN, K. C.**, Rotating fluidized-bed research reactor, 20: 3598
**HOFMANN, F.**, Experimental investigations of fast-neutron decay times in lead assemblies, 20: 2950
**HOFMANN, P. L.**, Physics aspects of fast-flux test reactor, 20: 3597
**HOFMANN, P. L.**, Safety and nuclear considerations in design of FTR, 20: 3581 (BNWL-SA-340)
**HOGAN, O. L.**, Dose models for evaluating the radiation hazard from reactor debris, 20: 2091
**HOGG, C. H.**, Measurement of resonance neutron flux and spectra by activation technique, 20: 2971
**HOH, J. C.**, 160,000-Curie $^{60}$Co facility, 20: 1929
**HOLCOMB, W. F.**, Startup experience with the EBR-II fuel cycle facility. I., 20: 3522
**HOLL, R. J.**, Fuels for gaseous-core nuclear rockets, 20: 3462
**HOLLANDER, J. M.**, Effect of chemical state on lifetime of 24-second isomer of $^{90}$Nb, 20: 3088
**HOLLEY, W. L.**, Cyclotron isotope production and other service irradiations, 20: 2212
**HOLLINGSWORTH, J. W.**, Correlations between tests of aging in Hiroshima subjects—attempt to define physiologic age, 20: 1587
**HOLLINGSWORTH, J. W.**, Effects of 1-$\beta$-D-arabinofuranosylcytosine hydrochloride on regenerating bone marrow, 20: 1687
**HOLM, Dale M.**, Gamma scanning with anticoincidence spectrometers, 20: 2172
**HOLM, Dale M.**, Measurement of the microscopic distribution of oxygen and carbon in metals by $^{3}$He activation, 20: 2227
**HOLM, Hans I.**, Bibliography on preventive maintenance in chemical and mining industries, 20: 1976 (VDDIT-94)
**HOLMES, J. T.**, Fluid-bed fluoride volatility processing of irradiated fuels in hot cells, 20: 1971
**HOLMES, Robert S.**, Isthmian canal studies, 1964, 20: 1983 (PNE-2000)
**HOLOWACH, J.**, Alkali metal. Refractory alloy component and compatibility evaluation tests, 20: 2271
**HOLOWACH, J.**, Design and operation of an alkali metal. Refractory alloy corrosion test facility, 20: 2272
**HOLROYD, Louis V.**, F centers in SrO and quadrupole moment of $^{87}$Sr, 20: 3087
**HOLT, E. H.**, Microwave lens system for plasma diagnostics, 20: 3169 (NASA-CR-319)
**HOLZBECHER, Zevis**, Fluorometric determination of scandium and gallium with derivatives of salicylaldehyde, 20: 1773
**HOLZBERLEIN, T. M.**, Lifetime of the $3^1$P state of helium, 20: 2621
**HONECK, H. C.**, Heterogeneous analysis by multigroup methods of epithermal reactions, 20: 2992
**HONNOLD, Vincent R.**, Prog. rpt. on semiconductor design effects on radiation resistance, 12/15/64–3/15/65, 20: 2411 (AD-618078)
**HONSAKER, John Leonard**, Investigation of $^{6}$Li(p,n)$^{6}$Be reaction by neutron threshold technique, 20: 3140
**HOOPER, M. B.**, Deuteron stripping at low energies according to prior formalism, 20: 3070
**HOOT, Charles G.**, Levels of $^{58}$Ni from reaction $^{58}$Ni(p,t)$^{56}$Ni at 28 Mev, 20: 3041
**HOOTMAN, H. E.**, Diffusivity of uranium in liquid metal solutions, 20: 2368
**HORA, H.**, Estimation of heating of plasma by lasers, 20: 3185 (TT-1193)
**HORAN, John R.**, Safety first in quest for economic nuclear power, 20: 2093
**HORESOVSKY, O.**, Measurement of soft $\beta$ radiation in biological material with aid of liquid scintillators. III., 20: 1758
**HORN, D.**, Bookstrap calculation for mass of the intermediate vector boson, 20: 2721
**HORNE, R. E.**, Low-power shield measurements on Enrico Fermi reactor, 20: 3524
**HORNE, R. W.**, Fine structure of Micrococcus radiodurans, 20: 1584
**HORSKI, Jozef**, Removal of radioisotopes from the water solutions by use of silica gel, 20: 1742 (INR-636/XIII/J)
**HORST-MEYER, H. zur**, Effect of single radiation exposure on blood picture of guinea-pigs in dependence on dose and time, 20: 1670
**HORST-MEYER, H. zur**, Examinations of blood picture after intracavitary administration of $^{198}$Au, 20: 1672
**HORVAT, Robert J.**, Bulgur wafer and adjuncts for fallout shelter rations, 20: 2067 (AD-614824)
**HOSHIAI, Yoichi**, Flow of slurry through a pipe. I., 20: 2020
**HOSHIZAKI, Norio**, Range of validity of the one-boson-exchange model, 20: 2726
**HOSOKAWA, Iwao**, Effect of space charge convection on magnetic field transition toward the plasma regime, 20: 2856
**HOUGHTON, G. K.**, Fast-neutron spectra in paraffin shields, 20: 3257
**HOUGHTON, G. K.**, Fast-neutron spectra in liquid hydrogen, 20: 2967
**HOUGHTON, G. K.**, Neutron spectrum measurements in $H_2O$ as a function of temperature, 20: 2966
**HOURANY, E.**, Momentum distribution of recoil nuclei in reaction $^{12}$C(p,2p)$^{11}$B, 20: 3081
**HOUSLEY, Robert Melvin**, Moessbauer effect of $^{57}$Fe in beryllium and copper, 20: 3145
**HOUSTON, D. H.**, Neutron spectrum measurements in $H_2O$ as a function of temperature, 20: 2966
**HOWARD, C. J.**, Effect of radiation damage on 23.8 kev Moessbauer transition in $^{119}$Sn, 20: 3065
**HOWARD, R. A.**, Fuel elements for Arbeitsge-Meinschaft Versuchs reaktor (AVR), 20: 3494
**HOWARD, Robert**, Development of solar flares within the calcium network, 20: 2578
**HOWES, B. W.**, Measurement of resonance neutron flux and spectra by activation technique, 20: 2971
**HOWES, J. E. Jr.**, Fission-product behavior in fuel-element cladding materials, 20: 2389
**HOYLE, F.**, Surface boundary condition for stars, 20: 2581
**HOYLE, Fred**, Synthesis and destruction of elements in peculiar stars of types A and B, 20: 2565
**HSU, L. S.**, Microscopic models for vibrational states in even nickel isotopes, 20: 3083
**HUANG, M. N.**, Visual and frictional pressure-drop study of natural-circulation single-component two-phase flow at low pressures, 20: 2021
**HUBBELL, W. H.**, Livermore slug fabrication facility, 20: 2298
**HUBER, D. L.**, Energy transfer mechanisms between rare-earth impurity ions, 20: 2627
**HUBER, O.**, Some measurements on hot particles during 1962 and 1963, 20: 2049
**HUBER, P.**, Energy loss per ion pair in various gases for nitrogen and oxygen ions from 0.14 to 0.7 Mev, 20: 2602
**HUBER, P.**, T(d,n)$^{4}$He reaction with polarized deuterons, 20: 3039
**HUBER, P.**, Use of coincidence method for determination of total conversion coefficients, 20: 3038
**HUDSON, F. M.**, Nitration and succinoylation of tritium-labeled toluene, 20: 1950
**HUERLIMANN, T.**, Measurements of generation-time variations, 20: 3386
**HUGGINS, R. A.**, Influence of finely dispersed second phase on recrystallization, 20: 2325 (HW-SA-3767)
**HUGGINS, R. A.**, Structure of deformed internally oxidized alloys, 20: 2324 (HW-SA-3765)
**HUGHES, D. S.**, Quantitative reduction of data from high-speed stereoscopic photographs, 20: 3624 (LA-DC-7088)
**HUGHES, J.**, Cleaning blocked coolant passages in water-cooled magnets, 20: 1992
**HUIZENGA, J. R.**, Structure of the transition state nucleus in nuclear fission, 20: 3154
**HULL, D. E.**, Use of $^{14}$C to measure $CO_2$ removal in a synthetic ammonia plant, 20: 1836
**HULM, J. K.**, Superconductivity of barium tungsten bronze, 20: 2901
**HULM, J. K.**, Superconducting technetium–tungsten alloys, 20: 2907
**HULUBEL, H.**, Mechanism of reaction $^{26}$Mg(p,p',$\gamma$) at low energy, 20: 3092
**HUMPHREY, J. Richard**, Determination of magnesium in uranium by atomic absorption spectrometry, 20: 1753
**HUNDHAUSEN, E.**, Rainbow effect and interference patterns in molecular collisions, 20: 2636
**HUNT, E. C.**, 630A–Mark IV. A nuclear fueled steam generator-superheater for merchant ship propulsion, 20: 3546 (GE-TM-64-12-12)
**HUNT, Thomas Kintzing**, Fluxoid conservation by superconducting thin film rings, 20: 2927
**HUNTER, Raymond Eugene**, Final state pion-nucleon interactions at 2.27 Bev, 20: 2745
**HUNTINGTON, H. B.**, Thermal diffusion of platinum in temperature gradient, 20: 3628 (RPI-1044-1)
**HURE, Geoffroy Graham Jacques**, Process for dispersion of uniform droplets of a liquid in a second liquid, 20: 1800(P)
**HURSH, John B.**, Body content of $^{232}$Th daughters after Thorotrast injection, 20: 1596
**HURST, G. S.**, Application of the generalized concept of dosimetry to space radiations, 20: 2133 (NASA-SP-71, pp 245-50)
**HUSSAIN, F.**, U(12) irregular coupling relations for stopped proton pair annihilation into mesons, 20: 2703
**HUSTER, E.**, Propagation of discharges in self-extinguishing counters. IV., 20: 2176
**HUXTABLE, G. B.**, Polarization in neutron-proton scattering, 20: 2701
**HYER, F. K.**, Annular-ring model for loft meltdown studies, 20: 3333
**HYMAN, N.**, Carbon and nitrogen transfer in type 316-stainless-steel Cb–1% Zr, liquid-potassium system, 20: 2239
**HYNDMAN, R.**, Monitoring reactor kinetics of EBR-II, 20: 3517
**HYNDMAN, R. W.**, EBR-II self-excited oscillations, 20: 3514

## I

**IAGOLNITZER, Daniel**, S-matrix theory and double scattering, 20: 2774
**IBARRA, H.**, The use of integral activation techniques to experimentally

determine $H_2O$–$H_3BO_3$ thermal-neutron spectra, 20: 2965
**ICHIKAWA, Yoshihiko,** Remark on kinetic equation in unstable plasma, 20: 3220
**ICONOMOU, N.,** Influence of radioactive rays on pharmaceuticals, 20: 1918
**IDE, H. M.,** Particle-size distributions from Rover fuel-element fragmentation studies, 20: 3574
**IDE, R. H.,** Production of tritium and $^3$He by proton bombardment of metals, solar origin of terrestrial tritium, 20: 3095
**IDEHARA, Toshitake,** Negative absorption of microwave radiation in weakly ionized xenon plasma in magnetic field, 20: 3204
**IL'IN, Yu. I.,** Distribution of specific ionization along the track as a function of initial energy of $^{235}$U fission fragments, 20: 3029
**IL'KOVA, S. B.,** Polarographic determination of europium and ytterbium in presence of potassium chloride, 20: 1795
**ILYASHENKO, V. S.,** Physico-chemical properties of crystal hydrates of terbium subgroup rare earth sulfates, 20: 1868
**IMRE, Kaya,** Pre-kinetic equations for plasma, 20: 3163 (CNAEM-26)
**INCH, W. R.,** Effect of inhaling 95% and 5% $CO_2$ on radiocurability of murine tumors, 20: 1683
**INOPIN, E. V.,** Optical potential for nucleus in excited state, 20: 3116
**INOUYE, H.,** Equilibrium solid solutions of nitrogen in Cb-1% Zr between 1200-1800°C, 20: 2337 (ORNL-P-1677)
**IRVINE, A. R.,** Thorium–uranium recycle facility, 20: 1994
**IRVINE, W. H.,** Safety of reactor pressure vessels, 20: 2401
**ISACCHINI, Franco,** Thermal conductivity of sodium from 90 to 850°C, 20: 2370
**ISETT, D. D.,** "Accel" automated circuit card etching layout, 20: 3635 (SC-TM-65-544)
**ISHIGURE, Kenkichi,** Radiation-induced copolymerization of tetrafluoroethylene with isobutene at low temperature, 20: 1915
**ISHINO, S.,** Defect mobility and annealing in irradiated germanium and silicon, 20: 2506
**ISRAEEL, Gerhard W.,** Thoron (Rn-220) measurements in the atmosphere and their application in meteorology, 20: 2860
**ISRAEL, H. I.,** Shielding considerations for proposed Los Alamos meson physics facility, 20: 2559
**IVANCEANU, I.,** Argon gas scintillation detector, 20: 2163
**IVANCHENKO, A. F.,** Lanthanum citrate complexes of 1:1 composition, 20: 1856
**IVANITZKAYA, E. A.,** Role of systems orthophenols–orthoquinones in initial radiation-induced processes in an organism, 20: 1647
**IVANOV, L. I.,** Effect of electron irradiation on mechanical properties of steel subjected to thermal mechanical treatment, 20: 2438
**IVANOV, V. S.,** Investigations of polymerization radiation. V., 20: 1930
**IVANOVSKII, N. N.,** Decontamination of sodium from products of reactions with water in the circulation loop, 20: 1960
**IVASCU, M.,** Mechanism of reaction $^{26}$Mg(p,p′,γ) at low energy, 20: 3092

## J

**JABLON, Seymour,** Correlations between tests of aging in Hiroshima subjects—attempt to define physiologic age, 20: 1587
**JACKSON III, D. C.,** Operating experience with the KAPL Radioactive Materials Lab. metallography facility, 20: 2247
**JACOBSON, C. H.,** Lifetime of the $^{31}$P state of helium, 20: 2621
**JACOBSON, M. E.,** Measurement of heat generation rate of highly radioactive calcined alumina, 20: 2425 (IDO-14665)
**JAFFEE, Max,** Relationship of wavelength of transfer system to quenching of radioisotopes in dyes, 20: 2189
**JAMES, A. P.,** Radiobiology of yeast, 20: 1663
**JAMES, D. J.,** Investigation of the pressure wave propagated from open end of a 30 × 18 in. shock tube, 20: 2822 (AWRE-O-60/65)
**JAMESON, A. S.,** BONUS reactor-operating performance, 20: 3520
**JANKOWSKI, K.,** Some remarks on correlated wave function method, 20: 2871
**JANSEN, D. H.,** Compatibility of refractory metals with boiling alkali metals, 20: 2236
**JANSEN, D. H.,** Screening tests of turbine nozzle and blade materials, 20: 2240
**JANSEN, J. F. W.,** Determination of conversion coefficient in $^{170}$Yb with scintillation methods, 20: 3155
**JARVIS, George A.,** Neutronic isolation characteristics of concrete, lead, wood, polyethylene and beryllium, 20: 3390
**JASINS, Alfred C.,** Development of radiac set AN/TDQ-2 for detection of pulsed x radiation from high-powered electronic equipment, 20: 2121 (AD-614832)
**JASON, R. H.,** Time-dependent perturbation theory approach to non-linear kinetics problem, 20: 3413
**JATCZAK, Jerzy,** Cosmic neutrinos, 20: 2587
**JAVARY, B.,** Central laboratory for hot chemistry at KFA-Juelich, 20: 1996
**JEAN, M.,** Double charge exchange with negative pions. Search for tetraneutron, 20: 3080
**JENKINS, Mansell John,** Improvements relating to manufacture of graphite, 20: 2249
**JENSEN, S. E.,** Influence of zirconium cladding on loft loss-of-coolant test, 20: 3334
**JOHNSON, A. A.,** Irradiation hardening and embrittlement in bcc transition metals, 20: 2472
**JOHNSON, Albert E.,** Cerebral blood flow monitoring by external detection of inhaled radioactive xenon, 20: 1711
**JOHNSON, C. C.,** Perturbation of disk-loaded waveguide modes by anisotropic plasma, 20: 3219
**JOHNSON, C. R.,** A device for outpile thermal simulation of reactor-fuel microstructures, 20: 2393
**JOHNSON, E. B.,** Critical experiments with SPERT-D fuel elements, 20: 3379 (ORNL-TM-1207)
**JOHNSON, Harold E.,** Investigation of waves of ionization in pulsed discharge, 20: 3162 (AD-618683)
**JOHNSON, J. H.,** Bremsstrahlung production in thick aluminum and iron targets by 0.5- to 3.0-Mev electrons, 20: 3247 (NASA-SP-71, pp 449-53)
**JOHNSON, N. R.,** Conversion coefficient measurements employing magnetic and solid-state spectrometers, 20: 3019 (ORNL-P-1657)
**JOHNSON, Peter,** Detection of phospholipids on paper chromatograms by neutron activation, 20: 1771
**JOHNSON, Quintin,** Crystal structure of tetramethyl ammonium hexahydrohexaborate, 20: 2347 (UCRL-12146)
**JOHNSON, R. A.,** Static control of SNAP reactors, 20: 3559
**JOHNSON, R. J.,** Calculating space-dependent reactor transfer functions using statics techniques, 20: 3421
**JOHNSON, Richard E.,** Fracture mechanics in design against brittle failure, 20: 3345
**JOHNSON, T. W.,** Investigation of thermoluminescent dosimetry for measuring γ heating in a critical assembly, 20: 2175
**JOHNSON, W. Reed,** Fission neutron age and thermal diffusion length in ordinary concrete, 20: 3255
**JOHNSON, Wiley A.,** Nuclear safety coordination within Oak Ridge operations facilities, 20: 3370 (CONF-651103-2)
**JOHNSTON, A. R.,** Polarization in elastic scattering at backward angles of 30-Mev protons from deuterons, 20: 2706
**JOHNSTON, Jean,** Superconductivity of the cubic modification of MoC, 20: 2346 (UCRL-11471)
**JOLLY, R. K.,** Isobaric analogue states via (p,p) and (p,n) on $^{144}$Sm, 20: 3084
**JONES, A. R.,** Estimate of electron density in plasma after-glow from study of electromagnetic scattering, 20: 3193
**JONES, D. A.,** Cost of remote fabrication of metal-clad metal-fuel fast-reactor fuel elements, 20: 3510
**JONES, E. D.,** $^{55}$Mn zero-field nuclear magnetic resonance in antiferromagnet MnSe, 20: 3295
**JONES, E. D. Jr.,** Conservation economics and reactor technology, 20: 3458
**JONES, H. G.,** Diffusion parameters of mixtures of light and heavy water at several temperatures, 20: 2951
**JONES, J. E.,** Control-rod systems for HFIR, 20: 3543
**JONES, J. R.,** Diffusion coefficient of water in water and in some alkaline earth chloride solutions at 25°C, 20: 1865
**JONES, Robert K.,** Radiobiological consequences of dose distributions produced by solar-flare-type spectra, 20: 2655 (NASA-SP-71, pp 85-96)
**JONES, Stuart M.,** Pressure tube neutronic reactor, 20: 3442
**JONES, W. D.,** Simple momentum probe for plasma studies, 20: 3179 (ORNL-P-1575)
**JONKERS, H. L.,** Backward scattering of alpha particles by $^{16}$O at medium energies, 20: 3056
**JOPSON, R. C.,** X-ray spectra from Scorpius (SCO-XR-1) and the sun observed above the atmosphere, 20: 2585
**JORDAN, E. D.,** Neutron production by (α,n) reaction from heterogeneous isotopic sources, 20: 2949
**JORDAN, P.,** Precision method for routine measurement of $^{14}$C and $^{3}$H in proportional counters, 20: 1768
**JORDAN, T. M.,** Energy-independent biasing functions for Monte Carlo transport calculations, 20: 2985
**JOST, Res,** Pauli principle and Lorentz group, 20: 2878
**JU, F. D.,** Analog model of wave propagation in open-end cylinder. Phase I of investigation in analog study of impact fracture of closed-end cylinders, 20: 3630 (SC-DC-65-1697)
**JUCYS, A. P.,** Two-electron matrix elements of spin-spin interaction energy operator, 20: 2605
**JUCYS, A. P.,** Two-electron matrix elements of spin-orbit interaction energy operator, 20: 2606
**JUDAY, R. D.,** Detectability of lunar x rays, 20: 2666
**JUDGE, Frank D.,** Neutron transport theory in pulsed multiplying assemblies, 20: 3001
**JULIA, Gaston,** Nuclear power applications and Hilbert-Schmidt applications in Banach spaces, 20: 2215
**JUNKERMANN, W.,** Consolidate nuclear steam generator III (CNSG III) a nuclear ships-propulsion, 20: 3552

**JURA, George,** Electrical resistance of bismuth from 25 to 80 kilobars, 20: 3642 (UCRL-11639)
**JURA, George,** Resistance measurements at high pressures, 20: 2345 (UCRL-11030)
**JUST, F.,** EBR-II dynamics, 20: 3590

# K

**KABAKCHI, A. M.,** Gamma and neutron dosimetry using colored polyvinyl alcohol films in nuclear reactors, 20: 2135
**KABIR, P. K.,** Particle-mixture theories of $K^0 \rightarrow 2\pi$ decay, 20: 2720
**KABLER, M. N.,** Concentrations of $\alpha$ and F centers in KBr irradiated at 5°K, 20: 1919
**KACHI, S.,** Moessbauer effect of $^{57}Fe$ doped in $V_2O_3$, 20: 3289
**KACZAROWSKI, R.,** Interactions of 9 Bev protons with large energy transfer to target nuclei, 20: 3047
**KADOMTSEV, B. B.,** Plasma turbulence, 20: 3236
**KAGIWADA, H.,** Numerical results for auxiliary equation of radiative transfer, 20: 2930 (AD-614636)
**KAHN, Bernard,** Prog. rpt. on slender-channel electrogasdynamics, 2/63--8/64, 20: 2667 (AD-614907)
**KALABA, R.,** Numerical results for auxiliary equation of radiative transfer, 20: 2930 (AD-614636)
**KALADE, Yu. A.,** Theory of the electromagnetic form factors in three-nucleon system, 20: 3119
**KALE, S. H.,** Leak testing of HWCTR containment building, 20: 2037 (DP-968)
**KALINICHEV, Yu. V.,** Investigation of $^{116*}In$ decay, 20: 3097
**KALINKIN, B. N.,** Angular distribution of inelastically scattered complex particles, 20: 3013 (JINR-P-2331)
**KALLENBACH, Reinhard,** Obrigheim nuclear power station, 20: 3488
**KALLMAN, Robert F.,** Cyclic fluctuations in radiosensitivity of mice after exposure to sublethal whole-body irradiation, 20: 1685
**KALMAN, M. P.,** Use of adiabatic approximation in prompt-critical, large-core reactor-excursion analyses, 20: 3417
**KALMUS, P. I. P.,** Evidence for $\kappa^0(725)$ in $\pi^-$p reactions, 20: 2715
**KAMERDZHIEV, S. P.,** Effective quadrupole charge in nuclei (matrix elements), 20: 3115
**KAMIGAITO, Osami,** Focusing of electron beam from biased electron gun, 20: 2110
**KAMINISI, Keisuke,** Adiabatic exponent for iron--helium transition and pair creation, 20: 2588
**KAMPHOUSE, J. L.,** Effect of neutron irradiation on hardness properties of tungsten and molybdenum, 20: 2457
**KANASEWICH, E. R.,** Lead isotope ratios from the Cobalt-Noranda Area, Canada, 20: 2051
**KANCHELI, O. V.,** Parity conserving amplitudes of hadron decays of baryons in the U(12) symmetry scheme, 20: 2697
**KANE, J. V.,** Data processing, 20: 2218
**KANEKAR, C. R.,** Moessbauer effect in Sn--Pt alloys, 20: 3290
**KANEVSKII, E. A.,** Kinetics of $UO_2$ and Fe(III) reactions in perchloric acids, 20: 1851
**KANTOLA, Martti,** Measurement of formation energy of electron-hole pair in n-type silicon, 20: 2362
**KAPCHIGASHEV, S. P.,** Cross sections of 1- to 50,000-ev neutron radiative capture by V, Zr, $^{90}Zr$, $^{91}Zr$, and $^{94}Zr$ nuclei, 20: 3032
**KAPITSA, S. P.,** Angular distribution of $^{238}U$ photofission fragments near fission threshold, 20: 3134
**KAPLAN, Arthur L.,** Basement radiation from infinite-plane gamma source, 20: 3272
**KAPLAN, Arthur M.,** Feasibility study of filtration unit for removal by the individual of CBR agents from water, 20: 2072 (AD-618006)
**KAPLAN, I.,** Criticality of bare slab of arbitrary size with anisotropic scattering, 20: 2986
**KAPLAN, I.,** Reactor physics measurements in slightly enriched uranium $D_2O$ lattices, 20: 3397
**KAPLAN, I.,** Studies of subcritical lattices with distributed neutron absorber by means of pulsed-neutron source technique, 20: 3432
**KAPLAN, J. I.,** Conduction electron spin resonance in superconductor, 20: 2899
**KAPLAN, S.,** Analogy between variational principles of reactor theory and those of classical mechanics, 20: 3331
**KAPLAN, Stanley,** Transport synthesis, 20: 2990
**KAR, K. C.,** Lorentz invariance and linearization of relativistic Hamiltonian, 20: 2874
**KAR, K. C.,** Vectors in theory of relativity, 20: 2875
**KARAZIJA, R. I.,** Two-electron matrix elements of spin-orbit interaction energy operator, 20: 2606
**KARCHER, R. H.,** Initial radiation shield requirements for hardened structures, 20: 3276
**KARR, H.,** Legal questions on the commercial entry of the Savannah into German waters, 20: 2088
**KARRA, James Sundararao,** Dynamic polarization of nuclear spins at low temperatures, 20: 3143
**KARTHEUSER, E.,** New approach to continuum polaron theory, 20: 3277 (BLG-328)
**KARTLUKE, H.,** Acoustic instrument for measuring subcooling in boiling systems, 20: 2014 (ORNL-P-1678)
**KARTSEV, V. P.,** Problem of heat fluxes in superconducting devices, 20: 2892
**KARWOWSKI, M.,** Charge-sensitive transistor preamplifier for use with semiconductor nuclear radiation detectors, 20: 2154
**KARZHAVIN, Yu. A.,** Wire spark chamber with external acoustic transducers, 20: 2132 (JINR-P-2368)
**KASCENKO, L. A.,** Reaction of ionizing radiation in the system of adenohypophysis—thyroid gland—gonads, 20: 1671
**KASSIERER, F.,** Crystal structure of rare earth and yttrium oxybromides, 20: 1834
**KASTEN, Paul R.,** Nuclear and fuel-cycle performance of molten-salt breeder reactors, 20: 3498
**KASTEN, Paul R.,** Nuclear fuel utilization and economic incentives, 20: 3513
**KASUGAI, Nobuo,** Chlorophyll chelate compounds as chemical protectors against radiation injury, 20: 1692
**KATO, H.,** High-melting point carbides (HfC), 20: 2351 (USBM-RC-1205, pp 3-7)
**KATO, H.,** W--Re--Mo alloy development, 20: 2354 (USBM-RC-1205 pp 15-19)
**KATO, Kiyoe,** Plasma ion oscillation in plasma beam system, 20: 3191
**KATTCHEE, N.,** Local film coefficients of turbulence promoted ML-1-type fuel elements, 20: 2022
**KATZOFF, S.,** Conference on thermal radiation of solids, San Francisco, Calif, 3/64, 20: 2427 (NASA-SP-55)
**KAWAGUCHI, Osamu,** Removal of iodine from atmosphere by spray. I., 20: 1966
**KAWASAKI, Setsuo,** Behavior of krypton and xenon in uranium metal, 20: 2358 (AERE-Trans-1034)
**KAYASHI, K.,** Hot laboratory of Japan Atomic Energy Research Institute, 20: 1997
**KAZACHKOVSKII, O. D.,** The BN-350 (Fast Neutron) Atomic Power Station, 20: 3475 (NP-15458)
**KAZANJIAN, Armen Roupen,** Hot atom chemistry of surfaces: chemical reactivity of isomeric radiobromine atoms, 20: 1934
**KAZI, A. H.,** Plutonium production and burnup calculation methods for light water moderated reactors, 20: 3535
**KAZI, A. Helim,** Approximation to space-energy slowing down through use of multigroup thermal self-shielding factors in $PuO_2$--$UO_2$ lattice calculations, 20: 3426
**KAZOVSKII, E. A.,** Problem of heat fluxes in superconducting devices, 20: 2892
**KEANE, B. E.,** Image contrast and radiation protection: A figure of merit. I., 20: 1698
**KECK, Carolyn A.,** Time-integrated model for reactor-excursion calculations, 20: 3418
**KEDEM, Ora,** Isotope flows and flux ratios in biological membranes, 20: 1585
**KEEFE, Denis,** Design of experimental facilities at proposed 200-Bev accelerator, 20: 2540 (UCRL-16223)
**KEENE, J. P.,** Effect of solvent on spectra produced by pulse radiolysis of solutions of organic electron scavengers, 20: 1920
**KEENEY, R. L.,** Environental effects on space structures, 20: 2036 (AD-618030)
**KEIRIM-MARKUS, I. B.,** Measurement of the background external radiation exposure of urban population in the USSR, 20: 2087
**KEITH, M. L.,** Systematic relationships between carbon and oxygen isotopes in carbonates deposited by modern corals and algae, 20: 1591
**KELBER, C. N.,** Group cross sections of fissile nuclides in unresolved energy range, 20: 2972
**KELBG, G.,** Observations on the quantum statistical ring sum of a system of punctiform charge carriers, 20: 2809
**KELLAR, A. A.,** Fuel elements for Arbeitsge-Meinschaft Versuchs reaktor (AVR), 20: 3494
**KELLER, C.,** Closed-cycle gas turbine for nuclear power plants, 20: 3343
**KELLER, F. L.,** The effect of charged-particle environments on manned military space systems, 20: 2656 (NASA-SP-71, pp 165-86)
**KELLER, R.,** Scientific program of laboratory for research on plasma physics, 20: 3206
**KELLERER, S.,** Feasibility of new procedure for biological dosimetry, 20: 1612 (EUR-2505.e)
**KELLOGG, H. B.,** Prog. rpt. on supercritical reactor, 7--9/62, 20: 3485 (WCAP-2120)
**KELLY, Hal J.,** Investigation of the system UC--UN--UO, 20: 2353 (USBM-RC-1205, pp 11-14)
**KELMAN, L. R.,** Compatibility of commercial cladding alloys with improved metallic fast reactor fuels, 20: 2229
**KELMAN, L. R.,** Improved metallic fast power breeder fuels, 20: 2386

**KEMMLER, Sibylle,** Ternary uranium(V) oxides, 20: 2400
**KEMP, T. J.,** Effect of solvent on spectra produced by pulse radiolysis of solutions of organic electron scavengers, 20: 1920
**KEMPER, R. S.,** Superconducting technetium–tungsten alloys, 20: 2907
**KENAHAN, C. B.,** Stress-corrosion cracking of vanadium, molybdenum, and a titanium–vanadium alloy, 20: 2254 (BM-RI-6680)
**KENDRICK, E. D.,** Adequacy of one-group three-dimensional model in core-following program, 20: 3501
**KENDRICK, E. D.,** Elk River lifetime—predicted and observed, 20: 3499
**KENNEDY, Kurt D.,** Grain boundary energy, 20: 2348 (UCRL-16051)
**KENZHEBAEV, Sh.,** Heavy monoatomic gas model and unsteady thermalization of neutrons in lead, 20: 2943
**KERIMOV, B. K.,** Lepton annihilation of proton-antiproton pairs with allowance for form factors and polarization correlations, 20: 2696
**KERLIN, T. W.,** Frequency response sensitivities in reactor dynamics studies, 20: 3377 (ORNL-P-1482)
**KERLIN, T. W.,** Frequency response sensitivities in reactor dynamics studies, 20: 3416
**KERLIN, T. W.,** Frequency response sensitivities in reactor dynamics studies, 20: 3380 (ORNL-TM-1305)
**KERPER, P.,** Scattered light in photothermo-elasticity, 20: 2026 (UCRL-13188)
**KERR, J. M.,** A device for outpile thermal simulation of reactor-fuel microstructures, 20: 2393
**KESHISHIAN, Vahe,** Criticality of $^{244}Cm$, 20: 2995
**KESSIE, R. W.,** Laboratory investigations in support of fluid-bed fluoride volatility processes. VIII., 20: 2076 (ANL-7068)
**KESSLER, W. E.,** Analysis of SNAP-10A/2 kinetic behavior using pulse reactivity excitations, 20: 3558
**KESTER, S. G.,** Weapons effects display system study, 20: 1987 (UCRL-13189)
**KESTIGIAN, M.,** Czochralski growth of rare-earth molybdates of type $M_2(MoO_4)_3$, 20: 1840
**KESZTHELYI, L.,** Investigations of ordering transformation in $Fe_3Al$ alloy by Moessbauer effect, 20: 3292
**KEY, Joseph A.,** Pulsed nuclear radiation induced transients in electrical cables, 20: 2186 (ECOM-2415)
**KHADR, F. H.,** Recurrent irradiation for oat breeding, 20: 1665
**KHARADZE, G. A.,** Passage of polarized neutrons through superconductor in mixed state, 20: 2998
**KHARLAMOV, S. P.,** Determination of isotopical components of the $\gamma + N \to N + \pi$ amplitude at $\gamma$ threshold, 20: 2737
**KHELASHVILI, A. A.,** Algebra of the currents and dispersion relations, 20: 2755 (JINR-E-2329)
**KHODEL, V. A.,** $\beta$-decay in nuclei, 20: 3101
**KHODEL, V. A.,** Calculation of magnetic moments of spherical nuclei, 20: 3118
**KHODEL', V. A.,** Single-particle 1-forbidden transitions in nuclei, 20: 3100
**KHOKHLOV, Yu. V.,** Influence of toroidal drift on plasma injection transversely to magnetic field, 20: 3205
**KHOMUTOVSKII, O. A.,** Microscopic and submicroscopic changes in adrenals in radiation sickness caused by radioactive strontium, 20: 1641
**KHRAMCHENKOV, V. A.,** Radiochemical processes taking place during radiolysis of carbon tetrafluorides, 20: 1899 (BNL-tr-23)
**KHVOROSTIN, Yu. S.,** Investigation of Ru(IV) solutions in perchloric and sulfuric acids, 20: 1853
**KHVOSTOVA, V. V.,** Mutants induced by ionizing radiations and ethyleneimine in winter wheat, 20: 1655
**KIBBLE, T. W. B.,** Elementary particle symmetries, 20: 2766
**KIEFER, H.,** Modern detectors in radiation protection, 20: 2143
**KIER, P. H.,** Group cross sections of fissile nuclides in unresolved energy range, 20: 2972
**KIGER, E. O.,** Leak testing of HWCTR containment building, 20: 2037 (DP-968)
**KIKIANI, B. I.,** Ionization produced in collisions between alkali metal atoms and gas molecules, 20: 2639
**KIKUCHI, C.,** Effect of neutron irradiation on electrical properties of $Mg_2Ge_{.8}Si_{.2}$, 20: 2502
**KIKUCHI, R.,** Lattice models for cooperative phenomena. I., 20: 1819 (UCRL-14287)
**KILIMANN, K.,** Stationary state of cylindrical plasmoid in external longitudinal magnetic field, 20: 3189
**KILLEN, D. A.,** Relative toxicity of angiographic contrast media, 20: 1724
**KILPATRICK, R. A.,** Current magnet design practice in the U.S.A., 20: 2533 (BNL-9536)
**KIM, Chong K.,** Determination of Hg in wheat and tobacco leaf by neutron activation analysis, 20: 1755
**KIM, H. J.,** $^{24}Mg(\alpha,\alpha)^{24}Mg$ reaction and a $J^{\pi} = 10^+$ state of $^{28}Si$, 20: 3069
**KIM, Hi-sang,** Radiation widths of intermediate nuclei, 20: 3133
**KIM, Y. S.,** Evidence for $\kappa^0(725)$ in $\pi^- p$ reactions, 20: 2715
**KIMBALL, D. S.,** Auroral morphology as shown by all-sky photographs, 20: 2852
**KIMURA, Masaomi,** Spectroscopic measurement of flame temperature in magnetohydrodynamic generator, 20: 2673
**KIMURA, Miwako,** Preparation of radium standard solutions, 20: 1941
**KINCINAS, J.,** Fluid-bed fluoride volatility processing of irradiated fuels in hot cells, 20: 1971
**KIND, A.,** New lattice calculation method for ORGEL-type reactors, 20: 3424
**KING, L. D. P.,** Some feasibility studies of nuclear destruct concept for Rover reactor disposal, 20: 3572
**KINGERY, W. D.,** Grain growth in porous compacts, 20: 2373
**KINGSBURY, F. D.,** Effect of thermal-neutron irradiation at fixed fast-neutron dose on creep-rupture properties of high-temperature alloys, 20: 2456
**KINGSLEY, V. V.,** Comparative sensitivity to $\gamma$ radiation of yeast mitosis and meiosis, 20: 1664
**KINNEY, W. E.,** Calculated fluxes of less than 50-Mev neutrons diffusing beneath shield of meson production facility, 20: 3262
**KINZER, Jackson,** Alpha-particle energized neutron-flux monitor, 20: 2173
**KIRILLOV, P. L.,** Decontamination of sodium from products of reactions with water in the circulation loop, 20: 1960
**KIRILYUK, A. L.,** Total neutron cross sections of $^{185}Re$ and $^{187}Re$, 20: 3030
**KIRIN, I. S.,** Lanthanum citrate complexes of 1:1 composition, 20: 1856
**KIRKBRIDE, J.,** Measurement of fast neutron spectra in infinite medium of $CH_2$, 20: 2931 (AD-616518)
**KIRKINSKII, V. A.,** System $UO_2$–$PbO_2$, 20: 1871
**KIRN, F. S.,** EBR-II self-excited oscillations, 20: 3514
**KIRN, F. S.,** EBR-II dynamics, 20: 3590
**KIRN, F. S.,** Monitoring reactor kinetics of EBR-II, 20: 3517
**KIRSANOVA, G. I.,** Radiation-induced brain necrosis (clinical observation), 20: 1713
**KIRSCHBAUM, H. S.,** NERVA reactor control, 20: 3569
**KISDI, David,** Landau theory of Fermi systems. II., 20: 2691
**KISER, Donald L.,** Anion exchange studies of Th, rare earths, and Sc, 20: 1959
**KISH, A. J.,** Metallurgical characteristics of weldments in 0.750-inch-thick 6061 aluminum, 20: 3609 (ACF-11)
**KITZES, S.,** Remote underwater devices for evaluation and reduction of irradiated Yankee fuel assemblies, 20: 2117
**KITZINGER, D. G.,** Aerospace nuclear safety: probability analysis of reactor power level and dose rate, 20: 3549 (SC-RR-65-417)
**KLAMUT, C. J.,** Relative aggressiveness of Li, Na, K, Rb, and Cs boiling and condensing in Nb–1Zr capsules, 20: 2268
**KLEFFNER, J. O.,** Startup experience with the EBR-II fuel cycle facility. I., 20: 3522
**KLEIN, A. H.,** Thermal diffusivity of armco iron by three methods, 20: 3622 (IS-1266)
**KLEIN, D.,** Measurement of fast advantage factors and intra-cell flux shapes in several eight-water-moderated slightly enriched uranium lattices, 20: 3396
**KLEIN, J. H.,** Chemonuclear loop removal from BGRR using semi-remote cutting technique, 20: 3599
**KLEIN, M. J.,** Influence of finely dispersed second phase on recrystallization, 20: 2325 (HW-SA-3767)
**KLEIN, Melvin,** Structure of socalled "ethylmetaphosphate" (langbeld ester), 20: 3640 (UCRL-11488)
**KLEIN, Melvin P.,** Paramagnetic resonance of $^{57}Fe$ in polycrystalline ferrichrome A, 20: 3643 (UCRL-11685)
**KLEPEIS, James,** Experimental studies of strong Hall effects and U x B induced ionization, 20: 2671
**KLIER, E. P.,** Prog. rpt. on irradiation effects on reactor structural materials, 11/64–1/65, 20: 2408 (AD-614899)
**KLINE, W.,** Operational practices in treatment of low and intermediate level radioactive wastes—Argonne and Los Alamos Laboratories, U. S. A., 20: 3603 (LA-DC-7249)
**KLINEBERG, Otto,** Social implications of peaceful uses of nuclear energy, 20: 2094
**KLONTZ, E. E.,** Electron irradiation of p-type Ge at 0°C, 20: 2485
**KLONTZ, E. E.,** Low-temperature irradiation of semiconductors and ionization effects, 20: 2482
**KLOPP, William D.,** Properties of arc-melted and electron-beam-melted tungsten, 20: 2396
**KNIGHT, Ford,** High-power operation of $PuO_2$–$UO_2$ fast reactor fuel, 20: 2448
**KNIGHTON, J. B.,** Preparation of metals by Mg–Zn reduction. III., 20: 2220 (ANL-7059)
**KNUTH, D. F.,** Neutron production by $(\alpha,n)$ reaction from heterogeneous isotopic sources, 20: 2949
**KOCH, H., Ruediger,** Neutron capture gamma spectrum and level scheme of $^{167}Er$, 20: 3127
**KOCH, Paul A.,** Relativistic shock structure, 20: 2844
**KOEHLER, W. C.,** Magnetic form factor of chromium, 20: 3280 (ORNL-P-1737)
**KOEHLER, W. C.,** Magnetic structure properties of Tb–Sc alloys,

20: 2338 (ORNL-P-1735)
**KOENIG, T. W.**, Deuterium isotope effects in decompositions of acetyl peroxide and two t-butyl peresters, 20: 1891
**KOERBLER, J.**, Generation and prevention of severe radiation lesions, 20: 1717
**KOGAN, V. S.**, Isotopic effect in values of molar volumes of LiF and LiH, 20: 3307
**KOHN, W.**, Self-consistent equations including exchange and correlation effects, 20: 3216
**KOLAR, J.**, Symptomatology of radiation-caused growth disturbances to vertebral column, 20: 1702
**KOLAR, O. C.**, Interaction in arrays of fissionable materials, 20: 2938 (UCRL-14245)
**KOL'GA, V. V.**, Strong-current high-energy particle accelerators—meson factories, 20: 2560
**KOLKUNOV, V. A.**, General method for calculations with phenomenological amplitudes, 20: 2804
**KOLOMIITSEVA, I. K.**, Role of systems orthophenols–orthoquinones in initial radiation-induced processes in an organism, 20: 1647
**KOLOPUS, James L.**, F centers in SrO and quadrupole moment of $^{87}Sr$, 20: 3087
**KOLOTYI, V. V.**, Total neutron cross sections of $^{185}Re$ and $^{187}Re$, 20: 3030
**KONAREV, M. I.**, Physico-chemical properties of crystal hydrates of terbium subgroup rare earth sulfates, 20: 1868
**KONAREVA, V. G.**, Viscosity of hydrogen isotope solutions, 20: 2922
**KONCZOS, G.**, Neutron diffraction studies on $(1-x)Fe_2O_{3-x}Rh_2O_3$ system, 20: 3293
**KONDO, M.**, Levels of $^{56}Ni$ from reaction $^{58}Ni(p,t)^{56}Ni$ at 28 Mev, 20: 3041
**KONOPLEVA, R. F.**, Ripening of defects, induced by fast neutrons in germanium, in course of low-temperature annealing, 20: 2509
**KONOPOLYANNIKOV, A. G.**, Action of protective agents following irradiation with sublethal doses, 20: 1688
**KONOVALOV, L. N.**, Physico-chemical properties of crystal hydrates of terbium subgroup rare earth sulfates, 20: 1868
**KONTOS, J.**, Analog computation of instability growth rates in finite conductivity magnetohydrodynamics, 20: 2836
**KOPITSCH, F.**, Propagation of thermal neutron bursts in diffusion media, 20: 2944
**KOPPEL, Joan U.**, Unified computational method for thermal-neutron scattering, 20: 3412
**KOPYLOV, V. A.**, Role of systems orthophenols–orthoquinones in initial radiation-induced processes in an organism, 20: 1647
**KORABLEVA, N. P.**, Influence of ionizing irradiation on growth and metabolism of nucleic acids in plants, 20: 1648
**KORCHACK, A. A.**, Electromagnetic radiation with continuous spectra during solar flares, 20: 2580
**KORENCHENKO, S. M.**, Displacement of spark chamber discharges in a magnetic field, 20: 2131 (JINR-P-2344)
**KORN, Dietrich**, Spin ordering of paramagnetic states in quenched condensed layers on superconductors, 20: 2918
**KORNBICHLER, Heinz**, Pressure release device to drench reactor core, 20: 3363
**KORNILOV, I. I.**, Physical metallurgy of titanium, 20: 2359 (NASA-TT-F-338)
**KOROBKOV, V. I.**, Dispersion method for relative measurements of radioactivity, 20: 1781
**KORSHUNOV, B. G.**, System $YCl_3$–NaCl–KCl, 20: 1872
**KORVER, John A.**, Isthmian canal studies, 1964, 20: 1985 (PNE-2003)
**KOSAREVA, K. V.**, Angular and energy distributions of $^{18}F$ recoil nuclei in reaction $^{19}F(\gamma,n)^{18}F$, 20: 3108
**KOSSIONIDES, S.**, First excited state of $^5He$, 20: 3078
**KOSTA, L.**, Determination of some impurities in nuclear-grade U, 20: 1784
**KOSTMAN, S.**, Carbon and nitrogen transfer in type 316-stainless steel Cb–1% Zr, liquid-potassium system, 20: 2239
**KOSUGE, K.**, Moessbauer effect of $^{57}Fe$ doped in $V_2O_3$, 20: 3289
**KOTANSKI, Andrzej**, Isotropic tensors, 20: 2761
**KOTHARI, N. C.**, Effect of particle size on sintering kinetics in alumina powder, 20: 2287
**KOVACIC, Evan C.**, Hydraulic studies with random-packed beds applicable to paste-fuel concept, 20: 3461
**KOVALEV, V. A.**, Geochemical aspects of Th/U ratio investigation in rocks, 20: 2052
**KOVARSKAYA, E. S.**, Stepwise excitation of fluorescence of $CaWO_4$ activated with $Er^{3+}$, 20: 1842
**KOVARSKII, A. P.**, Production and preparation of polymethylmethacrylate kryptonates, 20: 1862
**KOVBA, L. M.**, X-ray phase analysis of binary oxides in the $UO_2$–$MoO_2$–$MoO_3$ system, 20: 2384
**KOYAMA, K.**, Prog. rpt. on advanced, graphite-matrix, dispersion-type fuel systems and research on graphite, 8/15–11/14/64, 20: 2318 (GA-5918 (Pt. 1))
**KOZINA, G. S.**, Stepwise excitation of fluorescence of $CaWO_4$ activated with $Er^{3+}$, 20: 1842
**KOZLOV, F. A.**, Decontamination of sodium from products of reactions with water in the circulation loop, 20: 1960
**KOZLOVA, P. S.**, Two genetic types of post-magmatic thorium–rare earth deposits, 20: 2064
**KRAFFT, O.**, Propagation of discharges in self-extinguishing counters. IV., 20: 2176
**KRANER, Hobart W.**, Application of Li-drifted Ge detectors to neutron activation analysis—studies in geochemistry and of 15th century printing, 20: 2166
**KRASNOYAROV, N. V.**, The BN-350 (Fast Neutron) Atomic Power Station, 20: 3475 (NP-15458)
**KRAUSE, Manfred O.**, Electron shake-off resulting from K-shell ionization in Ne, 20: 2622
**KRAWCZYNSKI, S.**, Purification of uranium from fission products by means of fractional precipitation of $UO_2$ by reduction of $UO_2Cl_2$ from alkali chloride melt, 20: 1962
**KREMSER, Jacques**, ALECTO—results obtained with homogeneous critical experiments on $^{239}Pu$, $^{235}U$ and $^{233}U$, 20: 3369 (CEA-R-2814)
**KREN, E.**, Neutron diffraction studies $(1-x)Fe_2O_{3-x}Rh_2O_3$ system, 20: 3293
**KRESTOV, G. A.**, Entropy characteristics of smallest and largest hydrations of rare earth and actinide ions, 20: 1858
**KRESTOV, G. A.**, Thermal capacity of francium and astatine crystalline compounds at 0 to 300°K, 20: 1859
**KRIPYAKEVICH, P. I.**, New compounds of $MgCu_2$ type in alloys of rare-earth metals with Fe, Co, and Ni, 20: 2385
**KRIVKO, N. I.**, Local magnetic fields on surface of Nb–Zr superconductor in mixed state, 20: 2924
**KRIZAN, John E.**, Kinetic equation with relativistic interaction corrections for plasma, 20: 3218
**KRIZEK, R.**, Current magnet design practice in the U.S.A., 20: 2533 (BNL-9536)
**KROBER, M. S.**, Detection of phospholipids on paper chromatograms by neutron activation, 20: 1771
**KRUEGER, T. K.**, Atomic wave functions, collision cross sections, and transition probabilities of Fe ions, 20: 2609
**KRUGER, O. L.**, Phase relations in pseudo-ternary uranium–plutonium–fissium system, 20: 3493
**KRUMBEIN, A. D.**, Synthesis of spherical minimum-weight proton shields, 20: 3242 (NASA-SP-71, pp 225-8)
**KRUPP, William Edward**, Preparation of vanadium metal by aluminum reduction of $V_2O_5$, 20: 2225 (IS-T-40)
**KRUSKAL, Martin**, Explosion of a supernova into the interstellar magnetic field. II., 20: 2570
**KRUUV, J.**, Effect of inhaling 95% and 5% $CO_2$ on radiocurability of murine tumors, 20: 1683
**KRYLOV, L. I.**, Reaction of Pu with $H_2O_2$ in presence of other alloys, 20: 1857
**KUBIS, Joseph John**, Scattering amplitude for crossed-box ladder graphs in the Bethe-Salpeter equation, 20: 2818
**KUBIT, C. J.**, Behavior of water vapor $UO_2$ during irradiation, 20: 2468
**KUBO, Hiroshi**, Negative absorption of microwave radiation in weakly ionized xenon plasma in magnetic field, 20: 3204
**KUCERA, J.**, Radiolysis of acetone in the liquid phase. Quantitative study, 20: 1901
**KUCHERENKO, E. T.**, Low frequency oscillations in plasma of reflex discharge, 20: 3222
**KUDLACIK, Louis**, Mounting arrangements for casing-enclosed apparatus, 20: 3351
**KUECH, F.**, Microwave absorption and magnetic transition in $GdCl_3$, 20: 3288
**KUEHNE, D.**, Examinations of radioiodine uptake of human fetuses, 20: 1600
**KUGLER, E.**, Crowbar and power crowbar circuits and their calculation, 20: 2102 (JUL-273-PP)
**KUGLER, Tibor**, Plasma-jet gun, 20: 2251
**KUHL, O. A.**, Gamma radiation source and irradiator design, 20: 1937 (BNL-9281)
**KUKAVADZE, G. M.**, Search for anomalous hydrogen, 20: 2742
**KUKLIN, R. N.**, Mean widths for radiative transitions in heated nuclei, 20: 3114
**KUL'CHITSKII, L. A.**, Investigation of reaction $^{16}O(\gamma,p)^{15}N$, 20: 3107
**KULIK, M. I.**, Effect of temperature and oxygen on frequency of chromosome aberrations in irradiated tomato seeds, 20: 1638
**KULP, B. A.**, ESR center in ZnSe after electron bombardment at low temperature, 20: 2492
**KULP, B. A.**, Fluorescence studies on II-VI compound semiconductors, 20: 2498
**KULSRUD, Russell M.**, Explosion of a supernova into the interstellar magnetic field. I., 20: 2569
**KULSRUD, Russell M.**, Explosion of a supernova into the interstellar mag-

netic field. II., 20: 2570
KULSRUD, Russell M., Stability of negative $V^{-}$ systems, 20: 3167 (MATT-374)
KUNAISH, Hasson H., Time-, energy-, and space-dependent neutron thermalization theory, 20: 3003
KUNDU, S. K., Electromagnetic $2\pi$ decay of $K^0_2$, 20: 2692
KUNITOMI, Nobuhiko, Scattering of long wavelength neutrons by precipitations in $Al_{99.5}Cu_{0.5}$ alloys, 20: 3285
KURCHATOVA, L. N., Cross sections for nuclear reactions $^{45}Sc(n,\alpha)^{42}K$, $^{42}Ca(n,p)^{42}K$, and $^{43}Ca(n,p)^{43}K$. Production of carrier-free $^{42}K$ and $^{43}K$, 20: 1947
KUROI, H., EBR-II self-excited oscillations, 20: 3514
KUROI, H., Monitoring reactor kinetics of EBR-II, 20: 3517
KURSANOV, D. N., Isotopic exchange of hydrogen atoms in cyclopentadienyl rings of cobalticinium compounds, 20: 1828
KURSANOV, D. N., Replacement of a halogen by a proton in halogenoferrocenes, 20: 1830
KUSHNIRENKO, A. N., New method of calculating magnetic moment of the electron, 20: 2601
KUZHETSOV, E. P., Production of slow $\pi$ mesons on light nuclei and the $\pi\sigma$ interaction, 20: 2739
KUZIN, A. M., Role of systems orthophenols–orthoquinones in initial radiation-induced processes in an organism, 20: 1647
KUZ'MINA, S. S., Radiation polymerization of hexamethylcyclotrisiloxane in solid phase, 20: 1903
KUZ'MINOV, B. D., Kinetic energies of fragments with various masses in fission of $^{235}U$ by thermal and fast neutrons, 20: 3110
KUZNETSOV, B. S., Behavior of polonium in ketones and mixed aqueous-acetone solutions, 20: 1946
KUZNETSOV, B. S., Effects of ketones on polonium behavior in hydrochloric solutions, 20: 1777
KUZNETSOV, E. V., Production of slow $\pi$ mesons on light nuclei and the $\pi\sigma$ interaction, 20: 2739
KVITEK, Louis C., DEL—perturbation program written in FORTRAN, 20: 3366 (ANL-7052)
KYLE, M. L., Corrosion of refractory metals by zinc–magnesium–uranium and halide salt systems, 20: 2266
KYLE, Martin L., Corrosion of steels and tantalum by molten cadmium–magnesium–zinc systems, 20: 2265
KYONG, Sang H., Input-output approach to optimal control, 20: 3409

# L

LACEY, P. G., Comparison of calculated and measured burnup distributions and isotopic inventory in Yankee core, 20: 3504
LAGET, J. M., Study of levels of $^{63}Cu$ by inelastic scattering of 10 Mev deuterons, 20: 3073
LAHTI, J. A., Compatibility of commercial cladding alloys with improved metallic fast reactor fuels, 20: 2229
LAI, M. G., Compendium of radiochemical procedures for determination of selected fission products in sea water, 20: 1749 (USNRDL-TR-912)
LAL, Manohar, Extraction of thorium, protactinium, uranium, ruthenium, and zirconium by long-chain amines, 20: 1761
LALLEMAND, Andre, Calculation of collision [cross] sections of $2s \rightarrow np$ type in ions of isoelectronics series of lithium, 20: 2598
LAM, Carroll F., Pulse-shape discrimination technique for dual-crystal Compton reduction detector, 20: 2167
LAMBERT, Michel, Analogous isobaric states of $^{41}Ar$ in $^{41}K$, 20: 3036
LAMBERT, V. E., Recrystallization variables of flat-rolled molybdenum–cobalt alloys, 20: 2313 (AD-619208)
LAMOREE, D. J., Use of $^{14}C$ to measure $CO_2$ removal in a synthetic ammonia plant, 20: 1836
LANDGREBE, A. R., Determination of trace amounts of cadmium and silver by substoichiometric radioisotopic dilution analysis, 20: 1786
LANDSBERG, L. G., Elastic backward scattering of $\pi^-$ by neutrons, 20: 2700
LANDSBERG, L. G., $\pi^-$ meson-neutron elastic backward scattering at 1.4 to 4.0 Bev, 20: 2713
LANE, Frank O., Mathematical models of magnetic flux compression, 20: 2523 (SC-RR-65-449)
LANG, G., Energy transfer in $\gamma$ radiolysis of the benzene–benzophenone–isopropanol system, 20: 1931
LANG, J., $^{238}U$ fission induced by low-energy monochromatic $\gamma$-rays, 20: 3050
LANG, Peter M., Survey of high-temperature demineralization for dual-purpose BWR plants, 20: 3539 (ACNP-65558(Rev. 1))
LANG, S. M., Studies on monoclinic zirconium dioxide from room temperature to 1095°C, 20: 2314 (ARL-65-140)
LANGE, D., Decay of $^{58}Co$, $T_{1/2}$ = 18hr, 20: 3132
LANGE, H., Calculation of pressure drop in ducts and fuel elements with shroud, 20: 2010 (IPV-19)
LANGER, B. F., Use of materials properties by the reactor vessel designer, 20: 2479
LANGEVIN, M., De-excitation of states of giant dipolar resonance of $^{16}O$, 20: 3074
LANGHAM, Wright H., Biological aspects of use of spheroidized fuel in space nuclear power systems, 20: 1694
LANGSFORD, A., Polarization in neutron-proton scattering, 20: 2701
LANNING, D. D., Measurement of diffusion coefficient in highly anisotropic medium, 20: 2957
LANNING, D. D., Reactor physics measurements in slightly enriched uranium $D_2O$ lattices, 20: 3397
LANNING, D. D., Studies of subcritical lattices with distributed neutron absorber by means of pulsed-neutron source technique, 20: 3432
LANZ, R., Preparation of uranium dioxide and carbide particles by sol-gel methods, 20: 2226 (RT/CHI(65)-30)
LANZA, F., TESI—advanced power excursion reactor for research in reactor safety, 20: 3584 (EUR-2433.e)
LAPIN, V. A., Thermal capacity of francium and astatine crystalline compounds at 0 to 300°K, 20: 1859
LAPITSKII, A. V., Behavior of thorium, protactinium, and uranium during extraction by means of benzohydroxamic acid and n-benzoylphenylhydroxylamine, 20: 1776
LAPITSKII, A. V., Complexing of actinide elements, 20: 1855
LAPITSKII, A. V., Thorium, protactinium, and uranium extraction by means of neocupferron, 20: 1775
LARIONOVA, V. G., Determination of isotopical components of the $\gamma + N \rightarrow N + \pi$ amplitude at $\gamma$ threshold, 20: 2737
LARKIN, A. I., Nuclear rotational spectra at high momenta, 20: 3103
LA ROCQUE, D. D., Operating experience with the KAPL Radioactive Materials Lab. metallography facility, 20: 2247
LARSON, Robert, TRIST—tri-level multiprogramming executive involving real-time calculations and asynchronous on-line data source, 20: 3644 (UCRL-16199)
LASCARO, Charles P., Pulsed nuclear radiation effects on resistors and cables, 20: 2187 (ECOM-2545)
LASEEVA, G. S., Devices for spectral-isotopic determination of gases in metals, 20: 1793
LASHKO, N. F., Modification of magnesium alloys with zirconium and lanthanum, 20: 2399
LASKORIN, B. N., Extraction of U(VI) from carbonate solutions by quaternary phosphonium and arsonium bases, 20: 1782
LASSILA, K. E., Unstable boson exchange interactions and pole approximation for resonance particles, 20: 2779
LATHROP, K. D., Moments equations and equivalent discrete ordinates equations. I., 20: 2981
LATHROP, K. D., Moments equations and equivalent discrete ordinates equations. II., 20: 2982
LATIMER, I. D., Corpuscular bombardment and $N^+_2$ radiation, 20: 2859
LATTA, R. E., Determination of melting point of $UO_{2+x}$, 20: 2390
LATTMAN, Eaton E., Compact versatile x-ray collimator with adjustable pinholes, 20: 2162
LAUER, R. S., Extraction of rare earth amygdalate salts by butanol, 20: 1796
LAURITZEN, T. A., Effect of carbon-contaminated sodium on austenitic stainless steel, 20: 2244
LAUTZENHEISER, C. E., Prog. rpt. on evaluation of serviceability of Elk River reactor pressure vessel, 5–7/65, 20: 3482 (SWRI-1228-75)
LAVAL, G., Necessity of energy principles for magnetostatic stability, 20: 3211
LAVDANSKII, P. A., Shielding parameters of concretes, 20: 3253
LAVINE, Leroy S., Prog. rpt. on bioelectric effects in calcified tissues, 9/64–6/65, 20: 3625 (NYO-3282-1)
LAVRENCHIK, V. N., Global fallout of nuclear explosion products, 20: 2086 (BNL-tr-42)
LAVRENTOVICH, Ye. I., Gamma and neutron dosimetry using colored polyvinyl alcohol films in nuclear reactors, 20: 2135
LAVRINENKO, I. A., Capillary phenomena in densification process during sintering in presence of liquid phase, 20: 2286
LAX, Benjamin, Prog. rpt. on solid state research using high magnetic fields, 7/60–10/64, 20: 2519 (AD-615152)
LAYTON, J. K., Secondary-electron emission from molybdenum due to positive and negative ions of atmospheric gases, 20: 2628
LAZARENKO, V. R., Attempt to detect double $\beta$-decay in $^{48}Ca$, 20: 3137
LAZAREV, L. N., Investigation of Ru(IV) solutions in perchloric and sulfuric acids, 20: 1853
LEA, A. T., Evidence for pion-nucleon inelastic $S_{31}$ resonance, 20: 2716
LEA, D. A., Pairing forces with neutrons and protons, 20: 3066
LEADON, Bernard M., Measurements and calculations of hydrogen loss from hydrided zirconium–uranium fuel elements during transient heating to temperatures near melting point, 20: 3563
LEAMER, R. D., Calorimetric and spectrometric techniques to relate zone-wise power distributions in Pu–U multizoned cores, 20: 3388
LEBEAU, Paul, Thermal decomposition of uranyl nitrate, 20: 1820 (AEC-tr-6619)
LEBEDEV, A. I., Determination of isotopical components of the $\gamma + N \rightarrow$

$N + \pi$ amplitude at $\gamma$ threshold, 20: 2737

**LEBEDEVA, N. E.,** Role of systems orthophenols–orthoquinones in initial radiation-induced processes in an organism, 20: 1647

**LECHEVALLIER, Mewice,** Drive mechanism for nuclear reactor control rods, 20: 3356

**LECLERCQ, Daniel,** Improvements in beryllium–magnesium alloys, 20: 2277

**LEDDICOTTE, G. W.,** Radiochemistry of selenium, 20: 1744 (NAS-NS-3030(Rev.))

**LEE, Ikcheon,** Astatine isotopes produced in $^{3}$He bombardment of bismuth, 20: 1949

**LEFEBVRE, Gilbert,** System for mechanically mounting a radioactive sample, 20: 2006

**LEGAL, J.,** Device to facilitate threading of $^{60}$Co beads, 20: 1722

**LEGAR, F.,** Semi-automatic device for scanning and measuring spark chamber photographs, 20: 2130 (JINR-P-2340)

**LEGG, John Wallis,** Catalytic reactions of aliphatic alcohols over thorium oxide, 20: 1892

**LEIBFRIED, G.,** Convergence behavior of expansions in the classical collision theory, 20: 2808

**LEIGH, Gerald G.,** Simulation of air-blast-induced ground motion, phase I, 20: 1980 (AD-614990)

**LEIMGRUBER, R.,** Energy loss per ion pair in various gases from nitrogen and oxygen ions from 0.14 to 0.7 Mev, 20: 2602

**LEIPUNSKII, A. I.,** The BN-350 (Fast Neutron) Atomic Power Station, 20: 3475 (NP-15458)

**LEISTNER, M.,** Absolute standardization of electron-capturing radionuclide $^{54}$Mn by $4\pi$X(PC)- and $4\pi(X,e_K)$-$\gamma$-measurements, 20: 3034

**LEITH, D. W. G.,** Spin, parity and isospin of Y*(1760), 20: 2711

**LEMKEY, F. D.,** Phase-reinforced high-temperature alloys produced directly from the melt, 20: 2219 (AMRA-CR-64-05/4)

**LENOIR, Marcel,** Einstein-Schroedinger theory and its generalizations, 20: 2869

**LEONARD, Regis F.,** Elastic and inelastic scattering of 40-Mev alpha particles from even tin isotopes, 20: 3017 (NASA-TN-D-3067)

**LERNER, E.,** Properties of superconducting Mo–Re alloys, 20: 2890 (AFML-TR-65-154)

**LEROUX-HUGON, P.,** Effect of fast neutron irradiation on thermal conductivity of ternary arsenides, 20: 2488

**LETFUS, V.,** Determination of effective cross-section for collisions of neutral calcium with argon, 20: 2597

**LETOURNEA, R. O.,** Weight, center of gravity, and moment of inertia of geometric solids, 20: 3633 (SC-TM-64-1686)

**LEVANDO, L. K.,** Investigations of polymerization radiation. V., 20: 1930

**LEVCHENKO, A. V.,** Certain polonium *p*-anisyl derivatives, 20: 1854

**LEVCHENKO, A. V.,** Synthesis of some polonium $\alpha$-naphthyl derivatives, 20: 1850

**LEVIN, B. Yu.,** Origin of meteorites, 20: 2590

**LEVIN, V. I.,** Cross sections for nuclear reactions $^{45}$Sc(n,$\alpha$)$^{42}$K, $^{43}$Ca(n,p)$^{43}$K, and $^{43}$Ca(n,p)$^{43}$K. Production of carrier-free $^{42}$K and $^{43}$K, 20: 1947

**LEVIN, V. I.,** Preparation of specimens and corrections for self-absorption during measurement of activity of soft $\beta$ emitters, 20: 1780

**LEVINSON, C. A.,** Renormalization of the strangeness-changing axial-vector coupling constant and the Cabibbo form of universality, 20: 2722

**LEVIS, A. G.,** Prog. rpt. on cell survival as function of radiation dose, final 1959-62, 20: 1617 (NP-15149)

**LEVITT, Albert P.,** Infrared radiation of solids refractory materials, 20: 1823

**LEVON, A. I.,** Gamma and neutron dosimetry using colored polyvinyl alcohol films in nuclear reactors, 20: 2135

**LEVY, Peter M.,** Anisotropy of exchange in ytterbium iron garnet, 20: 1802 (AD-618038)

**LEVY, R. H.,** Diocotron instability in quasi-toroidal geometry, 20: 3252 (NP-15578)

**LEVY-LEBLOND, Jean-Marc,** N-particle kinematics and group-theoretical treatment of phase space. I., 20: 2772

**LEVY-LEBLOND, Jean-Marc,** Three-particle nonrelativistic kinematics and phase space, 20: 2773

**LEVY-NAHAS, Monique,** Three-particle nonrelativistic kinematics and phase space, 20: 2773

**LEW, Marion S.,** Determination of $^{155}$Eu in fission products using reduction by lithium amalgam, 20: 1752

**LEWINS, Jeffery,** Optimization theorems in reactor physics, 20: 3330

**LEWINS, Jeffery,** Optimum shielding theory, 20: 3346

**LEWINS, Jeffery,** Stationary calculation of ratios in reactor statics, 20: 3367 (BNWL-156)

**LEWIS, R. A.,** Doppler-effect measurements on dilute fast-carbide assembly, ZPR-6 assembly 4Z, 20: 2959

**LEWIS, R. A.,** Equipment and techniques for Doppler-effect measurements on fast critical assemblies, 20: 3401

**LEWIS, R. E.,** Reactor neutron cross sections for production of $^{33}$P from $^{36}$Cl and enriched $^{33}$S in Oak Ridge research reactor, 20: 3020 (ORNL-TM-1065)

**LEWIS, R. R.,** Particle-mixture theories of $K^0 \to 2\pi$ decay, 20: 2720

**LEWIS, Robert H.,** Post-accident recovery program, 20: 3339

**LIBBY, W. F.,** Production of tritium and $^{3}$He by proton bombardment of metals, solar origin of terrestrial tritium, 20: 3095

**LIBMAN, G.,** Analysis of $\pi^- + p \to \pi^- + \pi^+ + n$ and $\pi^- + p \to \pi^- + \pi^0 + p$ at 338 Mev, 20: 2682 (JINR-P-2320)

**LICHNEROWICZ, Andre,** Thermodynamic fluid in the Jordan-Thiry theory, 20: 2827

**LIEBERMAN, P.,** Prog. rpt. on reactor containment, 10/64–7/65, 20: 3324 (IITRI-578P21-13)

**LIEBLEIN, S.,** Material and geometry aspects of space radiators, 20: 3556

**LIFSON, H.,** $2^{1,3}$P, $3^{1,3}$P, and $4^{1,3}$P states of He and the $2^{1}$P state of $Li^{+}$, 20: 2626

**LIGENZA, S.,** Optical transitions of electrons in fast-neutron-irradiated antimony-doped germanium, 20: 2495

**LIKHACHEV, M. F.,** Elastic $\pi^{+}$-p scattering at 180° and high energies, 20: 2683 (JINR-P-2327)

**LILEY, B.,** Examination of relative merits of stochastic and nonstatistical methods of computing primary ionization doses, 20: 2658 (NASA-SP-71, pp 527-33)

**LILLETHUN, E.,** Real part of proton-neutron scattering amplitude at 19.3 Gev, 20: 2712

**LIM, M.,** Fission neutron age and thermal diffusion length in ordinary concrete, 20: 3255

**LIMIC, N.,** Remark on crossing symmetry and parastatistics, 20: 2751 (IC/65/51)

**LINARES, Robert C.,** Prog. rpt. on $CeO_2$ as laser host, 1965, 20: 2312 (AD-619197)

**LIND, Jan-Erik,** Bibliography on preventive maintenance in chemical and mining industries, 20: 1976 (VDDIT-94)

**LINDEN, D. B.,** Multipurpose $^{60}$Co $\gamma$ irradiation facility, 20: 2193

**LINDENBAUM, A.,** Colloidal properties of plutonium in dilute aqueous solution, 20: 1835

**LINDENFELD, P.,** Metallic heat conductivity below 1°K, 20: 2383

**LINEV, S. V.,** Distribution of specific ionization along the track as a function of initial energy of $^{235}$ fission fragments, 20: 3029

**LINZ, H.,** Analysis and data processing of multiparametric measurement values, 20: 2142

**LIPELES, M.,** Direct detection of two-photon emission from metastable state of singly ionized helium, 20: 2630

**LIPIS, L. V.,** Physico-chemical properties of crystal hydrates of terbium subgroup rare earth sulfates, 20: 1868

**LIPPMAA, E.,** Nuclear magnetic double resonance in analysis of high-resolution NMR spectra, 20: 2109

**LITHERLAND, A. E.,** Radiative transitions following nuclear reactions, 20: 3150

**LITMAN, A. P.,** Partitioning of oxygen between zirconium and liquid potassium, 20: 2367

**LITTLE, R.,** Attenuation of radiation from finite plane source by horizontal concrete slabs, 20: 3271

**LITTLE, W. W.,** Physics aspects of fast-flux test reactor, 20: 3597

**LITTLE, W. W. Jr.,** Safety and nuclear considerations in design of FTR, 20: 3581 (BNWL-SA-340)

**LITVINENKO, Yu. A.,** Magnetic flux jumps in hard superconductors in pulsed magnetic fields, 20: 2921

**LJUNGGREN, K.,** Radiotracer studies of industrial processes and waste discharges, 20: 2201

**LLOYD, D. B.,** Corrosion studies in the NaK 78 type-316 stainless-steel Cb–1% Zr alloy system, 20: 2273

**LLOYD, R. C.,** Criticality research on plutonium, 20: 3368 (BNWL-SA-214)

**LLOYD, R. C.,** Criticality studies with plutonium solutions, 20: 3395

**LLOYD, R. C.,** Recent exponential and critical approach experiments with slightly enriched uranium metal tubes in light water, 20: 3393

**LOAWHAKASETR, Pathom,** Influence of certain chemicals on sensitivity of rat embryos to x irradiation, 20: 1693

**LOBKOWICZ, F.,** Muon and antiproton trap at SLAC, 20: 2547 (UR-875-98)

**LOCKER, D. R.,** ESR center in ZnSe after electron bombardment at low temperature, 20: 2492

**LOFBERG, Robert T.,** Long-lived radiation-induced electron spin resonances in an aqueous biological system, 20: 1605

**LOFERSKI, J. J.,** Radiation defects in GaAs based on proton- and electron-bombardment induced light emission, 20: 2501

**LOGINOV, A. A.,** Biphenyl thermal turbines and their maximum power, 20: 2019

**LOISEAUX, J. M.,** De-excitation of states of giant dipolar resonance of $^{16}$O, 20: 3074

**LOKAJICEK, M.,** Symptomatology of radiation-caused growth disturbances to vertebral column, 20: 1702

**LOMER, P. D.,** High output neutron tubes, 20: 3005

**LONCHAMP, J. P.,** Production of hyperfragments and $^{8}$Li fragments, 20: 3062

**LONERGAN, J. A.,** Mean lives of excited states in $^{14}N$, 20: 3045
**LONG, E. L. Jr.,** Irradiation behavior of high-burnup $ThO_2$–4.45% $UO_2$ fuel rods, 20: 2429 (ORNL-3837)
**LONG, Everett,** Nuclear reactors, 20: 3538
**LONG, Robert L.,** Effects of reflectors on burst characteristics of WSMR fast-burst reactor, 20: 3589
**LONG, Robert L.,** Report of reactor excursion during test of modified WSMR fast-burst reactor core, 20: 3594
**LONSDALE, H. K.,** Prog. rpt. on advanced, graphite-matrix, dispersion-type fuel systems and research on graphite, 8/15–11/14/64, 20: 2318 (GA-5918(Pt. 1))
**LOO, P. Von,** Purification of uranium from fission products by means of fractional precipitation of $UO_2$ by reduction of $UO_2Cl_2$ from alkali chloride melt, 20: 1962
**LOOG, P. K.,** Tera-ohmeter with a radioactive generator current, 20: 2108
**LOOSCH, R.,** Legal questions on the commercial entry of the Savannah into German waters, 20: 2088
**LOPRIENO, Nicola,** Investigations on reversions to methionine independence induced by mutagens in Schizosaccharomyces pombe, 20: 1654
**LOSKUTOVA, N. G.,** $\gamma$-Spectrum from the reaction $^{54}Fe(n,\gamma)^{55}Fe$, 20: 3109
**LOTTS, A. L.,** Remote refabrication of reactor fuels, 20: 2282 (HW-SA-3755)
**LOTTS, A. L.,** Thorium–uranium recycle facility, 20: 1994
**LOU, K. H.,** Current magnet design practice in the U.S.A., 20: 2533 (BNL-9536)
**LOVE, Warner E.,** Compact versatile x-ray collimator with adjustable pinholes, 20: 2162
**LOVELACE, C.,** Evidence for pion-nucleon inelastic $S_{31}$ resonance, 20: 2716
**LOVELL, A. J.,** Effect of thermal-neutron irradiation at fixed fast-neutron dose on creep-rupture properties of high-temperature alloys, 20: 2456
**LOVTSEVICH, E. L.,** Comparative resistance of enteroviruses and B. coli in water disinfection with $\gamma$ radiation, 20: 1645
**LOWDER, W. M.,** Direct-field $\gamma$ spectrometry for rapid quantitative assessment of environmental contamination, 20: 2171
**LOWENBERG, A. L.,** Prog. rpt. on evaluation of serviceability of Elk River reactor pressure vessel, 5–7/65, 20: 3482 (SWRI-1228-75)
**LOWRIE, L. M.,** Strong-motion seismic measurements. Project Dugout, 20: 1981 (PNE-605F)
**LU, Chen-fu,** Cherenkov radiation in anisotropic media, 20: 2734
**LUCEY, J. W.,** Numerical solutions of transport equation, 20: 2984
**LUCIUS, J. L.,** Frequency response sensitivities in reactor dynamics studies, 20: 3377 (ORNL-P-1482)
**LUCIUS, J. L.,** Frequency response sensitivities in reactor dynamics studies, 20: 3416
**LUCIUS, J. L.,** Frequency response sensitivities in reactor dynamics studies, 20: 3380 (ORNL-TM-1305)
**LUDEWIG, H.,** Geometrical effects on neutron resonance absorption in heterogeneous system, 20: 2973
**LUDLOW, J. O.,** Inert-atmosphere enclosure for environmental testing, 20: 2246
**LUEBS, Eide-Dittmar,** Use of positron emitter in determination of coronary blood flow in man, 20: 1709
**LUHLEICH, H.,** Septum cap technique and its many-sided applications, 20: 1945
**LUKASZUK, L.,** Resonances in Y-$\pi$ scattering, 20: 2694
**LUKENS, H. R.,** The determination of vanadium in blood by neutron activation analysis with preirradiation separation, 20: 1791
**LUKENS, H. R., Jr.,** Activation analysis simultaneous determination of manganese, copper and zinc in blood serum, 20: 1586
**LUKENS, H.R. Jr.,** Neutron activation determination of rare-earth elements in silicate ores, 20: 2056
**LUKYANOV, S. Yu.,** Attempt to detect double $\beta$-decay in $^{48}Ca$, 20: 3137
**LUK'YANOV, V. B.,** Dispersion method for relative measurements of radioactivity, 20: 1781
**LUNDGREN, Donald G.,** Prog. rpt. on production and study of asporogenic mutants, annual, 1965, 20: 1582 (NYO-2038-2)
**LUNDQUIST, D.,** Polarization measurements on recoil proton from $\pi^0$ photoproduction, 20: 2679 (AD-618664)
**LUNGU, S.,** Study of liquidus diagrams and thermodynamic properties of $SiO_2$–$ThO_2$ and $SiO_2$–$ThO_2$–$UO_2$ systems, 20: 2326 (IFA-FR-39)
**LURCAT, Francois,** N-particle kinematics and group-theoretical treatment of phase space. I., 20: 2772
**LURIE, H.,** Geometrical effects on neutron resonance absorption in heterogeneous system, 20: 2973
**LURIE, H.,** Time-dependent monoenergetic neutron transport in two adjacent semi-infinite media, 20: 2987
**LUSEBRINK, T. R.,** Analysis of nuclear magnetic resonance spectroscopic data: four-membered ring compounds, 20: 3645 (UCRL-16344)
**LUSHCHIKOV, V. I.,** Dynamic polarization of protons in rotating lanthanum–magnesium nitrate crystal, 20: 3311
**LUTON, J. N. Jr.,** Problems in design of an 8th order power optimized coil, 20: 2522 (ORNL-P-1516)
**LYAPUNOV, O. I.,** Effects of reactor radiation on thermophysical properties of monoisopropyldiphenyl, 20: 1923
**LYKOUREZOS, A. P.,** Precision method for routine measurement of $^{14}C$ and $^{3}H$ in proportional counters, 20: 1768
**LYNAM, L.,** Behavior of blanket $UO_2$ fuel rods in PWR core I, 20: 3495
**LYNTON, E. A.,** Metallic heat conductivity below 1°K, 20: 2383
**LYON, W. L.,** Melting point of plutonia–urania mixed-oxide fuels, 20: 2391
**LYONS, L.,** Deuteron–deuteron interaction at 270 to 507 Mev/c, 20: 3042
**LYONS, M. F.,** New evidence to delineate the $UO_2$ molten boundary, 20: 2392
**LYS, J. E. A.,** Deuteron–deuteron interaction at 270 to 507 Mev/c, 20: 3042
**LYUBIMOV, A. L.,** Elastic $\pi^+$-p scattering at 180° and high energies, 20: 2683 (JINR-P-2327)
**LYUBIMOV, V. A.,** Elastic backward scattering of $\pi^-$ by neutrons, 20: 2700
**LYUBIMOV, V. A.,** $\pi^-$ meson-neutron elastic backward scattering at 1.4 to 4.0 Bev, 20: 2713
**LYUBOSHITS, V. L.,** Scattering of neutrons on polarized targets, 20: 3120

# M

**MAAS, M. E.,** Aqueous radioactive waste treatment plant at Rocky Flats, 20: 1940 (RFP-638)
**MACDONALD, D. R.,** Biological interactions associated with spruce budworm infestations, 20: 1589 (BNL-917, pp 61-8)
**MAC DONALD, N.,** Dalitz diagrams and decay of $^{12}C$ states, 20: 3067
**MAC DONALD, N.,** Nuclear structure and electromagnetic interactions, 20: 3147
**MAC DONALD, R. D.,** Re-irradiation of a high burnup $UO_2$–Zircaloy fuel element at an increased heat rating, 20: 2421 (EXP-NRX-22902)
**MAC DONALD, R. N.,** Calculating space-dependent reactor transfer functions using statics techniques, 20: 3421
**MAC EWAN, J. R.,** An in-pile study of the thermal conductivity and electrical properties of $UO_2$ and $UO_{2-x}$, 20: 2452
**MAC EWAN, J. R.,** Fission-product gas pressures in $UO_2$ fuel elements during irradiation, 20: 2462
**MACHARADZE, T. S.,** Photodisintegration theory for lightest nuclei, 20: 3105
**MACKAY, J. W.,** Application of hot carrier techniques to study of radiation damage in germanium, 20: 2483
**MAC KAY, J. W.,** Electron irradiation of p-type Ge at 0°C, 20: 2485
**MAC KAY, J. W.,** Low-temperature irradiation of semiconductors and ionization effects, 20: 2482
**MACKINTOSH, A. R.,** Observation of resonant lattice modes by inelastic neutron scattering, 20: 3302
**MAC PHERSON, R. E.,** Screening tests of turbine nozzle and blade materials, 20: 2240
**MADELL, John T.,** Breeder reactors—tomorrow's power plants, 20: 3491
**MADEY, Richard,** Quality factors for degraded proton spectra, 20: 3243 (NASA-SP-71, pp 229-34)
**MADIGAN, Sandra,** Prog. rpt. on applications of neutron-activation analysis to scientific crime detection, 2–4/63, 20: 1739 (GA-4297)
**MADIGAN, Sandra,** Prog. rpt. on application of neutron-activation analysis to scientific crime detection, 5–7/63, 20: 1740 (GA-4576)
**MAECK, William J.,** Prog. rpt. on burnup determination of nuclear fuels, 4–6/65, 20: 3010 (IDO-14663)
**MAEKAWA, Tatsuo,** Removal of iodine from atmosphere by spray. I., 20: 1966
**MAERKER, R. E.,** Differential fast-neutron albedos for concrete. I., 20: 2932 (ORNL-3822(Vol.1))
**MAERKER, R. E.,** Differential fast-neutron albedos for concrete. II., 20: 2933 (ORNL-3822(Vol.2))
**MAERKER, R. E.,** Differential fast-neutron albedos for concrete. III., 20: 2934 (ORNL-3822(Vol.3))
**MAERKER, R. E.,** Differential fast-neutron albedos for concrete. IV., 20: 2935 (ORNL-3822(Vol.4))
**MAERKER, R. E.,** Differential fast-neutron albedos for concrete. V., 20: 2936 (ORNL-3822(Vol.5))
**MAERKER, R. E.,** Differential fast-neutron albedos for concrete. VI., 20: 2937 (ORNL-3822(Vol.6)
**MAERKER, R. E.,** Single-velocity calculation and measurement of differential angular thermal-neutron albedos for concrete, 20: 3266
**MAGNUS, D. K.,** UC fabrication cost data for Hallam second core, 20: 3509
**MAGNUSON, G. D.,** Secondary-electron emission from molybdenum due to positive and negative ions of atmospheric gases, 20: 2628
**MAGNUSON, G. D.,** Space electron radiation shielding—bremsstrahlung and electron transmission, 20: 3248 (NASA-SP-71, pp 455-63)
**MAGYAR, John,** Large-angle collisions in an aluminum surface bombarded by 50-kev argon ions, 20: 2629
**MAHADEVAN, P.,** Secondary-electron emission from molybdenum due to positive and negative ions of atmospheric gases, 20: 2628

**MAHAGIN, D. E.,** Remote determination of gas pressure and volume for encapsulated fuel elements, 20: 2116

**MAHAGIN, D. E.,** Startup experience with the EBR-II fuel cycle facility. III., 20: 2297

**MAILING, L.,** Selection rules for nuclear reactions involving nucleon associations in SU(3) scheme, 20: 3117

**MAISON, J. M.,** De-excitation of states of giant dipolar resonance of $^{16}O$, 20: 3074

**MAJUMDAR, Rabi,** Some consequences of the De Santis model for weak interactions, 20: 2784

**MAKAROV, A. A.,** Meson current in broken symmetry U(12) and experiments with colliding beams, 20: 2753 (JINR-P-2300)

**MAKAROV, E. S.,** System $UO_2$–$PbO_2$, 20: 1871

**MAKAROV, V. M.,** Decontamination of sodium from products of reactions with water in the circulation loop, 20: 1960

**MAKASHEV, Yu. A.,** Lanthanum citrate complexes of 1:1 composition, 20: 1856

**MAKHAN'KOV, V. G.,** Surface wave in plasma with current of limited radius, 20: 3165 (JINR-P-2352)

**MAKI, H.,** An in-pile study of the thermal conductivity and electrical properties of $UO_2$ and $UO_{2-x}$, 20: 2452

**MAKI, Kazumi,** Gapless superconductivity induced by metallic contacts, 20: 2910

**MAKIN, Myer,** Chronic synovial effusions treated with intra-articular radioactive gold, 20: 1706

**MAKOVETSKII, K. L.,** Synthesis of trimethylbenzenes for measuring natural radiocarbon by means of scintillation method, 20: 2062

**MAKOWSKA, E.,** Interactions of 9 Bev protons with large energy transfer to target nuclei, 20: 3047

**MALAKHOV, S. G.,** Problem of hot particles in atmospheric air (a survey), 20: 2053

**MALANIFY, J. J.,** Measurement of $C_{NN}$ in neutron-proton scattering at 23 Mev, 20: 2685 (LA-DC-7250)

**MALAVIYA, B. K.,** Studies of subcritical lattices with distributed neutron absorber by means of pulsed-neutron source technique, 20: 3432

**MALECHA, R. F.,** Inert-atmosphere enclosure for environmental testing, 20: 2246

**MALININ, A. B.,** Destruction of the otolith apparatus by ionizing radiation, 20: 1628

**MALKIN, I. A.,** Structure of $Sp_4$ and $SO_5$ multiplets, 20: 2795

**MALKIN, I. A.,** Unitary and spin content of SU(6) supermultiplets, 20: 2802

**MAL'KOV, V. V.,** Shielding parameters of concretes, 20: 3253

**MALLIKARJUNA RAO, K. R. P.,** Moessbauer effect in Sn–Pt alloys, 20: 3290

**MALM, J.,** Cleaning blocked coolant passages in water-cooled magnets, 20: 1992

**MALMAISON, Roeil,** Apparatus for treating interior of a tubular element, 20: 2304

**MAL'TSEV, E. I.,** Radiative kaon decays, 20: 2684 (JINR-P-2374)

**MAL'TSEVA, N. S.,** Production of $^{205}At$ and $^{203}At$ during bombardment of bismuth by 400-Mev protons, 20: 1948

**MALVICINI, A.,** Environmental radioactivity, Ispra 1964, 20: 2047 (EUR-2509.e)

**MALY, M.,** Semi-automatic device for scanning and measuring spark chamber photographs, 20: 2130 (JINR-P-2340)

**MALYUTA, Yu. M.,** Shell model of hadrons, 20: 2781

**MAMALADZE, Yu. G.,** Passage of polarized neutrons through superconductor in mixed state, 20: 2998

**MAMASAKHLISOV, V. M.,** Photodisintegration theory for lightest nuclei, 20: 3105

**MAMIYA, Takeyoshi,** Thermal conductivity of superconducting and normal lanthanum, 20: 2893

**MANDEL'TSVEIG, V. G.,** Structure of $Sp_4$ and $SO_5$ multiplets, 20: 2795

**MANFREDINI, A.,** $^{238}U$ fission induced by low-energy monochromatic $\gamma$-rays, 20: 3050

**MANKO, V. I.,** Oscillator model for elementary particles, 20: 2800

**MANKO, V. I.,** Relativistic oscillator models of elementary particles, 20: 2778

**MAR, B. W.,** Evaluation of radiation shielding by vehicle orientation, 20: 3249 (NASA-SP-71, pp 473-6)

**MARCHENKO, B. N.,** Possibility of stabilization of synchrocyclotron intensity, 20: 2536 (JINR-P-2341)

**MARCUS, S.,** Level-crossing spectroscopy with an electric field, 20: 2619

**MARCUS, Y.,** Solvent extraction, 20: 1741 (IA-1031)

**MARGOLIS, S. G.,** Control-induced xenon oscillations, 20: 3326 (WAPD-T-1732)

**MARIN, G.,** Prog. rpt. on cell survival as function of radiation dose, final 1959-62, 20: 1617 (NP-15149)

**MARINESCU, L.,** Argon gas scintillation detector, 20: 2163

**MARK, Hans,** X-ray spectra from Scorpius (SCO-XR-1) and the sun observed above the atmosphere, 20: 2585

**MARKAROV, E. F.,** Analysis of $^{119}Sn$ nuclear charge radius based on Moessbauer spectra, 20: 3136

**MARKLEY, F.,** Cleaning blocked coolant passages in water-cooled magnets, 20: 1992

**MARKOCZY, G.,** Temperature distribution and heat transfer in rod of bundle fuel element for nuclear reactors, 20: 3450

**MARKVART, J., PARAMETRY II** for calculation of physical parameters of gas cooled heavy-water reactor, 20: 3381 (UJV-1309b/65)

**MARSHAK, R. E.,** Field-theoretic models of elementary particles, 20: 2758 (UR-875-100)

**MARSHAK, R. E.,** Present status of weak interactions, 20: 2759 (UR-875-102)

**MARSHALL, R. C.,** Vibration of fuel assemblies in parallel flow, 20: 1978

**MARTALOGU, N.,** Mechanism of reaction $^{26}Mg(p,p',\gamma)$ at low energy, 20: 3092

**MARTIN, J. J.,** Thermal diffusivity of platinum, 20: 3621 (IS-1261)

**MARTIN, W. R.,** Irradiation effects in stainless steels at high temperatures, 20: 2430 (ORNL-P-1713)

**MARTIN, W. R.,** Post-irradiation stress-strain behavior of stainless steel, 20: 2477

**MAS, Roland,** Automatic tilting device for radioactive articles, 20: 2002

**MASHKOVA, E. S.,** Energy spectra of scattered ions as influenced by crystal structure of the target, 20: 2600

**MASON, D. R.,** Effect of neutron irradiation on electrical properties of $Mg_2Ge_xSi_{1-x}$, 20: 2502

**MASON, Edward A.,** Interpretation of radiolysis of terphenyls—apparent kinetics and fast-neutron effect, 20: 1927

**MASSAGLIA, A.,** Electrochemical labeling of proteins, 20: 1939 (EUR-2476.i)

**MASSET, M.,** Radiosensitivity of rice seed in relation to water content and free radicals, 20: 1669

**MASTERS, Christopher F.,** Asymptotic reactor-theory analysis of Garelis-Russell experiment, 20: 3385

**MASUTANI, Takeye,** Striated column appearing in high-frequency gas discharge, 20: 3203

**MATAS, J.,** Moessbauer spectra of alkaline ferrocyanides, 20: 3296

**MATERIKOVA, R. B.,** Isotopic exchange of hydrogen atoms in cyclopentadienyl rings of cobalticinium compounds, 20: 1828

**MATERS, M.,** Molecular weight of Factor XII (Hageman factor) estimated with ionizing radiation, 20: 1673

**MATEVOSYN, E. M.,** Ionization measurement in a streamer chamber, 20: 2128 (JINR-E-2324)

**MATHAY, P. W.,** Performance of defected low-density powder $UO_2$ fuels in reactor service, 20: 2232

**MATHE, G.,** Adoptive immunotherapy of acute leukemia: Experimental and clinical results, 20: 1701

**MATHEWS, D. R.,** Invariant imbedding solutions for energy-dependent neutron transport in heterogeneous anisotropically scattering shields, 20: 2989

**MATINYAN, S. G.,** Parity conserving amplitudes of hadron decays of baryons in the U(12) symmetry scheme, 20: 2697

**MATINYAN, S. G.,** Photonic decays of hyperons and $SU_6$ symmetry, 20: 2738

**MATLACK, George M.,** Determination of $^{155}Eu$ in fission products using reduction by lithium amalgam, 20: 1752

**MATSUMOTO, T.,** Hot laboratory of Japan Atomic Energy Research Institute, 20: 1997

**MATTHEWS, C. M. E.,** Tumor uptake and distribution of niobium isotopes in rats, 20: 1595

**MATTHIAE, G.,** Real part of proton-neutron scattering amplitude at 19.3 Bev, 20: 2712

**MATTHIAS, B. T.,** Superconductivity of barium tungsten bronze, 20: 2901

**MATTOX, D. M.,** Ion-plated coatings for corrosion protection of uranium, 20: 2260 (SC-DR-65-519)

**MATTSSON, H.,** Radiotracer studies of industrial processes and waste discharges, 20: 2201

**MATULENKO, Yu. A.,** Elastic $\pi^+$-p scattering at 180° and high energies, 20: 2683 (JINR-P-2327)

**MATVEEV, V. A.,** Algebra of the currents and dispersion relations, 20: 2755 (JINR-E-2329)

**MATYUSHIN, A. T.,** Symmetric system of wire electrodes for an isotropic spark chamber, 20: 2129 (JINR-P-2312)

**MATYUSHIN, A. T.,** Wire spark chamber with external acoustic transducers, 20: 2132 (JINR-P-2368)

**MATYUSHIN, V. T.,** Symmetric system of wire electrodes for an isotropic spark chamber, 20: 2129 (JINR-P-2312)

**MATYUSHIN, V. T.,** Wire spark chamber with external acoustic transducers, 20: 2132 (JINR-P-2368)

**MATYYA, G.,** Interdiffusion in nickel–uranium system, 20: 2328 (INR-625/XIV/R)

**MAUE, Marilyn J.,** Radioactive gas disposal, 20: 3608

**MAUSHART, R.,** Modern detectors in radiation protection, 20: 2143

**MAY, Robert M.,** Magnetic properties of charged ideal quantum gases in n dimensions, 20: 2833

**MAYBURG, S.,** Radiation-induced fluctuations in base resistance and emitter efficiency of Si transistors, 20: 2188
**MAYBURG, Sumner,** Radiation facility support and solid-state studies, 20: 2531 (AD-618304)
**MAYER, I.,** Crystal structure of rare earth and yttrium oxybromides, 20: 1834
**MAYER, R.,** Optical properties of $TlO_2$ as reflector for plastic scintillators, 20: 2327 (IKF-12)
**MAYNARD, C. Douglas,** Demonstration of extracranial neoplasms with $^{99m}Tc$ pertechnetate, 20: 1712
**MAYO, S.,** Elastic scattering of 27.5 Mev deuterons and its optical model analysis, 20: 3057
**MAYO, T. J.,** Electrolytic generation of fluorine from uranium hexafluoride, 20: 1954 (KY-287)
**MAYOR, Richard P.,** Non-linear response of reinforced concrete spherical domes to air blast loading, 20: 2035 (AD-615017)
**MAZURIK, V. K.,** Concerning the disturbance of thymidine and desoxyuridine metabolism in irradiated rats, 20: 1630
**MC CALL, Richard C.,** Development of radiac set AN/TDQ-2 for detection of pulsed x radiation from high-powered electronic equipment, 20: 2121 (AD-614832)
**MC CARTAN, J.,** Electrostatic screening in theta-pinch coil, 20: 3190
**MC CLELLAN, R. O.,** Age related changes in hematological and serum biochemical parameters in miniature swine, 20: 1581 (BNWL-SA-341)
**MC CLENDON, L. T.,** Determination of trace amounts of cadmium and silver by substoichiometric radioisotopic dilution analysis, 20: 1786
**MC CLINTOCK, D. R.,** Behavior of water vapor in $UO_2$ during irradiation, 20: 2468
**MC CONKEY, J. W.,** Corpuscular bombardment and $N_2^+$ radiation, 20: 2859
**MC CONNELL, Harden M.,** Isotope effect on paramagnetic resonance of triplet excitons, 20: 1841
**MC CONVILLE, T.,** Ginzburg-Landau parameters of type-II superconductors, 20: 2906
**MC CORKLE, G. Lewis,** Compact versatile x-ray collimator with adjustable pinholes, 20: 2162
**MC CORMACK, Francis Joseph,** Microscopic theory of molecular and ionized gases, 20: 2842
**MC CREDIE, J. A.,** Effect of inhaling 95% and 5% $CO_2$ on radiocurability of murine tumors, 20: 1683
**MC CRELESS, Thomas G.,** Neutronic isolation characteristics of concrete, lead, wood, polyethylene and beryllium, 20: 3390
**MC CUTCHAN, D. A.,** Comparison of analytical and experimental power distribution of NERVA reactors, 20: 3568
**MC DONALD, D. L.,** Thermal resistance due to microcracking in neutron-irradiated beryllium oxide, 20: 2443
**MC DONALD, F. B.,** Review of galactic and solar cosmic rays, 20: 2653 (NASA-SP-71, pp 19-29)
**MC DONALD, G. Corry,** Nuclear electrical power for sea-level canal construction, 20: 3481 (SC-RR-65-121A)
**MC DONALD, J. E.,** Ion-plated coatings for corrosion protection of uranium, 20: 2260 (SC-DR-65-519)
**MC DONALD, R. E.,** $^{17}O$ and $^{19}O$ lifetimes by particle-gamma coincidence technique, 20: 3156
**MC DOWELL, C. A.,** Photoelectron spectroscopy with a spherical analyzer. Vibrational energy levels of $H_2^+$, 20: 2633
**MC ELEARNEY, J. N.,** Phase shift analysis of $^3H(p,p)$, $^3H(p,n)$ and $^3He(n,n)$ reactions, 20: 3060
**MC ELLISTREM, M. T.,** Automated system for rapid and precise fast neutron activation analysis, 20: 1765
**MC EWAN, J.,** Unstable boson exchange interactions and pole approximation for resonance particles, 20: 2779
**MC GOFF, D. J.,** Static control of SNAP reactors, 20: 3559
**MC GOWAN, F. K.,** Gamma-ray energies determined with lithium-drifted germanium detector, 20: 3043
**MC GRATH, R. A.,** Effects of x irradiation on DNA of E. coli. An autoradiographic study, 20: 1639
**MC GRATH, Robert G.,** Method of operating reactor during start-up or shutdown, 20: 3361
**MC GUIRE, S. W.,** Improved model for least-squares analysis of $\gamma$ spectra in activation analysis, 20: 1787
**MC KEE, J.,** Carbon and nitrogen transfer in type-316 stainless-steel Cb–1% Zr, liquid-potassium system, 20: 2239
**MC KENNA, J.,** Quantum mechanical microscopic Brownian motion, 20: 2881
**MC KENNA, Susan M. P.,** Correlation between optical and radio aspects of a class 3 flare, 20: 2582
**MC KIBBEN, J. L.,** Design of source of negative polarized hydrogen ions using charge exchange in cesium and argon, 20: 2537 (LA-DC-7268)
**MC KINLEY, John C.,** Post-accident recovery program, 20: 3339
**MC LAUGHLIN, J.,** Stray neutron spectra at large pulsed-particle accelerator sites, 20: 2553
**MC LEAN, E. A.,** Optical interferometric and spectroscopic measurements of electron density in plasma, 20: 3214
**MC LEOD, N. B.,** Direct substitute plutonium fuel for commercial water reactors, 20: 3511
**MC LEOD, N. B.,** Economic potential of direct nuclear superheat, 20: 3508
**MC QUEEN, H. S.,** Remotely operated test equipment for materials testing in combined cryogenic and nuclear radiation environment, 20: 2032
**MC RAE, I. F.,** Ontario economic and nuclear mission, 20: 3451
**MC REYNOLDS, A. W.,** Space electron radiation shielding—bremsstrahlung and electron transmission, 20: 3248 (NASA-SP-71, pp 455-63)
**MEAD, James F.,** Lipids of Ruvettus pretiosus muscle and liver, 20: 3637 (UCLA-12-534)
**MEASOR, Ernest Oliver,** Improvements in concrete pressure vessels, 20: 3349
**MEASOR, Ernest Oliver,** Improvements in concrete pressure vessels, 20: 3350
**MECHAM, William J.,** Engineering development of fluid-bed fluoride volatility processes. IV., 20: 1952 (ANL-6859)
**MEGAW, J. H. P. C.,** Polarization in elastic scattering at backward angles of 30-Mev protons from deuterons, 20: 2706
**MEICHLE, R. H.,** Clean $^{233}U$ production-methods and parameters, 20: 3542
**MEIER, K.,** Neutron spectra in heterogeneous media, 20: 2942
**MEIER, V. A.,** Results of x-ray-radiometric well-logging in central Kazakhstan, 20: 2063
**MEKERS, J.,** Working conditions and safety in laboratories of Department of Radioisotopes at Mol, 20: 2192 (BLG-68-11)
**MEKHEDOV, V. N.,** Production of $^{205}At$ and $^{203}At$ during bombardment of bismuth by 400-Mev protons, 20: 1948
**MEKHTIEV, R. F.,** X-ray and $\gamma$ conductivity of GaSe single crystals, 20: 2439
**MELIKHOV, L. L.,** Complex emanation-thermal method, 20: 1779
**MELIKOV, Yu. V.,** The $^{12}C(d,\alpha)^{10}B$ reaction as a nucleon association replacement process, 20: 3106
**MEL'NIKOVA, G. N.,** Gamma and neutron dosimetry using colored polyvinyl alcohol films in nuclear reactors, 20: 2135
**MEL'NIKOVA, S. K.,** Role of systems orthophenols–orthoquinones in initial radiation-induced processes in an organism, 20: 1647
**MEMELOVA, L. Yu.,** Search for anomalous hydrogen, 20: 2742
**MENDELSON, M. R.,** Infinite medium spectrum-weighted group constants for gamma heating calculations, 20: 3268
**MENDELSON, Max Richard,** Solutions of one-speed neutron transport equation in plane geometry, 20: 3000
**MENEGHETTI, David,** Calculational studies of effects of thin-slab heterogeneities upon spectral reactivity component of Na-voiding, 20: 3414
**MENELEY, D. A.,** Calculational checks of plutonium cross sections by comparison with critical-assembly results, 20: 3394
**MENKES, C. K.,** Low-dose measurements with modified silver–phosphate glass dosimeter reader, 20: 2122 (AD-622626)
**MENNIG, J.,** Use of recursion formulas for Lie-Series method, 20: 2941
**MENO, F.,** ($^{90}Sr$ + $^{90}Y$)/uranium radiation gage for hydrocarbon density measurements, 20: 2115
**MENSKII, M. B.,** Mass relations in reducible unitary multiplets, 20: 2796
**MENTZONI, Michael H.,** Waveguide admittance for radiation into plasma layers—theory and experiment, 20: 2098 (AD-618398)
**MERCHANT, A. E.,** Lithium isotope ratio in two Hyades F stars, 20: 2577
**MERCIER, C.,** Necessity of energy principles for magnetostatic stability, 20: 3211
**MERGELYAN, O. S.,** Cherenkov radiation of charged particles in circular waveguide with gyrotropic ferrite filing, 20: 2550
**MERLI, E.,** Tank type organic cooled and moderated reactor, 20: 3440 (RT/ING(65)16)
**MERRIAM, Virginia,** Photoreactivation of tobacco mosaic virus RNA following near uv irradiation, 20: 1659
**MERRILL, E. T.,** Calibration of high-speed burnup code for nuclear fuel surveys, 20: 3455
**MERRILL, E. T.,** Monte Carlo calculation of optimum loading of plutonium in fuels, 20: 3456
**MERRILL, M.,** BLOOST-5: Combined reactor kinetics-heat transfer code for IBM-7044. Preliminary description, 20: 3323 (GAMD-6644)
**MERRILL, O. H.,** High-energy electron (10–60 Mev) and proton (20–130 Mev) radiation damage in silicon and germanium, 20: 2517
**MERTE, Herman Jr.,** Prog. rpt. on liquid metal boiling heat transfer, 5–8/65, 20: 2008 (AD-622825)
**MESSIER, J.,** Formation of defects at low temperature in Si irradiated by $^{60}Co$ $\gamma$ rays, 20: 2496
**METLIZKII, L. V.,** Influence of ionizing irradiation on growth and metabolism of nucleic acids in plants, 20: 1648
**METZ, H. J.,** Experiences and developments in instrumentation for liquid metal experiments, 20: 2013 (ORNL-P-1661)
**MEUNIER, R.,** Double charge exchange with negative pions. Search for tetraneutron, 20: 3080
**MEYER, A. S. Jr.,** Gas chromatographic determination of permanent gases in helium at reduced sample pressures, 20: 1751

**MEYERHOF, W. E.**, Phase shift analysis of $^3H(p,p)$, $^3H(p,n)$ and $^3He(n,n)$ reactions, 20: 3060
**MEZENTSEV, A. F.**, Experimental detection of isotopic shift of the molybdenum $K_{\alpha 1}$ x-ray line, 20: 2641
**MEZI, E.**, Preparation of uranium dioxide and carbide particles by sol-gel methods, 20: 2226 (RT/CHI(65)-30)
**MICHAEL, B. D.**, Rate constant for reaction of $O^-$ with oxygen, 20: 1917
**MICHEL, G.**, T(d,n)$^4$He reaction with polarized deuterons, 20: 3039
**MICHIYOSHI, Ituro**, Flow of slurry through a pipe. I., 20: 2020
**MICKEY, W. V.**, Strong-motion seismic measurements. Project Dugout, 20: 1981 (PNE-605F)
**MIDURA, Thaddeus Francis**, Resistance of Clostridium perfringens type A spores to $\gamma$ radiation, 20: 1679
**MIGDAL, A. B.**, $\beta$-decay in nuclei, 20: 3101
**MIGICOVSKY, Bert B.**, Removal of radioactive strontium and cesium from milk, 20: 1975
**MIHAI, I.**, Argon gas scintillation detector, 20: 2163
**MIHALCZO, John T.**, Critical uranium-metal annuli reflected with polyethylene and graphite, 20: 3892
**MIKHAILOVSKII, A. B.**, Drift cyclotron instability of plasma with hot ions, 20: 3208
**MIKULINSKII, M. A.**, Relation between nuclear masses, 20: 3102
**MILEY, G. H.**, Pulse-propagation experiments using fast-burst reactor, 20: 2955
**MILLAR, D. D.**, Experimental studies of J × B ionizing fronts propagation over pressure range 10 to 800 millitorr, 20: 3177 (NP-15570)
**MILLER, Carl F.**, Physical damage from nuclear explosions, 20: 2078 (BNL-917, pp 1-10)
**MILLER, D. C.**, Tensile properties of plutonium–gallium alloys at 20 to 100°C, 20: 2378
**MILLER, J. J.**, Comparative sensitivity to $\gamma$ radiation of yeast mitosis and meiosis, 20: 1664
**MILLER, L. F.**, Charged-particle slowing-down spectra for fast-neutron irradiation of water, 20: 1924
**MILLER, Morton W.**, Radiosensitivity of Marchantia thalli as related to nuclear and interphase chromosome volumes, 20: 1610 (BNL-9611)
**MILLER, R. R.**, High-temperature properties of sodium, 20: 1815 (NRL-6241)
**MILLER, R. V.**, Radiative properties of gases. I., 20: 1803 (AD-619266)
**MILLIKEN, John Crosby**, Magnetoresistance of thallium, 20: 2329 (IS-T-35)
**MILLS, C. B.**, Kiwi temperature coefficient, 20: 3566
**MILLS, C. B.**, Some feasibility studies of nuclear destruct concept for Rover reactor disposal, 20: 3572
**MILNER, W. T.**, Gamma-ray energies determined with lithium-drifted germanium detector, 20: 3043
**MILOVIDOV, I. V.**, The BN-350 (Fast Neutron) Atomic Power Station, 20: 3475 (NP-15458)
**MINAMI, Shigeo**, Recently discovered resonant states in the meson family, 20: 2727
**MINER, D.**, Remote underwater devices for evaluation and reduction of irradiated Yankee fuel assemblies, 20: 2117
**MIODOWNIK, A. P.**, Mechanism of strain-aging in commercially pure niobium, 20: 2376
**MIR-KASIMOV, R. M.**, Focusing singularity in p-space of constant curvature, 20: 2813
**MISENTA, R.**, Kinetic theory and calculations for accelerator booster with periodically varying multiplication factor, 20: 3371 (EUR-2492.e)
**MISHIMA, Nobuhiko**, Note on the four-particle scattering theory, 20: 2791
**MITANI, Kouji**, Experiment of gaseous breakdown in a longitudinal magnetic field, 20: 2835
**MITANI, Kouji**, Negative absorption of microwave radiation in weakly ionized xenon plasma in magnetic field, 20: 3204
**MITCHELL, D. L.**, Startup experience with the EBR-II fuel cycle facility. II., 20: 3523
**MITCHELL, E. W. J.**, Radiation damage produced by fast electron in silicon carbide, 20: 2504
**MITCHELL, E. W. J.**, Thresholds and cross sections, 20: 2513
**MITTLER, Sidney**, Prog. rpt. on chemical protection against radiation-induced chromosome aberrations, final, 9/61–8/65, 20: 1619 (TID-22293)
**MIZUNO, Kenichi**, Flow of slurry through a pipe. I., 20: 2020
**MOELLER, Erna**, Plaque-formation by non-immune and x-irradiated lymphoid cells on monolayers of mouse embryo cells, 20: 1658
**MOELLER, Gooran**, Plaque-formation by non-immune and x-irradiated lymphoid cells on monolayers of mouse embryo cells, 20: 1658
**MOELLER, H. Bjerrum**, Observation of resonant lattice modes by inelastic neutron scattering, 20: 3302
**MOHR, W. C.**, Design of Argonne isotopic source neutron facility, 20: 2997
**MOISEEV, A. A.**, Measurement of the background external radiation exposure of urban population in the USSR, 20: 2087
**MOLCHANOV, V. A.**, Energy spectra of scattered ions as influenced by crystal structure of the target, 20: 2600
**MOLENDA, Robert P.**, Long-lived radiation-induced electron spin resonances in an aqueous biological system, 20: 1605
**MOLINSKI, V. J.**, Radiochemistry of selenium, 20: 1744 (NAS-NS-3030 (Rev.))
**MOLL, A.**, Preservation of irradiated meat, 20: 2203
**MONK, C. G.**, Diffusion coefficient of water in water and in some alkaline earth chloride solutions at 25°C, 20: 1865
**MONTENAY-GARESTIER, M. T.**, Effects on proton irradiation on silicon, 20: 2489
**MONTGOMERY, D.**, Simple momentum probe for plasma studies, 20: 3179 (ORNL-P-1575)
**MOOLENAAR, Robert J.**, Cesium production, 20: 1883
**MOON, R. M.**, Magnetic form factor of chromium, 20: 3280 (ORNL-P-1737)
**MOORE, C. F.**, Isobaric analogue states via (p,p) and (p,n) on $^{144}Sm$, 20: 3084
**MOORE, Charles R.**, Hydraulic studies with random-packed beds applicable to paste-fuel concept, 20: 3461
**MOORE, Charles R.**, Operation of sodium loop with circulation of stainless-steel paste, 20: 3460
**MOORE, M. J.**, Radiation damage produced by fast electrons in silicon carbide, 20: 2504
**MOORE, M. N.**, Dispersion law of moderator, 20: 2991
**MORAN, H. S.**, Electron-photon cascade calculations and neutron yields from electrons in thick targets, 20: 3261
**MORE, K. A.**, Cosmic-ray shower production in manned space vehicles—copper, 20: 3240 (NASA-SP-71, pp 183-8)
**MOREH, R.**, Level structure of $^{18}O$ and $^{19}O$ by stripping reactions, 20: 3052
**MORGAN, J. G.**, Irradiation evaluation of fuel elements for PBRE and AVR reactors, 20: 2464
**MORI, Hazime**, Continued-fraction representation of the time-correlation functions, 20: 2846
**MORIUCHI, Yasuyuki**, Standard $\gamma$ irradiation facilities and measurements of dose rates distribution, 20: 1942
**MORLEY, H.**, Radiolytic reaction between graphite and carbon dioxide. VI., 20: 1895 (AERE-R-4988)
**MOROZOV, A. G.**, Displacement of spark chamber discharges in a magnetic field, 20: 2131 (JINR-P-2344)
**MOROZOVA, G. I.**, Modification of magnesium alloys with zirconium and lanthanum, 20: 2399
**MOROZOVA, I. K.**, Influence of thermal neutron radiation on potential of oximercury electrode, 20: 1932
**MORRIS, J. R.**, Uranium corrosion studies. II., 20: 1804 (AWRE-O-68/65)
**MORRIS, John L.**, Materials development for sliding-contact applications in 1000°F potassium space power systems, 20: 2242
**MORRIS, W.**, Channeling of 13-kev $D^+$ ions in gold crystals, 20: 2616
**MORRIS, W. R.**, NERVA reactor control, 20: 3569
**MORRISON, D. L.**, Fission-product behavior in fuel-element cladding materials, 20: 2389
**MORRISON, G. H.**, Preconcentration of trace elements by precipitation ion exchange using organic-hydrochloric acid systems, 20: 1958
**MORROW, Kenneth John Jr.**, Basis of variation of purine analog resistance in established murine cell line, 20: 1678
**MORSELT, G.**, Molecular weight of Factor XII (Hageman factor) estimated with ionizing radiation, 20: 1673
**MORTION, Maurice**, Prog. rpt. on low-temperature polymerization, 4–6/65, 20: 1893 (AD-618228)
**MORTON III, J. R.**, Interaction in arrays of fissionable materials, 20: 2938 (UCRL-14245)
**MORTON, Maxwell R.**, Bulk-grain-irradiator design, 20: 2194
**MOSHINSKY, M.**, Recursion relations for Wigner coefficients of unitary groups, 20: 2770
**MOSKALENKO, V. A.**, Determination of critical temperature of a superconductor with impurity in two-band model, 20: 2925
**MOSS, W. D.**, Particle-size distributions from Rover fuel-element fragmentation studies, 20: 3574
**MOTEFF, J.**, Effect of neutron irradiation on hardness properties of tungsten and molybdenum, 20: 2457
**MOTEFF, J.**, Effect of thermal-neutron irradiation at fixed fast-neutron dose on creep-rupture properties of high-temperature alloys, 20: 2456
**MOTEFF, J.**, Recovery of defects in neutron-irradiated tungsten, 20: 2475
**MOTT, W. E.**, Bromine-82 tagged bromobenzene as an industrial tracer, 20: 2202
**MOTT, W. E.**, Radiotracer study of product contamination by catalytic nickel, 20: 1889
**MOTT, W. E.**, ($^{90}Sr$ + $^{90}Y$)/uranium radiation gage for hydrocarbon density measurements, 20: 2115
**MOTTLEY, J. D.**, Model for predicting effect of loop geometry on corrosion rate of materials in sodium, 20: 2295
**MOUGEY, Jean**, Results and interpretation of spectral indices measurements made with aquilon, 20: 3582 (CEA-R-2482)
**MOULET, Elisee**, Bibliography on Be isotopes—nuclear reactions, 20: 3007 (CEA-Bib-32)
**MOUNTFORD, L. A.**, Doppler coefficients of fertile and refractory materials, 20: 2958

**MOWERY, A. L.,** Comparison of analytical and experimental operating reactivity of NERVA reactors, 20: 3567
**MOWERY, A. L.,** Design and analysis of poison system for safe shipping NERVA reactor, 20: 3576
**MOYER, Robert Findley,** Effect of x irradiation on extractable cellular components of the lung, 20: 1675
**MOZHAEVA, V. S.,** Mutants induced by ionizing radiations and ethyleneimine in winter wheat, 20: 1655
**MUCHNIK, M.,** $^{238}U$ fission induced by low-energy monochromatic $\gamma$-rays, 20: 3050
**MUCKA, V.,** Influence of physiological inoculum age on growth of microbe culture in $H_2O$ and 50% $D_2O$, 20: 1601
**MUCKENTHALER, F. J.,** Differential fast-neutron albedos for concrete. I., 20: 2932 (ORNL-3822(Vol.1))
**MUCKENTHALER, F. J.,** Single-velocity calculation and measurement of differential angular thermal-neutron albedos for concrete, 20: 3266
**MUEHE, C. E.,** AC breakdown in gases, 20: 3160 (AD-618503)
**MUELLER, A.,** ESR measurements on irradiated bacteriophages and their nuclei acids, 20: 1623
**MUELLER, H.,** Measurement of $\beta$-$\gamma$ angular correlation for $^{198}Au$, 20: 3129
**MUELLER, Heinz,** Measurement of beta–gamma directional correlation of $^{22}Na$ and $^{56}Co$, 20: 3054
**MUELLER, R.,** $^{238}U$ fission induced by low-energy monochromatic $\gamma$-rays, 20: 3050
**MUELLER, V. F.,** Low energy baryon-nucleon scattering, 20: 2707
**MUENCH, E.,** Behavior of FRJ-1(MERLIN) as result of forced cooling, 20: 3585 (JUL-259-RE)
**MUENCHOW, H.,** Late changes of skin after irradiation of haemangiomas, 20: 1719
**MUHS, M. A.,** Purities of some commercially available $^{14}C$-labeled hydrocarbons, 20: 1764
**MUIR, A. H. Jr.,** Moessbauer effect data index, 20: 3146
**MUKASHEV, F. A.,** Determination of uranium in ores, 20: 1794
**MUKHAMEDOV, T.,** Effect of combined action of $^{131}I$ and noise on cardiac activity, 20: 1629
**MUKHERJEE, S.,** Slow surface wave along compressible plasma slab, 20: 3195
**MUKHTAROVA, T. A.,** System of equations for plasma jet with account of reaction of decomposition of methane in it, 20: 3197
**MUKUNDA, N.,** Group theory of the Kepler problem, 20: 2612
**MUKUNDA, N.,** Reduction of the product $(\lambda,\mu) \oplus (3,0)$ of irreducible representations of SU(3), 20: 2771
**MULLER, A. C.,** Measurement of negarad doses of $^{60}Co$ gamma rays with UVT lucite, 20: 2165
**MULLER, Albert C.,** Calorimetric calibrations of high-specific-activity $\gamma$ sources, 20: 2195
**MULLER, Harry D.,** Prog. rpt. on x irradiation of developing avian embryo as factor of aging, 9/20/64–9/10/65, 20: 1611 (COO-1119-4)
**MULLER, J.,** Superconductivity in beryllium–rhenium system, 20: 2898
**MUNNO, Frank J.,** General time-dependent perturbation theory for reactor physics, 20: 3436
**MUNRO, R.,** Mass spectrometer source loading lock and isolation valve, 20: 2159
**MUNSHI, Kailash N.,** Chromotrope 2B in photometric determination of rare earths, 20: 1772
**MURAKAMI, M.,** Hot laboratory of Japan Atomic Energy Research Institute, 20: 1997
**MURAKAWA, Kiyoshi,** Ionization potential of Tm(I), 20: 2603
**MURAMATSU, Takio,** Uranium ore refining plant, 20: 1964
**MURANO, Tohru,** Radioactive equilibrium in Ningyotoge uranium ores, especially between ionium and uranium, 20: 2066
**MURAYAMA, T.,** Range distribution of cosmic-ray muons underground, 20: 2664
**MURFIN, Walter B.,** Use of shock spectrum technique for non-linear systems, 20: 3631 (SC-DC-65-1723)
**MURPHY, H. J.,** Electron-beam tube-to-tubesheet welding, 20: 2283 (KAPL-3110)
**MURPHY, Raymond E.,** An organic plastic, localizing whole-body counter, 20: 1710
**MURPHY, W. J.,** Handling hazardous materials, 20: 1727
**MURRAY, J. L.,** Prog. rpt. on EVESR fuel development, 3–5/65, 20: 3472 (GEAP-4891)
**MURRAY, K.,** Shielding problems at the NRL linac facility, 20: 2556
**MUSTACCHI, C.,** Interaction of krypton with uranium oxide surfaces, 20: 1813 (EUR-2515.e)
**MUSTACCHI, C.,** Thermal and mechanical studies of solid-solid contacts, 20: 1811 (EUR-2486.e)
**MUZINICH, I.,** Renormalization of the strangeness-changing axial-vector coupling constant and the Cabibbo form of universality, 20: 2722
**MYERS, E. June,** An organic plastic, localizing whole-body counter, 20: 1710
**MYERSCOUGH, Valerie P.,** Elastic scattering of slow electrons by atomic oxygen, 20: 2617
**MYTTENAERE, C.,** Radiosensitivity of rice seed in relation to water content and free radicals, 20: 1669

# N

**NAGASAKI, Ryukichi,** Behavior of krypton and xenon in uranium metal, 20: 2358 (AERE-Trans-1034)
**NAGELS, P.,** Effect of fast neutron bombardment on electrical properties of p- and n-type silicon carbide, 20: 2503
**NAGLE, Darragh E.,** High-energy proton linear accelerators, 20: 2538 (LA-DC-7281)
**NAGY, Gabor,** Gamma-initiated polymerization of N-vinylsuccinimide in the liquid phase, 20: 1912
**NAHAVANDI, Amir N.,** Solution of nonlinear vibration problems in reactor components, 20: 3328
**NAIDICH, Yu. V.,** Capillary phenomena in densification process during sintering in presence of liquid phase, 20: 2286
**NAIL, James H.,** New fuel configuration to increase plutonium value in thermal reactors, 20: 3457
**NAIR, P. P.,** Rapid method for dissolving tissue for liquid scintillation counting, 20: 1767
**NAIR, V.,** Interactive effects of x irradiation and barbiturates, 20: 1662
**NAKACHE, F. R.,** Synthesis of spherical minimum-weight proton shields, 20: 3242 (NASA-SP-71, pp 225-8)
**NAKAJIMA, Saburo,** Radiation dosimeter, 20: 2181
**NAKAMURA, Sadaoi,** Experiment of gaseous breakdown in a longitudinal magnetic field, 20: 2835
**NAKAMURA, Y.,** Moessbauer effect of $^{57}Fe$ doped in $V_2O_3$, 20: 3289
**NAKATA, Junji,** Striated column appearing in high-frequency gas discharge, 20: 3203
**NAKAYAMA, Toshio,** Kinetic structure of plasma, 20: 3164 (IPPJ-39)
**NAKHABTZEV, V. S.,** Results of x-ray-radiometric well-logging in central Kazakhstan, 20: 2063
**NAKHUTIN, I. E.,** Sorption of radioactive substance in a chromatographic column, 20: 1770
**NALIBOFF, David,** Unified computational method for thermal-neutron scattering, 20: 3412
**NASTUK, William L.,** Effect of allogeneic bone marrow on lethally irradiated thymectomized mice, 20: 1660
**NASYROV, F.,** Distribution of specific ionization along the track as a function of initial energy of $^{235}U$ fission fragments, 20: 3029
**NATAF, R.,** Models in nuclear spectroscopy, 20: 3139
**NATELSON, M.,** Importance of space and energy effects in neutron-fluctuation experiments, 20: 3420
**NATH, R. J.,** Calorimetric and spectrometric techniques to relate zonewise power distributions in Pu–U multizoned cores, 20: 3388
**NAUDET, Roger,** Results and interpretation of spectral indices measurements made with aquilon, 20: 3582 (CEA-R-2482)
**NAUMANN, H. H.,** Shielding for radioisotope bremsstrahlung sources $^{90}Sr + ^{90}Y$, 20: 3254
**NAUMOV, A. N.,** Isotopic effect in diffusion of lithium in sodium, 20: 3305
**NAUMOV, A. N.,** Methods for determining isotopic diffusion effect in solid, 20: 3304
**NAZARENKO, V. A.,** Mass spectra of water ionized in a strong electrical field, 20: 1829
**NAZARYAN, A. A.,** Ionization measurement in a streamer chamber, 20: 2128 (JINR-E-2324)
**NEAGU, D. V.,** Interpretation of Wilson chamber photographs by the reprojection method. A., 20: 2728
**NEAGU, D. V.,** Interpretation of Wilson chamber photographs by the reprojection method. B., 20: 2729
**NEAL, L. G.,** Hydrodynamic stability of natural circulation boiling-water reactors, 20: 3516
**NEAL, M.,** Preparation of ceramic-refractory metal seals for space power systems, 20: 2292
**NEAL, P. E.,** NERVA reactor experiment (NRX) reactor testing, 20: 3565
**NEAMU, I.,** Mechanism of reaction $^{26}Mg(p,p',\gamma)$ at low energy, 20: 3092
**NEED, John L.,** Elastic and inelastic scattering of 40-Mev alpha particles from even tin isotopes, 20: 3017 (NASA-TN-D-3067)
**NEEF, W. I.,** Conservation economics and reactor technology, 20: 3458
**NEFEDOV, V. D.,** Certain polonium *m*-anisyl derivatives, 20: 1854
**NEFEDOV, V. D.,** Synthesis of some polonium *a*-naphthyl derivatives, 20: 1850
**NEFEDOVA, M. N.,** Replacement of a halogen by a proton in halogeno-ferrocenes, 20: 1830
**NEGANOV, B. S.,** Dynamic polarization of protons in rotating lanthanum–magnesium nitrate crystal, 20: 3311
**NEI, Masatoshi,** Genetic effects of x rays on population of Drosophila, 20: 1642
**NEILL, J. M.,** Differential neutron scattering from $D_2O$ and $ZrH_{1.85}$, 20: 2963
**NEILL, J. M.,** Neutron spectrum measurements in $H_2O$ as a function of

temperature, 20: 2966
**NEILL, J. M.,** Neutron spectra in beryllium metal, 20: 2968
**NEJEDLIK, J. F.,** Material resistance to mercury corrosion, 20: 2264
**NEKRASOV, K. G.,** Displacement of spark chamber discharges in a magnetic field, 20: 2131 (JINR-P-2344)
**NELSON, P. A.,** Corrosion of refractory metals by zinc–magnesium–uranium and halide salt systems, 20: 2266
**NELSON, Paul A.,** Corrosion of steels and tantalum by molten cadmium–magnesium–zinc systems, 20: 2265
**NELSON, V. G.,** Mechanical properties of wrought depleted uranium and of welds joining this material, 20: 2342 (SC-DR-58-61)
**NEMENOV, L. L.,** Analysis of $\pi^- + p \to \pi^- + \pi^+ + n$ and $\pi^- + p \to \pi^- + \pi^- + p$ at 338 Mev, 20: 2682 (JINR-P-2320)
**NEMILOV, Yu. A.,** Angular anisotropy of fission by sub-barrier deuterons, 20: 3122
**NERGE, WILHELM,** Drying process and apparatus therefor for removing solids from liquid mixtures, 20: 3607
**NESMEYANOV, A. N.,** Replacement of a halogen by a proton in halogenoferrocenes, 20: 1830
**NESMEYANOV, An. N.,** Reactions of tritium recoil atoms and $^{14}C$ with heterocyclic amines, 20: 1921
**NESS, Nathan,** Explosion of a supernova into the interstellar magnetic field. II., 20: 2570
**NESTOR, C. W. Jr.,** Heating in infinite cylinders by uniform gamma sources, 20: 3269
**NESTOR, C. W. Jr.,** Heating in infinite cylinders by uniform gamma sources, 20: 3325 (ORNL-P-1480)
**NEUBERT, Theodore J.,** Color centers in sodium fluoride, 20: 1908
**NEUDATCHIN, V. G.,** Selection rules for nuclear reactions involving nucleon associations in SU(3) scheme, 20: 3117
**NEVENZEL, Judd C.,** Lipids of Ruvettus pretiosus muscle and liver, 20: 3637 (UCLA-12-534)
**NEVSKII, V. A.,** Two genetic types of post-magmatic thorium–rare earth deposits, 20: 2064
**NEWBERG, Joseph,** Pulsed nuclear radiation induced transients in electrical cables, 20: 2186 (ECOM-2415)
**NEWBERG, Joseph,** Pulsed nuclear radiation effects on resistors and cables, 20: 2187
**NEWTON, J. O.,** Coulomb excitation, 20: 3153
**NEY, E. J.,** NERVA reactor experiment (NRX) reactor testing, 20: 3565
**NEZRICK, Frank A.,** Positron spectrum from fission antineutrinos on protons, 20: 2680 (COO-818-58)
**NG, Hawkins,** Bulgur wafer and adjuncts for fallout shelter rations, 20: 2067 (AD-614824)
**NGUYEN VAN DONG,** Study of recombination processes of electron-hole pairs in Ge irradiated by $^{60}Co$ $\gamma$ rays by means of photovoltaic effect in p-n junctions, 20: 2512
**NGUYEN VAN HIEU,** Asymptotic equality of the cross section of $\pi^{\pm}$ meson generation from the neutrino and antineutrino, 20: 2733
**NGUYEN VAN HIEU,** Electromagnetic decays and the mass-splitting of vector mesons in unitary symmetry, 20: 2801
**NGUYEN VAN HIEU,** Form factors and interaction constants for the 56-plet of the group SL(6), 20: 2803
**NGUYEN VAN HIEU,** Meson current in broken symmetry U(12) and experiments with colliding beams, 20: 2753 (JINR-P-2300)
**NICHOLSON, Richard B.,** Diffusion and losses of electrons in astron E-layer, 20: 3183 (UCRL-14275)
**NICKEL, H.,** Physico-chemical analysis methods for study of reactor materials and nuclear fuels, 20: 1743 (JUL-216-RW)
**NICOLAE, Marieta,** Preparation and characteristics of the IFA $EN_2$ nuclear emulsion, 20: 2158
**NIELSEN, H. L.,** Isobaric-spin impurity in $^{170}Lu$ ground state, 20: 3072
**NIGRO, M.,** Positive pion photoproduction with coherent bremsstrahlung, 20: 2718
**NIHOUL, Jacques C. J.,** Cold-plasma induction motors for propulsion of spacecraft, 20: 2041
**NIKITINE, S.,** Effects of neutron and proton bombardments on the exciton spectrum of $Cu_2O$, 20: 2505
**NIKOLAEV, V. M.,** Radiocolloids in sorption systems. II., 20: 1968
**NIKOLAEV, V. S.,** Calculation of effective cross section for loss of K-electrons by fast hydrogen-like ions during encounters with hydrogen and helium atoms, 20: 2642
**NIKOLAEV, V. S.,** Capture and loss of electrons by fast ions in atomic collisions, 20: 2634
**NIKOLOV, A. V.,** Mass formula in SU(12) contains $Sp(6) \times SU(2)$ symmetry, 20: 2756 (JINR-P-2342)
**NIKOL'SKII, B. P.,** Reaction of Pu with $H_2O_2$ in presence of other alloys, 20: 1857
**NILSSON, G.,** Observations on Fermi surface of aluminum by neutron spectrometry, 20: 3303
**NISHIYAMA, Yoshio,** Proposal for quantum mechanical orbit equation, 20: 2883
**NISHIZAWA, Yukinori,** Removal of iodine from atmosphere by spray. I., 20: 1966
**NOBILI, D.,** Isochronal recovery of work hardening in aluminum–alumina alloys, 20: 2375
**NODVIK, R. J.,** Comparison of calculated and measured burnup distributions and isotopic inventory in Yankee core, 20: 3504
**NORDLINGER, S. G.,** United States nuclear power programme, 20: 3492
**NORDYKE, Milo D.,** Isthmian canal studies, 1964, 20: 1983 (PNE-2000)
**NORDYKE, Milo D.,** Isthmian canal studies, 1964, 20: 1985 (PNE-2003)
**NORMAN, S. J.,** Auroral spectrograph data, 20: 2851
**NORRIS, E. B.,** Prog. rpt. on evaluation of serviceability of Elk River reactor pressure vessel, 5–7/65, 20: 3482 (SWRI-1228-75)
**NORRIS, F. W.,** Effects of high levels of $\gamma$ irradiation on lipids of wheat, 20: 1637
**NORWITZ, George,** Determination of Zr in Zr metal and Zr powder, 20: 1729 (AD-619244)
**NOSANOW, L. H.,** Calculations of sound velocities in crystalline helium at zero temperature, 20: 2912
**NOTLEY, M. J. F.,** An in-pile study of the thermal conductivity and electrical properties of $UO_2$ and $UO_{2-x}$, 20: 2452
**NOTLEY, M. J. F.,** Fission-product gas pressures in $UO_2$ fuel elements during irradiation, 20: 2462
**NOVAK, P. E.,** Evaluation of thermocouples for use to 2600°C in mixed-oxide fuel, 20: 2114
**NOVAK, P. E.,** Survey for high temperature sensor for SEFOR, 20: 3473 (GEAP-4903)
**NOVICK, R.,** Direct detection of two-photon emission from metastable state of singly ionized helium, 20: 2630
**NOVICK, R.,** Level-crossing spectroscopy with an electric field, 20: 2619
**NOVIKOV, M. T.,** Profound stripping and scattering of $Kr^+$ ions in single collisions with Ne, Ar, Kr and Xe atoms, 20: 2644
**NOVIKOV, S. R.,** Ripening of defects, induced by fast neutrons in germanium, in course of low-temperature annealing, 20: 2509
**NOWAK, M.,** Preliminary studies on neutron activation of tetraethyl germanium, 20: 1944
**NOYES, H. Pierre,** Interaction effect in n-p capture, 20: 3059
**NOZAWA, Masao,** Preliminary design work of 2 Mw Na loop, 20: 3479 (NP-15556)
**NUNN, L. R. Jr.,** Measurement of neutron-flux spectra using Fermi chopper, 20: 2994
**NURMIA, M.,** Half-life of $^{147}Sm$; comparison of ionization chamber and liquid scintillation results, 20: 3028
**NUZHDIN, N. I.,** Effect of space flight factors on Evonymus europaea seeds, 20: 1649
**NYAGU, D.,** An experimental determination of $K_2^0 \to 2\pi$ decay probability in sloped $K_2^0$ beam, 20: 2865 (JINR-P-2325)

# O

**OAKBERG, Theodore Cameron,** Atomic transition probabilities using a d-c arc plasma jet, 20: 2649
**OAKES, L. C.,** Control-rod systems for HFIR, 20: 3543
**OAKES, Melvin Ervin Louis,** Interaction of electromagnetic waves in partially ionized gas, 20: 2814
**OBERMEYER, Ronald W.,** Measurements and calculations of hydrogen loss from hydrided zirconium–uranium fuel elements during transient heating to temperatures near melting point, 20: 3563
**O'BRIEN, H. G.,** Control system for gas-cooled nuclear power plant, 20: 3480 (ORNL-P-1679)
**O'BRIEN, K.,** Stray neutron spectra at large pulsed-particle accelerator sites, 20: 2553
**OBRUTSKY, D.,** Properties of copper alloys of high resistance and high conductivity, 20: 2334 (NP-15530)
**OCHKIN, D. V.,** Sorption of radioactive substance in a chromatographic column, 20: 1770
**ODA, H.,** Range distribution of cosmic-ray muons underground, 20: 2664
**ODIAN, George,** Radiation crosslinking of nylon 66 and poly(vinyl alcohol), 20: 1909
**OERTEL, W.,** Mixed systems of lanthanide and actinide elements. III., 20: 2379
**OETJEN, Georg-Wilhelm,** Drying process and apparatus therefor for removing solids from liquid mixtures, 20: 3607
**OEZIZMIR, Ercument,** Pre-kinetic equations for plasma, 20: 3163 (CNAEM-26)
**OGURTSOV, G. N.,** Ionization produced in collisions between alkali metal atoms and gas molecules, 20: 2639
**OHANIAN, Mihran J.,** Eigenfunction analysis of hydrogenous neutron spectra, 20: 2999
**OKAMURA, Seizo,** Gamma-induced polymerization of formaldehyde, 20: 1914
**OKONOV, E. O.,** An experimental determination of $K_2^0 \to 2\pi$ decay probability in sloped $K_2^0$ beam, 20: 2865 (JINR-P-2325)
**OKUN, L. B.,** Baryon charge degeneracy in the Quark model with even-charge mesons, 20: 2806

**OKUN, L. B.,** Possible non-conservation of CP parity and the nature of the $\Delta T = \frac{1}{2}$ rule, 20: 2798

**OLANDER, D. R.,** Effect of natural convection upon temperature transient following loss-of-coolant accident, 20: 3515

**OLDHAM, S. B.,** Radiation-induced decomposition of millimolar concentrations of hydrogen peroxide in aerated pure water, 20: 1894 (AD-623095)

**OLIVER, J.,** Auroral spectrograph data, 20: 2851

**OLIVER, Thomas,** TRIST—tri-level multiprogramming executive involving real-time calculations and asynchronous on-line data source, 20: 3644 (UCRL-16199)

**OLIVIERI, G.,** Mutagenic effect of tritiated uridine in Drosophila spermatocytes, 20: 1657

**OLSEN, A. R.,** Thorium–uranium recycle facility, 20: 1994

**OLSEN, C. E.,** Neutron-diffraction study of antiferromagnetism in $UO_2$, 20: 3301

**OLSSON, Martin G.,** Confirmation of an SU(6)$_w$ scattering relation, 20: 2788

**OLTMANN, A.,** Gamma radiation source and irradiator design, 20: 1937 (BNL-9281)

**OMAROV, T. G.,** Isotopic effect in values of molar volumes of LiF and LiH, 20: 3307

**OMBERG, R. P.,** Effect of natural convection upon temperature transient following loss-of-coolant accident, 20: 3515

**O'NEILL, G. L.,** High-power operation of $PuO_2$–$UO_2$ fast reactor fuel, 20: 2448

**ORAEVSKII, A. N.,** Spontaneous particle radiation in resonator with several coupled modes, 20: 2527

**O'RAIFEARTAIGH, L.,** Group theory of the Kepler problem, 20: 2612

**ORBAN, Gyula,** Radiation crosslinking of nylon 66 and poly(vinyl alcohol), 20: 1909

**O'REILLY, Richard J.,** Accumulation of radioactive fission products in hair, 20: 1695

**ORIANI, R. A.,** Thermal diffusion of dissolved hydrogen isotopes in iron and nickel, 20: 2397

**ORMAN, P. R.,** Fast electronics in nuclear physics, 20: 2118

**ORR, P. B.,** Separation of Curie quantities of $^{90}Y$ from $^{90}Sr$ by an elution process, 20: 2211

**ORR, Raymond Leonard,** Aspects of alloy thermochemistry: A and B, 20: 2349 (UCRL-16320)

**ORR, W. L.,** Comparison of analysis with experiment for Saxton plutonium critical experiments, 20: 3389

**ORSZAG, Steven A.,** Neutron-star atmospheres, 20: 2568

**ORTENBERG, L.,** Comparison of analytical and experimental power distribution of NERVA reactors, 20: 3568

**ORTENBERG, L. I.,** Comparison of analytical and experimental operating reactivity of NERVA reactors, 20: 3567

**ORTENBERG, L. I.,** Design and analysis of poison system for safe shipping NERVA reactor, 20: 3576

**OSBORN, R. K.,** Importance of space and energy effects in neutron-fluctuation experiments, 20: 3420

**OSBORNE, Carol,** TRIST—tri-level multiprogramming executive involving real-time calculations and asynchronous on-line data source, 20: 3644 (UCRL-16199)

**OSBORNE, M. F.,** Irradiation behavior of high-burnup $ThO_2$–4.45% $UO_2$ fuel rods, 20: 2429 (ORNL-3837)

**OSHIMA, K.,** Radiation-induced liquid- and solid-phase polymerization of acetylene, 20: 1913

**OSHIMA, Keiichi,** Radiation-induced copolymerization of tetrafluoroethylene with isobutene at low temperature, 20: 1915

**OSKAM, H. J.,** Prog. rpt. on collision processes in gaseous plasmas, semiannual, 7/64–1/65, 20: 3158 (AD-614923)

**OSTANEVICH, J.,** Investigations of ordering transformation in $Fe_3Al$ alloy by Moessbauer effect, 20: 3292

**OSTERTAG, Werner,** Absorption of blue solutions of europium and beryllium in liquid ammonia, 20: 1867

**OTTER, J. M.,** Structure in Doppler effect as a function of surface, mass ratio in $^{197}Ag$, 20: 2975

**OTTEWITTE, E. H.,** Effect of revisions to multigroup representations of the beryllium (n,2n) and beryllium (n,α) reactions, 20: 2960

**OTTEWITTE, Eric H.,** Criticality of $^{244}Cm$, 20: 2995

**OUELLETTE, Robert P.,** The determination of iodinated compounds by neutron activation of $^{129}I$-description of the technique, 20: 1790

**OWNBY, P. Darrell,** Hot isostatic compaction of graphite, 20: 2278 (BMI-1746)

**OZERNOI, L. M.,** Gravitational radiation of explosive origin, 20: 2877

**OZISIK, M. Necati,** Theoretical investigations of fission-product deposition from flowing gas streams, 20: 3344


## P


**PACHOLCZYK, A. G.,** Relativistic stability of a magneto-turbulent massive star, 20: 2579

**PACK, D. C.,** Research on magneto-gasdynamics, 20: 2821 (AD-618296)

**PADILLA, Andrew Jr.,** Prog. rpt. on liquid metal boiling heat transfer, 5–8/65, 20: 2008 (AD-622825)

**PAIGE, D. M.,** Startup experience with the EBR-II fuel cycle facility. I., 20: 3522

**PAIK, N. C.,** Criticality of bare slab of arbitrary size with anisotropic scattering, 20: 2986

**PAL, L.,** Investigations of ordering transformation in $Fe_3Al$ alloy by Moessbauer effect, 20: 3292

**PAL, S.,** Dispersion of lattice waves in tungsten, 20: 3294

**PALATNIK, L. S.,** Mechanism of formation of growth textures in beryllium condensates, 20: 3306

**PALCOS, M. C.,** Preparation of a $^{99m}Tc$ labeled colloid, 20: 1696 (CONF-641126-1)

**PALECEK, L.,** Symptomatology of radiation-caused growth disturbances to vertebral column, 20: 1702

**PALISTRANT, M. E.,** Determination of critical temperature of a superconductor with impurity in two-band model, 20: 2925

**PALOWITCH, B. L.,** Measurement of effective resonance integral and Doppler coefficient of thorium–oxide rods, 20: 2976

**PANDIT, L. K.,** Reduction of the product $(\lambda,\mu) \oplus (3,0)$ of irreducible representations of SU(3), 20: 2771

**PANISKO, F. E.,** Irradiation of $UO_2$–$PuO_2$ high-power-density fuel elements in PRTR, 20: 2449

**PANKOV, A. M.,** Effects of gas macrocomponent on the distribution of $^{85}Kr$ and $^{133}Xe$ between gaseous phase and solid carbon sorbent, 20: 1969

**PANKOV, A. M.,** Production and preparation of polymethylmethacrylate kryptonates, 20: 1862

**PANTYUSHIN, A. A.,** Relativistic generalization of SU(3) symmetry. Baryon current, 20: 2777

**PAPAC, R. J.,** Effects of 1-β-D-arabinofuranosylcytosine hydrochloride on regenerating bone marrow, 20: 1687

**PAPE, R.,** Protracted x irradiations in bronchial carcinoma, 20: 1720

**PAPE, R.,** X-ray diagnosis radiation burdens to youths and adults, 20: 1703

**PAPIROV, I. I.,** Change of beryllium properties after aging treatment, 20: 2363

**PARFENOV, L. B.,** Dynamic polarization of protons in rotating lanthanum–magnesium nitrate crystal, 20: 3311

**PARISER, Bert,** Cesium plasma diode, 20: 2675

**PARISKAYA, L. V.,** Automodel motion of rarefied plasma, 20: 3228

**PARK II, Young,** Genetic effects of irradiation on preweaning and postweaning gains of pigs, 20: 1677

**PARKER, E. N.,** Cosmic rays and their formation of a galactic halo, 20: 2662

**PARKER, Earl R.,** Superconductivity of the cubic modification of MoC, 20: 2346 (UCRL-11471)

**PARKER, G. W.,** Release and adsorption of methyl iodide in HFIR maximum credible accident, 20: 3586 (ORNL-TM-1291)

**PARKINSON, R. Y.,** 1.5 Mwe thermionic reactor space power system, 20: 3547 (NAA-SR-Memo-7581)

**PARKS, Charles E.,** Blowdown models application to loss-of-fluid test facility (Loft) evaluation, 20: 3335

**PARKS, J. G.,** Inelastic proton-proton scattering at 5.10 Bev, 20: 2688 (UCRL-14335)

**PARKS, P. B.,** Pulsed measurements of neutron-diffusion parameters in $D_2O$, 20: 2954

**PARKS, R. D.,** Quantum effects in superconductors, 20: 2914

**PARRISH, Marvin L.,** Fracture mechanics in design against brittle failure, 20: 3345

**PARSONS, D. S.,** Reduction of tungsten oxides by hydrogen, 20: 1831

**PASCHALL, R. K.,** Age of fission neutrons to indium resonance energy in aluminum–water mixtures, 20: 2970

**PASHNEVA, G. E.,** Rare earth and thorium content in soils of Tomsk region, 20: 2065

**PASHOS, T. J.,** Development fuel assembly irradiation testing in Big Rock Point Reactor, 20: 3452

**PASHOS, T. J.,** Fuel performance in boiling-water reactors, 20: 3497

**PASHOS, T. J.,** New evidence to delineate the $UO_2$ molten boundary, 20: 2392

**PASHOS, T. J.,** Performance of defected low-density powder $UO_2$ fuels in reactor service, 20: 2232

**PASIERB, E. J.,** Considerations on annealing of irradiated pressure-vessel steel, 20: 2455

**PASKIN, A.,** Magnetic field penetration and breakdown of surface superconductivity. II., 20: 2900

**PASTUSHENKO-STRELETS, N. A.,** Effect of space flight factors on Evonymus europaea seeds, 20: 1649

**PATARAYA, A. D.,** Plasma bremsstrahlung, 20: 3200

**PATHAK, Keshava Chandra,** Electrometric study on the quantitative precipitation of samarium(III) as normal tellurite, 20: 1760

**PATHAK, M.,** Radiation effects on free radical properties of melanin, 20: 1684

**PATIMO, C.**, Method of gas-chromatographic analysis of polyphenyls in lithium chloride columns, 20: 1745 (RT/CHI(65)-25)
**PATRICK, Richard M.**, Plasma generator, 20: 2042
**PATT, H. H.**, Rapid method for dissolving tissue for liquid scintillation counting, 20: 1767
**PATT, H. J.**, Theory of gas heating in axially symmetric wall-stabilized luminous arcs. I., 20: 2840
**PATTORET, A.**, Thermodynamic study of the uranium–oxygen system by mass spectrometry. Heat of sublimation of uranium, 20: 1810 (EUR-2458.f)
**PAUL, S. D.**, Labeling of glycine by direct exchange with heavy water, 20: 1833
**PAULSON, Dantos L.**, Investigation of the system UC–UN–UO, 20: 2353 (USBM-RC-1205, pp 11-14)
**PAULY, H.**, Measurement of velocity dependence of total scattering cross sections for scattering of He, $H_2$, and $D_2$ molecular beams on rare gases, 20: 2614
**PAULY, H.**, Rainbow effect and interference patterns in molecular collisions, 20: 2636
**PAULY, J.**, Identification chart for $\gamma$-emitting radionuclides formed by (n,$\gamma$) reactions, 20: 1735 (EUR-2408.e)
**PAUNOVIC, R.**, Possibility of using radiations in preservation of wine, 20: 2197
**PAVELESCU, M.**, Method for solution of neutron transport equation within framework of Sn approximation, 20: 2940
**PAVLICA, R. T.**, Vibration of fuel assemblies in parallel flow, 20: 1978
**PAVLICK, J. E.**, Recovery of yield stress in Pu-1 wt.% Ga, 20: 2374
**PAVLICK, J. E.**, Recovery and strain-hardening of alpha-phase plutonium, 20: 2380
**PAWLIW, J.**, CANDU fuel performance in NPD, 20: 3496
**PAWLOWSKI, Z.**, Charge-sensitive transistor preamplifier for use with semiconductor nuclear radiation detectors, 20: 2154
**PEAK, J. C.**, Tungsten water-moderated rocket critical assembly, analytical method and experimental results, 20: 3571
**PEARS, C. D.**, Lateral strain behavior of graphite—an anisotropic material, 20: 2315 (CONF-650632-3)
**PEDDIE, R. A.**, Commissioning programmes and procedures, 20: 3529
**PED'KO, A. A.**, Magnetostriction in gadolinium crystal, 20: 3312
**PEKAREK, L.**, Exact solution in theory of decay of pulse disturbance in one-dimensional diffusion plasma, 20: 3187
**PEKERIS, C. L.**, $2^{1,3}P$, $3^{1,3}P$, and $4^{1,3}P$ states of He and the $2^1P$ state of $Li^+$, 20: 2626
**PEKERMAN, S. M.**, Immunological reactivity in monkeys after recovery from acute radiation sickness, 20: 1631
**PEKRUL, P. J.**, Dynamic measurements of SNAP-8ER feedback coefficients, 20: 3557
**PELLAT, R.**, Necessity of energy principles for magnetostatic stability, 20: 3211
**PENG, C. T.**, Significance of exponential function in quenching correction in liquid-scintillation counting and its application to channels-ratio method, 20: 2168
**PENNISI, F.**, Electrochemical labeling of proteins, 20: 1939 (EUR-2476.i)
**PENTSCHEV, P.**, Concentrated serial irradiation method for treating carcinoma of the skin, 20: 1718
**PERELOMOV, A. M.**, Unitary and spin content of SU(6) supermultiplets, 20: 2802
**PERESSINI, Eugene Ramon**, Validity of Thomas-Fermi model of finite nuclear matter, 20: 2819
**PEREVALOVA, E. G.**, Replacement of a halogen by a proton in halogenoferrocenes, 20: 1830
**PERRY, B. John**, Radioisotope scanning display, 20: 1715
**PERRY, G. S.**, Sorption of methanol by corroded uranium, 20: 1805 (AWRE-O-69/65)
**PERRY, K. J.**, Effective axial and radial thermal expansion of $UO_2$ with a radial thermal gradient, 20: 2234
**PETERSEN, D. F.**, Synchronized mammalian cells. II., 20: 1594 (LA-DC-6507)
**PETERSEN, M.**, Studies on sandy surfcoasts with $^{46}Sc$, 20: 2060
**PETERSON, Dorothy C.**, An organic plastic, localizing whole-body counter, 20: 1710
**PETKOV, I.**, Amplitude of inelastic scattering of electrons by nuclei, 20: 3124
**PETRAS, M.**, Self-consistent calculation of magnetic moments of nucleons, 20: 2704
**PETRASCU, M.**, Argon gas scintillation detector, 20: 2163
**PETROFF, C. P.**, Rapid method for dissolving tissue for liquid scintillation counting, 20: 1767
**PETROFF, Ch.**, Effect of single radiation exposure on blood picture of guinea-pigs in dependence on dose and time, 20: 1670
**PETROV, A. A.**, Devices for spectral-isotopic determination of gases in metals, 20: 1793
**PETROV, N. I.**, An experimental determination of $K_2^0 \rightarrow 2\pi$ decay probability in sloped $K_2^0$ beam, 20: 2865 (JINR-P-2325)
**PETROVA, N. N.**, Strengths and polarities of magnetic fields of sunspots during IGY, 20: 2563
**PFANN, J.**, PARAMETRY II for calculation of physical parameters of gas cooled heavy-water reactor, 20: 3381 (UJV-1309b/65)
**PFISTER, J. C.**, Radiation-enhanced diffusion in silicon, 20: 2508
**PHALANGAS, C. J.**, Radiation-induced polymerization of styrene at low temperatures, 20: 1925
**PHILLIPS, David**, Electrical resistance of bismuth from 25 to 80 kilobars, 20: 3642 (UCRL-11639)
**PHILLIPS, Donald H.**, Transient effects in dielectric materials caused by electron irradiation, 20: 1897 (NASA-TN-D-3032)
**PICART, Renee**, Autoradiography of incorporation of tritiated leucine, 20: 1597
**PICKLESIMER, M. L.**, Deformation, creep, and fracture in alpha-zirconium alloys, 20: 2339 (ORNL-P-1753)
**PIETRZYK, Donald J.**, Anion exchange studies of Th, rare earths, and Sc, 20: 1959
**PIGACHE, D. R.**, Reflex ionization in torus, 20: 3180 (SEL-63-116)
**PIGEAUD, Pierre**, Thermodynamic fluid in the Jordan-Thiry theory, 20: 2827
**PIKELNER, L. B.**, Radiation widths of intermediate nuclei, 20: 3133
**PIKVER, R. I.**, Tera-ohmeter with a radioactive generator current, 20: 2108
**PILARSKI, E. M.**, Nonremote fabrication of $^{233}U$ fuel elements, 20: 2289
**PILAT, E. E.**, Measurement of diffusion coefficient in highly anisotropic medium, 20: 2957
**PINAJIAN, J. J.**, Conversion coefficient measurements employing magnetic and solid-state spectrometers, 20: 3019 (ORNL-P-1657)
**PINDOR, M.**, Electromagnetic mass formulae in unitary symmetry, 20: 2764
**PINKHASIK, M. S.**, The BN-350 (Fast Neutron) Atomic Power Station, 20: 3475 (NP-15458)
**PIONTKOVSKII, I. A.**, Changes in higher nervous activity of dogs after irradiation, 20: 1627
**PIPIRAITE, P. P.**, Theory of the electromagnetic form factors in three-nucleon system, 20: 3119
**PIRANI, F. A. E.**, Note on bouncing photons, 20: 2870
**PITAEVSKII, L. P.**, Automodel motion of rarefied plasma, 20: 3228
**PITAEVSKII, L. P.**, Space physics with artificial satellites, 20: 2863
**PITOT, Henry C.**, Effect of $\gamma$ radiation on dietary and hormonal induction of enzymes in rat, 20: 1674
**PIVOVAR, L. I.**, Profound stripping and scattering of $Kr^+$ ions in single collisions with Ne, Ar, Kr and Xe atoms, 20: 2644
**PIZZELLA, R.**, Self-radiolysis and methods for storage of tritiated organic compounds, 20: 1938
**PLATT, Robert B.**, Ionizing radiation and homeostasis of ecosystems, 20: 2081 (BNL-917, pp 39-60)
**PLEINEVAUX, C.**, Main technical characteristics of graphite–gas and light boiling- or pressurized-water type plants, 20: 3322 (EUR-2448.f)
**PLESHANOV, A. S.**, Optical magnetohydrodynamic generator, 20: 2674
**PLESSER, Th.**, Convergence behavior of expansions in the classical collision theory, 20: 2808
**PLETNEV, V. D.**, Principal hypotheses concerning origin of earth's radiation belts, 20: 2861
**PLOUGH, H. H.**, Genetic effects of fast neutrons from nuclear detonations, 20: 1622 (WT-820)
**PLUMLEE, K. E.**, Linear relationship between cadmium ratio and reactor core moderating ratio, 20: 3439
**PLUNKETT, T. F.**, Fuels for gaseous-core nuclear rockets, 20: 3462
**PLYSHEVSKAYA, E. G.**, Role of systems orthophenols–orthoquinones in initial radiation-induced processes in an organism, 20: 1647
**POBELL, Frank**, Investigations on tin and indium–tin alloys in superconducting state with help of Moessbauer effect, 20: 2919
**PODOLSKI, W. F.**, 160,000-Curie $^{60}Co$ facility, 20: 1929
**POEYHOENEN, R.**, Half-life of $^{147}Sm$; comparison of ionization chamber and liquid scintillation results, 20: 3028
**POGDORETSKII, M. I.**, Scattering of neutrons on polarized targets, 20: 3120
**POIDO, M. S.**, The BN-350 (Fast Neutron) Atomic Power Station, 20: 3475 (NP-15458)
**POKORSKI, S.**, Possible influence of the channel $\gamma + N \rightarrow \pi + N$ on the photoproduction amplitude, 20: 2695
**POKROVSKII, V. A.**, Mass spectra of water ionized in a strong electrical field, 20: 1829
**POLAK, L. S.**, System of equations for plasma jet with account of reaction of decomposition of methane in it, 20: 3197
**POLFEROV, E. A.**, Duty cycle improvement of particle beams at 680-Mev JINR synchrocyclotron, 20: 2548
**POLFEROV, E. A.**, Possibility of stabilization of synchrocyclotron intensity, 20: 2536 (JINR-P-2341)
**POLLACK, Louis R.**, Absolute counting with well-type scintillation detectors, 20: 2170
**POLLACK, Louis R.**, Recommended delay in counting after neutron activation, 20: 1788
**POLLAK, F. H.**, Band structure of gallium arsenide: spin-orbit splitting, 20: 3287

**POLLARD, H. E.,** Nuclear environmental effects on spacecraft thermal control coatings, 20: 2428 (NASA-SP-55, pp 365-79)
**POLUEKTOV, N. S.,** Extraction of rare earth amygdalate salts by butanol, 20: 1796
**POLYAKOV, V. K.,** Studies of startup conditions of I. V. Kurchatov Beloyarsk Nuclear Power Station performed at test rig, 20: 3486
**POLYAKOV, V. P.,** Application of complex emanation-thermal method for studying the KCl–$CaCl_2$ constitution diagram, 20: 1860
**POLYAKOV, V. P.,** Application of complex emanation-thermal method in studies of the CaO–$Fe_2O_3$ constitution diagram, 20: 1861
**POMERANTZ, Martin A.,** Prog. rpt. on solid state investigations utilizing electron-bombardment phenomena, annual, 1965, 20: 2434 (TID-22342)
**POMRANING, G. C.,** A flexible numerical approach to linear transport problems, 20: 2983
**POMRANING, G. C.,** Effective thermal-neutron cross sections for materials with grain structure, 20: 2993
**PONCELET, C. G.,** Evaluation of calculational models and thermal cross-section data in analysis of $PuO_2$–$UO_2$–$H_2O$ lattices, 20: 3425
**PONOSOV, A. K.,** Production of slow $\pi$ mesons on light nuclei and the $\pi$-$\pi$ interaction, 20: 2739
**POP, Rodica,** Preparation and characteristics of the IFA $EN_2$ nuclear emulsion, 20: 2158
**POPA, M. S.,** Gamma rays from $^{75}As(n,\gamma)^{76}As$ reaction, 20: 3011 (IFA-NR-22)
**POPOV, V. S.,** Unitary and spin content of SU(6) supermultiplets, 20: 2802
**POPPLE, R. T.,** CANDU fuel performance in NPD, 20: 3496
**PORATH, W. W.,** Calibration of high-speed burnup code for nuclear fuel surveys, 20: 3455
**PORGES, K.,** Fuel-element failure detection in EBR-II, 20: 3518
**PORIES, Walter J.,** Accumulation of radioactive fission products in hair, 20: 1695
**PORTAL, A.,** New Fontenay-aux-Roses $\alpha$-$\beta$-$\gamma$ radiometallurgy laboratory—design and construction, 20: 1999
**PORTAL, Pierre,** A method of fabrication of finned tubes and apparatus therefor, 20: 2303
**PORTYANOI, V. A.,** Complex emanation-thermal method, 20: 1779
**POSSAGNO, E.,** Self-radiolysis and methods for storage of tritiated organic compounds, 20: 1938 (EUR-2452.e)
**POSTMA, H.,** Lorentz dissociation of $H_3^+$ in DCX-1, 20: 3213
**POSVOL'SKII, M. V.,** Reaction of Pu with $H_2O_2$ in presence of other alloys, 20: 1857
**POTSCHWADEK, B.,** Examinations of radioiodine uptake of human fetuses, 20: 1600
**POTTS, G.,** Fluid-bed fluoride volatility processing of irradiated fuels in hot cells, 20: 1971
**POULOPOULOS, P.,** The positive excess of $\mu$ mesons at high energies, 20: 2702
**POUSMA, J. G.,** Thermal properties of selected metals at ambient temperature, 20: 2343 (SC-TM-65-242)
**POZDNYAKOV, A. A.,** Adsorption of Tc from aqueous solutions onto anion exchange resin, 20: 1963
**POZWOLSKI, Alexandre Edgar,** Measuring permeability of porous barriers, 20: 2120
**PRADDAUDE, H. C.,** Bloch electrons in external electric and magnetic fields, 20: 3298
**PRADOS, J. W.,** Mathematical model for predicting coated-particle behavior, 20: 2235
**PRADOS, J. W.,** Partitioning of oxygen between zirconium and liquid potassium, 20: 2367
**PRAEL, R. E.,** SNAPTRAN-2 destructive test predictions, 20: 3561
**PRASAD, K. G.,** X-ray yields from K-shell ionization by $\alpha$ particles, 20: 2625
**PRASAD, Sorju,** Electrometric study on the quantitative precipitation of samarium(III) as normal tellurite, 20: 1760
**PRATVIEL, Pierre,** Improvements in remote control and automation devices for plant in radioactive surroundings, 20: 2003
**PREISER, H. S.,** On cavitation damage in liquid-metal pumps, 20: 2243
**PRESSLEY, R. J.,** Factor of conduction electrons in metallic lithium, 20: 3297
**PRESSMAN, D.,** Computer programs for paired and triad radioiodine label techniques in radioimmunochemistry, 20: 1943
**PRESSMAN, R.,** Computer programs for paired and triad radioiodine label techniques in radioimmunochemistry, 20: 1943
**PRESTON, Roger G.,** Isthmian canal studies, 1964, 20: 1985 (PNE-2003)
**PRETZEL, Frank E.,** Radiation damage to alkali-halides and other simple ionic crystals, 20: 2426 (LA-3387)
**PRICE, R. J.,** Prog. rpt. on advanced, graphite-matrix, dispersion-type fuel systems and research on graphite, 8/15–11/14/64, 20: 2318 (GA-5918 (Pt. 1))
**PRICE, R. J.,** Young's modulus of pyrolytic carbon in relation to preferred orientation, 20: 2446
**PRINCE, A.,** Neutron cross sections for tantalum and tungsten, 20: 2961
**PRINCE, B. E.,** Predicted and observed nuclear characteristics of Molten Salt Reactor Experiment, 20: 3505
**PROFIO, A. E.,** Fast-neutron spectra in paraffin shields, 20: 3257
**PROFIO, A. E.,** Measurement of fast neutron spectra in infinite medium of $CH_2$, 20: 2931 (AD-616518)
**PROKOF'EV, N. S.,** Economic efficiency of nuclear radiation in production and processing of agricultural products, 20: 2198
**PROSAD, R.,** Separation of Mo from Re by the extraction of Mo(VI) from Re(IV) with amyl acetate, 20: 1965
**PROSINA, T. I.,** Measurement of the background external radiation exposure of urban population in the USSR, 20: 2087
**PROTASOV, V. P.,** Production of slow $\pi$ mesons on light nuclei and the $\pi$-$\pi$ interaction, 20: 2739
**PRUETT, R. G.,** The effect of charged-particle environments on manned military space systems, 20: 2656 (NASA-SP-71, pp 265-86)
**PRUGOVECKI, Eduard Slavko,** Empirical and mathematical foundations of quantum mechanics, 20: 2887
**PRUVOST, N. L.,** Interaction in arrays of fissionable materials, 20: 2938 (UCRL-14245)
**PRYOR, A. W.,** Thermal resistance due to microcracking in neutron-irradiated beryllium oxide, 20: 2443
**PRYOR, William A.,** Nuclear safety coordination within Oak Ridge operations facilities, 20: 3370 (CONF-651103-2)
**PRZYBORSKI, Vincenty,** Semiconductor nuclear radiation detectors and applications, 20: 2155
**PTASHNIK, V. B.,** Methods for determining isotopic diffusion effect in solid, 20: 3304
**PULACCI, A.,** Automatic control system for ISPRA-1 reactor, 20: 3587 (RT/ING(65)-3)
**PULLAN, B.,** Radioisotope scanning display, 20: 1715
**PUSANKO, Zh. I.,** Total neutron cross sections of $^{185}Re$ and $^{187}Re$, 20: 3030
**PUTT, G. D.,** Angular distributions in reactions $^{11}B(d,p)^{12}B$ and $^{11}B(d,\alpha)^{9}Be$, 20: 3035
**P'YANOV, I. I.,** Angular distribution of fragments, 20: 3111

## Q

**QUIDORT, J.,** Study of levels of $^{63}Cu$ by inelastic scattering of 10 Mev deuterons, 20: 3073

## R

**RABE, B.,** Self-radiolysis and methods for storage of tritiated organic compounds, 20: 1938 (EUR-2452.e)
**RABE, G.,** Self-radiolysis and methods for storage of tritiated organic compounds, 20: 1938 (EUR-2452.e)
**RABIN, S. A.,** High-power operation of $PuO_2$–$UO_2$ fast reactor fuel, 20: 2448
**RABIN, S. A.,** Irradiation behavior of high-burnup $ThO_2$–4.45% $UO_2$ fuel rods, 20: 2429 (ORNL-3837)
**RABINOVICH, Harris,** Partial wave calculation of diatomic molecule $(HeH)^{++}$, 20: 2595 (NASA-TN-D-3050)
**RABINOWITZ, P.,** $2^{1,3}P$, $3^{1,3}P$, and $4^{1,3}P$ states of He and the $2^1P$ state of $Li^+$, 20: 2626
**RADCLIFFE, R. E.,** Comparison of calculated and measured burnup distributions and isotopic inventory in Yankee core, 20: 3504
**RADICELLA, R.,** Preparation of a $^{99m}Tc$ labeled colloid, 20: 1696 (CONF-641126-1)
**RAFFO, Peter L.,** Properties of arc-melted and electron-beam-melted tungsten, 20: 2396
**RAGAN, H. A.,** Age related changes in hematological and serum biochemical parameters in miniature swine, 20: 1581 (BNWL-SA-341)
**RAHE, E. P. Jr.,** Measurement and analysis of SM-1A core-3, 20: 3503
**RAHEJA, Krishan,** Bibliography on wholesomeness of irradiated food, 20: 2196 (AD-614910)
**RAHM, D. C.,** Observation of a peak in $K^- + p \rightarrow \Lambda + \eta$ near threshold, 20: 2724
**RAJU, Mudundi R.,** Studies of Vicia faba root meristems irradiated with a $\pi^-$ beam, 20: 1621 (UCRL-16387)
**RALLS, K. M.,** Microstructure and superconducting properties of 45 Nb–55 Zr alloy, 20: 2395
**RAMAMURTHY, J.,** Labeling of glycine by direct exchange with heavy water, 20: 1833
**RAMANATHAN, P.,** Economic method of obtaining photoscan, 20: 1705
**RAMAYYA, A. V.,** Conversion coefficient measurements employing magnetic and solid-state spectrometers, 20: 3019 (ORNL-P-1657)
**RAMIREZ, C.,** Comparative sensitivity to $\gamma$ radiation of yeast mitosis and meiosis, 20: 1664
**RAMORINO, C.,** $^{238}U$ fission induced by low-energy monochromatic $\gamma$-rays, 20: 3050
**RAMQVIST, Lars,** Wetting of metallic carbides by liquid, copper, nickel, cobalt and iron, 20: 1837

**RAMSDEN, S. A.,** Optical interferometric and spectroscopic measurements of electron density in plasma, 20: 3214
**RAMSEY, Frank K.,** Inhalation study of pathogenesis of neodymium oxide in mice and guinea pigs, 20: 1593 (COO-1170-4)
**RANCITELLI, L.,** Nondestructive activation analysis of cobalt in iron meteorites, 20: 2055
**RAND, R. E.,** Inelastic electron scattering from alpha particle, 20: 3086
**RANDEN, K. G.,** Modification of shield test and irradiation reactor for one-megawatt operation, 20: 3595
**RANKIN, M.,** Simple momentum probe for plasma studies, 20: 3179 (ORNL-P-1575)
**RANNIGER, Klaus,** Long-term angiographic and clinical evaluation after irradiation of one kidney in dogs, 20: 1686
**RANSHOFF, J. A.,** Producing large quantities of $^{237}$Np and $^{238}$Pu in commercial power reactors, 20: 2210
**RANTALA, Veikko,** Measurement of formation energy of electron-hole pair in n-type silicon, 20: 2362
**RAO, B. Rama,** Antenna inside a magneto-plasma-filled parallel-plate waveguide, 20: 2096 (AD-617928)
**RAO, V. Udaya Shanker,** Moessbauer effect in Sn–Pt alloys, 20: 3290
**RAPOPORT, V. B.,** Calorimetric analysis of kinetics of radiation polymerization, 20: 1904
**RASMUSSEN, J. O.,** Effect of chemical state on lifetime of 24-second isomer of $^{90}$Nb, 20: 3088
**RASMUSSEN, N. C.,** Nondestructive analyses of irradiated MIT reactor fuel elements by $\gamma$ spectroscopy, 20: 2030
**RASSKAZOV, D. S.,** Effects of reactor radiation on thermophysical properties of monoisopropyldiphenyl, 20: 1923
**RASZILLIER, I.,** Irreducible representations of the group $C_2$, 20: 2793
**RATNIKOVA, M. G.,** Preparation of specimens and corrections for self-absorption during measurement of activity of soft $\beta$ emitters, 20: 1780
**RAUCH, H.,** Neutron spectra of cooled moderators, 20: 2945
**RAVETS, J.,** Comparison of analytical and experimental power distribution of NERVA reactors, 20: 3568
**RAVETS, J. M.,** WANL experience with r-$\theta$ calculations, 20: 3429
**RAYFIELD, George T.,** Measurements and calculations of hydrogen loss from hydrided zirconium–uranium fuel elements during transient heating to temperatures near melting point, 20: 3563
**RAYMES, Frederick,** Apollo spacecraft nuclear radiation protection status report, 20: 3244 (NASA-SP-71, pp 365-75)
**RAYMOND, James P.,** Prog. rpt. on semiconductor radiation response prediction, 12/15/64–3/15/65, 20: 2412 (AD-618079)
**RAYMOND, L.,** Prog. rpt. on fabrication and properties of W singe crystals, final, 3/64–2/65, 20: 2284 (NP-15093)
**RAYSKI, Jerzy,** Quantization and physical interpretation of the gravitational field, 20: 2866
**REBER, Elwood F.,** Bibliography on wholesomeness of irradiated food, 20: 2196 (AD-614910)
**REBER, L. H.,** Lorentz dissociation of $H_2^+$ in DCX-1, 20: 3213
**REBOUX, J.,** High-frequency induction currents and their uses at very high temperatures, 20: 2525
**REDMAN, W. C.,** Direct measurement of effective capture-to-fission ratio at low flux, 20: 3430
**REED, G. L.,** Economic potential of direct nuclear superheat, 20: 3508
**REED, Jack W.,** Isthmian canal studies, 1964, 20: 1985 (PNE-2003)
**REEDY, R. K. Jr.,** Critical experiments with SPERT-D fuel elements, 20: 3379 (ORNL-TM-1207)
**REETZ, Arthur Jr.,** Conference on protection against radiations in space, Gatlinburg, 10/64, 20: 3239 (NASA-SP-71)
**REIBACK, Earl,** Bulk-grain-irradiator design, 20: 2194
**REICHERT, E.,** Angular dependence of polarization of 3.5 ev electrons on free Hg atoms, 20: 2615
**REIER, M.,** Pulsed-neutron measurements in diphenyl at 85 and 105°C, 20: 2953
**REIKHSFEL'D, V. O.,** Synthesis of trimethylbenzenes for measuring natural radiocarbon by means of scintillation method, 20: 2062
**REIN, James E.,** Prog. rpt. on burnup determination of nuclear fuels, 4–6/65, 20: 3010 (IDO-14663)
**REISER, W.,** Spin determination on $^{144}$Pr by angular correlation measurements, 20: 3033
**REITHEL, R. J.,** Particle-size distributions from Rover fuel-element fragmentation studies, 20: 3574
**REKALO, M. P.,** Relations between electromagnetic amplitudes according to the unitary symmetry model, 20: 2732
**RENERO, I.,** Recursion relations for Wigner coefficients of unitary groups, 20: 2770
**RESNICK, Lazer,** Effects of $\pi$ and $\rho$ exchange in peripheral model of isobar production, 20: 2817
**RESNICK, R.,** Diffusivity of carbon in tantalum and Nb carbides, 20: 2398
**REUSCHER, Jon Arthur,** Transient thermal stresses in liquid metal cooled reactor fuel elements, 20: 3463
**REUTER, R. A.,** Fuel elements for Arbeitsge-Meinschaft Versuchs reaktor (AVR), 20: 3494
**REYNOLDS, W. N.,** Nucleation of radiation damage in graphite, 20: 2447
**REZBEN, V. A.,** Tera-ohmeter with a radioactive generator current, 20: 2108
**RHEA, G. W.,** Relative toxicity of angiographic contrast media, 20: 1724
**RHODES, D. W.,** Measurement of heat generation rate of highly radioactive calcined alumina, 20: 2425 (IDO-14665)
**RHUDE, H. V.,** Improved metallic fast power breeder fuels, 20: 2386
**RICCHENA, R.,** TESI—advanced power excursion reactor for research in reactor safety, 20: 3584 (EUR-2433.e)
**RICE, T. M.,** Superconductivity in one and two dimensions, 20: 2889 (AD-618203)
**RICHARDS, P.,** Technetium-99m generator, 20: 1730 (BNL-9601)
**RICHARDS, W. Bruce,** Total and differential cross sections for reaction $\pi^- p \to \eta n$, 20: 2689 (UCRL-16140)
**RICHARDSON, James H.,** Thermal expansion of three group IVA carbides to 2700°C, 20: 1839
**RICHEY, C. R.,** Criticality research on plutonium, 20: 3368 (BNWL-SA-214)
**RICHEY, C. R.,** Criticality studies with plutonium solutions, 20: 3395
**RICHEY, C. R.,** Neutron interaction between multiplying media separated by various materials, 20: 3391
**RICHMAN, Chaim,** Studies of Vicia faba root meristems irradiated with a $\pi^-$ beam, 20: 1621 (UCRL-16387)
**RICHMAN, Stephen P.,** Studies of Vicia faba root meristems irradiated with a $\pi^-$ beam, 20: 1621 (UCRL-16387)
**RICHMOND, Donald R.,** Biological tolerance to air blast and related biomedical criteria, 20: 2083 (CEX-65.4)
**RICKEY, M. E.,** Levels of $^{58}$Ni from reaction $^{58}$Ni(p,t)$^{56}$Ni at 28 Mev, 20: 3041
**RIDDLE, R. A. J.,** Polarization in neutron-proton scattering, 20: 2701
**RIDLEY, R. G.,** Mass spectrometer source loading lock and isolation valve, 20: 2159
**RIEBOLD, W.,** TESI—advanced power excursion reactor for research in reactor safety, 20: 3584 (EUR-2433.e)
**RIEDEL, Jozef Tadeusz,** Determination of isotopic composition of natural B isotopes, 20: 1774
**RIGNY, Paul,** Anisotropy of the fluorine chemical shift tensor in $UF_6$, 20: 1807 (CEA-R-2827)
**RILEY, L. W.,** Stimulated emission from 4.3 percent abundant $^{50}$Cr ions in ruby, 20: 3283
**RILEY, R. E.,** Compatibility of refractory metals with solid solution (UC)(ZrC) at elevated temperatures, 20: 2332 (LA-3307)
**RINALDINI, C.,** TESI—advanced power excursion reactor for research in reactor safety, 20: 3584 (EUR-2433.e)
**RINN, F. H.,** Fast method in $\gamma$ spectrometry, 20: 2150
**RIPLING, E. J.,** Use of strain softening to improve properties of refractory metals, 20: 2311 (AD-618925)
**RITSON, D. M.,** Polarization measurements on recoil proton from $\pi^0$ photoproduction, 20: 2679 (AD-618664)
**RITTINGHAUS, K. F.,** Telecommunication equipment of the nuclear research establishment at Juelich, 20: 2111
**RITZ, V. H.,** Concentrations of $\alpha$ and F centers in KBr irradiated at 5°K, 20: 1919
**RIZZO, F. X.,** Measurement of megarad doses of $^{60}$Co gamma rays with UVT lucite, 20: 2165
**RIZZO, Francis X.,** Calorimetric calibrations of high-specific-activity $\gamma$ sources, 20: 2195
**ROBERTS, A.,** Evidence for $\kappa^0(725)$ in $\pi^-$ p reactions, 20: 2715
**ROBERTS, A. C.,** Nature and annealing behavior of irradiation damage in molybdenum, 20: 2476
**ROBERTS, Franklin L.,** Genetic segregation in unisexual wasp Devorgilla, 20: 1643
**ROBERTS, J. T.,** Development of the Excer Process. I., 20: 1956 (ORNL-1696)
**ROBERTS, John J.,** Limitations to applicability of restricted space, time-optimal xenon shutdown problem, 20: 3410
**ROBERTS, T. R.,** Measurement of $C_{NN}$ in neutron-proton scattering at 23 Mev, 20: 2685 (LA-DC-7250)
**ROBERTSON, James S.,** Role of computers in processing scanning data, 20: 2213 (BNL-9609)
**ROBESON, A.,** Diffusion parameters of mixtures of light and heavy water at several temperatures, 20: 2951
**ROBIN, Gordon C.,** Chronic synovial effusions treated with intra-articular radioactive gold, 20: 1706
**ROBINSON, L. E.,** Fast reactor safety experiments on EBR-II samples in flowing sodium environment, 20: 3506
**ROBINSON, R. L.,** Gamma-ray energies determined with lithium-drifted germanium detector, 20: 3043
**ROBINSON, W. R.,** Linear relationship between cadmium ratio and reactor core moderating ratio, 20: 3439
**ROBINSON, William Courtney Jr.,** Reactions of uranium carbide in a fused KCl–LiCl/zinc system, 20: 2404
**ROBKIN, M. A.,** Burnup analysis of lumpy fuel, 20: 2454

**ROCHE, T. K.,** Evaluation of niobium–vanadium alloys for application in high-temperature reactor systems, 20: 2340 (ORNL-TM-1131)
**RODEGKER, Waldtraut,** Lipids of Ruvettus pretiosus muscle and liver, 20: 3637 (UCLA-12-534)
**RODERICK, Hilliard,** Thermonuclear power, 20: 3196
**RODINA, I. B.,** Study of diffusion of carbon and molybdenum in chromium, 20: 2357 (AERE-Trans-1032)
**RODIONOV, K. P.,** Effect of uniform compression on Curie temperature of ferromagnetic compound EuO, 20: 3313
**RODRIGUEZ PASQUES, Rafael H.,** Tritiation of furfural, 20: 1887 (NP-15523)
**ROEDER, P. J.,** Semiconductivity in glass systems $V_2O_3$–$P_2O_5$ and $V_2O_5$–$P_2O_5$, 20: 2316 (COO-1198-220)
**ROGERS, Morris R.,** Feasibility study of filtration unit for removal by the individual of CBR agents from water, 20: 2072 (AD-618006)
**ROGERS, W. B.,** Buckling measurements by successive substitution in subcritical assembly, 20: 3399
**ROMANO, A. J.,** Relative aggressiveness of Li, Na, K, Rb and Cs boiling and condensing in Nb–1Zr capsules, 20: 2268
**ROMANOWSKI, T. A.,** Evidence for $\kappa^0(725)$ in $\pi^-$p reactions, 20: 2715
**ROOS, J.,** Prog. rpt. on boiling flow regimes and critical heat flux, 6/16–9/15/65, 20: 2012 (NYO-3304-6)
**ROOT, J. W.,** Abstraction of H atoms by energetic recoil tritium atoms, 20: 1907
**ROSA, Richard J.,** Experimental studies of strong Hall effects and U x B induced ionization, 20: 2671
**ROSA, U.,** Electrochemical labeling of proteins, 20: 1939 (EUR-2476.i)
**ROSE, R. M.,** Microstructure and superconducting properties of 45 Nb–55 Zr alloy, 20: 2395
**ROSE, R. P.,** Annular-ring model for loft meltdown studies, 20: 3333
**ROSE, R. P.,** Loft semi-scale blowdown tests, 20: 3336
**ROSE, R. P.,** SNAPTRAN-2 destructive test predictions, 20: 3561
**ROSEN, A.,** Effect of temperature, strain rate and structure on flow stress of an iron–2 percent manganese alloy, 20: 3641 (UCRL-11512(Rev.))
**ROSEN, Louis,** Elastic scattering of polarized nucleons, 20: 3014 (LA-DC-7386)
**ROSENBLATT, J.,** Elastic scattering of 27.5 Mev deuterons and its optical model analysis, 20: 3057
**ROSHOLT, John N. Jr.,** Fractionation of U isotopes and daughter products in U-bearing sandstone, 20: 2057
**ROSNER, L. G.,** Superconducting $H_c$-$J_c$ characteristics of nitrided Nb–Zr wire to 130 kOe, 20: 2891
**ROSOFF, Betty,** Removal of radioisotopes from man, 20: 1691
**ROSSMASSLER, W. R.,** Electrolytic generation of fluorine from uranium hexafluoride, 20: 1954 (KY-287)
**ROSTOVTSEV, A. A.,** Distribution of specific ionization along the track as a function of initial energy of $^{235}U$ fission fragments, 20: 3029
**ROTELLI, P.,** U(12) irregular coupling relations for stopped proton pair annihilation into mesons, 20: 2703
**ROTHBART, Michael A.,** Calorimetric calibrations of high-specific-activity $\gamma$ sources, 20: 2195
**ROUSE, Robert Lindsay,** Improvements relating to solid-state radiation detectors, 20: 2182
**ROUSSET, Pierre,** Improvements in refractory uranium compounds, 20: 2250
**ROUT, Reginald Harold,** Improvements relating to nuclear reactors, 20: 3465
**ROWLAND, F. S.,** Abstraction of H atoms by energetic recoil tritium atoms, 20: 1907
**ROWLANDS, D. L. G.,** Diffusion coefficient of water in water and in some alkaline earth chloride solutions at 25°C, 20: 1865
**ROY, C.,** Nucleation and growth of hydrides in zirconium alloys, 20: 2253 (AECL-2297)
**ROY, Gerald,** Direct reaction analysis of $^{15}N(p,\alpha_0)^{12}C$ reaction, 20: 3061
**ROZANOV, E. I.,** Duty cycle improvement of particle beams at 680-Mev JINR synchrocyclotron, 20: 2548
**ROZHKOVA, R. S.,** Magnetic properties of Ni–Eu alloys, 20: 2369
**RUARK, Arthur E.,** Thermonuclear power, 20: 3196
**RUBIN, B.,** Behavior of blanket $UO_2$ fuel rods in PWR core I, 20: 3495
**RUBINOVA, E. E.,** Ripening of defects, induced by fast neutrons in germanium, in course of low-temperature annealing, 20: 2509
**RUBY, Lawrence,** Applications of nuclear energy—new course for humanities, 20: 3329
**RUCH, R. R.,** Preconcentration of trace elements by precipitation ion exchange using organic-hydrochloric acid systems, 20: 1958
**RUCH, R. R.,** Prog. rpt. on applications of neutron-activation analysis to scientific crime detection, 10/62, 20: 1737 (GA-3664)
**RUCH, R. R.,** Prog. rpt. on applications of neutron-activation analysis to scientific crime detection, 11/62–1/63, 20: 1738 (GA-4041)
**RUCH, R. R.,** Prog. rpt. on applications of neutron-activation analysis to scientific crime detection, 2–4/63, 20: 1739 (GA-4297)
**RUCH, R. R.,** Prog. rpt. on application of neutron-activation analysis to scientific crime detection, 5–7/63, 20: 1740 (GA-4576)
**RUCKDESCHEL, W.,** Prog. rpt. on development of $ZrNb_3Sn_1$ for use as cladding material, 10–12/64, 20: 2255 (EURAEC-1323)
**RUDENKO, N. P.,** Behavior of thorium, protactinium, and uranium during extraction by means of benzohydroxamic acid and n-benzoylphenyl-hydroxylamine, 20: 1776
**RUDENKO, N. P.,** Investigation of radiation of $^{113}Cd$, 20: 3113
**RUDENKO, N. P.,** Thorium, protactinium, and uranium extraction by means of neocupferron, 20: 1775
**RUDENKO, N. S.,** Viscosity of hydrogen isotope solutions, 20: 2922
**RUDENKO, V. S.,** Irreversible polymorphic transformations of rare earth oxides, 20: 1827
**RUDO, F. S.,** Nondestructive electrical method of studying density distribution of a randomly packed bed, 20: 1977
**RUDY, Erwin,** High-temperature nuclear fuel structures and their production, 20: 2305
**RUDY, Erwin,** Superconductivity of the cubic modification of MoC, 20: 2346 (UCRL-11471)
**RUDZIKAS, Z. B.,** Two-electron matrix elements of spin-spin interaction energy operator, 20: 2605
**RUDZIKAS, Z. B.,** Two-electron matrix elements of spin-orbit interaction energy operator, 20: 2606
**RUEDENAUER, F.,** Numerical method for calculation of image aberrations of inhomogeneous magnetic sector fields between conical pole faces, 20: 2209 (SGAE-PH-26/1965)
**RUEDORFF, Walter,** Absorption of blue solutions of europium and beryllium in liquid ammonia, 20: 1867
**RUEGG, F. C.,** Absolute-velocity Moessbauer spectrometer, 20: 2113
**RUEHL, W.,** Transition temperatures of superconductors of various metals under influence of very thin oxide layers, 20: 2915
**RUMBLES, William E.,** Radiation shelter, 20: 2040
**RUPBERT, George N.,** Advanced high-temperature thermal analysis apparatus employing derivative and differential techniques, 20: 1863
**RUSAKOV, V. A.,** An experimental determination of $K_2^0 \to 2\pi$ decay probability in sloped $K_2^0$ beam, 20: 2865 (JINR-P-2325)
**RUSLING, D. H.,** Importance of space radiation shielding weight, 20: 3245 (NASA-SP-71, pp 407-14)
**RUSSELL, B.,** Helium gas precipitation in irradiated Cu–B alloys, 20: 2441
**RUSSELL, B.,** Measurement of helium content in neutron-irradiated copper–boron alloys, 20: 2444
**RUSSELL, Irving J.,** Radiobiological consequences of dose distributions produced by solar-flare-type spectra, 20: 2655 (NASA-SP-71, pp 85-96)
**RUSSELL, J. L. Jr.,** Accelerator-pulsed fast-assembly operating experience, 20: 2956
**RUSSELL, J. L. Jr.,** Fast-neutron spectra in paraffin shields, 20: 3257
**RUTBERG, Blanka,** Role of superinfecting phage in lysis inhibition with phage T4 in E. coli, 20: 1650
**RUTBERG, Lars,** Role of superinfecting phage in lysis inhibition with phage T4 in E. coli, 20: 1650
**RUTHERFORD, Charles H.,** PWR-2 flux wire measurements and comparison to calculations, 20: 3519
**RUTTER, R. L.,** Commissioning programmes and procedures, 20: 3529
**RUZICKA, T.,** Exact solution in theory of decay of pulse disturbance in one-dimensional diffusion plasma, 20: 3187
**RYABCHENKO, V. A.,** Comparative resistance of enteroviruses and B. coli in water disinfection with $\gamma$ radiation, 20: 1645
**RYABCHIKOV, D. I.,** Adsorption of Tc from aqueous solutions onto anion exchange resin, 20: 1963
**RYAN, E. S.,** Aqueous radioactive waste treatment plant at Rocky Flats, 20: 1940 (RFP-638)
**RYNBRANDT, J. D.,** Correlated EPR-optical spectra of potassium in ethylamine–ammonia mixtures, 20: 1808 (COO-958-5)
**RYS'EV, O. A.,** Determination of $^7Be$ in samples of atmospheric aerosols and atmospheric precipitation in presence of fission fragments, 20: 1778
**RYSKIN, G. Ya.,** Isotopic effect in diffusion of lithium in sodium, 20: 3305
**RYVKIN, S. M.,** Ripening of defects, induced by fast neutrons in germanium, in course of low-temperature annealing, 20: 2509
**RZEWUSKI, H.,** Metastable defect annealing in germanium, 20: 2484
**RZEWUSKI, J.,** Technique of normal products in terms of functional integrals, 20: 2765

## S

**SAAVEDRA, I.,** Ehrenfest's theorem in scattering theory, 20: 2785
**SACHENKO, V. P.,** Satellites of x-ray spectra, 20: 2645
**SADYKHOV, F. S.,** Lepton annihilation of proton-antiproton pairs with allowance for form factors and polarization correlations, 20: 2696
**SAED, Abdel Gawad,** Thorium, protactinium, and uranium extraction by means of neocupferron, 20: 1775
**SAED, Abdel Gawad,** Behavior of thorium, protactinium, and uranium during extraction by means of benzohydroxamic acid and n-benzoylphenyl-hydroxylamine, 20: 1776
**SAENKO, V. A.,** Low frequency oscillations in plasma of reflex discharge, 20: 3222

**SAFONOV, A. N.,** Possibility of stabilization of synchrocyclotron intensity, 20: 2536 (JINR-P-2341)
**SAINT-JAMES, Rose,** Process for dispersion of uniform droplets of a liquid in a second liquid, 20: 1800
**SAITO, B.,** Radiation-induced liquid- and solid-phase polymerization of acetylene, 20: 1913
**SAKAI, Yoshiro,** Electron spin resonance of irradiated methacrylic acid, 20: 1916
**SAKAKURA, A.,** Hot laboratory of Japan Atomic Energy Research Institute, 20: 1997
**SAKAMOTO, Masanobu,** Scattering of long wavelength neutrons by precipitations in $Al_{99.5}Cu_{0.5}$ alloys, 20: 3285
**SAKHAROVA, N. N.,** Water solubility of complex compounds of lanthanum, cerium, praseodymium, neodymium, and samarium acetates with thiourea, 20: 1869
**SAKHAROVA, Yu. G.,** Water solubility of complex compounds of lanthanum, cerium, praseodymium, neodymium, and samarium acetates with thiourea, 20: 1869
**SAKO, Kiyoshi,** Preliminary design work of 2 Mw Na loop, 20: 3479 (NP-15556)
**SAKORINA, N. A.,** Devices for spectral-isotopic determination of gases in metals, 20: 1793
**SAKS, O. V.,** Tera-ohmeter with a radioactive generator current, 20: 2108
**SALAH, Sagid,** Neutron spectrum measurements in heterogeneous media, 20: 3600
**SALAITA, G. N.,** Diffusion parameters of mixtures of light and heavy water at several temperatures, 20: 2951
**SALESSE, Marc,** Improvements in beryllium–magnesium alloys, 20: 2277
**SALKIND, M. J.,** Phase-reinforced high-temperature alloys produced directly from the melt, 20: 2219 (AMRA-CR-64-05/4)
**SALMON, G. A.,** Effect of solvent on spectra produced by pulse radiolysis of solutions of organic electron scavengers, 20: 1920
**SALSIG, William W.,** 200 Bev accelerator handling systems in regions of high residual radioactivity, 20: 2542 (UCRL-16236)
**SAMOKHVALOVA, N. S.,** Effect of space flight factors on Evonymys europaea seeds, 20: 1649
**SAMOKHVALOV, A. A.,** Effect of uniform compression on Curie temperature of ferromagnetic compound EuO, 20: 3313
**SANDERS, V. D.,** Pressure drop for flowing vapors condensing in a straight horizontal tube, 20: 1814 (NAA-SR-6333)
**SANDERS, W. Mort,** Gamma scanning with anticoincidence spectrometers, 20: 2172
**SANDERSON, E. A.,** Nuclear ground states in random phase approximation, 20: 3085
**SANDLER, S. R.,** The use of organometallic compounds in plastic scintillators for detection and resolution of $\gamma$ rays, 20: 1905
**SANGAL, Satendra P.,** Chromotrope 2B in photometric determination of rare earths, 20: 1772
**SANNA, R.,** Stray neutron spectra at large pulsed-particle accelerator sites, 20: 2553
**SANNIKOV, S. S.,** Representations of the rotation group with complex spin, 20: 2805
**SANTAVY, J. A.,** Remote underwater devices for evaluation and reduction of irradiated Yankee fuel assemblies, 20: 2117
**SANTOS, Ibarra S.,** Reduction of sensitivity to $^{60}Co$ $\gamma$ rays in Phaseolus mungo through pre- or post-irradiation heat treatment of the seed, 20: 1690
**SANTY, M. J.,** Behavior of beryllium metal in simulated launch pad abort environments, 20: 2341 (SC-DC-65-1637)
**SAPERSHTEIN, E. E.,** Calculation of magnetic moments of spherical nuclei, 20: 3118
**SAPHAR, Pierre,** Nuclear power applications and Hilbert-Schmidt applications in Banach spaces, 20: 2215
**SARASON, Leonard,** Hydromagnetic switch-on shocks, 20: 2834
**SARGENT, G. A.,** Irradiation hardening and embrittlement in bcc transition metals, 20: 2472
**SARGIS, D. A.,** Analytic error estimates for integral-equation Eigenvalue problems, 20: 3411
**SARGOOD, D. G.,** Angular distributions in reactions $^{11}B(d,p)^{12}B$ and $^{11}B(d,\alpha)^{9}Be$, 20: 3035
**SARI, C.,** Preparation of Zr and U–Mo alloys, 20: 2222 (EURAEC-1390)
**SARRATE, M.,** Properties of copper alloys of high resistance and high conductivity, 20: 2334 (NP-15530)
**SASAKAWA, Tetsuya,** Symmetry property of the S matrix on basis of the Jost function method, 20: 2790
**SASAKI, Y.,** Hot laboratory of Japan Atomic Energy Research Institute, 20: 1997
**SASLAW, William C.,** Statistical model of formation of stars and interstellar clouds, 20: 2574
**SASTRE, C.,** HFBR physics startup manual, 20: 3580 (BNL-9591)
**SATCHLER, G. R.,** Polarization-asymmetry equality and measurement of spin-flip in inelastic scattering from nuclei, 20: 3076
**SATO, Masatomo,** Higher order corrections to Alfven wave instability, 20: 3221
**SAVAGE, H.,** Improved metallic fast power breeder fuels, 20: 2386
**SAVIN, E. P.,** The isotopic exchange of cyclohexane with deuterium over evaporated films of germanium and silicon, 20: 1838
**SAVIN, I. A.,** Elastic $\pi^+$-p scattering at 180° and high energies, 20: 2683 (JINR-P-2327)
**SAWADA, T.,** Elastic scattering of deuterons from complex nuclei at high energies, 20: 3044
**SAWATZKY, A.,** Effect of neutron irradiation and hydrogen concentration on tensile properties of CANDU coolant tube spacer alloy, 20: 2414 (AECL-2272)
**SAWYER, J. C.,** Prog. rpt. on creep of refractory alloys at elevated temperatures, 20: 2333 (NASA-CR-54457)
**SAYER, M.,** Scintillation decay in calcium tungstate, 20: 1900
**SAYRE, Edward V.,** Refinement in methods of neutron activation analysis of ancient glass objects, 20: 1731 (BNL-9614)
**SCANLON, J. P.,** Real part of proton-neutron scattering amplitude at 19.3 Bev, 20: 2712
**SCASSELLATI, G.,** Electrochemical labeling of proteins, 20: 1939 (EUR-2476.i)
**SCAVUZZO, R. J.,** Structural analysis of fuel growth in fuel plates, 20: 3453
**SCAVUZZO, R. J.,** Post-buckling behavior of hydraulically collapsed assembly fuel plates, 20: 3459
**SCHAEDLE, G. C.,** Examination of relative merits of stochastic and non-statistical methods of computing primary ionization doses, 20: 2658 (NASA-SP-71, pp 527-33)
**SCHAEFER, Hermann J.,** Local dose from proton and alpha particle enders behind complex shield systems, 20: 3251 (NASA-SP-71, pp 507-12)
**SCHAEFFER, Riley,** Crystal structure of tetramethyl ammonium hexahydrohexaborate, 20: 2347 (UCRL-12146)
**SCHAFFHAUSER, A. C.,** Low-temperature ductility and strength of vapor-deposited tungsten, 20: 2388
**SCHAMBERGER, R.,** Comparison of shield leakage obtained from 3-D calculations and measurements, 20: 3348
**SCHENZ, R. F.,** Cryogenic irradiation of resistance temperature transducers for NERVA, 20: 2191
**SCHIAGER, Keith Jerome,** Alpha-active fallout particles: Physical characteristics related to pulmonary exposure, 20: 1601
**SCHIAVUTA, E.,** Positive pion photoproduction with coherent bremsstrahlung, 20: 2718
**SCHIFF, B.,** $2^{1,3}P$, $3^{1,3}P$, and $4^{1,3}P$ states of He and $2^{1}P$ state of $Li^+$, 20: 2626
**SCHINKMANN, M.,** Microwave absorption and magnetic transition in $GdCl_3$, 20: 3288
**SCHINZ, H. R.,** Patient dosimetry in x-ray diagnosis, 20: 1704
**SCHLAIN, David,** Stress-corrosion cracking of vanadium, molybdenum, and a titanium–vanadium alloy, 20: 2254
**SCHLITZ, Jean-Claude,** Computer processing of $\gamma$ spectra and determination of radioelements, 20: 1732 (CEA-R-2850)
**SCHLOESSER, L.,** Central laboratory for hot chemistry at KFA-Juelich, 20: 1996
**SCHLOSSER, William,** Pulsed nuclear radiation induced transients in electrical cables, 20: 2186 (ECOM-2415)
**SCHLOSSER, William,** Pulsed nuclear radiation effects on resistors and cables, 20: 2187 (ECOM-2545)
**SCHMELTEKOPF, A. L.,** A new speculation on terrestrial helium loss, 20: 2857
**SCHMID, B. K.,** Radiotracer study of product contamination by catalytic nickel, 20: 1889
**SCHMIDT, H.,** Neutron spectra of cooled moderators, 20: 2945
**SCHMITT, H.,** Spin dependence of Rayleigh scattering, 20: 3082
**SCHMITZ, G.,** Theory of gas heating in axially symmetric wall-stabilized luminous arcs. I., 20: 2840
**SCHNEIDER, M.,** Adoptive immunotherapy of acute leukemia: Experimental and clinical results, 20: 1701
**SCHNELL, W.,** Missing bunch phaselock system for proton storage rings, 20: 2535 (CERN-65-31)
**SCHNITZEL, R. H.,** Recrystallization variables of flat-rolled molybdenum–cobalt alloys, 20: 2313 (AD-619208)
**SCHOENEBERG, R.,** Delayed neutrons in decay of $^{9}Li$, 20: 3130
**SCHOENMAKERS, J.,** Molecular weight of Factor XII (Hageman factor) estimated with ionizing radiation, 20: 1673
**SCHOPPER, H.,** Measurement of $\beta$-$\gamma$ angular correlation for $^{198}Au$, 20: 3129
**SCHRAIDT, J. H.,** Inert-atmosphere enclosure for environmental testing, 20: 2246
**SCHREINER, Sheldon,** Numerical comparison of higher order variational principles, 20: 2980
**SCHROCK, V. E.,** Effect of natural convection upon temperature transient following loss-of-coolant accident, 20: 3515
**SCHROEDER, Gerald L.,** Application of Li-drifted Ge detectors to neutron activation analysis—studies in geochemistry and of 15th century printing,

20: 2166
**SCHULT, O. W. B.**, Optimum measuring condition of $\gamma$ and $\beta$ spectrometers, 20: 2148
**SCHULTE-FROHLINDE, D.**, Energy transfer in $\gamma$ radiolysis of the benzene–benzophenone–isopropanol system, 20: 1931
**SCHUNICHT, Bernard F.**, Numerical methods for solution of complex $\gamma$ spectra, 20: 1792
**SCHWAB, C.**, Effects of neutron and proton bombardments on the exciton spectrum of $Cu_2O$, 20: 2505
**SCHWARTZ, Bernard**, Studies of Vicia faba root meristems irradiated with a $\pi^-$ beam, 20: 1621 (UCRL-16387)
**SCHWARTZ, K.-D.**, Examinations of radioiodine uptake of human fetuses, 20: 1600
**SCHWARZ, R. W.**, Cost estimating magnet systems with the aid of a computer, 20: 2545 (UCRL-16386)
**SCHWARZ, Steven Emanuel**, Plasma diagnosis by means of photon-electron scattering, 20: 3232
**SCHWARZENBERG, L.**, Adoptive immunotherapy of acute leukemia: Experimental and clinical results, 20: 1701
**SCHWEITZER, D. G.**, Magnetic field penetration and breakdown of surface superconductivity. II., 20: 2900
**SCHWOERER, F.**, Economic potential of direct nuclear superheat, 20: 3508
**SCINTEI, N.**, Mechanism of reaction $^{26}Mg(p,p',\gamma)$ at low energy, 20: 3092
**SCOTT, J. L.**, Irradiation evaluation of fuel elements for PBRE and AVR reactors, 20: 2464
**SCOTT, J. L.**, Mathematical model for predicting coated-particle behavior, 20: 2235
**SCOTT, W. C.**, Energy transfer mechanisms between rare-earth impurity ions, 20: 2627
**SCOTT, Walter P.**, Cobalt-60 rotational therapy calculator, 20: 1723
**SEARASHI, T.**, Repair of damage induced by uv light in Bacillus subtilis, 20: 1624
**SEARS, John Thomas**, Energy deposition by fission fragments: optical excitation of nitrogen, 20: 1933
**SEGRE, Gino**, Sum rules for massive vector gauge fields, 20: 2783
**SEGUIN, Maurice**, General views about sample irradiations in reactors, 20: 2418 (CEA-R-2801)
**SENGAL, Bal Raj**, Intermediate resonance absorption in heterogeneous media including moderator scattering, 20: 2974
**SEIDEL, W.**, Dosimetry of high-energy electrons, 20: 2156
**SEIGLE, L.**, Diffusivity of carbon in tantalum and Nb carbides, 20: 2398
**SELENGUT, D. S.**, Higher order variational principles, 20: 2979
**SELENGUT, D. S.**, Numerical comparison of higher order variational principles, 20: 2980
**SELF, S. A.**, Numerical solution of collisionless plasma-sheath equation in cylindrical geometry, 20: 3168 (ML-1185)
**SELIG, Walter**, Some analytical methods for explosives and explosive simulants, 20: 3638 (UCRL-7873)
**SELIS, Sidney M.**, Thermodynamic properties of molybdenum(III) chloride in molten alkali metal chlorides, 20: 1882
**SELITSKII, Yu. A.**, Angular anisotropy of fission by sub-barrier deuterons, 20: 3122
**SELIVANOV, G. I.**, Analysis of $\pi^- + p \rightarrow \pi^- + \pi^+ + n$ and $\pi^- + p \rightarrow \pi^- + \pi^0 + p$ at 338 Mev, 20: 2682 (JINR-P-2320)
**SELLE, J. E.**, Internal friction at high temperatures and diffusion of vacancies between dislocations, 20: 3281(T) (ML-M-1276(tr))
**SELTZER, S. M.**, Results of recent transport calculations for electrons and bremsstrahlung, 20: 3246 (NASA-SP-71, pp 437-48)
**SEMAL, M.**, Isotopic effect of tritium in the form of tritiated thymidine on the activity of ATP, 20: 1583
**SEMAN, D. J.**, Considerations on annealing of irradiated pressure-vessel steel, 20: 2455
**SEREBRENNIKOV, V. V.**, Rare earth and thorium content in soils of Tomsk region, 20: 2065
**SERGEEV, A. G.**, Energies and relative intensities of 2201, 2490, and 2508 kev $\gamma$ lines in spectrum of $^{72}Ga$, 20: 3040
**SERGEEV, A. G.**, Investigation of $^{113m}In$ decay, 20: 3097
**SERGEEV, F. M.**, Production of slow $\pi$ mesons on light nuclei and the $\pi\sigma$ interaction, 20: 2739
**SERGEYEV, V. O.**, Decay of $^{149}Eu$, 20: 3075
**SERIN, B.**, Ginzburg-Landau parameters of type-II superconductors, 20: 2906
**SERPAN, C. Z. Jr.**, Prog. rpt. on irradiation effects on reactor structural materials, 11/64–1/65, 20: 2408 (AD-614899)
**SESHADRI, S. R.**, Propagation constant along a cylindrical antenna immersed in a warm plasma. I and II., 20: 2097 (AD-618396)
**SESHADRI, S. R.**, Radiation from electric dipole in infinite column of warm plasma, 20: 3161 (AD-618520)
**SESSIONS, C. E.**, Compatibility of some refractory alloys in flowing nonisothermal lithium, 20: 2238
**SESSIONS, R. T.**, Relative toxicity of angiographic contrast media, 20: 1724
**SETKINA, V. N.**, Isotopic exchange of hydrogen atoms in cyclopentadienyl rings of cobalticinium compounds, 20: 1828
**SETKINA, V. N.**, Replacement of a halogen by a proton in halogenoferrocenes, 20: 1830
**SEVASTYANOV, A. I.**, Investigation of radiation of $^{111}Cd$, 20: 3113
**SEVRYUKOVA, L. M.**, Effects of fast neutron irradiation on silicon electric properties during p-n transitions in fused diodes prepared with silicon base, 20: 2440
**SEWARD, F. D.**, X-ray spectra from Scorpius (SCO-XR-1) and the sun observed above the atmosphere, 20: 2585
**SEXL, Theodor**, Energy pool in magnetohydrodynamics, 20: 2823
**SHA, William T.**, A non-iterative nuclear-thermal interaction method, 20: 3500
**SHABAD, A. Yu.**, Coulomb Regge poles in quantum electrodynamics, 20: 2782
**SHABLYGIN, M. V.**, Formation of ordered PVC by radiation polymerization from the gas phase onto an ordered polymer film, 20: 1902
**SHAFFER, C. R.**, Effects of x irradiation on DNA of E. coli. An autoradiographic study, 20: 1639
**SHAFRANOV, V. D.**, Plasma confinement in toroidal magnetic field and with conducting diaphragm, 20: 3209
**SHAH, D.**, Interactive effects of x irradiation and barbiturates, 20: 1662
**SHAI, Isaac**, Prog. rpt. on effect of surface conditions on pool boiling heat transfer of Na, 3–10/65, 20: 2017 (TID-22312)
**SHALAMOV, Yu. Yu.**, Production of slow $\pi$ mesons on light nuclei and the $\pi\sigma$ interaction, 20: 2739
**SHAM, L. J.**, Self-consistent equations including exchange and correlation effects, 20: 3216
**SHANK, E. M.**, Eurochemic sampling system, 20: 1955 (NP-15403)
**SHANKAR, J.**, Extraction of thorium, protactinium, uranium, ruthenium, and zirconium by long-chain amines, 20: 1761
**SHANKER, R.**, Extraction of thorium, protactinium, uranium, ruthenium, and zirconium by long-chain amines, 20: 1761
**SHANKS, H. R.**, Thermal diffusivity of armco iron by three methods, 20: 3622 (IS-1266)
**SHANTAROVICH, V. P.**, Effect of complex formation on reactions between positronium and inorganic ions, 20: 1844
**SHAPIRO, I. S.**, Two-nucleon transfer in direct reactions, 20: 3121
**SHAPIRO, J. L.**, Design study of fission-electric cell reactor for space power, 20: 3577
**SHAPOSHNIKOVA, E. F.**, Strengths and polarities of magnetic fields of sunspots during IGY, 20: 2563
**SHAPOVAL, E. A.**, Critical fields of thin superconducting films, 20: 2926
**SHARAPOV, E. I.**, Radiation widths of intermediate nuclei, 20: 3133
**SHARKHATUNYAN, R. O.**, Ionization measurement in a streamer chamber, 20: 2128 (JINR-E-2324)
**SHARMA, N. K.**, Relativistic variational principle for a charged hydromagnetic compressible fluid, 20: 2829
**SHARMA, P. K.**, Dispersion of lattice waves in tungsten, 20: 3294
**SHARMA, R. P.**, X-ray yields from K-shell ionization by $\alpha$ particles, 20: 2625
**SHARMA, S. M.**, Economic method of obtaining photoscan, 20: 1705
**SHARMA, S. R.**, Relativistic variational principle for a charged hydromagnetic compressible fluid, 20: 2829
**SHARP, D. G.**, Effect of particle aggregation on survival of irradiated Vaccinia virus, 20: 1651
**SHARP, Rodman A.**, System design in low background internal gas sample counting of $^{14}C$ and tritium, 20: 2179
**SHARP, W. T.**, Racah algebra for an arbitrary group, 20: 2775
**SHAVTVALOV, L. Ya.**, Investigation of radiation of $^{111}Cd$, 20: 3113
**SHAWHAN, Stanley D.**, Method of determining $\alpha = n(H+)/n_e$ and ion temperature from measurement of proton-whistlers, 20: 2847 (AD-614716)
**SHCHEBOLEV, V. T.**, Method of small solid angle for measuring $\alpha$-particle flux, 20: 2147
**SHEIKO, I. N.**, Behavior of $ZrCl_2$ in molten mixtures of alkali and alkali earth metals, 20: 1822 (ANL-Trans-233)
**SHELDON, W. R.**, Fractional cell lethality approach to space radiation hazards, 20: 1616 (NASA-SP-71, pp 219-23)
**SHELEPIN, L. A.**, Theory of transformation matrices, 20: 2604
**SHELKOV, L. S.**, Efficiency of $^3H/Zr$ sources in nondispersive x-ray spectrometric analysis, 20: 2136
**SHEN, B. S. P.**, Some experimental data on nuclear cascade in thick absorbers, 20: 3015 (NASA-SP-71, pp 357-62)
**SHEN, L. Yun Lung**, Specific heat of superconducting transition metals, 20: 2905
**SHEPHERD, Allen D.**, Bulgur wafer and adjuncts for fallout shelter rations, 20: 2067 (AD-614824)
**SHEPPARD, C. W.**, Genetic effects of fast neutrons from nuclear detonations, 20: 1622 (WT-820)
**SHER, R.**, The use of integral activation techniques to experimentally determine $H_2O$–$H_3BO_3$ thermal-neutron spectra, 20: 2965
**SHERCLIFF, J. A.**, Demonstration of the Hartmann layer, 20: 2831
**SHERIDAN, J. R.**, Vibration and rotation of $N_2$ excited by 10- to 65-kev

ions, 20: 2618
**SHERMAN, Arthur,** Non-equilibrium ionization and magnetohydrodynamic flow phenomena, 20: 3233
**SHERMAN, L. E.,** On propagation of resonance neutrons in uranium, 20: 3031
**SHERRILL, F. A.,** X-ray topograph examination of vacancy clusters in nearly perfect copper crystals, 20: 3279 (ORNL-P-1704)
**SHESTAKOVA, I. A.,** Solubility of certain actinium compounds. I., 20: 1846
**SHESTAKOVA, I. A.,** Solubility of certain actinium compounds. II., 20: 1847
**SHESTOV, A. V.,** Possibility of stabilization of synchrocyclotron intensity, 20: 2536 (JINR-P-2341)
**SHETET, T.,** Account of the pulsed mode in intermediate memories, 20: 2101 (JINR-P-2319)
**SHEVCHENKO, A. P.,** Formation of polymers labeled with $^{14}C$ during ethylene-ammonia irradiated in nuclear reactor, 20: 1922
**SHEVELEV, A. S.,** Effect of transplantation of homologous hematopoietic cells on antibody synthesis in irradiated animals, 20: 1632
**SHEVTSOVA, Z. N.,** System $YCl_3$–NaCl–KCl, 20: 1872
**SHIBAEV, V. D.,** Account of the pulsed mode in intermediate memories, 20: 2101 (JINR-P-2319)
**SHIBANO, H.,** Radiation-induced liquid- and solid-phase polymerization of acetylene, 20: 1913
**SHIBAYAMA, Tetsuo,** Removal of iodine from atmosphere by spray. I., 20: 1966
**SHIELD, E.,** Polarization in p-$^4$He scattering between 27 and 63 Mev, 20: 3022 (UCRL-16216)
**SHIGA, M.,** Moessbauer effect of $^{57}Fe$ doped in $V_2O_3$, 20: 3289
**SHIMOTAKE, H.,** Static and dynamic corrosion by tin, bismuth, and bismuth–sodium alloy up to 1000°C, 20: 2275
**SHINJO, T.,** Moessbauer effect of $^{57}Fe$ doped in $V_2O_3$, 20: 3289
**SHIRANE, G.,** Neutron-diffraction study of antiferromagnetism in $UO_2$, 20: 3301
**SHIRLEY, D. A.,** Paramagnetic resonance of $^{57}Fe$ in polycrystalline ferrichrome A, 20: 3643 (UCRL-11685)
**SHON, O.,** Semi-automatic device for scanning and measuring spark chamber photographs, 20: 2130 (JINR-P-2340)
**SHOROSHEV, Yu. G.,** Application of complex emanation-thermal method for studying the KCl–$CaCl_2$ constitution diagram, 20: 1860
**SHOROSHEV, Yu. G.,** Application of complex emanation-thermal method in studies of the CaO–$Fe_2O_3$ constitution diagram, 20: 1861
**SHOSHEV, P.,** Wire spark chamber with external acoustic transducers, 20: 2132 (JINR-P-2368)
**SHOTKIN, Louis M.,** Autonomous power oscillations in reactors, 20: 3408
**SHUCK, A. B.,** Remote refabrication of reactor fuels, 20: 2282 (HW-SA-3755)
**SHUGUROV, V. K.,** Theory of the electromagnetic form factors in three-nucleon system, 20: 3119
**SHUINOV, Yu. N.,** Studies of startup conditions of I. V. Kurchatov Beloyarsk Nuclear Power Station performed at test rig, 20: 3486
**SHUKOVSKY, H. B.,** Microstructure and superconducting properties of 45 Nb–55 Zr alloy, 20: 2395
**SHULER, W. B.,** New measurement of lifetime of the positive pion, 20: 2714
**SHURE, F.,** Importance of space and energy effects in neutron-fluctuation experiments, 20: 3420
**SHURE, K.,** Few group and multigroup calculations of neutron penetration, 20: 2939 (WAPD-T-1710)
**SHUVALOV, O. N.,** Effects of salting-out agents on uranium and plutonium activity coefficients in nitric acid solutions, 20: 1967
**SHVARTSBURG, A. B.,** Theory of nonlinear interaction of waves in magneto-active anisotropic plasma, 20: 3230
**SHVETSOV, I. K.,** Neptunium(V) complexing ability, 20: 1848
**SIDLES, P. H.,** Thermal diffusivity of platinum, 20: 3621 (IS-1261)
**SIDORIV, I. V.,** $\pi^-$ meson-neutron elastic backward scattering at 1.4 to 4.0 Bev, 20: 2713
**SIDOROV, I. V.,** Elastic backward scattering of $\pi^-$ by neutrons, 20: 2700
**SIEGEL, R. T.,** New measurement of lifetime of the positive pion, 20: 2714
**SIEWERT, C. E.,** Exact solution of equations of radiative transfer, 20: 2731
**SIFFERT, P.,** New levels in $^{58}Co$, 20: 3077
**SIGMAN, Donald Ray,** Electron densities determined by measurement of Thomson scattering of laser light from plasma, 20: 3234
**SILINI, Giovanni,** Cyclic fluctuations in radiosensitivity of mice after exposure to sublethal whole-body irradiation, 20: 1685
**SILVERMAN, Joseph,** Absolute efficiencies and radiation damage in polycrystalline phosphors irradiated with high-energy electrons, 20: 2164
**SILVERMAN, Joseph,** Determination of Hg in wheat and tobacco leaf by neutron activation analysis, 20: 1755
**SILVERMAN, Joseph,** Radiation-induced polymerization of styrene at low temperatures, 20: 1925
**SILVERMAN, Joseph,** Semi-empirical equation for external bremsstrahlung yield from $\beta$ emitters, 20: 2730
**SILVERMAN, Leslie,** Performance of air cleaning system for U. S. Bureau of Mines Bomaec-30 incinerator, 20: 1989 (NYO-841-2)
**SILVERT, W.,** Surface states and high-temperature surface superconductivity, 20: 2903
**SIMEK, J.,** Effects of external irradiation of the heart on cardiac output, venous pressure and arterial pressure, 20: 1652
**SIMKINA, A. P.,** Specific heat of Gd near Curie point, 20: 2920
**SIMMONS, J. E.,** Measurement of $C_{NN}$ in neutron-proton scattering at 23 Mev, 20: 2685 (LA-DC-7250)
**SIMMONS, Richard L.,** Effect of allogeneic bone marrow on lethally irradiated thymectomized mice, 20: 1660
**SIMON, D.,** Approach to electron-pion scattering, 20: 2678 (AD-614843)
**SIMPSON, J. A.,** Tables of IGY cosmic ray data. I., 20: 2659
**SIMPSON, J. A.,** Tables of IGY cosmic ray data. II., 20: 2660
**SIMPSON, J. A.,** Tables of IGC cosmic ray data. III., 20: 2661
**SIMPSON, R. E.,** Response of lithium fluoride to reactor neutrons, 20: 2178
**SINCLAIR, D. A.,** Estimation of heating of plasma by lasers, 20: 3185 (TT-1193)
**SINGER, T.,** Prog. rpt. on reactor containment, 10/64–7/65, 20: 3324 (IITRI-578P21-13)
**SINGWI, K. S.,** Kohn anomaly and coherent scattering of slow neutrons in liquid metals, 20: 2948
**SINHA, Surendra N.,** Chromotrope 2B in photometric determination of rare earths, 20: 1772
**SIRAZHET, Kh.,** Radiation widths of intermediate nuclei, 20: 3133
**SKALSKI, Stanislaus,** Two problems in theory of superconductivity, 20: 2929
**SKAVARIL, Russell Vincent,** Effects of total-body irradiation of Mesocricetus auratus, 20: 1676
**SKAVDAHL, R. E.,** FFTF driver fuel—$PuO_2$ stainless-steel cermet, 20: 3588
**SKAVDAHL, R. E.,** Irradiation of $UO_2$–$PuO_2$ high-power-density fuel elements in PRTR, 20: 2449
**SKEEN, D. R.,** Criticality studies with plutonium solutions, 20: 3395
**SKELLY, David W.,** Ionic processes in $\gamma$-irradiated organic solids, 20: 1906
**SKISLAK, A. H.,** A ferromagnetic resonance magnetometer, 20: 2104 (MATT-362)
**SKOROBOGATOV, G. A.,** Formal kinetics of some competitive bimolecular reactions and calculation of kinetic isotope effect in distribution of isotopic molecules, 20: 1866
**SKOROVAROV, D. I.,** Extraction of U(VI) from carbonate solutions by quaternary phosphonium and arsonium bases, 20: 1782
**SKURIDIN, G. A.,** Principal hypotheses concerning origin of earth's radiation belts, 20: 2861
**SKVORTSOV, N. V.,** Extraction of U(VI) from carbonate solutions by quaternary phosphonium and arsonium bases, 20: 1782
**SKVORTZOVA, G. V.,** Devices for spectral-isotopic determination of gases in metals, 20: 1793
**SLAVNINA, T. P.,** Rare earth and thorium content in soils of Tomsk region, 20: 2065
**SLAVNOV, A. A.,** Solution of the Bethe-Salpeter equation in charged vector meson theory, 20: 2797
**SLAWECKI, M. A.,** Inert-atmosphere enclosure for environmental testing, 20: 2246
**SLICHTER, Charles P.,** Lectures on spin temperature, 20: 2864 (COO-1198-300)
**SLOBODRIAN, R. J.,** Polarization in p-$^4$He scattering between 27 and 63 Mev, 20: 3022 (UCRL-16216)
**SLOBODRIAN, R. J.,** Study of $^4He(p,d)^3He$ reaction with polarized protons at 55 and 63 Mev, 20: 3023 (UCRL-16218)
**SLONE, Hasel James Jr.,** The far infrared spectrum of $D_2O$, 20: 1877
**SMALLWOOD, K. L.,** Sunspot cycle and ionospheric storms, 20: 2848 (AD-615111)
**SMIRENKIN, G. N.,** Angular distribution of $^{238}U$ photofission fragments near fission threshold, 20: 3134
**SMIRNOV, B. M.,** Destruction of atomic particles by an electric field and by electron impact, 20: 2646
**SMIRNOV, V. I.,** Duty cycle improvement of particle beams at 680-Mev JINR synchrocyclotron, 20: 2548
**SMIRNOV, V. I.,** Kinetic energies of fragments with various masses in fission of $^{235}U$ by thermal and fast neutrons, 20: 3110
**SMIRNOV, Yu. F.,** Selection rules for nuclear reactions involving nucleon associations in SU(3) scheme, 20: 3117
**SMITH, C. K.,** 1.5 Mwe thermionic reactor space power system, 20: 3547 (NAA-SR-Memo-7581)
**SMITH, C. V.,** UNPACK. Neutron cross section data retrieval program, 20: 3009 (GA-6685)
**SMITH, David R.,** Neutronic isolation characteristics of concrete, lead, wood,

polyethylene and beryllium, 20: 3390
**SMITH, Gordon S.,** Crystal structure of tetramethyl ammonium hexahydroborate, 20: 2347 (UCRL-12146)
**SMITH, H. H.,** Mutations induced by ethyl methane-sulfonate in maize, 20: 1656
**SMITH, Harold P. Jr.,** Limitations to applicability of restricted space, time-optimal xenon shutdown problem, 20: 3410
**SMITH, J. P.,** Effect of neutron irradiation on hardness properties of tungsten and molybdenum, 20: 2457
**SMITH, J. P.,** Recovery of defects in neutron-irradiated tungsten, 20: 2475
**SMITH, Lloyd,** Design study for a 200-Bev accelerator facility, 20: 2543 (UCRL-16238)
**SMITH, M. L.,** Measurement of filter efficiency with condensation nuclei counter, 20: 3340
**SMITH, R. R.,** EBR-II self-excited oscillations, 20: 3514
**SMITH, R. R.,** EBR-II dynamics, 20: 3590
**SMITH, R. R.,** Fuel-element failure detection in EBR-II, 20: 3518
**SMITH, R. R.,** Monitoring reactor kinetics of EBR-II, 20: 3517
**SMITH, William R.,** Analysis of elastic and inelastic scattering of neutrons from $^{206}Pb$, $^{208}Pb$, and $^{209}Bi$ below 4.5 Mev, 20: 3021 (ORNL-TM-1238)
**SMOES, S.,** Thermodynamic study of the uranium–oxygen system by mass spectrometry. Heat of sublimation of uranium, 20: 1810 (EUR-2458.f)
**SMOLIN, V. N.,** Studies of startup conditions of I. V. Kurchatov Beloyarsk Nuclear Power Station performed at test rig, 20: 3486
**SMOOT, Perry R.,** Effect of deformation and heat treatment on mechanical properties of Ti–6Al–6V–2Sn–4Zr–1Fe–1Cu alloy, 20: 2309 (AD-615024)
**SMORODINSKII, J. A.,** Form factors and interaction constants for the 56-plet of the group SL(6), 20: 2803
**SNOW, G. A.,** Absorption time of $\Sigma^-$ hyperons in liquid hydrogen, 20: 2723
**SNYDER, B. J.,** Geometrical effects on efficiencies of well-type $\gamma$ scintillation detectors, 20: 2169
**SOBUE, H.,** Radiation-induced liquid- and solid-phase polymerization of acetylene, 20: 1913
**SOCHOR, Vaclav,** Microtron—an effective accelerator, 20: 2549
**SOFER, G. A.,** Plutonium production and burnup calculation methods for light water moderated reactors, 20: 3535
**SOFTLEY, Eric James,** Relativistic free molecule flow, 20: 2841
**SOKOLOV, A. A.,** Lepton annihilation of proton-antiproton pairs with allowance for form factors and polarization correlations, 20: 2696
**SOKOLOVA, G. K.,** Effect of uniform compression on Curie temperature of ferromagnetic compound EuO, 20: 3313
**SOLBRIG, A. W., Jr.,** Topics in nuclear reactor theory, 20: 3375 (IDO-17120)
**SOLDATOV, A. S.,** Angular distribution of $^{238}U$ photofission fragments near fission threshold, 20: 3134
**SOLOMON, Y.,** Development of photogrammetric techniques for measuring surface contours of small samples, 20: 2033
**SOLOV'EV, S. M.,** Angular anisotropy of fission by sub-barrier deuterons, 20: 3122
**SOLOV'EV, V. G.,** Binding energy anomalies for last two neutrons in region N = 86–92, 20: 3098
**SONDHAUS, Charles A.,** Effect of high-energy protons and $\alpha$ particles on small mammals, 20: 1614 (NASA-SP-71, pp 97-103)
**SONG, K. S.,** Effects of neutron and proton bombardments on the exciton spectrum of $Cu_2O$, 20: 2505
**SOOD, P. M.,** Spurious scattering in nuclear emulsions, 20: 2145
**SOSHKA, V.,** Energy spectra of scattered ions as influenced by crystal structure of the target, 20: 2600
**SOSO, F.,** Positive pion photoproduction with coherent bremsstrahlung, 20: 2718
**SOUCEK, B.,** Megachannel analyzers, 20: 2124 (BNL-9590)
**SOUCEK, Branko,** Application of pile-up distortion calculations, 20: 2160
**SOULEN, R.,** Metallic heat conductivity below 1°K, 20: 2383
**SOULIS, R.,** Local film coefficients of turbulence promoted ML-1-type fuel elements, 20: 2022
**SOUTHWOOD, J. R. M.,** Berkeley nuclear power station, 20: 3528
**SOVKA, J. A.,** Nondestructive analyses of irradiated MIT reactor fuel elements by $\gamma$ spectroscopy, 20: 2030
**SOWA, E. S.,** Development of small integral loop for in-pile fuel-failure studies in presence of flowing sodium, 20: 3347
**SOWINSKI, Mieczyslaw,** Semiconductor nuclear radiation detectors and their applications, 20: 2155
**SOXHLET, P.,** Effects of neutron and proton bombardments on the exciton spectrum of $Cu_2O$, 20: 2505
**SPALARIS, C. N.,** Radiation damage in Incoloy-800, 20: 2458
**SPANN, J. R.,** High-temperature properties of sodium, 20: 1815 (NRL-6241)
**SPANNER, J. C.,** Applications of eddy current testing at Battelle-Northwest, 20: 2025 (BNWL-SA-349)
**SPARROW, A. H.,** Effects of ionizing radiation on ecological systems, 20: 2080 (BNL-917, pp 20-38)
**SPARROW, A. H.,** Reproductive integrity in the stamen hair and root meristem of Tradescantia paludosa following acute $\gamma$ irradiation, 20: 1668
**SPARROW, Arnold H.,** Radiosensitivity of Marchantia thalli as related to nuclear and interphase chromosome volumes, 20: 1610 (BNL-9611)
**SPEICHER, B. R.,** Genetic segregation in unisexual wasp Devorgilla, 20: 1643
**SPEICHER, Kathryn G.,** Genetic segregation in unisexual wasp Devorgilla, 20: 1643
**SPEIS, T. P.,** Design and analysis of poison system for safe shipping NERVA reactor, 20: 3576
**SPENCER, Herta,** Removal of radioisotopes from man, 20: 1691
**SPERANSKII, N. M.,** Magnetic properties of Ni–Eu alloys, 20: 2369
**SPERNOL, A.,** Precise redetermination of $P_K\omega_K$ value and fluorescence yield of Cr, 20: 2593 (EUR-2524.e)
**SPEZHAKOVA, G. E.,** On the effect of $H_2^+$ excitation on the cross section for the ion-molecular reaction $H_2^+ + H_2 \rightarrow H_3^+ + H$, 20: 1843
**SPIEGLER, G.,** Image contrast and radiation protection: A figure of merit. I., 20: 1698
**SPIGHEL, M.,** Double charge exchange with negative pions. Search for tetraneutron, 20: 3080
**SPIGT, C. L.,** Analysis of boiling system dynamics, 20: 3532
**SPIJKERMAN, J. J.,** Absolute-velocity Moessbauer spectrometer, 20: 2113
**SPILLANTINI, P.,** Positive pion photoproduction with coherent bremsstrahlung, 20: 2718
**SPINRAD, R. J.,** Megachannel analyzers, 20: 2124 (BNL-9590)
**SPITZLI, P.,** Superconductivity in beryllium–rhenium system, 20: 2898
**SPOERL, Edward,** Glucose control of an x-radiation-induced difference in $CO_2$ production by yeast cells, 20: 1653
**SPRINGER, T. H.,** Doppler coefficients of fertile and refractory materials, 20: 2958
**SRINIVASAN, S.,** Radiation-induced polymerization of styrene at low temperatures, 20: 1925
**SRIVASTAVA, P. S.,** Technique using radioactive tracers for studies in physical oceanography, 20: 2061
**STAAS, F. A.,** New kind of transverse voltage in type II superconductor, 20: 2897
**STAB, L.,** New levels in $^{58}Co$, 20: 3077
**STAFFORD, G. H.,** Recent advances in elementary particle physics, 20: 2693
**STAHLHOFEN, W.,** Bibliography on radiation effects on living tissues and organisms, 20: 1607 (AED-C-04-18)
**STAHLHOFEN, W.,** Bibliography on radiation effects on living tissues and organisms, 20: 1608 (AED-C-04-19)
**STALINSKI, B.,** PMR studies of hydrogen diffusion in Nb–H system, 20: 2365
**STAMBLER, Irwin,** Power for deep space, 20: 3553
**STANEK, L. J.,** Method for calculation of core temperature following loss of coolant, 20: 3332
**STANFORD, G. S.,** Investigation of thermoluminescent dosimetry for measuring $\gamma$ heating in a critical assembly, 20: 2175
**STANFORD, G. S.,** Linear relationship between cadmium ratio and reactor core moderating ratio, 20: 3439
**STARBUCK, J. W.,** Effect of Soller slits on x-ray intensity in a diffractometer, 20: 2161
**STARIK, I. E.,** Behavior of polonium in ketones and mixed aqueous-acetone solutions, 20: 1946
**STARIK, I. E.,** Effects of ketones on polonium behavior in hydrochloric solutions, 20: 1777
**STARR, Victor P.,** Structure and energetics of large-scale hydromagnetic disturbances in the solar photosphere, 20: 2589
**STASEK, Vl,** Symptomatology of radiation-caused growth disturbances to vertebral column, 20: 1702
**STATHOPLOS, A.,** Performance optimization of fast-burst reactor core, 20: 3593
**STAVINSKII, V. S.,** Elastic $\pi^+$-p scattering at 180° and high energies, 20: 2683 (JINR-P-2327)
**STAVISSKII, Yu. Ya.,** On propagation of resonance neutrons in uranium, 20: 3031
**STECKI, J.,** Divergence of ternary scattering operator in two dimensions, 20: 2786
**STEDMAN, R.,** Observations on Fermi surface of aluminum by neutron spectrometry, 20: 3303
**STEELE, L. E.,** Prog. rpt. on irradiation effects on reactor structural materials, 2–4/65, 20: 2409 (AD-617319)
**STEELE, L. E.,** Prog. rpt. on irradiation effects on reactor structural materials, 11/64–1/65, 20: 2408 (AD-614899)
**STEIDL, H.,** Angular dependence of polarization of 3.5 ev electrons on free Hg atoms, 20: 2615
**STEIGERWALD, E. A.,** Prog. rpt. on creep of refractory alloys at elevated temperatures, 3/26–6/26/65, 20: 2333 (NASA-CR-54457)
**STEIN, R. S.,** Transmission of light by crystal aggregates between polarizers. II., 20: 3636 (TID-22319)

**STEIN, Richard S.,** Scattering of light by anisotropic discs with their principal polarizability direction at an angle to the radius, 20: 1817 (TID-22323)
**STEINDLER, M. J.,** Fluorination of $UO_2$–$PuO_2$ fission-product oxide pellets in a fluidized-bed reactor, 20: 1970
**STEINDLER, M. J.,** Laboratory investigations in support of fluid-bed fluoride volatility processes. VIII., 20: 2076 (ANL-7068)
**STEINITZ, R.,** Diffusivity of carbon in tantalum and Nb carbides, 20: 2398
**STEINKULLER, E. W.,** High-temperature properties of sodium, 20: 1815 (NRL-6241)
**STEINMAN, O.,** Calculation of pressure drop in ducts and fuel elements with shroud, 20: 2010 (IPV-19)
**STEKLER, Joan,** TRIST—tri-level multiprogramming executive involving real-time calculations and asynchronous on-line data source, 20: 3644 (UCRL-16199)
**STEKLY, Z. J. J.,** Magnetic radiation shielding using superconducting coils, 20: 3241 (NASA-SP-71, pp 199-209)
**STEKOL'NIKOV, V. V.,** The BN-350 (Fast Neutron) Atomic Power Station, 20: 3475 (NP-15458)
**STELSON, P. H.,** Gamma-ray energies determined with lithium-drifted germanium detector, 20: 3043
**STEPANOV, V. E.,** Strengths and polarities of magnetic fields of sunspots during IGY, 20: 2563
**STEPHANY, W.,** Fast reactor safety experiments on EBR-II samples in flowing sodium environment, 20: 3506
**STEPHEN, M. J.,** Theory of motion of vortices in superconductors, 20: 2908
**STEPHENSON, R. L.,** Comparative creep-rupture properties of D-43 and B-66 alloys, 20: 2336 (ORNL-P-1634)
**STEPHENSON, Thomas E.,** Quality factors for degraded proton spectra, 20: 3243 (NASA-SP-71, pp 229-34)
**STERNBERG, H. I.,** Comparison of analysis with experiment for Saxton plutonium critical experiments, 20: 3389
**STEUNENBERG, R. K.,** Preparation of metals by Mg–Zn reduction. III., 20: 2220 (ANL-7059)
**STEVENSON, C. E.,** Startup experience with the EBR-II fuel cycle facility. I., 20: 3522
**STEWARD, Palmer G.,** Results of computations of depth dose in tissue irradiated by protons, 20: 1620 (UCRL-16154)
**STEWART, D. C.,** Design of Argonne isotopic source neutron facility, 20: 2997
**STEWART, William M.,** Elastic and inelastic scattering of 40-Mev alpha particles from even tin isotopes, 20: 3017 (NASA-TN-D-3067)
**STEYN, J. J.,** Experimental differential number, energy and dose albedos for semi-infinite media, for normally-incident gamma radiation, 20: 3273
**STIEFEL, U.,** Temperature distribution and heat transfer in rod of bundle fuel element for nuclear reactors, 20: 3450
**STIRN, R. C.,** Use of adiabatic approximation in prompt-critical, large-core reactor-excursion analyses, 20: 3417
**STIRSKY, Pavel,** Automation in the first Czechoslovak nuclear power plant, 20: 3534
**STOECKER, W. C.,** Effect of Soller slits on x-ray intensity in a diffractometer, 20: 2161
**STONE, H. L.,** Effects of external irradiation of the heart on cardiac output, venous pressure and arterial pressure, 20: 1652
**STONE, J. P.,** High-temperature properties of sodium, 20: 1815 (NRL-6241)
**STONEHILL, D. L.,** Observation of a peak in $K^- + p \to \Lambda + \eta$ near threshold, 20: 2724
**STOREBOE, P. B.,** Particulate nuclear bomb debris as a meteorological tracer, 20: 2044 (NDRE-51)
**STORTI, George M.,** Transient effects in dielectric materials caused by electron irradiation, 20: 1897 (NASA-TN-D-3032)
**STRAHLE, Erwin,** Waterproof nuclear radiation screening substance, 20: 2248
**STRAIN, William H.,** Accumulation of radioactive fission products in hair, 20: 1695
**STRAKA, J.,** PARAMETRY II for calculation of physical parameters of gas cooled heavy-water reactor, 20: 3381 (UJV-1309b/65)
**STRASHININ, A. S.,** General reaction and radiation injuries in radiotherapy of patients with cervical carcinoma, 20: 1725
**STRATTON, K.,** Radiation-induced inactivation of ribonuclease, 20: 1682
**STRATTON, K.,** Radiation effects on free radical properties of melanin, 20: 1684
**STRAUMANN, N.,** Branching rules and Clebsch-Gordon series of semi-simple Lie algebras, 20: 2216
**STRAUSS, B.,** Repair of damage induced by uv light in Bacillus subtilis, 20: 1624
**STRAWBRIDGE, L. E.,** Xenon induced core instabilities, 20: 3383 (WCAP-3269-48)
**STRIEBEL, H. R.,** T(d,n)$^4$He reaction with polarized deuterons, 20: 3039
**STROHL, G. E.,** Total ionization in nitrogen by heavy ions of energies 25 to 50 kev, 20: 2623
**STROM, S. E.,** Temperature structure of early-type model stellar atmospheres. II., 20: 2564
**STRONGIN, M.,** Magnetic field penetration and breakdown of surface superconductivity. II., 20: 2900
**STROOT, J. P.,** Double charge exchange with negative pions. Search for tetraneutron, 20: 3080
**STRUTT, M. J. O.,** Spontaneous radiation-emission fluctuations of gas discharges and their measurement using a suitable radiation detector, 20: 2828
**STUART, Malcolm R.,** Evaluation of beginning-of-life measured and calculated reactivity characteristics of PWR core-2 seed-1, 20: 3502
**STUVE, J. M.,** Heat of formation of neodymium trichloride, 20: 1806 (BM-RI-6697)
**SUBBARAMAN, P. R.,** Ion exchange behaviour of U(VI) in aqueous sodium triphosphate and its separation from rare earths, 20: 1762
**SUBBA RAO, V. V.,** Calcination and sintering study of ceria, 20: 1832
**SUBBOTIN, V. I.,** Decontamination of sodium from products of reactions with water in the circulation loop, 20: 1960
**SUBOTOWITZ, Mieczyslaw,** Measurement of matrix elements for singly forbidden beta transitions, 20: 3090
**SUBRAMANYAN, V.,** Extraction of thorium, protactinium, uranium, ruthenium, and zirconium by long-chain amines, 20: 1761
**SUCHOZA, B. P.,** Shippingport atomic power station disposition of radioactive waste, 20: 3521
**SUELZLE, L. R.,** Inelastic electron scattering from alpha particle, 20: 3086
**SUGANO, Reiji,** Recently discovered resonant states in the meson family, 20: 2727
**SUGAR, Robert Louis,** Variational bounds for multichannel scattering, 20: 2815
**SUHR, Harold,** Absorption of blue solutions of europium and beryllium in liquid ammonia, 20: 1867
**SUICH, John E.,** Generalized equivalence principle for resonance integral calculations, 20: 2977
**SUICH, John E.,** Heterogeneous analysis by multigroup methods of epithermal reactions, 20: 2992
**SULC, P.,** PARAMETRY II for calculation of physical parameters of gas cooled heavy-water reactor, 20: 3381 (UJV-1309b/65)
**SUMBAEV, O. I.,** Experimental detection of isotopic shift of the molybdenum $K\alpha_1$ x-ray line, 20: 2641
**SUMITANI, Shozo,** Uranium ore refining plant, 20: 1964
**SUNAKAWA, Sigenobu,** Collective description of a system of interacting Bose particles, 20: 2792
**SUNDARSHAN, E. C. G.,** Group theory of the Kepler problem, 20: 2612
**SUNDERMAN, D. N.,** Fission-product behavior in fuel-element cladding materials, 20: 2389
**SUNDERMAN, D. N.,** Promethium-147 betavoltaic electrical power sources, 20: 2206
**SUNG, C. C.,** Specific heat of superconducting transition metals, 20: 2905
**SURINDAR, Singh,** Effect of ion gyration radius on magnetogravitational instability of infinite homogeneous medium, 20: 2885
**SUSOROVA, N. A.,** Determination of $^7$Be in samples of atmospheric aerosols and atmospheric precipitation in presence of fission fragments, 20: 1778
**SUSSKIND, Leonard,** Quantum mechanical approach to strong interactions, 20: 2816
**SUTALA, Veeinee,** Measurement of formation energy of electron-hole pair in n-type silicon, 20: 2362
**SUTTER, G.,** New levels in $^{58}$Co, 20: 3077
**SUVOROV, L. Ya.,** Search for anomalous hydrogen, 20: 2742
**SUVOROV, N. N.,** Action of protective agents following irradiation with sublethal doses, 20: 1688
**SVARCER, Vesna,** Exit doses for lung fields measured by LiF thermoluminescence, 20: 1699
**SVEC, Harry J.,** Electronics in mass spectrometry, 20: 2100 (IS-1193)
**SVIMONISHVILI, V. I.,** Plasma bremsstrahlung, 20: 3200
**SVIRSKII, M. S.,** Theory of s-f exchange for nonvanishing orbital momenta, 20: 2643
**SVISTUNOV, V. M.,** Interaction of alternating Josephson current with resonant modes in superconducting tunnel structure, 20: 2895
**SWAIN, A. D.,** Safety as a design feature in systems, 20: 2085 (SC-R-65-991)
**SWANSON, Kenneth MacGregor,** Improvements relating to radiographic examination, 20: 2034
**SWARTZ, Harold M.,** Long-lived radiation-induced electron spin resonances in an aqueous biological system, 20: 1605
**SWARTZ, J. M.,** High-sensitivity fast neutron dosimeter, 20: 2134 (TID-22335)
**SWEEDLER, A. R.,** Superconductivity of barium tungsten bronze, 20: 2901
**SWIECKI, M.,** Resonance Y* from self-consistency and broken unitary symmetry, 20: 2710
**SWIFT, Arthur R.,** Mixing of Regge poles and cuts in field-theory model, 20: 2768

**SWIFT, C. D.,** X-ray spectra from Scorpius (SCO-XR-1) and the sun observed above the atmosphere, 20: 2585
**SYCHEV, B. S.,** Shielding parameters of concretes, 20: 3253
**SYROMYATNIKOV, N. G.,** Determination of uranium in ores, 20: 1794
**SZABO, P.,** Neutron diffraction studies on $(1-x)Fe_2O_{3-x}Rh_2O_3$ system, 20: 3293
**SZKOPIAK, Z. C.,** Mechanism of strain-aging in commercially pure niobium, 20: 2376

# T

**TABATA, Y.,** Radiation-induced liquid- and solid-phase polymerization of acetylene, 20: 1913
**TABATA, Yoneho,** Radiation-induced copolymerization of tetrafluoroethylene with isobutene at low temperature, 20: 1915
**TABOADA, A.,** Corrosion studies in the NaK 78 type-316 stainless-steel Cb–1% Zr alloy system, 20: 2273
**TABUSSE, E.,** Space explorations and the radiation belts, 20: 2663
**TAEBEL, W. A.,** Recrystallization variables of flat-rolled molybdenum-cobalt alloys, 20: 2313 (AD-619208)
**TAKAHASHI, Isao,** Negative absorption of microwave radiation in weakly ionized xenon plasma in magnetic field, 20: 3204
**TAKAHASHI, Yasutaro,** Note on the four-particle scattering theory, 20: 2791
**TAKAKI, H.,** Moessbauer effect of $^{57}Fe$ doped in $V_2O_3$, 20: 3289
**TAKANAMI, M.,** Size of ribosomal site for messenger RNA binding, 20: 1592 (BNL-7903)
**TAKEBE, Masahiro,** Standard $\gamma$ irradiation facilities and measurements of dose rates distribution, 20: 1942
**TAKEMIYA, Toshinori,** Angular distribution of nucleons scattered from $^{14}N$, 20: 3091
**TAKENAKA, Eiji,** Striated column appearing in high-frequency gas discharge, 20: 3203
**TAKHTAMYSHEV, G. G.,** An experimental determination of $K_2^0 \rightarrow 2\pi$ decay probability in sloped $K_2^0$ beam, 20: 2865 (JINR-P-2325)
**TALBERT, W. L. Jr.,** Circular polarization measurements of gamma rays following the beta decay of $^{124}Sb$ and $^{134}Cs$, 20: 3051
**TALLMAN, C. R.,** Analytical model for study of thermocouple error attributed to electrical conduction in insulation, 20: 2103 (LA-DC-7055)
**TALVITIE, N. A.,** Radiochemical determination of $^{90}Sr$ in water using ion exchange, 20: 1754
**TALWAR, S. P.,** Two-stream instability in gravitating plasmas with magnetic field and rotation, 20: 3170 (NASA-TN-D-3052)
**TAMBURINO, L.,** Lorentz-covariant gravitational energy-momentum linkages, 20: 2882
**TANDON, J. N.,** Hydromagnetic stability of two superposed plasma columns with anisotropic pressure, 20: 3224
**TANUMA, Seiichi,** Thermal conductivity of superconducting and normal lanthanum, 20: 2893
**TAO, Wong-tyk,** Electromagnetic decays and the mass-splitting of vector mesons in unitary symmetry, 20: 2801
**TARAN, Yu. V.,** Dynamic polarization of protons in rotating lanthanum–magnesium nitrate crystal, 20: 3311
**TARBE DE ST. HARDOUIN, A.,** Central laboratory for hot chemistry at at KFA-Juelich, 20: 1996
**TASTE, Jean,** Results and interpretation of spectral indices measurements made with aquilon, 20: 3582 (CEA-R-2482)
**TATARONIS, J. A.,** Absolute instabilities of obliquely-propagating cyclotron harmonic plasma waves, 20: 3181 (SU-IPR-20)
**TAUB, J. M.,** Compatibility of refractory metals with solid solution (UC)(ZrC) at elevated temperatures, 20: 2332 (LA-3307)
**TAUSEND, A.,** Determination of chlorine and sodium in selenium by non-destructive neutron activation analysis, 20: 1769
**TAVKHELIDZE, A. N.,** Algebra of the currents and dispersion relations, 20: 2755 (JINR-E-2329)
**TAYLOR, C. A.,** High-energy electron (10–60 Mev) and proton (20–130 Mev) radiation damage in silicon and germanium, 20: 2517
**TAYLOR, Edward J.,** Evaluation of beginning-of-life measured and calculated reactivity characteristics of PWR core-2 seed-1, 20: 3502
**TAYLOR, J. B.,** End losses from theta pinch, 20: 3212
**TAYLOR, J. G.,** $\phi$ suppression in $K^-p$ reactions, 20: 2719
**TAYLOR, J. H.,** N. S. Savannah containment integrity—its measurement and improvement, 20: 3551 (TID-22316)
**TAYLOR, J. W.,** Quantitative reduction of data from high-speed stereoscopic photographs, 20: 3624 (LA-DC-7088)
**TAYLOR, Roderick,** Radiation shielding material, 20: 2301
**TEAS, H. J.,** Multipurpose $^{60}Co$ $\gamma$ irradiation facility, 20: 2193
**TEATS, R.,** High-temperature tensile testing machine for irradiated structural materials, 20: 2031
**TEICHMANN, Jiri,** Interaction between a field and a plasma, 20: 3207
**TEITEL, R. J.,** Determination of solubility of several transition metals in molten potassium, 20: 2237
**TELLIER, Henry, ALECTO—results obtained with homogeneous critical experiments on $^{239}Pu$, $^{235}U$ and $^{233}U$,** 20: 3369 (CEA-R-2814)
**TEMPERLEY, Archibald Angus,** Moessbauer effect in iron compounds with Marcasite type structure, 20: 3317
**TERA, Fouad,** Preconcentration of trace elements by precipitation ion exchange using organic-hydrochloric acid systems, 20: 1958
**TEREKHOVA, V. F.,** Magnetic properties of Ni–Eu alloys, 20: 2369
**TERUMICHI, Yasushi,** Negative absorption of microwave radiation in weakly ionized xenon plasma in magnetic field, 20: 3204
**TESLYUK, M. Yu.,** New compounds of $MgCu_2$ type in alloys of rare-earth metals with Fe, Co, and Ni, 20: 2385
**TESTONI, J.,** Elastic scattering of 27.5 Mev deuterons and its optical model analysis, 20: 3057
**TESTOV, V. G.,** Duty cycle improvement of particle beams at 680-Mev JINR synchrocyclotron, 20: 2548
**THEISON, Roger,** Improvements in or relating to niobium-coated uranium carbide articles, 20: 2300
**THEVENET, B.,** Observation of a peak in $K^- + p \rightarrow \Lambda + \eta$ near threshold, 20: 2724
**THIRUVENGADAM, A.,** On cavitation damage in liquid-metal pumps, 20: 2243
**THOMAS, E. D.,** Bone marrow transplantation in acute leukemia, 20: 1700
**THOMAS, J. T.,** Experimental and calculated system criticality, 20: 3378 (ORNL-P-1680)
**THOMAS, Martin R.,** Accumulation of radioactive fission products in hair, 20: 1695
**THOMASON, I. D.,** Sodium flame photometer test for high-efficiency filters, 20: 2077 (AWRE-O-41/65)
**THOME, Paul,** Apparatus for treating interior of a tubular element, 20: 2304
**THOMPSON, T. J.,** Reactor physics measurements in slightly enriched uranium $D_2O$ lattices, 20: 3397
**THOMPSON, T. J.,** Studies of subcritical lattices with distributed neutron absorber by means of pulsed-neutron source technique, 20: 3432
**THOMSON, D. B.,** Los Alamos flux compression program from its origin, 20: 3166 (LA-DC-7252)
**THOMSON, D. H.,** Radiation-induced inactivation of ribonuclease, 20: 1682
**THORNLEY, Margaret J.,** Fine structure of Micrococcus radiodurans, 20: 1584
**THOSAR, B. V.,** X-ray yields from K-shell ionization by $\alpha$ particles, 20: 2625
**THROWER, P. A.,** Nucleation of radiation damage in graphite, 20: 2447
**THRUN, E.,** Distribution of gaseous impurities and carbon transport in gas cooled atomic reactors, 20: 3327
**THURSTON, M. O.,** High-sensitivity fast neutron dosimeter, 20: 2134 (TID-22335)
**TIFFANY, O. L.,** Cosmic-ray shower production in manned space vehicles—copper, 20: 3240 (NASA-SP-71, pp 183-8)
**TIKHINSKII, G. F.,** Change of beryllium properties after aging treatment, 20: 2363
**TIKHOVA, N. M.,** Modification of magnesium alloys with zirconium and lanthanum, 20: 2399
**TILL, C. E.,** Doppler-effect measurements on dilute fast-carbide assembly, ZPR-6 assembly 4Z, 20: 2959
**TILL, C. E.,** Equipment and techniques for Doppler-effect measurements on fast critical assemblies, 20: 3401
**TIMASHEV, S. F.,** Two-nucleon transfer in direct reactions, 20: 3121
**TIMMINS, Tom H.,** Interpretation of radiolysis of terphenyls—apparent kinetics and fast-neutron effect, 20: 1927
**TINGEY, F. H.,** Nuclear safety and criticality control, 20: 2095
**TINLOT, J.,** Muon and antiproton trap at SLAC, 20: 2547 (UR-875-98)
**TIPPLES, K. H.,** Effects of high levels of $\gamma$ irradiation on lipids of wheat, 20: 1637
**TIRELLI, Sebastian,** Radiation crosslinking of nylon 66 and poly(vinyl alcohol), 20: 1909
**TIRSELL, Kenneth Glenn,** Circular polarization measurements of gamma rays following the beta decay of $^{124}Sb$ and $^{134}Cs$, 20: 3051
**TISHCHENKO, M. A.,** Extraction of rare earth amygdalate salts by butanol, 20: 1796
**TITTEL, Klaus,** Measurement of effective cross section for line broadening of h-f transitions in $6\,^3P_2$ state of mercury by sollisions with rare gas ions, 20: 2637
**TIXIER-VIDAL, Andree,** Autoradiography of incorporation of tritiated leucine, 20: 1597
**TJIN A DJIE, H. R. E.,** Optical model analysis of 26 Mev deuteron scattering, 20: 3053
**TKACHEV, L. G.,** Meson current in broken symmetry U(12) and experiments with colliding beams, 20: 2753 (JINR-P-2300)
**TOBARI, Izuo,** Genetic effects of x rays on population of Drosophila, 20: 1642
**TODD, Paul,** Biological effects of heavy ions, 20: 1615 (NASA-SP-71, pp 105-14)
**TODOROV, I. T.,** Mass formula in SU(12) contains $Sp(6) \times SU(2)$ symmetry,

20: 2756 (JINR-P-2342)
**TOKAREVA, L. G.,** Formation of ordered PVC by radiation polymerization from the gas phase onto an ordered polymer film, 20: 1902
**TOKARSKAYA, V. I.,** Role of systems orthophenols–orthoquinones in initial radiation-induced processes in an organism, 20: 1647
**TOLK, N.,** Direct detection of two-photon emission from metastable state of singly ionized helium, 20: 2630
**TOMASCH, W. J.,** Geometrical resonance in tunneling characteristics of superconducting Pb, 20: 2909
**TOMIMURA, K.,** Hot laboratory of Japan Atomic Energy Research Institute, 20: 1997
**TOMONTO, J. R.,** Plutonium production and burnup calculation methods for light water moderated reactors, 20: 3535
**TOMONTO, James R.,** Approximation to space-energy slowing down through use of multigroup thermal self-shielding factors in $PuO_2$–$UO_2$ lattice calculations, 20: 3426
**TOROPOVA, M. A.,** Certain polonium *n*-anisyl derivatives, 20: 1854
**TOROPOVA, M. A.,** Synthesis of some polonium α-naphthyl derivatives, 20: 1850
**TOTH, Arpad,** Radon measurements by scintillation methods, 20: 2152
**TOTH, L. E.,** Superconducting $H_c$-$J_c$ characteristics of nitrided Nb–Zr wire to 130 kOe, 20: 2891
**TOTH, Louis E.,** Superconductivity of the cubic modification of MoC, 20: 2346 (UCRL-11471)
**TOUGH, James Thomas,** Non-linear thermo-hydrodynamic of He(II) in wide channels, 20: 2928
**TRAECHSLIN, W.,** T(d,n)$^4$He reaction with polarized deuterons, 20: 3039
**TRAHEY, Nancy M.,** Post-irradiation chemical analysis of SNAP-8 experimental reactor coolant, 20: 3564
**TRAININ, L. Ya.,** Magnetic mirror trap for prolonged confinement of electrons, 20: 3225
**TRAMMELL, M. R.,** Analysis for correlating ground destruct tests with in-flight destruct of nuclear rockets, 20: 3575
**TRAVELLI, A.,** Criticality of bare slab of arbitrary size with anisotropic scattering, 20: 2986
**TRAVELLI, Armando,** Thermal neutron transients in Various order P-N approximations, 20: 3002
**TREGO, A. L.,** Magnetic form factor of chromium, 20: 3280 (ORNL-P-1737)
**TREHERNE, Jacqueline,** Isobaric-spin impurity in $^{170}$Lu ground state, 20: 3072
**TREVORROW, L. E.,** Laboratory investigations in support of fluid-bed fluoride volatility processes. VIII., 20: 2076 (ANL-7068)
**TRIEULE, Andre,** A method of fabrication of finned tubes and apparatus therefor, 20: 2303
**TRIMBLE, G. D.,** Fast-neutron spectra in paraffin shields, 20: 3257
**TRIMBLE, G. D.,** Fast-neutron spectra in liquid hydrogen, 20: 2967
**TRIPLETT, John R.,** Unified computational method for thermal-neutron scattering, 20: 3412
**TROFIMOV, A. M.,** Effects of gas macrocomponent on the distribution of $^{85}$Kr and $^{133}$Xe between gaseous phase and solid carbon sorbent, 20: 1969
**TROFIMOVA, A. M.,** Production and preparation of polymethylmethacrylate kryptonates, 20: 1862
**TROFIMOVA, G. M.,** Radiation polymerization of hexamethylcyclotrisiloxane in solid phase, 20: 1903
**TROFIMOVA, N. A.,** Total neutron cross sections of $^{185}$Re and $^{187}$Re, 20: 3030
**TROSTINA, K. A.,** Analysis of $\pi^-$ + p reactions, 20: 2690 (AEC-tr-6591)
**TROYANOV, M. F.,** The BN-350 (Fast Neutron) Atomic Power Station, 20: 3475 (NP-15458)
**TRUNOV, V. K.,** X-ray phase analysis of binary oxides in the $UO_2$–$MoO_2$–$MoO_3$ system, 20: 2384
**TRUSCELLO, Vincent C.,** Semi-empirical equation for external bremsstrahlung yield from β emitters, 20: 2730
**TSAREV, V. A.,** Analysis of reaction $\gamma + p \rightarrow K^+ + \Sigma^0$, 20: 2735
**TSETLIN, B. L.,** Formation of ordered PVC by radiation polymerization from the gas phase onto an ordered polymer film, 20: 1902
**TSIPENIUK, Yu. M.,** Angular distribution of $^{238}$U photofission fragments near fission threshold, 20: 3134
**TSUKAMOTO, Tetsuo,** Symmetry property of the S matrix on basis of the Jost function method, 20: 2790
**TSUYA, Hideki,** Superconducting properties of Fe–Sn superimposed films, 20: 2894
**TSVANKIN, D. Ya.,** Formation of ordered PVC by radiation polymerization from the gas phase onto an ordered polymer film, 20: 1902
**TSYTOVICH, V. N.,** Possibility of statistical acceleration of photons in turbulent plasma, 20: 3199
**TSYTOVICH, V. N.,** Theory of nonlinear interaction of waves in magneto-active anisotropic plasma, 20: 3230
**TUCKER, Charles T.,** Prog. rpt. on Hawaiian Run-Up program, 10/15/65, 20: 2058 (NVO-98-10)
**TULCZYJEW, W. M.,** Abstract formulation of quantum dynamics, 20: 2872
**TULCZYJEW, W. M.,** Abstract formulation of nonrelativistic quantum dynamics, 20: 2873
**TULINOV, A. F.,** One effect accompanying nuclear reactions in single crystals and its use in different physical investigations, 20: 3037
**TULINOV, A. F.,** The $^{12}$C(d,α)$^{10}$B reaction as a nucleon association replacement process, 20: 3106
**TUNITSKII, N. N.,** On the effect of $H_2^+$ excitation on the cross section for the ion-molecular reaction $H_2^+ + H_2 \rightarrow H_3^+ + H$, 20: 1843
**TURNER, Gary F.,** Beryllium radiator fabrication, 20: 2293
**TURNER, K. S.,** Fluid-bed fluoride volatility processing of irradiated fuels in hot cells, 20: 1971
**TURNER, P. P.,** Internal conversion BeO-base fuel element, 20: 2467
**TUTTLE, R. J.,** Doppler coefficients of fertile and refractory materials, 20: 2958
**TYLUTKI, N. J.,** Studies on monoclinic zirconium dioxide from room temperature to 1095°C, 20: 2314 (ARL-65-140)

## U

**UEDA, Hiroshi,** Preliminary design work of 2 Mw Na loop, 20: 3479 (NP-15556)
**UEMATSU, K.,** Direct substitute plutonium fuel for commercial water reactors, 20: 3511
**UGLIRZH,** Meson current in broken symmetry U(12) and experiments with colliding beams, 20: 2753 (JINR-P-2300)
**UHRIG, Robert E.,** Digital computer controlled data-acquisition and processing system for nuclear experiments, 20: 2996
**UHRIG, Robert E.,** Use of exponential cosine autocorrelation functions in processing nuclear-system test data, 20: 3342
**ULLMANN, J. W.,** Irradiation behavior of high-burnup $ThO_2$–4.45% $UO_2$ fuel rods, 20: 2429 (ORNL-3837)
**UNGER, B.,** Microwave absorption and magnetic transition in $GdCl_3$, 20: 3288
**UPSON, U. L.,** Fixation of high-level radioactive waste in phosphate glass, 20: 3606
**URRUTIA, Jose Luis,** Hydromagnetic stability of a liquid layer under the action of a magnetic field and a gravitational force, 20: 2820 (AD-614645)
**UTTERBACK, Nyle G.,** Charge-transfer excitation of (Co)$^+$ comet-tail bands by slow $N_2^+$ ions, 20: 2631
**UYEKI, Edwin M.,** Effect of x rays on hemolysin plaque forming cells, 20: 1661
**UYESUGI, G. S.,** Simultaneous assay of $^{90}$Sr and $^{90}$Y by liquid scintillation spectrometry, 20: 1766

## V

**VACHET, Pierre,** Improvements in beryllium–magnesium alloys, 20: 2277
**VAGINA, N. S.,** Solubility of yttrium and erbium phosphates, 20: 1873
**VALENTE, V.,** Positive pion photoproduction with coherent bremsstrahlung, 20: 2718
**VALENTIN, A.,** New Fontenay-aux-Roses α-β-γ radiometallurgy laboratory—design and construction, 20: 1999
**VALEVA, S. A.,** Mutants induced by ionizing radiations and ethyleneimine in winter wheat, 20: 1655
**VALLI, K.,** Half-life of $^{147}$Sm; comparison of ionization chamber and liquid scintillation results, 20: 3028
**VALLIER, J. C.,** Reestablishment of normal state in different superconducting alloys subjected to variable magnetic fields, 20: 2902
**VAN BOCKSTAEL, G.,** Main technical characteristics of graphite–gas and light boiling- or pressurized-water type plants, 20: 3322 (EUR-2448.f)
**VANCE, J. N.,** Aqueous radioactive waste treatment plant at Rocky Flats, 20: 1940 (RFP-638)
**VAN DER EIJK, W.,** Precise redetermination of $P_K\omega_K$ value and fluorescence yield of Cr, 20: 2593 (EUR-2524.e)
**VANDERMEER, R. A.,** Grain boundary migration, 20: 3626 (ORNL-P-1722)
**VAN DER STRICHT, E.,** Environmental radioactivity, Ispra 1964, 20: 2047 (EUR-2509.e)
**VANDERVELDE, V. D.,** Buckling measurements by successive substitution in subcritical assembly, 20: 3399
**VANDERVOORT, Peter O.,** Prog. rpt. on expansion of H(II) regions, final, 10/63–12/64, 20: 2562 (AD-614715)
**VANDERVOORT, Peter O.,** Properties of non-stationary ionization fronts. I., 20: 2571
**VANDERVOORT, Peter O.,** Properties of non-stationary ionization fronts. II., 20: 2572
**VANDERVOORT, Richard R.,** High-temperature plastic deformation of polycrystalline BeO, 20: 2371
**VANDEVYVER, M.,** Effects of fast neutrons on the thermal conductivity of silicon, 20: 2487
**VAN GERVEN, Lieven,** Conference on nuclear magnetic resonance, Leuven, 9/64, 20: 3316
**VAN HAGAN, Thomas H.,** SNAP-50/SPUR boiler development, 20: 3554
**VANINBROUKX, R.,** Precise redetermination of $P_K\omega_K$ value and fluorescence

yield of Cr, 20: 2593 (EUR-2524.e)
VAN LINT, V. A. J., Carrier lifetime studies in high-energy electron-irradiated silicon, 20: 2518
VAN NIFTRIK, G. J. C., Backward scattering of alpha particles by $^{16}O$ at medium energies, 20: 3056
VAN NOOIJEN, B., Conversion coefficient measurements employing magnetic and solid-state spectrometers, 20: 3019 (ORNL-P-1657)
VAN OERS, W. T. H., Backward scattering of alpha particles by $^{16}O$ at medium energies, 20: 3056
VAN STEENBERGEN, A., Evaluation of phase-space density measurement techniques, 20: 2534 (BNL-9587)
VARDYA, M. S., Pressure dissociation and molecular hydrogen, 20: 2610
VARGA, Dezsoe, Semiconductor particle detectors, 20: 2138
VARGA, Jozsef, Gamma-initiated polymerization of N-vinylsuccinimide in the liquid phase, 20: 1912
VARGAFTIK, N. B., Thermal conductivity of helium at temperatures 0 to 1000°C and pressures 1 to 200 atm, 20: 1824
VARGO, E. J., Material resistance to mercury corrosion, 20: 2264
VASIL'EV, A. N., Characteristic of the generalized free field, 20: 2812
VASIL'EV, S. S., Investigation of radiation of $^{113}Cd$, 20: 3113
VASSILIOU, Basil Emmanuel, Radiation shielding material, 20: 2301
VAUGHAN, R. D., Bradwell nuclear power station, 20: 3527
VAUGOYEAU, Henri, System uranium–uranium monocarbide, 20: 2366
VAVILOV, V. S., Interaction of radiation defects with impurities and other defects in semiconductors, 20: 2491
VDOVENKO, V. M., Investigation of Ru(IV) solutions in perchloric and sulfuric acids, 20: 1853
VDOVENKO, V. M., Physico-chemical studies of some Ra compounds. I., 20: 1852
VEAZEY, Sidney Edwin, Rotational spectroscopy of alkali fluorides, 20: 1876
VELLETRI, J., Attenuation of radiation from finite plane source by horizontal concrete slabs, 20: 3271
VENERUS, Ernest R., Theoretical investigations of fission-product deposition from flowing gas streams, 20: 3344
VENINGA, T. S., X-ray reactions with regard to chemoprotection. X., 20: 1646
VENKATESWARLU, K. S., Extraction of thorium, protactinium, uranium, ruthenium, and zirconium by long-chain amines, 20: 1761
VERBINSKI, V. V., Fast-neutron scattering from small cylinders of steel, aluminum, graphite, concrete and lithium hydride, 20: 3265
VERDONE, M., Neutron and gamma irradiations of indium antimonide at 70°K. Annealing of defects, 20: 2500
VERHEUGEN, A. H. J., Analysis of boiling system dynamics, 20: 3532
VERKHOVSKII, B. I., Efficiency of $^{3}H/Zr$ sources in nondispersive x-ray spectrometric analysis, 20: 2136
VERRIERE, Philippe, ALECTO—results obtained with homogeneous critical experiments on $^{239}Pu$, $^{235}U$ and $^{233}U$, 20: 3369 (CEA-R-2814)
VERTEBNYI, V. P., Total neutron cross sections of $^{185}Re$ and $^{187}Re$, 20: 3030
VERTUT, Jean, Device for the transmission of movements and application of said device to remote-handling appliances, 20: 2004
VESELKINA, M. N., Quantitative analysis of DNA in cells of the corneal epithelium in rats irradiated with x rays, 20: 1633
VESELOVSKII, G. S., Production of slow $\pi$ mesons on light nuclei and the $\pi\pi$ interaction, 20: 2739
VESELY, Vladimir, Plasma-jet gun, 20: 2251
VESNA, V. A., Investigation of $^{116*}In$ decay, 20: 3097
VETTE, James I., Updating and dissemination of knowledge of trapped radiation—model environments, 20: 2654 (NASA-SP-71, pp 47-55)
VICHEK, I., Discovery of damage in uranium fuel elements in nonactive test in $CO_2$, 20: 1748 (UJV-1369/65)
VICKERS, Anthony A., Restriction of obstetric radiology, 20: 1689
VIDELA, Gerardo J., Preparative chromatograph of moving-gas phases, 20: 1886 (CONF-641123-1)
VIEHBOECK, F. P., Numerical method for calculation of image aberrations of inhomogeneous magnetic sector fields between conical pole faces, 20: 2209 (SGAE-PH-26/1965)
VILLARS, Felix M. H., Elementary quantum theory of nuclear collective rotation, 20: 3048
VITMAN, V. D., Determination of intensities and multipolarities in high-energy $^{182}Ta$ decay $\gamma$ transitions, 20: 3112
VITMAN, V. D., Energies and relative intensities of 2201, 2490, and 2508 kev $\gamma$ lines in spectrum of $^{72}Ga$, 20: 3040
VITTORIO, P. V., Effect of damage on cell conductivity in electronic cell size distribution, 20: 1636
VIZBARAITE, Ya. I., Two-electron matrix elements of spin-spin interaction energy operator, 20: 2605
VIZBARAITE, Ya. I., Two-electron matrix elements of spin-orbit interaction energy operator, 20: 2606
VLASOV, A. N., Stepwise excitation of fluorescence of $CaWO_4$ activated with $Er^{3+}$, 20: 1842
VLASOV, A. V., Formation of ordered PVC by radiation polymerization from the gas phase onto an ordered polymer film, 20: 1902
VLASOV, M. F., Total neutron cross sections of $^{185}Re$ and $^{187}Re$, 20: 3030
VOGT, Gleada S., Age related changes in hematological and serum biochemical parameters in miniature swine, 20: 1581 (BNWL-SA-341)
VOGT, J. R., Automated system for rapid and precise fast neutron activation analysis, 20: 1765
VOINOVA, N. A., Determination of intensities and multipolarities in high-energy $^{182}Ta$ decay $\gamma$ transitions, 20: 3112
VOINOVA, N. A., Investigation of $^{116*}In$ decay, 20: 3097
VOLKOV, M. K., Investigation of infrared singularities in cross sections by functional integration method, 20: 2754 (JINR-P-2309)
VOLKOVYSKII, P. Yu., Sensitivity of scintillation method in $\gamma$ defectoscopy, 20: 2027
VOLTA, G., TESI—advanced power excursion reactor for research in reactor safety, 20: 3584 (EUR-2433.e)
VON BRAUN, Wernher, Man-made radiations in space, 20: 2652 (NASA-SP-71, pp 1-4)
VON BUTTLAR, H., Yield of $(\gamma,t)$ reaction in oxygen with 50-Mev Bremsstrahlung, 20: 3126
VONDRA, B. L., Development of $ThO_2$–pellet fabrication, 20: 2291
VONDRA, Benedict L. Jr., Method of dissolving ceramics containing beryllia, 20: 2252
VON EHRENSTEIN, D., Proposal for source of completely polarized deuterons, 20: 2528
VON SONNTAG, C., Energy transfer in $\gamma$ radiolysis of the benzene–benzophenone–isopropanol system, 20: 1931
VONSOVSKII, S. V., Theory of s-f exchange for nonvanishing orbital momenta, 20: 2643
VON WANGENHEIM, K. H., Electron microscopic study on development of normal and x-irradiated cells of wheat embryos, 20: 1666
VOOK, F. L., Structural properties of defects in semiconductors, 20: 2486
VOROBIEV, A. M., Determination of $^{233}Pa$ in the air, 20: 1759
VORONEL, A. V., Specific heat of Gd near Curie point, 20: 2920
VORTMAN, Luke J., Isthmian canal studies, 1964, 20: 1985 (PNE-2003)
VOTA, A. V., WIGL2. A program for the solution of the one-dimensional, two-group, space-time diffusion equations accounting for temperature, xenon, and control feedback, 20: 3382 (WAPD-TM-532)
VOVENKO, A. S., Elastic $\pi^+$ -p scattering at 180° and high energies, 20: 2683 (JINR-P-2327)
VROOM, D. A., Photoelectron spectroscopy with a spherical analyzer. Vibrational energy levels of $H_2^+$, 20: 2633
VYALOV, G. N., Acceleration of particles with variables charges in an electrostatic field, 20: 2561

# W

WADE, David C., Conditions for probabilistic boundedness of reactors with random macroscopic cross sections, 20: 3404
WADMAN, William W., Shielding attenuation of neutrons from 80-Mev $\alpha$-particle bombardment of Ta, 20: 2554
WAECHTER, K. H., Shielding for radioisotope bremsstrahlung sources $^{90}Sr$ + $^{90}Y$, 20: 3254
WAGNER, E. B., Application of the generalized concept of dosimetry to space radiations, 20: 2133 (NASA-SP-71, pp 245-50)
WAGNER, Paul R., Absolute counting with well-type scintillation detectors, 20: 2170
WAGNER, R. J., Analytical model for predicting pressure-temperature history within containment vessel in response to loss-of-coolant accident, 20: 3337
WAHL, H., Interaction of krypton with uranium oxide surfaces, 20: 1813 (EUR-2515.e)
WAHLGREN, M. A., Design of Argonne isotopic source neutron facility, 20: 2997
WAIDE, C. H., Chemonuclear loop removal from BGRR using semi-remote cutting technique, 20: 3599
WAINERDI, Richard E., Improved model for least-squares analysis of $\gamma$ spectra in activation analysis, 20: 1787
WAINERDI, Richard E., Pulse-shape discrimination technique for dual-crystal Compton reduction detector, 20: 2167
WAITE, R. J., Radiolytic reaction between graphite and carbon dioxide. VI., 20: 1895 (AERE-R-4988)
WALDMAN, L. A., Fatigue and burst tests on irradiated in-pile stainless steel pressure tubes, 20: 2435 (WAPD-T-1720)
WALKER, D. G., X-ray line broadening in neutron-irradiated magnesium oxide, 20: 2445
WALKER, V. A., Controlled irradiation testing of uranium–aluminum fuels for the Advanced Test Reactor, 20: 2465
WALL, James A., Radiation facility support and solid-state studies, 20: 2531 (AD-618304)
WALLERSTEIN, George, Lithium isotope ratio in two Hyades F stars, 20: 2577
WALSH, Patrick N., Prog. rpt. on behavior of solid materials in high-temperature environments, 7–9/65, 20: 2261 (UCRI-326)

**WALTER, C. M.**, Compatibility of commercial cladding alloys with improved metallic fast reactor fuels, 20: 2229
**WALTER, C. M.**, Improved metallic fast power breeder fuels, 20: 2386
**WALTHERT, A.**, Use of coincidence method for determination of total conversion coefficients, 20: 3038
**WAMBOLD, J. C.**, Analog model of wave propagation in open-end cylinder. Phase I of investigation in analog study of impact fracture of closed-end cylinders, 20: 3630 (SC-DC-65-1697)
**WANDERS, G.**, Sum rules for $\pi^0$-$\sigma^0$ scattering, 20: 2709
**WAPSTRA, A. H.**, Determination of conversion coefficient in $^{170}$Yb with scintillation methods, 20: 3155
**WARCH, Kenneth L.**, Direct reaction analysis of $^{15}N(p,\alpha_0)^{12}C$ reaction, 20: 3061
**WARRINGTON, James A.**, CURFIT. Curve fitting program, 20: 2214 (KAPL-M-6483)
**WARWICK, Constance S.**, Solar-flare frequency and observing-time patterns, 20: 2575
**WASA, Kiyotaka**, Discharges between coaxial cylinders in magnetic field, 20: 3202
**WASHBURN, D. F.**, Primary and secondary recrystallization of alpha Zircaloy-4, 20: 2330 (KAPL-3091)
**WASHBURN, D. F.**, Primary and secondary recrystallization of beta-quenched Zircaloy-4, 20: 2331 (KAPL-3103)
**WASSERMANN, Eberhard**, Superconducting lead films with additions of transition metals and their oxides, 20: 2916
**WATABE, Mitsuo**, Remark on kinetic equation in unstable plasma, 20: 3220
**WATKINS, G. D.**, Review of EPR studies in irradiated silicon, 20: 2490
**WATSON, H. E.**, Prog. rpt. on irradiation effects on reactor structural materials, 2–4/65, 20: 2409 (AD-617319)
**WATSON, H. E.**, Prog. rpt. on irradiation effects on reactor structural materials, 11/64–1/65, 20: 2408 (AD-614899)
**WATSON, Peter G.**, Techniques of magnetic-field measurement, 20: 2105 (UCRL-16357(Rev.))
**WATSON, R. W.**, Electronic band structure and optical properties of rare-earth metals, 20: 2592 (BNL-9556)
**WATSON-MUNRO, C. N.**, Experimental studies of J × B ionizing fronts propagation over pressure range 10 to 800 millitorr, 20: 3177 (NP-15570)
**WATTS, E. C.**, High-temperature tensile testing machine for irradiated structural materials, 20: 2031
**WEBB, F. J.**, Cooperative modes of motion in simple liquids, 20: 2837
**WEBER, D.**, Channeling of 13-kev $D^+$ ions in gold crystals, 20: 2616
**WEBER, Evelyn J.**, Detection of phospholipids on paper chromatograms by neutron activation, 20: 1771
**WEBER, J. N.**, Systematic relationships between carbon and oxygen isotopes in carbonates deposited by modern corals and algae, 20: 1591
**WEBER, T. A.**, Time-dependent perturbation theory, 20: 2776
**WEEKS, R. J.**, Operational performance, 20: 3531
**WEIDENBAUM, B.**, New evidence to delineate the $UO_2$ molten boundary, 20: 2392
**WEIGEL, F.**, Mixed systems of lanthanide and actinide elements. III., 20: 2379
**WEIGMANN, H.**, Delayed neutrons in decay of $^9$Li, 20: 3130
**WEIL, Louis**, Improvements in or relating to irradiation enclosures for swimming pool type reactors, 20: 3602
**WEILL, G.**, Effect of fast neutron irradiation on thermal conductivity of ternary arsenides, 20: 2488
**WEIR, J. R.**, Post-irradiation stress-strain behavior of stainless steel, 20: 2477
**WEIR, J. R. Jr.**, Irradiation effects in stainless steels at high temperatures, 20: 2430 (ORNL-P-1713)
**WEISS, Francis Joseph**, Nuclear notations, 20: 3096
**WEISS, H.**, Low-level device for measurement of high-energy $\beta$-radioactive gases, 20: 2139
**WEISS, H.**, Operation of halogen-filled G-M counters up to high $\gamma$ dose rates, 20: 2140
**WELCH, A. D.**, Effects of 1-$\beta$-D-arabinofuranosylcytosine hydrochloride on regenerating bone marrow, 20: 1687
**WELCH, J. Eddie**, Moving picture computer output, 20: 2011 (LA-DC-7189)
**WELEFF, W.**, Radiation effects on materials at liquid-hydrogen temperature, 20: 2459
**WELEFF, W.**, Remotely operated test equipment for materials testing in combined cryogenic and nuclear radiation environment, 20: 2032
**WELSH, R. E.**, New measurement of lifetime of the positive pion, 20: 2714
**WELT, M. A.**, Measurement of neutron-flux spectra using Fermi chopper, 20: 2994
**WEMPLE, B. D.**, Operating experience with the KAPL Radioactive Materials Lab. metallography facility, 20: 2247
**WENSEL, A.**, Optical properties of $TlO_2$ as reflector for plastic scintillators, 20: 2327 (IKF-12)
**WENTZ, L. B.**, Fixed-volume experiments on transient thermal pressure production in water, 20: 3338
**WENZEL, W. A.**, Improved Bevatron and its performance at high intensity, 20: 2541 (UCRL-16228)
**WERNER, M. M.**, Radiobiology of yeast, 20: 1663
**WERTHAMER, N. R.**, Calculations of sound velocities in crystalline helium at zero temperature, 20: 2912
**WESSEL, E. T.**, Embrittlement of irradiated pressure vessel steels. I., 20: 2436 (WERL-8844-4)
**WESSEL, E. T.**, Sensitivity to irradiation damage—pressure vessel steels. III., 20: 2437 (WERL-8844-6)
**WESSON, J. A.**, End losses from theta pinch, 20: 3212
**WEST, D. L.**, Use of adiabatic approximation in prompt-critical, large-core reactor-excursion analyses, 20: 3417
**WEST, David L.**, Process-scale separation of hydrogen isotopes by gas chromatography, 20: 1733 (DP-979)
**WEST, J. M.**, BONUS reactor-operating performance, 20: 3520
**WESTERN, G. T.**, Interactions of 14.6-Mev neutrons in iron, $^7$Li, and carbon, 20: 2962
**WESTFALL, W.**, Colloidal properties of plutonium in dilute aqueous solution, 20: 1835
**WESTHEAD, J. M.**, Computer alarm, monitoring, logging, and analysis system for Oldbury, 20: 3490
**WESTRUM, Edgar F. Jr.**, American Documentation Institute Document No. 0000. Supplementing: "The system tetramethylmethane–tetrachloromethane. Thermodynamics of mixing in the plastically crystalline region." and "heat capacities and thermodynamic properties of globular molecules. XV., 20: 3620 (COO-1149-27)
**WESTRUM, Edgar F. Jr.**, Heat capacities and thermodynamic properties of globular molecules. XIII., 20: 3616 (COO-1149-22)
**WESTRUM, Edgar F. Jr.**, Heat capacities and thermodynamic properties of globular molecules. XIV., 20: 3617 (COO-1149-23)
**WESTRUM, Edgar F. Jr.**, Heat capacities and thermodynamic properties of globular molecules. XV., 20: 3619 (COO-1149-26)
**WESTRUM, Edgar F. Jr.**, Heat capacity and thermodynamic properties of $ZrF_4$ from 5 to 307°K, 20: 1809 (COO-1149-30)
**WESTRUM, Edgar F. Jr.**, System tetramethylmethane–tetrachloromethane. Thermodynamics of mixing in plastically crystalline region, 20: 3618 (COO-1149-25)
**WESTRUM, Edgar F. Jr.**, 2-Methylfuran: heat capacity and thermodynamic properties from 5 to 350°K, 20: 3615 (COO-1149-17)
**WESTRUM, Edgar F. Jr.**, 2,5-Dimethylthiophene, heat capacities and thermodynamic properties from 5 to 300°K and fusion of stable and metastable phases, 20: 3614 (COO-1149-16)
**WETH, George**, Fixation of high-level radioactive waste in phosphate glass, 20: 3606
**WETHERELL, A. M.**, Real part of proton-neutron scattering amplitude at 19.3 Bev, 20: 2712
**WHAN, Glenn A.**, Effect of sample geometry on decay-constant measurements in water using pulsed-neutron technique, 20: 2952
**WHIPPMANN, M. L.**, Branching rules for simple Lie groups, 20: 2769
**WHITE, Clayton S.**, Biological tolerance to air blast and related biomedical criteria, 20: 2083 (CEX-65.4)
**WHITE, David Parker**, Existence of electromagnetic surface waves on planar plasma slab with finite transverse magnetic field, 20: 3231
**WHITE, Howard S.**, TRIST—tri-level multiprogramming executive involving real-time calculations and asynchronous on-line data source, 20: 3644 (UCRL-16199)
**WHITE, J. D.**, Neutron interaction between multiplying media separated by various materials, 20: 3391
**WHITE, J. L.**, Prog. rpt. on advanced, graphite-matrix, dispersion-type fuel systems and research on graphite, 7/15–11/14/64, 20: 2318 (GA-5918 (Pt. 1))
**WHITE, J. R.**, Calculational checks of plutonium cross sections by comparison with critical-assembly results, 20: 3394
**WHITE, J. S.**, Tensile properties of plutonium–gallium alloys at 20 to 100°C, 20: 2378
**WHITE, R.**, Mass formulae in U(6) ⊗ U(6) theory, 20: 2752 (IC/65/77)
**WHITESIDE, H.**, Absorption time of $\Sigma^-$ hyperons in liquid hydrogen, 20: 2723
**WHITFIELD, J. F.**, Feasibility of new procedure for biological dosimetry, 20: 1612 (EUR-2505.e)
**WHITLEY, Joseph E.**, Demonstration of extracranial neoplasms with $^{99m}$Tc pertechnetate, 20: 1712
**WHITLOW, W. H.**, Effect of Y on oxidation resistance of Fe–Cr base alloys, 20: 2263
**WHITTEMORE, W. L.**, Scattering of neutrons by polyethylene, 20: 2964
**WHITTUM, H. O.**, ML-1 shield study, 20: 3525
**WICHNER, R. P.**, Acoustic instrument for measuring subcooling in boiling systems, 20: 2014 (ORNL-P-1678)
**WICHNER, R. P.**, Pressure drop with forced-convection boiling of potassium, 20: 2015 (ORNL-P-1681)
**WICKMAN, H. Hollis**, Paramagnetic resonance of $^{57}$Fe in polycrystalline ferrichrome A, 20: 3643 (UCRL-11685)
**WIDEROE, R.**, Patient dosimetry in x-ray diagnosis, 20: 1704
**WIECZOREK, L. W.**, Plasma effects, multiplication and secondary emission

of anomalous hydrogen glow discharges, 20: 2826
**VIEDEMANN, K.**, Telecommunication equipment of the nuclear research establishment at Juelich, 20: 2111
**WIEDER, H.**, Cross section of spin exchange between $^{85}Rb$ and $^{87}Rb$, 20: 2613
**WIGHALL, J. W. G.**, Effect of radiation damage on 23.8 kev Moessbauer transition in $^{119}Sn$, 20: 3075
**WILCOX, B. A.**, Effect of strain rate on dislocation multiplication in polycrystalline molybdenum, 20: 3286
**WILDIN, Maurice W.**, Heat transfer and temperature distribution in finned radiators, 20: 2016 (SC-DC-65-1765)
**WILENSKY, S.**, Experimental investigations of fast-neutron decay times in lead assemblies, 20: 2950
**WILEY, R. C.**, Effects of alloying upon certain properties of 55.1 Nitinol, 20: 2310 (AD-618681)
**WILIP, Elmer K.**, Behavior of $ZrCl_2$ in molten mixtures of alkali and alkali earth metals, 20: 1822 (ANL-Trans-233)
**WILLERS, G.**, Determination of chlorine and sodium in selenium by nondestructive neutron activation analysis, 20: 1769
**WILLIAMS, A.**, Relative time distribution of pulses in $4\pi$ $\beta$-$\gamma$ coincidence technique, 20: 2146
**WILLIAMS, D. D.**, High-temperature properties of sodium, 20: 1815 (NRL-6241)
**WILLIAMS, Geoffrey Milson John**, Improvements in concrete pressure vessels, 20: 3349
**WILLIAMS, Geoffrey Milson John**, Improvements in concrete pressure vessels, 20: 3350
**WILLIAMS, J. E. C.**, Minimum propagating current of composite superconductor, 20: 2904
**WILLIAMS, J. R.**, Interactions of 14.6-Mev neutrons in iron, $^{7}Li$, and carbon, 20: 2962
**WILLIAMS, W. Jones**, Effect of radiation on nuclear phosphorylation in human malignant tumors, 20: 1626
**WILLIAMSON, H. E.**, Fuel performance in boiling-water reactors, 20: 3497
**WILLIAMSON, Marvin M.**, Isthmian canal studies, 1964, 20: 1983 (PNE-2000)
**WILLIAMSON, S. J.**, de Haas-van Alphen effect in pyrolytic and single-crystal graphite, 20: 3300
**WILLIAMSON, T. G.**, Fission neutron age and thermal diffusion length in ordinary concrete, 20: 3255
**WILLIS, L.**, Fast reactor safety experiments on EBR-II samples in flowing sodium environment, 20: 3506
**WILLIS, W. J.**, Observation of a peak in $K^- + p \rightarrow \Lambda + \eta$ near threshold, 20: 2724
**WILSKY, K.**, Isobaric-spin impurity in $^{170}Lu$ ground state, 20: 3072
**WILSON, A. R.**, New techniques for superconducting cables, 20: 3612 (CONF-651001-6)
**WILSON, George**, Prog. rpt. on Hawaiian Run-Up program, 10/15/65, 20: 2058 (NVO-98-10)
**WILSON, J. H.**, Initial radiation shield requirements for hardened structures, 20: 3276
**WILSON, P. R.**, Wilson effect and sunspot structure, 20: 2576
**WILSON, Robert M.**, Accumulation of radioactive fission products in hair, 20: 1695
**WINCHESTER, John W.**, Neutron activation analysis of halogens in the atmosphere, 20: 1789
**WINFREY III, E. W.**, Relative toxicity of angiographic contrast media, 20: 1724
**WINICOUR, J.**, Lorentz-covariant gravitational energy-momentum linkages, 20: 2882
**WINTERNITZ, P.**, Meson current in broken symmetry U(12) and experiments with colliding beams, 20: 2753 (JINR-P-2300)
**WIRTHS, Guenter**, Nuclear fuels and nuclear elements, 20: 3447
**WIT, R.**, Asymptotic and threshold values of the scattering amplitudes in some static models, 20: 2763
**WIT, R.**, Permissible rate of decrease of forward scattering amplitude at high energies, 20: 2810
**WIT, R.**, Some properties of the forward scattering amplitude at high energies, 20: 2762
**WITCOFSKI, Richard L.**, Demonstration of extracranial neoplasms with $^{99m}Tc$ pertechnetate, 20: 1712
**WITHERS, W. T.**, BONUS reactor-operating performance, 20: 3520
**WITTHAUS, J. K.**, ML-1 shield study, 20: 3525
**WITTMAACK, K.**, Effective cross section for excitation of molecular vibrations by fast electrons, 20: 2638
**WITZKE, Walter R.**, Properties of arc-melted and electron-beam-melted tungsten, 20: 2396
**WLODARSKI, W.**, Charge-sensitive transistor preamplifier for use with semiconductor nuclear radiation detectors, 20: 2154
**WOJACZEK, K.**, Approximation of velocity distributions of electrons in Maxwell distribution in region of inelastic collisions, 20: 3188
**WOLBERG, J. R.**, Prediction analysis of the exponential function, 20: 2217
**WOLF, G.**, Determination of the $\pi$-$\pi$ scattering phase shifts up to 1.3 Bev, 20: 2708
**WOLF, Sheldon M.**, Effect of allogeneic bone marrow on lethally irradiated thymectomized mice, 20: 1660
**WOLFF, U. E.**, Observations on microstructural changes with burnup in mixed-oxide fuels, 20: 2451
**WOMACK, Robert E.**, Babcock and Wilcox hot-cell facility, 20: 1998
**WONG, D. T.**, Gamma-emission data for calculation of exposure rates from nuclear debris. II., 20: 2048 (USNRDL-TR-888)
**WONG, Wen-Kuei**, Heat capacities and thermodynamic properties of globular molecules. XIII., 20: 3616 (CPP-1149-22)
**WOOD, J. D. L. H.**, High output neutron tubes, 20: 3005
**WOODBURY, H. H.**, Some electrical transport studies on n-type II-VI semiconductors, 20: 2499
**WOODING, E. R.**, Estimate of electron density in plasma after-glow from study of electromagnetic scattering, 20: 3193
**WOODS, F. R.**, Total ionization in nitrogen by heavy ions of energies 25 to 50 kev, 20: 2623
**WOODS, L. C.**, Ionizing shock waves in cylindrical plasma, 20: 3201
**WOODWELL, G. M.**, Ecological effects of nuclear war, 20: 1588 (BNL-917)
**WOODWELL, G. M.**, Effects of ionizing radiation on ecological systems, 20: 2080 (BNL-917, pp 20-38)
**WORK, Richard N.**, Dendritic erosion in dielectrics, 20: 2259 (SC-DC-65-1789)
**WORSHAM, H. J. Jr.**, Experimental evaluation of self-powered neutron-flux monitors for PWR in-core use, 20: 2174
**WORTMAN, O.**, Properties of copper alloys of high resistance and high conductivity, 20: 2334 (NP-15530)
**WOYSKI, Jon S.**, Dynamic performance of clustered nuclear engines, 20: 3570
**WOZNICKI, W.**, Some remarks on correlated wave function method, 20: 2871
**WRIGHT, H. A.**, Application of the generalized concept of dosimetry to space radiations, 20: 2133 (NASA-SP-71, pp 245-50)
**WRIGHT, R. W.**, Fixed-volume experiments on transient thermal pressure production in water, 20: 3338
**WRIGHT, Robert Andrew**, Improvements in or relating to refuelling machines for nuclear reactors, 20: 3355
**WRONSKI, A. S.**, Irradiation hardening and embrittlement in bcc transition metals, 20: 2472
**WU, Ming Hsien**, Radiation defects in GaAs based on proton- and electron-bombardment induced light emission, 20: 2501
**WU, Tai Tsun**, Electrodynamics of intermediate bosons and CP noninvariance, 20: 2789
**WUKUSICK, C. S.**, Mechanism of rhenium-alloying effect in group VI-A metals, 20: 2323 (GEMP-314)
**WULFF, W.**, Dosimetry of high-energy electrons, 20: 2156
**WUNG, Hao-ming**, Reactions of tritium recoil atoms and $^{14}C$ with heterocyclic amines, 20: 1921
**WU TSUN-FAN**, An experimental determination of $K_2^0 \rightarrow 2\pi$ decay probability in sloped $K_2^0$ beam, 20: 2865 (JINR-P-2325)
**WYLIE, R. D.**, Materials parameters affecting performance of nuclear reactor pressure vessels, 20: 2402
**WYNBLATT, P.**, Effect of temperature, strain rate and structure on flow stress of an iron–2 percent manganese alloy, 20: 3641 (UCRL-11512 (Rev.))
**WYNCHANK, S. A. R.**, Proton-thermal neutron capture cross section, 20: 3058
**WYNVEEN, R. A.**, Nonremote fabrication of $^{233}U$ fuel elements, 20: 2289

# Y

**YAGI, I.**, Separation of thorium from rare earths by use of anion exchange resins, 20: 1957 (CEA-tr-X-616)
**YAGUDINA, F. R.**, Determination of isotopical components of the $\gamma + N \rightarrow N + \pi$ amplitude at $\gamma$ threshold, 20: 2737
**YAKHYAEV, R. Sh.**, Lepton annihilation of proton-antiproton pairs with allowance for form factors and polarization correlations, 20: 2696
**YAKOVLEVA, I. V.**, Possibility of measuring magnetic moment of the $\Sigma^+$ hyperon, 20: 2744
**YAKUBIK, V. V.**, Measurement of the background external radiation exposure of urban population in the USSR, 20: 2087
**YAMADA, Kazuo**, Remark on kinetic equation in unstable plasma, 20: 3220
**YAMAMOTO, S. S.**, Observation of a peak in $K^- + p \rightarrow \Lambda + \eta$ near threshold, 20: 2724
**YAMANAKA, Nobuji**, Spectroscopic measurement of flame temperature in magnetohydrodynamic generator, 20: 2673
**YAMAOKA, Hitoshi**, Gamma-induced polymerization of formaldehyde, 20: 1914
**YANG, Gee-zheng**, Group $C_2$ and symmetry of weak interactions, 20: 2794
**YANSON, I. K.**, Interaction of alternating Josephson current with resonant modes in superconducting tunnel structure, 20: 2895
**YAO, I. G.**, Observations of the night airglow, 20: 2850

**YARBROUGH, James David,** Determination of $^{45}Ca$ and $^{89}Sr$ in Chlamydomonas reinhardti and Protosiphon botryoides, 20: 1603
**YARMONENKO, S. B.,** Action of protective agents following irradiation with sublethal doses, 20: 1688
**YAROSH, M. M.,** Experiences and developments in instrumentation for liquid metal experiments, 20: 2013 (ORNL-P-1661)
**YASUKAWA, S.,** Direct substitute plutonium fuel for commercial water reactors, 20: 3511
**YATES, Jarrell,** Effects of external irradiation of the heart on cardiac output, venous pressure and arterial pressure, 20: 1652
**YATES, M. J. L.,** $h_{11/2}$ Single proton hole state in $^{207}Tl$, 20: 3071
**YATIRAJAM, V.,** Separation of Mo from Re by the extraction of Mo(VI) from Re(IV) with amyl acetate, 20: 1965
**YEARIAN, M. R.,** Inelastic electron scattering from alpha particle, 20: 3086
**YELLIN, Joseph,** Optical pumping transients in $^{87}Rb$ and application to disorientation cross sections, 20: 2596 (UCRL-16241)
**YEN, C. M.,** Superconducting $H_c$-$J_c$ characteristics of nitrided Nb–Zr wire to 130 kOe, 20: 2891
**YEN, W. M.,** Energy transfer mechanisms between rare-earth impurity ions, 20: 2627
**YENIKOLOPYAN, N. S.,** Radiation polymerization of hexamethylcyclotrisiloxane in solid phase, 20: 1903
**YERANOS, Walter A.,** Normal coordinate analysis of $XeF_4$ in the Urey-Bradley field, 20: 1845
**YETCH, F. A.,** $\pi^-$ meson-neutron elastic backward scattering at 1.4 to 4.0 Bev, 20: 2713
**YOKOTO, Ryosuke,** Radiation dosimeter, 20: 2181
**YOSERI, Norihiro,** Plasma ion oscillation in plasma beam system, 20: 3191
**YOUDALE, T.,** Feasibility of new procedure for biological dosimetry, 20: 1612 (EUR-2505.e)
**YOUNG, F. W. Jr.,** X-ray topograph examination of vacancy clusters in nearly perfect copper crystals, 20: 3279 (ORNL-P-1704)
**YOUNG, George A.,** Micrometeorological phenomena of underwater nuclear explosions, 20: 1979 (AD-614814)
**YOUNG, J. C.,** Differential neutron scattering from $D_2O$ and $ZrH_{1.85}$, 20: 2963
**YOUNG, J. C.,** Neutron spectrum measurements in $H_2O$ as a function of temperature, 20: 2966
**YOUNG, J. C.,** Neutron spectra in beryllium metal, 20: 2968
**YOUNG, R. S.,** Observations concerning localized corrosion in pumped sodium systems, 20: 2296
**YOUNGQUIST, C. H.,** 160,000-Curie $^{60}Co$ facility, 20: 1929
**YOURD, R. B.,** Cost estimating magnet systems with the aid of a computer, 20: 2545 (UCRL-16386)
**YSO, Y.,** Hot laboratory of Japan Atomic Energy Research Institute, 20: 1997
**YUANG RUNG-FANG,** Analysis of $\pi^- + p \rightarrow \pi^- + \pi^+ + n$ and $\pi^- + p \rightarrow \pi^- + \pi^0 + p$ at 338 Mev, 20: 2682 (JINR-P-2320)
**YUASA, T.,** Momentum distribution of recoil nuclei in reaction $^{12}C(p,2p)^{11}B$, 20: 3081
**YUCKER, W. R.,** Empirical formulae for secondary nucleon-production cross sections, 20: 3259
**YUMOTO, R.,** Direct substitute plutonium fuel for commercial water reactors, 20: 3511
**YURA, Osamu,** Preparation of radium standard solutions, 20: 1941
**YUSHMANOV, E. E.,** Confinement of slow ions in mirror trap in plasma with positive potential, 20: 3227

## Z

**ZABABAKHIN, E. I.,** Cumulation of energy and its boundary, 20: 2839
**ZABIYAKIN, G. I.,** Account of the pulsed mode in intermediate memories, 20: 2101 (JINR-P-2319)
**ZABLOCKI, H. S.,** Nondestructive electrical method of studying density distribution of a randomly packed bed, 20: 1977
**ZABORENKO, K. B.,** Application of complex emanation-thermal method for studying the KCl–$CaCl_2$ constitution diagram, 20: 1860
**ZABORENKO, K. B.,** Application of complex emanation-thermal method in studies of the CaO–$Fe_2O_3$ constitution diagram, 20: 1861
**ZABORENKO, K. B.,** Complex emanation-thermal method, 20: 1779
**ZAGER, S.,** Use of strain softening to improve properties of refractory metals, 20: 2311 (AD-618925)
**ZAHEDI-MOGHADAM, A.,** Study of recombination processes of electron-hole pairs in Ge irradiated by $^{60}Co$ $\gamma$ rays by means of photovoltaic effect in p-n junctions, 20: 2512
**ZAIDMAN, S. A.,** Effects of fast neutron irradiation on silicon electric properties during p-n transitions in fused diodes prepared with silicon base, 20: 2440
**ZAIITS, V.,** Discovery of damage in uranium fuel elements in nonactive test in $CO_2$, 20: 1748 (UJV-1369/65)
**ZAITSEV, L. V.,** Shielding parameters of concretes, 20: 3253
**ZAITSEVA, L. L.,** Physico-chemical properties of crystal hydrates of terbium subgroup rare earth sulfates, 20: 1868
**ZAKATOV, L. P.,** Runaway electron collective interactions with plasma in stellarator S-1, 20: 3186
**ZAKHAROV, I. I.,** Biphenyl thermal turbines and their maximum power, 20: 2019
**ZAKOVSKY, J.,** X-ray diagnosis radiation burdens to youths and adults, 20: 1703
**ZAKRZEWSKI, J.,** Scattering of Ar ions in photographic emulsion, 20: 3063
**ZALESKI, Edward J.,** Use of positron emitter in determination of coronary blood flow in man, 20: 1709
**ZALEWSKI, Kacper,** Simple asymptotic formula for charge branching ratios in the statistical model, 20: 2760
**ZAMECNIK, Jiri,** Dependence of build-up ratio on field size and source-surface distance, 20: 1721
**ZAMOLODCHIKOV, B. I.,** Duty cycle improvement of particle beams at 680-Mev JINR synchrocyclotron, 20: 2548
**ZAMOLODCHIKOV, B. I.,** Strong-current high-energy particle accelerators—meson factories, 20: 2560
**ZAMPARO, Giuseppe,** Lattices of graphite moderated reactors, 20: 3434
**ZAMPARO, Giuseppe,** Verification of method for calculations of gas-cooled and graphite-moderated reactors, 20: 3441
**ZARE, Richard N.,** Dissociation of $H_2^+$ by electron impact, 20: 2632
**ZEBROSKI, E. L.,** Effective axial and radial thermal expansion of $UO_2$ with a radial thermal gradient, 20: 2234
**ZEHENDER, Otto,** Gamma radiation in capture of thermal neutrons in $^{143}Nd$ by means of sum-coincidence method, 20: 3131
**ZEL'DOVICH, B. Ya.,** Possible non-conservation of CP parity and the nature of the $\Delta T = \frac{1}{2}$ rule, 20: 2798
**ZEL'DOVICH, O. Ya.,** Elastic backward scattering of $\pi^-$ by neutrons, 20: 2700
**ZELDOVICH, O. Ya.,** $\pi^-$ meson-neutron elastic backward scattering at 1.4 to 4.0 Bev, 20: 2713
**ZELENSKAYA, N. S.,** Selection rules for nuclear reactions involving nucleon associations in SU(3) scheme, 20: 3117
**ZELEVINSKII, V. G.,** Green functions and transition probabilities in odd nuclei, 20: 3104
**ZEMCIK, T.,** Moessbauer spectra of alkaline ferrocyanides, 20: 3296
**ZEMSKII, S. V.,** Study of diffusion of carbon and molybdenum in chromium, 20: 2357 (AERE-Trans-1032)
**ZHILEIKIN, Yu. M.,** Calculation of effective cross section for loss of K-electrons by fast hydrogen-like ions during encounters with hydrogen and helium atoms, 20: 2642
**ZHMYROV, V. N.,** Ionization measurement in a streamer chamber, 20: 2128 (JINR-E-2324)
**ZHORNO, L. Ya.,** Inclusion of $^{3}H$-thymidine in cells of stratified flat epithelium in rats following x irradiation, 20: 1634
**ZHUKOV, V. A.,** Analysis of $\pi^- + p \rightarrow \pi^- + \pi^+ + n$ and $\pi^- + p \rightarrow \pi^- + \pi^0 + p$ at 338 Mev, 20: 2682 (JINR-P-2320)
**ZHURAVLEV, V. E.,** Certain polonium *m*-anisyl derivatives, 20: 1854
**ZHURAVLEV, V. E.,** Synthesis of some polonium $\alpha$-naphthyl derivatives, 20: 1850
**ZIEMACK, H.,** Examinations of blood picture after intracavitary administration of $^{198}Au$, 20: 1672
**ZILBERT, E. R.,** Chinese nuclear explosion, N-nation nuclear development and civil defense, 20: 2068 (AD-614895)
**ZIMINA, N. H.,** Thermal conductivity of helium at temperatures 0 to 1000°C and pressures 1 to 200 atm, 20: 1824
**ZIMMER, G. W.,** Shielding problems at the NRL linac facility, 20: 2556
**ZIV, D. M.,** Solubility of certain actinium compounds. I., 20: 1846
**ZIV, D. M.,** Solubility of certain actinium compounds. II., 20: 1847
**ZIVI, S. M.,** Hydrodynamic stability of natural-circulation boiling-water reactors, 20: 3516
**ZOGAL, O. J.,** PMR studies of hydrogen diffusion in Nb–H system, 20: 2365
**ZOLLINGER, H.,** Hydrogen isotope effects in aromatic substitution reactions, 20: 1888
**ZOLOTAR, B. A.,** Asymptotic reactor-theory analysis of Garelis-Russell experiment, 20: 3385
**ZOLOTAVIN, A. V.,** Decay of $^{146}Eu$, 20: 3075
**ZOLOTOV, S.,** Crystal structure of rare earth and yttrium oxybromides, 20: 1834
**ZOLOTUKHIN, V. G.,** Angular distribution of $^{238}U$ photofission fragments near fission threshold, 20: 3134
**ZORY, Peter,** Nuclear electric-field gradient determination utilizing the Moessbauer effect ($^{57}Fe$), 20: 3299
**ZUBAY, G.,** Size of ribosomal site for messenger RNA binding, 20: 1592 (BNL-7903)
**ZUMWALT, L. R.,** Prog. rpt. on advanced, graphite-matrix, dispersion-type fuel systems and research on graphite, 8/15–11/14/64, 20: 2318 (GA-5918(Pt. 1))
**ZWEIFEL, P. F.,** Exact solution of equations of radiative transfer, 20: 2731
**ZYL, Bert Van,** Dissociation of $H_2^+$ by electron impact, 20: 2632

# SUBJECT INDEX

Main entries in this index are generally specific materials, things, and processes. These are followed by modifiers that describe the properties of, and processes applied to, the main entries.

The number preceding the colon is the *NSA* volume number, and the number following is the abstract number. The designation (R) following the abstract number indicates that the abstract is of a progress report; (P) indicates a patent; and (T) indicates a translation. Abstracts for reports other than progress reports carry no letter designation. References to report numbers, where appropriate, are included after the abstract number of the citation. Published literature (journal article or book) is identifiable by the absence of a report number.

The user should bear in mind that the ideas presented in the original literature, rather than key words, have been indexed. The indexers have tried to select what seemed the most probable and logical place to look for typical information. Since it is not possible to anticipate where a user would look for information, numerous cross references are included in cumulative indexes to assist him in his search.

Experience in using an index of this type will be the best guide in obtaining the desired information, and a consideration of synonymous or closely related terms will prove valuable.

Information must be so indexed as to be of the greatest use to the greatest number of users. This requires that a topic be indexed to headings that most specifically describe it and not ordinarily to the headings that describe its ultimate use, nor to the general class headings that include the specific headings. For example, information on the treatment of thyroid disease with I-131 would be indexed under Thyroid Gland and under Iodine Isotopes I-131, but not necessarily under Radiotherapy. A study of the effects of x radiation on hair would be indexed under both X Radiation and Hair. However, the information would not be indexed under the experimental animal, e.g., Rats, unless the report discusses the effects on rat hair as compared with the effect on the hair of other animals.

The broad, general class headings are used only for general information or for comprehensive reports or articles.

## Subject Heading Styles

Generally, the direct form of subject entry is used rather than inverted headings, e.g., Amino Acids rather than Acids, Amino; Helium Isotopes He-4 rather than Helium—isotopes He-4 or Helium—He-4 isotopes. Note, however, that in some cases parenthetic modifying terms or inverted headings of the form Neutrons, Fast are used in preference to a direct entry that would result in the scattering of information. Organic compounds are usually entered in the index in the inverted form so that substituted compounds can be listed near the parent compound; e.g., Benzene, Bromo- rather than Bromobenzene. In general, the style of nomenclature used is that of Chemical Abstracts, except that some items listed in that publication as subheadings are elevated to form part of the main heading; e.g., Butyric Acid, Methyl Ester rather than Butyric Acid—methyl ester.

## Alphabetization

Main headings are alphabetized word-by-word. A parenthetic qualifier following a main heading is disregarded in alphabetizing unless there are two or more headings identical except for the parenthetic qualifier, in which case the qualifier determines the order. Headings involving Greek letters are arranged as if the names of the letters were spelled out.

Examples:

M-Capture
  see Electron Capture
Magnesium
Magnesium Alloys
Manganese Fluorides
Manganese(II) Fluorides
Mesons
Mesons ($\pi$)
Mesons ($\rho$)
3-Pentanol, 2,4-Dimethyl-
2-Pentanol, 2-Methyl-
2-Pentanol, 4-Methyl-

## Nomenclature of Inorganic Compounds

Inorganic compounds are indexed in the direct form, listing cations in the order of increasing valence in the case of polycationic salts of varying valence and in alphabetic order for polycationic salts in which all cations have the same valence; e.g., Sodium Aluminum Silicates and Potassium Sodium Sulfates.

## Multicomponent Alloys and Other Systems

Multicomponent alloys, except well-known trade names are indexed under a main heading in the form "element alloy" for each element in the alloy. The modifier begins with element symbols for each component arranged alphabetically as if the English name for the element were spelled out.

Example: Copper-Gold Alloy is indexed
  Copper Alloys
    Cu-Au...
  Gold Alloys
    Cu-Au...

Well-known alloys such as Zircaloy-2 are indexed directly to the trade name; cross references referring from each component of the alloy to the entry for the trade name appear in cumulative indexes.

Multicomponent systems of non-metallic elements are indexed in a manner similar to alloys except the main heading used contains the word "Systems" in place of "Alloys."

Example: Silicon–Tungsten Systems are indexed
  Silicon Systems
    Si-W...
  Tungsten Systems
    Si-W...

Multicompound systems and mixtures of compounds are indexed under the main heading for each component com-

pound; the modifiers begin with an alphabetical listing of compound formulas.

Example: Lead Titanate–Lead Zirconate is indexed
Lead Titanates
$PbTiO_3$-$PbZrO_3$...
Lead Zirconates
$PbTiO_3$-$PbZrO_3$...

A mixed system of compounds and elements is indexed using a combined form of the above conventions, e.g., a dispersion of copper and alumina would be indexed

Aluminum Oxides
$Al_2O_3$-Cu...
Copper Systems
$Al_2O_3$-Cu..

## Physical States and Configurations of Materials

Specification of the physical state, if other than normal, or geometric configuration of the material is included in the modifying phrase, i.e., liquid metals would be indexed to the metal with "liquid" in the modifier, and carbon crucibles would be indexed to Carbon with "crucibles" appropriately placed in the modifier and also to Crucibles if appropriate.

## Modifying Phrases

The modifiers appearing under a main heading are written specifically to describe the relation of the item being indexed to that main heading. The modifier, therefore, will generally contain more useful information about that relation than will a title or a phrase written to be used under every main heading assigned to the item. Effort is exerted to begin the modifier with the word judged to be of greatest use to the greatest number of users; this, however, does not obviate the need to consider all modifiers under the main heading(s) of interest.

Modifiers are usually intended to form a meaningful phrase when combined with the main heading. Some are intended to be read following the main heading, e.g., the entry Hydrogen—sorption by charcoal is read "hydrogen sorption by charcoal"; however, as a result of placing the important word first, many modifiers must be arranged for smooth reading, e.g., Formaldehyde—yields in radiolysis of ethyl ether, effects of deuterium on is read "effects of deuterium on formaldehyde yields in radiolysis of ethyl ether" and Uranium—crystal structure of, effect of cooling rate on allotropic transformations in is read "effect of cooling rate on allotropic transformations in crystal structure of uranium." Prepositions are sometimes omitted if no ambiguity results.

Special characters are added to modifiers in the field of physics; if the modifier does not establish the experimental or theoretical character of a reference, a symbol (E), (T), or (E/T) is placed immediately after the modifying phrase and before the journal reference number. The value of this identification has been established by the American Institute of Physics.

# A


**A-286 ALLOY**
radiation effects on creep-rupture properties of, neutron, 20: 2456
**ABSTRACTS**
of patents on production of heavy water, 20: 1951 (AECL-2279)
on radiation effects on glass, 20: 2432 (REIC-Memo-26)
**ACCELERATORS**
beam density in, phase-space techniques for measuring, (T), 20: 2534 (BNL-9587)
beam focusing of, symmetric quadrupole magnet triplets for, (T), 20: 2539 (SLAC-47)
bremsstrahlung shielding for electron, design of, (T), 20: 2557
component handling systems for high-energy, design of shielded, (E), 20: 2542 (UCRL-16236)
development of high-energy, for meson production, 20: 2560
experimental facilities for 200-Bev, design of, 20: 2540 (UCRL-16223)
magnet cost estimation for, computer program for, 20: 2545 (UCRL-16386)
magnet design of, computer program for, 20: 2546 (UCRL-16389)
magnets for, design of high-current-density septum, 20: 2544 (UCRL-16309)
magnets for, review of, 20: 2533 (BNL-9536)
neutron spectra outside shields of pulsed, 20: 2553
phase locking systems for proton storage rings, (E), 20: 2535 (CERN-65-31)
reactor boosting using pulsed, mean power density for, (T), 20: 3371 (EUR-2492.e)
remote-handling equipment for high-energy development of, 20: 2551
shielding design for tandem, (T), 20: 2558
shielding for high-energy electron, design of, (T), 20: 2555
shielding for, neutron attenuation in concrete and iron, (E), 20: 2554
shielding for, skyshine effects in, (T), 20: 2552
**ACCIDENTS**
criticality detection and alarm systems, review of design principles of, 20: 2075 (AHSB(S)R-92)
**ACETALDEHYDE**
yields in gamma radiolysis of liquid acetone, 20: 1901
yields of, from radiolysis of benzene–isopropanol–benzophenone mixtures, 20: 1931
**ACETIC ACID**
corrosive effects on molybdenum and vanadium, stress-, 20: 2254 (BM-RI-6680)
yields in gamma radiolysis of liquid acetone, 20: 1901
**ACETIC ACID, AMYL ESTER**
use in separation of molybdenum and rhenium, 20: 1965
**ACETIC ACID, [(CARBOXYMETHYLIMINO) BIS(ETHYLENENITRILO)] TETRA-**
effects on excretion of scandium-46 and zinc-65 by man, 20: 1691
trisodium calcium chelate of, radiosensitivity effects on rat fetuses, 20: 1693
**ACETIC ACID, CHLORO-**
corrosive effects on molybdenum, stress-, 20: 2254 (BM-RI-6680)
**ACETIC ACID, (ETHYLENEDIAMINE) TETRA-**
effects on excretion of scandium-46 and zinc-65 by man, 20: 1691
**ACETIC ACID, TRIFLUORO-**
deuterium exchange between deuterium-labeled, and halogens in halo-ferrocene, 20: 1830
reactions with fluorine, effects of water on, 20: 1881
**ACETIC ACID, TRIPHENYL-, *t*-BUTYL ESTER**
decomposition of, deuterium effects on, 20: 1891
**ACETONE**
effects on polonium separation from hydrochloric acid solutions, 20: 1777
radiolysis of liquid, yields in gamma, 20: 1901
solvent properties for polonium chloride, 20: 1946
yields of, from radiolysis of benzene–isopropanol–benzophenone mixtures, 20: 1931
**ACETYL FLUORIDE, TRIFLUORO-**
preparation of, effects of water vapor on, 20: 1881
**ACETYL PEROXIDE**
decomposition of, deuterium effects on, 20: 1891
**ACETYLENE**
determination of, factors affecting continuous on line, 20: 1734 (EG-Report-36)
production by methane decomposition in hydrogen plasma jets, (T), 20: 3197
radioinduced polymerization of liquid and solid, properties and spectra of products of, 20: 1913
yields in recoil reactions of carbon-11 in liquid hydrocarbons, 20: 1896 (IS-T-23)
acetylene–O, engineering drawings of spectrophotometer burner design using, 20: 1798
**ACRYLIC ACID, ESTERS**
radioinduced polymerization of trihydroperfluoroalkyl, 20: 1911
**ACRYLIC ACID POLYMERS**
radioinduced polymerization of, calorimetric analysis of kinetics of, 20: 1904
**ACRYLONITRILES**
radioinduced polymerization with formaldehyde, effects of dichloro-methane and ethyl ether on, 20: 1914
radioinduced polymerization of, at low temperatures, 20: 1893(R) (AD-618228)
**ACTINIDE COMPOUNDS**
stability, 20: 1855
**ACTINIDE IONS**
entropy of smallest and largest hydrations of, 20: 1858
**ACTINIDES**
electrophoretic properties of trivalent, in *α*-hydroxyisobutyric acid, 20: 1961
**ACTINIUM HYDROXIDES**
basicity of, determination of, 20: 1847
solubility in ammonium nitrate and water, aging effects on, 20: 1847
**ACTINIUM ISOTOPES Ac-227**
analysis for lead-210, electrophoretic, 20: 1756
decay products of, electrophoretic behavior in *α*-hydroxyisobutyric acid, 20: 1756
electrophoretic properties in *α*-hydroxyisobutyric acid, 20: 1756
**ACTINIUM OXALATES**
solubility in nitric acid and water, 20: 1846
**ACTINOMYCIN**
effects on nucleoside metabolism of, in Drosophila spermatocytes, 20: 1657
**ACTIVATION ANALYSIS**
counting delay time in neutron, 20: 1788
development for forensic and medical uses, 20: 2520(R) (IA-920)
equipment and methods development for, review of, 20: 1785
equipment for rapid and precise fast-neutron, automated, 20: 1765
gamma spectra for, tabulation of, 20: 1735 (EUR-2406.e)
gamma spectra in, least-squares analysis of, 20: 1787
neutron sources for, development of high-output, 20: 3005
of manganese, method for, 20: 2520(R) (IA-920)
use in crime detection, 20: 1736(R) (GA-3491)
use in crime detection, 20: 1740(R) (GA-4576)
use in determination of halogens in atmosphere, 20: 1789
use of lithium-drifted germanium detectors in, 20: 2166
**ACTIVATION DETECTORS**
development for reactor neutron flux measurements, 20: 3362(P)
development for simultaneous measurement of neutron dose equivalent and fluence, 20: 2123 (ANL-7085)
**ADDITION COMPOUNDS**
radiolysis and storage of tritium-labeled, self-, 20: 1938 (EUR-2452.e)
**ADENINE**
complexes with chlorophyllin and metal ions, radiosensitivity effects in mice, 20: 1692
**ADENOSINEPHOSPHORIC ACIDS**
activity of, effects of tritium-labeled thymidine on, 20: 1583
**ADRENAL GLANDS**
radiation effects from deposited strontium-89 or strontium-90 on guinea pig and rat, morphological, 20: 1641
**ADVANCED TEST REACTOR**
fuel elements for, irradiation testing of aluminum cermet–uranium oxide, 20: 2465
**AEROSOLS**
determination of uranium-containing, using carbon dioxides, 20: 1748 (UJV-1369/65)
inhalation of neodymium oxide, by guinea pigs and mice, effects of particle size and concentration on, 20: 1593 (COO-1170-4)
monitoring beta-active, design of coincidence counters for, 20: 2139
separation of beryllium-7 from atmospheric, method for, 20: 1778
**AGE**
physiological, tests for determination of, 20: 1587
**AGE ESTIMATION**
of lead minerals from Cobalt-Noranda area, Canada, 20: 2051
radiocarbon methods of, scintillation counting in, 20: 2062
**AGING**
effects on hematological and serum biochemical parameters, in miniature swine, 20: 1581 (BNWL-SA-341)
radiation effects on, of chickens exposed during embryonic development, x, 20: 1611(R) (COO-1119-4)
**AGRICULTURE**
radiosterilization of products of, economics of gamma, 20: 2198
**AIR**
analysis for argon-41 by adsorption on charcoal and gamma scintillation spectrometry, 20: 1763
corrosive effects on reactor fuel alloys, 20: 3320(R) (ANL-7082, pp 1-28)
effects on Zircaloy-4 corrosion by steam, 20: 2257(R) (GEMP-52A,

pp 47-52)
fallout particles in, alpha-active, 20: 1602
light scattering by, Rayleigh cross section for laser, 20: 3234
monitoring for plutonium-239, $\alpha-\beta$ pseudocoincidence method for, 20: 2151
oxidation of aluminum–chromium–iron–yttrium alloy at 900 and 1100°C, 20: 2223(R) (GEMP-51A)
reactions with beryllium in simulated launch pad abort environments at 800 to 1500°C, 20: 2341 (SC-DC-65-1637)
separation of krypton-85 and xenon-133 from, by sorption on activated carbon, 20: 1969
air–H, combustion of beryllium in flame system of, 20: 2341 (SC-DC-65-1637)
air–methane, combustion of beryllium in flame system of, 20: 2341 (SC-DC-65-1637)

**AIRCRAFT**
cosmic radiation effects on occupants of high-altitude, (T), 20: 2657 (NASA-SP-71, pp 287-99)

**ALANINE, PHENYL-**
radiolysis and storage of tritium-labeled, self-, 20: 1938 (EUR-2452.e)

**ALARM SYSTEMS**
design for criticality detection, 20: 2075 (AHSB(S)R-92)
design for radiation monitors, 20: 2121 (AD-614832)

**ALCOHOLS**
reactions with phosphorous pentoxide products from, 20: 2520(R) (IA-920)

**ALGAE**
analysis for calcium-45 and strontium-89 by liquid scintillation, 20: 1603
calcium-45 and strontium-89 uptake by, 20: 1603
carbon and oxygen isotopic ratios in carbonates deposited by, in Jamaican waters, 20: 1591

**ALKALI METALS**
compatibility with refractory metals at high temperatures, 20: 2236
corrosive effects on refractory alloys, facility for studying, 20: 2272
critical density and temperature of, 20: 3321(R) (ANL-7082, pp 29-53)
properties of hafnium–tantalum–zirconium alloys for use with, at high temperatures, 20: 2241
scattering by mercury and xenon atoms, cross sections and rainbow effect in, (E/T), 20: 2636

**ALKANES, HALO-**
effects on gamma radiolysis of hexane, 20: 2520(R) (IA-920)

**ALLOYS**
cavitation damage to refractory, in liquid metals, 20: 2243
corrosion of refractory, by alkali metals, 20: 2272

**ALPHA PARTICLES**
angular distributions from deuteron reactions (d,$\alpha$) with carbon-12 or 13 Mev, (E/T), 20: 3106
angular distributions from nitrogen-15 (p,$\alpha_0$) reactions at 3 to 12 Mev, 20: 3061
detection and measurement at small solid angles using proportional counters, 20: 2147
detection and measurement using semiconductor detectors, 20: 2154
detection of, scintillation detector for, 20: 2152
dose distributions behind spacecraft shields, (T), 20: 3251 (NASA-SP-71, pp 507-12)
effects on algal, biological, 20: 1681
effects on calcium tungstate, luminescence decay time for, (E), 20: 1900
effects on electric conductivity of diamond, (E), 20: 2434(R) (TID-22242)
effects on man, pathological evaluation using fractional cell lethality calculations, 20: 1616 (NASA-SP-71, pp 219-23)
effects on mice and rats at 910 Mev, pathological, 20: 1614 (NASA-SP-71, pp 97-103)
effects on n-type silicon at 5.147 Mev, formation energy of electron-hole pair in, (E), 20: 2362
effects on water vapor, 20: 1936
emission in samarium-147 decay, half-life and atomic stopping cross section for, (E), 20: 3028
ionization in K-shell of atoms of deformed even-even nuclei, x-ray yields from, (E), 20: 2625
ranges in mica, argon, helium, methane, and carbon dioxide, 20: 2147
reactions ($\alpha$,n) with oxygen-18, neutron spectra from, 20: 2520(R) (IA-920)
reactions with nitrogen, optical excitation in, 20: 1933
scattering by carbon-12 and magnesium-24 at 42 Mev, alpha-gamma coincidences in, 20: 3141
scattering by magnesium-24 at 18 to 21.4 Mev, silicon-28 levels from, (T), 20: 3069
scattering by oxygen-16 at 41.9 to 49.7 Mev, backward elastic, (E), 20: 3056
scattering by tin isotopes at 40 Mev, angular distributions from, (E), 20: 3017 (NASA-TN-D-3067)

**ALUMINUM**
argon-ion reactions at 50 kev, charged-particle emission in large-angle, (E), 20: 2629
bremsstrahlung and electron transport in, (T), 20: 3246 (NASA-SP-71, pp 437-48)
corrosion resistance to mercury at 900°F, 20: 2264
deposition on uranium for corrosion protection, method for, 20: 2260 (SC-DR-65-519)
determination in grease samples, activation, 20: 1738(R) (GA-4041)
deuteron scattering by, cross sections for, (T), 20: 3026
diffusion of uranium in liquid, at 700 to 850°C, 20: 2368
effects on hardness properties of Nitinol alloy, 20: 2310 (AD-618681)
electron diffraction by, (E), 20: 2434(R) (TID-22242)
electron scattering at 0.5 to 3.0 Mev, bremsstrahlung from, (E), 20: 3247 (NASA-SP-71, pp 449-53)
electron shielding properties of, at 0.2 to 2.5 Mev, (E), 20: 3248 (NASA-SP-71, pp 455-63)
gamma back-scattering from, albedos from, (E), 20: 3273
grain boundary migration in zone-refined, review on, 20: 3626 (ORNL-P-1722)
neutron scattering by cylinders of, fast, (E/T), 20: 3265
phonon dispersion relations in, Fermi surface structure from, (E), 20: 3303
proton reactions at 30 to 45 Mev, helium-3 and tritium production in, (E), 20: 3095
proton shielding performance of, for space vehicles, (T), 20: 3242 (NASA-SP-71, pp 225-8)
reduction of vanadium pentoxide by, preparation of vanadium by, 20: 2225 (IS-T-40)
superconducting transition temperature of thin films of, effect of thin oxide layer on, 20: 2915

**ALUMINUM ALLOYS**
welding of three-quarters in. thick 6061, methods for, 20: 3609 (ACF-11)
Al–Cr–Fe, diffusion of uranium through cladding of, research program for, 20: 2322(R) (GEMP-52A, pp 53-4)
Al–Cr–Fe, oxidation by carbon dioxide, effects of yttrium additions on, 20: 2263
Al–Cr–Fe–Y, corrosion by steam at 550°C, effects of pre-oxidation and strain on, 20: 2223(R) (GEMP-51A)
Al–Cr–Fe–Y, diffusion of uranium through cladding of, 20: 2223(R) (GEMP-51A)
Al–Cr–Fe–Y, oxidation by air at 900 and 1100°C, 20: 2223(R) (GEMP-51A)
Al–Cr–Fe–Y, radiation effects on mechanical properties of, 20: 2409(R) (AD-617319)
Al–Cu, neutron scattering at long wavelength by precipitations in, 20: 3285
Al–Cu–Fe–Sn–Ti–V–Zr, deformation and heat treatment effects on mechanical properties of, 20: 2309 (AD-615024)
Al–Fe, iron-57 Mössbauer effect in intermetalic compounds of, ordering transformation from, (E), 20: 3292
Al–La–Zr, crystal structure, 20: 2399
Al–Mg, crystal structure, 20: 2399
Al–Sn–Ti–V–Zr, formability characteristics and mechanical properties of, 20: 2308 (AD-614637)

**ALUMINUM CHLORIDES**
$AlCl_3$–$CdCl_2$, spectra of reduced melts of, 20: 3623 (IS-T-36)
$AlCl_3$–NaCl, stability of zirconium dichloride in, 20: 1822(T) (ANL-Trans-233)

**ALUMINUM IONS**
angular and energy spectra from argon-ion reactions on aluminum at 50 kev, (E), 20: 2629

**ALUMINUM ISOTOPES Al-27**
neutron reactions (n,d) and (n,p) at 8 to 22 Mev, distributions from, (E), 20: 3012 (IKF-11)
proton reactions (p,$\gamma$), resonance widths in, (E), 20: 3142

**ALUMINUM NITRATES**
effects on uranium and plutonium activity coefficients in nitric acid solutions, 20: 1967

**ALUMINUM OXIDES**
corrosion by bismuth and tin, 20: 2275
heat generation rate of highly radioactive calcined, 20: 2425 (IDO-14665)
promethium-147 diffusion in sintered, (E), 20: 2364
radiation effects of gamma rays and neutrons on, (E), 20: 3446(R) (GEST-2045)
sintering kinetics of alpha-, at 1200 to 1600°C, effects of particle size on, 20: 2287
spectra of, at 1300°K, infrared emission, 20: 1823
testing for use in shaft seals for potassium space power plants, 20: 2242
Al–$Al_2O_3$, hardening of, isochronal recovery of, 20: 2375

Al–$AlO_x$–Pb, superconducting film diodes of, geometrical resonance in tunneling characteristics of, (E), 20: 2909
$Al_2O_3$–Cu, annealing effects on structure of dispersion-hardened, 20: 2325 (HW-SA-3767)
$Al_2O_3$–Cu, structure of deformed, 20: 2324 (HW-SA-3765)
$Al_2O_3$–$H_2O$, flow in circular pipe, analysis of laminar, 20: 2020
$Al_2O_3$–$ZrO_2$, preparation of, for use at temperatures to 1750°C, 20: 2382

**ALUMINUM SYSTEMS**
Al–$Al_2O_3$, hardening of, isochronal recovery of, 20: 2375
Al–$AlO_x$–Pb, superconducting film diodes of, geometrical resonance in tunneling characteristics of, (E), 20: 2909
Al–Be–B, preparation and properties, 20: 2406(P)
Al–$H_2O$, fission-neutron age to indium resonance in, (E), 20: 2970

**AMERICIUM**
separation from aqueous lithium nitrate by solvent extraction using di(2-ethyl hexyl) phosphoric acid, 20: 2520(R) (IA-920)

**AMERICIUM COMPLEXES**
with bromine and chlorine, stability of, 20: 2520(R) (IA-920)

**AMERICIUM COMPOUNDS**
stability, 20: 1855

**AMERICIUM FLUORIDES**
melting points, 20: 1864

**AMERICIUM IONS**
spectra in lithium chloride solutions, absorption, 20: 2520(R) (IA-920)

**AMERICIUM ISOTOPES Am-241**
separation from thulium-170 and cerium-144, electrophoretic, 20: 1961

**AMIDE POLYMERS**
radioinduced crosslinking with polyvinyl alcohol in presence of allyl methacrylate–methanol–water system, 20: 1909

**AMINES**
radiation effects on ionic processes in solid, relation to delayed luminescence, 20: 1906
solvent properties of long chain, for protactinium, ruthenium, thorium, uranium, and zirconium, 20: 1761

**AMMINES**
complexes with chlorophyllin and metal ions, radiosensitivity effects in mice, 20: 1692

**AMMONIA**
determination of, factors affecting continuous on line, 20: 1734 (EG-Report-36)
preparation of, tracer studies of carbon dioxide removal in plants for, 20: 1836
spectra of blue solutions of beryllium and europium in liquid, absorption, 20: 1867
$NH_3$–ethylene, radioinduced polymerization of, recoil carbon-14 labeling in, 20: 1922
$NH_3$–ethylamine–K, spectra of metal in, electron paramagnetic resonance and optical, 20: 1808 (COO-958-5)

**AMMONIUM BOROHYDRIDES, TETRAALKYL-**
crystal structure of tetramethyl ammonium hexahydrohexaborate, 20: 2347 (UCRL-12146)

**AMMONIUM FERROCYANIDES**
iron-57 Mössbauer spectra from, (E), 20: 3296

**AMMONIUM NITRATES**
effects on uranium and plutonium activity coefficients in nitric acid solutions, 20: 1967
solvent properties for actinium hydroxide, aging effects on, 20: 1847

**AMPLIFIERS**
performance of transistorized pre-, for semiconductor detectors, 20: 2154

**AMYGDALIN**
complexes with rare earths, separation by solvent extraction using butanol, 20: 1796

**ANALYSIS**
methods for, of reactor fuel elements and materials, 20: 1743 (JUL-216-HW)

**ANIMAL CELLS**
effects of nitrogen mustard on survival of, in tissue culture, 20: 1617(R) (NP-15149)
growth rate patterns of, in tissue cultures, 20: 1594 (LA-DC-6507)
radiation effects on DNA synthesis in L-strain, in tissue culture, uv, 20: 1625
radiation effects on desoxyribonucleic acid content of, in rat corneal epithelium, 20: 1633
radiation effects on survival of, in tissue cultures, x, 20: 1617(R) (NP-15149)
radiation injuries of, induced by charged particles, 20: 1615 (NASA-SP-71, pp 105-14)
radiosensitivity of human, to alpha particles, charged particle, and protons, 20: 1616 (NASA-SP-71, pp 219-23)
resistance of murine cell line to purine analogs, 20: 1678
size distribution studies on, effects of membrane damage on Coulter electronic counter measurements, 20: 1636
tissue cultures of lymphoid cells, on monolayers of mouse embryo cells, 20: 1658

**ANIMALS**
radiation effects on, bibliography, 20: 1607 (AED-C-04-18)
radiation effects on, bibliography, 20: 1608 (AED-C-04-19)
radiation effects on, of flour beetles, Tribolium, 20: 1613 (HW-SA-3537)
radiation effects on ecology of, thermal, 20: 2079 (BNL-917, pp 11-19)
radiation effects on ecology of, 20: 2080 (BNL-917, pp 20-36)
radiation effects, biochemical, 20: 2520(R) (IA-920)

**ANION EXCHANGE MATERIALS**
sorptive properties for technetium, 20: 1963
use of Amberlite IRA-410 resin in separation of thorium from rare earths, 20: 1957(T) (CEA-tr-X-616)

**ANISOLE**
effects as diluent on perchloric and perrhenic acid extractions by tri-dodecylamine, 20: 1747 (UCRL-11616(Rev.))

**ANISOLE COMPLEXES**
with polonium, preparation of, 20: 1854

**ANTENNAS**
feed-point singularity and frequency of, effects of plasma sheath on, (E), 20: 2096 (AD-617928)
performance of cylindrical and spherical, (E), 20: 3632 (SC-DR-65-459)
propagation constant along cylindrical, in warm plasma, (T), 20: 2097 (AD-618396)

**ANTHRACENE**
radiolysis in alcoholic, aqueous, and hydrocarbon solutions, solvent effects on spectra of, 20: 1920

**ANTIBODIES**
radiation effects on formation of, in monkeys, 20: 1631
radiation effects on formation of, in mice and rats, 20: 1632
radiation effects on formation of, in mice injected with sheep erythrocytes, 20: 1661
radiation effects on response to protein antigens, 20: 1680

**ANTIGENS**
immune response to, recognition of antigenic determinants in, 20: 1680
radiation effects on immune reactions to injected homologous, in mice, 20: 1632
radiation effects on antibody response of rabbits to protein, 20: 1680

**ANTIMONY**
determination in gunpowder residues, oils, and river silts, activation, 20: 1739(R) (GA-4297)
effects of additions of, on steam corrosion of niobium–tin–zirconium alloys, 20: 2255(R) (EURAEC-1323)
effects on radioinduced defects in germanium at 100°C, 20: 2495

**ANTIMONY ALLOYS**
Sb–Fe, iron-57 isomer shift and quadrupole splitting in $FeSb_2$, 20: 3317
Sb–Ga, radioinduced defects in, structural properties of, 20: 2486
Sb–In, radiation effects on close-pair defects at 0 to 140°K in, 20: 2482
Sb–In, radiation effects on semiconducting, 20: 2497
Sb–In, radiation effects on n-type, at 78°K, 20: 2500
Sb–In, radioinduced defects in, structural properties of, 20: 2486

**ANTIMONY FLUORIDES**
reactions with xenon hexafluoride, 20: 1881

**ANTIMONY ISOTOPES Sb-117**
energy level at 157.9 kev, 20: 3043

**ANTIMONY ISOTOPES Sb-121**
energy-level transition probabilities of, E2, (T), 20: 3115
gamma transition at 572.8 kev following Coulomb excitation, (E), 20: 3043

**ANTIMONY ISOTOPES Sb-123**
energy-level transition probabilities of, E2, (T), 20: 3115
gamma transitions following Coulomb excitation, (E), 20: 3043

**ANTIMONY ISOTOPES Sb-124**
beta decay of, circular polarization of gamma rays following, (E), 20: 3051

**ANTIMONY SULFIDES**
preparation of technetium-99m-labeled colloidal, for tracer use in medicine, 20: 1696 (CONF-641126-1)

**ANTINEUTRINOS**
interactions with protons, positron spectra from, (E), 20: 2680 (COO-818-58)
interactions with neutrinos, bootstrap method for W boson exchange in, 20: 2721
interactions with protons at high energy, cross sections for meson ($\pi^-$) production in, (T), 20: 2733
interactions with protons, cross section for ($\mu^+\gamma$) production in, (T), 20: 2736

**ANTIPROTON BEAMS**
trapping of, quadrupole magnetic channel for, 20: 2547 (UR-375-98)

**ANTIPROTONS**
annihilation with protons, cross sections for lepton-pair production in, (T), 20: 2696
interactions with protons, U(12) symmetry for annihilation into mesons in, 20: 2703

**ARGON**

alpha stopping power of, for 5-Mev, 20: 2147
collisions of atoms of, with alkali metal atoms, ionization produced in, (E), 20: 2639
collisions of atoms of, with singly charged krypton ions, profound stripping and scattering in, (E), 20: 2644
determination of, factors affecting continuous on line, 20: 1734 (EG-Report-36)
diagnostics of cesium-seeded plasma of, in MHD cells, (E), 20: 2671
diffusion in potassium iodide monocrystals, 20: 2317 (EURAEC-1380)
effects on hydrogen yields in radiolysis of liquid ethylene, 20: 1898(R) (RRL-2310-164)
electric breakdown potential of, measurement of a-c, 20: 3160 (AD-618503)
electric discharge in, striated plasma column in h-f, (E), 20: 3203
electron density in afterglow plasma of, microwave diagnostics of, (E), 20: 3193
helium scattering on, velocity dependence of total cross sections for, (E), 20: 2614
neutron scattering by liquid, co-operative modes of motion from cold, (E), 20: 2837
nitrogen ion reactions at 0.14 to 0.7 Mev, energy loss in, (E), 20: 2602
oxygen ion reactions at 0.14 to 0.7 Mev, energy loss in, (E), 20: 2602
reactions with calcium atoms, cross sections for, 20: 2597
reactions with hydrogen, production of negative molecular ions by charge-exchange, 20: 2537 (LA-DC-7268)
reactions with mercury, cross sections for line broadening from, (E), 20: 2637
separation of krypton-85 and xenon-133 from, by sorption on activated carbon, 20: 1969
spectra of graphite vapor, mercury, and sulfur isolated in, at high temperatures, 20: 1818 (UCRL-11976)
use in gas scintillation detector for fission fragments, 20: 2163

**ARGON IONS**
ionization of nitrogen by 25- to 50-kev, total, (E), 20: 2623
reactions with aluminum surfaces at 50 kev, atomic-particle emission in large-angle, (E), 20: 2629
scattering by copper at 30 kev, effect of crystal structure on energy spectra of, 20: 2600
scattering in nuclear emulsions, particle-track production and momentum transfer in, (E), 20: 3063

**ARGON ISOTOPES Ar-40**
proton reactions (p,γ) at 1 to 3 Mev, potassium-41 isobaric energy levels from, (E), 20: 3036

**ARGON ISOTOPES Ar-41**
activity of, design of coincidence counters for, 20: 2139
determination in air by adsorption on charcoal and gamma scintillation spectrometry, 20: 1763
energy levels in, spins and parities of isobaric, (E), 20: 3036

**ARGON SYSTEMS**
Ar–$CCl_4$, reactions with uranium (IV–VI) oxide at 400 to 550°C, 20: 1816 (ORNL-TM-1258)
Ar–Hg, glow discharge initiation in, (E), 20: 3162 (AD-616683)
Ar–Rb, optical pumping of rubidium-87 in, 20: 2596 (UCRL-16241)

**ARGONNE ADVANCED RESEARCH REACTOR**
development and testing, 20: 3579(R) (ANL-7082, pp 54-61)

**ARGONNE FAST REACTOR EXPERIMENT TEST**
design and development of, July 1965, 20: 3320(R) (ANL-7082, pp 1-28)

**ARGONNE NATIONAL LAB., LEMONT, ILL.**
waste treatment practices at, comparison with Los Alamos, 20: 3603 (LA-DC-7249)

**ARMY REACTORS (ML-1)**
heat transfer from turbulence-promoted fuel elements for, 20: 2022
shielding of, performance of, (T), 20: 3525

**ARMY REACTORS (SM-1)**
measurements on SM-1A core-3, analysis of zero-power, 20: 3503

**ARSENAZO III**
analytical use for determination of uranium in ores, 20: 1794

**ARSENIC**
determination in hair, activation, 20: 1737(R) (GA-3664)
determination in oils, activation, 20: 1739(R) (GA-4297)
effects on radioinduced defects in germanium at 0°C, 20: 2494

**ARSENIC ISOTOPES As-75**
gamma transitions following Coulomb excitation, (E), 20: 3043
neutron reactions (n,γ) with, gamma spectra from, (E), 20: 3011 (IPA-NR-22)

**ARSENIC ISOTOPES As-76**
energy levels of, parity and spin, 20: 3011 (IPA-NR-22)

**ARSENIC SYSTEMS**
As–Cd–Sn, radiation effects on thermal conductivity of semiconducting $CdSnAs_2$, 20: 2488
As–Sn–Zn, radiation effects on thermal conductivity of superconducting, 20: 2488

**ARSONIUM COMPOUNDS**
extraction equilibria of tetraphenylarsonium salts in chloroform and water, 20: 2520(R) (IA-920)
solvent properties for uranium, effects of 8-hydroxyquinoline on, 20: 1782

**ASPHALT**
preparation and properties as waterproof radiation shielding, 20: 2248(P)

**ASTATINE ISOTOPES**
production in helium-3 bombardment of bismuth, 20: 1949

**ASTATINE ISOTOPES At-203**
production of, by irradiation of bismuth using 400-Mev protons, 20: 1948

**ASTATINE ISOTOPES At-205**
production of, by irradiation of bismuth using 400-Mev protons, 20: 1948

**ASTRONAUTS**
protection against protons, spherical shields for, (T), 20: 3243 (NASA-SP-71, pp 229-34)
protection from cosmic rays by copper shields, (T), 20: 3240 (NASA-SP-71, pp 183-8)
radiation effects of solar flares on, (T), 20: 2655 (NASA-SP-71, pp 85-96)
radiation hazard evaluation for, using fractional cell lethality calculations, 20: 1616 (NASA-SP-71, pp 219-23)
radiation protection of, in Apollo Command/Service Module, (T), 20: 3244 (NASA-SP-71, pp 365-75)
radiation protection of, (T), 20: 3245 (NASA-SP-71, pp 407-14)
radiation protection of, against solar flares, (T), 20: 3251 (NASA-SP-71, pp 507-12)

**ASTRONOMY**
gamma ray intensity in space, high-energy, (E/T), 20: 2586

**ATMOSPHERE**
airglow intensities of, IGY-IGC data tabulations of night, 20: 2850
analysis for halogens, using neutron activation analysis, 20: 1789
auroral spectra in, IGY data tabulations on, 20: 2851
electron reactions with nitrogen in, cross sections for, (E), 20: 2859
fallout particle activity and size in, 20: 2053
helium losses from, mechanism for, (T), 20: 2857
iodine removal from, by spraying, 20: 1966
particle diffusion in, tests on, 20: 2073(R) (AD-618101)
radioactivity of, analysis of 1962 to 1963, 20: 2049
radioactivity release to, calculation of deposition rates from, 20: 2074 (AHSB(RP)M-40)
radon-220 content in, correlation with meteorological variables, (E), 20: 2860
sampling of upper, development of cryogenic device for, 20: 2045 (UCRL-13162)
xenon-133 content in equal volumes of blood and, partition coefficients for, 20: 1599

**ATMOSPHERES**
simulation of inert, facility for, 20: 2246

**ATOMIC ENERGY**
book: *Economy and Perspectives of Atomic Energy*, in French, 20: 3648
book: *Social Implications of the Peaceful Uses of Nuclear Energy*, 20: 2094
legal aspects of entry of nuclear ships into foreign ports, 20: 2088
uses of, college course on, 20: 3329

**ATOMIC EXPLOSIONS**
description of Chinese, 20: 2068 (AD-614895)
design for nuclear excavation of sea-level Isthmian canal, 20: 1984 (PNE-2001)
effects of blast from, on man, 20: 2083 (CEX-65.4)
excavation of sea-level Isthmian canal, plan for nuclear, 20: 1983 (PNE-2000)
excavation of sea-level Isthmian canal, nuclear operations program for, 20: 1986 (PNE-2004)
fallout from, gamma dose distributions from, (T), 20: 2048 (USNRDL-TR-888)
ground motions from, methods for simulating air-blast-induced, 20: 1980 (AD-614990)
safety evaluation of, for excavation of sea-level Isthmian canal, 20: 1985 (PNE-2003)
surveillance of Handcar event, weather and radiological, 20: 1982 (PNE-607F)

**ATOMIC MODELS**
electron spin-orbit interaction energy operator in, reduced matrix elements for, 20: 2606
electronspin-spin interaction energy operator in, reduced matrix elements for, 20: 2605

**ATOMIC PHYSICS**
theory of inelastic collisions of slow atoms, (T), 20: 2624
theory of resonance broadening of spectral lines by atom-atom impacts, (T), 20: 2620
theory of s-f exchange for nonvanishing orbital momenta, 20: 2643

**ATOMIC WEAPONS**
effects of, display system for studying, 20: 1987 (UCRL-13139)
fallout from Chinese, in troposphere above Berlin, October 1964, 20: 2050

fragments produced by, trajectory analysis of structural, 20: 3610 (AD-622333)
radiation effects from, compilation of projects on, 20: 2433 (REIC-Memo-27)
**ATOMS**
collisions of slow, theory of inelastic, (T), 20: 2624
collisions of the type e + e + A and e + A + B, electron attachment in, (T), 20: 2647
collisions with negative ions at low energies, electron detachment in, (T), 20: 2648
destruction by electric fields and by electron impact, (T), 20: 2646
neutron cross sections of, tabulations, (E), 20: 3018 (NYO-72-27)
reactions with atomic oscillators, energy exchange in, (T), 20: 2594 (N64-23208)
reactions with atoms, theory of resonance broadening of spectral lines in, (T), 20: 2620
reactions with ions, electron capture and loss in, (T), 20: 2634
**AUDITORY ORGANS**
physiology of equilibrium-control by, 20: 1628(T)
radioinduced destruction of otolith apparatus of, in rabbits, 20: 1628(T)
**AURORAL STORMS**
morphology of, IGY all-sky photographs of, 20: 2852
properties, 20: 2859
spectra of, IGY data tabulations on, 20: 2851
**AUSTRALIA**
production and transport of radioisotopes by Atomic Energy Commission of, 20: 2208 (NP-15575)
**AVR REACTOR**
fuel element fabrication for, 20: 3494
fuel elements for, irradiation testing of, 20: 2464

# B

**BACTERIA**
cytology and control mechanisms for sporulation of *Bacillus cereus* and *B. subtilis*, 20: 1582(R) (NYO-2038-2)
effects of methyl methanesulfonate on desoxyribonucleic acid in *Bacillus subtilis* mutant, 20: 1624
radiation effects on immune reactions to injected homologous, in mice, 20: 1632
radiosensitivity effects of, fine structure in *Micrococcus radiodurans*, 20: 1584
radiosensitivity of *Clostridium perfringens* Type A spores, gamma, 20: 1679
radiosensitivity of, effects of sulfhydryl compounds on, 20: 1618 (NYO-2219-6)
radiosensitivity of, effects of p-hydroxymercuribenzoate binding on, 20: 1618 (NYO-3319-6)
**BACTERIOPHAGES**
radioinduced inactivation of, effects on lysis inhibition, 20: 1650
radioinduced radicals in dry, ESR of gamma and x, 20: 1623
**BARIUM**
determination in gunpowder residues, activation, 20: 1739(R) (GA-4297)
separation of trace elements from, by precipitation ion exchange, 20: 1958
**BARIUM CHLORATES**
deuterium NQR in hydrated, using chlorine-35 indicator, 20: 3144
radiolysis of isotopic exchange in, 20: 2520(R) (IA-920)
**BARIUM CHLORIDES**
diffusion of water in, coefficients of, 20: 1865
$BaCl_2$–NaCl, stability of zirconium dichloride in, 20: 1822(T) (ANL-Trans-233)
**BARIUM FLUORIDES**
charge compensation by fluoride ions in rare earth-doped, 20: 2520(R) (IA-920)
**BARIUM ISOTOPES Ba-135**
energy-level transitions in deuterated barium chlorate, NQR, 20: 3144
**BARIUM ISOTOPES Ba-137**
energy-level transitions in deuterated barium chlorate, NQR, 20: 3144
**BARIUM ISOTOPES Ba-140**
content in fallout particles, 20: 2053
determination in sea water, methods for, 20: 1749 (USNRDL-TR-912)
**BARIUM SULFATES**
use in bitumen-bound radiation shielding material, 20: 2248(P)
**BARIUM TUNGSTATES**
superconductivity of barium tungsten bronze, (E), 20: 2901
**BARLEY**
radiation effects on seeds of, biological, 20: 1667
**BARRIERS**
permeability of, system for measuring relative, 20: 2120(P)
**BARYONS**
interactions with photons, electromagnetic amplitudes for meson production in, (T), 20: 2732
interactions with neutrinos at high energy, De Santis model for, 20: 2784
interactions with mesons, $SU(6)_w$ scattering relation for S-wave isobar production in, 20: 2788
mass formulas from SU(12), (T), 20: 2756 (JINR-P-2342)
model for 56-plet SL(6), form factors and matrix elements in, 20: 2803
model for, mass relations and symmetry properties from oscillator, 20: 2800
model of, higher unitary symmetry groups for shell, 20: 2781
production in high-energy inelastic interactions, transverse momentum distribution of, (T), 20: 2681 (IFA-CR-55)
symmetry for, relativistic generalization of SU(3), 20: 2777(T)
**BARYONS, RESONANCE**
coupling constants and mass of $Y_1^*$, from self-consistency and broken unitary symmetry, (T), 20: 2710
interactions of Y particles with mesons ($\pi$), two-channel p-wave, (T), 20: 2694
isospin, parity, and spin of Y*(1760), (E), 20: 2711
mass spectra of $\Lambda(1238)$-$\pi$ and $\Sigma(1385)$-$\pi$ systems, (T), 20: 2741
model for 56-plet SL(6), form factors and matrix elements in, 20: 2803
model for, mass relations and symmetry properties from oscillator, 20: 2800
production in unstable boson exchange interactions, pole approximation for, 20: 2779
production of (114) and (1216), meson ($\pi^-$)-proton interactions at 7.0 Bev/c, 20: 2746
production of N*(1238) in meson ($\pi^-$)-proton interactions at 2.26 Bev/c, 20: 2745
production of $\Sigma$-$\pi$, by mesons ($K^-$) in complex nuclei, computer calculation of, (E/T), 20: 2520(R) (IA-920)
production of $Y_0^0$, in meson ($K^-$) capture by emulsion nuclei, (E), 20: 3064
production of Y*(1760) in meson (K)-proton interactions, (E), 20: 2711
**BEANS**
content of radioisotopes in, 20: 2520(R) (IA-920)
**BEARINGS**
materials testing for potassium-lubricated, for space power systems, 20: 3555
**BEHAVIOR**
radiation effects on conditioned-reflex activity of dogs exposed during fetal development, 20: 1627(T)
**BELGIUM**
radioisotope production facilities at Mol, 20: 2192 (BLG-63-11)
**BENZALDEHYDE**
radioinduced polymerization of, at low temperatures, 20: 1893(R) (AD-618228)
**BENZENE**
benzene–benzophenone–isopropanol, radiolysis of, energy transfer in, 20: 1931
benzene–methylcyclopentane, recoil reactions of carbon-11 in liquid, 20: 1896 (IS-T-23)
effects as diluents on perchloric and perrhenic acid extractions by tridodecylamine, 20: 1747 (UCRL-11616(Rev.))
effects on pulse radiolysis of organic solutes, spectra of, 20: 1920
neutron spectra in cooled, thermal, (E), 20: 2945
recoil reactions of carbon-11 in liquid, 20: 1896 (IS-T-23)
**BENZENE, BROMO-**
use of bromine-82-labeled, in tracer studies of industrial processes, 20: 2202
**BENZENE, CHLORO-**
effects as diluent on perchloric and perrhenic acid extractions by tridodecylamine, 20: 1747 (UCRL-11616(Rev.))
**BENZENE, DICHLORO-**
effects as diluent on perchloric and perrhenic acid extractions by tridodecylamine, 20: 1747 (UCRL-11616(Rev.))
**BENZENE, NITRO-**
effects as diluent on perchloric and perrhenic acid extractions by tridodecylamine, 20: 1747 (UCRL-11616(Rev.))
radiolysis in alcoholic, aqueous, and hydrocarbon solutions, solvent effects on spectra of pulse, 20: 1920
**BENZENE, TRIETHYL-**
effects as diluent on perchloric and perrhenic acid extractions by tridodecylamine, 20: 1747 (UCRL-11616(Rev.))
**BENZENE, 1,2,4-TRIPHENYL-**
preparation of, for measuring natural carbon-14 by scintillation methods, 20: 2062
**BENZENESULFONIC ACID**
heat of solution of sodium salt of, in heavy and light water, 20: 1825
**BENZOHYDROXAMIC ACID**
solvent properties for protactinium, thorium, and uranium, 20: 1776
**BENZOHYDROXAMIC ACID, *N*-PHENYL-**
solvent properties for protactinium, thorium, and uranium, 20: 1776
**BENZOIC ACID**
corrosive effects on molybdenum and vanadium, stress-, 20: 2254

(BM-RI-6680)
**BENZOIC ACID, p-(HYDROXYMERCURI)-**
binding by bacteria of, effects on radiosensitivity, 20: 1618 (NYO-3319-6)
**BENZOPHENONE**
benzene–benzophenone–isopropanol, radiolysis of, energy transfer in, 20: 1931
radiolysis in alcoholic, aqueous, and hydrocarbon solutions, solvent effects on spectra of, 20: 1920
benzophenone–naphthalene, radiolysis in alcoholic, aqueous, and hydrocarbon solutions, 20: 1920
**BENZOQUINONE**
effects on radioinduced polymerization of liquid and solid acetylene, 20: 1913
**p-BENZOQUINONE, TETRAMETHYL-**
radiolysis in alcoholic, aqueous, and hydrocarbon solutions, solvent effects on spectra of, 20: 1920
ethanol–$H_2SO_4$–tetramethyl-p-benzoquinone, radiolysis in aqueous solutions, 20: 1920
naphthalene–tetramethyl-p-benzoquinone, radiolysis in alcoholic, aqueous, and hydrocarbon solutions, 20: 1920
**BERYLLIUM**
combustion in flame environments, airborne contamination release by, 20: 2341 (SC-DC-65-1637)
condensation on sodium chloride crystals, formation of growth textures in, 20: 3306(T)
corrosion resistance to mercury at 900°F, 20: 2264
fabrication into radiators for space power systems, 20: 2293
grain refining of, by boron addition, 20: 2406(P)
iron-57 Mössbauer effect in, 20: 3145
mechanical properties and residual resistance of, 20: 2363
meson ($\pi^-$) reactions at 120 to 280 Mev, double charge exchange in, (E), 20: 3080
neutron reactions (n,$\alpha$) and (n,2n) with, multigroup cross sections for, 20: 2960
neutron scattering kernels and laws for, thermal, 20: 3412
neutron spectra in, (E/T), 20: 2968
properties as neutron reflector, 20: 3390
radiation effects on oxidation dioxide at 600 to 1000°C, 20: 2442
radiation effects on gas formation and compression fractures in, 20: 2478
reactions with combustion gases in simulated launch pad abort environments, 20: 2341 (SC-DC-65-1637)
separation from aqueous solutions by thiocyanate extraction, 20: 1974(P)
spectra of blue solutions of, in liquid ammonia, 20: 1867
**BERYLLIUM ALLOYS**
Be–Mg, corrosion in moist carbon dioxide at 650-750°C, 20: 2277(P)
Be–Ni, development of NiBe fiber-reinforced composites of, 20: 2219 (AMRA-CR-64-05/4)
Be–Re, superconductivity in, properties of, (E), 20: 2898
**BERYLLIUM IONS**
electron transitions in, collision cross sections for dipolar, 20: 2598
**BERYLLIUM ISOTOPES**
nuclear reactions of, bibliography, 20: 3007 (CEA-Bib-32)
**BERYLLIUM ISOTOPES Be-6**
production threshold for ground-state, in lithium-6 (p,n) reactions, (E), 20: 3140
**BERYLLIUM ISOTOPES Be-7**
gamma transition at 477.4 kev, (E), 20: 3043
production using ORNL 86-in. cyclotron, 20: 2212
separation from atmospheric aerosols and rain water, method for, 20: 1778
**BERYLLIUM ISOTOPES Be-9**
energy levels from delayed neutron spectra in decay of lithium-9, (E), 20: 3130
energy levels of, from boron-11 (d,$\alpha$) reactions, (E), 20: 3035
**BERYLLIUM OXIDE REACTOR EXPERIMENT**
component design modification, fabrication, and testing, 20: 3470(R) (GA-5499)
development, Apr.–June 1964, 20: 3470(R) (GA-5499)
**BERYLLIUM OXIDES**
density determination in diethylphthalate or toluene, soaking times required for, 20: 2424(R) (GEMP-52A, pp 37-42)
electric conductivity in thermocouple insulation of, analytical model for errors from, (T), 20: 2103 (LA-DC-7055)
electric conductivity at 1200 to 2000°C as function of oxygen pressure, 20: 2223(R) (GEMP-51A)
plastic deformation of polycrystalline, at 1400 to 1700°C, 20: 2371
radiation effects on properties of, effects of composition on fast neutron, 20: 2424(R) (GEMP-52A, pp 37-42)
radiation effects on reactions with graphite, at 1500°C, equipment and setup for studying, 20: 2431 (ORNL-TM-1255)
radiation effects on thermal conductivity due to microcracking, 20: 2443
radiation effects on electric conductivity of, 20: 2460
BeO–$ThO_2$–$UO_2$–$Y_2O_3$, irradiation testing of tubular fuel elements of, 20: 2467
BeO–$UO_2$, fission gas diffusion from, for 1 hr at 1400°C, 20: 3470(R) (GA-5499)
**BERYLLIUM SYSTEMS**
Al–Be–B, preparation and properties, 20: 2406(P)
Be–B, preparation and properties, 20: 2406(P)
Be–Cu–TaC, production of cermets of, 20: 2261(R) (UCRI-326)
**BETA DECAY**
matrix elements for singly forbidden transitions in, (T), 20: 3090
transitions in nuclei, interacting quasiparticle method for, (T), 20: 3101
**BETA PARTICLES**
absorption in samples of beta emitters, corrections for self-, 20: 1780
angular correlations with gamma rays from gold-198, (E), 20: 3129
detection and measurement by scintillation counting, dissolution of tissues for, 20: 1767
dose distributions from, in fallout, (T), 20: 2048 (USNRDL-TR-888)
effects of, from deposited strontium-89 or strontium-90, on adrenal glands of guinea pigs and rats, morphological, 20: 1641
effects on algal, biological, 20: 1681
effects on crystal structure of alkali halides, mechanism of, 20: 2426 (LA-3387)
effects on Drosophila spermatocytes, genetic, 20: 1657
effects on leukocyte blood picture of, 20: 1672
energy transfer to liquid phosphors, 20: 2189
use in therapy of benign joint diseases, 20: 1706
**BETA SHIELDING**
performance of aluminum and polythene as, for 0.2 to 2.5 Mev range, (E), 20: 3248 (NASA-SP-71, pp 455-63)
performance with selective vehicle orientation, for protecting space vehicles from cosmic particles, 20: 3249 (NASA-SP-71, pp 473-6)
**BETA SOURCES**
design of promethium-147, for radiobiological studies, 20: 1628(T)
measurement of gaseous, design of coincidence counters for, 20: 2139
**BETA SPECTROMETERS**
design and performance of photoelectron energy analyzer, 20: 2633
design of low-background scintillation, 20: 2180(P)
development, 20: 2520(R) (IA-920)
performance of semiconductor, for conversion coefficient measurements, 20: 3019 (ORNL-P-1657)
performance of, optimum measuring conditions for, 20: 2148
**BETATRONS**
use in radiography of heavy steel castings, 20: 2028
**BEVATRON**
development and performance of, 20: 2541 (UCRL-16228)
experimental facilities for, development of, 20: 2541 (UCRL-16228)
**BIBLIOGRAPHIES**
on a-c breakdown in gases, 20: 3160 (AD-618503)
on activation analysis, 20: 1785
on analysis of reactor fuel elements and materials, 20: 1743 (JUL-216-HW)
on annealing effects on structure of dispersion-hardened systems, 20: 2325 (HW-SA-2767)
on biological tolerance to air blast, 20: 2083 (CEX-65.4)
on creep, deformation, and fracture in alpha-zirconium alloys, 20: 2339 (ORNL-P-1753)
on direct conversion of nuclear into electrical energy, 20: 2669 (AED-C-15-07)
on fallout sample collection, 20: 2086(T) (BNL-tr-42)
on grain boundary migration in metals, 20: 3626 (ORNL-P-1722)
on heavy water production patents, 20: 1951 (AECL-2279)
on hot laboratories, 20: 1990 (TID-3545(Rev.1))
on hydrogen isotope effects on aromatic substitution reactions, 20: 1888
on hydrology of radioactive waste disposal in rivers, 20: 2082 (CEA-Bib.-59)
on methods for estimating thermodynamic properties of physico-chemical systems during phase transitions, 20: 1819 (UCRL-14287)
on Mössbauer effect data, 20: 3146
on nuclear reactions involving beryllium, 20: 3007 (CEA-Bib-32)
on plastic fatigue properties of heat resistant alloys, 20: 2320(R) (GEMP-52A, pp 23-5)
on plutonium technology, 20: 3611 (BNWL-113-8)
on preventive maintenance in chemical and mining industries, 20: 1976 (VDDIT-94)
on radiation effects on living tissues and organisms, 20: 1607 (AED-C-04-18)
on radiation effects on living tissues and organisms, 20: 1608 (AED-C-04-19)
on radiation effects on yeast, 20: 1663
on radiation effects on glass, 20: 2432 (REIC-Memo-26)
on radiochemistry of selenium, 20: 1744 (NAS-NS-3030(Rev.))
on structure of deformed internally oxidized alloys, 20: 2324 (HW-SA-3765)
on transplutonium elements, 20: 1726 (EUR-2508.e)

on wholesomeness of irradiated foods, 20: 2196 (AD-514910)
**BIG ROCK POINT POWER REACTOR**
fuel element irradiation testing in, uranium dioxide, 20: 3452
**BINDERS**
use of furfuryl alcohol-pitch in graphite fabrication, 20: 2302(P)
**BIOLOGICAL MATERIALS**
analysis for sulfur-35, method for, 20: 1758
**BIOLOGICAL MODELS**
of cell growth pattern in tissue cultures, 20: 1594 (LA-DC-6507)
**BIOLOGICAL STRESS**
radioinduced, in mammals, 20: 1716
**BIOLOGICAL SYSTEMS**
radiation injuries of, induced by charged particles, 20: 1615 (NASA-SP-71, pp 105-14)
**BIOTITES**
sorptive properties for cesium, 20: 1879
**BIPHENYL**
neutron diffusion parameters at 85 and 105°C, (E), 20: 2953
performance in thermal turbines, 20: 2019
radiolysis in alcoholic, aqueous, and hydrocarbon solutions, solvent effects on spectra of, 20: 1920
**BIPHENYL, ISOPROPYL-**
radiation effects on thermophysical properties of, neutron, 20: 1923
**BIRDS**
tritium uptake by hypophysis of organotypic culture of drake tissue, electron microscopy of, 20: 1597
**BISMUTH**
corrosive effects on structural materials, 20: 2275
diffusion of uranium in liquid, at 490 to 725°C, 20: 2368
electric conductivity at 25 to 80 kilobars, 20: 3642 (UCRL-11639)
helium-3 reactions with, yields of astatine isotopes in, 20: 1949
proton reaction with, at 400 Mev, production of astatine-203 and astatine-205 in, 20: 1948
superconductivity at 4.2°K, 20: 2521 (LNF-65/28)
**BISMUTH ALLOYS**
Bi–In, Ginzburg-Landau parameters of superconducting, (E/T), 20: 2906
Bi–In, specific heat of superconducting, in magnetic fields, (E), 20: 2906
Bi–Na, corrosive effects on carbon steel and stainless steel, 20: 2275
**BISMUTH ISOTOPES Bi-207**
gamma transitions at 569.5 and 1063.7 kev, (E), 20: 3043
**BISMUTH ISOTOPES Bi-209**
neutron scattering at 0.8 to 4.5 Mev, compound-nucleus analysis of, (T), 20: 3021 (ORNL-TM-1238)
**BISMUTH ISOTOPES Bi-214**
determination on filters by scintillation counting, 20: 2520(R) (IA-920)
**BISMUTH OXIDES**
use in bitumen-bound radiation shielding material, 20: 2248(P)
**BITUMINOUS MATERIALS**
use of pitch as binder in graphite fabrication, 20: 2302(P)
**BLAST EFFECTS**
biological tolerance of man to, from nuclear explosions, 20: 2083 (CEX-65.4)
display system for, 20: 1987 (UCRL-13139)
for nuclear excavation of sea-level Isthmian canal, evaluation, 20: 1985 (PNE-2003)
ground motion from nuclear explosion, methods for simulating air-blast-induced, 20: 1980 (AD-614990)
on reinforced concrete spherical domes, 20: 2035 (AD-615017)
physical effects of, from nuclear explosions, 20: 2078 (BNL-917, pp 1-10)
**BLOOD**
analysis for iodinated compounds using neutron activation of iodine-129, 20: 1790
analysis for vanadium with pre-irradiation separation, activation, 20: 1791
radioinduced ESR in aqueous system of human, long-lived, 20: 1605
xenon-133 content in equal volumes of air and, partition coefficients for, 20: 1599
**BLOOD CIRCULATION**
in tumors, effects of inhaled carbon dioxide on, 20: 1683
in tumors, effects of inhaled oxygen on, 20: 1683
measurement in heart of, using rubidium-84 as tracer, 20: 1709
measurements in brain of, using xenon-133 as tracer, 20: 1711
**BLOOD PICTURE**
effects of aging on, of miniature swine, 20: 1581 (BNWL-SA-341)
radiation effects on leukocyte, $\beta$-$\gamma$, 20: 1672
radiation effects on leukocyte, in guinea pigs, x, 20: 1670
**BLOOD PLASMA**
molecular weight of Factor XII in, estimated after proton irradiation, 20: 1673
**BLOOD SERUM**
activation analysis of human, for copper, manganese, and zinc, 20: 1586
effects of aging on biochemical composition of, in miniature swine, 20: 1581 (BNWL-SA-341)
**BLOOD VESSELS**
radiography of kidney, in radiation nephritis, 20: 1686
**BOILERS**
development for SNAP-50/SPUR, 20: 3554
**BOILING**
burnout and heat transfer for potassium, rubidium, and sodium saturated pool, 20: 2008(R) (AD-622825)
critical heat flux and flow regimes in water, (E), 20: 2012(R) (NYO-3304-6)
dynamics of, in power plant systems, 20: 2119
film, apparatus for, 20: 2008(R) (AD-622825)
heat transfer in sodium pool, effect of surface conditions on, (E), 20: 2017(R) (TID-22312)
pressure drop in forced-convection, of potassium in vertical tubes, (E/T), 20: 2015 (ORNL-P-1681)
subcooling measurement in water and potassium, tests of acoustic instrument for, 20: 2014 (ORNL-P-1678)
**BOILING REACTORS**
coolant decompression studies for, analysis of, (E), 20: 3324(R) (IITRI-578P21-13)
coolant demineralization for dual-purpose, 20: 3539 (ACNP-65558(Rev.1))
fuel element cans for, heat-transfer testing of "nuclear vapotron," (E), 20: 3443(R) (EURAEC-1356)
fuel element cans for, heat-transfer testing of "nuclear vapotron", 20: 3444(R) (EURAEC-1357)
fuel element cans for, heat-transfer testing of "nuclear vapotron," (E), 20: 3445(R) (EURAEC-1358)
fuel element performance in, 20: 3497
kinetic analysis of, analog and digital methods for, (E/T), 20: 3532
pressure relief device for, 20: 3363(P)
properties of graphite moderated, 20: 3322 (EUR-2448.f)
simulation of, one-group three-dimensional model for, 20: 3501
stability analysis for, (E/T), 20: 3373(R) (EURAEC-1353)
stability of natural-circulation, hydrodynamic, 20: 3516
use of plutonium fuel in, 20: 3511
**BONE MARROW**
chromium phosphate colloid distribution in, tracer studies of, 20: 1598
radiation effects on immune reactions to injected homologous, in mice, 20: 1632
radiation effects on immune reactions to injected allogenic and syngenic, in mice, 20: 1660
tissue transplants of, growth in irradiated mice, effects of arabinofurano-sylcytosine on, 20: 1687
transplants of, use for therapy of leukemia, 20: 1700
**BONES**
calcium-45 content in chicken, 20: 2520(R) (IA-920)
chromium phosphate colloid distribution in, tracer studies of, 20: 1598
electric properties of, 20: 3625(R) (NYO-3282-1)
radiotherapy of benign diseases of joint, using colloidal gold-198, 20: 1706
**BORIC ACID**
use in reactor poisoning compensation, 20: 3359(P)
boric acid–$H_3O_3$, thermal neutron spectra in, determination using integral activation techniques, (E), 20: 2965
**BORON**
content in concretes, gamma and neutron shielding parameter variations with, 20: 3253
effects on grain size of beryllium, 20: 2406(P)
effects on radioinduced embrittlement of steel, 20: 2474
separation from Incoloy 800 by electron beam melting, (E), 20: 3471(R) (GEAP-4861)
**BORON HYDRIDES**
handling of pentaborane, 20: 1727 (NASA-SP-5032)
toxicity of pentaborane, 20: 1727 (NASA-SP-5032)
**BORON ISOTOPES**
abundance of, mass spectrometric determination of relative, 20: 1774
**BORON ISOTOPES B-10**
helium-3 reactions (He-3,n), angular distributions from, (T), 20: 3121
neutron reactions with, production of helium-4 and lithium-7 in, 20: 2444
performance for nuclear pumping gas lasers, (T), 20: 2591 (ANL-7030)
triton reactions (t,p), angular distributions from, (T), 20: 3121
use in neutron capture therapy of tissues, 20: 1714
**BORON ISOTOPES B-11**
deuteron reactions (d,$\alpha$) and (d,p) at 390 to 700 kev, angular distributions from, (E), 20: 3035
proton reactions with, Dalitz diagram of carbon-12 3$\alpha$ decay in, (T), 20: 3067
recoil momentum from carbon-12 (p,2p) reactions, distribution of, (E), 20: 3081
**BORON ISOTOPES B-12**

energy levels of, from boron-11 (d,p) reactions, (E), 20: 3035
**BORON NITRIDES**
spectra of, at 1300°K, infrared emission, 20: 1823
**BORON OXIDES**
testing for use in shaft seals for potassium space power systems, 20: 2242
**BORON SYSTEMS**
Al–Be–B, preparation and properties, 20: 2406(P)
B–Cu, analysis of neutron-measurement of irradiated for helium, 20: 2444
B–Cu, radiation effects on lattice parameters and helium precipitation, 20: 2441
B–Cu, radiation effects on, 20: 2444
Be–B, preparation and properties, 20: 2406(P)
$B–UO_2(NO_3)_2–H_2O$, critical mass of, 20: 3379 (ORNL-TM-1207)
**BOSONS**
amplitudes in interactions with exchange of unstable, 20: 2779
decay of intermediate vector, De Santis model for, 20: 2784
electrodynamics of intermediate, 20: 2789
exchange in nucleon interactions, model for, (T), 20: 2726
interactions of higher-spin, with electrons, cross section for, (T), 20: 2799
interactions of system of, collective description of, (T), 20: 2792
interactions of W, coupling constant and Lagrangian for, 20: 2794
magnetic properties of charged ideal gases of, in n dimensions, (T), 20: 2833
mass of intermediate vector, bootstrap calculation of, 20: 2721
production of intermediate vector, in high-energy neutrino reactions, (T), 20: 2759 (UR-875-102)
**BRAIN**
blood circulation measurements in, tracer method using xenon-133, 20: 1711
radiation effects on developing, in dog fetus, 20: 1627(T)
radiation injuries of, induced by therapeutic x radiation doses, 20: 1713
**BRAZING**
methods for bonding graphite to niobium–zirconium alloy and stainless steel, 20: 2294
**BREATH**
thoron excretion in, after injection of thorotrast, 20: 1596
**BREEDER REACTORS**
development, 20: 3491
performance of molten-salt power, 20: 3498
**BREMSSTRAHLUNG**
attenuation in lead, 20: 3254
emission from plasma, anomalous, (E/T), 20: 3175(R) (NP-15562, pp 38-79)
emission from plasma, intensity of, (T), 20: 3200
emission of double, in electron-electron collisions at high energies, (T), 20: 2743
interactions with protons at 1 Bev, meson ($\pi^+$) production from, (E), 20: 2718
production by scattering of 0.5- to 3.0-Mev electrons by aluminum and iron, (E), 20: 3247 (NASA-SP-71, pp 449-53)
production by 0.2- to 2.5-Mev electrons on aluminum and polythene, (E), 20: 3248 (NASA-SP-71, pp 455-63)
reactions (γ,n) with fluorine-19 at 260 Mev, angular and energy distributions of fluorine-18 recoils in, (E), 20: 3108
reactions (γ,t) with oxygen-16 at 50 Mev, yield in, (E), 20: 3126
transport in matter, calculations of, (T), 20: 3246 (NASA-SP-71, pp 437-48)
yield from beta emitters, 20: 2730
**BREMSSTRAHLUNG SHIELDING**
design for electron accelerators, (T), 20: 2557
**BROMINE**
determination in food and grease samples activation, 20: 1738(R) (GA-4041)
radioinduced production in aqueous solutions, chemical behavior of atomic, 20: 2520(R) (IA-920)
reactions of, from isomeric transitions and (n,γ) reaction, 20: 1934
**BROMINE ISOTOPES Br-79**
gamma transitions following Coulomb excitation, (E), 20: 3043
**BROMINE ISOTOPES Br-82**
incorporation in bromobenzene for use in industrial tracer studies, 20: 2202
**BROMINE ISOTOPES Br-83**
decay measurements, 20: 2520(R) (IA-920)
**BROOKHAVEN ALTERNATING-GRADIENT SYNCHROTRON**
beam separator for, design of r-f, (E), 20: 2532 (BNL-9505)
**BROOKHAVEN BEAM RESEARCH REACTOR**
startup manual, 20: 3580 (BNL-9591)
**BROOKHAVEN REACTOR**
fuel burnups calculations for, 20: 3601
method for removal of in-pile loops from, 20: 3599
**BROWNIAN MOVEMENT**
quantum mechanics of, classical limit to Fokker-Planck equation in, (T), 20: 2881
**BUBBLE CHAMBERS**
uses for analyzing meson ($\pi^-$)-proton interactions, (T), 20: 2690(T) (AEC-tr-6591)
**BUBBLES**
growth in liquids, energy density in, 20: 2839
motion in BWR, analysis of, (E/T), 20: 3373(R) (EURAEC-1353)
**1,3-BUTADIENE, 2-METHYL- POLYMERS**
crystal structure of, determination of interplanar spacings using single-neutron diffraction, 20: 3308
**BUTANE, 1-CHLORO-**
butyl chloride–naphthalene, radiolysis in alcoholic, aqueous, and hydrocarbon solutions, 20: 1920
**BUTANE, 2,2-DIMETHYL-**
recoil reactions of carbon-11 in liquid, 20: 1896 (IS-T-23)
**BUTANE, 2,3-DIMETHYL-**
recoil reactions of carbon-11 in liquid, 20: 1896 (IS-T-23)
**BUTANEDIOLS**
yields in gamma radiolysis of liquid acetone, 20: 1901
**2,3-BUTANEDIONE**
yields in gamma radiolysis of liquid acetone, 20: 1901
2,3-butanedione–ethanol, radiolysis in aqueous solutions, 20: 1920
**1-BUTANOL**
dehydration over thorium oxide catalyst, 20: 1892
solvent properties for rare earth complexes with amygdalin, 20: 1796
**2-BUTANOL**
dehydration over thorium oxide catalyst, 20: 1892
**2-BUTANONE**
solvent properties for polonium chloride, 20: 1946
**2-BUTENE**
perfluoro-, radioinduced polymerization at low temperatures, 20: 1893(R) (AD-618228)
**BUTYL PHOSPHATES**
$HNO_3–TBP–H_2O$, nitric acid concentration in mixer-settler extractor as function of time, 20: 1953 (IS-T-34)
**BUTYRIC ACID, METHYL ESTER**
radiolysis and storage of tritium-labeled, self-, 20: 1938 (EUR-2452.e)

# C

**CABLES**
radiation effects on, pulsed neutron, 20: 2187 (ECOM-2545)
**CADMIUM**
determination of trace amounts of, by substoichiometric radioisotopic dilution analysis, 20: 1786
diffusion of uranium in liquid at 450 to 650°C, 20: 2368
separation of trace amounts of, from alkali metals, alkaline earths, and rare earths, 20: 1958
**CADMIUM ALLOYS**
Cd–Ag, mechanical properties of internally oxidized, 20: 3639 (UCRL-11194)
Cd–Au, entropy of formation of AuCd ordered phase, (T), 20: 2349 (UCRL-16320)
Cd–Mg, corrosive effects on carbon steel and stainless steel at 750°C, 20: 2265
Cd–Mg–Zn, corrosive effects on carbon steel, stainless steel, and tantalum at 500, 750, and 850°C, 20: 2265
**CADMIUM CHLORIDES**
$AlCl_3–CdCl_2$, spectra of reduced melts of, 20: 3623 (IS-T-36)
**CADMIUM ISOTOPES Cd-106**
gamma transition at 632.7 kev following Coulomb excitation, (E), 20: 3043
**CADMIUM ISOTOPES Cd-108**
gamma transition at 633.2 kev following Coulomb excitation, (E), 20: 3043
**CADMIUM ISOTOPES Cd-109**
production using ORNL 86-in. cyclotron, 20: 2212
**CADMIUM ISOTOPES Cd-110**
gamma transition at 657.9 kev following Coulomb excitation, (E), 20: 3043
**CADMIUM ISOTOPES Cd-111**
magnetic moment, (T), 20: 3118
**CADMIUM ISOTOPES Cd-112**
gamma transition at 617.4 kev following Coulomb excitation, (E), 20: 3043
**CADMIUM ISOTOPES Cd-114**
gamma transition at 558.5 kev following Coulomb excitation, (E), 20: 3043
**CADMIUM ISOTOPES Cd-116**
gamma transition at 513.1 kev following Coulomb excitation, (E), 20: 3043
**CADMIUM ISOTOPES Cd-117**
beta and gamma spectra of, (E), 20: 3113
**CADMIUM SULFIDES**
efficiency of silver-activated crystals of, for detection of high-energy electrons, 20: 2164
radiation effects on double acceptor defects in n-type, 20: 2499

radioinduced defects in, fluorescence studies of, 20: 2498

**CADMIUM SYSTEMS**
As–Cd–Sn, radiation effects on thermal conductivity of semiconducting $CdSnAs_2$, 20: 2488

**CADMIUM TELLURIDES**
radiation effects on double acceptor defects in n-type, 20: 2499

**CALCIUM**
corrosion resistance to mercury at 900°F, 20: 2264
determination in grease samples, activation, 20: 1738(R) (GA-4041)
deuteron elastic scattering at 26 Mev, optical model analysis of, (E/T), 20: 3053
reactions with argon atoms, cross section for, 20: 2597
separation of trace elements from, by precipitation ion exchange, 20: 1958

**CALCIUM CHLORIDES**
diffusion of water in, coefficients of, 20: 1865
$CaCl_2$–KCl, phase studies of, emanation-thermal method for, 20: 1860
$CaCl_2$–NaCl, stability of zirconium dichloride in, 20: 1822(T) (ANL-Trans-233)

**CALCIUM FLUORIDES**
radiation effects on crystal structure of, mechanism of beta, 20: 2426 (LA-3387)
thulium energy level transitions in, strain effects on, (E/T), 20: 3291

**CALCIUM ISOTOPES Ca-40**
electron inelastic scattering at 200 Mev, differential cross sections for, (T), 20: 3124

**CALCIUM ISOTOPES Ca-41**
energy-level transition probabilities of, E2, (T), 20: 3115

**CALCIUM ISOTOPES Ca-42**
neutron reactions (n,p) with, cross sections for, 20: 1947

**CALCIUM ISOTOPES Ca-43**
neutron reactions (n,p) with cross sections for, 20: 1947

**CALCIUM ISOTOPES Ca-45**
determination in algal cells by liquid scintillation, 20: 1603
uptake by dead and live algal cells, 20: 1603
uptake by hens, 20: 2520(R) (IA-920)

**CALCIUM ISOTOPES Ca-48**
beta decay of, search for double, (E), 20: 3137

**CALCIUM ISOTOPES Ca-49**
energy-level transition probabilities of, E2, (T), 20: 3115

**CALCIUM OXIDES**
hyperfine structure of, effects of cupric ions on, 20: 2520(R) (IA-920)
radiation effects on ESR of crystalline, 20: 2520(R) (IA-920)
CaO–$Fe_2O_3$, phase studies of, emanation-thermal method for, 20: 1861

**CALCIUM TUNGSTATES**
electron spin resonance of, 20: 2520(R) (IA-920)
erbium ion fluorescence in, stepwise excitation of, (E), 20: 1842(T)
magnetic resonance of trivalent ytterbium in, 20: 2520(R) (IA-920)
radioinduced luminescence in, decay time for alpha, beta, and gamma, (E), 20: 1900

**CALDER HALL REACTORS**
alarm analysis at Oldbury, computer for, 20: 3490
commissioning programs and procedures for Berkeley and Bradwell, 20: 3529
conference on Berkeley and Bradwell, 20: 3526
design of Berkeley Power Station, 20: 3528
design of Bradwell Power Station, 20: 3527
fuel management procedures, 20: 3530
performance of Berkeley and Bradwell, 20: 3531

**CALIBRATION**
of gamma sources with high specific activities, calorimetric, 20: 2195

**CALORIMETERS**
design for measurements of kinetics of radioinduced polymerization, 20: 1904
use in calibration of high-specific-activity gamma sources, 20: 2195

**CAMERAS**
design of stereoscopic framing, (E), 20: 3624 (LA-DC-7088)

**CANDU REACTOR**
control system for, 20: 3533
heavy water leak detector, 20: 2099 (AECL-2291)

**CAPTURE-TO-FISSION RATIOS**
measurement in enriched-uranium heavy-water lattices, 20: 3397
measurement in low-flux assemblies, method for direct, 20: 3430

**CARBON**
corrosion resistance to mercury at 900°F, 20: 2264
deuteron elastic scattering at 26 Mev, optical model analysis of, (E/T), 20: 3053
diffusion in chromium as function of temperature, 20: 2357(T) (AERE-Trans-1032)
diffusion in tantalum and niobium carbides at 1800 to 2700°C, layer-growth measurements of, 20: 2398
diffusion of metallic fission products in pyrolytic, method for measuring, 20: 2318(R) (GA-5915(Pt.1))
distribution in metals, determination by helium-3 activation, 20: 2227
effects on rupture of type 316 stainless steel of, in sodium, 20: 2258(R) (MSAR-65-149)
effects on strain-aging process in commercially pure niobium, 20: 2376
mass transfer from type-316 stainless steel to niobium–zirconium alloy by liquid potassium, 20: 2239
meson ($K^0$) regeneration in, 20: 2748
meson ($\pi^-$) capture reactions with, mechanism of, (E/T), 20: 3123
meson ($\pi^-$) reactions at 120 to 280 Mev, double charge exchange in, (E), 20: 3080
neutron inelastic scattering at 14.6 Mev, 20: 2962
neutron total cross section at 14.6 Mev, (E), 20: 2962
properties of pyrolytic, effects of structure on, 20: 2318(R) (GA-5915 (Pt.1))
proton shielding performance of, for space vehicles, (T), 20: 3242 (NASA-SP-71, pp 225-8)
structure of pyrolytic, deposited at 1900 to 2400°C, effects of methane concentration on, 20: 2318(R) (GA-5915(Pt.1))
transfer from stainless steels to niobium–zirconium alloy in potassium, 20: 2270
use in concretes for shielding materials, 20: 2305(P)
use with ferrous materials for fabrication of shielding materials, process for, 20: 2301(P)
Young's modulus of pyrolytic, (E/T), 20: 2446

**CARBON (ACTIVATED)**
sorptive properties for krypton-85 and xenon-133, in air, argon, carbon dioxide, and helium, 20: 1969

**CARBON DIOXIDES**
alpha stopping power of, 5-Mev, 20: 2147
corrosive effects on beryllium–magnesium alloys at 650-750°C, 20: 2277(P)
determination in helium at reduced sample pressures by gas chromatography, 20: 1751
determination of, factors affecting continuous on line, 20: 1734 (EG-Report-36)
effects of inhaled, on radiosensitivity of tumors in mice, 20: 1683
effects on deterioration of uranium fuel elements during testing in, 20: 1748 (UJV-1369/65)
effects on irradiated beryllium at 600 to 1000°C, 20: 2442
electron reactions with, vibrational excitation in fast, (E/T), 20: 2638
oxidation of chromium–iron alloys, effects of aluminum and yttrium additions on, 20: 2263
oxidation of graphite, kinetics of, 20: 2261(R) (UCRI-326)
production in irradiated and unirradiated yeasts, effects of glucose supplementation in starvation media on, 20: 1653
radioinduced reactions with graphite, effects of oxygen on, 20: 1895 (AERE-R-4988)
radiolysis mechanisms and yields of, 20: 2520(R) (IA-920)
reactions with beryllium in simulated launch pad abort environments at 800 to 1500°C, 20: 2341 (SC-DC-65-1637)
separation from ammonia in synthetic ammonia plant, tracer studies of efficiency of, 20: 1836
separation of krypton-85 and xenon-133 from, by sorption on activated carbon, 20: 1969
$CO_2$–CO–methane, effects of oxygen on radioinduced oxidation of graphite in, 20: 1895 (AERE-R-4988)

**CARBON IONS**
ionization of nitrogen by 25- to 50-kev, total, (E), 20: 2623

**CARBON ISOTOPES C-11**
recoil reactions in liquid hydrocarbons, 20: 1896 (IS-T-23)

**CARBON ISOTOPES C-12**
alpha inelastic scattering at 42 Mev, alpha-gamma coincidences in, 20: 3141
content in carbonates deposited by algae and corals in Jamaican waters, 20: 1591
decay of excited, Dalitz diagram for kinematics of $3\alpha$, (T), 20: 3067
deuteron reactions (d,$\alpha$) at 13 Mev, angular distributions from, (E/T), 20: 3106
gamma reactions ($\gamma$,n) in liquid hydrocarbons, recoil reactions of carbon-11 produced by, 20: 1896 (IS-T-23)
proton reactions (p,2p) at 50 to 110 Mev, recoil nuclei momentum distribution from, (E), 20: 3081
triton reactions (t,p), angular distributions from, (T), 20: 3121

**CARBON ISOTOPES C-13**
content in carbonates deposited by algae and corals in Jamaican waters, 20: 1591
helium-3 reactions (He-3,n), angular distributions from, (T), 20: 3121

**CARBON ISOTOPES C-14**
detection and measurement in gases, system design for low-background, 20: 2179
determination in global fallout samples, review on, 20: 2086(T) (BNL-tr-42)
determination of, precision of proportional counter for, 20: 1768

half life of, 20: 2062
incorporation in mesitylene and pseudocumene for scintillation counting of, for radiocarbon dating, 20: 2062
incorporation of recoil, in polymers formed by irradiation of ammonia–ethylene mixtures, 20: 1922
reactions with picoline and pyridine, stability and yields in, 20: 1921
uses as tracer to measure carbon dioxide removal in synthetic ammonia plant, 20: 1836

**CARBON MONOXIDES**
determination in helium at reduced sample pressures by gas chromatography, 20: 1751
nitrogen-ion reactions with, charge-transfer excitation in slow, (E), 20: 2631
reactions with beryllium in simulated launch pad abort environments at 800 to 1500°C, 20: 2341 (SC-DC-65-1637)
$CO_2$–CO–methane, effects of oxygen on radioinduced oxidation of graphite in, 20: 1895 (AERE-R-4988)
CO–O, combustion of beryllium in flame system of, 20: 2341 (SC-DC-65-1637)

**CARBON STEEL**
corrosion by bismuth and tin, 20: 2275
corrosion by bismuth-sodium alloy, 20: 2275
corrosion by molten cadmium–magnesium–zinc alloy at 500, 750, and 850°C, 20: 2265
corrosion by molten cadmium–magnesium alloys at 750°C, 20: 2265
C–Cr–Mn, radiation effects on mechanical properties of, 20: 2438

**CARBON SYSTEMS**
fabrication and phase studies on, 20: 2350(R) (USBM-RC-1205)
C–HfC, preparation and properties of, 20: 2351(R) (USBM-RC-1205, pp 3-7)
C–Hf–Ta, preparation and properties of, 20: 2351(R) (USBM-RC-1205, pp 3-7)
C–Hf–W, creep at 1800 to 2200°F of Silvania A, 20: 2333(R) (NASA-CR-54457)
C–Mo–Nb–Ta–Ti–W–Zr, creep properties at 1800 to 2200°F of Cb132M, 20: 2333(R) (NASA-CR-54457)
C–Mo–Ti–Zr, creep properties at 1800 to 2200°F of TZC, 20: 2333(R) (NASA-CR-54457)
C–Nb, phase studies on, thermal analysis of, (E), 20: 1863
C–NbC–UC, preparation as reactor fuel material, 20: 2305(P)
C–TaC, preparation and properties of, 20: 2351(R) (USBM-RC-1205, pp 3-7)
C–Ti, phase studies on, thermal analysis of, (E), 20: 1863
C–UC–ZrC, preparation as reactor fuel material, 20: 2305(P)
C–V, phase studies on, thermal analysis of, (E), 20: 1863

**CARBON TETRACHLORIDE**
Ar–$CCl_4$, reactions with uranium (IV–VI) oxide at 400 to 550°C, 20: 1816 (ORNL-TM-1258)
carbon tetrachloride–naphthalene, radiolysis in alcoholic, aqueous, and hydrocarbon solutions, 20: 1920
$CCl_4$–2,2-dimethyl propane, thermal capacities and thermodynamic properties at 5 to 300°K, 20: 3619 (COO-1149-26)
$CCl_4$–2,2-dimethyl propane, thermodynamic properties at 5 to 300°K, 20: 3618 (COO-1149-25)
$CCl_4$–2,2-dimethyl propane, thermodynamic properties of, 20: 3620 (COO-1149-27)
Cl–$CCl_4$, reactions with uranium (IV–VI) oxide at 400 to 550°C, 20: 1816 (ORNL-TM-1258)

**CARBON TETRAFLUORIDE**
neutron scattering by liquid, co-operative modes of motion from cold, (E), 20: 2837
radiolysis of liquid, electron spin resonance spectrum of oxygen fluoride radical formed in, 20: 1898(R) (RRL-2310-164)
radiolysis of, separation of molecular fluorine by, 20: 1899(T) (BNL-tr-23)

**CARBONATES**
carbon-12, carbon-13, oxygen-16, and oxygen-18 ratios in, deposited by algae and coral, 20: 1591
separation of uranium from, by solvent extraction using arsonium and phosphonium salts, 20: 1782
use in uranium yellow cake purification, 20: 1973(P)

**CARCINOGENS**
properties of fallout particles as, 20: 2053

**CARCINOMAS**
radiotherapy of bronchial, 20: 1720
radiotherapy of skin, using concentrated serial method, 20: 1718

**CARDIOGRAPHY**
effects of iodine-131 and noise on cardiac activity in dogs, 20: 1629

**CARIBBEAN SEA**
isotopic composition of algal and coral carbonates in, carbon and oxygen isotopic ratios in, 20: 1591

**CAROLINAS-VIRGINIA TUBE REACTOR**
development and operation, Jan.–March 1965, 20: 3469(R) (CVNA-242)

**CATALASES**
radiation effect on liver, in aqueous solutions, 20: 2520(R) (IA-920)

**CATHODES**
electron beam focusing from oxide-cored and tungsten hair-pin, 20: 2110

**CAVES**
bibliography on, 20: 1990 (TID-3545(Rev.1))
design for fabrication of irradiation capsules, 20: 2298
design for reactor fuel studies at BNL, 20: 2001
design for remote metallography, 20: 2247
design of KAPL remote annealing facility, modifications of, 20: 2299
design using high-level gamma source, for radiation chemistry, 20: 1929
development at Risö, Denmark, 20: 3646
development at Savannah River Laboratory, 20: 2000
filter removal system for Thorium–Uranium Recycle Facility, 20: 1995
fuel processing in, fluid-bed fluoride-volatility unit for, 20: 1971

**CAVITATION**
use in incipient boiling detector, 20: 2014 (ORNL-P-1678)

**CAVITY RESONATORS**
Q-values for, temperature dependence of, 20: 2521 (LNF-65/28)
radiation in, mode-coupling effects on spontaneous excited-particle, (T), 20: 2527

**CELLULOSE**
radiation effects on dielectric properties of, electron, 20: 1897 (NASA-TN-D-3032)

**CERAMIC COATINGS**
radiation effects on, for spacecraft, 20: 2428 (NASA-SP-55, pp 365-79)
spectra of, at 1300°K, infrared emission, 20: 1823

**CERAMIC MATERIALS**
dissolution of beryllia-containing, using mercury or silver catalyst, 20: 2252(P)
radiation effects on, compilation of projects on, 20: 2433 (REIC-Memo-27)
radiation effects on dielectric properties of, electron, 20: 1897 (NASA-TN-D-3032)
radioinduced electric conductivity in, 20: 3309

**CERIUM**
determination in rocks, spectrographic, 20: 2520(R) (IA-920)
determination using Chromotrope 2B, photometric, 20: 1772
deuteron elastic scattering at 26 Mev, optical model analysis of, (E/T), 20: 3053
ionization in K-shell by alpha particles at 3 to 4 Mev, x-ray yields from, (E), 20: 2625

**CERIUM ACETATES**
complexes with thiourea, solubility in water, 20: 1869

**CERIUM ALLOYS**
Ce–Mg, crystal structure, 20: 2399

**CERIUM CARBONATES**
thermal decomposition of, calcination and sintering study of, (E), 20: 1832

**CERIUM ISOTOPES**
yields in uranium-233 thermal fission, (E), 20: 3010(R) (IDO-14663)

**CERIUM ISOTOPES Ce-137**
yields in uranium-233 thermal fission, (E), 20: 3010(R) (IDO-14663)

**CERIUM ISOTOPES Ce-141**
content in atmosphere, 1962 to 1963, 20: 2049
content in fallout particles, 20: 2053
determination in sea water, methods for, 20: 1749 (USNRDL-TR-912)

**CERIUM ISOTOPES Ce-144**
beta decay of, praseodymium energy level spin from, (E), 20: 3033
content in atmosphere, 1962 to 1963, 20: 2049
content in fallout particles, 20: 2053
determination in sea water, methods for, 20: 1749 (USNRDL-TR-912)
distribution in uranium dioxide fuel rods, 20: 2450
separation from aqueous solutions, use of silica gel for, 20: 1742 (INR-636/XIII/J)
separation from milk by electrodialysis, 20: 1972(P)

**CERIUM OXIDES**
crystal growth and properties of, for use as laser host, 20: 2312 (AD-619197)
determination in ancient glass and natron using lithium drifted germanium diode detector, activation, 20: 1731 (BNL-9614)
thermal decomposition of hydrated, calcination and sintering study of, (E), 20: 1832

**CERIUM OXYBROMIDES**
preparation and crystal structure, 20: 1834

**CERMETS**
mechanical properties of nuclear, 20: 2381

**CESIUM**
collisions of atoms of, with rare gas atoms and hydrogen and nitrogen molecules, ionization in, (E), 20: 2639
corrosive effects on niobium–zirconium alloy at high temperatures, 20: 2268
performance in thermionic diodes, 20: 2675

production from cesium halides, 20: 1883(P)
reactions with hydrogen, production of negative molecular ions by charge-exchange, 20: 2537 (LA-DC-7268)
separation from milk, 20: 1975(P)
sorption by hydrobiotite, 20: 1879
temperature in MHD cell, (E), 20: 2673
**CESIUM ASTATIDES**
entropy and thermal capacity at 0 to 300°K, 20: 1859
**CESIUM FERROCYANIDES**
iron-57 Mössbauer spectra from, (E), 20: 3296
**CESIUM FLUORIDES**
spectroscopy of, measurement of rotational transitions in, 20: 1876
**CESIUM HALIDES**
use in the production of metallic cesium, 20: 1883(P)
**CESIUM IODIDES**
radiation effects on crystal structure of, mechanism of beta, 20: 2426 (LA-3387)
**CESIUM ISOTOPES Cs-134**
beta decay of, circular polarization of gamma rays following, (E), 20: 3051
**CESIUM ISOTOPES Cs-137**
content in milk, 20: 2046 (BIO/04/64)
content in milk in Israel, 20: 2520(R) (IA-920)
content in milk, Italy, 1964, 20: 2047 (EUR-2509.e)
deposition with respect to atmospheric release of, calculation of, 20: 2074 (AHSB(RP)M-40)
determination in sea water, methods for, 20: 1749 (USNRDL-TR-912)
distribution in uranium dioxide fuel rods, 20: 2450
separation from aqueous solutions, use of silica gel for, 20: 1742 (INR-636/XIII/J)
separation from milk by electrodialysis, 20: 1972(P)
**CHARCOAL**
sorption properties for iodine, 20: 3586 (ORNL-TM-1291)
sorptive properties for argon-41, 20: 1763
**CHARGED PARTICLE BEAMS**
density of, phase-space techniques for measuring, (T), 20: 2534 (BNL-9587)
focusing of, symmetric quadrupole magnet triplets for, (T), 20: 2539 (SLAC-47)
separation of high-energy, design of r-f separator for, (E), 20: 2532 (BNL-9505)
**CHARGED PARTICLES**
acceleration by hydromagnetic waves in slightly turbulent plasma, 20: 3192
acceleration in electrostatic fields, 20: 2561
charge and mass of, relativistic field equations for, 20: 2886
Cherenkov emission by, in circular waveguide filled with gyrotropic ferrite, (T), 20: 2550
diffusion in lower ionosphere, negative-ion effects on, (T), 20: 2853
effects on biological systems, pathological, 20: 1615 (NASA-SP-71, pp 105-14)
effects on man, pathological evaluation using fractional cell lethality calculations, 20: 1616 (NASA-SP-71, pp 219-23)
interactions with electromagnetic fields, Wightman formalism for, (T), 20: 2878
mass formula for, empirical, (T), 20: 2750 (AD-618659)
momentum in magnetic field, conic reprojection of photographs for calculating, 20: 2728
momentum in magnetic field, effects of field nonhomogeneity on photographic analysis of, 20: 2729
motion in nonuniform electromagnetic fields, (T), 20: 2529
motion in plasma, momentum probe for measuring, 20: 3179 (ORNL-P-1575)
motion of geomagnetically trapped, (T), 20: 2849
motion of, Einstein-Schroedinger theory for equations of, 20: 2869
reactions with nuclear Coulomb field, (T), 20: 3153
scattering in plasma, method of measuring, 20: 3158(R) (AD-614923)
slowing-down spectra from fast-neutron reactions in water, 20: 1924
systems of, quantum statistics of ring sum of, (T), 20: 2809
**CHELATION**
reagents for bone, tracer studies of, 20: 2520(R) (IA-920)
**CHEMICAL ANALYSIS**
methods for, of reactor fuel elements and materials, 20: 1743 (JUL-216-HW)
**CHEMICALS AND REAGENTS**
radiation effects on, compilation of projects on, 20: 2433 (REIC-Memo-27)
**CHEMISTRY**
preventive maintenance in industrial, bibliography on, 20: 1976 (VDDIT-94)
research programs on, at Risö nuclear research center, Denmark, 20: 3646
**CHERENKOV RADIATION**
emission by charged particles in circular waveguide filled with gyrotropic ferrite, (T), 20: 2550
emission in non-homogeneous plasma, effect on Landau damping of, 20: 3198
propagation in anisotropic media, 20: 2734
**CHICKENS**
calcium-45 uptake, 20: 2520(R) (IA-920)
radiation effects on aging of, exposed during embryonic development, x, 20: 1611(R) (COO-1119-4)
**CHIMERAS**
radiation effects on immune reactions in allogenic and syngenic bone marrow mouse, 20: 1660
**CHINA**
atomic explosion in, description of, 20: 2068 (AD-614895)
**CHLORELLA**
radiation effects on survival in, beta, 20: 1681
**CHLORIDES**
effects of molten, on corrosion of refractory metals by magnesium–uranium–zinc alloy and zinc, 20: 2266
**CHLORINE**
determination in drugs, hair, and oils, activation, 20: 1739(R) (GA-4297)
determination in grease samples, activation, 20: 1738(R) (GA-4041)
determination in selenium by neutron activation methods, 20: 1769
determination of, factors affecting continuous on line, 20: 1734 (EG-Report-36)
**CHLORINE COMPOUNDS**
difluorochlorine tetrafluoroborate, preparation and properties, 20: 2520(R) (IA-920)
**CHLORINE FLUORIDES**
handling of, 20: 1727 (NASA-SR-5032)
toxicity of, 20: 1727 (NASA-SP-5032)
**CHLORINE ISOTOPES Cl-35**
neutron reactions (n,$\alpha$) with, cross sections for phosphorus-32 production in, (E), 20: 3020 (ORNL-TM-1065)
nuclear quadrupole resonance and spin echo in sodium chlorates, 20: 3144
**CHLORINE ISOTOPES Cl-36**
neutron reactions (n,$\alpha$) with, cross sections for phosphorus-33 production in, (E), 20: 3020 (ORNL-TM-1065)
**CHLORINE SYSTEMS**
Cl–$CCl_4$, reactions with uranium (IV–VI) oxide at 400 to 550°C, 20: 1816 (ORNL-TM-1258)
**CHLOROPHYLLINS**
complexes with adenine and metal ions, radiosensitivity effects in mice of, gamma, 20: 1692
complexes with ammine and metal ions, radiosensitivity effects in mice of, gamma, 20: 1692
complexes with folic acid and metal ions, radiosensitivity effects in mice of, 20: 1692
complexes with metal ions, radiosensitivity effects in mice of, 20: 1692
complexes with metal ions and methionine, radiosensitivity effects in mice of, gamma, 20: 1692
**CHROMATOGRAPHIC SEPARATIONS**
description of apparatus for, of rare gases, 20: 2317 (EURAEC-1380)
**CHROMATOGRAPHY**
column sorption of radioactive substance in, calculation of, 20: 1770
equipment for preparative gaseous, 20: 1886 (CONF-641123-1)
gas, for determining deuterium content in water, 20: 1801(P)
method for, of groups of elements, 20: 1750(T) (UCRL-Trans-1245(L))
uses for analysis of carbon-14-labeled hydrocarbons for radioactive impurities, 20: 1764
**CHROMIC ACID**
corrosive effects on vanadium, stress-, 20: 2254 (BM-RI-6680)
**CHROMIUM**
corrosion resistance to mercury at 900°F, 20: 2264
crystal lattice resonant modes in, (E), 20: 3302
determination in hair, river silts, and soils, activation, 20: 1739(R) (GA-4297)
determination in soils, activation, 20: 1738(R) (GA-4041)
determination of trace amounts in uranium compounds by activation analysis, 20: 1784
diffusion of carbon and molybdenum in, as function of temperature, 20: 2357(T) (AERE-Trans-1032)
effects of additions of, on steam corrosion of niobium–tin–zirconium alloys, 20: 2255(R) (EURAEC-1323)
effects on superconducting transition temperature of lead, (E), 20: 2916
fluorescence yield of, determination of k-shell, (E), 20: 2593 (EUR-2524.e)
magnetic form factor of, method for measuring, 20: 3280 (ORNL-P-1737)
**CHROMIUM ALLOY COUPLES**
Cr–Os/Re–W, thermoelectric properties at 200 to 1800°C, 20: 2223(R) (GEMP-51A)
**CHROMIUM ALLOYS**
Al–Cr–Fe, diffusion of uranium through cladding of, research program

for, 20: 2322(R) (GEMP-52A, pp 53-4)
Al–Cr–Fe, oxidation by carbon dioxide, effects of yttrium additions on, 20: 2263
Al–Cr–Fe–Y, corrosion by steam at 550°C, effects pre-oxidation and strain on, 20: 2223(R) (GEMP-51A)
Al–Cr–Fe–Y, diffusion of uranium through cladding of, 20: 2223(R) (GEMP-51A)
Al–Cr–Fe–Y, oxidation by air at 900 and 1100°C, 20: 2223(R) (GEMP-51A)
Al–Cr–Fe–Y, radiation effects on mechanical properties of, 20: 2409(R) (AD-617319)
Cr–Fe, oxidation by carbon dioxide, effects of yttrium additions on, 20: 2263
Cr–Fe–Ni, electron-beam welding to tubesheet joints, 20: 2283 (KAPL-3110)
Cr–Ni, metallurgical properties of austenitic, (E), 20: 3471(R) (GEAP-4861)
Cr–Re, ductility, phase studies, and properties of, 20: 2323 (GEMP-314)
Cr–Ru, properties of, 20: 2323 (GEMP-314)
Cr–W, resonant lattice modes in, (E), 20: 3302

**CHROMIUM CARBIDES**
wetting by liquid cobalt, copper, iron, and nickel, 20: 1837

**CHROMIUM ISOTOPES Cr-50**
emission spectra of ions of, in ruby laser, (E), 20: 3283
gamma transition at 783.1 kev following Coulomb excitation, (E), 20: 3043

**CHROMIUM ISOTOPES Cr-51**
gamma transition at 319.8 kev, (E), 20: 3043

**CHROMIUM ISOTOPES Cr-52**
emission spectra of ions of, in ruby laser, (E), 20: 3283

**CHROMIUM ISOTOPES Cr-53**
magnetic moment, (T), 20: 3118

**CHROMIUM OXIDES**
effects on superconducting transition temperature of lead, (E), 20: 2916
spectra of, at 1300°K, infrared emission, 20: 1823
testing for use in shaft seals for potassium space power systems, 20: 2242

**CHROMIUM PHOSPHATES**
distribution of colloidal, in mice, tracer studies of, 20: 1598

**CHROMIUM STEEL**
C–Cr–Mn, radiation effects on mechanical properties of, 20: 2438
Cr–Mo, creep rupture of, effects of aging at 1100°F on, 20: 2258(R) (MSAR-65-149)
Cr–Mo, welding procedures for, electro-slag, 20: 2281(R) (EURAEC-1408)
Cr–Ni, loop corrosion tests at supercritical pressure and temperature on, 20: 2262 (WCAP-2056(Pt.6))

**CHROMOSOMES**
radioinduced aberrations of, in tomato seeds, 20: 1638
radioinduced aberrations in, of plant seedlings, 20: 1649
volume of, effects on radiosensitivity of plant cells, 20: 1610 (BNL-9611)

**CHROMOTROPE 2B**
analytical use for photometric determination of rare earths, 20: 1772

**CIRCUITS**
design of impedance-measuring devices for use in plasma, (E), 20: 3094
design of printed, computer program for, 20: 3635 (SC-TM-65-544)
design of single-wire, for remote-control devices, 20: 2003(P)
design of switching, for electric discharge control, 20: 2102 (JUL-273-PP)
development of fast, for nuclear physics, 20: 2118
performance of mass spectrometer, review of, 20: 2100 (IS-1193)

**CIVILIAN DEFENSE**
dose rates in underground structures from scattered fallout radiation, 20: 2038
fire damage to non-urban areas from nuclear attack, model for, (T), 20: 1590 (RM-3902-TAB)
food evaluation for fallout shelter rations, 20: 2067 (AD-614824)
gamma scattering into basement from infinite plane source, 20: 3272
occupancy tests in simulated fallout shelters, 20: 2071 (AD-615005)
occupancy tests in simulated community fallout shelters, environmental and organizational factors in, 20: 2070 (AD-615004)
shelter for, evaluation of survival without training in, 20: 2069 (AD-615003)
shelter program of U. S. Government, 20: 2068 (AD-614895)
shielding design for hardened structures, (T), 20: 3276
structural fragments produced by nuclear weapons, trajectory analysis of, 20: 3610 (AD-622333)

**CLAYS**
thorium and uranium abundances in, 20: 2052

**CLEANING**
method for coolant passages of water-cooled magnets, using fluorine, (E), 20: 1992
system for air, performance evaluation of BOMAEC-30 incinerator, 20: 1989 (NYO-841-2)

**CLEANING SOLUTIONS**
performance of low-pressure fluorine gas as, in coolant passages of water-cooled magnets, (E), 20: 1992

**COATINGS**
cracking of stainless steel pressure-vessel, 20: 3321(R) (ANL-7082, pp 29-53)
heat transfer testing of "nuclear vapotron" cans on fuel elements, (E), 20: 3443(R) (EURAEC-1356)
heat transfer testing of "nuclear vapotron" cans on fuel elements, (E), 20: 3444(R) (EURAEC-1357)
heat transfer testing of "nuclear vapotron" cans on fuel elements, (E), 20: 3445(R) (EURAEC-1358)
radiation effects on thermal control, for spacecraft, 20: 2428 (NASA-SP-55, pp 365-79)
removal from spent ceramic fuels, 20: 3321(R) (ANL-7082, pp 29-53)

**COAXIAL CABLES**
fabrication of superconducting, for use as delay lines, (E), 20: 3612 (CONF-651001-6)
radiation effects on, pulsed neutron, 20: 2187 (ECOM-2545)
signal transients in, radioinduced gamma and neutron, 20: 2186 (ECOM-2415)

**COBALT**
corrosion resistance to mercury at 900°F, 20: 2264
determination in iron meteorites using neutron activation analysis, 20: 2055
determination in oils and soils, activation, 20: 1739(R) (GA-4297)
determination of trace amounts in uranium compounds by activation analysis, 20: 1784
deuteron elastic scattering at 27.5 Mev, angular distribution for, (E/T), 20: 3057
effects on hardness properties of Nitinol alloy, 20: 2310 (AD-618681)
effects on superconducting transition temperature of lead, (E), 20: 2916
separation of trace amounts of, from alkali metals, alkaline earths, and rare earths, 20: 1958
wetting properties for metallic carbides, 20: 1837

**COBALT ALLOYS**
corrosion resistance to mercury at 900°F, 20: 2264
properties of V-36, strain softening effects on, 20: 2311 (AD-618925)
Co–Lu, preparation and structure of $MgCu_2$-type, 20: 2385(T)
Co–Mo, recrystallization variables of flat rolled, 20: 2313 (AD-619208)
Co–Yb, preparation and structure of $MgCu_2$-type, 20: 2385(T)

**COBALT COMPLEXES**
chlorophyllin, radiosensitivity effects in mice, gamma, 20: 1692

**COBALT COMPOUNDS**
deuterium exchange between cyclopentadienyl rings of, and methanol, 20: 1828

**COBALT ISOTOPES Co-55**
gamma spectra, (E), 20: 3132

**COBALT ISOTOPES Co-56**
beta decay of, beta–gamma directional correlation in, (E), 20: 3054
production using ORNL 86-in. cyclotron, 20: 2212

**COBALT ISOTOPES Co-58**
energy levels of, from proton reactions (p,nγ) with iron-58, (E), 20: 3077

**COBALT ISOTOPES Co-60**
beads of, automatic threading device for use in preparation of radio-applicators, 20: 1722
beta decay of, spin dependence of Rayleigh scattering from, (E), 20: 3082
determination in water, 20: 2520(R) (IA-920)
dosimetry of gamma radiation from, in tumors, calculator for, 20: 1723
use as tracer in physical oceanographic studies, 20: 2061
use in viscometers, 20: 2200

**COBALT OXIDES**
effects on superconducting transition temperature of lead, (E), 20: 2916

**COBALT URANATES**
crystal structure and density of, 20: 2400

**COELENTERATES**
carbon and oxygen isotopic ratios in carbonates deposited by coral in Jamaican waters, 20: 1591

**COINCIDENCE COUNTERS**
design for high-energy beta-active gases, 20: 2139
development of 50-channel, for fuel motion during TREAT meltdown, 20: 2221(R) (ANL-7082, pp 62-73)

**COKE**
production of particles of, for graphite manufacture, 20: 2249(P)

**COLLOIDS**
preparation of technetium-99m-labeled, for tracer use in medicine, 20: 1696 (CONF-641126-1)
radioactive, sorption of, isotherm of collective, 20: 1968

**COMMUNICATION SYSTEMS**
description and operation for German nuclear research establishment, 20: 2111

**COMPACTS**
grain growth in porous, 20: 2373
**COMPUTER PROGRAMS**
ACCEL, for printed circuit board design, for IBM-7090, 20: 3635 (SC-TM-65-544)
ALTHAEA, for burnup calculations, calibration of, 20: 3455
ASSIGN, for NMR spectral data analysis, in FORTRAN IV for IBM 7094, 20: 3645 (UCRL-16344)
BLOOST-5, for reactor kinetics and heat transfer, in FORTRAN IV for IBM-7044, 20: 3323 (GAMD-6644)
CARIBOU, for NRX fuel burnup, 20: 3583 (CRT-1187 B)
COMA, for accelerator magnet cost estimations, in FORTRAN, 20: 2545 (UCRL-16386)
CROWBAR, for electric discharge control, in FORTRAN, 20: 2102 (JUL-273-PP)
CURFIT, for fitting sets of data points, FORTRAN IV for Philco 2000-212, (E), 20: 2214 (KAPL-M-6485)
DECOMP, for NMR spectral data analysis, in FORTRAN IV for IBM-7094, 20: 3645 (UCRL-16344)
DEL, for neutron multiplication factor changes, in FORTRAN for IBM 704, 20: 3366 (ANL-7052)
for analysis of reactor excursions, 20: 3418
for calculation of derived working limits for release rates of cesium-137 and strontium-90 to atmosphere, 20: 2074 (AFSB(RP)M-40)
for hydrogen peroxide molecular properties, 20: 2520(R) (IA-920)
for properties of geometric solids, in FORTRAN for IBM 7090, 20: 3633 (SC-TM-64-1686)
for radioiodine label techniques in radioimmunochemistry in FORTRAN-II, 20: 1943
for radioisotope gamma spectra resolution, in FORTRAN II for IBM 7094, 20: 1732 (CEA-R-2850)
HAMMER, for neutron physics calculations on reactor matrices, 20: 2992
PARAMETRY II, for reactor lattice parameters, in ELLIOTT-ALGOL, 20: 3381 (UJV-1309b/65)
reactor power distribution calculations using ($r$-$\theta$) geometry, 20: 3429
SIBYL, for accelerator magnet design, in FORTRAN II for IBM 7090/94, 20: 2546 (UCRL-16389)
SNG-AD, for multigroup adjoint transport equation, 20: 2520(R) (IA-920)
SWEDE-I, for processing heat transfer data, 20: 3485(R) (WCAP-2120)
TRANSY, for solution of neutron transport equations, 20: 2990
TRIST, for IBM 7094 multiprogramming, 20: 3644 (UCRL-16199)
UNPACK, for retrieval of neutron cross section data, in FORTRAN IV and MAP for IBM-7044, 20: 3009 (GA-6685)
WIGL2, for neutron diffusion equation solutions, in FORTRAN II for Philco-2000, 20: 3382 (WAPD-TM-532)
**COMPUTERS**
data processing on SDS UO, 20: 2218
programming of IBM 7094, program for multi, 20: 3644 (UCRL-16199)
use for fluid dynamics calculations, 20: 2011 (LA-DC-7189)
use for proton depth-dose calculations for tissue, 20: 1620 (UCRL-16154)
use in nuclear radiation counting, 20: 2153
use in power plant control, 20: 2119
use in Weapons Effects Display System, 20: 1987 (UCRL-13139)
use of AEI-1040, in alarm system for Oldbury Nuclear Power Station, 20: 3490
use of analog, in model of wave propagation in open-end hollow cylinder, (T), 20: 3630 (SC-DC-65-1697)
use of analog, in finite conductivity magnetohydrodynamics, 20: 2836
use of digital, for on-line data reduction in reactor physics experiments, 20: 3433
use of digital, in on-line data analysis for Molten Salt Reactor Experiment, 20: 3591
use of digital, in nuclear data processing system, 20: 2996
use with megachannel analyzers, 20: 2123 (BNL-9590)
uses for processing scanning data, 20: 2213 (BNL-9609)
**CONCRETE AGGREGATES**
shielding parameters of, gamma and neutron, 20: 3253
**CONCRETES**
blast loading of spherical domes of reinforced, stress-strain effects of, 20: 2035 (AD-615017)
fabrication of lead- and carbon-containing, for radiation shielding, 20: 2306(P)
gamma attenuation by horizontal concrete slabs, from finite plane source, (E/T), 20: 3271
gamma dose albedos for, differential, 20: 3270
gamma dose albedos for, (T), 20: 3274
meson ($\mu$) ionization energy losses in, (T), 20: 3238 (JINR-P-2354)
neutron activation and spectra in, from accelerator neutron sources, 20: 3264
neutron age to resonance in, fission, (E), 20: 3255
neutron angular albedos for, differential thermal-, (T), 20: 3266
neutron attenuation in, from alpha reactions with tantalum, (E), 20: 2554
neutron diffusion length in, thermal, (E), 20: 3255
neutron reflection by, dose albedo distributions for fast, (E/T), 20: 2932 (ORNL-3822(Vol.1))
neutron reflection by, dose albedo distributions for fast, (E/T), 20: 2933 (ORNL-3822(Vol.2))
neutron reflection by, dose albedo distributions for fast, (E/T), 20: 2934 (ORNL-3822(Vol.3))
neutron reflection by, dose albedo distributions for fast, (E/T), 20: 2935 (ORNL-3822(Vol.4))
neutron reflection by, dose albedo distributions for fast, (E/T), 20: 2936 (ORNL-3822(Vol.5))
neutron reflection by, dose albedo distributions for fast, (E/T), 20: 2937 (ORNL-3822(Vol.6))
neutron scattering by cylinders of, fast, (E/T), 20: 3265
properties as neutron reflector, 20: 3390
shielding parameters of, gamma and neutron, 20: 3253
**CONFERENCES**
*see also introduction to Report Number Index*
Ecological Effects of Nuclear War, 20: 1588 (BNL-917)
Metallurgy, Physical Metallurgy, and Application of Titanium and its Alloys, Fifth Conference on, Moscow, March 1963, 20: 2359(T) (NASA-TT-F-338)
Metals and Alloys in Nuclear Environments, Symposium on Flow and Fracture of, ASTM, Chicago, Illinois, June 21 to 26, 1964, 20: 2470
Nuclear Magnetic Resonance and Relaxation in Solids, Proceedings of the XIIIth Colloque Ampere on, Leuven, Sept. 1964, 20: 3316
Radiation Damage in Semiconductors, 7th International Conference on Physics of Semiconductors, Paris, July 19 to 24, 1964, 20: 2480
**CONSTANTS AND CONVERSION FACTORS**
for atomic and plasma physics, 20: 3235
**CONVECTION**
effects on heat transfer in radioisotope propulsion systems, (E), 20: 2007 (AD-818026)
**CONVECTION (FORCED)**
boiling of potassium in vertical tubes, pressure drop in, (E/T), 20: 2015 (ORNL-P-1681)
burnout and hydrodynamic instability in, of water in round tubes, 20: 2009 (EUR-2490.e)
**COPPER**
argon ion scattering at 30 kev, effect of crystal structure on energy spectra of, 20: 2600
corrosion resistance to mercury at 900°F, 20: 2264
deposition on uranium carbide, 20: 2300(P)
determination in gunpowder residues, oils, and river silts, activation, 20: 1739(R) (GA-4297)
determination in human blood serum using neutron activation analysis, 20: 1586
determination in snake venom, activation, 20: 2520(R) (IA-920)
determination of trace amounts in uranium compounds by activation analysis, 20: 1784
electron-photon cascades in thick targets of, (T), 20: 3261
grain boundary energy at 200 to 1000°C, effects of silver additions on, 20: 2348 (UCRL-16051)
iron-57 Mössbauer effect in, 20: 3145
meson ($K_1^0$) regeneration in, 20: 2748
performance as cosmic-ray shielding for manned space vehicles, (T), 20: 3240 (NASA-SP-71, pp 183-8)
proton shielding performance of, for space vehicles, (T), 20: 3242 (NASA-SP-71, pp 225-8)
spectra in hollow cathode discharges, 20: 2520(R) (IA-920)
thermal conductivity of, below 1°K, (E), 20: 2383
vacancy clusters in nearly perfect crystals of, x-ray topography of, 20: 3279 (ORNL-P-1704)
wetting properties for metallic carbides, 20: 1837
**COPPER ALLOYS**
Al–Cu, neutron scattering at long wavelength by precipitations in, 20: 3285
Al–Cu–Fe–Sn–Ti–V–Zr, deformation and heat treatment effects on mechanical properties of, 20: 2309 (AD-615024)
Cu–Au, entropy of formation of AuCu ordered phase, (T), 20: 2349 (UCRL-16320)
Cu–Mn, spin ordering of paramagnetic states in superconducting, 20: 2918
Cu–Nb–Zr, radiation effects on tensile properties of, fast-neutron, 20: 2414 (AECL-2272)
Cu–W, sintering in presence of liquid phase, kinetics of, 20: 2286
Cu–Zr, conductivity, mechanical properties, and precipitation in, 20: 2334 (NP-15530)
**COPPER IONS**
effects on paramagnetic resonance of calcium oxide, 20: 2520(R) (IA-920)
**COPPER ISOTOPES Cu-63**
deuteron inelastic scattering at 10 Mev, energy levels from, (E), 20: 3073

**COPPER ISOTOPES Cu-65**
deuteron elastic scattering at 27.5 Mev, angular distribution for, (E/T), 20: 3057
**COPPER OXIDES**
radiation effects on exciton spectrum, 20: 2505
**COPPER SYSTEMS**
$Al_2O_3$–Cu, annealing effects on structure of dispersion-hardened, 20: 2325 (HW-SA-3767)
$Al_2O_3$–Cu, structure of deformed, 20: 2324 (HW-SA-3765)
B–Cu, analysis of neutron-measurement of irradiated for helium, 20: 2444
B–Cu, radiation effects on lattice parameters and helium precipitation, 20: 2441
B–Cu, radiation effects on, 20: 2444
Be–Cu–TaC, production of cermets of, 20: 2261(R) (UCRI-326)
Cu–Ag–TaC, production of cermets of, 20: 2261(R) (UCRI-326)
Cu–TaC, production of cermets of, 20: 2261(R) (UCRI-326)
**CORROSION LOOPS**
fabrication of high-temperature sodium, 20: 3321(R) (ANL-7082, pp 29-53)
operation of potassium, 20: 2008(R) (AD-622825)
tests on chromium–nickel steel in oxygenated water, at supercritical pressure and temperature, 20: 2262 (WCAP-2056(Pt.6))
**COSMIC ALPHA PARTICLES**
shielding solar-flare-produced, (T), 20: 3251 (NASA-SP-71, pp 507-12)
**COSMIC ELECTRONS**
shielding space vehicles from, use of selective vehicle orientation for, (T), 20: 3249 (NASA-SP-71, pp 473-6)
**COSMIC MESONS ($\mu$)**
production at high energies, charge ratio in, (T), 20: 2702
properties of, 20: 2665
range distribution of, underground, (T), 20: 2664
**COSMIC MESONS ($\pi$)**
production from interactions at $10^9$ kev, 20: 2665
**COSMIC PROTONS**
doses from solar-flare, calculation of, (T), 20: 2658 (NASA-SP-71, pp 527-33)
dosimetry of high-energy, performance of silicon-detector arrays for, (E), 20: 2133 (NASA-SP-71, pp 245-50)
shielding astronauts from, spherical shields for, (T), 20: 3243 (NASA-SP-71, pp 229-34)
shielding solar-flare-produced, (T), 20: 3251 (NASA-SP-71, pp 507-12)
shielding space vehicles from, minimum-mass spherical configurations for, (T), 20: 3242 (NASA-SP-71, pp 225-8)
shielding space vehicles from, use of selective vehicle orientation for, (T), 20: 3249 (NASA-SP-71, pp 473-6)
**COSMIC RADIATION**
data tabulations of, IGY, 20: 2659
data tabulations of, IGY, 20: 2660
data tabulations of, IGC, 20: 2661
distributions of trapped, engineering models for, (E), 20: 2654 (NASA-SP-71, pp 47-55)
effects on biological systems, pathological, 20: 1615 (NASA-SP-71, pp 105-14)
effects on man, pathological evaluation using fractional cell lethality calculations, 20: 1616 (NASA-SP-71, pp 219-23)
effects on manned space missions, 20: 2652 (NASA-SP-71, pp 1-4)
effects on manned military space vehicles, (T), 20: 2656 (NASA-SP-71, pp 265-86)
effects on mice and rats, pathological, 20: 1614 (NASA-SP-71, pp 97-103)
effects on occupants of high-altitude aircraft, (T), 20: 2657 (NASA-SP-71, pp 287-99)
effects on semiconductors, 20: 3239 (NASA-SP-71)
effects on space vehicles, estimates of magnitude and nature of, 20: 2036 (AD-618030)
production in galactic magnetic gas cloud, (T), 20: 2662
properties of galactic and solar, 20: 2653 (NASA-SP-71, pp 19-29)
shielding astronauts from, in Apollo Command/Service Module, (T), 20: 3244 (NASA-SP-71, pp 365-75)
shielding development for, conference, 20: 3239 (NASA-SP-71)
shielding manned space vehicles against, (T), 20: 3245 (NASA-SP-71, pp 407-14)
shielding performance for solar-flare-produced, (T), 20: 3251 (NASA-SP-71, pp 507-12)
shielding space vehicles from, use of selective vehicle orientation for, (T), 20: 3249 (NASA-SP-71, pp 473-6)
**COSMIC SHOWERS**
Lorentz factor for jets of, (T), 20: 2651 (INR-608/VI/PH)
production in copper manned-spacecraft shields, (T), 20: 3240 (NASA-SP-71, pp 183-8)
**COSMOLOGY**
energy balance in universe, neutrino radiation from stars for, (T), 20: 2587
singularities in open universes, occurrence of, 20: 2583
**CRATERS**
design for nuclear excavation of sea-level Isthmian canal, 20: 1984 (PNE-2001)
**CREEP**
equations for analysis of, 20: 2223(R) (GEMP-51A)
**CRITICAL ASSEMBLIES**
buckling measurements in sub-, by successive substitution, 20: 3399
calculation for fuel element storage, (E/T), 20: 3379 (ORNL-TM-1207)
critical dimensions for SPERT-D elements in handling and storage, 20: 3379 (ORNL-TM-1207)
critical masses and reactivity of, calculation by SNG-AD code, 20: 2520(R) (IA-920)
criticality studies of, for simulation of tungsten water-moderated rocket reactor, 20: 3571
design and development of ZPPR, 20: 3320(R) (ANL-7082, pp 1-28)
design and testing of FARET assembly 46, 20: 3320(R) (ANL-7082, pp 1-28)
design for fast reactor experiments, 20: 3376 (NP-15573)
Doppler effect measurements on fast, equipment and techniques for, 20: 3401
Doppler effect measurements in ZPR-VI, 4Z, 20: 2959
fuel fabrication for ZPR-III, 20: 2290
gamma heating in AARR, measurement using thermoluminescent detectors, 20: 2175
interactions in arrays of subcritical units, (E), 20: 2938 (UCRL-14245)
kinetics of, stationary calculations of parameters of, (T), 20: 3367 (BNWL-156)
neutron cadmium ratio and core moderating ratio in, relation between, 20: 3439
neutron Doppler measurements with ZPR-VI, 20: 3320(R) (ANL-7082, pp 1-28)
neutron transport theory in pulsed, 20: 3001
operations of MSSCEF, (E), 20: 3471(R) (GEAP-4861)
physics calculations for Borax-V and Hi-C lattices in ZPR-7, 20: 3321(R) (ANL-7082, pp 29-53)
physics measurements on AARR, 20: 3579(R) (ANL-7082, pp 54-61)
reactivity effects of sodium voids in heterogeneous slab cell, 20: 3414
**CRITICALITY STUDIES**
critical mass of curium-244 spheres, density dependence of, 20: 2995
criticality of bare slab with anisotropic scattering, (T), 20: 2986
data compilation from, 20: 3370 (CONF-651103-2)
interactions in arrays of subcritical units, (E), 20: 2938 (UCRL-14245)
neutron fission and flux distributions in light-water-moderated enriched-uranium lattices, 20: 3396
of aluminum–plutonium alloy-polyethylene lattices, 20: 3398
of enriched uranium fuel tubes in light water, 20: 3393
of graphite- and polyethylene-reflected uranium annuli, 20: 3392
of multi-region uranium dioxide and plutonium dioxide–uranium dioxide lattices, 20: 3389
of neutron reflector materials, 20: 3391
of plutonium and plutonium–uranium lattices, 20: 3394
of plutonium nitrate solutions in thin stainless steel spheres, 20: 3395
of reactor reflectors, 20: 3390
of subcritical lattices with distributed neutron absorber, using pulsed-neutron techniques, 20: 3432
on Molten Salt Reactor Experiment, 20: 3505
on simple geometrical arrays, 20: 3378 (ORNL-P-1680)
plutonium-239 and uranium-233 and -235, homogeneous, 20: 3369 (CEA-R-2814)
reactivity effects of sodium voids in heterogeneous slab cell, 20: 3414
reactivity measurements on irradiated uranium dioxide, 20: 3384
reactivity measurements by Garelis-Russell method, analysis using asymptotic reactor theory, 20: 3385
reactivity measurements on reactor media, interpretation of, 20: 3431
**CROSSROADS OPERATION**
underwater nuclear explosions in, above-surface phenomena and base surge in, 20: 1979 (AD-614814)
**CRYOSTATS**
design of liquid-helium, for Moessbauer-effect measurements, (E), 20: 3093
heat fluxes in liquid helium, calculation of, 20: 2892
**CRYSTAL DETECTORS**
crystal alignment and preparation for precision x-ray spectroscopy, 20: 2126 (CONF-650657-1)
**CRYSTAL STRUCTURE**
determination of interplanar spacings in polymers using single-neutron diffraction, 20: 3308
exciton resonance in ionic molecular crystals with nuclear hyperfine interactions, hydrogen isotope effects in, (E), 20: 1841
**CRYSTALLOGRAPHY**
dislocation arrays in heterogeneous materials, linear, (T), 20: 2335 (NYO-2394-9)
**CRYSTALS**
electron wave equations in external electric and magnetic fields, Bloch,

(T), 20: 3298
internal friction measurements in, effects of vacancy absorption and emission by lattice dislocations on, 20: 3281(T) (MLM-1276(tr))
light scattering by anisotropic spherulite–polymer discs, polarization effects in, (T), 20: 1817 (TID-22323)
light transmission by two-dimensional spherulite between crossed polaroids, 20: 3636 (TID-22319)
physical properties of plastically deformed, effects of edge dislocation dipoles on, 20: 3278 (COO-1198-222)
radiation effects on mechanical properties, 20: 2471
vibrational frequencies in distorted, sum rules for, 20: 2520(R) (IA-920)

**CURIUM FLUORIDES**
melting points, 20: 1864

**CURIUM ISOTOPES Cm-244**
critical mass of spheres of, density dependence of, 20: 2995

**CYCLOHEXANE**
deuterium exchange with hydrogen in, effects of germanium and silicon on, 20: 1838
effects on pulse radiolysis of organic solutes, spectra of, 20: 1920
radiolysis and storage of tritium-labeled, self-, 20: 1938 (EUR-2452.e)
recoil reactions of carbon-11 in liquid, 20: 1896 (IS-T-23)

**CYCLOHEXANE, METHYL-**
recoil reactions of carbon-11 in liquid, 20: 1896 (IS-T-23)

**CYCLOHEXENE**
recoil reactions of carbon-11 in liquid, 20: 1896 (IS-T-23)

**CYCLOPENTADIENYL COMPOUNDS**
deuterium exchange with methanol, 20: 1828

**CYCLOPENTANE, METHYL-**
benzene–methylcyclopentane, recoil reactions of carbon-11 in liquid, 20: 1896 (IS-T-23)
recoil reactions of carbon-11 in liquid, 20: 1896 (IS-T-23)

**CYCLOPENTENE**
octafluoro-, reactions with xenon hexafluoride, 20: 1881

**CYCLOPROPANE, METHYL-**
photolysis of, mercury-sensitized, 20: 1898(R) (RRL-2310-164)

**CYCLOTRON RADIATION**
emission from plasma, anomalous, (E/T), 20: 3175(R) (NP-15562, pp 38-79)
propagation in magnetoplasma, instabilities from oblique, (T), 20: 3181 (SU-IPR-20)

**CYCLOTRONS**
design and performance of microtron, review on, 20: 2549
use of ORNL 86-in., in radioisotope production, 20: 2212

**CYLINDERS**
elastic wave propagation in open-end hollow, analog model of, (T), 20: 3630 (SC-DC-65-1697)
gamma heating effects on infinite, (T), 20: 3325 (ORNL-P-1480)
gamma heating in infinite, with uniformly distributed gamma sources, 20: 3269

**CYTOLOGY**
cell size distribution studies using Coulter electronic counter for, 20: 1636

# D

**DATA RECORDING SYSTEMS**
design for measurement of hysteresis curves of superconductors, (E), 20: 2913
development for radiation measurements, 20: 2141

**DATA TABULATIONS**
auroral spectrograph, IGY, 20: 2851
Clebsch-Gordan coefficients for irreducible representations of SU(3), 20: 2771
cosmic-ray, IGC, 20: 2661
cosmic-ray, IGY, 20: 2659
cosmic-ray, IGY, 20: 2660
gamma intensities for radioisotope determination, 20: 1735 (EUR-2408.e)
Mössbauer effect index, 20: 3146
neutron cross sections of atoms, molecules, and nuclei, (E), 20: 3018 (NYO-72-27)
on night airglow intensities, IGY-IGC, 20: 2850
plasma thermodynamic equilibrium data, 20: 3235
radiation effects on capacitors, transient gamma, 20: 2410 (AD-617916)
spectroscopy formulas, 20: 3235
stellar atmosphere temperature structures, 20: 2564
thermal properties of metals at ambient temperature, 20: 2343 (SC-TM-65-242)
thermodynamic properties of sodium at high temperatures, 20: 1815 (NRL-6241)

**DELAY LINES**
fabrication of superconducting-cable, (E), 20: 3612 (CONF-651001-6)

**DENMARK**
fallout monitoring, 1961 to 1964, 20: 2054
nuclear research programs at Risö, review of, 20: 3646

**DENSITOMETERS**
design for liquid hydrocarbons, using x-ray transmission, 20: 2115

**DENSITY**
distribution in randomly packed beds, method for measuring, 20: 1977

**DEUTERIUM**
abstraction by tritium recoil atoms in ethylene, bond dissociation energies in, 20: 1907
crystal structure of n-, from electron diffraction, 20: 3310
determination in water, method for, 20: 1801(P)
deuteron elastic and inelastic scattering at 270 to 507 Mev/c, (E), 20: 3042
deuteron reactions (d,n) and (d,p) at 270 to 507 Mev/c, (E), 20: 3042
effects on aromatic substitution reaction, 20: 1888
effects on decompositions of acetyl peroxide, t-butyl, phenylperacetate, and t-butyl-α-phenyl perpropionate, 20: 1891
effects on exciton resonance in ionic molecular crystal, nuclear hyperfine interaction, (E), 20: 1841
exchange between methanol and cyclopentadienyl rings of cobalticinium compounds, 20: 1828
exchange with halogen in haloferrocene, 20: 1830
exchange with hydrogen in cyclohexane, effects of germanium and silicon on, 20: 1838
incorporation in glycine by direct exchange using heavy water, 20: 1833
neutron scattering by liquid, co-operative modes of motion from cold, (E), 20: 2837
nuclear quadrupole resonance in hydrated barium chlorates, 20: 3144
production of plasma jets of, by explosions, 20: 3166 (LA-DC-7252)
properties of plasma of, in two-phase radiofrequency system, 20: 3237
separation from hydrogen isotope mixtures by gas chromatography, 20: 1733 (DP-979)
separation from water by zone refining, 20: 2520(R) (IA-920)
thermal diffusion in alpha–iron and nickel at 400 to 600°C, 20: 2397

**DEUTERIUM HYDRIDES**
separation from hydrogen isotope mixtures by gas chromatography, 20: 1733 (DP-979)
D–HD, viscosity of liquid, (E), 20: 2922
H–HD, viscosity of liquid, (E), 20: 2922

**DEUTERIUM IONS**
reactions of monoatomic singly charged, with nitrogen at 10 to 65 kev, rotational and vibrational excitation of singly charged molecular nitrogen ions in, (E), 20: 2618

**DEUTERIUM SYSTEMS**
D–H, viscosity of liquid, (E), 20: 2922
D–HD, viscosity of liquid, (E), 20: 2922

**DEUTERIUM TRITIDES**
separation from hydrogen isotope mixtures by gas chromatography, 20: 1733 (DP-979)

**DEUTERONS**
interactions with protons at 30 Mev, polarization in backward elastic, (E), 20: 2706
interactions with protons at 19.3 Bev/c, neutron-proton amplitude from, (E), 20: 2712
interactions with neutrons at high energy, equation for partial amplitudes of, 20: 2740
production of polarized, design of apparatus for, 20: 2528
reactions (d,α) with carbon-12 at 13 Mev, angular distributions from, (E/T), 20: 3106
reactions (d,α) and (d,p) with boron-11 at 390 to 700 kev, angular distributions from, (E), 20: 3035
reactions (d,n) and (d,p) with deuterium at 270 to 507 Mev/c, (E), 20: 3042
reactions (d,n) with tritium at 150 to 580 kev, cross sections for polarized, (E), 20: 3039
reactions (d,p) with N = 88 to 90 nuclei, effect of deformation change on cross sections for, 20: 3125
reactions (d,p) with oxygen-18, lifetimes of oxygen-19 levels from, (E), 20: 3156
reactions (d,p) with oxygen-16, lifetimes of oxygen-17 levels from, (E), 20: 3156
reactions with lithium-7 at 380 Mev, helium-5 excited levels from, (E), 20: 3078
reactions with nuclei, angular anisotropy of fission, (E), 20: 3122
reactions with nuclei at low energies, formalism for stripping, (T), 20: 3070
scattering by aluminum and magnesium, cross sections for, (T), 20: 3026
scattering by complex nuclei at high energies, elastic, (T), 20: 3044
scattering by copper-63 at 10 Mev, energy levels from inelastic, (E), 20: 3073
scattering by deuterium at 270 to 507 Mev/c, elastic and inelastic, (E), 20: 3042

scattering by gold crystals at 13 kev, channeling in, (E), 20: 2616
scattering by nonspherical nuclei, diffraction, (T), 20: 3026
scattering by nuclei at 27.5 Mev, angular distribution for elastic, (E/T), 20: 3057
scattering by nuclei at 21.6 and 26 Mev, optical model analysis of elastic, (E/T), 20: 3053
**DIALYSIS**
use of electro-, in milk decontamination, 20: 1972(P)
**DIAMONDS**
electroluminescence of single-crystal, 20: 2520(R) (IA-920)
photoelectric effects in semiconducting, 20: 2520(R) (IA-920)
radiation effects on electric conductivity of, (E), 20: 2434(R) (TID-22242)
radiation effects on photocurrents in, 20: 2520(R) (IA-920)
radiation effects on, absorption and ESR spectra studies of, 20: 2493
**DIELECTRIC BREAKDOWN**
potentials for a-c, in gases, 20: 3160 (AD-618503)
**DIELECTRICS**
electric conduction of metal-insulator sandwich, (E/T), 20: 2405
erosion in, mechanism of dendritic, (T), 20: 2259 (SC-DC-65-1789)
radiation effects on, electron, 20: 1897 (NASA-TN-D-3032)
radioinduced electric conductivity in ceramic, 20: 3309
**DIET**
effects of radiation processed chicken, cabbage, and peaches in, on wholesomeness of rat, 20: 2199
effects on radiosensitivity of patients, 20: 1717
pyridoxine content of, effects on radiosensitivity of mice, 20: 1646
radiation effects on induction of enzymes by, in rat liver, 20: 1674
**DIFFERENTIAL EQUATIONS**
book: *Applications of Nonlinear Partial Differential Equations in Mathematical Physics*, 20: 2530
**DIFFERENTIAL THERMAL ANALYSIS**
instrumentation for high-temperature, (E), 20: 1863
**DIODES**
design and performance of cesium plasma, 20: 2675
radiation effects on, model for predicting transient, 20: 2412(R) (AD-618079)
radiation effects on, transient neutron, 20: 2190
tunneling characteristics of superconducting lead film, geometrical resonance in, (E), 20: 2909
**DIRECT ENERGY CONVERSION DEVICES**
bibliography on, 20: 2669 (AED-C-15-07)
design of electromagnetic, 20: 2676(P)
**DISASTERS**
hazards to public of major reactor, 20: 2520(R) (IA-920)
**DISTILLATION APPARATUS**
sampler for sodium, engineering drawings of, 20: 1799
**DOGS**
cardiac activity in, effects of iodine-131 and noise on, 20: 1629
radiation effects on conditioned-reflex activity of, exposed *in utero*, 20: 1627(T)
radiation effects on cardiac function in, $\gamma$, 20: 1652
radioinduced nephrosis in, pathology of, 20: 1686
toxic effects of nine radiographic contrast medias in, 20: 1724
**DOSIMETERS**
development of fast-neutron, semiconductor, 20: 2134 (TID-22335)
development of glass, 20: 2143
modification of silver-activated phosphate glass, for low dose measurements, 20: 2122 (AD-622626)
radiation effects on glass, bibliography on, 20: 2432 (REIC-Memo-26)
reading device for phosphate-glass-block, 20: 2181(P)
**DRESDEN POWER REACTOR**
control rod drive system for Unit 2, 20: 3476 (NP-15538(Vol.1))
coolant circulation in Unit 2, jet pump development for, 20: 3476 (NP-15538(Vol.1))
design and development of Unit 2, 20: 3476 (NP-15538(Vol.1))
design of Unit 2, engineering drawings for, 20: 3477 (NP-15538(Vol.2))
hazards analysis of Unit 2, 20: 3476 (NP-15538(Vol.1))
site analysis for Unit 2, 20: 3478 (NP-15538(Vol.3))
**DROPS**
dispersion of uniform, process for, 20: 1800
**DROSOPHILA**
radiation effects on immature and mature male, genetic, 20: 1644
radiation effects on spermatocytes, genetic, 20: 1657
radiation effects on, genetic, 20: 1622 (WT-820)
radiation effects on heterogeneous population of, genetic, 20: 1642
radiation effects, genetic, 20: 1619(R) (TID-22293)
radiation injuries of gonads of, protective effects of sulfhydryl compounds, 20: 1619(R) (TID-22293)
**DRUGS**
analysis in crime detection, activation, 20: 1739(R) (GA-4297)
analysis in crime detection, activation, 20: 1740(R) (GA-4576)
effects of arabinofuranosylcytosine, on growth of injected bone marrow cells in irradiated mice, 20: 1687
**DRYING APPARATUS**
design for freeze drying filterable radioactive waste products, 20: 3607(P)
**DUST HAZARDS**
from nuclear explosions, 20: 2083 (CEX-65.4)
**DUSTS**
gravitational collapse of sphere of charged, relativistic model for, (T), 20: 2879
**DYSPROSIUM**
determination in zirconium, spectrographic, 20: 2520(R) (IA-920)
determination using Chromotrope 2B, photometric, 20: 1772
**DYSPROSIUM CHLORIDES**
reactions with sodium fluosilicates, precipitation in, 20: 1870
**DYSPROSIUM OXIDES**
magnetic susceptibility at 4 to 300°K, 20: 3318
phase studies of, at 2200 to 2300°C, 20: 1827
**DYSPROSIUM OXYBROMIDES**
preparation and crystal structure, 20: 1834

# E

**ECOLOGY**
of boral forests, effects of spruce budworms and insecticides on, 20: 1589 (BNL-917, pp 61-8)
of forest fires from nuclear attack, model for, (T), 20: 1590 (RM-3902-TAB)
radiation effects on, thermal, 20: 2079 (BNL-917, pp 11-19)
radiation effects on, from nuclear explosions, 20: 2080 (BNL-917, pp 20-36)
radiation effects on, of forests, 20: 2081 (BNL-917, pp 39-60)
**EGGS**
calcium-45 content in chicken, 20: 2520(R) (IA-920)
**ELASTICITY**
equations in relativity theory, 20: 2868
**ELECTRIC ARCS**
gas heating by, (T), 20: 2840
**ELECTRIC CONDENSERS**
radiation effects on, data tabulations on transient gamma, 20: 2410 (AD-617916)
radiation effects on, transient neutron, 20: 2190
switching circuits for, crowbar, 20: 2102 (JUL-273-PP)
**ELECTRIC CONDUCTIVITY**
model for, of thermocouple insulation, (T), 20: 2103 (LA-DC-7055)
**ELECTRIC CONDUCTORS**
design for supplying power and support to mobile elements, 20: 3353(P)
magnetic flux compression in, models for, (T), 20: 2523 (SC-RR-65-449)
signal transients in, radioinduced gamma and neutron, 20: 2186 (ECOM-2415)
**ELECTRIC CURRENTS**
measurement of persistent, in superconducting rings, 20: 2927
**ELECTRIC DISCHARGE**
control of, crowbar circuits for, 20: 2102 (JUL-273-PP)
electron density in toroidal, microwave measurement of, 20: 3180 (SEL-63-116)
in argon, striated plasma column in h-f, (E), 20: 3203
magnetic field effects on, between coaxial cylinders, 20: 3202
microwave–plasma interactions in, (E/T), 20: 3157 (AD-614654)
spectroscopy of, design of fast shutters for, (E), 20: 2125 (CEA-R-2816)
**ELECTRIC FIELDS**
effects on plasma diffusion and drift, (T), 20: 2858
electron beam diocotron instability in crossed magnetic and, (T), 20: 3252 (NP-15578)
electron swarms in gases in uniform, Townsend energy ratio for, (E), 20: 2825
plasma flute instability in inhomogeneous, 20: 3210
plasma production in crossed magnetic and, (E), 20: 3177 (NP-15570)
screening effects in theta-pinch coils, 20: 3190
**ELECTRIC GENERATORS**
design of reheat turbo-, for 1000-Mw(e) plant, 20: 3485(R) (WCAP-2120)
performance of electrogasdynamic, (E), 20: 2667(R) (AD-614907)
pumps for space Rankine-cycle, development of thermoelectromagnetic, 20: 1988 (E) (NAA-SR-11198)
**ELECTRIC MOMENTS**
radiation from dipole, in warm plasma column, 20: 3161 (AD-618520)
**ELECTRIC POWER**
generation by slender channel electrohydrodynamics, (E), 20: 2667(R) (AD-614907)
production using MHD-reactor combinations, economics of, 20: 2670 (LA-DC-7330)
production using rocket engine exhaust streams, feasibility of devices for, 20: 2668 (AD-615124)
**ELECTRIC PROBES**

development of momentum, for plasma studies, 20: 3179 (ORNL-P-1575)
effects of resonance, in plasma, (E/T), 20: 3175(R) (NP-15562, pp 38-79)
production of, bibliography on direct-conversion, 20: 2669 (AED-C-15-07)
**ELECTRIC PROPERTIES**
of tissues, 20: 3625(R) (NYO-3282-1)
**ELECTRICITY**
production by direct conversion of heat from nuclear fission, 20: 2676(P)
**ELECTROCHEMICAL ANALYSIS**
equipment for sodium oxides, 20: 3321(R) (ANL-7082, pp 29-53)
**ELECTRODES**
design of grooved, for magnetohydrodynamic generators, 20: 2677(P)
plasma flow between cooled metal, (E), 20: 2672
radiation effects on potential of mercury oxide, 20: 1932
**ELECTROHYDRODYNAMICS**
energy conversion in slender channel, (E), 20: 2667(R) (AD-614907)
**ELECTROLYTES**
solvation in mixed solvents, ionic free energy of, 20: 2520(R) (IA-920)
**ELECTROMAGNETIC FIELDS**
charged-particle motion in nonuniform, (T), 20: 2529
equations for, Lorentz invariance of, 20: 2874
equations in relativity theory, 20: 2869
interactions with charged particles, Wightman formalism for, (T), 20: 2878
interactions with plasma, MHD theory for high-frequency, 20: 3207
**ELECTROMAGNETIC PUMPS**
development of thermoelectromagnetic, for Rankine-cycle space power plants, (E), 20: 1988 (NAA-SR-11198)
**ELECTROMAGNETIC SEPARATION**
magnetic sector field image aberrations in, (T), 20: 2209 (SGAE-PH-26/1965)
**ELECTROMAGNETIC WAVES**
detection and propagation along cylindrical antenna in warm plasma, (T), 20: 2097 (AD-618396)
emission from axially oriented electric dipole in column of warm plasma, (T), 20: 3161 (AD-618520)
emission with continuous spectra during solar flares, 20: 2580
energy density of converging shock, (T), 20: 2839
interactions in partially ionized gas, (T), 20: 2814
propagation in anisotropic plasma in disk-loaded waveguide, mode perturbation in, (E), 20: 3219
propagation on plasma surfaces, solution of equations for, 20: 3231
**ELECTROMAGNETISM**
theory of, vectors in relativistic, 20: 2875
**ELECTROMETERS**
design for measuring ionization chamber charges, 20: 2183(P)
**ELECTRON BEAMS**
dosimetry of, performance of photographic film detectors for, 20: 2156
effects on polymerization of styrene with polyvinyl ester, 20: 1910
effects on polymerization of 1,1,3-trihydroperfluoropropyl acrylate and 1,1,7-trihydroperfluoroheptyl acrylate, 20: 1911
focusing of, from oxide-cored and tungsten hair-pin cathodes, 20: 2110
interactions with electron and positron beams, theoretical aspects of, 20: 2687 (LNF-65/25)
reactions with hydrogen, oscillatory excitation in, 20: 1843
stability in crossed fields, diocotron, (T), 20: 3252 (NP-15578)
**ELECTRON MICROSCOPY**
study in *Micrococcus radiodurans*, 20: 1584
**ELECTRON PAIRS**
production in collapsing stars, (T), 20: 2588
**ELECTRON SOURCES**
beam focusing from oxide-cored and tungsten hair-pin, 20: 2110
**ELECTRONIC EQUIPMENT**
design for measuring collision processes in plasmas, 20: 3158(R) (AD-614923)
design of impedance-measuring devices for use in plasma, (E), 20: 3094
design of phase locking systems for proton storage rings, (E), 20: 2535 (CERN-65-31)
development, 20: 2107
packaging of, method for precision microballoon-filled epoxy, 20: 3634 (SC-TM-65-462)
radiation effects on, compilation of projects on, 20: 2433 (REIC-Memo-27)
radiation effects on, transient neutron, 20: 2190
x-ray emission from, monitor design for detection and measurement of, 20: 2121 (AD-614832)
**ELECTRONICS**
development of fast, for nuclear physics, 20: 2118
**ELECTRONS**
absorption by aluminum and polythene shields, at 0.2 to 2.5 Mev, (E), 20: 3248 (NASA-SP-71, pp 455-63)
bremsstrahlung emission by plasma, (T), 20: 3200
capture and loss by light fast ions in reactions with atoms, (T), 20: 2634
confinement for prolonged periods, magnetic mirror trap for, (E), 20: 3225
content in ionosphere, determination from proton-whistler measurements, (T), 20: 2847 (AD-614716)
density in afterglow plasma, microwave diagnostics of, (E), 20: 3193
density in ionospheric F(2) region during low and medium sunspot activity, 20: 2848 (AD-615111)
density in toroidal discharges, microwave measurement of, 20: 3180 (SEL-63-116)
density measurement in plasma using laser-light scattering, 20: 3234
diffraction by crystalline hydrogen, 20: 3310
diffusion and losses in Astron E-layer, (T), 20: 3183 (UCRL-14275)
distribution functions for gases of, calculation of radial, (T), 20: 2830
effects on algal, biological, 20: 1681
effects on calcium tungstate, luminescence decay time for, (E), 20: 1900
effects on diamonds, absorption and ESR spectra studies of, 20: 2493
effects on dielectrics, 20: 1897 (NASA-TN-D-3032)
effects on electric conductivity of diamond and rubidium and sodium bromides, (E), 20: 2434(R) (TID-22242)
effects on electron mobility in gallium arsenide, 20: 2514
effects on gallium arsenides, 20: 2501
effects on germanium, hot carrier techniques for studying, 20: 2483
effects on germanium, annealing of, 20: 2484
effects on germanium and silicon, 20: 2491
effects on germanium and silicon at 10 to 60 Mev, 20: 2517
effects on impurity diffusion in silicon, 20: 2508
effects on mechanical properties of carbon–chromium–manganese steel, 20: 2438
effects on n-type cadmium sulfide, cadmium telluride, and zinc selenide semiconductors, 20: 2499
effects on organic solutes in alcoholic, aqueous, and hydrocarbon solutions, solvent effects on spectra of, 20: 1920
effects on p-type germanium at 0°C, annealing of, 20: 2485
effects on semiconducting properties of silicon carbide, 20: 2504
effects on silicon, EPR studies of, 20: 2490
effects on silicon, annealing of, 20: 2507
effects on silicon junctions, 20: 2511
effects on silicon, anisotropy of displacement energy for, 20: 2515
effects on silicon at ~30 Mev, 20: 2518
effects on silicon transistor resistance, carrier removal in, (E), 20: 2188
effects on thorium desorption from rhenium and tungsten, (E), 20: 2434(R) (TID-22242)
effects on zinc selenides, ESR studies of, 20: 2492
emission from hydrogen ions, vibration energy levels from, (E), 20: 2633
energy spectra and flux of geomagnetically trapped, (T), 20: 2849
flux in gases in uniform electric fields, Townsend energy ratio for, (E), 20: 2825
interaction energy operator for, reduced matrix elements of spin-spin operator for, 20: 2605
interaction energy operator for, reduced matrix elements of spin-orbit, 20: 2606
interaction operator for, Feynman diagram for, 20: 2607
interaction operator for, Feynman diagrams for, 20: 2608
interactions of runaway, with plasma in S-1 stellarator, (E), 20: 3186
interactions with positrons, meson pair production cross sections for, (T), 20: 2753 (JINR-P-2300)
interactions with mesons ($\pi$), Mandelstam representation of, (T), 20: 2678 (AD-614843)
interactions with polarized protons, Born approximation for elastic, (T), 20: 2686 (LNF-65/22)
interactions with electrons and positrons, Coulomb Regge poles in, 20: 2782
interactions with particles of higher spin, cross section for, (T), 20: 2799
interactions with electrons at high energies, two-photon emission in, (T), 20: 2743
light scattering by, in plasma, 20: 3232
magnetic moment of, method for calculation of, 20: 2601
mass number of, involvement in empirical mass formula, (T), 20: 2750 (AD-618659)
mass of, Lorentz invariance for rest, 20: 2874
plasma of hot, containment in minimum-B and mirror fields, (E), 20: 3184 (UCRL-14310)
reactions in thick targets, electron-photon cascades in, (T), 20: 3261
reactions with atmospheric nitrogen, cross sections for, 20: 2859
reactions with atoms and ions, breakup in, (T), 20: 2646
reactions with atoms, attachment in, (T), 20: 2647
reactions with carbon dioxide, ethylene, and nitrogen oxides, vibrational excitation in fast, (E/T), 20: 2638
reactions with molecular hydrogen ions, dissociation cross sections for, (E), 20: 2632
reactions with potassium bromide crystals, $\alpha$ and F centers induced in,

20: 1919
scattering by aluminum and iron at 0.5 to 3.0 Mev, bremsstrahlung from, (E), 20: 3247 (NASA-SP-71, pp 449-53)
scattering by aluminum and tungsten, measurement of diffractive, (E), 20: 2434(R) (TID-22242)
scattering by helium-4 at 200 Mev, differential spectra of inelastic, (E), 20: 3086
scattering by hydrogen, s-wave phase shift bounds for, 20: 2815
scattering by nuclei at high and low energies, phase shifts for elastic, (T), 20: 2635
scattering by nuclei, (T), 20: 3152
scattering by nuclei, amplitude of inelastic, (T), 20: 3124
scattering of slow, by atomic oxygen, (T), 20: 2617
scattering on mercury at 3.5 ev, polarization in, (E), 20: 2615
self-consistent equations including exchange and correlation effects for homogeneous gas of, (T), 20: 3216
temperature in partially ionized gas, equations for, 20: 2814
transitions in diatomic molecules, methods for calculating spectral absorption coefficients of, 20: 1803 (AD-619266)
transport in matter, calculations of, (T), 20: 3246 (NASA-SP-71, pp 437-48)
velocity distribution in nonisothermal plasma, (T), 20: 3188
wave equation for Bloch, in external electric and magnetic fields, (T), 20: 3298
yields of secondary, from krypton ion reactions with uranium dioxide, 20: 1813 (EUR-2515.e)

**ELEMENTARY PARTICLES**
dispersion relations for, algebra of currents in, (T), 20: 2755 (JINR-E-2329)
interactions at high energies, properties of forward amplitudes for, (T), 20: 2762
interactions of higher-spin, with electrons, cross section for, (T), 20: 2799
interactions of, asymptotic and threshold values of amplitudes for, (T), 20: 2763
interactions of, amplitude for four-body, (T), 20: 2791
interactions of, boundary of Landau surface of arbitrary Feynman diagrams for, 20: 2780
interactions of, charge branching ratios in statistical model for, (T), 20: 2760
interactions of, $C_2$ group and symmetry of weak, 20: 2794
interactions of, calculation method using phenomenological amplitudes, 20: 2804
interactions of, De Santis model for weak, 20: 2784
interactions of, Nakanishi's inequality for, (T), 20: 2767
interactions of, pole approximation and unstable boson exchange in, 20: 2779
interactions of, quantum mechanical approach to strong, (T), 20: 2816
interactions of, review of, 20: 2665
interactions of, renormalization of strangeness-changing axial-vector coupling constant for, 20: 2722
interactions of, Regge poles and cuts mixing in model for, (T), 20: 2768
interactions of, S-matrix theory for double, (T), 20: 2774
interactions of, theory of weak, 20: 2759 (UR-875-102)
interactions of, transverse momentum distribution of secondaries from, (T), 20: 2681 (IFA-CR-55)
interactions of, time-dependent perturbation theory for, (T), 20: 2776
interactions of, three-particle partial amplitudes and unitarity conditions for complex values of angular momentum in, (T), 20: 2811
interactions of, unitary spin selection rules for weak, 20: 2520(R) (IA-920)
interactions of, Wolfenstein model for CP-nonconservation and $\Delta T = \frac{1}{2}$ rule in, 20: 2798
kinetics of many-body systems of, group theoretical treatment for phase space for nonrelativistic, (T), 20: 2772
kinetics of three-body systems of, phase space for nonrelativistic, (T), 20: 2773
mass formulas in nonrelativistic quark and SU(6) models for, 20: 2807
mass formulas in SU(3), electromagnetic, (T), 20: 2764
mass formulas in $U(6) \otimes U(6)$, 20: 2752 (IC/65/77)
mass of $Z^-$, in unitary symmetry models, 20: 2520(R) (IA-920)
mass relations in unitary multiplets for strongly-interacting, 20: 2796
model for 56-plet SL(6), form factors and matrix elements in, 20: 2803
model for, mass relations and symmetry properties from oscillator, 20: 2800
model for, spin and unitary content of SU(6) supermultiplets in, 20: 2802
model for, survey of quantum approach for, 20: 2758 (UR-875-100)
model of hadrons, higher unitary symmetry groups for shell, 20: 2781
models for, SU(3) scheme in relativistic oscillator, 20: 2778
motion in external gravitational field, one-point model for, 20: 2867
production mechanisms for, review of, 20: 2665
quark model with even-charged mesons, baryon charge degeneracy in SU(6), 20: 2806
representations with complex spin, rotation group in, 20: 2805
research on, review of, 20: 2693
scattering by nuclei, polarization asymmetry in spin-flip inelastic, (T), 20: 3076
scattering of, infrared singularities in cross sections from, (T), 20: 2754 (JINR-P-2309)
search for, with greater than proton mass, (E), 20: 2742
symmetries for, branching rules for simple Lie group, (T), 20: 2769
symmetries for, Clebsch-Gordan coefficients for irreducible representations of SU(3), 20: 2771
symmetries for, irreducible representations of $C_2$ group and Racah tensors for, (T), 20: 2793
symmetries for, isotropic tensors for, (T), 20: 2761
symmetries for, Racah algebra for arbitrary group, (T), 20: 2775
symmetries for, review of, (T), 20: 2766
symmetries for, recursion relations for Wigner coefficients of unitary group, (T), 20: 2770
symmetries of, sum rules for massive vector gauge fields in, 20: 2783
symmetry for, Dashen and Gell-Mann method in SU(6), (T), 20: 2787
symmetry for, parastatistics of, (T), 20: 2751 (IC/65/51)
symmetry for, relativistic generalization of SU(3), 20: 2777(T)
symmetry groups for, irreducible representations for $Sp_4$ and $SO_5$, 20: 2795
symmetry models for, U-spin in higher, 20: 2520(R) (IA-920)
theory for, normal products in terms of functional integrals in S-matrix, 20: 2765

**ELEMENTS**
distribution of heavy, in uranium dioxide fuel rods, 20: 2450
neutron cross sections of, tabulations, (E), 20: 3018 (NYO-72-27)
proton reactions at 160 and 450 Mev, nucleon spectra from, (T), 20: 3260
separation of groups of, by paper chromatography, 20: 1750(T) (UCRL-Trans-1245(L))
synthesis and destruction in stars, (T), 20: 2565

**ELK RIVER POWER REACTOR**
fuel burnup in, 20: 3499
pressure vessel serviceability, (E), 20: 3482(R) (SWRI-1228-75)

**EMBRYOS**
radiation effects on development of nervous system in dogs, 20: 1627(T)
radiation effects on development of wheat, 20: 1666
radiation effects on developing avian, x, 20: 1611(R) (COO-1119-4)

**EMISSION SPECTRA**
source for, use of d-c arc plasma jet as, 20: 2649

**ENDOCRINE GLANDS**
radiation effects on function and morphology of, x, 20: 1671

**ENERGY**
radiative transfer of, transport theory of, 20: 2731

**ENGINEERING TEST REACTOR**
fuel irradiation testing in, 20: 2429 (ORNL-3837)

**ENGLAND**
radon content in living and working environments in Finsbury Borough, 20: 2090

**ENZYMES**
radiation effects on tyrosine-tyrosinase systems, 20: 1647
radiation effects on dietary and hormonal induction of, in rat liver, 20: 1674
radiosensitivity of dry, correlation with molecular weight, 20: 1673

**EPITHELIUM**
radiation effects on desoxyribonucleic acid content of cells of corneal, in rats, 20: 1633
radiation effects on metabolism of desoxyribonucleic acid in tongue, of rats, 20: 1634

**EQUATION OF STATE**
for matter at supernuclear density, (T), 20: 3016 (NASA-TN-D-3020)

**ERBIUM**
determination using Chromotrope 2B, photometric, 20: 1772
reactions with potassium phosphate, 20: 1873
separation from thorium and other rare earths by ion exchange in ammonium thiocyanate–organic solvent–water systems, 20: 1959

**ERBIUM IONS**
fluorescence in calcium tungstate crystals, stepwise excitation of, 20: 1842(T)

**ERBIUM ISOTOPES Er-166**
neutron capture by, gamma spectra and erbium-167 level scheme from, (E), 20: 3127

**ERBIUM ISOTOPES Er-167**
energy levels and gamma spectra from neutron capture by erbium-166, 20: 3127

**ERBIUM OXIDES**
magnetic susceptibility at 4 to 300°K, 20: 3318

**ERBIUM OXYBROMIDES**
preparation and crystal structure, 20: 1834

**ERBIUM PHOSPHATES**
solubility in salt solutions, sulfuric acid, and water, 20: 1873
**EROSION**
mechanism of dendritic, in dielectrics, (T), 20: 2259 (SC-DC-65-1789)
**ESCHERICHIA COLI**
radiation effects on desoxyribonucleic acid synthesis in, x, 20: 1639
radiation effects on lysis inhibition by bacteriophage in, 20: 1650
radiosensitivity of, strain difference in, x, 20: 1639
radiosensitivity of, in water, gamma, 20: 1645
ribosomes of, messenger RNA binding by, 20: 1592 (BNL-7903)
**ESTERS**
ester–urea, ESR studies of irradiated, 20: 1935
**ETHANE**
photolysis of, far uv flash, 20: 1898(R) (RRL-2310-164)
yields in recoil reactions of carbon-11 in liquid hydrocarbons, 20: 1896 (IS-T-23)
**ETHANETHIOL, 2-AMINO-**
effects of, against radioinduced genetic damage in Drosophila, 20: 1619(R) (TID-22293)
radiosensitivity effects on rat fetuses, 20: 1693
**ETHANOL**
dehydration over thorium oxide catalyst, 20: 1892
effects on pulse radiolysis of organic solutes, spectra of, 20: 1920
separation from water by ion exchange, 20: 2520(R) (IA-920)
ethanol–naphthol–$H_2SO_4$, radiolysis in aqueous solutions, 20: 1920
ethanol–naphthalenesulfonic acid–$H_2SO_4$, radiolysis in aqueous solutions, 20: 1920
ethanol–$H_2SO_4$–tetramethyl-*p*-benzoquinone, radiolysis in aqueous solutions, 20: 1920
2,3-butanedione–ethanol, radiolysis in aqueous solutions, 20: 1920
**ETHENETETRACARBONITRILE**
radioinduced polymerization of, at low temperatures, 20: 1893(R) (AD-618228)
**ETHER, BIS(2-BUTOXYETHYL)**
uses in dissolution of tissues for scintillation counting, 20: 1767
**ETHERS**
ether–urea, ESR studies of irradiated, 20: 1935
**ETHYL ETHER**
effects on radioinduced polymerization of formaldehyde, 20: 1914
effects on radioinduced polymerization of formaldehyde with acrylonitrile, isobutene, methyl methacrylate, and styrenes, 20: 1914
**ETHYL PHOSPHATES**
composition of ethyl metaphosphate, spectral determination of, 20: 3640 (UCRL-11488)
**ETHYLAMINE**
$NH_3$–ethylamine–K, spectra of metal in, electron paramagnetic resonance and optical, 20: 1808 (COO-958-5)
**ETHYLENE**
determination of, factors affecting continuous on line, 20: 1734 (EG-Report-36)
electron reactions with, vibrational excitation in fast, (E/T), 20: 2638
photolysis of gaseous, 20: 1898(R) (RRL-2310-164)
radiolysis of liquid, effects of argon on hydrogen yields in, 20: 1898(R) (RRL-2310-164)
reactions with recoil tritium atoms, bond dissociation energies and hydrogen abstraction in, 20: 1907
yields in recoil reactions of carbon-11 in liquid hydrocarbons, 20: 1896 (IS-T-23)
$NH_3$–ethylene, radioinduced polymerization of, recoil carbon-14 labeling in, 20: 1922
**ETHYLENE, CHLORO- POLYMERS**
with dichloroethylene, radiation effects on dielectric properties, 20: 1897 (NASA-TN-D-3032)
**ETHYLENE, DICHLORO-**
radioinduced polymerization on stretched polyethylene film, 20: 1902
**ETHYLENE, DICHLORO- POLYMERS**
with chloroethylene, radiation effects on dielectric properties, 20: 1897 (NASA-TN-D-3032)
**ETHYLENE, DIFLUORO-**
radioinduced polymerization of, at low temperatures, 20: 1893(R) (AD-618228)
**ETHYLENE, FLUORO-**
radioinduced polymerization of, at low temperatures, 20: 1893(R) (AD-618228)
**ETHYLENE POLYMERS**
crystal structure of, determination of interplanar spacings using single-neutron diffraction, 20: 3308
electron shielding properties of, at 0.2 to 2.5 Mev, (E), 20: 3248 (NASA-SP-71, pp 455-63)
neutron scattering by crystals of, at 0.17 to 0.50 ev, (E/T), 20: 2964
neutron spectra in cooled, thermal, (E), 20: 2945
phonon frequencies in highly crystalline, 20: 3315
properties as neutron reflector, 20: 3390
properties as neutron reflectors, 20: 3391
proton shielding performance of, for space vehicles, (T), 20: 3242 (NASA-SP-71, pp 225-8)
radioinduced polymerization of vinylidene chloride on, 20: 1902
**ETHYLENE, TETRACHLORO-**
effects as diluent on perchloric and perrhenic acid extractions by tridodecylamine, 20: 1747 (UCRL-11616(Rev.))
**ETHYLENE, TETRAFLUORO-**
radioinduced polymerization with isobutene at low temperatures, 20: 1915
**ETHYLENE, TETRAFLUORO- POLYMERS**
radiation effects on dielectric properties of, electron, 20: 1897 (NASA-TN-D-3032)
**ETHYLENE, TRIFLUORO-**
radioinduced polymerization of, at low temperatures, 20: 1893(R) (AD-618228)
**ETHYLENIMINE**
mutagenic effects of, in wheat seeds, 20: 1655
**EUROPIUM**
determination in potassium chloride medium, polarographic, 20: 1795
determination in uranium and zirconium, spectrographic, 20: 2520(R) (IA-920)
determination using Chromotrope 2B, photometric, 20: 1772
spectra of blue solutions of, in liquid ammonia, 20: 1867
**EUROPIUM ALLOYS**
Eu–Ni, magnetic properties, 20: 2369
Eu–Ni, preparation, hardness, and microstructure, 20: 2369
**EUROPIUM ISOTOPES Eu-145**
energy levels, (E), 20: 3084
**EUROPIUM ISOTOPES Eu-146**
beta decay of, samarium-146 levels from, (E), 20: 3075
**EUROPIUM ISOTOPES Eu-155**
determination in fission products using reduction by lithium amalgam, 20: 1752
**EUROPIUM MOLYBDATES**
preparation of single crystals of, by Czochralski technique, 20: 1840
$Eu_2(MoO_4)_3$–$Gd_2(MoO_4)_3$, preparation of single crystals of, by Czochralski method, 20: 1840
$Eu_2(MoO_4)_3$–$Tb_2(MoO_4)_3$, preparation of single crystals of, by Czochralski method, 20: 1840
**EUROPIUM OXIDES**
Curie temperature in pressures up to 12 Katm, effects of uniform compression on, (E), 20: 3313
determination in ancient glass and natron using lithium drifted germanium diode detector, activation, 20: 1731 (BNL-9614)
$EuO_2$–$NpO_2$, phase studies by x-ray diffraction, 20: 2379
$EuO_2$–$PaO_2$, phase studies by x-ray diffraction, 20: 2379
$EuO_2$–$PuO_2$, phase studies by x-ray diffraction, 20: 2379
$EuO_2$–$ThO_2$, phase studies by x-ray diffraction, 20: 2379
$EuO_2$–$UO_2$, phase studies by x-ray diffraction, 20: 2379
**EUROPIUM OXYBROMIDES**
preparation and crystal structure, 20: 1834
**EUROPIUM SULFATES**
properties and structure of crystal hydrates of, 20: 1868
**EXCER PROCESS**
development of, for converting uranyl nitrate solutions to tetrafluoride, 20: 1956 (ORNL-1696)
**EXPERIMENTAL BREEDER REACTOR-II**
development and operation of, July 1965, 20: 3320(R) (ANL-7082, pp 1-28)
fuel cycle facility for, 20: 3522
fuel cycle facility for, fuel processing in, 20: 3523
fuel cycle facility for, fuel fabrication in, 20: 2297
fuel element fabrication and processing for, 20: 2282 (HW-SA-3755)
fuel element failure detection in, systems for, 20: 3518
fuel elements for, remote determination of gas pressure and volume in, 20: 2116
fuel meltdown in flowing sodium, TREAT tests on, 20: 3506
kinetics of, system for monitoring, 20: 3517
power oscillations in, self-excited, 20: 3514
transfer functions of, 20: 3590
**EXPLOSIONS**
analysis using stereoscopic framing-camera techniques, (E), 20: 3624 (LA-DC-7088)
**EXPLOSIVES**
analysis for gunpowder residues on hands in crime detection, activation, 20: 1739(R) (GA-4297)
analysis for gunpowder residues on hands in crime detection, activation, 20: 1740(R) (GA-4576)
analysis of gunpowder residues on hands, activation, 20: 1736(R) (GA-3491)
analysis of gunpowder residues on hands, activation, 20: 1737(R) (GA-3664)

use for magnetic flux compression, review of, 20: 3166 (LA-DC-7252)
**EXPONENTIAL PILES**
buckling measurements by successive substitution, 20: 3399
criticality studies of subcritical lattices, using pulsed-neutron techniques, 20: 3432
neutron spectra measurements in University of Florida, 20: 3600
reactivity measurements using pseudo-random-impulse methods, finite correlation times in, 20: 3387
**EXTRACTION APPARATUS**
performance of fused-salt molten-metal, 20: 2245
**EYES**
radiation effects on desoxyribonucleic acid content of cells of corneal epithelium, 20: 1633

# F

**FALLOUT**
deposition with respect to atmospheric release of, calculation of, 20: 2074 (AHSB(RP)M-40)
distribution of particles of, in atmosphere, 20: 2053
effects of radiation from, on ecological systems, 20: 2080 (BNL-917, pp 20-36)
effects of, from nuclear explosions, physical, 20: 2078 (BNL-917, pp 1-10)
gamma dose distribution over desert terrain, angular, 20: 2092
gamma dose distributions from, (T), 20: 2048 (USNRDL-TR-888)
gamma dose rates from, determination using gamma spectrometry, 20: 2171
monitoring in German troposphere following Chinese test of October 16, 1964, 20: 2050
monitoring in Israel, July to Dec. 1963, 20: 2520(R) (IA-920)
monitoring in Italy, 1963, 20: 2046 (BIO/04/64)
monitoring in Italy, 1964, 20: 2047 (EUR-2509.e)
monitoring in Scandinavian countries, 1961 to 1964, 20: 2054
monitoring of, 1962 to 1963, 20: 2049
physical properties of alpha-active particles in, 20: 1602
radiation from, attenuation by horizontal concrete slabs, (E/T), 20: 3271
sample collection and analysis of global, review on methods for, 20: 2086(T) (BNL-tr-42)
use as tracer in meteorology, 20: 2044 (NDRE-51)
**FAST BURST REACTOR FACILITY**
reflector effects on burst characteristics of, 20: 3589
**FAST REACTORS**
cooling system design for experimental 2 Mw sodium, 20: 3479 (NP-15556)
critical assemblies for, design of, 20: 3376 (NP-15573)
design of Fast Test Reactor, conceptual, 20: 3581 (BNWL-SA-340)
design of Soviet BN-350, 20: 3475 (NP-15458)
Doppler coefficient in, cross sections for calculating, (T), 20: 2972
feasibility of mixed-spectrum steam-superheat power reactors, (T), 20: 3471(R) (GEAP-4861)
fuel alloys for, phase studies of fissium–plutonium–uranium, 20: 3493
fuel element refabrication costs for, 20: 3510
fuel studies at BNL, facility for, 20: 2001
fuels for power-breeder, properties of metallic, 20: 2386
fuels for power-breeder, plutonium–thorium–uranium, 20: 2230
kinetics of mixed-spectrum steam-superheat, (E/T), 20: 3471(R) (GEAP-4861)
neutron Doppler coefficients of, sinusoidal fuel heating for determining, (T), 20: 3374 (IA-1053)
neutron Doppler effect in, 20: 2520(R) (IA-920)
neutron spectra in, (T), 20: 3402
operations of MSSCEF, (E), 20: 3471(R) (GEAP-4861)
reactivity of, effects of plutonium isotopic composition on, 20: 2520(R) (IA-920)
**FATTY ACIDS**
content of, in lipids of the gempylid fish, *Ruvettus pretiosus*, 20: 3637 (UCLA-12-534)
**FERMI FAST BREEDER REACTOR**
shielding measurements on, 20: 3524
**FERMIONS**
interactions of higher-spin, with electrons, cross section for, (T), 20: 2799
magnetic properties of charged ideal gases of, in n dimensions, (T), 20: 2833
systems of interacting, applications of Landau theory to, 20: 2691
**FERROCENES**
deuterium exchange with halogens in halogenated, 20: 1830
**FETUSES**
iodine-131 metabolism in human, 20: 1600
radiation effects on development of nervous system in dogs, 20: 1627(T)
radiation hazards from radiodiagnosis during pregnancy, 20: 1689
radiosensitivity of rat, effects of chemicals on x, 20: 1693
**FIELD THEORY**
decay modes of hadrons, unitary symmetry of leptonic, 20: 2520(R) (IA-920)
differential equations in, applications of partial, 20: 2530
elementary particle models in quantum, survey of, 20: 2758 (UR-875-100)
elementary particle weak interactions in, 20: 2759 (UR-875-102)
Feynman diagrams in, boundary of Landau surface of arbitrary, 20: 2780
focusing singularity in p-space of constant curvature, 20: 2813
models for quantum, survey of soluble, (T), 20: 2757 (NYO-2262-98)
permissible rate of decrease of forward scattering amplitude at high energies, (T), 20: 2810
Regge poles and cuts mixing in, (T), 20: 2768
S-matrix theory in quantum, normal product techniques for, 20: 2765
sum rules for massive vector gauge fields, 20: 2783
symmetry schemes higher than SU(3), weak currents from, 20: 2520(R) (IA-920)
three-particle partial amplitudes and unitarity conditions for complex values of angular momenta, (T), 20: 2811
transformations of generalized local free fields, 20: 2812
**FILMS**
critical fields of thin superconducting, 20: 2926
**FILTERS**
analysis for bismuth-214 and polonium-214, method for, 20: 2520(R) (IA-920)
contamination of glove box system of, by accidental plutonium hexafluoride release, 20: 2076 (ANL-7068)
efficiency in reactor containment system, measurement using condensation nuclei, 20: 3340
performance of charcoal, for methyl iodide sorption, 20: 3586 (ORNL-TM-1291)
system for removal of contaminated, from Thorium–Uranium Recycle Facility, 20: 1995
testing high-efficiency, sodium flare photometer method for, 20: 2077 (AWRE-O-41/65)
**FINLAND**
fallout monitoring, 1961 to 1964, 20: 2054
**FINNED TUBES**
design of helical, with baffles in fin channels, 20: 3467(P)
design of, with braces for splitter fins, 20: 3466(P)
fabrication with inclined fins, apparatus and method for, 20: 2303(P)
**FIRES**
effects on damage to non-urban areas from nuclear attack, model for, (T), 20: 1590 (RM-3902-TAB)
effects on ecosystems of moss, 20: 2079 (BNL-917, pp 11-19)
extinguishing in vertical reactor channels, device for, 20: 3364(P)
**FISH**
fatty acid content of *Ruvettus pretiosus*, 20: 3637 (UCLA-12-534)
**FISSION**
heat from, conversion to electric energy, 20: 2676(P)
model of, liquid drop, 20: 2520(R) (IA-920)
models of asymmetric and symmetric, 20: 2520(R) (IA-920)
nuclear structure at saddle configuration during, 20: 3154
**FISSION FRAGMENTS**
angular correlations between prompt neutrons and, methods for, 20: 3025
angular distribution from photofission of uranium-238 near threshold, (E), 20: 3134
angular distributions of, structure of transition state nucleus from, 20: 3154
detection using argon gas scintillation detector, 20: 2163
effects on molybdenum, annealing of, 20: 2476
energy distributions from fast and thermal neutron fission of uranium-235, (E), 20: 3110
energy losses of uranium-235, ionization, (E), 20: 3029
reactions with nitrogen, energy loss and optical excitation in, 20: 1933
**FISSION PRODUCTS**
analysis for europium-155 using reduction by lithium amalgam, 20: 1752
content in atmosphere, 1962 to 1963, 20: 2049
determination in sea water, methods for, 20: 1749 (USNRDL-TR-912)
diffusion from beryllia–urania fuels at 1400°C, 20: 3470(R) (GA-5499)
diffusion in cladding materials, 20: 2389
diffusion in pyrolytic carbon, method for measuring metallic, 20: 2318(R) (GA-5915(Pt.1))
distribution in reactor fuel elements, determination by gamma scanning with anticoincidence spectrometers, 20: 2172
distribution in uranium dioxide fuel rods, 20: 2450
effects on neutron capture cross section of uranium dioxide, 20: 3384
fixation in phosphate glass, 20: 3606
pressure of gaseous, in irradiated uranium dioxide fuel elements, 20: 2462
release from irradiated uranium–zirconium hydride SNAP fuel, 20: 3562
release of gaseous, from irradiated plutonium dioxide–uranium dioxide fuel under transient irradiation, 20: 2469
separation from protactinium by solvent extraction using 4-methyl-2-pentanone, 20: 1759

separation from uranium, method for, 20: 1962
sorption on surfaces from gas flow, 20: 3344
uptake by rat hair, 20: 1695
**FISSIONABLE MATERIAL**
handling of, criticality control and safety in, 20: 2095
safety during handling and shipping of, 20: 3370 (CONF-651103-2)
**FISSIUM**
Pu–U–fissium, phase studies of, 20: 3493
**FLUID FLOW**
dynamics calculation using computers, 20: 2011 (LA-DC-7189)
equations for relativistic charged fluid, 20: 2829
heat transfer and isothermal pressure drop for two phase potassium, 20: 2008(R) (AD-622825)
heat transfer in steam flow around rod bundles with turbulence promoters, (E), 20: 3471(R) (GEAP-4861)
in boiling water systems at high pressure, (E), 20: 2012(R) (NYO-3304-6)
magnetohydrodynamic, with temperature-dependent electric conductivity, (T), 20: 2824
pressure drop for vapors condensing in straight horizontal tube in quasi-static two-phase, 20: 1814 (NAA-SR-6333)
pressure drop in natural-circulation single-component two-phase, at low pressures, 20: 2021
**FLUID FLOW (LAMINAR)**
of Bingham plastic fluid in circular pipe, 20: 2020
**FLUIDIZATION**
density distribution in randomly packed beds, method for measuring, 20: 1977
development and properties of pilot-plant fluid-bed fluoride volatility processes, (E/T), 20: 1952 (ANL-6859)
paste flow studies using randomly packed beds, 20: 3461
**FLUIDS**
magnetohydrodynamics of, generalization of plasma wave theory in, 20: 2838
relativistic variational principle for charged hydromagnetic compressible, 20: 2829
thermodynamics of, Jordan-Thiry theory of, 20: 2827
**FLUOBORATES**
preparation and properties of $ClF_2^+$ ion, 20: 2520(R) (IA-920)
**FLUORAL**
radioinduced polymerization of, at low temperatures, 20: 1893(R) (AD-618228)
**FLUORESCENCE**
radioinduced in phosphate glass, measurement of, 20: 2181(P)
**FLUORIDE VOLATILITY PROCESSES**
development and properties of pilot-plant fluid-bed, (E/T), 20: 1952 (ANL-6859)
**FLUORINATION**
of plutonium dioxide–uranium dioxide pellets in fluidized bed, 20: 1970
**FLUORINE**
handling of, 20: 1727 (NASA-SP-5032)
performance as cleaning agent for coolant passages of water-cooled magnets, (E), 20: 1992
reactions with trifluoroacetic acid, effects of water on, 20: 1881
separation by radiolysis of carbon tetrafluoride and perfluorodienes, method for, 20: 1899(T) (BNL-tr-23)
separation from uranium hexafluoride waste by electrolysis, 20: 1954 (KY-287)
toxicity of, 20: 1727 (NASA-SP-5032)
**FLUORINE COMPOUNDS**
preparation of sulfur- and xenon-containing, effects of water on, 20: 1881
**FLUORINE ISOTOPES F-17**
energy-level transition probabilities of, E2, (T), 20: 3115
**FLUORINE ISOTOPES F-18**
angular and energy distribution of recoil, from fluorine-19 (γ,n) reactions at 260 Mev, (E), 20: 3108
**FLUORINE ISOTOPES F-19**
bremsstrahlung reactions (γ,n) at 260 Mev, angular and energy distributions of fluorine-18 recoils in, (E), 20: 3108
magnetic resonance in uranium hexafluoride, anisotropy of chemical shift tensors of, 20: 1807 (CEA-R-2827)
**FOLIC ACID**
complexes with chlorophyllin and metal ions, radiosensitivity effects in mice of, gamma, 20: 1692
**FOOD**
analysis for bromine, activation, 20: 1738(R) (GA-4041)
evaluation of bulgur wafer and adjuncts for fallout shelter rations, 20: 2067 (AD-614824)
radiation processing of, effects on wholesomeness, 20: 2199
radiation processing of meats, 20: 2203
radiosterilization of, bibliography on, 20: 2196 (AD-514910)
radiosterilization of, economics of gamma, 20: 2198
**FORESTS**
ecology of boral, effects of spruce budworm and insecticides on, 20: 1589 (BNL-917, pp 61-8)
effects of mass fires on ecology of, 20: 2079 (BNL-917, pp 11-19)
fire damage to, from nuclear attack, (T), 20: 1590 (RM-3902-TAB)
radiation effects on, ecological, 20: 2080 (BNL-917, pp 20-36)
radiation effects on, ecological, 20: 2081 (BNL-917, pp 39-60)
**FORMALDEHYDE**
radioinduced polymerization of, effects of ethyl ether, dichloromethane, and toluene solutions on, 20: 1914
radioinduced polymerization with acrylonitrile, isobutene, methyl methacrylate and styrenes, 20: 1914
yields in gamma radiolysis of liquid acetone, 20: 1901
**FORMAMIDE, *N,N*-DIMETHYL-**
effects on radioinduced polymerization of liquid and solid acetylene, 20: 1913
**FORMIC ACID**
corrosive effects on molybdenum, stress-, 20: 2254 (BM-RI-6680)
**FOSSILS**
carbon-12, carbon-13, oxygen-16, and oxygen-18 ratios in, deposited by algae and coral, 20: 1591
**FRANCIUM ASTATIDES**
entropy and thermal capacity at 0 to 300°K, 20: 1859
**FRANCIUM BROMIDES**
entropy and thermal capacity at 0 to 300°K, 20: 1859
**FRANCIUM CHLORIDES**
entropy and thermal capacity at 0 to 300°K, 20: 1859
**FRANCIUM FLUORIDES**
entropy and thermal capacity at 0 to 300°K, 20: 1859
**FRANCIUM IODIDES**
entropy and thermal capacity at 0 to 300°K, 20: 1859
**FREE RADICALS**
radioinduced in dry bacteriophages and nucleic acids, ESR of gamma and x, 20: 1623
radioinduced in melanin, 20: 1684
radioinduced in rice seeds, 20: 1669
radioinduced, electron spin resonance studies of, 20: 1898(R) (RRL-2310-164)
reactions with hydriodic acid in irradiated hydrocarbons, kinetics of, 20: 1898(R) (RRL-2310-164)
**FRUITS**
coating of, tracer study on, 20: 2520(R) (IA-920)
**FUMARIC ACID**
fumaric acid–urea, ESR studies of irradiated, 20: 1935
**FUNGI**
radiation effects on, genetic, 20: 1622 (WT-820)
radiosensitivity of, thermal, effects of uv and x radiations on, 20: 1640
**FURALDEHYDES**
labeling with tritium, 20: 1887 (NP-15523)
**FURAN**
2-methyl-, thermal capacity and thermodynamic properties at 5 to 350°K, 20: 3615 (COO-1149-17)
**FURAN, TETRAHYDRO-**
effects on pulse radiolysis of organic solutes, spectra of, 20: 1920
naphthalene–tetrahydrofuran, radiolysis in alcoholic, aqueous, and hydrocarbon solutions, 20: 1920
**FURFURYL ALCOHOLS**
use as binder in graphite fabrication, 20: 2302(P)
**FURNACES**
operation of high pressure-temperature, for metal–water reactions, 20: 2221(R) (ANL-7082, pp 62-73)
**FUSED SALTS**
cation exchange in, 20: 2520(R) (IA-920)
effects on corrosion of refractory metals by magnesium–uranium–zinc alloy and zinc, 20: 2266

## G

**GADOLINIUM**
determination in zirconium, spectrographic, 20: 2520(R) (IA-920)
determination using Chromotrope 2B, photometric, 20: 1772
magnetostriction in crystals of, 20: 3312
optical properties of, electronic band structure predictions of, (T), 20: 2592 (BNL-9556)
separation from thorium and other rare earths by ion exchange in ammonium thiocyanate–organic solvent–water systems, 20: 1959
specific heat near the Curie point, 20: 2920
**GADOLINIUM ALLOYS**
Gd–La, spin ordering of paramagnetic states in superconducting, 20: 2918
**GADOLINIUM CHLORIDES**
magnetic transition from microwave absorption in, (E), 20: 3288
reactions with sodium fluosilicates, precipitation in, 20: 1870
**GADOLINIUM IONS**
superconducting transition temperature of thin films of, effect of thin oxide

layer on, 20: 2915
**GADOLINIUM ISOTOPES Gd-160**
ionization in K-shell by alpha particles at 3 to 4 Mev, x-ray yields from, (E), 20: 2625
**GADOLINIUM MOLYBDATES**
preparation of single crystals of, by Czochralski technique, 20: 1840
$Eu_2(MoO_4)_3$–$Gd_2(MoO_4)_3$, preparation of single crystals of, by Czochralski method, 20: 1840
**GADOLINIUM OXIDES**
magnetic susceptibility at 4 to 300°K, 20: 3318
phase studies of, at 2200 to 2300°C, 20: 1827
**GADOLINIUM OXYBROMIDES**
preparation and crystal structure, 20: 1834
**GADOLINIUM SULFATES**
properties and structure of crystal hydrates of, 20: 1868
**GAGES**
use with machine tools, for fabrication and inspection, 20: 3627 (RFP-670)
**GALAXIES**
cosmic radiation properties in Milky Way, review, 20: 2653 (NASA-SP-71, pp 19-29)
cosmic ray halo around, magnetic gas cloud formation of, (T), 20: 2662
gas flow stability in disk and halo of, 20: 2573
gravitational radiation from, 20: 2877(T)
**GALENAS**
lead isotope ratios in, Cobalt-Noranda area, Canada, 20: 2051
**GALLIUM**
determination using derivatives of resorcylaldehyde and salicylaldehyde and 3-methyl-1-butanol, fluorometric, 20: 1773
**GALLIUM ALLOYS**
Ga–Fe–Pu, reactions with tantalum at high temperatures, 20: 2228
Ga–Pu, tensile properties of, at 20 to 100°C, 20: 2378
Ga–Pu, yield stress in, recovery of, 20: 2374
Sb–Ga, radioinduced defects in, structural properties of, 20: 2486
**GALLIUM ARSENIDES**
electron band structure of, effects of spin-orbit splitting on, (E), 20: 3287
radiation effects on semiconducting, 20: 2497
radiation effects on electron mobility in, 20: 2514
radioinduced conductivity in single crystals of, $\gamma$ and x-, 20: 2439
radioinduced defects in, spectroscopic study of, 20: 2501
radioinduced defects in, structural properties of, 20: 2486
radioinduced defects in, 20: 2516
**GALLIUM ISOTOPES Ga-72**
gamma spectra of, energies and relative intensities of lines in, (E), 20: 3040(T)
**GAMMA RADIATION**
angular correlation of, measuring device for, 20: 2520(R) (IA-920)
angular correlations in beta decay of gold-198, (E), 20: 3129
attenuation by horizontal concrete slabs, from finite plane source, (E/T), 20: 3271
detection and measurement of high-level, performance of halogen-filled G-M counters for, 20: 2140
detection and measurement in man of, performance of organic plastic scintillation counters for whole-body, 20: 1710
detection and resolution of, use of organometallic compounds in plastic scintillators for, 20: 1905
dose albedos for concrete and steel, differential, 20: 3270
dose albedos for concrete, iron, lead, and water, (T), 20: 3274
dose deposition in low-Z materials, low-energy component of, (T), 20: 3267
dose distribution from fallout over desert terrain, angular, 20: 2092
dose distribution in reflector and primary shield of New Production Reactor, 20: 3544
dose distributions from, in fallout, (T), 20: 2048 (USNRDL-TR-888)
dose distributions in compartmented structures, from external sources, 20: 3275
dose measurements using polymethylmethacrylate, 20: 2165
dose rates in environment, determination using gamma spectrometry, 20: 2171
dosimetry in reactors, using colored polyvinyl alcohol films, 20: 2135
dosimetry of, calculator for use with rotational cobalt-60 teletherapy unit, 20: 1723
dosimetry of, design and performance of facility for standards for, 20: 1942
dosimetry of, from cobalt-60 teletherapy unit, 20: 1721
dosimetry of, modified silver-activated phosphate glass dosimeter for low-dose, 20: 2122 (AD-622626)
dosimetry using lithium fluoride, 20: 2178
effects in aqueous human blood, ESR, 20: 1605
effects in mice, protective effects of chelated complexes against, 20: 1692
effects of cobalt-60, on mice and rats, pathological, 20: 1614 (NASA-SP-71, pp 97-103)
effects on aluminum oxides, (E), 20: 3446(R) (GEST-2045)
effects on arsenic-doped germanium at 0°C, 20: 2494
effects on bacteriophages, ESR spectra of, 20: 1623
effects on bacteriophage, physiological, 20: 1650
effects on benzene–benzophenone–isopropanol system, 20: 1931
effects on calcium tungstate, luminescence decay time for, (E), 20: 1900
effects on capacitors, data tabulations on transient, 20: 2410 (AD-617916)
effects on carbon tetrafluoride and perfluorodienes, separation of molecular fluorine by, 20: 1899(T) (BNL-tr-23)
effects on catalases and peroxidases, 20: 2520(R) (IA-920)
effects on cells of *Marchantia polymorpha*, biological, 20: 1610 (BNL-9611)
effects on crosslinking of nylon 66 and polyvinyl alcohol in presence of allyl methacrylate–methanol–water systems, 20: 1909
effects on dietary and hormonal induction of enzymes in rat liver, 20: 1674
effects on electric conductivity of gallium selenides, 20: 2439
effects on electric conductivity of beryllia, thoria, and zirconia, 20: 2460
effects on electric cables, signal transients from, 20: 2186 (ECOM-2415)
effects on enzyme systems, 20: 1647
effects on forests, ecological, 20: 2080 (BNL-917, pp 20-36)
effects on forests, ecological, 20: 2081 (BNL-917, pp 39-60)
effects on germanium p-n junction, 20: 2512
effects on heart function in dogs, therapeutic dose range, 20: 1652
effects on immune reactions in monkeys, 20: 1631
effects on ionic processes in solid organic compounds, relation to delayed luminescence, 20: 1906
effects on leukocyte blood picture of, 20: 1672
effects on liquid hydrocarbons, recoil reactions of carbon-11 produced in, 20: 1896 (IS-T-23)
effects on liquid methane and methane–propene, 20: 1898(R) (RRL-2310-164)
effects on liquid acetone, yields in, 20: 1901
effects on lithium-drifted p-i-n silicon junctions, 20: 2510
effects on meta- and ortho-terphenyl, 20: 1928
effects on millimolar concentrations of hydrogen peroxide in aerated water, 20: 1894 (AD-623095)
effects on n-type and p-type silicon, 20: 2496
effects on n-type antimony–indium alloy at 78°K, 20: 2500
effects on *Phaseolus mungo* seeds, heat treatment effects on, 20: 1690
effects on polymerization of monomers at low temperatures, 20: 1893(R) (AD-618228)
effects on polymerization of liquid *N*-vinyl-succinimide, kinetics of, 20: 1912
effects on polymerization of liquid and solid acetylene, properties and spectra of products of, 20: 1913
effects on polymerization of styrene at low temperatures, 20: 1925
effects on polymerization of isobutene with tetrafluoroethylene at low temperatures, 20: 1915
effects on polymerization of 4,4′-diphenylenedi- and *N*,*N*′-phenylenedimaleimide, yields in, 20: 1930
effects on potential of mercury oxide electrode, 20: 1932
effects on radioinduced polymerization of formaldehyde with acrylonitrile, isobutene, methyl methacrylate, and styrenes, 20: 1914
effects on radioinduced polymerization of formaldehyde, effects of ethyl ether, dichloromethane, and toulene on, 20: 1914
effects on resistance-temperature transducers at low temperatures, 20: 2191
effects on ribonuclease, inactivating, 20: 1682
effects on ribonuclease activity and molecular structure, 20: 1604(R) (TID-22291)
effects on seeds of tomatoes, genetic, 20: 1638
effects on seeds of wheat, genetic, 20: 1655
effects on seeds of barley, biological, effects of oxygen and moisture on, 20: 1667
effects on seeds, genetic, 20: 1649
effects on semiconductors, 20: 2516
effects on silicon junction diodes, 20: 2413 (AD-618688)
effects on terphenyls, interpretation of, 20: 1927
effects on thermal control coatings for spacecraft, 20: 2428 (NASA-SP-55, pp 365-79)
effects on tissues, physiological, 20: 1647
effects on Tradescantia, biological, 20: 1668
effects on transistors, physical parameters for predicting, 20: 2184(R) (AD-614618)
effects on tyrosine-tyrosinase systems, 20: 1647
effects on wheat lipids, effects of dose on, 20: 1637
effects on yeast, biological, 20: 1664
effects on yeast, biological, 20: 1663
emission by indium-116, (E), 20: 3097

emission in alpha inelastic scattering, alpha-gamma coincidences in, 20: 3141
heat deposition in reactor shielding, group constants for calculating, 20: 3268
heat deposition in infinite cylinders with uniformly distributed gamma sources, 20: 3269
heating effects on infinite cylinders, (T), 20: 3325 (ORNL-P-1480)
intensity of high-energy, in space, (E/T), 20: 2586
interactions with nucleons, meson (π) production amplitude from, (T), 20: 2695
interactions with protons, hyperon ($\Sigma^0$) and meson ($K^+$) production in, (E/T), 20: 2735
interactions with nucleon at 165 to 230 Mev, amplitudes and cross sections for mesons ($\pi^+$) production in, (E/T), 20: 2737
production in antineutrino interactions with protons, cross sections for, (T), 20: 2736
reactions (γ,f) with uranium-238 near threshold, fragment angular distributions from, (E), 20: 3134
reactions (γ,f) with uranium-238 at 5.43 to 7.72 Mev, cross sections for, (E), 20: 3050
reactions (γ,n) and (γ,p) with oxygen-16 giant dipole resonance from, (E), 20: 3074
reactions (γ,p) with oxygen-16 at 21.3 to 43.7 Mev, cross sections for, (E), 20: 3107
scattering by homogeneous plane slab, angular and spectral distributions of multiple Compton, 20: 2705
scattering from semi-infinite media, albedos from back-, (E), 20: 3273
scattering into basement from infinite plane source, 20: 3272
shielding by concretes, 20: 3253
spectra from electron capture decay of titanium-45, 20: 3128
spectra from thermal neutron reactions (n,γ) with iron-54, 20: 3109
spectra from thermal neutron capture by neodymium-143, (E), 20: 3131
therapeutic use of radium, for infantile hemangiomas, 20: 1719
transport in complex geometry, analysis by three-dimensional Monte Carlo calculations, (E/T), 20: 3348
use in scintillation defectoscopy, 20: 2027

**GAMMA SHIELDING**
design for hardened structures, (T), 20: 3276
dose albedos for semi-infinite media, (E), 20: 3273
dose deposition in, low-energy component of, (T), 20: 3267

**GAMMA SOURCES**
calibration of high-specific-activity, calorimetric, 20: 2195
design, fabrication, and operation of, 20: 1937 (BNL-9281)
design of cobalt-60 3000 C, 20: 1942
design of multipurpose cobalt-60, 20: 2193
preparation of cobalt-60 bead, automatic threading device for, 20: 1722
use for food radiosterilization, economics of, 20: 2198

**GAMMA SPECTRA**
analysis in activation analysis, model for least-squares, 20: 1787
analysis of complex, numerical methods for, 20: 1792
resolution for radioisotope determination, computer program for, 20: 1732 (CEA-R-2850)

**GAMMA SPECTROMETERS**
performance of anticoincidence-shielded scintillation, 20: 3006 (AD-613676)
performance of oscillographic, with linear and parabolic energy scale, 20: 2149
performance of oscillographic, 20: 2150
performance of, optimum measuring conditions for, 20: 2148
use in determination of environmental gamma dose rates, 20: 2171
use in nondestructive analysis of irradiated MITR fuel elements, 20: 2030
use of anticoincidence, in gamma scanning, 20: 2172

**GAMMA SPECTROSCOPY**
methods for single-channel, 20: 2150

**GARIGLIANO POWER REACTOR**
operations, 20: 3483(R) (TID-22201)

**GARNETS**
anisotropy of exchange in ytterbium iron, 20: 1802 (AD-618038)

**GAS ANALYZERS**
design and performance of continuous on line, 20: 1734 (EG-Report-36)

**GAS COOLED REACTORS**
control system and instrumentation for Czechoslovakian A 1, 20: 3534
control systems for power, (E), 20: 3480 (ORNL-P-1679)
coolant impurities and carbon transport in graphite-moderated, 20: 3327
criticality calculations for natural uranium-fueled, 20: 3434
design calculations for, 20: 3441
economics of MHD generators and, for commercial power, 20: 2670 (LA-DC-7330)
feasibility of mixed-spectrum steam-superheat power reactors, (T), 20: 3471(R) (GEAP-4861)
heat transfer in fuel-rod bundles in superheated-steam-cooled, (E), 20: 3471(R) (GEAP-4861)
kinetics of mixed-spectrum steam-superheat, (E/T), 20: 3471(R) (GEAP-4861)
operations of MSSCEF, 20: 3471(R) (GEAP-4861)
physics parameters of heavy water, computer program for calculating, 20: 3381 (UJV-1309b/65)

**GAS FLOW**
ionization fronts in stellar, boundary conditions at nonstationary, (T), 20: 2572
ionization fronts in stellar, model for nonstationary, (T), 20: 2571
magnetohydrodynamic, deflagrations and properties of ideal, 20: 2821 (AD-618296)
stability of, astrophysical theory of thermal, 20: 2573

**GAS HILLS AREA (WYO.)**
uranium isotope and daughter product fractionation in sandstone deposits in, 20: 2057

**GASES**
cosmic ray formation from galactic magnetic, halo from, (T), 20: 2662
determination in gases, equipment and methods for spectral-isotopic, 20: 1793
determination of, equipment and method for on line, 20: 1734 (EG-Report-36)
distribution functions for classical electron, calculation of radial, (T), 20: 2830
effects on surfaces, relativistic theory of, 20: 2841
electric breakdown potential of, bibliography on a-c, 20: 3160 (AD-618503)
electric discharges between coaxial cylinders in ,magnetic field effects on, 20: 3202
electromagnetic wave interactions in partially ionized, (T), 20: 2814
electron swarms in uniform electric fields, Townsend energy ratio for, (E), 20: 2825
gravitational collapse of spheres of ionized, relativistic model for, (T), 20: 2879
heating by electric arcs, (T), 20: 2840
kinetic theory of ionized and molecular, electron attachment, inelastic collisions, and ionization in, 20: 2842
magnetic properties of charged ideal quantum, in n dimensions, (T), 20: 2833
monitoring beta-active, design of coincidence counters for, 20: 2139
neutron differential scattering cross sections of molecules of, calculation of, (T), 20: 3135
properties of, time-correlation functions for, (T), 20: 2846
radiative properties of high temperature, spectra of, (T), 20: 1803 (AD-619266)

**GEIGER-MUELLER TUBES**
electric discharge propagation in self-extinguishing, 20: 2176
operation and performance of, 20: 2144
use in beta-particle measurements, 20: 2180(P)

**GENES**
analysis of, in chemically and ultraviolet induced mutations of *Schizosaccharomyces pombe*, 20: 1654
radiosensitivity effects of types of, in hamsters, 20: 1676

**GENETICS**
radiation effects on weight gain of swine progeny, x, 20: 1677

**GEOLOGY**
research on, Geological Survey Professional Paper 525-C, 20: 2043

**GEOMAGNETIC FIELDS**
disturbances in, correlation with spread-F echoes, 20: 2854
electron and proton trapping by, (T), 20: 2849

**GEOMAGNETIC STORMS**
occurrence of, correlation with spread-F echoes, 20: 2854
solar effects on, (E), 20: 2855

**GERMANIUM**
corrosion resistance to mercury at 900°F, 20: 2264
development of lithium-drifted detectors of, for activation analysis of glass, 20: 1731 (BNL-9614)
effects on isotopic exchange between cyclohexane and deuterium, 20: 1838
radiation effects on, 20: 2481
radiation effects on close-pair defects at 0 to 90°K, 20: 2482
radiation effects on hot carrier techniques for studying, 20: 2483
radiation effects on p-type, annealing of electron, 20: 2485
radiation effects on antimony-doped at 100°C, 20: 2495
radiation effects on semiconducting, 20: 2497
radiation effects on, high-energy electron and proton, 20: 2517
radioinduced defects in, annealing of metastable, 20: 2484
radioinduced defects in, structural properties of, 20: 2486
radioinduced defects in, effects of doping with gold on, 20: 2491
radioinduced defects in arsenic-doped, at 0°C, 20: 2494
radioinduced defects in, annealing of, 20: 2506
radioinduced defects in, 20: 2516
radioinduced defects in n-type and p-type, annealing of, 20: 2509

**GERMANIUM ALKYLS**
labeling with germanium-75 and germanium-77 by neutron activation, 20: 1944
**GERMANIUM ISOTOPES Ge-70**
gamma transition at 1039.8 kev following Coulomb excitation, (E), 20: 3043
**GERMANIUM ISOTOPES Ge-72**
gamma transition at 834.8 kev following Coulomb excitation, (E), 20: 3043
**GERMANIUM ISOTOPES Ge-74**
gamma transition at 596.0 kev following Coulomb excitation, (E), 20: 3043
**GERMANIUM ISOTOPES Ge-75**
incorporation in tetraethyl germanium by neutron activation, 20: 1944
**GERMANIUM ISOTOPES Ge-76**
gamma transition at 563.2 kev following Coulomb excitation, (E), 20: 3043
**GERMANIUM ISOTOPES Ge-77**
incorporation in tetraethyl germanium by neutron activation, 20: 1944
**GERMANIUM JUNCTIONS**
radiation effects on p-n, 20: 2512
**GERMANIUM SYSTEMS**
Ge–Mg–Si, radiation effects on electric properties of $Mg_2Ge_{0.8}Si_{0.2}$, 20: 2502
Ge–Si, preparation for radiation detectors, 20: 2182(P)
**GLASS**
analysis for rare earth oxides using lithium drifted germanium diode detector, activation, 20: 1731 (BNL-9614)
analysis in crime detection, activation, 20: 1738(R) (GA-4041)
preparation of, alumina–zirconia refractory material for use in furnaces for, 20: 2382
radiation effects on, bibliography on, 20: 2432 (REIC-Memo-26)
**GLOVE BOXES**
contamination of filter system in, by accidental plutonium hexafluoride release, 20: 2076 (ANL-7068)
**GLOW DISCHARGES**
cathode fall in hydrogen, plasma effects, multiplication and secondary emission from, 20: 2826
initiation in admixture of argon and mercury vapor, time history of, (E), 20: 3162 (AD-616683)
**GLUCOSE**
effects on differences in carbon dioxide production by irradiated and unirradiated yeasts, 20: 1653
**GLUTATHIONE**
effects of, against radioinduced genetic damage in Drosophila, 20: 1619(R) (TID-22293)
**GLYCEROL**
effects on pulse radiolysis of organic solutes, spectra of, 20: 1920
**GLYCINE**
labeling by direct exchange with heavy water, (E), 20: 1833
**GOLD**
corrosion resistance to mercury at 900°F, 20: 2264
determination in hair, activation, 20: 1739(R) (GA-4297)
deuteron elastic scattering at 25.3 Mev, optical model analysis of, (E/T), 20: 3053
deuteron elastic scattering at 27.5 Mev, angular distribution for, (E/T), 20: 3057
deuteron scattering at 13 kev, channeling in, (E), 20: 2616
effects on radioinduced defects in germanium, 20: 2491
**GOLD ALLOYS**
Au–Ag–Sn, solute interactions in dilute, (E/T), 20: 2349 (UCRL-16320)
Au–In–Sn, solute interactions in dilute, (E/T), 20: 2349 (UCRL-16320)
Au–Ni–Sn, solute interactions in dilute, (E/T), 20: 2349 (UCRL-16320)
Au–Sn, solute interactions in dilute, (E/T), 20: 2349 (UCRL-16320)
Cd–Au, entropy of formation of AuCd ordered phase, (T), 20: 2349 (UCRL-16320)
Cu–Au, entropy of formation of AuCu ordered phase, (T), 20: 2349 (UCRL-16320)
**GOLD COMPLEXES**
chlorophyllin, radiosensitivity effects in mice, gamma, 20: 1692
**GOLD ISOTOPES Au-197**
Doppler effect in, structure in, (E), 20: 2975
neutron reactions (n,γ), cross sections for resonance and thermal, (E), 20: 3031
**GOLD ISOTOPES Au-198**
beta decay of, angular correlations in, (E), 20: 3129
beta spectra at 420 to 940 kev, shape factor of, (E), 20: 3055
radiation effects from intracavitary, on leukocyte blood picture, 20: 1672
use of colloidal, in therapy of benign joint diseases, 20: 1706
**GONADAL HORMONES**
radiation effects on distribution and synthesis of, 20: 1671
**GONADS**
chromium phosphate colloid distribution in, tracer studies of, 20: 1598
radiation dose to, from diagnostic radiography, 20: 1703
radiation hazards to maternal, from radiodiagnosis during pregnancy, 20: 1689
radiation injuries of Drosophila, protective effects of sulfhydryl compounds, 20: 1619(R) (TID-22293)
radiosensitivity of, in immature and mature male Drosophila, 20: 1644
**GRAIN GROWTH**
pore migration and growth in, in compacts, 20: 2373
**GRAIN STRUCTURE**
effects on neutron resonance absorption in materials, (T), 20: 2993
migration in metals, review on, 20: 3626 (ORNL-P-1722)
**GRAPHITE**
bonding to niobium–zirconium alloy and stainless steel, brazing techniques for, 20: 2294
de Haas-van Alphen effect in pyrolytic and single-crystal, (E), 20: 3300
elastic properties of ATJ and CFZ grades of, 20: 2315 (CONF-650632-3)
fabrication by hot-working with additive carbides in liquid state, 20: 2318(R) (GA-5915(Pt.1))
fabrication by hot isostatic compaction, properties of products of, 20: 2278 (BMI-1746)
fabrication of shaped bodies of, from particulate material, 20: 2302(P)
gamma back-scattering from, albedos from, (E), 20: 3273
microstructure of, effects of hot-working with molybdenum and zirconium carbide additives on, 20: 2318(R) (GA-5915(Pt.1))
neutron pulse propagation in, thermal, 20: 2955
neutron scattering by cylinders of, fast, (E/T), 20: 3265
neutron scattering kernels and laws for, thermal, 20: 3412
neutron thermalization in, computation of, 20: 3003
oxidation by carbon dioxide, kinetics of, 20: 2261(R) (UCRI-326)
production of isotropic, preparation of coke particles for, 20: 2249(P)
radiation effects on different types of, at 800 to 1200°C, 20: 2417 (BNWL-112)
radiation effects on reactions with beryllium oxide at 1500°C, equipment and setup for studying, 20: 2431 (ORNL-TM-1255)
radiation effects on Young's modulus of, neutron, (E/T), 20: 2446
radioinduced effects in, nucleation of neutron, 20: 2447
radioinduced reactions with carbon dioxide, effects of oxygen on, 20: 1895 (AERE-R-4988)
spectra of vaporous, isolated in inert gas matrices at high temperatures, 20: 1818 (UCRL-11976)
tensile properties of tube specimens of, under combined stress, 20: 2372
thermal conductivity, 20: 2387
vaporization rate, 20: 2261(R) (UCRI-326)
**GRAPHITE MODERATED REACTORS**
coolant impurities and carbon transport in gas-cooled, 20: 3327
criticality calculations for natural uranium-fueled, 20: 3434
design calculations for, 20: 3441
properties of light boiling- and pressurized-water types, 20: 3322 (EUR-2448.f)
**GRAVITATION**
detection of gravitational radiation, (T), 20: 2884
effects on stability of electrically conducting liquid layer, 20: 2820 (AD-614645)
elementary particle motion in external field of, model for one-point, (T), 20: 2867
emission of waves of, from cosmic explosions, (T), 20: 2877(T)
energy-momentum linkages in, Lorentz-covariant, (T), 20: 2882
meson $K^o$ and $\overline{K}^o$ mass signs in, 20: 2865 (JINR-P-2325)
quantization of, noncovariant, (T), 20: 2866
stability of infinite homogeneous medium in magnetic fields, effect of ion gyration radius on, 20: 2885
**GREASES**
analysis in crime detection of activation, 20: 1736(R) (GA-3491)
analysis in crime detection, activation, 20: 1737(R) (GA-3664)
analysis in crime detection, activation, 20: 1738(R) (GA-4041)
**GROUND**
contamination from in-flight destruction of rocket reactors, 20: 3575
motions of, methods for simulating air-blast-induced, 20: 1980 (AD-614990)
**GROWTH**
effects of water-$d_2$ on yeast, as function of inoculum age, 20: 1601
radiation effects on swine progeny, x, 20: 1677
**GUANINE**
resistance to analogs of, in murine cell line, 20: 1678
**GUINEA PIGS**
inhalation of neodymium oxide aerosol by, 20: 1593 (COO-1170-4)
radiation effects on leukocyte blood picture in, effects of dose and time on, x, 20: 1670
radiation injuries of adrenal glands of, induced by deposited strontium-89 or strontium-90, 20: 1641

# H

**HAFNIUM**
corrosion by steam and water at 800 to 1500°F, (E), 20: 3471(R)

(GEAP-4861)
separation of trace amounts of, from alkali metals, alkaline earths, and rare earths, 20: 1958
**HAFNIUM ALLOYS**
Hf–Ta–W, corrosion by lithium at 1200°C, 20: 3321(R) (ANL-7082, pp 29-53)
Hf–Ta–W, properties for use with alkali metals at high temperatures, 20: 2241
Nb–Ta–V–Zr, strength at high temperatures, 20: 2407(P)
**HAFNIUM CARBIDES**
corrosion by hydrogen fluoride at 2000 to 3100°K, 20: 2261(R) (UCRI-326)
thermal expansion of, to 2700°C, 20: 1839
wetting by liquid cobalt, copper, iron, and nickel, 20: 1837
C–HfC, preparation and properties of, 20: 2351(R) (USBM-RC-1205, pp 3-7)
**HAFNIUM ISOTOPES Hf-166**
energy states of, large-spin rotational, (E/T), 20: 3008 (COO-1420-104)
**HAFNIUM ISOTOPES Hf-168**
energy states of, large-spin rotational, (E/T), 20: 3008 (COO-1420-104)
**HAFNIUM ISOTOPES Hf-170**
energy states of, large-spin rotational, (E/T), 20: 3008 (COO-1420-104)
**HAFNIUM ISOTOPES Hf-172**
energy states of, large-spin rotational, (E/T), 20: 3008 (COO-1420-104)
**HAFNIUM SYSTEMS**
C–Hf–Ta, preparation and properties of, 20: 2351(R) (USBM-RC-1205, pp 3-7)
C–Hf–W, creep at 1800 to 2000°F of Silvania A, 20: 2333(R) (NASA-CR-54457)
**HAIR**
analysis for arsenic, activation, 20: 1737(R) (GA-3664)
analysis in crime detection, activation, 20: 1739(R) (GA-4297)
analysis in crime detection, activation, 20: 1740(R) (GA-4576)
fission product uptake by rat, 20: 1695
radiation effects on free radical properties of melanin in, uv, 20: 1684
**HALLAM POWER REACTOR**
fuel element fabrication costs for Core 2, 20: 3509
**HALOGENS**
determination in atmosphere using neutron activation analysis, 20: 1789
fixation of radioactive, in water-unleachable rocklike products, 20: 3608(P)
**HAMSTERS**
radiosensitivity of, effects of genotype, liver homogenates, and sex on x, 20: 1676
**HANDBOOKS AND MANUALS**
startup manual for HFBR, 20: 3580 (BNL-9591)
**HANDLING AND STORAGE**
of fissionable material, safety measures for, 20: 3370 (CONF-651103-2)
**HANDS**
analysis for gunpowder residues, activation, 20: 1736(R) (GA-3491)
analysis for gunpowder residue, activation, 20: 1737(R) (GA-3664)
analysis for gunpowder residues in crime detection, activation, 20: 1739(R) (GA-4297)
analysis for gunpowder residues in crime detection, activation, 20: 1740(R) (GA-4576)
**HANFORD PRODUCTION REACTORS (N)**
gamma dose distributions in reflector and primary shield of, 20: 3544
neutron flux distributions in reflector and primary shield of, 20: 3544
operational modes for converted, 20: 3541 (RL-NRD-81(Suppl.1))
**HASTELLOY C**
conductivity of, temperature dependence of electric and thermal, 20: 3485(R) (WCAP-2120)
radiation effects at cryogenic temperatures, 20: 2459
**HASTELLOY F**
corrosion by steam and water at 800 to 1500°F, (E), 20: 3471(R) (GEAP-4861)
**HASTELLOY X**
compatibility with plutonium–uranium–zirconium alloys, 20: 2229
radiation effects on creep-rupture properties of, neutron, 20: 2456
reactions with plutonium–uranium–zirconium alloys at high temperatures, 20: 3320(R) (ANL-7082, pp 1-28)
welding to stainless steel, 20: 3472(R) (GEAP-4891)
**HAYNES 25 ALLOY**
testing for use in liquid-metal turbine blades and nozzles, 20: 2240
**HEAD**
radiation effects on rat, on response to barbiturates, 20: 1662
**HEALTH PHYSICS**
instrumentation for, 20: 2107
procedures for linear accelerators, 20: 2531 (AD-618304)
**HEART**
blood circulation measurements in, tracer method using rubidium-84, 20: 1709
radiation effects on function of, therapeutic doses of $\gamma$, 20: 1652
**HEAT**
conversion to electricity, direct method for, 20: 2676(P)
generation by radioactive wastes, 20: 3605
**HEAT EXCHANGERS**
cleaning blocked, in water-cooled magnets, (E), 20: 1992
performance of double-pipe, 20: 3321(R) (ANL-7082, pp 29-53)
**HEAT-RESISTING ALLOYS**
thermal properties at ambient temperature, data tabulation of, 20: 2343 (SC-TM-65-242)
**HEAT TRANSFER**
boiling, effects of surface conditions on, (E), 20: 2017(R) (TID-22312)
burnout in boiling liquid metal systems, 20: 2023
burnout of round tubes with forced water flow, 20: 2009 (EUR-2490.e)
by natural convection in reactor loss-of-coolant accidents, 20: 3515
critical heat flux and flow regimes in boiling water, (E), 20: 2012(R) (NYO-3304-6)
data on, computer code for processing, 20: 3485(R) (WCAP-2120)
effects on corrosion of alloys by steam and water at 800 to 1500°F, (E), 20: 3471(R) (GEAP-4861)
from "nuclear vapotron" fuel-element cans, (E), 20: 3443(R) (EURAEC-1356)
from "nuclear vapotron" fuel-element cans, (E), 20: 3444(R) (EURAEC-1357)
from "nuclear vapotron" fuel-element cans, (E), 20: 3445(R) (EURAEC-1358)
in boiling potassium, rubidium, and sodium, 20: 2008(R) (AD-622825)
in core of SNAP-8ER, 20: 3557
in irradiation capsules, feasibility of powder media of, 20: 2018 (TRG-Report-920)
in liquid-metal-cooled reactor channels, prediction of, 20: 3321(R) (ANL-7082, pp 29-53)
in radioisotope propulsion systems, combined effects of convection and radiation on, (E), 20: 2007 (AD-818026)
in reactor loss-of-coolant accidents, model for, 20: 3333
in reactors, computer program for calculating, 20: 3323 (GAMD-6644)
measurement in steam-cooled rod bundles with turbulence promoters, (E), 20: 3471(R) (GEAP-4861)
radiant, in finned radiators, 20: 2016 (SC-DC-65-1765)
**HEAT TRANSFER SYSTEMS**
design and fabrication of supercritical-pressure, 20: 3485(R) (WCAP-2120)
instrumentation of liquid metal, 20: 2013 (ORNL-P-1661)
**HEAVY WATER REACTORS**
fuel economics of, 20: 3451
**HELIUM**
alpha stopping power of, 5-Mev, 20: 2147
analysis for contaminant gases, gas chromatographic, 20: 1751
collisions of atoms of, with alkali metal atoms, ionization produced in, (E), 20: 2639
collisions of atoms of, with fast hydrogen-like ions, calculation of cross sections for K-electron loss in, (T), 20: 2642
determination in neutron-irradiated boron–copper system, 20: 2444
determination of, factors affecting continuous on line, 20: 1734 (EG-Report-36)
effects on lattice parameters of neutron-irradiated copper–boron system, 20: 2441
electric breakdown potential of, measurement of a-c, 20: 3160 (AD-618503)
electric discharge in spark chambers, displacement of, (E/T), 20: 2131 (JINR-P-2344)
flow of liquid II, critical heat currents in wide-channel, 20: 2928
heat fluxes in cryostat of liquid, calculation of, 20: 2892
ionization by protons in spark chambers, measurement of, (E), 20: 2128 (JINR-E-2324)
losses of terrestrial, mechanism for, (T), 20: 2857
meson ($\pi^-$) reactions at 120 to 280 Mev, double charge exchange in, (E), 20: 3080
nitrogen ion reactions at 0.14 to 0.7 Mev, energy loss in, (E), 20: 2602
oxygen ion reactions at 0.14 to 0.7 Mev, energy loss in, (E), 20: 2602
performance in gas turbines for nuclear power plants, 20: 3343
reactions with mercury, cross sections for line broadening from, (E), 20: 2637
scattering on rare gases, velocity dependence of total cross sections for, (E), 20: 2614
separation of krypton-85 and xenon-133 from, by sorption on activated carbon, 20: 1969
sound detection in solid, light scattering for second, (E), 20: 2896
sound velocities in crystalline, (T), 20: 2912
spectra of, lifetime of $3^1P$ state in, (E), 20: 2621
spectra of, $2^{1,3}P$, $3^{1,3}P$, and $4^{1,3}P$ states in, (E), 20: 2626
thermal conductivity at 0 to 1000°C and 1 to 200 atm, (E/T), 20: 1824
**HELIUM HYDRIDES**
wave equation for ionic, p-wave calculations for Schroedinger, (T),

20: 2595 (NASA-TN-D-3050)
**HELIUM IONS**
electron binding energy in negative, calculation of, (T), 20: 2646
ionization of nitrogen by 25- to 50-kev, total, (E), 20: 2623
reactions of monoatomic singly charged, with nitrogen at 10 to 65 kev, rotational and vibrational excitation of singly charged molecular nitrogen ions in, (E), 20: 2618
two-photon decay of metastable state of, 20: 2630
**HELIUM ISOTOPES He-3**
electromagnetic form factors, (T), 20: 3119
neutron reactions (n,n) to 1.5 Mev, phase-shift analysis of, 20: 3060
photodisintegration of, cross sections for total and two-particle, (T), 20: 3105
production by proton reactions with aluminum and iron, (E), 20: 3095
reactions (He-3,n) with light nuclei, angular distributions from direct, (T), 20: 3121
reactions with bismuth, yields of astatine isotopes from, 20: 1949
**HELIUM ISOTOPES He-4**
electron inelastic scattering at 200 Mev, differential spectra of, (E), 20: 3086
photodisintegration of, cross sections for total and two-particle, (T), 20: 3105
proton reactions (p,d) with, polarization effects in, (E/T), 20: 3023 (UCRL-16218)
proton scattering at 21 to 63 Mev, polarization effects in, (E/T), 20: 3022 (UCRL-16216)
reactions in collapsing stars, adiabatic exponent for equilibrium in, (T), 20: 2588
**HELIUM ISOTOPES He-5**
energy levels of, excited, (E), 20: 3078
**HELIUM SYSTEMS**
He–N, spectra of singly ionized nitrogen in plasma of, Stark profiles of, (E), 20: 3215
He–Ne, electric discharge in spark chambers, displacement of, (E/T), 20: 2131 (JINR-P-2344)
He–Rb, optical pumping of rubidium-87 in, 20: 2596 (UCRL-16241)
**HEMATOPOIETIC SYSTEM**
effects of aging on, of miniature swine, 20: 1581 (BNWL-SA-341)
radiation injuries of rat, protective effects of 5-hydroxytryptamine, 20: 1688
radiation injuries of rat, protective effects of aminoethylisothiuronium, 20: 1688
tissue transplants of, use for therapy of leukemia, 20: 1701
**HETEROGENEOUS REACTORS**
fire extinguishing system for, design of, 20: 3364(P)
neutron flux in cylindrical-cell approximation, fine structure in fast, 20: 3427
**HEXANE**
radiolysis of, effects of perfluoroalkanes on gamma, 20: 2520(R) (IA-920)
recoil reactions of carbon-11 in liquid, 20: 1896 (IS-T-23)
**2,5-HEXANEDIONE**
yields in gamma radiolysis of liquid acetone, 20: 1901
**HEXENE**
recoil reactions of carbon-11 in liquid, 20: 1896 (IS-T-23)
**HIGH ENERGY INJECTION DEVICES**
spectrometer design for use in DCX-2, (E), 20: 3178 (ORNL-P-1513)
**HIGH TEMPERATURE SEPARATION PROCESSES**
development of pyrochemical, for processing fast breeder fuels, 20: 3320(R) (ANL-7082, pp 1-28)
performance of fused-salt molten-metal extractor, 20: 2245
**HOLMIUM**
determination using Chromotrope 2B, photometric, 20: 1772
**HOLMIUM OXYBROMIDES**
preparation and crystal structure, 20: 1834
**HOLMIUM OXIDES**
magnetic susceptibility at 4 to 300°K, 20: 3318
**HOMOGENEOUS REACTORS**
control by fuel concentration variation in moderating vehicle, method for, 20: 3361(P)
**HORMONES**
radiation effects on induction of enzymes by, in rat liver, 20: 1674
**HYDRAULICS**
flow stability in round tubes, power distribution effects on forced water, 20: 2009 (EUR-2490.e)
**HYDRAZINE**
handling of, 20: 1727 (NASA-SP-5032)
toxicity of, 20: 1727 (NASA-SP-5032)
**HYDRAZINE, DIMETHYL-**
handling of, 20: 1727 (NASA-SP-5032)
toxicity of, 20: 1727 (NASA-SP-5032)
**HYDRAZINE, METHYL–**
handling of, 20: 1727 (NASA-SP-5032)
toxicity of, 20: 1727 (NASA-SP-5032)
**HYDRAZYL, DIPHENYLPICRYL-**
effects on nuclear spin polarization in polystyrene at low temperatures, (E/T), 20: 3143
effects on radioinduced polymerization of liquid and solid acetylene, 20: 1913
**HYDRIODIC ACID**
reactions with radioinduced radicals, kinetics of, 20: 1898(R) (RRL-2310-164)
**HYDROAROMATIC COMPOUNDS**
radiation effects on ionic processes in solid, relation to delayed luminescence, 20: 1906
substitution reactions of, isotopic effects on, 20: 1888
**HYDROBROMIC ACID**
HBr–HF, solvent properties for ignited plutonium dioxide, 20: 2344 (TRG-Report-1072)
**HYDROCARBONS**
analysis of carbon-14-labeled, for impurities, by radiochromatography, 20: 1764
density measurements on, x-ray transmission gage for, 20: 2115
radiolysis of, studies of free radicals produced in, 20: 1898(R) (RRL-2310-164)
**HYDROCHLORIC ACID**
corrosive effects on molybdenum, vanadium, and titanium–vanadium alloys, stress-, 20: 2254 (BM-RI-6680)
separation from polonium, effects of acetone on, 20: 1777
**HYDRODYNAMICS**
shock structure in relativistic, (T), 20: 2844
**HYDROFLUORIC ACID**
corrosive effects on tantalum at 2000 to 2800°K, 20: 2261(R) (UCRI-326)
corrosive effects on refractory metal carbides at 2000 to 3100°K, 20: 2261(R) (UCRI-326)
HBr–HF, solvent properties for ignited plutonium dioxide, 20: 2344 (TRG-Report-1072)
$HF–HNO_3$, solvent properties for ignited plutonium dioxide, 20: 2344 (TRG-Report-1072)
**HYDROGEN**
abstraction by tritium recoil atoms in ethylene, bond dissociation energies in, 20: 1907
collisions of atoms of, with fast hydrogen-like ions, calculation of cross sections for K-electron loss in, (T), 20: 2642
collisions of molecules of, with alkali metal atoms, ionization produced in, (E), 20: 2639
content in irradiated uranium dioxide fuel elements, 20: 2468
crystal structure of n-, p-, from electron diffraction, 20: 3310
determination in helium at reduced sample pressures by gas chromatography, 20: 1751
determination of, factors affecting continuous on line, 20: 1734 (EG-Report-36)
deuterium exchange with steam in presence of fissionable material, production of heavy water by, 20: 1884(P)
diffusion in hydrogen–niobium system, NMR spectra of, 20: 2365
effects on tensile properties of copper–niobium–zirconium alloy, 20: 2414 (AECL-2272)
effects on tungsten oxidation by water, 20: 2261(R) (UCRI-326)
electron scattering by, s-wave phase shift bounds for, 20: 2815
energy levels in stationary plasma of, population densities of excited, (T), 20: 3223
energy levels of atomic, group theory of Kepler problem for (T), 20: 2612
exchange reactions of, in nitration and succinoylation of tritium-labeled toluene, 20: 1950
glow discharges in, plasma effects, multiplication, and secondary emission of, 20: 2826
handling of liquid, 20: 1727 (NASA-SP-5032)
heating of plasma of, laser-beam, (T), 20: 3185(T) (TT-1193)
ionization of interstellar, by radiation from stars, (T), 20: 2562(R) (AD-614715)
light scattering by, Rayleigh cross section for laser, 20: 3234
molecular forces in diatomic, equations for, 20: 2650
neutron capture by, interaction effect in, (T), 20: 3059
neutron capture reactions (n,γ), cross section for thermal, (E), 20: 3058
neutron spectra in liquid, fast, (E), 20: 2967
neutron transport in media containing, eigenfunction analysis of, 20: 2999
nucleation and growth of hydrides in zirconium alloys, 20: 2253 (AECL-2297)
partition functions for molecular, pressure and temperature dependence of, (T), 20: 2610
photon reactions ($\gamma,\pi^0$) at 500 to 1000 Mev, proton polarization in, (E), 20: 2679 (AD-618664)
production of plasma of, at 10 to 800 mtorr, crossed-fields, (E), 20: 3177 (NP-15570)

radioinduced production from water, isotope effects in, 20: 2520(R) (IA-920)
reactions with beryllium in simulated launch pad abort environments at 800 to 1500°C, 20: 2341 (SC-DC-65-1637)
reactions with electron beams, oscillatory excitation in, 20: 1843
reactions with iron ions in various compounds, 20: 1844
reactions with isopropanol, isotope effects in, 20: 2520(R) (IA-920)
reactions with molecular hydrogen ions, effects of oscillatory excitation on, 20: 1843
reactions with tungsten oxide at 625°C, 20: 1831
reactions with Zircaloy-2, zirconium–niobium, and uranium–molybdenum alloys, kinetics, 20: 2222 (EURAEC-1390)
release in re-entry heating of uranium–zirconium hydride fuel elements, 20: 3563
scattering on krypton, velocity dependence of total cross sections for, (E), 20: 2614
separation from hydrogen isotope mixtures by gas chromatography, 20: 1733 (DP-979)
solubility in zirconium at 800°C, effects of oxygen on, 20: 2267
thermal diffusion in alpha–iron, nickel, and gamma–iron–nickel alloys at 400 to 600°C, 20: 2397
toxicity of liquid, 20: 1727 (NASA-SP-5032)
yields in radiolysis of liquid argon–ethylene, 20: 1898(R) (RRL-2310-164)
yields of, from radiolysis of benzene–isopropanol–benzophenone mixtures, 20: 1931
air–H, combustion of beryllium in flame system of, 20: 2341 (SC-DC-65-1637)

**HYDROGEN FERROCYANIDES**
iron-57 Mössbauer spectra from, (E), 20: 3296

**HYDROGEN IONS**
content in ionosphere, determination from proton-whistler measurements, (T), 20: 2847 (AD-614716)
dissociation of $H_3^+$ in DCX-1, proton trapping from Lorentz, (E), 20: 3213
electron reactions with molecular, dissociation cross sections for, (E), 20: 2632
energy levels of, photoelectron spectroscopy for vibrational, (E), 20: 2633
production of negative polarized, using charge exchange in argon and cesium, 20: 2537 (LA-DC-7268)
reactions of molecular, with hydrogen, effects of oscillatory excitation on, 20: 1843
reactions of monoatomic singly charged, with nitrogen at 10 to 65 kev, rotational and vibrational excitation of singly charged molecular nitrogen ions in, (E), 20: 2618
reactions of negative monatomic and positive diatomic and triatomic, with molybdenum surfaces, secondary-electron yields from, (E), 20: 2628
temperatures in ionosphere, determination from proton-whistler measurements, 20: 2847 (AD-614716)

**HYDROGEN ISOTOPES**
viscosity of liquid solutions of, (E), 20: 2922

**HYDROGEN ISOTOPES H-7**
production in meson ($\pi^-$) reactions with nuclei at 120 to 280 Mev, (E), 20: 3080

**HYDROGEN PEROXIDES**
molecular property calculations for, 20: 2520(R) (IA-920)
radiolysis of millimolar concentrations of, in aerated water, 20: 1894 (AD-623095)
reactions with plutonium in presence of different organic ligands, 20: 1857
reduction of ruthenium oxide in perchloric and sulfuric acids, ruthenium(IV) preparation by, 20: 1853

**HYDROGEN SYSTEMS**
D–H, viscosity of liquid, (E), 20: 2922
H–HD, viscosity of liquid, (E), 20: 2922
H–Nb, diffusion of hydrogen in, 20: 2365
H–O, combustion of beryllium in flame system of, 20: 2341 (SC-DC-65-1637)

**HYDROGEN TRITIDES**
separation from hydrogen isotope mixtures by gas chromatography, 20: 1733 (DP-979)
yields in hydrogen abstraction in ethylene reactions with tritium recoil atoms, 20: 1907

**HYDROLOGY**
problems in, from radioactive waste disposal in rivers, 20: 2082 (CEA-Bib.-59)
research on, Geological Survey Professional Paper 525-C, 20: 2043

**HYDROMAGNETIC WAVES**
kinetics and structure in solar photosphere, (T), 20: 2589
particle acceleration by, in slightly turbulent rarefied plasma, (T), 20: 3192
propagation in collisionless plasma, instabilities in, (T), 20: 3176(R) (NP-15562, pp 80-4)
shock behavior in one-dimensional flows of, switch-on, (T), 20: 2834
stability in plasma, higher order corrections for Alfven, (T), 20: 3221

**HYDROXIDES**
molecular structure of concentrated aqueous, 20: 2520(R) (IA-920)

**HYPERFRAGMENTS**
detection in nuclear emulsions, minimum momentum transfer for, (E), 20: 3063
production by lithium-6 reactions with mesons ($K^-$), (E), 20: 2520(R) (IA-920)
production in meson ($K^-$) interactions with emulsion nuclei at 5 Bev/c, (E), 20: 3062

**HYPERONS ($\Lambda$)**
decay in U(12) symmetry, parity-conserving amplitudes of hadron, (T), 20: 2697(T)
interactions with protons, effective-range and shape-dependent parameters for, (T), 20: 2707

**HYPERONS ($\Lambda^0$)**
decay of, De Santis model for, 20: 2784

**HYPERONS ($\Omega^-$)**
decay amplitudes of, SU(6) symmetry for photonic, 20: 2738
decay in $\bar{U}$(12) symmetry, parity-conserving amplitudes of hadron, (T), 20: 2697(T)
decay of, De Santis model for, 20: 2784
production in meson ($K^-$)-proton interactions at 6 Bev/c, lifetime and mass from, (E), 20: 2717

**HYPERONS ($\Sigma$)**
decay of, De Santis model for, 20: 2784

**HYPERONS ($\Sigma^-$)**
decay in $\bar{U}$(12) symmetry, parity-conserving amplitudes of hadron, (T), 20: 2697(T)
interactions with protons at rest, absorption time for, (E), 20: 2723

**HYPERONS ($\Sigma^0$)**
decay of, $G_2$ symmetry in, (E/T), 20: 2520(R) (IA-920)
photoproduction on protons, (E/T), 20: 2735

**HYPERONS ($\Sigma^+$)**
decay in $\bar{U}$(12) symmetry, parity-conserving amplitudes of hadron, (T), 20: 2697(T)
interactions with protons, effective-range and shape-dependent parameters for, (T), 20: 2707
magnetic moment of, possibility of measuring, (T), 20: 2744

**HYPERONS ($\Xi^-$)**
decay in $\bar{U}$(12) symmetry, parity-conserving amplitudes of hadron, (T), 20: 2697(T)

**HYPNOTICS**
radiation effects on response of rats to barbiturates, 20: 1662

**HYPOFLUORITES**
sulfur fluoride, effects of water on preparation of, 20: 1881

**HYPOXANTHINE**
resistance to analogs of, in murine cell line, 20: 1678

# I

**ICELAND**
fallout monitoring, 1961 to 1964, 20: 2054

**IMAGE BRIGHTNESS INTENSIFIERS**
development of neutron, 20: 3321(R) (ANL-7082, pp 29-53)

**IMMUNE REACTIONS**
protein transfer in, tracer studies of, 20: 1943
radiation effects on, in monkeys, 20: 1631
radiation effects on, in allogenic and syngenic bone marrow mouse chimeras, 20: 1660
radiation effects on, in mice injected with sheep erythrocytes, 20: 1661
radiation effects on, to transplanted bone marrow, 20: 1700
radiation effects on, to hematopoietic tissue transplants, 20: 1701
radiation effects on, in mice and rats, 20: 1632
to lymphoid cells, by mouse embryo cells in tissue culture, 20: 1658

**IMPACT SHOCK**
wave propagation in open-end hollow cylinder, analog model of, (T), 20: 3630 (SC-DC-65-1697)

**IN-PILE LOOPS**
design for fuel failure studies using sodium coolant, 20: 3347
method for removal from Brookhaven Graphite Research Reactor, 20: 3599
operation of sodium, with stainless steel paste, 20: 3460

**INCINERATORS**
air cleaning system and combustion of, performance evaluation of, 20: 1989 (NYO-841-2)

**INCOLOY**
compatibility of 800, with plutonium–uranium–zirconium alloys, 20: 2229
corrosion of 800, by steam and water at 800 to 1500°F, (E), 20: 3471(R) (GEAP-4861)
creep rupture testing of type 2, at 1100 to 1350°F, (E), 20: 3471(R) (GEAP-4861)

diffusion of fission products in 800, 20: 2389
radiation effects of fast neutrons on tensile properties of 800, (E), 20: 3471(R) (GEAP-4861)
radiation effects on mechanical properties of 800, neutron, 20: 2458
radiography of boron in, using neutrons, (E), 20: 3471(R) (GEAP-4861)
reactions with plutonium–uranium–zirconium alloys at high temperatures, 20: 3320(R) (ANL-7082, pp 1-28)
separation of 800, from boron by electron beam melting, (E), 20: 3471(R) (GEAP-4861)

**INCONEL**
corrosion of 625 and 718, by steam and water at 800 to 1500°F, (E), 20: 3471(R) (GEAP-4861)
radiation effects on 713-C and X-750, at cryogenic temperatures, 20: 2459
radiography of boron in, using neutrons, (E), 20: 3471(R) (GEAP-4861)
welding to stainless steel, 20: 3472(R) (GEAP-4891)

**INDEXES**
of Mössbauer effect data, 20: 3146

**INDIUM**
corrosion resistance to mercury at 900°F, 20: 2264
determination by spectrophotometry using bromopyrogallal red, 20: 2520(R) (IA-920)
determination in uranium, fluorometric, 20: 2520(R) (IA-920)
separation of trace amounts of, from alkali metals, alkaline earths, and rare earths, 20: 1958
superconducting transition temperature of films of lead on, (E), 20: 2917
superconducting transition temperature of thin films of, effect of thin oxide layer on, 20: 2915

**INDIUM ALLOYS**
Au–In–Sn, solute interactions in dilute, (E/T), 20: 2349 (UCRL-16320)
Bi–In, Ginzburg-Landau parameters of superconducting, (E/T), 20: 2906
Bi–In, specific heat of superconducting, in magnetic fields, (E), 20: 2906
In–Ag–Sn, solute interactions in dilute, (E/T), 20: 2349 (UCRL-16320)
In–Pb, voltage in superconducting type II, transverse, (E), 20: 2897
In–Sn, Mössbauer effect in superconducting, (E), 20: 2919
In–Sn, solute interactions in dilute, (E/T), 20: 2349 (UCRL-16320)
In–Sn, thermal conductivity below 1°K, (E), 20: 2383
Sb–In, radiation effects on close-pair defects at 0 to 140°K in, 20: 2482
Sb–In, radiation effects on semiconducting, 20: 2497
Sb–In, radiation effects on n-type, at 78°K, 20: 2500
Sb–In, radioinduced defects in, structural properties of, 20: 2486

**INDIUM ARSENIDES**
radiation effects on semiconducting, 20: 2497

**INDIUM ISOTOPES In-115**
neutron reactions (n,γ), cross sections for resonance and thermal, (E), 20: 3031

**INDIUM ISOTOPES In-116**
gamma spectra of, (E), 20: 3097

**INDIUM PHOSPHIDES**
radiation effects on semiconducting, 20: 2497

**5-INDOLOL, 3-(2-AMINOETHYL)-**
protective effects against radiation injuries in rats, low-dose exposure, 20: 1688

**INDUCTION FURNACES**
performance for cold-mold melting of refractory metals, 20: 2352(R) (USBM-RC-1205, pp-9-10)

**INDUCTION HEATING**
use of high-frequency, in chemistry, metallurgy, and physics, 20: 2525

**INFORMATION RETRIEVAL SYSTEMS**
development, 20: 2520(R) (IA-920)
neutron cross sections, computer program for, 20: 3009 (GA-6685)

**INFRARED RADIATION**
emission by solid refractory materials at 1300°K, 20: 1823

**INFRARED SPECTROMETERS**
development for nondestructive testing, 20: 3321(R) (ANL-7082, pp 29-53)

**INOR-8**
radiation effects on rupture life of, effects of irradiation temperature on fast neutron, 20: 2423(R) (GEMP-52A, pp 27-35)
radiation effects on rupture life of, effects of postirradiation annealing on fast neutron, 20: 2423(R) (GEMP-52A, pp 27-35)

**INSECTICIDES**
determination on grain samples, activation, 20: 1740(R) (GA-4576)
effects on ecology of boral forests, 20: 1589 (BNL-917, pp 61-8)

**INSECTS**
effects of spruce budworm on ecology of boral forests, 20: 1589 (BNL-917, pp 61-8)
radiation control of flour beetle, *Tribolium castaneum*, 20: 1613 (HW-SA-3537)
radiation effects on reproduction of Tribolium, effects of age and temperature, 20: 1613 (HW-SA-3537)

**INSTRUMENTATION**
conference on power plant, 20: 2119
design for photographic film-scanning, 20: 2130 (JINR-P-2340)
development for liquid metal power cycles, 20: 2013 (ORNL-P-1661)
development for microwave spectrometry, 20: 2106 (UJV-1346/65)
development of nuclear, 20: 2107
shipment of fragile, isolation of shock and vibrations for, (T), 20: 3613 (CONF-651016-1)

**INSTRUMENTS**
design for complex emanation-thermal analysis, 20: 1779
shipment of fragile, isolation of shock and vibrations for, (T), 20: 3613 (CONF-651016-1)

**INSULIN**
labeling with iodine-131, 20: 1890

**INTERMETALLIC COMPOUNDS**
thermodynamic properties of ordered, compositional variation of configurational, (T), 20: 2349 (UCRL-16320)

**INTERNAL FRICTION**
measurement in crystals, effects of vacancy absorption and emission by lattice dislocations on, 20: 3281(T) (NLM-1276(tr))

**IODIDE IONS**
effects on deamination of ethylenediamine, 20: 2520(R) (IA-920)

**IODINE**
determination in blood using neutron activation of iodine-129, 20: 1790
labeling of methyl iodide by fission-produced, selectivity effects in, 20: 2520(R) (IA-920)
separation from atmosphere by spraying, 20: 1966

**IODINE COMPOUNDS**
determination in blood using neutron activation of iodine-129, 20: 1790

**IODINE ISOTOPES I-123**
production using ORNL 86-in. cyclotron, 20: 2212

**IODINE ISOTOPES I-125**
incorporation in proteins, computer programs for immunochemical studies using paired and triad, 20: 1943
incorporation into proteins of, electrochemical, 20: 1939 (EUR-2476.i)

**IODINE ISOTOPES I-127**
neutron reactions (n,γ), cross sections for resonance and thermal, (E), 20: 3031

**IODINE ISOTOPES I-130**
incorporation in proteins, computer programs for immunochemical studies using paired and triad, 20: 1943

**IODINE ISOTOPES I-131**
beta decay of, spin dependence of Rayleigh scattering from, (E), 20: 3082
content in fallout particles, 20: 2053
determination in sea water, methods for, 20: 1749 (USNRDL-TR-912)
effects on cardiac activity in dogs, 20: 1629
incorporation in insulin, 20: 1890
incorporation in proteins, computer programs for immunochemical studies using paired and triad, 20: 1943
incorporation into proteins of, electrochemical, 20: 1939 (EUR-2476.i)
metabolism in human fetuses, 20: 1600
separation from aqueous solutions, use of silica gel for, 20: 1742 (INR-636/XIII/J)
separation from milk by electrodialysis, 20: 1972(P)
uptake by rat hair, 20: 1695

**ION BEAMS**
acceleration and production of high-intensity in electrostatic fields, 20: 2561
scattering of complex-nucleus, by heavy nuclei, collective levels from inelastic, (T), 20: 3013 (JINR-P-2331)

**ION EXCHANGE MATERIALS**
depletion in Savannah River reactors, 20: 2419 (DP-973)
properties of amberlite IR-120 for iron and thorium, 20: 1783

**ION EXCHANGE PROCESSES**
design for demineralization of dual-purpose boiling-water reactor coolant, 20: 3539 (ACNP-65558(Rev.1))
development for removal of cesium and strontium from milk, 20: 1975(P)

**ION SOURCES**
design of polarized negative hydrogen, 20: 2537 (LA-DC-7268)
design of polarized deuteron, 20: 2528

**IONIZATION**
calculation of cross sections for K-electron loss by fast hydrogen-like ions colliding with hydrogen and helium atoms, (T), 20: 2642

**IONIZATION CHAMBERS**
design and performance for measuring atmospheric radon-220 content, (E), 20: 2860
development, 20: 2177
efficiency in conducting medium, (T), 20: 2137
electric charges in, electrometer for measuring, 20: 2183(P)
use with radioactive source for high-resistance ohmmeter, 20: 2108

**IONOSPHERE**
charged-particle diffusion in lower, negative-ion effects on, (T),

20: 2853
electron density in F(2) region of, effects of sunspots on, 20: 2848 (AD-615111)
electron/hydrogen ion content ratio in, determination from proton-whistler measurements, (T), 20: 2847 (AD-614716)
ionization diffusion and drift motions in F2 region of, ambipolar, (T), 20: 2858
satellite motion in, plasma kinetics from, 20: 2863(T)
storms in, during low and medium sunspot activity, 20: 2848 (AD-615111)
**IONS**
collisions of fast hydrogen-like, with helium and hydrogen atoms, calculation of cross sections for K-electron loss in, (T), 20: 2642
collisions of negative, with atoms at low energies, electron detachment in, (T), 20: 2648
destruction by electric fields and by electron impact, (T), 20: 2646
model potential for positive, 20: 2611
motion in electric and magnetic fields, theory of, 20: 3237
oscillations in plasma beam system, 20: 3191
reactions with atoms, electron capture and loss by fast, (T), 20: 2634
solvation in mixed solvents, ionic free energy of, 20: 2520(R) (IA-920)
**IRIDIUM ISOTOPES Ir-192**
use in radiography, diffraction effects from, 20: 2029
**IRON**
compatibility with uranium–zirconium alloys, 20: 2229
content in concretes, gamma and neutron shielding parameter variations with, 20: 3253
corrosion by bismuth and tin, 20: 2275
corrosion resistance to mercury at 900°F, 20: 2264
deuteron elastic scattering at 26 Mev, optical model analysis of, (E/T), 20: 3053
deuteron elastic scattering at 27.5 Mev, angular distribution for, (E/T), 20: 3057
effects of additions of, on steam corrosion of niobium–tin–zirconium alloys, 20: 2255(R) (EURAEC-1323)
effects on hardness properties of Nitinol alloy, 20: 2310 (AD-618681)
electron scattering at 0.5 to 3.0 Mev, bremsstrahlung from, (E), 20: 3247 (NASA-SP-71, pp 449-53)
gamma dose albedos for, (T), 20: 3274
ion exchange by amberlite IR-120 in nitric acid solution, 20: 1783
meson ($K^0$) regeneration in, 20: 2748
neutron attenuation in, few- and multigroup P3 analyses of, (T), 20: 2939 (WAPD-T-1710)
neutron attenuation in, from alpha reactions with tantalum, (E), 20: 2554
neutron inelastic scattering at 14.6 Mev, (E/T), 20: 2962
neutron total cross section at 14.6 Mev, (E), 20: 2962
proton reactions at 1 to 3 Bev, distributions from, (E), 20: 3015 (NASA-SP-71, pp 357-62)
proton reactions at 1 and 3 Bev, nucleon-meson cascades in, (T), 20: 3258
proton reactions at 30 to 45 Mev, helium-3 and tritium production in, (E), 20: 3095
radiation effects on bcc alpha-, computer study of, 20: 2473
radiation effects on, neutron, 20: 2474
radiation effects on hardening and embrittlement of bcc, 20: 2472
reactions with uranium dioxide in perchloric acid solutions, kinetics of, 20: 1851
separation of trace amounts of, from alkali metals, alkaline earths, and rare earths, 20: 1958
solubility in molten potassium, 20: 2237
superconducting properties of superimposed films of tin and, 20: 2894
thermal diffusion of deuterium and hydrogen in alpha, at 400 to 600°C, 20: 2397
thermal diffusivity of Armco, at 25 to 1100°C, 20: 3622 (IS-1266)
wetting properties for metallic carbides, 20: 1837
**IRON ALLOYS**
corrosion resistance to mercury at 900°F, 20: 2264
fabrication of shielding materials of, 20: 2301(P)
Al–Cr–Fe, diffusion of uranium through cladding of, research program for, 20: 2322(R) (GEMP-52A, pp 53-4)
Al–Cr–Fe, oxidation by carbon dioxide, effects of yttrium additions on, 20: 2263
Al–Cr–Fe–Y, corrosion by steam at 550°C, effects of pre-oxidation and strain on, 20: 2223(R) (GEMP-51A)
Al–Cr–Fe–Y, diffusion of uranium through cladding of, 20: 2223(R) (GEMP-51A)
Al–Cr–Fe–Y, oxidation by air at 900 and 1100°C, 20: 2223(R) (GEMP-51A)
Al–Cr–Fe–Y, radiation effects on mechanical properties of, 20: 2409(R) (AD-617319)
Al–Cu–Fe–Sn–Ti–V–Zr, deformation and heat treatment effects on mechanical properties of, 20: 2309 (AD-615024)
Al–Fe, iron-57 Mössbauer effect in intermetalic compounds of, ordering transformation from, (E), 20: 3292
Cr–Fe, oxidation by carbon dioxide, effects of yttrium additions on, 20: 2263
Cr–Fe–Ni, electron-beam welding to tubesheet joints, 20: 2283 (KAPL-3110)
Fe–Lu, preparation and structure of $MgCu_2$-type, 20: 2385(T)
Fe–Mn, effects of strain rate, structure, and temperature on flow stress at 77 to 370°K, 20: 3641 (UCRL-11512(Rev.))
Fe–Ni, thermal diffusion of hydrogen in gamma-, at 400 to 600°C, 20: 2397
Fe–Tb, preparation and structure of $MgCu_2$-type, 20: 2385(T)
Fe–Yb, anisotropy of exchange in garnets of, 20: 1802 (AD-618038)
Ga–Fe–Pu, reactions with tantalum at high temperatures, 20: 2228
Sb–Fe, iron-57 isomer shift and quadrupole splitting in $FeSb_2$, 20: 3317
**IRON(II) CHLORIDES**
nuclear electric-field gradient in tetrahydrate of, (E), 20: 3299
**IRON(III) CHLORIDES**
corrosive effects on molybdenum, vanadium, and titanium–vanadium alloys, stress-, 20: 2254 (BM-RI-6680)
**IRON COMPOUNDS**
bonding in, Mössbauer study of, 20: 1874
nuclear electric-field gradient in, measurement using Mössbauer effect of iron-57, (E), 20: 3299
**IRON CYANIDES**
reactions with hydrogen and positronium, 20: 1844
**IRON HYDROXIDES**
reactions with uranium dioxide in perchloric acid solutions, kinetics of, 20: 1851
**IRON IONS**
atomic wave functions, collision cross sections, and transition probabilities for, 20: 2609
radiolysis of trivalent, in perchlorate solution, pulse, 20: 1898(R) (RRL-2310-164)
spectra in polycrystalline Ferrichrome A, paramagnetic resonance, 20: 3643 (UCRL-11685)
**IRON ISOTOPES Fe-54**
neutron reactions (n,γ) with, gamma spectra from thermal, 20: 3109
**IRON ISOTOPES Fe-55**
decay scheme from thermal neutron reactions (n,γ) with iron-54, 20: 3109
**IRON ISOTOPES Fe-56**
gamma transition at 846.8 kev following Coulomb excitation, (E), 20: 3043
neutron inelastic scattering at 14.6 Mev, (E/T), 20: 2962
reactions in collapsing stars, adiabatic exponent for equilibrium in, (T), 20: 2588
**IRON ISOTOPES Fe-57**
Mössbauer effect in vanadium oxides antiferromagnetism from, (E), 20: 3289
Mössbauer effect in aluminum–iron intermetallic compounds, ordering transformation from, (E), 20: 3292
Mössbauer effect in ferrous salts, use in nuclear electric-field gradient measurements, (E), 20: 3299
Mössbauer effect in marcasite-type iron compounds, 20: 3317
Mössbauer effect of, in beryllium and copper, 20: 3145
Mössbauer spectra in alkaline ferrocyanides, (E), 20: 3296
**IRON ISOTOPES Fe-58**
proton reactions (p,αγ), cobalt-58 levels from, (E), 20: 3077
**IRON OXIDES**
testing for use in shaft seals for potassium space power systems, 20: 2242
**IRON(III) OXIDES**
$CaO–Fe_2O_3$, phase studies of, emanation-thermal method for, 20: 1861
$F_2O_3–Rh_2O_3$, crystal and magnetic structure of, (E), 20: 3293
**IRON PERCHLORATES**
reactions with hydrogen and positronium, 20: 1844
**IRON SELENIDES**
iron-57 isomer shift and quadrupole splitting in marcasite, 20: 3317
**IRON SULFATES**
reactions with hydrogen and positronium, 20: 1844
**IRON SULFIDES**
iron-57 isomer shift and quadrupole splitting in marcasite and pyrite, 20: 3317
**IRON SYSTEMS**
C–Fe, fabrication of shielding materials of, process for, 20: 2301(P)
$Fe–H_2O$, neutron attenuation in, few- and multigroup P3 analyses of, (T), 20: 2939 (WAPD-T-1710)
$Fe–UO_2$, radioinduced swelling in, 20: 2223(R) (GEMP-51A)
**IRON TELLURIDES**
iron-57 isomer shift and quadrupole splitting in marcasite, 20: 3317
**IRRADIATION FACILITIES**
design for swimming-pool reactors, 20: 3602(P)
design of gamma, 20: 2193
design of gamma, for bulk grain irradiation, 20: 2194
design of high-level gamma, for radiation chemistry, 20: 1929

design using isotopic neutron sources, 20: 2997
**IRRADIATION TECHNIQUES**
for exposure of plant cells to cyclotron meson ($\pi^-$) beam, 20: 1621 (UCRL-16387)
**ISOPROPYL ETHER**
solvent properties for astatine, 20: 1949
**ISOTOPE EFFECTS**
kinetics of, in distribution of isotopic molecules, (T), 20: 1866
of deuterium on decomposition of acetyl peroxide, t-butyl phenyl peracetate, and t-butyl-α-phenylperpropionate, 20: 1891
of tritium on activity of adenosine triphosphate, 20: 1583
on aromatic substitution reactions, 20: 1888
**ISOTOPE SEPARATION METHODS**
electromagnetic, method for calculating image aberrations in, (T), 20: 2209 (SGAE-PH-26/1965)
zone refining applications in, 20: 2520(R) (IA-920)
**ISOTOPES**
diffusion in biological membranes, effects of flux on, 20: 1585
diffusion in solids, 20: 3304(T)
separation by electromigration, cost of, 20: 2520(R) (IA-920)
separation in inhomogeneous magnetic sector fields, method for calculating image aberrations in, (T), 20: 2209 (SGAE-PH-26/1965)
**ISOTOPIC EXCHANGE**
between cyclohexane and deuterium, effects of germanium and silicon on, 20: 1838
deuterium, between methanol and cyclopentadienyl rings of cobalticinium compounds, 20: 1828
**ISRAEL**
fallout monitoring, July to Dec. 1963, 20: 2520(R) (IA-920)
**ITALY**
fallout monitoring, 1963, 20: 2046 (BIO/04/64)
fallout monitoring, 1964, 20: 2047 (EUR-2509.e)
waste disposal in, technical and hygienic aspects of, 20: 3604 (RT/PROT(65)-12)

## J

**JETS**
development for Dresden reactor coolant circulation, 20: 3476 (NP-15538(Vol.1))

## K

**KETONES**
radiation effects on ionic processes in solid, relation to delayed luminescence, 20: 1906
ketone–urea, ESR studies of irradiated, 20: 1935
**KIDNEYS**
radiosensitivity of, in dogs, 20: 1686
radiosensitivity of human, to alpha particles, charged particle, and protons, 20: 1616 (NASA-SP-71, pp 219-23)
**KRYPTON**
collisions of atoms of, with alkali metal atoms, ionization produced in, (E), 20: 2639
collisions of atoms of, with singly charged krypton ions, profound stripping and scattering in, (E), 20: 2644
diffusion in irradiated uranium, coefficient of, 20: 2358(T) (AERE-Trans-1034)
diffusion in tantalum, 20: 2321(R) (GEMP-52A, pp 43-5)
helium scattering on, velocity dependence of total cross sections for, (E), 20: 2614
hydrogen scattering on, velocity dependence of total cross sections on, (E), 20: 2614
reactions with mercury, cross sections for line broadening from, (E), 20: 2637
spectra of graphite vapor, mercury, and sulfur isolated in, at high temperatures, 20: 1818 (UCRL-11976)
**KRYPTON IONS**
collisions of singly charged, with rare gas atoms, profound stripping and scattering in, (E), 20: 2644
reactions with uranium dioxide surfaces, saturation values, secondary electron yields, and sputtering ratios in, 20: 1813 (EUR-2515.e)
**KRYPTON ISOTOPES**
yields in uranium-233 thermal fission, (E), 20: 3010(R) (IDO-14663)
**KRYPTON ISOTOPES Kr-85**
precipitation as kryptonate on polymethylmethacrylate, activity from, 20: 1862
sorption on activated carbon, from air, argon, carbon dioxide, and helium, 20: 1969
**KRYPTONATES**
preparation of, on polymethylmethacrylate base, 20: 1862

## L

**LABORATORIES**
description of Babcock and Wilcox Hot-Cell Facility, 20: 1998
description of BNL alpha-gamma facility for reactor fuel studies, 20: 2001
description of central laboratory for hot chemistry at Julich, 20: 1996
description of Fontenay-aux-Roses Radiometallurgy Laboratory, 20: 1999
description of hot laboratory at Japan Atomic Energy Research Institute, 20: 1997
design of alpha, 20: 2089
development of high-level caves at Savannah River Laboratory, 20: 2000
radon content in, ventilation effects on, 20: 2090
**LABORATORY EQUIPMENT**
description of evaporator-collector for sampling water supplies, 20: 1757
**LACTIC ACID, 2-METHYL-**
electrophoretic properties in α-hydroxyisobutyric acid, 20: 1756
use in electrophoresis of radioactive rare earth gases, 20: 1961
**LANTHANUM**
determination in river silts and soils, activation, 20: 1739(R) (GA-4297)
determination in soils, activation, 20: 1738(R) (GA-4041)
determination of trace amounts in uranium compounds by activation analysis, 20: 1784
determination using Chromotrope 2B, photometric, 20: 1772
separation from thorium and other rare earths by ion exchange in ammonium thiocyanate–organic solvent–water systems, 20: 1959
separation of trace elements from, by precipitation ion exchange, 20: 1958
thermal conductivity of normal and superconducting, (E), 20: 2893
**LANTHANUM ACETATES**
complexes with thiourea, solubility in water, 20: 1869
**LANTHANUM ALLOYS**
Al–La–Zr, crystal structure, 20: 2399
Gd–La, spin ordering of paramagnetic states in superconducting, 20: 2918
**LANTHANUM CITRATES**
preparation, composition, and electric conductivity of hydrates, 20: 1856
**LANTHANUM FLUORIDES**
spectra of praseodymium–neodymium-doped, optical linewidth and line-shape studies of energy transfer mechanisms in, (E), 20: 2627
**LANTHANUM ISOTOPES La-140**
content in fallout particles, 20: 2053
**LANTHANUM OXYBROMIDES**
preparation and crystal structure, 20: 1834
**LEAD**
bremsstrahlung attenuation in, 20: 3254
effects on organic scintillator efficiency for gamma detection, 20: 1905
electron-photon cascades in thick targets of, (T), 20: 3261
gamma back-scattering from, albedos from, (E), 20: 3273
gamma dose albedos for, (T), 20: 3274
grain boundary migration in zone-refined, review on, 20: 3626 (ORNL-P-1722)
ionization in K-shell by alpha particles at 3 to 4 Mev, x-ray yields from, (E), 20: 2625
neutron diffusion in, heavy monoatomic gas model for, 20: 2943
neutron flux decay in slabs of, fast, (E), 20: 2950
properties as neutron reflector, 20: 3390
properties as neutron reflectors, 20: 3391
superconducting transition temperature of thin films of, effect of thin oxide layer on, 20: 2915
superconducting transition temperature of, effect of chromium, cobalt, and iron additives on, (E), 20: 2916
superconducting transition temperature of, effect of chromium-, manganese- and cobalt-oxides on, (E), 20: 2916
superconducting transition temperature of films of, on substrates, (E), 20: 2917
superconducting transition temperature of layers of indium, (E), 20: 2917
use in concretes for shielding materials, 20: 2306(P)
**LEAD ALLOYS**
In–Pb, voltage in superconducting type II, transverse, (E), 20: 2897
Mn–Pb, spin ordering of paramagnetic states in superconducting, 20: 2918
**LEAD ISOTOPES**
abundance ratios in galenas, Cobalt-Noranda Area, Canada, 20: 2051
**LEAD ISOTOPES Pb-208**
deuteron elastic scattering at 27.5 Mev, angular distribution for, (E/T), 20: 3057
energy level at 7.285 Mev, (E), 20: 2520(R) (IA-920)
neutron scattering at 0.8 to 4.5 Mev, compound-nucleus analysis of, (T), 20: 3021 (ORNL-TM-1238)
triton reactions (t,α) at 12 Mev, thallium-207 1.34-Mev level from, (E), 20: 3071
**LEAD ISOTOPES Pb-209**

neutron scattering at 0.8 to 4.5 Mev, compound-nucleus analysis of, (T), 20: 3021 (ORNL-TM-1238)

**LEAD ISOTOPES Pb-210**
determination in actinium-227 by electrophoresis, 20: 1756

**LEAD OXIDES**
use in bitumen-bound radiation shielding material, 20: 2248(P)

**LEAD(IV) OXIDES**
$PbO_2$–$UO_2$, phase studies on, 20: 1871

**LEAD SYSTEMS**
Al–$AlO_x$–Pb, superconducting film diodes of, geometrical resonance in tunneling characteristics of, (E), 20: 2909

**LEAK DETECTORS**
design of high-sensitivity infrared, for heavy water in light water, 20: 2099 (AECL-2291)

**LEAKS**
detection in HWCTR containment building, 20: 2037 (DP-968)

**LEPTONS**
interactions of, charged vector meson theory for, 20: 2797
production of pairs of, in proton-pair annihilation, (T), 20: 2696

**LEUKEMIA**
treatment of acute, in man and mice, use of whole-body x irradiation and bone marrow transplants for, 20: 1700
treatment of acute, in man and mice, use of whole-body x irradiation and hematopoietic tissue transplants, 20: 1701

**LEUKOCYTES**
chromium phosphate colloid distribution in, tracer studies of, 20: 1598
radiation effects on number of, in peripheral blood. 20: 1672
radiation effects on number of, in blood of guinea pigs, effects of dose and time on, x, 20: 1670

**LEVEL INDICATORS**
design of liquid metal, 20: 2013 (ORNL-P-1661)

**LIFE SPANS**
radiation effects on, of mammals, 20: 1716

**LIGHT**
effects on ionic processes in gamma irradiated solid organic compounds, relation to delayed luminescence, 20: 1906
effects on ribonucleic acid in tobacco mosaic virus exposed to ultraviolet radiation, reactivating, 20: 1659
scattering by plasma electrons, 20: 3232
scattering by polymer discs, polarization effects in, (T), 20: 1817 (TID-22323)
scattering of laser, in plasmas, 20: 3234
transmission by two-dimensional spherulite between crossed polaroids, 20: 3636 (TID-22319)

**LINEAR ACCELERATORS**
beam current of electron, device for measuring, 20: 2531 (AD-618304)
construction status of Frascati, 20: 2521 (LNF-65/28)
development of high-energy proton, review of, 20: 2538 (LA-DC-7281)
operation of, instrumentation and safety in, 20: 2531 (AD-618304)
shielding design for NRL 60-Mev electron, 20: 2556

**LIPIDS**
fatty acid content of, in the gempylid fish, *Ruvettus pretiosus*, 20: 3637 (UCLA-12-534)
radiation effects on wheat, effects of dose on gamma, 20: 1637

**LIQUID FLOW**
magnetohydrodynamic, Hartmann layer effects in, (E/T), 20: 2831

**LIQUID METAL COOLED REACTORS**
cooling apparatus for, design of, 20: 3537(P)
cooling system design for experimental 2 Mw sodium, 20: 3479 (NP-15556)
design of Soviet BN-350 power-breeder sodium, 20: 3475 (NP-15458)
fuel elements of, calculation of transient thermal stresses in, 20: 3463

**LIQUIDS**
bubble growth in, stability of energy density in, (T), 20: 2839
dispersion of uniform droplets of, process for, 20: 1800
flow of finitely conducting viscous, Hartmann layer effects in, (E/T), 20: 2831
properties of, time-correlation functions for, (T), 20: 2846
stability of electrically conducting layer of, magnetic field effects on, 20: 2820 (AD-614645)
thermodynamic properties of physico-chemical systems during phase transitions, methods for estimating, 20: 1819 (UCRL-14287)

**LITHIUM**
collision cross sections for dipole transitions in isoelectronic series of, 20: 2598
collisions of atoms of, with rare gas atoms and hydrogen and nitrogen molecules, ionization in, (E), 20: 2639
content in stars during pre-main-sequence contraction, depletion in, (T), 20: 2566
corrosive effects on refractory alloys at 1200°C, 20: 3321(R) (ANL-7082, pp 29-53)
corrosive effects on niobium–vanadium alloys, effects of oxygen on, 20: 2340 (ORNL-TM-1131)
corrosive effects on refractory alloys, 20: 2238
corrosive effects on niobium–zirconium alloy at high temperatures, 20: 2268
corrosive effects on molybdenum, rhenium, and tungsten alloys at high temperatures, 20: 2269
effects on radioinduced defects in silicon, 20: 2491
electron spin resonance, (E), 20: 3297
gyromagnetic ratio of conduction electrons in, (E), 20: 3297
meson ($\pi^-$) reactions at 120 to 280 Mev, double charge exchange in, (E), 20: 3080
positron annihilation in, (T), 20: 3314
separation of trace elements from, by precipitation ion exchange, 20: 1958
spectra in electron fields, Stark shift of $3^2P$ term in, (E), 20: 2619

**LITHIUM ALLOYS**
Li–Ag, diffusion of tritium in, 20: 2317 (EURAEC-1380)

**LITHIUM CHLORIDES**
radiation effects on crystal structure of, mechanism of beta, 20: 2426 (LA-3387)
LiCl–KCl, effects of molten, on thermodynamic properties of molybdenum(III) chloride, 20: 1882
LiCl–KCl–Zn–$ZnCl_2$, reactions of uranium monocarbide at 540 to 802°C in, 20: 2404
LiCl–KCl, stability of zirconium dichloride in, 20: 1822(T) (ANL-Trans-233)

**LITHIUM FERROCYANIDES**
iron-57 Mössbauer spectra from, (E), 20: 3296

**LITHIUM FLUORIDES**
isotope effect in molar volumes of, 20: 3307(T)
radiation effects on crystal structure of, mechanism of beta, 20: 2426 (LA-3387)
radioinduced thermoluminescence of gamma and thermal neutron, 20: 2178
spectroscopy of, measurement of rotational transitions in, 20: 1876

**LITHIUM HYDRIDES**
isotope effect in molar volumes of, 20: 3307(T)
neutron scattering by cylinders of, fast, (E/T), 20: 3265
radiation effects on crystal structure of, mechanism of beta, 20: 2426 (LA-3387)

**LITHIUM IONS**
spectra of, $2^1P$ state in, (E), 20: 2626

**LITHIUM ISOTOPES Li-6**
content in Hyades F stars, ratio to lithium-7, (E/T), 20: 2577
diffusion in sodium, isotope effect in, 20: 3305(T)
meson (K-) reactions with, hyperfragments from, (E), 20: 2520(R) (IA-920)
proton reactions (p,n), neutron threshold measurements of, (E), 20: 3140
reactions (Li-6,d) with oxygen-16, selection rules for, (T), 20: 3117

**LITHIUM ISOTOPES Li-7**
content in Hyades F stars, ratio to lithium-6, (E/T), 20: 2577
determination in neutron irradiated boron–copper system by atomic absorption methods, 20: 2444
deuteron reactions at 380 kev, helium-5 excited levels from, (E), 20: 3078
diffusion in sodium, isotope effect in, 20: 3305(T)
neutron inelastic scattering at 14.6 Mev, (E/T), 20: 2962

**LITHIUM ISOTOPES Li-8**
production in meson (K-) interactions with emulsion nuclei at 5 Bev/c, (E), 20: 3062

**LITHIUM ISOTOPES Li-9**
decay of, delayed neutron spectra from, (E), 20: 3130

**LITHIUM NITRATES**
ion exchange from aqueous nitric acid, effects of acidity on, 20: 2520(R) (IA-920)
solvent properties for water vapor, thermodynamics of, 20: 1812 (EUR-2495.e)
$LiNO_3$–$KNO_3$, solvent properties for water vapor, 20: 1812 (EUR-2495.e)
$LiNO_3$–$NaNO_3$, solvent properties for water vapor, 20: 1812 (EUR-2495.e)

**LITHIUM TRITIDES**
radiation effects on crystal structure of, mechanism of beta, 20: 2426 (LA-3387)

**LIVER**
chromium phosphate colloid distribution in, tracer studies of, 20: 1598
radiation effects on dietary and hormonal induction of enzymes in, of rats, $\gamma$, 20: 1674
radiosensitivity effects of injections of, on hamsters, 20: 1676

**LIVERWORTS**
radiosensitivity of *Marchantia polymorpha* cells, effects of chromosome and nucleus volumes on, 20: 1610 (BNL-9611)

**LOOPS**
development of TREAT, 20: 2221(R) (ANL-7082, pp 62-73)
fabrication of niobium–zirconium, 20: 3321(R) (ANL-7082, pp 29-53)

**LOS ALAMOS SCIENTIFIC LAB., N. MEX.**

waste treatment practices at, comparison with Argonne, 20: 3603 (LA-DC-7249)
**LUMINESCENT DETECTORS**
modification of silver-activated phosphate glass, for low dose measurements , 20: 2122 (AD-622626)
performance of lithium fluoride powder in gelatin capsule as, for dosimetry of exit x radiation during radiotherapy, 20: 1699
**LUNGS**
carcinogensis in, effects of fallout particles on, 20: 2053
plutonium retention in, following fallout exposure, 20: 1602
radiation effects on extractable cellular components of rabbit and rat, x, 20: 1675
radioinduced tumors in mouse, 20: 1606 (AD-623079)
radiotherapy of lesions of, dosimetry of exit dose during, 20: 1699
urethan-induced tumors in mouse, 20: 1606 (AD-623079)
**LUTETIUM**
determination using Chromotrope 2B, photometric, 20: 1772
**LUTETIUM ALLOYS**
Co–Lu, preparation and structure of $MgCu_2$-type, 20: 2385(T)
Fe–Lu, preparation and structure of $MgCu_2$-type, 20: 2385(T)
Lu–Ni, preparation and structure of, 20: 2385(T)
**LUTETIUM ISOTOPES Lu-170**
beta decay of, isobaric-spin impurity in ground state from, (E), 20: 3072
**LUTETIUM OXYBROMIDES**
preparation and crystal structure, 20: 1834
**LYMPH CELLS**
immune reactions to growth of, on monolayers of mouse embryo cells in culture, 20: 1658
radiation effects on nuclei of, morphological, 20: 1612 (EUR-2505.e)
radiation effects on growth of, on monolayers of mouse embryo cells in culture, 20: 1658

# M

**MACHINE TOOLS**
use with gages, for fabrication and inspection, 20: 3627 (RFP-670)
**MAGNESIUM**
corrosion resistance to mercury at 900°F, 20: 2264
crystal structure, effects of alloying additions of other metals on, 20: 2399
determination in uranium by atomic absorption spectrophotometry, 20: 1753
deuteron elastic scattering at 26 Mev, optical model analysis of, (E/T), 20: 3053
deuteron elastic scattering at 27.5 Mev, angular distribution for, (E/T), 20: 3057
deuteron scattering by, cross sections for, (T), 20: 3026
separation of trace elements from, by precipitation ion exchange, 20: 1958
**MAGNESIUM ALLOYS**
Al–Mg, crystal structure, 20: 2399
Be–Mg, corrosion in moist carbon dioxide at 650-750°C, 20: 2277(P)
Cd–Mg, corrosive effects on carbon steel and stainless steel at 750°C, 20: 2265
Cd–Mg–Zn, corrosive effects on carbon steel, stainless steel, and tantalum at 500, 750 and 850°C, 20: 2265
Ce–Mg, crystal structure, 20: 2399
Mg–Ag, entropy of formation of AgMg ordered phase, (T), 20: 2349 (UCRL-16320)
Mg–Ag, mechanical properties of internally oxidized, 20: 3639 (UCRL-11194)
Mg–Nd, crystal structure, 20: 2399
Mg–rare earths–Zn–Zr, crystal structure, 20: 2399
Mg–rare earths–Zr, crystal structure, 20: 2399
Mg–U–Zn, corrosive effects on refractory metals in presence of molten chlorides, 20: 2266
Mg–Zn, crystal structure, 20: 2399
Mg–Zn, reactions with plutonium dioxide, 20: 2220 (ANL-7059)
Mg–Zr, crystal structure, 20: 2399
**MAGNESIUM CERIUM NITRATES**
proton polarization and spin relaxation rates in, at low temperatures, (E/T), 20: 3143
**MAGNESIUM CHLORIDES**
corrosive effects on austenitic and austeno-ferritic stainless steels, stress, 20: 2256(R) (EURAEC-1449)
diffusion of water in, coefficients of, 20: 1865
thermal decomposition of, factors affecting, 20: 2520(R) (IA-920)
$MgCl_2$–KCl, stability of zirconium dichloride in, 20: 1822(T) (ANL-Trans-233)
$MgCl_2$–NaCl, stability of zirconium dichloride in, 20: 1822(T) (ANL-Trans-233)
**MAGNESIUM COMPLEXES**
chlorophyllin, radiosensitivity effects in mice, gamma, 20: 1692
**MAGNESIUM ISOTOPES Mg-24**
alpha inelastic scattering at 42 Mev, alpha-gamma coincidences in, 20: 3141
alpha scattering at 18 to 21.4 Mev, silicon-28 energy levels from, (T), 20: 3069
**MAGNESIUM ISOTOPES Mg-26**
proton reactions (p,p'γ) at 5.67 to 6.46 Mev, angular distributions and excitation functions for, (E), 20: 3092
**MAGNESIUM LANTHANUM NITRATES**
proton dynamic polarization in rotating crystals of, (E), 20: 3311
proton polarization and spin relaxation rates in, at low temperatures, (E/T), 20: 3143
**MAGNESIUM NITRATES**
effects on uranium and plutonium activity coefficients in nitric acid solutions, 20: 1967
**MAGNESIUM OXIDES**
radiation effects on crystal structure of, mechanism of beta, 20: 2426 (LA-3387)
radiation effects on, x-ray line broadening in fast neutron, (E), 20: 2445
MgO–Ag, annealing effects on structure of dispersion-hardened, 20: 2325 (HW-SA-3767)
MgO–Ag, structure of deformed, 20: 2324 (HW-SA-3765)
MgO–$SnO_2$, radiation damage effects on tin-119 Mössbauer effect in, neutron, 20: 3065
**MAGNESIUM SYSTEMS**
Ge–Mg–Si, radiation effects on electric properties of $Mg_2Ge_{0.8}Si_{0.2}$, 20: 2502
**MAGNET COILS**
design of eighth-order power optimized, analysis of, (E), 20: 2522 (ORNL-P-1516)
**MAGNETIC FIELDS**
charged particle momentum in, conic reprojection of photographs for calculating, 20: 2728
charged particle momentum in, effects of field nonhomogeneity on photographic analysis of, 20: 2729
compression of, mathematical models for, 20: 2523 (SC-RR-65-449)
effect on breakdown time lag of low pressure neon discharge, 20: 2835
effects of direction and magnitude on magnetoresistance of thallium at 1 and 4.2°K, 20: 2329 (IS-T-35)
effects on gas discharges between coaxial cylinders, 20: 3202
effects on nuclei in samarium compounds, temperature dependence of, 20: 2520(R) (IA-920)
effects on stability of dilute gases, (T), 20: 2573
effects on stability of electrically conducting liquid layer, 20: 2820 (AD-614645)
electron beam diocotron instability in crossed electric and, (T), 20: 3252 (NP-15578)
flux compression by explosives, review of, 20: 3166 (LA-DC-7252)
intensity and polarities of sunspots during IGY, 20: 2563
measurement by ferromagnetic resonance magnetometers, 20: 2104 (MATT-362)
measurement of, performance of scanning and recording systems for, (E), 20: 2105 (UCRL-16357(Rev.))
measurement of, using NMR field probes, (E), 20: 2112
penetration in type II superconductors, surface superconductivity breakdown from, (T), 20: 2900
plasma containment in minimum-B and saddle, (E), 20: 3184 (UCRL-14310)
plasma injection into, effects of toroidal drift on transverse, (E), 20: 3205(T)
plasma production in crossed electric and, (E), 20: 3177 (NP-15570)
space charge effect on transitions of, toward plasma regime, (T), 20: 2856
supernova explosion into interstellar, model for early stages of, (T), 20: 2569
supernova explosion into interstellar, weak-field limit for, (T), 20: 2570
use of high, in solid state research, 20: 2519(R) (AD-615152)
**MAGNETIC MIRROR MACHINES**
design for confinement of electrons for long periods, (E), 20: 3225
design of Heliotron C, 20: 3174(R) (NP-15562, pp 30-7)
development of MACETIE, 20: 3173(R) (NP-15562, pp 20-9)
development of QP machine, 20: 3172(R) (NP-15562, pp 4-19)
plasma stability in negative V, (T), 20: 3167 (MATT-374)
spectrometer design for use in DCX-2, (E), 20: 3178 (ORNL-P-1513)
**MAGNETIC MIRRORS**
containment of slow ions in, in a plasma with positive potential, (T), 20: 3227
ion escape from, due to instability connected with loss cone, (T), 20: 3229
plasma in, containment of hot-electron, (E), 20: 3184 (UCRL-14310)
**MAGNETIC RESONANCE**
of melanin, 20: 1684
spin temperature formalism for analysis of, (T), 20: 2864 (COO-1198-300)

**MAGNETIC SUSCEPTIBILITY**
measurement in rare earth oxides, apparatus for, 20: 3318
**MAGNETOHYDRODYNAMIC CELLS**
economics of reactors and, for commercial power, 20: 2670 (LA-DC-7330)
electrode design for, 20: 2677(P)
flame temperature in, spectroscopic measurement of, (E), 20: 2673
operation of, optimal, (T), 20: 2674
performance of, Hall effects and induced ionization in, (E), 20: 2671
plasma flow between electrodes in, boundary layer in, (E), 20: 2672
**MAGNETOHYDRODYNAMICS**
differential equations in, applications of partial, 20: 2530
energy balance in, equation for, 20: 2823
equations for quasineutral plasma, (T), 20: 3159 (AD-618138)
fluid flow with temperature-dependent electric conductivity, channel, (T), 20: 2824
gas flow in, deflagrations and properties of ideal, 20: 2821 (AD-618296)
liquid flow in, Hartmann layer effects on, (E/T), 20: 2831
plasma flow in, single fluid theory of, 20: 3233
stability in finite conductivity, analog computation for, 20: 2836
stability in, effect of ion gyration radius on gravitational, 20: 2885
stability of liquid layers, 20: 2820 (AD-614645)
theory for plasma interactions with high-frequency field, 20: 3207
two-fluid, equation development for, 20: 2838
**MAGNETOMETERS**
design and performance of ferromagnetic resonance, 20: 2104 (MATT-362)
design of NMR, for homogeneous and inhomogeneous fields, (E), 20: 2112
design of recording, for measurement of hysteresis curves of superconductors, (E), 20: 2913
performance of scanning, review, (E), 20: 2105 (UCRL-16357(Rev.))
**MAGNETOSPHERE**
boundary with solar wind effects of space charge convection on, (T), 20: 2856
**MAGNETS**
coolant system cleaning method for water-cooled, (E), 20: 1992
cost estimation of accelerator, computer program for, 20: 2545 (UCRL-16386)
design for accelerators, review of, 20: 2533 (BNL-9536)
design for accelerators, computer program for, 20: 2546 (UCRL-16389)
design of high-current-density septum, for accelerators, 20: 2544 (UCRL-16309)
design of linear accelerator, 20: 2521 (LNF-65/28)
design of 150-kOe cryogenic pulsed, 20: 1991
performance of superconducting, as space-vehicle dynamic radiation shield, (T), 20: 3241 (NASA-SP-71, pp 199-209)
power supply and support for mobile electro-, design, 20: 3353(P)
properties of symmetric quadrupole triplets, (T), 20: 2539 (SLAC-47)
**MAIZE**
mutations of, induced by ethyl methanesulfonate, 20: 1656
radioinduced mutations of, x, 20: 1656
**MALEIMIDE**
4,4′-diphenylenedi-, radioinduced polymerization of, 20: 1930
**MALEIMIDE, *N,N′*-PHENYLENEDI-**
radioinduced polymerization of, yields in, 20: 1930
**MALONIC ACID, DERIVATIVES**
2,5-cyclohexadiene-1,4-diylidenedimalonitrile, isotope effects on exciton resonance in morpholinium and methyltriphenylarsonium complexes of, (E), 20: 1841
**MAMMALS**
radiation effects on, delayed pathological, x, 20: 1716
**MAN**
cosmic radiation effects on, in high-altitude aircraft, 20: 2657 (NASA-SP-71, pp 287-99)
effects of blast on, pathological, 20: 2083 (CEX-65.4)
effects on vertebral column of radiotherapy during childhood, late pathological, 20: 1702
explosion effects on, display system for studying atomic, 20: 1987 (UCRL-13139)
iodine-131 metabolism in fetuses of, 20: 1600
leukemia treatment in, use of whole-body x irradiation and bone marrow transplants for, 20: 1700
leukemia treatment in, use of whole-body x irradiation and hematopoietic tissue transplants for, 20: 1701
physiological age tests for, 20: 1587
radiation dose measurements for, from diagnostic radiography, 20: 1703
radiation hazards from uranium carbide fuel particles, 20: 1694
radiation injuries of, diagnosis by morphological study of lymphocyte nuclei, 20: 1612 (EUR-2505.e)
radioactivity of, whole-body counting, 20: 1710
thorotrast metabolism in, 20: 1596
**MANGANESE**
corrosion resistance to mercury at 900°F, 20: 2264
determination in drugs, hair, oils, river silts, and tobacco, activation, 20: 1739(R) (GA-4297)
determination in greases and soils, activation, 20: 1738(R) (GA-4041)
determination in human blood serum using neutron activation analysis, 20: 1586
determination of trace amounts in uranium compounds by activation analysis, 20: 1784
neutron activation determination, 20: 2520(R) (IA-920)
separation of trace amounts of, from alkali metals, alkaline earths, and rare earths, 20: 1958
**MANGANESE ALLOYS**
Cu–Mn, spin ordering of paramagnetic states in superconducting, 20: 2918
Fe–Mn, effects of strain rate, structure, and temperature on flow stress at 77 to 370°K, 20: 3641 (UCRL-11512(Rev.))
Mn–Pb, spin ordering of paramagnetic states in superconducting, 20: 2918
Mn–Sn, spin ordering of paramagnetic states in superconducting, 20: 2918
**MANGANESE COMPLEXES**
chlorophyllin, radiosensitivity effects in mice, gamma, 20: 1692
**MANGANESE ISOTOPES Mn-54**
electron-capture decay of, absolute activity determination of, 20: 3034
gamma transition at 835.0 kev, (E), 20: 3043
uptake by rat hair, 20: 1695
**MANGANESE ISOTOPES Mn-55**
neutron reactions (n,γ), cross sections for resonance and thermal, (E), 20: 3031
nuclear magnetic resonance in manganese selenide, coupling constants from zero-field, (E), 20: 3295
**MANGANESE ISOTOPES Mn-56**
use in calibration of neutron sources, 20: 3321(R) (ANL-7082, pp 29-53)
**MANGANESE OXIDES**
effects on superconducting transition temperature of lead, (E), 20: 2916
**MANGANESE SELENIDES**
manganese-55 NMR in, coupling constants from zero-field, (E), 20: 3295
**MANGANESE STEEL**
welding procedures for, electro-slag, 20: 2281(R) (EURAEC-1408)
C–Cr–Mn, radiation effects on mechanical properties of, 20: 2438
Mn–Mo, radiation effects on deformation properties of A302B, neutron, 20: 2436 (WERL-8844-4)
Mn–Mo, welding procedures for A302B, electro-slag, 20: 2281(R) (EURAEC-1408)
Mn–Mo–Ni–V, welding procedures for, electro-slag, 20: 2281(R) (EURAEC-1408)
**MANGANESE SULFATES**
nuclear magnetic resonance in, uses for magnetic field measurements, (E), 20: 2112
**MANGANESE URANATES**
crystal structure and density of, 20: 2400
**MARITIME NUCLEAR STEAM GENERATOR**
development of CNSG III, 20: 3552
development of 630A Mark IV, 20: 3546 (GE-TM-64-12-12)
**MARITIME PRESSURIZED WATER REACTOR**
containment vessel leak rate tests on N.S. *Savannah*, 20: 3551 (TID-22316)
legal aspects of operation of Savannah, in foreign ports, 20: 2088
**MASERS (OPTICAL)**
beam reactions with plasma, heating effects of, (T), 20: 3185(T) (TT-1193)
chromium-50 and 52 emission spectra in ruby, (E), 20: 3283
hosts for, crystal growth and properties of cerium and thorium dioxides as, 20: 2312 (AD-619197)
nuclear pumping of gas, optimum design for, (T), 20: 2591 (ANL-7030)
optical pumping transients in rubidium-87 gas, 20: 2596 (UCRL-16241)
use in electron density measurement in plasma, 20: 3234
use in plasma diagnostics, 20: 3232
**MASS SPECTROGRAPHY**
use for isotopic analysis of water ionized in strong electrical field, 20: 1829
**MASS SPECTROMETERS**
circuits for, review of, 20: 2100 (IS-1193)
source handling systems for, design of vacuum seals and valves for, (E), 20: 2159
use for measuring relative abundances of isotopes, 20: 1774
**MATERIALS TESTING**
developments and uses of eddy-current, 20: 2025 (BNWL-SA-349)
equipment for tensile testing of irradiated structural materials at high temperatures, 20: 2031
equipment for tensile testing of irradiated materials at low temperatures, 20: 2032
photoelastic, nondestructive technique for, 20: 2026 (UCRL-13188)
**MATERIALS TESTING REACTOR**

fuel irradiation testing in, 20: 2429 (ORNL-3837)
**MATHEMATICS**
Banach spaces in, Hilbert-Schmidt and nuclear power applications in, 20: 2215
book: *Applications of Nonlinear Partial Differential Equations in Mathematical Physics*, 20: 2530
cross sections in $P_1$-age approximation of transport equation, 20: 2520(R) (IA-920)
Lie algebras in, branching rules and Clebsch-Gordon series for, 20: 2216
symmetry properties of matrices of summability theory, 20: 3629 (SC-DC-64-288)
theory of transformation matrices, 20: 2604
**MATTER**
energy levels of nuclear, with hard core interaction with neutron excess, (T), 20: 3079
equation of state of, at supernuclear density, (T), 20: 3016 (NASA-TN-D-3020)
model of finite nuclear, validity of Thomas-Fermi, 20: 2819
proton shielding properties of, calculations of dose, energy, and flux variation factors for, (T), 20: 3250 (NASA-SP-71, pp 493-505)
**MEATS**
radiation processing of, effects of fat content, previous cooking, and storage temperature on wholesomeness, 20: 2203
**MECHANICAL ENGINEERING**
photoelastic instruments for nondestructive stress analyses, 20: 2026 (UCRL-13188)
**MECHANICS**
shock-spectrum analysis of systems of oscillators in, 20: 3631 (SC-DC-65-1723)
variational principles of classical, analogies in reactor theory, 20: 3331
**MEIOSIS**
radiosensitivity of, in yeast, 20: 1664
**MEMBRANES**
isotope diffusion in biological, effects of flux on, 20: 1585
trauma of animal cell, effects on Coulter electronic cell size distribution, 20: 1636
use in leak-tight movement transmission through walls, 20: 2005(P)
**MEMORY DEVICES**
properties of intermediate, effects of pulsed mode on, (E/T), 20: 2101 (JINR-P-2319)
**MERCAPTO GROUP**
radiosensitivity effects of, in bacteria, 20: 1618 (NYO-3319-6)
**MERCURY**
alkali metal scattering by, cross sections and rainbow effect in, (E/T), 20: 2636
corrosive effects on alloys and metals, 20: 2264
determination in electrolytic cells, radiometric, 20: 2520(R) (IA-920)
determination in tobacco leaf and wheat by neutron activation methods, 20: 1755
determination in wheat, activation, 20: 1738(R) (GA-4041)
determination in wheat, activation, 20: 1739(R) (GA-4297)
effect on the dissolution of ceramics containing beryllium oxide, catalytic, 20: 2252(P)
electron scattering at 3.5 ev, polarization in, (E), 20: 2615
flow of liquid, Hartmann layer effects in MHD, (E/T), 20: 2831
rare gas reactions with, cross sections for line broadening in, (E), 20: 2637
spectra of, isolated in inert gas matrices at high temperature, 20: 1818 (UCRL-11976)
spectra of, measurement of transition probabilities in, 20: 2649
**MERCURY BROMIDES**
separation from molten nitrates by solvent extraction using polyphenyls, 20: 2520(R) (IA-920)
solubility and structure in organic solvents, 20: 2520(R) (IA-920)
**MERCURY CHLORIDES**
corrosive effects on molybdenum and vanadium, stress-, 20: 2254 (BM-RI-6680)
separation from molten nitrates by solvent extraction using polyphenyls, 20: 2520(R) (IA-920)
solubility and structure in organic solvents, 20: 2520(R) (IA-920)
**MERCURY HALIDES**
enthalpy of formation and stabilization constants of complex, 20: 2520(R) (IA-920)
**MERCURY IODIDES**
separation from molten nitrates by solvent extraction using polyphenyls, 20: 2520(R) (IA-920)
**MERCURY ISOTOPES Hg-198**
gamma transitions in, conversion coefficients for, (E), 20: 3038
**MERCURY ISOTOPES Hg-199**
energy levels in, radiative lifetime of $6^3P_0$, 20: 2599
**MERCURY ISOTOPES Hg-200**
electron inelastic scattering at 200 Mev, differential cross sections for, (T), 20: 3124
**MERCURY ISOTOPES Hg-201**
energy levels in, radiative lifetime of $6^3P_0$, 20: 2599
**MERCURY OXIDES**
radiation effects on potential of electrode of, 20: 1932
**MERCURY SYSTEMS**
Ar–Hg, glow discharge initiation in, (E), 20: 3162 (AD-616683)
**MESIC ATOMS**
scattering of ($p\mu$), by protons, (E), 20: 2640
**MESIC MOLECULES**
formation of ($pp\mu$), by proton-mesic atom ($p\mu$) scattering, (E), 20: 2640
**MESITYLENE**
effects as diluent on perchloric and perrhenic acid extractions by tri-dodecylamine, 20: 1747 (UCRL-11616(Rev.))
preparation of, for measuring natural carbon-14 by scintillation methods, 20: 2062
**MESON BEAMS**
trapping of ($\mu$), quadrupole magnetic channel for, 20: 2547 (UR-375-98)
**MESON PAIRS**
production in electron-positron beam interactions, cross sections for, (T), 20: 2753 (JINR-P-2300)
**MESON SHOWERS**
production in proton reactions with iron at 1 and 3 Bev, (T), 20: 3258
**MESONS**
interactions with baryons, $SU(6)_w$ scattering relation for S-wave isobar production in, 20: 2788
mass formulas from SU(12), (T), 20: 2756 (JINR-P-2342)
model of, higher unitary symmetry groups for shell, 20: 2781
photoproduction on baryons, electromagnetic amplitudes for, 20: 2732
production facility for, neutron flux beneath shield of, (T), 20: 3262
production in high-energy inelastic interactions, transverse momentum distribution of, (T), 20: 2681 (IFA-CR-55)
production of ($S^0$), in intermediate boson pole in meson (K) radiative decay, (T), 20: 2684 (JINR-P-2374)
symmetry for, matrix element of current in, (T), 20: 2753 (JINR-P-2300)
theory of vector, Bethe-Salpeter equation for lepton interactions in, 20: 2797
**MESONS, RESONANCE**
mass spectra of $\phi$-$\pi$ system, (T), 20: 2741
mass splitting of unitary-octet vector, electromagnetic decays for, (T), 20: 2801
production in meson ($\pi$) interactions, phase shift analysis for, (T), 20: 2708
production in unstable boson exchange interactions, pole approximation for, 20: 2779
production of $A_1$, $E_1(740)$, and $E_2(940)$ in meson ($\pi^-$)-proton interactions at 2.26 Bev/c, 20: 2745
production of $\kappa^0(725)$ in meson ($\pi^-$)-proton interactions, 20: 2715
symmetry for H, $K^+K^+$, and $K\pi\pi$, 20: 2727
**MESONS (B)**
production in meson ($\pi^-$)-proton interactions at 2.26 Bev/c, 20: 2745
**MESONS ($\eta$)**
decay of, $G_2$ symmetry in, (E/T), 20: 2520(R) (IA-920)
production in meson ($\pi^-$)-proton interactions at 2.26 Bev/c, 20: 2745
production with neutrons in meson ($\pi^-$)-proton interactions, (E), 20: 2689 (UCRL-16140)
**MESONS (f)**
production in meson ($\pi^-$)-proton interactions at 2.26 Bev/c, 20: 2745
**MESONS (K)**
interactions with protons, strangeness-conserving axial-vector coupling constant for, 20: 2722
interactions with protons, triangular diagrams for cross sections of, (T), 20: 2741
**MESONS ($K^-$)**
interactions with protons at 0.8 to 1.2 Bev/c, $Y^*(1760)$ production and properties, (E), 20: 2711
interactions with protons at 6 Bev/c, hyperon ($\Omega^-$) production from, (E), 20: 2717
interactions with protons, meson ($\phi$) suppression in, (T), 20: 2719
interactions with protons at 725 to 820 Mev/c, peak in cross sections for, (E), 20: 2724
reactions with emulsion nuclei at 5 Bev/c, hyperfragment and lithium-8-fragment production in, (E), 20: 3062
reactions with emulsion nuclei, $Y^0_0$ production in capture, (E), 20: 3064
reactions with lithium-6, hyperfragments from, (E), 20: 2520(R) (IA-920)
reactions with nuclei, baryons $\Sigma$-$\pi$ production in, (E/T), 20: 2520(R) (IA-920)
reactions with nuclear emulsions at 800 Mev/c, computer analysis of, 20: 2520(R) (IA-920)
**MESONS ($K^0$)**
decay ($2\pi$) of, particle-mixture theory for CP invariance in, 20: 2720
decay of $K^0_2$, alternatives to $2\pi$, (T), 20: 2692
decay of $K^0_2$, statistical irreversibility of $2\pi$, (T), 20: 2699(T)

decay of $K_2^0$, gravitational effects on, 20: 2865 (JINR-P-2325)
decay of, intermediate boson pole with meson ($S^0$) in radiative, (T), 20: 2684 (JINR-P-2374)
decays of, CP invariance violation and noninvariant vacuum in, (T), 20: 2698(T)
mass difference ($K_1^0$–$K_2^0$), measurement of, 20: 2748
mass sign of, comparison with $\overline{K}^0$, 20: 2865 (JINR-P-2325)
regeneration of $K_1$, in solid materials, 20: 2748

**MESONS ($\overline{K}^0$)**
mass sign of, comparison with $\overline{K}^0$, 20: 2865 (JINR-P-2325)

**MESONS ($K^+$)**
decay of, intermediate boson pole with meson ($S^0$) in radiative, (T), 20: 2684 (JINR-P-2374)
decay of, rare modes in, 20: 2749
photoproduction on protons, (E/T), 20: 2735

**MESONS ($\kappa$)**
production of (725), in meson ($\pi^-$)-proton interactions, 20: 2715

**MESONS ($\mu$)**
energy losses in concretes, (T), 20: 3238 (JINR-P-2354)
photoproduction on nucleons, amplitude of, (T), 20: 2695
production of, development of high-energy accelerators for, 20: 2560
trapping beams of, quadrupole magnetic channel for, 20: 2547 (UR-375-98)

**MESONS ($\mu^-$)**
production of cosmic, $(\mu^+)/(\mu^-)$ ratio in high-energy, (T), 20: 2702
production of meson ($\mu^-$)-meson ($\mu^+$) pairs in proton-pair annihilation, (T), 20: 2696

**MESONS ($\mu^+$)**
production in antineutrino interactions with proton, cross sections for, (T), 20: 2736
production of cosmic, $(\mu^+)/(\mu^-)$ ratio in high-energy, (T), 20: 2702
production of meson ($\mu^-$)-meson ($\mu^+$) pairs in proton-pair annihilation, (T), 20: 2696

**MESONS ($\omega$)**
decay of, $G_2$ symmetry in, (E/T), 20: 2520(R) (IA-920)
production in meson ($\pi^-$)-proton interactions at 2.26 Bev/c, 20: 2745

**MESONS ($\phi$)**
production in meson ($K^-$) interactions with protons, (T), 20: 2719

**MESONS ($\pi$)**
dosimetry of beam of, 20: 1621 (UCRL-16387)
effects on root meristem cells of *Vicia faba*, biological, 20: 1621 (UCRL-16387)
exchange contribution in peripheral model of isobar production, (T), 20: 2817
interactions with electrons, Mandelstam representation of, (T), 20: 2678 (AD-614843)
interactions with Y particles, two-channel p-wave, (T), 20: 2694
interactions with mesons ($\pi$), phase shifts to 1.3 Bev for, (T), 20: 2708
interactions with nucleons at 0 to 20 Bev, data review for, 20: 2725
photoproduction of pairs of, on protons, 20: 2747
production facility using proton linear accelerator, shielding for, 20: 2559
production in high-energy inelastic interactions, transverse momentum distribution of, (T), 20: 2681 (IFA-CR-55)
production of, development of high-energy accelerators for, 20: 2560

**MESONS ($\pi^-$)**
interactions in freon at 2.8 Bev/c, meson ($\pi^\pm$) production in, (E), 20: 2739
interactions with protons, elastic differential cross sections for, (E), 20: 2520(R) (IA-920)
interactions with protons, mesons ($\eta$) and neutrons from, (E), 20: 2689 (UCRL-16140)
interactions with protons, analysis using bubble chambers, (T), 20: 2690(T) (AEC-tr-6591)
interactions with protons, triangular diagrams for cross sections of, (T), 20: 2741
interactions with protons at 2.26 Bev/c, resonances and final states in, 20: 2745
interactions with protons at 7.0 Bev/c, 20: 2746
interactions with protons at 338 Mev, cross sections for, (E), 20: 2682 (JINR-P-2320)
interactions with neutrons at 1.4 to 4.0 Bev/c, backward elastic, (E), 20: 2700(T)
interactions with neutrons at 1.38 to 4.05 Bev/c, backward elastic, (E), 20: 2713
interactions with protons at 1.5 and 1.8 Bev/c, $\kappa^0$(725) production from, (E), 20: 2715
production at high energy, $(\mu^+)/(\mu^-)$ ratio from $(\pi^+)/(\pi^-)$ ratio in, (T), 20: 2702
production in antineutrino interactions with protons at high energy, cross section for, (T), 20: 2733
production in freon-meson ($\pi^-$) interactions at 2.8 Bev/c, (E), 20: 2739
production in meson ($\pi^-$)-proton interactions at 7.0 Bev/c, 20: 2746
reactions of stopped, with carbon, mechanism of absorption, (E/T), 20: 3123
reactions with nuclei at 120 to 280 Mev, double charge exchange in, (E), 20: 3080

**MESONS ($\pi^0$)**
decay of, $G_2$ symmetry in, (E/T), 20: 2520(R) (IA-920)
interactions with mesons ($\pi^0$), analyticity and crossing symmetry for sum rules for, (T), 20: 2709
photoproduction on protons at 500 to 1000 Mev, polarization in, (E), 20: 2679 (AD-618664)

**MESONS ($\pi^+$)**
interactions with protons, elastic differential cross sections for, (E), 20: 2520(R) (IA-920)
interactions with protons at 4.1 and 4.85 Bev/c, cross sections for elastic, (E), 20: 2683 (JINR-P-2327)
interactions with protons, inelastic $S_{31}$ resonance in, (T), 20: 2716
lifetime, (E), 20: 2714
photoproduction on protons at 1 Bev, 20: 2718
photoproduction on protons at 165 to 230 Mev, amplitudes and cross sections for, (E/T), 20: 2737
production at high energy, $(\mu^+)/(\mu^-)$ ratio from $(\pi^+)/(\pi^-)$ ratio in, (T), 20: 2702
production in freon-meson ($\pi^-$) interactions at 2.8 Bev/c, (E), 20: 2733
production in neutrino interactions with protons at high energy, cross section for, 20: 2733

**MESONS ($\rho$)**
exchange contribution in peripheral model of isobar production, (T), 20: 2817
production in meson ($\pi^-$)-proton interactions at 2.26 Bev/c, 20: 2745
production in meson ($\pi$) interactions, phase shift analysis for, (T), 20: 2708

**MESONS ($\rho^0$)**
photoproduction on protons, 20: 2747
production in meson ($\pi^-$)-proton interactions at 7.0 Bev/c, 20: 2746

**METAL COATINGS**
deposition of high-melting, plasma-jet-gun for, 20: 2251(P)
radiation effects on, for spacecraft, 20: 2428 (NASA-SP-55, pp 365-79)

**METALLOGRAPHY**
design of remote metallography cell, 20: 2247

**METALLURGY**
conference on physical, of titanium and its alloys, 20: 2359(T) (NASA-TT-F-338)
fabrication and phase studies on alloys, 20: 2350(R) (USBM-RC-1205)
research programs on, at Risö nuclear research center, Denmark, 20: 3646

**METALS**
analysis for gases, equipment and methods for spectral-isotopic, 20: 1793
cavitation damage in liquid sodium, 20: 2243
corrosion rates in flowing sodium, loop geometry effects on, 20: 2295
distribution of carbon and oxygen in, determination by helium-3 activation, 20: 2227
electric conduction of metal-insulator sandwich, (E/T), 20: 2405
grain boundary migration in, review on, 20: 3626 (ORNL-P-1722)
neutron coherent scattering in liquid, Kohn anomaly in slow, (T), 20: 2948
proton reactions with, radioactivity from, (E/T), 20: 3263
radiation effects on, compilation of projects on, 20: 2433 (REIC-Memo-27)
radiation effects on hardness of bcc, neutron, 20: 2457
radiation effects on, ASTM symposium on, 20: 2470
radiation effects on mechanical properties, 20: 2471
thermal properties at ambient temperature, data tabulation of, 20: 2343 (SC-TM-65-242)
transport effects in, research on, 20: 2519(R) (AD-615152)
tunneling characteristics of contacts of superconductors and normal, (T), 20: 2910

**METEORITES**
analysis for cobalt, activation, 20: 2055
effects on space vehicles, estimates of magnitude and nature of, 20: 2036 (AD-618030)
origin and properties of, review of, 20: 2590
proton reactions at 1 to 3 Bev with chondritic, distributions from, (E), 20: 3015 (NASA-SP-71, pp 357-62)

**METEOROLOGY**
phenomena in underwater nuclear explosions in Crossroads and Teapot Operations, 20: 1979 (AD-614814)
use of particulate nuclear bomb debris as tracer material in, 20: 2044 (NDRE-51)

**METHACRYLIC ACID**
radiolysis at –40 to 10°C, ESR spectra of yields in uv, 20: 1916

**METHACRYLIC ACID, ALLYL ESTERS**
allyl methacrylate–methanol–$H_2O$, effects on radioinduced crosslinking of nylon 66 and poly (vinyl alcohol), 20: 1909

**METHACRYLIC ACID, METHYL ESTER**
radioinduced polymerization with formaldehyde, effects of dichloromethane and ethyl ether on, 20: 1914
**METHACRYLIC ACID, METHYL ESTER POLYMERS**
proton reactions at 1 to 3 Bev, distributions from, (E), 20: 3015 (NASA-SP-71, pp 357-62)
use in gamma dose measurements, 20: 2165
uses in preparation of kryptonates, 20: 1862
**METHANE**
alpha stopping power of, 5-Mev, 20: 2147
decomposition in hydrogen plasma jets, acetylene production by, (T), 20: 3197
determination in helium at reduced sample pressures by gas chromatography, 20: 1751
determination of, factors affecting continuous on line, 20: 1734 (EG-Report-36)
effects on radioinduced oxidation of graphite in carbon dioxide, oxygen effects on, 20: 1895 (AERE-R-4988)
radiolysis of liquid, effects of propene on gamma, 20: 1898(R) (RRL-2310-164)
yields in recoil reactions of carbon-11 in liquid hydrocarbons, 20: 1896 (IS-T-23)
yields of, from radiolysis of benzene–isopropanol–benzophenone mixtures, 20: 1931
air–methane, combustion of beryllium in flame system of, 20: 2341 (SC-DC-65-1637)
$CO_2$–CO–methane, effects of oxygen on radioinduced oxidation of graphite in, 20: 1895 (AERE-R-4988)
**METHANE, DICHLORO-**
effects on radioinduced polymerization of liquid and solid acetylene, 20: 1913
effects on radioinduced polymerization of formaldehyde, 20: 1914
effects on radioinduced polymerization of formaldehyde with acrylonitrile, isobutene, methyl methacrylate, and styrenes, 20: 1914
**METHANE, IODO-**
labeling by fission-product iodine, selectivity effects in, 20: 2520(R) (IA-920)
release and sorption in HFIR maximum credible accident, 20: 3586 (ORNL-TM-1291)
**METHANESULFONIC ACID**
heat of solution of sodium salt of, in heavy and light water, 20: 1825
mutagenic effects of, on seeds or seedlings of *Zea mays*, 20: 1656
**METHANOL**
neutron spectra in cooled, thermal, (E), 20: 2945
sorption by uncorroded and corroded uranium, 20: 1805 (AWRE-O-69/65)
allyl methacrylate–methanol–$H_2O$, effects on radioinduced crosslinking of nylon 66 and poly (vinyl alcohol), 20: 1909
methanol–KOH, solvent properties for tissues, 20: 1767
**METHIONINE**
complexes with chlorophyllin and metal ions, radiosensitivity effects in mice of, gamma, 20: 1692
**METROLOGY**
machine gaging philosophy on instrumentation, 20: 3627 (RFP-670)
**MICA**
alpha range in, 5-Mev, 20: 2147
radiation effects on dielectric properties of paper of, effects of silicones on, 20: 1897 (NASA-TN-D-3032)
**MICE**
chromium phosphate colloid distribution in, tracer studies of, 20: 1598
inhalation of neodymium oxide aerosol by, 20: 1593 (COO-1170-4)
leukemia treatment in, use of whole-body x irradiation and bone marrow transplants for, 20: 1700
leukemia treatment in, use of whole-body x irradiation and hematopoietic tissue transplants for, 20: 1701
radiation effects on immune reactions in, 20: 1632
radiation effects on immune reactions of, to injected allogenic and syngenic bone marrow, 20: 1660
radiation effects on growth of bone marrow transplants in, effects of arabinofuranosylcytosine on, 20: 1687
radiation effects in, protective effects of chelated complexes against gamma, 20: 1692
radiation effects on, genetic, 20: 1622 (WT-820)
radiation effects on antibody formation in, injected with sheep erythrocytes, 20: 1661
radiation injuries in, recovery kinetics for, 20: 1685
radiation injuries of, induced by high-energy protons and alpha particles, 20: 1614 (NASA-SP-71, pp 97-103)
radioinduced lung tumors in, effects of urethan on incidence of, 20: 1606 (AD-623079)
radiosensitivity of, effects of dietary content of pyridoxine on, 20: 1646
radiosensitivity of transplanted tumors in, effects of inhalation of 5% carbon dioxide and 95% oxygen on, 20: 1683
**MICROSOMES**
binding site for messenger RNA in *Escherichia coli*, tracer study, 20: 1592 (BNL-7903)
**MICROWAVE EQUIPMENT**
Cherenkov emission by charged particles in circular waveguide filled with gyrotropic ferrite, (T), 20: 2550
design of r-f beam separator for Brookhaven AGS, (E), 20: 2532 (BNL-9505)
development of lenses for plasma diagnostics, 20: 3169 (NASA-CR-319)
frequency of antenna inside magneto-plasma-filled parallel-plate waveguide, (E), 20: 2096 (AD-617928)
plasma perturbation in disk-loaded wave-guide, (E), 20: 3219
waveguide admittance for radiation into plasma layers, (E/T), 20: 2098 (AD-618398)
waveguide development for proton linacs, 20: 2538 (LA-DC-7281)
**MICROWAVE SPECTROMETERS**
instrumentation for, development of, 20: 2106 (UJV-1346/65)
**MICROWAVES**
absorption in weakly ionized xenon plasma in magnetic fields, (E), 20: 3204
emission by excited particles in resonator with coupled modes, spontaneous, (T), 20: 2527
interactions with plasma in gas discharges and semiconductors, (E/T), 20: 3157 (AD-614654)
**MILITARY PERSONNEL**
radiation protection of, aboard space vehicles, (T), 20: 2656 (NASA-SP-71, pp 265-86)
**MILK**
cesium-137 and strontium-90 content in Israeli, 20: 2520(R) (IA-920)
cesium-137 content in, Italy, 1963, 20: 2046 (BIO/04/64)
cesium-137 content of, Italy, 1964, 20: 2047 (EUR-2509.e)
decontamination by electrodialysis, equipment and method for, 20: 1972(P)
separation of strontium and cesium from, 20: 1975(P)
strontium-90 content in, Italy, 1963, 20: 2046 (BIO/04/64)
strontium-90 content of, Italy, 1964, 20: 2047 (EUR-2509.e)
**MINING**
preventive maintenance in, bibliography on, 20: 1976 (VDDIT-94)
**MISSILES**
effects of, from nuclear explosions, traumatic, 20: 2083 (CEX-65.4)
trajectories of structural fragments produced by nuclear weapons, analysis, 20: 3610 (AD-622333)
**MITOSIS**
radiation effects on, in animal cells in tissue culture, x, 20: 1617(R) (NP-15149)
radiation effects on, in L-strain cells, uv, 20: 1625
radiosensitivity of, in yeast, 20: 1664
**MIXED SPECTRUM CRITICAL ASSEMBLY**
neutron spectra in, fast and thermal, 20: 3402
**MIXER-SETTLERS**
steady-state of, prediction of approach to, 20: 1953 (IS-T-34)
**MOLECULAR STRUCTURE**
diatomic forces and force constants in, equations for, 20: 2650
**MOLECULES**
distribution of isotopic, kinetics of isotope effects in, 20: 1866
electron transitions in diatomic, methods for calculating spectral absorption coefficients of, 20: 1803 (AD-619266)
flow of free, relativistic theory of, 20: 2841
neutron cross sections of, tabulations, (E), 20: 3018 (NYO-72-27)
neutron differential scattering cross sections of gaseous, calculation of, (T), 20: 3135
perturbation theory for symmetrical, field form of, 20: 2607
perturbation theory for symmetrical, field form of, 20: 2608
scattering by solids, transition probabilities for, (T), 20: 2594 (N64-23208)
**MOLTEN SALT REACTOR EXPERIMENT**
criticality studies on, 20: 3505
use of on-line digital computer in data analysis for, 20: 3591
**MOLTEN SALT REACTORS**
performance of breeder-power, 20: 3498
**MOLYBDENUM**
corrosion by bismuth and tin, 20: 2275
corrosion by lithium at 1200°C, 20: 3321(R) (ANL-7082, pp 29-53)
corrosion by zinc and magnesium–uranium–zinc alloy, effects of molten chlorides on, 20: 2266
corrosion cracking by inorganic and organic acids and inorganic salt solutions, stress-, 20: 2254 (BM-RI-6680)
corrosion resistance to mercury at 900°F, 20: 2264
determination of trace amounts in uranium compounds by activation analysis, 20: 1784
diffusion in chromium and nickel as function of temperature, 20: 2357(T) (AERE-Trans-1032)
dislocation multiplication in polycrystalline, effect of strain rate on, (E), 20: 3286

electric conductivity at 0 to 2000°C, 20: 2223(R) (GEMP-51A)
electron emission from surfaces of, by positive and negative ion bombardment, (E), 20: 2628
properties and uses of, review on, 20: 2307 (AD-613023)
radiation effects on hardness of, neutron, 20: 2457
radiation effects on, annealing of, at 60 to 1200°C, 20: 2476
radiation effects on hardening and embrittlement of bcc, 20: 2472
reactions with uranium carbide–zirconium carbide solid solutions at high temperatures, compatibility in, 20: 2332 (LA-3307)
separation from rhenium using amyl acetate, 20: 1965
spectra of, isotopic shift in K-series x-ray, (E), 20: 2641
testing for use in shaft seals for potassium space power plants, 20: 2242
thermal conductivity at 900 to 2000°C, 20: 2223(R) (GEMP-51A)

**MOLYBDENUM ALLOY COUPLES**
Mo–Os–Ru/Re–W, thermoelectric properties at 100 to 1400°C, 20: 2223(R) (GEMP-51A)

**MOLYBDENUM ALLOYS**
properties and uses of, review on, 20: 2307 (AD-613023)
Co–Mo, recrystallization variables of flat rolled, 20: 2313 (AD-619208)
Mo–Nb–V–Zr, creep-rupture properties of, 20: 2336 (ORNL-P-1634)
Mo–Pu–U, development and fabrication for ZPPR and ZPR-VI fuels, 20: 3320(R) (ANL-7082, pp 1-28)
Mo–Re, corrosion by lithium at high temperatures, 20: 2269
Mo–Re, corrosion by bismuth and tin, 20: 2275
Mo–Re, development, 20: 2223(R) (GEMP-51A)
Mo–Re, ductility, phase studies, and properties of, 20: 2323 (GEMP-314)
Mo–Re, superconducting properties of, (E/T), 20: 2890 (AFML-TR-65-154)
Mo–Re–W, creep at 1600 and 2200°C, 20: 2223(R) (GEMP-51A)
Mo–Re–W, ductility of, effects of composition on, 20: 2223(R) (GEMP-51A)
Mo–Re–W, fabrication and properties of, 20: 2354(R) (USBM-RC-1205, pp 15-19)
Mo–Re–W, sectioning of, method for submicron, 20: 2321(R) (GEMP-52A, pp 43-5)
Mo–Ti, strain softening effects on properties of, 20: 2311 (AD-618925)
Mo–Ti–Zr, cavitation damage to TZM, in liquid sodium, 20: 2243
Mo–Ti–Zr, compatibility of TZM, with niobium–zirconium alloy in flowing zirconium, 20: 2238
Mo–Ti–Zr, corrosion of TZM, by potassium at high temperatures, 20: 2271
Mo–Ti–Zr, testing of TZM, for use in liquid-metal turbine blades and nozzles, 20: 2240
Mo–U, hydridation of, kinetics, 20: 2222 (EURAEC-1390)
Mo–U, preparation of powders of, 20: 2222 (EURAEC-1390)
Mo–U, use in the preparation of uranium compounds, 20: 1885(P)
Mo–W, corrosion by lithium at 1200°C, 20: 3321(R) (ANL-7082, pp 29-53)
Mo–W, corrosion by zinc and magnesium–uranium–zinc alloy, effects of molten chlorides on, 20: 2266
Mo–W, corrosion by bismuth and tin, 20: 2275

**MOLYBDENUM CARBIDES**
effects on graphite microstructure, 20: 2318(R) (GA-5915(Pt.1))
wetting by liquid cobalt, copper, iron, and nickel, 20: 1837

**MOLYBDENUM CHLORIDES**
superconductivity of cubic modification of, 20: 2346 (UCRL-11471)
thermodynamic properties of, in molten alkali metal chlorides, 20: 1882

**MOLYBDENUM ISOTOPES Mo-99**
beta decay of, lifetime of 24-sec isomer of niobium-90 from, 20: 3088

**MOLYBDENUM ISOTOPES Mo-94**
gamma transition at 871.1 kev following Coulomb excitation, (E), 20: 3043

**MOLYBDENUM ISOTOPES Mo-95**
neutron resonances at 45.1 and 161.0 ev, radiation widths of, (E), 20: 3133

**MOLYBDENUM ISOTOPES Mo-96**
gamma transition at 778.5 kev following Coulomb excitation, (E), 20: 3043
neutron resonance at 132.6 ev, radiation width of, (E), 20: 3133

**MOLYBDENUM ISOTOPES Mo-97**
magnetic moment, (T), 20: 3118
neutron resonance at 71.6 ev, radiation width of, (E), 20: 3133

**MOLYBDENUM ISOTOPES Mo-98**
gamma transition at 786.8 kev following Coulomb excitation, (E), 20: 3043
neutron resonance at 12.15 ev, radiation width of, (E), 20: 3133

**MOLYBDENUM ISOTOPES Mo-99**
content in fallout particles, 20: 2053
determination in sea water, methods for, 20: 1749 (USNRDL-TR-912)
separation from technetium-99 by milking, equipment and process for, 20: 1730 (BNL-9601)

**MOLYBDENUM ISOTOPES Mo-100**
gamma transition at 535.5 kev following Coulomb excitation, (E), 20: 3043

**MOLYBDENUM OXIDES**
testing for use in shaft seals for potassium space power plants, 20: 2242
thermodynamic properties, 20: 1880
$MoO_2$–$MoO_3$–$UO_2$, phase studies, 20: 2384

**MOLYBDENUM STEEL**
Cr–Mo, creep rupture of, effects of aging at 1100°F, 20: 2258(R) (MSAR-65-149)
Cr–Mo, welding procedures for, electro-slag, 20: 2281(R) (EURAEC-1408)
Mn–Mo, radiation effects on deformation properties of A302B, neutron, 20: 2436 (WERL-8844-4)
Mn–Mo, welding procedures for A302B, electro-slag, 20: 2281(R) (EURAEC-1408)
Mn–Mo–Ni–V, welding procedures for, electro-slag, 20: 2281(R) (EURAEC-1408)

**MOLYBDENUM SYSTEMS**
C–Mo–Nb–Ta–Ti–W–Zr, creep properties at 1800 to 2200°F of Cb132M, 20: 2333(R) (NASA-CR-54457)
C–Mo–Ti–Zr, creep properties at 1800 to 2200°F of TZC, 20: 2333(R) (NASA-CR-54457)
Mo–O, phase diagrams, 20: 1880
Mo–Ti–Zr, creep at 1800 to 2200°F of TZM, 20: 2333(R) (NASA-CR-54457)

**MONKEYS**
radiation effects on immune reactions in, 20: 1631

**MONTE CARLO METHOD**
use in analysis of shielding effectiveness of compartmented structures, 20: 3275
use in analysis of gamma and neutron transport in complex geometry, 20: 3348
use in neutron transport calculations, energy-independent biasing functions for, 20: 2985
use in optimization of plutonium distribution in reactor fuels, 20: 3456

**MOON**
power supplies for base on, development of SNAP-50/SPUR, 20: 3553
x-ray generation by, theories on detection of, 20: 2666

**MÖSSBAUER EFFECT**
cryostats for measurement of, at liquid helium temperatures, (E), 20: 3093
data index on, 20: 3146
measurement of, spectrometer for, 20: 2113
measurement of, spectrometer and technique for, 20: 3145
radiation damage effects on tin-119, in magnesium–tin oxide crystals, 20: 3065
use in measuring nuclear electric-field gradient, (E), 20: 3299
use in relativity theory testing, (E), 20: 2880
use in study of bonding in iron compounds, 20: 1874

**MULTIPLICATION FACTOR**
calculation of, using reactor-statics methods, (T), 20: 3367 (BNWL-156)
changes in, computer program for calculation of, 20: 3366 (ANL-7052)

**MUTAGENS**
effects of chemical, on *Schizosaccharomyces pombe*, genetic, 20: 1654

**MUTATIONS**
chemically induced, of wheat, 20: 1655
chemically induced, of *Zea mays*, 20: 1656
genetic analysis of chemically and ultraviolet induced, of *Schizosaccharomyces pombe*, 20: 1654
in murine cell line resistant to purine analogs, 20: 1678
production of asporogenic, by *Bacillus cereus* and *B. subtilis*, 20: 1582(R) (NYO-2038-2)
radioinduced in animals and plants, fast neutron, 20: 1622 (WT-820)
radioinduced in Drosophila, effects of sulfhydryl compounds on, 20: 1619(R) (TID-22293)
radioinduced in oat seeds, 20: 1665
radioinduced in tomato seeds, effects of temperature and oxygen during storage on, 20: 1638
radioinduced in yeast, 20: 1663
radioinduced, in Drosophila population, 20: 1642
radioinduced, in Drosophila, 20: 1644
radioinduced, in maize, x, 20: 1656
radioinduced, in unisexual wasp Devorgilla, 20: 1643
radioinduced, of wheat, 20: 1655


## N


**NAPHTHALENE**
complexes with polonium and polonium bromides, chlorides, fluorides, and iodides, preparation of, 20: 1850
benzophenone–naphthalene, radiolysis in alcoholic, aqueous, and hydrocarbon solutions, 20: 1920
butyl chloride–naphthalene, radiolysis in alcoholic, aqueous, and hydrocarbon solutions, 20: 1920
carbon tetrachloride–naphthalene, radiolysis in alcoholic, aqueous, and hydrocarbon solutions, 20: 1920
naphthalene–tetrahydrofuran, radiolysis in alcoholic, aqueous, and hydrocarbon solutions, 20: 1920

naphthalene–$H_2SO_4$, radiolysis in alcoholic, aqueous, and hydrocarbon solutions, 20: 1920
naphthalene–tetramethyl-p-benzoquinone, radiolysis in alcoholic, aqueous, and hydrocarbon solutions, 20: 1920
**NAPHTHALENESULFONIC ACIDS**
ethanol–naphthalenesulfonic acid–$H_2SO_4$, radiolysis in aqueous solutions, 20: 1920
**NAPHTHOL**
ethanol–naphthol–$H_2SO_4$, radiolysis in aqueous solutions, 20: 1920
**NATIONAL REACTOR TESTING STATION**
reactor development and safety at, 20: 2093
**NEBULAE**
formation of, statistical model for, (T), 20: 2574
gas flow stability in planetary, dilute, (T), 20: 2573
**NEOCUPFERRON**
solvent properties for protactinium, thorium, and uranium in hydrochloric acid solutions, 20: 1775
**NEODYMIUM**
determination using Chromotrope 2B, photometric, 20: 1772
spectra of, specific mass effects on isotopic displacements in, 20: 1826
**NEODYMIUM ACETATES**
complexes with thiourea, solubility in water, 20: 1869
**NEODYMIUM ALLOYS**
Mg–Nd, crystal structure, 20: 2399
**NEODYMIUM CHLORIDES**
heat of formation of, 20: 1806 (BM-RI-6697)
**NEODYMIUM COMPLEXES**
with amygdalin, separation by solvent extraction using butanol, 20: 1796
**NEODYMIUM IONS**
electron spin resonance of, 20: 2520(R) (IA-920)
spectra in praseodymium–neodymium-doped lanthanum fluoride, optical linewidth and line-shape studies of energy transfer mechanisms in, (E), 20: 2627
**NEODYMIUM ISOTOPES**
yields in uranium-233 thermal fission, (E), 20: 3010(R) (IDO-14663)
**NEODYMIUM ISOTOPES Nd-142**
effects on spectrum of neodymium, mass, 20: 1826
**NEODYMIUM ISOTOPES Nd-143**
neutron capture by, gamma spectra from thermal, (E), 20: 3131
**NEODYMIUM ISOTOPES Nd-144**
effects on spectrum of neodymium, mass, 20: 1826
energy levels from thermal neutron capture by neodymium-143, (E), 20: 3131
**NEODYMIUM ISOTOPES Nd-146**
effects on spectrum of neodymium, mass, 20: 1826
**NEODYMIUM ISOTOPES Nd-147**
content in fallout particles, 20: 2053
**NEODYMIUM ISOTOPES Nd-148**
effects on spectrum of neodymium, mass, 20: 1826
**NEODYMIUM ISOTOPES Nd-150**
effects on spectrum of neodymium, mass, 20: 1826
**NEODYMIUM OXIDES**
inhalation of aerosol of, effects of particle size and concentration in guinea pigs and mice, 20: 1593 (COO-1170-4)
magnetic susceptibility at 4 to 300°K, 20: 3318
**NEODYMIUM OXYBROMIDES**
preparation and crystal structure, 20: 1834
**NEON**
collisions of atoms of, with alkali metal atoms, ionization produced in, (E), 20: 2639
collisions of atoms of, with singly charged krypton ions, profound stripping and scattering in, (E), 20: 2644
determination of, factors affecting continuous on line, 20: 1734 (EG-Report-36)
electric breakdown potential of, measurement of a-c, 20: 3160 (AD-618503)
electric discharge in spark chambers, displacement of, (E/T), 20: 2131 (JINR-P-2344)
electric discharges in, effects of magnetic fields on breakdown time lag of, 20: 2835
helium scattering on, velocity dependence of total cross sections for, (E), 20: 2614
ionization by protons in spark chambers, measurement of, (E), 20: 2128 (JINR-E-2324)
neutron scattering by liquid, co-operative modes of motion from cold, (E), 20: 2837
photoionization in the K-shell of, electron shake-off resulting from, (E), 20: 2622
reactions with mercury, cross sections for line broadening from, (E), 20: 2637
spectra of mercury and sulfur isolated in, at high temperatures, 20: 1818 (UCRL-11976)
**NEON IONS**
electron transitions in, collision cross sections for dipolar, 20: 2598
formation by K-shell photoionization of neon, electron shake-off in, (E), 20: 2622
reactions of monoatomic singly charged, with nitrogen at 10 to 65 kev, rotational and vibrational excitation of singly charged molecular nitrogen ions in, (E), 20: 2618
**NEON ISOTOPES Ne-20**
particle reactions with, selection rules for alpha-knockout, (T), 20: 3117
**NEON ISOTOPES Ne-21**
energy level at 350.2 kev, (E), 20: 3043
energy levels, 20: 2520(R) (IA-920)
**NEON SYSTEMS**
He–Ne, electric discharge in spark chambers, displacement of, (E/T), 20: 2131 (JINR-P-2344)
Ne–Rb, optical pumping of rubidium-87 in, 20: 2596 (UCRL-16241)
**NEPHROSIS**
radioinduced in dogs, pathology of, 20: 1686
**NEPTUNIUM**
properties for complexing, 20: 1848
**NEPTUNIUM COMPLEXES**
stability, 20: 1848
with bromine and chlorine, stability of, 20: 2520(R) (IA-920)
**NEPTUNIUM COMPOUNDS**
stability, 20: 1855
**NEPTUNIUM ISOTOPES Np-237**
production in commercial power reactors, process for, 20: 2210
**NEPTUNIUM ISOTOPES Np-239**
content in fallout particles, 20: 2053
**NEPTUNIUM OXIDES**
$EuO_2$–$NpO_2$, phase studies by x-ray diffraction, 20: 2379
**NERVES**
radiation effects on regenerative capacity of, 20: 1635
**NERVOUS SYSTEM**
radiation effects on developing, in dog fetus, 20: 1627(T)
**NEUTRINO PAIRS**
production in stars, (T), 20: 2587
**NEUTRINOS**
interactions with antineutrinos, bootstrap method for W boson exchange in, 20: 2721
interactions with protons at high energy, cross sections for meson ($\pi^+$) production in, (T), 20: 2733
interactions with baryons at high energy, De Santis model for, 20: 2784
production in stars, energy balance in universe from, (T), 20: 2587
production in thermonuclear reactions, (T), 20: 2587
reactions with matter, intermediate vector bosons from, (T), 20: 2759 (UR-875-102)
**NEUTRINOS ($\nu_e$)**
interactions with protons, positron spectra from, (E), 20: 2680 (COO-818-58)
**NEUTRON CAPTURE CROSS SECTIONS**
resonance effects in Doppler calculations, (T), 20: 2972
**NEUTRON CROSS SECTIONS**
calculation for tantalum-181 and tungsten from 1 kev to 14 Mev, (T), 20: 2961
data retrieval of, computer program for, 20: 3009 (GA-6685)
Doppler broadening integral for, derivation of, (T), 20: 3375 (IDO-17120)
tabulations, (E), 20: 3018 (NYO-72-27)
**NEUTRON-DIFFRACTION ANALYSIS**
use in determination of interplanar spacings in polymers, 20: 3308
**NEUTRON FISSION CROSS SECTIONS**
calculation of, multi-level model for, (T), 20: 3374 (IA-1053)
**NEUTRON SCATTERING CROSS SECTIONS**
calculation of differential, for gas molecules, (T), 20: 3135
**NEUTRON SHIELDING**
albedo distributions for fast, (E/T), 20: 2932 (ORNL-3822(Vol.1))
albedo distributions for fast, (E/T), 20: 2933 (ORNL-3822(Vol.2))
albedo distributions for fast, (E/T), 20: 2934 (ORNL-3822(Vol.3))
albedo distributions for fast, (E/T), 20: 2935 (ORNL-3822(Vol.4))
albedo distributions for fast, (E/T), 20: 2936 (ORNL-3822(Vol.5))
albedo distributions for fast, (E/T), 20: 2937 (ORNL-3822(Vol.6))
design for hardened structures, (T), 20: 3276
design for meson ($\pi$) production facility using proton linear accelerator, 20: 2559
performance of, few- and multigroup P3 analyses of, (T), 20: 2939 (WAPD-T-1710)
**NEUTRON SOURCES**
calibration, 20: 2520(R) (IA-920)
calibration of, with different spectral composition, 20: 2947
calibration using manganese-56, 20: 3321(R) (ANL-7082, pp 29-53)
development of high-output tubes for activation analysis, 20: 3005
neutron activation and spectra in concrete walls around accelerator, 20: 3264
neutron spectra and yields from ($\alpha$,n) reactions in heterogeneous isotopic,

(E), 20: 2949
performance of accelerator-pulsed, 20: 2956
use of isotopic, in irradiation facilities, 20: 2997
**NEUTRON SPECTRA**
determination outside shields of pulsed accelerators, 20: 2553
measurement in Aquilon reactor, (E/T), 20: 3582 (CEA-R-2482)
measurement in heterogeneous media, integral and differential, 20: 3600
measurement in paraffin, 20: 2931 (AD-616518)
measurement using resonance activation, 20: 2971
measurement using Fermi chopper, 20: 2994
**NEUTRON TOTAL CROSS SECTIONS**
calculation of, multi-level model for, (T), 20: 3374 (IA-1053)
measurement for carbon and iron at 14.6 Mev, (E), 20: 2962
**NEUTRONS**
absorption in heterogeneous systems, resonance integral for, (T), 20: 2973
absorption in heterogeneous media with moderator scattering, resonance integrals for, (T), 20: 2974
absorption in materials with grain structure, resonance, 20: 2993
absorption resonance integral calculations for, equivalence principle for, (T), 20: 2977
attenuation by matter, few- and multigroup P3 analyses of, (T), 20: 2939 (WAPD-T-1710)
binding energies in nuclei with N = 86 to 92, 20: 3098
buckling in light-water-uranium lattices, 20: 2520(R) (IA-920)
capture by erbium-166, gamma spectra and erbium-167 level scheme from, (E), 20: 3127
capture-to-fission ratios for plutonium-239 and -241 at epicadmium energies, 20: 3321(R) (ANL-7082, pp 29-53)
capture-to-fission ratio measurement in low-flux assemblies, method for direct, 20: 3430
diffusion equations for reactors, computer program for solving, 20: 3382 (WAPD-TM-532)
diffusion in lead, heavy monoatomic gas model for, 20: 2943
diffusion parameters for cylinders of water–heavy water, 20: 2951
diffusion parameters in water, sample geometry effects on, (E), 20: 2952
diffusion parameters in diphenyl at 85 and 105°C, (E), 20: 2953
diffusion theory representation of fuel clusters containing control rods, 20: 3428
dispersion law of moderators, (T), 20: 2991
Doppler coefficients of fertile and refractory materials, 20: 2958
dosimetry in reactors, using colored polyvinyl alcohol films, 20: 2135
effects on algal, biological, 20: 1681
effects on alloys and stainless steels cryogenic low temperatures, 20: 2459
effects on aluminum oxides, (E), 20: 3446(R) (GEST-2045)
effects on A302B steel, annealing effects on, 20: 2455
effects on bcc alpha-iron, computer study of, 20: 2473
effects on beryllium oxidation by carbon dioxide at 600 to 1000°C, 20: 2442
effects on bursting pressure and fatigue life of stainless steel pressure tubes, 20: 2435 (WAPD-T-1720)
effects on cables and resistors, 20: 2187 (ECOM-2545)
effects on deformation properties of A302B steel, 20: 2436 (WERL-8844-4)
effects on elastic properties of polycrystalline graphite, (E/T), 20: 2446
effects on electric properties of magnesium–germanium silicides, 20: 2502
effects on electric conductivity of beryllium, thoria, and zirconia, 20: 2460
effects on electric cables, signal transients from, 20: 2186 (ECOM-2415)
effects on electronic equipment, transient, 20: 2190
effects on exciton spectrum of copper oxide, 20: 2505
effects on forests, ecological, 20: 2080 (BNL-917, pp 20-36)
effects on forests, ecological, 20: 2081 (BNL-917, pp 39-60)
effects on formation of carbon-14-labeled polymers in ammonia–ethylene mixtures, 20: 1922
effects on graphite, defect nucleation in, 20: 2447
effects on hardening and embrittlement in body-centered-cubic transition metals, 20: 2472
effects on hardness of molybdenum and tungsten, 20: 2457
effects on hollow uranium dioxide pellets in collapsible Zircaloy-2 sheaths, 20: 2415 (AECL-2276)
effects on iron and steel, 20: 2474
effects on lattice parameter of copper–boron systems, 20: 2441
effects on mechanical properties of stainless steel at high temperatures, 20: 2430 (ORNL-P-1713)
effects on mechanical properties of Incoloy 800, 20: 2458
effects on melting tungsten–uranium dioxide and uranium dioxide fuel elements, 20: 2416 (AECL-2289)
effects on molybdenum, annealing of, 20: 2476
effects on n-p-n silicon transistors, 20: 2184(R) (AD-614618)
effects on n-p-n silicon transistors, 20: 2185(R) (AD-618194)
effects on n-type antimony–indium alloy at 78°K, 20: 2500
effects on thermal conductivity and electric properties of uranium dioxide, 20: 2452
effects on thermophysical properties of isopropylbiphenyl, 20: 1923
effects on tin-119 Mössbauer effect in magnesium–tin oxide crystals, damage, 20: 3065
effects on transistors, physical parameters for predicting, 20: 2184(R) (AD-614618)
effects on transistors, method for predicting, 20: 2185(R) (AD-618194)
effects on tungsten, 20: 2475
emission in proton reactions with lithium-6, (E), 20: 3140
energy spectra in heterogeneous nonabsorbing media, (T), 20: 2942
extrapolation length in slab geometry, (T), 20: 2988
flux beneath shield of meson production facility, (T), 20: 3262
flux distribution in light-water-moderated reactors, 20: 3500
flux distribution in Shippingport Pressurized Water Reactor, 20: 3519
flux distribution of, transport equation for, 20: 2940
flux distributions in reflector and primary shield of New Production Reactor, 20: 3544
flux in nonmultiplying medium, recursion formula in Lie-series method for, 20: 2941
flux in reactors, instrumentation for measuring, 20: 2107
flux measurements using resonance activation, 20: 2971
flux monitoring in reactors, device for, 20: 2173
flux monitoring in pressurized-water reactors, self-powered detectors for, 20: 2174
interactions with protons at 23 Mev, correlation function for, (E), 20: 2685 (LA-DC-7250)
interactions with neutrons at 1.4 to 4.0 Bev/c, backward elastic, (E), 20: 2700(T)
interactions with protons at 20 to 120 Mev, polarization in, (E), 20: 2701
interactions with protons at 19.3 Bev/c, amplitude for, (E/T), 20: 2712
interactions with mesons ($\pi^-$) at 1.38 to 4.05 Bev/c, backward elastic, (E), 20: 2713
interactions with deuterons at high energy, equation for partial amplitudes of, 20: 2740
magnetic moments of, self-consistent calculation of isovector part of, 20: 2704
nuclear generation time in reactors, variation with reactivity, 20: 3386
photoproduction in electron-photon cascades in thick targets, 20: 3261
production by ($\alpha$,n) reactions in heterogeneous isotopic neutron sources, (E), 20: 2949
reactions (n,$\alpha$) and (n,p) with chlorine-35 and -36 and sulfur-32 and -33, phosphorus-32 and -33 production in, (E), 20: 3020 (ORNL-TM-1065)
reactions (n,$\alpha$) with scandium-45, cross sections for, 20: 1947
reactions (n,$\alpha$) and (n,2n) with beryllium, multigroup cross sections for, 20: 2960
reactions (n,$\gamma$) with arsenic-75, gamma spectra from, (E), 20: 3011 (IPA-NR-22)
reactions (n,$\gamma$) with nuclei at 1 ev to 50 kev, cross sections for, (E), 20: 3032
reactions (n,n) with helium-3 to 1.5 Mev, phase-shift analysis of, 20: 3060
reactions (n,p) with calcium-42 and calcium-43, cross sections for, 20: 1947
reactions in collapsing stars, adiabatic exponent for equilibrium in, (T), 20: 2588
reactions with atoms, molecules, and nuclei, cross section tabulations for, (E), 20: 3018 (NYO-72-27)
reactions with hydrogen, interaction effect in capture, (T), 20: 3059
reactions with nuclei, Doppler broadening of cross sections for, (T), 20: 3375 (IDO-17120)
reactions with uranium-233 and -235 at 0.1 to 0.2 Mev, fission cross section structure from, (E), 20: 3089
scattering by carbon, iron, and lithium-7 at 14.6 Mev, inelastic, (E/T), 20: 2962
scattering by complex nuclei below 50 Mev, data survey for elastic polarized, 20: 3014 (LA-DC-7386)
scattering by crystals of polyethylene at 0.17 to 0.50 ev, (E/T), 20: 2964
scattering by nuclei at high energies, direct-interaction inelastic, (T), 20: 3256
scattering by polarized nuclei in external magnetic field, (T), 20: 3120
scattering by precipitations in aluminum–copper alloys at long wavelength, 20: 3285
scattering by zirconium hydrides and heavy water at 0.06 to 10 ev, differential cross sections for, (E), 20: 2963
shielding by concrete, 20: 3253
shielding space vehicles from secondary, produced in spherical proton shielding, (T), 20: 3242 (NASA-SP-71, pp 225-8)
spectra in beryllium, (E/T), 20: 2968
spectra in hydrogenous media, eigenfunction analysis of, 20: 2999
spectra in water containing erbium and gadolinium, temperature-dependent, (E/T), 20: 2966

thermalization in moderating assemblies, time-, energy-, and space-dependent theory of, 20: 3003
thermalization of, error estimates for integral-equation eigenvalue problems in, 20: 3411
transmission of polarized, through a superconductor in the mixed state, (T), 20: 2998
transport calculations using Monte Carlo method, energy-independent biasing functions for, 20: 2985
transport equation for critical slab, solution by perturbation theory, 20: 3423
transport equation for, variational vacuum boundary conditions for $P_N$ approximation to, 20: 2978
transport equation for, approximation by moments equations, 20: 2981
transport equation for, numerical method for solving linear, 20: 2983
transport equation for, method for solving, 20: 2984
transport equations for, computer program for solving, 20: 2990
transport equation for one-speed, solutions in plane geometry, 20: 3000
transport equation for, approximation by discrete ordinates equations, 20: 2982
transport in adjacent semi-infinite media, time-dependent, (T), 20: 2987
transport in complex geometry, analysis by three-dimensional Monte Carlo calculations, (E/T), 20: 3348
transport in finite slab geometries, source functions for, (T), 20: 2930 (AD-614636)
transport in heterogeneous anisotropically scattering shields, energy-dependent, (T), 20: 2989
transport in reactors, (T), 20: 3375 (IDO-17120)
transport in slab geometry with anisotropic scattering, (T), 20: 2986
transport in slab geometry, solution to one-velocity time-independent Boltzmann equation for, 20: 3004
transport theory for, variational principles in, 20: 2979
transport theory for, variational principles in, 20: 2980
transport theory in pulsed multiplying assemblies, 20: 3001
use for radiography of boron in reactor alloys, (E), 20: 3471(R) (GEAP-4861)
use in measurement of phonon frequencies in polyethylene, 20: 3315

**NEUTRONS, COLD**

reactions with rhenium-185 and -187, total cross sections for, (E), 20: 3030
scattering by liquids, cooperative modes of motion from, (E), 20: 2837

**NEUTRONS, DELAYED**

spectra in lithium-9 decay, (E), 20: 3130

**NEUTRONS, EPITHERMAL**

absorption in slabs of 1/v absorbers, (T), 20: 2946
production, properties, and use for therapy, 20: 1714
reaction rates in reactor matrices, computer program for calculating, 20: 2992

**NEUTRONS, FAST**

angular distribution and spectra in paraffin, measurement of, 20: 2931 (AD-616518)
detection and measurement of dose equivalent and fluence of, device for, 20: 2123 (ANL-7085)
dosimetry of, using semiconductor detectors, (E), 20: 2134 (TID-22335)
effects on animals and plants, genetic, 20: 1622 (WT-820)
effects on antimony-doped germanium single crystals at 100°C, 20: 2495
effects on beryllium oxide thermal conductivity due to microcracking, 20: 2443
effects on brittle-to-ductile transition temperature of polycrystalline tungsten, 20: 2422(R) (GEMP-52A, pp 11-21)
effects on creep-rupture properties of A-286 alloy and Hastelloy X, 20: 2456
effects on different type graphites at 800 to 1200°C, 20: 2417 (BNWL-112)
effects on ductility of Zircaloy-2, 20: 2420(R) (DPST-65-83-8)
effects on electric properties of silicon carbides, 20: 2503
effects on electric properties of silicon, annealing during fabrication of p-n junctions of, 20: 2440
effects on flour beetles, Tribolium, biological, 20: 1613 (HW-SA-3537)
effects on gas formation and compression fractures in beryllium, 20: 2478
effects on germanium, annealing of, 20: 2509
effects on hot-hardness of tungsten single crystals, dosage effects of, 20: 2422(R) (GEMP-52A, pp 11-21)
effects on magnesium oxides, x-ray line broadening in, (E), 20: 2445
effects on mechanical properties of stainless steel at 25 to 850°C, 20: 2477
effects on meta- and ortho-terphenyl, 20: 1928
effects on properties of beryllia, effects of composition on, 20: 2424(R) (GEMP-52A, pp 37-42)
effects on reactions between beryllium oxide and graphite at 1500°C, equipment and setup for studying, 20: 2431 (ORNL-TM-1255)
effects on resistance-temperature transducers at low temperatures, 20: 2191
effects on rupture life of tungsten–25 rhenium sheet, 20: 2422(R) (GEMP-52A, pp 11-21)
effects on rupture life of INOR-8, effects of postirradiation annealing on, 20: 2423(R) (GEMP-52A, pp 27-35)
effects on rupture life of INOR-8, effects of irradiation temperature on, 20: 2423(R) (GEMP-52A, pp 27-35)
effects on seeds of tomatoes, genetic, 20: 1638
effects on seeds of wheat, genetic, 20: 1655
effects on seeds of barley, biological, effects of oxygen and moisture on, 20: 1667
effects on tensile properties of Incoloy 800, (E), 20: 3471(R) (GEAP-4861)
effects on tensile properties of copper–niobium–zirconium alloy, 20: 2414 (AECL-2272)
effects on terphenyls, interpretation of, 20: 1927
effects on thermal conductivity of silicon monocrystals at 80 to 300°K, 20: 2487
effects on thermal conductivity of ternary arsenides, 20: 2488
effects on thermal control coatings for spacecraft, 20: 2428 (NASA-SP-55, pp 365-79)
flux decay in lead slabs, (E), 20: 2950
reactions (n,d) and (n,p) with nuclei at 8 to 22 Mev, distributions from, (E), 20: 3012 (IKF-11)
reactions in water, charged-particle slowing-down spectra from, 20: 1924
reactions with uranium-235 at 720 kev, fragment kinetic-energy distributions from, (E), 20: 3110
reflection by concretes, dose albedo distributions for, (E/T), 20: 2932 (ORNL-3822(Vol.1))
reflection by concretes, dose albedo distributions for, (E/T), 20: 2933 (ORNL-3822(Vol.2))
reflection by concretes, dose albedo distributions for, (E/T), 20: 2934 (ORNL-3822(Vol.3))
reflection by concretes, dose albedo distributions for, (E/T), 20: 2935 (ORNL-3822(Vol.4))
reflection by concretes, dose albedo distributions for, (E/T), 20: 2936 (ORNL-3822(Vol.5))
reflection by concretes, dose albedo distributions for, (E/T), 20: 2937 (ORNL-3822(Vol.6))
scattering by aluminum, concrete, graphite, lithium hydride, and steel cylinders, (E/T), 20: 3265
scattering by nuclei at 0.8 to 4.5 Mev, compound-nucleus analysis of, (T), 20: 3021 (ORNL-TM-1238)
spectra in liquid hydrogen, (E), 20: 2967
spectra in paraffin, (E/T), 20: 3257

**NEUTRONS, FISSION**

age to indium resonance in aluminum–water systems, (E), 20: 2970
age to resonance in concrete, (E), 20: 3255
slowing down in water, spin polarization effects on, (T), 20: 2969

**NEUTRONS, PROMPT**

angular correlations between fission fragments and, methods for, 20: 3025
lifetime in mixed spectrum critical assembly, 20: 3402

**NEUTRONS, RESONANCE**

diffusion in uranium, (E), 20: 3031
reactions (n,f) and (n,γ) with nuclei, cross sections for, (E), 20: 3031
reactions with rhenium-185 and -187, total cross sections for, (E), 20: 3030

**NEUTRONS, THERMAL**

angular albedos for concrete, differential, (T), 20: 3266
capture by neodymium-143, gamma spectra from, (E), 20: 3131
capture resonance scattering detection by gamma radiation from, (E/T), 20: 2520(R) (IA-920)
diffusion coefficient in heavy water containing voids, (E), 20: 2957
diffusion length in concrete, (E), 20: 3255
diffusion parameters in water, measurement using pulsed neutron techniques, 20: 2954
dosimetry using lithium fluoride, 20: 2178
effects on creep-rupture properties of A-286 alloy and Hastelloy X, 20: 2456
effects on mechanical properties of stainless steel at 25 to 850°C, 20: 2477
effects on potential of mercury oxide electrode, 20: 1932
effects on semiconductors, 20: 2516
flux of, distribution of eigenvalue curves in analysis of, (T), 20: 3002
genetic effects in oat seeds, 20: 1665
propagation of pulsed, in infinite water geometry, 20: 2944
pulse propagation in graphite, from reactors, 20: 2955
reactions (n,f) and (n,γ) with nucleic, cross sections for, (E), 20: 3031
reactions (n,f) with uranium-235, ionization energy losses of fragments from, (E), 20: 3029
reactions (n,γ) with iron-54, gamma spectra from, 20: 3109
reactions (n,γ) with hydrogen, cross section for, (E), 20: 3058
reactions with boron-10 in boron–copper system, production of helium-4 and lithium-7 by, 20: 2444
reactions with rhenium-185 and -187, total cross sections for, (E),

20: 3030
reactions with uranium-235, fragment kinetic-energy distributions from, (E), 20: 3110
scattering in liquid metals, Kohn anomaly in coherent, (T), 20: 2948
scattering kernels and laws for, method for calculating, 20: 3412
spectra in boric acid–water systems, determination using integral activation techniques, (E), 20: 2965
spectra in cooled moderators, (E), 20: 2945

**NICKEL**
corrosion resistance to mercury at 900°F, 20: 2264
deuteron elastic scattering at 26 Mev, optical model analysis of, (E/T), 20: 3053
diffusion of molybdenum in, as function of temperature, 20: 2357(T) (AERE-Trans-1032)
grain boundary migration in zone-refined, review on, 20: 3626 (ORNL-P-1722)
proton shielding performance of, for space vehicles, (T), 20: 3242 (NASA-SP-71, pp 225-8)
solubility in molten potassium, 20: 2237
thermal diffusion of deuterium and hydrogen in alpha, at 400 to 600°C, 20: 2397
wetting properties for metallic carbides, 20: 1837

**NICKEL ALLOYS**
corrosion resistance to mercury at 900°F, 20: 2264
Au–Ni–Sn, solute interactions in dilute, (E/T), 20: 2349 (UCRL-16320)
Cr–Fe–Ni, electron-beam welding to tubesheet joints, 20: 2283 (KAPL-3110)
Cr–Ni, metallurgical properties of austenitic, (E), 20: 3471(R) (GEAP-4861)
Eu–Ni, magnetic properties, 20: 2369
Eu–Ni, preparation, hardness, and microstructure, 20: 2369
Fe–Ni, thermal diffusion of hydrogen in gamma-, at 400 to 600°C, 20: 2397
Lu–Ni, preparation and structure of, 20: 2385(T)
Ni–Ti, effects of aluminum, cobalt, iron, silicon, and tungsten on properties of Nitinol, 20: 2310 (AD-618681)
Ni–Tm, preparation and structure of $MgCu_2$-type, 20: 2385(T)
Ni–U, diffusion in, activation energy for inter-, 20: 2328 (INR-625/XIV/R)

**NICKEL BORIDES**
$Ni–Ni_3B$, development of fiber-reinforced composites of, 20: 2219 (AMRA-CR-64-05/4)

**NICKEL CATALYSTS**
uses in hydrogenation, tracer studies of product contamination by, 20: 1889

**NICKEL ISOTOPES Ni-56**
energy levels from proton, reactions (p,t) with nickel-58 at 28 Mev, (E), 20: 3041

**NICKEL ISOTOPES Ni-58**
deuteron elastic scattering at 27.5 Mev, angular distribution for, (E/T), 20: 3057
energy levels of, microscopic models for vibrational, (T), 20: 3083
neutron reactions (n,d) and (n,p) at 8 to 22 Mev, distributions from, (E), 20: 3012 (IKF-11)
proton reactions (p,t) at 28 Mev, nickel-56 energy levels from, (E), 20: 3041

**NICKEL ISOTOPES Ni-60**
energy levels of, microscopic models for vibrational, (T), 20: 3083
energy-level transition probabilities of, E2, (T), 20: 3115

**NICKEL ISOTOPES Ni-62**
energy levels of, microscopic models for vibrational, (T), 20: 3083

**NICKEL ISOTOPES Ni-64**
energy levels of, microscopic models for vibrational, (T), 20: 3083

**NICKEL STEEL**
Cr–Ni, loop corrosion tests at supercritical pressure and temperature on, 20: 2262 (WCAP-2056(Pt.6))
Mn–Mo–Ni–V, welding procedures for, electro-slag, 20: 2281(R) (EURAEC-1408)

**NICKEL SYSTEMS**
$Ni–Ni_3B$, development of fiber-reinforced composites of, 20: 2219 (AMRA-CR-64-05/4)

**NICKEL URANATES**
crystal structure and density of, 20: 2400

**NIOBIUM**
corrosion by bismuth and tin, 20: 2275
corrosion resistance to mercury at 900°F, 20: 2264
deposition on uranium carbide, 20: 2300(P)
fabrication into superconducting delay lines, (E), 20: 3612 (CONF-651001-6)
Ginzburg-Landau parameters of superconducting, (E/T), 20: 2906
melting of, performance of induction furnace for cold-mold, 20: 2352(R) (USBM-RC-1205, pp 9-10)
properties and uses of, review on, 20: 2307 (AD-613023)
properties of pentavalent, in aqueous solution, 20: 1875
radiation effects on yielding and flow in bcc, 20: 2472
reactions with uranium carbide–zirconium carbide solid solutions at high temperatures, compatibility in, 20: 2332 (LA-3307)
solubility in molten potassium, 20: 2237
specific heat of superconducting, in magnetic fields, (E), 20: 2906
strain-aging process in, yield-point return and internal friction studies of, 20: 2376
thermal capacity of superconducting, (T), 20: 2905

**NIOBIUM ALLOYS**
properties and uses of, review on, 20: 2307 (AD-613023)
Be–Ni, development of NiBe fiber-reinforced composites of, 20: 2219 (AMRA-CR-64-05/4)
Cu–Nb–Zr, radiation effects on tensile properties of, fast-neutron, 20: 2414 (AECL-2272)
Mo–Nb–V–Zr, creep-rupture properties of, 20: 2336 (ORNL-P-1634)
Nb–Sn, magnetic flux jumps in superconducting $Nb_3Sn$ in pulsed magnetic fields, (E), 20: 2921
Nb–Sn–Zr, corrosion by steam, effects of antimony, chromium, iron, and vanadium additions on, 20: 2255(R) (EURAEC-1323)
Nb–Ta, Ginzburg-Landau parameters of superconducting, (E/T), 20: 2906
Nb–Ta, specific heat of superconducting, in magnetic fields, (E), 20: 2906
Nb–Ta–V–Zr, strength at high temperatures, 20: 2407(P)
Nb–Ti, superconducting-normal transitions in variable fields, mechanisms of, (E), 20: 2902
Nb–Ti–V–Zr, properties, effects of composition on, 20: 2340 (ORNL-TM-1131)
Nb–V, corrosion by lithium at 815°C, effects of oxygen on, 20: 2340 (ORNL-TM-1131)
Nb–W, corrosion by lithium at high temperatures, 20: 2269
Nb–W–Zr, corrosion by flowing lithium, 20: 2238
Nb–W–Zr, corrosion by bismuth and tin, 20: 2275
Nb–W–Zr, creep-rupture properties of, 20: 2336 (ORNL-P-1634)
Nb–W–Zr, stress effects in corrosion of D-43, by photassium, 20: 2270
Nb–Y–Zr, corrosion by steam at 400-500°C, 20: 2276(P)
Nb–Zr, brazing techniques for bonding to graphite, 20: 2294
Nb–Zr, compatibility with alkali metals at high temperatures, 20: 2236
Nb–Zr, compatibility with TZM alloy in flowing lithium, 20: 2238
Nb–Zr, corrosion by boiling and condensing alkali metals, 20: 2268
Nb–Zr, corrosion by potassium at high temperatures, 20: 2271
Nb–Zr, corrosion by potassium–sodium system, 20: 2273
Nb–Zr, corrosion by bismuth and tin, 20: 2275
Nb–Zr, fabrication into superconducting delay lines, (E), 20: 3612 (CONF-651001-6)
Nb–Zr, hydridation of, kinetics, 20: 2222 (EURAEC-1390)
Nb–Zr, hydride nucleation and growth in, 20: 2253 (AECL-2297)
Nb–Zr, magnetic flux jumps in superconducting NbZr in pulsed magnetic fields, (E), 20: 2921
Nb–Zr, magnetic fields on surface of superconducting, in external magnetic field, (E), 20: 2924
Nb–Zr, mass transfer of carbon and nitrogen to, from type-316 stainless steel in liquid potassium, 20: 2239
Nb–Zr, parameters for zirconium self-diffusion in, 20: 2356(T) (AERE-Trans-1030)
Nb–Zr, preparation of powders of, 20: 2222 (EURAEC-1390)
Nb–Zr, superconducting properties of, effects of heat treatments and microstructure on, 20: 2395
Nb–Zr, superconducting-normal transitions in variable fields, mechanisms of, (E), 20: 2902
Nb–Zr, testing for use in liquid-metal turbine blades and nozzles, 20: 2240
Nb–Zr, transfer of carbon and nitrogen to, from stainless steels in potassium, 20: 2270

**NIOBIUM CARBIDES**
corrosion by hydrogen fluoride at 2000 to 3100°K, 20: 2261(R) (UCRI-326)
diffusion of carbon in, at 1800 to 2700°C, layer-growth measurements of, 20: 2398
wetting by liquid cobalt, copper, iron, and nickel, 20: 1837
C–NbC–UC, preparation as reactor fuel material, 20: 2305(P)
NbC–TaC, wetting by liquid copper, 20: 1837

**NIOBIUM HYDRIDES**
structure of beta-, 20: 2365

**NIOBIUM ISOTOPES Nb-90**
energy levels in, effect of chemical state on lifetime of 24-second isomer, 20: 3088
metabolism of, in rats and rat sarcomas, 20: 1595

**NIOBIUM ISOTOPES Nb-91**
energy-level transition probabilities of, E2, (T), 20: 3115

**NIOBIUM ISOTOPES Nb-93**

magnetic moment, (T), 20: 3118
neutron resonances at 94 to 379 ev, radiation widths of, (E), 20: 3133
**NIOBIUM ISOTOPES Nb-95**
content in atmosphere, 1962 to 1963, 20: 2049
content in fallout particles, 20: 2053
metabolism of, in rats and rat sarcomas, 20: 1595
**NIOBIUM NITRIDES**
NbN–ZrN, superconductivity of wires of, (E), 20: 2891
**NIOBIUM OXIDES**
testing for use in shaft seals for potassium space power systems, 20: 2242
**NIOBIUM SYSTEMS**
C–Mo–Nb–Ta–Ti–W–Zr, creep properties at 1800 to 2200°F of Cb132M, 20: 2333(R) (NASA-CR-54457)
C–Nb, phase studies on, thermal analysis of, (E), 20: 1863
H–Nb, diffusion of hydrogen in, 20: 2365
Nb–N–Zr, equilibrium solid solutions at 1200 to 1800°C in, 20: 2337 (ORNL-P-1677)
**NITRAMIDES**
determination of HMX and RDX by nonaqueous titration with tetrabutylammonium hydroxide, 20: 3638 (UCRL-7873)
**NITRATION**
hydrogen exchange in, of tritium-labeled toluene, 20: 1950
**NITRIC ACID**
analytical use for ion exchange of iron and thorium by amberlite IR-120, 20: 1783
corrosive effects on molybdenum, vanadium, and titanium–vanadium alloys, stress-, 20: 2254 (BM-RI-6680)
solvent properties for actinium oxalate, 20: 1846
HF–$HNO_3$, solvent properties for ignited plutonium dioxide, 20: 2344 (TRG-Report-1072)
$HNO_3$–TBP–$H_2O$, nitric acid concentration in mixer-settler extractor as function of time, 20: 1953 (IS-T-34)
**NITROGEN**
collisions of molecules of, with alkali metal atoms, ionization produced in, (E), 20: 2639
determination in helium at reduced sample pressures by gas chromatography, 20: 1751
determination of, factors affecting continuous on line, 20: 1734 (EG-Report-36)
effects on radioinduced embrittlement of steel, 20: 2474
electron reactions with atmospheric, cross sections for, 20: 2859
ionization by heavy ions at 25 to 50 kev, total, (E), 20: 2623
mass transfer from type-316 stainless steel to niobium–zirconium alloy by liquid potassium, 20: 2239
nitrogen ion reactions at 0.14 to 0.7 Mev, energy loss in, (E), 20: 2602
oxygen ion reactions at 0.14 to 0.7 Mev, energy loss in, (E), 20: 2602
radioinduced luminescence of, alpha and fission-fragment, 20: 1933
reactions with beryllium in simulated launch pad abort environments at 800 to 1500°C, 20: 2341 (SC-DC-65-1637)
spectra of graphite vapor, mercury, and sulfur isolated in, at high temperatures, 20: 1818 (UCRL-11976)
transfer from stainless steels to niobium–zirconium alloys in potassium, 20: 2270
**NITROGEN IONS**
electron transitions in, collision cross sections for dipolar, 20: 2598
ionization of nitrogen by 25- to 50-kev, total, (E), 20: 2623
reactions of monoatomic singly charged, with nitrogen at 10 to 65 kev, rotational and vibrational excitation of singly charged molecular nitrogen ions in, (E), 20: 2618
reactions of positive monatomic and diatomic, with molybdenum surfaces, secondary-electron yields from, 20: 2628
reactions with argon, nitrogen, and helium at 0.14 to 0.7 Mev, energy loss in, 20: 2602
reactions with carbon monoxide, charge-transfer excitation in slow, (E), 20: 2631
rotational and vibrational excitation of singly charged molecular, by monoatomic ions at 10 to 65 kev, (E), 20: 2618
**NITROGEN ISOTOPES N-14**
energy levels at 2.31, 3.95, and 5.10 Mev, mean lives of, (E), 20: 3045
nucleon scattering by, differential cross section and polarization for, (T), 20: 3091
proton reactions (p,γ) at 0.97 to 1.96 Mev, oxygen-15 production in, (E), 20: 3006 (AD-613676)
radioinduced exchange with nitrogen-15, use in dosimeters, 20: 2520(R) (IA-920)
**NITROGEN ISOTOPES N-15**
energy levels from gamma reactions (γ,p) with oxygen-16 at 21.3 to 43.7 Mev, (E), 20: 3107
energy levels of, from oxygen-16 giant dipole resonance de-excitation, (E), 20: 3074
proton reactions (p,α) at 3 to 12 Mev, direct-reaction analysis of angular distributions from, (E/T), 20: 3061
radioinduced exchange with nitrogen-14, use in dosimeters, 20: 2520(R) (IA-920)
**NITROGEN ISOTOPES N-16**
activity of, design of coincidence counters for, 20: 2139
production and reactions of, 20: 2520(R) (IA-920)
**NITROGEN MUSTARDS**
effects on survival of animal cells in culture, 20: 1617(R) (NP-15149)
**NITROGEN OXIDES**
determination of, factors affecting continuous on line, 20: 1734 (EG-Report-36)
electron reactions with, vibrational excitation in fast, (E/T), 20: 2638
handling of, 20: 1727 (NASA-SP-5032)
reactions with beryllium in simulated launch pad abort environments at 800 to 1500°C, 20: 2341 (SC-DC-65-1637)
toxicity of, 20: 1727 (NASA-SP-5032)
**NITROGEN SYSTEMS**
He–N, spectra of singly ionized nitrogen in plasma of, Stark profiles of, (E), 20: 3215
Nb–N–Zr, equilibrium solid solutions at 1200 to 1800°C in, 20: 2337 (ORNL-P-1677)
**NOISE**
effects on cardiac activity in dogs, 20: 1629
**NORTH AMERICA**
effects of 20,000-MT nuclear attack on, ecological, 20: 2081 (BNL-917, pp 39-60)
effects of 20,000-MT nuclear attack on, physical, 20: 2078 (BNL-917, pp 1-10)
**NORTH CAROLINA RESEARCH REACTOR**
neutron spectra from, measurement using Fermi chopper, 20: 2994
**NORWAY**
fallout monitoring, 1961 to 1964, 20: 2054
**NPD REACTOR**
control system for, 20: 3533
fuel elements from, inspection of, 20: 3496
**NRX REACTOR**
fuel burnup in, computer program for calculating, 20: 3583 (CRT-1187 B)
fuel irradiation testing in, 20: 2429 (ORNL-3837)
**NUCLEAR BATTERIES**
design using solar cells with promethium-147 beta sources, 20: 2206
**NUCLEAR CHEMISTRY**
radioisotope decay measurements in multidimensional pulse analyser use in, 20: 2142
**NUCLEAR EMULSIONS**
argon-ion scattering in, particle-track production and momentum transfer in, (E), 20: 3063
mesons ($K^-$) reactions at 800 Mev/c with, computer analysis of, 20: 2520(R) (IA-920)
particle scattering in, non-planarity effects in spurious, (E), 20: 2145
preparation and properties of, 20: 2158
proton reactions at 9 Bev with heavy nuclei in, with large energy transfer, (E), 20: 3047
**NUCLEAR HEATING PLANTS**
coolant purification in boiling-water, BWR, survey of ion-exchange methods for, 20: 3539 (ACNP-65558(Rev.1))
turbines for dual-purpose, flexibility of back-pressure, 20: 3540 (ACNP-65573)
**NUCLEAR MAGNETIC RESONANCE**
book: *Nuclear Magnetic Resonance and Relaxation in Solids*, 20: 3316
energy levels and line intensities of NQR, in single crystals, (T), 20: 3284
spectra of, computer programs for analysis of, 20: 3645 (UCRL-16344)
spectral analysis of, performance of double-resonance spectrometer for, 20: 2109
use for measurement of homogeneous and inhomogeneous magnetic fields, (E), 20: 2112
**NUCLEAR MATERIALS MANAGEMENT**
criticality control and safety of fissionable materials, 20: 2095
criticality studies for fuel element handling and storage, 20: 3379 (ORNL-TM-1207)
gamma counting of unirradiated fuel elements, 20: 3464
procedures for Berkeley and Bradwell fuels, 20: 3530
reactor fuel inventory and control, 20: 3536
**NUCLEAR MODELS**
book: *Les Modeles en Spectroscopie Nucleaire*, 20: 3139
book: *Nuclear Structure and Electromagnetic Interactions*, 20: 3147
properties, 20: 3149
use for constructing wave functions and testing electromagnetic properties of nuclei, 20: 3148
validity of Thomas-Fermi, 20: 2819
**NUCLEAR MODELS (OPTICAL)**
potential for excited states in, using Fermi gas model, 20: 3116
use in analysis of deuteron elastic scattering, (E/T), 20: 3053

**NUCLEAR MODELS (SHELL)**
generalized quasi-spin in neutron-proton systems, 20: 3046
properties, 20: 3149
**NUCLEAR PHYSICS**
data processing system using digital computer, 20: 2996
research at Frascati, 20: 2521 (LNF-65/28)
research programs on, at Risö, Denmark, 20: 3646
terminology, 20: 3096
**NUCLEAR POWER**
development of, United States program for, 20: 3492
uses of, college course on, 20: 3329
**NUCLEAR POWER PLANTS**
control system and instrumentation for Czechoslovakian A 1, 20: 3534
control system for, having two load medium circuits, 20: 3357(P)
control systems for Canadian, 20: 3533
coolant purification in boiling-water, BWR, survey of ion-exchange methods for, 20: 3539 (ACNP-65558(Rev.1))
design study of fission-electric cell-reactor, 20: 3577
insulation problems for, materials and techniques for, 20: 3487
startup conditions of Beloyarsk, 20: 3486
turbine design and performance for, closed-cycle gas, 20: 3343
turbines for dual-purpose, flexibility of back-pressure, 20: 3540 (ACNP-65573)
**NUCLEAR REACTIONS**
angular distribution of fragments from, at 76 Mev to 25 Bev, (T), 20: 3111
book: *Nuclear Structure and Electromagnetic Interactions*, 20: 3147
of beryllium, bibliography, 20: 3007 (CEA-Bib-32)
photo-, analysis of, 20: 3151
radiative transitions from, 20: 3150
selection rules for, nucleon associations in SU(3) scheme for, 20: 3117
theory for deuteron stripping, 20: 3070
theory of polarization in direct, semiclassical, 20: 3049
**NUCLEAR SHOWERS**
distributions in 1- to 3-Bev proton-produced, (E), 20: 3015 (NASA-SP-71, pp 357-62)
**NUCLEAR SPECTRA**
book: *Les Modeles en Spectroscopic Nucleaire*, 20: 3139
rotational, at high momenta, 20: 3103
**NUCLEAR STRUCTURE**
book: *Les Modeles en Spectroscopic Nucleaire*, 20: 3139
book: *Nuclear Structure and Electromagnetic Interactions*, 20: 3147
determination using polarized nucleon elastic scattering, 20: 3014 (LA-DC-7386)
isomer shift and structure of metastable nuclear states, 20: 3138
**NUCLEAR THEORY**
generalized quasi-spin in neutron–proton systems, 20: 3046
Green functions and transition probabilities in odd nuclei, 20: 3104
isomer shift and structure of metastable nuclear states, 20: 3138
nuclear masses and interaction amplitudes in, relation between, 20: 3102
of deuteron elastic scattering by complex nuclei at high energies, 20: 3044
quantum, of nuclear collective rotation, 20: 3048
single-particle excitations in, model hamiltonians for, 20: 3099
single-particle 1-forbidden transitions in, 20: 3100
**NUCLEI**
beta decay of, allowed and forbidden transitions in, (T), 20: 3090
beta decay of, interacting quasiparticle method for, (T), 20: 3101
charged-particle reactions in Coulomb field of, (T), 20: 3153
deuteron elastic scattering by complex, at high energies, (T), 20: 3044
deuteron reactions (d,p) with N = 88 to 90, effect of deformation change on cross sections for, 20: 3125
deuteron reactions at low energies, formalism for stripping, (T), 20: 3070
deuteron scattering by nonspherical, (T), 20: 3026
electromagnetic form factors of three-nucleon, (T), 20: 3119
electromagnetic properties of nuclear models and wave functions for, 20: 3148
electron elastic scattering at high and low energies, phase shifts for, (T), 20: 2635
electron inelastic scattering by, amplitude for, (T), 20: 3124
electron scattering by, (T), 20: 3152
elementary particle scattering by, polarization-asymmetry in spin-flip inelastic, (T), 20: 3076
energy levels of, capture gamma detection of, (E), 20: 2520(R) (IA-920)
energy levels of, random phase approximation for ground-state, (T), 20: 3085
energy levels with hard core interaction with neutron excess, ground-state, (T), 20: 3079
energy states of deformed, large-spin rotational, (E/T), 20: 3008 (COO-1420-104)
generalized quasi-spin in neutron–proton systems, 20: 3046
helium-3 reactions (He-3,n) with light, angular distributions in direct, (T), 20: 3121
magnetic moments of spherical, corrections to equation for, 20: 3118
mass relations between, beta-transition frequencies for, 20: 3102
meson ($K^-$) reactions with emulsion, at 5 Bev/c, hyperfragment and lithium-8 production in, (E), 20: 3062
meson ($K^-$) reactions with emulsion, $Y_0^0$ production in capture, (E), 20: 3064
models for, 20: 3149
neutron binding energies in N = 86 to 92, 20: 3098
neutron cross sections of, tabulations, (E), 20: 3018 (NYO-72-27)
neutron inelastic scattering at high energies, direct-interaction, (T) 20: 3256
neutron scattering by polarized, in external magnetic field, (T), 20: 3120
nucleon elastic scattering below 50 Mev, data survey for polarized, 20: 3014 (LA-DC-7386)
nucleon interaction potentials in, shell model calculations for, (T), 20: 3068
nucleon pairing correlation at high momenta, 20: 3103
nucleon pairing forces in, (T), 20: 3066
nucleon reactions at high energies, nucleon production in, 20: 3259
nucleus inelastic scattering by, collective levels from, (T), 20: 3013 (JINR-P-2331)
optical potential for excited states of, Fermi gas model for, 20: 3116
photon reactions with, analysis of, 20: 3151
quadrupole charges and E2 transition probabilities of, (T), 20: 3115
radiative dipole transitions in heated, energy dependence of width of, (T), 20: 3114
radiative transitions of, probability of electric multipole relativistic, (T), 20: 3026
single-particle excitations in, model hamiltonians for, 20: 3099
transition probabilities in odd, Green functions and, 20: 3104
transitions in, single-particle 1-forbidden, 20: 3100
triton reactions (t,p) with light, angular distributions in direct, (T), 20: 3121
**NUCLEI (CELLS)**
radiation effects on morphology of lymphocyte, 20: 1612 (EUR-2505.e)
radiation effects on phosphorylation in tumor, x, 20: 1626
volume of, effects on radiosensitivity of plant cells, 20: 1610 (BNL-9611)
**NUCLEIC ACIDS**
radiation effects on plant metabolism of, 20: 1648
radioinduced radicals in dry, ESR of gamma and x, 20: 1623
**NUCLEON SHOWERS**
production in proton reactions with iron at 1 and 3 Bev, (T), 20: 3258
**NUCLEONS**
interaction potentials in nuclei, shell model calculations for, (T), 20: 3068
interactions with gamma rays, meson ($\pi$) production amplitude from, (T), 20: 2695
interactions with mesons ($\pi$) at 0 to 20 Bev, data review for, 20: 2725
interactions with nucleons, one-boson-exchange model for, (T), 20: 2726
interactions with gamma radiation at 165 to 230 Mev, amplitude and cross sections for meson ($\pi^+$) production, (E/T), 20: 2737
magnetic moments of, self-consistent calculation of isovector part of, 20: 2704
pairing forces in nuclei, (T), 20: 3066
production in nucleon reactions with nuclei at high energies, cross sections for, 20: 3259
scattering by complex nuclei below 50 Mev, data survey for elastic polarized, 20: 3014 (LA-DC-7386)
scattering by nitrogen-14, differential cross section and polarization for, (T), 20: 3091
spectra from proton reactions with elements at 160 and 450 Mev, (T), 20: 3260


## O


**OATS**
radioinduced mutations of, 20: 1665
**OBRIGHEIM POWER REACTOR** (*Germany*)
design and operational characteristics of, 20: 3489
development and characteristics of, 20: 3488
**OCEANOGRAPHY**
air–water interface oscillations, eddy diffusion, and water movement in, use of cobalt-60 for measurement, 20: 2061
**ODOR**
radiation effects on wine, effects of dose on, 20: 2197
**OHMMETERS**
design of high-resistance, with radioactive current generator, 20: 2108
**OILS**
analysis in crime detection, activation, 20: 1740(R) (GA-4576)
analysis in crime detection, activation, 20: 1739(R) (GA-4297)
**ONTARIO**
lead isotope ratios in galenas in, 20: 2051
**OPTICAL SYSTEMS**
design of stereoscopic framing-camera techniques, (E), 20: 3624 (LA-DC-7088)

design of 1.5- to 3000-μsec shutters for spectrographs, (E), 20: 2125 (CEA-R-2816)
use in dimensional location of reactor components, 20: 3341
**ORES**
analysis for rare earths, activation, 20: 2056
analysis for uranium by colorimetric method, 20: 1794
composition of, radiometric well logging method for studying, 20: 2063
**ORGANIC COMPOUNDS**
hydrogenation of, tracer studies of product contamination by nickel catalyst in, 20: 1889
radiation chemistry, 20: 1918
radiation effects on, compilation of projects on, 20: 2433 (REIC-Memo-27)
spectra of four-membered ring, computer programs for analysis of NMR, 20: 3645 (UCRL-16344)
**ORGANIC COMPOUNDS, METALLO-**
uses in plastic scintillators for detection and resolution of gamma rays, 20: 1905
**ORGANIC COOLED REACTORS**
design of 50-Mw(t) tank-type organic moderated, 20: 3440 (RT/ING(65)16)
**ORGANIC MODERATED REACTORS**
design of 50-Mw(t) tank-type organic cooled, 20: 3440 (RT/ING(65)16)
**ORGANISMS**
radiation effects on living, bibliography, 20: 1608 (AED-C-04-19)
**ORNL HIGH FLUX ISOTOPE REACTOR**
accidents in, methyl iodide release and sorption in maximum credible, 20: 3586 (ORNL-TM-1291)
control rod systems for, 20: 3543
filter system for, efficiency of charcoal, 20: 3586 (ORNL-TM-1291)
target element fabrication for, 20: 2282 (HW-SA-3755)
**OSMIUM ALLOY COUPLES**
Cr–Os/Re–W, thermoelectric properties at 200 to 1800°C, 20: 2223(R) (GEMP-51A)
Mo–Os–Ru/Re–W, thermoelectric properties at 100 to 1400°C, 20: 2223(R) (GEMP-51A)
**OXALIC ACID**
corrosive effects on molybdenum and vanadium, stress-, 20: 2254 (BM-RI-6680)
**OXYGEN**
determination by activation methods using automated equipment, 20: 1765
determination in helium at reduced sample pressures by gas chromatography, 20: 1751
determination in liquid potassium by gettering-vacuum fusion method, 20: 2367
determination in potassium–sodium and sodium, engineering drawings of sodium sampler design for, 20: 1799
determination in silicon, activation, 20: 2531 (AD-618304)
determination of, factors affecting continuous on line, 20: 1734 (EG-Report-36)
distribution between zirconium and liquid potassium at 815°C, 20: 2367
distribution in metals, determination by helium-3 activation, 20: 2227
effects of inhaled, on radiosensitivity of tumors in mice, 20: 1683
effects of internal, on mechanical properties of silver and its alloys, 20: 3639 (UCRL-11194)
effects on niobium–vanadium corrosion by lithium, 20: 2340 (ORNL-TM-1131)
effects on radioinduced chromosome aberrations in stored seed, 20: 1638
effects on radioinduced inactivation of ribonuclease, 20: 1682
effects on radioinduced oxidation of graphite in carbon dioxide, 20: 1895 (AERE-R-4988)
effects on rupture of type 316 stainless steel of, in sodium, 20: 2258(R) (MSAR-65-149)
effects on solubility of hydrogen in zirconium at 800°C, 20: 2267
effects on strain-aging process in commercially pure niobium, 20: 2376
electron elastic scattering by atomic, slow, (T), 20: 2617
oxidation of tungsten, kinetics of, 20: 2261(R) (UCRI-326)
reactions with beryllium in simulated launch pad abort environments at 800 to 1500°C, 20: 2341 (SC-DC-65-1637)
reactions with oxygen ion O⁻, radiolysis measurement of rate constant for, 20: 1917
O–propane, temperature in MHD cell, (E), 20: 2673
**OXYGEN FLUORIDES**
radioinduced in liquid carbon tetrafluoride in presence of oxygen, electron spin resonance spectrum of, 20: 1898(R) (RRL-2310-164)
**OXYGEN IONS**
ionization of nitrogen by 25- to 50-kev, total, (E), 20: 2623
reactions of negative monatomic and positive monatomic and diatomic, with molybdenum, secondary electrons from, (E), 20: 2628
reactions with argon, nitrogen, and helium at 0.14 to 0.7 Mev, energy loss in, (E), 20: 2602
reactions with oxygen, radiolysis measurement of rate constant for, 20: 1917
**OXYGEN ISOTOPES O-15**
energy levels of, decay schemes for, (E), 20: 3006 (AD-613676)
energy levels of, from oxygen-16 giant dipole resonance de-excitation, (E), 20: 3074
**OXYGEN ISOTOPES O-16**
alpha elastic scattering at 41.9 to 49.7 Mev, backward, (E), 20: 3056
bremsstrahlung reactions (γ,t) at 50 Mev, yield in, (E), 20: 3126
content in carbonates deposited by algae and corals in Jamaican waters, 20: 1591
deuteron reactions (d,p) with, lifetimes of oxygen-17 levels from, (E), 20: 3156
gamma reactions (γ,p) at 21.3 to 43.7 Mev, cross sections for, (E), 20: 3107
gamma reactions (γ,n) and (γ,p) giant dipole resonance from, (E), 20: 3074
lithium-6 reactions (Li-6,d), selection rules for, (T), 20: 3117
particle reactions with, selection rules for alpha-knockout, (T), 20: 3117
triton reactions (t,p), angular distributions from, (T), 20: 3121
**OXYGEN ISOTOPES O-17**
deuteron reactions (d,p) at 5.56 Mev, Q values and proton angular distributions for, (E), 20: 3052
energy levels from deuteron reactions (d,p) with oxygen-16, lifetimes of, (E), 20: 3156
energy-level transition probabilities of, E2, (T), 20: 3115
**OXYGEN ISOTOPES O-18**
alpha reactions (α,n), neutron spectra from, 20: 2520(R) (IA-920)
content in carbonates deposited by algae and corals in Jamaican waters, 20: 1591
deuteron reactions (d,p) with, lifetimes of oxygen-19 levels from, (E), 20: 3156
deuteron reactions (d,p) at 5.56 Mev, Q values and proton angular distributions for, (E), 20: 3052
energy levels from stripping reactions, (E), 20: 3052
**OXYGEN ISOTOPES O-19**
energy levels from deuteron reactions (d,p) with oxygen-18, lifetimes of, (E), 20: 3156
energy levels from stripping reactions, (E), 20: 3052
**OXYGEN SYSTEMS**
acetylene–O, engineering drawings of spectrophotometer burner design using, 20: 1798
CO–O, combustion of beryllium in flame system of, 20: 2341 (SC-DC-65-1637)
H–O, combustion of beryllium in flame system of, 20: 2341 (SC-DC-65-1637)
Mo–O, phase diagrams, 20: 1880
O–Re, phase diagrams, 20: 1880
**OZONE**
handling of, 20: 1727 (NASA-SP-5032)
toxicity of, 20: 1727 (NASA-SP-5032)

# P

**PACIFIC OCEAN**
seismic data collection and analysis in, near Hawaii, 20: 2058(R) (NVO-98-10)
**PACKAGE POWER REACTORS**
economics for canal construction, 20: 3481 (SC-RR-65-121A)
**PACKAGING**
materials for, molding epoxy, 20: 3634 (SC-TM-65-462)
**PAINTS**
analysis in crime detection, activation, 20: 1740(R) (GA-4576)
analysis in crime detection, activation, 20: 1738(R) (GA-4041)
development of self-luminous, 20: 2520(R) (IA-920)
**PALLADIUM ISOTOPES Pd-104**
gamma transition at 555.4 kev following Coulomb excitation, (E), 20: 3043
**PALLADIUM ISOTOPES Pd-106**
gamma transition at 511.7 kev following Coulomb excitation, (E), 20: 3043
**PALLADIUM ISOTOPES Pd-108**
gamma transition at 433.9 kev following Coulomb excitation, (E), 20: 3043
**PALLADIUM ISOTOPES Pd-110**
gamma transition at 373.8 kev following Coulomb excitation, (E), 20: 3043
**PAPER**
analysis in crime detection, activation, 20: 1738(R) (GA-4041)
**PARAFFIN**
neutron angular distribution and spectra in, (E), 20: 2931 (AD-616518)
neutron spectra in, fast, (E/T), 20: 3257
neutron spectra in cooled, thermal, (E), 20: 2945
**PARTICLE STATISTICS**
statistical mechanics of a system of quasiparticles, (T), 20: 2843
**PARTICLE TRACKS**
determination in spark chambers, using symmetric wire electrodes, 20: 2129 (JINR-P-2312)

**PARTICLES**
diffusion in atmosphere, tests on, 20: 2073(R) (AD-618101)
radiation hazards from uranium carbide, 20: 1694
radioactivity and size of, in fallout, 20: 2053
size and transport in atmosphere from nuclear explosions, use as meteorological tracers, 20: 2044 (NDRE-51)
size distributions from destruct tests of ROVER fuel elements, 20: 3574
**PATENTS**
abstracts of, on production of heavy water, 20: 1951 (AECL-2279)
**PEBBLE BED REACTOR EXPERIMENT (ORNL)**
fuel elements for, irradiation testing of, 20: 2464
**PENTANE, 2-METHYL-**
recoil reactions of carbon-11 in liquid, 20: 1896 (IS-T-23)
**PENTANE, 3-METHYL-**
recoil reactions of carbon-11 in liquid, 20: 1896 (IS-T-23)
**2,4-PENTANEDIOL**
2-methyl-, yields in gamma radiolysis of, 20: 1901
**2,4-PENTANEDIONE**
yields in gamma radiolysis of liquid acetone, 20: 1901
**PENTANES**
recoil reactions of carbon-11 in liquid, 20: 1896 (IS-T-23)
**2-PENTANOL, 4-METHYL-**
solvent properties for polonium chloride, 20: 1946
**2-PENTANONE**
4-hydroxy-4-methyl-, yields in gamma radiolysis of liquid acetone, 20: 1901
**2-PENTANONE, 4-METHYL-**
solvent properties for fission products, protactinium, thorium, and uranium, 20: 1759
**PEPTIDES**
spectra of iron(III) ions in polycrystalline Ferrichrome A, paramagnetic resonance, 20: 3643 (UCRL-11685)
**PERCHLORIC ACID**
separation by solvent extraction using tridodecylamine, effects of aromatic diluents on, 20: 1747 (UCRL-11616(Rev.))
**PERFLUOROORGANIC COMPOUNDS**
radiolysis of, separation of molecular fluorine by, 20: 1899(T) (BNL-tr-23)
**PERMEABILITY**
measurement of porous barrier, 20: 2120(P)
**PEROXIDASES**
radiation effects on horse-radish, 20: 2520(R) (IA-920)
**PEROXIDES**
sulfur fluoride, effects of water on preparation of, 20: 1881
**PERRHENIC ACID**
separation by solvent extraction using tridodecylamine, effects of aromatic diluents on, 20: 1747 (UCRL-11616(Rev.))
**PERSONNEL**
cosmic radiation effects on, in high-altitude aircraft, 20: 2657 (NASA-SP-71, pp 287-99)
protection against protons, spherical shields for, (T), 20: 3243 (NASA-SP-71, pp 229-34)
radiation protection of, in alpha laboratories, 20: 2089
radiation protection of, aboard space vehicles, (T), 20: 3245 (NASA-SP-71, pp 407-14)
radiation protection of spacecraft, against solar flares, (T), 20: 3251 (NASA-SP-71, pp 507-12)
**PERTURBATION THEORY**
formalism for sudden and time-independent, for scattering, (T), 20: 2776
general time-dependent, for reactor physics, 20: 3436
use in solution of neutron transport equation for critical slab, 20: 3423
use in weight optimization of reactor shielding, 20: 3346
use of time-dependent, in nonlinear reactor kinetics problems, 20: 3413
**PHARMACEUTICALS**
radiation effects on, 20: 1918
radiosterilization, 20: 1918
**PHASE STUDIES**
thermodynamic properties of physico-chemical systems during phase transitions, methods for estimating, 20: 1819 (UCRL-14287)
**PHONONS**
dispersion relations in aluminum, Fermi surface structure from, (E), 20: 3303
interactions with phonons in graphite, 20: 2387
motion of, equations for, (T), 20: 2883
**PHOSPHATE GLASS**
radiation dosimetry with, reading device for use in, 20: 2181(P)
use of silver-activated, in low dose measurements, 20: 2122 (AD-622626)
waste fixation in, 20: 3606
**PHOSPHATES**
radiation effects on metabolism of, in nuclei of tumor cells, x, 20: 1626
**PHOSPHATIDES**
determination on paper chromatograms by activation, 20: 1771
**PHOSPHONIUM COMPOUNDS**
solvent properties for uranium, effects of 8-hydroxyquinoline on, 20: 1782
**PHOSPHORIC ACID**
corrosive effects on vanadium, stress-, 20: 2254 (BM-RI-6680)
**PHOSPHORIC ACID, BIS(2-ETHYLHEXYL) ESTERS**
solvent properties for americium, 20: 2520(R) (IA-920)
**PHOSPHORIC ACID, ESTERS**
production by alcohol-phosphoric pentoxide reactions, 20: 2520(R) (IA-920)
**PHOSPHORS**
efficiency of polycrystalline, for high-energy electrons, 20: 2164
energy transfer to liquid, by beta particles, 20: 2189
reflector for plastic, optical properties of titanium dioxide for use as, 20: 2327 (IKF-12)
response of lithium fluoride, to reactor gammas and thermal neutrons, 20: 2178
uses of lead- and tin-loaded liquid and plastic, for detection and resolution of gamma rays, 20: 1905
**PHOSPHORUS ISOTOPES P-31**
energy-level transition probabilities of, E2, (T), 20: 3115
**PHOSPHORUS ISOTOPES P-32**
production in chlorine-35 (n,$\alpha$) and sulfur-32 (n,p) reactions, (E), 20: 3020 (ORNL-TM-1065)
**PHOSPHORUS ISOTOPES P-33**
production in chlorine-36 (n,$\alpha$) and sulfur-33 (n,p) reactions, (E), 20: 3020 (ORNL-TM-1065)
**PHOSPHORUS OXIDES**
reactions with alcohols, products from, 20: 2520(R) (IA-920)
testing for use in shaft seals for potassium space power systems, 20: 2242
$P_2O_5$–$V_2O_3$, electric conductivity of glass systems of, 20: 2316 (COO-1198-220)
$P_2O_5$–$V_2O_5$, electric conductivity of glass systems of, 20: 2316 (COO-1198-220)
**PHOSPHORUS SELENIDES**
thermal capacity and thermodynamic properties of tetraphosphorus triselenide at 5 to 350°K, 20: 3617 (COO-1149-23)
**PHOSPHORUS SULFIDES**
thermal capacities and thermodynamic properties of tetraphosphorus deca- and trisulfides at 5 to 350°K, 20: 3617 (COO-1149-23)
**PHOTOCONDUCTIVITY**
of diamonds, radiation effects on, 20: 2520(R) (IA-920)
**PHOTOELECTRIC EFFECT**
in semiconducting diamonds, 20: 2520(R) (IA-920)
**PHOTOGRAPHIC FILM**
development for photoscanning, 20: 1705
scanning of spark chamber, semiautomatic device for, 20: 2130 (JINR-P-2340)
**PHOTOGRAPHIC FILM DETECTORS**
performance of, for dosimetry of high-energy electrons, 20: 2156
**PHOTOGRAPHY**
design of stereoscopic framing-camera techniques, (E), 20: 3624 (LA-DC-7088)
methods for measuring surface contours of small samples, 20: 2033
**PHOTOMETRY**
use of sodium flame, in testing high-efficiency filters, 20: 2077 (AWRE-O-41/65)
**PHOTONS**
acceleration in turbulent plasma, statistical, (T), 20: 3199
emission from plasma, statistical fluctuations in, (T), 20: 2828
emission in decay of helium ion metastable state, 20: 2630
emission in hyperon ($\Omega^-$) decay, SU(6) symmetry for, 20: 2738
interactions with protons, meson ($\rho^0$) production in, 20: 2747
interactions with baryons, electromagnetic amplitudes for meson production in, (T), 20: 2732
motion of, equations for, (T), 20: 2883
reactions ($\gamma,\pi^0$) with hydrogen at 500 to 1000 Mev, proton polarization in, 20: 2679 (AD-618664)
reactions with nuclei, analysis of, 20: 3151
transport of, bouncing in, (T), 20: 2870
**PHOTOSENSITIVITY**
of ultraviolet-irradiated virus ribonucleic acid, 20: 1659
**PHYSICAL CHEMISTRY**
methods for estimating thermodynamic properties of systems during phase transitions, 20: 1819 (UCRL-14287)
**PHYSICS**
book: *Applications of Nonlinear Partial Differential Equations in Mathematical Physics*, 20: 2530
research activities at Department of General and Applied Sciences, USSR, 20: 2524(T) (NP-tr-1292(Draft))
research in solid state, use of high magnetic fields in, 20: 2519(R) (AD-615152)
**PHYSIOLOGY**
function, effects of age in man, 20: 1587

of equilibrium by auditory organ, 20: 1628(T)
**PICKERING POWER REACTOR**
control system design for, 20: 3533
**PICOLINES**
reactions with carbon-14 and tritium recoil atoms, stability and yields in, 20: 1921
**PIGMENTS**
radiation effects on free radical properties of melanin, ESR study of uv, 20: 1684
**PINACOL**
yields in gamma radiolysis of liquid acetone, 20: 1901
**PINCH DEVICES**
electrostatic screening in theta, shield design, (T), 20: 3190
**PIPERAZINE**
deamination of, effects of iodides on, 20: 2520(R) (IA-920)
**PIPES**
pressure drop in, with shrouds, 20: 2010 (IPV-19)
**PITUITARY GLAND**
radiotherapy of tumors of, 20: 1708
**PITUITARY HORMONES**
radiation effects on distribution and synthesis of, 20: 1671
**PLACENTA**
iodine-131 metabolism in human, 20: 1600
**PLANT CELLS**
effects of meson ($\pi^-$) beam on, biological, 20: 1621 (UCRL-16387)
radiosensitivity of flower and root, in Tradescantia, 20: 1668
radiosensitivity of *Marchantia polymorpha*, effects of chromosome and nucleus volumes on, 20: 1610 (BNL-9611)
**PLANTS**
electric properties of tissues of bamboo, 20: 3625(R) (NYO-3282-1)
radiation effects on, bibliography, 20: 1607 (AED-C-04-18)
radiation effects on, bibliography, 20: 1608 (AED-C-04-19)
radiation effects on metabolism of nucleic acids in, 20: 1648
radiation effects on *Phaseolus mungo* by seed exposure, heat treatment effects on, 20: 1690
radiation effects on ecology of, thermal, 20: 2079 (BNL-917, pp 11-19)
radiation effects on ecology of, 20: 2080 (BNL-917, pp 20-36)
radioinduced chromosome aberrations in root cells of, 20: 1649
radiosensitivity of, effects of chromosome volume on, 20: 2080 (BNL-917, pp 20-36)
**PLASMA**
book: *Data for Plasmas in Local Thermodynamic Equilibrium*, 20: 3235
book: *Plasma Turbulence*, 20: 3236(T)
boundary layer with magnetic fields, effects of space charge convection on, (T), 20: 2856
bremsstrahlung intensity from, (T), 20: 3200
charged-particle motion in, momentum probe for measuring, 20: 3179 (ORNL-P-1575)
Cherenkov radiation from, effect on Landau damping of, 20: 3198
containment in QP machine, (E), 20: 3172(R) (NP-15562, pp 4-19)
containment in toroidal magnetic field with conducting diaphragm, 20: 3209
containment of hot-electron, in minimum-B and mirror fields, (E), 20: 3184 (UCRL-14310)
containment of slow ions in mirror trap in, with positive potential, (T), 20: 3227
containment of, design of Heliotron C for, 20: 3174(R) (NP-15562, pp 30-7)
containment of, stability of negative V systems for, (T), 20: 3167 (MATT-374)
current sheath in, boundary conditions for, (T), 20: 3165 (JINR-P-2352)
cyclotron wave propagation in, instabilities from oblique, (T), 20: 3181 (SU-IPR-20)
density of theta-pinch, gas laser interferometer measurement of, 20: 3173(R) (NP-15562, pp 20-9)
diagnostics of cesium-seeded argon, in MHD cells, (E), 20: 2671
diagnostics of, electron-photon scattering in, 20: 3232
diagnostics of, MACETIE Project on, (E), 20: 3173(R) (NP-15562, pp 20-9)
diagnostics of, microwave lens system for, 20: 3169 (NASA-CR-319)
diffusion and drift in magnetic fields, external electric field effects on, (T), 20: 2858
diffusion of neutral particles in, effect on population densities of excited hydrogen levels, (T), 20: 3223
distribution functions for, calculation of radial, (T), 20: 2830
electric dipole in column of warm, radiation characteristics of axially oriented, (T), 20: 3161 (AD-618520)
electric discharges between coaxial cylinders in, magnetic field effects on, 20: 3202
electric impedance at 40 to 300 Mc, instruments for measuring, (E), 20: 3094
electric probe resonance effects on, (E/T), 20: 3175(R) (NP-15562, pp 38-79)
electromagnetic surface waves on slab of, solution of equations for, 20: 3231
electromagnetic wave propagation in loaded waveguide, mode perturbation in, (E), 20: 3219
electron density in argon afterglow, microwave diagnostics of, (E), 20: 3193
electron density in, optical interferometric and spectroscopic measurements of, (E), 20: 3214
electron density measurement in, using laser-light scattering, 20: 3234
electron velocity distribution in nonisothermal, (T), 20: 3188
electron–electron instabilities in, growth rates for, (T), 20: 3182 (UCRL-12447)
electron–ion instabilities in, growth rates for, (T), 20: 3182 (UCRL-12447)
equation for collisionless sheath, cylindrical geometry solution for, 20: 3168 (ML-1185)
equations for quasineutral, magnetohydrodynamic, (T), 20: 3159 (AD-618138)
flow between cooled metal electrodes, (E), 20: 2672
flow in, single fluid theory of, 20: 3233
heating in two-phase radiofrequency system, 20: 3237
heating of hydrogen, laser-beam, (T), 20: 3185(T) (TT-1193)
hydromagnetic stability of superposed columns of, with anisotropic pressure, 20: 3224
hydromagnetic wave propagation in collisionless, instabilities in, (T), 20: 3176(R) (NP-15562, pp 80-4)
hydromagnetic wave instability in, higher order corrections to Alfven, (T), 20: 3221
injection into magnetic fields, effects of toroidal drift on transverse, (E), 20: 3205(T)
interactions with microwaves in gas discharges and semiconductors, (E/T), 20: 3157 (AD-614654)
interactions with runaway electrons, (E), 20: 3186
interactions with high-frequency electromagnetic field, MHD theory of stationary, 20: 3207
ion cyclotron resonance in low-density, (E), 20: 3172(R) (NP-15562, pp 4-19)
ion escape from magnetic mirror traps in, due to instability connected with loss cone, (T), 20: 3229
ion oscillations in discharge, 20: 3191
ionic sound waves in reflex discharge, 20: 3222
ionization phenomena in, nonequilibrium, 20: 3233
kinetic equation with relativistic interaction corrections for, (T), 20: 3218
kinetic equations for, Bogoliubov theory for pre-, 20: 3163 (CNAEM-26)
kinetics of ionospheric, from satellite motion, 20: 2863(T)
kinetics of unstable equation for, (T), 20: 3220
longitudinal waves in inhomogeneous, damping of, (T), 20: 3226
losses from ends of theta pinch, (T), 20: 3212
magnetostatic stability of, energy principles for, 20: 3211
microwave absorption in weakly ionized xenon, in magnetic fields, (E), 20: 3204
microwave frequency in sheath of, (E), 20: 2096 (AD-617928)
motion in rarefied, automodel, (T), 20: 3228
noise in magneto-, dynamic, (T), 20: 3194
oscillations of, research on, (E/T), 20: 3175(R) (NP-15562, pp 38-79)
particle acceleration by MHD waves in slightly turbulent rarefied, (T), 20: 3192
particle collision processes in, method for measuring, 20: 3158(R) (AD-614923)
particle distribution in cylindrical, in external longitudinal magnetic field, (T), 20: 3189
photon acceleration in turbulent, statistical, (T), 20: 3199
photon emission from, statistical fluctuations in, (T), 20: 2828
production by toroidal reflex discharge, electron density in, (E), 20: 3180 (SEL-63-116)
production of hydrogen, at 10 to 800 mtorr, crossed-fields, (E), 20: 3177 (NP-15570)
production of stable, methods for, 20: 3175(R) (NP-15562, pp 38-79)
properties in thermonuclear reactors, 20: 3196
pulse disturbances in one-dimensional diffusion, decay of, (T), 20: 3187
radiation from, anomalous bremsstrahlung and cyclotron, (E/T), 20: 3175(R) (NP-15562, pp 38-79)
radio transmission in layers of, (E/T), 20: 2098 (AD-618398)
research, (T), 20: 3176(R) (NP-15562, pp 80-4)
research in Japan, (E/T), 20: 3171(R) (NP-15562)
research on, use of high magnetic fields in, 20: 2519(R) (AD-615152)
research program on, 20: 3206
research programs on, at Risö, Denmark, 20: 3646
self-consistent equations including exchange and correlation effects for an electron gas, (T), 20: 3216
shock waves in cylindrical, ionizing, (T), 20: 3201
spectra of singly ionized nitrogen in helium–nitrogen, Stark profiles of, (E), 20: 3215

spectra of, theory of wing broadening of hydrogen Lyman $\alpha$ line by electrons and ions in, (T), 20: 3217
stability of dense anisotropic, with magnetically supported velocity-space, (T), 20: 3182 (UCRL-12447)
stability of dilute, in inhomogeneous electric field, 20: 3210
stability of gravitating, two-stream, (T), 20: 3170 (NASA-TN-D-3052)
stability of, drift cyclotron, 20: 3208
striations in argon h-f discharge, (E), 20: 3203
structure of, kinetic, (T), 20: 3164 (IPPJ-39)
use in fabrication of reactor fuel spheres, 20: 2288
wave detection and propagation along cylindrical antenna in warm, (T), 20: 2097 (AD-618396)
wave interactions in magnetoactive anisotropic, theory of nonlinear, 20: 3230
wave propagation along compressible slab of, slow surface, (T), 20: 3195

**PLASMA JETS**
design, 20: 2042(P)
design for deposition of high-melting metallic coatings, 20: 2251(P)
methane decomposition in hydrogen, acetylene production by, (T), 20: 3197
performance of cold-plasma induction, for space propulsion, 20: 2041
production by explosions, review of, 20: 3166 (LA-DC-7252)
use of d-c arc, as source of emission spectra, 20: 2649

**PLASTIC COATINGS**
radiation effects on, for spacecraft, 20: 2428 (NASA-SP-55, pp 365-79)

**PLASTIC-FILM DETECTORS**
performance of colored polyvinyl alcohol, for gamma and neutron dosimetry, 20: 2135

**PLASTICS**
analysis in crime detection of activation, 20: 1736(R) (GA-3491)
analysis in crime detection, activation, 20: 1737(R) (GA-3664)

**PLATES**
stability in hydraulically collapsed fuel assemblies, 20: 3459

**PLATINUM**
corrosion resistance to mercury at 900°F, 20: 2264
thermal conductivity at 300 to 1200°K, 20: 3621 (IS-1261)
thermal diffusion of, marker motion study, 20: 3628 (RPI-1044-1)

**PLATINUM ALLOYS**
Pt–Sn, tin-119 Mössbauer effect in intermetallic compounds of isomer shifts and quadrupole splittings from, (E), 20: 3290

**PLATINUM ISOTOPES Pt-195**
gamma transition following Coulomb excitation, (E), 20: 3043

**PLOWSHARE PROJECT**
excavation of sea-level Isthmian canal, plan for nuclear, 20: 1983 (PNE-2000)
excavation of sea-level Isthmian canal, design of nuclear explosions for, 20: 1984 (PNE-2001)
excavation of sea-level Isthmian canal, safety evaluation of nuclear, 20: 1985 (PNE-2003)
excavation of sea-level Isthmian canal, nuclear operations program for, 20: 1986 (PNE-2004)
seismic measurements of Dugout row-charge cratering experiment, 20: 1981 (PNE-605F)
surveillance of Handcar event, weather and radiological, 20: 1982 (PNE-607F)

**PLUTONIUM**
burnup and production in water moderated reactors, calculation methods for, 20: 3535
content in fallout, 20: 1602
criticality studies on lattices of metallic cylinders of, (E), 20: 2938 (UCRL-14245)
distribution in fuel rods for water-moderated reactors, optimization of, 20: 3457
distribution in reactor fuels, Monte Carlo calculations on optimum, 20: 3456
distribution in uranium dioxide fuel rods, 20: 2450
isotopic composition of, effects on fast reactor reactivity, 20: 2520(R) (IA-950)
neutron cross sections for, testing by criticality studies, 20: 3394
production by reduction of dioxide using magnesium–zinc alloy, 20: 2220 (ANL-7059)
properties as reactor fuels, 20: 3449
reactions with hydrogen peroxide in presence of different organic ligands, 20: 1857
reactions with tantalum at high temperatures, 20: 2228
recovery from spent fuels by pyrochemical processes, 20: 3320(R) (ANL-7082, pp 1-28)
recovery from spent fuels by fluidization and volatility processes, 20: 3321(R) (ANL-7082, pp 29-53)
retention in lungs of persons exposed to fallout, 20: 1602
separation from nitric acid solutions, effects of salting-out agents on, 20: 1967
strain hardening of alpha-, recovery from, 20: 2380
technology of, bibliography on, 20: 3611 (BNWL-113-8)
use in boiling-water reactors, 20: 3511

**PLUTONIUM ALLOYS**
desorption and sorption by silica gel, acidity effects on, 20: 1849
Ga–Fe–Pu, reactions with tantalum at high temperatures, 20: 2228
Ga–Pu, tensile properties of, at 20 to 100°C, 20: 2378
Ga–Pu, yield stress in, recovery of, 20: 2374
Mo–Pu–U, development and fabrication for ZPPR and ZRP-VI fuels, 20: 3320(R) (ANL-7082, pp 1-28)
Pu–Th–U, properties as fast power-breeder fuel, 20: 2230
Pu–Ti–U, corrosion by air, effects of exposure-time on, 20: 3320(R) (ANL-7082, pp 1-28)
Pu–Ti–U, properties as fast power-breeder fuels, 20: 2386
Pu–U–fissium, phase studies of, 20: 3493
Pu–U–Zr, compatibility with Hastelloy-X, Incoloy-800, and type-304 stainless steels, 20: 2229
Pu–U–Zr, properties as fast power-breeder fuels, 20: 2386
Pu–U–Zr, reactions with Hastelloy, Incoloy, and stainless steel at high temperatures, 20: 3320(R) (ANL-7082, pp 1-28)

**PLUTONIUM CARBIDES**
PuC–UC, fabrication into rods for irradiation testing, 20: 3320(R) (ANL-7082, pp 1-28)
PuC–UC, preparation methods, 20: 3321(R) (ANL-7082, pp 29-53)
PuC–UC, radiation effects on clad, at 510 to 650°C, 20: 3321(R) (ANL-7082, pp 29-53)

**PLUTONIUM COMPLEXES**
peroxide, thermodynamic stability, 20: 1857

**PLUTONIUM COMPOUNDS**
stability, 20: 1855

**PLUTONIUM(VI) FLUORIDES**
penetration through glove box filter system by accidental release, 20: 2076 (ANL-7068)

**PLUTONIUM HALIDES**
stability of complex trivalent, 20: 2520(R) (IA-920)

**PLUTONIUM IONS**
colloidal properties of, in dilute aqueous solutions, 20: 1835
spectra in lithium bromide solutions, absorption, 20: 2520(R) (IA-920)

**PLUTONIUM ISOTOPES Pu-238**
production in commercial power reactors, process for, 20: 2210

**PLUTONIUM ISOTOPES Pu-239**
criticality studies of homogeneous, 20: 3369 (CEA-R-2814)
determination in air, $\alpha$–$\beta$ pseudocoincidence method for, 20: 2151
deuteron fission reactions, angular anisotropy of, (E), 20: 3122
distribution in uranium dioxide fuel rods, 20: 2450
neutron capture-to-fission ratio, epicadmium, 20: 3321(R) (ANL-7082, pp 29-53)
neutron reactions (n,f), cross sections for resonance and thermal, (E), 20: 3031

**PLUTONIUM ISOTOPES Pu-241**
neutron capture-to-fission ratio, epicadmium, 20: 3321(R) (ANL-7082, pp 29-53)

**PLUTONIUM NITRATES**
criticality studies of spherical aqueous solutions of, 20: 3368 (BNWL-SA-214)
criticality studies of solutions of, in stainless steel spheres, 20: 3395

**PLUTONIUM(IV) NITRATES**
colloidal properties of, in citrate solutions, 20: 1835

**PLUTONIUM OXIDES**
$EuO_2$–$PuO_2$, phase studies by x-ray diffraction, 20: 2379

**PLUTONIUM(IV) OXIDES**
reduction to metal by magnesium–zinc alloy, 20: 2220 (ANL-7059)
solubility of ignited, methods for, 20: 2344 (TRG-Report-1072)
$PuO_2$–polystyrene, criticality studies on compacts of, 20: 3368 (BNWL-SA-214)
$PuO_2$–$UO_2$, fluorination of, facility for, 20: 3321(R) (ANL-7082, pp 29-53)
$PuO_2$–$UO_2$, fluorination in fluidized beds, 20: 1970
$PuO_2$–$UO_2$, in-pile thermal conductivity of stoichiometric and hypo-stoichiometric, 20: 2453
$PuO_2$–$UO_2$, irradiation testing of fuel elements in Plutonium Recycle Test Reactor, 20: 2449
$PuO_2$–$UO_2$, irradiation testing of vibrationally compacted fuel rods of, 20: 2461
$PuO_2$–$UO_2$, isotopic burnup analysis of, 20: 2454
$PuO_2$–$UO_2$, melting point of, 20: 2391
$PuO_2$–$UO_2$, performance as fuels in mixed-spectrum superheat reactors, (E/T), 20: 3471(R) (GEAP-4861)
$PuO_2$–$UO_2$, structure variations with burnup, 20: 2451
$PuO_2$–$UO_2$, testing as fast reactor fuel, 20: 2448
$PuO_2$–$UO_2$, thermocouples for temperature measurements on, 20: 2114
$PuO_2$–$UO_2$, transient performance of pre-irradiated, 20: 2469

**PLUTONIUM RECYCLE TEST REACTOR**
fuel element fabrication for, methods for, 20: 2282 (HW-SA-3755)

fuel element irradiation testing in, 20: 2449
**PLUTONIUM SYSTEMS**
Pu–$H_2O$, criticality of, effects of plutonium-240 concentrations on, 20: 3368 (BNWL-SA-214)
Pu–$H_2O$, criticality studies on, 20: 3368 (BNWL-SA-214)
**PNEUMATIC SYSTEMS**
design for transfer of irradiated samples, 20: 2520(R) (IA-920)
development of air springs, for instrumentation shipping, 20: 3613 (CONF-651016-1)
**POLARISCOPES**
design of scattered-light photoelastic instruments for nondescructive stress analyses, 20: 2026 (UCRL-13188)
**POLAROGRAPHY**
sensitivity of incremental derivative, 20: 1746 (TID-22199)
**POLARONS**
theory of, continuum, 20: 3277 (BLG-328)
**POLISHING**
mounting system for radioactive sample, 20: 2006(P)
**POLLEN**
radiation effects on maize, genetic, 20: 1656
radiation effects on, genetic, 20: 1622 (WT-820)
**POLONIUM**
separation from hydrochloric acid solutions, effects of acetone on, 20: 1777
**POLONIUM BROMIDES**
complexes with naphthalene, preparation of, 20: 1850
**POLONIUM CHLORIDES**
complexes with naphthalene, preparation of, 20: 1850
dissolution in anhydrous ketones and aqueous acetone solutions, complexing in, 20: 1946
**POLONIUM COMPLEXES**
formation in anhydrous ketone solutions, 20: 1946
with anisole, preparation of, 20: 1854
with naphthalene, preparation of, 20: 1850
**POLONIUM FLUORIDES**
complexes with naphthalene, preparation of, 20: 1850
**POLONIUM IODIDES**
complexes with naphthalene, preparation of, 20: 1850
**POLONIUM ISOTOPES Po-204**
alpha branching ratios for, 20: 3024 (UCRL-16324)
gamma spectra, (E), 20: 3024 (UCRL-16324)
**POLONIUM ISOTOPES Po-214**
determination on filters by scintillation counting, 20: 2520(R) (IA-920)
**POLYMERIZATION**
radioinduced, design of calorimeter for studying kinetics of, 20: 1904
**POLYMERS**
crystal structure of, determination of interplanar spacings using single-neutron diffraction, 20: 3308
light scattering by anisotropic discs of, polarization effects in, (T), 20: 1817 (TID-22323)
radiation effects on, compilation of projects on, 20: 2433 (REIC-Memo-27)
radioinduced formation of carbon-14-recoil-labeled, 20: 1922
**POLYPHENYL SYSTEMS**
radiolysis of Santowax WR, 20: 1927
**POLYPHENYLS**
separation by gas chromatography on lithium chloride columns, 20: 1745 (RT/CHI(65)-25)
solvent properties for mercury halides, 20: 2520(R) (IA-920)
**POPULATIONS**
physiological age tests for human, 20: 1587
radiation exposure of Soviet urban, background, 20: 2087
radioinduced mutations in heterogeneous Drosophila, 20: 1642
**POSITRON BEAMS**
interactions with electron and positron beams, theoretical aspects of, 20: 2687 (LNF-65/25)
**POSITRONIUM**
reactions with iron ions in various compounds, 20: 1844
**POSITRONS**
annihilation in lithium, (T), 20: 3314
interactions with electrons, meson pair production cross section for, (T), 20: 2753 (JINR-P-2300)
interactions with electrons, Coulomb Regge poles in, 20: 2782
production in antineutrino interactions with protons, spectra from, (E), 20: 2680 (COO-818-58)
**POTASSIUM**
analysis of liquid, for oxygen, by gettering-vacuum fusion method, 20: 2367
boiling detection in, tests of acoustic instrument for, 20: 2014 (ORNL-P-1678)
boiling in vertical tubes, pressure drop in forced-convection, (E/T), 20: 2015 (ORNL-P-1681)
collisions of atoms of, with rare gas atoms and hydrogen and nitrogen molecules, ionization in, (E), 20: 2639
compatibility with refractory metals at high temperatures, 20: 2236
corrosion resistance to mercury at 900°F, 20: 2264
corrosive effects on niobium–zirconium alloy at high temperatures, 20: 2268
corrosive effects on D-43 alloy, stress effects in, 20: 2270
corrosive effects on refractory alloys at high temperatures, 20: 2271
determination in drugs and tobacco, activation, 20: 1739(R) (GA-4297)
heat transfer and isothermal pressure drop for two phase flow of, 20: 2008(R) (AD-622825)
heat transfer in film boiling, 20: 2008(R) (AD-622825)
mass transfer of carbon and nitrogen by liquid, from type-316 stainless steel to niobium–zirconium alloy, 20: 2239
separation of trace elements from, by precipitation ion exchange, 20: 1958
solvent properties for oxygen at 815°C, 20: 2367
solvent properties of molten, for transition metals, 20: 2237
temperature in MHD cell, (E), 20: 2673
use as working fluid in nuclear power cycles, 20: 2013 (ORNL-P-1661)
**POTASSIUM ACID PHOSPHATES**
spectra of, infrared, 20: 2520(R) (IA-920)
**POTASSIUM ALLOYS**
K–Na, analysis for oxygen, 20: 1799
**POTASSIUM ASTATIDES**
entropy and thermal capacity at 0 to 300°K, 20: 1859
**POTASSIUM BROMIDES**
radiation effects on crystal structure of, mechanism of beta, 20: 2426 (LA-3387)
radioinduced $\alpha$ and F centers in, relative concentration variation of electron and x, (E), 20: 1919
**POTASSIUM CHLORIDES**
analysis for europium and ytterbium, polarographic, 20: 1795
radiation effects on crystal structure of, mechanism of beta, 20: 2426 (LA-3387)
$CaCl_2$–KCl, phase studies of, emanation-thermal method for, 20: 1860
KCl–NaCl–$YCl_3$, phase studies on, 20: 1872
KCl–NaCl, stability of zirconium dichloride in, 20: 1822(T) (ANL-Trans-233)
KCl–NaCl–$ZrCl_4$, stability of zirconium dichloride in, 20: 1822(T) (ANL-Trans-233)
LiCl–KCl, effects of molten, on thermodynamic properties of molybdenum(III) chloride, 20: 1882
LiCl–KCl–Zn–$ZnCl_2$, reactions of uranium monocarbide at 540 to 802°C in, 20: 2404
LiCl–KCl, stability of zirconium dichloride in, 20: 1822(T) (ANL-Trans-233)
$MgCl_2$–KCl, stability of zirconium dichloride in, 20: 1822(T) (ANL-Trans-233)
**POTASSIUM FERROCYANIDES**
iron-57 Mössbauer spectra from, (E), 20: 3296
**POTASSIUM FLUORIDES**
spectroscopy of, measurement of rotational transitions in, 20: 1876
**POTASSIUM HYDROXIDES**
methanol–KOH, solvent properties for tissues, 20: 1767
**POTASSIUM IODIDES**
diffusion of argon in monocrystals of, 20: 2317 (EURAEC-1380)
radiation effects on crystal structure of, mechanism of beta, 20: 2426 (LA-3387)
**POTASSIUM ISOTOPES K-39**
energy-level transition probabilities of, E2, (T), 20: 3115
**POTASSIUM ISOTOPES K-41**
energy levels from proton reactions (p,$\gamma$) with argon-40 at 1 to 3 Mev, isobaric, 20: 3036
magnetic moment, (T), 20: 3118
**POTASSIUM ISOTOPES K-42**
production by neutron irradiation of calcium-42 and scandium-45, cross sections for, 20: 1947
**POTASSIUM ISOTOPES K-43**
production by neutron irradiation of calcium-43, cross sections for, 20: 1947
**POTASSIUM NITRATES**
$LiNO_3$–$KNO_3$, solvent properties for water vapor, 20: 1812 (EUR-2495.e)
**POTASSIUM PHOSPHATES**
reactions with erbium and yttrium salts, 20: 1873
**POTASSIUM SYSTEMS**
K–Na, chemistry in experimental SNAP-8 reactor, 20: 3564
K–Na, corrosive effects on niobium–zirconium alloy and type-316 stainless steel, 20: 2273
$NH_3$–ethylamine–K, spectra of metal in, electron paramagnetic resonance and optical, 20: 1808 (COO-958-5)
**POWDERS**
use as heat transfer media in irradiation capsules, feasibility study, 20: 2018 (TRG-Report-920)

**POWER BREEDER REACTORS**
design of Soviet BN-350, 20: 3475 (NP-15458)
**POWER CYCLES**
instrumentation development for Rankine, 20: 2013 (ORNL-P-1661)
**POWER PLANTS**
control and instrumentation for, symposium on, 20: 2119
radiators for space, 20: 3556
**POWER REACTORS**
control system and instrumentation for Czechoslovakian A 1, 20: 3534
control systems for gas-cooled, (E), 20: 3480 (ORNL-P-1679)
cooling apparatus for liquid metal, design, 20: 3537(P)
design and development of SNAP-50/SPUR for lunar bases, 20: 3553
design of Fast Test Reactor, conceptual, 20: 3581 (BNWL-SA-340)
design using two fuels and two coolant temperatures, 20: 3538(P)
economics of superheat, 20: 3508
feasibility of mixed-spectrum steam-superheat, 20: 3471(R) (GEAP-4861)
fuel costs for, with uranium–thorium spherical fuel elements, 20: 3448
fuel cycle costs using crossed-progeny fuels, 20: 3512
fuel for Candu-type, economics of plutonium, 20: 3449
fuel management for, 20: 3536
fuel utilization in, economics of, 20: 3513
heat transfer in loss-of-coolant accidents, by natural convection, 20: 3515
neptunium-237 and plutonium-238 production in, process for, 20: 2210
performance of molten-salt breeder, 20: 3498
plutonium burnup and production in water-moderated, calculation methods for, 20: 3535
power excursions from high power levels, 20: 3507
safety of, effects of major disasters on, 20: 2520(R) (IA-920)
stability of natural-circulation boiling-water, hydrodynamic, 20: 3516
use of plutonium fuel in boiling-water, 20: 3511
**POWER SUPPLIES**
pumps for space Rankine-cycle, development of thermoelectromagnetic, (E), 20: 1988 (NAA-SR-11198)
**PRASEODYMIUM**
determination using Chromotrope 2B, photometric, 20: 1772
separation from thorium and other rare earths by ion exchange in ammonium thiocyanate–organic solvent–water systems, 20: 1959
**PRASEODYMIUM ACETATES**
complexes with thiourea, solubility in water, 20: 1869
**PRASEODYMIUM FLUORIDES**
preparation of tetravalent, 20: 2520(R) (IA-920)
**PRASEODYMIUM IONS**
spectra in praseodymium–neodymium-doped lanthanum fluoride, optical linewidth and line-shape studies of energy transfer mechanism in, (E), 20: 2627
**PRASEODYMIUM ISOTOPES Pr-143**
content in fallout particles, 20: 2053
**PRASEODYMIUM ISOTOPES Pr-144**
energy level spins from beta–gamma angular correlation, (E), 20: 3033
**PRASEODYMIUM NITRATES**
preparation of tetravalent, 20: 2520(R) (IA-920)
**PRASEODYMIUM OXIDES**
phase studies of, at 2200 to 2300°C, 20: 1827
**PRASEODYMIUM OXYBROMIDES**
preparation and crystal structure, 20: 1834
**PREGNANCY**
radiodiagnosis during, hazards to fetus and maternal gonads from, 20: 1689
**PRESSURE**
effects on radioinduced polymerization of solid trioxanes, 20: 1926
**PRESSURE DROP**
calculation for ducts and fuel elements with shrouds, 20: 2010 (IPV-19)
in forced- convection boiling of potassium in vertical tubes, (E/T), 20: 2015 (ORNL-P-1681)
in saturated vapor flowing in straight round tube, calculation of static, 20: 1814 (NAA-SR-6333)
**PRESSURE GAGES**
design for liquid metal systems, 20: 2013 (ORNL-P-1661)
**PRESSURE VESSELS**
design against brittle failure, fracture mechanics in, 20: 3345
design for submarine PWR, 20: 3578(P)
design of cylindrical prestressed concrete, 20: 3350(P)
development and testing for plutonium recycle reactors, 20: 3321(R) (ANL-7082, pp 29-53)
end wall for prestressed concrete, design of, 20: 3349(P)
failure mechanisms in reactor, 20: 2402
fracture mechanics in steel, for reactors, 20: 2401
materials, study of radiation sensitivity of A302B steel, 20: 2437 (WERL-8844-6)
radiation effects on A302B steel for, 20: 2455
radiation effects on materials for, review of, 20: 2479
support design for, 20: 3351(P)
testing of ERR, (E), 20: 3482(R) (SWRI-1228-75)
**PRESSURIZED WATER REACTORS**
coolant decompression studies for, analysis of, (E), 20: 3324(R) (IITRI-578P21-13)
design, 20: 3442(P)
design of submarine, with horizontal pressure vessel, 20: 3578(P)
fuel element performance in, 20: 2231
neutron flux monitoring in, self-powered detectors for, 20: 2174
pressure relief device for, 20: 3363(P)
properties of graphite moderated, 20: 3322 (EUR-2448.f)
xenon oscillations in, control of, (E/T), 20: 3383 (WCAP-3269-48)
**PROMETHIUM ISOTOPES Pm-141**
gamma transitions in, conversion coefficients for, (E), 20: 3038
**PROMETHIUM ISOTOPES Pm-147**
diffusion in sintered alumina, (E), 20: 2364
use in beta-voltaic batteries, 20: 2206
**PROPANE**
determination of, factors affecting continuous on line, 20: 1734 (EG-Report-36)
O–propane, temperature in MHD cell, (E), 20: 2673
**PROPANE, 1,3-DIBROMO-2,2-BIS(BROMOMETHYL)-**
thermodynamic properties of crystalline and liquid, above 290°K, 20: 3616 (COO-1149-22)
**PROPANE, 1,3-DICHLORO-2,2-BIS(CHLOROMETHYL)-**
thermodynamic properties of crystalline and liquid, above 290°K, 20: 3616 (COO-1149-22)
**PROPANE, 1,3-DIIODO-2,2-BIS(IODOMETHYL)-**
thermodynamic properties of crystalline, above 290°K, 20: 3616 (COO-1149-22)
**PROPANE, 2,2-DIMETHYL-**
$CCl_4$–2,2-dimethyl propane, thermal capacities and thermodynamic properties at 5 to 300°K, 20: 3619 (COO-1149-26)
$CCl_4$–2,2-dimethyl propane, thermodynamic properties at 5 to 300°K, 20: 3618 (COO-1149-25)
$CCl_4$–2,2-dimethyl propane, thermodynamic properties of, 20: 3620 (COO-1149-27)
**1-PROPANOL**
dehydration over thorium oxide catalyst, 20: 1892
radiolysis and storage of tritium-labeled, self-, 20: 1938 (EUR-2452.e)
**2-PROPANOL**
benzene–benzophenone–isopropanol, radiolysis of, energy transfer in, 20: 1931
dehydration over thorium oxide catalyst, 20: 1892
effects on pulse radiolysis of organic solutes, spectra of, 20: 1920
reactions with hydrogen, isotope effects in, 20: 2520(R) (IA-920)
yields in gamma radiolysis of liquid acetone, 20: 1901
**PROPENE**
effects on radiolysis of liquid methane, 20: 1898(R) (RRL-2310-164)
**PROPENE, HEXAFLUORO-**
radioinduced polymerization of, at low temperatures, 20: 1893(R) (AD-618228)
**PROPENE, 2-METHYL-**
radioinduced polymerization with formaldehyde, effects of dichloromethane and ethyl ether on, 20: 1914
radioinduced polymerization with tetrafluoroethylene at low temperatures, 20: 1915
**PROPIONIC ACID, PENTAPHENYL-, *t*-BUTYL ESTER**
decomposition of, deuterium effects on, 20: 1891
**PROPORTIONAL DETECTORS**
design and performance of $\alpha$–$\beta$ pseudocoincidence, for plutonium-239 monitoring, 20: 2151
development, 20: 2143
performance for determination of carbon-14 and hydrogen-3, 20: 1768
performance for 5-Mev alpha particles at small solid angles, 20: 2147
**PROPULSION**
radiation effects on systems for, compilation of projects on, 20: 2433 (REIC-Memo-27)
systems for radioisotope, effects of convection and radiation on heat transfer in, (E), 20: 2007 (AD-818026)
**PROTACTINIUM**
separation by solvent extraction using long chain amines, 20: 1761
separation from fission products, thorium, and uranium by solvent extraction using 4-methyl-2-pentanone, 20: 1759
separation from hydrochloric acid solutions by solvent extraction using neocupferron, 20: 1775
separation from thorium and uranium by solvent extraction using benzohydroxamic acid, 20: 1776
separation from thorium by solvent extraction using *N*-benzoylphenylhydroxylamine, 20: 1776
**PROTACTINIUM COMPOUNDS**
stability, 20: 1855
**PROTACTINIUM ISOTOPES Pa-231**
abundance ratio to uranium-235 in sandstone deposits in Gas Hills,

Wyoming, 20: 2057
**PROTACTINIUM ISOTOPES Pa-233**
determination in atmosphere, 20: 1759
**PROTACTINIUM OXIDES**
$EuO_2$–$PaO_2$, phase studies by x-ray diffraction, 20: 2379
**PROTEINS**
incorporation of iodine-125 and iodine-131 into, electrochemical, 20: 1939 (EUR-2476.i)
labeling with iodine-125, iodine-130, and iodine-131, computer programs for immunochemical studies using, 20: 1943
molecular weight of blood plasma Factor XII, 20: 1673
**PROTON BEAMS**
effects on enzymes, molecular weight estimations from, 20: 1673
pulse duration of JINR synchrocyclotron, increasing, (E/T), 20: 2548
storage rings for, phase locking systems for, (E), 20: 2535 (CERN-65-31)
use in radiotherapy of, review, 20: 1707
**PROTON PAIRS**
annihilation of polarized, cross section for lepton, (T), 20: 2696
**PROTON SHIELDING**
design of minimum-mass spherical, (T), 20: 3242 (NASA-SP-71, pp 225-8)
dose distributions behind cosmic-, (T), 20: 3251 (NASA-SP-71, pp 507-12)
dose quality factors for spherical, (T), 20: 3243 (NASA-SP-71, pp 229-34)
performance of, calculations of dose, energy, and flux variation factors for, (T), 20: 3250 (NASA-SP-71, pp 493-505)
performance with selective vehicle orientation, for protecting space vehicles from cosmic particles, 20: 3249 (NASA-SP-71, pp 473-6)
**PROTONS**
annihilation with antiprotons, cross sections for lepton-pair production in, (T), 20: 2696
dosimetry of, in tissues, 20: 1620 (UCRL-16154)
effects on algal, biological, 20: 1681
effects on biological systems, 20: 1707
effects on exciton spectrum of copper oxide, 20: 2505
effects on gallium arsenides, 20: 2501
effects on germanium and silicon at 20 to 130 Mev, 20: 2517
effects on impurity diffusion in silicon, 20: 2508
effects on man, pathological evaluation using fractional cell lethality calculations, 20: 1616 (NASA-SP-71, pp 219-23)
effects on mice and rats at 730 Mev, pathological, 20: 1614 (NASA-SP-71, pp 97-103)
effects on silicon at 0.7 Mev, 20: 2489
energy spectra and flux of geomagnetically trapped, (T), 20: 2849
interactions with antineutrinos, positron spectra from, (E), 20: 2680 (COO-818-58)
interactions with neutrons at 23 Mev, correlation function for, (T), 20: 2685 (LA-DC-7250)
interactions with mesons ($\pi^-$), analysis using bubble chambers, (T), 20: 2690(T) (AEC-tr-6591)
interactions with protons at 5.10 Bev, cross sections for inelastic, (T), 20: 2688 (UCRL-14336)
interactions with mesons ($\pi^-$), mesons ($\eta$) and neutrons from, (E), 20: 2689 (UCRL-16140)
interactions with protons, elastic differential cross sections for, (E), 20: 2520(R) (IA-920)
interactions with mesons ($\pi^+$), elastic differential cross sections for, (E), 20: 2520(R) (IA-920)
interactions with protons, diffraction patterns of inelastic, (E), 20: 2520(R) (IA-920)
interactions with mesons (K) and ($\pi^-$), triangular diagrams for cross sections of, (T), 20: 2741
interactions with mesons ($\pi^-$) at 2.26 Bev/c, resonances and final states in, 20: 2745
interactions with mesons ($\pi^-$) at 338 Mev, cross sections for, (E), 20: 2682 (JINR-P-2320)
interactions with mesons ($\pi^+$) at 4.1 and 4.85 Bev/c, cross sections for elastic, (E), 20: 2683 (JINR-P-2327)
interactions with electrons, Born approximation for elastic, (T), 20: 2686 (LNF-65/22)
interactions with neutrons at 20 to 120 Mev, polarization in, (E), 20: 2701
interactions with antiprotons, U(12) symmetry for annihilation into mesons in, 20: 2703
interactions with deuterons at 30 Mev, polarization in backward elastic, (E), 20: 2706
interactions with hyperons ($\Lambda$) and ($\Sigma^+$), effective-range and shape-dependent parameters for, (T), 20: 2707
interactions with mesons ($K^-$) at 0.8 to 1.2 Bev/c, Y*(1760) production and properties from, (E), 20: 2711
interactions with deuterons at 19.3 Bev/c, neutron-proton amplitude from, (E), 20: 2712
interactions with mesons ($\pi^+$), inelastic $S_{31}$ resonance in, (T), 20: 2716
interactions with mesons ($K^-$) at 6 Bev/c, hyperon ($\Omega^-$) production from, (E), 20: 2717
interactions with coherent bremsstrahlung at 1 Bev, meson ($\pi^+$) production from, (E), 20: 2718
interactions with mesons ($K^-$) meson ($\phi$) suppression in, (T), 20: 2719
interactions with mesons (K), strangeness conserving axial-vector coupling constant for, 20: 2722
interactions with hyperons ($\Sigma^-$) at rest, absorption time for, (E), 20: 2723
interactions with mesons ($K^-$) at 725 to 820 Mev/c, peak in cross sections for, (E), 20: 2724
interactions with neutrinos and antineutrinos at high energy, cross sections for meson ($\pi^\pm$) production in, (T), 20: 2733
interactions with gamma radiation, hyperon ($\Sigma^0$) and meson ($K^+$) production in, (E/T), 20: 2735
interactions with antineutrinos, cross section for ($\mu^+\gamma$) production in, (T), 20: 2736
interactions with neutrons at 19.3 Bev/c, amplitude for, (E/T), 20: 2712
interactions with mesons ($\pi^-$) at 1.5 and 1.8 Bev/c, $\kappa^0$(725) production from, (E), 20: 2715
interactions with meson ($\pi^-$) at 7.0 Bev/c, 20: 2746
interactions with photons, meson ($\rho^0$) production in, 20: 2747
interactions with protons at 2 to 10 Bev, peripheral model for isobar production in, (T), 20: 2817
ionization of nitrogen by 25- to 50-kev, total, (E), 20: 2623
magnetic moments of, self-consistent calculation of isovector part of, 20: 2704
mesic atom ($p\mu$) scattering by, (E), 20: 2640
polarization and spin relaxation rates in polystyrene at low temperatures, (E/T), 20: 3143
polarization in meson ($\pi^0$) photoproduction on hydrogen at 500 to 1000 Mev, (E), 20: 2679 (AD-618664)
polarization in rotating lanthanum magnesium nitrate crystal, dynamic, (E), 20: 3311
production of polarized targets of, (E), 20: 2686 (LNF-65/22)
reactions (p,$\alpha$) with nitrogen-15 at 3 to 12 Mev, direct-reaction analysis of angular distributions from, (E/T), 20: 3061
reactions (p,d) with helium-4, polarization effects in, (E/T), 20: 3023 (UCRL-16218)
reactions (p,$\gamma$) with aluminum-27, resonance widths in, (E), 20: 3142
reactions (p,$\gamma$) with argon-40 at 1 to 3 Mev, potassium-41 isobaric energy levels from, (E), 20: 3036
reactions (p,$\gamma$) with nitrogen-14 at 0.97 to 1.96 Mev, oxygen-15 production 20: 3006 (AD-613676)
reactions (p,n$\gamma$) with iron-58, cobalt-58 levels from, (E), 20: 3077
reactions (p,n) and (p,p) with tritium to 1.5 Mev, phase-shift analysis of, 20: 3060
reactions (p,n) and (p,p) with samarium-144 at 9.2 to 10.8 Mev, isobaric analog states from, (E), 20: 3084
reactions (p,n) with lithium-6, neutron threshold measurements of, (E), 20: 3140
reactions (p,p'$\gamma$) with magnesium-26 at 5.67 to 6.46 Mev, angular distributions and excitation function for, (E), 20: 3092
reactions (p,t) with nickel-58 at 28 Mev, nickel-56 energy levels from, (E), 20: 3041
reactions (p,2p) with carbon-12 at 50 to 110 Mev, recoil nuclei momentum distribution from, (E), 20: 3081
reactions with bismuth at 400 Mev, production of astatine-203 and astatine-205 in, 20: 1948
reactions with boron-11, Dalitz diagram of carbon-12 3$\alpha$ decay in, 20: 3067
reactions with chondritic material, iron, and plexiglass at 1 to 3 Bev, (E), 20: 3015 (NASA-SP-71, pp 357-62)
reactions with elements at 160 and 450 Mev, nucleon spectra from, (T), 20: 3260
reactions with emulsion nuclei at 9 Bev with large energy transfer, (E), 20: 3047
reactions with helium and neon, ionization measurements from, (E), 20: 2128 (JINR-E-2324)
reactions with iron at 1 and 3 Bev, nucleon-meson cascades in, (T), 20: 3258
reactions with metals, radioactivity from, (E/T), 20: 3263
reactions with molybdenum surfaces, secondary-electron yields from, (E), 20: 2628
scattering by complex nuclei below 50 Mev, data survey for elastic polarized, 20: 3014 (LA-DC-7386)
scattering by helium-4 at 21 to 63 Mev, polarization effects in, (E/T), 20: 3022 (UCRL-16216)
scattering by tungsten at 3 Mev, angular distributions for elastic, (E), 20: 3037

shielding of, dose, energy, and flux variation factors for analysis of, (T), 20: 3250 (NASA-SP-71, pp 493-505)
spectra from gamma reactions (γ,p) with oxygen-16 at 21.3 to 43.7 Mev, cross sections for, (E), 20: 3107
trapping in DCX-1 by Lorentz dissociation of triatomic hydrogen ions, (E), 20: 3213

**PSEUDOUREA, 2-(2-AMINOETHYL)-2-THIO-**
effects of, against radioinduced genetic damage in Drosophila, 20: 1619(R) (TID-22293)
protective effects against radiation injuries in rats, low-dose exposure, 20: 1688
radiosensitivity effects on rat fetuses, 20: 1693

**PUERTO RICO POWER REACTOR**
operation, July 1964, 20: 3474(R) (GNEC-364)
performance, 20: 3520

**PULSE ANALYZERS**
design and performance of megachannel, 20: 2123 (BNL-9590)
design of pulse-shape discriminator for scintillation detectors, 20: 2167
performance of oscillographic, with gamma spectrometers, 20: 2149
use for measurement of relative time distribution of pulses in 4π beta-gamma coincidence system, 20: 2146
use of multidimensional, in nuclear chemistry, 20: 2142

**PUMPS (LIQUID METAL)**
cavitation damage in, 20: 2243

**PYRENE**
electron spin resonance of triplet state of, 20: 1935

**PYRIDINE**
reactions with carbon-14 and tritium recoil atoms, stability and yields in, 20: 1921

**PYRIDOXINE**
dietary content of, effects on radiosensitivity of mice, 20: 1646

**PYROMELLITIMIDE POLYMERS**
radiation effects on dielectric properties of, electron, 20: 1897 (NASA-TN-D-3032)


# Q


**QUANTUM ELECTRODYNAMICS**
Lorentz invariance in, 20: 2878
scattering amplitudes in, Coulomb Regge poles in, 20: 2782

**QUANTUM MECHANICS**
book: *Wave Mechanics of a Free Particle*, 20: 2888
bootstrap theory in, 20: 2816
Brownian motion formulation in, classical limit to Fokker-Planck equation for, 20: 2881
generalized quasi-spin in neutron–proton systems, 20: 3046
kinetics in, abstract formulation of, (T), 20: 2872
kinetics in, abstract formulation of nonrelativistic, (T), 20: 2873
of nuclear collective rotation, 20: 3048
orbit equation for quantum motion, 20: 2883
Pauli exclusion principle in, 20: 2878
principles of, critical reconsideration of fundamental, 20: 2887
spin temperature formalism in, (T), 20: 2864 (COO-1198-300)
thermodynamic functions in microcanonical ensemble in, (T), 20: 2832
wave equations in, correlation method for poles in Schroedinger, (T), 20: 2871

**QUARTZ**
photoluminescence of silver-activated, (E/T), 20: 3282

**QUATERPHENYL**
preparation of pure isomers of, method for, 20: 1745 (RT/CHI(65)-25)

**QUEBEC**
lead isotope ratios in galenas in, 20: 2051

**8-QUINOLINOL**
effects on solvent properties of arsonium and phosphonium salts for uranium, 20: 1782

**QUINONES**
effects of ortho, on living tissues, 20: 1647
radioinduced conversion of tyrosine to, 20: 1647


# R


**RABBITS**
radiation effects on antibody response to protein antigens in, 20: 1680
radiation effects on extractable cellular components of lungs of, x, 20: 1675
radioinduced destruction of otolith apparatus of auditory organ, 20: 1628(T)

**RADIATION**
attenuation of, radiative transfer in, (T), 20: 2930 (AD-614636)
detection and measurement of, automation in, 20: 2141
detection and measurement of, digital computer uses for analyzing, 20: 2153
dosimetry of background, in Soviet urban population, 20: 2087
dosimetry of, development and review of detectors for, 20: 2143
effects of direct, from nuclear explosion, ecological, 20: 2081 (BNL-917, pp 39-60)
effects of fallout, on ecological systems, 20: 2080 (BNL-917, pp 20-36)
effects of, compilation of projects on, 20: 2433 (REIC-Memo-27)
effects of, from nuclear explosions, physical, 20: 2078 (BNL-917, pp 1-10)
effects on alloys and metals in nuclear environments, ASTM symposium on, 20: 2470
effects on chemicals, pharmaceuticals, and pharmaceutical preparations, 20: 1918
effects on clad plutonium–uranium carbides, 20: 3321(R) (ANL-7082, pp 29-53)
effects on diodes and semiconductors, model for predicting transient, 20: 2412(R) (AD-618079)
effects on ferric perchlorate solutions, 20: 1898(R) (RRL-2310-164)
effects on germanium and silicon, annealing of, 20: 2506
effects on glass, bibliography on, 20: 2432 (REIC-Memo-26)
effects on kidneys in dogs, 20: 1686
effects on living tissues and organisms, bibliography, 20: 1607 (AED-C-04-18)
effects on living tissues and organisms, bibliography, 20: 1608 (AED-C-04-19)
effects on mechanical properties of reactor materials, 20: 2471
effects on mechanical properties of aluminum–chromium–iron–yttrium alloy and steels, 20: 2409(R) (AD-617319)
effects on metabolism of deoxyuridine in rats, 20: 1630
effects on metabolism of thymidine in rats, 20: 1630
effects on metabolism of nucleic acids in plants, 20: 1648
effects on oxidation of graphite in carbon dioxide and methane, oxygen effects on, 20: 1895 (AERE-R-4988)
effects on polymerization of monomers, calorimetric analysis of, 20: 1904
effects on properties of materials for pressure vessels, 20: 2479
effects on resin depletion in Savannah River reactors, 20: 2419 (DP-973)
effects on semiconductors, 20: 2481
effects on semiconductors, threshold energy for, 20: 2513
effects on semiconductors, surface design effects on, 20: 2411(R) (AD-618078)
effects on steel reactor structures, 20: 2408(R) (AD-614899)
effects on tumors in mice, effects of inhalation of 5% carbon dioxide and 95% oxygen on, 20: 1683
effects on uranium dioxide–Zircaloy-2 burnup at increased heat rating, 20: 2421 (EXP-NRX-22902)
effects on wines, preservative, 20: 2197
energy transfer by, transport theory of, 20: 2731
use in agriculture and industry in Denmark, 20: 3646

**RADIATION CHEMISTRY**
hot atom reactions in, effects of containment by surrounding molecules on, 20: 1934
research program on, 20: 1898(R) (RRL-2310-164)

**RADIATION DETECTION INSTRUMENTS**
design for criticality detection and alarm systems, review, 20: 2075 (AHSB(S)R-92)
design for low-background internal gas sample counting of carbon-14 and tritium, 20: 2179
design for neutron flux monitoring in reactors, 20: 2173
development, 20: 2107
development of, review of, 20: 2143
measurements with criteria for best, 20: 2127 (ISS-64/15)
use of self-powered, for neutron flux monitoring in pressurized-water reactors, 20: 2174

**RADIATION DETECTION INSTRUMENTS (PULSE TYPE)**
beta detection by, method of tissue dissolution for, 20: 1767
design for high-energy beta-active gases, 20: 2139
design for pulsed or steady x radiation, 20: 2121 (AD-614832)
operation and performance of G-M, 20: 2144
performance of halogen-filled G-M, for high gamma dose rates, 20: 2140
performance of, effects of pulse pile-up distortion on, (T), 20: 2160
pulse time distributions in 4π beta-gamma coincidence system using, 20: 2146

**RADIATION DETECTORS**
development, 20: 2177

**RADIATION EXPOSURE CHAMBERS**
design for gamma radiography, 20: 2520(R) (IA-920)

**RADIATION INJURIES**
diagnosis of, by morphological study of lymphocyte nuclei, 20: 1612 (EUR-2505.e)
evaluation of, fractional cell lethality calculations for, 20: 1616 (NASA-SP-71, pp 219-23)
in animal cells, genetic control of, 20: 1617(R) (NP-15149)
of *Bacillus subtilis*, repair mechanisms for ultraviolet-induced, 20: 1624

of skin, protective effects of melanin against ultraviolet-induced, 20: 1684
pathology of brain, induced by therapeutic x radiation doses, 20: 1713
pathology of delayed, 20: 1716
pathology of delayed, of vertebral column after radiotherapy during childhood, 20: 1702
pathology of, in swine skin, 20: 1609 (BNL-9477)
pathology of, induced by deposited strontium-89 or strontium-90 in adrenal glands, 20: 1641
pathology of, induced by radiotherapy, 20: 1717
pathology of, induced by high-energy protons in mice and rats, 20: 1614 (NASA-SP-71, pp 97-103)
pathology of, induced by high-energy alpha particles in mice and rats, 20: 1614 (NASA-SP-71, pp 97-103)
pathology of, induced by charged particles in biological systems and animal cells, 20: 1615 (NASA-SP-71, pp 105-14)
pathology of, induced by radiotherapy of cervical carcinomas, 20: 1725
protection against, effects of aminoethylisothiuronium in rats, 20: 1688
protection against, effects of 5-hydroxytryptamine in rats, 20: 1688
protection against, effects of sulfhydryl compounds on genetic damage in Drosophila, 20: 1619(R) (TID-22293)
reaction mechanisms involved in genetic, 20: 1619(R) (TID-22293)
recovery kinetics of, in mice, 20: 1685

**RADIATION PROTECTION**
design of shielded vehicles for work in radiation areas of high-energy accelerators, (E), 20: 2542 (UCRL-16236)
development of fast-neutron dosimeters for personnel, (E), 20: 2134 (TID-22335)
dose quality factors for spherical proton shields, (T), 20: 3243 (NASA-SP-71, pp 229-34)
during diagnostic radiography, 20: 1698
of astronauts from cosmic radiation, by copper shields, (T), 20: 3240 (NASA-SP-71, pp 183-8)
of astronauts in Apollo Command/Service Module, (T), 20: 3244 (NASA-SP-71, pp 365-75)
of personnel of military space vehicles, (T), 20: 2656 (NASA-SP-71, pp 265-86)
of personnel of space vehicles, (T), 20: 3245 (NASA-SP-71, pp 407-14)
of spacecraft personnel from solar flares, (T), 20: 2655 (NASA-SP-71, pp 85-96)

**RADIATION SICKNESS**
pathological effects in mammals of, delayed, 20: 1716

**RADIATION SOURCES**
preparation and calibration of standard radium, 20: 1941
use in ionization chamber for high-resistance ohmmeter, 20: 2108

**RADIATION TARGET CANS**
design of, calculational methods in, 20: 2418 (CEA-R-2801)
fabrication of, facility for, 20: 2298
heat transfer media in capsules, feasibility of powders as, 20: 2018 (TRG-Report-920)
properties of, survey of, 20: 2418 (CEA-R-2801)

**RADIATION TARGETS**
design of rotating, for photonuclear scattering studies, 20: 2520(R) (IA-920)
fabrication of, for HFIR, 20: 2282 (HW-SA-3755)
preparation of polarized proton, 20: 2686 (LNF-65/22)

**RADIATORS**
development for space power systems, 20: 3556
fabrication of beryllium, for space power systems, 20: 2293
fabrication of space, graphite brazing techniques for, 20: 2294
heat transfer and temperature distribution in finned, radiant, 20: 2016 (SC-DC-65-1765)

**RADICALS**
electron spin resonance of ion radical salt, 20: 1935

**RADIO WAVES**
effects of solar, on terrestrial events, 20: 2855
emission from solar flares, (T), 20: 2582
transmission in plasma layers, (E/T), 20: 2098 (AD-618398)

**RADIOACTIVE CONTAMINATION**
measurement in water supplies, evaporator-collector sampler for, 20: 1757
separation from water supplies, feasibility of filtration unit for, 20: 2072 (AD-616006)

**RADIOACTIVE MATERIALS**
analysis by emanation-thermal method, 20: 1779
polishing of, mounting system for, 20: 2006(P)

**RADIOACTIVITY**
diffusion in atmosphere, tests on, 20: 2073(R) (AD-618101)
gamma radiation doses from fallout, (T), 20: 2048 (USNRDL-TR-888)
measurement of background in Soviet Union, 20: 2087
measurement of, criteria for, 20: 2127 (ISS-64/15)
measurements of, dispersion method for, 20: 1781
sorption by chromatographic column, calculation of, 20: 1770

**RADIOAPPLICATORS**
design of promethium-147, for radiobiological studies, 20: 1628(T)
preparation of cobalt-60 bead, automatic threading device for, 20: 1722

**RADIOCHEMICAL PROCESSING PLANTS**
operation of aqueous, at Rocky Flats, Colorado, 20: 1940 (RFP-638)
sampling of process solutions at Eurochemic, system for, 20: 1955 (NP-15403)

**RADIOCHEMISTRY**
experimental facilities for, septum cap technique for air exclusion in, 20: 1945

**RADIODIAGNOSIS**
exposure during pregnancy, effects of Adrian and Medical Research Council Reports on, 20: 1689
hazards to fetus and maternal gonads during pregnancy, 20: 1689
photoscanning methods in, economics of, 20: 1705
scanning in, display system for, 20: 1715

**RADIOFREQUENCY SPECTROMETERS**
design and performance of double-resonance, 20: 2109

**RADIOGRAPHY**
betatron for, of heavy steel castings, 20: 2028
contrast media for, relative toxicity of nine, in dogs, 20: 1724
diffraction effects in gamma, 20: 2029
dosimetry during diagnostic, performance of rate meters for, 20: 1697
of blood vessels of kidney, in radiation nephritis, 20: 1686
radiation dose during diagnostic, 20: 1703
radiation dose of skin during diagnostic, 20: 1704
sensitivity of gamma scintillation, for defect detection, 20: 2027
shield for gamma, design of pivotable spherical, 20: 2034(P)
techniques for image contrast during diagnostic, 20: 1698

**RADIOISOTOPES**
bremsstrahlung yield from beta-emitting, 20: 2730
content and movement in garden crops, 20: 2520(R) (IA-920)
decay measurements for, multidimensional pulse analyser use in, 20: 2142
determination by gamma spectra resolution, computer program for, 20: 1732 (CEA-R-2850)
determination in labeled compounds by emanation-thermal method, 20: 1779
determination in water supplies, evaporator-collector for, 20: 1757
determination of beta-emitting corrections for self-absorption, 20: 1780
determination of, tabulations of gamma intensity data for, 20: 1735 (EUR-2406.e)
excretion by man, effects of chelating agents on, 20: 1691
gamma radiation doses from fallout, (T), 20: 2048 (USNRDL-TR-888)
handling of alpha-emitting, laboratory for, 20: 2089
neutron fission and total cross sections for heavy, multi-level model for calculating, (T), 20: 3374 (IA-1053)
production facilities at Mol, Belgium, 20: 2192 (BLG-63-11)
production in Israel, July–Dec. 1963 summary, 20: 2520(R) (IA-920)
production using ORNL 86-in. cyclotron, 20: 2212
production, properties, and transport, of, by AAEC, 20: 2208 (NP-15575)
propulsion systems using, effects of convection and radiation on heat transfer in, (E), 20: 2007 (AD-818026)
use in agriculture and industry in Denmark, 20: 3646
use in instruments, 20: 2107
uses in pharmacy, 20: 1918

**RADIOLOGICAL WARFARE**
ecological effects of, in North America, 20: 2081 (BNL-917, pp 36-60)
effects of fire on ecosystems during, 20: 2079 (BNL-917, pp 11-19)
effects on fire damage to non-urban areas, model for, (T), 20: 1590 (RM-3902-TAB)
physical damage from nuclear explosions during, review, 20: 2078 (BNL-917, pp 1-10)

**RADIOMETRIC ANALYSIS**
dispersion methods for, 20: 1781

**RADIOPROTECTIVE COMPOUNDS**
effects on low-dose injuries in rats, 20: 1688
protective effects of sulfhydryl, against genetic damage in Drosophila, 20: 1619(R) (TID-22293)

**RADIOSENSITIVITY**
of animal cells, effects of environment on, 20: 1617(R) (NP-15149)
of bacteria, effects of sulfhydryl compounds on, 20: 1618 (NYO-3319-6)
of bacteria, effects of p-hydroxymercuribenzoate binding on, 20: 1618 (NYO-3319-6)
of barley seeds, effects of oxygen and moisture, 20: 1667
of plant cells, effects of chromosome and nucleus volumes on, 20: 1610 (BNL-9611)
of plants, effects of chromosome volume on, 20: 2080 (BNL-2080, pp 20-36)
of rice seeds, effects of moisture content and variety, 20: 1669
thermal, of fungi and yeast, effects of uv and x radiations on, 20: 1640

**RADIOSTERILIZATION**
effects on wholesomeness of foods, bibliography on, 20: 2196 (AD-514910)
of meats, effects of fat content, previous cooking, and storage temperature

on wholesomeness, 20: 2203
of pharmaceuticals, 20: 1918
**RADIOTHERAPY**
dose calculations for gamma radiation for, 20: 1723
effectiveness of concentrated serial method of, in skin carcinomas, 20: 1718
effects on vertebral column of, during childhood, late pathological, 20: 1702
neutron capture, development and use of, 20: 1714
of carcinoma of the cervix, late pathological effects, 20: 1725
of lung lesions, dosimetry of exit dose during, 20: 1699
pathological effects of, delayed, 20: 1717
technique of, for bronchial carcinomas, 20: 1720
use of colloidal gold-198 for benign joint diseases, 20: 1706
use of proton beams for, 20: 1707
use of radium for, of infantile hemangiomas, 20: 1719
**RADIUM**
ion refraction in aqueous solutions, calculation of, 20: 1852
preparation and calibration of standard solutions of, 20: 1941
therapeutic use of, for infantile hemangiomas, 20: 1719
**RADIUM BROMIDES**
density and molar refraction of aqueous solutions of, 20: 1852
**RADIUM CHLORIDES**
density and molar refraction of aqueous solutions of, 20: 1852
**RADON**
content in living and working environments in Finsbury Borough, England, factors affecting, 20: 2090
diffusion in synthetic sandstone, 20: 1878
**RADON ISOTOPES Rn-219**
determination of, scintillation detector for, 20: 2152
**RADON ISOTOPES Rn-220**
content in atmosphere, correlation with meteorological variables, (E), 20: 2860
determination of, scintillation detector for, 20: 2152
excretion in breath of, after injection of thorotrast, 20: 1596
**RADON ISOTOPES Rn-222**
determination of, scintillation detector for, 20: 2152
**RAIN WATER**
analysis for halogens, using neutron activation analysis, 20: 1789
fission product content in Berlin following Chinese test of October 16, 1964, 20: 2050
separation of beryllium-7 and strontium-89 and -90 from, method for, 20: 1778
**RARE EARTH ALLOYS**
Mg–rare earths–Zn–Zr, crystal structure, 20: 2399
Mg–rare earths–Zr, crystal structure, 20: 2399
**RARE EARTH COMPLEXES**
with amygdalin, separation by solvent extraction using butanol, 20: 1796
**RARE EARTH IONS**
entropy of smallest and largest hydrations of, 20: 1858
**RARE EARTH MOLYBDATES**
preparation of single crystals of, by Czochralski method, 20: 1840
**RARE EARTH OXYBROMIDES**
preparation and crystal structure, 20: 1834
**RARE EARTHS**
content in soils of Tomsk region, 20: 2065
deposits properties of postmagmatic, with thorium, 20: 2064
determination in silicate ores using neutron activation analysis, 20: 2056
determination using Chromotrope 2B, photometric, 20: 1772
optical properties of heavy, electronic band structure predictions of, (T), 20: 2592 (BNL-9556)
separation from uranium by ion exchange in sodium triphosphate, 20: 1762
separation of mixtures of, electrophoretic, 20: 1961
separation of thorium from, by anion exchange, 20: 1957(T) (CEA-tr-X-616)
**RARE GASES**
diffusion in solids, effects of traps on, (T), 20: 2360(T) (ORNL-tr-314)
effects on mechanical properties of reactor materials, 20: 2471
fixation of radioactive, in water-unleachable rocklike products, 20: 3608(P)
**RATE METERS**
performance of, for patient dosimetry during diagnostic radiography, 20: 1697
**RATS**
diet, effects of radiation processed chicken, cabbage, and peaches on wholesomeness of, 20: 2199
niobium-90 metabolism in, 20: 1595
niobium-95 metabolism in, 20: 1595
radiation effects on immune reactions in, 20: 1632
radiation effects on desoxyribonucleic acid content of cells of corneal epithelium, 20: 1633
radiation effects on metabolism of desoxyribonucleic acid in tongue epithelium of, 20: 1634
radiation effects on metabolism of thymidine in, 20: 1630
radiation effects on metabolism of deoxyuridine in, 20: 1630
radiation effects on response to barbiturates of, 20: 1662
radiation effects on dietary and hormonal induction of enzymes in liver of, 20: 1674
radiation effects on extractable cellular components of lungs of, x, 20: 1675
radiation injuries of, diagnosis by morphological study of lymphocyte nuclei, 20: 1612 (EUR-2505.e)
radiation injuries of adrenal glands of, induced by deposited strontium-89 or strontium-90, 20: 1641
radiation injuries of, protective effects of aminoethylisothiuronium, 20: 1688
radiation injuries of, induced by high-energy protons and alpha particles, 20: 1614 (NASA-SP-71, pp 97-103)
radiation injuries of, protective effects of 5-hydroxytryptamine, 20: 1688
radiosensitivity of fetuses of, effects of chemicals on, 20: 1693
**REACTOR COMPONENTS**
alignment using optical tooling, 20: 3341
development for AARR, 20: 3579(R) (ANL-7082, pp 54-61)
evaluation of alloys for use as, (E/T), 20: 3471(R) (GEAP-4861)
**REACTOR CONTROL ELEMENTS**
effectiveness of linear arrays of absorber tubes as control-rod blades, 20: 3400
**REACTOR CONTROL RODS**
calibration using on-line computers, 20: 3320(R) (ANL-7082, pp 1-28)
drive mechanism design for coarse, fine, and safety, 20: 3356(P)
magnets for, design of support for, 20: 3353(P)
reactivity worth in Molten Salt Reactor Experiment, 20: 3505
**REACTOR CONTROL SYSTEMS**
description of, for gas-cooled power reactors, (E), 20: 3480 (ORNL-P-1679)
design for ORNL High Flux Isotope Reactor, 20: 3543
design using fuel concentration variations, 20: 3361(P)
design using neutron absorber in primary fluid, 20: 3359(P)
effects on xenon spatial oscillations, 20: 3326 (WAPD-T-1732)
**REACTOR COOLANTS**
analysis of water for heavy water leaks, infrared detector for, 20: 2099 (AECL-2291)
chemistry of experimental SNAP-8, 20: 3564
density profile in light-water-moderated reactors, 20: 3500
flow control system for, 20: 3357(P)
flow through subassemblies, temperature-sensitive device for control of, 20: 3365(P)
radiolysis of terphenyls, interpretation of, 20: 1927
**REACTOR COOLING SYSTEMS**
design of liquid metal, for power reactors, 20: 3537(P)
design of 2 Mw sodium, for experimental fast reactor, 20: 3479 (NP-15556)
design using heat output and neutron flux measurements, 20: 3358(P)
design with flow control, 20: 3365(P)
fission product sorption on surfaces in gaseous, 20: 3344
**REACTOR FUEL ALLOYS**
development, 20: 3320(R) (ANL-7082, pp 1-28)
fabrication of clad molybdenum–plutonium–uranium, for ZPR-III, 20: 2290
phase studies of fissium–plutonium–uranium, 20: 3493
**REACTOR FUEL ELEMENTS**
analysis for uranium-235, gamma counting for nondestructive, 20: 3464
analysis of irradiated MITR, using gamma spectrometry, 20: 2030
analysis of solid, physico-chemical methods for, 20: 1743 (JUL-216-HW)
annealing of, facility for remote, 20: 2299
burnup calculations for, 20: 3601
design for Fast Flux Test Reactor, 20: 3588
design for operation at 1700 to 1800°F, 20: 3472(R) (GEAP-4891)
design of, with fuel cans in graphite sleeve, 20: 3465(P)
design with braced splitter fins, 20: 3466(P)
design with helically arranged fins and baffle in fin channels, 20: 3467(P)
design with tubular assembly within casing, 20: 3468(P)
diffusion of fission products in cladding for, 20: 2389
fabrication and processing of, methods for, 20: 2282 (HW-SA-3755)
fabrication costs of uranium carbide, for Hallam Power Reactor, 20: 3509
fabrication costs for fast reactors, 20: 3510
fabrication for AVR Reactor, 20: 3494
fabrication in Germany, 20: 3447
fabrication of uranium-233, nonremote, 20: 2289
failure detection in Experimental Breeder Reactor-II, systems for, 20: 3518
fission gas pressure in irradiated uranium dioxide, 20: 2462
fuel can assembly design with graphite sleeve, 20: 3465(P)
gamma heating effects on cylindrical, (T), 20: 3325 (ORNL-P-1480)

gamma scanning using anticoincidence spectrometers, 20: 2172
gas pressure and volume in, device for remote determination of, 20: 2116
handling of, design of tilting device for, 20: 2002(P)
heat transfer by 7-rod, 20: 3472(R) (GEAP-4891)
heat transfer from turbulence-promoted, for gas-cooled reactors, 20: 2022
heat transfer in steam-cooled rod bundles with turbulence promoters, (E), 20: 3471(R) (GEAP-4861)
heat-transfer testing of "nuclear-vapotron" cans for, (E), 20: 3443(R) (EURAEC-1356)
heat-transfer testing of "nuclear-vapotron" cans for, (E), 20: 3444(R) (EURAEC-1357)
heat-transfer testing of "nuclear-vapotron" cans for, (E), 20: 3445(R) (EURAEC-1358)
inspection of irradiated, remote-control equipment for underwater, 20: 2117
inspection of, from NPD Reactor, 20: 3496
irradiation testing of uranium dioxide, in Big Rock Point Power Reactor, 20: 3452
irradiation testing of AVR and PBRE, 20: 2464
irradiation testing of tubular beryllia–thoria–urania–yttria, 20: 2467
particle-size distributions from destruct tests of ROVER, 20: 3574
performance in boiling-water reactors, 20: 3497
performance in pressurized-water reactors, 20: 2231
pressure drop in, with shrouds, 20: 2010 (IPV-19)
re-entry heating of uranium–zirconium hydride, hydrogen release in, 20: 3563
re-entry heating of SNAP-10A, 20: 3560
testing in flowing carbon dioxide, deterioration of uranium during, 20: 1748 (UJV-1369/65)
testing of plutonium dioxide–uranium dioxide, in Plutonium Recycle Test Reactor, 20: 2449
testing of stainless-steel-clad plutonium dioxide–uranium dioxide, 20: 2448
thermal properties of fuel-pellet-clad interaction in, (E/T), 20: 1811 (EUR-2486.e)
thermal stresses in liquid-metal-cooled, calculation of transient, 20: 3463
vibrations in parallel water flow, flow-induced, 20: 1978
water-vapor effects in irradiated uranium dioxide, 20: 2468

**REACTOR FUEL ELEMENTS (CERAMIC)**

cladding removal and fluorination of, 20: 3321(R) (ANL-7082, pp 29-53)
development for SEFOR, 20: 3320(R) (ANL-7082, pp 1-28)
fabrication and processing of, methods for, 20: 2282 (HW-SA-3755)
fabrication of niobium-coated uranium carbide, 20: 2300(P)
radiation effects on melting tungsten–uranium dioxide and uranium dioxide, 20: 2416 (AECL-2289)
reactions of stainless steel- and Zircaloy-2-clad, with steam, 20: 2221(R) (ANL-7082, pp 62-73)
thermal stability of Incoloy-clad uranium dioxide, 20: 3472(R) (GEAP-4891)

**REACTOR FUEL ELEMENTS (DISPERSION)**

irradiation testing of aluminum cermet–uranium oxide, for ATR, 20: 2465

**REACTOR FUEL ELEMENTS (THERMOELECTRIC)**

development, (E), 20: 3446(R) (GEST-2045)
performance for space uses, 20: 3547 (NAA-SR-Memo-7881)

**REACTOR FUEL PINS**

meltdown in flowing sodium, TREAT tests on, 20: 3506

**REACTOR FUEL PLATES**

fabrication for ZPR-III, 20: 2290
fuel expansion in, structural analysis of, 20: 3453
stability in hydraulically collapsed assemblies, 20: 3459

**REACTOR FUEL RODS**

dimensional measurements on, systems for remote, 20: 1993
fabrication for EBR-II experiments, 20: 3320(R) (ANL-7082, pp 1-28)
fabrication in EBR-2 Fuel Cycle Facility, remote, 20: 2297
fission-product distribution in uranium dioxide, 20: 2450
heat transfer and temperature distribution in, 20: 3450
heat transfer in steam-cooled rod bundles with turbulence promoters, (E), 20: 3471(R) (GEAP-4861)
inspection of, from blanket region of Shippingport Pressurized Water Reactor, 20: 3495
irradiation testing of vibrationally compacted plutonium dioxide–uranium dioxide, 20: 2461
irradiation testing of clad uranium dioxide, in Big Rock Point Power Reactor, 20: 3452
performance of clad, in boiling-water reactors, 20: 3497
plutonium distribution in, optimization for water-moderated reactors, 20: 3457
vibrations in parallel water flow, flow-induced, 20: 1978

**REACTOR FUEL SPHERES**

fabrication using arc plasma, 20: 2288

**REACTOR FUEL TUBES**

criticality studies of enriched uranium, in light water, 20: 3393
fabrication of uranium dioxide, for irradiation in VBWR, 20: 2280 (DP-989)
irradiation testing zircaloy–2-clad uranium–zirconium alloy, 20: 2466

**REACTOR FUELS**

burnup analysis of plutonium–uranium dioxide, isotopic, 19: 2454
burnup calculations using synthesis approximations, 20: 3454
burnup calculations, calibration of computer program for, 20: 3455
burnup in Elk River Power Reactor, 20: 3499
burnup in Yankee Power Reactor, 20: 3504
burnup of thorium–uranium, cost analysis for high-temperature reactors from, 20: 3448
burnup of uranium-233, measurement of, (E), 20: 3010(R) (IDO-14663)
cycle facility for, maintenance and operation of, 20: 3320(R) (ANL-7082, pp 1-28)
development of plutonium and thorium, in Canada, 20: 3449
development of thorium, facility for, 20: 1994
economics of crossed-progeny, 20: 3512
expansion in fuel plates, structural analysis of, 20: 3453
expansion of hollow uranium dioxide pellets in collapsible zircaloy cladding, 20: 2463
fabrication of sintered thorium dioxide pellets, 20: 2291
fission product release from irradiated uranium–zirconium hydride, 20: 3562
melting of uranium dioxide, molten boundary in, 20: 2392
melting point of plutonium dioxide–uranium dioxide, 20: 2391
microstructure variations with temperature, device for studying, 20: 2393
neutron resonance absorption in, with grain structure, (T), 20: 2993
paste flow studies using randomly packed beds, 20: 3461
performance of irradiated plutonium dioxide–uranium dioxide, under transient irradiation, 20: 2469
plutonium distribution in, Monte Carlo calculations on optimum, 20: 3456
preparation of coated-particle carbide, 20: 2305(P)
processing and shipping spent, regulations for, 20: 2084 (EURAEC-374(Vol.2))
processing in ER-2 Fuel Cycle Facility, 20: 3523
processing in Germany, 20: 3447
processing in hot cell, fluid-bed fluoride-volatility unit for, 20: 1971
processing of irradiated, methods for, 20: 3320(R) (ANL-7082, pp 1-28)
representation of fuel clusters containing control rods, using neutron diffusion theory, 20: 3428
stress analysis of pyrolytic-carbon coatings for particulate, model for, 20: 2235
structure of plutonium dioxide–uranium dioxide, variations with burnup, 20: 2451
temperature distribution in, calculation method, 20: 2221(R) (ANL-7082, pp 62-73)
testing of low-density compacted-powder uranium dioxide, in Vallecitos Boiling Water Reactor, 20: 2232
testing of plutonium dioxide–uranium dioxide, for fast reactors, 20: 2448
thermal conductivity of stoichiometric and hypostoichiometric plutonium dioxide–uranium dioxide, 20: 2453
thermal expansion of uranium dioxide pellets with radial temperature gradient, 20: 2234

**REACTOR MATERIALS**

analysis of solid, physico-chemical methods for, 20: 1743 (JUL-216-HW)
evaluation of alloys for use as, (E/T), 20: 3471(R) (GEAP-4861)
radiation effects on steel, 20: 2408(P) (AD-614899)
radiation effects on mechanical properties, 20: 2471
tensile testing at high temperatures, equipment for, 20: 2031

**REACTOR MATRICES**

buckling measurements in subcritical, by successive substitution, 20: 3399
criticality studies of multi-region uranium dioxide and plutonium dioxide–uranium dioxide, 20: 3389
criticality studies of plutonium and plutonium–uranium, 20: 3394
criticality studies of enriched-uranium heavy-water, using pulsed-neutron techniques, 20: 3432
criticality studies of aluminum–plutonium alloy-polyethylene, 20: 3398
neutron buckling in light-water-uranium, 20: 2520(R) (IA-920)
neutron fission and flux distributions in light-water-moderated enriched-uranium, 20: 3396
neutron flux in heterogeneous, fine structure in fast, 20: 3427
neutron kinetics calculations for plutonium dioxide–uranium dioxide, using multigroup thermal self-shielding factors, 20: 3426
neutron kinetics measurements in enriched-uranium heavy-water, 20: 3397
neutron kinetics of ORGEL, method for calculating, 20: 3424
neutron kinetics of water-moderated plutonium dioxide–uranium dioxide, (T), 20: 3425
neutron physics calculations on, computer program for, 20: 2992
performance of fast-burst, optimization of, 20: 3593
power distributions in multi-region plutonium–uranium, 20: 3388
reactivity coefficient of, interpretation of, 20: 3431

**REACTOR MODERATORS**
neutron dispersion law of, (T), 20: 2991
**REACTOR REFLECTORS**
criticality studies of, 20: 3390
effects on burst characteristics of WSMR Fast-Burst Reactor, 20: 3589
**REACTOR SAFETY**
accident-recovery equipment, 20: 3339
containment pressure and temperature in loss-of-coolant accidents, 20: 3337
core temperature in loss-of-coolant accident, method for calculating, 20: 3332
evaluation for power generation, AEC, 20: 2093
evaluation of IRR-1, 20: 2520(R) (IA-920)
excursion in modified WSMR Fast-Burst Reactor, prompt-burst, 20: 3594
fire extinguishing system for heterogeneous reactors, 20: 3364(P)
hazards analysis of AARR, 20: 3579(R) (ANL-7082, pp 54-61)
**REACTOR SAFETY EXPERIMENTS**
blowdown model for LOFT, 20: 3335
blowdown tests on LOFT, semi-scale, 20: 3336
containment pressure and temperature in LOFT, 20: 3337
design of TESI, 20: 3584 (EUR-2433.e)
effects of zirconium cladding in LOFT, 20: 3334
fuel element handling for SPERT-D, criticality studies for, (E), 20: 3379 (ORNL-TM-1207)
fuel meltdown in flowing sodium, TREAT tests on, 20: 3506
meltdown studies in LOFT, annular-ring model for, 20: 3333
operation of TREAT, July 1965, 20: 2221(R) (ANL-7082, pp 62-73)
power excursions from high power levels in SPERT-III, 20: 3507
pressure pulse production in fixed water volume, by pulse heating, 20: 3338
**REACTOR SHIELDING**
design of crushable, analysis of, (E/T), 20: 3324(R) (IITRI-578P21-13)
design of, weight optimization theory for, 20: 3346
gamma and neutron transport in complex geometry, (E/T), 20: 3348
gamma dose deposition in, low-energy component of, (T), 20: 3267
gamma heating in, group constants for calculation, 20: 3268
measurements on Fermi Fast Breeder Reactor, 20: 3524
performance of ML-1, (T), 20: 3525
**REACTOR SLURRIES**
operation of sodium loop with stainless steel paste, 20: 3460
paste flow studies using randomly packed beds, 20: 3461
**REACTOR THERMAL COLUMNS**
loading equipment for, 20: 2520(R) (IA-920)
**REACTOR TUBES**
design of calandria, for liquid-moderated reactors, 20: 3354(P)
radiation effects on bursting pressure and fatigue life of stainless steel, neutron, 20: 2435 (WAPD-T-1720)
**REACTORS**
containment filter system efficiency in, measurement using condensation nuclei, 20: 3340
containment of, research on, (E/T), 20: 3324(R) (IITRI-578P21-13)
containment pressure and temperature in loss-of-coolant accidents, 20: 3337
control of, input-output methods in optimal, 20: 3409
control of, optimization by Maximum Principle, (T), 20: 3372 (EUR-2508.e)
core temperature in loss-of-coolant accident, method for calculating, 20: 3332
development summary for, July 1965, 20: 3319(R) (ANL-7062)
economics of MHD generators and, for commercial power, 20: 2670 (LA-DC-7330)
effects of zirconium cladding in loss-of-coolant accidents, 20: 3334
fuel burnup calculations using synthesis approximations, 20: 3454
fuel burnup calculations for, calibration of computer program for, 20: 3455
fuel cycles for, facility for studying thorium, 20: 1994
heat transfer and kinetics in, computer program for calculating, 20: 3323 (GAMD-6644)
instrumentation development for, 20: 2107
kinetics and stability of, prompt-jump approximation for, 20: 3437
kinetics equations for, approximate solutions of, 20: 3436
kinetics experiments on, on-line data reduction using digital computers, 20: 3433
kinetics of coupled-core, transfer functions for, 20: 3422
kinetics of large, excursion analysis using adiabatic approximation, 20: 3417
kinetics of large, spatial dependence of, 20: 3419
kinetics of, frequency response sensitivities in, 20: 3377 (ORNL-P-1482)
kinetics of, frequency response sensitivities in analysis of, 20: 3416
kinetics of, Liapunov function for prompt-jump approximation in, 20: 3407
kinetics of, performance of frequency-response analyses of, 20: 3380 (ORNL-TM-1305)
kinetics of, stationary calculations of parameters of, (T), 20: 3367 (BNWL-156)
kinetics of, time-dependent perturbation theory for nonlinear, 20: 3413
loading device for, design of, 20: 3352(P)
loading machine for fluid-cooled, design of, 20: 3355(P)
loading machine for, design of, 20: 3360(P)
neutron diffusion equations for, computer program for solving, 20: 3382 (WAPD-TM-532)
neutron Doppler effect and transport parameters for, (T), 20: 3375 (IDO-17120)
neutron flux distribution in, activation method for determining, 20: 3362(P)
neutron flux distributions in, energy and space effects in, 20: 3420
neutron flux in, effect of scattering kernel on, 20: 3435
neutron flux measurements in, instrumentation for, 20: 2107
neutron flux monitoring in, device for, 20: 2173
neutron physics of, error estimates for integral-equation eigenvalue problems in, 20: 3411
neutron spectra in, measurement using Fermi chopper, 20: 2994
neutron transport in, variational vacuum boundary conditions for $P_N$ approximation in, 20: 2978
neutron transport theory for, variational principles in, 20: 2979
neutron transport theory for, variational principles in, 20: 2980
nuclear generation time in, variation with reactivity, 20: 3386
physics of, optimization theorems in, 20: 3330
physics parameters of, temperature dependence of, 20: 3435
poisoning by xenon-135, method of compensating, 20: 3359(P)
power density of accelerator boosted, kinetic theory of, (T), 20: 3371 (EUR-2492.e)
power distributions in, calculation using computer programs with $(r\text{-}\theta)$ geometry, 20: 3429
power excursions in, time-integrated model for, 20: 3418
power oscillations in, 20: 3408
power spectral-density measurements in, analysis using exponential cosine autocorrelation functions, 20: 3342
pressure vessel design against brittle failure, fracture mechanics in, 20: 3345
reactivity excursions in, temperature variation in ramp-insertion, 20: 3415
reactivity measurements by Garelis-Russell method, analysis using asymptotic reactor theory, 20: 3385
safety aspects of chemo-nuclear, 20: 2520(R) (IA-920)
shutdown modes for, analysis for near-optimum, 20: 3438
shutdown of, control of xenon buildup in, 20: 3410
simulation of, one-group three-dimensional model for, 20: 3501
stability of, criterion for nonlinear asymptotic, 20: 3406
stability of, Lagrange, 20: 3405
stability with randomly fluctuating macroscopic cross sections, 20: 3404
structural vibrations in, method for analyzing nonlinear, 20: 3328
testing in, eddy-current method for vibration, 20: 2025 (BNWL-SA-349)
theory of, variational principle analogies in classical mechanics, 20: 3331
transfer functions of, method for calculating space-dependent, 20: 3421
xenon spatial oscillations in, control-rod effects on, 20: 3326 (WAPD-T-1732)
**RECOIL IONS**
reactivity of, effects of containment by surrounding molecules on, 20: 1934
**REFRACTORY MATERIALS**
bonding to yttrium oxides, 20: 2292
compatibility with alkali metals at high temperatures, 20: 2236
dislocation arrays in heterogeneous, linear, (T), 20: 2335 (NYO-2394-9)
fabrication and phase studies on systems of, 20: 2350(R) (USBM-RC-1205)
melting of, performance of induction furnace for cold-mold, 20: 2352(R) (USBM-RC-1205, pp 9-10)
properties and uses of, review on, 20: 2307 (AD-613023)
properties of, strain softening effects on, 20: 2311 (AD-618925)
testing for use in potassium-lubricated bearings for space power systems, 20: 3555
**RELATIVITY THEORY**
differential equations in, applications of partial, 20: 2530
Einstein's equations, generalization of, (T), 20: 2876(T)
electromagnetic field equations and Einstein-Schroedinger theory in, 20: 2869
electromagnetic field vectors in, 20: 2875
equations of elasticity in, 20: 2868
field equations for particle rest mass and charge, 20: 2886
gravitational energy-momentum linkages in, Lorentz-covariant, (T), 20: 2882
gravitational radiation in, detection of, (T), 20: 2884
Lorentz invariance and linearization of relativistic hamiltonian in, 20: 2874
Mössbauer effect for verification of, (E), 20: 2880

photon bouncing in, (T), 20: 2870
shock structure in relativistic fluid dynamics, (T), 20: 2844
**REMOTE-CONTROL EQUIPMENT**
coupling device for use in, design and application, 20: 2004(P)
design and development of master-slave components for, 20: 3321(R) (ANL-7082, pp 29-53)
design for dimensional measurements on reactor fuel rods, 20: 1993
design for leak-tight movement transmission through walls, 20: 2005(P)
design for mounting and polishing radioactive samples, 20: 2006(P)
design for tensile testing of irradiated materials at low temperatures, 20: 2032
design for tilting irradiated fuel elements, 20: 2002(P)
design for work in radiation areas of high-energy accelerators, (E), 20: 2542 (UCRL-16236)
design of single-wire circuit for, 20: 2003(P)
development for underwater disassembly and inspection of irradiated fuel assemblies, 20: 2117
development of manipulators for high-energy accelerators, 20: 2551
performance in EBR-II Fuel Cycle Facility, 20: 3522
**RENE-62**
corrosion by steam and water at 800 to 1500°F, (E), 20: 3471(R) (GEAP-4861)
**REPTILES**
venom from, activation analysis for copper and zinc, 20: 2520(R) (IA-920)
**RESEARCH REACTORS**
control system design for Ispra-1, 20: 3587 (RT/ING(65)-3)
coolant pump breakdown in MERLIN, analysis of, (E), 20: 3585 (JUL-259-RE)
design modifications to SNAP Shield Test and Irradiation Reactor, 20: 3595
design of Fast Flux Test Reactor, 20: 3596
design of Fast Flux Test Reactor, physics aspects of, 20: 3597
design of Fast Test Reactor, conceptual, 20: 3581 (BNWL-SA-340)
design of high-flux, using rotating fluidized bed, 20: 3598
development of Danish, review of, 20: 3646
excursion in modified WSMR Fast-Burst Reactor, prompt-burst, 20: 3594
fuel element design for Fast Flux Test Reactor, 20: 3588
fuel element fabrication and processing for, 20: 2282 (HW-SA-3755)
neutron pulse propagation from, thermal, 20: 2955
neutron spectra measurements in University of Florida, 20: 3600
operation of IRR-1, July–Dec. 1963, 20: 2520(R) (IA-920)
performance of fast-burst, optimization of, 20: 3593
reflector effects on burst characteristics of WSMR Fast-Burst Reactor, 20: 3589
**RESINS**
molding precision microballoon-filled epoxy, method for, 20: 3634 (SC-TM-65-462)
performance of ion exchange, for demineralization of boiling reactor coolant plants, 20: 3539 (ACNP-65558(Rev.1))
**RESISTORS**
radiation effects on, pulsed neutron, 20: 2187 (ECOM-2545)
radiation effects on, transient neutron, 20: 2190
**RESPIRATORY TRACTS**
neodymium deposition in, after inhalation of neodymium oxide aerosol by guinea pigs and mice, 20: 1593 (COO-1170-4)
radiotherapy of carcinomas of, 20: 1720
**RHENIUM**
desorption of thorium from, by electron bombardment, (E), 20: 2434(R) (TID-22242)
effects on ductility of chromium, molybdenum, and tungsten, 20: 2323 (GEMP-314)
separation from molybdenum using amyl acetate, 20: 1965
**RHENIUM ALLOY COUPLES**
Cr–Os/Re–W, thermoelectric properties at 200 to 1800°C, 20: 2223(R) (GEMP-51A)
Mo–Os–Ru/Re–W, thermoelectric properties at 100 to 1400°C, 20: 2223(R) (GEMP-51A)
**RHENIUM ALLOYS**
Be–Re, superconductivity in, properties of, (E), 20: 2898
Cr–Re, ductility, phase studies, and properties of, 20: 2323 (GEMP-314)
Mo–Re, corrosion by lithium at high temperatures, 20: 2269
Mo–Re, corrosion by bismuth and tin, 20: 2275
Mo–Re, development, 20: 2223(R) (GEMP-51A)
Mo–Re, ductility, phase studies, and properties of, 20: 2323 (GEMP-314)
Mo–Re, superconducting properties of, (E/T), 20: 2890 (AFML-TR-65-154)
Mo–Re–W, creep at 1600 and 2200°C, 20: 2223(R) (GEMP-51A)
Mo–Re–W, ductility of, effects of composition on, 20: 2223(R) (GEMP-51A)
Mo–Re–W, fabrication and properties of, 20: 2354(R) (USBM-RC-1205, pp 15-19)
Mo–Re–W, sectioning of, method for submicron, 20: 2321(R) (GEMP-52A, pp 43-5)
Re–W, chemical compatibility with urania, (E), 20: 3446(R) (GEST-2045)
Re–W, corrosion by lithium at high temperatures, 20: 2269
Re–W, creep at 1800 to 2200°F, 20: 2333(R) (NASA-CR-54457)
Re–W, creep rate to rupture time, equation for relating, 20: 2422(R) (GEMP-52A, pp 11-21)
Re–W, ductility, phase studies, and properties of, 20: 2323 (GEMP-314)
Re–W, fabrication and properties of, 20: 2354(R) (USBM-RC-1205, pp 15-19)
Re–W, fabrication of sheets and tubing of, procedure for, 20: 2223(R) (GEMP-51A)
Re–W, radiation effects on rupture life of, fast neutron, 20: 2422(R) (GEMP-52A, pp 1-21)
Re–W, use in thermocouples for measurements on plutonium dioxide–uranium dioxide fuel, 20: 2114
**RHENIUM ISOTOPES Re-185**
neutron total cross sections, cold, resonance, and thermal, (E), 20: 3030
**RHENIUM ISOTOPES Re-187**
neutron total cross sections, cold, resonance, and thermal, (E), 20: 3030
**RHENIUM OXIDES**
thermodynamic properties, 20: 1880
**RHENIUM SYSTEMS**
O–Re, phase diagrams, 20: 1880
**RHODIUM ISOTOPES Rh-102**
gamma spectra of, measurement using lithium-drifted germanium detector, (E), 20: 3043
**RHODIUM ISOTOPES Rh-106**
gamma spectra of, measurement using lithium-drifted germanium detector, (E), 20: 3043
**RHODIUM OXIDES**
$Fe_2O_3$–$Rh_2O_3$, crystal and magnetic structure of, (E), 20: 3293
**RIBONUCLEASE**
effects on metabolism of uridylic acid in *Escherichia coli* ribosomes, tracer study, 20: 1592 (BNL-7903)
radiation effects on activity and structure of molecules of, 20: 1604(R) (TID-22291)
radioinduced inactivation of, effects of oxygen and temperature on, 20: 1682
**RIBONUCLEIC ACID**
messenger, binding site in *Escherichia coli* ribosomes, tracer study, 20: 1592 (BNL-7903)
radioinduced inactivation of tobacco mosaic, photoreactivation, 20: 1659
**RIBONUCLEIC ACID, DESOXY-**
inactivation of transforming, by methyl methanesulfonate, in *Bacillus subtilis*, 20: 1624
radiation effects on synthesis of, in L-strain cells, uv, 20: 1625
radiation effects on content of, in cells of corneal epithelium of rats, 20: 1633
radiation effects on synthesis in *Escherichia coli* of, x, 20: 1639
radiation effects on metabolism of, in tongue epithelium cells of rats, 20: 1634
**RICE**
radiosensitivity of seeds of, effects of moisture content and variety, 20: 1669
**ROCKET MOTOR NOZZLES**
tensile properties of graphite, 20: 2372
**ROCKET MOTORS**
exhaust streams from, feasibility of electric energy extraction from, 20: 2668 (AD-615124)
performance of clustered nuclear, 20: 3570
**ROCKET REACTORS**
core destruction using high explosives, ground contamination from, 20: 3575
fuel selection for gaseous-core, 20: 3462
performance of clustered, 20: 3570
radiation hazards from debris of, dose models for evaluating, 20: 2091
safety analysis for, review of, 20: 3548 (SC-DC-65-1752)
simul of tungsten water-moderated, criticality studies of critical assembly for, 20: 3571
**ROCKET REACTORS (KIWI)**
control system of NERVA, 20: 3569
core destruct tests of NERVA, using high explosives, 20: 3573
core destruction by rapid excursions, feasibility studies of, 20: 3572
fuel element destruct tests using high explosives, particle-size distributions from, 20: 3574
poisoning system for NERVA, 20: 3576
power distributions in NERVA, 20: 3568
reactivity effects of tantalum rods in NERVA, (T), 20: 3403
reactivity of NERVA, 20: 3567
reactivity of, temperature coefficient of, 20: 3566
testing of NERVA, 20: 3565
**ROCKETS**

use in space research, 20: 2862
**ROCKS**
analysis for cerium, spectrographic, 20: 2520(R) (IA-920)
analysis in crime detection of activation, 20: 1736(R) (GA-3491)
thorium and uranium abundances in, 20: 2052
weathering of, use of thorium–uranium ratio for estimating, 20: 2052
**ROCKY FLATS PLANT, DENVER**
radiochemical processing facility at, operation of, 20: 1940 (RFP-638)
**ROOTS**
radioinduced chromosome aberrations in tomato, 20: 1638
**RUBBER**
analysis of automobile-tire, activation, 20: 1737(R) (GA-3664)
**RUBIDIUM**
compatibility with niobium–zirconium alloys at high temperatures, 20: 2236
corrosive effects on niobium–zirconium alloy at high temperatures, 20: 2268
heat transfer by boiling, burnout heat flux in, 20: 2023
heat transfer in saturated pool boiling, 20: 2008(R) (AD-622825)
separation of trace elements from, by precipitation ion exchange, 20: 1958
**RUBIDIUM ASTATIDES**
entropy and thermal capacity at 0 to 300°K, 20: 1859
**RUBIDIUM BROMIDES**
radiation effects on electric conductivity of, (E), 20: 2434(R) (TID-22242)
**RUBIDIUM FERROCYANIDES**
iron-57 Mössbauer spectra from, (E), 20: 3296
**RUBIDIUM FLUORIDES**
spectroscopy of, measurement of rotational transitions in, 20: 1876
**RUBIDIUM ISOTOPES Rb-84**
production using ORNL 86-in. cyclotron, 20: 2212
tracer use of, for cardiac circulation studies, 20: 1709
**RUBIDIUM ISOTOPES Rb-85**
neutron resonances at 528 and 1210 ev, radiation widths of, (E), 20: 3133
spin exchange cross section between rubidium-87 and, (E), 20: 2613
**RUBIDIUM ISOTOPES Rb-87**
neutron resonance at 378 ev, radiation width of, (E), 20: 3133
optical pumping in, alone and mixed with noble gases, 20: 2596 (UCRL-16241)
spin exchange cross section between rubidium-85 and, (E), 20: 2613
**RUBIDIUM SYSTEMS**
Ar–Rb, optical pumping of rubidium-87 in, 20: 2596 (UCRL-16241)
He–Rb, optical pumping of rubidium-87 in, 20: 2596 (UCRL-16241)
Ne–Rb, optical pumping of rubidium-87 in, 20: 2596 (UCRL-16241)
**RUSSIAN REACTORS**
design of BN-350 power breeder, 20: 3475 (NP-15458)
**RUTHENIUM**
preparation in perchloric and sulfuric acids by hydrogen peroxide reduction of ruthenium oxide, 20: 1853
separation by solvent extraction using long chain amines, 20: 1761
**RUTHENIUM ALLOY COUPLES**
Mo–Os–Ru/Re–W, thermoelectric properties at 100 to 1400°C, 20: 2223(R) (GEMP-51A)
**RUTHENIUM ALLOYS**
Cr–Ru, properties of, 20: 2323 (GEMP-314)
**RUTHENIUM ISOTOPES Ru-96**
gamma transition at 832.6 kev following Coulomb excitation, (E), 20: 3043
**RUTHENIUM ISOTOPES Ru-100**
gamma transition at 539.6 kev following Coulomb excitation, (E), 20: 3043
**RUTHENIUM ISOTOPES Ru-103**
content in fallout particles, 20: 2053
determination in sea water, methods for, 20: 1749 (USNRDL-TR-912)
**RUTHENIUM ISOTOPES Ru-104**
gamma transition at 357.7 kev following Coulomb excitation, (E), 20: 3043
**RUTHENIUM ISOTOPES Ru-106**
separation from aqueous solutions, use of silica gel for, 20: 1742 (INR-636/XIII/J)
**RUTHENIUM OXIDES**
reactions with sulfuric acid, complex formation in, 20: 1853
reduction by hydrogen peroxide in perchloric and sulfuric acids, ruthenium(IV) preparation by, 20: 1853

## S

**SACLAY REACTORS (AQUILON)**
neutron spectra in lattices of, (E/T), 20: 3582 (CEA-R-2482)
**SAFETY**
criticality detection and alarm systems, review of design principles of, 20: 2075 (AHSB(S)R-92)
evaluation of nuclear excavation of sea-level Isthmian canal, 20: 1985 (PNE-2003)
in handling and shipping fissionable material, 20: 3370 (CONF-651103-2)
preventive maintenance in chemical and mining industries, bibliography on, 20: 1976 (VDDIT-94)
regulations for shipping spent fuels, 20: 2084 (EURAEC-374(Vol.2))
systems design for, 20: 2085 (SC-R-65-991)
**SAFETY HAZARDS**
from rocket reactor debris, dose models for evaluating, 20: 2091
**SALTS**
electron spin resonance of ion radical salt, 20: 1935
**SAMARIUM**
determination by precipitation as normal tellurite, 20: 1760
determination in uranium and zirconium, spectrographic, 20: 2520(R) (IA-920)
determination using Chromotrope 2B, photometric, 20: 1772
**SAMARIUM ACETATES**
complexes with thiourea, solubility in water, 20: 1869
**SAMARIUM COMPOUNDS**
magnetic fields in, temperature dependence of effective, 20: 2520(R) (IA-920)
**SAMARIUM ISOTOPES**
yields in uranium-233 thermal fission, (E), 20: 3010(R) (IDO-14663)
**SAMARIUM ISOTOPES Sm-144**
ionization in K-shell by alpha particles at 3 to 4 Mev, x-ray yields from, (E), 20: 2625
proton reactions (p,n) and (p,p) at 9.2 to 10.8 Mev, isobaric analog states from, (E), 20: 3084
**SAMARIUM ISOTOPES Sm-146**
energy levels of, from europium-146 decay, (E), 20: 3075
**SAMARIUM ISOTOPES Sm-147**
alpha decay of, half-life and atomic stopping cross sections for, (E), 20: 3028
**SAMARIUM ISOTOPES Sm-152**
ionization in K-shell by alpha particles at 3 to 4 Mev, x-ray yields from, (E), 20: 2625
**SAMARIUM ISOTOPES Sm-154**
ionization in K-shell by alpha particles at 3 to 4 Mev, x-ray yields from, (E), 20: 2625
**SAMARIUM OXIDES**
phase studies of, at 2200 to 2300°C, 20: 1827
**SAMARIUM OXYBROMIDES**
preparation and crystal structure, 20: 1834
**SAMPLING**
equipment and methods for fallout, review on, 20: 2086(T) (BNL-tr-42)
equipment for air at high altitudes, development of cryogenic, 20: 2045 (UCRL-13162)
equipment for continuous, evaporator-collector, 20: 1757
equipment for sodium, engineering drawings of, 20: 1799
system for falling stream, engineering drawings of, 20: 1797
system for process solutions at Eurochemic process plant, 20: 1955 (NP-15403)
**SANDIA PULSED REACTOR**
shock forces in, inertial, 20: 3592
**SANDS**
thorium and uranium abundances in, 20: 2052
transport of surf coast, tracer methods for measuring, 20: 2060
**SANDSTONE**
permeability and radon diffusion in synthetic, 20: 1878
**SANDSTONE DEPOSITS**
uranium isotope fractionation in, Gas Hills, Wyoming, 20: 2057
**SAP (SINTERED ALUMINUM PRODUCTS)**
hardening of, isochronal recovery of, 20: 2375
**SARCOMAS**
niobium-90 metabolism in rat, 20: 1595
niobium-95 metabolism in rat, 20: 1595
**SATELLITES**
book: *Space Physics with Artificial Satellites*, 20: 2863(T)
**SAVANNAH RIVER COMPONENTS TEST REACTOR**
containment building for, leak testing of, 20: 2037 (DP-968)
fuel tubes for, irradiation testing of uranium–zirconium alloy, 20: 2466
**SAVANNAH RIVER PRODUCTION REACTORS**
resin depletion in heavy water purification system of, 20: 2419 (DP-973)
**SCANDIUM**
determination in river silts, soils, and tobacco, activation, 20: 1739(R) (GA-4297)
determination in silicate ores using neutron activation analysis, 20: 2056
determination in soils, activation, 20: 1738(R) (GA-4041)
determination using Chromotrope 2B, photometric, 20: 1772
determination using derivatives of resorcylaldehyde and salicylaldehyde and 3-methyl-1-butanol, fluorometric, 20: 1773
separation from thorium and other rare earths by ion exchange in ammonium thiocyanate–organic solvent–water systems, 20: 1959
separation of trace elements from, by precipitation ion exchange,

20: 1958
**SCANDIUM ALLOYS**
Sc–Tb, magnetic structure properties of, 20: 2338 (ORNL-P-1735)
**SCANDIUM ISOTOPES Sc-41**
energy-level transition probabilities of, E2, (T), 20: 3115
**SCANDIUM ISOTOPES Sc-45**
energy levels from electron capture decay of titanium-45, 20: 3128
neutron reactions (n,α) with, cross sections for, 20: 1947
**SCANDIUM ISOTOPES Sc-46**
excretion by man, effects of chelating agents on, 20: 1691
use as tracer in studies on erosion and sand transport on surf coasts, 20: 2060
**SCANDIUM ISOTOPES Sc-49**
energy-level transition probabilities of, E2, (T), 20: 3115
**SCANDIUM TELLURIDES**
radiative transfer in, equation of, 20: 2930 (AD-614636)
**SCATTERING**
amplitude for crossed-box ladder graphs in the Bethe-Salpeter equation, 20: 2818
amplitudes for four-body, (T), 20: 2791
amplitudes in high-energy, properties of forward, (T), 20: 2762
amplitudes of, asymptotic and threshold values in static models for, (T), 20: 2763
amplitudes of, calculation method using phenomenological, 20: 2804
cross sections for elastic and inelastic, temperature dependence of, 20: 3435
cross sections for, infrared singularities in, 20: 2754 (JINR-P-2309)
distributions from light-nucleus–heavy-nucleus, 20: 3013 (JINR-P-2331)
focusing singularity in p-space of constant curvature, 20: 2813
operators in two dimensions for, divergence of ternary, (T), 20: 2786
permissible rate of decrease in amplitude of forward, at high energies, (T), 20: 2810
perturbation theory for, time-dependent, 20: 2776
potential, variational bounds for multichannel, 20: 2815
potentials in, expansions in classical collision theory for, 20: 2808
Regge poles and cuts in field theory model for, (T), 20: 2768
symmetry properties of S matrix, Jost function method for, (T), 20: 2790
theory for, normal products in terms of functional integrals in S-matrix, 20: 2765
theory of double, S-matrix, 20: 2774
theory of, identities from Ehrenfest theorem and Lippman-Schwinger equation in, (T), 20: 2785
theory of, Nakanishi's inequality for, (T), 20: 2767
three-particle partial amplitudes and unitarity conditions for complex values of angular momenta, (T), 20: 2811
**SCINTILLATION DETECTORS**
design and performance of zinc sulfide (silver) for alpha counting, 20: 2152
design and performance of argon-gas, for fission fragments, 20: 2163
development, 20: 2177
efficiency for gamma radiation using well-type crystals, geometrical effects on, 20: 2169
efficiency of well-type, for absolute counting, 20: 2170
energy transfer in, by beta particles, 20: 2189
performance of anticoincidence-shielded, for gamma spectroscopy, 20: 3006 (AD-613676)
performance of organic plastic, for whole-body counting of man, 20: 1710
performance of, as x radiation dosimeters, 20: 2157
pulse-shape discriminator for dual-crystal Compton reduction, 20: 2167
quenching corrections for liquid, exponential function in, 20: 2168
use in beta-particle measurements, 20: 2180(P)
**SEA WATER**
analysis and sampling of Israel-shore, 20: 2520(R) (IA-920)
analysis for fission products, methods for, 20: 1749 (USNRDL-TR-912)
**SEALS AND GLANDS**
design for leak-tight movement transmission through walls, 20: 2005(P)
development for shafts in potassium space power systems, materials testing in, 20: 2242
preparation of ceramic-refractory metal, for space power systems, 20: 2292
**SEED**
effects of ethylenimine on wheat, genetic, 20: 1655
effects of space flight environment on, genetic, 20: 1649
mutagenic effects of ethyl methanesulfonate in maize, 20: 1656
radiation effects on, genetic, 20: 1649
radiation effects on wheat, genetic, γ, 20: 1655
radiation effects on wheat, genetic, fast neutrons, 20: 1655
radiation effects in oat, genetic, 20: 1665
radiation effects on barley, biological, 20: 1667
radiation effects on, genetic, 20: 1622 (WT-820)
radioinduced chromosome aberrations of tomato, 20: 1638
radiosensitivity of rice, effects of moisture content and variety, 20: 1669
radiosensitivity of *Phaseolus mungo*, post- and pre-irradiation heat treatment effects on, 20: 1690
**SEEDLINGS**
mutagenic effects of ethyl methanesulfonate in maize, 20: 1656
radiation effects on development of wheat, 20: 1666
radiation effects on growth of barley, 20: 1667
radioinduced chromosome aberrations in roots of tomato, 20: 1638
radioinduced chromosome aberrations in root tips of, 20: 1649
**SEIGNETTOELECTRIC MATERIALS**
conference on ferroelectricity, 20: 2526
**SEISMIC WAVES**
detection of tsunami, system design and development for, 20: 2058(R) (NVO-98-10)
measurement of tsunami, pressure sensors for, 20: 2059(R) (NVO-98-11)
**SEISMOLOGY**
measurements of Dugout row-charge cratering experiments, strong-motion, 20: 1981 (PNE-605F)
**SELENIUM**
analysis for traces of chlorine and sodium by neutron activation, 20: 1769
properties of, review on chemical and nuclear, 20: 1744 (NAS-NS-3030 (Rev.))
radiochemistry of, review on, 20: 1744 (NAS-NS-3030(Rev.))
semiconductor properties of, effects of chlorine and sodium on, 20: 1769
**SELENIUM ISOTOPES Se-76**
gamma transition at 559.3 kev following Coulomb excitation, (E), 20: 3043
**SELENIUM ISOTOPES Se-77**
gamma spectra following Coulomb excitation, (E), 20: 3043
gamma transitions following Coulomb excitation, (E), 20: 3043
**SELENIUM ISOTOPES Se-78**
gamma transition at 614.2 kev following Coulomb excitation, (E), 20: 3043
**SELENIUM ISOTOPES Se-80**
gamma transition at 666.2 kev following Coulomb excitation, (E), 20: 3043
**SELENIUM ISOTOPES Se-82**
gamma transition at 655.4 kev following Coulomb excitation, (E), 20: 3043
**SEMICONDUCTOR DETECTORS**
amplifier for, performance of transistorized pre-, 20: 2154
development, 20: 2143
development, 20: 2177
development, 20: 2520(R) (IA-920)
development of fast-neutron dosimeters using, (E), 20: 2134 (TID-22335)
development, properties, and use of, 20: 2155
fabrication and performance of germanium-silicon, 20: 2182(P)
performance in β-spectrometers for conversion coefficient measurements, 20: 3019 (ORNL-P-1657)
performance of silicon-array, as cosmic-proton dosimeters, (E), 20: 2133 (NASA-SP-71, pp 245-50)
review on, 20: 2138
use of lithium-drifted germanium, in neutron activation analysis, 20: 2166
use of lithium-drifted germanium, for precision gamma energy measurements, 20: 3043
**SEMICONDUCTORS**
electric conductivity measurements on, methods and uses of, 20: 2345 (UCRL-11030)
microwave–plasma interactions in, (E/T), 20: 3157 (AD-614654)
radiation effects of cosmic radiation on, 20: 3239 (NASA-SP-71)
radiation effects on, conference on, 20: 2480
radiation effects on, 20: 2481
radiation effects on, at 0 to 140°K, 20: 2482
radiation effects on, 20: 2497
radiation effects on double acceptor defects in n-type, 20: 2499
radiation effects on silicon carbide, 20: 2503
radiation effects on, threshold energy for, 20: 2513
radiation effects on, surface design effects on, 20: 2411(R) (AD-618078)
radiation effects on, model for predicting transient, 20: 2412(R) (AD-618079)
radioinduced defects in, structural properties of, 20: 2486
radioinduced defects in, fluorescence studies of, 20: 2498
radioinduced defects in, 20: 2516
radioinduced electron-hole pairs in n-type silicon, formation energy for alpha, (E), 20: 2362
transport effects in, research on, 20: 2519(R) (AD-615152)
**SENA POWER REACTOR**
development, April–June 1965, 20: 3484(R) (TID-22329)
**SERVOMECHANISMS**
development of manipulators for high-energy accelerators, 20: 2551
**SEWAGE**
disposal of, tracer studies of, 20: 2201
**SEX**
radiosensitivity effects of, in hamsters, 20: 1676
**SHELLS**
elastic wave propagation in open-end cylinder, analog model of, (T), 20: 3630 (SC-DC-65-1697)

**SHELTERS**
design of prefabricated roof structure for fallout, 20: 2039(P)
design of prefabricated fallout, 20: 2040(P)
design of, for protection against blast effects, 20: 2083 (CEX-65.4)
food evaluation for rations in fallout, 20: 2067 (AD-614824)
occupancy tests in simulated community fallout, environmental and organizational factors in, 20: 2070 (AD-615004)
occupancy tests in simulated fallout, 20: 2071 (AD-615005)
survival in fallout, without trained manager, 20: 2069 (AD-615003)
**SHIELDED CONTAINERS**
design for shipping spent fuels, 20: 2084 (EURAEC-374(Vol.2))
for fissionable material, safety, 20: 3370 (CONF-651103-2)
**SHIELDING**
analysis and development of cosmic-radiation, conference, 20: 3239 (NASA-SP-71)
design for high-energy electron accelerators, (T), 20: 2555
design for meson ($\pi$) production facility using proton linear accelerator, 20: 2559
design for NRL 60-Mev electron linear accelerator, 20: 2556
design for tandem accelerators, (T), 20: 2558
design of shielded vehicles for work in radiation areas of high-energy accelerators, (E), 20: 2542 (UCRL-16236)
electron beam diocotron instabilities in, (T), 20: 3252 (NP-15578)
gamma attenuation by horizontal concrete slabs, from finite plane source, (E/T), 20: 3271
mass calculations for cosmic-ray, for manned space vehicles, (T), 20: 3245 (NASA-SP-71, pp 407-14)
meson ($\mu$) ionization energy losses in, (T), 20: 3238 (JINR-P-2354)
neutron attenuation in concrete and iron, from alpha reactions with tantalum, (E), 20: 2554
neutron spectra in paraffin, fast, (E/T), 20: 3257
neutron spectra outside pulsed-accelerator, 20: 2553
neutron transport in heterogeneous, with anisotropic scattering, (T), 20: 2989
of gonads, during diagnostic radiography, 20: 1703
performance of copper for cosmic-ray, on manned space vehicles, (T), 20: 3240 (NASA-SP-71, pp 183-8)
performance of cosmic-ray, on Apollo Command/Service Module, (T), 20: 3244 (NASA-SP-71, pp 365-75)
performance of superconducting-magnet dynamic, for space vehicles, (T), 20: 3241 (NASA-SP-71, pp 199-209)
radiation attenuation by proton accelerator, 20: 2552
requirements for manned military space missions, (T), 20: 2656 (NASA-SP-71, pp 265-86)
requirements for protecting astronauts from solar flares, (T), 20: 2655 (NASA-SP-71, pp 85-96)
**SHIELDING MATERIALS**
fabrication of concrete containing carbon and lead, 20: 2306(P)
fabrication of ferrous-carbon type, process for, 20: 2301(P)
neutron transport in finite slab, source functions for, (T), 20: 2930 (AD-614636)
preparation and uses of asphalt, 20: 2248(P)
**SHIPPING**
cask design and regulations for spent fuel, 20: 2084 (EURAEC-374 (Vol.2))
of fissionable material, safety measures for, 20: 3370 (CONF-651103-2)
**SHIPPINGPORT PRESSURIZED WATER REACTOR**
fuel rods from blanket region of Core I, inspection of, 20: 3495
neutron flux distribution in, 20: 3519
reactivity of Core-2 Seed 1, 20: 3502
waste disposal from, 20: 3521
**SHIPS**
nuclear, legal aspects of entry into foreign ports, 20: 2088
**SHOCK TUBES**
pressure wave measurement from, technique for, (E), 20: 2822 (AWRE-O-60/65)
**SHOCK WAVES**
behavior of switch-on, in one-dimensional hydromagnetic flows, (T), 20: 2834
effects of ionizing, in cylindrical plasmas, (T), 20: 3201
effects on man, pathological, 20: 2083 (CEX-65.4)
energy density in converging, stability of, (T), 20: 2839
measurement from shock tubes, technique for, (E), 20: 2822 (AWRE-O-60/65)
physical effects of, from nuclear explosions, 20: 2078 (BNL-917, pp 1-10)
reactions with styrofoam, analysis of, (E/T), 20: 3324(R) (IITRI-578P21-13)
structure in relativistic fluid dynamics, (T), 20: 2844
**SILANE, TRIETHOXYVINYL-**
radioinduced polymerization of, at low temperatures, 20: 1893(R) (AD-618228)
**SILICATE ROCKS**
analysis for rare earths, activation, 20: 2056
**SILICATES**
radiation effects on coatings of, for spacecraft, 20: 2428 (NASA-SP-55, pp 365-79)
**SILICON**
analysis for oxygen, activation, 20: 2531 (AD-618304)
corrosion resistance to mercury at 900°F, 20: 2264
determination by activation methods using automated equipment, 20: 1765
effects on hardness properties of Nitinol alloy, 20: 2310 (AD-618681)
effects on isotopic exchange between cyclohexane and deuterium, 20: 1838
radiation effects on crystal structure of, mechanism of beta, 20: 2426 (LA-3387)
radiation effects on, 20: 2481
radiation effects on close-pair defects at 0 to 90°K, 20: 2482
radiation effects on thermal conductivity of monocrystals of, at 80 to 300°K, 20: 2487
radiation effects on, proton, 20: 2489
radiation effects on, EPR studies of, 20: 2490
radiation effects on n-type and p-type, 20: 2496
radiation effects on semiconducting, 20: 2497
radiation effects on diffusion of impurities in, 20: 2508
radiation effects on, anisotropy of displacement energy for, 20: 2515
radiation effects on, high-energy electron and proton, 20: 2517
radiation effects on, high-energy electron, 20: 2518
radiation effects on electric properties of, annealing during fabrication of p-n junctions of fast-neutron, 20: 2440
radioinduced defects in, structural properties of, 20: 2486
radioinduced defects in, effects of doping with lithium on, 20: 2491
radioinduced defects in, annealing of, 20: 2506
radioinduced defects in, 20: 2516
radioinduced defects in, annealing and drift mobility of, 20: 2507
radioinduced electron-hole pairs in n-type, formation energy for alpha, 20: 2362
radioinduced resistance fluctuations in transistors of, carrier removal effects on electron, (E/T), 20: 2188
**SILICON CARBIDES**
radiation effects on electric properties of n-type and p-type, 20: 2503
radiation effects on semiconducting properties, 20: 2504
**SILICON JUNCTIONS**
radiation effects on lithium-drifted p-i-n, 20: 2510
radiation effects on p-n, charge and field dependence of, 20: 2511
radiation effects on, for semiconductors, 20: 2413 (AD-618688)
radiation effects on n-p-n, neutron, 20: 2184(R) (AD-614618)
radiation effects on n-p-n, neutron, 20: 2185(R) (AD-618194)
**SILICON OXIDES**
analytical use for decontamination of aqueous solutions, 20: 1742 (INR-636/XIII/J)
sorptive properties for plutonium, acidity effects on, 20: 1849
testing for use in shaft seals for potassium space power systems, 20: 2242
$SiO_2$–$ThO_2$, liquidus curves and thermodynamic properties, 20: 2326 (IFA-FR-39)
$SiO_2$–$ThO_2$–$UO_2$, liquidus curves and thermodynamic properties, 20: 2326 (IFA-FR-39)
**SILICON SYSTEMS**
Ge–Mg–Si, radiation effects on electric properties of $Mg_2Ge_{0.8}Si_{0.2}$, 20: 2502
Ge–Si, preparation for radiation detectors, 20: 2182(P)
**SILICONES**
effects on radioinduced changes in dielectric properties of mica paper, 20: 1897 (NASA-TN-D-3032)
radiation effects on coatings of, for spacecraft, 20: 2428 (NASA-SP-55, pp 365-79)
radioinduced polymerization of hexamethylcyclotrisiloxane in solid phase, 20: 1903
**SILTS**
analysis in surface waters, activation, 20: 1739(R) (GA-4297)
**SILVER**
corrosion resistance to mercury at 900°F, 20: 2264
determination of trace amounts of, by substoichiometric radioisotopic dilution analysis, 20: 1786
deuteron elastic scattering at 25.3 Mev, optical model analysis of, (E/T), 20: 3053
deuteron elastic scattering at 27.5 Mev, angular distribution for, (E/T), 20: 3057
effect on the dissolution of ceramics containing beryllium oxide, catalytic, 20: 2252(P)
effects on grain boundary of copper at 200 to 1000°C, 20: 2348 (UCRL-16051)
mechanical properties of internally oxidized, 20: 3639 (UCRL-11194)
separation of trace amounts of, from alkali metals, alkaline earths, and

rare earths, 20: 1958
**SILVER ALLOYS**
Ag–W, sintering in presence of liquid phase, kinetics of, 20: 2286
Au–Ag–Sn, solute interactions in dilute, (E/T), 20: 2349 (UCRL-16320)
Cd–Ag, mechanical properties of internally oxidized, 20: 3639 (UCRL-11194)
In–Ag–Sn, solute interactions in dilute, (E/T), 20: 2349 (UCRL-16320)
Li–Ag, diffusion of tritium in, 20: 2317 (EURAEC-1830)
Mg–Ag, entropy of formation of AgMg ordered phase, (T), 20: 2349 (UCRL-16320)
Mg–Ag, mechanical properties of internally oxidized, 20: 3639 (UCRL-11194)
**SILVER CHLORIDES**
radiation effects on crystal structure of, mechanism of beta, 20: 2426 (LA-3387)
**SILVER COMPLEXES**
chlorophyllin, radiosensitivity effects in mice, gamma, 20: 1692
**SILVER NITRATES**
Ag–$AgNO_3$, cation exchange in molten, 20: 2520(R) (IA-920)
**SILVER SYSTEMS**
Ag–$AgNO_3$, cation exchange in molten, 20: 2520(R) (IA-920)
Cu–Ag–TaC, production of cermets of, 20: 2261(R) (UCRI-326)
MgO–Ag, annealing effects on structure of dispersion-hardened, 20: 2325 (HW-SA-3767)
MgO–Ag, structure of deformed, 20: 2324 (HW-SA-3765)
**SINGLE CRYSTALS**
nuclear quadrupole resonance in, energy levels and line intensities from, (T), 20: 3284
**SINTERING**
kinetics of, in the presence of liquid phase, 20: 2286
**SKELETON**
radiation injuries of vertebrae column, after radiotherapy during childhood, 20: 1702
**SKIN**
radiation dose to, during diagnostic radiography, 20: 1704
radiation effects on free radical properties of melanin in, uv, 20: 1684
radiation injuries of swine, pathology, 20: 1609 (BNL-9477)
radiotherapy of carcinomas of, 20: 1718
radiotherapy of hemangiomas of, in infants, 20: 1719
**SODIUM**
analysis for oxygen, engineering drawings of sodium sampler design for, 20: 1799
cavitation damage in liquid, 20: 2243
collisions of atoms of, with rare gas atoms and hydrogen and nitrogen molecules, ionization in, (E), 20: 2639
compatibility with niobium–zirconium alloys at high temperatures, 20: 2236
corrosion resistance to mercury at 900°F, 20: 2264
corrosive effects on titanium–vanadium alloys, 20: 3320(R) (ANL-7082, pp 1-28)
corrosive effects on metals, dependence on polarization, 20: 3321(R) (ANL-7082, pp 29-53)
corrosive effects on niobium–zirconium alloy at high temperatures, 20: 2268
corrosive effects of flowing, on type-316 stainless steel at high temperatures, 20: 2274
corrosive effects on metals, loop geometry effects on, 20: 2295
corrosive effects on austenitic and ferritic steel, in pumped systems, 20: 2296
determination in drugs, hair, oils, river silts, soils, and tobacco, activation, 20: 1739(R) (GA-4297)
determination in greases and soils, activation, 20: 1728(R) (GA-4041)
determination in selenium by neutron activation methods, 20: 1769
determination of trace amounts in uranium compounds by activation analysis, 20: 1784
diffusion of lithium-6 and -7 in, isotope effect in, 20: 3305(T)
effects of carbon-contaminated, on austenitic stainless steel, 20: 2244
effects on rupture of type 316 stainless steel of high-carbon or -oxygen, 20: 2258(R) (MSAR-65-149)
heat transfer at high heat fluxes, 20: 2008(R) (AD-622825)
heat transfer by boiling, burnout heat flux in, 20: 2023
heat transfer of boiling, effect of surface conditions on, (E), 20: 2017(R) (TID-22312)
purification in circulation loops, reaction-product, 20: 1960
separation of trace elements from, by precipitation ion exchange, 20: 1958
temperature in MHD cell, (E), 20: 2673
thermal conductivity of, at 90 to 850°C, 20: 2370
thermodynamic properties of, at high temperatures, 20: 1815 (NRL-6241)
**SODIUM ALLOYS**
Bi–Na, corrosive effects on carbon steel and stainless steel, 20: 2275
K–Na, analysis for oxygen, 20: 1799
**SODIUM ASTATIDES**
entropy and thermal capacity at 0 to 300°K, 20: 1859
**SODIUM BROMIDES**
activity of coefficients of highly concentrated aqueous, 20: 2520(R) (IA-920)
radiation effects on crystal structure of, mechanism of beta, 20: 2426 (LA-3387)
radiation effects on electric conductivity of, (E), 20: 2434(R) (TID-22242)
**SODIUM CARBONATES**
analysis for rare earth oxides in natron, activation, 20: 1731 (BNL-9614)
**SODIUM CHLORATES**
chlorine-35 spin echo and NQR in monocrystalline, 20: 3144
**SODIUM CHLORIDES**
beryllium growth textures on, 20: 3306(T)
corrosive effects on molybdenum and vanadium, stress-, 20: 2254 (BM-RI-6680)
heat of solution in heavy and light water, (E), 20: 1825
radiation effects on crystal structure of, mechanism of beta, 20: 2426 (LA-3387)
$AlCl_3$–NaCl, stability of zirconium dichloride in, 20: 1822(T) (ANL-Trans-233)
$BaCl_2$–NaCl, stability of zirconium dichloride in, 20: 1822(T) (ANL-Trans-233)
$CaCl_2$–NaCl, stability of zirconium dichloride in, 20: 1822(T) (ANL-Trans-233)
KCl–NaCl–$YCl_3$, phase studies on, 20: 1872
KCl–NaCl, stability of zirconium dichloride in, 20: 1822(T) (ANL-Trans-233)
KCl–NaCl–$ZrCl_4$, stability of zirconium dichloride in, 20: 1822(T) (ANL-Trans-233)
$MgCl_2$–NaCl, stability of zirconium dichloride in, 20: 1822(T) (ANL-Trans-233)
**SODIUM FERROCYANIDES**
iron-57 Mössbauer spectra from, (E), 20: 3296
**SODIUM FLUORIDES**
heat of solution in heavy and light water, (E), 20: 1825
radioinduced color center formation in crystals of, 20: 1908
spectroscopy of, measurement of rotational transitions in, 20: 1876
**SODIUM FLUOSILICATES**
reactions with dysprosium, gadolinium, and yttrium chlorides, precipitation in, 20: 1870
**SODIUM HYDRIDES**
separation from sodium in circulation loops, 20: 1960
**SODIUM HYDROXIDES**
corrosive effects on molybdenum and vanadium, stress-, 20: 2254 (BM-RI-6680)
**SODIUM IODIDES**
radiation effects on crystal structure of, mechanism of beta, 20: 2426 (LA-3387)
**SODIUM ISOTOPES Na-22**
beta decay of, beta–gamma directional correlation in, (E), 20: 3054
beta decay of, spin dependence of Rayleigh scattering from, (E), 20: 3082
gamma transition at 1274.6 kev, (E), 20: 3043
**SODIUM NITRATES**
$LiNO_3$–$NaNO_3$, solvent properties for water vapor, 20: 1812 (EUR-2495.e)
**SODIUM OXIDES**
impurities in, equipment for control of, 20: 3321(R) (ANL-7082, pp 29-53)
separation from sodium in circulation loops, 20: 1960
**SODIUM PHOSPHATES**
complexes with uranium, separation rare earths by ion exchange, 20: 1762
**SODIUM SYSTEMS**
K–Na, chemistry in experimental SNAP-8 reactor, 20: 3564
K–Na, corrosive effects on niobium–zirconium alloy and type-316 stainless steel, 20: 2273
**SOILS**
analysis in crime detection of activation, 20: 1736(R) (GA-3491)
analysis in crime detection, activation, 20: 1738(R) (GA-4041)
analysis in crime detection, activation, 20: 1739(R) (GA-4297)
rare earth, thorium, and yttrium contents in Tomsk region, 20: 2065
**SOLAR FLARES**
detection of, frequency and observing-time patterns in, (E), 20: 2575
effects on manned military space vehicles, (T), 20: 2656 (NASA-SP-71, pp 265-86)
effects on terrestrial events, (E), 20: 2855
electromagnetic wave emission with continuous spectra during, 20: 2580
occurrence of, correlation with pre-existing calcium network, (E), 20: 2578
properties of class 3, correlation between optical and radio, (T), 20: 2582
proton doses from, calculation of, (T), 20: 2658 (NASA-SP-71, pp 527-33)

radiation effects on spacecraft personnel, (T), 20: 2655 (NASA-SP-71, pp 85-96)
shielding alpha particles and protons from, (T), 20: 3251 (NASA-SP-71, pp 507-12)
shielding manned space vehicles against, (T), 20: 3245 (NASA-SP-71, pp 407-14)
shielding space vehicle personnel from, using superconducting-magnet dynamic shielding, (T), 20: 3241 (NASA-SP-71, pp 199-209)

**SOLAR RADIATION**
properties of, review, 20: 2653 (NASA-SP-71, pp 19-29)

**SOLENOIDS**
design of eighth-order power optimized, analysis of, (E), 20: 2522 (ORNL-P-1516)

**SOLID PROPELLANTS**
combustion of, effects of additives on rates in, 20: 2668 (AD-615124)
development for space research, 20: 2862

**SOLIDS**
book: *Nuclear Magnetic Resonance and Relaxation in Solids*, 20: 3316
contacts by, mechanical and thermal properties of, (E/T), 20: 1811 (EUR-2486.e)
diffusion of rare gases in, effects of traps on, (T), 20: 2360(T) (ORNL-tr-314)
isotopic diffusion effect in, 20: 3304(T)
properties of geometric, computer program for calculating, 20: 3633 (SC-TM-64-1686)
radiation effects on, thermal, 20: 2427 (NASA-SP-55)

**SOLUTIONS**
decontamination of aqueous, use of silica gel for, 20: 1742 (INR-636/XIII/J)

**SOLVATION**
mechanism of selective, in mixed solvents, 20: 2520(R) (IA-920)

**SOLVENT EXTRACTION PROCESSES**
design of thiocyanate, for beryllium in aqueous solutions, 20: 1974(P)
developments in, review on, 20: 1741 (IA-1031)
equipment for uniform droplet dispersion in, 20: 1800

**SOLVENTS**
electrolyte solvation in mixed, ionic free energy of, 20: 2520(R) (IA-920)

**SOUND**
velocity in crystalline helium, (T), 20: 2912

**SOUTHWEST EXPERIMENTAL FAST OXIDE REACTOR**
fuel temperature of, survey of sensors for measuring, 20: 3473 (GEAP-4903)

**SOVIET UNION**
rare earth, thorium, and yttrium contents in soils in Tomsk region, 20: 2065

**SPACE**
book: *Advances in Space Research*, 20: 2862
book: *Space Physics with Artificial Satellites*, 20: 2863(T)
gamma ray intensity in, high-energy, (E/T), 20: 2586
radiation distributions in, effects on manned space missions, 20: 2652 (NASA-SP-71, pp 1-4)
radiation effects in, compilation of projects on, 20: 2433 (REIC-Memo-27)

**SPACE FLIGHT**
cosmic radiation effects on manned, 20: 2652 (NASA-SP-71, pp 1-4)
cosmic radiation effects on manned military, (T), 20: 2656 (NASA-SP-71, pp 265-86)
effects on seeds, genetic, 20: 1649
power plants for, development of thermoelectromagnetic pumps for Rankine-cycle, (E), 20: 1988 (NAA-SR-11198)
power systems for, waste-heat radiators for, 20: 3556
radiation doses from inner and outer radiation belts during manned, 20: 2663

**SPACE VEHICLES**
cosmic proton dosimetry in, using silicon-detector arrays, (E), 20: 2133 (NASA-SP-71, pp 245-50)
cosmic radiation effects on manned military, (T), 20: 2656 (NASA-SP-71, pp 265-86)
cosmic radiation effects on occupants of high-altitude aircraft, (T), 20: 2657 (NASA-SP-71, pp 287-99)
effects of meteoric particles, radiation, and space vacuum on, estimates of magnitude and nature of, 20: 2036 (AD-618030)
power systems for, bearing materials for Rankine-cycle, 20: 3555
power systems for, design study of fission-electric cell-reactor, 20: 3577
power systems for, ceramic-refractory metal seals for, 20: 2292
power systems for, fabrication of beryllium radiators for, 20: 2293
propulsion of, cold-plasma induction system for, 20: 2041
radiation doses from solar-flare protons in, calculations of, (T), 20: 2658 (NASA-SP-71, pp 527-33)
radiation effects of solar flares on personnel in, (T), 20: 2655 (NASA-SP-71, pp 85-96)
radiation effects on thermal control coatings for, 20: 2428 (NASA-SP-55, pp 365-79)
radiation environment from trapped particles, 20: 2849
radiation protection of astronauts in Apollo Command/Service Module, (T), 20: 3244 (NASA-SP-71, pp 365-75)
shielding against protons, design of spherical minimum-mass configurations for, (T), 20: 3242 (NASA-SP-71, pp 225-8)
shielding against protons, spherical configurations for, (T), 20: 3243 (NASA-SP-71, pp 229-34)
shielding against solar-flare alpha particles and protons, (T), 20: 3251 (NASA-SP-71, pp 507-12)
shielding by selective orientation in anisotropic cosmic-particle fluxes, (T), 20: 3249 (NASA-SP-71, pp 473-6)
shielding for manned, performance of copper as, (T), 20: 3240 (NASA-SP-71, pp 183-8)
shielding for manned, mass calculations for, (T), 20: 3245 (NASA-SP-71, pp 407-14)
shielding for, performance of superconducting-magnet dynamic, (T), 20: 3241 (NASA-SP-71, pp 199-209)

**SPARK CHAMBERS**
design of wire, with external acoustic transducers, 20: 2132 (JINR-P-2368)
particle track measuring in, semiautomatic scanning device for, 20: 2130 (JINR-P-2340)
performance of symmetric wire, for track coordinate determination, 20: 2129 (JINR-P-2312)
proton ionizing power in helium and neon filled, measurement of, (E), 20: 2128 (JINR-E-2324)
spark displacement in magnetic fields, (E/T), 20: 2131 (JINR-P-2344)

**SPECTROMETERS**
design of scanning collimated, for measuring particle energy spectra in DCX-2, (E), 20: 3178 (ORNL-P-1513)
shutters for, design of 1.5- to 3000-$\mu$sec, (E), 20: 2125 (CEA-R-2816)

**SPECTROPHOTOMETERS**
burner design for, engineering drawings of acetylene–oxygen, 20: 1798

**SPECTROPHOTOMETRY**
of indium and tantalum, use of bromopyrogallal red in, 20: 2520(R) (IA-920)

**SPECTROSCOPY**
theory of resonance broadening of spectral lines by atom-atom impacts, (T), 20: 2620
theory of wing broadening of hydrogen Lyman $\alpha$ line by electrons and ions in a plasma, (T), 20: 3217
transformation matrices for atomic, 20: 2604

**SPERM**
radiation effects on Drosophila spermatocytes, from incorporated tritium-labeled thymidine or uridine, $\beta$, 20: 1657

**SPHERES**
gravitational collapse of charged dust, relativistic model for, (T), 20: 2879
proton depth-dose measurements in tissue-equivalent, 20: 1620 (UCRL-16154)

**SPLEEN**
radiation effects on immune reactions to injected cells of, in rats, 20: 1632

**SPORES**
cytology and control mechanisms for formation of, by *Bacillus cereus* and *B. subtilis*, 20: 1582(R) (NYO-2038-2)
radiation effects on formation of, by yeast, 20: 1664
radiation effects on, genetic, 20: 1622 (WT-820)
radiosensitivity of *Clostridium perfringens* Type A, gamma, 20: 1679

**SPRINGS**
development of pneumatic, for vibration damping and isolation, (T), 20: 3613 (CONF-651016-1)

**STAINLESS STEEL**
bonding of 316, to graphite, brazing techniques for, 20: 2294
cavitation damage to 316, in liquid sodium, 20: 2243
compatibility of 304, with plutonium–uranium–zirconium alloys, 20: 2229
compatibility of 304, with plutonium–thorium–uranium alloys, 20: 2230
corrosion by bismuth-sodium alloy, 20: 2275
corrosion by bismuth and tin, 20: 2275
corrosion by molten cadmium–magnesium–zinc alloy at 500, 750, and 850°C, 20: 2265
corrosion by molten cadmium–magnesium alloys at 750°C, 20: 2265
corrosion cracking by magnesium chloride of austenitic and austeno-ferritic, stress-, 20: 2256(R) (EURAEC-1449)
corrosion of 310, by steam and water at 800 to 1500°F, 20: 3471(R) (GEAP-4861)
corrosion of 316, by potassium–sodium system, 20: 2273
corrosion of 316, by flowing sodium at high temperatures, 20: 2274
corrosion of 316, in pumped sodium systems, 20: 2296
cracking of 304 cladding, on reactor vessels, 20: 3321(R) (ANL-7082, pp 29-53)
diffusion of fission products in 304, 20: 2389
effects of carbon-contaminated sodium on austenitic, 20: 2244

fatigue of type 304, at 800°C, plastic, 20: 2320(R) (GEMP-52A, pp 23-5)
flow of paste of, in sodium loop, 20: 3460
mass transfer of carbon and nitrogen from 316, to niobium–zirconium alloy in liquid potassium, 20: 2239
mechanical properties of austenitic and austeno-ferritic, effects of test temperature on, 20: 2256(R) (EURAEC-1449)
radiation effects at cryogenic temperatures, 20: 2459
radiation effects on bursting pressure and fatigue life of pressure tubes of, neutron, 20: 2435 (WAPD-T-1720)
radiation effects on mechanical properties of, at high temperatures, 20: 2430 (ORNL-P-1713)
radiation effects on mechanical properties of types 304 and 347, at 25 to 850°C, 20: 2477
radiography of boron in 304, using neutrons, (E), 20: 3471(R) (GEAP-4861)
reactions with plutonium–uranium–zirconium alloys at high temperatures, 20: 3320(R) (ANL-7082, pp 1-28)
rupture of type 316, effects of high-carbon or -oxygen sodium at 1200°F on, 20: 2258(R) (MSAR-65-149)
testing of 316, for use in liquid-metal turbine blades and nozzles, 20: 2240
transfer of carbon and nitrogen to niobium–zirconium alloy in potassium, 20: 2270
welding to Hastelloy X and Inconel, 20: 3472(R) (GEAP-4891)

**STANDARDS**
preparation and calibration of radium, 20: 1941

**STANFORD LINEAR ACCELERATOR**
beam storage ring for, antiproton and meson ($\mu$) trapping by, 20: 2547 (UR-375-98)

**STARS**
atmospheres of neutron, x-ray spectra of, (T), 20: 2568
element synthesis and destruction in types A and B, (T), 20: 2565
energy of neutron, correlation with light curves of type-I supernova, (T), 20: 2584
evolution of medium-mass, processes in early, (T), 20: 2567
explosion of supernova, into interstellar magnetic field, (T), 20: 2569
explosion of supernova, into interstellar magnetic field, (T), 20: 2570
formation of, statistical model for, (T), 20: 2574
gas flow in, boundary conditions at nonstationary ionization front in, (T), 20: 2572
gas flow in, model for nonstationary ionization fronts for, (T), 20: 2571
gravitational radiation from novas, quasars, and supernovas, (T), 20: 2877(T)
gravitational radiation emission by, (T), 20: 2884
lithium depletion during pre-main-sequence contraction, (T), 20: 2566
lithium isotope ratio in Hyades F, (E/T), 20: 2577
neutrino emission from, energy balance in universe by, (T), 20: 2587
photosphere boundary conditions for, method for integration downward from, (T), 20: 2581
radiation from newly formed, hydrogen ionization by, (T), 20: 2562(R) (AD-614715)
stability of magnetoturbulent massive, relativistic, (T), 20: 2579
stability of, adiabatic exponent for helium-iron transition and pair creation for, (T), 20: 2588
temperature structure of atmospheric model calculations of, 20: 2564
x-ray spectra of Scorpius (SCO-XR-1), (E), 20: 2585

**STATISTICS**
prediction analysis of exponential functions, 20: 2217
spin temperature formalism in quantum, (T), 20: 2864 (COO-1198-300)

**STEAM**
corrosive effects on aluminum–chromium–iron–yttrium alloy, effects of pre-oxidation and strain on, 20: 2223(R) (GEMP-51A)
corrosive effects on niobium–tin–zirconium alloys, effects of alloy additions on, 20: 2255(R) (EURAEC-1323)
corrosive effects on Zircaloy-4, effects of air introduction on, 20: 2257(R) (GEMP-57A, pp 47-52)
deuterium exchange with hydrogen in presence of fissionable material for production of heavy water, 20: 1884(P)
effects on niobium–yttrium–zirconium alloy at 400-500°C, 20: 2276(P)
embrittlement of Zircaloy-4 during dynamic heating, 20: 2257(R) (GEMP-52A, pp 47-52)
heat transfer properties in rod bundles with turbulence promoters, (E), 20: 3471(R) (GEAP-4861)
pressure drop in condensing flow of, method for calculating static, 20: 1814 (NAA-SR-63333)
reactions with clad urania fuels, 20: 2221(R) (ANL-7082, pp 62-73)
separation from water, design of device for, 20: 2024(P)
steam–water, pressure drop in natural-circulation single-component flow at low pressures, 20: 2021

**STEARIC ACID, METHYL ESTER**
radiolysis and storage of tritium-labeled, self-, 20: 1938 (EUR-2452.e)

**STEEL**
corrosion of austenitic and ferritic, in pumped sodium systems, 20: 2296
fabrication of shielding materials of, 20: 2301(P)
failure mechanisms in, in reactor pressure vessels, 20: 2402
fracture mechanics in, in reactor pressure vessels, 20: 2401
gamma dose albedos for, differential, 20: 3270
neutron scattering by cylinders of, fast, (E/T), 20: 3265
properties of radiation-sensitive and insensitive A302B, 20: 2437 (WERL-8844-6)
properties of, strain softening effects on, 20: 2311 (AD-618925)
radiation effects on reactor structures of, 20: 2408(P) (AD-614899)
radiation effects on A302B, annealing effects on, 20: 2455
radiation effects on, neutron, 20: 2474
radiation effects on, in pressure vessels, 20: 2479
radiation effects on mechanical properties of, 20: 2409(R) (AD-617319)
radiation effects on hardening and embrittlement of bcc, 20: 2472

**STELLARATORS**
plasma of S-1, interactions of runaway electrons and, (E), 20: 3186

**STELLARATORS (C)**
development of, review of, 20: 3196

**STRESS ANALYSIS**
of air blast loading of spherical reinforced concrete domes, 20: 2035 (AD-615017)
of pyrolytic-carbon coatings for fuel particles, model for, 20: 2235
of reactor fuel plate cladding, 20: 3453
photoelastic nondestructive methods for experimental, 20: 2026 (UCRL-13188)

**STRONTIUM**
separation from milk, 20: 1975(P)
separation of trace elements from, by precipitation ion exchange, 20: 1958

**STRONTIUM CHLORIDES**
diffusion of water in, coefficients of, 20: 1865

**STRONTIUM FLUORIDES**
charge compensation by fluoride ions in rare earth-doped, 20: 2520(R) (IA-920)

**STRONTIUM ISOTOPES Sr-85**
production using ORNL 86-in. cyclotron, 20: 2212
uptake by rat hair, 20: 1695

**STRONTIUM ISOTOPES Sr-87**
nuclear quadrupole moment, (E), 20: 3087

**STRONTIUM ISOTOPES Sr-89**
content in fallout particles, 20: 2053
determination in algal cells by liquid scintillation, 20: 1603
determination in sea water, methods for, 20: 1749 (USNRDL-TR-912)
separation from milk by electrodialysis, 20: 1972(P)
separation from rain water, method for, 20: 1778
uptake by algal cells, 20: 1603

**STRONTIUM ISOTOPES Sr-90**
content in fallout particles, 20: 2053
content in milk, 20: 2046 (BIO/04/64)
content in milk in Israel, 20: 2520(R) (IA-920)
content in milk, Italy, 1964, 20: 2047 (EUR-2509.e)
content in teeth of Israeli children born 1950 to 1956, 20: 2520(R) (IA-920)
deposition with respect to atmospheric release of, calculation of, 20: 2074 (AHSB(RP)M-40)
determination in presence of yttrium-90 by liquid scintillation spectrometry, 20: 1766
determination in sea water, methods for, 20: 1749 (USNRDL-TR-912)
determination in water radiochemical, 20: 1754
separation from aqueous solutions, use of silica gel for, 20: 1742 (INR-636/XIII/J)
separation from milk by electrodialysis, 20: 1972(P)
separation from rain water, method for, 20: 1778
separation from yttrium-90 by election process, 20: 2211
shielding of, bremsstrahlung attenuation factors for, 20: 3254

**STRONTIUM OXIDES**
spectra of F centers in single crystals of, paramagnetic-resonance, (E), 20: 3087

**STRUCTURES**
blast effects on, trajectory analysis of fragments produced by, 20: 3610 (AD-622333)
blast loading of spherical domes of reinforced concrete, stress-strain effects of, 20: 2035 (AD-615017)
gamma dose distributions in compartmented, from external sources, 20: 3275
shielding for hardened, design of, (T), 20: 3276

**STYRENE**
*p*-nitro-, radioinduced polymerization at low temperatures, 20: 1893(R) (AD-618228)
radioinduced polymerization with polyvinyl ester, 20: 1910
radioinduced polymerization at low temperatures, gamma, 20: 1925
radioinduced polymerization with formaldehyde, effects of dichloro-

methane and ethyl ether on, 20: 1914
**STYRENE, α-METHYL-**
radioinduced polymerization with formaldehyde, effects of dichloromethane and ethyl ether on, 20: 1914
**STYRENE POLYMERS**
proton polarization and spin relaxation rates in, at low temperatures, (E/T), 20: 3143
radiation effects on dielectric properties of, electron, 20: 1897 (NASA-TN-D-3032)
shock impingement studies on styrofoam, (E/T), 20: 3324(R) (IITRI-578P21-13)
$PuO_2$–polystyrene, criticality studies on compacts of, 20: 3368 (BNWL-SA-214)
**SUBMARINE REACTORS**
design of PWR, with horizontal pressure vessel, 20: 3578(P)
**SUCCINIMIDES**
*N*-vinyl-, radioinduced polymerization of liquid, 20: 1912
**SULFONATES**
effects of methyl methanesulfonate, in *Bacillus subtilis*, 20: 1624
**SULFUR**
spectra of, isolated in inert gas matrices at high temperature, 20: 1818 (UCRL-11976)
**SULFUR COMPOUNDS**
preparation of fluorine-containing, effects of water on, 20: 1881
**SULFUR ISOTOPES S-32**
neutron reactions (n,p) with, cross sections for phosphorus-32 production in, (E), 20: 3020 (ORNL-TM-1065)
**SULFUR ISOTOPES S-33**
energy-level transition probabilities of, E2, (T), 20: 3115
neutron reactions (n,p) with, cross sections for phosphorus-33 production in, (E), 20: 3020 (ORNL-TM-1065)
**SULFUR ISOTOPES S-35**
determination in biological materials, method for, 20: 1758
**SULFURIC ACID**
corrosive effects on molybdenum and vanadium, stress-, 20: 2254 (BM-RI-6680)
reactions with ruthenium oxide, complex formation in, 20: 1853
solvent properties for erbium and yttrium phosphates, 20: 1873
ethanol–naphthol–$H_2SO_4$, radiolysis in aqueous solutions, 20: 1920
ethanol–naphthalenesulfonic acid–$H_2SO_4$, radiolysis in aqueous solutions, 20: 1920
ethanol–$H_2SO_4$–tetramethyl-p-benzoquinone, radiolysis in aqueous solutions, 20: 1920
naphthalene–$H_2SO_4$, radiolysis in alcoholic, aqueous, and hydrocarbon solutions, 20: 1920
**SULFURYL FLUORIDE**
peroxydi-, properties as fluorinating agent, 20: 1881
**SUN**
activity of, correlation with solar-terrestrial events, (E), 20: 2855
gas flow stability in corona and prominences of, dilute, (T), 20: 2573
photosphere boundary conditions for, method for integration downward from, (T), 20: 2581
photosphere of, kinetics and structure of hydrodynamic disturbances in, (T), 20: 2589
spot magnetic field strengths and polarities during IGY, 20: 2563
spot structure on, intensity profiles for, (T), 20: 2576
sunspot activity of, ionospheric effects of, 20: 2848 (AD-615111)
x-ray spectra, (E), 20: 2585
**SUPERCONDUCTIVITY**
effect of metallic contacts on gapless, (T), 20: 2910
magnetic field penetration effects on breakdown of surface, (T), 20: 2900
paramagnetic-impurity and spin-orbit-coupling effects in, Abrikosov-Gor'kov theory for, 20: 2929
surface states correlation with high-temperature, review of, (T), 20: 2903
**SUPERCONDUCTORS**
critical fields of thin films of, (T), 20: 2926
critical temperature of, with an impurity in the two-band model, (T), 20: 2925
current propagation in composite, minimum, (T), 20: 2904
electron spectrum of intermediate state of, (T), 20: 2923
electron spin resonance in, model for conduction, (T), 20: 2899
electron tunneling in, resonant mode interactions with a-c Josephson, (E/T), 20: 2895
fabrication into cables, (E), 20: 3612 (CONF-651001-6)
fluxoid conservation in thin-film ring, 20: 2927
Ginzburg-Landau parameters of type-II, (E/T), 20: 2906
magnetic flux jumps in hard, in pulsed magnetic fields, (E), 20: 2921
magnetic hysteresis curves of, instruments for recording, (E), 20: 2913
Meissner effect and vortices in, (T), 20: 2914
neutron transmission through, in the mixed state, depolarization in, (T), 20: 2998
paramagnetic-impurity and spin-orbit-coupling effects in, Abrikosov-Gor'kov theory for, 20: 2929
vehicles, (T), 20: 3241 (NASA-SP-71, pp 199-209)
performance in dynamic magnetic-field radiation shields for space
properties of barium tungsten bronze, (E), 20: 2901
properties of beryllium–rhenium alloy, (E), 20: 2898
properties of molybdenum–rhenium alloy, (E/T), 20: 2890 (AFML-TR-65-154)
properties of nitrided niobium–zirconium wires, (E), 20: 2891
thermal conductivity of lathanum, (E), 20: 2893
thermodynamics of, in one and two dimensions, (T), 20: 2889 (AD-618203)
transition temperature of superimposed films of iron and tin, 20: 2894
transition temperature of, effect of Suhl-Abrikosov resonance on, 20: 2911
transition temperature of lead, effect of transition metals and transition-metal oxides on, 20: 2916
transition temperature of lead films on superconducting substrates, (E), 20: 2917
transition temperatures of thin-film, effect of thin oxide layer on, 20: 2915
transition to normal state in variable fields, mechanisms of, (E), 20: 2902
tunneling characteristics of aluminum–aluminum oxide–lead, geometrical resonance in, (E), 20: 2909
tunneling characteristics of contacts of normal metals and, (T), 20: 2910
voltage in type II, transverse, (E), 20: 2897
vortex motion in type-II, theory of, (T), 20: 2908
**SUPERCRITICAL ONCE-THRU TUBE REACTOR**
design and development, 20: 3485(R) (WCAP-2120)
**SUPERHEATERS (NUCLEAR)**
economics, 20: 3508
feasibility of mixed-spectrum steam-superheat power reactors, (T), 20: 3471(R) (GEAP-4861)
kinetics of mixed-spectrum steam-cooled, (E/T), 20: 3471(R) (GEAP-4861)
operations of MSSCEF, (E), 20: 3471(R) (GEAP-4861)
**SURFACE WATERS**
analysis for pollution, activation, 20: 1739(R) (GA-4297)
radioactive waste disposal in, hydrological problems in, 20: 2082 (CEA-Bib.-59)
**SURFACES**
contour measurements on small samples, photogrammetric techniques for, 20: 2033
gas-particle effects on, relativistic theory of, 20: 2841
**SURGERY**
effects on radiosensitivity of patients, 20: 1717
**SWEDEN**
fallout monitoring, 1961 to 1964, 20: 2054
**SWIMMING POOL REACTORS**
irradiation enclosure design for, 20: 3602(P)
**SWINE**
effects of aging on biochemical and hematological parameters in, 20: 1581 (BNWL-SA-341)
radiation effects on weight gain of progeny of, x, 20: 1677
radiation injuries of skin of, pathology, 20: 1609 (BNL-9477)
**SYNCHROCYCLOTRONS**
beam intensity of, method for stabilizing, (E), 20: 2536 (JINR-P-2341)
beam pulse duration in JINR, method for increasing, (E/T), 20: 2548
**SYNCHROTRONS**
component handling systems for 200-Bev, design of shielded, (E), 20: 2542 (UCRL-16236)
design of 200-Bev proton, 20: 2543 (UCRL-16238)
experimental facilities at Frascati, 20: 2521 (LNF-65/28)
operation of Frascati, 6-64 to 7-65, 20: 2521 (LNF-65/28)
proton storage rings for CERN, phase locking systems of, (E), 20: 2535 (CERN-65-31)
**SYRINGES**
use in radiochemistry, septum cap technique for, 20: 1945
**SYSTEMS FOR NUCLEAR AUXILIARY POWER**
control of SNAP reactors, static, 20: 3559
description, 20: 2862
performance of thermionic reactors, 20: 3547 (NAA-SR-Memo-7881)
re-entry flight demonstration (RFD-2) for, heating data from, 20: 2207
reactor dose rates and power level for, probability analysis of, (T), 20: 3549 (SC-RR-65-417)
safety analysis for, review of, 20: 3548 (SC-DC-65-1752)
testing of, SNAPTRAN-2 destructive, 20: 3561
**SYSTEMS FOR NUCLEAR AUXILIARY POWER (SNAP-2)**
fission product release from irradiated uranium–zirconium hydride fuel for 2/10A, 20: 3562
**SYSTEMS FOR NUCLEAR AUXILIARY POWER (SNAP-8)**
coolant chemistry of experimental reactor S8ER, 20: 3564
reactivity coefficients of SNAP-8ER, dynamic measurement of, 20: 3557
testing facility for Flight Prototype of, design, (E), 20: 3550 (TID-21994)
**SYSTEMS FOR NUCLEAR AUXILIARY POWER (SNAP-10)**

fission product release from irradiated uranium–zirconium hydride fuel for 2/10A, 20: 3562
kinetics of SNAP-10A/2, with reactivity pulse excitation, 20: 3558
re-entry heating of fuel elements for 10A, 20: 3560
**SYSTEMS FOR NUCLEAR AUXILIARY POWER (SNAP-15)**
design, development, and performance of 15A, 20: 2204 (GA-6695)
**SYSTEMS FOR NUCLEAR AUXILIARY POWER (SNAP-19)**
re-entry heating of, 20: 2207
support structure design, development, and testing, 20: 2205 (MND-3169-52)
**SYSTEMS FOR NUCLEAR AUXILIARY POWER (SNAP-50)**
development of boiler for SNAP-50/SPUR, 20: 3554
development of SNAP-50/SPUR for lunar bases and space propulsion, 20: 3553
testing facilities for, design of, 20: 3545 (CNLM-5729)

# T

**TACHOMETERS**
design for enclosed turbine, 20: 2013 (ORNL-P-1661)
**TANTALUM**
bremsstrahlung and electron transport in, (T), 20: 3246 (NASA-SP-71, pp 437-48)
corrosion by bismuth and tin, 20: 2275
corrosion by hydrogen fluoride at 2000 to 2800°K, 20: 2261(R) (UCRI-326)
corrosion by lithium at 1200°C, 20: 3321(R) (ANL-7082, pp 29-53)
corrosion by molten cadmium–magnesium–zinc alloy at 500, 750, and 850°C, 20: 2265
corrosion by zinc and magnesium–uranium–zinc alloy, effects of molten chlorides on, 20: 2266
corrosion resistance to mercury at 900°F, 20: 2264
creep at 1680 to 2650°C, 20: 2394
determination by spectrophotometry using bromopyrogallal red, 20: 2520(R) (IA-920)
deuteron elastic scattering at 26 Mev, optical model analysis of, (E/T), 20: 3053
diffusion of krypton in, 20: 2321(R) (GEMP-52A, pp 43-5)
Doppler coefficients at 20 to 600°C, 20: 2958
electron-photon cascades in thick targets of, (T), 20: 3261
properties and uses of, review on, 20: 2307 (AD-613023)
radiation effects on hardening and embrittlement of bcc, 20: 2472
reactions with plutonium and gallium–iron–plutonium alloy at high temperatures, 20: 2228
reactivity effects in NERVA reactor, (T), 20: 3403
solubility in molten potassium, 20: 2237
**TANTALUM ALLOYS**
properties and uses of, review on, 20: 2307 (AD-613023)
Hf–Nb–Ta–V, strength at high temperatures, 20: 2407(P)
Hf–Ta–W, corrorsion by lithium at 1200°C, 20: 3321(R) (ANL-7082, pp 29-53)
Hf–Ta–W, properties for use with alkali metals at high temperatures, 20: 2241
Nb–Ta, Ginzburg-Landau parameters of superconducting, (E/T), 20: 2906
Nb–Ta, specific heat of superconducting, in magnetic fields, (E), 20: 2906
Nb–Ta–V–Zr, strength at high temperatures, 20: 2407(P)
Ta–W, corrosion by zinc and magnesium–uranium–zinc alloy, effects of molten chlorides on, 20: 2266
Ta–Zr, parameters for zirconium self-diffusion in, 20: 2356(T) (AERE-Trans-1030)
**TANTALUM BORIDES**
phase diagrams for, equilibrium, 20: 2403
**TANTALUM CARBIDES**
corrosion by hydrogen fluoride at 2000 to 3100°K, 20: 2261(R) (UCRI-326)
diffusion of carbon in, at 1800 to 2700°C, layer-growth measurements of, 20: 2398
reactivity effects in NERVA reactor, (T), 20: 3403
wetting by liquid cobalt, copper, iron, and nickel, 20: 1837
Be–Cu–TaC, production of cermets of, 20: 2261(R) (UCRI-326)
C–TaC, preparation and properties of, 20: 2351(R) (USBM-RC-1205, pp 3-7)
Cu–Ag–TaC, production of cermets of, 20: 2261(R) (UCRI-326)
Cu–TaC, production of cermets of, 20: 2261(R) (UCRI-326)
NbC–TaC, wetting by liquid copper, 20: 1837
Ta–$Ta_2C$, development of fiber-reinforced composites of, 20: 2219 (AMRA-CR-64-05/4)
**TANTALUM IODIDES**
phase diagrams for, equilibrium, 20: 2403
**TANTALUM ISOTOPES Ta-181**
**TANTALUM ISOTOPES Ta-182**
neutron cross sections from 1 kev to 14 Mev, (T), 20: 2961
beta decay of, gamma intensities and multipolarities from, (E), 20: 3112
energy levels of, from tantalum-182 decay, (E), 20: 3112
**TANTALUM OXIDES**
electric conduction of thin films of, in metal-insulator sandwich, (E/T), 20: 2405
testing for use in shaft seals for potassium space power systems, 20: 2242
**TANTALUM SYSTEMS**
structure of alpha pentoxide, defect, 20: 1880
C–Hf–Ta, preparation and properties of, 20: 2351(R) (USBM-RC-1205, pp 3-7)
C–Mo–Nb–Ta–Ti–W–Zr, creep properties at 1800 to 2200°F of Cb132M, 20: 2333(R) (NASA-CR-54457)
Ta–$Ta_2C$, development of fiber-reinforced composites of, 20: 2219 (AMRA-CR-64-05/4)
**TASTE**
radiation effects on wine, effects of dose on, 20: 2197
**TEAPOT OPERATION**
underwater nuclear explosions in, above-surface phenomena and base surge in, 20: 1979 (AD-614814)
**TECHNETIUM**
separation from aqueous waste solutions by ion exchange, 20: 1963
**TECHNETIUM ALLOYS**
Tc–W, superconducting properties, (E), 20: 2907
**TECHNETIUM ISOTOPES Tc-99**
incorporation of metastable, into colloid for tracer use in medicine, 20: 1696 (CONF-641126-1)
preparation of isomeric, by milking molybdenum-99, 20: 1730 (BNL-9601)
tracer use of, for diagnosis of tumors, 20: 1712
**TECHNICAL REPORTS**
list of Israel Atomic Energy Commission, 20: 2520(R) (IA-920)
**TEETH**
strontium-90 content in Israeli children, born 1950 to 1956, 20: 2520(R) (IA-920)
**TELLURIUM**
ionization in K-shell by alpha particles at 3 to 4 Mev, x-ray yields from, (E), 20: 2625
**TELLURIUM ISOTOPES Te-122**
gamma transition at 564.4 kev following Coulomb excitation, (E), 20: 3043
**TELLURIUM ISOTOPES Te-123**
energy-level transition probabilities of, E2, (T), 20: 3115
**TELLURIUM ISOTOPES Te-124**
gamma transition at 602.8 kev following Coulomb excitation, (E), 20: 3043
**TELLURIUM ISOTOPES Te-126**
gamma transition at 666.5 kev following Coulomb excitation, (E), 20: 3043
**TELLURIUM ISOTOPES Te-128**
gamma transition at 743.2 kev following Coulomb excitation, (E), 20: 3043
**TELLURIUM ISOTOPES Te-130**
gamma transition at 839.9 kev following Coulomb excitation, (E), 20: 3043
**TELLURIUM ISOTOPES Te-132**
content in fallout particles, 20: 2053
**TEMPERATURE**
effects on radioinduced chromosome aberrations in stored seed, 20: 1638
effects on radioinduced inactivation of ribonuclease, 20: 1682
effects on reactor physics parameters and scattering kernels, 20: 3435
**TENDONS**
electric properties of, 20: 3625(R) (NYO-3282-1)
**TERBIUM**
determination using Chromotrope 2B, photometric, 20: 1772
**TERBIUM ALLOYS**
Fe–Tb, preparation and structure of $MgCu_2$-type, 20: 2385(T)
Sc–Tb, magnetic structure properties of, 20: 2338 (ORNL-P-1735)
**TERBIUM MOLYBDATES**
$Eu_2(MoO_4)_3$–$Tb_2(MoO_4)_3$, preparation of single crystals of, by Czochralski method, 20: 1840
**TERBIUM OXIDES**
phase studies of, at 2200 to 2300°C, 20: 1827
**TERBIUM OXYBROMIDES**
preparation and crystal structure, 20: 1834
**TERBIUM SULFATES**
properties and structure of crystal hydrates of, 20: 1868
**TEREPHTHALIC ACID, ETHYLENE POLYMER ESTERS**
crystal structure of, determination of interplanar spacings using single-neutron diffraction, 20: 3308
radiation effects on dielectric properties of, electron, 20: 1897 (NASA-TN-D-3032)
**TERPHENYL**
radiolysis of meta- and ortho-, 20: 1928
radiolysis of, interpretation of, 20: 1927
**TETRANEUTRONS**
production in meson ($\pi^-$) reactions with nuclei at 120 to 280 Mev, (E),

20: 3080
**THALLIUM**
magnetoresistance at 1 and 4.2°K, effects of magnetic field direction and magnitude on, 20: 2329 (IS-T-35)
superconducting transition temperature of thin films of, effect of thin oxide layer on, 20: 2915
**THALLIUM ISOTOPES Tl-203**
gamma transitions in, conversion coefficients for, (E), 20: 3038
**THALLIUM ISOTOPES Tl-207**
energy levels in, $h_{11/2}$ single proton hole, (E), 20: 3071
**THERMAL CONDUCTIVITY CELLS**
design for measurements on linear accelerator targets, 20: 2531 (AD-618304)
**THERMAL INSULATION**
electric conduction in, analytical model for thermocouple error from, (T), 20: 2103 (LA-DC-7055)
**THERMAL RADIATION**
effects of, from nuclear explosions, physical, 20: 2078 (BNL-917, pp 1-10)
effects of, from nuclear explosions, pathological, 20: 2083 (CEX-65.4)
effects on ecosystems of, from nuclear explosions, physical, 20: 2079 (BNL-917, pp 11-19)
effects on heat transfer in radioisotope propulsion systems, (E), 20: 2007 (AD-818026)
effects on solids, 20: 2427 (NASA-SP-55)
sensitivity of fungi and yeast to, effects of uv and x radiations on, 20: 1640
**THERMAL REACTORS**
feasibility of mixed-spectrum steam-superheat power reactors, (T), 20: 3471(R) (GEAP-4861)
kinetics of mixed-spectrum steam-superheat, (E/T), 20: 3471(R) (GEAP-4861)
operations of MSSCEF, 20: 3471(R) (GEAP-4861)
plutonium distribution in fuel rods for, optimization, 20: 3457
uranium utilization in, conservation and economic aspects of, 20: 3458
**THERMAL STRESSES**
calculation of transient, in liquid-metal-cooled reactor fuel elements, 20: 3463
**THERMIONIC CELLS**
design and performance of cesium plasma diode, 20: 2675
development of nuclear-, (E), 20: 3446(R) (GEST-2045)
**THERMOCOUPLES**
insulation of, analytical model for electric conduction in, (T), 20: 2103 (LA-DC-7055)
performance for SEFOR fuel temperature measurements, 20: 3473 (GEAP-4903)
performance in reactor cores, 20: 3472(R) (GEAP-4891)
testing for use with plutonium dioxide–uranium dioxide fuel to 2600°C, 20: 2114
**THERMODYNAMIC PROPERTIES**
of ordered intermetallic phases, compositional variation of configurational, (T), 20: 2349 (UCRL-16320)
of sodium at high temperatures, 20: 1815 (NRL-6241)
**THERMODYNAMICS**
calculation of Yang-Lee distribution of zeros of the grand partition function, (T), 20: 2845
entropy limit in quantum microcanonical ensemble, infinite-volume, (T), 20: 2832
irreversible processes in, time correlation functions for, (T), 20: 2846
of superconductivity in one and two dimensions, (T), 20: 2889 (AD-618203)
spin temperature formalism in quantum, (T), 20: 2864 (COO-1198-300)
statistical mechanics of a system of quasiparticles, (T), 20: 2843
**THERMOELECTRIC CELLS**
uses in thermoelectromagnetic pumps for Rankine-cycle space power plants, (E), 20: 1988 (NAA-SR-11198)
**THERMOLUMINESCENT DETECTORS**
use in measurement of gamma heating in AARR critical assembly, 20: 2175
**THERMONUCLEAR EXPLOSIONS**
ecological effects of, 20: 2081 (BNL-917, pp 39-60)
effects of blast from, on man, 20: 2083 (CEX-65.4)
physical effects of, 20: 2078 (BNL-917, pp 1-10)
thermal radiation from, physical effects on ecosystems, 20: 2079 (BNL-917, pp 11-19)
**THERMONUCLEAR REACTIONS**
neutrino production in, (T), 20: 2587
research on, review of, 20: 3196
**THERMONUCLEAR REACTORS**
development of, review of, 20: 3196
electron diffusion and losses in Astron E-layer, (T), 20: 3183 (UCRL-14275)
**THIETANE, 3-ACETYL-**
spectra of, computer programs for analysis of NMR, 20: 3645 (UCRL-16344)
**THIETANE, 3-CHLORO-**
spectra of, computer programs for analysis of NMR, 20: 3645 (UCRL-16344)
**THIOCYANATES**
solvent properties for beryllium in aqueous solutions, 20: 1974(P)
**THIOPHENE, 2,5-DIMETHYL-**
heat of fusion, thermal capacity, and thermodynamic properties at 5 to 300°K, 20: 3614 (COO-1149-16)
**THORIUM**
abundance ratio to uranium in sedimentary deposits, weathering estimation from, 20: 2052
content in soils of Tomsk region, 20: 2065
desorption from rhenium and tungsten surfaces, by electron bombardment, (E), 20: 2434(R) (TID-22242)
determination of trace amounts in uranium compounds by activation analysis, 20: 1784
diffusion in pyrolytic carbon, effects of structure on, 20: 2318(R) (GA-5915(Pt.1))
Doppler coefficients at 20 to 600°C, 20: 2958
ion exchange by amberlite IR-120 in nitric acid solution, 20: 1783
properties as reactor fuels, 20: 3449
separation by solvent extraction using long chain amines, 20: 1761
separation from hydrochloric acid solutions by solvent extraction using neocupferron, 20: 1775
separation from protactinium by solvent extraction using 4-methyl-2-pentanone, 20: 1759
separation from protactinium by solvent extraction using *N*-benzoylphenylhydroxylamine, 20: 1776
separation from protactinium and uranium by solvent extraction using benzohydroxamic acid, 20: 1776
separation from rare earths by anion exchange, 20: 1957(T) (CEA-tr-X-616)
separation from rare earths by ion exchange in ammonium thiocyanate–organic solvent–water systems, 20: 1959
**THORIUM ALLOYS**
Pu–Th–U, properties as fast power-breeder fuel, 20: 2230
**THORIUM CARBIDES**
fabrication into reactor fuel spheres using arc plasma, 20: 2288
$ThC_2$–$UC_2$, fabrication and processing reactor fuels of, 20: 2282 (HW-SA-3755)
**THORIUM COMPOUNDS**
stability, 20: 1855
**THORIUM DEPOSITS**
properties of postmagmatic, with rare earths, 20: 2064
**THORIUM(IV) FLUORIDES**
shipping of, safety during, 20: 3370 (CONF-651103-2)
**THORIUM ISOTOPES Th-230**
abundance ratio to uranium-234 in sandstone deposits in Gas Hills, Wyoming, 20: 2057
determination of radioactive equilibrium in ningyotoge uranium ores between uranium and, 20: 2066
**THORIUM ISOTOPES Th-232**
burnup in high-temperature reactors, fuel cost analysis from, 20: 3448
deuteron fission reactions, angular anisotropy of, (E), 20: 3122
metabolism in man, 20: 1596
**THORIUM OXIDES**
properties as catalyst for aliphatic-alcohol dehydration, 20: 1892
radiation effects on electric conductivity of, 20: 2460
use in bitumen-bound radiation shielding material, 20: 2248(P)
$EuO_2$–$ThO_2$, phase studies by x-ray diffraction, 20: 2379
**THORIUM(IV) OXIDES**
crystal growth and properties of, for use as laser host, 20: 2312 (AD-619197)
Doppler coefficients at 20 to 600°C, 20: 2958
Doppler coefficient of rods of, (E), 20: 2976
fabrication into sintered pellets, 20: 2291
metabolism in man, 20: 1596
neutron resonance absorption integrals of rods of, (E), 20: 2976
optical properties for use as reflector for plastic scintillators, 20: 2327 (IKF-12)
uranium-233 production by irradiation of, uranium-232 yield in, 20: 3542
$BeO$–$ThO_2$–$UO_2$–$Y_2O_3$, irradiation testing of tubular fuel elements of, 20: 2467
$SiO_2$–$ThO_2$, liquidus curves and thermodynamic properties, 20: 2326 (IFA-FR-39)
$SiO_2$–$ThO_2$–$UO_2$, liquidus curves and thermodynamic properties, 20: 2326 (IFA-FR-39)
$ThO_2$–$UO_2$, fabrication and processing reactor fuels of, 20: 2282 (HW-SA-3755)
$ThO_2$–$UO_2$, microstructure variations with temperature, 20: 2393
$ThO_2$–$UO_2$, radiation effects on pellets of, 20: 2429 (ORNL-3837)
$ThO_2$–$UO_2$–$ZrO_2$, phase studies on, 20: 2361(T) (WAPD-Trans-21)

**THRESHOLD DETECTORS**
design for criticality detection, 20: 2075 (AHSB(S)R-92)
**THULIUM**
determination using Chromotrope 2B, photometric, 20: 1772
ionization potential from hfs of, 20: 2603
separation from thorium and other rare earths by ion exchange in ammonium thiocyanate–organic solvent–water systems, 20: 1959
**THULIUM ALLOYS**
Ni–Tm, preparation and structure of $MgCu_2$-type, 20: 2385(T)
**THULIUM IONS**
energy level transitions in calcium fluoride crystals, strain effects on, (E/T), 20: 3291
**THULIUM ISOTOPES Tm-170**
beta decay of, ytterbium-170 conversion coefficient from, 20: 3155
**THULIUM OXYBROMIDES**
preparation and crystal structure, 20: 1834
**THYMIDINE**
incorporation in ATP, tritium effects on, 20: 1583
metabolism in Drosophila spermatocytes of, 20: 1657
radiation effects on metabolism of, in rats, 20: 1630
**THYROID HORMONES**
radiation effects on distribution and synthesis of, 20: 1671
**THYROXINE**
deiodination in humans, tracer studies of, 20: 2520(R) (IA-920)
**TIN**
corrosion resistance to mercury at 900°F, 20: 2264
corrosive effects on structural materials, 20: 2275
effects on organic scintillator efficiency for gamma detection, 20: 1905
electron tunneling in superconducting junctions of, resonant mode interactions with a-c Josephson, (E/T), 20: 2895
grain boundary migration in zone-refined, review on, 20: 3626 (ORNL-P-1722)
ionization in K-shell by alpha particles at 3 to 4 Mev, x-ray yields from, (E), 20: 2625
separation of trace amounts of, from alkali metals, alkaline earths, and rare earths, 20: 1958
superconducting properties of superimposed films of iron and, 20: 2894
superconducting transition temperature of thin films of, effect of thin oxide layer on, 20: 2915
**TIN ALLOYS**
Al–Cu–Fe–Sn–Ti–V–Zr, deformation and heat treatment effects on mechanical properties of, 20: 2309 (AD-615024)
Al–Sn–Ti–V–Zr, formability characteristics and mechanical properties of, 20: 2308 (AD-614637)
Au–Ag–Sn, solute interactions in dilute, (E/T), 20: 2349 (UCRL-16320)
Au–In–Sn, solute interactions in dilute, (E/T), 20: 2349 (UCRL-16320)
Au–Ni–Sn, solute interactions in dilute, (E/T), 20: 2349 (UCRL-16320)
Au–Sn, solute interactions in dilute, (E/T), 20: 2349 (UCRL-16320)
In–Ag–Sn, solute interactions in dilute, (E/T), 20: 2349 (UCRL-16320)
In–Sn, Mössbauer effect in superconducting, (E), 20: 2919
In–Sn, solute interactions in dilute, (E/T), 20: 2349 (UCRL-16320)
In–Sn, thermal conductivity below 1°K, (E), 20: 2383
Mn–Sn, spin ordering of paramagnetic states in superconducting, 20: 2918
Nb–Sn, magnetic flux jumps in superconducting $Nb_3Sn$ in pulsed magnetic fields, (E), 20: 2921
Nb–Sn–Zr, corrosion by steam, effects of antimony, chromium, iron, and vanadium additions on, 20: 2255(R) (EURAEC-1323)
Pt–Sn, tin-119 Mössbauer effect in intermetallic compounds of isomer shifts and quadrupole splittings from, (E), 20: 3290
Sn–Zr, parameters for zirconium self-diffusion in, 20: 2356(T) (AERE-Trans-1030)
**TIN ISOTOPES Sn-112**
gamma transition at 1257.3 kev following Coulomb excitation, (E), 20: 3043
**TIN ISOTOPES Sn-116**
alpha scattering at 40 Mev, angular distributions from, (E), 20: 3017 (NASA-TM-D-3067)
gamma transition at 1293.3 kev following Coulomb excitation, (E), 20: 3043
**TIN ISOTOPES Sn-117**
gamma transitions following Coulomb excitation, (E), 20: 3043
**TIN ISOTOPES Sn-118**
alpha scattering at 40 Mev, angular distributions from, (E), 20: 3017 (NASA-TN-D-3067)
gamma transition at 1230.2 kev following Coulomb excitation, (E), 20: 3043
**TIN ISOTOPES Sn-119**
gamma transitions following Coulomb excitation, (E), 20: 3043
Mössbauer effect in magnesium–tin oxide crystals, neutron damage effects on, 20: 3065
Mössbauer effect in superconducting, (E), 20: 2919
Mössbauer effect in platinum–tin intermetallic compounds, isomer shifts and quadrupole splittings from, (E), 20: 3290
nuclear charge radius of, based on Mossbauer spectra, (E), 20: 3136
**TIN ISOTOPES Sn-120**
alpha scattering at 40 Mev, angular distributions from, (E), 20: 3017 (NASA-TN-D-3067)
gamma transition at 1171.5 kev following Coulomb excitation, (E), 20: 3043
**TIN ISOTOPES Sn-121**
energy levels, (E), 20: 2520(R) (IA-920)
**TIN ISOTOPES Sn-122**
alpha scattering at 40 Mev, angular distributions from, (E), 20: 3017 (NASA-TN-D-3067)
gamma transition at 1140.2 kev following Coulomb excitation, (E), 20: 3043
**TIN ISOTOPES Sn-124**
gamma transition at 1131.4 kev following Coulomb excitation, (E), 20: 3043
**TIN OXIDES**
MgO–$SnO_2$, radiation damage effects on tin-119 Mössbauer effect in, neutron, 20: 3065
**TIN SYSTEMS**
As–Cd–Sn, radiation effects on thermal conductivity of semiconducting $CdSnAs_2$, 20: 2488
As–Sn–Zn, radiation effects on thermal conductivity of superconducting, 20: 2488
**TISSUE CULTURES**
effects of nitrogen mustard on survival of animal cells in, 20: 1617(R) (NP-15149)
growth rate patterns of animal cells in, 20: 1594 (LA-DC-6507)
of lymphoid cells on monolayers of mouse embryo cells, 20: 1658
radiation effects on survival of animal cells in, effects of dose, x, 20: 1617(R) (NP-15149)
radiation effects on DNA synthesis in L-strain cells in, uv, 20: 1625
**TISSUE TRANSPLANTS**
bone marrow, use in therapy of leukemia, 20: 1700
growth of bone marrow, in irradiated mice, effects of arabinofuranosylcytosine on, 20: 1687
hematopoietic, use in therapy of leukemia, 20: 1701
**TISSUES**
dissolution of, for liquid scintillation counting, 20: 1767
effects of orthoquinones on, physiological, 20: 1647
electric properties of calcified, 20: 3625(R) (NYO-3282-1)
electric properties of ivory, 20: 3625(R) (NYO-3282-1)
plutonium distribution in animal, effects of colloidal properties of plutonium solutions on, 20: 1835
proton dosimetry in, 20: 1620 (UCRL-16154)
radiation effects on, bibliography, 20: 1608 (AED-C-04-19)
radiation effects on, physiological, 20: 1647
radioinduced ablation of, using soft beta applicator, 20: 1628(T)
radiotherapy of, penetration in epithermal neutron beam, 20: 1714
tritium uptake by hypophysis of organotypic culture of drake, electron microscopy of, 20: 1597
**TITANIUM**
corrosion resistance to mercury at 900°F, 20: 2264
incorporation into furfural, 20: 1887 (NP-15523)
melting of, performance of induction furnace for cold-mold, 20: 2352(R) (USBM-RC-1205, pp 9-10)
physical metallurgy of, 20: 2359(T) (NASA-TT-F-338)
solubility in molten potassium, 20: 2237
**TITANIUM ALLOYS**
physical metallurgy of, 20: 2359(T) (NASA-TT-F-338)
Al–Cu–Fe–Sn–Ti–V–Zr, deformation and heat treatment effects on mechanical properties of, 20: 2309 (AD-615024)
Al–Sn–Ti–V–Zr, formability characteristics and mechanical properties of, 20: 2308 (AD-614637)
Mo–Ti, strain softening effects on properties of, 20: 2311 (AD-618925)
Mo–Ti–Zr, cavitation damage to TZM, in liquid sodium, 20: 2243
Mo–Ti–Zr, compatibility of TZM, with niobium–zirconium alloy in flowing zirconium, 20: 2238
Mo–Ti–Zr, corrosion by lithium at high temperatures, 20: 2269
Mo–Ti–Zr, corrosion of TZM, by potassium at high temperatures, 20: 2271
Mo–Ti–Zr, testing of TZM, for use in liquid-metal turbine blades and nozzles, 20: 2240
Nb–Ti, superconducting-normal transitions in variable fields, mechanisms of, (E), 20: 2902
Nb–Ti–V–Zr, properties, effects of composition on, 20: 2340 (ORNL-TM-1131)
Ni–Ti, effects of aluminum, cobalt, iron, silicon, and tungsten on properties of Nitinol, 20: 2310 (AD-618681)
Pu–Ti–U, corrosion by air, effects of exposure-time on, 20: 3320(R) (ANL-7082, pp 1-28)
Pu–Ti–U, properties as fast power-breeder fuels, 20: 2386

Ti–V, compatibility with plutonium–thorium–uranium alloys, 20: 2230
Ti–V, corrosion by sodium at high temperatures, 20: 3320(R) (ANL-7082, pp 1-28)
Ti–V, corrosion by oxygenated sodium at 540°C, effects of polarization on, 20: 3321(R) (ANL-7082, pp 29-53)
Ti–V, corrosion cracking by ferric chloride, hydrochloric acid, and nitric acid solutions, stress-, 20: 2254 (BM-RI-6680)

**TITANIUM BORIDES**
Ti–TiB, development of fiber-reinforced composites of, 20: 2219 (AMRA-CR-64-05/4)

**TITANIUM CARBIDES**
corrosion by hydrogen fluoride at 2000 to 3100°K, 20: 2261(R) (UCRI-326)
radiation effects on crystal structure of, mechanism of beta, 20: 2426 (LA-3387)
testing for use in shaft seals for potassium space power plants, 20: 2242
thermal expansion of, to 2700°C, 20: 1839
wetting by liquid cobalt, copper, iron, and nickel, 20: 1837
TiC–VC, wetting by liquid copper, 20: 1837
WC–TiC, wetting by liquid cobalt and copper, 20: 1837

**TITANIUM ISOTOPES Ti-44**
production using ORNL 86-in. cyclotron, 20: 2212

**TITANIUM ISOTOPES Ti-45**
beta decay of, scandium-45 energy levels and gamma spectra from, 20: 3128

**TITANIUM ISOTOPES Ti-48**
gamma transition at 983.1 kev following Coulomb excitation, (E), 20: 3043

**TITANIUM OXIDES**
testing for use in shaft seals for potassium space power systems, 20: 2242

**TITANIUM SYSTEMS**
C–Mo–Nb–Ta–Ti–W–Zr, creep properties at 1800 to 2200°F of Cb132M, 20: 2333(R) (NASA-CR-54457)
C–Mo–Ti–Zr, creep properties at 1800 to 2200°F of TZC, 20: 2333(R) (NASA-CR-54457)
C–Ti, phase studies on, thermal analysis of, (E), 20: 1863
Mo–Ti–Zr, creep at 1800 to 2200°F of TZM, 20: 2333(R) (NASA-CR-54457)
Ti–TiB, development of fiber-reinforced composites of, 20: 2219 (AMRA-CR-64-05/4)

**TOBACCO**
analysis for mercury by neutron activation, 20: 1755
analysis in crime detection, activation, 20: 1739(R) (GA-4297)

**TOLUENE**
effects on radioinduced polymerization of formaldehyde, 20: 1914
nitration and succinoylation of tritium-labeled, hydrogen exchange and isotope effects in, 20: 1950
recoil reactions of carbon-11 in liquid, 20: 1896 (IS-T-23)

**TOLUENE, VINYL- POLYMERS**
use as plastic scintillator for gamma detection, effects of tin on photopeak resolution in, 20: 1905

**TOLUENESULFONIC ACID**
heat of solution of sodium salt of, in heavy and light water, 20: 1825

**TOMATOES**
radioinduced chromosome aberrations of seeds of, 20: 1638

**TOPOLOGY**
Banach spaces in, Hilbert-Schmidt and nuclear power applications in, 20: 2215

**TOXINS**
analysis of snake venom for copper and zinc by activation, 20: 2520(R) (IA-920)

**TRACER APPLICATIONS**
use in determination of trace amounts of cadmium and silver, 20: 1786

**TRACER TECHNIQUES**
use in studies of waste discharges and industrial processes, 20: 2201
use of bromine-82-labeled bromobenzene in industrial studies, 20: 2202

**TRACER TECHNIQUES (AGRICULTURE)**
for fruit coating, 20: 2520(R) (IA-920)

**TRACER TECHNIQUES (CHEMISTRY)**
for anion exchange of complexes from mixed solvents, 20: 2520(R) (IA-920)

**TRACER TECHNIQUES (HYDROLOGY)**
erosion and sand transport on surf coasts, 20: 2060

**TRACER TECHNIQUES (MEDICINE)**
for cerebral blood flow measurements, 20: 1711
for coronary blood flow studies, 20: 1709
for tumor localization, 20: 1712
performance of organic plastic scintillation detectors for whole-body counting for, 20: 1710

**TRACER TECHNIQUES (METEOROLOGY)**
use of fallout in, 20: 2044 (NDRE-51)

**TRACER TECHNIQUES (OCEANOGRAPHY)**
use of air–water interface and eddy-diffusion, 20: 2061

**TRADESCANTIA**
radiation effects on stamen hairs and root meristem cells of, 20: 1668
radiation effects on, genetic, 20: 1622 (WT-820)

**TRANSDUCERS**
design for water wave measurements, 20: 2059(R) (NVO-98-11)
radiation effects on resistance-temperature, at low temperatures, 20: 2191
use of acoustic, with wire spark chambers, 20: 2132 (JINR-P-2368)

**TRANSISTORS**
radiation effects on n-p-n silicon, neutron, 20: 2184(R) (AD-614618)
radiation effects on, physical parameters for predicting gamma and neutron, 20: 2184(R) (AD-614618)
radiation effects on, method for predicting neutron, 20: 2185(R) (AD-618194)
radiation effects on, transient neutron, 20: 2190
radiation effects on n-p-n silicon, neutron, 20: 2185(R) (AD-618194)
radioinduced resistance fluctuations in silicon, carrier removal effects on electron, (E), 20: 2188

**TRANSITION METALS**
radiation effects on hardening and embrittlement of bcc, 20: 2472
solubility in molten potassium, 20: 2237

**TRANSPLUTONIC ELEMENTS**
bibliography on, 20: 1726 (EUR-2508.e)

**TRAUMA**
induced by blast effects, missiles, and thermal radiation from nuclear explosions, 20: 2083 (CEX-65.4)
of cell membranes, effects on size distribution studies with Coulter electronic counter, 20: 1636

**TRIDODECYLAMINE**
solvent properties for perchloric and perrhenic acids, effects of aromatic diluents on, 20: 1747 (UCRL-11616(Rev.))

**TRIETHYLAMINE**
effects on pulse radiolysis of organic solutes, spectra of, 20: 1920

**TRIOCTYLAMINE**
solvent properties for protactinium, ruthenium, thorium, uranium, and zirconium, 20: 1761

**TRIOXANES**
radioinduced polymerization of solid, pressure effects on, 20: 1926

**TRIPHENYLAMINE**
radiation effects on ionic processes in solid, relation to delayed luminescence, 20: 1906

**TRITIUM**
concentration in water, review on methods for, 20: 1728 (AD-618562)
detection and measurement in gases, system design for low-background, 20: 2179
determination in global fallout samples, review on, 20: 2086(T) (BNL-tr-42)
determination in water, review on methods for, 20: 1728 (AD-618562)
determination of, precision of proportional counter for, 20: 1768
deuteron reactions (d,n) at 150 to 580 kev, cross sections for polarized, (E), 20: 3039
diffusion in lithium–silver alloys, 20: 2317 (EURAEC-1380)
effects on aromatic substitution reaction, 20: 1888
effects on self-radiolysis and storage of organic compounds, 20: 1938 (EUR-2452.e)
electromagnetic form factors, (T), 20: 3119
production by proton reactions with aluminum and iron, (E), 20: 3095
proton reactions (p,n) and (p,p) to 1.5 Mev, phase-shift analysis of, 20: 3060
recoil reactions with ethylene, bond dissociation energies and hydrogen abstraction in, 20: 1907
recoil reactions with picoline and pyridine, stability and yields in, 20: 1921
separation from hydrogen isotope mixtures by gas chromatography, 20: 1733 (DP-979)
uptake by hypophysis of organotypic culture of drake tissue, electron microscopy of, 20: 1597

**TRITIUM SYSTEMS**
T–Zr, efficiency as x-ray spectroscopy source, 20: 2136

**TRITONS**
reactions (t,$\alpha$) with lead-208 at 12 Mev, thallium-207 1.34-Mev level from, (E), 20: 3071
reactions (t,p) with light nuclei, angular distributions from direct, (T), 20: 3121
yield in bremsstrahlung reactions ($\gamma$,t) with oxygen-16 at 50 Mev, (E), 20: 3126

**TROPOSPHERE**
radioactivity in German, resulting from Chinese test of October 16, 1964, 20: 2050

**TUBES**
boiling of potassium in vertical, pressure drop in forced-convection, (E/T), 20: 2015 (ORNL-P-1681)

burnout and hydrodynamic instability in round, with forced water flow, 20: 2009 (EUR-2490.e)
joining by internal welding, device for, 20: 2304(P)
pressure drop measurement for condensing vapor flow in, method for calculating static, 20: 1814 (NAA-SR-6333)
testing of, eddy-current methods for, 20: 2025 (BNWL-SA-349)
welding to tubesheet, electron-beam, 20: 2283 (KAPL-3110)

**TUMORS**
diagnosis of, using technetium-99 and external counting, 20: 1712
radiation dose calculations for gamma radiotherapy of, 20: 1723
radiation effects on phosphorylation in, x, 20: 1626
radioinduced, in mouse lungs, 20: 1606 (AD-623079)
radiosensitivity of transplanted, effects of inhalation of 5% carbon dioxide and 95% oxygen on, in mice, 20: 1683
radiotherapy of hemangiomas, in infants, using radium, evaluation of, 20: 1719
radiotherapy of pituitary gland, 20: 1708
radiotherapy of uterine, late pathological effects, 20: 1725
radiotherapy of, radiation hazards from, 20: 1717
urethan-induced, in mouse lungs, 20: 1606 (AD-623079)

**TUNGSTEN**
bremsstrahlung and electron transport in, (T), 20: 3246 (NASA-SP-71, pp 437-48)
corrosion by bismuth and tin, 20: 2275
corrosion by zinc and magnesium–uranium–zinc alloy, effects of molten chlorides on, 20: 2266
corrosion resistance to mercury at 900°F, 20: 2264
creep and tensile properties at 2250 to 4140°F, effects of grain size on, 20: 2396
creep at 1800 to 2200°F, 20: 2333 (NASA-CR-54457)
creep of arc-cast, activation energy for, 20: 2223(R) (GEMP-51A)
crystal lattice waves dispersion in, (T), 20: 3294
desorption of thorium from by electron bombardment, (E), 20: 2434(R) (TID-22242)
determination of trace amounts in uranium compounds by activation analysis, 20: 1784
Doppler coefficients at 20 to 600°C, 20: 2958
effects on properties of Nitinol alloy, 20: 2310 (AD-618681)
electron diffraction by, (E), 20: 2434(R) (TID-22242)
erosion by rocket exhaust gases, 20: 2261(R) (UCRI-326)
fabrication procedures for single-crystal sheets of, 20: 2284(R) (NP-15093)
mechanical properties of vapor-deposited, at low temperatures, 20: 2388
meson ($K_2^0$) regeneration in, 20: 2748
neutron cross sections from 1 kev to 14 Mev, (T), 20: 2961
oxidation by oxygen, kinetics of, 20: 2261(R) (UCRI-326)
oxidation by water, mass spectrometric study of, 20: 2261(R) (UCRI-326)
oxidation by water, effects of hydrogen on, 20: 2261(R) (UCRI-326)
properties and uses of, review on, 20: 2307 (AD-613023)
proton elastic scattering at 3 Mev, angular distributions for, (E), 20: 3037
proton shielding performance of, for space vehicles, (T), 20: 3242 (NASA-SP-71, pp 225-8)
radiation effects on hot-hardness of single-crystal, dosage effects of fast neutron, 20: 2422(R) (GEMP-52A, pp 11-21)
radiation effects on brittle-to-ductile transition temperature of polycrystalline, fast neutron, 20: 2422(R) (GEMP-52A, pp 11-21)
radiation effects on hardness of, neutron, 20: 2457
radioinduced defects in, recovery spectra of neutron, 20: 2475
reactions with uranium carbide–zirconium carbide solid solutions at high temperatures, compatibility in, 20: 2332 (LA-3307)

**TUNGSTEN ALLOY COUPLES**
Cr–Os/Re–W, thermoelectric properties at 200 to 1800°C, 20: 2223(R) (GEMP-51A)
Mo–Os–Ru/Re–W, thermoelectric properties at 100 to 1400°C, 20: 2223(R) (GEMP-51A)

**TUNGSTEN ALLOYS**
properties and uses of, review on, 20: 2307 (AD-614023)
Ag–W, sintering in presence of liquid phase, kinetics of, 20: 2286
Cr–W, resonant lattice modes in, (E), 20: 3302
Cu–W, sintering in presence of liquid phase, kinetics of, 20: 2286
Hf–Ta–W, corrosion by lithium at 1200°C, 20: 3321(R) (ANL-7082, pp 29-53)
Hf–Ta–W, properties for use with alkali metals at high temperatures, 20: 2241
Mo–Re–W, creep at 1600 and 2200°C, 20: 2223(R) (GEMP-51A)
Mo–Re–W, ductility of, effects of composition on, 20: 2223(R) (GEMP-51A)
Mo–Re–W, fabrication and properties of, 20: 2354(R) (USBM-RC-1205, pp 15-19)
Mo–Re–W, sectioning of, method for submicron, 20: 2321(R) (GEMP-52A, pp 43-5)
Mo–Ti–Zr, corrosion by lithium at high temperatures, 20: 2269
Mo–W, corrosion by lithium at 1200°C, 20: 3321(R) (ANL-7082, pp 29-53)
Mo–W, corrosion by zinc and magnesium–uranium–zinc alloy, effects of molten chlorides on, 20: 2266
Mo–W, corrosion by bismuth and tin, 20: 2275
Nb–W, corrosion by lithium at high temperatures, 20: 2269
Nb–W–Zr, corrosion by flowing lithium, 20: 2238
Nb–W–Zr, corrosion by bismuth and tin, 20: 2275
Nb–W–Zr, creep-rupture properties of, 20: 2336 (ORNL-P-1634)
Nb–W–Zr, stress effects in corrosion of D-43, by potassium, 20: 2270
Re–W, chemical compatibility with urania, (E), 20: 3446(R) (GEST-2045)
Re–W, corrosion by lithium at high temperatures, 20: 2269
Re–W, creep at 1800 to 2200°F, 20: 2333(R) (NASA-CR-54457)
Re–W, creep rate to rupture time, equation for relating, 20: 2422(R) (GEMP-52A, pp 11-21)
Re–W, ductility, phase studies, and properties of, 20: 2323 (GEMP-314)
Re–W, fabrication and properties of, 20: 2354(R) (USBM-RC-1205, pp 15-19)
Re–W, fabrication of sheets and tubing of, procedure for, 20: 2223(R) (GEMP-51A)
Re–W, radiation effects on rupture life of, fast neutron, 20: 2422(R) (GEMP-52A, pp 11-21)
Re–W, use in thermocouples for measurements on plutonium dioxide–uranium dioxide fuel, 20: 2114
Ta–W, corrosion by zinc and magnesium–uranium–zinc alloy, effects of molten chlorides on, 20: 2266
Tc–W, superconducting properties, (E), 20: 2907

**TUNGSTEN CARBIDES**
wetting by liquid cobalt, copper, iron, and nickel, 20: 1837
WC–TiC, wetting by liquid cobalt and copper, 20: 1837

**TUNGSTEN ISOTOPES W-174**
energy states of, large-spin rotational, (E/T), 20: 3008 (COO-1420-104)

**TUNGSTEN ISOTOPES W-176**
energy states of, large-spin rotational, (E/T), 20: 3008 (COO-1420-104)

**TUNGSTEN ISOTOPES W-182**
neutron cross sections from 1 kev to 14 Mev, (T), 20: 2961

**TUNGSTEN ISOTOPES W-183**
neutron cross sections from 1 kev to 14 Mev, (T), 20: 2961

**TUNGSTEN ISOTOPES W-184**
neutron cross sections from 1 kev to 14 Mev, (T), 20: 2961

**TUNGSTEN ISOTOPES W-186**
ionization in K-shell by alpha particles at 3 to 4 Mev, x-ray yields from, (E), 20: 2625
neutron cross sections from 1 kev to 14 Mev, (T), 20: 2961

**TUNGSTEN OXIDES**
reduction by hydrogen at 625°C, 20: 1831
testing for use in shaft seals for potassium space power systems, 20: 2242

**TUNGSTEN SYSTEMS**
C–Hf–W, creep at 1800 to 2200°F of Silvania A, 20: 2333(R) (NASA-CR-54457)
C–Mo–Nb–Ta–Ti–W–Zr, creep properties at 1800 to 2200°F of Cb132M, 20: 2333(R) (NASA-CR-54457)
W–$UO_2$, radiation effects on melting fuel elements of, 20: 2416 (AECL-2289)

**TURBINES**
design and performance of closed-cycle gas, for nuclear power plants, 20: 3343
flexibility of back-pressure, for dual-purpose nuclear plants, (E), 20: 3540 (ACNP-65573)
properties of biphenyl thermal, 20: 2019

**TYROSINE**
radioinduced conversion to orthoquinones, 20: 1647

**TYROSINE, 3,5-DIIODO-**
determination in blood using neutron activation of iodine-129, 20: 1790

**TYROSINE, IODO-**
determination in blood using neutron activation of iodine-129, 20: 1790


## U


**ULTRASONICS**
equipment for nondestructive testing by wave measurement, 20: 3321(R) (ANL-7082, pp 29-53)

**ULTRAVIOLET RADIATION**
effects in *Bacillus subtilis*, biological, 20: 1624
effects melanins of hair and skin, 20: 1684
effects of flashes of far, on ethane, 20: 1898(R) (RRL-2310-164)
effects on algal, biological, 20: 1681
effects on bacteriophage, physiological, 20: 1650
effects on DNA synthesis in L-strain cells, 20: 1625
effects on ethylene gas, 20: 1898(R) (RRL-2310-164)
effects on mutation rate in murine cell line resistant to purine analogs, 20: 1678
effects on ribonucleic acid in tobacco mosaic virus, photoreactivation,

20: 1659
effects on *Schizosaccharomyces pombe*, genetic, 20: 1654
effects on solar reflector coatings for spacecraft, 20: 2428 (NASA-SP-55, pp 365-79)
effects on solid methacrylic acid at −40 to 10°C, ESR spectra of yields in, 20: 1916
effects on thermal sensitivity of fungi and yeast, 20: 1640
effects on Vaccinia viruses, biological, 20: 1651
effects on yeast, biological, 20: 1663
**UNDERGROUND EXPLOSIONS**
design for nuclear excavation of sea-level Isthmian canal, 20: 1984 (PNE-2001)
excavation of sea-level Isthmian canal, plan for nuclear, 20: 1983 (PNE-2000)
excavation of sea-level Isthmian canal, nuclear operations program for, 20: 1986 (PNE-2004)
safety evaluation of, for excavation of sea-level Isthmian canal, 20: 1985 (PNE-2003)
seismic measurements of Dugout row-charge cratering experiment, 20: 1981 (PNE-605F)
surveillance of Handcar event, weather and radiological, 20: 1982 (PNE-607F)
**UNDERGROUND STRUCTURES**
dose rates from scattered fallout radiation, 20: 2038
gamma scattering into basement from infinite plane source, 20: 3272
**UNDERWATER EXPLOSIONS**
above-surface phenomena and base surge in nuclear, in Crossroads and Teapot Operations, 20: 1979 (AD-614814)
**UPSHOT-KNOTHOLE OPERATION**
effects of fast neutrons, genetic, on biological specimens studied during, 20: 1622 (WT-820)
**URANATES**
production of high-purity di-, from yellow cake, 20: 1973(P)
**URANIUM**
abundance ratio to uranium in sedimentary deposits, weathering estimation from, 20: 2052
analysis for europium and samarium spectrographic, 20: 2520(R) (IA-920)
analysis for indium, fluorometric, 20: 2520(R) (IA-920)
analysis for magnesium by atomic absorption spectrophotometry, 20: 1753
casting of, carbide dissolution and precipitation in, 20: 2285
corrosion protection films on, method for deposition of aluminum, 20: 2260 (SC-DR-65-519)
criticality studies of graphite- and polyethylene-reflected annuli of, 20: 3392
crystal structure on surface of B-quenched, 20: 2377
deterioration of fuel elements of, during testing in flowing carbon dioxide, 20: 1748 (UJV-1369/65)
determination in aerosols using carbon dioxide, radiometric, 20: 1748 (UJV-1369/65)
determination in ores by colorimetric method, 20: 1794
diffusion in liquid aluminum, bismuth, cadmium, and zinc, 20: 2368
diffusion of krypton and xenon in irradiated, coefficient of, 20: 2358(T) (AERE-Trans-1034)
diffusion through iron–chromium–aluminum cladding, research program for, 20: 2322(R) (GEMP-52A, pp 53-4)
diffusion through aluminum–chromium–iron–yttrium alloy cladding, 20: 2223 (GEMP-51A)
distribution in uranium dioxide fuel rods, 20: 2450
gamma back-scattering from, albedos from, (E), 20: 3273
oxidation of powdered, at low temperatures, 20: 2279 (CEA-R-2828)
reactions with water vapor at 30 to 80°C, kinetics, 20: 1804 (AWRE-O-68/65)
recovery from spent fuels by skull reclamation, 20: 3320(R) (ANL-7082, pp 1-28)
recovery from spent fuels by pyrochemical processes, 20: 3320(R) (ANL-7082, pp 1-28)
recovery from spent fuels by fluidization and volatility processes, 20: 3321(R) (ANL-7082, pp 29-53)
separation by solvent extraction using long chain amines, 20: 1761
separation from carbonate solutions by solvent extraction using arsonium and phosphonium salts, 20: 1782
separation from hydrochloric acid solutions by solvent extraction using neocupferron, 20: 1775
separation from nitric acid solutions, effects of salting-out agents on, 20: 1967
separation from protactinium and thorium by solvent extraction using benzohydroxamic acid, 20: 1776
separation from protactinium by solvent extraction using 4-methyl-2-pentanone, 20: 1759
sorptive properties for methanol, effects of corrosion by water vapor on, 20: 1805 (AWRE-O-69/65)
tensile properties in wrought depleted, design allowables for, 20: 2342 (SC-DR-58-61)
tensile properties in welds joining wrought depleted, design allowables for, 20: 2342 (SC-DR-58-61)
use in thermal reactors, conservation and economic aspects of, 20: 3458
U–Zr, irradiation testing of reactor fuel tubes of, 20: 2466
**URANIUM ALLOYS**
casting of, carbide dissolution and precipitation in, 20: 2285
Mg–U–Zn, corrosive effects on refractory metals in presence of molten chlorides, 20: 2266
Mo–Pu–U, development and fabrication for ZPPR and ZPR-VI fuels, 20: 3320(R) (ANL-7082, pp 1-28)
Mo–U, hydridation of, kinetics, 20: 2222 (EURAEC-1390)
Mo–U, preparation of powders of, 20: 2222 (EURAEC-1390)
Mo–U, use in the preparation of uranium compounds, 20: 1885(P)
Ni–U, diffusion in, activation energy for inter-, 20: 2328 (INR-625/XIV/R)
Pu–Th–U, properties as fast power-breeder fuel, 20: 2230
Pu–Ti–U, corrosion by air, effects of exposure-time on, 20: 3320(R) (ANL-7082, pp 1-28)
Pu–Ti–U, properties as fast power-breeder fuels, 20: 2386
Pu–U–fission, phase studies of, 20: 3493
Pu–U–Zr, compatibility with Hastelloy-X, Incoloy-800, and type-304 stainless steels, 20: 2229
Pu–U–Zr, properties as fast power-breeder fuels, 20: 2386
Pu–U–Zr, reactions with Hastelloy, Incoloy, and stainless steel at high temperatures, 20: 3320(R) (ANL-7082, pp 1-28)
U–Zr, compatibility with iron, 20: 2229
**URANIUM BROMIDE COMPLEXES**
stability of trivalent, 20: 2520(R) (IA-920)
**URANIUM CARBIDES**
coating with niobium, method for, 20: 2300(P)
diffusion of xenon in monocrystals of, 20: 2317 (EURAEC-1380)
dissolution and precipitation of, in casting of uranium or its alloys, 20: 2285
fabrication costs for Hallam Power Reactor fuel elements, 20: 3509
fabrication into reactor fuel spheres using arc plasma, 20: 2288
preparation of powdered, by cermet disintegration, 20: 2250(P)
preparation of spherical particles of, sol-gel process for, 20: 2226 (RT/CHI(65)-30)
radiation hazards from particles of, 20: 1694
reactions in lithium chloride–potassium chloride–zinc–zinc chloride system at 580 to 802°C, 20: 2404
reactions with liquid zinc at 540 to 800°C, phase formations in, 20: 2404
C–NbC–UC, preparation as reactor fuel material, 20: 2305(P)
C–UC–ZrC, preparation as reactor fuel material, 20: 2305(P)
PuC–UC, fabrication into rods for irradiation testing, 20: 3320(R) (ANL-7082, pp 1-28)
PuC–UC, preparation methods, 20: 3321(R) (ANL-7082, pp 29-53)
PuC–UC, radiation effects on clad, at 510 to 650°C, 20: 3321(R) (ANL-7082, pp 29-53)
$ThC_2$–$UC_2$, fabrication and processing reactor fuels of, 20: 2282 (HW-SA-3755)
UC–UN–UO, phase studies, 20: 2353(R) (USBM-RC-1205, pp 11-14)
$UC_2$–US, phase studies, 20: 3321(R) (ANL-7082, pp 29-53)
UC–ZrC, compatibility of molybdenum, niobium, and tungsten at high temperatures in, 20: 2332 (LA-3307)
U–UC, phase diagram, 20: 2366
**URANIUM CHLORIDE COMPLEXES**
stability of trivalent, 20: 2520(R) (IA-920)
**URANIUM(IV) CHLORIDES**
formation in chlorination of uranium (IV–VI) oxide by chlorine–carbon tetrachloride, 20: 1816 (ORNL-TM-1258)
**URANIUM(V) CHLORIDES**
formation in chlorination of uranium (IV–VI) oxide by chlorine–carbon tetrachloride, 20: 1816 (ORNL-TM-1258)
**URANIUM(VI) CHLORIDES**
formation in chlorination of uranium (IV–VI) oxide by chlorine–carbon tetrachloride, 20: 1816 (ORNL-TM-1258)
**URANIUM COMPLEXES**
with sodium triphosphate, separation from rare earths by ion exchange, 20: 1762
**URANIUM COMPOUNDS**
analysis for trace impurities by activation methods, 20: 1784
stability, 20: 1855
**URANIUM CONCENTRATES**
sampling system for, engineering drawings of, 20: 1797
**URANIUM(IV) FLUORIDES**
preparation by reaction of Mo–U alloys with gaseous hydrofluoric acid and oxygen-containing gas, 20: 1885(P)
production from uranyl nitrate, development of Excer process for, 20: 1956 (ORNL-1696)
**URANIUM(VI) FLUORIDES**
electrolysis in fused salt melts for fluorine recovery, 20: 1954 (KY-287)

magnetic resonance of fluorine-19 in, anisotropy of chemical shift tensors of, 20: 1807 (CEA-R-2827)

**URANIUM ISOTOPES**
burnup in Yankee Power Reactor, 20: 3504

**URANIUM ISOTOPES U-232**
yield in uranium-233 production by irradiation of thorium dioxide, 20: 3542

**URANIUM ISOTOPES U-233**
criticality studies for use in gaseous-core rocket reactors, 20: 3462
criticality studies of homogeneous, 20: 3369 (CEA-R-2814)
deuteron fission reactions, angular anisotropy of, (E), 20: 3122
fabrication into fuel elements, nonremote, 20: 2289
neutron fission cross section structure at 0.1–0.2 Mev, (E), 20: 3089
neutron fission of, fragment yields from thermal, (E), 20: 3010(R) (IDO-14663)
processing of, safety measures for, 20: 3370 (CONF-651103-2)
production in irradiation of thorium dioxide uranium-232 yield in, 20: 3542

**URANIUM ISOTOPES U-234**
abundance ratio to thorium-230 and uranium-238 in sandstone deposits in Gas Hills, Wyoming, 20: 2057
effects on equilibrium between ionium and uranium in ningyotoge uranium ores, 20: 2066

**URANIUM ISOTOPES U-235**
abundance ratio to protactinium-231 in sandstone deposits, Gas Hills, Wyoming, 20: 2057
burnup in high-temperature reactors, fuel cost analysis from, 20: 3448
criticality studies of homogeneous, 20: 3369 (CEA-R-2814)
determination in fuel elements, gamma counting for nondestructive, 20: 3464
deuteron fission reactions, angular anisotropy of, (E), 20: 3122
neutron fission cross section structure at 0.1–0.2 Mev, (E), 20: 3089
neutron fission of, fragment kinetic-energy distributions from fast and thermal, (E), 20: 3110
neutron fission of, ionization energy losses of fragments from thermal, (E), 20: 3029
neutron reactions (n,f), cross sections for resonance and thermal, (E), 20: 3031
performance for nuclear pumping gas lasers, (T), 20: 2591 (ANL-7030)

**URANIUM ISOTOPES U-237**
content in fallout particles, 20: 2053

**URANIUM ISOTOPES U-238**
abundance ratio to uranium-234 in sandstone deposits in Gas Hills, Wyoming, 20: 2057
deuteron fission reactions, angular anisotropy of, (E), 20: 3122
Doppler coefficients at 20 to 600°C, 20: 2958
neutron reactions (n,f), cross sections for resonance and thermal, (E), 20: 3031
neutron reactions (n,γ), cross sections for resonance and thermal, (E), 20: 3031
photofission cross section at 5.43 to 7.72 Mev for monochromatic gamma rays, (E), 20: 3050
photofission near threshold, fragment angular distributions from, (E), 20: 3134

**URANIUM LEACH PRECIPITATES**
purification of yellow cake by carbonic acid salt treatment, 20: 1973(P)

**URANIUM NITRIDES**
preparation of powdered, by cermet disintegration, 20: 2250(P)
UC–UN–UO, phase studies, 20: 2353(R) (USBM-RC-1205, pp 11-14)

**URANIUM ORE PROCESSING PLANTS**
design of Japanese, 20: 1964

**URANIUM ORES**
radioactive equilibrium between ionium and uranium in Ningyotoge, 20: 2066

**URANIUM OXIDES**
analysis for trace impurities by activation methods, 20: 1784
mechanical properties of, effects of oxygen content on, 20: 3321(R) (ANL-7082, pp 29-53)
preparation from Mo–U alloys, 20: 1885(P)
testing for use in sheft seals for potassium space power systems, 20: 2242
$EuO_2$–$UO_2$, phase studies by x-ray diffraction, 20: 2379
UC–UN–UO, phase studies, 20: 2353(R) (USBM-RC-1205, pp 11-14)

**URANIUM(IV) OXIDES**
antiferromagnetism in, neutron-diffraction study of, (E), 20: 3301
chemical compatibility with rhenium–tungsten cladding, (E), 20: 3446(R) (GEST-2045)
expansion of hollow irradiated pellets of, in collapsible zircaloy cladding, 20: 2463
fabrication into reactor fuel spheres using arc plasma, 20: 2288
fabrication of fuel tubes of, for irradiation in VBWR, 20: 2280 (DP-989)
grain growth in porous compacts of, 20: 2373
melting of, molten boundary in, 20: 2392
melting point, 20: 2390
microstructure variations with temperature, device for studying, 20: 2393
preparation of spherical particles of, sol-gel process for, 20: 2226 (RT/CHI(65)-30)
radiation effects on pellets of, 20: 2429 (ORNL-3837)
radiation effects on hollow pellets of, in collapsible Zircaloy-2, 20: 2415 (AECL-2276)
radiation effects on melting fuel elements of, neutron, 20: 2416 (AECL-2289)
radiation effects on thermal conductivity and electric properties of, 20: 2452
reactions with iron(III) and iron hydroxide ions in perchloric acid solutions, kinetics of, 20: 1851
reactions with krypton ions, saturation values, secondary electron yields, and sputtering ratios in, 20: 1813 (EUR-2515.e)
reactions with Zircaloy-4 at 1900°C, 20: 2257(R) (GEMP-52A, pp 47-52)
reactivity measurements on irradiated, 20: 3384
separation from fission products by chlorination in alkali chloride melt, 20: 1962
testing in temperature gradient between 1600 and 2400°C, 20: 2233
thermal expansion with radial temperature gradient, 20: 2234
thermodynamic behavior of hypostoichiometric, 20: 2319 (GE-TM-65-6-13)
BeO–$ThO_2$–$UO_2$–$Y_2O_3$, irradiation testing of tubular fuel elements of, 20: 2467
BeO–$UO_2$, fission gas diffusion from, for 1 hr at 1400°C, 20: 3470(R) (GA-5499)
Fe–$UO_2$, radioinduced swelling in, 20: 2223(R) (GEMP-51A)
$MoO_2$–$MoO_3$–$UO_2$, phase studies, 20: 2384
$PbO_2$–$UO_2$, phase studies on, 20: 1871
$PuO_2$–$UO_2$, fluorination of, facility for, 20: 3321(R) (ANL-7082, pp 29-53)
$PuO_2$–$UO_2$, fluorination in fluidized beds, 20: 1970
$PuO_2$–$UO_2$, in-pile thermal conductivity of stoichiometric and hypostoichiometric, 20: 2453
$PuO_2$–$UO_2$, irradiation testing of fuel elements in Plutonium Recycle Test Reactor, 20: 2449
$PuO_2$–$UO_2$, irradiation testing of vibrationally compacted fuel rods of, 20: 2461
$PuO_2$–$UO_2$, isotopic burnup analysis of, 20: 2454
$PuO_2$–$UO_2$, melting point of, 20: 2391
$PuO_2$–$UO_2$, performance as fuels in mixed-spectrum superheat reactors, (E/T), 20: 3471(R) (GEAP-4861)
$PuO_2$–$UO_2$, structure variations with burnup, 20: 2451
$PuO_2$–$UO_2$, testing as fast reactor fuel, 20: 2448
$PuO_2$–$UO_2$, thermocouples for temperature measurements on, 20: 2114
$PuO_2$–$UO_2$, transient performance of pre-irradiated, 20: 2469
$SiO_2$–$ThO_2$–$UO_2$, liquidus curves and thermodynamic properties, 20: 2326 (IFA-FR-39)
$ThO_2$–$UO_2$, fabrication and processing reactor fuels of, 20: 2282 (HW-SA-3755)
$ThO_2$–$UO_2$, microstructure variations with temperature, 20: 2393
$ThO_2$–$UO_2$, radiation effects on pellets of, 20: 2429 (ORNL-3837)
$ThO_2$–$UO_2$–$ZrO_2$, phase studies on, 20: 2361(T) (WAPD-Trans-21)
$UO_2$–UP, fabrication for strength tests, 20: 3321(R) (ANL-7082, pp 29-53)
$UO_2$–Zircaloy-2, radiation effects on burnup at increased heat rating, 20: 2421 (EXP-NRX-22902)
U–$UO_2$, preparation and sintering of powdered, 20: 2279 (CEA-R-2828)
U–$UO_2$, thermodynamic studies on, 20: 1810 (EUR-2458.f)
W–$UO_2$, radiation effects on melting fuel elements of, 20: 2416 (AECL-2289)

**URANIUM(IV-VI) OXIDES**
chlorination by mixtures of carbon tetrachloride with argon or chlorine at 400 to 550°C, 20: 1816 (ORNL-TM-1258)

**URANIUM PHOSPHIDES**
corrosion by air at room temperature, 20: 3321(R) (ANL-7082, pp 29-53)
corrosion by boiling water, 20: 3321(R) (ANL-7082, pp 29-53)
$UO_2$–UP, fabrication for strength tests, 20: 3321(R) (ANL-7082, pp 29-53)

**URANIUM SILICIDES**
preparation of powdered, by cermet disintegration, 20: 2250(P)

**URANIUM SULFIDES**
oxidation by helium–oxygen mixtures at 700°C, 20: 3321(R) (ANL-7082, pp 29-53)
$UC_2$–US, phase studies, 20: 3321(R) (ANL-7082, pp 29-53)

**URANIUM SYSTEMS**
U–UC, phase diagram, 20: 2366
U–$UO_2$, preparation and sintering of powdered, 20: 2279 (CEA-R-2828)
U–$UO_2$, thermodynamic studies on, 20: 1810 (EUR-2458.f)

**URANYL CHLORIDES**
formation in chlorination of uranium (IV–VI) oxide by chlorine–carbon tetrachloride, 20: 1816 (ORNL-TM-1258)

**URANYL FLUORIDES**
preparation by reaction of Mo–U alloys with gaseous hydrofluoric acid and oxygen-containing gas, 20: 1885(P)
**URANYL NITRATES**
conversion to tetrafluoride, development of Excer process for, 20: 1956 (ORNL-1696)
decomposition and dehydration of hydrates of, formation of monohydrate in, 20: 1821(T) (AEC-tr-6620)
thermal decomposition of, temperature effects on, 20: 1820(T) (AEC-tr-6619)
$B$–$UO_2(NO_3)_2$–$H_2O$, critical mass of, 20: 3379 (ORNL-TM-1207)
**UREA**
ester–urea, ESR studies of irradiated, 20: 1935
ether–urea, ESR studies of irradiated, 20: 1935
fumaric acid–urea, ESR studies of irradiated, 20: 1935
ketone–urea, ESR studies of irradiated, 20: 1935
**UREA, THIO-, COMPLEXES**
with cerium, lanthanum, neodymium, praseodymium, and samarium acetates, solubility in water, 20: 1869
**URETHANS**
effects on mouse lungs, carcinogenic, 20: 1606 (AD-623079)
**URIDINE**
metabolism in Drosophila spermatocytes of, 20: 1657
**URIDINES, 2'-DEOXY-**
radiation effects on metabolism of, in rats, 20: 1630
**URIDYLIC ACID**
metabolism in *Escherichia coli* ribosomes, tracer study, 20: 1592 (BNL-7903)
**UTERUS**
radiotherapy of carcinoma of, late pathological effects, 20: 1725

# V

**VACUUM**
effects on space vehicles, estimates of magnitude and nature of, 20: 2036 (AD-618030)
**VACUUM SEALS**
design for mass-spectrometer source-handling systems, (E), 20: 2159
**VACUUM VALVES**
design for mass-spectrometer source-handling systems, (E), 20: 2159
**VALLECITOS BOILING WATER REACTOR**
fuel testing in, on low-density compacted powder uranium dioxide, 20: 2232
fuel tube fabrication for irradiation in, 20: 2280 (DP-989)
**VALLECITOS SUPERHEAT REACTOR**
fuel development for, 20: 3472(R) (GEAP-4891)
power distribution analysis of, 20: 3472(R) (GEAP-4891)
**VAN ALLEN RADIATION BELTS**
effects on manned military space vehicles, (T), 20: 2656 (NASA-SP-71, pp 265-86)
origin and properties of, review of hypotheses on, 20: 2861
radiation distributions in, engineering models for, (E), 20: 2654 (NASA-SP-71, pp 47-55)
radiation doses from inner and outer, 20: 2663
shielding manned space vehicles against, (T), 20: 3245 (NASA-SP-71, pp 407-14)
shielding space vehicles from, use of selective vehicle orientation for, (T), 20: 3249 (NASA-SP-71, pp 473-6)
**VANADIUM**
corrosion cracking by inorganic and organic acids and inorganic salt solutions, stress-, 20: 2254 (BM-RI-6680)
corrosion resistance to mercury at 900°F, 20: 2264
determination in blood using neutron activation analysis with pre-irradiation separation, 20: 1791
determination in oils, activation, 20: 1739(R) (GA-4297)
deuteron elastic scattering at 27.5 Mev, angular distribution for, (E/T), 20: 3057
effects of additions of, on steam corrosion of niobium–tin–zirconium alloys, 20: 2255(R) (EURAEC-1323)
neutron reactions $(n,\gamma)$ at 1 ev to 50 kev, cross sections for, (E), 20: 3032
preparation by aluminum reduction of vanadium pentoxide, 20: 2225 (IS-T-40)
**VANADIUM ALLOYS**
Al–Cu–Fe–Sn–Ti–V–Zr, deformation and heat treatment effects on mechanical properties of, 20: 2309 (AD-615024)
Al–Sn–Ti–V–Zr, formability characteristics and mechanical properties of, 20: 2308 (AD-614637)
Mo–Nb–V–Zr, creep-rupture properties of, 20: 2336 (ORNL-P-1634)
Nb–Ta–V–Zr, strength at high temperatures, 20: 2407(P)
Nb–Ti–V–Zr, properties, effects of composition on, 20: 2340 (ORNL-TM-1131)
Nb–V, corrosion by lithium at 815°C, effects of oxygen on, 20: 2340 (ORNL-TM-1131)
Ti–V, compatibility with plutonium–thorium–uranium alloys, 20: 2230
Ti–V, corrosion by sodium at high temperatures, 20: 3320(R) (ANL-7082, pp 1-28)
Ti–V, corrosion by oxygenated sodium at 540°C, effects of polarization on, 20: 3321(R) (ANL-7082, pp 29-53)
Ti–V, corrosion cracking by ferric chloride, hydrochloric acid, and nitric acid solutions, stress-, 20: 2254 (BM-RI-6680)
**VANADIUM CARBIDES**
wetting by liquid cobalt, copper, iron, and nickel, 20: 1837
TiC–VC, wetting by liquid copper, 20: 1837
**VANADIUM COMPLEXES**
chlorophyllin, radiosensitivity effects in mice, gamma, 20: 1692
**VANADIUM OXIDES**
magnetic properties of, from iron-57 Mössbauer effect in, (E), 20: 3289
reduction by aluminum, preparation of vanadium by, 20: 2225 (IS-T-40)
testing for use in shaft seals for potassium space power systems, 20: 2242
$P_2O_5$–$V_2O_3$, electric conductivity of glass systems of, 20: 2316 (COO-1198-220)
$P_2O_5$–$V_2O_5$, electric conductivity of glass systems of, 20: 2316 (COO-1198-220)
**VANADIUM STEEL**
Mn–Mo–Ni–V, welding procedures for, electro-slag, 20: 2281(R) (EURAEC-1408)
**VANADIUM SYSTEMS**
C–V, phase studies on, thermal analysis of, (E), 20: 1863
**VENTILATION**
effects on radon content in living and working environments, 20: 2090
**VESPIDAE**
radiation effects on unisexual wasp Devorgilla, genetic, 20: 1643
radiation effects on, genetic, 20: 1622 (WT-820)
**VIBRATION TESTING**
method for, eddy-current, 20: 2025 (BNWL-SA-349)
**VINYL ALCOHOL POLYMERS**
performance in colored films for gamma and neutron dosimetry, 20: 2135
radiation effects on dielectric properties of, electron, 20: 1897 (NASA-TN-D-3032)
radioinduced crosslinking with nylon 66 in presence of allyl methacrylate–methanol–water system, 20: 1909
**VINYL COMPOUNDS**
radioinduced polymerization with sytrene, 20: 1910
**VIRUSES**
photoreactivation of ribonucleic acid in tobacco mosaic, after ultraviolet inactivation, 20: 1659
radiation effects on survival of Vaccinia, effects of particle aggregation on, ultraviolet, 20: 1651
radiosensitivity of, in water, gamma, 20: 1645
**VISCOMETERS**
design of radiometric, using cobalt-60, 20: 2200

# W

**WASTE DISPOSAL**
at Argonne and Los Alamos, comparison of operational practices in low- and intermediate-level, 20: 3603 (LA-DC-7249)
at Shippingport Atomic Power Station, 20: 3521
fixation in phosphate glass, 20: 3606
fixation of radioactive gases in water-unleachable rocklike products, 20: 3608(P)
in Italy, technical and hygienic aspects of, 20: 3604 (RT/PROT(65)-12)
in rivers, hydrological problems in, 20: 2082 (CEA-Bib.-59)
liquid storage, use of asphalt composition in, 20: 2248(P)
storage in salt mines, heat generation by, 20: 3605
**WASTE PROCESSING**
at Argonne and Los Alamos, comparison of operational practices in low- and intermediate-level, 20: 3603 (LA-DC-7249)
filtration and vacuum freeze drying, apparatus for, 20: 3607(P)
fixation in phosphate glass, 20: 3606
methods in Denmark, 20: 3646
plant at Rocky Flats for, operation of aqueous, 20: 1940 (RFP-638)
**WASTE SOLUTIONS**
separation of technetium from, by ion exchange, 20: 1963
**WATER**
analysis for deuterium, 20: 1801(P)
analysis for heavy water, leak detector for, 20: 2099 (AECL-2291)
analysis for strontium-90, 20: 1754
analysis for tritium, review on methods for, 20: 1728 (AD-618562)
antenna performance in fresh, cylindrical and spherical, 20: 3632 (SC-DR-65-459)
boiling detection in, tests of acoustic instrument for, 20: 2014 (ORNL-P-1678)
bremsstrahlung and electron transport in, (T), 20: 3246 (NASA-SP-71, pp 437-48)

content in concretes, gamma and neutron shielding parameter variations with, 20: 3253
corrosion effects of oxygenated, on chromium–nickel steel, 20: 2262 (WCAP-2056(Pt.6))
critical heat flux and flow regimes in boiling, (E), 20: 2012(R) (NYO-3304-6)
decompression in reactors, analysis of, (E), 20: 3324(R) (IITRI-578P21-13)
demineralization of boiling-reactor cooling, 20: 3539 (ACNP-65558 (Rev.1))
diffusion in alkaline earth chlorides and water at 25°C, coefficients of, 20: 1865
effects on pulse radiolysis of organic solutes, spectra of, 20: 1920
flow in round tubes, power distribution effects on burnout and hydrodynamic instability forced, 20: 2009 (EUR-2490.e)
gamma dose albedos for, (T), 20: 3274
heat transfer by boiling, burnout heat flux in, 20: 2023
heat transfer by supercritical, 20: 3485(R) (WCAP-2120)
mass spectra of ionized, in strong electrical fields, 20: 1829
molecular structure model of, 20: 2520(R) (IA-920)
neutron diffusion in, pulsed thermal, 20: 2944
neutron diffusion parameters in, sample geometry effects on, (E), 20: 2952
neutron scattering kernels and laws for, thermal, 20: 3412
neutron slowing down in, spin polarization effects on fission, (T), 20: 2969
neutron spectra in cooled, thermal, (E), 20: 2945
neutron spectra in, containing erbium and gadolinium, temperature-dependent, (E/T), 20: 2966
oxidation of tungsten, effects of hydrogen on, 20: 2261(R) (UCRI-326)
oxidation of tungsten, mass spectrometric study of, 20: 2261(R) (UCRI-326)
pressure pulse production in fixed volume of, by pulse heating, 20: 3338
radiolysis of, isotope effects on hydrogen production by, 20: 2520(R) (IA-920)
radiolysis of, properties of excited molecules from, 20: 2520(R) (IA-920)
reactions with sodium in loops, separation of products of, 20: 1960
reactions with xenon di- and hexafluorides, 20: 1881
sampling of tap, evaporator collector for continuous, 20: 1757
separation from ethanol by ion exchange, 20: 2520(R) (IA-920)
separation from steam, design of device for, 20: 2024(P)
sodium compounds heats of solution in, 20: 1825
solvent properties for actinium oxalate, 20: 1846
solvent properties for rare earth acetates, temperature effects on, 20: 1869
solvent properties for erbium and yttrium phosphates, 20: 1873
solvent properties of actinium hydroxide, aging effects on, 20: 1847
tritium concentration in, review on methods for, 20: 1728 (AD-618562)
Al–$H_2O$, fission-neutron age to indium resonance in, (E), 20: 2970
allyl methacrylate–methanol–$H_2O$, effects on radioinduced crosslinking of nylon 66 and poly (vinyl alcohol), 20: 1909
$Al_2O_3$–$H_2O$, flow in circular pipe, analysis of laminar, 20: 2020
boric acid–$H_2O$, thermal neutron spectra in, determination using integral activation techniques, (E), 20: 2965
B–$UO_2(NO_3)_2$–$H_2O$, critical mass of, 20: 3379 (ORNL-TM-1207)
Fe–$H_2O$, neutron attenuation in, few- and multigroup P3 analyses of, (T), 20: 2939 (WAPD-T-1710)
$HNO_3$–TBP–$H_2O$, nitric acid concentration in mixer-settler extractor as function of time, 20: 1953 (IS-T-34)
$H_2O$–$D_2O$, neutron diffusion parameters for cylinders of, 20: 2951
Pu–$H_2O$, criticality studies on, 20: 3368 (BNWL-SA-214)
Pu–$H_2O$, criticality of, effects of plutonium-240 concentrations on, 20: 3368 (BNWL-SA-214)
steam–water, pressure drop in natural-circulation single-component flow at low pressures, 20: 2021

**WATER-$d_2$**
detection in water, leak detector for, 20: 2099 (AECL-2291)
effects on growth of yeasts as function of inoculum age, 20: 1601
mass spectra of ionized, in strong electrical fields, 20: 1829
neutron diffusion parameters in, measurement using pulsed neutron techniques, 20: 2954
neutron diffusion coefficient in, containing voids, thermal, (E), 20: 2957
neutron scattering at 0.05 to 10 ev, differential cross section for, 20: 2963
production by catalytic exchange between steam and hydrogen in the presence of fissionable material, 20: 1884(P)
production of, abstracts of patents on, 20: 1951 (AECL-2279)
sodium compounds heats of solution in, 20: 1825
spectra of, for infrared, 20: 1877
$H_2O$–$D_2O$, neutron diffusion parameters for cylinders of, 20: 2951

**WATER COOLED REACTORS**
feasibility of mixed-spectrum steam-superheat power reactors, (T), 20: 3471(R) (GEAP-4861)
heat transfer in fuel-rod bundles in superheated-steam-cooled, (E), 20: 3471(R) (GEAP-4861)
kinetics of mixed-spectrum steam-superheat, (E/T), 20: 3471(R) (GEAP-4861)
operations of MSSCEF, 20: 3471(R) (GEAP-4861)
plutonium burnup and production in, calculation methods for, 20: 3535

**WATER MODERATED REACTORS**
calandria arrangement for, design of, 20: 3354(P)
neutron flux distribution and coolant density profile of, method for calculating, 20: 3500
physics parameters of gas-cooled, computer program for calculating, 20: 3381 (UJV-1309b/65)
plutonium distribution in fuel rods for, optimization, 20: 3457

**WATER PURIFICATION EQUIPMENT**
feasibility of filtration unit for, 20: 2072 (AD-616006)

**WATER SUPPLIES**
decontamination of, feasibility of filtration unit for, 20: 2072 (AD-616006)
radiation disinfection of, gamma, 20: 1645

**WATER VAPOR**
corrosive effects on uranium, 20: 1805 (AWRE-O-69/65)
effects in irradiated uranium dioxide fuel elements, 20: 2468
effects on fluorine–trifluoroacetic acid reaction, 20: 1881
effects on preparation of sulfur- and xenon-containing fluorine compounds, 20: 1881
radiolysis of, ion yields in alpha, 20: 1936
reactions with beryllium in simulated launch pad abort environments at 800 to 1500°C, 20: 2341 (SC-DC-65-1637)
reactions with uranium at 30 to 80°C, kinetics, 20: 1804 (AWRE-O-68/65)
solubility in alkali nitrates, thermodynamics of, 20: 1812 (EUR-2495.e)

**WATER WAVES**
detection of tsunami, system design and development for, 20: 2058(R) (NVO-98-10)
measurement of tsunami, pressure sensors for, 20: 2059(R) (NVO-98-11)

**WELDING**
electron-beam, of tube to tubesheet joints, 20: 2283 (KAPL-3110)
equipment for tubular elements, 20: 2304(P)
methods for, of three-quarters in. thick 6061 aluminum alloy, 20: 3609 (ACF-11)
procedures for reactor steels, process development for electro-slag, 20: 2281(R) (EURAEC-1408)

**WELDS**
tensile properties for joining wrought depleted uranium, design allowables for, 20: 2342 (SC-DR-58-61)

**WELL LOGGING**
radiometric, performance in analysis of ore composition, 20: 2063

**WHEAT**
analysis for mercury, activation, 20: 1738(R) (GA-4041)
analysis for mercury contamination, activation, 20: 1739(R) (GA-4297)
analysis for mercury by neutron activation, 20: 1755
ethylenimine-induced mutations of, 20: 1655
radiation effects on lipids in, effects of dose on gamma, 20: 1637
radiation effects on development of embryos of, 20: 1666
radioinduced mutations of, $\gamma$ and fast neutron, 20: 1655

**WHISTLERS**
measurements on proton, hydrogen ion/electron content ratio from, (T), 20: 2847 (AD-614716)

**WINES**
radiopreservation of, effects of dose on organoleptic qualities in, 20: 2197

**WOOD**
analysis in crime detection, activation, 20: 1738(R) (GA-4041)
properties as neutron reflector, 20: 3390
properties as neutron reflectors, 20: 3391

**WYOMING (NATRONA CO.)**
uranium isotope and daughter product fractionation in sandstone deposits in, 20: 2057

# X

**X RADIATION**
detection and measurement of pulsed or steady, monitor design for, 20: 2121 (AD-614832)
detection of lunar, theories on, 20: 2666
dose distributions from, in fallout, (T), 20: 2048 (USNRDL-TR-888)
dose of incident and gonads, during diagnostic radiography, 20: 1703
dose to skin of, during diagnostic radiography, 20: 1704
dosimetry of exit dose for lungs, during radiotherapy, 20: 1699
dosimetry of, performance of scintillation detectors for, 20: 2157
effects in mammals, delayed pathological, 20: 1716
effects of embryonic exposure to, on aging of chickens, 20: 1611(R) (COO-1119-4)
effects on algal, biological, 20: 1681

effects on antibody formation in mice, injected with sheep erythrocytes, 20: 1661
effects on antibody response of rabbits to antigens, 20: 1680
effects on bacteriophages, ESR spectra of, 20: 1623
effects on bacteria, biological, effects of p-hydroxymercuribenzoate on, 20: 1618 (NYO-3319-6)
effects on brain tissues of therapeutic doses of, delayed, 20: 1713
effects on carbon dioxide production in starved yeasts, effects of glucose supplementation on, 20: 1653
effects on carcinomas of skin, concentrated serial exposure, 20: 1718
effects on carcinomas of bronchi, protracted exposure, 20: 1720
effects on cell membranes, traumatic, 20: 1636
effects on color center formation in sodium fluoride crystals, 20: 1908
effects on conditioned-reflex activity of dogs exposed *in utero*, 20: 1627(T)
effects on course of leukemia in man and mice, whole-body, 20: 1700
effects on course of leukemia in man and mice, whole-body, 20: 1701
effects on desoxyribonucleic acid content of cells of corneal epithelium of rats, 20: 1633
effects on desoxyribonucleic acid synthesis in *Escherichia coli*, 20: 1639
effects on development of wheat embryos, 20: 1666
effects on Drosophila population, genetic, 20: 1642
effects on Drosophila males, genetic, 20: 1644
effects on Drosophila, genetic, 20: 1619(R) (TID-22293)
effects on electric conductivity of gallium selenides, 20: 2439
effects on function and morphology of endocrine glands, 20: 1671
effects on growth of bone marrow transplants in mice, effects of arabinofuranosylcytosine on, 20: 1687
effects on growth of lymphoid cells, on monolayers of mouse embryo cells in culture, 20: 1658
effects on immune reactions in mice to injected allogenic and syngenic bone marrow, 20: 1660
effects on immune reactions in mice and rats, 20: 1632
effects on leukocyte blood picture in guinea pigs, effects of dose and time on, 20: 1670
effects on lungs of rabbits and rats, 20: 1675
effects on lymphocyte nuclei, morphological, 20: 1612 (EUR-2505.e)
effects on man of therapeutic doses of, pathological, 20: 1717
effects on mice and rats at 250 kev, pathological, 20: 1614 (NASA-SP-71, pp 97-103)
effects on mouse lungs, carcinogenic, 20: 1606 (AD-623079)
effects on mutation rate in murine cell line resistant to purine analogs, 20: 1678
effects on nerve regeneration, 20: 1635
effects on phosphorylation in nuclei of tumor cells, 20: 1626
effects on pituitary tumors, therapeutic, 20: 1708
effects on pollen of maize, genetic, 20: 1656
effects on polymerization of vinylidene chloride on polyethylene film, 20: 1902
effects on polymerization of hexamethylcyclotrisiloxane in solid phase, 20: 1903
effects on response to barbiturates by rats, 20: 1662
effects on rice seeds, biological, 20: 1669
effects on skin of swine, pathological, 20: 1609 (BNL-9477)
effects on survival of animal cells in tissue culture, dose effects on, 20: 1617(R) (NP-15149)
effects on the ichneumonid wasp, Devorgilla, genetic, 20: 1643
effects on thermal sensitivity of fungi and yeast, 20: 1640
effects on weight gain of swine progeny, 20: 1677
effects on yeast, biological, 20: 1663
emission from solar flares, correlation with radio and visible emission, 20: 2582
energy spectra from Scorpius (SCO-XR-1) and sun, (E), 20: 2585
radiation effects on metabolism of desoxyribonucleic acid in epithelial cells of rats, 20: 1634
reactions with potassium bromide crystals, $\alpha$ and F centers induced in, 20: 1919

**X-RAY BEAMS**
collimation of, design of adjustable-aperture devices for, (E), 20: 2162
dosimetry of, from accelerator, 20: 1721
use of narrow, for reduction of patient dose during diagnostic radiography, 20: 1698

**X-RAY DIFFRACTOMETERS**
radiation intensity distributions in, effects of Soller slits on, 20: 2161

**X-RAY EQUIPMENT**
design of variable-aperture collimators, (E), 20: 2162

**X-RAY SOURCES**
efficiency of tritium–zirconium, for excitation in x-ray spectroscopy, 20: 2136

**X-RAY SPECTRA**
intensity of satellites in, (T), 20: 2645

**X-RAY SPECTROMETERS**
crystal alignment and preparation for precision, 20: 2126 (CONF-650657-1)

**X-RAY SPECTROSCOPY**
source for, efficiency of tritium–zirconium, 20: 2136

**XENON**
alkali metal scattering by, cross sections and rainbow effect in, (E/T), 20: 2636
buildup in reactor shutdown, control of, 20: 3410
collisions of atoms of, with alkali metal atoms, ionization produced in, (E), 20: 2639
collisions of atoms of, with singly charged krypton ions, profound stripping and scattering in, (E), 20: 2644
diffusion in irradiated uranium, coefficient of, 20: 2358(T) (AERE-Trans-1034)
diffusion in uranium carbide monocrystals, 20: 2317 (EURAEC-1380)
distributions in reactors, spatial oscillations of, 20: 3326 (WAPD-T-1732)
electric breakdown potential of, measurement of a-c, 20: 3160 (AD-618503)
helium scattering on, velocity dependence of total cross sections for, (E), 20: 2614
microwave absorption in weakly ionized plasma of, in magnetic fields, (E), 20: 3204
reactions with mercury, cross sections for line broadening from, (E), 20: 2637
reactor criticality effects in PWR, (E/T), 20: 3383 (WCAP-3269-48)
spectra of mercury and sulfur isolated in, at high temperatures, 20: 1818 (UCRL-11976)

**XENON FLUORIDES**
bond vibration modes of, Bradley-Urey force constants for, (T), 20: 1845
preparation, 20: 2520(R) (IA-920)
reactions with antimony fluoride, octafluorocyclopentene, and water, 20: 1881

**XENON ISOTOPES**
yields in uranium-233 thermal fission, (E), 20: 3010(R) (IDO-14663)

**XENON ISOTOPES Xe-129**
gamma transitions in, conversion coefficients for, (E), 20: 3038

**XENON ISOTOPES Xe-133**
beta decay of, spin dependence of Rayleigh scattering from, (E), 20: 3082
content in equal volumes of air and blood, partition coefficients for, 20: 1599
sorption on activated carbon, from air, argon, carbon dioxide, and helium, 20: 1969
tracer use of, for cerebral blood flow measurements, 20: 1711

**XENON ISOTOPES Xe-135**
reactor poisoning by, method of compensating, 20: 3359(P)

# Y

**YANKEE POWER REACTOR**
fuel assemblies from, remote-control equipment for underwater inspection of irradiated, 20: 2117
fuel burnup in, 20: 3504

**YEASTS**
effects of water-$d_2$ on growth of, as function of inoculum age, 20: 1601
mutations of *Schizosaccharomyces pombe*, genetic analysis of chemically-induced, 20: 1654
radiation effects on carbon dioxide production in starved, effects of glucose on, 20: 1653
radiation effects on, biological, 20: 1663
radiation effects on wine, effects of dose on, 20: 2197
radioinduced mutations of *Schizosaccharomyces pombe*, ultraviolet, 20: 1654
radiosensitivity of, thermal, effects of uv and x radiations on, 20: 1640
radiosensitivity of mitosis in, 20: 1664
radiosensitivity of meiosis in, 20: 1664

**YTTERBIUM**
determination in potassium chloride medium, polarographic, 20: 1795
determination using Chromotrope 2B, photometric, 20: 1772

**YTTERBIUM ALLOYS**
Co–Yb, preparation and structure of $MgCu_2$-type, 20: 2385(T)
Fe–Yb, anisotropy of exchange in garnets of, 20: 1802 (AD-618038)
Nb–Y–Zr, corrosion by steam at 400-500°C, 20: 2276(P)

**YTTERBIUM IONS**
magnetic resonance in calcium tungstate, 20: 2520(R) (IA-920)

**YTTERBIUM ISOTOPES Yb-164**
energy states of, large-spin rotational, (E/T), 20: 3008 (COO-1420-104)

**YTTERBIUM ISOTOPES Yb-166**
energy states of, large-spin rotational, (E/T), 20: 3008 (COO-1420-104)

**YTTERBIUM ISOTOPES Yb-170**
gamma transition in, conversion coefficient of 84-kev, 20: 3155

**YTTERBIUM OXIDES**
magnetic susceptibility at 4 to 300°K, 20: 3318

**YTTRIUM**
content in soils of Tomsk region, 20: 2065
determination in silicate ores using neutron activation analysis, 20: 2056
determination using Chromotrope 2B, photometric, 20: 1772
effects on chromium–iron alloys oxidation by carbon dioxide, 20: 2263
reactions with potassium phosphate, 20: 1873
separation from thorium and other rare earths by ion exchange in ammonium thiocyanate–organic solvent–water systems, 20: 1959
separation of trace elements from, by precipitation ion exchange, 20: 1958
**YTTRIUM ALLOYS**
Al–Cr–Fe–Y, corrosion by steam at 550°C, effects of pre-oxidation and strain on, 20: 2223(R) (GEMP-51A)
Al–Cr–Fe–Y, diffusion of uranium through cladding of, 20: 2223(R) (GEMP-51A)
Al–Cr–Fe–Y, oxidation by air at 900 and 1100°C, 20: 2223(R) (GEMP-51A)
Al–Cr–Fe–Y, radiation effects on mechanical properties of, 20: 2409(R) (AD-617319)
**YTTRIUM CHLORIDES**
reactions with sodium fluosilicates, precipitation in, 20: 1870
KCl–NaCl–$YCl_3$, phase studies on, 20: 1872
**YTTRIUM FERRATES**
performance in magnetometers for point field measurements, 20: 2104 (MATT-362)
**YTTRIUM ISOTOPES Y-86**
gamma spectra of, conversion coefficients from, (E/T), 20: 3019 (ORNL-P-1657)
**YTTRIUM ISOTOPES Y-88**
gamma transitions at 898.2 and 1836.2 kev, (E), 20: 3043
production using ORNL 86-in. cyclotron, 20: 2212
**YTTRIUM ISOTOPES Y-90**
determination in presence of strontium-90 by liquid scintillation spectrometry, 20: 1766
separation from strontium-90 by elution process, 20: 2211
shielding of, bremsstrahlung attenuation factors for, 20: 3254
**YTTRIUM ISOTOPES Y-91**
determination in sea water, methods for, 20: 1749 (USNRDL-TR-912)
**YTTRIUM OXIDES**
bonding to refractory metals, 20: 2292
BeO–$ThO_2$–$UO_2$–$Y_2O_3$, irradiation testing of tubular fuel elements of, 20: 2467
**YTTRIUM OXYBROMIDES**
preparation and crystal structure, 20: 1834
**YTTRIUM PHOSPHATES**
solubility in salt solutions, sulfuric acid, and water, 20: 1873

# Z

**ZINC**
corrosion resistance to mercury at 900°F, 20: 2264
corrosive effects on refractory metals in presence of molten chlorides, 20: 2266
determination in grease samples, activation, 20: 1738(R) (GA-4041)
determination in human blood serum using neutron activation analysis, 20: 1586
determination in snake venom, activation, 20: 2520(R) (IA-920)
deuteron elastic scattering at 26 Mev, optical model analysis of, (E/T), 20: 3053
diffusion of uranium in liquid, at 600 to 800°C, 20: 2368
reactions with uranium monocarbide at 540 to 800°C, phase formations in, 20: 2404
separation of trace amounts of, from alkali metals, alkaline earths, and rare earths, 20: 1958
**ZINC ALLOYS**
Cd–Mg–Zn, corrosive effects on carbon steel, stainless steel, and tantalum at 500, 750, and 850°C, 20: 2265
Mg–rare earths–Zn–Zr, crystal structure, 20: 2399
Mg–U–Zn, corrosive effects on refractory metals in presence of molten chlorides, 20: 2266
Mg–Zn, crystal structure, 20: 2399
Mg–Zn, reactions with plutonium dioxide, 20: 2220 (ANL-7059)
**ZINC CHLORIDES**
LiCl–KCl–Zn–$ZnCl_2$, reactions of uranium monocarbide at 540 to 802°C in, 20: 2404
**ZINC COMPLEXES**
chlorophyllin, radiosensitivity effects in mice, gamma, 20: 1692
**ZINC ISOTOPES Zn-64**
gamma transition at 991.7 kev following Coulomb excitation, (E), 20: 3043
neutron resonance at 288 ev, radiation width of, (E), 20: 3133
**ZINC ISOTOPES Zn-65**
excretion by man, effects of chelating agents on, 20: 1691
gamma transition at 1115.6 kev, (E), 20: 3043
uptake by rat hair, 20: 1695
**ZINC ISOTOPES Zn-66**
gamma transition at 1039.2 kev following Coulomb excitation, (E), 20: 3043
neutron resonance at 328 ev, radiation width of, (E), 20: 3133
**ZINC ISOTOPES Zn-67**
neutron resonance at 226 ev, radiation width of, (E), 20: 3133
neutron resonance at 456 ev, radiation width of, (E), 20: 3133
**ZINC ISOTOPES Zn-68**
gamma transition at 1077.6 kev following Coulomb excitation, (E), 20: 3043
neutron resonance at 530 ev, radiation width of, (E), 20: 3133
**ZINC ISOTOPES Zn-70**
gamma transition at 883.7 kev following Coulomb excitation, (E), 20: 3043
**ZINC SELENIDES**
radiation effects on, ESR studies of, 20: 2492
radiation effects on double acceptor defects in n-type, 20: 2499
radioinduced defects in, fluorescence studies of, 20: 2498
**ZINC SULFIDES**
efficiency of copper-activated crystals of, for detection of high-energy electrons, 20: 2164
**ZINC SYSTEMS**
As–Sn–Zn, radiation effects on thermal conductivity of superconducting, 20: 2488
LiCl–KCl–Zn–$ZnCl_2$, reactions of uranium monocarbide at 540 to 802°C in, 20: 2404
**ZIRCALOY-2**
hydride nucleation and growth in, 20: 2253 (AECL-2297)
preparation of powders of, 20: 2222 (EURAEC-1390)
radiation effects on ductility of, fast neutron, 20: 2420(R) (DPST-65-83-8)
radiation effects on collapsible sheaths of, 20: 2415 (AECL-2276)
structure of alpha-, effects of preferred orientation on creep, deformation, and fracture in, 20: 2339 (ORNL-P-1753)
$UO_2$–Zircaloy-2, radiation effects on burnup at increased heat rating, 20: 2421 (EXP-NRX-22902)
**ZIRCALOY-4**
corrosion by steam, effects of air introduction on, 20: 2257(R) (GEMP-52A, pp 47-52)
diffusion of fission products in, 20: 2389
embrittlement by steam during dynamic heating, 20: 2257(R) (GEMP-52A, pp 47-52)
hydride precipitation in, effects of stress on habit planes for, 20: 2355 (WAPD-T-1757(Rev.))
reactions with urania at 1900°C, 20: 2257(R) (GEMP-52A, pp 47-52)
recrystallization of cold-worked alpha-, primary and secondary, 20: 2330 (KAPL-3091)
recrystallization of as-quenched and beta-quenched, primary and secondary, 20: 2331 (KAPL-3103)
**ZIRCONIUM**
analysis for rare earths, spectrographic, 20: 2520(R) (IA-920)
corrosion resistance to mercury at 900°F, 20: 2264
determination in zirconium metal and powders, method for, 20: 1729 (AD-619244)
deuteron elastic scattering at 26 Mev, optical model analysis of, (E/T), 20: 3053
diffusion in, parameters for self-, 20: 2356(T) (AERE-Trans-1030)
effects in reactor loss-of-coolant accidents, 20: 3334
hydridation of, at 800°C, effects of oxygen on, 20: 2267
hydridation of, kinetics, 20: 2222 (EURAEC-1390)
hydride nucleation and growth in, 20: 2253 (AECL-2297)
hydride precipitation in alpha-, habit planes for, 20: 2355 (WAPD-T-1757(Rev.))
melting of, performance of induction furnace for cold-mold, 20: 2352(R) (USBM-RC-1205, pp 9-10)
neutron reactions (n,γ) at 1 ev to 50 kev, cross sections for, (E), 20: 3032
preparation of powders of, 20: 2222 (EURAEC-1390)
reactions with hydrogen in irradiated uranium dioxide fuel elements, 20: 2468
separation by solvent extraction using long chain amines, 20: 1761
solubility in molten potassium, 20: 2237
sorptive properties for oxygen in liquid potassium at 815°C, 20: 2367
structure of alpha-, effects of preferred orientation on creep, deformation, and fracture in, 20: 2339 (ORNL-P-1753)
Nb–Sn–Zr, corrosion by steam, effects of antimony, chromium, iron, and vanadium additions on, 20: 2255(R) (EURAEC-1323)
U–Zr, irradiation testing of reactor fuel tubes of, 20: 2466
**ZIRCONIUM ALLOYS**
Al–Cu–Fe–Sn–Ti–V–Zr, deformation and heat treatment effects on mechanical properties of, 20: 2309 (AD-615024)
Al–La–Zr, crystal structure, 20: 2399
Al–Sn–Ti–V–Zr, formability characteristics and mechanical properties of, 20: 2308 (AD-614637)

Cu–Nb–Zr, radiation effects on tensile properties of, fast-neutron, 20: 2414 (AECL-2272)
Cu–Zr, conductivity, mechanical properties, and precipitation in, 20: 2334 (NP-15530)
Mg–rare earths–Zn–Zr, crystal structure, 20: 2399
Mg–rare earths–Zr, crystal structure, 20: 2399
Mg–Zr, crystal structure, 20: 2399
Mo–Nb–V–Zr, creep-rupture properties of, 20: 2336 (ORNL-P-1634)
Mo–Ti–Zr, cavitation damage to TZM, in liquid sodium, 20: 2243
Mo–Ti–Zr, compatibility of TZM, with niobium–zirconium alloy in flowing zirconium, 20: 2238
Mo–Ti–Zr, corrosion by lithium at high temperatures, 20: 2269
Mo–Ti–Zr, corrosion of TZM, by potassium at high temperatures, 20: 2271
Mo–Ti–Zr, testing of TZM, for use in liquid-metal turbine blades and nozzles, 20: 2240
Nb–Ta–V–Zr, strength at high temperatures, 20: 2407(P)
Nb–Ti–V–Zr, properties, effects of composition on, 20: 2340 (ORNL-TM-1131)
Nb–W–Zr, corrosion by flowing lithium, 20: 2238
Nb–W–Zr, corrosion by bismuth and tin, 20: 2275
Nb–W–Zr, creep-rupture properties of, 20: 2336 (ORNL-P-1634)
Nb–W–Zr, stress effects in corrosion of D-43, by potassium, 20: 2270
Nb–Y–Zr, corrosion by steam at 400-500°C, 20: 2276(P)
Nb–Zr, brazing techniques for bonding to graphite, 20: 2294
Nb–Zr, compatibility with alkali metals at high temperatures, 20: 2236
Nb–Zr, compatibility with TZM alloy in flowing lithium, 20: 2238
Nb–Zr, corrosion by boiling and condensing alkali metals, 20: 2268
Nb–Zr, corrosion by potassium at high temperatures, 20: 2271
Nb–Zr, corrosion by potassium–sodium system, 20: 2273
Nb–Zr, corrosion by bismuth and tin, 20: 2275
Nb–Zr, fabrication into superconducting delay lines, (E), 20: 3612 (CONF-651001-6)
Nb–Zr, hydridation of, kinetics, 20: 2222 (EURAEC-1390)
Nb–Zr, hydride nucleation and growth in, 20: 2253 (AECL-2297)
Nb–Zr, magnetic flux jumps in superconducting NbZr in pulsed magnetic fields, (E), 20: 2921
Nb–Zr, magnetic fields on surface of superconducting, in external magnetic field, (E), 20: 2924
Nb–Zr, mass transfer of carbon and nitrogen to, from type-316 stainless steel in liquid potassium, 20: 2239
Nb–Zr, parameters for zirconium self-diffusion in, 20: 2356(T) (AERE-Trans-1030)
Nb–Zr, preparation of powders of, 20: 2222 (EURAEC-1390)
Nb–Zr, superconducting properties of, effects of heat treatments and microstructure on, 20: 2395
Nb–Zr, superconducting-normal transitions in variable fields, mechanisms of, (E), 20: 2902
Nb–Zr, testing for use in liquid-metal turbine blades and nozzles, 20: 2240
Nb–Zr, transfer of carbon and nitrogen to, from stainless steels in potassium, 20: 2270
Pu–U–Zr, compatibility with Hastelloy-X, Incoloy-800, and type-304 stainless steels, 20: 2229
Pu–U–Zr, properties as fast power-breeder fuels, 20: 2386
Pu–U–Zr, reactions with Hastelloy, Incoloy, and stainless steel at high temperatures, 20: 3320(R) (ANL-7082, pp 1-28)
Sn–Zr, parameters for zirconium self-diffusion in, 20: 2356(T) (AERE-Trans-1030)
Ta–Zr, parameters for zirconium self-diffusion in, 20: 2356(T) (AERE-Trans-1030)
U–Zr, compatibility with iron, 20: 2229

**ZIRCONIUM CARBIDES**
corrosion by hydrogen fluoride at 2000 to 3100°K, 20: 2261(R) (UCRI-326)
effects on graphite microstructure, 20: 2318(R) (GA-5915(Pt.1))
thermal expansion of, to 2700°C, 20: 1839
wetting by liquid cobalt, copper, iron, and nickel, 20: 1837
C–UC–ZrC, preparation as reactor fuel material, 20: 2305(P)
UC–ZrC, compatibility of molybdenum, niobium, and tungsten at high temperatures in, 20: 2332 (LA-3307)

**ZIRCONIUM CHLORIDES**
stability in molten mixtures of alkali and alkaline earth metals, 20: 1822(T) (ANL-Trans-233)
KCl–NaCl–$ZrCl_4$, stability of zirconium dichloride in, 20: 1822(T) (ANL-Trans-233)

**ZIRCONIUM FLUORIDES**
thermal capacity and thermodynamic properties of tetravalent, at 5 to 307°K, 20: 1809 (COO-1149-30)

**ZIRCONIUM HYDRIDES**
neutron scattering at 0.06 to 10 ev, differential cross section for, 20: 2963
nucleation and growth in zirconium alloys, 20: 2253 (AECL-2297)

**ZIRCONIUM ISOTOPES Zr-90**
energy levels of, existence of low-lying 4-, 20: 3141
neutron reactions (n,γ) at 1 ev to 50 kev, cross sections for, (E), 20: 3032

**ZIRCONIUM ISOTOPES Zr-91**
energy-level transition probabilities of, E2, (T), 20: 3115
neutron reactions (n,γ) at 1 ev to 50 kev, cross sections for, (E), 20: 3032

**ZIRCONIUM ISOTOPES Zr-94**
neutron reactions (n,γ) at 1 ev to 50 kev, cross sections for, (E), 20: 3032

**ZIRCONIUM ISOTOPES Zr-95**
content in atmosphere, 1962 to 1963, 20: 2049
content in fallout particles, 20: 2053
determination in sea water, methods for, 20: 1749 (USNRDL-TR-912)
separation from aqueous solutions, use of silica gel for, 20: 1742 (INR-636/XIII/J)

**ZIRCONIUM NITRIDES**
NbN–ZrN, superconductivity of wires of, (E), 20: 2891

**ZIRCONIUM OXIDES**
radiation effects on electric conductivity of, 20: 2460
spectra of, at 1300°K, infrared emission, 20: 1823
structure of monoclinic, from room temperature to 1095°C, 20: 2314 (ARL-65-140)
testing for use in shaft seals for potassium space power systems, 20: 2242
$Al_2O_3$–$ZrO_2$, preparation of, for use at temperatures to 1750°C, 20: 2382
$ThO_2$–$UO_2$–$ZrO_2$, phase studies on, 20: 2361(T) (WAPD-Trans-21)

**ZIRCONIUM SYSTEMS**
C–Mo–Nb–Ta–Ti–W–Zr, creep properties at 1800 to 2200°F of Cb132M, 20: 2333(R) (NASA-CR-54457)
C–Mo–Ti–Zr, creep properties at 1800 to 2200°F of TZC, 20: 2333(R) (NASA-CR-54457)
Mo–Ti–Zr, creep at 1800 to 2200°F of TZM, 20: 2333(R) (NASA-CR-54457)
Nb–N–Zr, equilibrium solid solutions at 1200 to 1800°C in, 20: 2337 (ORNL-P-1677)
T–Zr, efficiency as x-ray spectroscopy source, 20: 2136

# REPORT NUMBER INDEX

Reports, conference papers and proceedings, numbered translations, and patents abstracted during the period are included in this index. Each item is listed by report number; this is followed by the abstract number and a brief notation regarding public availability. The index entries show which reports are on file in the depository libraries, which reports have been published in open-literature journals (journal citation given), and which reports can be purchased (source and price). Whenever a report is identified by more than one number, cross references from secondary to primary report numbers are cited.

The report number codes apply to AEC reports unless designated otherwise. Non-AEC reports are identified by parenthetical notes after the report codes; e.g., (non-AEC), (British), (Canadian), (French). The note (Misc.) identifies those codes used for both USAEC and non-AEC reports. Patents are listed under the heading "PATENTS"; the country of origin is included in parentheses.

A comprehensive listing of both AEC and non-AEC report codes is contained in TID-85(5th Rev.), *Report Number Series Used by the Division of Technical Information in Cataloging Reports*. This information is also included in the Cumulative Report Number Index (issued annually).

## Public Availability of USAEC Reports

All USAEC reports abstracted in *NSA* are available to the public through one or more of the following sources:

(1) Depository libraries in the United States, in other countries, and in international agencies. A list of these depositories appears on the inside covers of each issue of *NSA*.

(2) Scientific and technical journals or other publications.

(3) Microcard Editions, Inc., in Microcard and micronegative form. Orders and inquiries should be sent to: Accounting and Shipping Department, West Salem, Wisconsin 54669.

(4) Clearinghouse for Federal Scientific and Technical Information, U. S. Department of Commerce, Springfield, Virginia 22151.

(5) Superintendent of Documents, U. S. Government Printing Office, Washington, D. C. 20402.

## Public Availability of Non-AEC Reports

*U. S. Reports*. Many reports of U. S. Government agencies are available to the public from the Clearinghouse for Federal Scientific and Technical Information (CFSTI). This availability is given when known. Such reports should be ordered by AD number or NASA-N number. If availability is not shown, inquiries may be directed to CFSTI. In the case of NP numbers, inquiries should be by title and author.

*Non-U. S. Reports*. Many reports of atomic energy establishments of other countries are deposited in the libraries listed on the inside covers of each issue of *NSA*.

Additionally, the following have made their reports available as indicated.

AUSTRALIA

*Australian Atomic Energy Commission Research Establishment*. Available upon request from the Library, Australian Atomic Research Establishment, Private Mail Bag, Sutherland, New South Wales, Australia.

BELGIUM

*Centre d'Étude de l'Énergie Nucléaire*. Available upon request to individuals and organizations, from the Centre d'Étude de l'Énergie Nucléaire (CEN), 31, Rue Belliard, Bruxelles, Belgium.

CANADA

*Atomic Energy of Canada Limited*. For sale by the Technical Information Officer, Atomic Energy of Canada Limited, Chalk River, Ontario, Canada. Copies are also deposited in libraries in the United Kingdom.

*National Research Council of Canada*. Available from the National Research Council of Canada, Ottawa 2, Ontario, Canada.

DENMARK

*Atomic Energy Commission Research Establishment, Risø*. Available on exchange from the Library, Danish Atomic Energy Commission, Risø, Roskilde, Denmark. Also for sale by Jul. Gjellerup, Booksellers, 87 Sölvgade, København K., Denmark.

*Danatom*. Available on loan from Research Establishment, Risø, Roskilde, Denmark. Copies are available from Danatom, Aurehøjvej 2, Hellerup, Denmark.

EURATOM

Reports from the Commission of the European Atomic Energy Community are available from: Presses academiques europeennes, 98, chaussee de Charleroi, Brussels 6, Belgium; and Office central de vente des publications des Communautes eurodeennes 2, place de Metz, Luxemburg.

FRANCE

*Commissariat à l'Énergie Atomique*. Inquiries for reports numbered 1-2199 should be addressed to Commissariat à l'Énergie Atomique, Service Central de Documentation, Centre d'Études Nucléaires de Saclay, Boite Postale No. 2, Gif-sur-Yvette (S. et O.), France. Reports numbered 2200 and above are available from La Documentation Francaise, 16 Rue Lord-Byron, Paris VIII, France.

*Service Central de Protection contre les Rayonnements Ionisants*. Copies are available from Ministère de la Santé Publique, Service Central de Protection contre les Rayonnements Ionisants, B. P. n° 35—LE VESINET (S. et O.), France.

GERMANY

*Deutsches Elektronen-Synchrotron DESY*. Copies are available from Deutsches Elektronen-Synchrotron Desy, Dokumentation, 2000 Hamburg-Gr. Flottbek 1, Notkestieg 1, Germany.

*Gesellschaft für Kernforschung mbH (KFK)*. Copies are available from Gesellschaft für Kernforschung mbH, 75 Karlsruhe, Postfach 947, Germany. Copies are also deposited in many national nuclear centers in the world.

*Kernforschungsanlage*. Copies may be ordered from Zentralbibliothek der Kernforschungsanlage Jülich, Jülich, Bundesrepublik Deutschland.

*Hahn-Meitner-Institute für Kernforschung*. Available without charge from Hahn-Meitner-Institute für Kernforschung Berlin, Bibliothek, Glienicker Strasse 100, 1 Berlin

39, Germany. Copies are deposited in many national nuclear centers in the world.

*Johann-Wolfgang-Goethe Universität, Frankfurt Am Main, Institut für Kernphysik, (IKF).* Copies are available from Gmelin Institut, 40-42 Varrentrappstrasse, Frankfurt (Main), West Germany.

ISRAEL

*Israel Atomic Energy Commission.* Available without charge from Ministry of Defence/Atomic Energy Commission, Soreq Research Establishment, Yavne, Israel. Copies are deposited in libraries in Israel and in other countries.

ITALY

*Centro Informazioni Studi Esperienze (CISE).* For sale at CISE Press Office, Casella Postale 3986, Milano, Italy. Copies are deposited in libraries in Italy.

*Comitato Nazionale per l'Energia Nucleare.* Copies are available from Comitato Nazionale per l'Energia Nucleare, Divisione Affari Internazionali e Studi Economici, Ufficio Pubblicazioni, Via Belisario, 15, Roma, Italy.

JAPAN

*Japan Atomic Energy Research Institute (JAERI).* Available from the Staff Supply Cooperative of Japan Atomic Energy Research Institute (JAERI), 1-1 Tamura-Cho, Shiba, Minato-Ku, Tokyo, Japan. Copies are deposited in depositories in Tokyo, Nagoya, and Osaka.

*Nagoya University.* Copies are available from Research Information Center, Institute of Plasma Physics, Nagoya University, Nagoya, Japan.

*University of Tokyo.* Available free of charge from Institute for Nuclear Study, University of Tokyo, Tanashi-Machi, Kitatama-gun, Tokyo, Japan.

NETHERLANDS

*Reactor Centrum Nederland.* For sale by Reactor Centrum Nederland, 112 Scheveningseweg, 's-Gravenhage, The Netherlands. Copies are deposited in university libraries in Holland and in many national nuclear centers in the world.

NEW ZEALAND

*Institute of Nuclear Sciences.* Copies are available from Librarian, Institute of Nuclear Sciences, D.S.I.R., Private Bag, Lower Hutt, New Zealand. Copies are deposited in other countries.

NORWAY

*Forsvarets Forskningsinstitutt.* Copies available from Norwegian Defence Research Establishment, Library, P. O. Box 25, Kjeller, Norway.

*Institutt for Atomenergi.* "KR" reports are available on an exchange basis from the Library, Institutt for Atomenergi, Box 40, Kjeller, Norway. Other series are not generally available to the public.

*Norwegian Reactor School.* Copies are available from The Library, Institutt for Atomenergi, P. O. Box 40, Kjeller, Norway.

PAKISTAN

*Atomic Energy Center.* Copies are available from Atomic Energy Center, P. O. Box 658, Lahore, (West Pakistan).

POLAND

Reports of the Polish nuclear institutes are published by the Nuclear Energy Information Center of the Government Commissioner for Use of Nuclear Energy. Copies are available from Ośrodek Informacji o Energii Jądrowej, Warszawa, PKiN, Poland.

SPAIN

*Junta de Energia Nuclear.* "JEN" reports are available without charge from Servicio de Documentation, Junta de Energia Nuclear, Ciudad Universitaria, Madrid (3), Spain.

SWEDEN

*Aktiebolaget Atomenergi.* "AE" reports are for sale from Aktiebolaget Atomenergi, Library Section, Box 43041, Stockholm 43, Sweden. Bibliographies and literature surveys of the VDDIT- series may be obtained from Aktiebolaget Atomenergi, Information Office, Scientific and Technical Information, Box 43041, Stockholm 43, Sweden. Other series are not generally available to the public. Organizations in the atomic energy field may obtain copies from Aktiebolaget Atomenergi. Microcopy of AE reports is available from the International Documentation Centre, Tumba, Sweden.

SWITZERLAND

*CERN European Organization for Nuclear Research.* Available without charge from CERN European Organization for Nuclear Research, Geneva 23, Switzerland. Copies are deposited in libraries in 13 countries.

*Eidgenössisches Institut für Reaktorforschung.* "EIR" reports are available from Eidgenössiches Institut für Reaktorforschung, c/o Bibliothek, Würenlingen/Ag, Switzerland.

TURKEY

*Turkish Atomic Energy Commission.* Copies are available free of charge from T.A.E.C., Çekmece Nuclear Research Center, P. O. Box 1, Airport, Istanbul, Turkey.

UNITED KINGDOM

*United Kingdom Atomic Energy Authority.* Some reports are for sale in the United States by the British Information Service (BIS), 845 Third Avenue, New York, N. Y. 10022. United Kingdom reports generally may be purchased from Her Majesty's Stationery Office, London. Copies not for sale by Her Majesty's Stationery Office may be purchased in microcopy form from Micro Methods Limited, East Ardsley, Wakefield, Yorks, England. Report copies are deposited in a large number of libraries in England.

## Conferences

Published conference proceedings as well as individual unpublished papers from conferences are included in this index. A CONF number is assigned to the conference if published proceedings are received and also if only a single paper is received. The base number used is year-month-sequence. Thus, the number CONF-650101 would indicate that the conference was held in 1965, in January, and that this was the first January 1965 conference so received. This number would be assigned to complete published proceedings, or if individual papers are received, the base number would be extended to include a paper number, i.e., CONF-650101-1. As additional papers are received, they will be assigned consecutive numbers in the series, CONF-650101-1, 2, 3, 4, etc. This numbering system ensures that all papers received from a conference will be associated with that conference in this index.

If published proceedings are received after the receipt of individual papers, the complete proceedings will be abstracted and the abstract number will appear in this index with the base CONF number.

## Abbreviations Used in Availability Column

| | |
|---|---|
| AECL | For sale by Atomic Energy of Canada Ltd., Chalk River, Ontario, Canada. |
| BIS | For sale by British Information Service, 845 Third Avenue, New York, N. Y. 10022 |
| CFSTI | For sale by the Clearinghouse for Federal Scientific and Technical Information, U. S. Department of Commerce, Spring- |

field, Virginia 22151. The symbol "cy" indicates that the format of the item sold may be either a printed document or a photographic reproduction (two-thirds of original size) depending upon the availability of printed stock. The indicated price is for either format. The symbol "mn" is used to indicate that copy is also available in the form of micronegatives (microfiche).

Dep. AEC reports: Full-size copy is on deposit in the depository libraries both inside and outside the United States. These reports are also for sale by Microcard Editions, Inc., Accounting and Shipping Department, West Salem, Wisconsin 54669.

Non-AEC reports: Full-size copy on deposit in the depository libraries in the United States only.

Dep.(mn) Same as for Dep., except copy is in micronegative (microfiche) form.

DSIR For sale by the National Lending Library for Science and Technology (D.S.I.R.), Boston Spa, Yorkshire, England.

DTI Extension Available from the U. S. Atomic Energy Commission, Division of Technical Information Extension, P. O. Box 62, Oak Ridge, Tennessee 37830.

EM Blueprints and microcopy of AEC engineering drawings are available from Clearinghouse for Federal Scientific and Technical Information, U. S. Department of Commerce, Springfield, Virginia 22151. Current prices of the CAPE- packages may be obtained from this address. TID-4100, available from the Division of Technical Information Extension, P. O. Box 62, Oak Ridge, Tennessee 37831, contains information on all the CAPE- packages for sale.

Gmelin Available at a nominal charge and under the AED- number shown from Atomic Energy Documentation Center, Gmelin Institute, 40-42 Varrentrappstrasse Frankfurt (Main), West Germany.

GPO For sale by the Superintendent of Documents, Government Printing Office, Washington, D. C. 20402.

HMSO Her Majesty's Stationery Office, London.

IAEA Available from the International Atomic Energy Agency, Vienna, Austria, and from its sales agencies in various countries throughout the world. A list of these agencies is found in each STI/DOC and STI/PUB publication.

JCL For sale by the Special Libraries Association Translation Center, John Crerar Library, 35 West 33rd Street, Chicago, Illinois 60616.

NAS National Academy of Sciences, National Research Council, Washington, D. C. 20418.

NRC For sale by the National Research Council of Canada, Ottawa, Ontario, Canada.

ORAU Available on interlibrary loan from the Library, Oak Ridge Associated Universities, Post Office Box 117, Oak Ridge, Tennessee 37830.

ORINS See ORAU.

UKAEA, London Available from United Kingdom Atomic Energy Authority, 11 Charles II Street, London, S. W. 1.

UN United Nations Bookshop, United Nations Headquarters, New York, New York.

USGS Available free of charge from the U. S. Geological Survey, Washington, D. C. 20242.

[The symbols "ph," "mf," and "fs" are used to designate that copy is available only in photostat, microfilm, or facsimile form. The symbol "mn" is used to designate that copy is available in micronegative (microfiche) form. The symbol "cy" is used to designate full size or photographically enlarged copy (two-thirds of original size).]

| Report No. | Abstract No. | Availability |
|---|---|---|
| **A&ES–** | **(Non-AEC)** | |
| 64-4 | 20-2594 | See N64-23208 |
| **ACF–** | | |
| 11 | 20-3609 | Dep. mn; CFSTI $2.00 cy, $0.50 mn |
| 412-253 | 20-3609 | See ACF-11 |
| **ACNP–** | **(Misc.)** | |
| 65558(Rev.1) | 20-3539 | Dep. mn; CFSTI $2.00 cy, $0.50 mn |
| 65573 | 20-3540 | Dep. mn; CFSTI $2.00 cy, $0.50 mn |
| **AD–** | **(Misc.)** | |
| 613023 | 20-2307 | CFSTI $2.00 cy, $0.50 mn |
| 614618 | 20-2184 | CFSTI $3.00 cy, $0.75 mn |
| 614636 | 20-2930 | CFSTI $2.00 cy, $0.50 mn |
| 614637 | 20-2308 | CFSTI $1.00 cy, $0.50 mn |
| 614645 | 20-2820 | CFSTI $3.00 cy, $0.75 mn |
| 614654 | 20-3157 | CFSTI $5.00 cy, $1.00 mn |
| 614715 | 20-2562 | CFSTI $1.00 cy, $0.50 mn |
| 614716 | 20-2847 | CFSTI $2.00 cy, $0.50 mn |
| 614814 | 20-1979 | CFSTI $2.00 cy, $0.50 mn |
| 614824 | 20-2067 | CFSTI $3.00 cy, $0.50 mn |
| 614832 | 20-2121 | CFSTI $3.00 cy, $0.75 mn |
| 614843 | 20-2678 | |
| 614895 | 20-2068 | CFSTI $2.00 cy, $0.50 mn |
| 614899 | 20-2408 | CFSTI $1.00 cy, $0.50 mn |
| 614907 | 20-2667 | CFSTI $3.00 cy, $0.75 mn |
| 614910 | 20-2196 | CFSTI $1.00 cy, $0.50 mn |
| 614923 | 20-3158 | CFSTI $1.00 cy, $0.50 mn |
| 614990 | 20-1980 | CFSTI $3.00 cy, $0.75 mn |
| 615003 | 20-2069 | CFSTI $4.00 cy, $1.00 mn |
| 615004 | 20-2070 | CFSTI $4.00 cy, $1.00 mn |
| 615005 | 20-2071 | CFSTI $1.00 cy, $0.50 mn |
| 615017 | 20-2035 | CFSTI $5.00 cy, $1.00 mn |
| 615024 | 20-2309 | CFSTI $1.00 cy, $0.50 mn |
| 615111 | 20-2848 | CFSTI $2.00 cy, $0.50 mn |
| 615124 | 20-2668 | |
| 615152 | 20-2519 | CFSTI $2.00 cy, $0.50 mn |
| 616518 | 20-2931 | CFSTI $4.00 cy, $1.00 mn |
| 617319 | 20-2409 | CFSTI $2.00 cy, $0.50 mn |
| 617918 | 20-2410 | CFSTI $5.00 cy, $1.25 mn |
| 617928 | 20-2096 | CFSTI $1.00 cy, $0.50 mn |
| 618006 | 20-2072 | CFSTI $3.60 cy, $0.50 mn |
| 618026 | 20-2007 | CFSTI $4.00 cy, $1.00 mn |
| 618030 | 20-2036 | CFSTI $3.00 cy, $0.75 mn |
| 618038 | 20-1802 | CFSTI $1.00 cy, $0.50 mn |
| 618078 | 20-2411 | CFSTI $3.00 cy, $0.75 mn |
| 618079 | 20-2412 | CFSTI $5.00 cy, $1.00 mn |
| 618101 | 20-2073 | CFSTI $4.00 cy, $0.75 mn |
| 618138 | 20-3159 | CFSTI $1.00 cy, $0.50 mn |
| 618194 | 20-2185 | CFSTI $1.00 cy, $0.50 mn |
| 618203 | 20-2889 | CFSTI $1.00 cy, $0.50 mn<br>Phys. Rev., 140: A1889-91(1965) |
| 618228 | 20-1893 | CFSTI $3.00 cy, $0.75 mn |
| 618296 | 20-2821 | CFSTI $1.00 cy, $0.50 mn |
| 618304 | 20-2531 | CFSTI $3.00 cy, $0.75 mn |
| 618396 | 20-2097 | CFSTI $2.00 cy, $0.50 mn |
| 618398 | 20-2098 | CFSTI $2.00 cy, $0.50 mn |
| 618503 | 20-3160 | CFSTI $1.00 cy, $0.50 mn |
| 618520 | 20-3161 | CFSTI $2.00 cy, $0.50 mn |
| 618552 | 20-1728 | CFSTI $3.00 cy, $0.75 mn |
| 618659 | 20-2750 | CFSTI $1.00 cy, $0.50 mn |
| 618664 | 20-2679 | CFSTI $1.00 cy, $0.50 mn |
| 618676 | 20-3006 | CFSTI $5.00 cy, $1.00 mn |
| 618681 | 20-2310 | CFSTI $2.00 cy, $0.50 mn |
| 618683 | 20-3162 | CFSTI $3.00 cy, $0.75 mn |
| 618688 | 20-2413 | CFSTI $4.00 cy, $1.00 mn |
| 618925 | 20-2311 | CFSTI $2.00 cy, $0.50 mn |
| 619197 | 20-2312 | CFSTI $1.00 cy, $0.50 mn |
| 619208 | 20-2313 | CFSTI $1.00 cy, $0.50 mn |
| 619244 | 20-1729 | CFSTI $1.00 cy, $0.50 mn |
| 619266 | 20-1803 | CFSTI $6.00 cy, $1.25 mn |
| 622333 | 20-3610 | CFSTI $4.00 cy, $0.75 mn |
| 622626 | 20-2122 | CFSTI $2.00 cy, $0.50 mn |
| 622825 | 20-2008 | CFSTI $2.00 cy, $0.50 mn |
| 623079 | 20-1606 | CFSTI $1.00 cy, $0.50 mn |
| 623095 | 20-1894 | CFSTI $1.00 cy, $0.50 mn |
| **AEC-tr–** | **(For complete listing see TID-4025)** | |
| 6591 | 20-2690 | Dep. mn; CFSTI $1.00 cy, $0.50 mn; JCL $1.60 fs, $0.80 mf |
| 6619 | 20-1820 | Dep. mn; JCL $1.10 fs, $0.80 mf |
| 6620 | 20-1821 | Dep. mn; JCL $1.10 fs, $0.80 mf |

| Report No. | Abstract No. | Availability |
|---|---|---|
| **AECL–** | **(Canadian)** | |
| 2272 | 20-2414 | Dep.; AECL $1.00 |
| 2276 | 20-2415 | Dep.; AECL $1.50 |
| 2277 | 20-2421 | See EXP-NRX-22902 |
| 2279 | 20-1951 | Dep.; AECL $1.00 |
| 2289 | 20-2416 | Dep.; AECL $1.00 |
| 2291 | 20-2099 | Dep.; AECL $1.50 |
| 2296 | 20-3583 | See CRT-1187 B |
| 2297 | 20-2253 | Dep.; AECL $1.00 |
| **AED-C–** | **(Non-AEC)** | |
| 04-18 | 20-1607 | Dep. mn |
| 04-19 | 20-1608 | Dep. mn |
| 15-07 | 20-2669 | Dep. mn |
| **AERE-R–** | **(British)** | |
| 4862 | 20-2447 | Phil. Mag. (8), 12: 573-93(1965) |
| 4973 | 20-2701 | Nucl. Phys., 74: 241-60(1965) |
| 4988 | 20-1895 | Dep.; BIS $0.60; HMSO 3s. 0d. |
| **AERE-Trans–** | **(British)** | |
| 1030 | 20-2356 | Dep.; BIS $0.30; HMSO 1s. 9d. |
| 1032 | 20-2357 | Dep.; BIS $0.30; HMSO 1s. 9d. |
| 1034 | 20-2358 | Dep.; BIS $0.80; HMSO 4s. |
| **AFCRL–** | **(Non-AEC)** | |
| 65-125 | 20-2848 | See AD-615111 |
| 65-371 | 20-2097 | See AD-618396 |
| 65-373 | 20-2098 | See AD-618398 |
| 65-375 | 20-2531 | See AD-618304 |
| 65-401 | 20-2096 | See AD-617928 |
| 65-409 | 20-3161 | See AD-618520 |
| **AFML-TR–** | **(Non-AEC)** | |
| 64-334 | 20-2307 | See AD-613023 |
| 65-154 | 20-2890 | |
| **AFOSR–** | **(Misc.)** | |
| 65-0649 | 20-2678 | See AD-614843 |
| 65-0733 | 20-2519 | See AD-615152 |
| 65-1069 | 20-2821 | See AD-618296 |
| 65-1314 | 20-3159 | See AD-618138 |
| **AHSB(RP)–** | **(British)** | |
| M-40 | 20-2074 | Dep. |
| **AHSB(S)–** | **(British)** | |
| R-92 | 20-2075 | Dep.; BIS $1.60; HMSO 8s. |
| **AMRA-CR–** | **(Non-AEC)** | |
| 64-05/4 | 20-2219 | CFSTI $3.00 cy, $0.50 mn |
| **AMRA-TR–** | **(Non-AEC)** | |
| 65-04 | 20-2309 | See AD-615024 |
| 65-05 | 20-2308 | See AD-614637 |
| **ANL–** | | |
| 6859 | 20-1952 | Dep. mn; CFSTI $4.00 cy, $1.00 mn |
| 7030 | 20-2591 | Dep. mn; CFSTI $2.00 cy, $0.50 mn |
| 7052 | 20-3366 | Dep. mn; CFSTI $2.00 cy, $0.50 mn |
| 7059 | 20-2220 | Dep. mn; CFSTI $1.00 cy, $0.50 mn |
| 7068 | 20-2076 | Dep. mn; CFSTI $1.00 cy, $0.50 mn |
| 7082 | 20-3319 | Dep. mn; CFSTI $3.00 cy, $0.75 mn |
| 7085 | 20-2123 | Dep. mn; CFSTI $1.00 cy, $0.50 mn |
| **ANL-Trans–** | | |
| 233 | 20-1822 | Dep. mn; CFSTI $1.00 cy, $0.50 mn; JCL $1.10 fs, $0.80 mf |
| **ARL–** | **(Non-AEC)** | |
| 65-4 | 20-2667 | See AD-614907 |
| 65-140 | 20-2314 | |
| **AWRE-O–** | **(British)** | |
| 41/65 | 20-2077 | Dep.; BIS $1.40; HMSO 7s. |
| 60/65 | 20-2822 | Dep.; BIS $1.60; HMSO 8s. 0d. |
| 68/65 | 20-1804 | Dep.; BIS $0.65; HMSO 3s. 3d. |
| 69/65 | 20-1805 | Dep.; BIS $0.60; HMSO 3s. |
| **BIO–** | **(Italian)** | |

| Report No. | Abstract No. | Availability |
|---|---|---|
| 04/64 | 20-2046 | Dep. mn |
| **BLG–** | **(Belgian)** | |
| 68-11 | 20-2192 | Dep. mn |
| 328 | 20-3277 | Dep. mn |
| **BM-RI–** | **(Misc.)** | |
| 6680 | 20-2254 | Bureau of Mines Free |
| 6697 | 20-1806 | Bureau of Mines Free |
| **BMI–** | **(Misc.)** | |
| 1746 | 20-2278 | Dep. mn; CFSTI $1.00 cy, $0.50 mn |
| **BN–** | **(Misc.)** | |
| 6408-2 | 20-2222 | See EURAEC-1390 |
| **BNL–** | | |
| 917 | 20-1588 | Dep. mn; CFSTI $3.00 cy, $0.75 mn |
| 7903 | 20-1592 | Dep. mn; CFSTI $1.00 cy, $0.50 mn |
| 8260 | 20-1714 | Phys. Med. Biol., 10: 491-504(1965) |
| 8824 | 20-1656 | Mutat. Res., 2: 344-51(1965) |
| 9015 | 20-2160 | Rev. Sci. Instrum., 36: 1582-7(1965) |
| 9281 | 20-1937 | Dep. mn; CFSTI $2.00 cy, $0.50 mn |
| 9283 | 20-1668 | Radiat. Bot., 5: 423-30(1965) |
| 9318 | 20-3301 | Phys. Rev., 140: A1448-52(1965) |
| 9477 | 20-1609 | Dep. mn; CFSTI $3.00 cy, $0.75 mn |
| 9481 | 20-2724 | Phys. Rev. Letters, 15: 641-5(1965) |
| 9505 | 20-2532 | Dep. mn; CFSTI $1.00 cy, $0.50 mn |
| 9536 | 20-2533 | Dep. mn; CFSTI $2.00 cy, $0.50 mn |
| 9556 | 20-2592 | Dep. mn; CFSTI $1.00 cy, $0.50 mn |
| 9569 | 20-2900 | Phys. Lett., 19: 277-9(1965) |
| 9587 | 20-2534 | Dep. mn; CFSTI $1.00 cy, $0.50 mn |
| 9590 | 20-2124 | Dep. mn; CFSTI $1.00 cy, $0.50 mn |
| 9591 | 20-3580 | Dep. mn; CFSTI $2.00 cy, $0.50 mn |
| 9601 | 20-1730 | Dep. mn; CFSTI $2.00 cy, $0.50 mn |
| 9609 | 20-2213 | Dep. mn; CFSTI $1.00 cy, $0.50 mn |
| 9611 | 20-1610 | Dep. mn; CFSTI $1.00 cy, $0.50 mn |
| 9614 | 20-1731 | Dep. mn; CFSTI $2.00 cy, $0.50 mn |
| **BNL-tr–** | | |
| 23 | 20-1899 | Dep. mn; CFSTI $1.00 cy, $0.50 mn; JCL $1.10 fs, $0.80 mf |
| 42 | 20-2086 | Dep. mn; CFSTI $2.00 cy, $0.50 mn; JCL $4.60 fs, $1.52 mf |
| **BNWL–** | | |
| 112 | 20-2417 | Dep. mn; CFSTI $3.00 cy, $0.75 mn |
| 113-8 | 20-3611 | Dep. mn; CFSTI $2.00 cy, $0.50 mn |
| 156 | 20-3367 | Dep. mn; CFSTI $2.00 cy, $0.50 mn |
| **BNWL-SA–** | | |
| 133 | 20-1661 | Proc. Soc. Exp. Biol. Med., 120: 115-17 (1965) |
| 214 | 20-3368 | Dep. mn; CFSTI $2.00 cy, $0.50 mn |
| 340 | 20-3581 | Dep. mn; CFSTI $2.00 cy, $0.50 mn |
| 341 | 20-1581 | Dep. mn; CFSTI $1.00 cy, $0.50 mn |
| 349 | 20-2025 | Dep. mn; CFSTI $2.00 cy, $0.50 mn |
| **CAPE–** | | |
| 1261 | 20-1797 | |
| 1268 | 20-1799 | |
| 1271 | 20-1798 | |
| **CCDN-CI–** | | |
| 1 | 20-3018 | See NYO-72-27 |
| **CEA-Bib–** | **(French)** | |
| 32 | 20-3007 | Dep. mn |
| 59 | 20-2082 | Dep. mn |
| **CEA-R–** | **(French)** | |
| 2482 | 20-3582 | Dep. mn |
| 2801 | 20-2418 | Dep. mn |
| 2814 | 20-3369 | Dep. mn |
| 2816 | 20-2125 | Dep. mn |
| 2827 | 20-1807 | Dep. mn |
| 2828 | 20-2279 | Dep. mn |
| 2850 | 20-1732 | Dep. mn |
| **CEA-tr–** | **(French)** | |
| X-616 | 20-1957 | Dep. mn; JCL $2.60 fs, $1.04 mf |

| Report No. | Abstract No. | Availability |
|---|---|---|
| **CERN–** | **(European Organization for Nuclear Research)** | |
| 65-31 | 20-2535 | Dep. mn |
| **CEX–** | | |
| 65.4 | 20-2083 | Dep. mn; CFSTI $2.75 cy, $1.25 mn |
| **CNAEM–** | **(Turkish)** | |
| 26 | 20-3163 | Dep. mn |
| **CNLM–** | **(Misc.)** | |
| 5729 | 20-3545 | Dep. mn; CFSTI $300 cy, $0.75 mn |
| **CONF-512–** | **20-2470** | **(American Society for Testing of Materials, 67th Annual Meeting, Chicago, June 1964)** |
| **CONF-532–** | **20-2427** | **(Symposium on Thermal Radiation of Solids, San Francisco, Mar. 1964) See NASA-SP-55** |
| **CONF-608–** | **20-3316** | **(International Conference on Nuclear Magnetic Resonance and Relaxation in Solids, 13th Colloque Ampere, Leuven, Belgium, Sept. 1964)** |
| **CONF-679** | **20-1345**<br>**20-1346**<br>**20-2480** | **(International Conference on the Physics of Semiconductors, Paris, July 1964)** |
| | | 10-2 |
| **CONF-720–** | **20-3239** | **(2nd Symposium on Protection Against Radiation Hazards in Space, Gatlinburg, Oct. 1964) See NASA-SP-71** |
| **CONF-747–** | **(4th Symposium on Radioactivity in Scandinavia, Risø, Denmark, Oct. 5–6, 1964)** | |
| 6 | 20-2044 | See NDRE-51 |
| **CONF-601101–** | **20-2862** | **(1st Inter-American Symposium on Space Research, Buenos Aires, Nov. 1960)** |
| **CONF-630603–** | **20-3526** | **(Symposium on Berkeley and Bradwell Nuclear Power Stations, Westminster, England, June 27, 1963)** |
| **CONF-630805–** | **(13th Meeting of the American Inst. of Biological Sciences, Amherst, Mass., Aug. 1963)** | |
| 1 | 20-1588 | See BNL-917 |
| **CONF-631005–** | **(23rd Congress of the Italian National Assn. for Hygiene and Public Health, Catania, Italy, Oct. 1963)** | |
| 1 | 20-3604 | See RT/PROT(65)-12 |
| **CONF-640402–** | **20-2530** | **(American Mathematical Society Symposium on Application of Partial Differential Equations in Mathematical Physics, New York, Apr. 1964)** |
| **CONF-640917–** | **20-2526** | **(4th All-Union Conference on Ferroelectricity, Rostov-on-the-Don, U.S.S.R., Sept. 12–18, 1964)** |
| **CONF-641123–** | **(11th Argentina Chemical Conference, Bahia Blanca, Argentina, Nov. 1964)** | |
| 1 | 20-1886 | Dep. mn |
| **CONF-641126–** | **(1st Symposium on Nuclear Medicine, Mendoza, Argentina, Nov. 1964)** | |
| 1 | 20-1696 | Dep. mn |
| **CONF-641220–** | **(Society of Naval Architects and Marine Engineers, Southern California Section, Los Angeles, Dec. 3, 1964)** | |
| 1 | 20-3546 | See GE-TM-64-12-12 |
| **CONF-650117–** | **(2nd Conference on Solid State Physics, Bristol, England, Jan. 5–8, 1965)** | |
| 1 | 20-3277 | See BLG-328 |
| **CONF-650328–** | **(11th Annual Gas Turbine Conference and Products Show, Zurich, Mar. 13–17, 1965)** | |
| 1 | 20-2670 | See LA-DC-7330 |
| **CONF-650401–** | **(American Chemical Society, Detroit, Apr. 4–9, 1965)** | |

| Report No. | Abstract No. | Availability |
|---|---|---|
| 16 | 20-1808 | See COO-958-5 |
| **CONF-650405–** | **(International Conference on Modern Trends in Activation Analysis, College Station, Tex., Apr. 19–22, 1965)** | |
| 2 | 20-3005 | Gmelin, AED-CONF-65-040-29 |
| **CONF-650410–** | **(American Physical Society, Washington, D. C., Apr. 26–29, 1965)** | |
| 42 | 20-3156 | Gmelin, AED-CONF-65-073-72 Phys. Rev., 140: B1198-1201(1965) |
| **CONF-650422–** | **(American Geophysical Union, Program for Section of Seismology Annual Meeting, Washington, D. C., Apr. 19–22, 1965)** | |
| 16 | 20-2666 | Gmelin, AED-CONF-65-118-36 |
| **CONF-650502–** | **(Electrochemical Society, San Francisco, May 9–14, 1965)** | |
| 8 | 20-1882 | Gmelin, AED-CONF-65-169-11 |
| 9 | 20-1812 | See EUR-2495.e |
| **CONF-650512–** | **19-37944** | **(Symposium on Engineering Problems of Controlled Thermonuclear Research, Livermore, Calif., May 4–7, 1965)** |
| 8 | 20-3178 | See ORNL-P-1513 |
| 12 | 20-2104 | See MATT-362 |
| 14 | 20-2522 | See ORNL-P-1516 |
| **CONF-650536–** | **20-2119** | **(8th National Power Instrumentation Symposium, New York, May 12–14, 1965)** |
| **CONF-650544–** | **(Symposium on Fundamental Problems in Scanning, Chicago, May 1965)** | |
| 2 | 20-2213 | See BNL-9609 |
| **CONF-650560–** | **(13th Annual Meeting of the Radiation Research Society, Philadelphia, May 23–26, 1965)** | |
| 1 | 20-1683 | Gmelin, AED-CONF-65-157-8 |
| 2 | 20-1685 | Gmelin, AED-CONF-65-157-12 |
| 4 | 20-1686 | Gmelin, AED-CONF-65-157-9 |
| 5 | 20-1684 | Gmelin, AED-CONF-65-157-14 |
| 6 | 20-1682 | Gmelin, AED-CONF-65-157-11 |
| **CONF-650563–** | **(International Conference on the Internal Conversion Process, Nashville, Tenn., May 10–13, 1965)** | |
| 2 | 20-3155 | Gmelin, AED-CONF-65-117-4 |
| 3 | 20-3019 | See ORNL-P-1657 |
| **CONF-650564–** | **(Theoretical Automatics Congress, Saclay, May 4–7, 1965)** | |
| 1 | 20-3372 | See EUR-2506.e |
| **CONF-650602–** | **(American Nuclear Society 11th Annual Meeting, Gatlinburg, Tenn., June 20–24, 1965)** | |
| 61 | 20-3438 | Gmelin, AED-CONF-65-125-42 |
| 63 | 20-3437 | Gmelin, AED-CONF-65-125-35 |
| 68 | 20-3439 | Gmelin, AED-CONF-64-219-135 |
| **CONF-650620–** | **(Sodium Components Development Program Information Meeting, Chicago, June 16–17, 1965)** | |
| 2 | 20-2430 | See ORNL-P-1713 |
| **CONF-650632–** | **(7th Biennial Conference on Carbon, Cleveland, June 21–25, 1965)** | |
| 3 | 20-2315 | Dep. mn; CFSTI $2.00 cy, $0.50 mn |
| **CONF-650637–** | **(International Conference on Luminescent Dosimetry, Palo Alto, Calif., June 21–23, 1965)** | |
| 4 | 20-2178 | Gmelin, AED-CONF-65-151-2 |
| **CONF-650640–** | **(7th International Glass Congress, Brussels, June 28–July 3, 1965)** | |
| 2 | 20-1731 | See BNL-9614 |
| **CONF-650652–** | **(International $^{14}C$ and $^{3}H$ Dating Conference, Pullman, Wash., June 7–11, 1965)** | |
| 8 | 20-2179 | Gmelin, AED-CONF-65-158-11 |
| **CONF-650653–** | **(American Physical Society, Summer Meeting, New York, June 23–25, 1965)** | |
| 6 | 20-2757 | See NYO-2262-98 |
| 10 | 20-3184 | See UCRL-14310 |
| **CONF-650657–** | **(International Conference on Physics of X-Ray Spectra, Ithaca, N. Y., June 1965)** | |
| 1 | 20-2126 | Dep. mn; CFSTI $1.00 cy, $0.50 mn |
| **CONF-650704–** | **(IAEA Symposium on Thermodynamics, Vienna, July 22–27, 1965)** | |
| 34 | 20-2319 | See GE-TM-65-6-13 |
| **CONF-650715–** | **(Panel on Coordination of Research in Radiation Sensitization of Microorganisms in Food Preservation, Vienna, July 5–9, 1965)** | |
| 1 | 20-1618 | See NYO-3319-6 |
| **CONF-650718–** | **(Symposium on Swine in Biomedical Research, Richland, Wash., July 19–21, 1965)** | |
| 1 | 20-1581 | See BNWL-SA-341 |
| 2 | 20-1609 | See BNL-9477 |
| **CONF-650803–** | **(IAEA Symposium on Nuclear Materials Management, Vienna, Aug. 30–Sept. 3, 1965)** | |
| 14 | 20-3601 | ORINS |
| 15 | 20-3464 | ORINS |
| 16 | 20-3536 | ORINS |
| 45 | 20-3535 | ORINS |
| 46 | 20-2095 | ORINS |
| **CONF-650804–** | **(5th Rare Earth Research Conference, Ames, Iowa, Aug. 30–Sept. 1, 1965)** | |
| 10 | 20-2592 | See BNL-9556 |
| **CONF-650806–** | **(7th International Conference on Phenomena in Ionized Gases, Belgrade, Aug. 22–27, 1965)** | |
| 1 | 20-3182 | See UCRL-12447 |
| 15 | 20-3179 | See ORNL-P-1575 |
| **CONF-650812–** | **(ASME–AIChE Heat Transfer Conference and Exhibit, Los Angeles, Aug. 8–11, 1965)** | |
| 13 | 20-2023 | ORINS |
| **CONF-650814–** | **(Symposium on Mutational Process, Prague, Aug. 9–11, 1965)** | |
| 3 | 20-1610 | See BNL-9611 |
| **CONF-650908–** | **(International Conference on Thermionic Electrical Power Generation, London, Sept. 20–25, 1965)** | |
| 10 | 20-2687 | See LNF-65/25 |
| **CONF-650915–** | **(Systems Engineering Conference, Chicago, Sept. 20–23, 1965)** | |
| 2 | 20-2085 | See SC-R-65-991 |
| **CONF-650922–** | **(1st International Symposium on Magnet Technology, Stanford, Calif., Sept. 8–10, 1965)** | |
| 4 | 20-2544 | See UCRL-16309 |
| 16 | 20-2546 | See UCRL-16389 |
| 17 | 20-2533 | See BNL-9536 |
| 18 | 20-2105 | See UCRL-16357(Rev.) |
| 19 | 20-2545 | See UCRL-16386 |
| **CONF-650923–** | **(5th International Conference on High Energy Accelerators, Frascati, Italy, Sept. 9–16, 1965)** | |
| 8 | 20-2532 | See BNL-9505 |
| 10 | 20-2542 | See UCRL-16236 |
| 13 | 20-2541 | See UCRL-16228 |
| 14 | 20-2534 | See BNL-9587 |
| 15 | 20-2540 | See UCRL-16223 |
| 19 | 20-2547 | See UR-875-98 |
| 20 | 20-2538 | See LA-DC-7281 |
| 23 | 20-2543 | See UCRL-16238 |
| **CONF-650924–** | **(Workshop Conference on Space Radiation Biology, Berkeley, Calif., Sept. 7–10, 1965)** | |
| 5 | 20-1621 | See UCRL-16387 |
| **CONF-650927–** | **(American Physical Society, Honolulu, Hawaii, Sept. 2–4, 1965)** | |
| 3 | 20-2689 | See UCRL-16140 |
| 4 | 20-3279 | See ORNL-P-1704 |
| **CONF-650928–** | **(International Conference on Polarization Phenomena of Nucleons, Karlsruhe, Germany, Sept. 6–10, 1965)** | |
| 8 | 20-2537 | See LA-DC-7268 |

| Report No. | Abstract No. | Availability |
|---|---|---|
| 9 | 20-3014 | See LA-DC-7386 |
| 10 | 20-2685 | See LA-DC-7250 |
| 11 | 20-3022 | See UCRL-16216 |
| 12 | 20-3023 | See UCRL-16218 |
| **CONF-650934–** | **(7th International Congress on High-Speed Photography, Zurich, Sept. 12–18, 1965)** | |
| 1 | 20-3624 | See LA-DC-7088 |
| **CONF-650935–** | **(2nd IAEA Conference on Plasma Physics and Controlled Nuclear Fusion Research, Culham, England, Sept. 6–10, 1965)** | |
| 44 | 20-3167 | See MATT-374 |
| **CONF-650937–** | **(Conference on Megagauss Magnetic Field Generation by Explosives and Related Experiments, Frascati, Italy, Sept. 21–23, 1965)** | |
| 4 | 20-3166 | See LA-DC-7252 |
| **CONF-650946–** | **(4th High Temperature Liquid-Metal Heat Transfer Technology Conference, Argonne, Ill., Sept. 28–29, 1965)** | |
| 2 | 20-2013 | See ORNL-P-1661 |
| 3 | 20-2014 | See ORNL-P-1678 |
| 4 | 20-2015 | See ORNL-P-1681 |
| **CONF-650947–** | **(International Conference on Elementary Particles, Kyoto, Sept. 24–30, 1965)** | |
| 1 | 20-2758 | See UR-875-100 |
| 2 | 20-2759 | See UR-875-102 |
| **CONF-651001–** | **(IEEE Nuclear Science Symposium, San Francisco, Oct. 1965)** | |
| 4 | 20-2204 | See GA-6695 |
| 5 | 20-2124 | See BNL-9590 |
| 6 | 20-3612 | Dep. mn; CFSTI $1.00 cy, $0.50 mn |
| 7 | 20-3480 | See ORNL-P-1679 |
| **CONF-651002–** | **(Instrument Society of America, 20th Annual Conference, Los Angeles, Oct. 4–7, 1965)** | |
| 7 | 20-2103 | See LA-DC-7055 |
| **CONF-651009–** | **(Conference on Safety, Fuels and Core Design in Large Fast Power Reactors, Argonne, Oct. 11–14, 1965)** | |
| 2 | 20-3581 | See BNWL-SA-340 |
| **CONF-651011–** | **(IMOG and Metrology Subgroup Meeting, Las Vegas, Nev., Oct. 11, 1965)** | |
| 2 | 20-3627 | See RFP-670 |
| **CONF-651013–** | **(Shock and Vibration Symposium, New Orleans, Oct. 26–28, 1965)** | |
| 2 | 20-3631 | See SC-DC-65-1723 |
| **CONF-651016–** | **(35th Symposium on Shock and Vibration, New Orleans, Oct. 11, 1965)** | |
| 1 | 20-3613 | Dep. mn; CFSTI $1.00 cy, $0.50 mn |
| **CONF-651017–** | **(Electrochemical Society Meeting, Buffalo, Oct. 10–14, 1965)** | |
| 2 | 20-2339 | See ORNL-P-1753 |
| **CONF-651020–** | **(5th Thermal Conductivity Conference, Denver, Oct. 20–22, 1965)** | |
| 2 | 20-3621 | See IS-1261 |
| 3 | 20-3622 | See IS-1266 |
| **CONF-651022–** | **(Users of Automatic Information Display Equipment, Annual Meeting, New York, Oct. 11–14, 1965)** | |
| 1 | 20-2011 | See LA-DC-7189 |
| **CONF-651025–** | **(Symposium on Physical Metallurgy of Refractory Metals, French Lick, Ind., Oct. 3–5, 1965)** | |
| 1 | 20-2337 | See ORNL-P-1677 |
| 2 | 20-2336 | See ORNL-P-1634 |
| **CONF-651026–** | **(1st AIAA Rankine Circle Space Power System Specialists Conference, Cleveland, Oct. 26, 1965)** | |
| 1 | 20-3548 | See SC-DC-65-1752 |
| **CONF-651028–** | **(Conference on Electrical Insulation, Buck Hill Falls, Penna., Oct. 25–27, 1965)** | |
| 1 | 20-2259 | See SC-DC-65-1789 |
| **CONF-651031–** | **(American Society of Metals Meeting, Detroit, Oct. 19, 1965)** | |
| 1 | 20-2025 | See BNWL-SA-349 |
| 2 | 20-3626 | See ORNL-P-1722 |
| **CONF-651101–** | **20-3647** | **(American Nuclear Society, Winter Meeting, Washington, D. C., Nov. 15–18, 1965) (Revised 11-8-65)** |
| 36 | 20-3380 | See ORNL-TM-1305 |
| **CONF-651103–** | **(IAEA Symposium on Criticality Control of Fissile Materials, Stockholm, Nov. 1–5, 1965)** | |
| 2 | 20-3370 | Dep. mn; CFSTI $1.00 cy, $0.50 mn |
| 10 | 20-3368 | See BNWL-SA-214 |
| 11 | 20-3378 | See ORNL-P-1680 |
| 12 | 20-2938 | See UCRL-14245 |
| **CONF-651104–** | **(Joint Computer Conference, Las Vegas, Nov. 30–Dec. 2, 1965)** | |
| 1 | 20-3644 | See UCRL-16199 |
| **CONF-651106–** | **(Conference on Magnetism and Magnetic Materials, San Francisco, Nov. 16–19, 1965)** | |
| 2 | 20-2338 | See ORNL-P-1735 |
| 3 | 20-3280 | See ORNL-P-1737 |
| **CONF-651110–** | **(American Society of Mechanical Engineers, Annual Winter Meeting, Chicago, Nov. 7–11, 1965)** | |
| 3 | 20-1937 | See BNL-9281 |
| **CONF-651202–** | **(Symposium on Practices in the Treatment of Low and Intermediate Level Radioactive Waste, Vienna, Dec. 6–10, 1965)** | |
| 3 | 20-3603 | See LA-DC-7249 |
| 4 | 20-1940 | See RFP-638 |
| **COO–** | | |
| 818-58 | 20-2680 | Dep. mn; CFSTI $4.00 cy, $1.00 mn |
| 958-5 | 20-1808 | Dep. mn; CFSTI $3.00 cy, $0.75 mn |
| 1044-11 | 20-1908 | J. Phys. Chem. Solids, 26: 1615-19(1965) |
| 1119-4 | 20-1611 | Dep. mn; CFSTI $2.00 cy, $0.50 mn |
| 1149-16 | 20-3614 | Dep. mn; CFSTI $2.00 cy, $0.50 mn |
| 1149-17 | 20-3615 | Dep. mn; CFSTI $1.00 cy, $0.50 mn |
| 1149-22 | 20-3616 | Dep. mn; CFSTI $1.00 cy, $0.50 mn |
| 1149-23 | 20-3617 | Dep. mn; CFSTI $2.00 cy, $0.50 mn |
| 1149-25 | 20-3618 | Dep. mn; CFSTI $2.00 cy, $0.50 mn |
| 1149-26 | 20-3619 | Dep. mn; CFSTI $2.00 cy, $0.50 mn |
| 1149-27 | 20-3620 | Dep. mn; CFSTI $2.00 cy, $0.50 mn |
| 1149-30 | 20-1809 | Dep. mn; CFSTI $1.00 cy, $0.50 mn |
| 1170-4 | 20-1593 | Dep. mn; CFSTI $3.00 cy, $0.75 mn |
| 1198-222 | 20-3278 | Dep. mn; CFSTI $2.00 cy, $0.50 mn |
| 1198-220 | 20-2316 | Dep. mn; CFSTI $1.00 cy, $0.50 mn |
| 1198-300 | 20-2864 | Dep. mn; CFSTI $2.00 cy, $0.50 mn |
| 1261-18 | 20-2715 | Phys. Lett., 19: 350-2(1965) |
| 1420-104 | 20-3008 | Dep. mn; CFSTI $1.00 cy, $0.50 mn |
| **CP–** | **(Misc.)** | |
| 19 | 20-2072 | See AD-618006 |
| **CRT–** | **(Canadian)** | |
| 1187 B | 20-3583 | Dep.; AECL $1.00 |
| **CTO–** | **(Non-AEC)** | |
| 201(Draft) | 20-2524 | For translation see NP-tr-1292(Draft) |
| **CVNA–** | **(Misc.)** | |
| 242 | 20-3469 | Dep. mn; CFSTI $3.00 cy, $0.75 mn |
| **DASA–** | **(Misc.)** | |
| 1442 | 20-2035 | See AD-615017 |
| **DP–** | | |
| 968 | 20-2037 | Dep. mn; CFSTI $2.00 cy, $0.50 mn |
| 973 | 20-2419 | Dep. mn; CFSTI $1.00 cy, $0.50 mn |
| 979 | 20-1733 | Dep. mn; CFSTI $1.00 cy, $0.50 mn |
| 989 | 20-2280 | Dep. mn; CFSTI $1.00 cy, $0.50 mn |
| **DPST–** | | |
| 65-83-8 | 20-2420 | Dep. mn; CFSTI $1.00 cy, $0.50 mn |

| Report No. | Abstract No. | Availability |
|---|---|---|
| **DUBNA REPORTS** | **(Russian)** | |
| See JINR (Russian) | | |
| **EANDC–** | **(European-American Nuclear Data Committee)** | |
| 46(U) | 20-3018 | See NYO-72-27 |
| **ECOM–** | **(Non-AEC)** | |
| 00423-1 | 20-2412 | See AD-618079 |
| 2415 | 20-2186 | CFSTI $2.00 cy, $0.50 mn |
| 2545 | 20-2187 | CFSTI $2.00 cy, $0.50 mn |
| **EG-Report–** | **(English)** | |
| 36 | 20-1734 | Dep ; BIS $2.40; HMSO 12s. 6d. |
| **ER–** | **(Misc.)** | |
| 16 | 20-3177 | See NP-15570 |
| **ETR–** | **(Belgian)** | |
| 169 | 20-1955 | See NP-15403 |
| **EUR–** | **(European Atomic Energy Community)** | |
| 2305 | 20-2255 | See EURAEC-1323 |
| 2328 | 20-3373 | See EURAEC-1353 |
| 2331 | 20-3443 | See EURAEC-1356 |
| 2332 | 20-3444 | See EURAEC-1357 |
| 2333 | 20-3445 | See EURAEC-1358 |
| 2343 | 20-2317 | See EURAEC-1380 |
| 2349 | 20-2222 | See EURAEC-1390 |
| 2367 | 20-2281 | See EURAEC-1408 |
| 2383 | 20-2256 | See EURAEC-1449 |
| 2408.e | 20-1735 | Dep. mn |
| 2433.e | 20-3584 | Dep. mn |
| 2440.f | 20-2125 | See CEA-R-2816 |
| 2448.f | 20-3322 | Dep. mn |
| 2452.e | 20-1938 | Dep. mn |
| 2458.f | 20-1810 | Dep. mn |
| 2476.i | 20-1939 | Dep. mn |
| 2486.e | 20-1811 | Dep. mn |
| 2490.e | 20-2009 | Dep. mn |
| 2492.e | 20-3371 | Dep. mn |
| 2495.e | 20-1812 | Dep. mn |
| 2505.e | 20-1612 | Dep. mn |
| 2506.e | 20-3372 | Dep. mn |
| 2508.e | 20-1726 | Dep. mn |
| 2509.e | 20-2047 | Dep. mn |
| 2515.e | 20-1813 | Dep. mn |
| 2524.e | 20-2593 | Dep. mn |
| **EURAEC–** | | |
| 374(Vol.2) | 20-2084 | Dep. mn; CFSTI $5.00 cy, $1.00 mn |
| 1323 | 20-2255 | Dep. mn; CFSTI $1.00 cy, $0.50 mn |
| 1353 | 20-3373 | Dep. mn; CFSTI $3.00 cy, $0.75 mn |
| 1356 | 20-3443 | Dep. mn; CFSTI $2.00 cy, $0.50 mn |
| 1357 | 20-3444 | Dep. mn; CFSTI $2.00 cy, $0.50 mn |
| 1358 | 20-3445 | Dep. mn; CFSTI $1.00 cy, $0.50 mn |
| 1380 | 20-2317 | Dep. mn; CFSTI $1.00 cy, $0.50 mn |
| 1390 | 20-2222 | Dep. mn; CFSTI $3.00 cy, $0.75 mn |
| 1408 | 20-2281 | Dep. mn; CFSTI $4.00 cy, $0.75 mn |
| 1449 | 20-2256 | Dep. mn; CFSTI $2.00 cy, $0.50 mn |
| **EXP-NRX–** | **(Canadian)** | |
| 22902 | 20-2421 | Dep.; AECL $1.00 |
| **FZK–** | **(Non-AEC)** | |
| 206 | 20-2073 | See AD-618101 |
| **GA–** | **(Misc.)** | |
| 3491 | 20-1736 | Dep. mn; CFSTI $2.00 cy, $0.50 mn |
| 3664 | 20-1737 | Dep. mn; CFSTI $2.00 cy, $0.50 mn |
| 4041 | 20-1738 | Dep. mn; CFSTI $1.00 cy, $0.50 mn |
| 4297 | 20-1739 | Dep. mn; CFSTI $1.00 cy, $0.50 mn |
| 4576 | 20-1740 | Dep. mn; CFSTI $1.00 cy, $0.50 mn |
| 5499 | 20-3470 | Dep. mn; CFSTI $2.00 cy, $0.50 mn |
| 5918(Pt.1) | 20-2318 | Dep. mn; CFSTI $3.00 cy, $0.75 mn |
| 5973 | 20-2931 | See AD-616518 |
| 6053 | 20-2446 | Phil. Mag. (8), 12: 561-71(1965) |
| 6685 | 20-3009 | Dep. mn; CFSTI $2.00 cy, $0.50 mn |
| 6695 | 20-2204 | Dep. mn; CFSTI $1.00 cy, $0.50 mn |
| **GAMD–** | **(Misc.)** | |
| 6644 | 20-3323 | Dep. mn; CFSTI $2.00 cy, $0.50 mn |
| **GE-TM–** | | |
| 64-12-12 | 20-3546 | Dep. mn; CFSTI $3.00 cy, $0.75 mn |
| 65-6-13 | 20-2319 | Dep. mn; CFSTI $2.00 cy, $0.50 mn |
| **GEAP–** | **(Misc.)** | |
| 4861 | 20-3471 | Dep. mn; CFSTI $3.00 cy, $0.75 mn |
| 4891 | 20-3472 | Dep. mn; CFSTI $4.00 cy, $1.00 mn |
| 4903 | 20-3473 | Dep. mn; CFSTI $2.00 cy, $0.50 mn |
| **GEMP–** | **(Misc.)** | |
| 51A | 20-2223 | Dep. mn; CFSTI $3.00 cy, $0.75 mn |
| 52A | 20-2224 | Dep. mn; CFSTI $3.00 cy, $0.50 mn |
| 314 | 20-2323 | Dep. mn; CFSTI $1.00 cy, $0.50 mn |
| **GEST–** | **(Misc.)** | |
| 2045 | 20-3446 | |
| **GGC-EE–** | **(Non-AEC)** | |
| 65-7 | 20-3162 | See AD-618683 |
| **GNEC–** | | |
| 364 | 20-3474 | Dep. mn; CFSTI $2.00 cy, $0.50 mn |
| **GSP–** | **(Non-AEC)** | |
| 65A/ME/65-1 | 20-2007 | See AD-618026 |
| **HEPL–** | **(Misc.)** | |
| 382 | 20-2750 | See AD-618659 |
| 388 | 20-2679 | See AD-618664 |
| **HW-SA–** | | |
| 3537 | 20-1613 | Dep. mn; CFSTI $1.00 cy, $0.50 mn |
| 3755 | 20-2282 | Dep. mn; CFSTI $4.00 cy, $1.00 mn |
| 3765 | 20-2324 | Dep. mn; CFSTI $2.00 cy, $0.50 mn |
| 3767 | 20-2325 | Dep. mn; CFSTI $2.00 cy, $0.50 mn |
| **IA–** | **(Non-AEC)** | |
| 920 | 20-2520 | Dep. mn |
| 1031 | 20-1741 | Dep. mn |
| 1053 | 20-3374 | Dep. mn |
| **IC–** | **(Misc.)** | |
| 65/51 | 20-2751 | Dep. mn |
| 65/77 | 20-2752 | Dep. mn |
| **IDO–** | | |
| 14663 | 20-3010 | Dep. mn; CFSTI $2.00 cy, $0.50 mn |
| 14665 | 20-2425 | Dep. mn; CFSTI $1.00 cy, $0.50 mn |
| 17120 | 20-3375 | Dep. mn; CFSTI $2.00 cy, $0.50 mn |
| **IFA-CR–** | **(Rumanian)** | |
| 55 | 20-2681 | Dep. mn |
| **IFA-FR–** | **(Rumanian)** | |
| 39 | 20-2326 | Dep. mn |
| **IFA-NR–** | **(Rumanian)** | |
| 22 | 20-3011 | Dep. mn |
| **IITRI** | **(Misc.)** | |
| 578P21-13 | 20-3324 | Dep. mn; CFSTI $3.00 cy, $0.75 mn |
| T6042 | 20-3324 | See IITRI-578P21-13 |
| **IKF–** | **(German)** | |
| 11 | 20-3012 | Dep. mn |
| 12 | 20-2327 | Dep. mn |
| **INR–** | **(Non-AEC)** | |
| 608/VI/PH | 20-2651 | |
| 625/XIV/R | 20-2328 | Dep. |
| 636/XIII/J | 20-1742 | Dep. |
| **IPPJ–** | **(Japanese)** | |
| 39 | 20-3164 | Dep. mn |
| **IPV–** | **(Swedish)** | |
| 19 | 20-2010 | Dep. mn |
| **IS–** | | |
| 807 | 20-2776 | J. Math. Phys. (N. Y.), 6: 1591-?(1965) |
| 1173 | 20-3051 | Nucl. Phys., 74: 385-402(1965) |
| 1193 | 20-2100 | Dep. mn; CFSTI $3.00 cy, $0.75 mn |

| Report No. | Abstract No. | Availability |
|---|---|---|
| 1201 | 20-3302 | Phys. Rev. Letters, 15: 623-5(1965) |
| 1251 | 20-3621 | Dep. mn; CFSTI $1.00 cy, $0.50 mn |
| 1266 | 20-3622 | Dep. mn; CFSTI $1.00 cy, $0.50 mn |
| **IS-T–** | | |
| 23 | 20-1896 | Dep. mn; CFSTI $3.00 cy, $0.75 mn |
| 34 | 20-1953 | Dep. mn; CFSTI $3.00 cy, $0.75 mn |
| 35 | 20-2329 | Dep. mn; CFSTI $3.00 cy, $0.75 mn |
| 36 | 20-3623 | Dep. mn; CFSTI $3.00 cy, $0.50 mn |
| 40 | 20-2225 | Dep. mn; CFSTI $3.00 cy, $0.75 mn |
| **ISS–** | **(Italian)** | |
| 64/15 | 20-2127 | Dep. mn |
| **JINR–** | **(Russian)** | |
| E-2324 | 20-2128 | Dep. mn |
| E-2329 | 20-2755 | Dep. mn |
| P-2300 | 20-2753 | Dep. mn |
| P-2309 | 20-2754 | Dep. mn |
| P-2312 | 20-2129 | Dep. mn |
| P-2319 | 20-2101 | Dep. mn |
| P-2320 | 20-2682 | Dep. mn |
| P-2325 | 20-2865 | Dep. mn |
| P-2327 | 20-2683 | Dep. mn |
| P-2331 | 20-3013 | Dep. mn |
| P-2340 | 20-2130 | Dep. mn |
| P-2341 | 20-2536 | Dep. mn |
| P-2342 | 20-2756 | Dep. mn |
| P-2344 | 20-2131 | Dep. mn |
| P-2352 | 20-3165 | Dep. mn |
| P-2354 | 20-3238 | Dep. mn |
| P-2368 | 20-2132 | Dep. mn |
| P-2374 | 20-2684 | Dep. mn |
| **Jül–** | **(German)** | |
| 216-RW | 20-1743 | Dep. mn |
| 259-RE | 20-3585 | Dep. mn |
| 273-PP | 20-2102 | Dep. mn |
| **KAPL–** | | |
| 3091 | 20-2330 | Dep. mn; CFSTI $2.00 cy, $0.50 mn |
| 3103 | 20-2331 | Dep. mn; CFSTI $2.00 cy, $0.50 mn |
| 3110 | 20-2283 | Dep. mn; CFSTI $2.00 cy, $0.50 mn |
| **KAPL-M–** | | |
| 6483 | 20-2214 | Dep. mn; CFSTI $2.00 cy, $0.50 mn |
| **KY–** | | |
| 287 | 20-1954 | Dep. mn; CFSTI $2.00 cy, $0.50 mn |
| **LA–** | | |
| 3307 | 20-2332 | Dep. mn; CFSTI $1.00 cy, $0.50 mn |
| 3387 | 20-2426 | Dep. mn; CFSTI $1.00 cy, $0.50 mn |
| **LA-DC–** | | |
| 6507 | 20-1594 | Dep. mn; CFSTI $1.00 cy, $0.50 mn |
| 6508 | 20-1752 | Anal. Chem., 37: 1574-6(1965) |
| 7022 | 20-1863 | Rev. Sci. Instrum., 36: 1629-36(1965) |
| 7055 | 20-2103 | Dep. mn; CFSTI $2.00 cy, $0.50 mn |
| 7088 | 20-3624 | Dep. mn; CFSTI $1.00 cy, $0.50 mn |
| 7099 | 20-2394 | Trans. Met. Soc. AIME, 233: 1818-25(1965) |
| 7189 | 20-2011 | Dep. mn; CFSTI $2.00 cy, $0.50 mn |
| 7249 | 20-3603 | Dep. mn; CFSTI $1.00 cy, $0.50 mn |
| 7250 | 20-2685 | Dep. mn; CFSTI $1.00 cy, $0.50 mn |
| 7252 | 20-3166 | Dep. mn; CFSTI $2.00 cy, $0.50 mn |
| 7268 | 20-2537 | Dep. mn; CFSTI $1.00 cy, $0.50 mn |
| 7281 | 20-2538 | Dep. mn; CFSTI $2.00 cy, $0.50 mn |
| 7330 | 20-2670 | Dep. mn; CFSTI $2.00 cy, $0.50 mn |
| 7386 | 20-3014 | Dep. mn; CFSTI $3.00 cy, $0.50 mn |
| **LNF–** | **(Italian)** | |
| 65/22 | 20-2686 | Dep. mn |
| 65/25 | 20-2687 | Dep. mn |
| 65/28 | 20-2521 | Dep. mn |
| **MATT–** | | |
| 295 | 20-2569 | Astrophys. J., 142: 479-90(1965) |
| 362 | 20-2104 | Dep. mn; CFSTI $1.00 cy, $0.50 mn |
| 374 | 20-3167 | Dep. mn; CFSTI $1.00 cy, $0.50 mn |
| **MD–** | **(Misc.)** | |
| 65-5 | 20-2026 | See UCRL-13188 |
| **MIT–** | **(Misc.)** | |
| 2098-112 | 20-3093 | Rev. Sci. Instrum., 36: 1607-10(1965) |
| 2098-154 | 20-1991 | Rev. Sci. Instrum., 36: 1529-35(1965) |
| **ML–** | **(Misc.)** | |
| 1185 | 20-3168 | |
| **ML-TDR–** | **(Non-AEC)** | |
| 64-159 | 20-2427 | See NASA-SP-55 |
| **MLM–** | | |
| 1276(tr) | 20-3281 | Dep. mn; JCL $1.60 fs, $0.80 mf |
| **MND–** | **(Misc.)** | |
| 3169-52 | 20-2205 | Dep. mn; CFSTI $3.00 cy, $0.75 mn |
| **MSAR–** | **(Misc.)** | |
| 65-149 | 20-2258 | Dep. mn; CFSTI $2.00 cy, $0.50 mn |
| **N–** | **(Misc.)** | |
| 64-23208 | 20-2594 | |
| **NAA-SR–** | | |
| 6333 | 20-1814 | Dep. mn; CFSTI $1.00 cy, $0.50 mn |
| 11198 | 20-1988 | Dep. mn; CFSTI $3.00 cy, $0.75 mn |
| **NAA-SR-Memo–** | | |
| 7581 | 20-3547 | Dep. mn; CFSTI $2.00 cy, $0.50 mn |
| **NAS-NS–** | **(Misc.)** | |
| 3030(Rev.) | 20-1744 | Dep. mn; CFSTI $1.00 cy, $0.50 mn |
| **NASA-CR–** | **(Misc.)** | |
| 319 | 20-3169 | CFSTI $1.00 cy, $0.50 mn |
| 54384 | 20-3443 | See GEST-2045 |
| 54457 | 20-2333 | |
| **NASA-SP–** | **(Misc.)** | |
| 55 | 20-2427 | CFSTI $3.75 cy, $2.75 mn |
| 71 | 20-3239 | GPO $3.25 |
| 5032 | 20-1727 | GPO $0.45 |
| **NASA-TN–** | **(Misc.)** | |
| D-3020 | 20-3016 | CFSTI $1.00 cy, $0.50 mn |
| D-3032 | 20-1897 | CFSTI $3.00 cy, $0.75 mn |
| D-3050 | 20-2595 | CFSTI $1.00 cy, $0.50 mn |
| D-3052 | 20-3170 | CFSTI $1.00 cy, $0.50 mn |
| D-3067 | 20-3017 | CFSTI $2.00 cy, $0.50 mn |
| **NASA-TT–** | **(Non-AEC)** | |
| F-338 | 20-2359 | CFSTI $7.00 cy, $1.75 mn |
| **NAVORD–** | **(Non-AEC)** | |
| 3073 | 20-2313 | See AD-619208 |
| **NDRE–** | **(Norwegian)** | |
| 51 | 20-2044 | Dep. |
| **NOLTR–** | **(Misc.)** | |
| 64-187 | 20-1979 | See AD-614814 |
| 64-235 | 20-2310 | See AD-618681 |
| 65-72 | 20-3006 | See AD-618676 |
| **NP–** | **(AEC File No. for Non-AEC Reports)** | |
| 15093 | 20-2284 | |
| 15149 | 20-1617 | Dep. mn |
| 15403 | 20-1955 | Dep. mn; CFSTI $4.00 cy, $0.75 mn |
| 15458 | 20-3475 | Dep. mn |
| 15523 | 20-1887 | Dep. mn |
| 15530 | 20-2334 | Dep. mn |
| 15538(Vol.1) | 20-3476 | Dep. mn; CFSTI $6.00 cy, $1.50 mn |
| 15538(Vol.2) | 20-3477 | Dep. mn; CFSTI $4.00 cy, $0.75 mn |
| 15538(Vol.3) | 20-3478 | Dep. mn; CFSTI $6.00 cy, $1.50 mn |
| 15556 | 20-3479 | Dep. mn |
| 15562 | 20-3171 | Dep. mn |
| 15570 | 20-3177 | Dep. mn |
| 15573 | 20-3376 | Dep. mn |
| 15575 | 20-2208 | Dep. mn; Australian AEC Free |
| 15578 | 20-3252 | Phys. Fluids, 8: 2298-2300(1965) |
| **NP-tr–** | **(AEC File No. for Non-AEC Translations)** | |
| 1292(Draft) | 20-2524 | Dep. mn; CFSTI $3.00 cy, $0.50 mn; JCL |

| Report No. | Abstract No. | Availability<br>$5.60 fs, $1.91 mf |
|---|---|---|
| **NRC–** | **(Canadian)** | |
| 8613 | 20-1825 | Can. J. Chem., 43: 3100-3(1965) |
| **NRL–** | **(Misc.)** | |
| 6241 | 20-1815 | CFSTI $3.00 cy, $0.75 mn |
| **NRL-Memo–** | **(Misc.)** | |
| 1611 | 20-2409 | See AD-617319 |
| **NRL-MR–** | **(Non-AEC)** | |
| 1593 | 20-2408 | See AD-614899 |
| **NYO–** | | |
| 98-10 | 20-2058 | Dep. mn; CFSTI $3.00 cy, $0.75 mn |
| 98-11 | 20-2059 | Dep. mn; CFSTI $2.00 cy, $0.50 mn |
| **NYR–** | **(Non-AEC)** | |
| 3840 | 20-2412 | See AD-618079 |
| **NYO–** | | |
| 72-27 | 20-3018 | CFSTI $12.78 cy, $4.00 mn |
| 841-2 | 20-1989 | Dep. mn; CFSTI $5.00 cy, $1.00 mn |
| 2038-2 | 20-1582 | Dep. mn; CFSTI $3.00 cy, $0.50 mn |
| 2262-98 | 20-2757 | Dep. mn; CFSTI $1.00 cy, $0.50 mn |
| 2394-9 | 20-2335 | Dep. mn; CFSTI $1.00 cy, $0.50 mn |
| 3282-1 | 20-3625 | Dep. mn; CFSTI $1.00 cy, $0.50 mn |
| 3304-6 | 20-2012 | Dep. mn; CFSTI $2.00 cy, $0.50 mn |
| 3319-6 | 20-1618 | Dep. mn; CFSTI $1.00 cy, $0.50 mn |
| **ORNL–** | | |
| 1696 | 20-1956 | Dep. mn; CFSTI $3.00 cy, $0.50 mn |
| 3822(Vol.1) | 20-2932 | Dep. mn; CFSTI $2.00 cy, $0.50 mn |
| 3822(Vol.2) | 20-2933 | Dep. mn; CFSTI $6.00 cy, $1.25 mn |
| 3822(Vol.3) | 20-2934 | Dep. mn; CFSTI $6.00 cy, $1.25 mn |
| 3822(Vol.4) | 20-2935 | Dep. mn; CFSTI $6.00 cy, $1.25 mn |
| 3822(Vol.5) | 20-2936 | Dep. mn; CFSTI $6.00 cy, $1.25 mn |
| 3822(Vol.6) | 20-2937 | Dep. mn; CFSTI $6.00 cy, $1.25 mn |
| 3837 | 20-2429 | Dep. mn; CFSTI $3.00 cy, $0.75 mn |
| **ORNL-P–** | **(Misc.)** | |
| 649 | 20-1639 | Exp. Cell Res., 39: 604-6(1965) |
| 706 | 20-2133 | See NASA-SP-71, pp 245-50 |
| 984 | 20-2367 | Electrochem. Technol., 3: 228-33(1965) |
| 1036 | 20-1751 | Anal. Chem., 37: 1543-6(1965) |
| 1161 | 20-3213 | Nucl. Fusion, 5: 164-5(1965) |
| 1330 | 20-1643 | Genetics, 52: 1035-41(1965) |
| 1400 | 20-2622 | Phys. Rev., 140: A1057-64(1965) |
| 1437 | 20-3094 | Rev. Sci. Instrum., 36: 1659-60(1965) |
| 1480 | 20-3325 | Dep. mn; CFSTI $1.00 cy, $0.50 mn |
| 1482 | 20-3377 | Dep. mn; CFSTI $1.00 cy, $0.50 mn |
| 1513 | 20-3178 | Dep. mn; CFSTI $1.00 cy, $0.50 mn |
| 1516 | 20-2522 | Dep. mn; CFSTI $1.00 cy, $0.50 mn |
| 1518 | 20-3043 | Nucl. Phys., 74: 281-8(1965) |
| 1575 | 20-3179 | Dep. mn; CFSTI $1.00 cy, $0.50 mn |
| 1634 | 20-2336 | Dep. mn; CFSTI $1.00 cy, $0.50 mn |
| 1657 | 20-3019 | Dep. mn; CFSTI $1.00 cy, $0.50 mn |
| 1661 | 20-2013 | Dep. mn; CFSTI $2.00 cy, $0.50 mn |
| 1677 | 20-2337 | Dep. mn; CFSTI $1.00 cy, $0.50 mn |
| 1678 | 20-2014 | Dep. mn; CFSTI $1.00 cy, $0.50 mn |
| 1679 | 20-3480 | Dep. mn; CFSTI $1.00 cy, $0.50 mn |
| 1680 | 20-3378 | Dep. mn; CFSTI $2.00 cy, $0.50 mn |
| 1681 | 20-2015 | Dep. mn; CFSTI $1.00 cy, $0.50 mn |
| 1704 | 20-3279 | Dep. mn; CFSTI $1.00 cy, $0.50 mn |
| 1713 | 20-2430 | Dep. mn; CFSTI $1.00 cy, $0.50 mn |
| 1718 | 20-3076 | Phys. Lett., 19: 312-13(1965) |
| 1722 | 20-3626 | Dep. mn; CFSTI $4.00 cy, $0.75 mn |
| 1735 | 20-2338 | Dep. mn; CFSTI $1.00 cy, $0.50 mn |
| 1737 | 20-3280 | Dep. mn; CFSTI $1.00 cy, $0.50 mn |
| 1753 | 20-2339 | Dep. mn; CFSTI $3.00 cy, $0.75 mn |
| **ORNL-TM–** | | |
| 906 | 20-2477 | pp 251-68 of Flow and Fracture of Metals and Alloys in Nuclear Environments. ASTM Special Technical Publication No. 380. Philadelphia, American Society for Testing and Materials, 1965. |
| 1065 | 20-3020 | Dep. mn; CFSTI $1.00 cy, $0.50 mn |
| 1131 | 20-2340 | Dep. mn; CFSTI $2.00 cy, $0.50 mn |
| 1207 | 20-3379 | Dep. mn; CFSTI $1.00 cy, $0.50 mn |
| 1238 | 20-3021 | Dep. mn; CFSTI $1.00 cy, $0.50 mn |
| 1255 | 20-2431 | Dep. mn; CFSTI $3.00 cy, $0.75 mn |
| 1258 | 20-1816 | Dep. mn; CFSTI $1.00 cy, $0.50 mn |
| 1291 | 20-3586 | Dep. mn; CFSTI $2.00 cy, $0.50 mn |
| 1305 | 20-3380 | Dep. mn; CFSTI $1.00 cy, $0.50 mn |
| **ORNL-tr–** | | |
| 814 | 20-2360 | Dep. mn; JCL $2.60 fs, $0.95 mf |
| **P–** | **(Misc.)** | |
| 3074(RAND) | 20-2068 | See AD-614895 |
| **PATENTS** | **(British)** | **4s. 6d. each, U. K. Patent Office** |
| 1,004,205 | 20-2276 | |
| 1,004,206 | 20-2120 | |
| 1,004,248 | 20-2248 | |
| 1,004,262 | 20-2034 | |
| 1,004,482 | 20-3349 | |
| 1,004,483 | 20-3350 | |
| 1,004,499 | 20-2002 | |
| 1,004,546 | 20-3351 | |
| 1,004,547 | 20-2277 | |
| 1,004,755 | 20-3352 | |
| 1,004,867 | 20-2003 | |
| 1,004,904 | 20-2249 | |
| 1,004,993 | 20-3353 | |
| 1,005,102 | 20-2300 | |
| 1,005,125 | 20-1972 | |
| 1,005,133 | 20-3354 | |
| 1,005,196 | 20-2301 | |
| 1,005,393 | 20-2250 | |
| 1,005,416 | 20-3355 | |
| 1,005,436 | 20-2406 | |
| 1,005,489 | 20-3537 | |
| 1,005,514 | 20-3356 | |
| 1,005,541 | 20-3465 | |
| 1,005,551 | 20-3602 | |
| 1,005,582 | 20-2180 | |
| 1,005,850 | 20-3357 | |
| 1,005,871 | 20-2302 | |
| 1,005,881 | 20-3466 | |
| 1,005,940 | 20-3358 | |
| 1,005,948 | 20-2181 | |
| 1,006,007 | 20-1973 | |
| 1,006,187 | 20-3359 | |
| 1,006,233 | 20-2182 | |
| 1,006,272 | 20-2004 | |
| 1,006,322 | 20-3360 | |
| 1,006,414 | 20-2005 | |
| 1,006,471 | 20-3538 | |
| 1,006,475 | 20-2183 | |
| 1,006,484 | 20-2006 | |
| 1,006,571 | 20-2024 | |
| 1,006,613 | 20-2676 | |
| 1,006,644 | 20-2303 | |
| 1,006,799 | 20-2677 | |
| 1,006,900 | 20-1974 | |
| **PATENTS** | **(Canadian)** | |
| 712,562 | 20-1800 | |
| **PATENTS** | **(U. S.)** | **$0.25 each, U. S. Patent Office** |
| 3,201,229 | 20-1883 | |
| 3,205,588 | 20-3607 | |
| 3,206,305 | 20-2407 | |
| 3,206,365 | 20-1884 | |
| 3,206,371 | 20-3361 | |
| 3,206,409 | 20-3608 | |
| 3,206,587 | 20-2251 | |
| 3,206,896 | 20-2039 | |
| 3,207,408 | 20-2304 | |
| 3,207,607 | 20-1975 | |
| 3,207,667 | 20-3362 | |
| 3,207,671 | 20-3363 | |
| 3,207,672 | 20-3364 | |
| 3,207,673 | 20-3467 | |
| 3,207,697 | 20-2305 | |
| 3,207,705 | 20-2306 | |
| 3,208,410 | 20-2040 | |
| 3,208,815 | 20-1885 | |
| 3,208,816 | 20-2252 | |
| 3,208,826 | 20-1801 | |
| 3,208,913 | 20-3365 | |

| Report No. | Abstract No. | Availability |
|---|---|---|
| 3,208,914 | 20-3578 | |
| 3,208,915 | 20-3442 | |
| 3,208,917 | 20-3468 | |
| 3,209,189 | 20-2042 | |
| **PNE–** | | |
| 605F | 20-1981 | Dep. mn; CFSTI $2.00 cy, $0.50 mn |
| 807F | 20-1982 | Dep. mn; CFSTI $3.00 cy, $0.50 mn |
| 2000 | 20-1983 | Dep. mn; CFSTI $1.00 cy, $0.75 mn |
| 2001 | 20-1984 | Dep. mn; CFSTI $1.25 cy, $0.75 mn |
| 2003 | 20-1985 | Dep. mn; CFSTI $1.00 cy, $0.50 mn |
| 2004 | 20-1986 | Dep. mn; CFSTI $1.00 cy, $0.50 mn |
| **R–** | (Misc.) | |
| 63-53 | 20-2035 | See AD-615017 |
| **RADC-TDR–** | (Misc.) | |
| 64-259 | 20-2121 | See AD-614832 |
| **RADC-TR–** | (Non-AEC) | |
| 65-173 | 20-3157 | See AD-614654 |
| **REIC-Memo–** | (Misc.) | |
| 26 | 20-2432 | Dep. mn; CFSTI $2.00 cy, $0.50 mn |
| 27 | 20-2433 | Dep. mn; CFSTI $4.00 cy, $0.75 mn |
| **RFP–** | | |
| 638 | 20-1940 | Dep. mn; CFSTI $1.00 cy, $0.50 mn |
| 670 | 20-3627 | Dep. mn; CFSTI $1.00 cy, $0.50 mn |
| **RL-NRD–** | | |
| 81(Suppl.1) | 20-3541 | Dep. mn; CFSTI $1.00 cy, $0.50 mn |
| **RM–** | (Misc.) | |
| 3902-TAB | 20-1590 | Dep. mn; CFSTI $1.00 cy, $0.50 mn |
| 4572-PR | 20-2930 | See AD-614636 |
| **RPI–** | (Misc.) | |
| 1044-1 | 20-3628 | Dep. mn; CFSTI $1.00 cy, $0.50 mn |
| **RR–** | (Misc.) | |
| 451 | 20-2098 | See AD-618398 |
| **RRL–** | | |
| 2310-164 | 20-1898 | Dep. mn; CFSTI $1.00 cy, $0.50 mn |
| **RT-CHI–** | (Italian) | |
| (65)-25 | 20-1745 | Dep. mn |
| (65)-30 | 20-2226 | Dep. mn |
| **RT-ING–** | (Italian) | |
| (65)-3 | 20-3587 | Dep. mn |
| (65)16 | 20-3440 | Dep. mn |
| **RT-PROT–** | (Italian) | |
| (65)-12 | 20-3604 | Dep. mn |
| **SC-DC–** | | |
| 64-288 | 20-3629 | Dep. mn; CFSTI $1.00 cy, $0.50 mn |
| 65-1637 | 20-2341 | Dep. mn; CFSTI $6.00 cy, $1.25 mn |
| 65-1697 | 20-3630 | Dep. mn; CFSTI $2.00 cy, $0.50 mn |
| 65-1723 | 20-3631 | Dep. mn; CFSTI $2.00 cy, $0.50 mn |
| 65-1752 | 20-3548 | Dep. mn; CFSTI $1.00 cy, $0.50 mn |
| 65-1765 | 20-2016 | Dep. mn; CFSTI $3.00 cy, $0.75 mn |
| 65-1789 | 20-2259 | Dep. mn; CFSTI $1.00 cy, $0.50 mn |
| **SC-DR–** | | |
| 58-61 | 20-2342 | Dep. mn; CFSTI $2.00 cy, $0.50 mn |
| 65-459 | 20-3632 | Dep. mn; CFSTI $1.00 cy, $0.50 mn |
| 65-519 | 20-2260 | Dep. mn; CFSTI $2.00 cy, $0.50 mn |
| **SC-R–** | | |
| 65-991 | 20-2085 | Dep. mn; CFSTI $1.00 cy, $0.50 mn |
| **SC-RR–** | | |
| 65-121A | 20-3481 | Dep. mn; CFSTI $2.00 cy, $0.50 mn |
| 65-417 | 20-3549 | Dep. mn; CFSTI $1.00 cy, $0.50 |
| 65-449 | 20-2523 | Dep. mn; CFSTI $2.00 cy, $0.50 mn |
| **SC-TM–** | | |
| 64-1686 | 20-3633 | Dep. mn; CFSTI $2.00 cy, $0.50 mn |
| 65-242 | 20-2343 | Dep. mn; CFSTI $1.00 cy, $0.50 mn |
| 65-462 | 20-3634 | Dep. mn; CFSTI $1.00 cy, $0.50 mn |
| 65-544 | 20-3635 | Dep. mn; CFSTI $2.00 cy, $0.50 mn |
| **SEL–** | (Misc.) | |
| 63-116 | 20-3180 | Dep. mn; CFSTI $1.00 cy, $0.50 mn |
| **SGAE-PH–** | (Austrian) | |
| 26/1965 | 20-2209 | Dep. mn |
| **SLAC–** | | |
| 47 | 20-2539 | Dep. mn; CFSTI $2.00 cy, $0.50 mn |
| **SM–** | (Misc.) | |
| 66-83 | 20-2319 | See GE-TM-65-6-13 |
| 70/38 | 20-3370 | See CONF-651103-2 |
| 71-24 | 20-3603 | See LA-DC-7249 |
| 71-43 | 20-1940 | See RFP-638 |
| **SMUPA-TK–** | (Non-AEC) | |
| 935 | 20-2413 | See AD-618688 |
| **SR–** | (Misc.) | |
| 6 | 20-2097 | See AD-618396 |
| 8 | 20-2098 | See AD-618398 |
| **SRM–** | (Non-AEC) | |
| 65-1 | 20-3610 | See AD-622333 |
| **STS–** | | |
| 3 | 20-3551 | See TID-22316 |
| **SU-IPR–** | | |
| 20 | 20-3181 | Dep. mn; CFSTI $2.00 cy, $0.50 mn |
| **SUDAER–** | (Non-AEC) | |
| 218 | 20-2820 | See AD-614645 |
| **SWRI–** | | |
| 1228-75 | 20-3482 | Dep. mn; CFSTI $2.00 cy, $0.50 mn |
| **TID–** | | |
| 3545(Rev.1) | 20-1990 | Dep. mn; CFSTI $5.00 cy, $1.00 mn |
| 21994 | 20-3550 | Dep. mn; CFSTI $6.00 cy, $1.25 mn |
| 22199 | 20-1746 | Dep. mn; CFSTI $1.00 cy, $0.50 mn |
| 22201 | 20-3483 | Dep. mn; CFSTI $1.00 cy, $0.50 mn |
| 22234 | 20-1587 | Yale J. Biol. Med., 38: 11-26(1965) |
| 22291 | 20-1604 | Dep. mn; CFSTI $1.00 cy, $0.50 mn |
| 22293 | 20-1619 | Dep. mn; CFSTI $2.00 cy, $0.50 mn |
| 22312 | 20-2017 | Dep. mn; CFSTI $1.00 cy, $0.50 mn |
| 22316 | 20-3551 | Dep. mn; CFSTI $3.00 cy, $0.50 mn |
| 22319 | 20-3636 | Dep. mn; CFSTI $2.00 cy, $0.50 mn |
| 22323 | 20-1817 | Dep. mn; CFSTI $3.00 cy, $0.50 mn |
| 22329 | 20-3484 | Dep. mn; CFSTI $3.00 cy, $0.75 mn |
| 22335 | 20-2134 | Dep. mn; CFSTI $2.00 cy, $0.50 mn |
| 22342 | 20-2434 | Dep. mn; CFSTI $3.00 cy, $0.75 mn |
| 22362 | 20-2723 | Phys. Rev. Lett., 15: 639-41(1965) |
| **TM–** | (Misc.) | |
| 1633 | 20-2413 | See AD-618688 |
| **TR–** | (Misc.) | |
| 24 | 20-1802 | See AD-618038 |
| 32 | 20-2889 | See AD-618203 |
| 380 | 20-3160 | See AD-618503 |
| **TRG-Report–** | (British) | |
| 920 | 20-2018 | Dep.; BIS $0.50; HMSO 2s. 6d. |
| 1072 | 20-2344 | Dep.; BIS $0.40; HMSO 2s. |
| **TT–** | (Canadian) | |
| 1193 | 20-3185 | Dep. mn; JCL $2.60 fs, $0.86 mf |
| **UACRL–** | (Non-AEC) | |
| D910261-4 | 20-2219 | See AMRA-CR-64-05/4 |
| **UCLA–** | | |
| 12-534 | 20-3637 | Dep. mn; CFSTI $1.00 cy, $0.50 mn |
| **UCRI–** | (Non-AEC) | |
| 326 | 20-2261 | |

| Report No. | Abstract No. | Availability |
|---|---|---|
| **UCRL–** | | |
| 7873 | 20-3638 | Dep. mn; CFSTI $3.00 cy, $0.75 mn |
| 11030 | 20-2345 | Dep. mn; CFSTI $1.00 cy, $0.50 mn |
| 11194 | 20-3639 | Dep. mn; CFSTI $3.00 cy, $0.50 mn |
| 11471 | 20-2346 | Dep. mn; CFSTI $1.00 cy, $0.50 mn |
| 11488 | 20-3640 | Dep. mn; CFSTI $1.00 cy, $0.50 mn |
| 11512(Rev.) | 20-3641 | Dep. mn; CFSTI $1.00 cy, $0.50 mn |
| 11516(Rev.) | 20-1747 | Dep. mn; CFSTI $2.00 cy, $0.50 mn |
| 11639 | 20-3642 | Dep. mn; CFSTI $1.00 cy, $0.50 mn |
| 11685 | 20-3643 | Dep. mn; CFSTI $1.00 cy, $0.50 mn |
| 11976 | 20-1818 | Dep. mn; CFSTI $4.00 cy, $1.00 mn |
| 12146 | 20-2347 | Dep. mn; CFSTI $1.00 cy, $0.50 mn |
| 12447 | 20-3182 | Dep. mn; CFSTI $1.00 cy, $0.50 mn |
| 13162 | 20-2045 | Dep. mn; CFSTI $4.00 cy, $1.00 mn |
| 13188 | 20-2026 | Dep. mn; CFSTI $1.00 cy, $0.50 mn |
| 13189 | 20-1987 | Dep. mn; CFSTI $2.00 cy, $0.50 mn |
| 14245 | 20-2938 | Dep. mn; CFSTI $2.00 cy, $0.50 mn |
| 14275 | 20-3183 | Dep. mn; CFSTI $2.00 cy, $0.50 mn |
| 14287 | 20-1819 | Dep. mn; CFSTI $2.00 cy, $0.50 mn |
| 14310 | 20-3184 | Dep. mn; CFSTI $1.00 cy, $0.50 mn |
| 14335 | 20-2688 | Dep. mn; CFSTI $2.00 cy, $0.50 mn |
| 14369-T | 20-3089 | Phys. Rev. Letters, 15: 637-9(1965) |
| 14390 | 20-2585 | Phys. Rev. Letters, 15: 605-7(1965) |
| 16051 | 20-2348 | Dep. mn; CFSTI $2.00 cy, $0.50 mn |
| 16140 | 20-2689 | Dep. mn; CFSTI $1.00 cy, $0.50 mn |
| 16154 | 20-1620 | Dep. mn; CFSTI $4.00 cy, $0.75 mn |
| 16199 | 20-3644 | Dep. mn; CFSTI $1.00 cy, $0.50 mn |
| 16216 | 20-3022 | Dep. mn; CFSTI $1.00 cy, $0.50 mn |
| 16218 | 20-3023 | Dep. mn; CFSTI $1.00 cy, $0.50 mn |
| 16223 | 20-2540 | Dep. mn; CFSTI $1.00 cy, $0.50 mn |
| 16228 | 20-2541 | Dep. mn; CFSTI $1.00 cy, $0.50 mn |
| 16236 | 20-2542 | Dep. mn; CFSTI $1.00 cy, $0.50 mn |
| 16238 | 20-2543 | Dep. mn; CFSTI $1.00 cy, $0.50 mn |
| 16241 | 20-2596 | Dep. mn; CFSTI $5.00 cy, $1.00 mn |
| 16298 | 20-2905 | Phys. Letters, 19: 101-2(1965) |
| 16309 | 20-2544 | Dep. mn; CFSTI $1.00 cy, $0.50 mn |
| 16319 | 20-3088 | Phys. Rev. Lett., 15: 680-3(1965) |
| 16320 | 20-2349 | Dep. mn; CFSTI $3.00 cy, $0.75 mn |
| 16324 | 20-3024 | Dep. mn; CFSTI $2.00 cy, $0.50 mn |
| 16344 | 20-3645 | Dep. mn; CFSTI $5.00 cy, $1.25 mn |
| 16357(Rev.) | 20-2105 | Dep. mn; CFSTI $1.00 cy, $0.50 mn |
| 16386 | 20-2545 | Dep. mn; CFSTI $1.00 cy, $0.50 mn |
| 16387 | 20-1621 | Dep. mn; CFSTI $1.00 cy, $0.50 mn |
| 16389 | 20-2546 | Dep. mn; CFSTI $1.00 cy, $0.50 mn |
| **UCRL-Trans–** | | |
| 1245(L) | 20-1750 | Dep. mn; JCL $1.60 fs, $0.80 mf |
| **UJV–** | **(Czechoslovakian)** | |
| 1309b/65 | 20-3381 | Dep. mn |
| 1346/65 | 20-2106 | Dep. mn |
| 1369/65 | 20-1748 | Dep. mn |
| **UR–** | | |
| 875-73 | 20-2771 | J. Math. Phys. (N. Y.). 6: 1547-57(1965) |
| 875-98 | 20-2547 | Dep. mn; CFSTI $1.00 cy, $0.50 mn |
| 875-100 | 20-2758 | Dep. mn; CFSTI $2.00 cy, $0.50 mn |
| 875-102 | 20-2759 | Dep. mn; CFSTI $2.00 cy, $0.50 mn |
| **USBM-RC–** | | |
| 1205 | 20-2350 | Dep. mn; CFSTI $2.00 cy, $0.50 mn |
| **USNRDL-TR–** | **(Misc.)** | |
| 888 | 20-2048 | Dep. mn; CFSTI $3.00 cy, $0.75 mn |
| 889 | 20-2122 | See AD-622626 |
| 903 | 20-1894 | See AD-623095 |
| 911 | 20-1606 | See AD-623079 |
| 912 | 20-1749 | Dep. mn; CFSTI $2.00 cy, $0.50 mn |
| **VDDIT–** | **(Swedish)** | |
| 94 | 20-1976 | Dep. mn |
| **WAPD-T–** | | |
| 1710 | 20-2939 | Dep. mn; CFSTI $1.00 cy, $0.50 mn |
| 1720 | 20-2435 | Dep. mn; CFSTI $2.00 cy, $0.50 mn<br>Nucl. Appl., 1: 439-45(1965) |
| 1732 | 20-3326 | Dep. mn; CFSTI $1.00 cy, $0.50 mn |
| 1757(Rev.) | 20-2355 | Dep. mn; CFSTI $2.00 cy, $0.50 mn |
| **WAPD-TM–** | **(Misc.)** | |
| 532 | 20-3382 | Dep. mn; CFSTI $3.00 cy, $0.50 mn |
| **WAPD-Trans–** | | |
| 21 | 20-2361 | Dep. mn; JCL $1.60 fs, $0.80 mf |
| **WCAP–** | **(Misc.)** | |
| 2056(Pt.6) | 20-2262 | Dep. mn; CFSTI $5.00 cy, $1.00 mn |
| 2120 | 20-3485 | Dep. mn; CFSTI $2.00 cy, $0.75 mn |
| 3269-48 | 20-3383 | Dep. mn; CFSTI $3.00 cy, $0.75 mn |
| **WERL–** | **(Misc.)** | |
| 8844-4 | 20-2436 | Dep. mn; CFSTI $2.00 cy, $0.50 mn |
| 8844-6 | 20-2437 | Dep. mn; CFSTI $6.00 cy, $1.25 mn |
| **WL-TR–** | **(Non-AEC)** | |
| 64-156 | 20-2073 | See AD-618101 |
| 64-180 | 20-2931 | See AD-616518 |
| 65-11 | 20-1980 | See AD-614990 |
| **WT–** | **(Misc.)** | |
| 820 | 20-1622 | Dep. mn; CFSTI $3.00 cy, $0.75 mn |

# DEPOSITORIES OF USAEC REPORTS

## In Countries Other than the U.S.

**ARGENTINA**
Buenos Aires, Comisión Nacional de Energía Atómica
**AUSTRALIA**
Canberra, Australian National Library
Sutherland, New South Wales, Australian Atomic Energy Commission
**AUSTRIA**
Vienna, Zentral Bibliothek der Physikalischen Institute der Universität
**BELGIUM**
Mol-Donk, Centre d'Etude de l'Energie Nucleaire
**BOLIVIA**
La Paz, Comisión Nacional de Energia Nuclear
**BRAZIL**
Rio de Janeiro, Instituto Brasileiro de Bibliografia e Documentacao
São Paulo, Instituto de Energia Atomica, Cidade Universitaria São Paulo
**BURMA**
Rangoon, Union of Burma Applied Research Institute, Atomic Energy Center Library
**CANADA**
Hamilton, McMaster University
Ottawa, National Research Council Library
Vancouver, University of British Columbia
**CHILE**
Santiago, Instituto de Fisica y Matematicas, Universidad de Chile
**CHINA**
Hsinchu, Taiwan, Free China, National Tsing Hua University
**COLOMBIA**
Bogota, Instituto De Asuntos Nucleares
**COSTA RICA**
San Pedro, University of Costa Rica Library
**DENMARK**
Risö, Danish Atomic Energy Commission
**ECUADOR**
Quito, Escuela Politécnica Nacional
**EL SALVADOR**
San Salvador, Universidad de El Salvador, Biblioteca de Energia Nuclear
**FINLAND**
Helsinki, Teknillisen Korkeakoulun Kirjasto
**FRANCE**
Gif-sur-Yvette, Centre d'Etudes Nucléaires de Saclay
Paris, Académie des Sciences
**GERMANY**
Berlin, Hahn-Meitner-Institut für Kernforschung Berlin
Frankfurt/Main, Gmelin-Institut
Munich, Technische Hochschule, Bibliothek
**GHANA**
Accra, University College of Ghana
**GREECE**
Athens, Nuclear Research Center "Democritus"
**GUATEMALA**
Guatemala, Comisión Nacional de Energía Nuclear
**INDIA**
Bombay, Department of Atomic Energy
**INDONESIA**
Djogjakarta, Java, Science Faculty, Gadjah Mada University
**IRAN**
Tehran, Tehran University Nuclear Centre
**IRAQ**
Baghdad, Iraqi Atomic Energy Commission
**IRELAND**
Dublin, University College
**ISRAEL**
Rehovoth, Israel Atomic Energy Commission
**ITALY**
Rome, Centro di Studi Nucleari della Casaccia
Rome, Comitato Nazionale per l'Energia Nucleare
**JAPAN**
Tokyo, National Diet Library
**KOREA**
Seoul, Office of Atomic Energy
**LEBANON**
Beirut, Lebanese National Council for Scientific Research
**LUXEMBOURG**
Luxembourg, Ministry of Transport and Electricity
**MALAYSIA**
Kuala Lumpur, University of Malaysia
**MEXICO**
Mexico, D.F., Comisión Nacional de Energía Nuclear
**NETHERLANDS**
The Hague, Reactor Centrum Nederland
**NEW ZEALAND**
Lower Hutt, Institute of Nuclear Sciences
**NIGERIA**
Ibadan, University of Ibadan
**NORWAY**
Lillestrom, Institutt för Atomenergi
**PAKISTAN**
Lahore, West Pakistan, Atomic Energy Centre
**PERU**
Lima, Junta de Control de Energia Atomica
**PHILIPPINE REPUBLIC**
Manila, Philippine Atomic Energy Commission
**POLAND**
Warsaw, Biura Pelnomocnika Rzadu do Spraw Wykorzystania Energii Jadrowej
**PORTUGAL**
Sacavem, Junta de Energía Nuclear
**REPUBLIC OF SOUTH AFRICA**
Pretoria, Atomic Energy Board Library
**REPUBLIC OF THE CONGO**
Leopoldville, Université Lovanium
**SPAIN**
Madrid, Junta de Energía Nuclear, Biblioteca Documentación y Publicaciones, Ciudad Universitaria
**SWEDEN**
Nyköping, Aktiebolaget Atomenergi
**SWITZERLAND**
Zürich, Eidgenössische Technische Hochschule, Bibliothek
**THAILAND**
Bangkok, Office of the Thai Atomic Energy Commission, Department of Science
**TURKEY**
Ankara, Turkish Atomic Energy Commission, Atomic Energy Library
**UNITED ARAB REPUBLIC**
Cairo, Atomic Energy Commission
**UNITED KINGDOM**
Belfast, City Library
Birmingham, Central Library
Boston Spa, National Lending Library for Science and Technology
Bristol, Central Library
Glasgow, Mitchell Library
Kingston upon Hull, Central Library
Leeds, Central Library
Liverpool, Central Library
London, Central Library, Acton
London, Science Museum Library, South Kensington
Manchester, Central Library
Newcastle upon Tyne, Central Library
Nottingham, Central Library
Sheffield, Central Library
**URUGUAY**
Montevideo, Comision Nacional de Energia Atomica
**VENEZUELA**
Caracas, Instituto Venezolano de Investigaciones Científicas
**VIET-NAM**
Saigon, Atomic Energy Office
**YUGOSLAVIA**
Belgrade, Federal Commission for Nuclear Energy

## In International Agencies

**AUSTRIA**
Vienna, International Atomic Energy Agency
**BELGIUM**
Brussels, La Bibliotheque EURATOM
**FRANCE**
Paris, European Nuclear Energy Agency, O.E.C.D.
**ITALY**
Ispra, EURATOM Research Center
**SWITZERLAND**
Geneva, United Nations Library

UNITED STATES
GOVERNMENT PRINTING OFFICE
DIVISION OF PUBLIC DOCUMENTS
WASHINGTON, D.C. 20402

OFFICIAL BUSINESS

POSTAGE AND FEES PAID
U.S. GOVERNMENT PRINTING OFFICE

# TECHNICAL PROGRESS REVIEWS

The Division of Technical Information, U. S. Atomic Energy Commission, also publishes the Technical Progress Reviews, a series of five quarterly journals on nuclear technology. These journals, compiled by specialists and recognized authorities, summarize, evaluate, and reference the progress of development in five important fields.

**Isotopes and Radiation Technology** P. S. Baker, A. F. Rupp, and associates, Oak Ridge National Laboratory. Reviews AEC-sponsored projects and related significant worldwide developments in radioisotopes and radiation technology.

**Nuclear Safety** Wm. B. Cottrell, W. H. Jordan, and associates, Oak Ridge National Laboratory. Covers topics relevant to the analysis and control of hazards associated with nuclear reactors and with operations involving fissionable materials and the products of nuclear fission.

**Power Reactor Technology** Argonne National Laboratory. Reviews research, development, design practices, and operating experiences associated with power reactors, including aerospace applications.

**Reactor Fuel Processing** Stephen Lawroski and associates, Argonne National Laboratory. Reviews all aspects of the fuel-processing field, including aqueous and nonaqueous processing and waste disposal.

**Reactor Materials** R. W. Dayton, E. M. Simons, and associates, Battelle Memorial Institute. Covers the properties, behavior, and fabrication processes of materials used in nuclear reactors and associated equipment.

## Availability

*SUBSCRIPTION RATE:* The Technical Progress Reviews may be purchased from the Superintendent of Documents, U. S. Government Printing Office, Washington, D. C. 20402, at $2.50 per year for each subscription or $0.70 per issue.

*POSTAGE:* Postpaid within the United States, Canada, Mexico, and all Central and South American countries except Argentina, Brazil, British and French Guiana, Surinam, and British Honduras. For these Central and South American countries and all other countries, add $0.75 per year or $0.20 per single issue.

*REMITTANCE:* Payment should be by check, money order, or document coupons and MUST accompany order. Remittances from foreign countries should be made by international money order or draft on an American bank payable to the Superintendent of Documents or by UNESCO book coupons.

7687